

①

AGARD-CP-322

AGARD-CP-322

AD A 123814

# AGARD

ADVISORY GROUP FOR AEROSPACE RESEARCH & DEVELOPMENT

7 RUE ANCELLE 92200 NEUILLY SUR SEINE FRANCE

AGARD CONFERENCE PROCEEDINGS No. 322

## Impact Injury Caused by Linear Acceleration: Mechanisms, Prevention and Cost

DTIC  
ELECT  
JAN 25 1983  
S E

NORTH ATLANTIC TREATY ORGANIZATION



DTIC FILE COPY

DISTRIBUTION AND AVAILABILITY  
ON BACK COVER

This document has been approved  
for public release and sales its  
distribution is unlimited.

83 01 25 033

**NORTH ATLANTIC TREATY ORGANIZATION  
ADVISORY GROUP FOR AEROSPACE RESEARCH AND DEVELOPMENT  
(ORGANISATION DU TRAITE DE L'ATLANTIQUE NORD)**

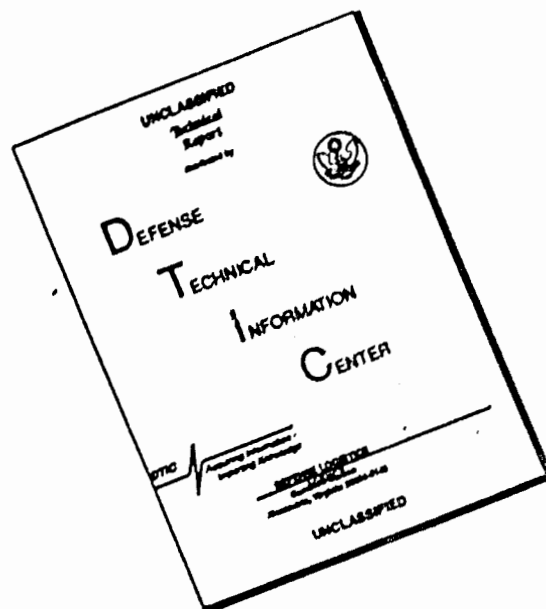
**ERRATA  
CONFERENCE PROCEEDINGS No.322**

Please note that in Paper 12 of the above publication the following alterations should be made to the figures in Tables 2 and 5: in the columns headed "Caractérisation du crâne Minéralisation ( $\text{g/cm}^2$ )" the figures should be divided by 2.

Veillez noter que dans la papier 12 de l'ouvrage mentionné ci-dessus, il faudrait effectuer les changements suivants dans les Tableaux 2 et 5: dans les colonnes intitulées "Caractérisation du crâne Minéralisation ( $\text{g/cm}^2$ )" les chiffres doivent être divisés par 2.



# DISCLAIMER NOTICE



THIS DOCUMENT IS BEST QUALITY AVAILABLE. THE COPY FURNISHED TO DTIC CONTAINED A SIGNIFICANT NUMBER OF PAGES WHICH DO NOT REPRODUCE LEGIBLY.

NORTH ATLANTIC TREATY ORGANIZATION  
ADVISORY GROUP FOR AEROSPACE RESEARCH AND DEVELOPMENT  
(ORGANISATION DU TRAITE DE L'ATLANTIQUE NORD)

AGARD Conference Proceedings No. 322

**IMPACT INJURY CAUSED BY LINEAR ACCELERATION:  
MECHANISMS, PREVENTION AND COST**

Edited by

J.L.Haley, Jr  
USAARL  
Fort Rucker, AL 36362  
USA

<b>Accession For</b>	
NTIS GRA&I	<input checked="" type="checkbox"/>
DTIC TAB	<input type="checkbox"/>
Unannounced	<input type="checkbox"/>
Justification	
By	
Distribution/	
Availability Codes	
Dist	Avail and/or Special
A	

Papers presented at the Aerospace Medical Panel Specialists' Meeting held  
in Cologne, West Germany, from 26-29 April 1982.

This document has been approved  
for public release and sale; its  
distribution is unlimited.



## THE MISSION OF AGARD

The mission of AGARD is to bring together the leading personalities of the NATO nations in the fields of science and technology relating to aerospace for the following purposes:

- Exchanging of scientific and technical information;
  - Continuously stimulating advances in the aerospace sciences relevant to strengthening the common defence posture;
  - Improving the co-operation among member nations in aerospace research and development;
  - Providing scientific and technical advice and assistance to the North Atlantic Military Committee in the field of aerospace research and development;
- Rendering scientific and technical assistance, as requested, to other NATO bodies and to member nations in connection with research and development problems in the aerospace field;
- Providing assistance to member nations for the purpose of increasing their scientific and technical potential;
- Recommending effective ways for the member nations to use their research and development capabilities for the common benefit of the NATO community.

The highest authority within AGARD is the National Delegates Board consisting of officially appointed senior representatives from each member nation. The mission of AGARD is carried out through the Panels which are composed of experts appointed by the National Delegates, the Consultant and Exchange Programme and the Aerospace Applications Studies Programme. The results of AGARD work are reported to the member nations and the NATO Authorities through the AGARD series of publications of which this is one.

Participation in AGARD activities is by invitation only and is normally limited to citizens of the NATO nations.

The content of this publication has been reproduced directly from material supplied by AGARD or the authors.

Published October 1982

Copyright © AGARD 1982  
All Rights Reserved

ISBN 92-835-0317-0



*Printed by Technical Editing and Reproduction Ltd  
5-11 Mortimer Street, London, W1N 7RH*

## PREFACE

Eleven years ago, an AGARD conference was convened in Oporto, Portugal which brought together experts in linear acceleration effects. Impact injury research and impact protection design have advanced to the point that a follow-up conference was deemed appropriate. In the intervening decade the need for impact injury protection in NATO aircraft has increased, largely because many of NATO aircraft are helicopters in which the only method of emergency escape is a landing of the vehicle under less than ideal conditions. Impact protection is important also in fixed wing aircraft and land vehicles in these accidents in which the living space of the occupants is maintained.

With the above facts for emphasis, the Aerospace Medical Panel initiated plans in 1979 to convene this conference. The Biodynamics Committee of the Aerospace Medical Panel selected Impact Injury as the title. The committee then selected the session organizers to determine the content and scope of the conference. Author's were sought who could best present the progress on impact research and impact protection. The session organizers sent requests for abstracts to highly qualified people to insure that enough abstracts were available to permit an optimum selection. The number of abstracts submitted was gratifying, indeed about twice as many abstracts were submitted as could be accepted. In addition, to the keynote paper, a total of 39 papers were finally accepted.

The conference was held at Porz-Wahn (near Cologne) West Germany on 24-28 April 1982. The host for this meeting was the Deutsche Forschungs-und Versuchsanstalt für Luft-und Raumfahrt e. V. (DFVLR), the German Aerospace Research Establishment. The meeting facilities were excellent, for which the organizers are indebted to our host, the DFVLR.

The papers were presented in four sessions during the four-day conference. The attendees were provided the opportunity to ask speakers questions at the end of their presentations. The recordings of these question-answer dialogues, as well as the opening and closing speeches, have been transcribed, condensed, and edited prior to publication.

Your editor wishes to apologize to those speakers to whom the printed and edited word does not match the thought the speaker wished to convey to the attendees. Rest assured that all changes made from the oral to the printed words were intended to clarify the idea and not to change it. In any event, your editor assumes responsibility for deletions and errors in the transcription process. If grave errors are noted, please contact AGARD Headquarters at the address noted on the cover page and ask for a correction.

Your editor wishes to thank Ms. Je. nnette Hinkle of the U.S. Army Aeromedical Research Laboratory, Fort Rucker, Alabama, for the transcription and typing of the opening ceremony, question-answer dialogue, and Round Table Discussions; her devotion to this task made my work far easier. In addition, I wish to thank my co-workers of the Programme Organization Committee and the Session Chairman for their outstanding efforts.

#### **AEROSPACE MEDICAL PANEL**

Chairman:           Medecin Colonel J.L.Bande, BE  
Deputy Chairman:   Air Commodore P.Howard, UK  
Executive:           Squadron Leader J.M.Mullaney, UK

#### **MEETING ORGANISATION**

Session Organiser:     Mr J.L.Haley, Jr, US  
Host Nation Coordinator:   Mr H.Bubenzer, FRG

PROGRAMME CHAIRMAN

Mr. J. L. Haley, Jr.  
Biodynamics Research Division  
US Army Aeromedical Research Laboratory (USAARL)  
P.O. Box 577  
Fort Rucker, AL 36362, USA

SESSION CHAIRMAN

Session I: Dr. H. E. von Gierke  
U.S. Air Force Aerospace Medical Research Laboratory  
Wright-Patterson Air Force Base, OH 45433

Session II: Dr. D. J. Thomas  
U.S. Naval Biodynamics Laboratory  
Michoud Station (NASA)  
P.O. Box 29407  
New Orleans, LA 70189

Session III: Dr. D. H. Glaister  
R.A.F. Institute of Aviation Medicine  
Farnborough, Hampshire GU14  
England

Session IV: Dr. R. Auffret  
Centre d'Essais en Vol  
BP No. 2, 91220 Bretigny Air  
France

ROUND TABLE DISCUSSION

Chairman: Dr. H. E. von Gierke, US Air Force Aeromedical Research Laboratory,  
Dayton, OH 45433

Members:

Professor Dr. Bier, Forensic Institute, University of Munich, Munich 2, FRG

Mr. B. Carnell, Sikorsky Aircraft Corporation, Stratford, Connecticut 06602

Mr. E. Franchini, FIAT Automobiles, Turin, Italy

Dr. D. J. Thomas, Naval Biodynamics Laboratory, New Orleans, LA 70189

# CONTENTS

	Page
PREFACE	iii
PANEL AND MEETING OFFICERS	iv
SESSION ORGANISER AND SUB-CHAIRMAN	v
TECHNICAL EVALUATION REPORT by J.L.Haley, Jr.	ix
REVIEW OF IMPACT ACCELERATION MEETING IN OPORTO, PORTUGAL IN JUNE 1971 by S.C.Knapp	xi
IMPACT PROTECTION IN HELICOPTERS DESIGN SPECIFICATIONS VS PERFORMANCE by J.L.Haley, Jr.	xiv
	Reference
CHRONIC EFFECTS OF +G <sub>z</sub> IMPACT ON THE BABOON SPINE by D.C. Van Sickle and L.E.Kazarian	1
MECHANISMS OF HEAD IMPACT INJURY AND MODIFICATION BY HELMET PROTECTION by A.M.Nahum and C.Ward	2
DYNAMIC FRONTO-OCCIPITAL HEAD LOADING OF HELMET-PROTECTED CADAVERS by R.Mattern, F.Schueler and G.Schmidt	3
TEMPORAL CHARACTERISTICS OF TRANSLATIONAL ACCELERATION IN THE PREDICTION OF HELMETED HEAD INJURY by J.A.Newman	4
Paper 5 Withdrawn	
ETUDE EN REGIME IMPULSIONNEL ET "IN VIVO" DE LA TRANSMISSIBILITE DES DISQUES INTERVERTEBRAUX LOMBAIRES D'UN PRIMATE par P.Quandieu, L.Pellieux et al.	6
HUMAN CADAVERIC RESPONSE TO SIMULATED HELICOPTER CRASHES by A.I.King and R.S.Levine	7
Paper 8 Withdrawn	
INJURY MECHANISMS IN FRONTAL COLLISIONS INVOLVING GLANCE-OFF by W.Reidelbach and F.Zeidler	9
ACCELERATION DAMAGE TO THE BRAIN by T.A.Gennarelli and L.E.Thibault	10
THE DEVELOPMENT OF INTRACRANIAL TISSUE COMPONENT FAILURE CRITERIA AS A CONSEQUENCE OF CONTROLLED INERTIAL LOADING by L.E.Thibault and T.A.Gennarelli	11
INFLUENCES RESPECTIVES DE L'ACCELERATION, DU JERK ET DE L'AMPLITUDE DE LA FLEXION DU COU SUR LA SURVENUE DES LESIONS CEREBRALES par C.Tarriere, G.Walfisch et al.	12
HEAD AND SPINE INJURIES by A.Sances, Jr, J.Myklebust et al.	13

	Reference
NEUROPHYSIOLOGICAL EFFECTS OF -X IMPACT ACCELERATION by M.S.Weiss and M.D.Berger	14
INSTRUMENTATION REQUIREMENTS FOR ASSESSING OCCUPANT RESPONSE TO THREE DIMENSIONAL HIGH ACCELERATION ENVIRONMENTS by G.D.Frisch and L.A.D'Aulerio	15
EVOKED POTENTIAL STUDIES OF CENTRAL NERVOUS SYSTEM INJURY DUE TO IMPACT ACCELERATION by B.Saltzberg, W.D.Burton, Jr, et al.	16
NEUROPATHOLOGY OF THE RHESUS MONKEY UNDERGOING -Gx IMPACT ACCELERATION by F.Unterharnscheidt	17
Paper 18 Withdrawn	
RECHERCHE CONCERNANT LA PROTECTION DE LA COLONNE VERTEBRALE AUX ACCELERATIONS DE L'EJECTION par F.Coussau, B.Vettes et G.Bezamat	19
Paper 20 Withdrawn	
THE U.S. NAVY APPROACH TO CRASHWORTHY SEATING SYSTEMS by M.Schulman	21
DEVELOPMENT OF IMPROVED CRITERIA FOR ENERGY-ABSORBING AIRCRAFT SEATS by S.P.Desjardins, J.W.Coltman and D.H.Laananen	22
EFFECT OF REEL-TYPE WEBBING RETRACTORS AND SHOULDER-BELT SLACK ON DUMMY DYNAMICS DURING SIMULATED FRONTAL VEHICLE IMPACTS by T.J.Bowden, J.K.Reichert and A.K.Nassim	23
MADYMO - A CRASH VICTIM SIMULATION COMPUTER PROGRAM FOR BIOMECHANICAL RESEARCH AND OPTIMIZATION OF DESIGNS FOR IMPACT INJURY PREVENTION by J.Wismans, J.Maitha, J.J. van Wijk and E.G.Janssen	24
Paper 25 Withdrawn	
ADVANCED RESTRAINT SYSTEM CONCEPTS by W.Reidelbach and H.Scholz	26
RECENT IMPROVEMENTS IN CRASH RESTRAINT IN UK HELICOPTERS by A.P.Steele-Perkins	27
EVALUATION SUR BANC D'ACCELERATION HORIZONTAL ET LORS D'UN CRASH SIMULE DE L'EFFICACITE DE SIEGES ANTICRASH D'HELICOPTERES - ETUDE SUR MANNEQUINS ANTHROPOMORPHIQUES par B.Vettes et G.Bezamat	28
SOME LIMITATIONS OF ADULT SEAT BELTS WHEN USED TO RESTRAIN CHILD DUMMIES IN SIMULATED FRONTAL IMPACTS by A.P.Roy, K.J.Hill and G.M.Mackay	29
VALIDATION OF A BIODYNAMIC INJURY PREDICTION MODEL OF THE HEAD-SPINE SYSTEM by E.Privitzer, R.R.Hosey and J.E.Ryerson	30
EVIDENCE FOR THE UTILIZATION OF DYNAMIC PRELOAD IN IMPACT INJURY PREVENTION by B.F.Hearon, J.H.Raddin, Jr and J.W.Brinkley	31

	Reference
HEAD PROTECTION FOR ROAD USERS WITH PARTICULAR REFERENCE TO HELMETS FOR MOTORCYCLISTS by J.B.Pedder, S.B.Hagues and G.M.Mackay	32
THE DEVELOPMENT AND INITIAL EVALUATION OF AN OBLIQUE-IMPACT TEST FOR PROTECTIVE HELMETS by D.H.Glaister	33
ANALYSIS OF US ARMY AVIATION MISHAP INJURY PATTERNS by J.E.Hicks, B.H.Adams and D.F.Shanahan	34
Paper 35 Not Available	
BACKFACE SIGNATURE FROM BODY ARMOR by R.F.Rolsten and D.J.Karl	36
COST EFFECTIVENESS OF BODY ARMOR by R.H.Holmes	37
TRAUMATISMES PAR IMPACT EN SERVICE AERIEN ET APTITUDE AU VOL A LA FORCE AERIENNE BELGE par A.Flion	38
IMPACT INJURIES FROM LINEAR ACCELERATION SUSTAINED BY AN F-5 MAN/MACHINE COLLIDING WITH THE TERRAIN AT 45 KIAS by H.T.Andersen	39
ROUND TABLE DISCUSSION	RTD
LIST OF PARTICIPANTS	P

## TECHNICAL EVALUATION REPORT

### GENERAL

By and large, this was a data-oriented conference. The papers presented on spinal column injury, head injury, torso injury, restraint systems, ballistic armor, crashworthy vehicles and accident investigation techniques all provided new data or new ideas on how to prevent or alleviate impact injuries. Whether or not one agrees with all the ideas presented is a moot point, because the ideas are now committed to posterity for judgement!

### SPINAL COLUMN INJURIES UNDER COMPRESSIVE AND/OR BENDING LOAD

A paper is included on spinal column arthritis (spondylosis deformans) as found in baboons several years after exposure to  $+40g_z$  of 13-16 milliseconds duration. Another paper describes a unique method of spinal column instrumentation with accelerometers mounted on each vertebra, so that, the response to vibratory or impact input at the buttocks can be evaluated.

The effect of high acceleration onset rate (1500-2000 g/sec) for "eyeballs down and forward" ( $g_z$  combined with 30%  $g_x$  vector) on cadavers is addressed in two papers. Although these tests were conducted primarily to evaluate the adequacy of a vertically stroking (load-limiting) seat, the effect on the seat occupant is similar to that of the ejection seat occupant during ejection except that the onset rate is about one-third that of the shock-absorbing seat, and the pulse duration is nearly twice as great. In any event, these fully instrumented crashworthy seat and cadaver tests may provide useful comparative vertebral fracture data for future ejection seat tests.

Inflatable head-neck "bracing" devices are discussed in several papers from Europe and America, indicating the universal recognition of the spinal column compressive and bending loading problem.

### SPINAL COLUMN INJURIES UNDER TENSILE LOAD

One paper presented data on human whole neck (in situ) static load capacity. These tests, on seven specimens, revealed basilar skull, cervical, and several T2 fractures at maximum loads ranging from 1535N up to 3892N.

If a mass of 5 Kg is assumed for the head, these loads range up to 80 g for a severe injury range in the eyeballs up ( $-g_z$ ) direction. These tensile fracture limits may be compared to the 105-125 g fracture (fatal) limits for rhesus monkeys stated by Dr. Thomas in the round table discussion for  $-g_x$  tolerance (converts to  $+g_z$  as head rotates forward  $90^\circ$ ). In short, this tensile data may be compared to volunteer ( $-g_x$ ) tolerance values to show the range for the unrestrained head and neck.

### LEG INJURY

Only one paper is presented on this topic. Lower leg injuries are discussed indirectly with regard to structural protection in an automobile in glanc-off accidents.

### HEAD AND NECK INJURY

No less than 12 papers (one-third of total papers) are included on head and/or neck injury! Obviously, this is a well-recognized problem, and obviously it is receiving some attention. This is not surprising since numerous aircraft accident statistics reveal the head to be a large injury producer; for example, for U.S. Army fliers in the past decade, two of five fatalities were caused by head injury. Several papers discuss the impact of unembalmed cadaver heads with the circulatory system perfused with a particulate such as india ink. This technique permits the identification, extent and location of hemorrhage in the head/neck circulatory system in the post-impact autopsy. Since minute hemorrhage is equivalent to some degree of head injury, this method provides an impact injury threshold for the particular specimen under test. Of course, mortality and biological age effects must be considered. One paper uses this data in the development of a finite element head model in which intracranial pressure and acceleration are compared to input energy at the threshold of hemorrhage of blood vessels.

The data presented in one paper supports the concept that the head c.g. acceleration is more important than any other measurement being made at current helmet testing facilities. This paper pleads for the use of acceleration as the best measurement to be used in the evaluation of impact helmets, in view of the myriad number of conflicting time evaluation schemes.

Mechanisms of head injury are classified from mild concussion to structural damage in two papers. These papers provide not only head injury mechanisms, but also very good research techniques in microtrauma.

A new and unique helmeted-headform test method is discussed in which the helmeted headform is permitted to truly free fall without use of guiding cables or wires. The method permits tangential impacts and also eliminates the friction associated with all types of guiding devices.

Several papers discussed the neurological effects of monkey head impacts and the techniques used to measure these effects. The cortical evoked potential values showed changes at a threshold of approximately  $600 \text{ m/s}^2$ .

Unfortunately, as noted by Dr. von Gierke in the Round Table Discussion, although much good research has been done, no agreement was reached on head impact evaluation criteria. Such agreement still awaits the future.



## INJURY DATA COLLECTION

Several papers provided descriptions of accident/injury investigations. One paper described an improved crash injury identification (coding) and reporting system as developed for U.S. Army aviation; this system appears to offer simplicity of presentation with enough detail to clarify injury causes. If the proposed injury-cause coding system is fully implemented, the cost effectiveness of injury-preventing hardware can be determined more easily in the future.

## INJURY-PREVENTING HARDWARE

The keynote paper by the writer outlined the features and the preliminary indication of crashworthiness in the U.S. Army's new UH-60 "Blackhawk" helicopter by comparison to the older UH-1 Helicopter. The data shows that a pilot actually received no back injury, in fact no injury at all, in a crash so severe that the same kinematics in a UH-1 would have resulted in a severe back injury or maybe a fatality.

Several papers outlined the development of crashworthy seats, designed to meet stringent new specifications. Both the U.S. Army and Navy have developed pilot and troop seats to "limit" the loads in the vertical (z axis) to approximately 15 g on occupants. Such crashworthy seats are currently in production, a noteworthy achievement in the past decade!

The effect of too much harness slack and the effects of dynamic preload were addressed and revealed the increase and decrease respectively of the "dynamic overshoot" in the output loads as would be expected.

Crash-sensing air bags combined with conventional harnesses were shown to be effective. Nevertheless, the production cost of approximately 600 dollars appears to be a deterrent to usage in small, low-cost automobiles.

One paper described the crash test of a French "Puma" helicopter. Crashworthy seats with instrumented dummies demonstrated their performance in the test.

The use of webbing as an energy-absorbing device, via the "tearing" of the material, was discussed in one paper. The method appears to be a low-cost and effective "load-limiting" device.

## VERIFICATION OF SEAT/MAN MODELS

Two papers are included on this topic, one from the Netherlands, and one from the United States. The Netherlands MADYMO Crash Victim Simulator appears to be a highly versatile model. Simulations as diverse as pedestrian impact to children's seats are demonstrated.

The U.S. Human Spine Model (HSM) is the most detailed model known of the human spine. This model has been validated up to the level of human volunteer tests, but not into the injury range.

## CAN CRASHWORTHINESS BE COST EFFECTIVE?

This question is addressed and partially answered in Session IV. The two papers on body armor certainly reveal the cost effectiveness of simple upper torso protection against exploding ammunition. In addition, one paper provides the methods to obtain detailed injury and hardware damage costs associated with helicopter crashes so that cost effectiveness can be estimated based on accident histories.

## CONCLUSIONS

Based on discussions in this proceedings, it is concluded that:

- a. Crash injury data collection at the scene of aircraft accidents varies from none to fragmented approaches in most AGARD nations represented.
- b. Methods to encourage the use of impact protective harnesses already available in automobiles and aircraft should be intensified.
- c. The tolerance of the seated human spinal column and cord to compressive and transverse load, with a helmeted head both unrestrained and restrained, should be studied further.
- d. The tolerance of the seated torso, with upper and lower torso restraint, to transverse loads should be studied further. The helmeted head should be unrestrained and compared with the restrained head.
- e. The cost effectiveness of various head restraint methods for use by pilots in aircraft should be analyzed.
- f. Contact head injury mechanisms should be studied further; however, the existing data should be applied to headgear design and evaluation. A large communication gap appears to exist between head injury researchers and helmet test method researchers.
- g. Body armor is highly effective, especially against exploding ammunition, and is well worth the modest cost.

REVIEW OF IMPACT ACCELERATION MEETING IN  
Oporto, Portugal in June 1971

by

Col. S.C. Knapp  
Commander  
U.S. Army Aeromedical Research Laboratory  
(USAARL)  
P.O. Box 577  
Fort Rucker, AL 36362

Since Dr. Richard Snyder from the University of Michigan is not able to be here for this "kick off" address, your session chairman asked that I offer a prelude to this symposium by reviewing a very significant meeting that was held in Oporto, Portugal in 1971. This Oporto meeting was held under the leadership of Dr. Edward J. Baldes (deceased), who was well known as a physician, physicist, and physiologist of great credit. Many of us attended this 1971 meeting. This earlier meeting is published as AGARD Conference Proceedings CP88-71, "Linear Acceleration of Impact Type." History is an important part of the advisory group for aerospace research and development. It's no less important for the aerospace medical panel, one of the original panels of the advisory group, and it is significant that the Biodynamics Subcommittee was one of the first Biodynamics Subcommittees formed, and I believe the first two chairmen of the committee were Dr. Walter Jones of the United States and Dr. David Glaister of the United Kingdom. In 1961, at Brooks AFB, Texas, the National Research Council of the National Academy of Science in conjunction with the National Aeronautics and Space Administration in the United States held a symposium called, "Impact Acceleration Stress." It is interesting as we review the history, that at approximate 10 year intervals the group assembled here, and the science that you represent, have seen the need to review the advancements that have been made in our particular area of biodynamics.

I've reviewed some of the significant events that occurred in that 1971 meeting and I would like to relate some of them because I think they are very important. We must look back on history and see what we thought were the problems 11 years ago if we are to gain some sense of accomplishment for what we will talk about in this meeting 11 years later. We have to ask ourselves, "Have any advancements been made? Have any problems been solved? What are the new problems? And where do we go from here?" Dr. Baldes in his opening comments made the following statement, "Words fail me when I attempt to express the IMPACT on civilization of the man-wrought epidemic which our science and technology has created." Dr. Baldes went on to describe in some detail the problems in translating Newton's original 3 laws of motion from the Latin into English, and he made note that in all of the historical translations, nowhere is there a translation from original Latin into English that uses any term that relates to the human body. I think that is interesting because the things that you, ladies and gentlemen, will talk about in this meeting, involve a human body and its relationship between these three fundamental human laws of motion. We will talk about cannonballs in terms of bullets and impact. We will talk about high velocities. We will talk about sudden stops. We will talk about forces placed upon the human body and how the human body responds to them.

Those of you that attended the 1971 meeting will remember that at least six major topics were covered as shown in Fig. 1-1. There was a session on the various sled test devices in use in 1971. There was some discussion of automotive and aircraft crashworthiness. Improved crash sensor devices were developed which helped to make air bags and other crashworthy devices more feasible.

We were at the threshold of the development of the first crashworthy aircraft, specifically helicopters designed for purely military use. Some joint agreements were consummated for looking at crashworthy engineering as a way of reducing injury and death. The US Army published a new military standard for crashworthiness. Crashworthy fuel systems were installed in most US Army helicopters and I can tell you that 11 years later, in US Army helicopters so equipped, there has not been a fire-related fatality in a survivable type crash, a very significant advance. Aircraft seats with integral stroking devices was an idea that had not yet been employed in actual aircraft; this is no longer the case. Several helicopter manufacturers now sell this type seating in their commercial aircraft and the US military services now require them.

The question is how much progress have we made? Where have we come since Oporto 1971? In Oporto, it was decided that we had come a long way from NRC meeting that was held at Brooks AFB in 1961. I am interested to see where we are today and I am sure you will give us insight into the significant advances since that 1971 meeting. See Fig. 1-2

## '71 MEETING REVIEW

- o SLED TEST DEVICES
- o AIRCRAFT & AUTO CRASH TESTS
- o INJURY MECHANISMS
- o CRASHWORTHY HARDWARE DEVELOPMENT
- o BIODYNAMIC MODELS
- o HEADGEAR DEVELOPMENT

Fig. 1-1 Topics Covered in AGARD Symposium in Oporto, Portugal

## IMPACT PROTECTION ADVANCES IN THE 70's

- o AUTOMOBILES - RESTRAINT, PADDING & STRUCTURE
- o HELICOPTER - UH-60 UTILITY & AH-64 ATTACK DEVELOPED TO CRASHWORTHY CRITERIA
- o TRANSPORT AIRCRAFT - DELETED CAM-TYPE BELTS, IMPROVED BELT GEOMETRY, & IMPROVED EMERGENCY EGRESS
- o JOINT AGREEMENT BETWEEN U. S., FR, & GE TO CO-ORDINATE HELICOPTER CRASHWORTHY DEVELOPMENT
- o MIL-STD 1290 "LIGHT FIXED & ROTARY-WING AIRCRAFT CRASHWORTHINESS" PUBLISHED
- o CRASHWORTHY FUEL SYSTEMS INSTALLED IN U. S. ARMY HELICOPTERS
- o AIRCRAFT SEATS WITH INTEGRAL "STROKING" DEVICES (LOAD-LIMITER) DEVELOPED & PRODUCED
- o ROCKET-POWERED EJECTION SEATS PERFECTED
- o FEDERAL AVIATION ADMIN. REQUIRED SHOULDER HARNESSSES IN ALL FIXED WING
- o U. S. ARMY LOWERED PASS-FAIL HELMET CRITERIA FROM 400g TO 150g FOR FUTURE DESIGN
- o IMPROVED CRASH SENSOR DEVICES DEVELOPED

## IMPACT PROTECTION IN HELICOPTERS DESIGN SPECIFICATIONS VS PERFORMANCE

J. L. Haley, Jr., Aerospace Engineer  
Biodynamics Research Division, USAARL  
Fort Rucker, Alabama 36362

### INTRODUCTION

In the previous introductory paper, a summary of crashworthy improvements in air and ground vehicles over the past decade has been outlined, and since this is a conference to bring together impact research results rather than a history of accident injuries, I have chosen to provide a very brief description of the actual crash performance of a specific US Army helicopter, the UH-60. This aircraft was conceived and developed in the 70's by Sikorsky Helicopter under the US Army competitive selection process as a replacement aircraft for the aging UH-1, which was developed in the 50's.

The UH-60 was developed to the most stringent requirements for crashworthiness of any aircraft yet developed of either fixed or rotary wing type. The UH-60 has now been in service for enough time so that several severe accidents have occurred. This paper will review the impact protection provided by the UH-60 in these accidents and compare the protection to that of the UH-1 in a similar crash.

### UH-1 D/H AND UH-60A GENERAL DESCRIPTION

The standard 13-place UH-1 and 14-place UH-60 would appear to be of similar size, but the data of Table 1-3 reveals the UH-60 to be a larger, heavier, and faster aircraft. The UH-60 has more floor space to accommodate 51 cm wide troop seats compared to 43 cm seats in the UH-1. The larger troop seats facilitate ingress-egress in the UH-60.

### CRASHWORTHY PERFORMANCE

A total of five UH-60 crashes were selected for this paper. These crashes were selected because a wide range of severe impact conditions are covered and personnel injuries did occur in the crashes. The crashworthy performance of these five UH-60's is summarized in Table 1-4 by showing the terrain impact conditions, aircraft orientation (attitude), floor acceleration against landing gear/seat stroke, and aircrew injuries. The same data for two UH-1 aircraft crashes is also included in Table 1-4 as points of reference.

Although case one might have been deleted in this comparison since no one survived and the cabin living space was destroyed, the writer chose to retain it because the impact conditions do show an upper limit to the protection provided by the UH-60. It was clear that the roof was separated from the floor due to the combined impact and hydraulic loads and that survival was doubtful with no protective cage.

A review of the impact conditions in Table 1-4 shows that the horizontal impact velocity was generally low by comparison to fixed wing aircraft (1), varying from zero up to 17 meters per second, if the nonsurvivable case is deleted. This is clearly not the case for vertical velocity at impact which varies from six to 17 meters per second, clearly beyond the three meter per second capacity of most aircraft landing gear. The crash path distance (distance traversed from terrain contact to rest point) is indicative of the low horizontal velocity at impact varying up to nine meters. The terrain is very typical of that seen by military aircraft at off-airport crash sites.

The aircraft attitude at impact varies considerably, but it should be noted that cases 1, 3, and 6 struck the terrain under uncontrollable conditions. Cases 2, 5, and 6 point out the fact that a pitch up at impact is desirable for improved survivability. The excessive sink velocity in cases 2 and 5 caused excessive floor acceleration but the load level on the occupants was reduced to tolerable values by the stroking landing gear and seats of the UH-60.

The floor acceleration estimates were made for the area of floor near the seats. Since these values are estimates, the values shown are equal to or greater than some known event(s). For example, in case four, the vertical g peak is based on the fact that the energy absorbing pilot seat, designed to limit the seat to 14.5 g did not stroke, indicating that the load did not exceed 15 g on the pilots.

Landing gear energy absorption is indicated by the displacement (stroke) of the gear and the average force level applied to the fuselage during the stroke. Note that the UH-60 provides approximately 14 times more energy absorption than does the UH-1. This capacity will hopefully be helpful in preventing expensive airframe damage caused

by fuselage belly and/or main rotor terrain contact in high sink speed and roll-over crashes.

The vertical displacement (stroke) of the UH-60 seats is an excellent indicator of crash performance. If the seat does not stroke, and the occupant sustains lower spinal column fractures, it may be hypothesized that the load-limiting shock-absorbers have provided too much resistance. The current production UH-60 seats are designed to provide a load level of 14.5 g on a 50th percentile mass occupant. Table 1-4 shows that these seats stroked to the maximum depth available in case two (0.37 m) and almost the maximum depth in case five (0.34 m and 0.25 m); even though injuries were sustained, it is noteworthy that no spinal column fractures occurred\*. The absence of spinal injuries in cases 2 and 5\* provide some assurance that the tolerance of these pilots, even when exposed to simultaneous forward and sideward loads, can sustain a 14.5 g input acceleration without spinal column fracture. A U.S. tri-service program is currently underway at Wayne State University with an objective to establish the threshold of injury level for combined vertical and forward loads (see papers by Desjardins and King in this proceedings).

The item in Table 1-4 labeled Protective Container provides a gross indication of volume change in the aircraft's living space due to inward deformation. It should be noted that a reduction of five percent, as in case three, was critical because the change occurred in the cockpit alone and the inwardly deformed structure caused contact and/or crushing injuries.

Although the four survivable UH-60 cases do not provide enough injuries with which to make statistically valid conclusions, some tentative comments are appropriate. Overall, it can be seen that four of 16 people aboard the UH-60 (in cases two through five) were fatalities; the four fatalities died due to contact injuries rather than inertial acceleration from the seats. Since some of these accidents occurred recently, injury analysis is not yet complete, but the absence of spinal column injury in the pilot's seat is noteworthy\*. By comparison, it can be seen that seven of eight occupants in the two UH-1 accidents sustained spinal column fractures even though the impact conditions are less severe. Based on this preliminary data, it is clear that the UH-60 will reduce injuries, especially spinal injuries.

TABLE 1-3  
GENERAL CHARACTERISTICS OF UH-1 D/H AND UH-60A HELICOPTERS

Category	Item	UH-1	UH-60
WEIGHTS	Design Gross Weight	4300 kg	9200 kg
	Empty Weight	2400 kg	6100 kg
PERFORMANCE	Dive Speed ( $V_{NE}$ )	124 kn	193 kn
	Number Engines	1	2
	Number Main Rotor Blades	2 Rigid "Teeter" Type	4 Articulated
	Min. Descent Rate in	595 meters/min	732 meters/min
	Autorotation (100% rpm)	(63 kn I.A.S.)	(80 kn I.A.S.)
CRASHWORTHY STRUCTURE	Turn-Over Capability	4g Vertical Only	4g <sub>z</sub> , 4g <sub>x</sub> , 4g <sub>y</sub> simultaneous
	Landing Gear Type	Cross Tubes & Skids	Conventional Type, Trailing Arm, Wheel
	Max. Sink Speed at Total Fuselage Collapse	7-9 meters/sec (estimate)	12.3 meters/sec (design)
	Main Transmission Tie-Down Strength	8g, all axes	20g Vertical, and Forward, 18g Sideward
	Pilots	15g Vertical, 15g Forward, 10g Side	48g Vertical, * 30g Forward, 18g Side
PERSONNEL RESTRAINT	Troop & Gunners	11g Vertical, 10g Forward, 10g Side	48g Vertical, ** 24g Forward, 18g Side
CRASHWORTHY FUEL SYSTEM	Number Tanks & Location	2 Belly Tanks 3 Above Belly	2 Above Belly

\*~Seat provides 31 cm minimum vertical stroke at approx 15g load on occupant.

\*\*~Seat provides 38 cm minimum vertical stroke at approx 15g load on occupant.

\*A spinal fracture did occur in case two, but our initial analysis indicates that the injury was caused by failure of the stroking device when struck by a nine cm diameter tree limb which permitted the seat to "free fall" a distance of approximately three cm.

TABLE I-4

## CRASHWORTHINESS PERFORMANCE COMPARISON

ITEM	ACCIDENT REF. NO.	UH-60 "BLACKHAWK"					UH-1	
		1	2	3	4	5	6	7
IMPACT CONDITIONS	Horiz Vel. (m/s)	45-60 <sup>b</sup>	3-4	≤2	ZERO	14-17	5-8	≤2
	Vert. Vel. (m/s)	>15 <sup>a</sup>	>17	9-11	6	15	11-12	6-9
	Crash Path Distance	2-3 meters	≤2 meters	≤2 meters	≤2 meters	9 meters	3-6 meters	≤2 meters
	Terrain	Water, 3m deep	Swamp & Trees	Sand & Trees	Earth	Sod & Trees	Grassy Sod	Grassy Sod
AIRCRAFT ATTITUDE	Pitch (degree)	90° <sup>a</sup> to 135° Down	15° to 20° Up	30°-40° Down	4° Down	5° Up	50° Up	2° Up
	Roll (degree)	≤15°	≤3°	130°-140° Right	5° Left	8° Left	5° Right	2° Right
	Yaw (degree)	≤15°	3° Left	20°-30° Right	5° Right	13° Left	90° Right	Spinning to Right
FLOOR ACCELE- RATION	Horiz. (g)	>40	≤15	20-30	≤3	20-30	10-15 Rearward	≤5
	Vertical (g)	>20 Up	>50	>10 Up	<15	50	15-25	15-20
	Side (g)	>5	>4	>10	≤3	10-15	5-10	≤5
LDG GEAR STROKE	Displacement (meters)	Unknown	0.7m @ 12g	None	Unknown	0.7m @ 12g	0.2m @ 3g	0.2m @ 3g
SEAT STROKE	Vert. Displ. (meters)	None	0.37 Lt 0.34 Rt	None	None	0.34 Lt 0.25 Rt	Zero	Zero
PROTECTIVE CONTAINER	Living Space Remaining	20% at rear	20% <sup>b</sup> at rear	95% at rear	100%	60% <sup>b</sup> at rear & front	60% <sup>b</sup> at rear	95% <sup>c</sup>
PERSONNEL INJURY	Total Aboard	3	4	2	7	3	4	4
	Lt Front	Fatal	Major	Fatal	Minor	Minor <sup>e</sup>	Fatal	Major <sup>d</sup>
	Rt Front	Fatal	Critical <sup>d</sup>	Fatal	Minor	Major <sup>f</sup>	Major <sup>d</sup>	Major <sup>d</sup>
	Lt Gunner	Not Used	Critical	Not Used	Major	Not Used	Not Used	Not Used
	Rt Gunner	Not Used	Not Used	Not Used	Minor	Critical <sup>g</sup>	Not Used	Not Used
	Center "Jump"	Fatal	Fatal	Not Used	Minor	Not Used	Not Used	Not Used
	Troop	Not Used	Not Used	Not Used	Two w/Minor	Not Used	Two w/Major <sup>d</sup>	Two w/Major <sup>d</sup>

a - These conditions (velocity and attitude) are deemed nonsurvivable.

b - Roof collapse.

c - Cockpit roof collapse

d - Spinal vertebra fracture

e - Struck helmet, dazed

f - Rt Elbow crushed, Rt side helmet impact, fibula superior end fx, ankle fx and sternum.

g - T12 fx, cardiac contusion, pulmonary contusions, sternum contusion and concussion.

## REFERENCES

Turnbow, J. W., Carroll, D. F., Haley, J. L., Robertson, S. H., USAAVLABS TR 70-22, "Crash Survival Design Guide", August 1969, U.S. Army Aviation Material Laboratories, Fort Eustis, Virginia

CHRONIC EFFECTS OF +G<sub>z</sub> IMPACT ON THE BABOON SPINE

D. C. Van Sickle, Professor of Anatomy, Purdue University, W. Lafayette, IN 47907  
 L. E. Kazarian, Biodynamic Effects Branch, AFAMRL, Wright-Patterson AFB, OH 45433

## SUMMARY

In 1974, eight male baboons weighing 20 kg. were subjected to subcritical (i.e., no direct injury producing) +G<sub>z</sub> impact of 40 G for 13-16 msec. and euthanatized in 1979 and 1980. From the serial radiographic and gross pathological data validated by histopathology and histochemistry, the experimental condition was classified in all 8 animals as spondylosis deformans traumatica. This paper provides a detailed time lapse anatomical study of degenerative changes very similar to human spondylosis deformans and answers the question can traumatic spondylosis deformans occur without radiographically detectable vertebral fracture. The results of this study indicate that in the baboon, radiographic examination on the day of exposure to excessive mechanical stress will reveal no significant radiographic changes, but that the subsequent appearance of spondylosis deformans strongly suggests that the pathological changes are the direct result of trauma.

## INTRODUCTION

The role of impact or repeated impact producing acute clinical injury as an etiologic factor initiating or accelerating intervertebral disk deterioration has not been systematically studied in the military service. In an attempt to explore a potential relationship of subacute trauma to spondylosis deformans, this initial study was conducted to demonstrate and identify the developed intensification of objective radiographic signs following controlled spinal impact in the baboon.

Spondylosis deformans traumatica is a disorder of the spinal column initially characterized by the presence of focal or diffuse bony spurs, ledges or shelves developing at the junction of the cortex with the upper and/or lower marginal ridges of the vertebral bodies adjacent to degenerating disks.

The appraisal of spondylosis deformans remains difficult considering that it is an age related phenomenon whose occurrence is also conditional by such factors as sex and occupation.

The purpose of this paper is to provide time lapse anatomical study of degenerative changes very similar to human spondylosis deformans and answer the following question: Can traumatic spondylosis deformans occur without radiographically detectable spinal damage in the baboon?

## MATERIALS AND METHODS

The animals had been purchased from an authorized dealer, quarantined, tested periodically for TB, examined for internal parasites and treated with the appropriate parasiticide when necessary, and maintained on a special formulated diet of commercial monkey food. During July and August of 1974, eight male baboons (*Papio anubis*) designated E-16, E-18, E-20, E-24, E-26, E-28, E-30, E-34 and weighing 20 kg., were radiographically screened to insure normalcy and that no congenital or acquired anomalies were present which might be misinterpreted post-impact as induced traumas. The Veterinary Sciences Division, AFAMRL, was responsible for the preceding care as well as the radiography.

Prior to impact each animal was radiographed in the anterior-posterior (AP) and lateral positions. This radiographic data provided base line data for comparison with post-impact serial radiographs as suggested by Schmoll and Junghans (1).

At the time of impact, the animals were tranquilized with ketamine hydrochloride (mg/kg IM) and transported to the drop tower. Each baboon was placed in a seat in a sitting position. The chest was restrained by a torso harness (about the nipple line) and a lap belt was used to secure the lower torso. The legs were secured with ankle belts, the head was nestled between the arms which were acutely flexed at the elbow, and the wrists were fastened to the top of the chair. The deceleration forces on the free falling guided impact vehicle with the seat were generated by impacting aluminum honeycomb core material with sufficient energy to produce up to 60% crushing. The rectangular deceleration-time history was stipulated by the vehicle drop height as well as the engineering specifications of the honeycomb material. To assure the desired deceleration-time history was executed, a whole system calibration was carried out before each experiment. The calibration signal and deceleration-time history were photographed. The impact time histories were recorded using piezoelectric accelerometers located beneath the seat pan and impact vehicle base. The deceleration-time history resulted in an average plateau of 40 G's with a time of duration of 10-13 msec. Each baboon was then removed from the seat, radiographed, placed back in the cage and closely monitored until recovery from the tranquilizer.

Serial radiographs were accomplished at 15, 30, 45 and 60 days post-impact and then every six months until euthanasia.

In 1979, five of the animals were euthanatized and necropsied, and their spines were photographed and then quickly frozen. In 1980, the remaining three baboons plus a control were radiographed, and hemograms as well as serum chemistries were done. These animals were euthanatized and necropsied, and hard and soft tissues were processed for histopathology.

## RESULTS

Clinically, the baboons did not appear to suffer any post-impact discomfort. Radiographically, the spinal alterations ranged from no apparent damage to a minor subluxation in the thoracolumbar transregion



(E34, E30, E18, E16). Within 12 months an increased density within the anterior portion of the annulus fibrosus was evident in E34, E30 and E18. E34 also had decreased waisting of the anterior surface of L2. In the lumbar region of E18, the anterior-superior border of the vertebrae appeared indistinct. In many of the animals, decreased IVD spaces were evident. By 1977, E34 had very evident osteophytes of the caudal-inferior aspect of L3-L5 while L2 had increased density of the centrum indicative of a healed pressure fracture. In the spine of E18, the T12-T13 IVD space was abolished, and increased densities were present in the anterior portion of the annulus fibrosus of T10-L5. In the inferior lumbar IVD spaces, the ossification of the annulus fibrosus (trabecular pattern visible) was less dense, while in the inferior thoracic region they were more dense. L1-L2, L1-T13 and T12-T13 IVD spaces had bridging osteophytes. Also in this time frame, the articular facets of the lumbar vertebrae were enlarging as were those of the T11, T12 and T13. By 1979, all the spinal columns of the experimental animals had varying degrees of pathology, with E24 having the least amount of reaction.

Following necropsy the isolated spine was radiographed in the AP and lateral positions using high contrast film. The following data are examples:

- E-30: Bridging osteophyte - T13-L5, C7-T1
- Mineralization of annulus fibrosus, decreased IVD space T5-L5
- Increased density of centrum T11-L3
- Schmorl's node - T11-T12
- Anterior lateral osteophyte - L3-L5 (L2-L3 & T12-T13 bridging)
- E-18: Osteophytes L3-L7, L3-L4 & L1-T13 (bridging) possibly broken. Large bulbous articular facets in lumbar area.
- E-34: Densities of the anterior portion of the annulus fibrosus throughout the T-region, with T10-T11, T12, T12-T13 the most reactive. Loss of IVD space T12-T13 & L1-L2. Osteophytes in the lumbar region; intense reaction on superior surface of each lumbar vertebrae, initiating in the region behind the epiphyseal line. Greater osteophytosis on right lateral side of spinal column than left, which corresponded to the fractured side of the pelvis resulting in secondary osteoarthritis of the right coxofemoral joint.

Grossly, the spines from the thoracolumbar area to the sacrum were represented by bulbous intervertebral spaces between vertebral bodies with concave contours. Since the lumbar vertebrae are larger, more inferiorly in the spine, it appeared as if the osteophytic reaction was greater more inferiorly. However, if one would compare the degree of osteophytosis with the size of the centrum, the greatest reaction was at the thoracolumbar region, decreasing in intensity either superiorly or inferiorly. A Schmorl's node was observed in the medullary cavity of L1 of several baboons originating from the T13-L1 IVD space. The muscle mass of the dorsum of the baboons did not appear atrophied. The soft tissues were unremarkable, except for E-18 where the visceral and parietal pleura were adhered from T3 to T12. No underlying pulmonary pathology was observed.

The histopathology verified the radiographic and gross pathological findings. The thoracolumbar area of E16 was divided horizontally exposing a white nodule in the medullary cavity of L1. Upon microscopic examination, a circumscribed nodule of material, apparently a degenerated portion of the nucleus pulposus had penetrated the end plate and had secondarily become surrounded by bone trabeculae of varying size. The medullary tissue reaction around the nodule was fibrous, changing to adipose and merging with hemopoietic. The portion of the cortical bone adjacent to the centrum was attached by the periosteum. The medullary cavity, which the bone chip had covered was filled with adipose bone marrow. There was a number of enlarged trabeculae extending axially as well as in the superior and inferior ends of the centrum. The trabeculae were composed of lamellar bone, and some were large enough to contain osteons. The osteophytes were composed of cancellous bone and red bone marrow. On one lateral side of the spine, the osteophytes were mature and bridging the annulus, while on the other side there was vascular invasion of the annulus with no osteophytic formation. In general, a large initial osteophyte appeared to develop inferior to the superior edge of the vertebrae. One large bone section from E-18 contained four IVD spaces and three bodies. One IVD space had collapsed, one was degenerating, and two were in fair condition. In the collapsed IVD space, a remnant of the nucleus pulposus was found under the posterior ligament in the vertebral canal. There was chondroid metaplasia in the center of the annulus fibrosus with the chondrocytes arranged in chondrones. There was a great amount of ossification in the anterior portion of the annulus fibrosus where the glycosaminoglycans were either absent or localized in cystic areas. There was an apparent fracture of the superior edge of the vertebrae which was repaired by trabeculae of irregular size and arrangement and surrounded by adipose bone marrow. This area was enclosed in hematopoietic bone marrow. The articular cartilage of the facets had an uneven articular surface. The superficial layer of the articular cartilage was missing in some areas, or was acellular in others. There were areas of multiple tide marks indicating progressive remodelling.

#### DISCUSSION

From the preceding data, it is apparent that the spines of the baboons developed a time-dependent spondylosis accompanied by osteophytosis, hyperostosis and articular facet osteoarthritis. Epstein (2) suggests that "spondylosis" refers to a pathological condition arising from discal degeneration resulting in osteophytosis and deformities of the discs. He also states that osteophytes are usually asymptomatic and that large paravertebral ligamentous calcification appear, particularly at the thoracolumbar region when laborers are engaged in excessive bending and/or strain. Hadley (3) correlated the radiology and histopathology of articular facets, and Lewin (4) described osteoarthritis of the facets in the lumbar region of the spine. Recently, the IVD and the two facet joints have been described as a tripod joint where failure in one will have secondary effects on the other two components (5). In Schmorl and

Junghanns (1), a number of animal experiments are listed where investigators discussed the relationship between spondylosis and a single trauma. Many of these experiments required invasive techniques which severely compromises the animal response.

Therefore, in view of our serial radiographic, gross pathologic as well as histopathologic results indicating a decrease IVD space at the thoracolumbar transregion, the secondary margination of anterolateral osteophytes, the secondary osteoarthritis of articular facets and the presence of Schmorl's nodules in and around the thoracolumbar region, it has been decided to classify this condition - Spondylosis Deformans Traumatica. This is the first report of this condition being experimentally produced non-invasively in a sub-human primate. Further study of this model should provide definitive knowledge relative to the initial observations listed in this paper plus provide a model from which the initial histochemical and biochemical lesions in the intervertebral disc can be learned.

Operationally, this lends credence to the most common site of injury (T12-L1) by man upon ejection from aircraft and will provide background to better understand the pathology of injuries suffered by aircrewmembers. It also supports the conclusion that systematic standardized radiographic skeletal overviews should be accomplished on all aircrewmembers recommended for flying in high performance aircraft. If a single traumatic incidence can induce spondylosis in healthy animals, then those aircrewmembers who have congenital or acquired spinal anomalies may weaken the integrity of their entire spine and may be in jeopardy following exposure to ejection forces. Likewise, those aircrewmembers who have ejected should have their spines monitored more closely than other line personnel. If an aircrewman has ejected more than once, then it becomes imperative that his or her spine be monitored very closely. As stated in Schmorl and Junghanns --- "The possible deterioration of a generalized spondylosis deformans following trauma can not be denied."

#### REFERENCES

1. Schmorl, G. and Junghanns, H. The Human Spine in Health and Disease. 5th German Edition, New York, Grune & Stratton, 1971, 300-305.
2. Epstein, B. S. The Spine a Radiographical Text and Atlas. 4th, Philadelphia, Lea & Febiger, 1976, 377-381.
3. Hadley, L. A. Anatomico-roentgenographic studies of the posterior spinal articulations. *Am. J. Roentgen. Rad. Therapy and Nuc. Med.*, 86, 1961, 270-276.
4. Lewin, T. Osteoarthritis in lumbar synovial joints. *Acta Orth. Suppl.* 73, 1964, 5-95.
5. Kazarian, L. E. AFAMRL. Injuries to the human spinal column: biomechanics and injury classification. AFAMRL-TR-80-53, 1980, WPAFB, Ohio.
6. Kazarian, L. E. and Belk, W. F. AFAMRL. Flight physical standards of the 1980's: spinal column considerations. AMRL-TR-79-74, 1979, p 1-18, WPAFB, Ohio.

The experiment reported herein was conducted according to the principles described in "Guide for the Care and Use of Laboratory Animals" prepared by the Committee on Care and Use of Laboratory Animals of the Institute of Laboratory Animal Resources, National Research Council, DHEW Publications No (NIH) 78-23, Revised 1978.

## DISCUSSION

## UNIDENTIFIED QUESTIONER

A question was asked about the location of the spinal column degeneration.

## AUTHOR'S REPLY

Well, I'd say the degeneration of intervertebral discs. I'm not sure if it's the annulus or the nuclei.

## DR. THOMAS (USA)

Is it possible that the loss of this kind is due to the displacement of the disk into the adjacent vertebral bodies?

## AUTHOR'S REPLY

Yes.

## DR. THOMAS (USA)

Do you get displacement or prolapse of the disk through the annulus-fibrosis laterally or posteriorly or anteriorly in any of these baboons?

## AUTHOR'S REPLY

Well, it looks like it is prolapsing into the vertebral body.

## DR. THOMAS (USA)

But you didn't see any prolapse into the spinal canal?

## AUTHOR'S REPLY

No. We reported one in our preprint where it appeared that the nucleus had come up underneath the posterior ligament.

## DR. THOMAS (USA)

But it didn't break through and become a free body in the spinal canal?

## AUTHOR'S REPLY

No, it didn't appear to. It appeared to undergo chondroid metaplasia in-situ.

## DR. UNTERHARNSCHIEDT (USA)

Is it correct that some of the material penetrated the anterior ligament?

## AUTHOR'S REPLY

I did not see any that penetrated the anterior.

## DR. UNTERHARNSCHIEDT (USA)

Didn't some part of it penetrate the inner part of the ligament? I had that impression in some of the photos

## AUTHOR'S REPLY

I did not see any.  
in the annulus.

We're now on phase three of this and are seeing some changes

## GEN BURCHARD (GE)

How does the aging process of the baboon compare to humans, and how fast would changes like this appear in humans compared to baboons?

## AUTHOR'S REPLY

We are in the process of doing a developmental study on aged spines in the baboon. I think that's very important. We have made arrangements with the Southeast Research Institute to get their aged baboon spines and we will have a better answer to that question hopefully in another year or two. As to the change rate for human, that's beyond me. I can only report what I see here i.e., baboon. We are seeing changes like you saw

in the helicopter pilots that may match these very closely. To put myself way out on a limb, I'll say two or three years, because we used 40g while most of our people receive less than 20g when they eject. So, I would almost double the time, but I think it happens. We are also concerned that people flying high performance aircraft begin their careers with excellent spines. Because it's going to happen on normal spines and the individual has hemovertebra or some other spinal abnormality. I think it would be very bad for a pilot to begin training with an undiagnosed spinal abnormality; it would intensify the pathology.

DR. VON GIERKE (USA) COMMENT

We know the baboon can stand higher acceleration levels. That was presented at the Oporto meeting where we showed tolerance curves of the baboon versus man. So the baboon was selected to more or less simulate just below what we call fracture tolerance in a baboon.

AUTHOR'S REPLY

However, we hope to get a better handle on this point during the developmental anatomy so that we can stage a better chronology.

COL KNAPP (USA)

Would you postulate the effect of chronic whole body vibration on acceleration of this process?

AUTHOR'S REPLY

I do not know. I don't have any idea what vibration would do to this. I think after we have done the impact work it would be very interesting to do the vibration plus impact work to see if there is an additive effect or even a synergistic effect.

COL KNAPP (USA)

Based on your findings, are you prepared to recommend that all pilot-patients who have sustained a significant but subclinical  $+g_z$  spinal fracture should have yearly, long-term, radiologic follow-up?

AUTHOR'S REPLY

It is unknown at this time how widespread this problem is in pilots who have sustained significant  $+g_z$  impact. However, our initial research indicates that the primate spine has the potential to react to impact by causing spondylosis. By performing an epidemiological study on those individuals who have suffered impact and by increased research on the biological potential of the spine a more definitive answer could be given.

COL KNAPP (USA)

Will the accumulated X-ray dose justify the early diagnosis of arthritic disease and follow-up data derived thereof?

AUTHOR'S REPLY

The radiation hazard would have to be submitted to radiological experts for this evaluation.

GEN ORD (USA)

Concerning any proposal for annual radiographic examination of the spines of aviators involved with impact incidents, there is a highly significant medicolegal problem related to the radiation exposure.

AUTHOR'S REPLY

Radiation hazards should be determined by radiological experts prior to such exposure. If a risk should be determined, another approach should be taken.

DR. LEVINE (USA) COMMENT

I will argue about the value of X-rays. I look at an awful lot of people who have various kinds of back trauma in my practice. I cannot correlate X-ray findings with pain. I see some terrible looking X-rays and the patient has no pain. I see some X-rays that are clean and beautiful and the patient lies there with a ruptured disk. I question what the X-rays mean on follow-up.

COL KNAPP (USA)

I think the issue here goes beyond. It goes to the issue of retaining a pilot who is demonstrating architectural changes in his load-bearing spine to force environments that may aggravate a clinical/orthopedic problem or may cause a more serious problem if he is to sustain a second injury problem. So this is both an epidemiologic

and occupational problem. My earlier question was baited because I knew what Dr. Kazarian had recommended, but only a few countries, primarily here in Europe, are doing the X-ray follow-up. I am hopeful that this one thing will come out of this meeting: a clear statement of the importance of some type of follow-up after a sub-clinical fracture.

#### UNIDENTIFIED QUESTIONER

I would wonder if we might work up some more clinical-like flexibility. I think if we could determine how much the spine could move or how stiff it is we might have more useful data rather than looking at an X-ray.

#### AUTHOR'S REPLY

I think you have to recognize that if you're going to have a decrease in intervertebral disk space you have to have an increase in articular facet joint area, which brings about a decrease in total range of motion over a period of time. And if you have decreased range of motion, you're going to bring about a decrease in tolerance to impact. So, then, the question is, should an individual be subjected to an acceleration-time history in an area where you know there's a high range of motion which in turn is saying there is a high risk area. I think that's what it boils down to. And I don't think we've recognized it as a problem.

#### DR. VON GIERKE (USA) COMMENT

I would like to add, we recommend this primarily with respect to ejectiones from aircraft where we have a much more controlled situation than we have normally in clinical injuries you might see. So, certainly the research results we would get out of such follow-up studies would be much better controlled than in general practice.

#### DR. UNTERHARNSCHEIDT (USA)

We should not only look at these problems from the orthopedical standpoint but also from the neurological standpoint, because compression of the disk means compression of the posterior roots. Therefore, pain and perhaps compression of the anterior roots and **atrophies**.

#### DR. THOMAS (USA) COMMENT

We have aviators who do eject and sustain vertebral fractures and as far as I know if they are healed, that is basically symptom free, they return to flight. The general feeling is that they are a higher risk of further back injuries if they have to eject again, but on the other hand they are extremely valuable people because they cost so much money to train. I don't think that the line services regardless of architectural damage to an aviator, provided he could do his job; I don't think they would consider not using him again, because of his value.

## MECHANISMS OF HEAD IMPACT INJURY AND MODIFICATION BY HELMET PROTECTION

Alan M. Nahum, M.D., Professor of Surgery, University of California Medical Center, San Diego, California 92103 and  
Carley Ward, Ph.D., Biodynamics/Engineering, Inc., Pacific Palisades, California 90272

### SUMMARY

Head protection provided by helmets or padding on the impacted cadaver skull surface was examined. Using unembalmed human cadaver subjects, frontal and lateral head impacts were conducted. Head acceleration and intracranial pressures were measured in order to determine the head and brain responses. Brain response was further analyzed with the aid of a finite element brain model; each impact was simulated on the computer to determine brain stresses and displacement during the impact. The degree of protection provided can be quantified by comparing head acceleration and brain pressures for equivalent energy impacts.

### INTRODUCTION

Using both the human cadaver and a mathematical simulation, a series of helmeted and non-helmeted impacts were conducted.

### EXPERIMENTAL METHODOLOGY

#### FRONTAL IMPACTS

Seated, stationary cadaver subjects were impacted by a rigid mass traveling at a constant velocity. The blow was delivered to the frontal bone in the mid-sagittal plane in an anterior-posterior direction. The skull was rotated forward so that the Frankfort anatomical plane was inclined 45 degrees to the horizontal. Various padding materials were interposed between the skull and impactor to vary the duration of the applied load. The input force and the biaxial acceleration-time histories of the skull were recorded during the impact event. Static fluid pressurization of the cranial vascular network and cerebral spinal fluid space to in vivo pressure levels at impact was also performed. Following the impact exposure the brain was perfused with a 10 per cent formalin and carbon particle solution. Injury to the contents of the cranium, as evidenced by extravasation of the carbon particles into the brain tissue, was then assessed by pathologic examination.

In some experiments a ventriculostomy technique was employed to provide input and monitoring sites for cerebral spinal fluid simulation. An alternate method of pressurization by entering the dura over the superior surface of the brain for addition and removal of saline via No. 8 French catheters was also employed.

In addition to the dynamic measurements of input force and head acceleration, a series of intracranial pressure-time histories were recorded. Endevco model 8510 piezo-resistive pressure transducers (resonant frequency: 180KHz) were used to monitor the dynamic intracranial pressure during the impact event. A 5 mm diameter hole was made in the skull and the bone thickness measured. A stainless steel nipple was inserted a distance equal to the bone thickness and the pressure transducer threaded into the nipple such that the diaphragm of the transducer was flush with the inner surface of the skull to prevent bruising of the brain due to protrusion of the transducer into the cranium. In all but one (Experiment 36; occipital pressure #2) of the pressure transducer placements, the dura was opened at the insertion site to allow subdural pressure measurement. Transducers were placed in the frontal bone adjacent to the impact contact area, immediately posterior and superior to the coronal and squamosal sutures respectively in the parietal bone, and inferior to the lambdoidal suture in the occipital bone. Additionally, transducers were placed in the occipital bone at the posterior fossa. A second type of dynamic pressure measurement was obtained by insertion of a Kulite model MCP-808-9R (resonant frequency: 150 KHz) catheter tip pressure transducer in the internal carotid artery at the level of the carotid siphon.

Due to the limited number of transducers available for a given experiment and the desire to acquire information at various anatomic sites, pressure measurements were not duplicated at all locations for each experiment. Certain measurements were specifically paired to examine questions of pressure pulse symmetry and recording accuracy. Bilateral occipital (Experiments 37, 38) pressures were monitored to gain information on pulse symmetry. Transducers were also placed adjacent to each other in the posterior region (Experiments 46-52) and occipital (Experiment 36) to determine if the measurement technique would yield similar results in essentially the same anatomical area of the skull.

#### SIDE IMPACTS

In this series impacts were conducted on the lateral aspect of unembalmed cadaver heads. The cadaver specimen was seated in an upright position. The Frankfort plane was maintained in a horizontal position by resting the mandible on a styrofoam support block prior to impact. The skull was impacted laterally in the

area of the parietal bone by a 12.38 kg pneumatically actuated piston. The impactor surface was a circular disc, 12.5 cm in diameter. Paired tests were conducted in protected and unprotected modes. Impactor terminal velocity was measured by a magnetic probe. Intracranial pressure was regulated by both intravascular and intracranial (subdural) catheters connected to saline reservoirs. Just prior to impact the intravascular pressure was adjusted to approximately 100 mm Hg via a catheter inserted in the common carotid artery. Intracranial pressure was monitored by a water manometer and was adjusted to 0 mm Hg prior to impact.

As in the frontal impacts, intracranial pressure was measured dynamically at the time of head impact by piezo resistive pressure transducers (Endevco model 8510, resonant frequency 180 KHz) which were inserted into the subdural space at designated locations. Head acceleration was measured by nine Endevco piezo resistive accelerometers (model 2264-2000; resonant frequency: 27 KHz) mounted on an Endevco triaxial bracket (model 21419).

In the unprotected tests the impactor surface was covered by a composite of two padding materials: 1.5 cm Ensolite and 1.5 cm open cell polystyrene. In the protected tests, the head was fitted with a Bell model R-T helmet [Helmets supplied courtesy of Bell Helmets, Inc.] This helmet utilizes an expanded polystyrene bead liner material.

The accelerometer bracket was rigidly attached to the head opposite the side of impact by drilling a clearance hole through the skull and securing the apex of the bracket by means of an expanding collet at the end of a threaded shaft. Two of the three accelerometer mount legs were also attached to the skull using threaded studs which terminated in drilled and tapped holes. Dental acrylic applied at each of the three attachment points acted to distribute the transmitted loads to a larger surface area of the skull. A portion of the helmet shell opposite the side of impact was removed to accommodate the accelerometer mount. Following the experiment the head was affixed in a measuring jig to establish the coordinate of the accelerometer bracket legs relative to the origin of the anatomic coordinate system. These components of linear and rotational acceleration at the point of attachment of the mounting bracket were calculated from the nine accelerometer array output using the analysis reported by Padgaonkar et al. [1] A coordinate transformation was then implemented to represent these data at the origin of the anatomic axes. The sign convention followed for the anatomic axes was positive x, y and z directions being posterior-anterior, laterally right to left, and inferior-superior respectively. All acceleration data discussed subsequently represents values at the origin of the anatomic axes.

## RESULTS

### HEAD ACCELERATION

Acceleration traces differ in shape, magnitude and duration for the helmeted and non-helmeted impacts. The short duration, spike-shaped trace shown in Figure 1 is typical of the resultant head accelerations for the unprotected head. Pulse duration is increased with thicker padding. The longer, rounded trace shown in Figure 2 is characteristic of a helmeted impact, where the helmet liner dissipates impact energy. In some impacts an oscillation occurs at the top of the trace (near the peak value). This is caused by the helmet moving with respect to the head, shifting position on the head.

In the frontal impacts, the resultant head acceleration vector lies in the midsagittal plane, the acceleration components being in the antero-posterior and superior-inferior directions. In the side impacts the head is accelerated in all three directions. Thus the resultant head acceleration vector does not remain in a plane, but changes direction as the head translates and rotates. The largest acceleration component is in the impact direction.

### INTRACRANIAL PRESSURE

The maximum positive pressures occur near the impact site regardless of the impact direction. Maximum pressure and head acceleration traces are similar in shape and duration. In the unprotected head, the brain experiences a sharp spike-shaped pressure pulse. In the helmeted head, the brain pressures are lower and last longer. (For a discussion of these pressure differences refer to the brain response analysis section of this paper.) In regions surrounding the impact site, the magnitude of the pressure decreases as the distance from the impact site increases. Opposite the impact, the initial dynamic pressures are negative when measured relative to the atmosphere. Tension stresses develop in the tissue. The internal folds of dura influence the pressure response. Closely spaced transducers on opposite sides of the membranes recorded different pressures. The most significant difference was between the right and left side of the falx cerebri in the lateral impact series. Pressures are also affected by the foramen magnum; pressures near this opening and in the posterior fossa were low.

### FRONTAL IMPACT SERIES

Important variables for the frontal series are recorded in Table 1 and compared graphically in Figures 3-9. In these plots kinetic energy refers to the following product:  $1/2 \times \text{impactor mass} \times \text{impactor velocity}^2$ . Skull fracture cases were not

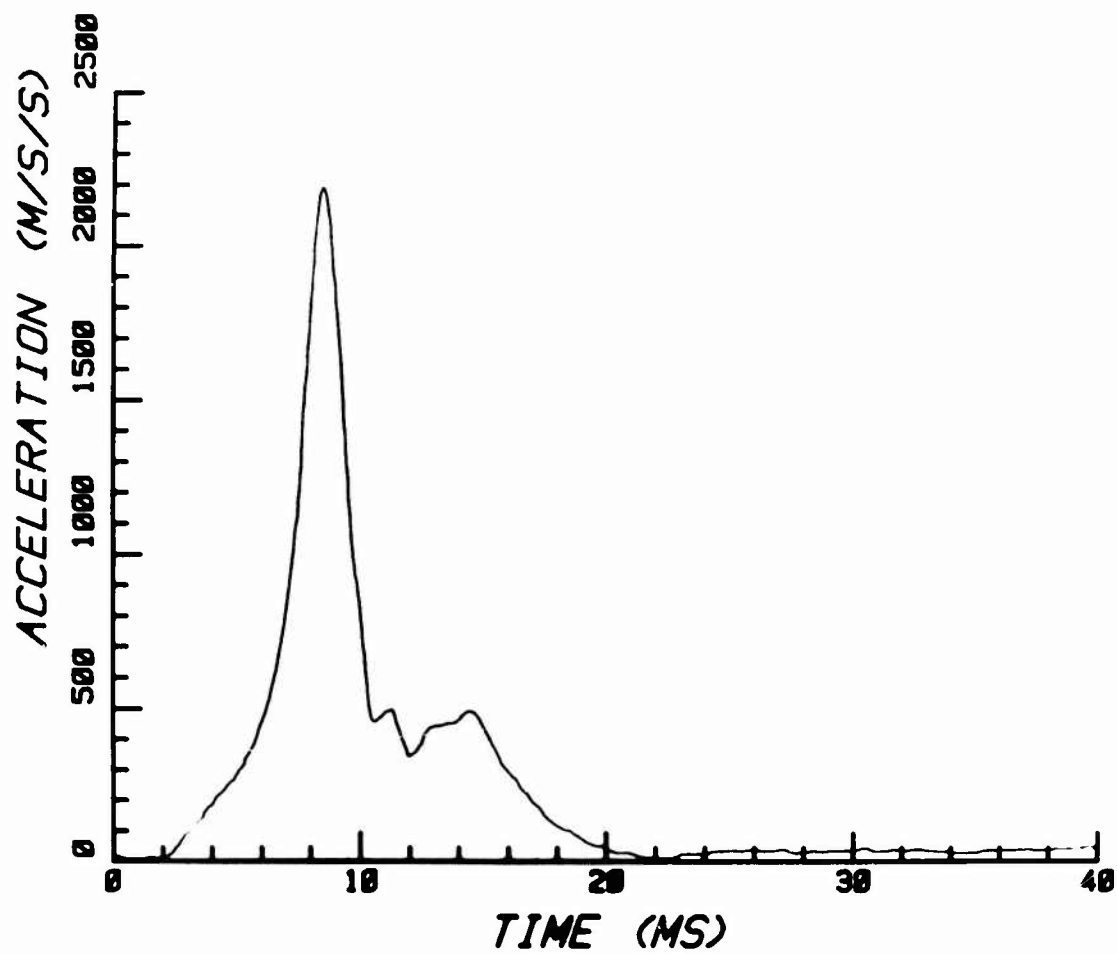


FIGURE 1. RESULTANT HEAD ACCELERATION. EXPT. #43W. UNHELMETED.



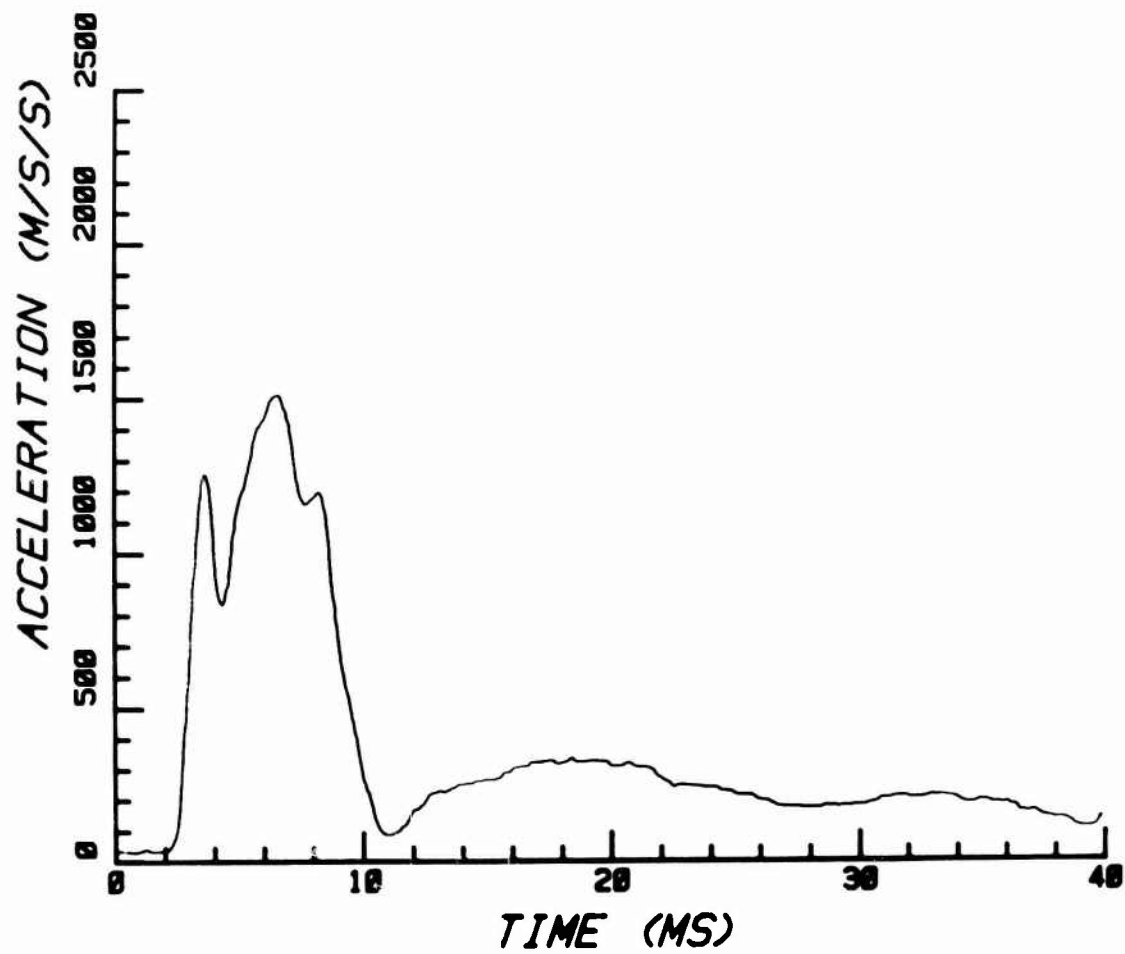


FIGURE 2. RESULTANT HEAD ACCELERATION. EXPT. #68W. HELMETED.

included.

(1) Peak Head Acceleration vs. Kinetic Energy

The comparison of impact energy and head acceleration in Figure 3 demonstrates the protection provided by the helmet. Head accelerations are low in the helmeted impacts even at high energies. The helmet effectively dissipates the impact energy. Non-helmeted impacts dissipate equivalent energy when a thick padding, 5.08 cm of polystyrene, is used on the impactor. This is shown by the overlapping of helmeted and non-helmet data points. In the high energy range, unpadded or minimally padded impacts could not be performed for comparison, because the skull would have fractured. Data scatter in Figure 3 is related to differences in impact interfaces.

(2) The U.S. Federal Head Injury Criterion (HIC) and the Gadd Severity Index (GSI) vs. Kinetic Energy

The relationships between these impact severity measures and the impact energy are shown in Figures 4 and 5. In calculating the GSI and HIC the acceleration is integrated with respect to time. The longer helmeted acceleration traces result in higher severity values, and the advantage afforded by the helmet is less apparent. The helmeted data points are still clustered on the low side, however. As in Figure 3, the non-helmeted data points for a thickly padded impactor overlap helmeted data.

(3) Peak Frontal Pressure vs. Kinetic Energy

The relationship between maximum intracranial pressures and impact energy are shown in Figure 6. Frontal pressures in these helmeted frontal impacts could not be measured because the helmet would destroy the transducer. The pressures in Figure 6 were obtained from the finite element model. Since the model accurately predicted the pressures at other locations in the impact, these frontal values are considered reliable. The results show that pressures are low in the helmeted head.

In Figure 6, horizontal lines representing moderate and severe injury levels were drawn. These pressure levels were obtained from an analysis of brain injuries in frontal and occipital impacts [2]. The study showed that when peak pressures were above 1758 Hg-mm (34 psi) the brain could be seriously injured. Between 1293 (25 psi) and 1758 Hg-mm (34 psi) moderate brain injuries occurred, and below 1293 Hg mm (25 psi) the injuries were only minor. Comparing the helmeted results to these injury levels shows that the helmet prevented severe injury.

(4) Peak Frontal Pressure vs. Head Acceleration

A linear relationship between head acceleration and peak pressure is shown in Figure 7. Pressure increases as acceleration increases, and the data can be approximated with a regression line. As in Figure 6 the peak pressures were obtained from the finite element model simulation. But even without these points, the linear trend is apparent. Some scatter is attributed to differences in head size and impact locations.

(5) The Federal Head Injury Criterion (HIC) and Gadd Severity Index (GSI) vs. Peak Head Acceleration

The relationships between these severity measures and peak head acceleration is shown in Figures 8 and 9. Since the HIC and GSI are exponential functions of head acceleration the data exhibits an exponential trend.

#### SIDE (LATERAL) IMPACT SERIES

Results from the side impact experiments are listed in Table 2, and relationships between the measured quantities are graphed in Figures 10-16. In all of the non-helmeted tests a thick layer of padding was used on the impactor, the thinnest layer being 3 cm thick. Although the range of interface conditions is not as extensive as in the frontal impacts, the same trends in the data are observed.

(1) Peak Head Acceleration and Kinetic Energy

Figure 10 shows that accelerations of the helmeted heads are low. The peak accelerations are only about half those of the non-helmeted heads in the high energy impacts. Some of this difference could be attributed to the mass of the helmet, but not reductions of this magnitude. The weight of the helmet is only 1000 gms.

(2) Maximum Angular Acceleration About the Y-Axis vs. Impactor Kinetic Energy

The helmet also reduces the angular acceleration as shown in Figure 11. For the same impact energies, helmeted head rotational accelerations are lower. As in Figure 10, differences between helmeted and non-helmeted impacts increase at higher energy impacts.

(3) HIC and GSI vs. Impactor Kinetic Energy

Relationships between the head injury criterion and impact energy are shown in Figure 12 A & B. As in the frontal impacts (Figure 4) the helmeted HIC values tend to be below the non-helmeted values. Because the HIC and GSI are integrated functions, the differences between the helmeted and non-helmeted data points are not

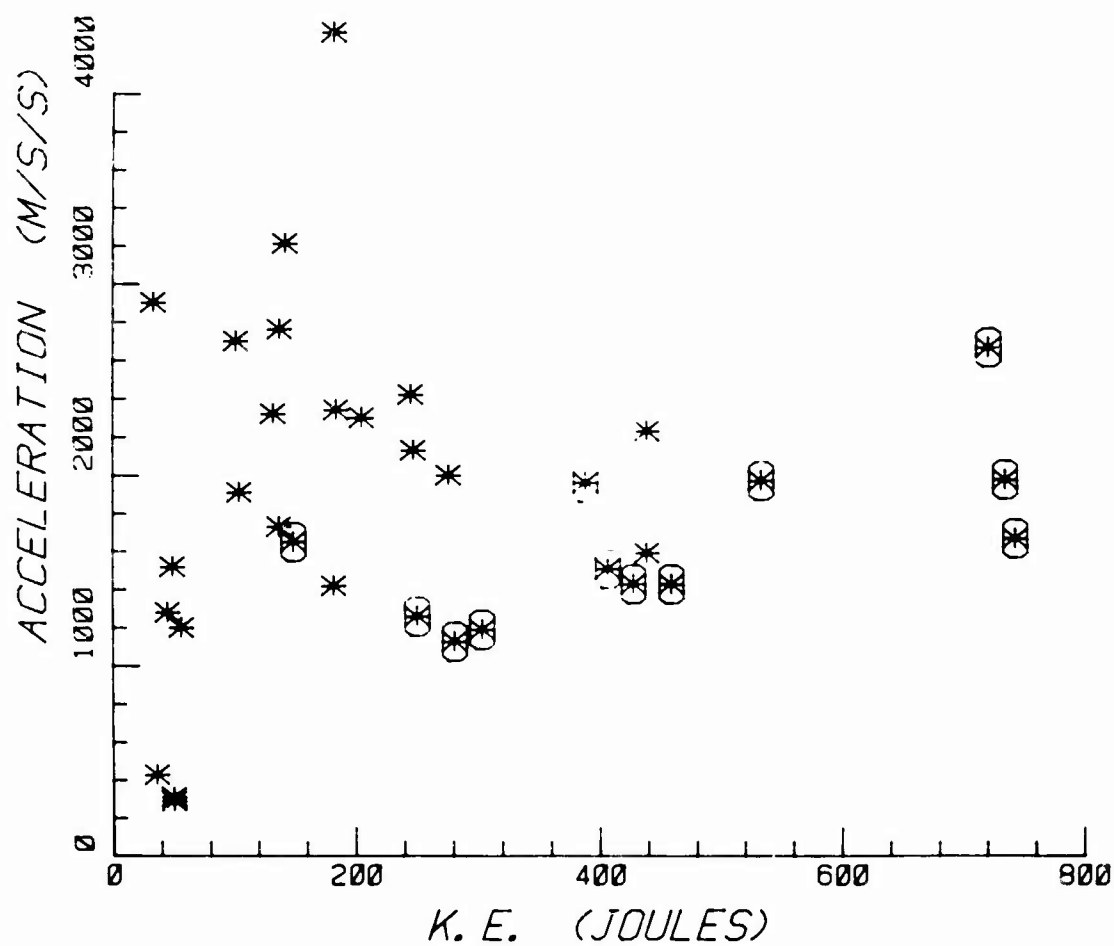


FIGURE 3. FRONTAL IMPACT. IMPACTOR KINETIC ENERGY VS. PEAK HEAD ACCELERATION.

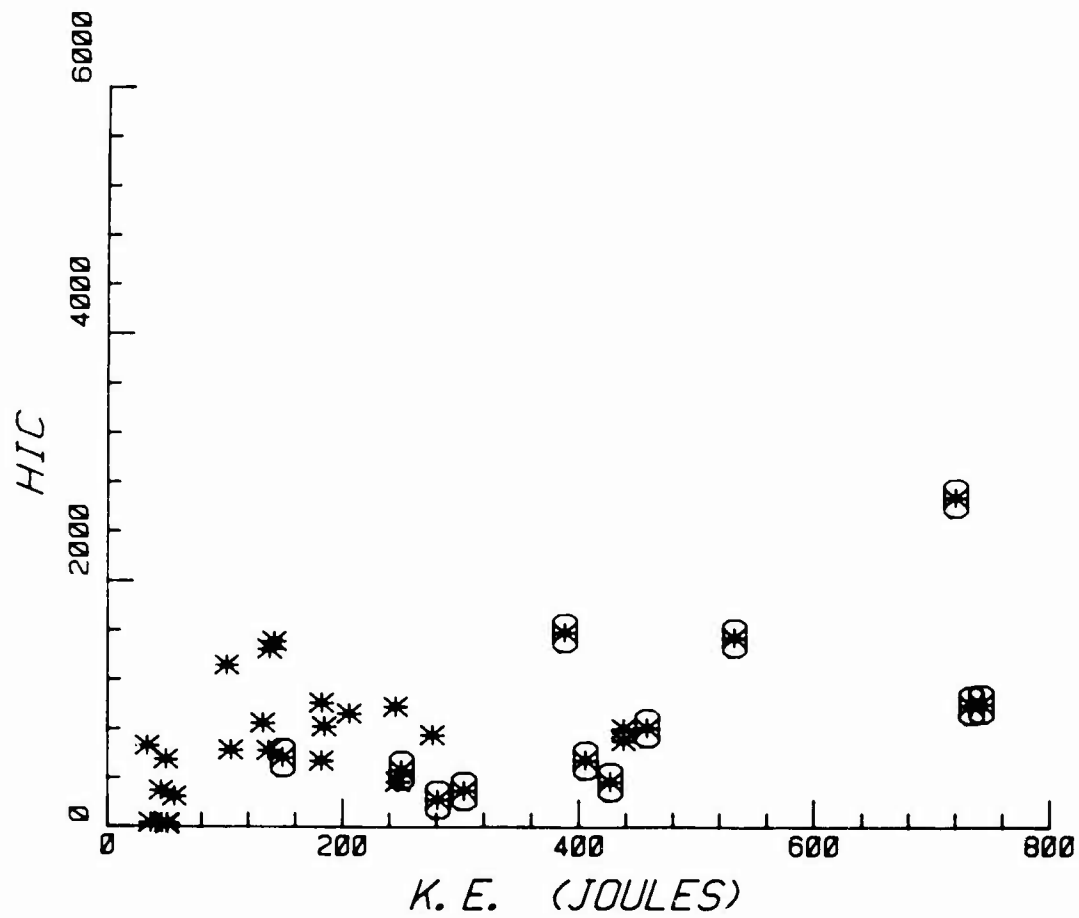
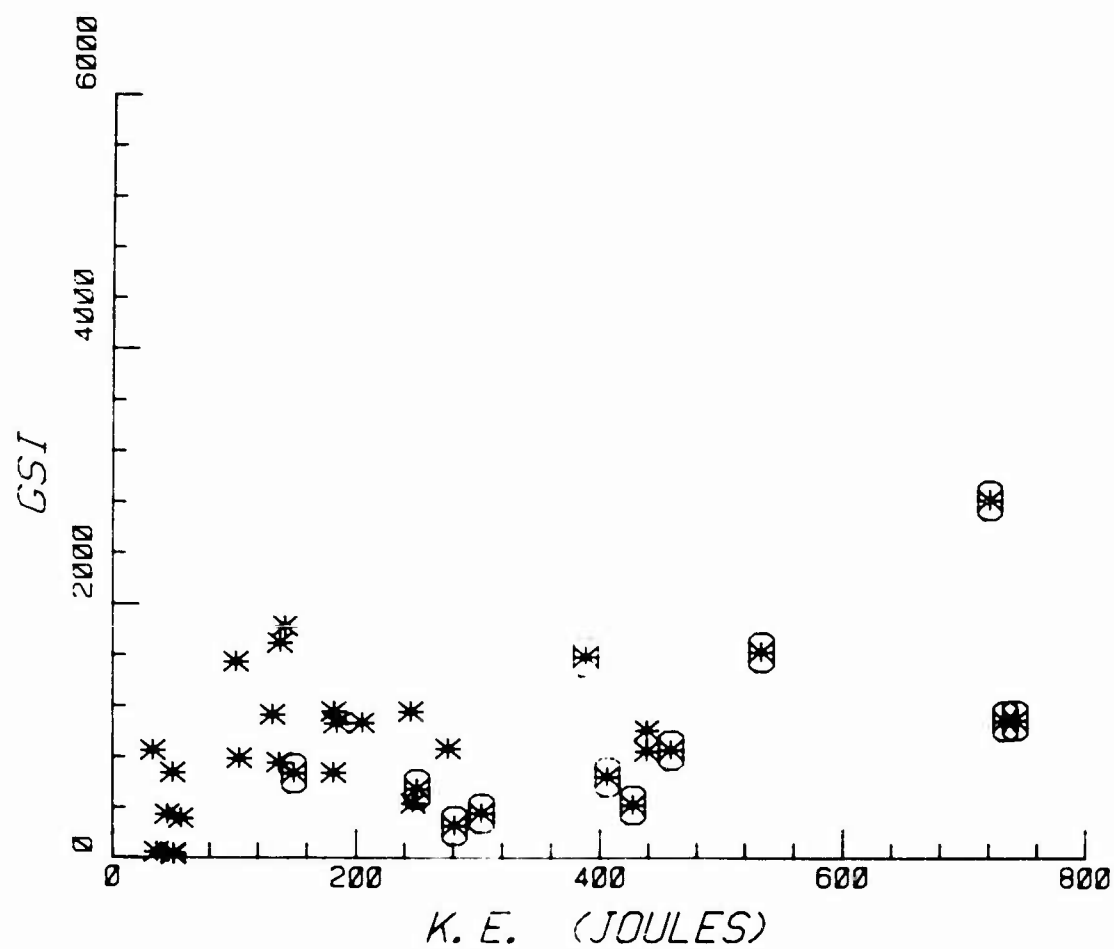


FIGURE 4. FRONTAL IMPACT. IMPACTOR KINETIC ENERGY VS. HIC.



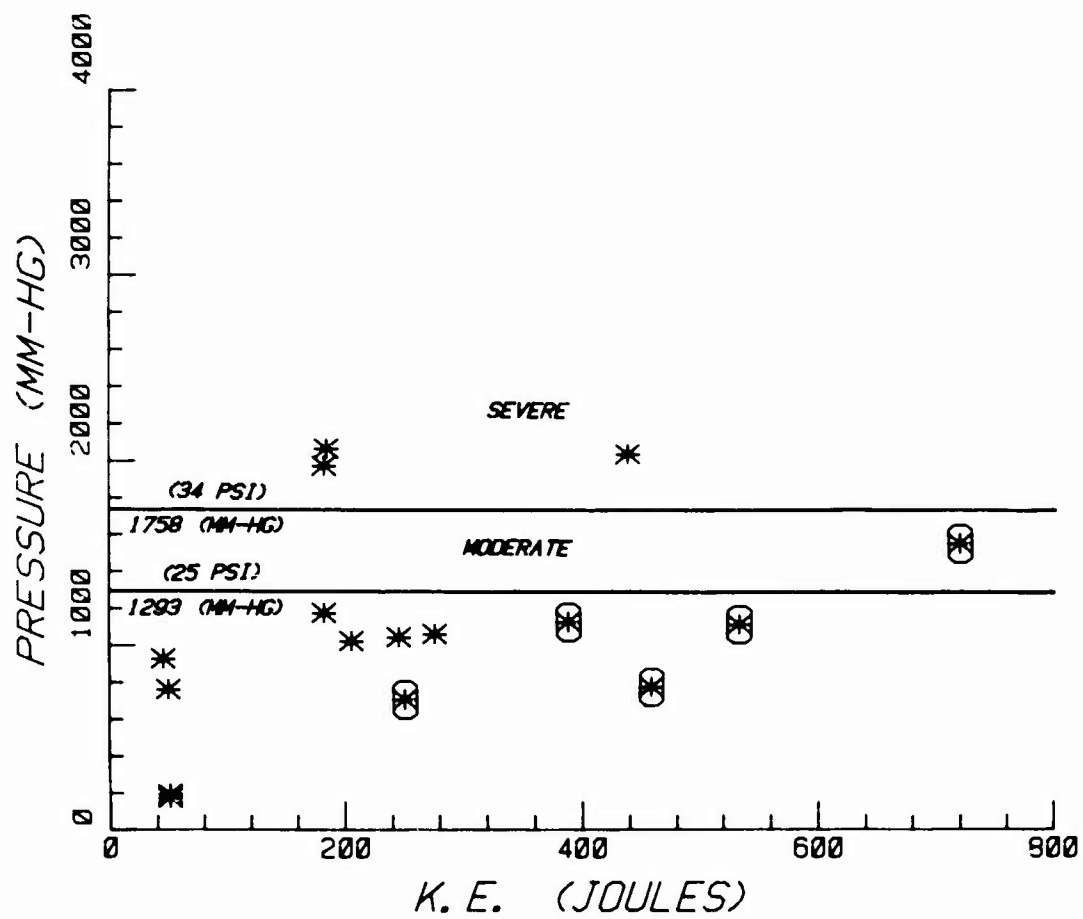


FIGURE 6. FRONTAL IMPACT. IMPACTOR KINETIC ENERGY VS. PEAK FRONTAL PRESSURE.

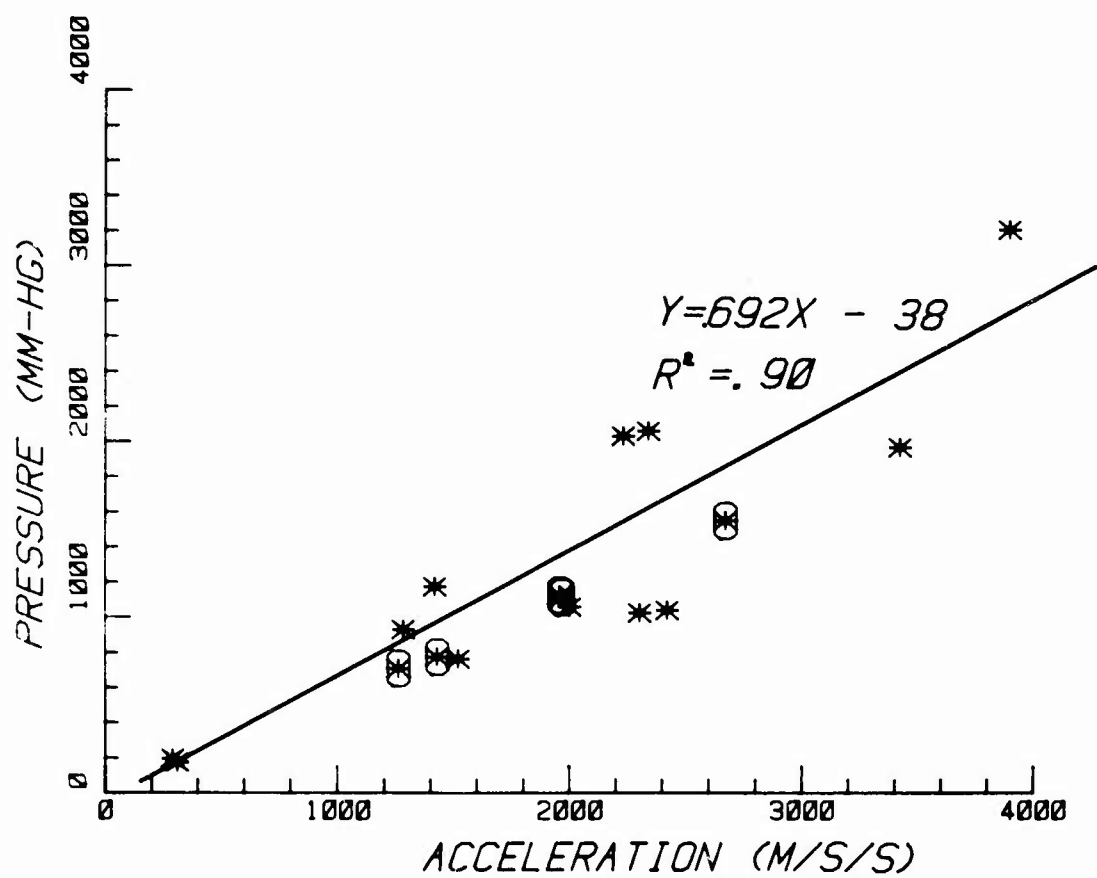


FIGURE 7. FRONTAL IMPACT. PEAK HEAD ACCELERATION VS. PEAK FRONTAL PRESSURE.

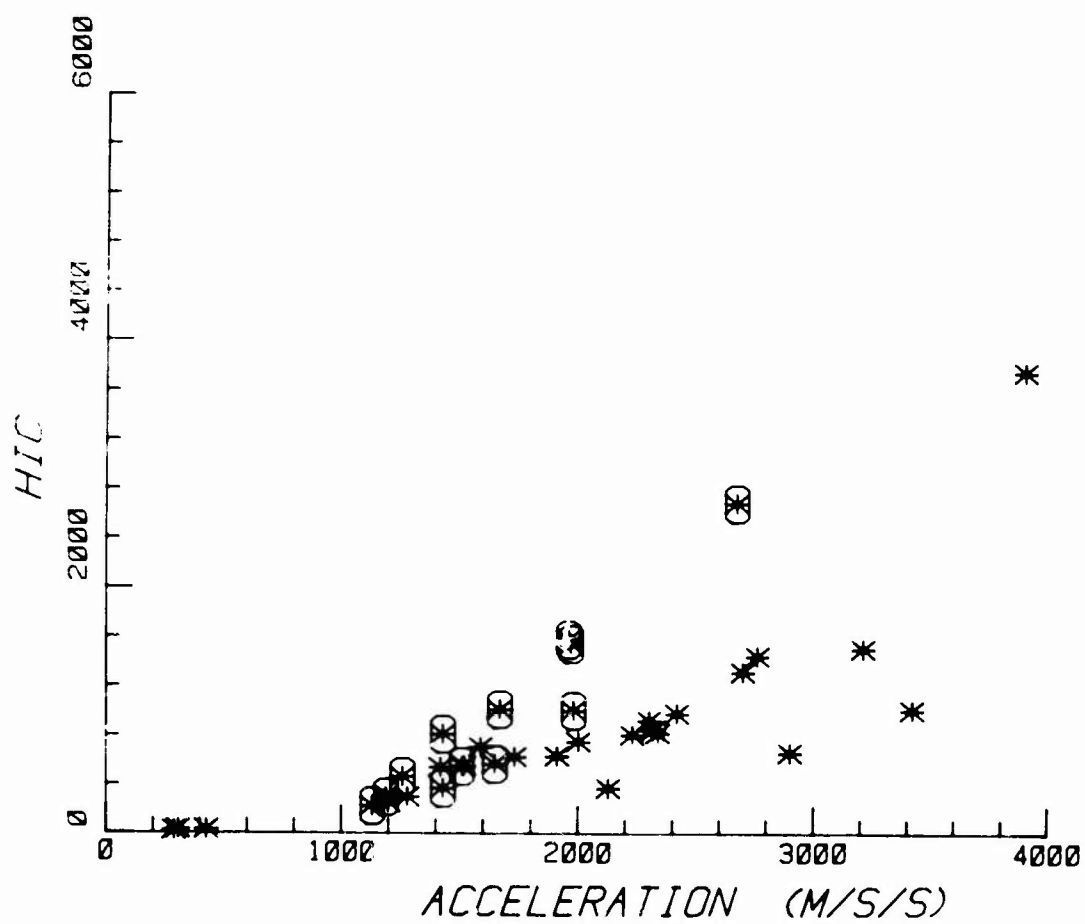


FIGURE 8. FRONTAL IMPACT. PEAK HEAD ACCELERATION VS. HIC.



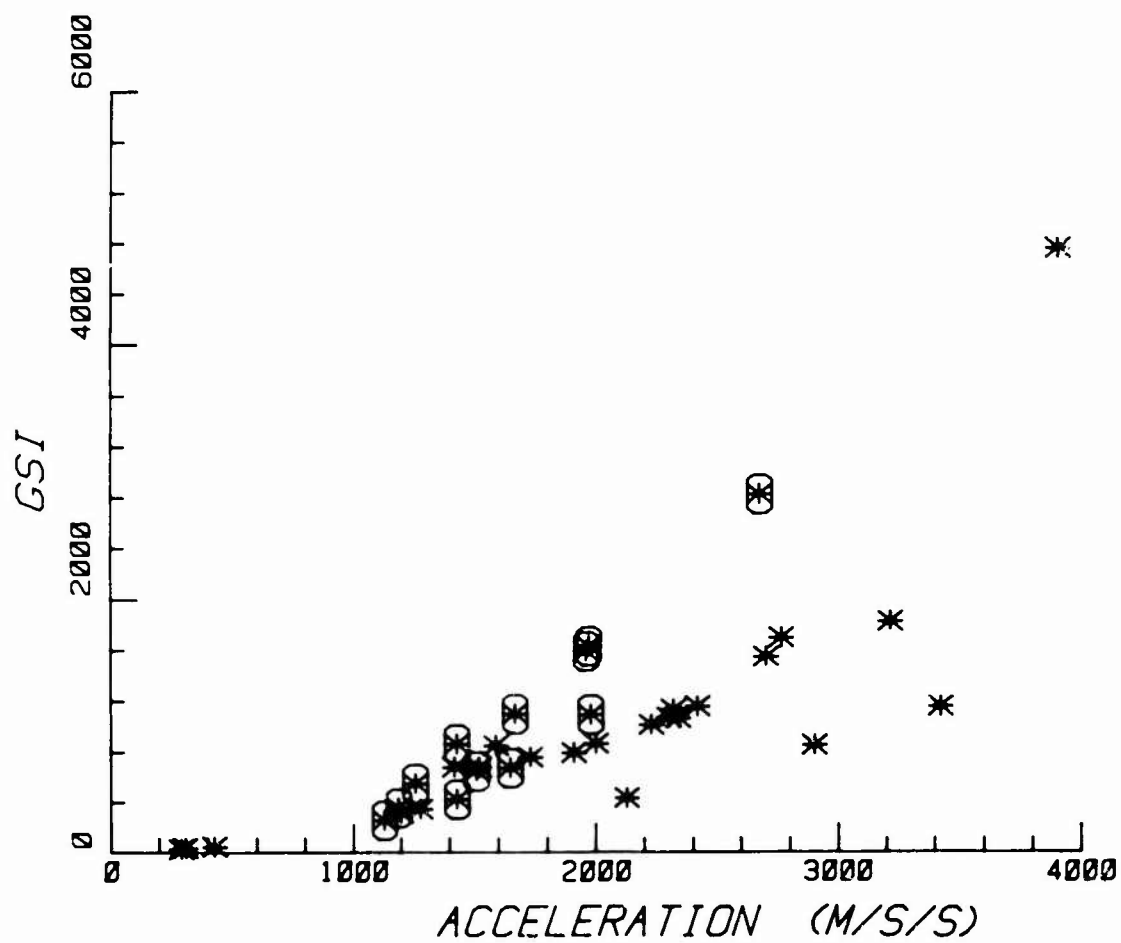


FIGURE 9. FRONTAL IMPACT. PEAK HEAD ACCELERATION VS. GADD SEVERITY INDEX.

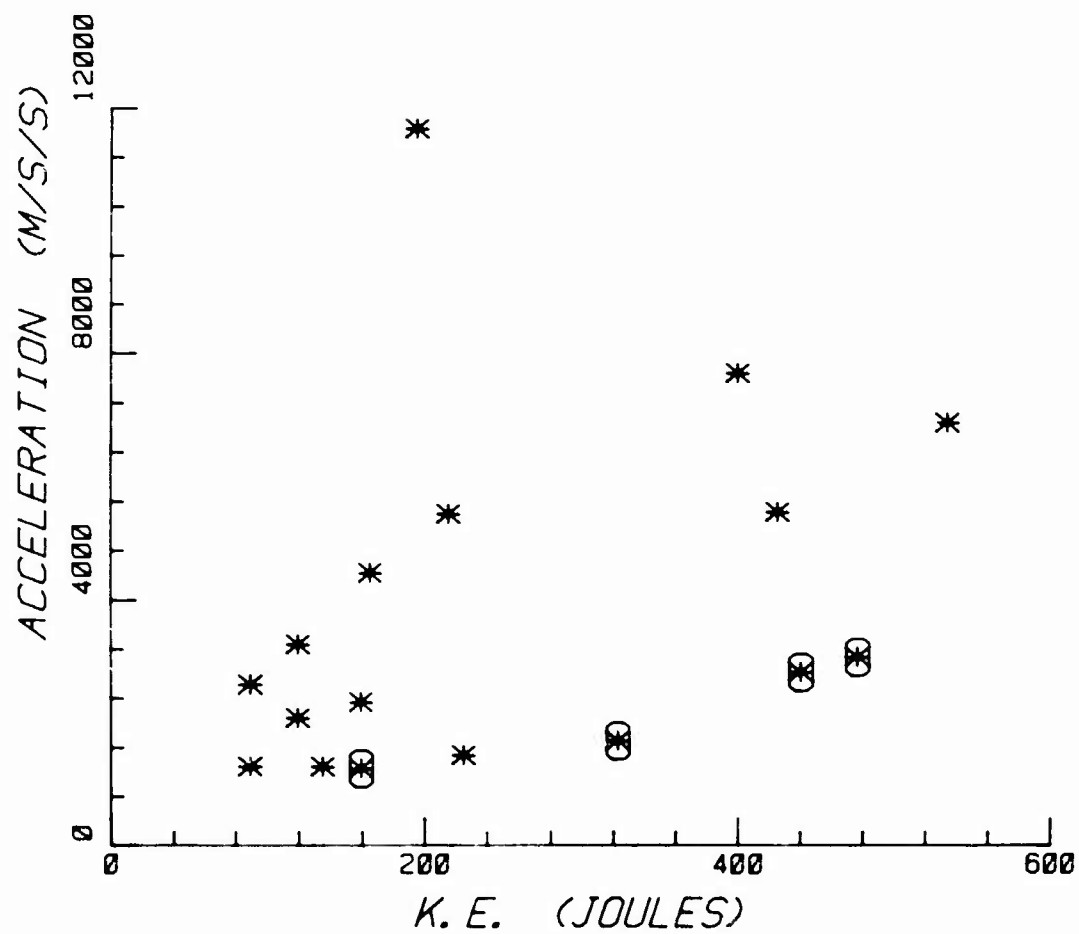


FIGURE 10. LATERAL IMPACT. IMPACTOR KINETIC ENERGY VS. PEAK HEAD ACCELERATION.

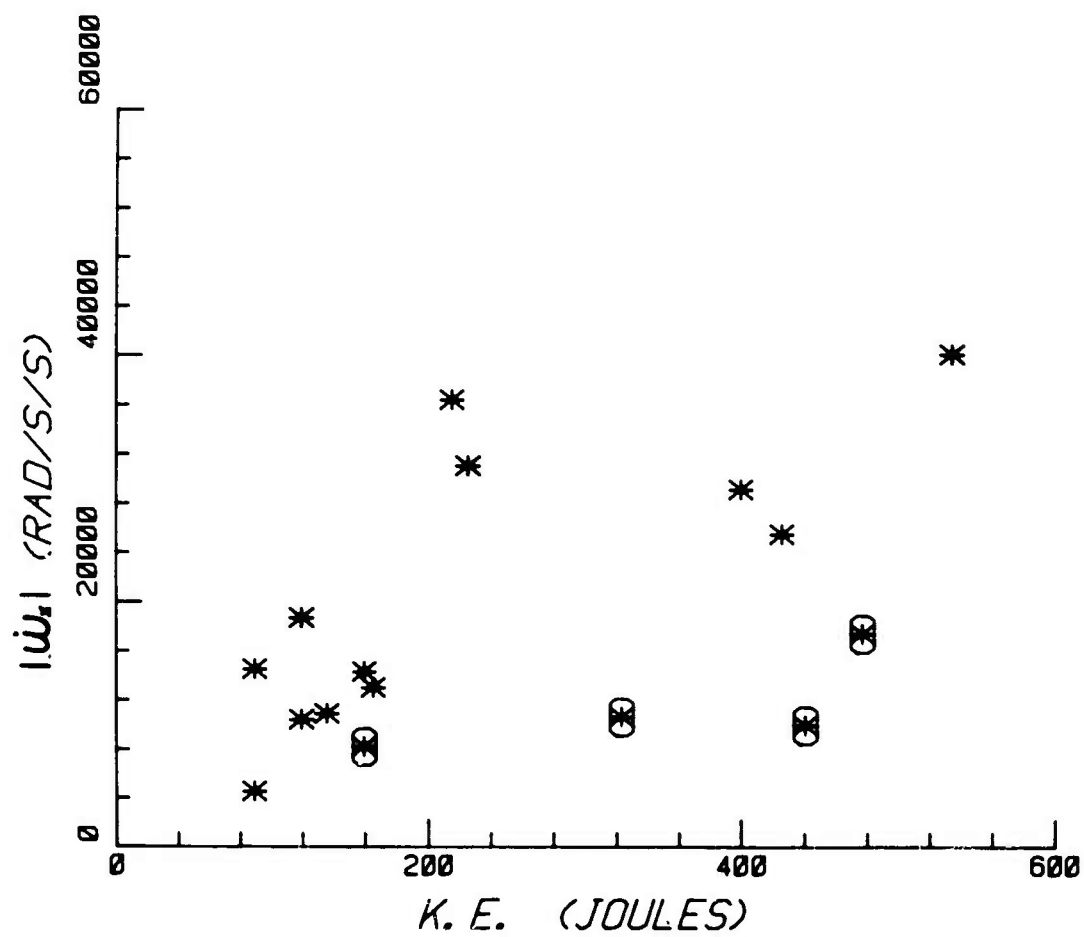


FIGURE 11. LATERAL IMPACT. IMPACTOR KINETIC ENERGY VS. MAXIMUM ANGULAR ACCELERATION.

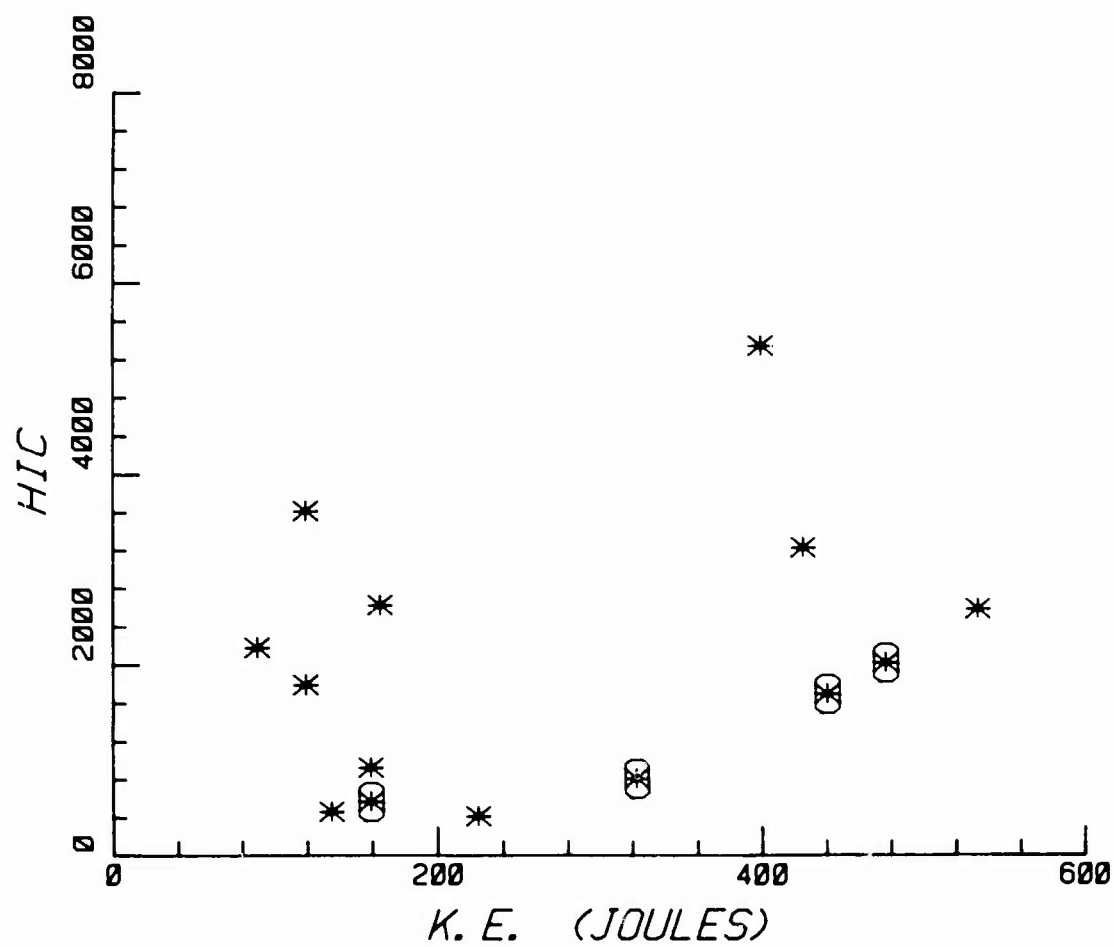


FIGURE 12 A. LATERAL IMPACT. IMPACTOR KINETIC ENERGY VS. HIC.

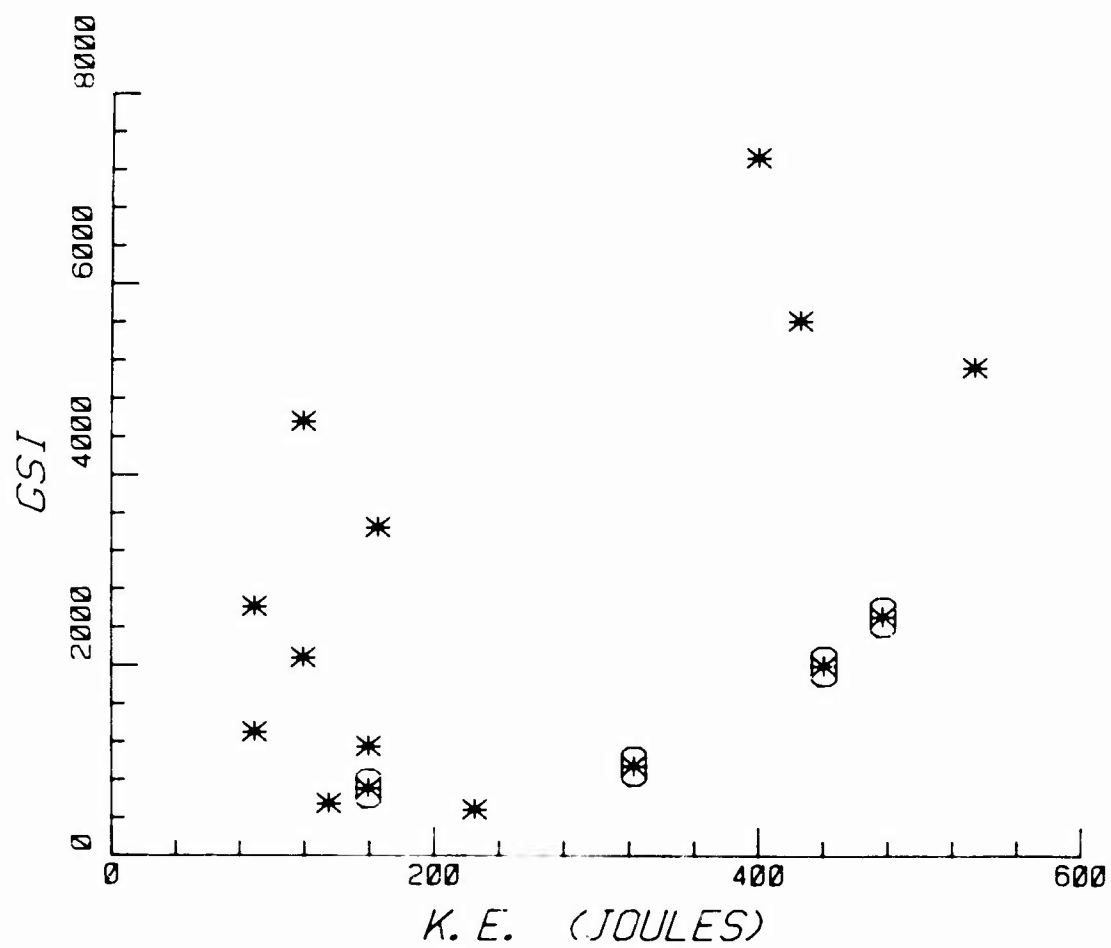


FIGURE 12 B. LATERAL IMPACT. IMPACTOR KINETIC ENERGY VS. GADD SEVERITY INDEX.

as great as in the acceleration peak, Figure 10.

(4) Peak Frontal Pressure vs. Impact Kinetic Energy

Intracranial pressure is related to impact energy in Figure 13. These measured frontal pressures, on the struck side of the head, approximate the maximum positive pressure at the impact site. For the same impact energy, pressures are lower in the helmeted head. Since injury is related to pressure magnitude, reducing the pressure reduces the occurrence and severity of brain injuries.

(5) Peak Frontal Pressure vs. Peak Head Acceleration

The relationship between pressure and acceleration tends to be linear for both helmeted and non-helmeted cases, as shown in Figure 14. This linearity is similar to that shown by the frontal impact data (Figure 7), but in this comparison the helmeted pressures were measured. One important observation is that for the same head acceleration, pressures in the laterally struck head are lower, approximately one-half the magnitude obtained in the frontal series. This is due to the falx cerebri. This membrane divides the upper brain into two compartments reducing the pressure responses in the lateral direction. The lengths of the individual sections of brain accelerated are one-half the brain width.

(6) The HIC and GSI vs. Peak Head Acceleration

These impact severity measures are related to head acceleration in Figures 15 and 16. The trend is similar to the frontal impact series, Figures 8 and 9. Again the relationship appears to be exponential which would be consistent with the HIC and GSI derivation. GSI values are higher than HIC values for the same impacts, especially at higher accelerations. This is due to the maximization procedure, which limits the portion of the acceleration trace used in the HIC calculation.

### BRAIN RESPONSE ANALYSIS

#### FINITE ELEMENT BRAIN MODEL

Stresses and displacements throughout the brain were calculated in computer simulations. An analysis procedure known as the finite element method was employed. Using this technique the structure or substance to be analyzed is mathematically divided into small pieces or elements. Equations for each element are generated in the computer and then combined to form the matrix system equation of motion. In this study the brain and contained fluids are divided into six sided, eight corner (node) brick elements. The assembled elements approximate the irregular shape of the brain where the edges of the elements form a grid of intersecting lines. Refer to Figure 17. Four node membrane elements are assembled to simulate the internal folds of dura, the falx and the tentorium. In all elements the mass is considered concentrated at the element corners or nodes.

The internal shape of the skull is simulated to form a container for the brain. An opening representing the foramen magnum is modeled and allows movement of the cervical cord into and out of the cranial cavity. In these test simulations the container or skull is mathematically moved in space as the head moved in the impact.

#### MATERIAL PROPERTIES

Material constants for the composite intracranial material - brain, vasculature and contained fluids, were obtained from a parametric study in which measured and computed intracranial pressures were compared. Properties which provided good correlation were selected. Although the selection was based on a series of thirteen tests (tests 36-38, 41-44, 46-50 and 54) subsequent simulations have demonstrated good correlation using these properties. A Young's modulus of  $5 \times 10^3$  mm-Hg has provided good results for all tests.

Compressibility of the material was shown to be strain or loading rate dependent. At higher rates of onset, the intracranial material becomes less compressible. This is thought to be a function of flow into and out of the cranial cavity; at a slow rate of onset, the pressure-relieving flow has a greater influence on response. In the brain material elements, the compressibility, as defined by Poisson's ratio, is varied between the values 0.48 and 0.499. Value selection is based on the head acceleration rise time, rise time being inversely proportional to rate of onset for equivalent head accelerations. A non-linear approach which would automatically select a value based on instantaneous element strain rate is being considered, but unfortunately it would increase the cost of solution by a factor of five.

Whether manually or automatically selected, these higher values of Poisson's ratio require a special element. Ordinarily, finite element equations become unstable as the material idealization approaches incompressibility (Poisson's ratio approaching 0.5). To avoid this instability, a split energy element was developed, verified, and implemented. This element is stable for all values of Poisson's ratio and can more accurately predict response.

#### SOLUTION PROCEDURE

The equations are generated in terms of a skull fixed axis. Head motion is

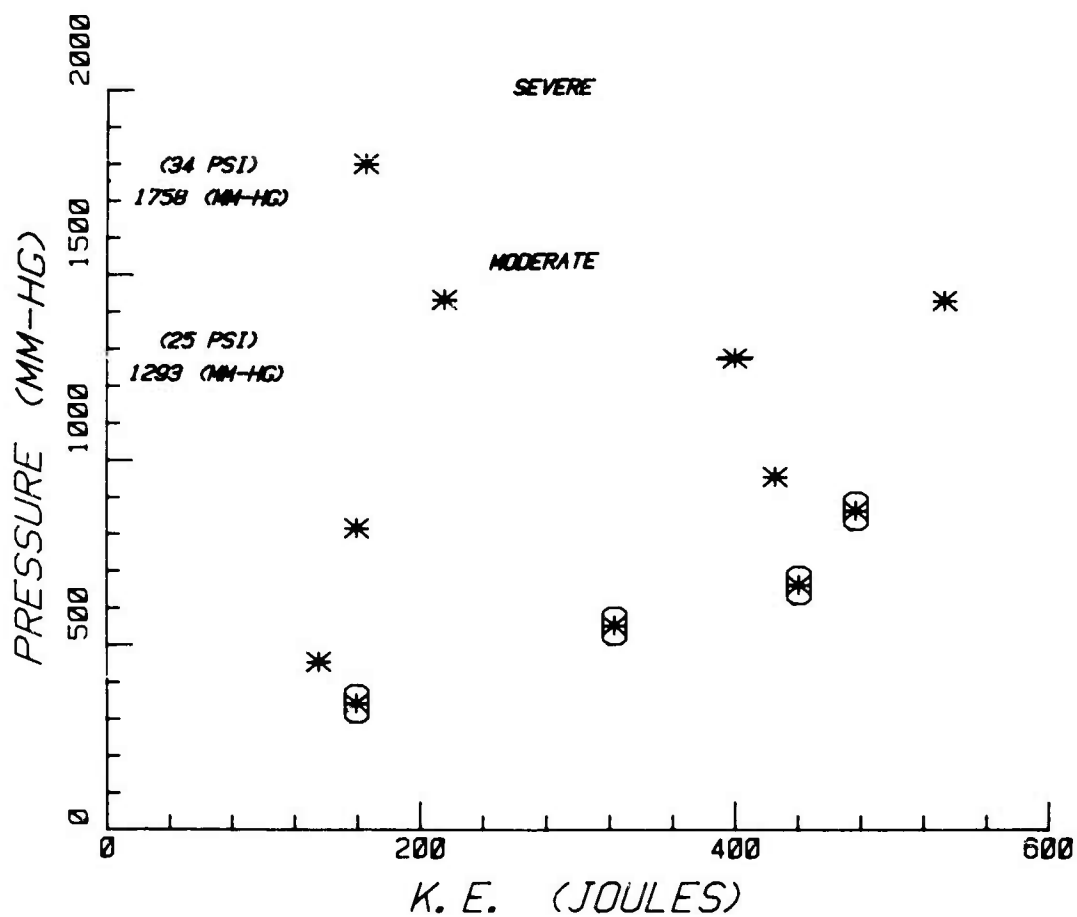


FIGURE 13. LATERAL IMPACT. IMPACTOR KINETIC ENERGY VS. PEAK FRONTAL PRESSURE.

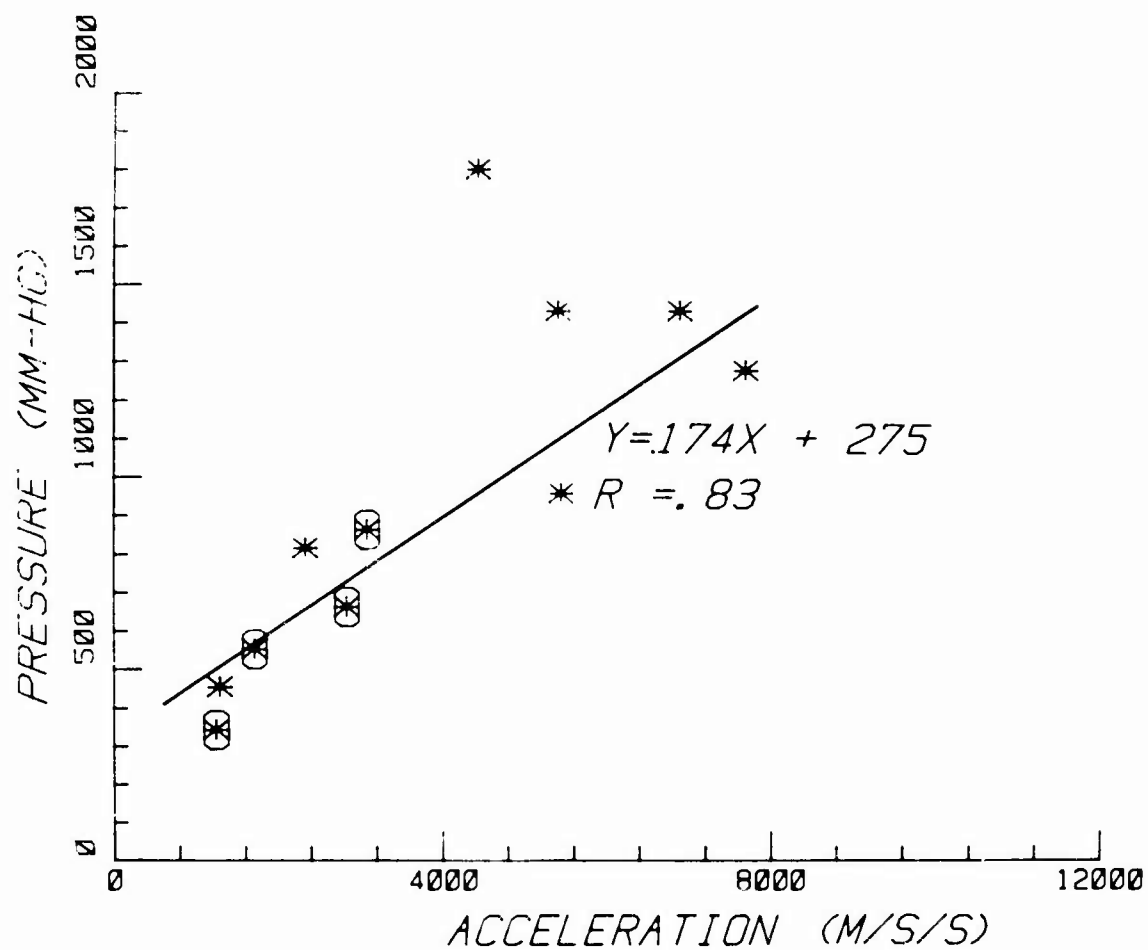


FIGURE 14. LATERAL IMPACT. PEAK HEAD ACCELERATION VS. PEAK FRONTAL PRESSURE.



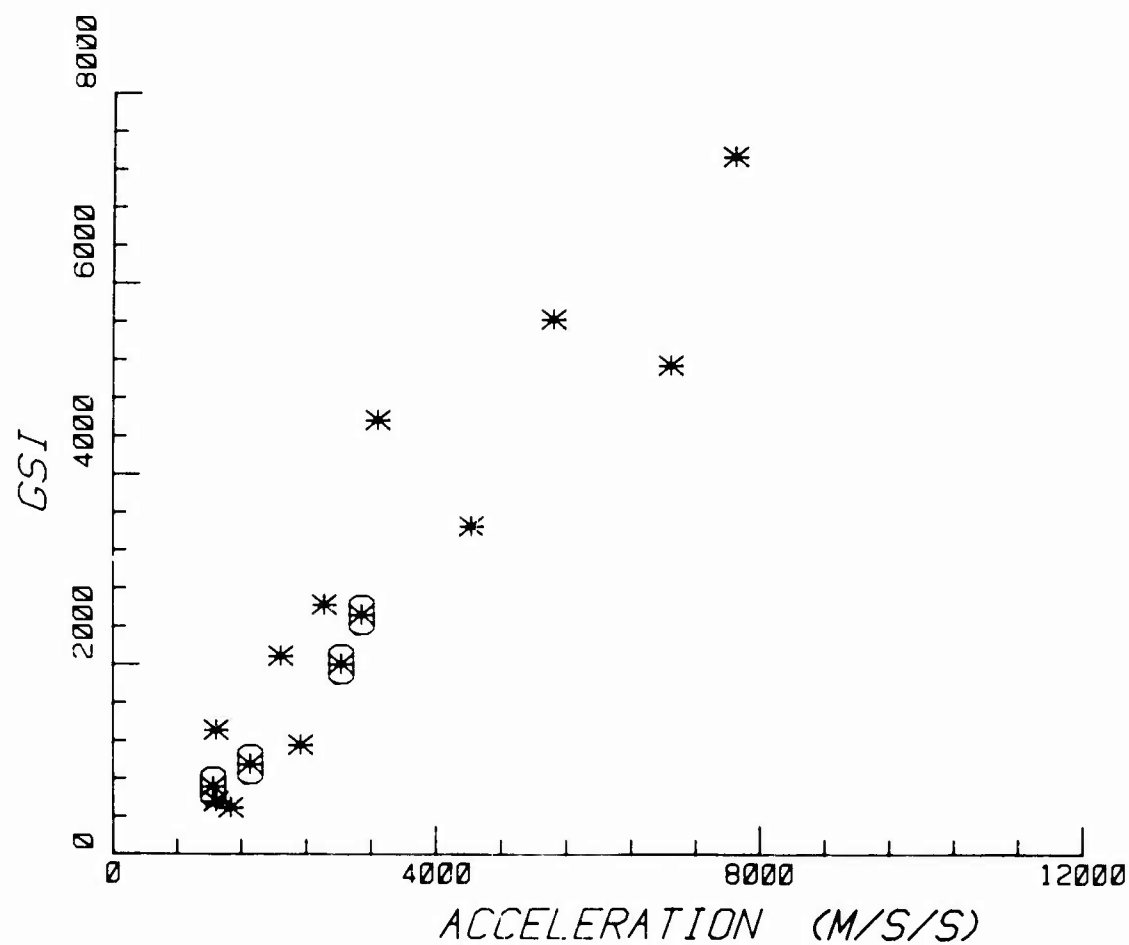


FIGURE 15. LATERAL IMPACT. PEAK HEAD ACCELERATION VS. GADD SEVERITY INDEX.

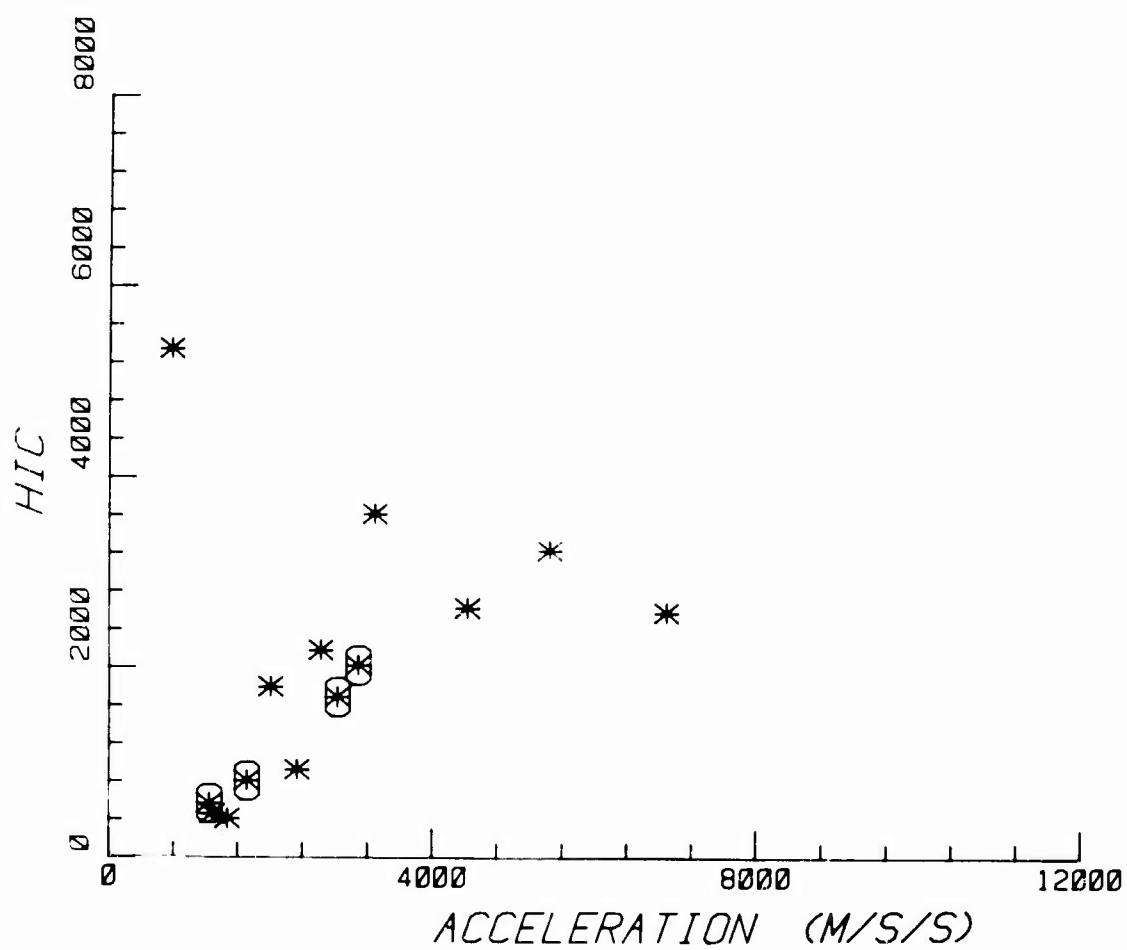


FIGURE 16. LATERAL IMPACT. PEAK HEAD ACCELERATION VS. HIC.

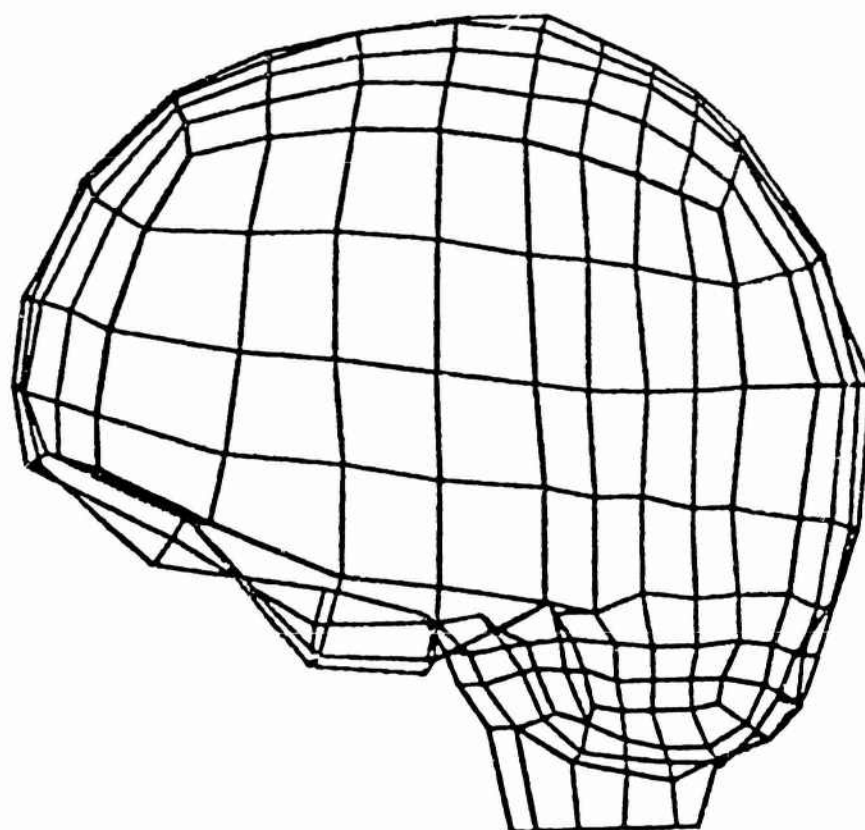


FIGURE 17. FINITE ELEMENT MODEL OF THE HUMAN BRAIN.

imposed by mathematically translating and rotating the axis frame as the head translates and rotates in the impact experiment. Using this procedure the nonlinear terms due to large rotation and displacements of the head are eliminated. Measured head rotations and displacement are incorporated as known forces on the right side of the system equation of motion. Since displacements of the brain relative to the skull are small, and the events are of short duration (less than 10 msec) the response can be approximated with a linear relationship.

The resulting system equation of motion is solved using direct integration. A general purpose finite element program named EASE 2 is used. EASE 2 was especially modified for the brain model calculations and is available internationally through the Control Data Corporation Cybernet system.

#### BRAIN MODEL RESULTS

The model-predicted brain response is shown for a helmeted and unhelmeted impact, Figures 18 and 19. In these two frontal impacts, the pressure or stress responses show that the brain tends to lag the skull. Brain tissue compresses against the skull near the impact site, and is in tension opposite the impact. The result is a pressure gradient. When the head translates along all three axes, as in the lateral impacts, three superimposed pressure gradients develop. Each gradient is proportional to the acceleration along its axis.

The brain also lags the skull in rotation, producing shear stresses and strains along the brain skull interface. In both head rotation and translation, the falx and tentorium help position the brain. In effect, they partition the intracranial cavity. Instead of a single rotational displacement of the brain as hypothesized by Holbourn [3], separate rotational motions develop in each compartment. These rotations in the cerebrum and cerebellum produce a complex interaction with the brainstem, the interconnecting brain structure.

Brain displacements are small, a few millimeters in most cases. Though the displacements depend on the event, in general, they are largest in the brain stem and cerebral cortex. When a superior-inferior component of motion is present, displacements of the cervical cord influence the brain response. In these impacts the brainstem may be stretched or compressed.

#### BRAIN RESPONSE AND INJURY

The injuries observed in this test series can be related to the brain motion. Contusions develop in the high pressure regions near the impact. Focal injuries develop opposite the impact where brain tension stresses are high. Subarachnoid and subpial hemorrhage occur in high shear strain regions and where tension stresses develop on the brain surface. Petechial hemorrhages were observed in the high shear strain regions of the brain stem.

Using the maximum intracranial pressure (hydrostatic stress) values as a quantitative measure of the brain responses, a relationship between injury severity and brain response was formulated for frontal impacts. Compression stresses of 1758 mm-Hg (34 psi) are associated with serious brain trauma. This compressive stress can produce brain contusions near the impact site. Responses of this magnitude are also associated with hemorrhages in the brain stem and in the material surrounding the brain. If the brain stresses are between 1293 mm-Hg (25 psi) and 1758 mm-Hg (34 psi) the injuries, if they occur, are moderate. Below 1293 mm-Hg, the injuries are no more than minor.

#### CONCLUSIONS

1. Unembalmed pressurized cadaver subjects were successfully used in an investigation of head protection measures and brain response.
2. Padding on the impacted surface and helmets significantly reduce the head acceleration and intracranial pressures in a head impact. Higher energy impacts can be tolerated without injury. The degree of protection can be assessed by comparing the head acceleration and/or the peak intracranial pressure for equivalent energy impacts.
3. The relationship between intracranial pressure and head acceleration tends to be linear. The Gadd Severity Index and Head Injury Criterion are exponential functions of head acceleration and therefore tend to be exponentially related to the peak head acceleration and intracranial pressure.
4. The finite element model can accurately predict intracranial pressure (stress) for both lateral and finite impacts. To obtain good correlation the model must approximate the size and shape of the brain, simulate the partitioning internal folds of dura, have an opening for the foramen magnum, and provide some effective compressibility.
5. The experimental and model results show that the brain tends to lag the skull producing pressure gradients. In the side impact where the head accelerates along all three axis, the pressure gradients are superimposed. The magnitude of each gradient is proportional to the magnitude of the acceleration along its axis. The largest component in both the lateral and frontal tests is in the direction of impact.
6. In frontal impacts, a relationship exists between brain response as defined by the peak intracranial pressure, and injury. Severe injuries only occur when the pressures or stresses exceed 1758 mm-Hg. Moderate injuries occur between 1758 and 1293 mm-Hg. Below 1293 mm-Hg the injuries, if they occur, are only minor.

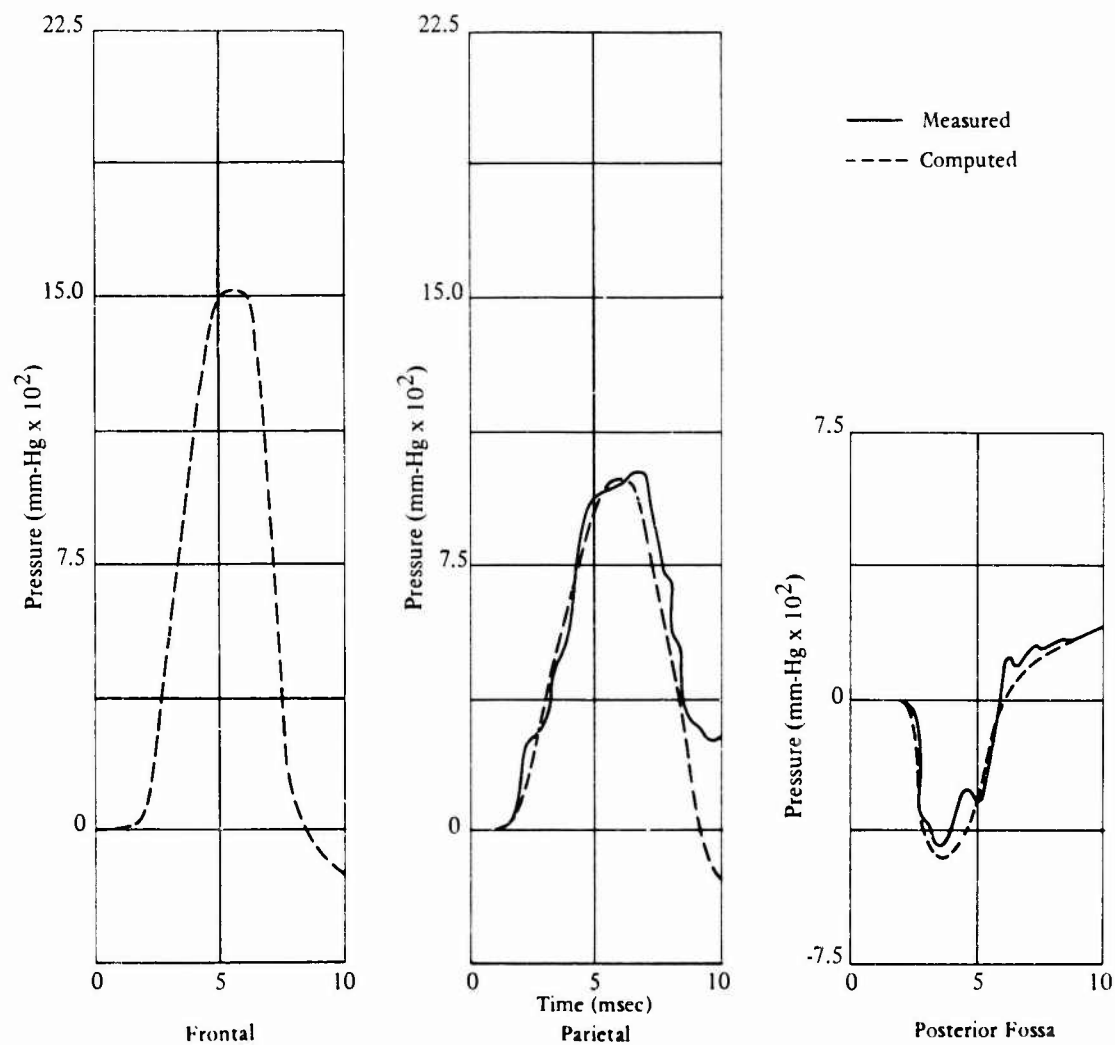


FIGURE 18. MEASURED AND COMPUTED INTRACRANIAL PRESSURES IN HELMETED FRONTAL IMPACTS.

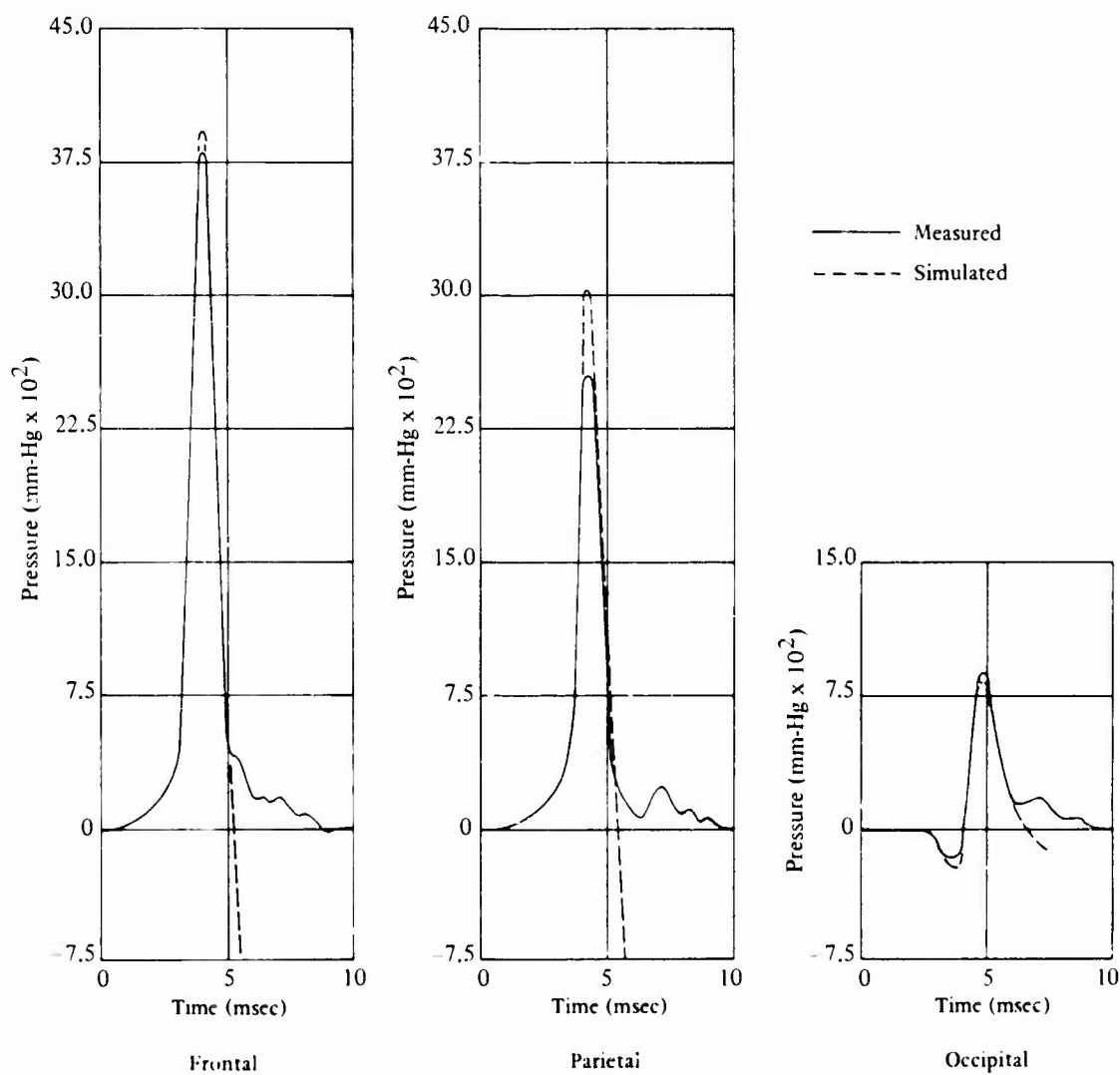


FIGURE 19. MEASURED AND COMPUTED INTRACRANIAL PRESSURES IN INEFFECTUALLY PADDED FRONTAL IMPACT.

## REFERENCES

1. Padgaonkar, A.J., Kreiger, K.W. and King, A.I. Measurement of angular acceleration of a rigid body using linear accelerometers. J. of Applied Mechanics 42:552-556, 1975.
2. Ward, C., Chan, M. and Nahum, A. Intracranial pressure - A brain injury criterion. Proc. 24th Stapp Car Crash Conference, Troy, MI, 1980.
3. Holbourn, A.H. Mechanics of head injuries. Lancet, p. 438, Oct. 9, 1943.
4. Nahum, A.M. and Smith, R.W. An experimental model for closed head impact injury. Proc. 20th Stapp Car Crash Conference, Troy, MI, 1976.
5. Nahum, A.M., Smith, R.W. and Ward, C.C. Intracranial pressure dynamics during head impact. Proc. 21st Stapp Car Crash Conference, Troy, MI, 1977.
6. Ward, C.C. and Nahum, A.M. 1979. Correlation between brain injury and intracranial pressure in experimental head impacts. In Proc. of the IVth International Conference on Biomechanics of Trauma, Goteborg, Pp. 1-10.
7. Nahum, A.M., Ward, C.C., Smith, R. and Raasch, F. Intracranial pressure relationships in the protected and unprotected head. Proc. 23rd Stapp Car Crash Conference, Troy, MI, 1979.
8. Nahum, A., Ward, C., Raasch, F., Adams, S. and Schneider, D. Experimental studies of side impact to the human head. Proc. 24th Stapp Car Crash Conference, 1980.
9. Nahum, A., Ward, C., Schneider, D., Raasch, F. and Adams, S. A study of impacts to the lateral protected and unprotected head. Proc. 25th Stapp Car Crash Conference, 1981.
10. Nahum, A.M. and Ward, C. 1981. Injury scaling of brain trauma. In Proc. of The Sixth International IRCOBI Conference on The Biomechanics of Impacts. Bron, France. Accepted for publication.
11. Nahum, A.M., Raasch, F. and Ward, C. Impact responses of the protected and unprotected head. In Proc. Consensus Workshop on Head and Neck Injury Criteria. Department of Transportation, Washington, D.C. Accepted for publication.

TABLE 1.  
FRONTAL IMPACTS

EXPT.	SPECIMEN SPEC#/SEX	CONDITION (INTERFACE) (cm)	KINETIC ENERGY (Joules)	PEAK HEAD ACCELERATION (M <sup>2</sup> Sec <sup>2</sup> x 10 <sup>3</sup> )	HIC	GADD	FRONTAL PRESSURE (mm-Hg)
15	78M	Isomode 1.4	105	1.91	627	787	-
17	79M	Isomode .7	142	3.21	1507	1882	-
18	81M	Rubber .2	247	2.13	366	432	-
19	82F	Isomode 1.4	132	2.32	845	1131	-
26	85M	Isomode 1.4	57	1.20	251	313	-
27	86M	Ensolute 2.54	37	.43	31	45	-
28	89F	Isomode 1.4	102	2.70	1316	1544	-
29	91M	Rubber .2	34	2.90	657	847	-
31	94M	Isomode 2.1	137	1.73	624	750	-
32	95F	Isomode 1.4	138	2.76	1443	1691	-
36	101F	Isomode 1.4	205	2.30	923	1068	1022
37	108F	Isomode 2.1	276	2.00	744	861	1059
38	109F	Isomode 1.4	245	2.42	980	1153	1041
41	111F	Polystyrene 5.08	1900	3.90	3765	4756	3207
42	112F	Polystyrene 5.08	438	1.59	703	842	-
43	115F	Polystyrene 5.08	438	2.23	804	1008	2031
44	117F	Polystyrene 5.08	50	1.52	551	675	764
46	120M	Polystyrene 5.08	51	.31	32	36	174
47	120M	Ensolute 2.54	51	.29	21	24	194
48	120M	Isomode 1.3	46	1.28	297	342	929
49	120M	Rubber .2	182	3.42	1008	1153	1969
50	120M	Polystyrene 5.08	182	1.42	539	675	1175
54	122M	Polystyrene 5.08	184	2.34	820	1061	2059
55	* 132F	Helmeted + Isomode .7	149	1.65	563	669	-



EXPT.	SPECIMEN SPEC#/SEX	CONDITION (INTERFACE) (cm)	KINETIC ENERGY (Joules)	PEAK HEAD ACCELERATION (M $\text{Sec}^2 \times 10^3$ )	HIC	GADD	FRONTAL PRESSURE (mm-Hg)
56	* 132D	Helmeted + Isomode .7	281	1.13	221	252	-
57	* 132F	Helmeted + Isomode .7	427	1.43	367	421	-
58	* 132F	Helmeted + Isomode .7	303	1.19	298	351	-
59	* 132F	Helmeted + Isomode .7	406	1.51	546	641	-
60	* 132F	Helmeted + Isomode .7	741	1.67	1010	1092	-
63	* 132F	Helmeted + Isomode .7	733	1.98	1000	1087	-
64	139M	Helmeted + Isomode .7	719	2.67	2685	2820	1548**
65	140M	Helmeted + Isomode .7	532	1.97	1542	1627	1113**
66	141M	Helmeted + Isomode .7	250	1.26	462	544	707**
67	142F	Helmeted + Isomode .7	388	1.96	1581	1585	1126**
68	144F	Helmeted + Isomode .7	458	1.43	807	857	775**

\* Indicates Embalmed Specimen

\*\*From Finite Model

TABLE 2.  
SIDE IMPACTS

EXPT.	SPECIMEN SPEC#/SEX	CONDITION (INTERFACE) (cm)	KINETIC ENERGY (Joules)	PEAK HEAD ACCELERATION (M/Sec <sup>2</sup> x 10 <sup>3</sup> )	HIC	GADD	PEAK FRONTAL PRESSURE (mm-Hg)
70W	147M	Ensolute (3)	89	1.29	-	1308	-
71W	147M	Ensolute (3)	119	2.08	1796	2085	-
72W	147M	Polystyrene (3.1)	119	3.28	3613	4566	-
73W	147M	Polystyrene (3.1)	89	2.62	2179	2624	-
74W	150F	Ensolute (3)	135	1.29	456	553	454
76W	152F	Ensolute (3)	165	4.43	2625	3452	1800
77W	153F	Polystyrene (3.1)	195	11.66	-	-	-
78W	154F	Polystyrene (3.1)	215	5.4	-	-	-
84W	158F	Polystyrene + Ensolute (4.1)	225	1.47	411	488	-
85W	158F	Helmeted	159	1.25	564	711	342
87W	158F	Polystyrene + Ensolute (4.1)	159	2.33	923	1152	815
88W	158F	Polystyrene + Ensolute (4.1)	399	7.69	5337	7343	1276
89W	158F	Helmeted	323	1.71	810	945	552
90W	158F	Helmeted	440	2.83	1690	2001	662
91W	158F	Helmeted	476	3.08	2022	2517	863
92W	158F	Polystyrene + Ensolute (4.1)	425	5.44	3234	5620	957
93W	158F	Polystyrene + Ensolute (4.1)	533	6.89	2584	5142	1432

## DISCUSSION

DR. SHANAHAN (USA)

You are really comparing in these tests, the effect of the helmet shell in that you are using a padded impactor for your unprotected samples and a helmet with built-in padding for the other. I was wondering if you have considered using this particular set-up to compare the effect of different types of materials for helmet shells.

AUTHOR'S REPLY

Yes, I think it's very appropriate to use it for different helmet shells. We have done different types of helmets; however, this data was only from the polystyrene. I think in addition to the helmet though we have a different contact area when the head hits a flat surface, it's a rather finite area with a helmeted liner, the more the head deforms into that liner, the more contact area you're getting, and so I think that's also included in the protection that was provided by the helmet.

UNIDENTIFIED QUESTIONER

If I understand one of your curves correctly, you showed the HIC and the GADD indices for frontal impact as being higher than for unprotected head. Did I read those curves correctly? I did notice that the HIC and the GADD indices seemed to be higher and you explained that because they were exponentials.

AUTHOR'S REPLY

I showed two comparisons with them, whether it was relative to the energy of the impactor, or relative to the head acceleration. I think if it was the exponential, it was comparing it to the head acceleration.

UNIDENTIFIED QUESTIONER

Yes, because it seemed to imply that with the helmeted impact with a longer time duration, you would get a higher HIC or GADD index number than you would with the unhelmeted head. What does that imply? Would you expect a higher index number because of the time duration?

AUTHOR'S REPLY

No. You would expect a higher HIC in unhelmeted impact of the same energy, but the difference is not as significant as if you were just comparing head accelerations because of the integration that tends to increase the HIC in the helmeted case. But time is not as significant as the peak g value.

UNIDENTIFIED QUESTIONER

The automotive industry looks at a HIC of more than 1000 as injurious, and certainly significant, and if I were to wear a helmet and the helmet gave me a HIC more than 1000, it would be unacceptable. That's what I am asking. If I were wearing a helmet in an automobile, the HIC that I would expect would be higher than if I were not wearing a helmet in an automobile with the same impact.

AUTHOR'S REPLY

I think there is a risk in using the HIC on a helmeted head case because of this problem. You can stay below the injury level and still have a high HIC.

DR. THOMAS (USA)

The original American National Standards ANSI (Z90) standards for helmet protection were based on linear acceleration measurements and the duration of that linear acceleration. That standard has existed for years and is based upon experimental work conducted at Wayne State University in the 40s and 50s era. The HIC is a creation of a bureaucracy. As far as I know, there is no experimental information to determine that the HIC discriminates between injury and noninjury better than linear acceleration. The data that you present here indicates that peak linear acceleration is a much better discriminator. Therefore, why use the HIC at all?

AUTHOR'S REPLY

Well, I'm not a member of the bureaucracy that created the HIC and I probably would use linear acceleration as a criteria.

UNIDENTIFIED QUESTIONER

Ms. Ward, can you say something about the test center and how you did the impacts?

AUTHOR'S REPLY

The subject is seated in front of an impactor and the impactor is traveling at constant velocity when it impacts the head. We use different padding material on the impactor and different weights of impactor to obtain different energy levels. The accelerations were recorded during the impact.

UNIDENTIFIED QUESTIONER

With cerebral injuries, are you sure there are no artifacts with your methods?

AUTHOR'S REPLY

Well, we did run controls and found that there were no injuries in the controls, but you don't always injure the brain. Some brains seem to be able to tolerate a great deal more than others, so that not every brain is injured at the injury level shown in our paper.

UNIDENTIFIED QUESTIONER

What level of errors would you expect in measuring dynamic pressures in the brain?

AUTHOR'S REPLY

We did do tests about four years ago, not in the skull, but in water on transducers, comparing them to others at impact. I don't think that our technicians found any major problems. I know that a number of other people are using the same pressure transducers, the University of Michigan uses them, and they haven't found any errors of significance. I might expect maybe 10% at most.

DR. VON GIERKE (USA)

I basically disagree when you say you have good correlation between pressure and head injury. I don't think the pressures produce any injury. It's a pressure gradient which would produce the injury; therefore I think you have the same injury mechanism in front and back. This comment might not be so important for your specific results and comparisons for this impactor for this weight and this helmet, but basically you have a pressure wave as you showed it on the last slide. The one with the higher peak has a higher pressure gradient and a pressure gradient causes the injury. If you compressed the whole brain uniformly, you would have no injury.

AUTHOR'S REPLY

Well, I'm sure if you applied the pressure very slowly and didn't let the brain move as it was being compressed, you probably wouldn't injure the brain. Perhaps our statement is too simple. What we're saying is you can get a dynamic stress that's high in a specific area and when you look at the brain you see an injury in that area. Whether it's the high pressure or the gradient in that pressure, I wouldn't say, but that's what we observed.

DR. VON GIERKE (USA)

But you agree it is a pressure wave traveling through the skull and if you assume compression of the brain tissue, it is not really the compressibility. That is a mathematical compressibility you introduced because your theory does not take care of the deformation of the skull and the accompanying shear in the brain tissue. The damage can only come from pressure gradients.

AUTHOR'S REPLY

No. I think that's where the misunderstanding is. We're not dealing primarily with the pressure wave transmitted through the brain. If we hit the skull on this side, the skull comes up against the brain and pushes it along and develops high contact pressure. In a way it's like an inertia of the brain. The bigger the brain is, the harder it pushes on the skull, and that's apparent in the side impacts.

DR. VON GIERKE (USA)

It is important when you go to blunt impacts where your time duration is longer; therefore, your wave has a longer time, and you have a different situation. I don't think the pressure criteria at all levels can be transmitted, and applied to completely different types of impacts to the skull.

AUTHOR'S REPLY

We used the pressure criteria (pressure values) as a measure of brain response. If the brain moves a lot, it has high pressures on one side, and low pressures on the other. So, it's a measure of what's going on inside the head. Some injuries don't occur at the high pressure regions like in the brain stem, and we know it is shear strain in response to what's going on and response to how the brain is moving. The more the brain moves the

more the shear strain and the higher the pressure. So, in a sense we're using pressures as a measure of brain response. We are not saying that because it's under a lot of pressure, it fails. It does fail under high pressure but I won't say that it's because it's a constant pressure, it's a changing pressure.

DR. VON GIERKE (USA)

Thank you very much.

UNIDENTIFIED QUESTIONER

Please discuss the analysis of the pressure curve on the contrecoup side of the brain where you had a decrease in pressure and a plateau effect within a large positive spike. What do you suppose causes the spike?

AUTHOR'S REPLY

Well, it's been a mystery and now we have seen the same thing happen in the University of Michigan Highway Safety Research Institute monkey data. I thought it might be some kind of artifact, but now we've also seen it in the monkey data and it seems to me that the tissue fails. It occurs around one atmosphere negative pressure. It may be cavitating, it may just be separating, it may be gases expanding, but then it ends when the load is off, and then fails.

UNIDENTIFIED QUESTIONER

Non transcribable sentence; however, question is asked about rebound.

AUTHOR'S REPLY

In the model, of course, it doesn't have a failure mechanism and it would rebound before that failure. I'm sorry I don't have something to draw on, but the model would respond faster. The only way I can make the model respond that slowly is if I let it fail, let part of the model release as a failure; I could then permit it to be a failure mode. In the human data, we've seen subchoroidal hemorrhage in all of those cases that demonstrated that failure mechanism.

UNIDENTIFIED QUESTIONER

You have some problems with vibrations in your accelerometers. I seem to recall that there was discussion in the literature that the nine accelerometers scheme might also be unstable. I haven't the faintest idea as to what extent these drift phenomenon are applicable to our tests. Could you comment on that please?

AUTHOR'S REPLY

To my knowledge it's the six accelerometer scheme that could be unstable and the nine are stable. When you mount these accelerometers very close together, and subtract one from the other, you could be reading "noise" in the system. If you could mount the accelerometers far apart, having three here, and three there, like the University of Michigan does, you eliminate that problem. I have never had that problem in using the University of Michigan data. The problem occurs when you mount them close together on a mechanism and then mount the mechanism at one point in the skull so that the mechanism can rotate and then you are just getting a lot of errors. So the best thing we could do because we were forced to under contract was to tie it down and wrap it with acrylic. In summary, I don't think that the system was unstable.

DYNAMIC FRONTO-OCCIPITAL HEAD LOADING  
OF HELMET-PROTECTED CADAVERS

Rainer Mattern                      Florian Schueler

Georg Schmidt

Institute of Forensic Medicine  
(Director: Prof.Dr.med.Gg.Schmidt)

UNIVERSITY OF HEIDELBERG

Voss str. 2

6900 HEIDELBERG

ABSTRACT:

Eleven dynamic fronto-occipital impact tests on helmet-protected cadavers were conducted with a deceleration trolley to which a quasi-rigid wall was installed. Effective head impact velocity lay between 32 and 45 km/h. The maximum deceleration of the head was on average 136 g in x-direction and 105 g in z-direction. The deceleration of the vertebral column reached values of 146 g for the 1st thoracic vertebra and 77 g for the 12th thoracic vertebra (average value of the maxima). Examination of the vertebral column showed 6 cases of severe compression fractures of the upper and middle thoracic part; signs of strain and flexion could be detected in the form of minor injuries in all cases. Discrete skull injuries were detected in only two cases. Injury to the brain could not be found but cannot be excluded in view of the test object. All the full-faced safety helmets used were of the same type and manufacture. The polycarbonate outer shell did not break in any of the tests. The polystyrol inner liner showed plastic compressions of a maximum of 30 % of the thickness of the damping liner at contact point.

INTRODUCTION

The head as one of the most critically-exposed parts of the human body in accidents, however they may occur, can be protected by a safety-helmet. In order to reduce impact severity and the resulting injuries to the head with brain and to the spine with spinal cord as head support and force transducing system, the helmet must be adjusted in accordance with technic-biomechanical criteria.

These criteria must on the one hand take account of the probability of certain types of accident (outer construction design recommendations) and, on the other hand, the possible injury patterns to be expected (inner construction design recommendation) in order to reduce the injury level.

At the Institute of Forensic Medicine of the University of Heidelberg, research into this question has been commenced on the basis of analysis of traffic accidents involving two-wheeled vehicles. After studying more than 350 accidents and closely analysing helmet damage and injury patterns related to the "accident input", we planned to carry out biomechanical tests with PMTOs (Post Mortem Test Object) on the Institute's own Impact Test Facility.

The opportunity of carrying out this work showed that the assumption is correct that the interaction of the helmet-head-vertebral column system cannot in fact be easily deduced from analysis of traffic accidents involving motorcyclists. There are difficulties in quantifying the mechanical accident interferences with sufficient precision, e.g. the acting forces, the occurring deceleration and the reconstruction of effective directions. Statistical investigations of accidents involving two-wheel vehicles carried out so far have rarely given a systematic analysis of the effects of the accident on the helmet (FELDKAMP et al. 1977, LANGWIEDER, 1977, HURT et al. 1981, SCHUELER et al. 1982, OTTE and SUREN, 1979).

Biomechanical investigations under standardized conditions are therefore necessary in order to determine the effect of different helmet design parameters on the risk of injury and also to develop injury criteria for helmet standards.

It is quite evident that safety helmet standards and test regulations have so far only rarely been based on injury patterns and biomechanical tolerance limits.

So the ultimate aim of the HD Project - to extend over a period of three years until the end of 83 - can be defined by the following three points:

1. the description of injury mechanisms on helmet-protected men,
2. the development of adequate, adapted safety helmet structures in both design and material,
3. cooperation on the development of safety helmet standards, base data and test regulations.

Point 1 implies the construction of adequate safety helmet impact test dummies.

Previous experimental investigations, using either cadaver heads protected by a helmet or complete corpses, have generally been in the form of impact or drop tests and have tended either to neglect the reactions to the vertebral column or have solely concentrated on the vertebral column. In the course of these experiments the reaction of the helmet itself has not been the subject of detailed analysis. ALDMAN (1976) examined the influence of various helmet-shell materials on isolated dummy heads with respect to the kinematics of the head, in particular angular acceleration.

There is a lack of experimental investigations which closely correspond to the real situations and use post mortal test objects in which the helmet, head and vertebral column have been subject to intensive technical and medical examination under defined loading impact conditions.

As a first configuration of the test series we chose a fronto-occipital impact situation which had been frequently found in real accident situations.

#### EXPERIMENTAL SET UP

The PMTOs or dummies were placed on the deceleration trolley by means of an appropriate support device.

A polystyrole support bloc was made to maintain the PMTO in position while a support for the back, pelvis and the feet was used to hold the PMTO during the acceleration phase of approximately 1,5 g (fig. 1).

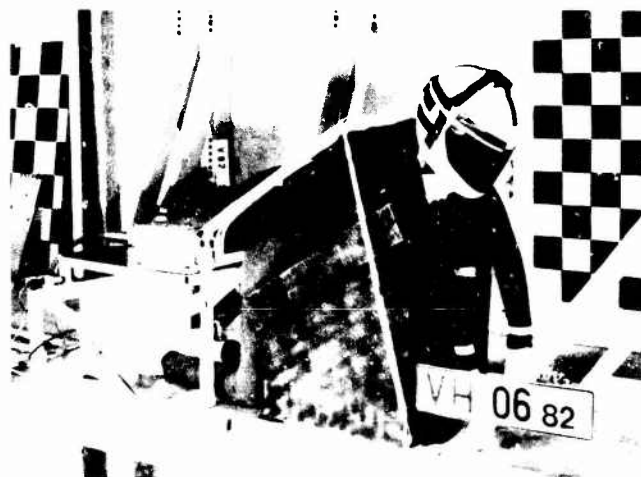


Fig. 1  
Experimental set up

Following deceleration of the trolley by means of a braking metal sheet, the PMTO slid and then hit against a quasi-rigid wall. The acceleration necessary for the desired impact and trolley-velocity was attained by hauling up a dropping weight of 13 tonnes which was connected to the trolley and then fixed at the appropriate distance when testing preparations had been completed (KALLIERIS, 1974).

The impact wall - 0,8 m wide, 0,9 m high - was fixed to the trolley. The material used was a 30 mm multiplex panel, reinforced on the side of impact by a 2,5 mm aluminium sheet and screwed unto a frame of 30 x 50 mm square bar steel. In the initial testing position the distance between the head and the impact wall was about 1,2 m.

A mosaic screen of 1 x 1,5 m, fixed unto the trolley, was used to facilitate the assessment of the high-speed films.

The transmitter was placed as close to the test object as possible. Its input was provided by the transducers' cables; its output by a trailing cable leading to the permanent control room.

Full-faced safety helmets of the same model and manufacturer were used in all tests. The material of the helmets used corresponded in construction and technology to the latest technical (although not biomechanical) developments. The outer shell was of polycarbonate, the damping liner of polystyrole. It was found that it was typical for the manufacture of the helmets that the foaming density of the damping liner, determined following the impact test, was different in the various test-runs although the helmets were in fact fresh from the factory. The specific density was between about 25 and 50 mg/ccm.

## TEST OBJECTS

Fresh, not embalmed or otherwise preserved human cadavers were used as PMTOs. The post mortal period was between 19 and 105 hours with an average of 62 hours. The stages of rigor mortis accordingly varied from an advanced stage to starting decline.

PMTOs in an advanced stage of rigor mortis had to be adjusted into the necessary position by gentle bending of the extremities.

There were no signs of decomposition in the sense of macroscopically visible putrefaction of tissue, especially in the region of the head, vertebral column and thorax, areas of special interest.

In the 11 dynamic tests performed so far the age ranges reached from 15-41 years, with an average of 29 years.

Since the population bracket prone to motorcycle accidents generally tends to be younger (18-20 years old), the PMTOs used in these tests correspond more closely to the real situation than those used in other similar experiments.

Before experimental trauma, the PMTOs had to be free of injury. This was diagnosed by examination, palpation, x-raying of the head (3-planes), the spinal column (2-planes) and the thorax. Careful consideration was also taken of case history.

## INSTRUMENTATION

The topographical position of the mounted accelerometers and pressure transducers is illustrated in fig. 2. The transducer-mounts, constructed for this test purpose, were fixed unto the skull bone after thread cutting following a slit-shaped incision and preparation of the scalp. The processus spinosus of the 12 th thoracic vertebra was used to fix the accelerometer base with a 5 cm bone screw. The accelerometer of the 1st vertebra, however, was mounted on a disk fixed by two screws in the vertebral joints of the 1st thoracic vertebral body.

So far no simulation of blood pressure by means of a catheter into the cervical arteries and puncturing of the side ventricles has been performed.

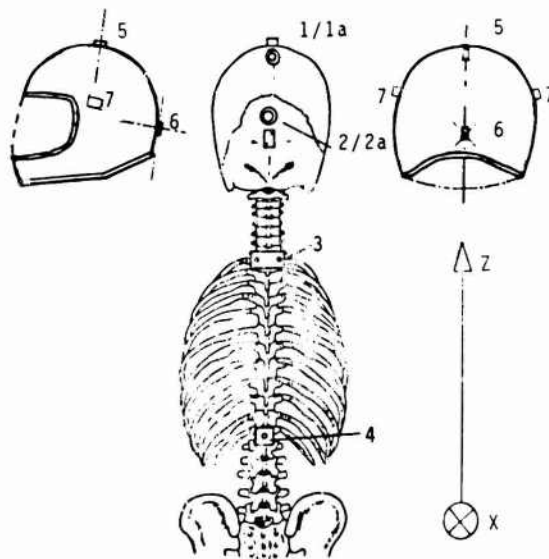


Fig. 2

Position of the ACCELEROMETERS AND PRESSURE TRANSDUCERS on head and helmet.

1. z-direction: central parietal bone
- 1.a) Pressure transducer in the parietal epidural space, level with the tabula interna.
2. x-direction: immediately above theinion (protuberantia occipitalis externa)
- 2.a) Pressure transducer central occipital bone
3. x-direction: 1st thoracic vertebra (T 1)
4. x-direction: 12th thoracic vertebra (T 12)
5. z-direction: top of the helmet
6. x-direction: posterior margin of helmet
7. x-direction: both lateral sides of helmet



## DUMMY

A TNO 10-type dummy was used for preliminary tests to check the experimental set-up and testing techniques and to carry out specific helmet examinations. Although this dummy was specifically designed for safety-belt testing, it proved surprisingly useful in these tests. A dummy of the whole body to meet the specific requirements of simulating motorcycle accidents and head-impacts has not yet been designed.

Another motorcycle dummy at present in use is a combination of elements from Hybrid II and Hybrid III and does not provide a satisfactory solution. The effectiveness of existing dummies must be re-examined so that they can be designed and adjusted in accordance with the requirements found in the cadaver tests.

## TESTING TECHNIQUE

The transmission of test data from the moving test object via the moving test trolley to the permanent control room is conducted by an IRIG standard telemetry plant.

Piezoresistive accelerometers (ENDEVCO) - types 2264/2000 or 7264/2000 - are fixed to the test object, the helmet, the impact point to the rear of the impact wall and the trolley. Along with the 603 B Kistler quartz crystal pressure transducer - or, alternatively, the ENDEVCO pressure transducer type 8510-100, they are first connected to the telemetry transmitter or a corresponding charge amplifier. Since the test object is in considerable motion before reaching its impact position an individual cable pulley had to be installed. From this point onwards, the amplified and frequency-coded signals of the accelerometers and pressure transducers, in the form of a frequency-multiplex signal, are connected to an analogue tape-computer.

In order to evaluate acceleration-time-history, the multiplex signal, stored on magnetic tape after demodulation, is printed by a UV printer or displayed and photographed by a memory-display oscillograph. When a sufficient number of these tests has been conducted, the digitalisation of this test data is to be carried out in October 1982. Following this, it will be possible to adequately assess and evaluate the head-impact data.

## Velocity measurement

The velocity of the test trolley is measured by a reflection-light-barrier-trigger-counting mechanism immediately before deceleration in the phase between acceleration and deceleration.

As this velocity does not precisely correspond to the actual impact velocity of the test object on the impact wall - it is in fact too low (rebound of the trolley!) - the slipping velocity of the test object immediately before impact is also measured. This is carried out as follows: another light barrier is interrupted. The so-called impact switch is short-circuited at the moment of impact. This impact switch consists of 2 parallel electrically-isolated aluminium foils which come into contact at the moment of impact.

## MEDICAL EVALUATIONS

## x-ray-examinations

After the test, every PMTO is x-rayed in the same way as in the pre-test examination, i.e. the head in 3 planes; the spinal column in 3 parts: cerebral, thoracic and lumbar part in 2 planes. When the head and brain venous system has been filled with contrast-medium by catheterisation of the venae jugulares internae, another x-ray examination of the head is performed in 3 planes (BARZ, MATTERN, 1975).

This diagnostic procedure provides evidence for venal lacerations in the region of the great dural veins and in particular the representation of ruptures of bridging veins. Lacerations of the great intracranial veins could also be diagnosed with patho-anatomical methods. It was however to be considered that even using careful preparatory methods there might be artefacts in the removal process of the circular-sawed calotte. These artefacts might not be distinguishable afterwards from traumatic lacerations of the PMTO. If the lesions had resulted from the dynamic load of the head even before preparation, they may be distinguished by applying venous contrast media - in this case the contrast media spills out of the lacerated vessel and forms an unusual opacity showing the laceration in the x-ray. Similarly arterial lacerations may be ascertained by filling the internal cerebral arteries with a contrast media.

## Autopsy

After the x-ray examination, a forensic pathological autopsy is performed with special attention to the traumatological findings. Part of this autopsy technique involves not only the opening of three body cavities of head, thorax and abdominal cavity but also an extensive preparation of the skeleton system by opening the body from back and front and preparation of the subcutaneous fatty tissue and the muscular system.

Special attention is paid to the examination of the spinal column. According to a special technique (MATTERN, 1977, 1980), the entire spinal column including the occiput is removed, the muscles are then removed in layers until a bone-ligament-specimen remains and, following deep freezing, sawed in 3 sagittal-parallel planes (fig. 5).

This makes it possible not only to observe all laceration of muscles in their segmental allocation but also to detect ruptures or strains of the ligamentous apparatus, bleedings and splicing of the intervertebral disks, subluxations, luxations, bleedings of the vertebral joints, contusion or bleeding of the spinal medulla and the spinal canal and fractures of vertebral bodies, processus and vertebral arches, even if barely visible.

Thus a complete recording of the injuries is possible which is not achieved by any other method, and in particular not by traditional x-ray techniques. More slight fractures important for the evaluation and understanding of the kinematic and injury mechanism, may sometimes only be verified in the x-ray if the slim sagittal-parallel cuts of the vertebral column, already described, are subject to further x-ray methods (fig. 5 c).

The examination of the brain starts with the inspection of the unfixed fresh specimen. It is then fixed in formalin to be cut into frontal-parallel slices and re-examined. The histological examinations refer to the more strained areas, which are known from the recent experience in brain traumatology.

#### Scaling of findings

Evaluation of the diagnosed injuries follows the AIS 80 and is based exclusively on patho-anatomical and x-ray findings. The assessment of multiple injuries follows the MAIS.

In the evaluation of findings of the spinal column, which is more complex than what is quoted in the dictionary of the 1980 Revision of the AIS, a grading was developed and used following the basic system of the AIS-evaluation (MATTERN, 1980).

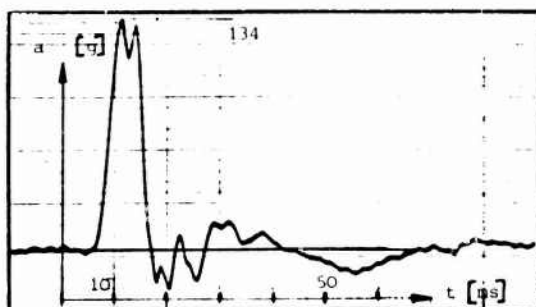
### TEST DATA

TEST No.	1	2	3	4	5	6	7	8	9	10	11	AVERAGE VALUES
TROLLEY velocity (km/h)	36	38	36	37	38	38	38,5	31	33	34	34	-
TROLLEY deceleration (-g)	19	16	-	19	18	-	18	17	17	20	19	-
IMPACT-WALL acceleration (+/-g)	90/94	111/107	-	116/113	115/94	-	127/94	123/73	106/84	114/77	134/81	-
HEAD velocity (km/h)	(43)	(45)	(43)	44	45	43	44	32	34	38	38	-
HEAD (-/+g) x-dir.	143/44	122/76	-	127/46	119/23	-	155/46	141/50	145/26	-	134/24	136
deceleration z-dir.	-	106/35	-	117/41	116/15	-	-	97/35	86/20	104/23	106/36	105
Deceleration on VERTEBRAL-BODIES (-/+g) T1, z	-	140/112	-	126/79	121/79	-	152/80	117/99	-	186/135	181/169	146
T12, z	-	82/86	-	65/35	67/32	-	91/55	57/44	-	103/34	72/41	77
Decelerations on HELMET	Maximal values of the HELMET deceleration between 550 and 700 g											
Size of HELMET	S,55/56	XS,53/54	XS,53/54	S,55/56	L,59/60	S,55/56	S,55/56	S,55/56	S,55/56	L,59/60	S,55/56	-
Density of DAMPING-LINER (mg/ccm)	27	51	50	50	27	28	28	29	29	28	28	-
Plastic Compression of DAMPING-LINER (mm) / %	5/19,3	6/23,1	6,5/24,5	7,5/27,7	7/26,9	8,7/30	8,5/29,3	7,5/25,9	7,4/25,5	7,4/25,5	6,8/23,5	-

Tab. 1

Measurement Data

3 a) head in x-direction



3 b) head in z-direction

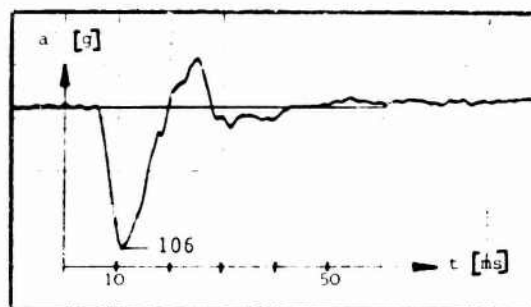


Fig. 3

Typical acceleration-time-history (Test No.11)

TEST No.	1	2	3	4	5	6	7	8	9	10	11
PMTO dates											
Age/sex (years/m,f)	24/m	15/m	33/m	25/m	25/f	27/m	41/m	37/m	32/m	34/m	28/m
weight/length (kg/cm)	81/170	46/170	59/174	67/178	75/178	65/178	75/172	67/170	74/178	94/193	55/170
MAIS	3	2	3	3	4	5	5	5	3	5	5
Regional AIS											
EXTERNAL	1	1	2	1	1	1	1	1	1	1	0
HEAD	3	0	3	0	0	2	4	0	0	0	0
visceral cranium	2					2	2				
neurocranium	3		3								
brain							4				
NECK	0	0	0	0	0	0	0	0	0	0	0
THORAX	0	0	0	0	0	4	4	1	0	4	2
AIS/Amount of fractures						4/17	4/27	1/2	0	4/13	2/5
Organs											
Abdomen	0	0	0	0	0	0	0	0	0	0	0
SPINAL COLUMN	1	1	3	3	4	5	5	5	3	5	5
Skelet			3	3	4	3	3	3	3	3	3
Ligaments/disks	1	1	2	2	3	3	3	3	3	3	3
spinal cord					4	5	5	5		5	5
EXTREMITIES	0	0	0	0	0	0	2	0	0	0	0

Tab. 2  
Medical Data

#### MEDICAL FINDINGS

In the 11 dynamic impact tests the frequencies of the injury levels according to MAIS and regional AIS were as follows:

	MAIS	Regional AIS			
Injury-level		Head	Thorax	Spine	External
0	0	7	6	0	1
1	2	0	1	2	9
2	0	1	1	0	1
3	3	2	1	3	0
4	1	1	2	1	0
5	5	0	0	5	0
> 0	11	4	5	11	10
> 3	6	1	2	6	0

Tab. 3

Frequencies of the injury levels 1-5 according to MAIS and Regional AIS.

The list of the individual injuries assessed according to AIS can be found in tab. 3. No PMTO remained unscathed. In six cases the degree of injury had reached the level of fatal injury (AIS > 3). With one exception the sole or partial reason for the overall injury level was traumatization of the spine.

Dehiscences of the dorsum of the nose and the middle of the forehead provided recurrent findings of head injury. In three cases these were combined with fractures of the nasal bone (open nasal bone fracture = AIS 2).

When the side of the helmet was adjusted at the upper visor, these injuries could be reduced and finally completely eradicated in test 11.

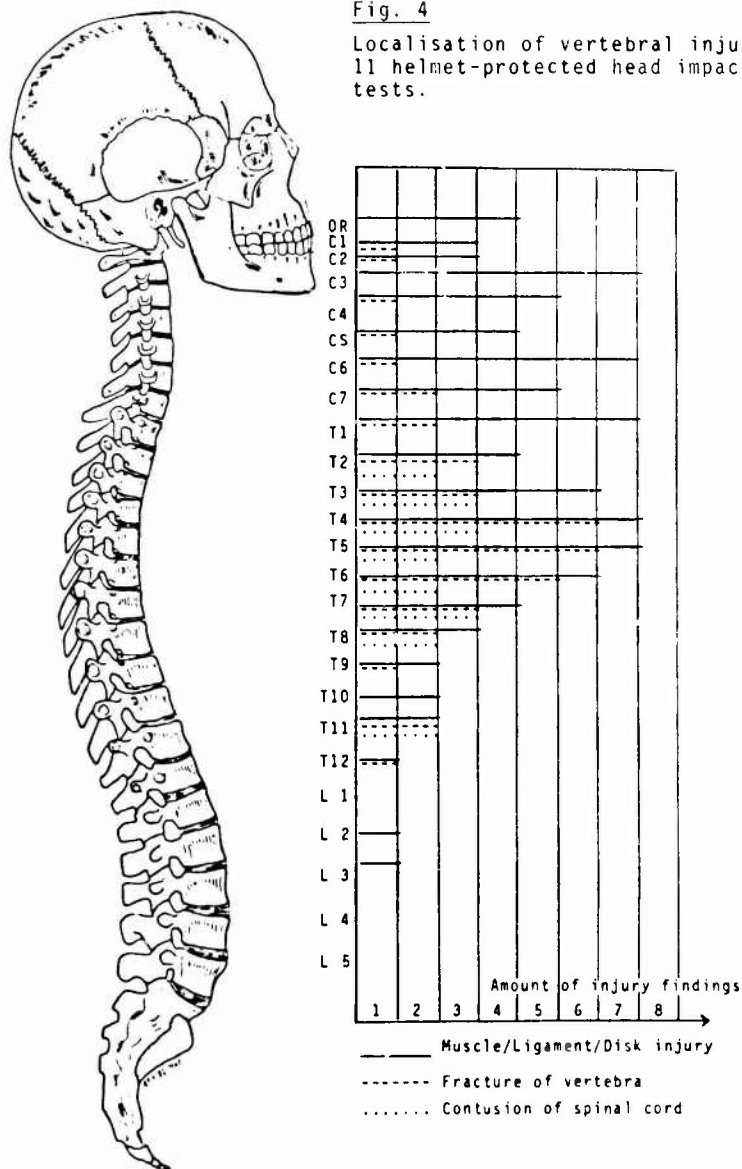
Fractures of the neurocranium were found in two cases only: in both cases these were merely discreet, minor fractures of the fossa crani anterior, less than 1 mm thick in the areas of the affected structures. (V 1: planum ethmoidale; V 3: planum sphenoidale).

In the AIS scaling of injuries these injuries as fractures of the skull base are in fact to be attributed grade AIS 3 since such fractures are qualified as serious damage to health due to the direct danger of the formation of a fluid fistula or ascending infection.

It should nevertheless be pointed out that these fractures are rarely detectable by clinical x-ray. Despite knowledge of the injuries, in the x-rays of the PMTOs the fractures could not be detected in the main axes in a second examination following the autopsy.

Fig. 4

Localisation of vertebral injuries.  
11 helmet-protected head impact  
tests.



The absence of patho-anatomically detectable cerebral lesions on the PMTO in these dynamic tests was surprising. Precisely in the case of PMTOs, however, this must be interpreted with some caution: in view of the amplitude and duration of the decelerations measured on the head, it can by no means be ruled out that considerable malfunctioning of the central nervous system - at least concussion, probably combined with contusion, intracerebral bleeding and cerebral oedema - would also have been observed at the same loading level in the case of a living being. Since these conditions are linked to circulation and the metabolism, it is difficult to simulate them on a PMTO (NAHUM 1976, FAYON, 1976, WARD 1980).

Rupture of the right anterior bridging vein (vena cerebri anterior superior), along with longitudinal ruptures of the anterior falx cerebri, was ascertained in one case only (V 7).

Spinal injuries, indicative of the overall degree of injury, appeared in the form of usually extreme comminuted fractures of the vertebra with compression of the spinal cord in the upper and central thoracic part of the spine.

Fig. 4 gives an outline of the localisation of segmental injuries in the essential injury findings. Tab. 4 gives an analysis of the frequencies of multisegmental injuries affected in each case. In connection with this table it should be emphasised that the bony injuries and the lesions of the ligamentous apparatus usually affected more than one segment, e.g. in two cases (V 8, V 9) injury to the ligaments occurred in 10 segments. In one case (V 7) the spinal medulla was compressed over 5 thoracic segments.

Injured structure	Amount of injured segments										
	0	1	2	3	4	5	6	7	8	9	10
Ligaments	1		2	2	1	1		1		1	2
Disks	2			1	2	3		1	1	1	
Vertebral bodies	2		4	3	2						
Vertebral processus	2	1	2	3	2		1				
Spinal cord	5		3	1		1	1				
Destabilisation	4	4	2	1							

Tabl. 4

Analysis of the injury pattern: Frequency of multisegmental spine injuries

Six cases showed uni- or multisegmental destabilisations and dislocations along with a number of spinal fractures. Most of these fractures of the thoracic vertebral column were in the form of extensive compression fractures with edge snapping towards the spinal channel, combined with serious damage to the neighbouring intravertebral disks and fractures of the accessory archs and joints. Fig. 5 shows a typical example of this combination of extensive injury to the central area of the thoracic spinal column.

Compared to the thoracic vertebral column, injuries detected in the cervical spine were of secondary importance. No morphological lesion of the cervical medulla could be detected and there were no signs of dislocation or destabilisation of the intervertebral motor segments.

The vertebra fractures detected - e.g. segment C 1 in V 5 - were in the form of a non-dislocated fracture of the anterior arch of the atlas. Fractures to vertebra C 4-C 7 were in the form of minor fractures of the lower edges of the vertebral body. The width of the vertebral body was not compressed and there were no further fractures of vertebral processes.

Injuries to the vertebral disks and ligamentous apparatus were roughly as frequent as those in the thoracic spinal column. However these various findings were generally not particularly extensive. Examples found were minor bleeding and cracking but there was no total collapse of the vertebral disks. One exception was the anterior longitudinal ligament, broken in 4 cases, mostly in several neck segments.

Injuries to the thoracic skeleton had occurred in five cases. Three of these were multiple rib fractures which had led to a destabilisation of the thorax (AIS 4). With 27 rib fractures, V 7 showed the most extensive thorax traumatisation. Rib fractures, when they occurred, were always paravertebral, in close vicinity to the vertebral segments, also seriously damaged. In addition however there were further fractures of the same and other ribs in the axillary line. The paravertebral fractures frequently took the form of torsion fractures.

It is to be assumed that the high number of rib fractures in V 7 was due to the age of this particular PMTO. At 41 it was the oldest of all the PMTOs tested. This case also showed the highest number of vertebral fractures: 4. No injury to the organs in the thoracic area could be detected in any test case.

#### PATHOMECHANICS of the spine injuries

It can be concluded from the intersegmental combination of injuries to the affected anatomic spinal structures that the cervical spine was subjected to a retroflective load and the thoracic vertebral column to a high hyperflective load in the sense of hyperkyphosis.

We can draw this conclusion, confirmed by kinematic analysis of the high-speed kinematography, on the basis of the fact that on the cervical spine the structures lying in a ventral position to the flexion axis failed by fracture as a result of stress-loading. On the other hand, on the thoracic spinal column the dorsal ligamentous structures showed signs of stress-loading and the ventral bony structures showed signs of pressure-loading.

The localisation of the most serious injuries is given by the double-S-shape of the spine. The distribution of lesser injuries on the cervical spine and by far the most serious injuries on the thoracic vertebral column, must be explained by the geometrical position of the main axes of impact vis-à-vis the vertices of the physiological curvatures. When the PMTO is in starting position in the stretched position of the neck, this direction of impact varies only slightly from the z-axis of the cervical spine. On the thoracic vertebral column, however, a by far greater bending impact point is established due to the unequal distance between the impact axis and the vertex of the spinal column. This leads to an asymmetrical loading of the vertebral body which means that it is not hit in the direction of maximum load capacity.

Fig. 5

TYPICAL SPINE INJURY PATTERN, prepared according to the saw-cutting technique.



a) View of the central cut and both lateral cuts, injuries concentrated on 2nd thoracic segment.



b) Detail of left central cut: serious comminuted fractures of the 2nd thoracic vertebral body. Fracture of the lower edge of the 3rd thoracic vertebral body. Fracture of the upper surface of the 4th thoracic vertebral body. Excessive compression of the spinal cord. (3 segments) Dislocation of fractured pieces of the bone in the vertebral channel.



c) Contact x-ray of the left central cut (see b).

If we compare the decelerations measured on the spine and the head in z-direction, we can see that no appreciable contribution has been made towards energy reduction by the cervical spine interposed between the testing points, head and 1st thoracic vertebra. The thoracic spinal column, on the other hand, reduces the middle level of decelerations measured at T 1 up to test point T 12 by approximately a half.

With regard to the anatomical structures, this damping ability of the spine in the physiological area is essentially due to two factors: the material damping of the vertebral disks and the shape - adjusting damping of hyperkyphosis, affected in addition by the bony thorax.

In these injury-inducing loading tests the vertebra and ribs also contribute towards material damping when the bony structures fail by fracture.

For anatomical reasons - the horizontal arrangement of the side joints - the damping of the vertebral disks in the cervical spine is almost without effect since the side joints come to rest very quickly, passing on the impact force via bony structures with low compressive power. The loading level in the spinal column of the neck was obviously too low to permit failure of these bony structures.

When we consider that under axial compression loading of isolated cervical vertebrae the ultimate fracture loads are generally less than those found in the thoracic vertebral column, the apparently reverse observation in these tests can only be explained by the loading direction which coincides with the direction of the highest, i.e. axial, loading capacity on the cervical spine but which on the thoracic vertebral column has primarily a bending impact due to the considerable distance from the main loading axes.

## DISCUSSION

The aim of this study was to simulate traffic accidents close to reality. In this first series we therefore chose an effective impact speed between 32 km/h and 45 km/h and a fronto-occipital impact configuration. However in our accident investigations the injury patterns of apparently comparable types of accident were in fact seldom found. To explain this finding, it seems that we must take into consideration the fact that the total accident input energy was absorbed by one single impact of the body through the helmet-protected head. A distribution of the accident energy is rather given by different accident phases, in particular by considerable throwing ranges of the motorcyclist. On the other hand, the tests were conducted in such a way that as a result of the body being held in position by a support bloc, force induction was established. This was essentially axial and passed over the head into the spine. Of particular note in the injury pattern was the high level of traumatisation of the thoracic vertebral column. The skull and the upper cervical spine hereby remained either unscathed or with little injury. No ring-fractures on the base of the skull were detected although it can be assumed that impact intensity was sufficiently high to have produced such fractures. We are of the opinion that in view of the test facts given there are two possible explanations for the absence of these fractures:

- a) impact absorption caused by dissipation of energy by the helmet,
- b) failure of the thoracic vertebral column and the energy absorption caused thereby.

It appears necessary to carry out a reference test with P.TOs without helmet protection. This has so far not been possible. As a result of this test we expect to find serious impression fractures and/or skull-base ring fractures. The effect of these injuries on the bony part of the head also damps the head impact input. This damping effect is equal to, or even greater than that of the helmet. Although a safety helmet is able to protect skull and brain, the transduced impact input by the helmet-protected head seems to aggravate the injury level of the thoracic spine. This is a theoretical point for discussion.

The given impact velocity change  $\Delta v$  between 32 km/h and 45 km/h produced maximum decelerations on the head in x-direction of an average value of 136 g and in z-direction of an average value of 105 g. As the amplifiers of the helmet accelerometers run into limitation we have had to reconstruct the peak-values. The reconstructed values of the outer shell of helmet was found to be between 550 g and 700 g.

The accelerometers on the vertebral column for the first thoracic vertebra T 1 gave peak-values similar to those measured on the head in x-direction: the average peak-value was 146 g. The result of measuring on the lower spine T 12 finally gave an average peak level of 77 g. The interpretation of the relationship of the upper and lower spine g-values is given under point "PATHOMECHANICS". The measurement of the epidural intracranial brain-pressure was undertaken with different pressure-transducers, but so far the results are not sure enough to be published. Further tests are required.

Whereas the outer polycarbonate shell showed no breakages or relevant plastic deformations in any test case, the inner polystyrol damping liner was plastically compressed at the region of impact between 19,3 and 30,0 % (average of liner width: 26 mm) and broke at this point.

The whole compression on the damping liner (both plastic and elastic deformation) was observed at a level of between 50 and 60 %. This value appears to be too low, related to the effective impact velocity and the acceleration-time-history of head acceleration. We are convinced that the material so far used for safety helmet liners must be replaced by a damping or energy-absorbing material which could work much more effectively, when adjusted to the technic-mechanical properties of head and brain. By further investigation of injury patterns and mechanisms under helmet protection, we must in our work therefore draw more conclusions concerning not only the outer construction design recommendations (accident "input") but also the inner construction design recommendations (technic-mechanical) properties of the head-brain and neck system) of a safety-helmet. Furthermore we want to verify whether the Heidelberg SAFETY HELMET PROTECTION CRITERION

$$\eta_{SH} = \frac{HIC_{(-SH)} - HIC_{(+SH)}}{HIC_{(-SH)}}$$

(whereby HIC (+/-SH) means the Head Injury Criterion number with/without safety-helmet) is adequate as a biomechanical helmet effectivity value.

Acknowledgement

This project is being sponsored in part by the European Community, Brussels and the Bundesanstalt für Straßenwesen, Cologne/Germany.

Authors

Priv.-Doz. Dr. med. R. Mattern  
Dipl. Ingenieur F. Schueler  
Prof. Dr. med. Gg. Schmidt

Institut für Rechtsmedizin  
im Klinikum der Universität Heidelberg  
Postfach 103069, D-6900 Heidelberg

## REFERENCES

- Aldman, B.  
Lundell, B.  
Thorngren, L. Non-perpendicular Impacts - An Experimental Study on crash-helmets. Proc. of the Meeting on Biomechanics of Injury to pedestrian, cyclists and motorcyclists, (IRC0BI Amsterdam) S. 322-340 (1976)
- AIS The Abbreviated Injury Scale 1980 Revision. American Association for Automotive Medicine, Morton, Grove, Illinois, 60 053 USA
- Barz, J.  
Mattern, R. Angiographische Untersuchungen an Leichen zur Diagnose von Gefäßverletzungen, Beiträge zur Gerichtl. Medizin, 33, 298 (1975)
- Fayon, A.  
Tarrière, C.  
Walfish, G.  
Got, C. Performance of helmets and contribution to the definition of the tolerances of human head to impact. Proc. of the Meeting on Biomechanics of Injury to pedestrian, cyclists and motorcyclists (IRC0BI Amsterdam), S. 291-300 (1976)
- Feldkamp, G.  
Prall, W.D.  
Bühler, E.  
Junghanns, K. Unfälle m. motorisierten Zweirädern - Epidemiologie, Klinik, Schutzmöglichkeiten -. Eine retrospektive u. prospektive Studie Unfallheilkunde 80, 1-19 (1977)
- Hurt, jr., H.H.  
Ouellet, J.V.  
Wagar, I.J. Effectiveness of motorcycle safety helmets and protective clothing. American Association for Automotive Medicine, S. 223-235 (1981)
- Kallieris, D. Eine Fallgewichtbeschleunigungsanlage zur Simulation von Aufprallunfällen - Prinzip u. Arbeitsweise - Z. Rechtsmed. 74, 25-30 (1974)
- Langwieder, K. Collision characteristics and injuries to motorcyclists and moped drivers. Proc. of the 21th Stapp Car Crash Conf., S. 261-301 (1977)
- Mattern, R.  
Schmidt, Gg.  
Kallieris, D. Dissection technique, description of injuries, evaluation of injuries, preparation for the loading test and selection criteria of the test subjects. Fifth Annual International Workshop on Human Subjects for Biomechanical Research, New Orleans, Louisiana 28(1977)
- Mattern R. Wirbelsäulenverletzungen angegurteter Fahrzeuginsassen bei Frontalkollisionen - Auswertungen von 228 Modellversuchen nach postmortalen Traumatisierungen. Med. Habilitationsschrift, 246 S., Heidelberg 1980
- Nahum, A.  
Ward, C.  
Schneider, D.  
Raasch, F.  
Adams, S. A Study of Impacts to the Lateral protected and unprotected head. Proc. of the 25th Stapp Car Crash Conf., S. 241-268 (1981)
- Nahum, A.  
Smith, R.W. An experimental model for closed head impact injury. Proc. of 20th Stapp Car Crash Conf., S. 785-814 (1976)
- Otte, D.  
Suren, E. Analyse motorisierter Zweiradunfälle. Der Verkehrsunfall, Heft 7/8, 1949-153 (1979)
- Otte D. A review of different kinematic forms in two-wheel accidents - their influence on effectiveness of protective measures. Proc. of the 24th Stapp Car Crash Conf., S. 561-605 (1980)
- Schmidt, Gg.  
Kallieris, D.  
Barz, J.  
Mattern, R.  
Schulz, F. Belastbarkeitsgrenze und Verletzungsmechanik des angegurteten Fahrzeuginsassen. Schriftenreihe d. Forschungsvereinigung Automobiltechnik eV (FAT) Nr. 6, 144 S. (1978).
- Schmidt, Gg.  
Kallieris, D.  
Barz, J.  
Mattern, R.  
Schulz, F.  
Schueler, F. Belastbarkeitsgrenzen des angegurteten Fahrzeuginsassen bei der Frontalkollision. Schriftenreihe d. Forschungsvereinigung Automobiltechnik eV. (FAT) Nr. 15, 113 S. (1981)
- Schueler F. et al. Optimierung des passiven Unfallschutzes für motorisierte Zweiradfahrer - Analyse v. Verkehrsunfällen. FP 7806/6 im Auftrag der Bundesanstalt für Straßenwesen, Köln.
- Ward, C.  
Chan, M.  
Nahmu, A. Intracranial pressure - A Brain injury criterion. Proc. of the 24th Stapp Car Crash Conf., S 163-185 (1980)



## DISCUSSION

DR. GENNARELLI (USA)

Please discuss the validity of the biomechanics of your neck-torso angulation upon impact. Are you considering different angulations of the neck-torso to get more cervical injuries which would be expected?

AUTHOR'S REPLY

The introduced force is mostly parallel to the axis whereas the curvature of the thoracic spine leads to bending forces and these bending forces lead to the failure and/or fractures of this region.

DR. GENNARELLI (USA)

From a clinical point of view, fractures in the middle of the thoracic spine are very unusual for vertex or forehead impacts compared to the frequency of fractures in the cervical spine.

AUTHOR'S REPLY

Do you relate your words to helmeted heads? I feel that the helmet impact is even less likely to cause injury in the thoracic spine.

UNIDENTIFIED QUESTIONER

In our studies of a similar nature, I can only think of two reported injuries (fractures) to the thoracic spine; on the whole we're not seeing injuries of that type so low down the spine.

DR. SANCES (USA)

It appeared in your high speed movie that the body was allowed to follow-up while the head was essentially pocketed and this allowed the thoracic column to buckle. Could this account for your injuries?

AUTHOR'S REPLY

Yes. In our opinion the buckling of the thoracic vertebral column seems to be the main injury mechanism for the multi-segmental fractures of the vertebral bodies.

DR. SANCES (USA)

Do you think the head was allowed to slide off because of the helmet, and so that would reduce the pressure on the cervical spine?

AUTHOR'S REPLY

We have to say that the helmet was very well fitted and so far the high speed movie didn't show relative movement of helmet to head.

DR. VON GIERKE (USA) COMMENT

But certainly a slight change in the neck curvature would change the results considerably, and it looks to me that a live subject might be more inclined to bend the head and try to look forward; thus, you would have a considerable higher load on the cervical spine.

FRISCH (USA) COMMENT

I noticed that you had a full helmet and from the film it appeared that the helmet pushed against the shoulder area. Did you, in fact, exhibit or see any damage to the shoulder area?

AUTHOR'S REPLY

No. In general, we did not see any damage to the shoulder area.

NEWMAN (CA)

Forgive me if I didn't quite catch what you said, but what was the nature and extent of brain injury sustained in that particular test?

AUTHOR'S REPLY

We didn't see injury to the brain, but in the case of PMTO's, however, it can by no means be ruled out that concussion, probably combined with contusion, intracerebral bleeding and oedema would also have been observed at the same loading level of a living being. Since these conditions are linked to circulation and metabolism, it is difficult to simulate them on a PMTO.

DR. VON GIERKE (USA)

Did you in any way fix or enforce the neck?

AUTHOR'S REPLY

No; however, we held the head into position until the moment of impact against the wall, the head was then free of every supporting system.

DR. VON GIERKE (USA)

And you did not try different neck positions?

AUTHOR'S REPLY

No, but we did try to position the head so that each impact was reproducible.

DR. VON GIERKE (USA)

I assume this (head position) will be the main difference to the cause of the injuries, the slight differences of the head alignment with respect to the thoracic spine.

Temporal Characteristics of Translational  
Acceleration in the Prediction of Helmeted Head Injury

James A. Newman, Ph.D., P. Eng.,  
Director of Engineering  
Biokinetics and Associates Ltd.  
1481 Cyrville Road  
Ottawa, Ontario  
Canada  
K1B 3L7

Impact performance criteria employed in the evaluation of protective headgear often consider the temporal characteristics of the translational acceleration induced in the helmeted head-form during impact. These implicit criteria may appear as limits on the time during which the test headform acceleration is allowed to exceed certain values, or may be inherent in the pass/fail criterion itself.

The present study examines the significance of time as a parameter in the prediction of head injury likelihood or severity. It is shown that since the temporal characteristics of the acceleration waveform is simply a reflection of the mechanical characteristics of the headform/helmet assembly it bears only a trivial relation to the input forcing function and thus is generally uncorrelatable to head injury severity.

It is concluded therefore that upper limits on translational acceleration alone, though not without certain restrictions, constitutes a sufficient criteria for evaluating helmet performance. The use of a time parameter is shown to be unsupportable and can lead to unnecessarily complex criteria and inferior helmet performance.

#### INTRODUCTION

It has long been regarded that the temporal characteristics of the translational acceleration imparted to a head (helmeted or otherwise) is related to the nature and severity of the accompanying head injury. That is, if a head undergoes an acceleration, the resulting head injury is somehow related to the manner by which this acceleration varies in time. The literature abounds with examples wherein reference is made to how head injury depends upon things such as the time duration of the acceleration pulse, rate of onset of acceleration, etc. (1-4)\*. Though less extensively studied, similar relationships have been proposed in a rotational acceleration field (5, 6). These latter considerations shall not be dwelt upon here. However, the thrust of the following remarks are generally applicable to both types of motion.

Notwithstanding the title of this symposium, it is the author's contention that impact injuries to the head are not caused by acceleration. Rather, impact injury and the accompanying acceleration of the head are both responses to a particular input or forcing function. This may appear to be a rather mundane point. However, it is very significant when attempting to quantify any relationship between injury and acceleration. Whatever  $a(t)$  is produced in a head impact, it is merely a kinematic response. A response that is dictated by the mechanical characteristics of the head/helmet and of the impact object and by all the other external motion limiting constraints.

Brain injury is due to the disturbance or disruption of the central nervous system caused by local deformation induced by physical stresses (7). Stress waves in the brain may be induced by skull deformation and/or by skull acceleration. In the absence of significant skull deformation, brain stresses are induced solely by inertial effects. These can be characterized by the acceleration of the skull (assumed to be rigid). Given the same set of motion limiting constraints, it is generally to be expected that in the latter case, higher levels of head injury will be associated with higher levels of acceleration which reflect higher imposed forces.

Given different motion limiting features, such as those that may be associated with direct blows to different parts of the head,\*\* the same head injury level may well be associated with entirely different levels of acceleration. Since  $a(t)$  merely provides a measure of the change in velocity of the head associated with the impact, it cannot, by itself, provide any information about the magnitude of the impact phenomenon (i.e., the induced stresses). For example, a firearms projectile or a blunt impact to the top of

\* Numbers in parantheses designate references at end of paper.

\*\* Thereby changing the motion-limiting effects of the neck.

the head will both produce head injuries. In neither case will the head be caused to accelerate substantially. The injury mechanism in these situations is not related to inertial loading but rather to stresses induced by deformation (and in the extreme; permanent physical disruption) of tissue.

Hence, one might expect to be able to correlate head injury to acceleration only when -

1. The stress (and hence injury)-inducing mechanism is dominantly of an inertial characteristic.
2. Skull deformation is small, and
3. Head motion limiting features are controlled.

If all of these conditions are fulfilled (and in many cases of helmeted or other padded impacts to the front, rear or side of the head, they are approximated), there remains only the question as to the relative significance of the head (or test headform) acceleration waveform shape (i.e.,  $a(t)$ ).

#### TEST METHODS

The usual approach to evaluating the impact protection afforded by a helmet is as follows: The helmet to be assessed is placed upon a headform of specific physical and geometric properties. The entire headform and the supporting assembly has some fixed mass. The helmeted headform is allowed to fall in guided free-fall from some pre-determined height onto some pre-determined surface. These kinds of controls should provide the necessary basis for measuring the relative performance of different helmet systems. Without such controls, the observation of a kinematic parameter alone (i.e.,  $a(t)$ ) would be insufficient to judge the helmet's performance. However, even the mechanical characteristics of the headform support assembly will affect the shape of the  $a(t)$  curve and different support structures can produce substantially different responses for identical impact circumstances (8). Since one cannot eliminate entirely the effects of the support structure, one has at best a tool to measure relative helmet performance only.

Similar points are relevant in, for example, the testing of automotive dashboards (19). Again the mechanical structure of the test device is fixed, as are the kinematic characteristics of the impact. The resulting  $a(t)$  for different dashboards will provide a relative measure of impact performance. If the mechanical characteristics of the test equipment are changed, then the apparent performance of the dashboard will change.

In any case, the observed  $a(t)$  is no more than an expression of the rate of which head velocity is changing during impact. The principal issue here then is; for a given total velocity change, within a given time interval, does it matter precisely how that velocity change is achieved in terms of the expected head injury (or the inferred protective capacity of the system). That is, should the shape of the acceleration time curve be incorporated into the failure criterion for the system and if so, how?

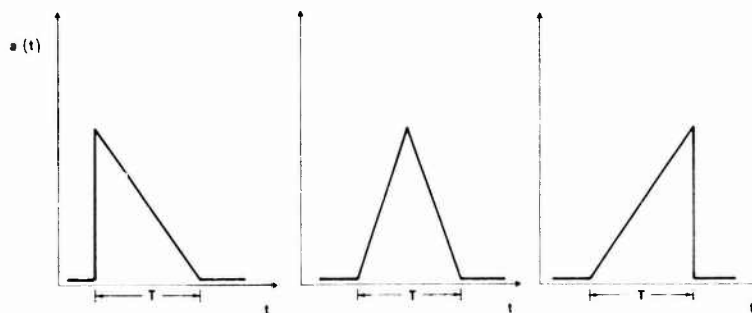


Figure 1: Triangular Acceleration Pulses

A simple illustrative example of these considerations is shown in Figure 1. Each of these hypothetical  $a(t)$ 's corresponds to the same velocity change. Each has the same maximum acceleration, same average acceleration  $\bar{a}$  and the same pulse duration  $T$ . Most head injury criteria would regard these pulses to be of equal severity. However, as first discussed by Brinn and Staffield (9), "Conventional impact analysis would demonstrate that they would each have a different effect on typical spring-mass systems" ... and thus similar effects on the human head. The fallacy of their approach is in the assumption that these acceleration pulses are inputs to the system rather than responses by it. Their system is assumed to be deformable and their measure of severity is the amount of deformation. Hence the conclusions are not applicable to inertial loading.

Before proceeding further with these kinds of considerations, a brief review of head injury criteria is appropriate.

# FAILURE CRITERIA

Most head injury models have an implicit if not explicit functional dependence on time (9-15). Included among these models are the Wayne State Tolerance Curve - WST (10) and the JARI Head Injury Tolerance Curve - JHTC (11). Others include the lumped-parameter models of Brinn and Staffield (9), Slattenscheck, et al (12), Fan (13) and the Maximum Strain Criteria - MSC of Stalnaker, et al (14). The most recent head injury model is the finite element brain model of Ward and Co-workers (15). Excellent reviews of these various models have been published elsewhere and need not be repeated here (15, 16).

Time  $t$  may occur in the failure criteria of these models usually in one of three ways:

1. Given a certain average acceleration during the impact pulse, the total time duration of the pulse may not exceed some value. The forebearer of most head injury models, the Wayne State Tolerance Curve (10) was initially intended to provide such a dependence based on this criteria. The recent work of Ono, et al (11), has provided similar correlations between average acceleration and time duration (JHTC). Such correlations have no explicit dependence on acceleration waveform shape. It can be inferred from such curves only that the total time during which the head accelerates is a factor in the resulting head injury. However, average acceleration vs time duration criteria have never been formally invoked. In fact, such curves provide no more than a limiting change in velocity that the head may undergo during a certain time interval. Within the range of 1 to 10 msec however, this velocity change is not greatly sensitive to time duration. Figure 2 illustrates the WST, the JHTC and a line of constant velocity change equal to approximately 5.5 m/sec. In light of the degree of experimental scatter associated with the WST and the JHTC, time duration dependence is not clear from these curves.

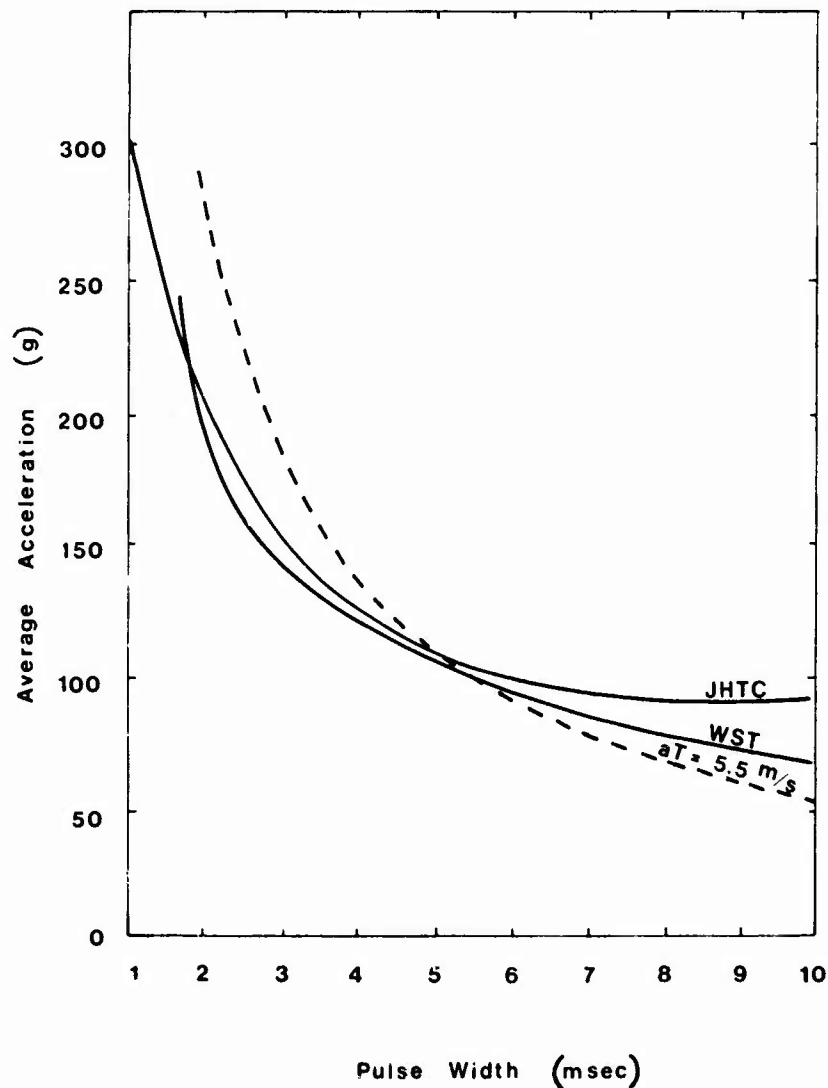


Figure 2: Comparison of the WST, the JHTC and a Fixed Change of Velocity

Since most other models are dependent on waveform shape, comparisons between the WST (and JHTC) and the predictions of these models can only be made for specific assumed  $a(t)$ 's. Such a comparison for several different head injury models for a triangular acceleration waveform shape is provided later on.

2. Given a certain  $a(t)$ , the time during which 'a' exceeds a limiting value may not be exceeded. Examples of this are MVSS 201 and 218 (17, 18). The respective criteria are:

- a) MVSS 201: The deceleration of the test headform shall not exceed 80g continuously for more than 3 milliseconds.
- b) MVSS 218:
  - i) Peak acceleration shall not exceed 400g.
  - ii) Acceleration in excess of 200g shall not exceed a cumulative duration of 2.0 milliseconds, and,
  - iii) Acceleration in excess of 150g shall not exceed a cumulative duration of 4.0 milliseconds.

In the case of MVSS 201, the specification is intended to restrict the bulk of the deceleration below 80g while allowing brief excursions above it. The rationale for the 3ms exemption appears to be in the belief that the head has a much higher tolerance to very short acceleration pulses than to long ones (see Figure 2). However, extracting a portion of a pulse (the part over 80g's) and applying the perceived rules applicable to pulses of short total duration is questionable.

With respect to MVSS 218, the purpose of the specifications are not absolutely clear. Limiting peak headform acceleration to 400g's is in effect limiting the peak force that can be applied through a helmet to approximately 4400 lb. (The test headform weighs nominally 11 lbs). The imposition of time-duration limits at the 200 and 150g level have the effect of "shaping" the acceleration waveform to some presumably desirable shape. Whether or not this is achieved in practice is debatable for it is certainly possible to "tailor" the headform response to meet the standard without necessarily providing a better helmet.\*

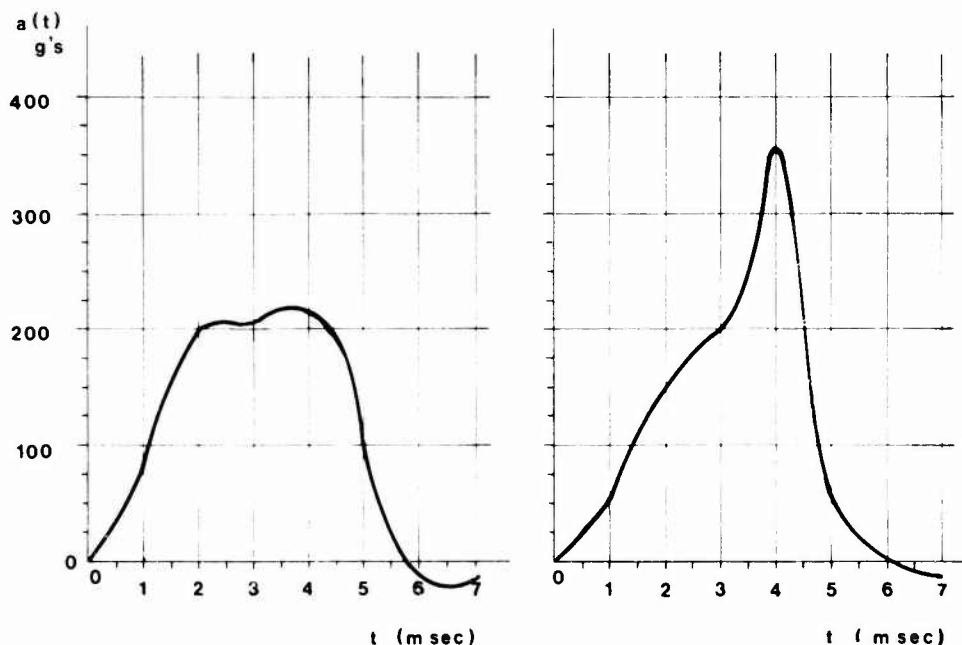


Figure 3: Helmeted Headform Response:  
 a) MVSS 218 Time Duration Failure  
 b) MVSS 218 Passing Acceleration Trace

Figure 3 illustrates two acceleration waveforms produced in random helmet testing. Both correspond to the same impact energy. The helmet in 3(a) would fail according to the above criteria while that of 3(b) would pass. This result can only be acceptable if the  $a(t)$  of 3(a) constitutes a greater head injury threat than that of 3(b).

\* It should be noted that simply limiting headforms acceleration to 80g's in MVSS 201 and to 150g's in MVSS 218 would obviate the need to invoke time-duration criteria per se.

The sharply rising peak of 3(b) could be interpreted as a spurious "spike" in the trace and hence disregarded. It is however an actual response of a helmet undergoing incipient bottoming. Whether or not this necessarily constitutes a more serious head injury threat is discussed further on.

3. A third form of  $a(t)$  and  $t$  correlation to head injury severity is that the value of some functional relationship between the two not be exceeded. Examples of this are the Gadd Severity Index - GSI (19) and the Head Injury Criteria - HIC (20). These are expressed as follows:-

$$GSI = \int a(t)^{2.5} dt \leq 1,000$$

$$HIC = \left( \frac{1}{t_2 - t_1} \int_{t_1}^{t_2} a(t) dt \right)^{2.5} (t_2 - t_1) \leq 1,000$$

where  $t_1$  and  $t_2$  are chosen to maximize HIC

The GSI is currently employed as the failure criterion of the NOCSAE standard for football helmets (21) (though the failure limit has been set at 1500). The HIC is referenced in MVSS 208 for head injury protection in automotive crash testing (22).

Both the GSI and the HIC heavily weigh the acceleration (by the 2.5 power) and thus both would result in higher values for the  $a(t)$  of Figure 3(b) than for 3(a). The higher these values, the more likely is it that the failure criterion would be exceeded and hence both would appear to identify the waveform shape of Figure 3(b) as being the greater head injury hazard. However, from a fundamental point of view, it is not clear that this conclusion is necessarily valid; for the GSI and the HIC suffer from serious theoretical flaws (23, 24). Some independent assessment of waveform shape is required.

#### FINITE ELEMENT BRAIN MODEL

The Ward brain model (15) can be used to simulate the response of the brain to dynamic loading. Employing a finite element structural analysis, the model can predict, for a prescribed skull acceleration, the pressure distribution, stresses and strains within the cranial cavity. The model must generally accept the approximation that the skull be rigid. Hence it is especially suitable for inertial loading or for impacts to a helmeted head. (Skull deformation in the latter case is significant only in cases of severe overloading of the helmet).

An essential postulate of the model, one which has some experimental validation (25), is that brain injury is directly related to the peak intracranial pressure. Moderate brain injury has been correlated to a peak pressure of 24 psi. Severe injury occurs if peak pressure exceeds 35 psi. No suggestion has been made that the time during which the pressure exceeds these (or any other) values has any bearing on the head injury severity.

For purposes solely of comparing the predicted  $\bar{a}$  vs  $T$  of the finite element model to those of other models, Ward has exercised the model for a series of triangular acceleration pulses each producing the same peak intracranial pressure of 24 psi. These predictions (labelled Ward MI) along with those of the HIC, SI, WST, JHTC and the MSC, are shown in Figure 4. Detailed discussions of the differences in the various predictions have been provided by Ward (25).

What she has not pointed out however, are the reasons for these differences. They presumably must lie in the different predictive capabilities of the various models. Such extraordinary variation in predictions of the same phenomenon, i.e., head injury, can only be explained by what must be termed inaccuracies in the models. Given an essentially triangular acceleration pulse, it is simply not possible to determine from all of these models, a tolerable time duration for a given average acceleration. Therefore, it seems highly unlikely that one could rely on any head injury criterion which invokes a functional relation between  $a(t)$  and  $t$ .

Every model does however have one common feature. For any given time duration, head injury severity or likelihood increases with average or peak acceleration. The "acceptable" performance of Figure 3(b) will in fact correspond to substantially higher intracranial pressures than the "failure" of Figure 3(a). Hence in the final analysis, the only currently meaningful criterion for translational helmeted head impact injury appears to be simply that of peak acceleration.

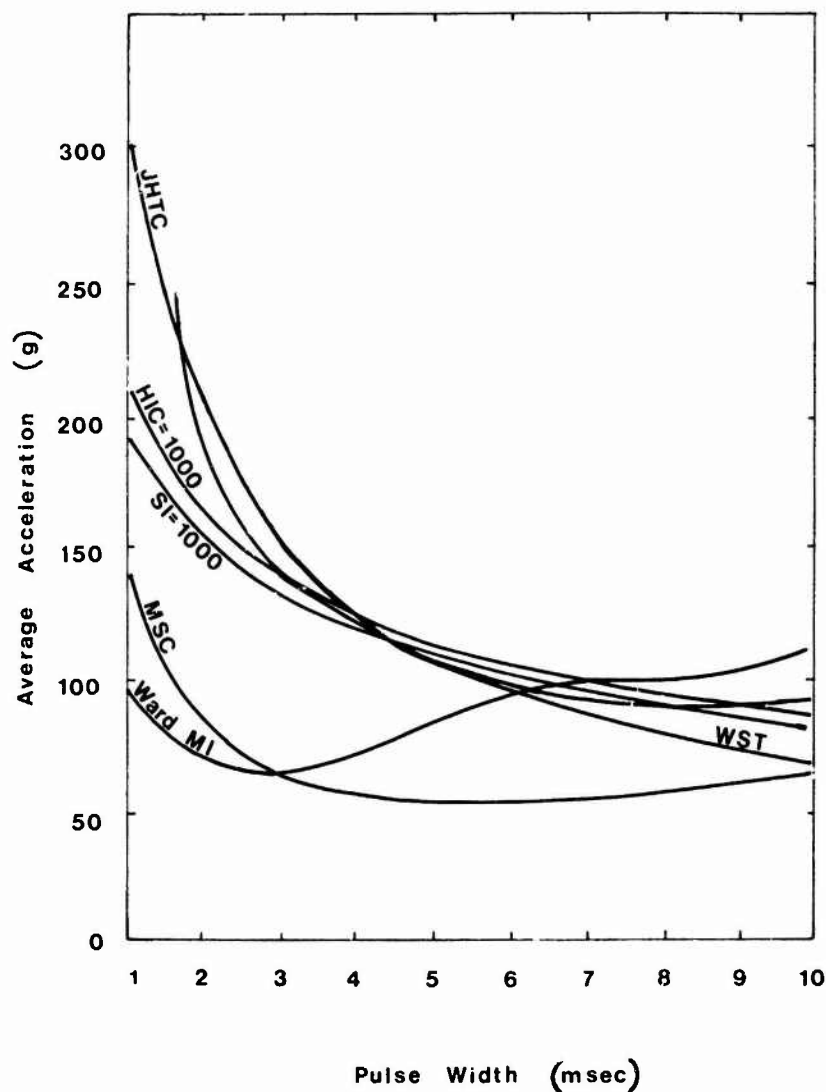


Figure 4: Tolerance Boundary Predictions of Various Head Injury Models

#### CONCLUSIONS

Given the present state-of-knowledge of head injury mechanisms of head injury models and of helmet test techniques, it is not possible to assign any special significance to the details of the manner by which headform translational acceleration varies with time. The safest, most reasonable approach to assessing helmet impact performance is to monitor the peak headform acceleration and to take whatever steps are necessary to minimize that acceleration.

#### REFERENCES

1. A.H.S. Holbourne, "Mechanics of the Head Injury", Lancet, Vol. 2., No. 438, October, 1943.
2. J.P. Stapp, "Human Exposures to Linear Deceleration", AF Tech. Rep. No. 5915, No. 2, Wright-Patterson AFB, December, 1951.
3. V.R. Hodgson, and L.M. Thomas, "Effect of Long-Duration Impact on Head", SAE Paper No. 720956, Proceedings of the Fourteenth Stapp Car Crash Conference, November, 1972.
4. A.N. Mucciardi, J.D. Sanders, and R.H. Eppinger, "Prediction of Brain Injury Measures from Head Motion Parameters", SAE Paper No. 770923, Proceedings of the Twenty-First Stapp Car Crash Conference, October, 1977.



5. A.K. Ommaya, and A.E. Hirsch, "Tolerances for Cerebral Concussion from Head Impact and Whiplash in Primates", *Journal of Biomechanics*, Volume 4, No. 13, 1971.
6. B. Aldman, B. Lundell, and L. Thorngren, "Non-Perpendicular Impacts - An Experimental Study on Crash Helmets", *Proceedings of the International Research Committee on the Biokinetics of Impacts*, Amsterdam, September, 1976.
7. W. Goldsmith, "Some Aspects of Head and Neck Injury and Protection", *Progress in Biomechanics*, Sijthoff and Noordhoff, 1979.
8. G. Henderson, "Correlation Anomalies Between Helmet Drop-Test Systems", Report to the Safety Helmet Council of America, January 15, 1974.
9. J. Brinn and S.E. Staffield, "Evaluation of Impact Test Accelerations: A Damage Index for the Head and Torso", SAE Paper No. 700902, *Proceedings of the Fourteenth Stapp Car Crash Conference*, November, 1970.
10. E.S. Gurdjian, V.L. Roberts, and L.M. Thomas, "Tolerance Curves of Acceleration and Intracranial Pressure and Protective Index in Experimental Head Injury", *Journal of Trauma*, pg. 600, 1964.
11. K. Ono, A. Kikuchi, M. Nakamura, H. Kobayashi and N. Kanamura, "Human Head Tolerance to Sagittal Impact Reliable Estimation Deduced from Experimental Head Injury Using Subhuman Primates and Human Cadaver Skulls", SAE Paper No. 801303, *Proceedings of the Twenty-Fourth Stapp Car Crash Conference*, October, 1980.
12. A. Slattenscheck, W. Tauffkirchen, and G. Benedikter, "The Quantification of Internal Head Injury by Means of the Phantom Head and the Impact Assessment Methods", SAE Paper No. 710879, *Proceedings of the Fifteenth Stapp Car Crash Conference*, November, 1971.
13. W.R.S. Fan, "Internal Head Injury Assessment", *Proceedings of the Fifteenth Stapp Car Crash Conference*, pg. 645, 1971.
14. R.L. Stalnaker, J.H. McElhaney and V.L. Roberts, "MSC Tolerance Curves for Human Head Impacts", ASME Paper 71-WA/BHF-10, 1971.
15. A.M. Nahum, C. Ward, R. Smith and F. Raasch, "Intracranial Pressure Relationships in the Protected and Unprotected Head", SAE Paper No. 791024, *Proceedings of the Twenty-Third Stapp Car Crash Conference*, October, 1979.
16. J.W. Melvin, D. Mohan and R.L. Stalnaker, "Occupant Injury Assessment Criteria", SAE Paper No. 750914, Presented at the Automobile Engineering Meeting, Detroit, October, 1975.
17. CMVSS Part III, 200-201 Occupant Protection/Head Impact Area, November, 1979.
18. FMVSS No. 218, "Motorcycle Helmets", *Federal Register*, Volume 38, No. 160, August, 1973.
19. C.W. Gadd, "Use of a Weighted-Impulse Criterion for Estimating Injury Hazard", *Proceedings of the Tenth Stapp Car Crash Conference*, pg. 164, 1966.
20. J. Versace, "A Review of the Severity Index", *Proceedings of the Fifteenth Stapp Car Crash Conference*, pg. 771, 1971.
21. "Standard Method of Impact Test and Performance Requirements for Football Helmets", Prepared by the National Operating Committee on Standards for Athletic Equipment, Inc., September, 1973.
22. Department of Transportation NHTSA Docket Number 69-7; Notice 19, Occupant Crash Protection Head Injury Criterion S6.2 of MVSS 208.
23. J.A. Newman, "On the Use of the Head Injury Criterion (HIC) in Protective Headgear Evaluation", *Proceedings of the Nineteenth Stapp Car Crash Conference*, pp. 615-640, November, 1975.
24. J.A. Newman, "Head Injury Criteria in Automotive Crash Testing", *Proceedings of the Twenty-Fourth Stapp Car Crash Conference*, pp. 701-747, SAE Paper No. 801317, October, 1980.
25. C. Ward, M. Chan, and A. Nahum, "Intracranial Pressure - A Brain Injury Criterion", *Proceedings of the Twenty-Fourth Stapp Car Crash Conference*, pp. 161-185, SAE Paper No. 801304, October, 1980.

#### ACKNOWLEDGEMENTS

The author expresses his sincere thanks to Dr. Carley Ward, Biodynamics/Engineering, Inc., for her helpful assistance in setting up and running the finite element brain model. This study emanates from research conducted under contract to Transport Canada.

## DISCUSSION

WARD (USA)

Would you please comment on the rate of change of acceleration (jerk)?

## AUTHOR'S REPLY

The point is very well taken and I know precisely that of which you are speaking, but indeed the peak intracranial pressure is also a function of how quickly the curve is rising. Perhaps manufacturers and helmet testers should not only look at the peak  $g$ , but they should also look at how quickly that peak is achieved. There are other considerations which might become necessary to take into account. I'd rather not get into them at this point.

DR. GLAISTER (UK)

One of the factors that determines peak acceleration in helmet tests is the frequency response of the equipment used. I wonder if all laboratories have standardized on such equipment.

## AUTHOR'S REPLY

The precise acceleration-time behavior is dependent not only upon the helmet and the thing that it strikes, but the entire test apparatus to which this helmet is attached; the headform, and the structure to which the headform is attached, etc. In 1974, the Z-90 Committee in the United States did a round-robin test on a number of laboratories in the United States and Canada and found that because of specific and relatively subtle mechanical differences in test equipment, that indeed the changes, the differences in acceleration versus time, were quite remarkable.

DR. VON GIERKE (USA) COMMENT

I don't want to defend the HIC standards we have, but I would like to remind you that we had the same discussion at the Oporto meeting with respect to the full body response, and some of us felt when you have duration of impulse or acceleration, to the left-hand side somewhere the curve has to rise. This is just a fact of nature. It has to be proportioned to  $\Delta V$ , once you have an impulse shorter than the mechanical response of your system. There was a long debate at Oporto and you have several papers in this conference proceedings, and I think by this time that it is well accepted by the whole community (and we showed it in human experiments) that the human body can stand 400g and more when the pulse is short enough. I'm sure the same thing will apply to the skull as long as you don't break the skull. There is a good theoretical basis for the terminal shape of the Wayne State University curve, and I think we should not jump to the opposite and suddenly say constant acceleration is all we need. Somewhere in the short range, I am sure we have to allow the curve to rise and there is some justification, at least for the testing method, certainly not for the HIC and the overemphasis on the acceleration.

DR. PRIVITZER (USA)

In your slides comparing Dr. Ward's tolerance curve with previously developed curves, I was under the impression that Dr. Ward's curve was based on triangular acceleration profiles, thus exhibiting a characteristic "dip," while the other curves were based on primarily rectangular acceleration profiles, which exhibit an exponential increase in acceleration with decreasing duration times to the left of roughly one-half the fundamental period of the system. Did I understand this correctly?

## AUTHOR'S REPLY

In the slide to which you refer, the MSC, HIC, GSI and Ward model were all exercised with triangular acceleration pulses. The WST and JHIC are based on experimental data; the  $a(t)$  for each point on those curves being whatever they were. The Ward model has, however, been exercised for a variety of waveform shapes and it always possesses the characteristic "dip". Its position on an  $a-t$  plot would be different for different pulse shapes.

DR. GLAISTER (UK)

A further factor which determines the peak acceleration monitored during helmet testing is the frequency response at the measurement system. How well do you think that this is standardized between different test centers?

## AUTHOR'S REPLY

The frequency response of the measurement system can affect not only the peak acceleration but the entire shape of the  $a(t)$  curve. Both Irving and Henderson have undertaken to establish the effects of the variables at various test labs and have found they can be substantial. Even, however, if all test labs had equipment of the same frequency response, the precise nature of  $a(t)$  would be dependent upon the particular characteristics of the test equipment.

DR. THOMAS (USA)

The gentlemen who did the work on the comparison between laboratories was Marshal Irving from Dayton T. Brown Co. (Z90 Committee Consultant) and he came up in that process with a system for the comparison testing between laboratories which involved a particular elastomeric impact pad, which was used to compare the accelerometer response in the drop tests for helmets. The issue about the test criteria that you're talking about has involved helmet manufacturers for over 20 years; it is only a test criteria and not a design criteria. That test criteria used to its ultimate insanity can come up with some very peculiar helmets. The US Army has had bitter experience in this area. During the sixties a helmet grew to more than four pounds as a result of carrying these things too far. Although the helmet limited the acceleration applied to the man, it was rejected by the flyers due to operational suitability. The Army then went back to an efficiency criteria of how much energy absorption you can get within the ANSI standard per unit of weight of the helmet, which became an operating design criteria for the SPH-4 helmet.

AUTHOR'S REPLY

I do realize that there are very practical considerations with respect to design. The 1979 ANSI revision did do away with time duration criteria. The Snell Foundation and ISO Standard have also dropped the time requirement. To my knowledge, the only agency that still retains it is the US D.O.T. Standard. For a design point of view perhaps it's nice to have a helmet such as that.

# ETUDE EN REGIME IMPULSIONNEL ET "IN VIVO" DE LA TRANSMISSIBILITE DES DISQUES INTERVERTEBRAUX LOMBAIRES D'UN PRIMATE

Méd.Chef P.QUANDIEU \* D.èsSc. ; L.PELLIEUX\* Ing. ;  
B.GARNIER \*\* Ing. ; Méd.Chef P.BORREDON \* D.èsSc.  
Avec la participation de B.VALEZY\* ; B.PIEDECOCQ\* ;  
A.BRUNET \*

- \* Laboratoire Central de Biologie Aérospatiale  
Service de Biomécanique  
5bis, Avenue de la Porte de Sèvres  
75731 PARIS CEDEX 15 AIR (FRANCE)
- \*\* Société METRAVIB  
24bis, Chemin des Mouilles  
69130 ECULLY (FRANCE)

## RESUME

Par analogie avec les méthodes d'analyse du comportement des structures industrielles, les auteurs posent l'hypothèse selon laquelle la propagation des chocs et des vibrations dans la colonne vertébrale peut être appréhendée par la détermination de la fonction de transfert du disque intervertébral. Après avoir rappelé les définitions et les conditions d'utilisation de la fonction de transfert, ils exposent la méthode employée, le protocole retenu pour l'étude de la propagation des vibrations consécutives à un choc appliqué directement sur le sacrum d'un primate de faible poids. La linéarité de la réponse vertébrale est étudiée, les vitesses de groupe et de phase des ondes propagées sont calculées. Ce travail constitue le complément des travaux effectués antérieurement concernant le comportement discal étudié, in vivo et in situ, en régime vibratoire chez un animal chroniquement bioinstrumenté.

## INTRODUCTION

L'étude des effets des chocs et des vibrations mécaniques sur le corps humain conserve à ce jour toute son importance en physiologie et en ergonomie aéronautique. Cet intérêt lié à la lutte contre les nuisances se justifie tant au plan de la connaissance fondamentale des effets biologiques des chocs et des vibrations qu'en ce qui concerne ses nombreuses applications - médicales, ergonomiques, socio-économiques et industrielles - civiles et militaires.

Evoquons le cas d'un certain nombre de postes de travail rencontré en Aéronautique.

"Le problème de l'étude de l'effet des vibrations sur l'homme en milieu aéronautique ne diffère pas fondamentalement de la même étude en ergonomie générale... le pilote d'hélicoptère soumis aux vibrations engendrées essentiellement par le rotor de l'appareil et cela plusieurs dizaines d'heures par mois, pendant des années, pourra ressentir une fatigue diffuse avec baisse des performances et souvent raideur du rachis à la fin de chaque mission, puis à plus longue échéance une douleur permanente accompagnée d'une contracture de la musculature paravertébrale, de signes d'arthrose vertébrale et de troubles de la mobilité du rachis.

Le pilote d'hélicoptère ou d'avion soumis à de fortes turbulences, ou encore plus les pilotes d'avion de pénétration à grande vitesse et basse altitude seront soumis à un intense régime vibratoire de basse fréquence" : Auffret et Coll. (1)

La relation entre la survenue de lombalgies et l'activité trépidante est certaine. Malheureusement les données relatives à la biodynamique vertébrale sont encore très parcellaires. La connaissance des contraintes et des déformations subies par l'organisme est, sans nul doute, le premier pas vers une explication rationnelle (celle qui relie causes et conséquences) de la pathologie rhumatismale ou traumatique. Mais, parce que les propriétés les plus importantes de la colonne vertébrale sont essentiellement liées à ses caractéristiques fonctionnelles, il est indispensable, en biomécanique, d'en étudier ses spécifications dynamiques et non seulement cinématiques, statiques ou quasistatiques.

Lorsque la sollicitation mécanique (choc ou vibration entretenue) est transmise à un sujet par le siège sur lequel il est assis, une onde vibratoire se propage dans l'ensemble du corps. Dans la colonne vertébrale cette onde chemine depuis les vertèbres les plus basses (sacrolombaires) jusqu'aux vertèbres cervicales. Cette propagation intéresse forcément les disques intervertébraux. A long terme, les sollicitations auxquelles sont soumises les articulations discales provoquent l'apparition de troubles dont la compréhension impose la connaissance du comportement dynamique de l'organe : celle-ci peut être abordée par l'étude de la fonction de transfert discal.

## DEFINITION DE LA FONCTION DE TRANSFERT DU DISQUE INTERVERTEBRAL

Etudions la propagation d'une onde vibratoire  $e(t)$ , fonction du temps, entre deux vertèbres adjacentes. On peut dire que  $e(t)$  est un signal émis par la première vertèbre dite émettrice E :  $e(t)$  est donc le signal d'entrée dans le disque intervertébral. De la même façon, le signal reçu par la vertèbre adjacente ou réceptrice R est considéré comme le signal de sortie  $s(t)$  du disque intercalaire (figure 1).

Si le disque possède certaines propriétés, il peut être considéré comme un opérateur de convolution qui présente un comportement  $h(t)$ . Ceci signifie que la connaissance de  $e(t)$  et de  $h(t)$  permet de calculer  $s(t)$  grâce à une opération dite de convolution (notée \*)

$$s(t) = e(t) * h(t)$$

Mais les caractéristiques de transfert d'un opérateur sont toujours obtenues en fonction des grandeurs d'entrée  $e(t)$  et de sortie  $s(t)$ . Dans notre étude, ce que l'on se propose de définir c'est  $h(t)$ , caractéristique de transfert de l'opérateur discal.

Il s'ensuit pratiquement la nécessité de mesurer  $e(t)$ ,  $s(t)$  puis de calculer  $h(t)$  par l'intermédiaire d'une opération dite de déconvolution (notée  $\div$ ) cf. figure 2.

Traditionnellement les études de vibrations (réponses impulsionnelles ou entretenues) se réfèrent non à l'évolution du signal dans le temps mais à son contenu en fréquence. Les caractéristiques de trans-

fert sont alors analysées en utilisant la Transformée de Fourier ;  $h(t)$  dans le domaine des fréquences devient  $H(\omega)$ .

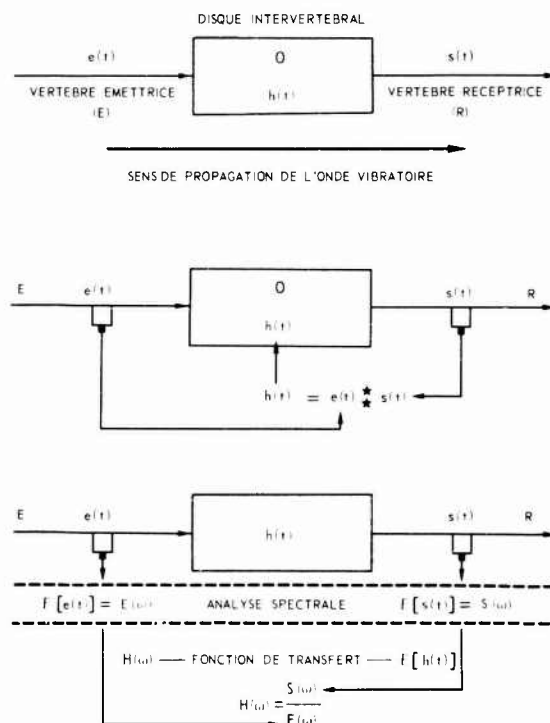


Fig.1-2-3 : Définition de la fonction de transfert du disque intervertébral



Fig. 4 : La fonction de transfert  $H(\omega)$  d'un disque intervertébral lombaire est calculée à partir de signaux délivrés par des accéléromètres fixés sur les corps des deux vertèbres situées de part et d'autre du disque

La fonction de transfert du disque  $H(\omega)$  est définie, comme le rapport de la Transformée de Fourier  $\mathcal{F}$  du signal de sortie  $\mathcal{F}(s(t))$  ou  $S(\omega)$  à la Transformée de Fourier du signal d'entrée  $\mathcal{F}(e(t))$  ou  $E(\omega)$  cf. figure 3.

Remarque : Cette définition est "stricte sensu" un abus de langage, car mathématiquement la fonction de transfert est définie exactement comme la Transformée de Laplace de la réponse du disque  $O$  à une impulsion appliquée en  $E$ .  $H(\omega)$  n'est donc pas vraiment la fonction de transfert du disque intervertébral ; il vaudrait mieux parler de comportement en fréquence. Cependant, l'appellation "fonction de transfert" est conservée dans la suite de l'étude car :

- La Transformée de Fourier n'est qu'un cas particulier de la Transformée de Laplace.
- Elle est passée dans le langage courant des ingénieurs ; ainsi les électroniciens associent le concept de fonction de transfert à la notion de filtre et les biomécaniciens ont de tout temps assimilé le disque intervertébral à un filtre mécanique.
- Enfin, de nombreux auteurs comme Max ( 2 ), Papoulis ( 3 ), Roddier ( 5 ), Roubine ( 6 ) ont apporté toutes les justifications nécessaires à l'utilisation de la Transformée de Fourier dans les études du comportement en fréquence des structures.

#### METHODOLOGIE

La lutte contre les vibrations entraîne une mise en jeu musculaire physiologiquement bien régulée qui implique la participation d'un capteur périphérique (récepteur physiologique) : le fuseau neuromusculaire. Cette lutte entraîne une dépense d'énergie en rapport avec le temps d'application du stimulus vibratoire et de son intensité. On peut également penser que les variations - même minimes - de contraction musculaire provoquant des variations de rigidité de la colonne s'accompagneront de variations des caractéristiques de transfert de la structure puisqu'une partie importante des muscles du tronc, du cou et des ceintures sont insérés sur cette poutre maîtresse de la charpente corporelle qu'est la colonne vertébrale.

Pour étudier la relation entrée-sortie d'un disque, telle qu'elle vient d'être définie, il faut considérer le système dans son intégrité anatomique, c'est-à-dire recueillir les signaux "in situ". Mais pour obtenir la réponse du système dans son intégrité biologique il faut recueillir les signaux "in vivo". Pour ce faire, il faut implanter des capteurs par voie chirurgicale sur une colonne vertébrale normalement vascularisée. Une telle méthode, sanglante, impose l'utilisation d'un bon modèle de colonne vertébrale humaine : le rachis d'un primate. Celui-ci équipé de ses capteurs vertébraux peut être soumis à une impulsion à l'aide d'une broche directement implantée sur le sacrum de l'animal profondément anesthésié.

Dès lors si deux signaux  $x(t)$  et  $y(t)$  représentent, par exemple, les accélérations vertébrales (fig. 4) de part et d'autre d'un disque, le calcul de  $H(\omega)$  détermine la fonction de transfert de ce disque. A partir des fonctions de corrélation on calcule la Densité spectrale de puissance (autocorrélation) et une mesure du Transfert d'énergie (intercorrélation) entre les deux points d'acquisition des signaux.

Toutefois, un certain nombre de conditions préalables doivent être vérifiées. Ainsi on ne peut parler de fonction de transfert que si l'opérateur auquel s'applique cette fonction est un opérateur de convolution qui présente les

propriétés de linéarité, d'invariance et de continuité.

De plus, il n'est licite d'utiliser l'intégrale de Fourier sur un temps fini que si les signaux auxquels elle s'applique présentent certaines propriétés statistiques de stationnarité et d'ergodicité. Ces tests statistiques bien qu'indispensables à la validité de l'étude ne seront pas rapportés ici ; longuement étudiés en régime vibratoire et discutés par ailleurs - Quandieu (4) - ils font l'objet de publications en cours.

Un protocole appliqué à une méthode appropriée a été mis au point pour définir le domaine de linéarité de l'ensemble ostéoligamentomusculaire étudié en régime impulsif.

#### METHODE PROTOCOLE

Théoriquement, un système est linéaire s'il obéit au principe de superposition.

$$L \left[ \lambda_1 f_1(n) + \lambda_2 f_2(n) \right] = \lambda_1 L[f_1(n)] + \lambda_2 L[f_2(n)]$$

Dans cette relation existe deux propriétés :

- l'homogénéité : si les entrées sont multipliées par un même facteur constant, les sorties sont également multipliées par ce même facteur (proportionnalité des effets aux causes).
- l'additivité : les sorties résultantes des diverses entrées sont la somme des sorties résultant séparément des entrées (les causes ajoutent leurs effets).

La linéarité est étudiée à l'aide de tests dont aucun n'est suffisant par lui-même mais dont la convergence d'ensemble fait fortement suspecter cette propriété du comportement discal en régime dynamique :

- a) Etude de la distorsion harmonique
- b) Etude de la superposition réduite à l'homogénéité dans laquelle les réponses vertébrales des divers animaux soumis à des excitations d'amplitude variable sont étudiées.
- c) Etude de la fonction de cohérence : la fonction de transfert effectivement calculée par notre analyseur réalise, par elle-même, une linéarisation du système puisqu'il s'agit du calcul d'une fonction de transfert cohérente. L'importance de cette approximation est évaluée par l'intermédiaire de l'étude de la fonction de cohérence. Celle-ci est égale au rapport du carré du module de l'interspectre (Transformée de Fourier de la fonction d'intercorrélation) des deux signaux, au produit des densités spectrales de ces signaux. C'est donc une fonction, continue, réelle comprise entre zéro et un. Si la valeur de la fonction de cohérence est inférieure à l'unité, trois possibilités peuvent être envisagées :
  - le système reliant les deux signaux n'a pas un comportement linéaire
  - le système est linéaire mais du bruit se superpose au signal
  - du bruit se superpose sur une réponse non linéaire du système

Mais la réciproque n'est pas vraie : une fonction de cohérence égale à l'unité n'implique pas la linéarité.

Le protocole consiste donc à fixer chirurgicalement des accéléromètres miniatures sur la face antérieure des corps vertébraux d'un animal profondément anesthésié ; à fixer une broche munie d'un accéléromètre et d'un capteur de force dans le sacrum ; à appliquer sur cette broche des chocs d'intensité variable et de richesse en harmoniques différente et d'étudier les fonctions qui viennent d'être définies et qui sont représentées sur le synoptique de la figure 5.

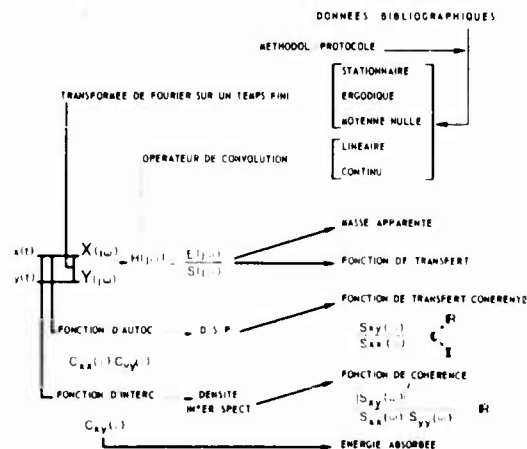


Fig. 5

#### MOYENS MIS EN OEUVRE :

##### 1 - Implantation chirurgicale des accéléromètres :

##### - Choix de l'animal :

Il s'agit d'un jeune babouin de 8 à 9 kg, capable de supporter une intervention chirurgicale de longue durée. Généralement quadrupède, sa position de repos est une position verticale. Parce qu'il n'est pas un brachiateur habituel, il ne présente pas de développement excessif de la ceinture scapulaire.

Cet animal possède sept vertèbres lombaires. Comparativement à l'homme, il possède un abdomen de



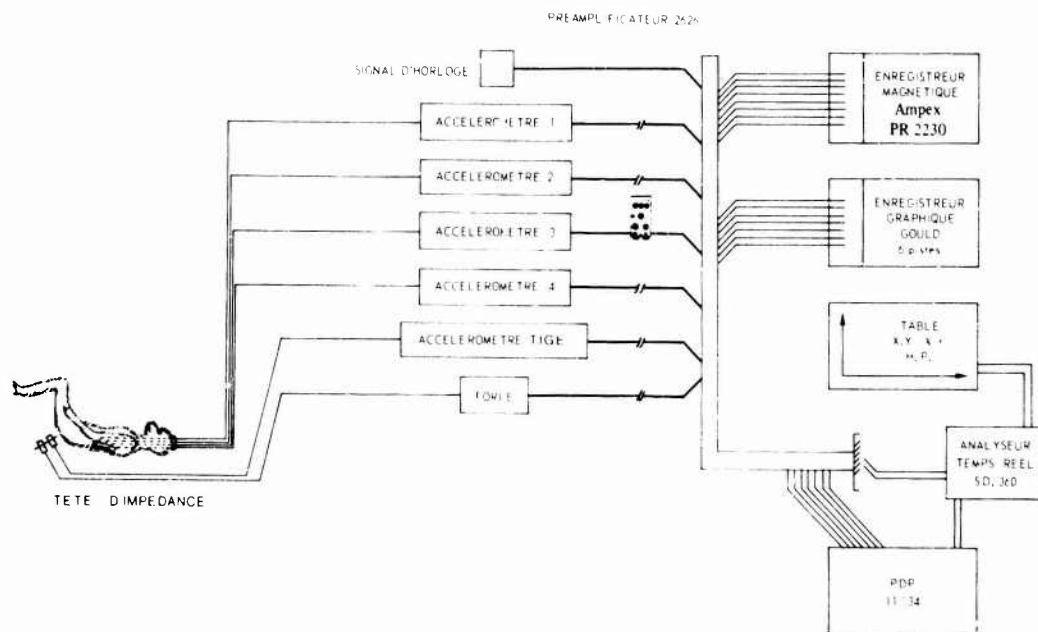


Fig. 8 : Moyens mis en oeuvre

PDP 11/34 plus spécialement destiné à réaliser les calculs statistiques.

- Le traitement en temps réel est réalisé par un Analyseur Spectral Dynamic 360 bicanal capable, en outre, d'afficher sur un scope la valeur de la fonction de cohérence des signaux recueillis.

#### RESULTATS :

Les résultats analysés dans cette étude proviennent de trois séries d'expériences pratiquées sur trois primates de masse respective assez variable :

- . Animal n°1 très robuste (environ 15 kg)
- . Animal n°2 environ 8 kg
- . Animal n°3 environ 11 kg

Après implantation des accéléromètres et de la broche les animaux sont radiographiés (fig. 9).

Les percussions réalisent des chocs dits "durs" ou "mous" (fig. 10).

- Chocs "durs" : acier-acier de spectre à peu près plat entre 800 et 4 kHz.

Ces chocs métalliques sont provoqués soit à l'aide d'un morceau de métal soit à l'aide d'une bille d'acier qui frappe la broche après cheminement sur un plan incliné.

- Chocs "mous" : élastomère-acier, dont le spectre d'excitation présente une amplitude maximale vers 1,3 kHz et décroissant au delà (ref 0 dB=1G/Hz ou 1N/Hz).

Les vibrations aléatoires (pot vibrant) entraînent sur la broche une densité spectrale recueillie sur la broche est représentée fig. 11 (ref 0dB=1G<sup>2</sup>/Hz)

Les informations recueillies sur les différents accéléromètres (fig.12) nécessitent un premier traitement de simplification d'acquisition des données.

#### - Acquisition des données :

Les signaux d'accéléromètres et de la force (8 voies dans une bande de 0 à 4000 Hz) sont enregistrés à grande vitesse sur l'enregistreur magnétique d'instrumentation (mode F.M.). A la relecture la vitesse de déroulement est divisée par 64. La nouvelle bande passante des signaux destinés à être digitalisés (12 bits) est alors compatible avec la fréquence d'échantillonnage du PDP 11/34 (2000 points par seconde par voie). Les données numériques sont stockées sur une unité magnétique numérique.

Parmi ces signaux, plusieurs types d'anomalies peuvent survenir : l'application d'un choc trop intense sur la broche provoque une saturation de



Fig. 9 : Animal n°2. La radiographie prise en per opératoire montre la présence de quatre accéléromètres sur la colonne lombaire - un accéléromètre sur le crâne et la broche implantée dans le sacrum.



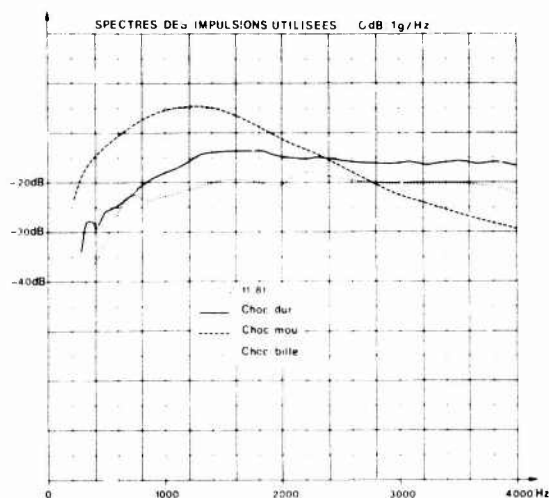


Fig. 10

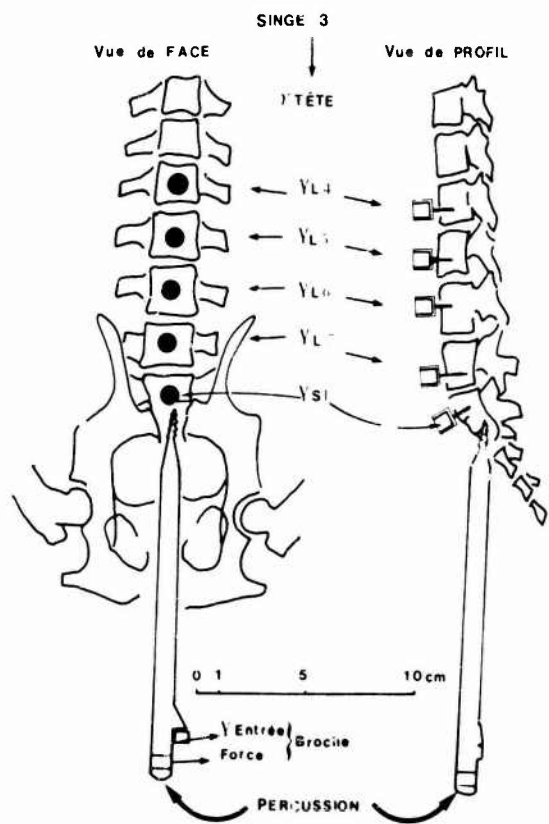


Fig. 12 : Schéma relevé à partir d'une radiographie pratiquée sur l'animal n° 3

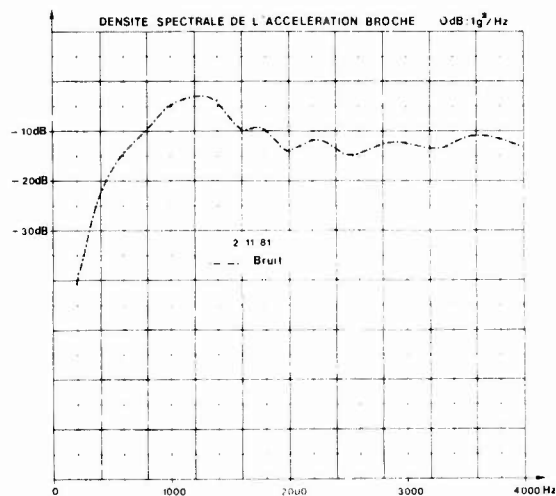


Fig. 11

l'électronique qui provoque la décapitation d'une portion originelle du signal ; un défaut de bande magnétique peut parfois en imposer pour une pseudo-impulsion. Un programme informatique permet de trier les impulsions reconnues correctes sur l'ensemble des voies. Chacune d'entre elles est transférée en 2048 points sur disque dur.

L'intérêt essentiel de cette méthode - outre de conserver les données sous leur forme analogique et digitale - est d'isoler et de répertorier chaque impulsion pour les calculs et visualisation ultérieure.

#### - Visualisation :

Pour visualiser un signal échantillonné sans utilisation d'interpolation plus ou moins complexe il faut utiliser une fréquence d'échantillonnage bien supérieure à celle préconisée par le Théorème de Shannon. Ainsi, pour obtenir une erreur relative sur l'amplitude inférieure à 1 % il faut une fréquence d'échantillonnage supérieure à 22 fois la fréquence de coupure.

Du fait de la lecture à vitesse lente de l'enregistreur magnétique et de la vitesse d'acquisition du PDP, c'est en fait 128000 points qui sont acquis sur une seconde du signal réel. Ceci justifie l'absence de filtres antirepliements dans le traitement des données. Il s'agit, bien entendu, d'une constatation expérimentale car il est clair qu'en toute rigueur il est impossible d'échantillonner un transitoire dont le spectre de fréquence s'étend à l'infini.

A 128 kHz les 2000 points/voie ont été acquis en 16 ms, ce qui est largement suffisant vis à vis du signal temporel. Au-delà de 7 ms après le choc, seul le bruit est enregistré. Pour l'accéléromètre de tête cependant, les 16 ms sont nécessaires.

Cette appropriation temporelle permet de conserver la totalité de l'information "pertinente" contenue dans le signal. Le triage et la réduction des signaux à 16 ms permet de faire une économie notable de disques.

#### ANALYSE SPECTRALE

L'ensemble des spectres, fonction de transfert et de cohérence, est obtenu après calcul par l'analyseur SD 360 commandé par le PDP. Cependant, en l'absence d'accès à l'étage post-convertisseur de l'analyseur, l'acheminement du fichier disque se fait après conversion numérique-analogique. Si cette méthode n'améliore évidemment pas la précision du traitement (elle oblige les expérimentateurs à comparer un grand nombre de signaux traités aux signaux d'origine pour affirmer leur identité) elle a l'avantage d'obtenir au même moment des représentations du signal dans le domaine temporel et dans le domaine fréquentiel.

L'analyse est faite par calcul d'une Transformée de Fourier rapide (F.F.T.) sur 1024 points du signal, ce qui représente une période mémoire d'une durée de 130 ms i.e.

. fréquence d'analyse : 4000 Hz

. fréquence d'échantillonnage  $4000 \cdot 2,048 = 8192$  Hz

Soit 1 point toutes les 0,12 ms environ.

Soit  $0,12 \times 1024 = 130$  ms pour remplir une mémoire d'entrée (période mémoire).

Or, nous l'avons vu, 16 ms de signal contiennent de l'information. Il faut donc compléter les 114ms restants par des signaux d'amplitude nulle. En fait, on complète le signal par une succession de points d'amplitude constante correspondant à la moyenne des valeurs prises par le signal calculée juste avant le début de l'impulsion. Le retrait de cette composante continue constitue, en fait et numériquement, la compensation d'offset inhérent à toute l'électronique.

#### LES SIGNAUX TEMPORELS :

Un exemple des réponses enregistrées sur la colonne et la tête est représenté fig. 13. Ils ont été obtenus sur l'animal n° 3. Sur les 8 voies il faut lire respectivement de bas en haut :

- la force et l'accélération de la broche d'excitation
- les accélérations de  $S_1$ ,  $L_7$ ,  $L_6$ ,  $L_5$  et  $L_4$
- en haut, l'accélération du crâne.

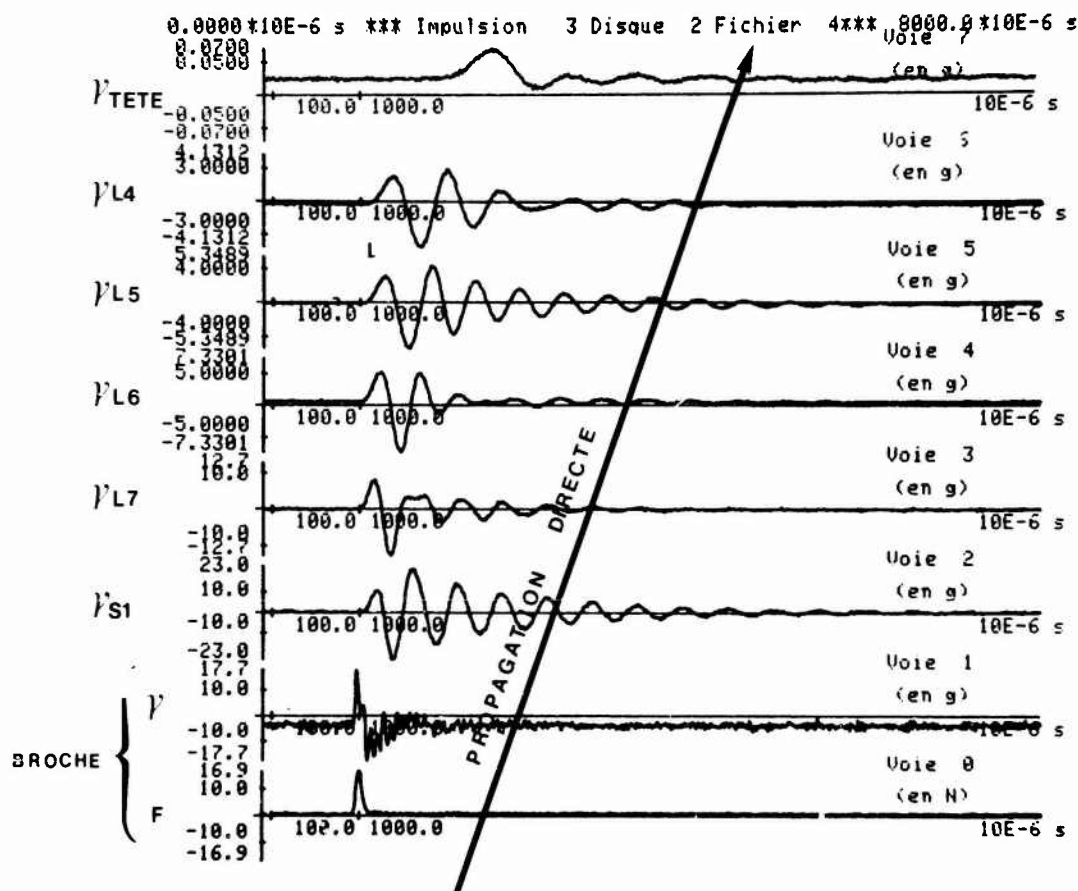


Fig. 13 : Enregistrement du signal temporel des ondes propagées depuis le sacrum  $S_1$  jusqu'à la tête  $Tête$ . Les deux enregistrements du bas sont respectivement, l'accélération et la force de l'excitation sur la broche d'implantation.

Le temps total de visualisation (abscisse) de l'enregistrement est de 8000 microsecondes. Sur le montage de la figure 13, les ordonnées sont normées (l'amplitude crête du signal de chaque voie occupe la totalité de la dynamique de l'enregistrement). Pour une force appliquée sur la broche de 16,9 N, soumise à une accélération de 17,7 G crête, les maxima des réponses vertébrales et de la Tête sont respectivement aux signes près.

$$S_1 = 23 \text{ G} \quad L_7 = 12,7 \text{ G} \quad L_6 = 7,3 \text{ G} \quad L_5 = 5,34 \text{ G} \quad L_4 = 4,13 \text{ G} \quad Tête = 0,07 \text{ G}$$

Cette représentation donne une bonne visualisation du retard d'apparition des impulsions sur les différentes vertèbres.

La figure 14 visualise mieux l'amortissement de la colonne lombaire. Sur ce montage, l'amplitude maximale de 23,3 G ( $S_1$ ) est conservée sur l'ensemble des voies.

En pratique, nous sommes limités à 7 enregistrements simultanés ; c'est le nombre d'amplificateurs conditionneurs que nous possédons. Aussi les enregistrements sont-ils toujours couplés deux par deux (fig. 15 choc dur - fig. 16 choc mou).

A gauche toutes les voies sont enregistrées sauf  $L_5$ , à droite tous les enregistrements sauf la Tête. Nous sommes tenus à cette représentation (et les montages des figures 13 et 14 n'ont qu'une valeur démonstrative) car il s'agit forcément de deux chocs différents enregistrés après commutation de la voie de  $L_5$ . Par conséquent, on ne saurait affirmer, d'une part, que deux chocs consécutifs sont parfaitement identiques en amplitude et en fréquence et, d'autre part, la représentation parfaitement synchrone de l'ensemble des enregistrements sur le papier ne peut être que subjective vis à vis de l'origine des temps.

Dans le choc mou (fig. 16) le deuxième accident en fin d'enregistrement (environ 7000 microsecondes)

ne constitue pas une onde de réflexion mais simplement une deuxième excitation (un rebond) qui est expérimentalement très difficile à éliminer.

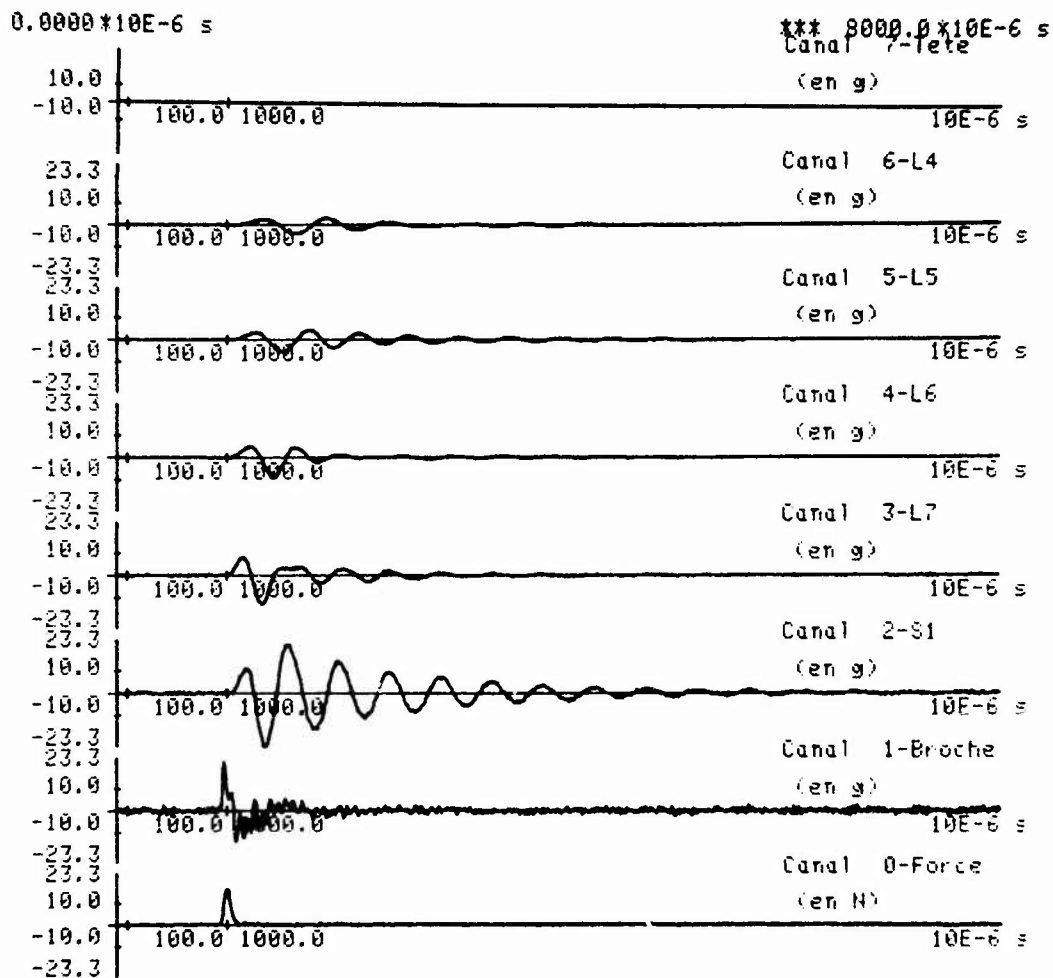


Fig. 14 : Même enregistrement que le précédent mais l'amplitude maximale de l'accélération de  $S_1$  ayant été conservée sur l'ensemble des voies on visualise beaucoup mieux l'amortissement des vibrations le long de la colonne vertébrale.

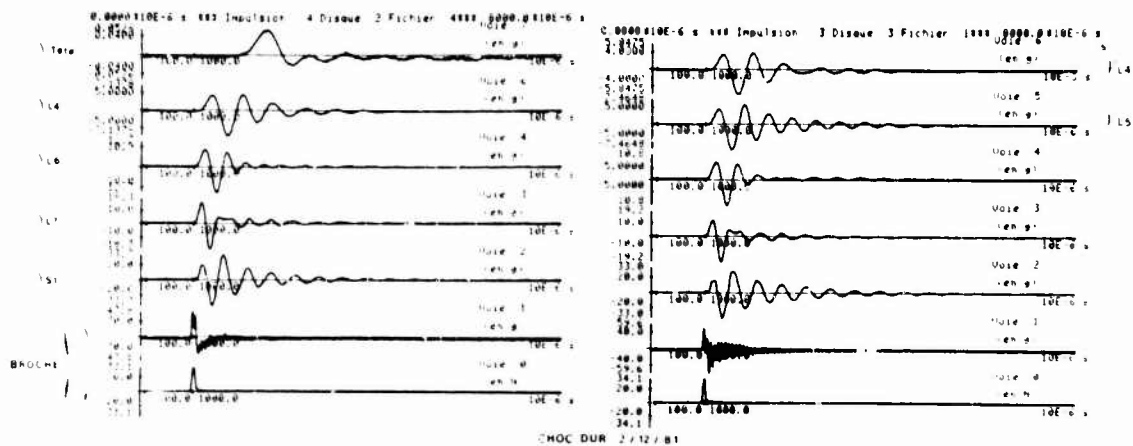


Fig. 15

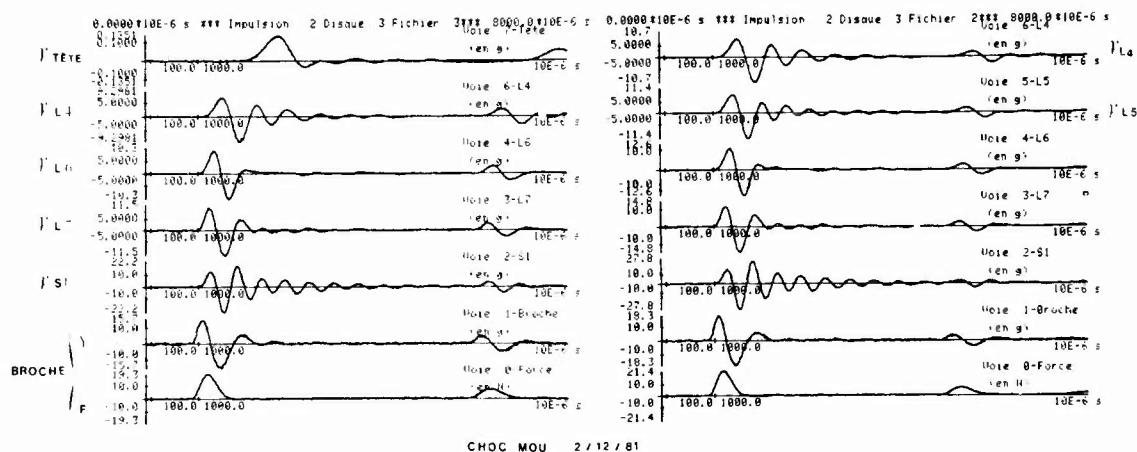


Fig. 16

### LES FONCTIONS DE TRANSFERT :

La figure 17 est un exemple d'enregistrement de la fonction de Transfert calculée entre les accélérations de la sixième et la septième vertèbre lombaire.

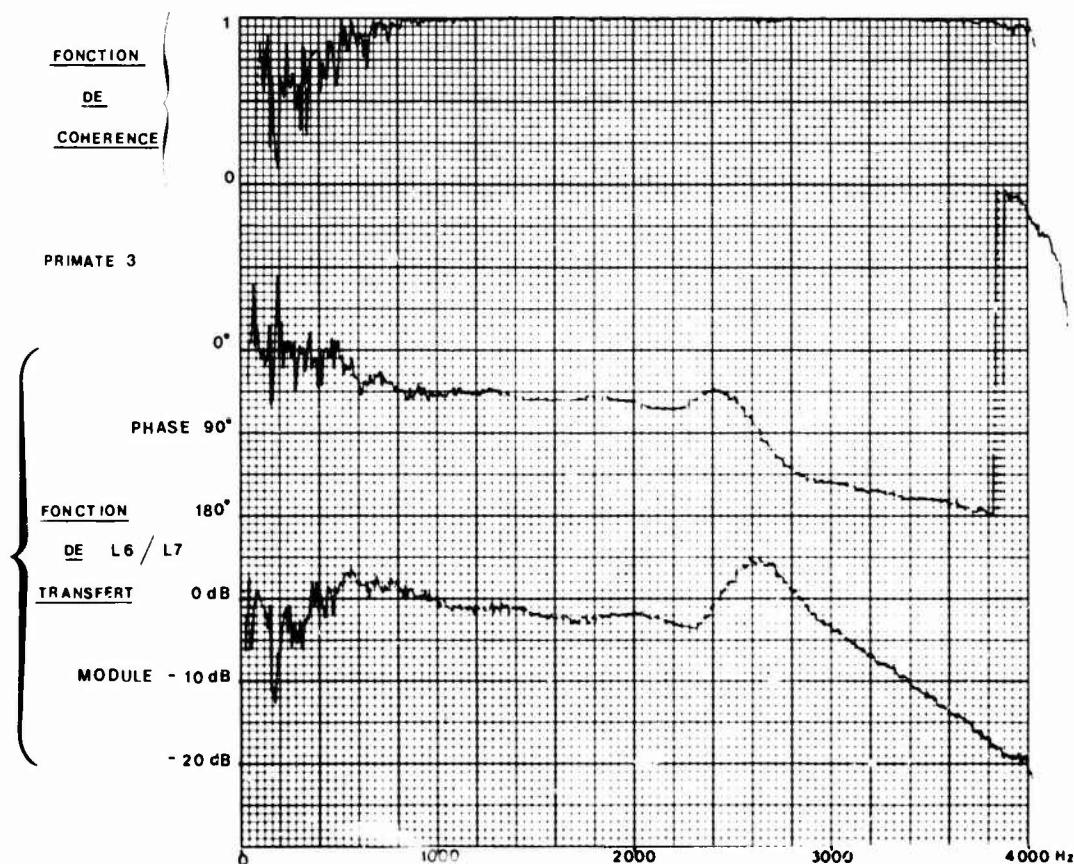


Fig. 17

Ramenées en abscisse à une bande d'analyse de 0 - 4000 Hz on lit en bas les variations du module en dB ( $\text{ndB} = 20 \log F_6/F_7$ ), au centre les variations de la phase en degrés, en haut la valeur de la fonction de cohérence qui témoigne de l'existence d'une bonne relation linéaire entre les signaux émis par L7 et ceux reçus par L6. Sa variabilité entre 0 et 1 est également en relation avec la valeur du rapport signal sur bruit. Ainsi l'énergie contenue dans les basses fréquences étant très faible la valeur de la fonction de cohérence devient très faible en-dessous de 200 Hz.

Les figures 18 (a, b, c, d, e et f) comparent les différentes fonctions de transfert en fonction des chocs. Dans cette représentation ont été comparés les portions d'enregistrements dans lesquelles les

fonctions de cohérence sont supérieures à 0,97.

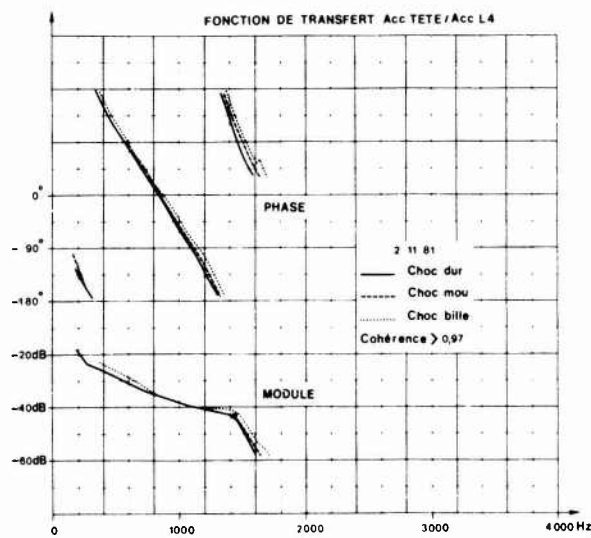


Fig. 18a

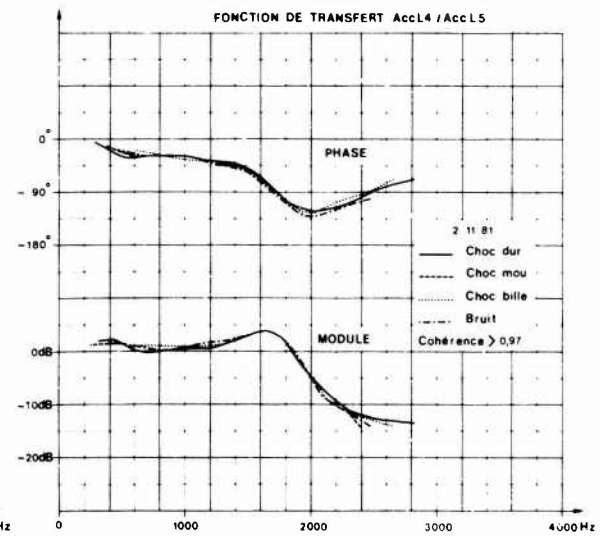


Fig. 18b

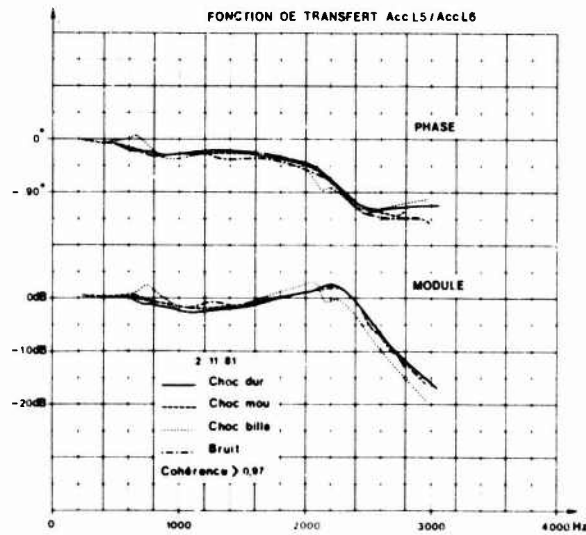


Fig. 18c

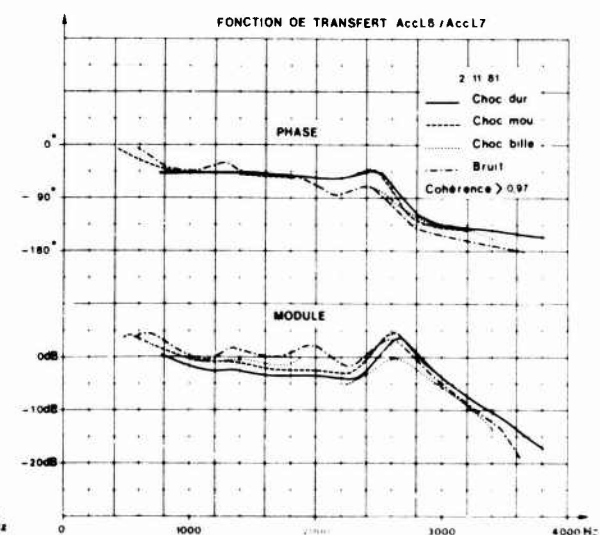


Fig. 18d

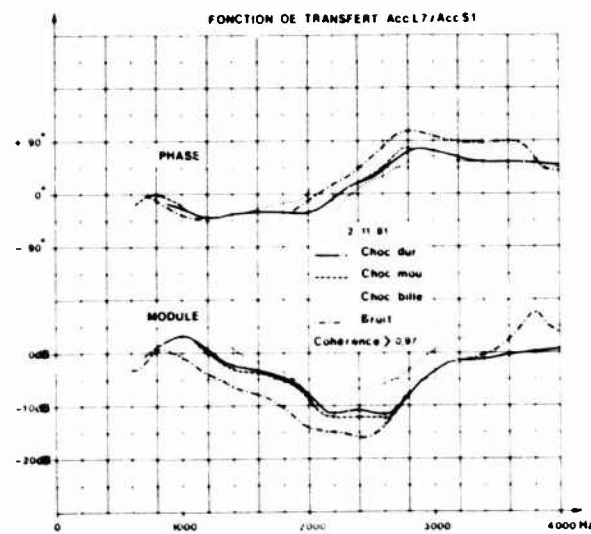


Fig. 18e

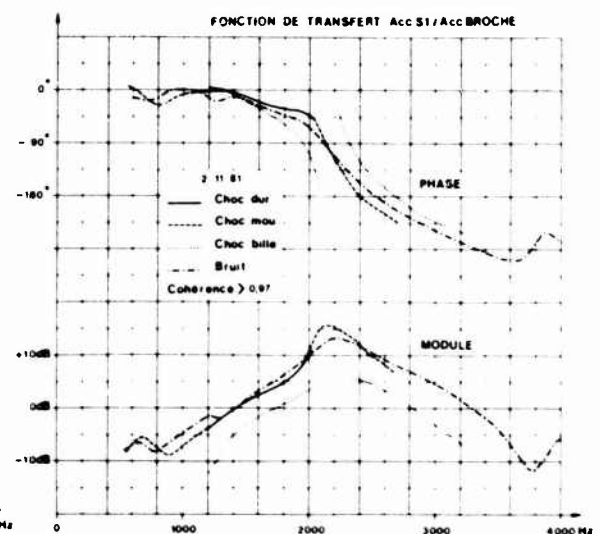


Fig. 18f

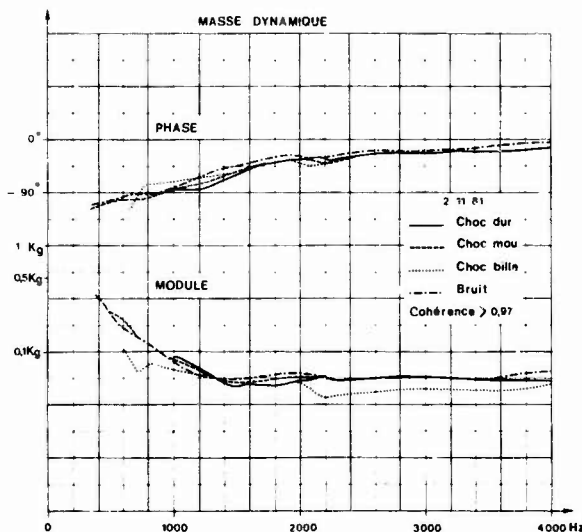


Fig. 19

La figure 19 est l'enregistrement des différentes masses dynamiques (ou effectives) de la broche. A une intégration près elles ont valeurs d'impédance d'entrée du système - colonne osseuse-muscle - ligaments. Le module en bas est donné en kilogramme, la phase (en haut) en degré.

Enfin, une autre représentation des fonctions de transfert est donnée après sommation des différents segments vertébraux. Pour une excitation aléatoire de la broche, on peut constater (fig. 20a) que l'adjonction d'une unité vertébrale complémentaire provoque une amélioration du caractère passe-bas du système.

La fig. 20b est la représentation en phase de ces fonctions de transfert.

#### ANALYSE - DISCUSSION :

##### 1) Linéarité :

Un test de linéarité est généralement réalisé à l'aide d'une excitation sinusoïdale. La mesure de la distorsion harmonique de la réponse du système testé est effectuée pour des niveaux d'excitation croissants. Il est clair que le signal d'excitation doit être très pur et en tout cas sa distorsion harmonique propre doit être infiniment plus faible que celle qui sera inhérente au système testé. Ce qui n'est pas le cas dans notre expérience ; en effet, l'excitateur (pour des raisons de maniabilité) est un mini pot vibrant électrodynamique aux performances nécessairement limitées en force maximale et en distorsion.

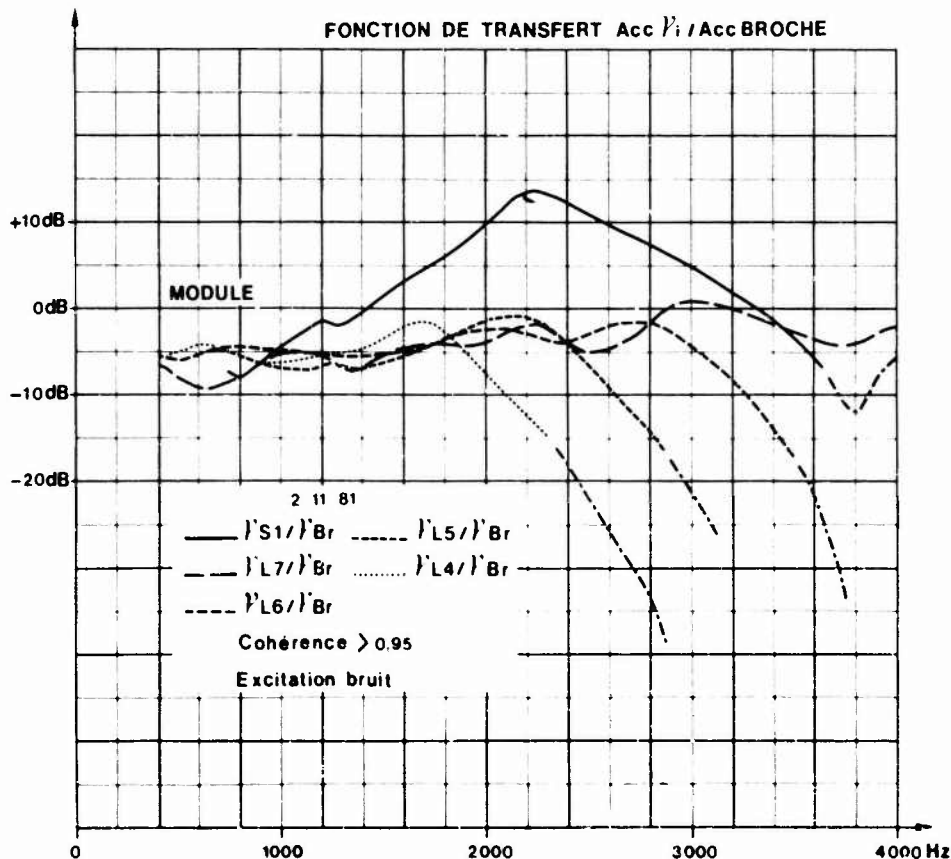


Fig. 20a

Aussi la linéarité a-t-elle été testée selon trois modalités :

- Calcul du taux de distorsion
- Etude de la proportionnalité entre les composantes spectrales de l'excitation et de la réponse
- Examen des variations des fonctions de transfert avec les divers types d'excitations utilisés.

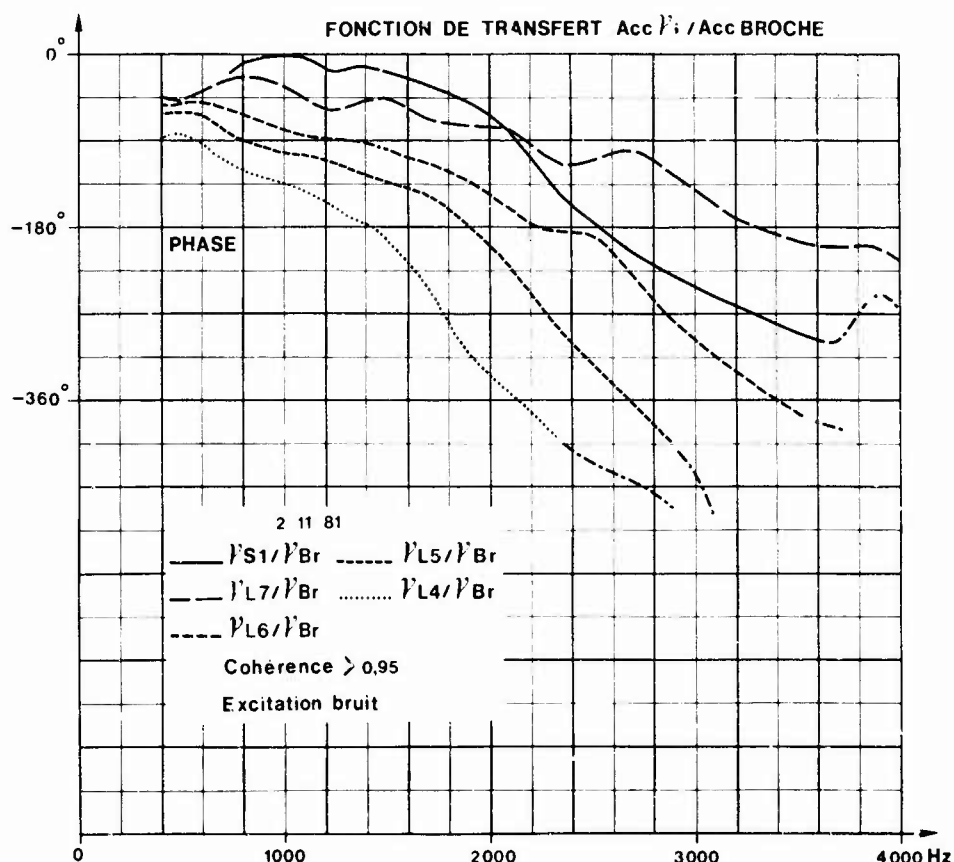


Fig. 20b

## a) Distorsion harmonique :

Le tableau 1 représente la distorsion de chaque échelon vertébral pour des accélérations croissantes au niveau de la broche. Ces accélérations sont celles de la broche données en G efficace à la fréquence fondamentale de l'excitation ici 832 Hz.

Accélération Broche :						
G eff.	1,213	2,392	3,458	4,558	5,805	6,009
Distorsion en %	Animal n° 2					
Broche	0,97	1,58	2,06	2,65	2,42	x
S <sub>1</sub>	5,25	9,06	12,63	15,44	14,35	x
L <sub>6</sub>	0,89	1,37	1,66	1,91	1,90	x
L <sub>5</sub>	0,59	1,21	1,70	1,92	1,88	x
L <sub>4</sub>	0,97	1,76	2,49	2,89	3,06	x
Tête	x	x	x	x	0,24	x

Tableau 1

Les cases du tableau remplies par des croix correspondent à des niveaux soit trop faibles pour être mesurés, soit trop élevés pour être atteints dans les conditions de l'expérience.

D'une façon très générale, il convient d'être extrêmement prudent dans l'analyse de ces données. Remarquons d'emblée que la distorsion harmonique du signal de la Tête est bien inférieure à celle du signal d'excitation (0,24 au lieu de 2,42 %). L'explication en est simple : la fonction de transfert Tête - L<sub>4</sub> (fig. 18) calculée chez l'animal n° 3 montre un module constamment décroissant et de façon rapide vers les hautes fréquences. Les harmoniques de distorsion à 1600 Hz, 2400 Hz, etc... sont donc très faibles et, par conséquent, abaissent la distorsion en-dessous de celle de l'excitation.

C'est le phénomène inverse que l'on constate lors de l'examen de la distorsion calculée sur le signal délivré par l'accéléromètre fixé sur le sacrum. La distorsion harmonique y est beaucoup plus élevée que celle de l'excitation (15,44 % et 2,65 % respectivement à 4,5 G eff.). En examinant la fonction de transfert S<sub>1</sub> / Broche, on constate que pour un fondamental à 800 Hz atténué à - 7 dB les harmoniques de rang 2 et 3 sont considérablement amplifiés (+ 10 dB). Dès lors, une faible augmentation des harmoniques de l'excitation (liée aux non linéarités du pot vibrant) se traduit par une très forte augmentation des harmoniques de la réponse, même si le système vertébral considéré est linéaire.

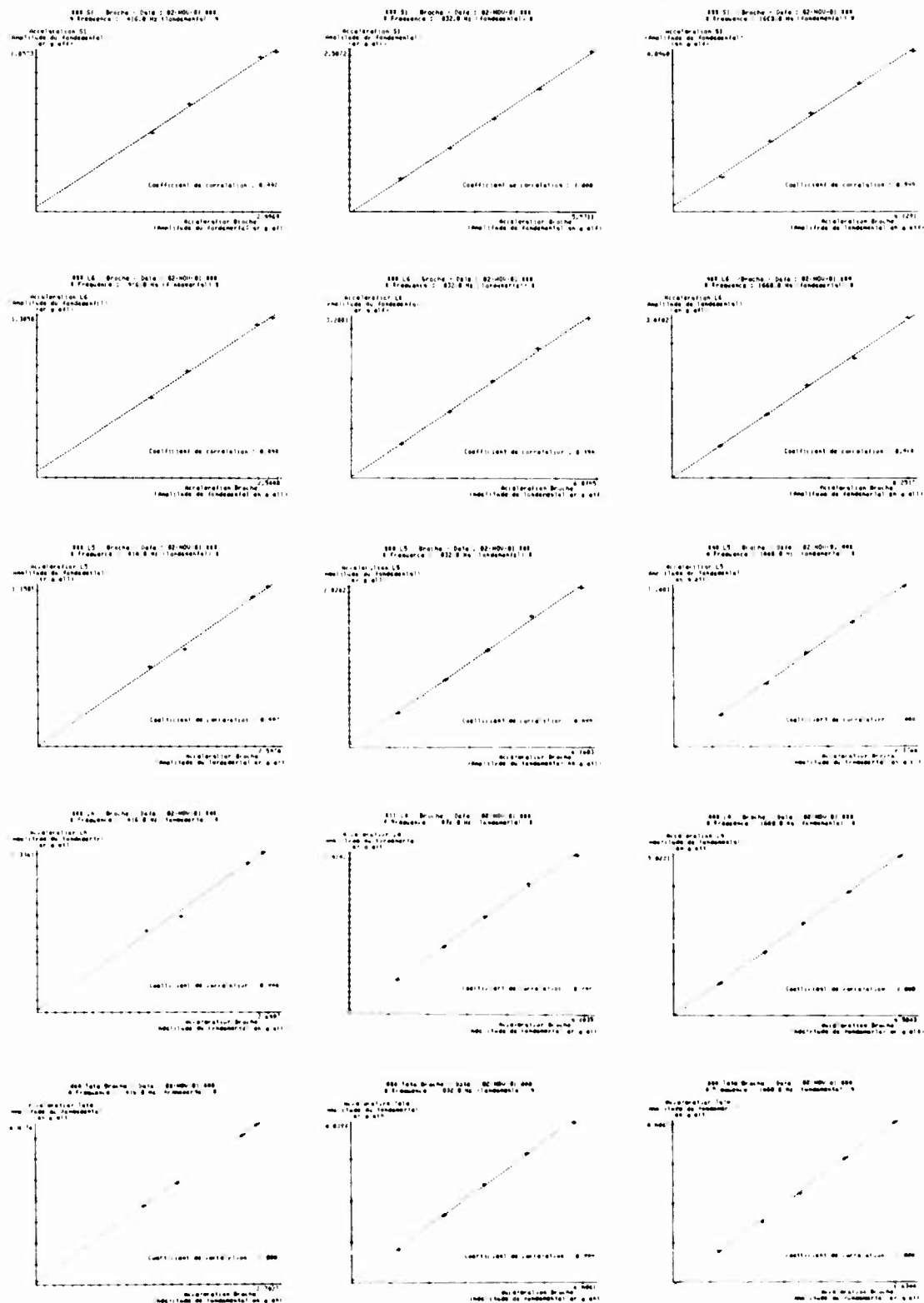
## b) Proportionnalité entrée-sortie :

L'étude est conduite en mesurant l'amplitude de la fréquence fondamentale et des harmoniques de rang 2 et 3 de l'excitation (broche) et des accélérations vertébrales. Les graphiques de la figure 21 intéressent les résultats obtenus sur le fondamental et sur lesquels il faut lire en abscisses les

accélérations imposées à la broche et en ordonnées les accélérations vertébrales ( à chaque colonne il correspond une fréquence fondamentale respectivement : 416, 832, 1660, 3320 et 4520.

La droite tracée est celle obtenue après approximation des moindres carrés. Les coefficients de corrélation en rapport avec ces droites sont données sur le tableau 2.

Fig. 21





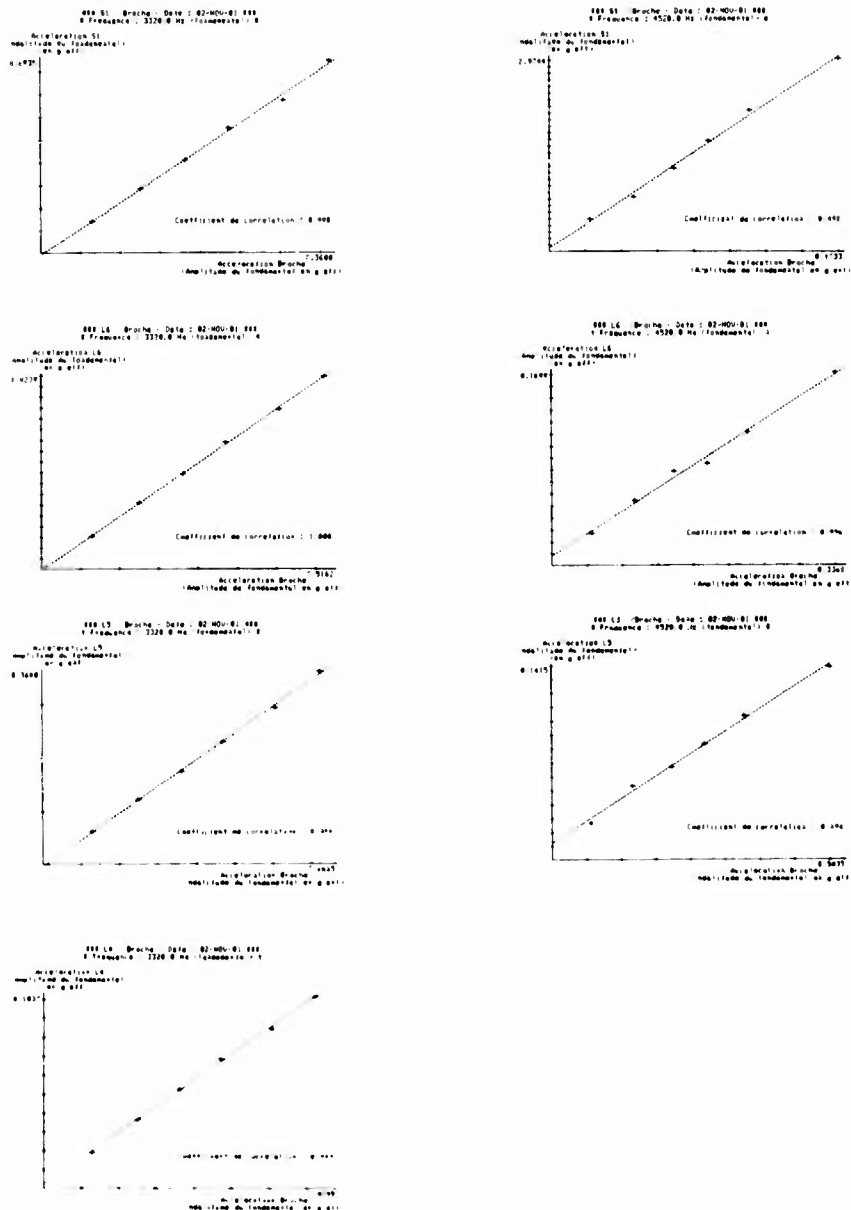


Fig. 51 (suite)

Sur le tableau 1, le chiffre placé en haut et à droite de chaque coefficient indique le nombre de points de mesure d'accélération qui ont été retenus pour le calcul jusqu'à la valeur limite maximale indiquée dans la dernière colonne de droite. Ainsi pour une accélération dont la fréquence fondamentale se trouve à 416 Hz, 4 points ont pu être relevés jusqu'à une amplitude max. d'accélération sur la broche de 2,448 G. Cette valeur dans les basses fréquences reste faible car la force maximale délivrée par le pot vibrant est d'une dizaine de Newtons. En basse fréquence - 208 Hz - le pot vibrant excite directement l'ensemble de la colonne vertébrale et des masses musculaires correspondantes. C'est donc bien la force qui limite l'étude (accélération maximale atteinte 0,256 G). Dans de telles conditions expérimentales il n'est pas douteux que la valeur des coefficients de corrélation qui diminue aux environs de 0,70 soit liée à un mauvais rapport signal sur bruit. Par contre, dès que la fréquence s'élève, la masse dynamique mesurée au niveau de l'entrée (broche) diminue. A 400 Hz, elle ne vaut plus que 0,3 kg, ce qui permet d'atteindre une accélération ( $a = F/m = 10/0,3$ ) environ égale à 3 G.

Dès lors à l'examen de ce tableau, la linéarité est bonne chaque fois que la mesure présente un bon rapport signal sur bruit, c'est-à-dire dans toutes les fréquences supérieures à 208 Hz. A l'extrémité inférieure droite du tableau (coefficient de corrélation Tête-broche à très haute fréquence) on constate l'absence de valeurs en relation avec l'absence de mesure possible. Déjà la corrélation entre  $L_4$  et la broche à 4520 Hz présentait une valeur basse voisine de 0,74 calculée seulement sur trois valeurs. Or, le niveau maximum d'accélération appliqué à la broche est élevé 8 G.

A cette fréquence, la colonne vertébrale joue parfaitement son rôle de filtre passe-bas (cf. fig. 21a) et le signal délivré par l'accéléromètre fixé sur le crâne devient extrêmement faible. C'est encore un mauvais rapport signal sur bruit qui est la cause d'une mauvaise corrélation entre les entrées et les sorties.

Les tableaux 3 et 4 concernent les coefficients de corrélation obtenus entre les entrées et réponses examinées cette fois sur les harmoniques 2 et 3.

Les remarques précédentes s'appliquent à ces résultats. Les corrélations sont excellentes chaque

fois que la mesure a pu être effectuée dans de bonnes conditions (jusqu'à 1600 Hz pour l'harmonique de rang 2 et 800 Hz pour l'harmonique de rang 3 - la corrélation unitaire de L<sub>4</sub>/Broche à 4520 Hz pour L<sub>4</sub>/Broche n'a évidemment aucune valeur puisqu'elle est calculée sur 2 points).

Frequence Fondamental (en Hz)	S1 /Broche	L6 /Broche	L5 /Broche	L4 /Broche	Tete/ /Broche	Niveau Broche Max (g) Fondamen.
208.0	0.73579 - <sup>!4</sup>	0.82046 - <sup>!4</sup>	0.81553 - <sup>!4</sup>	0.80962 - <sup>!4</sup>	0.66972 - <sup>!4</sup>	0.256
416.0	0.99735 - <sup>!4</sup>	0.99897 - <sup>!4</sup>	0.99697 - <sup>!4</sup>	0.99417 - <sup>!4</sup>	0.99988 - <sup>!4</sup>	2.448
832.0	0.99963 - <sup>!5</sup>	0.99941 - <sup>!5</sup>	0.99984 - <sup>!5</sup>	0.99981 - <sup>!5</sup>	0.99933 - <sup>!5</sup>	5.805
1660.0	0.99866 - <sup>!5</sup>	0.99921 - <sup>!5</sup>	0.99976 - <sup>!5</sup>	0.99992 - <sup>!5</sup>	0.99968 - <sup>!5</sup>	6.009
3320.0	0.99841 - <sup>!6</sup>	0.99980 - <sup>!6</sup>	0.99945 - <sup>!6</sup>	0.99944 - <sup>!6</sup>	***** - <sup>!0</sup>	7.224
4520.0	0.99791 - <sup>!6</sup>	0.99639 - <sup>!6</sup>	0.99755 - <sup>!6</sup>	0.74311 - <sup>!3</sup>	***** - <sup>!0</sup>	8.013

Coefficient de corrélation entre les amplitudes du FONDAMENTAL  
de l'excitation et de la réponse vertébrale . Date : 02-NOV-81

Tableau 2

Coefficient de corrélation entre les amplitudes de l'HARMONIQUE 2  
de l'excitation et de la réponse vertébrale . Date : 02-NOV-81

Frequence Fondamental (en Hz)	S1 /Broche	L6 /Broche	L5 /Broche	L4 /Broche	Tete/ /Broche	Niveau Broche Max (g) Harmon. 2
208.0	1.00000 - <sup>!2</sup>	0.99853 - <sup>!3</sup>	1.00000 - <sup>!2</sup>	1.00000 - <sup>!2</sup>	0.91200 - <sup>!3</sup>	0.029
416.0	0.99964 - <sup>!4</sup>	0.99856 - <sup>!4</sup>	0.99931 - <sup>!4</sup>	0.99705 - <sup>!4</sup>	0.99979 - <sup>!3</sup>	0.153
832.0	0.99914 - <sup>!4</sup>	0.99141 - <sup>!5</sup>	0.99936 - <sup>!4</sup>	0.99727 - <sup>!5</sup>	***** - <sup>!0</sup>	0.126
1660.0	0.99166 - <sup>!4</sup>	0.98903 - <sup>!3</sup>	0.96032 - <sup>!3</sup>	1.00000 - <sup>!2</sup>	***** - <sup>!0</sup>	0.116
3320.0	0.99527 - <sup>!5</sup>	***** - <sup>!0</sup>	***** - <sup>!0</sup>	***** - <sup>!0</sup>	***** - <sup>!0</sup>	0.201
4520.0	0.91423 - <sup>!5</sup>	***** - <sup>!0</sup>	0.95946 - <sup>!3</sup>	***** - <sup>!0</sup>	***** - <sup>!0</sup>	0.019

Tableau 3

**Coefficient de corrélation entre les amplitudes de l'HARMONIQUE 3  
de l'excitation et de la réponse vertébrale. Date : 02-NOV-81**

Frequence Fondamentale (en Hz)	S1 / Broche	L6 / Broche	L5 / Broche	L4 / Broche	Tête / Broche	Niveau Broche Max (g) Harmon. 3
208.0	0.99694 - <sup>14</sup>	0.99768 - <sup>14</sup>	0.99804 - <sup>14</sup>	0.99851 - <sup>14</sup>	0.99689 - <sup>14</sup>	1.857
416.0	1.00000 - <sup>13</sup>	1.00000 - <sup>13</sup>	0.99992 - <sup>13</sup>	0.99998 - <sup>13</sup>	0.99928 - <sup>13</sup>	4.353
832.0	0.98532 - <sup>15</sup>	0.96004 - <sup>15</sup>	0.97935 - <sup>15</sup>	0.99459 - <sup>13</sup>	***** - <sup>10</sup>	0.063
1660.0	0.31994 - <sup>14</sup>	1.00000 - <sup>12</sup>	***** - <sup>10</sup>	***** - <sup>10</sup>	***** - <sup>10</sup>	0.069
3320.0	0.09976 - <sup>16</sup>	0.36994 - <sup>14</sup>	0.02322 - <sup>15</sup>	***** - <sup>10</sup>	0.16739 - <sup>15</sup>	0.021
4520.0	0.69823 - <sup>16</sup>	0.67163 - <sup>15</sup>	0.81031 - <sup>16</sup>	1.00000 - <sup>12</sup>	0.98952 - <sup>13</sup>	0.048

Télégramme

c) Variations des fonctions de transfert obtenues avec divers types d'excitation :

La fonction de transfert d'un système linéaire doit être indépendante de l'excitation utilisée, puisqu'elle caractérise complètement le système. Faire varier le type d'excitation est donc un autre moyen de tester la linéarité. C'est ainsi que nous avons superposé les fonctions de transfert obtenues avec des chocs durs (acier contre acier), mous (acier contre élastomère). Les résultats présentés portent chaque fois sur une moyenne de 4 impulsions choisies pour leur ressemblance, en forme et en amplitude. Les courbes n'ont été tracées que dans le domaine de fréquence où les valeurs des fonctions de cohérence sont supérieures à 0,97. Si l'on constate une bonne superposition des courbes tête/L<sub>4</sub>, L<sub>4</sub>/L<sub>5</sub> et L<sub>5</sub>/L<sub>6</sub>, il existe ensuite une dégradation progressive sur L<sub>7</sub> et S<sub>1</sub>. Les résultats obtenus sur S<sub>1</sub> au moyen des billes sont surprenants. L<sub>7</sub>/S<sub>1</sub> paraît décalé d'environ 5 dB, ce qui peut faire suspecter une erreur de calibration, toujours possible malgré les multiples vérifications des divers commutateurs, tout au long de la manipulation. Cependant, l'examen des courbes de phase montre une altération identique, ce qui semble éliminer une erreur matérielle. Quoiqu'il en soit au niveau de la charnière lombo-sacrée les courbes se superposent plus ou moins. Que faut-il déduire en matière de linéarité ?

Il semble bien que l'on puisse affirmer que dans la bande 500 à 4000 Hz, la colonne vertébrale (intégralement associée à son système musculo-ligamentaire, normalement vascularisée) étudiée en régime impulsif se comporte linéaire. Ceci complète et confirme les résultats obtenus antérieurement dans la bande 5 - 100 Hz étudiés en régime vibratoire.

Il n'en va pas de même en ce qui concerne les fonctions de transfert de L<sub>7</sub>/S<sub>1</sub> et S<sub>1</sub>/Broche. A ce propos, il convient de remarquer qu'il faut sortir l'étude du sacrum de l'analyse vertébrale car anatomiquement, la vertèbre sacrée est bien reliée à la dernière lombaire, mais également aux os iliaques et d'une façon générale à la ceinture pelvienne porteuse des membres inférieurs.

2) Méthode d'analyse : le rachis est considéré comme un guide d'ondes

La propagation d'une sollicitation dynamique est étudiée d'un bout à l'autre du rachis, c'est-à-dire de S<sub>1</sub> à la tête. Toutefois, on n'a pu instrumenter au stade actuel que le niveau lombaire (L<sub>4</sub> à L<sub>5</sub>, S<sub>1</sub>) et la tête à l'autre extrémité. Une extension des mesures à des niveaux vertébraux intermédiaires est en projet.

On postule, à priori, qu'entre le bassin et la tête, le rachis complet (vertèbres - disques - ligaments - muscles) constitue un milieu dont les caractéristiques évoluent suffisamment progressivement pour constituer globalement un guide d'ondes mécaniques continu. Le guide s'ouvre à chaque extrémité sur des impédances nettement différentes, la tête et le bassin respectivement. On ignore volontairement les propagations parallèles possibles par l'ensemble des viscères (cavités abdominales et thoraciques) en se limitant à des excitations directes du rachis non susceptibles d'appropriser ces dernières. On postule aussi que la perturbation provoquée par l'attache des côtes et des ensembles omoplates-membres supérieurs n'est plus perceptible aux fréquences considérées dans l'étude actuelle, ces différents éléments étant mécaniquement découplés au-delà de 100 à 200 Hz. Le schéma du système étudié se ramène alors à la fig. 22.

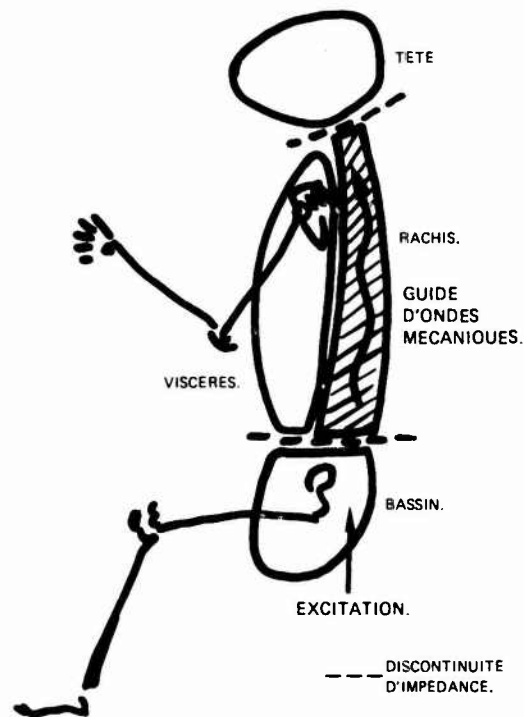
Le comportement d'un tel guide d'onde est facile à prévoir pour un milieu élastique homogène comme, par exemple, un barreau d'acier dans l'air : en appliquant un choc bref (relativement au temps de propagation dans le barreau) à une de ses extrémités, on voit (au moyen de capteurs disposés tout au long) se propager cet ébranlement de plusieurs façons (cf. fig. 23) :

- à vitesse élevée et sans déformation du signal sinon une infime atténuation : onde de compression à 5000 m/s (et éventuellement une onde de torsion à 3300 m/s sous réserve qu'elle soit appropriée par le choc excitateur)

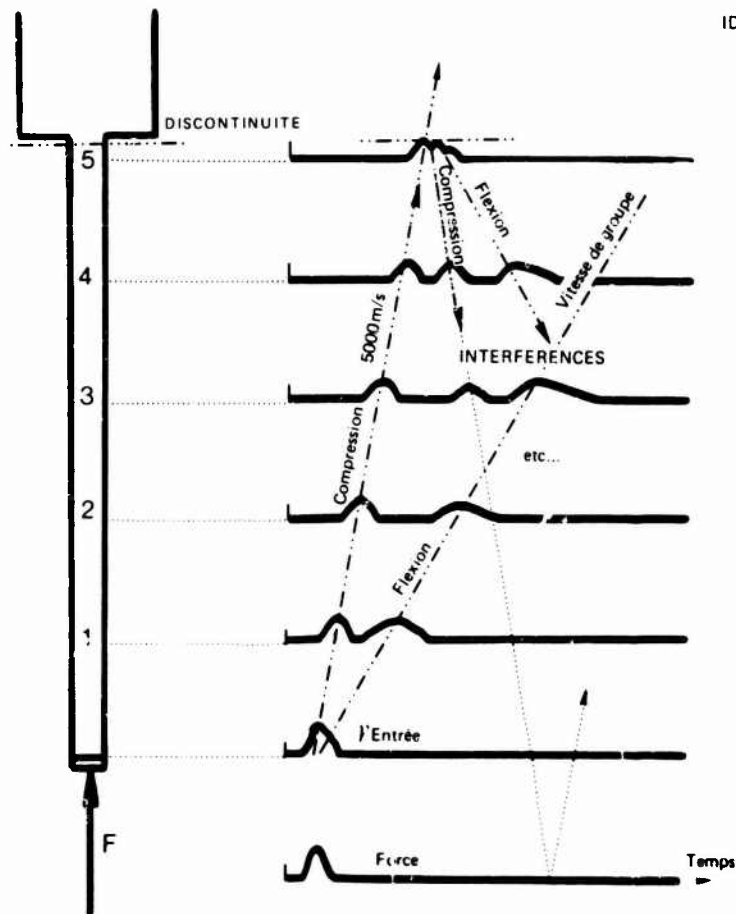
- à vitesse plus lente et avec déformation progressive de la forme du signal : onde de flexion.

La vitesse de propagation du maximum de l'enveloppe d'amplitude du signal correspond assez bien à la vitesse de groupe. Elle dépend à priori du spectre du signal excitateur. Elle est différente (proche du double au centre de la bande dans cet exemple) de la vitesse de phase du signal, qui ne peut se définir que fréquence à fréquence en résolvant l'équation de propagation, et mesurer en excitant par exemple le barreau en fréquence pure entretenue.

Lorsque l'onde la plus rapide (compression) arrive à la discontinuité d'impédance terminale, elle est pour une part appréciable, réfléchie en sens inverse tant sous la même forme (onde de compression inverse) que sous la forme d'ondes plus



IDEALISATION DU SYSTEME ETUDIE.



Exemple idéal : PROPAGATION HF DANS UNE BARRE LONGUE.

lentes si les diverses ondes sont couplées à l'interface.

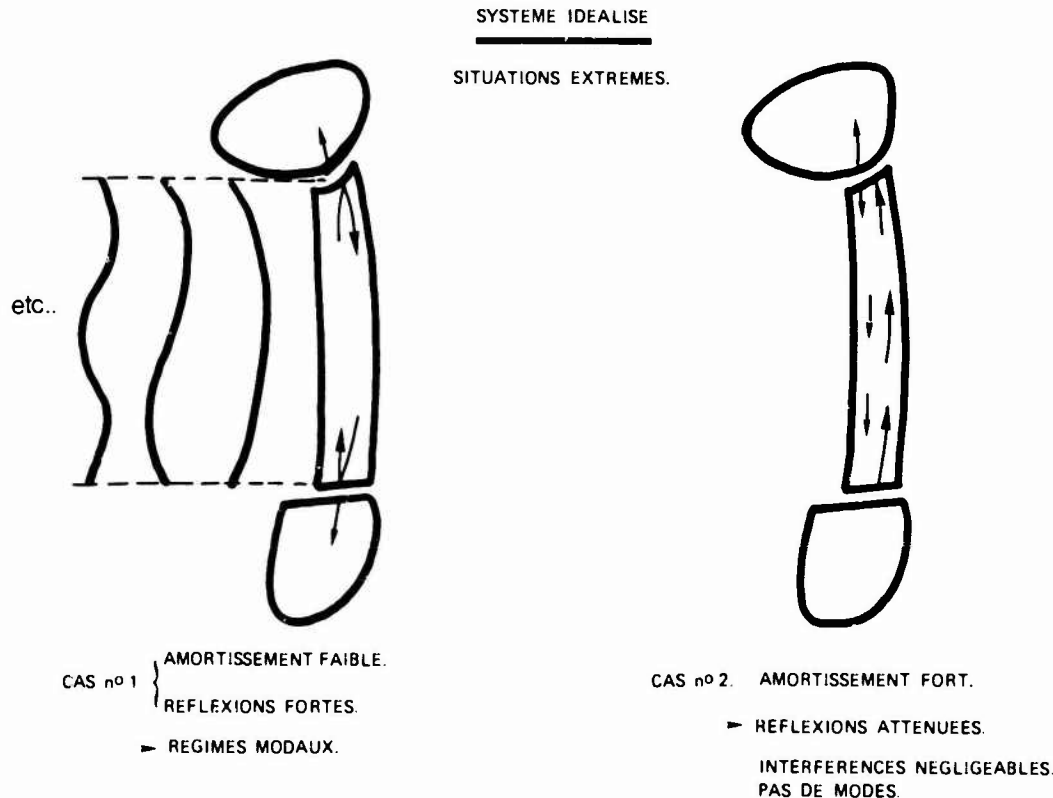
Lorsque ces ondes inverses rencontrent les ondes directes on n'observe plus que le résultat des interférences.

On voit alors dans notre schématisation du rachis que deux cas très différents sont possibles (cf. fig. 24) :

- le milieu est peu amorti et les réflexions aux extrémités fortes : le système stationnaire qui s'établit se traduit par une situation dominée par l'existence de modes propres à des fréquences discrètes, qui occasionnent un renforcement considérable de la réponse du système à une excitation quelconque sur ces fréquences singulières. C'est typiquement le cas du barreau acier présenté en exemple.

- le milieu est nettement amorti et les ondes réfléchies ont rapidement une amplitude négligeable par rapport aux ondes directes : l'interférence est négligeable et le milieu ne présente que des propagations directes comme s'il s'étendait jusqu'à l'infini. Il n'y a alors aucune singularité particulière relativement au domaine des fréquences.

On verra plus loin que les rachis étudiés se rapportent typiquement à cette situation.



### 3) L'accès au rachis : comportement et ancrage de la broche

#### 3.a) Ondes impliquées dans la broche

La broche utilisée ( $l = 0,18$  m,  $\rho = 0,008$  m, acier inox) correspond déjà en elle-même à un guide d'onde.

L'enregistrement du signal d'accélération sur la broche montre que dans le cas d'un choc bref, on excite très nettement un mode de résonance de la broche à 14,5 kHz, qui est typiquement la résonance en 1/2 onde en compression. Aucune mesure ne fait, par contre, apparaître de résonance perceptible à des fréquences inférieures : les modes de flexion ne sont donc appropriés ni par les excitations créées, ni par la disposition et l'orientation du capteur. On en conclut que pour sa plus grande part l'énergie injectée au singe est portée par une onde de compression de la broche, ce qui permet de connaître précisément l'instant d'application du choc sur  $S_1$ .

#### 3.b) Qualité de l'ancrage Broche- $S_1$ :

L'allure de la courbe de masse apparente au droit de la broche (cf. fig.19) laisse craindre à priori une perte de raideur de l'ancrage dès 1,5 kHz puisqu'on ne mesure plus qu'une masse de l'ordre de celle de la broche seule. La mesure sur la broche ne serait plus alors représentative du signal effectivement transmis sur  $S_1$ .

Mais on constate simultanément que la fonction de transfert accélération  $L_7$ /accélération broche reste constante pratiquement jusqu'à 4 kHz (cf. fig.25) : ceci suffit à prouver que le lien

Broche -  $S_1$  -  $L_7$  reste rigide jusqu'à ces fréquences mais que, compte tenu de la faible masse de ces pièces anatomiques, inférieure à la précision absolue de la courbe de masse apparente, elles n'y sont pas perceptibles à priori.

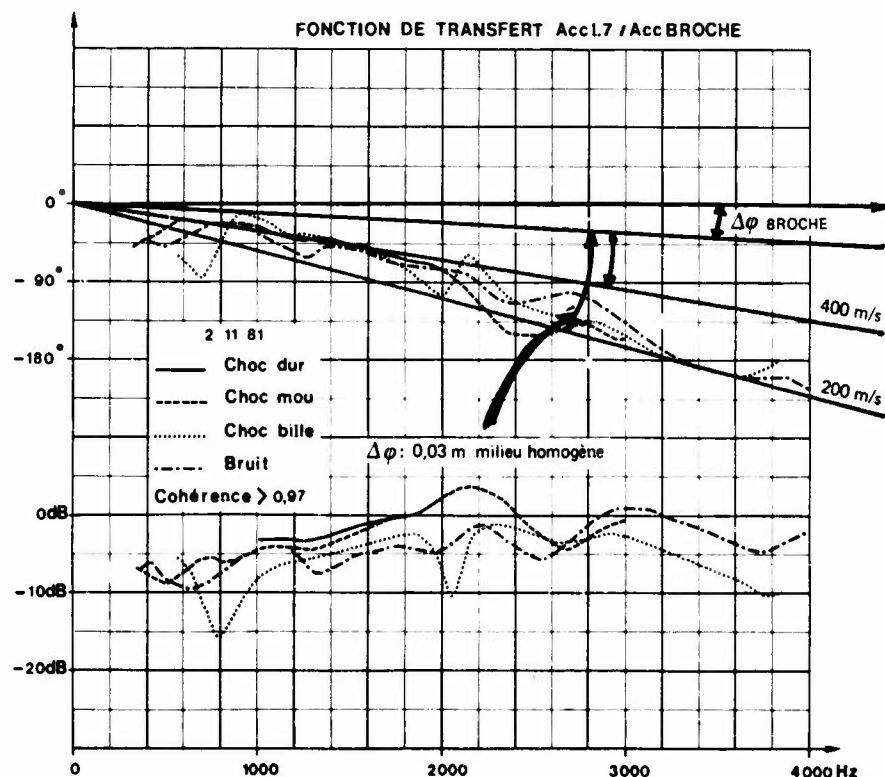
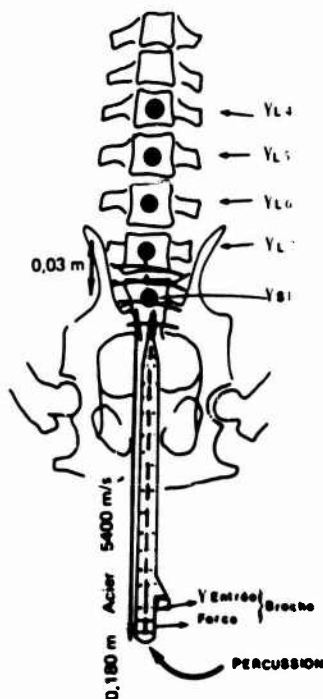


Fig. 26



#### 4) Examen des enregistrements directs des signaux. Vitesses de groupe :

L'examen des données sous la forme des courbes présentées aux figures 13 à 16 permet d'établir les résultats suivants relativement au modèle du barreau (cf. fig. 23)

- on n'enregistre qu'une seule onde et dans le seul sens direct.
- cette onde se modifie au cours de la propagation (étalement croissant des signaux) : le milieu est donc nettement dispersif.
- on peut procéder au calcul d'une vitesse de groupe, connaissant par ailleurs la distance effective entre capteurs.

La détermination de l'enveloppe des signaux étant en soi imprécise, et ne pouvant être améliorée faute de relevés expérimentaux directs d'une grandeur énergétique (forces ou contraintes étant trop difficiles à mesurer "in vivo", on ne dispose que des accélérations), on ne propose ici que des estimations grossières qui seront affinées par l'exploitation d'un plus grand nombre d'expériences :

- . singe 1 :  $230 \text{ m/s} < V_{gpe} < 325 \text{ m/s}$
- . singe 2 :  $180 \text{ m/s} < V_{gpe} < 220 \text{ m/s}$
- . singe 3 :  $250 \text{ m/s} < V_{gpe} < 400 \text{ m/s}$

La limite haute correspond à chaque fois à un trajet complet jusqu'à la tête.

Dans le cas du singe 1, on a observé entre  $L_6$  et  $L_7$  une vitesse de groupe de 1500 m/s. On rappelle que le singe 1 est le plus robuste (15 kg).

#### 5) Examen des fonctions de transfert :

L'examen des fig. 20a et 20b, en particulier, et 18a à 18f, permet de remonter à deux informations essentielles :

- l'atténuation des échelons vertébraux successifs ou cumulés en fonction de la fréquence ;

- la vitesse de phase de la propagation, par comparaison fréquence à fréquence entre le déphasage des signaux et la distance parcourue (dans le cas de capteurs distants, cela suppose des mesures assez précises vers les basses fréquences pour éliminer toute incertitude de  $2\pi$  sur l'angle total de rotation de phase).

Résultats :

5.a) Atténuations :

On a déjà relevé le caractère passe-bas caractéristique des différents échelons vertébraux, la fréquence de coupure étant plus ou moins nette selon l'animal étudié. Dans tous les cas il est caractéristique que cette fréquence de coupure s'abaisse quand on s'élève dans le rachis : 2,8 kHz pour L<sub>6</sub>, 2,4 kHz pour L<sub>5</sub>, 1,9 kHz pour L<sub>4</sub> dans le cas du singe 3.

En-deça de ces fréquences il n'y a pratiquement ni atténuation ni amplification des sollicitations, alors qu'au-delà l'atténuation est très rapide (supérieure à 20 dB/octave).

5.b) Vitesses de phase :

Là encore la précision des déterminations obtenues est limitée par le nombre insuffisant de mesures dont on dispose à l'heure actuelle.

Les seuls éléments certains pour l'instant sont les suivants :

- sur l'ensemble de la gamme de fréquences, la vitesse de phase mesurée est comprise entre 200 m/s et 400 m/s pour des fréquences entre 300 Hz et 4 kHz.

- plus précisément, elle serait très proche de 400 m/s jusqu'aux environs de la "fréquence de coupure" des échelons vertébraux (cf. ci-dessus) et décroîtrait alors sensiblement jusqu'à 200 m/s vers 3 à 4 kHz.

- la mesure globale entre broche et tête fournit une courbe de la vitesse de phase de l'ensemble du rachis qui est d'abord croissante de 200 à 400 m/s entre 100 et 800 Hz, très proche de 400 m/s entre 800 et 1400 Hz, décroissante de 400 à 200 m/s entre 1400 et 2800 Hz dans le cas du singe 3.

Les mesures sur le singe 1 ne sont disponibles que jusqu'à 1200 Hz. Elles suivent la même tendance avec des valeurs légèrement inférieures, de 160 à 350 m/s environ.

6) Cas particulier : cinématique de S<sub>1</sub>

Cette vertèbre S<sub>1</sub> n'a été équipée d'un accéléromètre sur sa face antérieure que dans le cas du singe 3.

Les relevés obtenus à partir de cet accéléromètre sont nettement singuliers (cf. courbes 18e et 18f), bien que la fixation du capteur ne laisse aucun doute.

L' "anomalie" la plus notable de ces mesures tient au fait que le maximum du signal est reçu sur L<sub>7</sub> près de 20  $\mu$ s plus tôt que sur ce capteur pourtant plus proche a priori de l'excitation.

L'examen plus attentif des relevés de ces signaux montre en fait l'arrivée sur ce capteur S<sub>1</sub> d'une première onde de faible amplitude sensiblement plus tôt (60  $\mu$ s environ) cf. fig. 26.

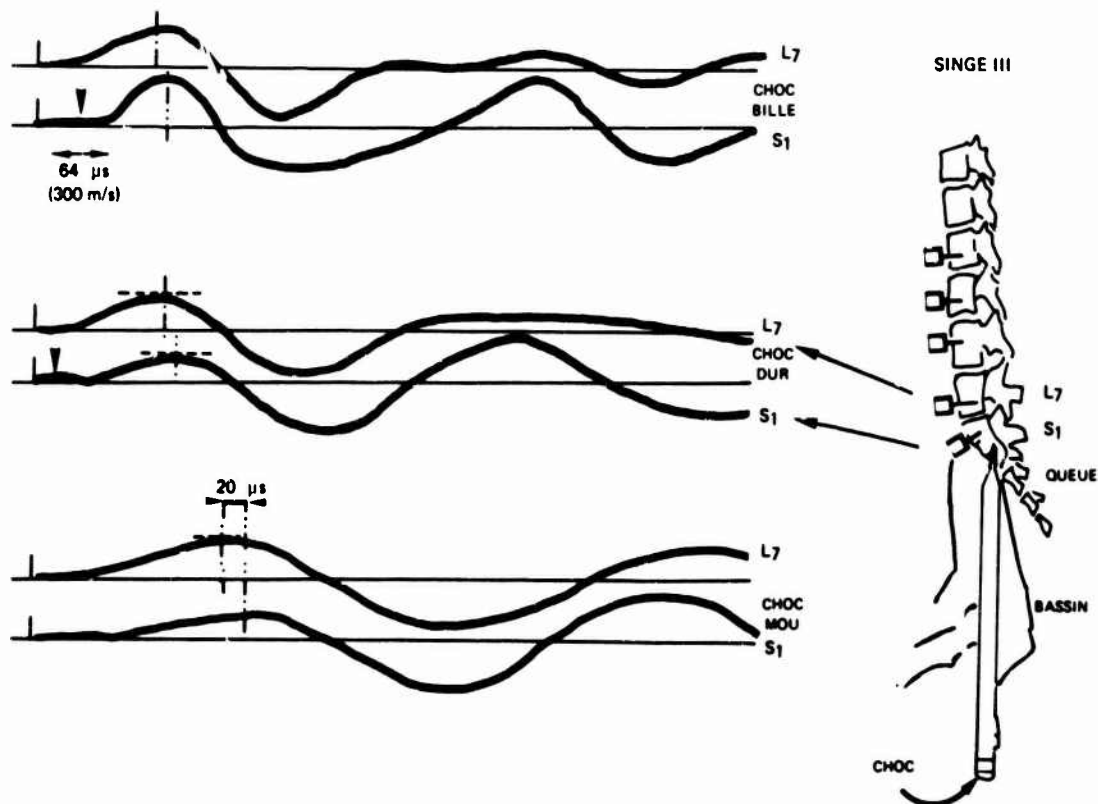


Fig. 26

On propose donc, sous réserve d'une analyse plus approfondie, l'explication suivante :

- l'ébranlement initial appliqué sur  $S_1$  se propage d'abord sous la forme d'une onde rapide de type compression. Cette onde crée un champ de déplacement faible sur l'os, mais porte l'essentiel de l'énergie du choc.

- ce n'est qu'en atteignant les limites de  $S_1$  (disque  $S_1L_7$ , surface articulaire de l'apophyse...) que cette onde se modifie en onde plus lente, à champ de déplacement en surface de l'os plus important. C'est cette nouvelle onde qu'on mesure sur  $L_7$ .

- la partie rétrodiffusée de cette onde atteint plus tardivement le capteur de la face antérieure de  $S_1$ , perturbée de plus par des interférences.

L'existence d'un champ interférentiel sur  $S_1$  est attestée par l'oscillation durable du signal enregistré (cf. fig. 14). Cette résonance a une fréquence de 2,2 kHz.

Sans instrumenter de façon plus complète cette vertèbre pour pouvoir préciser sa cinématique, il n'est pas possible de préciser la nature de cette résonance bien perceptible sur la fig. 18f.

#### 7) Problème de l'ancrage des capteurs :

On a montré plus haut que l'ancrage de la broche était sûr dans la gamme 0 - 4 kHz.

La qualité de l'ancrage des capteurs pose des questions analogues, bien que les masses mises en jeu soient beaucoup plus faibles, d'autant que cette fois le phénomène à craindre est une flexion du système capteur-vis sur la raideur de l'ancrage dans l'os.

Cette liaison n'a été vérifiée pour l'instant que jusqu'à des fréquences plus basses. Elle sera étendue jusqu'à 4 kHz dans les mesures à venir, la méthode étant de sacrifier l'animal, de prélever l'ensemble vertèbre-capteur et de le vibrer directement.

Comme il n'y a, à priori, aucune raison pour que ce type de résonance varie sensiblement en fonction du léger changement de dimension d'un corps vertébral à l'autre, mais présente plutôt une dispersion aléatoire, les auteurs ont le sentiment qu'un tel défaut d'ancrage ne saurait expliquer les courbes de filtrage régulièrement espacées des différents étages vertébraux, et que les phénomènes précités ne sont pas un artéfact du protocole expérimental. Ce qui ne saurait dispenser de cette vérification.

#### CONCLUSIONS :

Dans un premier temps, ce travail va être poursuivi dans le même esprit avec le souci de compléter les données actuelles et de préciser tout ce qui peut l'être.

Le but essentiel de cette caractérisation est avant tout le développement d'un modèle du rachis dans cette perspective "guide d'ondes".

Les principaux résultats acquis à ce jour sont les suivants :

- le rachis ne présente pas de phénomènes modaux perceptibles, et en particulier les vertèbres ne se comportent pas en résonateurs sur la raideur des disques voisins.

- les atténuations propres au rachis considéré comme un milieu de propagation sont très sélectives selon la fréquence, et donnent à ce dernier un caractère de passe-haut à pente de filtrage très rapide. Dans le cas des primates étudiés, la fréquence de coupure est de l'ordre de 2 kHz au niveau lombaire. Elle décroît continuellement quand on s'élève dans le rachis vers la tête.

- les ondes de compression volumique des matériaux constitutifs du rachis ne se propagent pas d'un étage vertébral à l'autre (on serait tenté d'y voir un cas de type "bande interdite" analogue à ce qu'on obtient dans l'étude de la propagation dans des milieux périodiques...).

- les sollicitations dynamiques sont du coup véhiculées par une onde lente, 200 à 400 m/s, dispersive, que l'on serait tenté de nommer "flexion" sous réserve de bien considérer :

. que l'on considère un milieu composite

. qu'il ne s'agit pas de la flexion du rachis au sens statique où les pièces osseuses ne se déforment pas, mais de la propagation d'une onde élastique dans un milieu composite, anisotrope, à caractéristiques continuellement variables.

Enfin, la linéarité observée jusqu'à des niveaux de sollicitation élevés (8 G crête) n'est pas la moindre surprise apportée par cette étude et laisse envisager la possibilité de modèles relativement simples applicables à des chocs très réalistes.

#### BIBLIOGRAPHIE :

- 1 - Auffret R., Poirier J.L., Tingaud A., Pellouard G., 1978 : "Effets sur l'homme des vibrations de basse fréquence" - Compte-rendu d'étude n°1067/CEV/LAMAS 91 Bretigny-sur-Orge (France), 41p.
- 2 - Max J., 1977 : "Méthodes et techniques de traitement du signal et applications aux mesures physiques" - Paris, Masson Ed., 379p.
- 3 - Papoulis A., 1977 : "Signal analysis", N.Y., Mac Graw Hill Book Company Ed., 431p.
- 4 - Quandieu P., 1981 : "Etude en régime vibratoire des fonctions de transfert des disques intervertébraux lombaires et de la masse apparente d'un primate" - Thèse Dr.ès.Sciences n°19, Paris VI, 276p.
- 5 - Roddier F., 1971 : "Distributions et Transformée de Fourier", Edisciences Ed., Paris, 286p.
- 6 - Roubine E., 1971 : "Introduction à la théorie de la communication", Tome III - "Théorie de l'information, Chap. 1 et 2 - Masson et Cie Ed., Paris, 159p.



## DISCUSSION

DR. VON GIERKE (USA)

Do you think your findings, the high frequency response of the spine, can be correlated with the injury patterns which have been observed in various subhuman primates?

## AUTHOR'S REPLY

We haven't been making any correlations on that which we observed because we made a preliminary study which is a global one. The response was not an impact response but a vibration response. So we thought about it and we came to the following conclusion; there exists a different phenomenon when it comes to the effect of a brief shock or a brief impact directly applied through the pelvis and this probably brings about a significant drop in the pass band of the signal sent to the spine. And we have the totality of the pass band which is applied. Moreover, in this type of study, for physical reasons, which you're well aware of, we cannot study the response of the spine in the 0-250hz because the energy contained in that band is much too weak and the signal to noise ratio is also very low; therefore, the correlation function becomes very low indeed and we can't draw any conclusions.

(UNKNOWN QUESTIONER) (UNCLEAR STATEMENT)

## AUTHOR'S REPLY

In the transfer function which has been studied here, first of all, this is a transfer function which is a particular type since this is a coherent transfer function. So there is a linearization of this system in this case. In both cases we only considered the results when the coherent transfer function is sufficiently high, that is, higher than 0.95. All the data below 0.95 of the coherent function have been rejected.

DR. VON GIERKE (USA)

The animals were sitting upright and not supine as in your drawing?

## AUTHOR'S REPLY

We prepared a seat which will enable us to make shock studies and vibration studies according to different positions from the supine to the erect.

DR. VON GIERKE (USA) (RECORDING UNCLEAR)

# HUMAN CADAVERIC RESPONSE TO SIMULATED HELICOPTER CRASHES

A.I. King and R.S. Levine  
Wayne State University  
Bioengineering Center  
Detroit, MI 48202, U.S.A.

## ABSTRACT

The use of energy absorbers in crew seats of military helicopters has the potential of minimizing spinal injuries during a crash. The determination of human response during such simulated crashes was attempted using a Black Hawk crew seat. A total of 28 impacts with 10 different cadavers were carried out to determine the injury pattern and the biodynamic response. Head and pelvic accelerations were measured along with sled and seat acceleration. Floor board and belt loads were also monitored. High speed film was taken to obtain head and torso kinematics. The predominant mode of failure was the anterior wedge fracture from T8 to L3. Generally, there was only one fracture per spine. One of the disturbing observations is the rolling of the shoulders within the restraint system resulting in hyperflexion of the thoraco-lumbar spine and anterior wedge fractures. An associated potential problem area is the observed large head excursions which can lead to significant head and neck acceleration injuries.

## INTRODUCTION

Spinal injuries, even those without significant injury to the enclosed neural structures, can lead to significant impairment. During helicopter crashes the spine is subjected to high levels of +G acceleration which causes spinal compression and flexion. Anterior wedge fractures of the lower thoracic and upper lumbar vertebrae are commonly seen. These injuries can be attenuated by using an energy absorbing (EA) seat. Due to limitations on the physical size of the cabin, it may not be possible to design an EA seat which can bring the loads down to a safe level for all crew members, that is, a constant load limiter can bottom out before the total energy is absorbed from a heavy crew member. The object of this project is to study the response of helicopter crews during combined +G and -G accelerations simulating a helicopter crash. A secondary objective is the determination of a reasonable EA setting for human cadavers which were used as surrogates for crew members. A preliminary series of runs were made using a rigid seat to determine cadaveric fracture g-levels which were to form the basis for using the 14.5-g setting designed for these helicopter seats or for testing cadavers at a lower level.

## METHODS

All tests were performed on WHAM III (Wayne Horizontal Acceleration Mechanism) with the seat and cadaver positioned as shown in Figure 1. The sled started at one end of the track, was brought to the desired velocity slowly and was decelerated rapidly at the opposite end of the track by a hydraulic snubbing device. The EA test seat was positioned so that its bottom pointed toward the front of the sled and the back was set at various angles with respect to the horizontal between 4 and 21 degrees (Figure 1). This system provided a +G acceleration component to a seated cadaver on a horizontal sled (horizontalized +G). The cadaver was positioned in the seat and held with a standard military harness used in helicopters. All belts were hand tightened. The cadaver was positioned with the head and neck were placed in slight flexion, simulating a pilot sitting upright.

The seat used in these tests was a standard helicopter seat with a thin foam cushion between the buttocks and seat pan. The EA's were changed after each run. EA settings were at 14.5 g and 11.5 g. Prior to using the EA's, several runs were made with a rigid seat set at 90 degrees. Two configurations were used for the EA seat to simulate a helicopter crash on a horizontal sled. The 'purely' vertical (+G) impact should be simulated by setting the seat back tangent line parallel to the horizontal surface of the sled. However, in order to account for gravitational acceleration which would act normal to the spinal axis, the seat back was tipped up 4 deg for a 14.5-g run.\* In the combined mode, simulating +G and -G accelerations, the seat back tangent line was tipped up an additional 17 deg to 21 deg. The g-levels for EA settings were subsequently reduced but the seat configurations were not altered since small rotational adjustments of one or two degrees were difficult to attain in structures designed to withstand high loads.

The cadavers were obtained from the Willed-Body Program of Wayne State University, School of Medicine.\*\* A total of 10 cadavers were used. A total of 28 runs (rigid and EA) were made. Initially, cadavers were subjected to more than one run, with five cadavers being used for 23 runs. Five of the 10 cadavers were used only once. Prior to use, the cadavers were X-rayed to rule out any spinal abnormalities, arthritis and/or osteoporosis; all of which disqualified the subject. Anthropometric measurements were made on each cadaver, after which it was instrumented with head and pelvic accelerometers and dressed in a tight fitting garment. The head and face were covered to preserve anonymity. A procedure to place the cadaver in the test seat was developed to ensure repeatable positioning. The lap belts were hand tightened to about 220 N and the shoulder straps to about 130 N. No helmets were used and the feet were strapped to bi-axial load cells which measured foot loads in the antero-posterior (x-axis) and superior-inferior (z-axis) directions. After each run, X-rays were taken and; for multiple runs, the cadaver was not reused if a fracture was identified. All cadavers were autopsied at the termination of the final run. During the autopsy, careful attention was paid to the spine. Specimens of vertebral bodies were sent to a testing laboratory to determine the compression strength at failure and their mineral content.

\* The arcsine of  $1/14.5$  is approximately 4 deg.

\*\*The protocol for the use of cadavers in this study was reviewed by the Human and Animal Investigation Committee of Wayne State University. It follows guidelines established by the U. S. Public Health Service and those recommended by the National Academy of Sciences/National Research Council.

The maximum number of data channels recorded was 32. They are:

Head accelerometers	9
Pelvic accelerometers	3
Seat pan accelerometers	3
Sled accelerometers	2
Lap belt load cells	2
Shoulder belt load cells	2
Tie-down strap load cell	1
Foot load cells	4
Energy absorber load cells	2
Displacement potentiometers	4

The head accelerometers were arranged in a 3-2-2-2 configuration for the measurement of linear and angular acceleration. Tri-axial pelvic and seat pan accelerations were measured along with sled deceleration which was monitored by a redundant accelerometer. The 5 belt loads were measured by clip-on type load cells while the x- and z-axis foot loads were measured by 2 multi-axis load cells. The performance of the 2 energy absorbers were monitored by EA load cells and up to a maximum of 4 string potentiometers which provided a quantitative measure of the loads sustained by the absorbers and the extent of the collapse of the seat. In many runs only one or two seat displacement measurements were made. All transducer data were transmitted to an analog tape recorder via trailing cables. Ten channels of data were digitized during the run, permitting an instant review of the results. All data were digitized at 1,600 samples/second after they were filtered at 800 Hz. The digital data were subjected to a 100-Hz low pass filter before they were plotted as results for this paper.

## RESULTS

Table 1 summarizes the 19 non-EA runs that were made with a rigid seat with a 90-degree seat back to seat pan angle. The seat back was parallel to the sled surface. Repeated runs were made on each of the three cadaveric subjects until a fracture was detected on lateral X-rays taken after each run. Cadaver 4612 was used for 3 runs. This 52-year old male cadaver sustained a fracture of T9 at 7.5 g, as shown in Figure 2 which was taken after the spine had been excised. The release of load and the removal of surrounding tissues permitted the vertebral body to rebound and lose its wedged shape. Cadaver 4654 was run 11 times up to 28.5 g. A typical fracture of T10 and T11 occurred during the last run. A total of 5 runs were made on Cadaver 4660 which sustained a small wedge fracture of T8 during the fourth run. However, this injury was initially overlooked and it was subjected to a fifth run at 21.4 g. A catastrophic fracture of T8 occurred.

The acceleration and load cell data presented in this paper are based on a set of body-fixed coordinate axes, the positive directions of which are directed anteriorly, left laterally and superiorly for the x-, y- and z-axis respectively. Figure 3 shows z-component accelerations of the pelvis, seat pan and input sled acceleration for a 12.8-g non-injury producing run on Cadaver 4654 (Run 7). Accelerations along the z-axis for a 28.5-g run on Cadaver 4654 are shown in Figure 4. Injuries to T10 and T11 were noted after this run. Because of the fact that the fracture level for this cadaver was so high, the average level for the three subjects was 16.0 g. Since the setting for the crew seat EA's was only 14.5 g, it was decided that this setting should be used for the second and principal phase of the study in which cadaveric responses were measured using an energy-absorbing seat. This set of non-EA runs also demonstrated the feasibility of simulating vertical accelerations on a horizontal sled and of producing injury patterns consistent with observations in the field.

The nine runs made with an EA seat are summarized in Table 2. A total of seven unembalmed cadavers were used in two different seat configurations. Two of the cadavers were tested in both the purely vertical mode and the combined mode while the remaining five were tested only once.

The nominal peak value of the sled pulse was set at 40 g. The velocity change was 46 km/hr and the stopping distance was 356 mm. A typical deceleration pulse is shown in Figure 5. Data from one of the nine runs (Run 25) were lost due to a malfunction of the tape recorder. The data from the remaining 8 runs can be divided into 3 groups. There were 3 purely vertical runs with an EA setting of 14.5 g (Runs 20, 28 and 31). Examples of head, pelvic and seat pan accelerations are shown in Figures 6 and 7 for the x- and z-components respectively. A 44-year old female cadaver (No. 4784) was used in Run 20. No gross spinal injury was detected. In Run 28, the test subject was a 61-year old female cadaver (No. 4850) which did not sustain any spinal injury. A 63-year old female cadaver was used in the third run of this series (Run 31). Figure 8 shows a compression fracture of T8 sustained by this cadaver. Again, this is an x-ray of the excised spine. Cadaver 4840 sustained a wedge fracture of L3 during Run 25 for which the transducer data were lost.

In the second group of two runs, the seat was tipped up 21 deg to simulate a combined mode of acceleration. In Run 21, Cadaver 4784 underwent a second run but was not injured. Run 29 was made with Cadaver 4850 which sustained an anterior wedge fracture of T12. Pelvic, head and seat-pan accelerations along the x- and z-axis for Run 29 are shown in Figures 9 and 10 respectively.

The three cadavers used in the last series of runs were impacted only once. They were subjected to a combined mode of deceleration with the EA's set at 11.5 g. The reduced EA level was an attempt to seek a g-level at which no spinal injuries among the cadaveric population would occur. All three cadavers sustained anterior wedge fractures, two of L1 and one of L3. The x- and z-components of the head, pelvis and seat pan for Run 33 are shown in Figures 11 and 12 respectively.

## DISCUSSION

In cadavers, fractures of the spine occur at about 10 g in the z-direction. Without an EA, the acceleration of the sled and seat pan are almost in phase, with the latter having a higher peak due to ringing. Pelvic response was delayed and magnified. The delay is due to the presence of soft tissue

covering the ischial tuberosities which need to be compressed before the inertial load can be transmitted to the bony pelvis. The higher acceleration experienced by the pelvis is attributable to the bottoming out of the tuberosities against a rigid seat pan. The z-component accelerations shown in Figure 3 are typical of all runs made in the non-EA mode at all g-levels. The spinal fracture patterns observed in this series of rigid seat runs on a horizontal sled were similar to that reported by Ewing et al (1) who performed cadaveric experiments on a vertical accelerator at Wayne State University. Shanahan (2) also indicated that the pattern of fracture seen in helicopter pilots is also similar to that of the cadaver. Thus, the simulation of helicopter crashes using cadavers on a horizontal sled is a viable method for injury studies. However, the difficulty of establishing human tolerance levels from cadaveric data still remains.

The data from the eight EA runs are more difficult to interpret. High speed movies of these runs show that the head and torso undergo severe hyperflexion. The sequence photograph in Figure 13 shows the head between the knees at the peak of its excursion (Run 28). For a comparable run without EA's, the amount of rotation of the head and torso is considerably less, as shown in the sequence photograph for Run 18 (Figure 14). The absence of significant spinal flexion was observed in previous studies in both the vertical acceleration mode and the combined mode. Prasad and King (3) made a large number of cadaveric runs on the vertical accelerator without encountering severe spinal flexion. Begeman (4) performed  $-G_x$  and combined  $-G_x$  and  $+G_z$  runs using a rigid seat but failed to observe the subject rolling inside the shoulder restraints. One of the major differences between the runs made on the Black Hawk seat and those performed previously is the manner in which the shoulder belts were pre-tightened before the run. During the Black Hawk test series, the pre-tension was kept at a relatively low level of about 130 N. In the rigid seat series and in previous experiments, the shoulder harness was tightened manually to about 400 N. Belt pre-tension may be a contributing factor to the observed head excursions.

The peak accelerations sustained by the head occurred near the end of the impact after the head had undergone a rotation in excess of 90 deg. The body-fixed accelerations in the x- and z- direction were both negative as the whipping head was brought to an abrupt stop by the shoulder belts. Peak head accelerations occurred at about the same time as that of the shoulder belt loads. A typical example of this is shown in Figure 15 for Run 33. Pelvic accelerations along the spinal axis were of the same order of magnitude as that of the seat. The seat cushion may have prevented the overshoot observed in the rigid seat runs.

The distribution of spinal fractures among the three groups of test conditions is not consistent with g-level or test mode. In the vertical mode, the fracture rate was 50% at an EA setting of 14.5 g. Two of the four cadavers sustained a spinal fracture in this series. At the same g-level in the combined mode, the fracture rate was also 50% (one out of two runs). However, the fracture rate was 100% for the 11.5-g setting in the combined mode. A much larger sample size is needed before a satisfactory explanation can be found.

#### CONCLUSIONS

The following conclusions can be made:

1. The use of a horizontal sled to simulate vertical impact accelerations has been shown to be a viable method in injury research involving the use of cadavers.
2. Human tolerance to combined accelerations cannot be deduced from these results. It is expected to be lower than that for  $+G_z$  acceleration.
3. The rolling of the shoulders inside the restraint system is a disturbing phenomenon which may aggravate spinal injuries. This was not observed in previous studies in which the shoulder harness was pre-tightened to 400 N. More research is needed to ascertain if powered inertial reels or an inflatable restraint system can be effective in reducing head excursion and upper torso rotation.
4. The energy absorbers functioned properly in all of the tests in which they were used. They appear to be an effective means of attenuating spinal injuries.
5. EA settings for cadaveric tests in the combined mode should be less than 11.5-g.

#### ACKNOWLEDGMENTS

This research was supported in part by a Tri-Service Contract (No. F33615-73-C-530), monitored by the U.S. Air Force. The work reported herein was coordinated by Lt. Paul France, Wright-Patterson Air Force Base and received technical support and advice from Dr. Leon Kazarian, Wright-Patterson Air Force Base; Mr. Joe Haley and Dr. Dennis Shanahan, U.S. Army Aeromedical Research Laboratory; Dr. Channing L. Ewing, Naval Biodynamics Laboratory; Messrs. George Singley and Kent Smith, U. S. Army Research and Technology Labs; and Messrs. Stanley DesJardins and Joe Colman, Simula, Inc. The contributions of each of the above-named persons are gratefully acknowledged.

#### REFERENCES

1. Ewing, C. L., King, A. I. and Prasad, P., 'Structural Considerations of the Human Vertebral Column under  $+G_z$  Impact Acceleration, J. of Aircraft, Vol. 9(1), pp. 84-90, 1972.
2. Shanahan, D., Personal Communication, 1982.
3. Prasad, P. and King, A. I., 'The Role of Articular Facets During  $+G_z$  Acceleration,' J. Appl. Mech., Vol. 41(2), pp. 321-326, 1974.
4. Begeman, P.C., 'The Effect of Energy Absorbing Devices on Spinal Loads Resulting from  $-G_x$  Acceleration,' Ph.D. Dissertation, Wayne State University, 1977.

TABLE 1 - SUMMARY OF RIGID SEAT RUNS

RUN #	CAD #	PEAK ACCEL	SEX	AGE	HT (mm)	WT (N)	INJURY
1	461	4.1	M	52	1775	716	
2		5.8					
3		7.5					Fracture of T9
4	4654	3.9	M	49	1695	899	
5		5.9					
6		8.7					
7		12.8					
8		15.5					
9		16.9					
10		18.8					
11		20.8					
12		24.0					
13		27.0					
14		28.5					Fracture of T10 and T11
15	4660	4.1	M	51	1705	961	
16		5.0					
17		8.8					
18		13.0					Anterior Wedge Fracture of T8
19		21.4					Catastrophic Fracture of T8

TABLE 2 - SUMMARY OF BLACK HAWK SEAT RUNS

RUN NO.	CAD NO.	PEAK ACCEL	SEX	AGE	HT (mm)	WT (N)	INJURY	SEAT CONFIG
20	4784	45.0	F	44	1600	738		VERT
21	4784	44.0						COMB
25	4840	LOST	M	55	1710	711	Fracture of L3	VERT
28	4850	42.3	F	61	1615	623		VERT
29	4850	41.6					Wedge Fracture of T12	COMB
31	4875	43.9	F	63	1660	657	Comp. Fracture of T8	VERT
33	4921	45.0	M	52	1750	971	Wedge Fracture of L1	COMB
35	4975	44.0	M	63	1715	628	Wedge Fracture of L3	COMB
37	4983	43.0	F	58	1620	718	Wedge Fracture of L1	COMB

VERT = Vertical (+G<sub>z</sub>) Acceleration, 4 deg seat back angle

COMB = Combined (+G<sub>z</sub> and -G<sub>x</sub>) Acceleration, 21 deg seat back angle



Figure 1 - Black Hawk Seat Assembly on WHAM III Sled.



Figure 2 - X-ray of Spinal Segment of Cadaver 4612 - Fracture of T9 at 7.5 g.

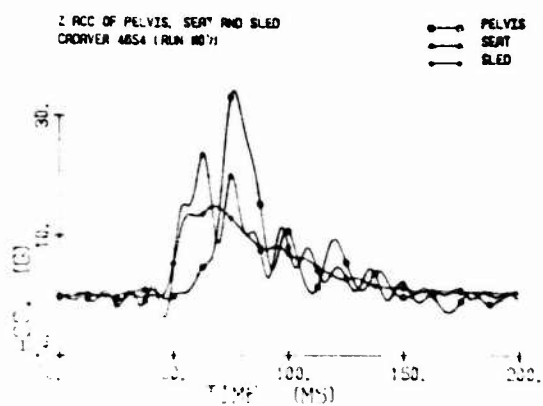


Figure 3 - Z-Component Accelerations of the Pelvis, Seat and Sled for Cadaver 4654 (Run 7) at 12.8 g.

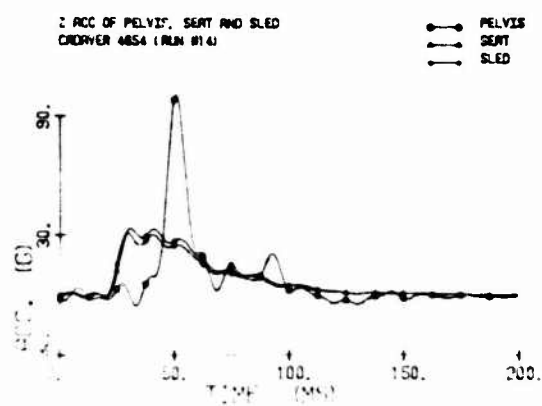


Figure 4 - Z-Component Accelerations of the Pelvis, Seat and Sled for Cadaver 4654 (Run 14) at 28.5 g.

TYPICAL SLED DECELERATION PULSE

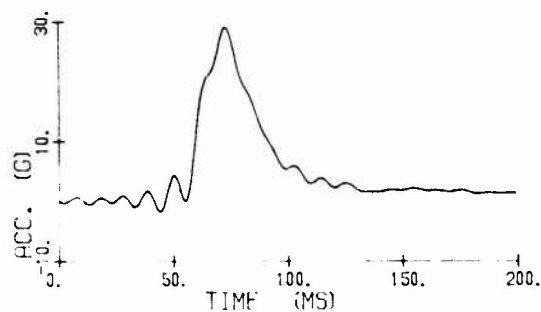


Figure 5 - A Typical Sled Deceleration Pulse Used for Black Hawk Seat Runs.

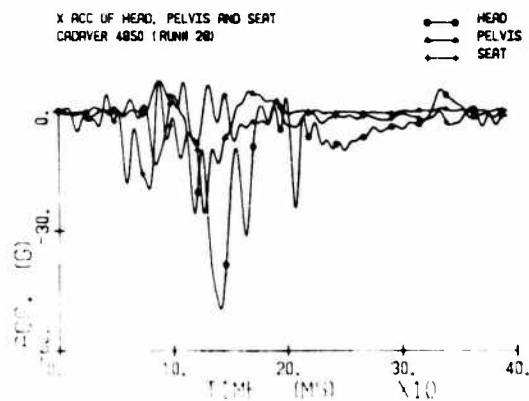


Figure 6 - X-Component Accelerations of the Head, Pelvis and Seat for Cadaver 4850 (Run 28) at 14.5 g EA Setting.

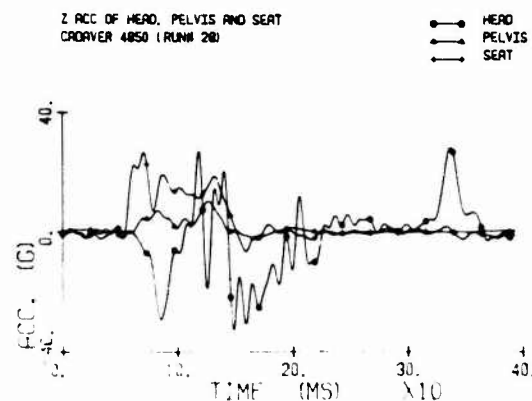


Figure 7 - Z-Component Accelerations of the Head, Pelvis and Seat for Cadaver 4850 (Run 28) at 14.5 g EA Setting.



Figure 8 - X-ray of A Spinal Segment of Cadaver 4875 - Fracture of T8

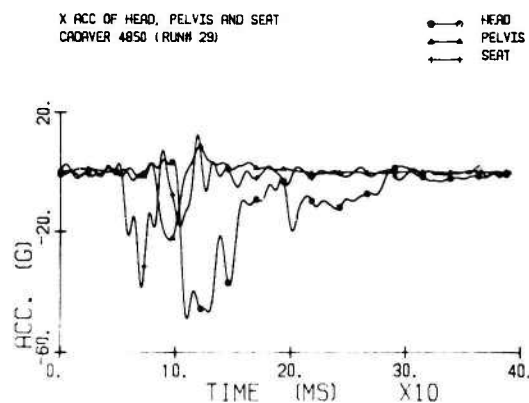


Figure 9 - X-Component of Acceleration of the Head, Pelvis and Seat for Cadaver 4850 (Run 29) at 14.5 g EA Setting.

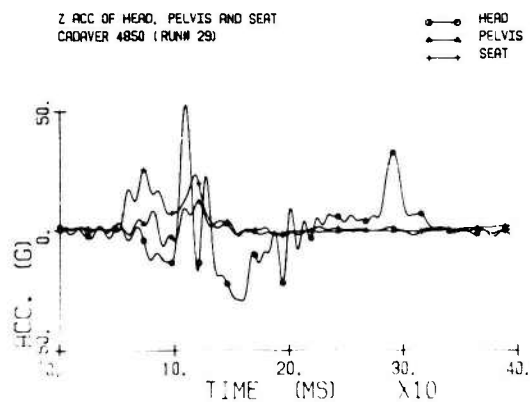


Figure 10 - Z-Component of Acceleration of the Head, Pelvis and Seat for Cadaver 4850 (Run 29) at 14.5 g EA Setting.

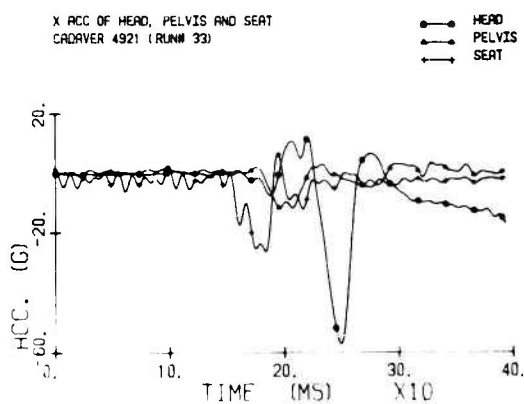


Figure 11 - X-Component of Accelerations of the Head, Pelvis and Seat for Cadaver 4921 (Run 33) at 11.5 g EA Setting

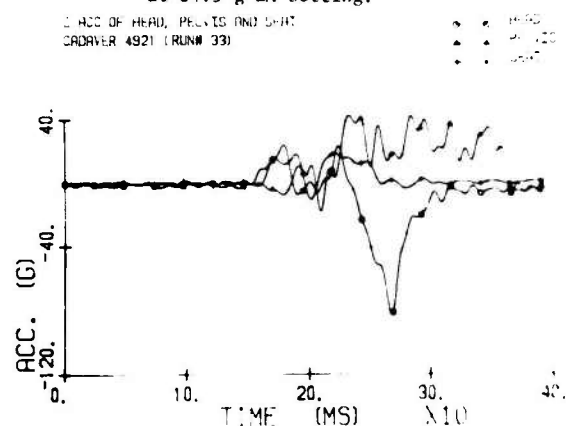


Figure 12 - Z-Component of Accelerations of the Head, Pelvis and Seat for Cadaver 4921 (Run 33) at 11.5 g EA Setting.

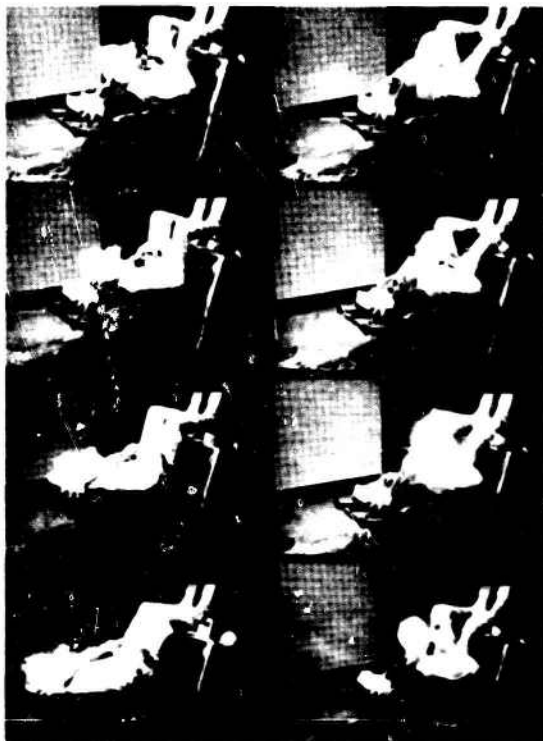


Figure 13 - Sequence Photograph of Run 28, Showing Large Head Rotation and Excursion.

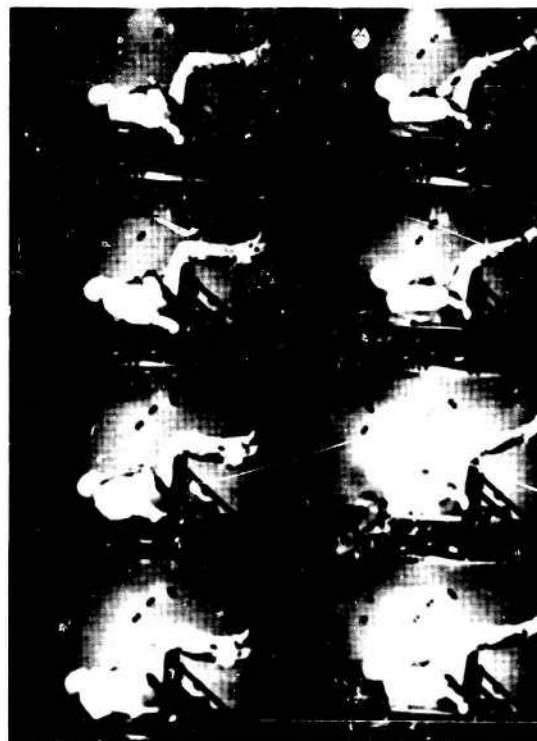


Figure 14 - Sequence Photograph of Run 18, Showing Considerably Less Head Rotation and Excursion.



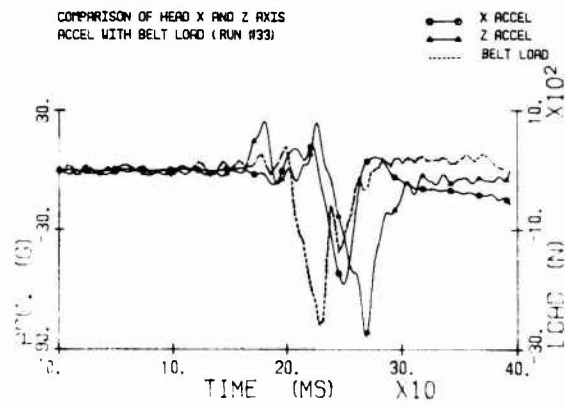


Figure 15 - Time Correlation of Peak Head Accelerations  
with Peak Shoulder Belt Load.

## DISCUSSION

## UNIDENTIFIED QUESTIONER

Can you give detailed information about the energy absorbing mechanism or energy materials in the seat system itself?

## AUTHOR'S REPLY

I request that Mr. DesJardins, the seat manufacturer's representative, discuss the material.

## DESJARDIN'S (USA)

The energy-absorbing mechanism used are inversion tubes. The material of the inversion tube is annealed aluminum tube, the device operates much like reaching into a sock and pulling it inside-out, the tube is pulled inside-out. The seat is attached to the bottom of these devices and the devices are attached to the top of the seat frame. The devices are elongated by the inertial load of the seat occupant.

## UNIDENTIFIED QUESTIONER

Did you see any ligamentous injuries and disk injuries?

## AUTHOR'S REPLY

We didn't see any ligamentous injuries nor did we see any disk injuries. Although I expect they should occur in the end-plate. I would expect to see these injuries in a larger series.

## INJURY MECHANISMS IN FRONTAL COLLISIONS INVOLVING GLANCE-OFF

Reidelbach, W.  
Zeidler, F.  
Daimler-Benz AG, 7032 Sindelfingen / Germany

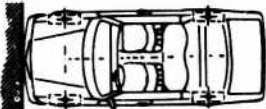
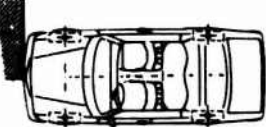
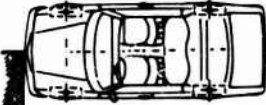
## SUMMARY

Among frontal car collisions offset impact collisions are three times more frequent than symmetrical ones. In case of small overlap and high collision speed the colliding vehicles glance-off. The definition and application of the energy equivalent speed helps to evaluate crash severity and to distinguish glance-off from non-glance-off collisions. The investigation of frequency and severity of injuries to belted occupants unveils that in case of glance-off, due to the "impact-shock syndrome", the injury risk of lower extremities is increased, the injury risk of remaining body regions is reduced when compared to non-glance-off cases.

## SOME RESULTS FROM ACCIDENT STATISTICS

Accident investigations have repeatedly shown that about 60 % of road traffic accidents involving injuries to car occupants are frontal collisions, this collision type therefore accounting for the greatest share of personal damage. Besides this general research result a more detailed knowledge of collision mechanisms was requested in order to identify the injury causing parts and kinematics and to design and perform realistic accident simulations.

So Daimler-Benz started in-depth accident analyses about 20 years ago and has now more than 1200 case reports on file. From there we have learned that about two thirds of the vehicles deformed by these frontal collisions can be allocated to one of three typical impact configurations.

impact configuration	rate of vehicles allocated
 100 % overlap (flat barrier)	25 %
 30 to 50 % overlap asymmetrical left (left offset barrier)	50 %
 30 to 50 % overlap asymmetrical right (right offset barrier)	25 %

Because of this 3:1 proportion of asymmetrical to symmetrical collision types, the offset impact deserves priority. Therefore Daimler-Benz for instance has included in its car engineering program the left side offset barrier impact test in addition to the flat barrier test required by law.

## ACCIDENT SEVERITY AND ENERGY EQUIVALENT SPEED

Since the beginning of accident research many attempts have been made to rate collision severity and correlate some to occupant injury severity. Among other approaches the change  $\Delta v$  of vehicle speed  $v$  during the collision (together with other parameters like mean acceleration and intrusion) is considered indicative for crash severity.

Our analyses led us to the opinion that for crash severity the exchange of kinetic energy and in particular the amount of energy absorbed by the deformed car structure is more significant than  $\Delta v$  [1]. The reason is the energy being a square function of the velocity. Be  $v$  the vehicle speed at the beginning and  $v - \Delta v$  the speed at the end of the collision. Then the vehicle's kinetic energy is reduced during the collision by

$$\Delta E = \frac{1}{2} m [v^2 - (v - \Delta v)^2] = \frac{1}{2} m (2v\Delta v - \Delta v^2).$$

For an equal amount of  $\Delta v$ , the dissipated energy  $\Delta E$  increases with  $v$ : the greater the "input speed", the greater the energy to be "managed".

The energy  $W$  absorbed by the car structure is in principle not identical to  $\Delta E$  described above but obviously of the same magnitude. So again, the greater  $v$ , the greater is  $W$ , and this quantity to our experience appropriately evaluates crash severity. Consequently, the "energy equivalent speed" [2]

$$EES = \sqrt{\frac{2W}{m}}$$

is a better collision severity indicator than  $\Delta v$ .  $W$  and thus EES can be estimated by experienced analysers in many cases with sufficient accuracy. Future application will validate this approach. Here it is used on a selected sample of frontal collisions.

#### THE FRONTAL COLLISION INVOLVING GLANCE-OFF

For further analysis of the prevailing offset frontal collision we selected from our files those cases which met the following criteria:

- Front structure damage indicates a left side offset impact with up to two thirds overlap.
- The deformation pattern of the case vehicle was to resemble the crush configuration resulting from offset barrier tests so that the EES could be estimated.
- The driver was to be belted which in many countries is compulsory.

82 cases complied with these conditions. Among them 12 were characterized by rather high input velocities and small overlap so that after a glancing blow the colliding vehicles separated from each other and continued their path with only a minor deviation (Fig. 1). We call it a frontal collision involving glance-off or, shortly, a glance-off-collision (GOC) in contrast to a non-glance-off-collision (NGOC).

After having determined  $\Delta v$  and EES for all 82 case vehicles, we realized that for those 12 GOC vehicles  $\Delta v$  was considerably smaller than EES whereas for the remaining 70 NGOC vehicles  $\Delta v$  was almost equal to EES. This led us to the definition of the parameter  $k = \Delta v/EES$  and a preliminary criterion  $k \approx 0.7$  indicating a typical GOC.

The significant data for the twelve GOC cases are compiled in tables 1 and 2. The cars were involved in accidents between 1975 and 1980. The weight given in each case is the empty vehicle weight. Worthy of note is the high relative speed  $v_{rel}$  which varies from 100 to 175 km/h. It can be found by adding the two collision speeds. The occupant injuries are ranked using the Abbreviated Injury Scale (AIS) [3].

#### COMPARISON OF GOC AND NGOC DATA

In the left side offset frontal collision sample considered here - 82 cases with all car drivers belted - no injuries of AIS above 3 are recorded.

In 70 NGOCs the drivers suffered  
 58 head, neck or thorax injuries, AIS 1 to 3  
 39 injuries to the lower extremities, in particular  
 13 injuries to knee and thigh, AIS 1 to 3  
 13 injuries to foot and lower leg, AIS 1 to 3  
 13 combined upper/lower leg injuries, AIS 1 to 3

Obviously in NGOCs the injury risk is almost equally distributed over the whole body with injury severity up to 3 in all body regions.

In 12 GOCs the drivers suffered  
 7 head, neck or thorax injuries, AIS 1  
 10 injuries to the lower extremities, in particular  
 1 knee injury, AIS 2  
 7 injuries to foot and lower leg, AIS 2 and 3  
 2 combined upper/lower leg injuries, AIS 3

In contrast to the NGOC sample the GOC sample, though a small number yet, indicates a concentration of serious injuries in the lower leg area and only a minor risk in the upper body region. 9 of the 12 drivers had foot/lower leg injuries some of which we consider to be more severe than is induced by being classified AIS 3. The large intrusion of the footwell/firewall area of the car body structure observed in all GOC cases was the first hint to a particular mechanism causing the prevailing lower leg injuries. We name it the "impact shock syndrome".

#### THE IMPACT SHOCK SYNDROME

It is characterized by a high peak/short duration impact force exerted on the feet by the footwell or pedals which in turn is due to the large closing speed between the feet and the quickly intruding structure elements in the footwell area at the moment of contact (contact speed). In this moment both feet and footwell move relative to the passenger compartment, the feet in forward direction, the footwell in rearward direction due to the intrusion. During GOCs the footwell intrusion speed is extraordinary large because of the small overlap and the high collision speeds involved. So also the contact speed is high, but the masses of body parts involved are low, resulting in the high peak/short duration impact.

Using some elementary equations of applied mechanics together with plausible assumptions on car crash behavior [1] it can be shown that the contact speed  $v_c$  can be approximated by the formula

$$v_c = \frac{1}{2} EES \left( k + \frac{1}{k} \right).$$

In Fig. 2 the severity of foot/lower leg injuries is plotted against  $v_c$  for all 82 cases. The scatter range of NGOC data is indicated here by the upper and lower limit value only, for each AIS level. We realize that many GOC data points fall within the NGOC data ranges except at AIS 3 level. Here it seems to be obvious that the data points allocated to  $v_c$  above 70 km/h indicate injury severity above 3. But after the revision of the Abbreviated Injury Scale in 1980, classification of injuries below the knee in AIS levels above 3 is not possible any more. Besides this irregularity the contact speed has successfully served as a means to clarify a previously unrecorded injury mechanism. Future investigations should include any attempt to determine  $v_c$  more precisely, not only from accident analysis using EES evaluations, but also experimentally through improved crash testing. It can be expected that in case of unbelted occupants also the severity of head/thorax injuries properly correlates to a contact speed, then being the closing speed between upper body regions and an intruding steering wheel or dashboard.

#### REFERENCES

- [1] Zeidler, F., et al., Injury Mechanisms in Head-On Collisions Involving Glance-Off P-97, San Francisco, Society of Automotive Engineers, Inc., 400 Commonwealth Drive, Warrendale, Pennsylvania 15096, 1981.
- [2] Burg, Zeidler; EES - Ein Hilfsmittel zur Unfallrekonstruktion und dessen Auswirkungen auf die Unfallforschung. Der Verkehrsunfall, Heft 4, 1980.
- [3] The Abbreviated Injury Scale (1980 Revision), Copyright 1980 American Association for Automotive Medicine, Morton Grove, Illinois 60053, USA.

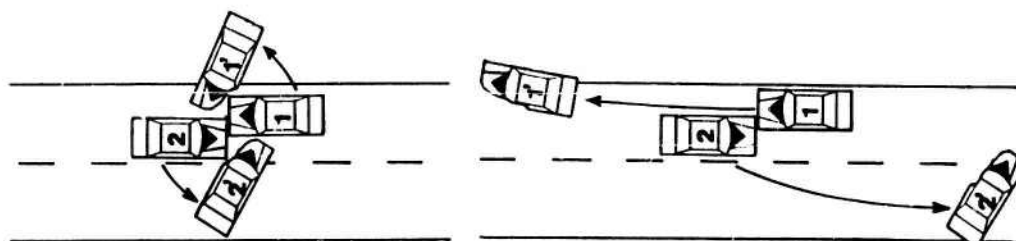


Fig. 1 Non-glance-off-collision

Glance-off-collision

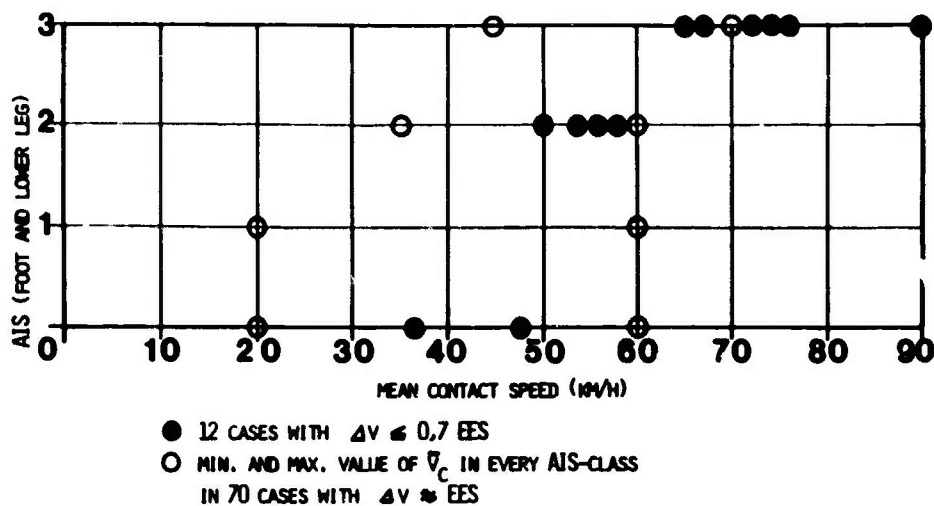


Fig. 2 Foot/lower leg injury severity versus contact speed

NO	WEIGHT (KG)		SPEED (KM/H)		OCC CASE VEH. OCC OTHER VEH.	V <sub>REL</sub> (KM/H)	EES (KM/H)	ΔV (KM/H)	AV OVER EES LAP %	
	CASE VEHICLE	OTHER VEHICLE	CASE VEHICLE	OTHER VEHICLE						
1	1525	820	60	100	12F06/77 12F07/85	160	55	25	0,46	25
2	1390	1240	65	75	12F09/88 12F05/83	140	60	37	0,62	28
3	1370	820	65	65	12F06/83 12F09/88	130	40	17	0,43	23
4	1345	1360	85	90	11F07/86 11F07/82	175	80	50	0,62	38
5	1375	1260	65	65	12F06/87 12F06/78	130	60	40	0,67	28
6	1340	1180	55	45	12F05/82 11F04/80	100	35	15	0,43	28
7	1755	950	110	65	11F06/73 11F08/80	175	60	30	0,5	40
8	1385	1430	50	70	12F03/88 12F08/82	120	50	30	0,6	30
9	1430	1385	70	50	12F08/82 12F08/88	120	50	30	0,6	31
10	1375	910	35	65	12F05/86 12F07/89	100	20	6	0,3	18
11	1375	810	65	45	12F03/88 12F08/88	110	30	10	0,33	30
12	1740	1360	85	75	11F06/89 11F06/77	160	70	50	0,7	45

Table 1 Vehicle data of 12 GOCs

NO	DATA OF DRIVER			INJURIES				
	AGE	WEIGHT (kg)	HEIGHT (cm)	LOWER EXTREMITIES	(AIS)	THORAX (AIS)	HEAD(AIS) NECK	PTS
1	41	80	180	FRACTURE AND DISLOCATION OF LEFT AND RIGHT ANKLE FRACTURE RIGHT TIBIA, FIBULA	(3)	NONE	LACERATION (1)	3
2	42	64	165	FRACTURES OF LEFT AND RIGHT TALO-CALCANEAL-NAVICULAR JOINT FRACTURE OF LEFT TIBIA	(3)	NONE	NONE	3
3	20	66	184	FRACTURE OF LEFT MALLEOLUS MEDIALIS	(2)	NONE	NONE	2
4	25	95	192	FRACTURES OF LEFT FEMUR, PATELLA, TIBIA, FIBULA, METATARSUS	(3)	ABRASION (1)	NONE FRACTURE (1)	3
5	22	95	175	CRUSH OF LEFT ANKLE DISLOCATION OF RIGHT ANKLE	(3)	NONE	NONE	3
6	20	65	174	NONE		BRUISE (1)	WHIPLASH (1) BRUISE	1
7	48	88	184	CRUSH OF LEFT ANKLE AND CALCANEUS DISLOCATION OF RIGHT ANKLE	(3)	NONE	NONE	3
8	54	95	174	DISLOCATION AND FRACTURE OF LEFT ANKLE	(2)	BRUISE (1)	WHIPLASH (1)	2
9	56	84	157	LACERATION INTO RIGHT KNEE-JOINT	(2)	BRUISE (1)	NONE	2
10	49	72	182	NONE		BRUISE (1)	NONE	1
11	38	65	170	DISLOCATION OF RIGHT MALLEOLUS MEDIALIS, FRACTURE OF MALLEOLUS LAT., PROX. FRACTURE OF RIGHT FIBULA	(2)	NONE	NONE	2
12	36	70	170	CRUSH OF RIGHT ANKLE, LACERATION RIGHT KNEE, FRACTURE OF LEFT METATARSUS	(3)	RIB FRACTURES(1)	LACERAT. (1) BRUISE (1)	3

Table 2 Driver data of 12 GOCs

## DISCUSSION

DR. LEVINE (USA)

These are severe injuries. I treat them. These fractures, although the AIS is only two or three, have long-term and lifetime impairments. These people have painful joints, they spend months in casts, and some do not heal. These are clinically very severe, impairing injuries, not life threatening, but they impair people. Many people will never be the same after a severe ankle fracture. They can't walk or run like they could before.

AUTHOR'S REPLY

We know this from cases, and that is the reason we consider it to be important, to be an objective for the automobile engineer to do something in that area.

DR. VON GIERKE (USA)

Would you propose a similar treatment of the absorbed energy, for example, for a multiple-impact helicopter crash?

AUTHOR'S REPLY

I have no idea what a helicopter crash is, except what I've seen today at this meeting. It may be that there is a way of reconstruction using some physical properties.

CARNELL (USA)

Can you give any idea of why the feet and legs were injured? Is it because flailing of the feet, or loss of living space in the space under the dashboard? Or is it just the impact loads on the pedals themselves? What is the cause of injury on the lower extremities?

AUTHOR'S REPLY

It is the impact with the feet and pedal or footwell in these particular cases where the rest of the vehicle, I should say, except a very small mass continues its path with only a minor reduction of speed. Whereas the footwell, or the intruding of the opposing vehicle into the compartment is very fast, very hard, high peak and short duration impact.

DR. VON GIERKE (USA)

I guess the question was, "Is it more the relative motion of the feet or is it more the compression of the free space?"

AUTHOR'S REPLY

The mechanism of injury is about 50-50.

DR. VON GIERKE (USA)

If the compartment would not collapse, would you always have the same ratio?

AUTHOR'S REPLY

No. You would not have the same contacts because we only have analyzed cases where the driver was belted. So that the belted driver may have a relative motion of his feet with respect to the compartment, but it may be attenuated by using a belt. If you started a similar analysis with unbelted drivers, I don't think you obtain any result. By using the upper torso restraint, the upper body is protected and legs are a significant remaining problem.

FRISCH (USA)

In the glance-off situation, you have a greater frequency of lower limb injuries than you do in frontal collisions?

AUTHOR'S REPLY

Not absolutely, but relatively; the distribution is different.

FRISCH (USA)

Is that due to the fact that in a frontal impact the car deforms uniformly and you have a breakaway engine and you don't have the sideward intrusion into the vehicle?

AUTHOR'S REPLY

Yes, we have a tremendous intrusion into the leg space at a high intrusion speed in the glance-off situation.

# ACCELERATION DAMAGE TO THE BRAIN

Thomas A. Gennarelli, M.D. and  
Lawrence E. Thibault, Sc.D.  
Departments of Neurosurgery and Bioengineering  
University of Pennsylvania,  
Philadelphia, Pa. 19104 U.S.A.

**Summary:** On the basis of 150 primate experiments utilizing controlled head acceleration the authors conclude that a unitary tolerance for head injury is unrealistic. Rather, a series of tolerance criteria exist that define two fundamentally different kinds of mechanically induced intracranial injury --- vascular and axonal. The mixture of these two injury types is largely determined by the magnitude and the time-history of the loading condition because of differences in the material properties of the vascular and axonal elements. The topographical distribution of the injured elements will be determined by the kinematics of the loading condition because of asymmetries of geometry, anatomy and constitutive behavior of the intracranial contents. In light of these findings the effect of acceleration on the brain is presented for the continuum of diffuse brain injuries and for acute subdural hematoma.

## Acceleration Damage to the Brain

In 1974 Ommaya and Gennarelli proposed an hypothesis for cerebral concussion and traumatic unconsciousness. (1) (Figure 1A). This hypothesis suggested that cerebral concussion and prolonged traumatic unconsciousness formed a continuum of increasingly severe clinical syndromes which were graded into six varieties. Our work since that time has been targeted to a more comprehensive understanding of this continuum of injuries and has placed special emphasis on the more severe varieties of traumatic unconsciousness. This paper reviews our approach to this problem and demonstrates our current concepts of tolerances of the brain to acceleration based on results synthesized from 150 acceleration head injuries in a primate model (2-5).

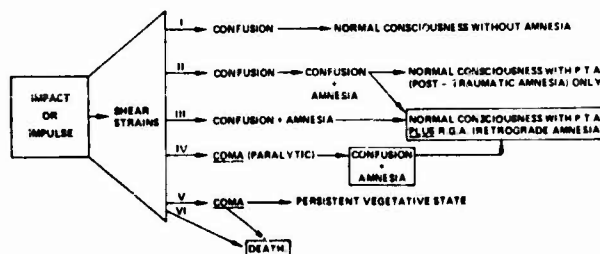
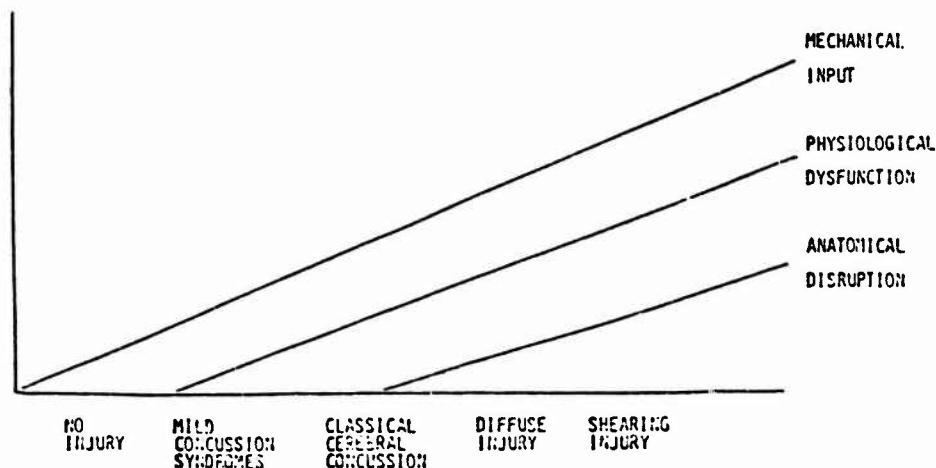


Figure 1A

Figure 1B





### Cerebral Concussion and Prolonged Traumatic Coma: a continuum

The conceptual format for our understanding of these injuries is presented in Figure 1B. Thus it is postulated that as the mechanical input to the head and brain progressively increases, the clinical result is that of progressively more severe traumatic unconsciousness. Thus very low levels of trauma cause no injury whatsoever but at some point as input is increased, temporary reversible neurological dysfunction without loss of consciousness occurs. Thus grades 1, 2, and 3 in Figure 1A are lumped together in Figure 1B under the heading Mild Concussion Syndromes. Further increases in the mechanical input to the head results in transient reversible loss of consciousness previously called paralytic coma (Figure 1A) but now called classical cerebral concussion (Figure 1B). As mechanical input increases further, prolonged traumatic unconsciousness occurs (Grade 5 and 6 in Figure 1A). Though clinicians tend to lump all such patients who have prolonged unconsciousness and no mass lesion under the term "diffuse brain injuries" or simply "diffuse injuries", it is important to recognize at least two varieties of prolonged traumatic unconsciousness. For want of better terms, in Figure 1B these are called diffuse injury and shearing injury. Diffuse injury in this scheme refers to those patients who are unconscious for more than 24 hours who have normal motor responses while shearing injury includes patients with prolonged coma who exhibit inappropriate decorticate or decerebrate spontaneous or reflexive motor movements. Thus it is clear from clinical observations that physiological dysfunction begins quite early in this scheme (with the mild concussion syndromes) and progresses along the injury severity continuum so that at the end of the spectrum, patients with shearing injury have very large amounts of physiological dysfunction.

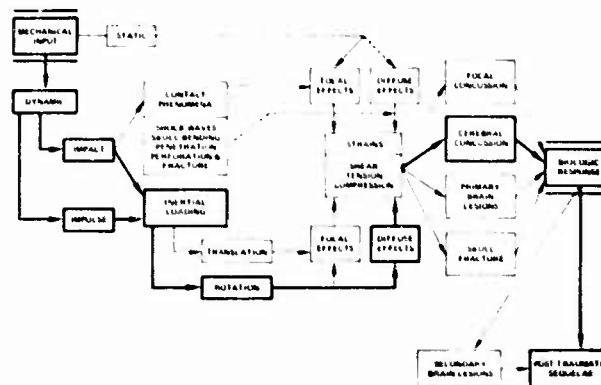
At the severe end of the severity spectrum a characteristic neuropathological lesion complex is well recognized and it is therefore a reasonable assumption that if the clinical symptomatology is progressively more severe so must the pathological spectrum. It is therefore postulated that anatomical disruption is very minimal at some point in this spectrum but that it progressively increases until the classical findings associated with shearing injury occur. These have been described by Strich (6-9) and by Adams et al. (10-12) and include minimal, but highly significant, focal macroscopic injuries in the corpus callosum and rostral brainstem adjacent to the superior cerebellar peduncle. The hallmark of this lesion is, however, the microscopic appearance of disrupted axons manifest by axonal retraction balls. If survival is longer, microglial clusters occur where axons have been injured. The distribution of axonal retraction balls and microglial clusters is widespread throughout the hemispheres and brainstem, hence a justification of the term diffuse. Long survival is compatible with functional recovery to vegetative or severely impaired existence and is associated with demyelination and long tract degeneration.

That these diffuse brain injuries are important was recently pointed out by Gennarelli et al. in a series of 1107 severely head injured patients (13). Patients with prolonged traumatic unconsciousness of more than 6 hours duration who had no mass lesions comprised 44% of severely head injured patients and had a mortality rate of 32%. This mortality was substantially higher in the shearing injury patients (57%). It was found that the patients with prolonged traumatic unconsciousness (>24 hours), because of their high incidence and because of their high mortality, were responsible for 32% of all head injury deaths, a number only exceeded by acute subdural hematoma. This study demonstrated that subdural hematoma and prolonged traumatic unconsciousness (diffuse brain injury) accounted for more deaths than all other head injury lesions combined.

### Development of a Model of Prolonged Traumatic Unconsciousness:

Because of the clinical importance of this group of diffuse brain injuries, it was felt that an appropriate laboratory model of these injuries should be created for further in-depth studies. In order to do so, a concept of the mechanisms which cause head injury was reviewed (Figure 2). Because of the extreme complexity of clinical head injury it

Figure 2

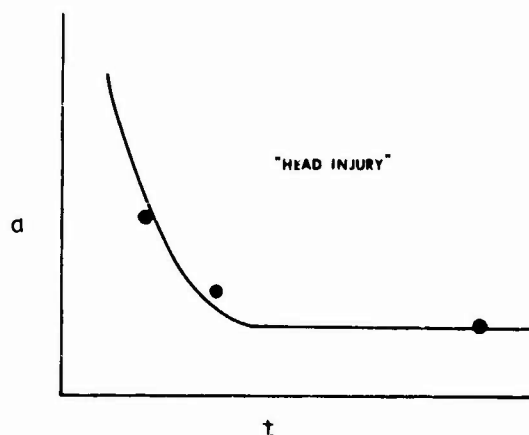


was thought most prudent to study individual injurious mechanisms as separately as possible. In 1971 Gennarelli, Ommaya and Thibault demonstrated that cerebral concussion could be readily produced by non-impact inertial loading of the head utilizing angular acceleration only (2). Since it was felt (Figure 1B) that cerebral concussion was along the same continuum of injury as the desired shearing injury, it was reasonable to assume that all that had to be done was to increase the acceleration level above that which causes cerebral concussion and diffuse injury with prolonged unconsciousness would result.

Relation to existing Tolerance Criteria:

Our initial experiments proceeded with this concept in mind and were based on the accepted concept of injury tolerance. Figure 3A demonstrates the currently accepted injury tolerance curve which demonstrates an acceleration-time dependence. The shape of this curve was initially generated by Gurdjian and co-workers to represent a threshold of "head injury" and was based on three data points from widely differing situations (14, 15).

Figure 3A



One data point had a very short pulse duration (t); one data point was near the end of the downslope of this curve and one data point was far to the right at the low acceleration, long pulse duration end of the curve. These three data points were then connected to form this familiar curve. The curve however did have some basis in mechanics, since this curve, in effect, provides for equivalent energy inputs into the head. Unfortunately, the three points comprised markedly differing data: cadaver drop experiments, impact to dog's skull, and human acceleration sled rides with acceleration measured on the chest and not the head.

Figure 3B

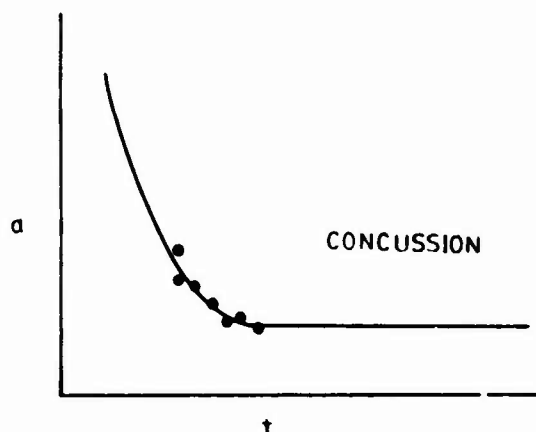
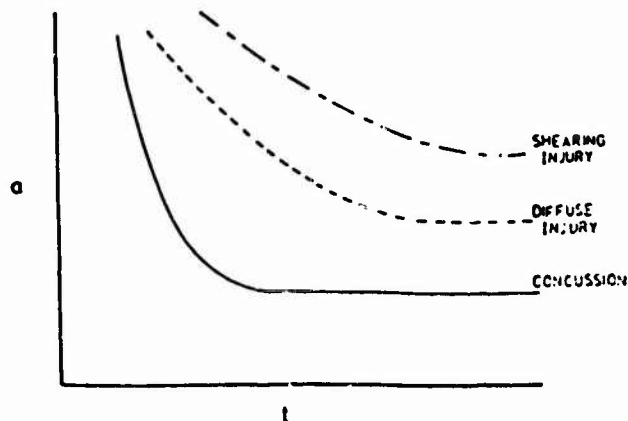


Figure 3C



However, further workers, notably Ommaya and Hirsch, did provide a similar shaped acceleration time curve for experimental cerebral concussion in the sub-human primate (16) (Figure 3B). This work however also presumed the curve shape, for the data was, in fact, limited to the lower part of the downslope and very first part of the horizontal asymptote. Nevertheless, a tolerance curve of this shape became the standard in the head injury tolerance field. Based on this working presumption, we assumed that in order to create the desired diffuse and shearing injuries one had to simply increase the acceleration levels to create the entire continuum of injury (Figure 3C).

#### The Acute Subdural Hematoma (SDH):

Based upon the assumption that diffuse injury and shearing injury were a more severe injury than concussion, we began to increase acceleration levels above those which cause concussion. To our disappointment increased acceleration levels at the short durations dictated by our injury apparatus did not create prolonged traumatic unconsciousness. There appeared to be no prolongation of the relatively standard 5 to 30 minute transient unconsciousness of the classical cerebral concussion. However as acceleration was increased further, first small, then quite massive subdural hematomas were produced. The size of these hematomas was sufficient to cause prompt death of the animals and careful neuropathological examination disclosed no evidence of internal brain injury. Gross pathological dissection did document the cause of the subdural hematoma however. This was shown to be due to rupture and failure of the parasagittal subdural bridging veins. (17)

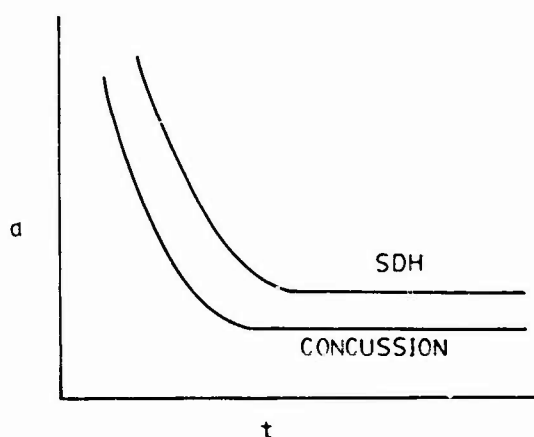


Figure 4A

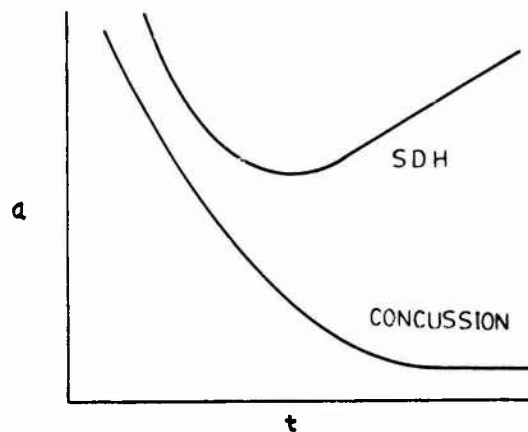


Figure 4B

We therefore concluded that a tolerance for subdural hematoma existed slightly above the tolerance threshold for concussion as depicted in Figure 4A. This hypothetical construct conformed to the existing concept of brain injury tolerances, but it soon became apparent that such a construct could not be valid. The situation depicted in Figure 4A would demand that there could never exist a shearing injury in the absence of subdural hematoma since the threshold for subdural hematoma was lower than that for shearing injury. This however could not be the case since clinical experience shows quite readily that the shearing injury can occur in the absence of subdural hematoma. It therefore became obvious that a tolerance curve for subdural hematoma must differ from the shape of that of concussion such as shown in Figure 4B. In fact on review of our experimental data such a tolerance curve for subdural hematoma seemed to exist. Our data defined a linear relationship between acceleration and pulse duration that begins at 3.5 msec acceleration duration at  $1.5 \times 10^5$  radians/sec<sup>2</sup> and increases with a slope of  $3 \times 10^4$  radians/sec<sup>2</sup> per millisecond of increasing pulse duration.

The mechanical reasons why this curve should be so are found in an evaluation of the properties of subdural veins. Lowenhielm demonstrated the viscoelastic nature of the subdural bridging veins in 1974 (18, 19). He reported that subdural bridging veins exhibit marked strain rate sensitivity, similar in nature to the viscoelastic behavior of other biological tissue. Thus, ultimate strain to mechanical failure is low when strain rates are high and increases as strain rate decreases. Translated to the more familiar acceleration-duration expression of the head injury tolerance curve, acceleration is proportional to ultimate strain to failure and acceleration duration is related to strain rate given the same shape of the acceleration-time history. Thus a tolerance curve for subdural hematoma of the shape shown in Figure 4B is explainable by the viscoelastic nature of the bridging veins whose rupture cause the subdural hematoma. Based on Lowenhielm's data, a simplified mathematical model was exercised and a tolerance curve for subdural hematoma was achieved (20). As shown in Figure 4C, our experimental data for SDH fall within the zone predicted by this model.

Figure 4C

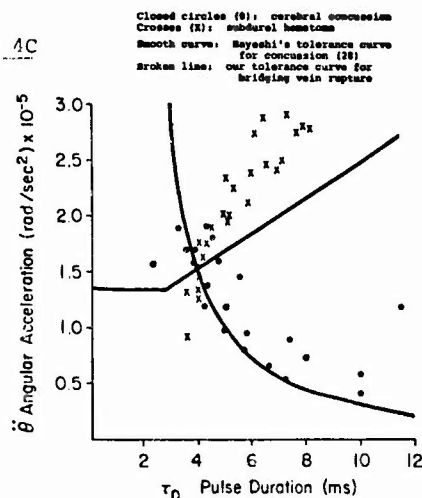
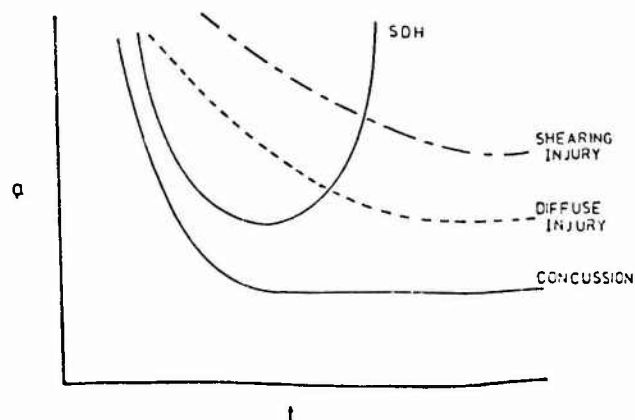


Figure 4D



#### Prolonged Coma and Diffuse Axonal Injury:

A second hypothetical construct to explain our findings was then proposed and is shown in Figure 4D. Here the shape of the tolerance curves of concussion and subdural hematoma interact with proposed tolerance curves for diffuse injury and shearing injury. This allows a window of acceleration-time history that can produce concussion alone, subdural hematoma alone, subdural hematoma plus either diffuse injury or shearing injury and finally diffuse injury or shearing injury alone. Through this working hypothesis our acceleration apparatus was modified to provide longer pulse duration (and lower strain rate) at the same acceleration level. In increasing the pulse duration, prolonged traumatic unconsciousness was produced for the first time in any experimental model. By appropriate manipulation of acceleration-time-direction of input, traumatic unconsciousness could be extended from the usual 5 to 30 minutes to, at first, several hours without any abnormal motor movements (diffuse injury) and finally to traumatic unconsciousness lasting for several days accompanied by decorticate and decerebrate responses (shearing injury). The neuropathological observations in this latter group of animals demonstrated an identical picture to the shearing injury seen in human cases. That is, macroscopic tears in the corpus callosum and rostral brainstem were present in association with widespread diffuse axonal retraction balls in the cerebral hemispheres and upper brainstem. Thus the entire spectrum of cerebral concussion and traumatic unconsciousness (Figure 1A and B) could be in fact be duplicated in an experimental model.

Our current data favors a model with tolerances such as depicted in Figure 5A. This can be viewed as our specific hypothesis and demonstrates that at acceleration levels which are applied rapidly, subdural hematoma occurs due to rupture of bridging veins because of their strain-rate sensitivity. At similar accelerations applied for longer time periods the clinical syndromes of traumatic prolonged unconsciousness (diffuse injury and shearing injury) begin to occur. An intermediate acceleration-time history will provide superimposition of these two phenomena and an intermediate zone which results in clinical injuries which have both subdural hematoma and evidence of axonal injury. These cases have been reported by Clark (21), Peerless (22) and others (23-26) and are probably more frequent if careful neuropathological examination of patients with subdural hematoma were performed. That our data support this concept is shown in Figure 5B.

Figure 5A

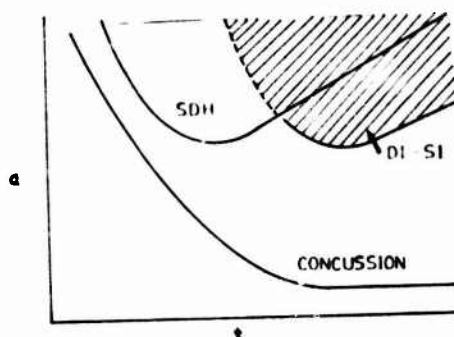
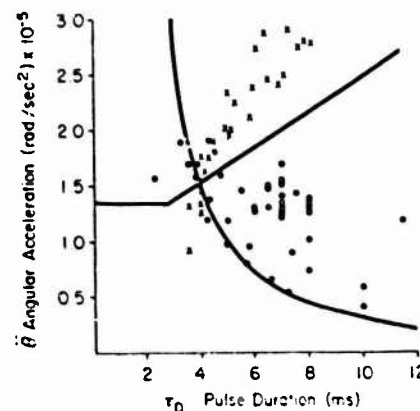


Figure 5B

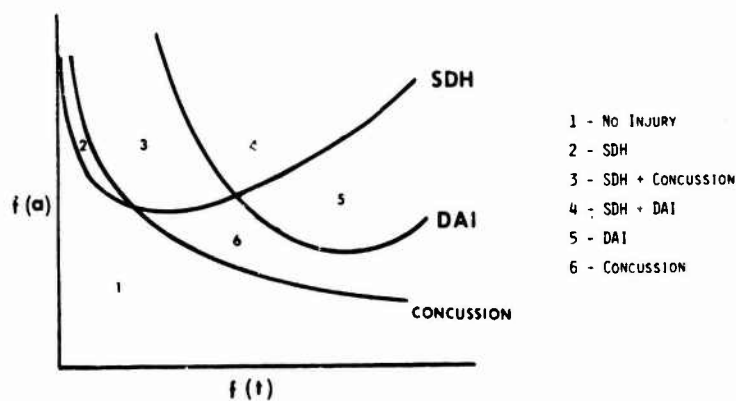
Open circles (○): prolonged coma  
All other symbols are as in Figure 4C



It also became apparent that one could begin to generalize this specific hypothesis. Since diffuse injury and shearing injury are parts of a clinical spectrum that correlate with a pathological spectrum of axonal injury manifest by increasing numbers of axonal retraction balls, this clinical complex could be viewed as differing amounts of the same injury to axons. Since axons exhibit the same type of viscoelastic behavior as do subdural bridging veins, it is reasonable to assume that the tolerance curve shape would be similar to that of subdural hematoma. This was corroborated in the mathematical model of Liu who demonstrated that materials with different viscoelastic properties all exhibit a similar wave shape which differs only in its placement on the acceleration-time axis (27). This allows us to conceptualize the injury not in clinical terms but in pathological-mechanical terms and to consider the diffuse-shearing injury tolerance as that of axons, to which we have applied the term diffuse axonal injury (DAI).

That DAI does, in fact, have a pathological spectrum was recently confirmed by a careful clinical-pathological examination of our animal material. We therefore suggest that the spectrum of DAI is responsible for the clinical spectrum proposed in Figure 1B. Axonal injury without disruption would be responsible for the lesser degrees of clinical injury (mild concussion and possibly classical cerebral concussion) while disruptive axonal injury causes the more severe injuries. (See also Figure 7B)

Figure 6A

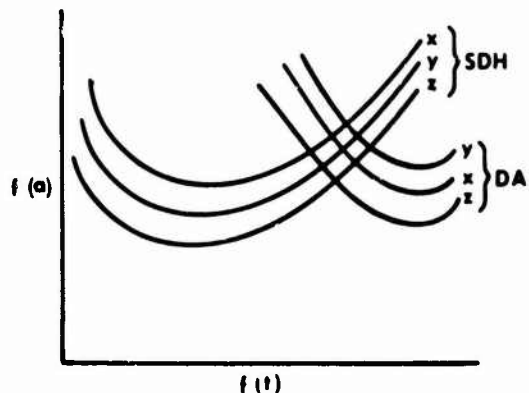


#### Current Concepts of the Effects of Acceleration on the Brain: Families of Head Injury Tolerances:

In general, Figure 6A summarizes our current conceptualization of the effect of acceleration on the brain. Acceleration is the principal mechanism leading to the two greatest causes of head injury death and disability--subdural hematoma and diffuse axonal injury. The determinants of these injuries reflect the mechanical properties of the

Figure 6B

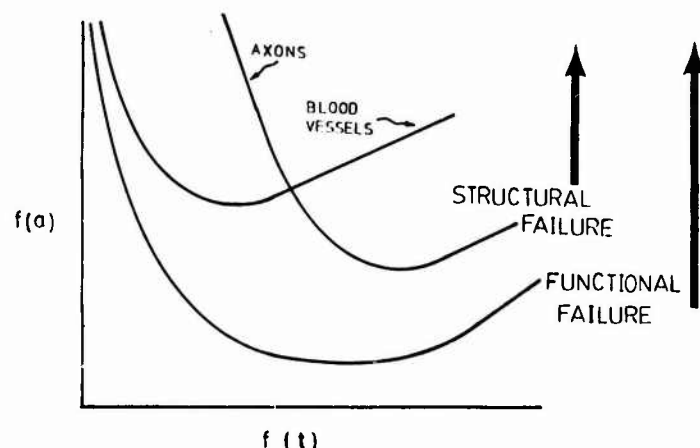
xyz indicate axis of acceleration



injured elements - bridging veins and axons respectively. As a first approximation the determinants are acceleration magnitude and strain rate, the latter being related to acceleration duration if the wave shape of the acceleration-time history is constant. These structural failure tolerance curves interact with a functional failure tolerance for reversible traumatic unconsciousness (cerebral concussion) to predict several types of injury combinations (as shown in Figure 6A).

This simplified view of injury tolerances is, of course, only an approximation and kinematic considerations can be added to the kinetic considerations as shown diagrammatically in Figure 6B. Thus axonal or bridging vein tolerances, because of tissue inhomogeneity and geometric peculiarities, will differ in magnitude, in location and in relative proportion depending on the direction of head acceleration.

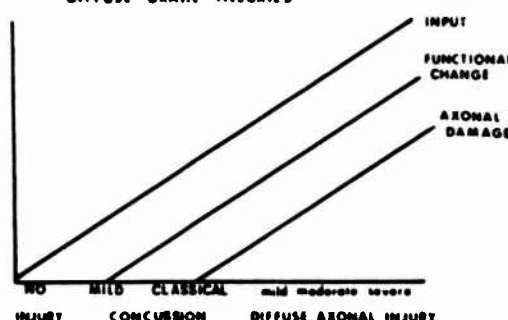
Figure 7A



Furthermore, we have noted that, as our experimental model produced more axonal injury and less subdural hematoma, fewer and fewer contusions were present. The experimental model in a few instances did reproduce the transition zone where subdural hematoma and axonal injury are combined. This zone produced a contusional state intermediate between the large deep contusions associated with the pure subdural hematoma and the virtually non-existent contusional state which accompanied severe DAI. Thus Figure 7A is a general hypothesis of head injury which generalizes the subdural hematoma curve to include all blood vessels of the brain and the DAI curve to represent diffuse axonal injury in general. This general hypothesis then explains not only the three conditions of pure subdural hematoma, pure axonal injury and a combination of both, but it also demonstrates that vascular elements that are disrupted within the brain (causing contusions) may follow a similar injury tolerance curve as do the subdural bridging veins. Thus Figure 7A becomes our current formulation of head injury mechanisms in kinetic terms. It can be related to Figure 7B where a zone of functional failure occurs without obvious structural disruption. Clinically this corresponds to the mild concussion syndrome and perhaps some of the classical cerebral concussion. Soon however, if the appropriate acceleration-time history is delivered to the head, structural failure begins, either of the axons or of the blood vessels. If the acceleration-time history is appropriate, pure axonal injury begins and causes the more severe types of cerebral concussion and prolonged unconsciousness of either the diffuse injury (moderate DAI) or shearing injury (severe DAI) clinical types. As these occur, structural failure increases in magnitude to the point where the classical injury described by Strich and Adams et al. occurs. Thus the spectrum of diffuse brain injuries can, in fact, occur with the appropriate loading conditions. In the general hypothesis the precise tolerance shapes are not yet known and are yet to be determined. Similarly, the precise function of acceleration and of time which best fit this hypothesis need to be further investigated.

DIFFUSE BRAIN INJURIES

Figure 7B



1. Ommaya, AD, Gennarelli, TA: Cerebral concussion and traumatic unconsciousness. Correlation of experimental and clinical observations on blunt head injuries. Brain 97:633-654, 1974.
2. Gennarelli, TA, Ommaya, AK, Thibault, LE: Comparison of linear and rotation acceleration in experimental cerebral concussion. In Proceeding of the 15th Stapp Car Crash Conference, New York, Society of Automotive Engineers, pp.802, 1971.
3. Gennarelli, TA, Thibault, LE, Ommaya, AK: Pathophysiologic responses to rotation and translational acceleration of the head. 16th Stapp Car Crash Conference. New York, Society of Automotive Engineers, pp. 296-308, 1972.
4. Abel, J, Gennarelli, TA, Segawa, H: Incidence and severity of cerebral concussion in the rhesus monkey following sagittal plane angular acceleration. in 22nd Stapp Car Crash Conference Proceedings, SAE, New York, 1978, pp. 33-53.
5. Gennarelli, TA, Adams, JH, Graham, DI: Acceleration induced head injury in the monkey: The model, its mechanical and physiological correlates. Acta Neuropath. Suppl. VII, Experimental and Clinical Neuropathology, Jellinger, K. (ed), Springer-Verlag, 23-25, 1981.
6. Stritch, SJ: Diffuse degeneration of the cerebral white matter in severe dementia following head injury. J. Neurol. Neurosurg. Psychiat. 19:163-185, 1956.
7. Strich, SJ: Lesions in the cerebral hemispheres after blunt head injury. J. Clin. Path. 23, Suppl., 4:166-171, 1970.
8. Strich, SJ: Shearing of nerve fibers as a cause of brain damage due to head injury. Lancet 2:443-448, 1961.
9. Strich, SJ: The pathology of brain damage due to blunt head injuries. In Walker, A.E. Caveness, W.F., Critchley, M. (eds), The Late Effects of Head Injury. Thomas, Springfield, pp. 501-524.
10. Adams, JH, Mitchell, DE, Graham, DI, Doyle, D: Diffuse brain damage of immediate impact type. Brain 100:489-502, 1977.
11. Adams, JH, Graham, DI, Scott, G, et al: Brain damage in fatal non-missile head injury. J. Clin. Path. 33:1132-1145, 1980.
12. Gennarelli, TA, Ommaya, AK, Thibault, LE: Comparison of linear and rotation acceleration in experimental cerebral concussion. In Proceedings of the 15th Stapp Car Crash Conference, New York, Society of Automotive Engineers, pp. 797-802, 1971.
13. Gennarelli, TA, Spielman, G, Langfitt, TW, et al: Influence of the type of intracranial lesion on outcome from severe head injury: A multicenter study using a new classification system. J. Neurosurg. 56:26-32, 1982.
14. Gurdjian, ES, Webster, JE: Experimental head injury with special reference to mechanical factors in acute trauma. Surg. Gynec. Obstet. 76:623-624, 1943.
15. Lissner, HR, Lebor, M, Evans, FG: Experimental studies on the relation between acceleration and intracranial pressure changes in man. Surg. Gynecol. Obstet. 111:329-338, 1960.
16. Ommaya, AK, Hirsch, AE, Martinez, JL: The role of whiplash in cerebral concussion. in The 10th Stapp Car Crash Conference, SAE, New York, pp. 314-324, 1966.
17. Adams, JH, Graham, DI, Gennarelli, TA: Acceleration induced head injury in the monkey: Neuropathology. Acta Neuropath. Suppl. VII:26-28, 1981.
18. Lowenhielm, P: Strain tolerance of the Vv cerebri sup. (bridging veins) calculated from head-on collision tests with cadavers. Z. Rechtsmedizin 75:131-144, 1974.
19. Lowenhielm, P: Mathematical simulation of gliding contusions. J. Biomechanics, 8:351-356, 1975.
20. Gennarelli, TA, Thibault, LE, Thompson, C, et al: Diffuse axonal injury produced by angular acceleration in the subhuman primate. New Eng. J. Med., submitted 1981.
21. Clark, JM: Distribution of microglial clusters in the brain after head injury. J. Neurol. Neurosurg. Psychiat. 37:463-474, 1974.
22. Peerless, SJ, Rewcastle, NB: Shear injuries of the brain. Canadian Med. Assn. J. 96:577-582, 1967.

23. Nevin, NC: Neuropathological changes in the white matter following head injury.  
J. Neuropathol. Exp. Neurol. 26:77-84, 1967.
24. Clark, JM: Distribution of microglial clusters in the brain after head injury.  
J. Neurol. Neurosurg. Psychiat. 37:463-474, 1974.
25. Oppenheimer, DR: Microscopic lesions in the brain following head injury.  
J. Neurol. Neurosurg. Psychiat. 31:299-306, 1968.
26. Rand, CS, Corville, CB: Histologic changes in the brain in cases of fatal injury to the head. Arch. Neurol. Psychiat. (Chicago) 31:527-555, 1934.
27. Liu, YK, Chandran, KB, von Rosenberg, DV: Angular acceleration of viscoelastic (Kelvin) material in a rigid spherical shell - a rotational head injury model.  
Math. Biosci. 6:473-486, 1970.
28. Hayashi, T: Brain shear theory of head injury due to rotational impact.  
J. of the Faculty of Engineering, Univ. of Tykyo (B), 30:4, 1970.



## DISCUSSION

DR. VON GIERKE (USA)

You spoke about a very controlled inertia loading input, but if I understand the set up correctly, you have the bending of the spinal cord involved. This has been shown to be potential input to concussion which is called acceleration concussion, but the focus is in the bending speed of the spinal cord and not cerebral.

## AUTHOR'S REPLY

I think that it will still be many, many years before the focus or location of concussion is agreed upon by all. What we can tell you is that when we increase the input that we see the axonal pathology that I demonstrated in the white matter of the hemispheres in the upper brain stem; but even under microscopic examination, we do not see it in the cervical spine. One would anticipate that if the cervical spine was the first thing to be injured, then as one increases the impact energy, we would expect to see something in the area. I certainly agree that the influence of the cervical spinal cord may have quite a bit to do with brain injury.

## UNIDENTIFIED QUESTIONER

You didn't say what kind of animal you used?

## AUTHOR'S REPLY

We used the baboon because of the brain size, but we have used squirrel monkeys, rhesus monkeys, and various species. We've not used subprimates.

DR. UNTERHARN SCHIEDT (USA)

We propose a family of at least three different concussion types. I think before I discuss this, I present my paper, and we can discuss this with questions later.

The Development of Intracranial Tissue Component  
Failure Criteria as a Consequence of Controlled Inertial Loading

Lawrence E. Thibault, Sc.D. \*  
Thomas A. Gennarelli, M.D. \*\*

\* Department of Bioengineering  
\*\* Department of Neurosurgery  
University of Pennsylvania  
Philadelphia, Pennsylvania 19104, U.S.A.

### Summary

Acute subdural hematoma and diffuse axonal injury have been shown (1) to be responsible for the large majority of deaths and/or disabilities associated with head injuries. In order to develop a set of criteria which describe the tolerance of the head to mechanical loading (and thereby gain better insight into methods of protection) it appears that it is necessary to describe, and to understand discretely the behavior of those components which constitute the intracranial contents. Specifically, the behavior of the vascular and neuronal elements under dynamic loading conditions needs to be further elucidated.

Physical and animal experimental models conducted in conjunction with isolated tissue studies will then permit us to relate the more macroscopic phenomena, such as the input force-time history or kinematical response of the head, to the variation of the field parameters within the intracranial vault and the concomitant changes in neurophysiology and neurohistology.

### Introduction

A well distributed impulsive load or an almost purely inertial loading condition applied to the head can produce a broad spectrum of injury modalities. The specific nature of these acceleration-induced brain injuries and the associated pathophysiological consequences can often be described in terms of failure of the discrete tissue elements which constitute this structure. In order to be able to protect the intracranial contents from damage it is essential that those loading conditions which are responsible for the high incidence of mortality and morbidity are well defined and that the relationships between the generalized mechanical input conditions and the resulting variations in the field parameters are understood. Once the spatial and temporal variations in the strain for example can be determined as a function of the loading it is then possible to examine a set of relevant failure criteria for the isolated tissue components. This report presents a three phase approach directed toward achieving these goals.

Figure 1. shows in diagrammatic form the elements of the subject study. The first phase consists of a series of primate experiments in which a system has been developed with the capability of producing those forms of injury which result in the highest rates of mortality and morbidity (acute subdural hematoma and diffuse axonal injury). The loading conditions in this experiment can be finely controlled, i.e., the acceleration amplitude, pulse duration and rise time are adjustable and the kinematical conditions such as center of rotation, axis of rotation and degree of angular excursion can be independently adjusted. The details of these experiments and the sensitivity of the animal model to the parameters mentioned will be discussed.

The second phase, which is designed to provide the necessary data to relate the input loading to the variation in the field parameters, is an experimental study of physical models of the skull and surrogate brain under identical loading conditions that the animal model experiences. These data can also serve to validate existing mathematical models and to perhaps provide necessary scaling information to be able to transfer findings from the subhuman primate studies to man.

The third phase of the program is designed to investigate the sensitivity of isolated vascular and neuronal tissue elements to mechanical deformation. Failure of these tissue components in response to mechanical deformation is not restricted to the more classical engineering failure criteria, which are structural in nature, but, must include functional changes in these living systems. Isolated neural tissue studies will be discussed in this context.

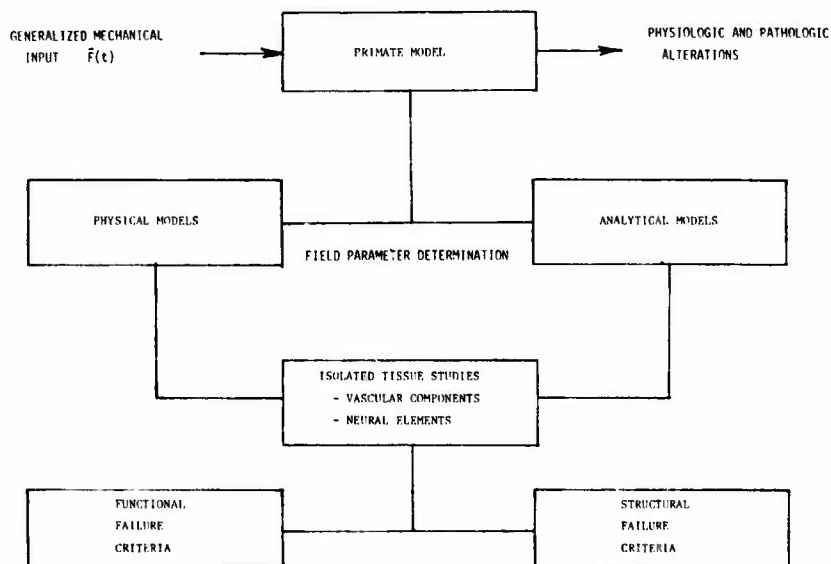


Figure 1

### Methods

Angular acceleration of the head was first used by Unterharnscheidt (2) to produce controlled forms of head injury in the primate. Subsequently, this model was extended to discretely examine cerebral concussion (3), (4) and more recently, subdural hematoma (5). In all cases the head was captured rigidly by a fixture and the driving mechanism produced an angular acceleration which was restricted to the sagittal plane. Further, the acceleration waveforms were relatively symmetric with respect to the acceleration and deceleration phase. The pulse durations in most cases were less than 4 msec and the rates of onset were approximately  $10^6$  g's per second and greater.

The system described herein is capable of shaping the acceleration-time history of the load and extending the deceleration phase pulse duration to beyond 10 msec. The device is also designed to produce a variety of kinematical conditions with respect to the head motion. We believe that because of the asymmetry of the head/neck structure this will undoubtedly alter the resulting variation in the field parameters.

The prime mover used in this system is a six-inch diameter HYGE<sup>R</sup> linear actuator (Consolidated Vacuum Corp., U.S.A.). The Hyge design permits wave shaping by modifying the internal acceleration and deceleration metering pins. The normal stroke of this unit is six inches. The design modifications to the standard Hyge unit include: decreased stroke length to 3.25 inches by modifying the deceleration pin length, redesign the acceleration pin contour to increase terminal velocity and thereby compensate for decreased stroke length, and finally, redesign of the deceleration pin contour to control deceleration phase pulse duration. Figure 2. depicts the system in schematic form. The cut-away view of the Hyge actuator shows the thrust column, piston, acceleration and deceleration metering pins. The unit is coupled to a linkage which converts the translational motion of the thrust column into an angular motion of the fixture which rigidly supports the head. In the case shown the motion is restricted to the sagittal plane. The linkage assembly is fabricated primarily from titanium for high strength to weight ratio. Relatively simple alterations prior to an experiment permits one to vary the center of rotation and the degree of angular excursion independently. Also shown in the figure are two calibration curves where the "set pressure" (the pressure on the downstream face of the piston) is varied to determine the peak deceleration amplitude. The two curves represent two different metering pin contours, both of which are half sines with deceleration pulse durations of approximately 8 and 11 msec. As can be seen the deceleration amplitude is a linear function of the set-pressure on the system.

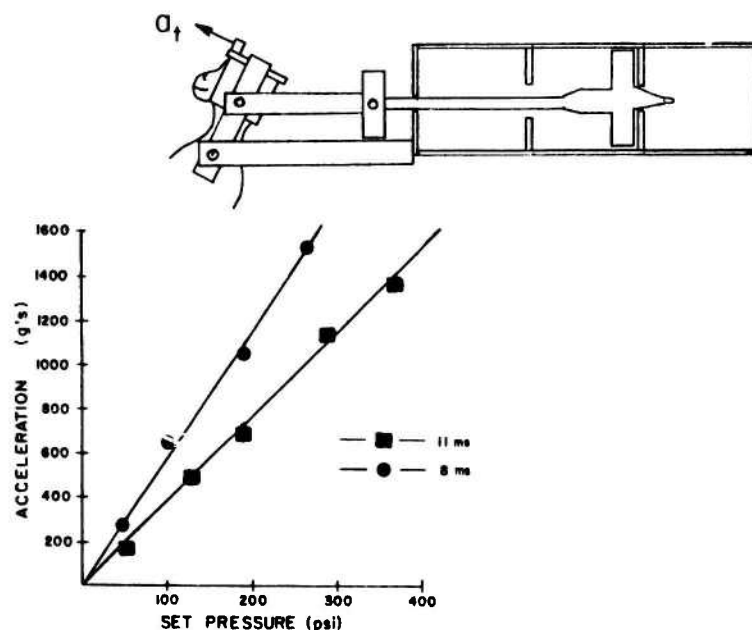


Figure 2

Acceleration measurements are made using piezoelectric accelerometers and appropriate amplifiers and recording system (ENDEVCO, U.S.A.). The accelerometers are fastened to the linkage in such a way that the sensitive axis is oriented tangentially at a fixed radial location. The animal's head is captured into a helmet by using dental cement as a potting compound. The head location and orientation is fixed relative to the helmet with the aid of ear canal pins. The helmet is then attached to the kinematic linkage.

Figure 3 shows a typical acceleration time history experienced by the animal model. As can be seen the acceleration and deceleration phases are approximately sinusoidal but asymmetric with respect to amplitude and duration. The deceleration amplitude in this case is approximately 1700 g's at the transducer which translates into 1150 g's at the center of mass of the brain and it is directed tangentially. The pulse duration of the deceleration phase in this case is approximately 8 msec with a rate of onset of  $2.8 \times 10^5$  g's per second. As discussed previously, this loading can be applied in the  $w_x$ ,  $w_y$  or  $w_z$  directions. In these experiments the  $w_x$  and  $w_y$  directions were used exclusively with the center of rotation in both cases located at approximately T-1, the first thoracic vertebral element.

Conventional physiological monitoring is performed and supplemented with neurological and behavioral examinations. The somatosensory evoked response using median nerve stimulation is measured bilaterally with the aid of a PDP-11 (Digital Equipment Corp., U.S.A.) computer.

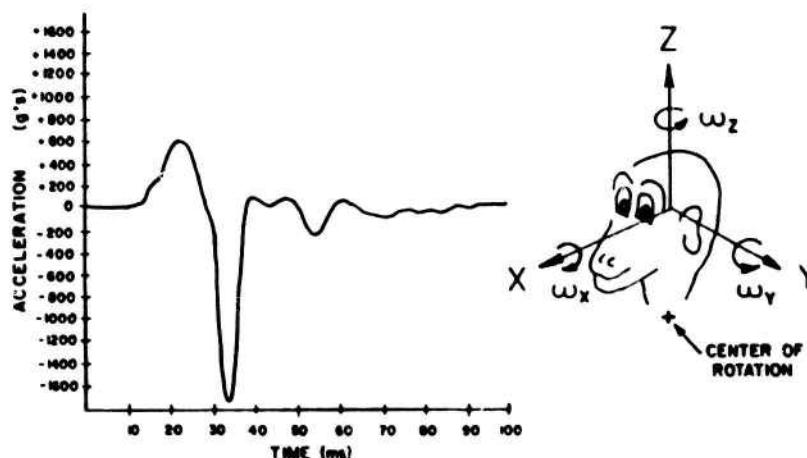


Figure 3

Phase II of the study focuses on the experimental determination of the field parameters utilizing physical models of the baboon. The models are constructed by taking sagittal, coronal or horizontal sections through a baboon skull, thereby obtaining a geometrically accurate boundary. A surrogate brain material (Sylgard dielectric gel, Dow Chemical) is cast into the skull sections. This material is optically transparent and can be cast in layers which adhere upon curing. On any given layer a grid may be printed to provide a means of measuring displacement of the elements of the plane of interest. The physical models are then subjected to the identical loading condition as the animal model. High speed photography of the physical models is obtained using a HYCAM camera at 4000 frames per second. Again, these models can be run in the sagittal, lateral or torsional modes similar to the animal model.

Phase III of this study is designed to investigate the mechanical properties of isolated neural and vascular tissue, though the primary emphasis here will be placed on the former. The intention is to develop a set of failure criteria for isolated tissue which may be described in structural and/or functional terms.

A system has been developed which is capable of applying either axial or torsional loads to an isolated nerve fiber while monitoring the compound action potential elicited by electrical stimulation. Desirable features of this system include: an atraumatic method of gripping the fiber which provides uniform load distribution at the point of attachment, a suitable environmental condition in order to maintain a viable tissue preparation, the ability to obtain any desired initial state of fiber strain, a method to produce a programmable displacement-time history of the movable fiber end, and last a monitoring system for both the mechanical and physiological variables. This system is shown in block diagram form in Figure 4. The system in essence is a miniature materials testing machine, capable of applying loads from static conditions to relatively high strain rates. The displacement is measured optically with an MTI-KD-100 Fotonic Sensor which provides a non-contact, high frequency response method of obtaining strain and strain rate. The load is measured by a Statham UC 2 "Green Cell" ( $\pm 30$  gm,  $\pm .06$  mm) force transducer and amplifier. The load cell is attached to the stationary end of the nerve fiber fixture and is relatively isometric as can be seen from the above specifications. The physiological instrumentation includes a Grass Stimulator Model 98, Isolation Unit SI05A and Physiological Amplifier P511J. A record of the compound action potential was obtained by periodically photographing the CRT trace from a Tektronix Oscilloscope.

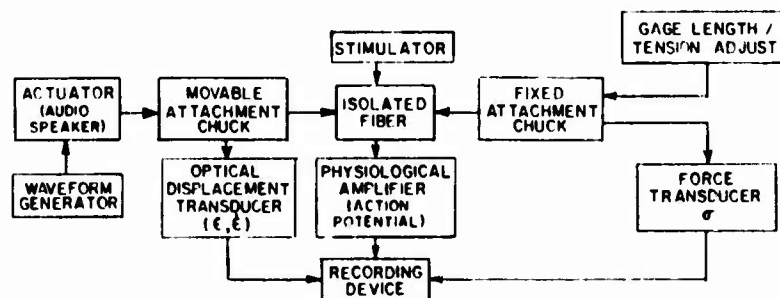


Figure 4

Depicted in Figure 5 is the apparatus which was developed to apply the loading to the nerve fiber. The nerve is attached to a pair of plattens by adhesive (cyanoacrylate) at the edge of each platten. The section of nerve between these points of attachment defines the gage length of the fiber. The plattens are attached to the load cell on one end and the actuator on the other. The load cell end can be moved statically through a spring-loaded micrometer drive and the gauge length of the fiber can therefore be adjusted over the range of zero to four centimeters. The actuator consists of an audio speaker (Poly Paks, Inc.) and linkage which attaches to the movable platten. The linkage design produces either axial or torsional displacement of the movable platten. The audio speaker is driven by a waveform generator and an emitter-follower circuit. The amplitude of the displacement and the pulse duration and rise time are adjustable. This system can be operated in a single shot or oscillating mode.

Contained within the plattens are pairs of stimulating and recording electrodes for the electrophysiological studies. Once a nerve fiber is bonded in place the electrodes are insulated with petrolatum. Both plattens are contained within a well assembly which is filled with a solution consisting of 205 mM Na Cl, 20 mM CaCl<sub>2</sub>, 5 mM KCl and 5 mM Trizma (7.50), adjusted to pH 7.55. All

chemicals were obtained from Sigma Chemical, St. Louis. The solution temperature was approximately 15°C.

The fiber selected for study was the spinal cord of the crayfish (cambarus). The preparations used were approximately 6 cm in length containing four giant axons approximately 60 microns in diameter. The crayfish were obtained from Monterey Bay Hydrocultural farms.

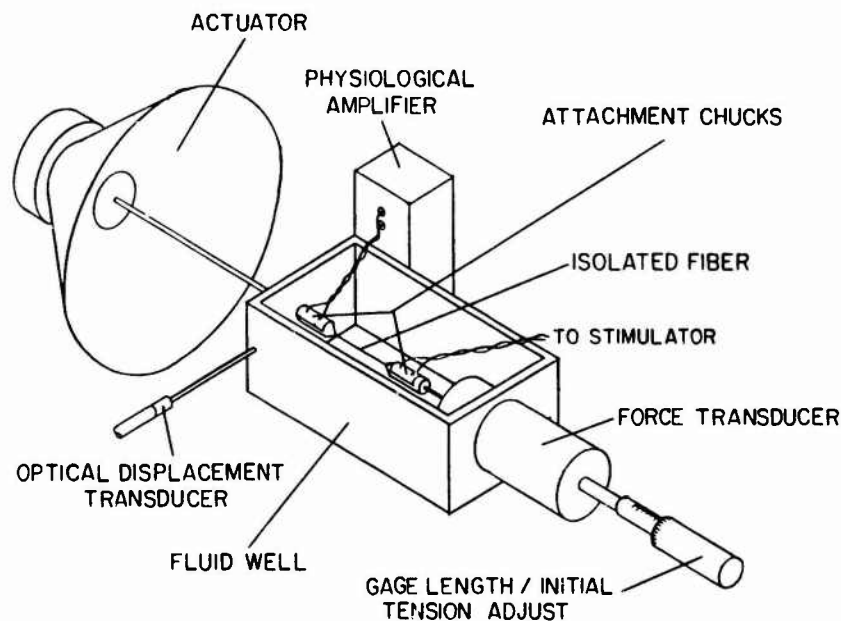


Figure 5

### Results

Figure 6 represents a summary of 68 animal experiments conducted using the HYPE device with modifications described herein. In all cases the animals were concussed to varying degrees of severity. The symbols (X) indicate subdural hematoma, (●) indicate mild to moderate concussion, and (O) indicate prolonged unconsciousness for periods up to six weeks. Also shown are the results of two analytical expressions which predict concussion threshold. The solid line is the result of an analytical model of Hyashi's (6) and the more conservative dashed line is that of Bycroft's (7). Both models seem to agree with the experimental data if the end point determination is to be some degree of cerebral concussion. However, it is important to note that there exist three subsets of data within the experimental population. Those animals which experienced subdural hematoma were subjected to high rates of onset of acceleration (of the order of  $10^6$  g's per second) while all other animals experienced approximately  $10^5$  g's per second. This can be accomplished with a variation of the metering pin configuration as discussed previously. Another distinction can be drawn between those animals which were run in the purely sagittal plane (●) which correlate with mild to moderate concussion and reduced rate of onset of acceleration, and those animals which were run in a lateral or oblique mode (O) which correlate with prolonged unconsciousness. The latter group was also subjected to reduced rate of onset of acceleration.

It is therefore suggested that specific injury modalities exist either independently or in concert with one another and that tolerance levels for each injury mechanism may be different. High rates of onset of acceleration suggest that high strain rates may be generated and therefore the viscoelastic properties of the discrete elements (vascular and neural) must be taken into account. Direction of the angular acceleration relative to an anatomical coordinate system may indeed influence the relative magnitudes of the components of the strain tensor since the brain is asymmetric, inhomogeneous and perhaps anisotropic.

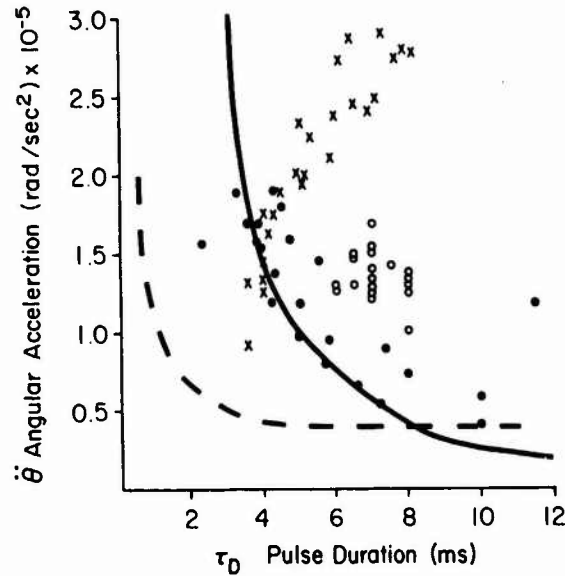


Figure 6

In the case of subdural hematoma one may view these data in a slightly different fashion. Figure 7 depicts the head subjected to an angular acceleration in the sagittal plane. The parasagittal bridging veins which couple the brain and skull undergo an elongation which is proportional to the relative angular displacement between the brain and skull. If the deceleration phase of the loading is symmetric with respect to time then the rise time of the deceleration pulse may be related to the strain rate which is experienced by the parasagittal bridging vein. It has been shown by Lowenhielm (8) that these vessels exhibit a markedly viscoelastic response to mechanical loading. As characterized by Lowenhielm, the ultimate strain to failure decreases by almost one order of magnitude as the strain-rate is increased from zero to three hundred  $\text{sec}^{-1}$ . If this experimental data is applied to the elastic case developed by Hyashi it is possible to incorporate the strain-rate dependence of the bridging vein into a tolerance curve for subdural hematoma. This result is depicted in Figure 8.

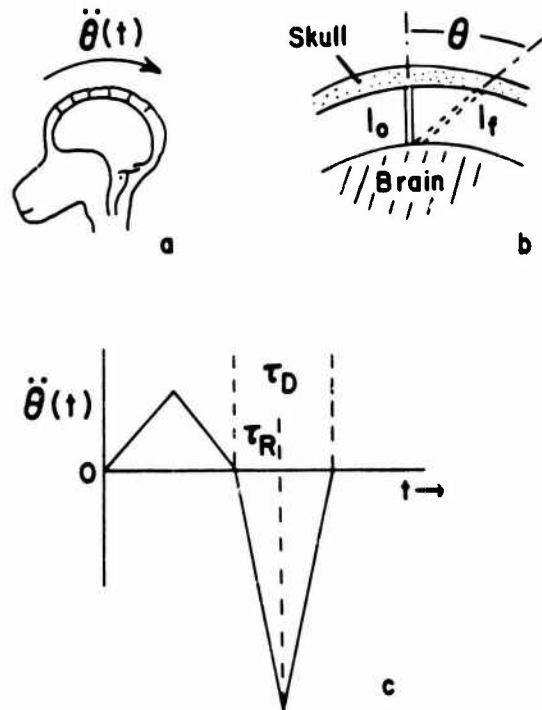


Figure 7

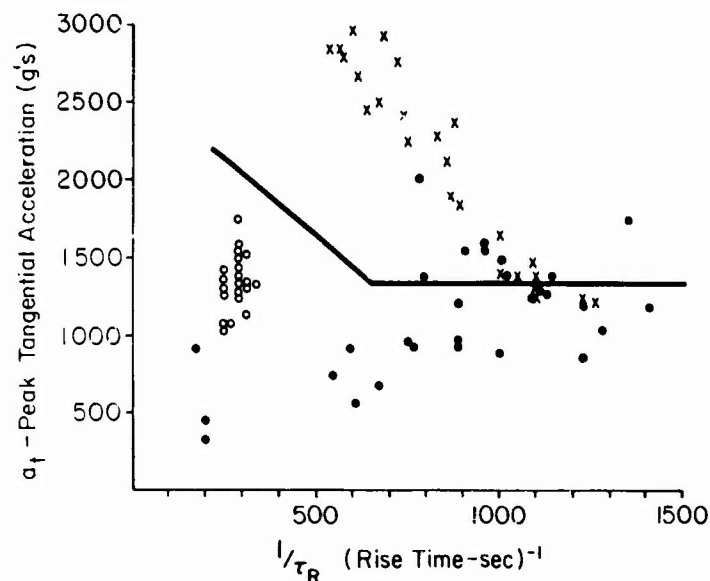


Figure 8

The difference in the physiological responses of the animals subjected to sagittal and lateral plane accelerations can be seen in the somatosensory evoked response changes. These differences are shown in Figure 9. The evoked response returns to normal in the first 5 minutes (post-trauma) in the case of the sagittal experiment, while the evoked response remains absent through 30 minutes in the case of the lateral plane acceleration. These experiments were conducted at comparable levels of acceleration and pulse duration (approximately 900 g's peak tangential deceleration at the center of mass of the brain with 8 msec pulse duration). The only parameter which is different in the two cases is the direction of the angular acceleration.

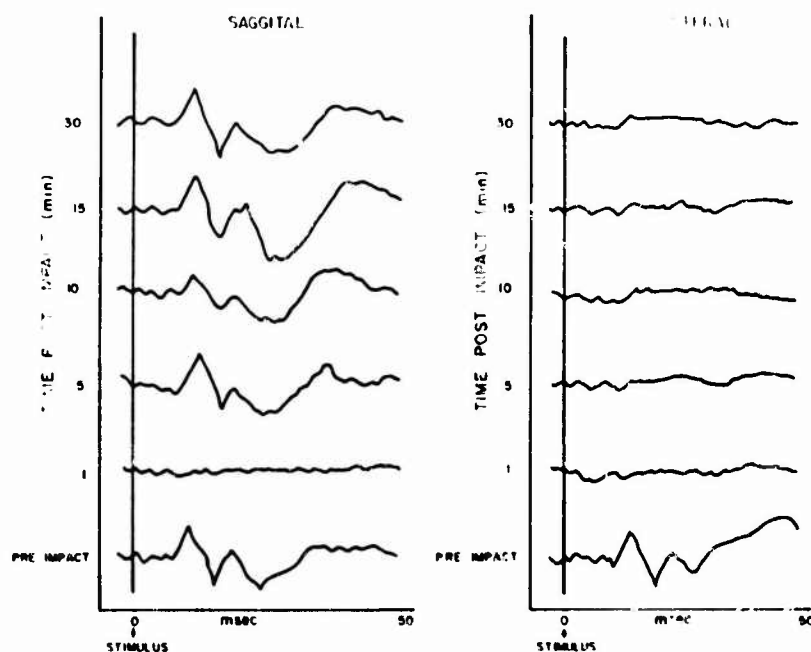


Figure 9



These experiments suggest that it is not sufficient to describe an injury tolerance level only in terms of the peak or average acceleration and the duration of the acceleration pulse, but that the pulse shape and direction of the acceleration vector need to be included.

The physical model experiments provide a method of determining the field parameters and their spatial and temporal variation as a function of the mechanical input conditions. Once these data are obtained from the physical model studies it becomes possible to test the isolated tissue preparations in order to develop a rational set of failure criteria for vascular and neuronal elements which are consistent with the loading conditions experienced in-situ.

These resulting deformations can then be applied to the isolated tissue and a evaluation of the tissue response from both a structural and functional point of view can be made. The system to perform these tests has been described previously.

Figure 10 shows the calibration curve of the optical displacement transducer which is used to determine the strain and strain-rate experienced by the tissue specimen.

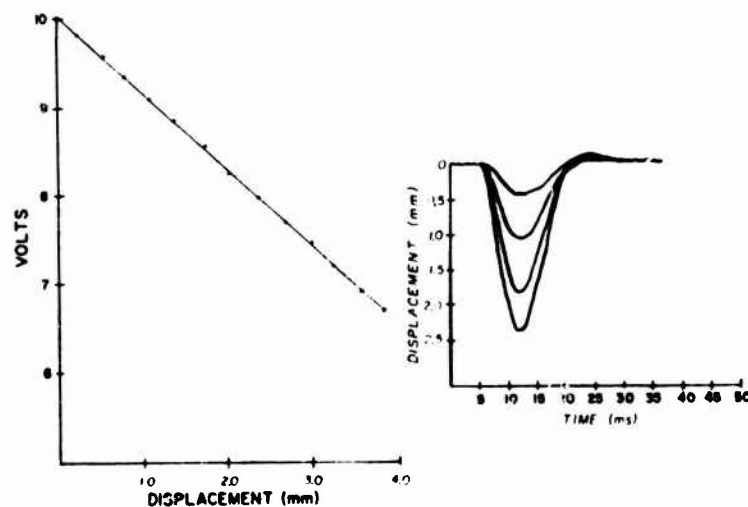


Figure 10

The transducer is displaced from the moving target by a "stand-off" distance of 2.0 mm which produces a full scale output of 10.0 volts. This voltage decreases with platten displacement and is linear ( $r = .9971$ ) over the range of zero to 3.8 mm. Also shown in the figure are typical displacement waveforms representative in terms of amplitude and wavelshape of those used during the study. The maximum strain rate used thus far is approximately  $300 \text{ sec}^{-1}$ , with maximum strains of 125%. The waveforms shown represent displacements of 0.8, 2.0, 3.6 and 4.7 mm with pulse durations of approximately 12 ms.

When the fiber is dissected free and ligated, it is transferred into the plattens of the apparatus where electrical stimulation and physiological recording are performed to establish fiber viability and baseline (control) conditions. The cyanoacrylate adhesive is then applied and recording continues in order to measure any time varying toxic effects. Fibers in this study have been monitored for up to 24 hours with no adverse effects observed as a result of manipulation or bonding to the plattens.

Figure 11a shows the results of an experiment which subjected the nerve fiber to a high strain rate uniaxial extension. The baseline compound action potential is recorded prior to loading the specimen. Sequentially the next signal was obtained at 30 sec post injury while continuing to stimulate the fiber with 3 volts, duration 60  $\mu\text{sec}$  at 1 Hz. The action potential in this case was virtually obliterated. The next signal obtained at 1.5 min shows spontaneous recovery where the signal amplitude is 200 mV with a latency of 6 ms. Figure 11b shows a similar experiment where the level of strain was increased. Control compound action potential is shown with amplitude 200 mV and a latency of 4 ms. The next signal is again approximately 30 sec post injury with no response to stimulus. The third signal shown is representative of the condition which persisted at 20 min. Under this loading condition (80% strain, strain rate  $250 \text{ sec}^{-1}$ ) the fiber did not recover. This fiber did not show macroscopic signs of structural damage which we have shown to occur at approximately 150 % strain in this preparation at comparable levels of strain rate.

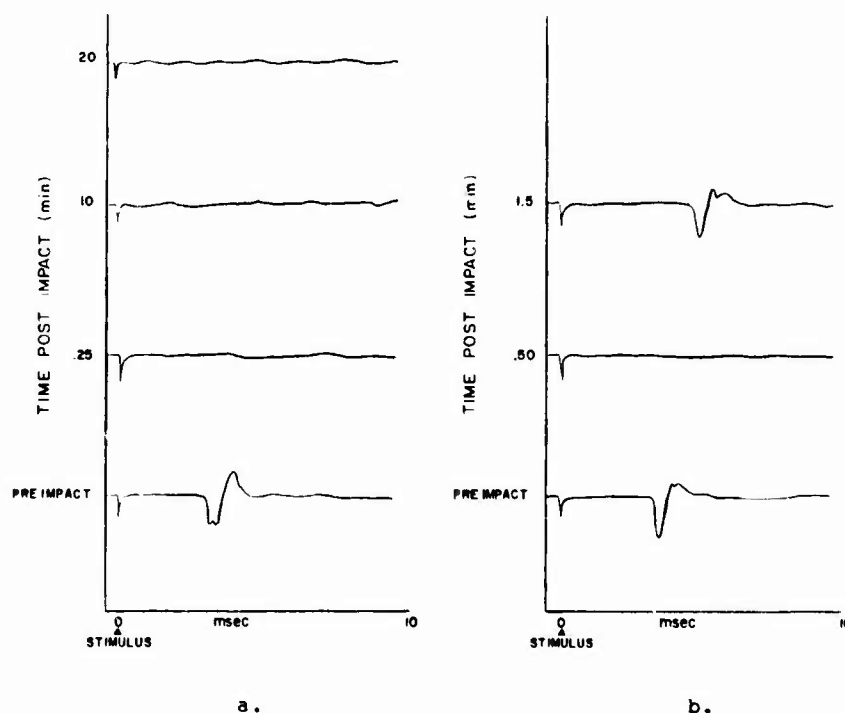


Figure 11

### Discussion

In order to develop rational criteria for injury to the structures of the head and neck when subjected to a variety of mechanical loading conditions, it is necessary to understand how these loads translate into the spatial and temporal variation of the field parameters such as strain, and, then, to determine what the structural and/or functional failure criteria are for the component tissues in terms of these parameters.

In this study it has been shown that controlled inertial loading can produce subdural hematoma, mild to moderate concussion and prolonged coma with concomitant diffuse axonal injury. These injuries may be dependent upon the amplitude of the acceleration, the pulse duration, the rise time (which is proportional to the strain-rate) and the direction of the acceleration vector with respect to the anatomical reference system. Physical model studies promise to provide insight into the details of the strain field in this regard.

It has also been shown that the ability of the isolated neural tissue element to propagate electrical signals can be impaired in a reversible or irreversible manner depending upon the levels of strain/strain-rate imposed. It is important to note that this functional response occurs before the nerve fails completely in a structural sense. The mechanism by which the normal electrophysiology is disrupted is not known and remains an area of great interest to the authors.

# References

- 1.) Gennarelli, T. A., Spielman, G., Langfitt, T. W. et. al.: Influences of the type of intracranial lesion on outcome from severe head injury: a multicenter study using a new classification system. J. Neurosurg. (in press).
- 2.) Unterharnscheidt, F. and Higgins, L. S.: Traumatic lesions of brain and spinal cord due to nondeforming angular acceleration of the head. Texas Reports on Biology and Medicine, Vol. 27, No. 1, pp 127-166.
- 3.) Gennarelli, T. A., Ommaya, A. K. and Thibault, L. E.: Comparison of translational and rotational head motions in experimental cerebral concussion. Proceedings of the 15th Stapp Conference, S. A. E., pp 797-803.
- 4.) Gennarelli, T. A., Thibault, L. E. and Ommaya, A. K.: Pathophysiologic response to rotational and translational acceleration of the head. Proceedings of the 16th Stapp Conference, S. A. E. pp. 296-308, 1972.
- 5.) Abel, J. M., Gennarelli, T. A. and Segawa, H.: Incidence and severity of cerebral concussion in the Rhesus Monkey following sagittal plane angular acceleration. Proceedings of the 22nd Stapp Conference, S. A. E., pp. 35-53, 1978.
- 6.) Hyashi, T.: Brain shear theory of head injury due to rotational impact. J. Fac. of Eng., University of Tokyo (B) Vol. XXX, No. 4, 1970.
- 7.) Bycroft, G. N.: Mathematical model of a head subjected to an angular acceleration. J. Biomech. 6, pp. 487-495, 1973.
- 8.) Lowenheilm, P.: Strain tolerance of the Vv cerebri sup. (bridging veins) calculated from head-on collision tests with cadavers. Z. Rechtsmedizin 75:131-144, 1974.

## DISCUSSION

UNIDENTIFIED QUESTIONER

(Non transcribable sentence).

DR. GENNARELLI'S (USA) REPLY TO ABOVE QUESTION

The first question was whether the cerebral bridging veins could rupture in the lateral mode. The answer is certainly, yes. If we deliver roughly the same wave shape in terms of posturation and amplitude in the lateral direction, we will also rupture bridging veins. They will be different bridging veins than the parasagittal bridging veins. As best we can tell, no difference exists in the mechanical tolerance of the different veins. The second question was whether the intracranial pressure that occurs after injury changes the viscoelastic properties of the veins. I don't know. We're talking of the slide that Dr. Thibault showed of post-impact intracranial pressure, not the instantaneous intracranial pressure, that Dr. Ward showed yesterday. We're talking about pressure that is probably due to venous congestion; the cause of the high pressure is probably distention of the veins and in our model does not occur instantaneously, but only after several seconds after injury. So we feel that if the vein is going to rupture, it will rupture in the first few milliseconds after the injury depending on the mechanical input rather than later. It may bleed more or less.

AUTHOR'S COMMENT

We are interested in also looking at a functional criteria for the bridging vein so to speak. We believe it may be possible that if the vein is subjected to a transient uniaxial extension, that it may in fact, dilate in response to that mechanical input, but not fail. At levels of strain below which it would ordinarily fail, it still may have a functional response, a basic dilatation, which may have an associated relaxation time constant.

UNIDENTIFIED QUESTIONER

From what you said, I think there are two different phenomenon. First of all, the dilatation phenomenon which is a physiological one. I believe the primary phenomenon is related to a hypertension, even a small one, but must exist due to the flexion of the head. The median parasinoidal characteristics of the vein change from flat to cylindrical and are probably much more sensitive to a possible rupture. This is the primary phenomenon. It's a purely mechanical phenomena, at least I think so.

DR. GENNARELLI (USA)

I agree that the bridging veins may be under different geometric configurations to begin with, and that certainly accounts for what we call biological variability in experiments; however, we feel that we need more data to prove that. The primary cause of increased intracranial pressure shown by Dr. Thibault is, in fact, the increased blood pressure and the blood pressure is the primary response to the acceleration forces and bending of the neck, etc. The intracranial pressure is a reflection of the increased blood pressure because of basal dilation or loss of cerebral autoregulation. We believe this is the mechanical response of the blood vessels to injury, just as lack of propagation of action potential is a response of the neuroelement to injury. Much more data is necessary to prove that.

DR. WARD (USA) QUESTION INADVERTENTLY NOT RECORDED.

AUTHOR'S REPLY

We are in the process of doing dynamic testing on both brain tissue and with the dielectric gel. The gel is strain rate sensitive. Whether or not we can match the viscoelastic properties, i.e., the relaxation modulus characterization, we have not yet been able to determine. We feel confident because you can vary the catalyst in a gel and change the gel elastic modulus three orders of magnitude. We also see variations in the viscoelastic properties. So we think we'll be able to do them.

DR. UNTERHARNSCHEIDT (USA)

First, I wish to congratulate Dr. Thibault and Dr. Gennarelli on their very fine and solid experiment work. Which technique did you use for the axon staining technique? I would like to comment that we should take into consideration that bridging veins have a tremendous variation in anatomy and in the location from animal to animal and man to man.

DR. GENNARELLI (USA) COMMENT

These photomicrographs that Dr. Thibault showed of the nerve cord of the crayfish were performed

in our peripheral nerve laboratory, not in our own laboratory. These were semi-thin cut sections of acrylic-embedded nerve. I plead ignorance to the particular stain that was used. The material was fixed in situ, in glutaraldehyde while under load, and then was prepared in the standard fashion for peripheral nerve material. I don't know the particular membrane stain that was used. Actually, the morphologist who did the work with us was much more convinced than perhaps was apparent, that those were real and not artifactual changes. He has had considerable experience with this particular fixation preparation method in human and other animal peripheral nerves, and has never seen the kind of disruptions of the axoplasm from the inner membrane of the neuron than was seen in these. It still could be artifactual but perhaps not.

DR. UNTERHARNSCHEIDT (USA) COMMENT

I am convinced that these were not artifacts.

DR. THIBAUT (USA) COMMENT

I am very interested in the behavior of a single cell undergoing mechanical deformation at very low levels of strain, where we believe any cell, bone, muscle or skin tissue experiences deformation and somehow can communicate that to the cell machinery. So we are trying to study this problem also in culture where we're subjecting cells to mechanical strain in culture and looking at changes in biochemistry. For example, in bone cells we're looking at Collagen synthesis as a function of mechanical strain, but to continue the concept that Dr. Gennarelli presented ultimately has to be verified at the cellular level. A response which starts out, perhaps as membrane phenomenon, but shows up as an inability to propagate electrical information. Perhaps a little further up the scale of mechanical deformation is an internal structural problem, failure perhaps of the cellular-skeletal network and ultimately at the limit to some membranes torn and disrupted which is as far as we know an irreversible phenomenon. This is the approach we are presently exploring.

# INFLUENCES RESPECTIVES DE L'ACCELERATION, DU JERK ET DE L'AMPLITUDE DE LA FLEXION DU COU SUR LA SURVENUE DES LESIONS CEREBRALES.

C. Tarrière, G. Walfisch, A. Fayon, Laboratoire de Physiologie et de biomécanique de l'Association Peugeot S.A./Renault, 147 ave. Paul Doumer, 92501 Rueil-Malmaison, France.

C. Got, F. Guillon, A. Patel, Institut de Recherches Orthopédiques, Hôpital Raymond Poincaré, 104 Bd Raymond Poincaré, 92380 Garches, France.

J. Hureau, Laboratoire d'Anatomie de l'U.E.R. Biomédicale des Saints-Pères, Faculté de Médecine, 75005 PARIS

## Résumé.

Les Auteurs présentent une synthèse de résultats expérimentaux obtenus sur cadavres humains frais dont la pression vasculaire moyenne a été rétablie avant de subir des impacts directs de tête.

L'influence des paramètres tels que l'accélération linéaire et l'accélération angulaire, le jerk, l'amplitude de la flexion du cou, la durée du choc, est analysée et discutée.

Les conclusions sont relatives à la tolérance de la tête humaine et aux critères de performance utilisables pour tester la qualité de la protection offerte par un casque ou un élément d'habitacle aménagé (padding).

La connaissance de la tolérance de la tête humaine à l'impact est nécessaire pour la réalisation de dispositifs de protection bien adaptés, qu'il s'agisse de casques pour usagers de deux-roues ou des parties d'un véhicule susceptibles d'être heurtées par la tête de ses occupants (ou celle de piétons). Les paramètres physiques mis en relation avec la sévérité des blessures cérébrales sont, le plus souvent, déduits de la loi d'accélération/temps de la tête (accélérations linéaires, HIC (head injury criterion), accélérations angulaires, jerk, etc...)

L'objectif de cette communication est de faire la synthèse de données expérimentales obtenues par le Laboratoire de Physiologie et de Biomécanique Peugeot S.A./Renault et l'Institut de Recherches Orthopédiques de l'Hôpital Raymond Poincaré de Garches.

Ces données permettront d'évaluer la tolérance de la tête à l'impact à partir de la loi accélération/temps; L'utilisation de cette loi nous paraît d'autant plus intéressante à prendre en considération que les paramètres qui s'en déduisent (accélération, HIC, etc...) sont assez aisément transposables sur mannequin de choc et, par conséquent, utilisables pour déterminer un critère de protection.

En plus de la commotion, ils pourraient permettre aussi d'évaluer le risque de fracture du crâne lorsque les efforts appliqués à la tête sont répartis sur une surface suffisante, ce qui est généralement le cas dans les accidents de véhicules à moteur. Les données utilisées ont été obtenues soit dans des simulations ou reconstitutions d'accidents réels, soit lors de chutes libres de sujets humains frais, non embaumés et instrumentés.

Une partie des résultats acquis lors de ces expériences a déjà fait l'objet de publications (1)(2)(3)(4)(5) dans lesquelles la méthodologie utilisée pour chaque type d'essais était décrite.

Par rapport à ces publications, l'analyse des résultats a été complétée et approfondie; en particulier certaines données ont été vérifiées.

Cette communication concerne la tolérance de la tête humaine à l'impact; la transposition au mannequin de choc doit être envisagée dans un deuxième temps.

## I - METHODOLOGIE

Rappelons brièvement quelques points importants:

### 1. Description des essais

Les reconstitutions d'accidents réels prises en compte étaient des collisions latérales et frontales à vitesse élevée pour les chocs latéraux (comprise entre 45 et 70 km/h). Pour les chocs frontaux, la vitesse d'impact était comprise entre 50 et 65 km/h. Dans les chocs latéraux, la tête de l'occupant du véhicule heurté était impactée dans sa partie pariéto-temporale; dans les chocs frontaux, la tête de l'occupant était heurtée dans sa partie frontale.

Pour les essais de chutes libres, au nombre de 53, schématisées sur les figures 1 et 2, les sujets humains étaient maintenus au moyen d'un dispositif adéquat, la tête casquée ou non, dans le prolongement du corps.

Ils sont tombés en chute libre, la tête heurtant une surface plane et rigide revêtue ou non de matériau amortissant.

Le reste du corps était arrêté par un épais matelas dont l'épaisseur et la raideur étaient choisies afin de contrôler le mouvement de flexion de la tête par rapport au thorax.

Les essais de chute réalisés peuvent être classés en deux catégories suivant la direction principale de l'impact:

- a) impacts pariéto-temporaux (au nombre de 17 dont 1 contre une surface rigide non aménagée (n° 76)). La hauteur de chute a varié entre 1,83 m et 3 m (1).

- b) impacts frontaux (au nombre de 20). Pour ces essais, la hauteur de chute était de 3 m.

## 2. Préparation des sujets

Il s'agit des corps de personnes en ayant fait don de leur vivant. Chaque sujet a fait l'objet de la préparation présentée ci-après.

a) relevés anthropométriques - Un relevé anthropométrique précis précède chaque essai.

Outre l'âge et le sexe, on note la circonférence et le diamètre antéro-postérieur de la tête, mesurés en passant par la partie la plus basse de l'os frontal (au niveau des sinus) et la protubérance occipitale externe.

Le diamètre transversal de la tête, également noté, correspond au maximum de la distance entre les parties temporales droite et gauche.

Après chaque essai, la tête et le cou sont prélevés suivant des techniques déjà décrites (6) pour la recherche d'éventuelles blessures cérébrales, crâniennes ou cervicales. Les masses de la tête et du cou, de la tête seule, du crâne et du cerveau sont prélevées afin d'aider à la compréhension des phénomènes de masse équivalente et à la caractérisation de la boîte crânienne.

L'ensemble des données disponibles est reporté dans les tableaux 2 et 5.

b) Rétablissement de la pression artérielle - Une perfusion de l'encéphale suivant la méthode déjà décrite (1) a été effectuée avec succès sur l'ensemble des sujets pris en compte dans l'analyse (20 essais en choc frontal, 17 en choc latéral). Cela a permis d'évaluer la sévérité des blessures cérébrales dans l'échelle des AIS (7).

## 3. Calcul des accélérations

Des accéléromètres sont vissés sur le crâne des sujets. Afin de pouvoir calculer les accélérations linéaires et angulaires au centre de gravité de la tête des cadavres, nous avons utilisé pour tous les essais postérieurs à l'essai n° 76, 9 voies d'accélération obtenues par l'intermédiaire de 3 capteurs tri-directionnels fixés sur le crâne, à distance de la zone impactée de la tête. Un programme de calcul permet, à partir de ces neuf voies, de reconstituer les accélérations au centre de gravité de la tête.

La mise en oeuvre de ce programme a été modifiée depuis le début de son utilisation, en particulier par l'incorporation d'orientations plus précises des capteurs. De ce fait, certaines valeurs antérieurement publiées se sont vues quelquefois retouchées.

L'ensemble des chaînes de mesure accélérométriques était conforme à la procédure SAE J 211 b (classe 1000).

## 4. Calcul du jerk

Il n'existe pas de procédure standardisée de calcul du jerk à partir de la loi accélération/temps. Plusieurs méthodes ont été décrites dans la littérature (8). Elles concernent la partie ascendante de la courbe de décélération de la tête; l'intervalle de temps choisi pour le calcul dépendant alors, dans une large mesure, de l'intuition de l'auteur. La méthode utilisée ici est définie comme suit:

- à partir du maximum de l'accélération résultante, on détermine sur la partie ascendante de la courbe accélération/temps deux points correspondant respectivement à 0.2 et 0.8 d'accélération résultante maximum.

- Puis, entre ces deux points, on détermine une droite définissant un jerk "moyen" par la méthode des moindres carrés, en échantillonnant la courbe suivant des longueurs d'arc constantes (20 à 25 points par courbe ont été ainsi utilisés).

Cette méthode s'est révélée bien adaptée aux sorties graphiques, une précaution devant être prise qui concerne les échelles; elles doivent, en effet, rester dans un rapport constant quel que soit l'essai considéré. Dans nos essais, il était tel que 1 g correspondait à  $25.10^{-5}$  secondes sur l'autre axe.

Ceci n'a été effectué que pour les essais avec impact frontal.

## 5. Mesure des efforts

Cette mesure est particulière aux essais de chute libre. Un plateau dynamométrique est placé sous le matériau amortissant impacté par la tête et mesure uniquement la composante verticale de l'effort appliqué à la tête.

Dans le cas où le sujet d'essai est porteur d'un casque, la tête impacte directement le plateau dynamométrique. Dans les autres cas, on interpose le plus souvent une couche de matériau amortissant.

# II - RESULTATS DES ESSAIS DE CHUTE LIBRE

## 1. Cinématique de la tête et du cou

D'une manière générale, la cinématique de la tête et du cou peut être décrite d'une façon simplifiée comme suit:

- une première phase, qui est un mouvement vertical de la tête dans le matériau (ou le casque), sans rotation importante par rapport à son orientation initiale. La durée de cette phase est voisine de 6 à 7 ms.

- Puis, au cours du rebond, on observe un mouvement de rotation de la tête par rapport au thorax (fig. 3 et 4).

On notera que les maxima des accélérations linéaires et angulaires sont atteints pendant la première phase décrite ci-dessus et que les vitesses angulaires n'ont pas excédé 96,2 rd/s (89 rd/s pendant 3 ms), valeur qui sera à rapprocher des limites envisagées pour garantir l'absence de blessure.

## 2. Analyse des blessures

a) au niveau du crâne - Pour les impacts frontaux, 3 sujets sur 21 présentaient une fracture du crâne. Il s'agit des essais 166, 250 et 251 qui étaient de sexe féminin avec une tête de petite dimension. Des essais mécaniques seront effectués sur des parties d'os crânien à des fins d'explication des fractures observées.

Pour les impacts pariéto-temporaux, sur les 17 sujets ayant subi un impact dans cette zone de la tête, seul un sujet est tombé tête nue sur une surface rigide, et il présentait une fracture du crâne (essai n° 76). Parmi les 16 autres, un seul sujet révéla une fracture du crâne. Ce sujet, de sexe féminin, est tombé casqué d'une hauteur de 3 m. Il s'agit du sujet qui présentait la plus faible épaisseur moyenne du crâne (3,65 mm) relevée parmi tous les sujets d'expérience. De plus, la minéralisation de sa boîte crânienne était également parmi les plus faibles observées (0,7 g/cm<sup>2</sup>). Les données sont rapportées dans le tableau n° 5; il s'agit du sujet n° 83.

b) Lésions du cou - Pour les impacts pariéto-temporaux, un sujet sur les 17 testés présentait des blessures ostéo-ligamentaires de la colonne cervicale pour un angle d'inclinaison latérale de la tête par rapport au thorax voisin de 61° (n° 67, sexe féminin, 82 ans). On doit noter que, plusieurs fois, des angles proches de 70° ont été atteints sans blessure de la colonne cervicale. Ces angles ont été relevés à partir de films tournés à 1000 images/seconde.

Pour les impacts frontaux, quatre sujets présentaient le même type de blessure ostéo-ligamentaire pour des angles d'hyperextension de la tête par rapport au thorax supérieurs à 65° (de 66° à 90°) pour des HIC variant de 1000 à 2000. Il s'agit des sujets 104 et 142 pour lesquels l'injection cérébrale a été un échec (1), et des sujets 110 et 143 (Cf. tableau 3).

c) Lésions cérébrales - Sur les 53 sujets impactés, on n'a pris en compte que les sujets pour lesquels le cerveau était bien conservé et bien injecté. Ils sont au nombre de 20 en chocs frontaux et de 17 en chocs latéraux. Une synthèse de la localisation des blessures cérébrales est reportée dans le tableau 1 où l'on peut constater la prédominance des blessures du tronc cérébral (près de 70 % des blessures observées) quelle que soit la direction des forces appliquées à la tête.

Ces blessures se situent souvent au niveau protubérantiel: la position de la protubérance, en saillie par rapport aux autres éléments du tronc cérébral et au contact des structures osseuses (corps de l'occipital en avant et partie antérieure du rocher latéralement) favorise son implication, que les efforts soient dirigés d'avant en arrière ou transversalement.

Des mécanismes du type "engagement" du tronc cérébral dans le trou occipital, consécutifs à certaines cinématiques de la tête par rapport au cou, peuvent être évoqués pour l'explication du nombre relativement élevé de blessures observées dans cette région.

Des recherches complémentaires seraient nécessaires pour préciser ce point.

## 3. Résultats des mesures concernant les impacts frontaux

L'ensemble des résultats utilisés dans l'analyse est reporté dans les tableaux 2 et 3. Dans ce qui suit, on a successivement cherché à mettre en relation les blessures observées, exprimées en termes de AIS, avec des paramètres liés à la violence et aux circonstances de l'impact: HIC, accélérations linéaires et angulaires, hyperextension de la tête par rapport au thorax, jerk d'accélération linéaire, etc...

La considération des données anthropométriques de la tête des sujets d'expérience et de données morphométriques relatives à leur boîte crânienne a permis une analyse plus fine des résultats. Ces dernières données sont la quantité de sels minéraux par unité de surface de l'os crânien et l'épaisseur moyenne du crâne.

Tous les sujets qui ont subi un impact frontal sont tombés d'une hauteur de chute de 3 m. La variation de vitesse de la tête dans ces essais était voisine de 10 m/s, et la durée totale du choc comprise entre 5 et 15 ms; ces durées de choc sont réalistes si l'on se réfère aux données expérimentales obtenues lors des reconstitutions d'accidents de voitures, de piétons ou de deux-roues (2)(4)(9)(10).

Le tableau 4 résume les principaux résultats obtenus, classés suivant la sévérité des blessures cérébrales observées (AIS).

On a respectivement relevé les minima, maxima et la valeur arithmétique moyenne pour chaque paramètre physique considéré, ainsi que le nombre de sujets pris en compte. Quelques observations peuvent être faites, paramètre par paramètre, à partir de ce tableau. Auparavant, on attirera l'attention sur deux sujets:

- le sujet 103, qui avait le crâne le plus épais et le plus minéralisé parmi tous les sujets d'expérience (Cf. tableau 2) et pour lequel, en l'absence de toute blessure, les paramètres utilisés dans l'analyse des résultats ont atteint des valeurs très élevées (Cf. tableau 3);

- le sujet 107, qui avait la plus petite tête, un crâne de très faible épaisseur et très peu minéralisé par rapport à l'ensemble des sujets (Cf. Tableau 2). Dans l'analyse qui suit, nous ne tiendrons pas compte des résultats relatifs à ce sujet car, de par ses caractéristiques, il s'écarte beaucoup trop de la moyenne des sujets d'expérience.

Nous attacherons une importance particulière aux sujets indemnes à chaque fois que leur nombre sera suffisant par rapport au nombre d'essais effectués et à chaque fois qu'il n'aura pas été possible d'isoler l'influence d'un paramètre parmi les autres, car l'association de plusieurs paramètres physiques qui ont atteint des niveaux élevés interdit toute conclusion sur l'éventuelle influence d'un paramètre sur le bilan lésionnel.



a) L'accélération linéaire est le premier paramètre examiné. On le considère selon qu'il est associé à des blessures sévères ou non.

- associée à des blessures sévères, AIS  $\geq 3$  - La plus petite valeur d'accélération maximum relevée était de 182 g (122 g pendant 3 ms). Il s'agit du sujet 174, qui associait à un jerk d'accélération linéaire élevé ( $0,99 \times 10^5$  g/s) une accélération angulaire (3 ms) importante (12936 rd/s<sup>2</sup>) et dont la sévérité des blessures était classée entre 3 et 4 dans l'échelle des AIS.

Pour les blessures ici les plus sévères, correspondant à des AIS 4 et 5 (sujets 102 et 108), les accélérations maxima étaient, respectivement, de 232 et 313 g (147 et 144 g pendant 3 ms). Ces deux sujets ont subi, par ailleurs, des accélérations angulaires très élevées et des hyperextensions de la tête par rapport au thorax très importantes (Cf. tableau 3). Associées à une absence totale de blessures cérébrales (AIS 0), les accélérations linéaires sont souvent élevées. Quatre fois sur dix, des accélérations linéaires résultantes maxima ont dépassé 250 g. La valeur la plus élevée de l'accélération maximale était de 349 g et, pour une durée de 3 ms de 149 g.

- pour les dix sujets indemnes, le maximum d'accélération a varié de 126 g à 349 g (valeur arithmétique moyenne = 217 g); l'accélération dépassée pendant 3 ms a varié de 102 à 169 g (moyenne arithmétique = 130 g).

La considération de ces résultats relatifs à l'accélération linéaire entraîne une critique du critère 80 g/3 ms. Il est en effet encore courant de le voir utiliser comme "critère de protection" de la tête à l'impact. Or, en impact frontal, nous n'avons jamais trouvé de blessure cérébrale pour des accélérations linéaires appliquées pendant 3 ms inférieures ou égales à 100 g.

b) HIC - L'on considère ici le HIC d'une manière privilégiée parce que c'est le paramètre le plus souvent examiné en relation avec la sévérité des blessures. On a trouvé un cas sur 20 où un HIC modéré (inférieur à 1500) peut être associé à des blessures sévères. Il s'agit du sujet 174 (HIC = 1156) qui a subi un jerk d'accélération linéaire très élevé ( $0,99 \times 10^5$  g/s), dont on verra l'influence probable sur le bilan lésionnel plus loin. Il a subi, en outre, une valeur d'accélération angulaire dépassée pendant 3 ms atteignant 12936 rd/s<sup>2</sup> (pic à 18922 rd/s<sup>2</sup>). L'association du jerk élevé et de cette accélération angulaire a pu contribuer à la sévérité des blessures cérébrales de ce sujet humain car aucun des autres paramètres physiques pris en compte dans l'analyse des résultats (HIC et hyperextension de la tête par rapport au thorax) n'a atteint un niveau suffisant pour rendre évidente cette sévérité de blessures (AIS 3 ou 4). Inversement, des HIC élevés supérieurs à 2000 ont été supportés par une tête humaine sans qu'il leur soit associé de blessures (Cf. Tableau 3). On n'a pas alors les associations jerk et les accélérations angulaires élevées notées précédemment (à l'exception du sujet 103 déjà cité).

c) Accélérations et vitesses angulaires (tableau 3) - Si l'on considère les trois sujets qui présentaient des blessures classées supérieures ou égales à 3 dans l'échelle des AIS, on trouve d'abord le sujet 174 qui associait à une accélération angulaire élevée (12940 rd/s<sup>2</sup> / 3 ms) un jerk élevé ( $0,99 \times 10^5$  g/s), et les sujets 102 et 108 pour lesquels l'ensemble des paramètres physiques mesurés était très élevé: HIC, accélérations linéaire et angulaire, vitesse angulaire, hyperextension, etc...

Si l'on considère maintenant les sujets dont la sévérité des blessures était 2 ou 3 dans l'échelle des AIS, on se heurte au même écueil que précédemment, c'est-à-dire la difficulté d'imputer les blessures à un paramètre isolé en raison des associations observées. [A titre d'exemple, hyperextension forcée de la tête et vitesse angulaire importante pour les essais 110 et 143.] Ne pouvant isoler l'influence d'un paramètre, on s'intéressera plus particulièrement aux sujets indemnes: quelques observations intéressantes peuvent être alors effectuées.

Pour les 10 sujets indemnes qui ont subi des HIC compris entre 690 et 2350, des jerks d'accélération linéaire entre 0,16 et  $2,49 \times 10^5$  g/s et une hyperextension de la tête peu importante (à l'exception du sujet 251), les maxima de leurs vitesses angulaires ont varié de 22 à 63 rd/s (valeur arithmétique moyenne = 34 rd/s).

Les maxima des accélérations angulaires ont varié de 8950 à 35780 rd/s<sup>2</sup> (valeur arithmétique moyenne = 16808 rd/s<sup>2</sup>), et les accélérations angulaires dépassées pendant 3 ms de 4300 à 15110 rd/s<sup>2</sup> (valeur arithmétique moyenne = 8161 rd/s<sup>2</sup>).

Ces résultats sont intéressants à prendre en compte en raison du peu de données disponibles relatives aux niveaux d'accélération angulaire et de vitesse angulaire supportables par un être humain sans qu'il leur soit associé de blessure cérébrale.

d) Jerk d'accélération linéaire -

Le maximum de jerk relevé en l'absence de blessure a été voisin de  $2,4 \times 10^5$  g/s.

Le minimum de jerk associé à des blessures a été voisin de  $0,17 \times 10^5$  g/s; il s'agit du sujet 143 qui associe une hyperextension de la tête élevée à une vitesse angulaire maximum élevée. Si l'on considère tous les essais où le jerk était élevé ( $> 10^5$  g/s) et l'AIS cérébral inférieur à 3, la moyenne arithmétique des jerks était voisine de  $1,2 \times 10^5$  g/s.

e) Hyperextension de la tête par rapport au thorax (angle  $\theta$  dans le tableau 3) - Si l'on considère les sujets indemnes, on peut constater que leur absence de blessure cérébrale s'accompagne d'une hyperextension inférieure ou voisine de l'hyperextension naturelle (60 à 65°), à l'exception du sujet 251 pour lequel l'hyperextension a atteint 76°. Ces résultats ont été obtenus pour des HIC compris entre 700 et 2350, des jerks inférieurs à  $1,52 \times 10^5$  g/s et des accélérations angulaires dépassées pendant 3 ms inférieures à 15000 rd/s<sup>2</sup>.

Pour les autres sujets (AIS 3, 4 ou 5), il n'a pas été possible de dégager l'influence de l'hyperextension sur le bilan lésionnel en raison du niveau élevé atteint par les autres paramètres.

Relations entre les paramètres physiques pris en compte et la sévérité des blessures observées, exprimée en termes d'AIS.

Dans les paragraphes précédents, on a analysé, par classe d'AIS, les niveaux atteints par chaque paramètre. Or l'interprétation de l'éventuelle influence d'un paramètre sur le bilan lésionnel ne peut se faire ici sans prendre en compte les autres paramètres physiques utilisés pour juger de la sévérité d'un impact crânien. Dans ce qui suit, on s'attachera à mettre en relation chaque paramètre physique avec la sévérité des blessures exprimée dans l'échelle des AIS en utilisant les essais où les autres paramètres étaient les plus voisins possibles.

a) Influence du jerk d'accélération Les sujets qui ont été sélectionnés pour analyser l'influence du jerk d'accélération linéaire sur le bilan lésionnel sont tous ceux qui ont supporté des HIC voisins de 1500 et des accélérations angulaires dépassées pendant 3 ms inférieures à 9000 rd/s<sup>2</sup> (à l'exception du sujet 174). De plus, pour tous ces essais, les conditions de choc étaient choisies de telle sorte qu'aucune hyperextension excessive de la tête par rapport au thorax n'a été provoquée (5). Les jerks classés comme élevés étaient compris entre 10<sup>5</sup> g/s et 1.5x10<sup>5</sup> g/s: un tel niveau de jerk avait été atteint lors d'une série d'essais antérieurs aux essais présentés ici, avec des sujets humains porteurs d'un casque dont les propriétés amortissantes s'étaient révélées insuffisantes par suite de la faible distance entre le point d'impact et le bord du casque (1). Les jerks "modérés" étaient voisins de 0.5x10<sup>5</sup> g/s: ce niveau avait été atteint lors de la série d'essais déjà citée, avec des sujets humains porteurs d'un casque dont la partie antérieure recouvrait 3 cm de polystyrène (1):

- Tous les essais effectués dans ce but ont été reportés sur la figure 5 où sont représentés le jerk, le HIC et la sévérité des blessures observées. Nous rappelons ici que ces résultats ont été obtenus pour des accélérations angulaires que l'on peut considérer comme tolérables par une tête humaine (inférieures à 9000 rd/s<sup>2</sup> pendant 3 ms), et qu'aucune hyperextension de la tête n'a été provoquée. Quelques observations peuvent être faites:

- pour une classe de HIC donnée, il n'y a pas de relation simple entre le jerk et la sévérité des blessures cérébrales. Ceci n'est pas étonnant car le jerk, comme cela a été constaté précédemment, n'est qu'un des paramètres physiques qui décrivent les sollicitations de la tête dans les essais réalisés.

- Néanmoins, on peut remarquer que, pour les jerks élevés (supérieurs à 10<sup>5</sup> g/s) et pour une même classe de HIC, 1 sujet ou 2 présentaient des blessures cérébrales. Ces blessures ne sont pas très sévères à l'exception du sujet 174 (AIS 3 ou 4) pour lequel une explication de la sévérité des blessures a déjà été proposée. Il semble donc, sur la base du petit nombre d'essais rapportés, qu'au delà d'une valeur voisine de 10<sup>5</sup> g/s, le jerk d'accélération linéaire ait une influence aggravante sur le bilan lésionnel (probabilité d'apparition d'une blessure cérébrale voisine de 50 %).

Cette hypothèse peut être prise en compte car on ne voit pas de paramètre auquel on puisse attribuer les blessures de façon évidente. Toutefois, il n'apparaît ni indispensable, ni possible, sur la base de ces résultats, de définir un critère spécifique à cette fonction, déduite de la loi d'accélération en fonction du temps, dans la mesure où la condition HIC 1500 est satisfaite. Les raisons sont, la très faible probabilité d'apparition d'une blessure cérébrale, dans ces conditions d'impact réalistes, lorsque le HIC est inférieur ou égal à 1500 (voir fig. 5) et l'absence de blessures parfois observées même lorsque le HIC et le jerk atteignent des valeurs élevées (essais 103 et 177, par exemple). Ces points seront repris à propos de la relation HIC/AIS.

b) Relations entre le HIC et l'AIS - L'ensemble des résultats est reporté sur la figure 6. Si l'on analyse cette figure, on n'observe pas de relation simple entre le HIC et la sévérité des blessures cérébrales exprimée en termes d'AIS. Cela n'est pas surprenant car les dispersions propres aux tolérances et l'absence de linéarité dans l'échelle des AIS expliquent en partie cette absence de relation HIC/AIS.

Néanmoins, l'analyse de la figure 6 permet de justifier l'utilisation du HIC comme limite pour la tolérance humaine. En effet, si l'on raisonne en termes de "seuil" de tolérance au lieu d'utiliser une définition statistique du niveau tolérable pour le paramètre choisi, par exemple un niveau tel que 50 % des sujets présentent un AIS < 3, on ne peut obtenir, pour le seuil, qu'une valeur inférieure de la tolérance. Il apparaît qu'un seul sujet (n° 174) sur les 20 pris en compte associait un HIC relativement faible (HIC = 1150) à des blessures cérébrales sévères (AIS 3 ou 4). Ce sujet présentait des particularités dont nous avons déjà parlé.

En conclusion sur la relation HIC/AIS en cas d'impact frontal et dans l'attente d'une fonction déduite de la loi accélération/temps de la tête mieux corrélée aux blessures que le HIC, on peut dire que la probabilité d'apparition d'une blessure sévère (AIS ≥ 3) est très faible lorsque la condition HIC ≤ 1500 est respectée.

En l'absence de paramètre mieux adapté, notre avis est que le HIC peut être utilisé comme limite pour la tolérance humaine, et que le niveau 1500 est d'autant plus acceptable qu'il est obtenu avec des cadavres qui, d'une manière générale, ne donnent qu'une sous-estimation de la tolérance des vivants exposés aux risques d'accidents. La validité de ces conclusions s'entend en l'absence de fracture du crâne, pour des accélérations linéaires maximales comprises entre 120 et 350 g (100 et 170 g pendant 3 ms), des accélérations angulaires maximales inférieures à 43200 rd/s<sup>2</sup> (17200 rd/s<sup>2</sup> pendant 3 ms), des hyperextensions de la tête par rapport au thorax inférieures à 80° et, enfin, des durées totales de choc comprises entre 5 et 15 ms.

#### 4. Résultats relatifs aux impacts latéraux

L'ensemble des données sont rassemblées dans les tableaux 5 et 6. On a considéré successivement les accélérations linéaires, les HIC et les inclinaisons latérales de la tête par rapport au thorax (angle α° dans le tableau 6); les autres données examinées pour les

chocs frontaux ne sont pas disponibles.

Pour ces essais, la hauteur de chute a varié de 1,83 à 3 m.

a) Résultats concernant les accélérations linéaires - Ceux-ci sont résumés dans le tableau 7 où ils ont été classés suivant la sévérité des blessures cérébrales observées. Quelques constatations peuvent être faites:

- dans le cas de blessures sévères ( $AIS > 3$ ), l'accélération maximale a varié de 210 à 580 g (moyenne arithmétique: 328 g), et l'accélération maximale dépassée pendant 3 ms de 136 g à 200 g (moyenne arithmétique 157 g).

- Inversement, des accélérations élevées peuvent être associées à une absence totale de blessures ( $AIS = 0$ ): pour les 9 sujets indemnes, le maximum d'accélération linéaire a varié de 150 à 350 g (moyenne arithmétique 218 g), et l'accélération linéaire dépassée pendant 3 ms de 110 à 175 g (moyenne arithmétique 144 g).

On peut noter sur le tableau 7 que les accélérations relevées dans chaque classe d'AIS sont assez voisines (surtout pour les accélérations 3 ms). Cela confirme que, comme en choc frontal, il n'est pas satisfaisant d'utiliser le seul maximum (pic ou 3 ms) de l'accélération linéaire à des fins de définition d'un critère de tolérance cérébrale de la tête humaine à l'impact.

En outre, il faut noter que pour ce type de sollicitation de la tête, il n'a jamais été observé de blessure cérébrale pour des accélérations appliquées pendant 3 ms inférieures à 110 g: ceci confirme l'inadaptation du critère "80 g pendant 3 ms" quand il s'agit des tolérances cérébrales.

b) Résultats concernant le HIC - Les HIC obtenus, classés suivant la sévérité des blessures cérébrales, sont également résumés dans le tableau 7. Quelques remarques peuvent être faites: lorsque les blessures sont d'un niveau d'AIS  $> 3$ , les HIC ont varié de 1255 à 5000 (moyenne arithmétique 2287).

Un seul sujet associait à ce niveau de sévérité de blessures un HIC relativement faible (1255): il s'agit du sujet 83 qui a été éliminé de l'analyse car il présentait un crâne particulièrement mince, le plus mince parmi tous les sujets d'expérience (Cf. tableau 5). L'impact crânien de ce sujet était localisé dans une zone pratiquement translucide qui s'est fracturée à cet endroit. Cette fracture explique en partie le faible niveau de HIC pour ce sujet. Tous les autres sujets ont supporté des HIC compris entre 1600 et 5000. Inversement, des HIC élevés ont été supportés par des têtes humaines en l'absence de blessure.

Pour les 9 sujets indemnes, le HIC était compris entre 1000 et 1990 (moyenne arithmétique 1400).

c) Résultats concernant l'inclinaison latérale de la tête (angle  $\alpha$  dans le tableau 6).

Si l'on considère les sujets indemnes, on peut constater que leur absence de blessure cérébrale s'accompagne d'une inclinaison latérale de la tête qui est restée inférieure ou égale à  $64^\circ$ , quelle que soit la valeur de HIC. Pour tous les autres sujets (AIS 3, 4 et 5) à l'exception du sujet 83 dont on a déjà parlé, il n'y a pas eu d'inclinaison latérale forcée de la tête par rapport au thorax, et les blessures peuvent être mises en relation avec le niveau de HIC atteint, compris entre 1600 et 5000.

#### Relation entre le HIC et la sévérité des blessures cérébrales, exprimée en termes d'AIS

La figure 7 illustre les résultats obtenus, à savoir que la probabilité d'apparition d'une blessure cérébrale sévère est très faible lorsque le HIC est  $\leq 1500$  et, qu'inversement, des HIC élevés peuvent fréquemment être supportés par une tête humaine lors d'impacts latéraux sans que leur soient associées de blessures cérébrales sévères. Comme dans le cas des impacts frontaux, la validité de ces conclusions s'entend en l'absence de fractures du crâne, pour des durées de choc comprises entre 5 ms et 15 ms et des accélérations linéaires comprises entre 150 g et 350 g (110 g et 180 g pendant 3 ms).

#### 5. Synthèse des résultats des essais de chute libre

Si l'on se réfère aux accélérations et HIC obtenus, il apparaît que pour une même classe de blessures, les valeurs atteintes sont plus faibles en choc frontal qu'en choc latéral. On admettra que l'on peut, dans l'attente de la disponibilité des données de la même famille en choc latéral (accélérations angulaires, jerk), extrapoler les seuils de tolérance qui apparaissent pour les impacts frontaux.

Pour les sujets indemnes, les valeurs moyennes arithmétiques étaient les suivantes:

- . accélération linéaire maxi  $\sim 220$  g ( $\sim 130$  g 3 ms pour 11 impacts frontaux et 9 latéraux),
- . accélération angulaire maxi  $\sim 16800$   $rd/s^2$  ( $\sim 8160$  3 ms pour 9 impacts frontaux).

Ces résultats ont été obtenus pour des HIC compris entre 900 et 2350.

Lorsque le HIC est de l'ordre de 1500, on peut dire qu'au delà de la valeur  $10^5$  g/s pour le jerk d'accélération linéaire, la probabilité d'apparition d'une blessure cérébrale sévère d'AIS 2 ou 3 est voisine de 50%.

En cas d'impact frontal, il semble qu'au dessous de  $65^\circ$  pour l'hyperextension de la tête, il n'y ait pas de risque supplémentaire d'apparition de lésion.

Un grand nombre d'essais permettrait de préciser ces points.

Dans le cas général où plusieurs des paramètres étudiés doivent être considérés pour décrire la sévérité de l'impact, il apparaît que le HIC est le paramètre le mieux adapté pour permettre d'évaluer la probabilité d'apparition d'une blessure cérébrale, et que la valeur  $HIC \leq 1500$  pourrait être utilisée comme limite acceptable pour la tolérance de la tête humaine à l'impact en cas de choc frontal et latéral. La figure 8 illustre ce résultat.

#### III - RESULTATS RELATIFS AUX RECONSTITUTIONS ET SIMULATIONS D'ACCIDENTS

Les résultats acquis lors de ces essais ont été reportés sur la figure 9. Ils con-

firmement les conclusions relatives à l'utilisation du HIC et de la valeur 1500.

Ces reconstitutions sont celles de collisions réelles choisies pour leur caractère représentatif en violence et en configuration. Pour les collisions frontales, la vitesse de rapprochement des véhicules était comprise entre 100 et 120 km/h. Pour les collisions latérales, le véhicule heurtant, centré sur l'occupant situé du côté du choc, avait une vitesse comprise entre 45 et 70 km/h suivant l'essai. Ceux des occupants dont les lésions apparaissaient les plus intéressantes à reproduire étaient remplacés par des sujets humains frais préparés comme pour les essais de chute libre. Ces recherches ont été présentées dans des publications récentes (2)(4).

#### IV - DISCUSSION

a) HIC en l'absence d'impact de la tête - En collisions frontales avec sujets humains instrumentés, retenus par une ceinture de sécurité trois points, nous n'avons jamais trouvé de blessures cérébrale ou cervicale en l'absence d'impact de la tête, bien que les HIC aient parfois atteint des niveaux élevés ( $1000 \leq HIC \leq 2000$ )(11)(3). Des conclusions identiques ont été obtenues par l'analyse des accidents réels (12-13) ce qui confirme qu'il n'est pas fondé d'utiliser le HIC (ou un autre paramètre accélérométrique) à des fins de prédiction d'une blessure cérébrale en l'absence d'impact.

Cependant, en collision latérale voiture contre voiture, nous avons observé deux fois des blessures cérébrales d'AIS  $\geq 4$  alors que le déplacement de la tête par rapport au thorax n'était pas limité. Les résultats de mesures ne sont disponibles que pour un cas, où les valeurs atteintes par les paramètres physiques étaient très faibles ( $HIC = 100$  mais flexion latérale =  $75^\circ$ ).

b) Critère de protection de la tête à l'impact - Dans l'attente de disposer d'un mannequin suffisamment "biofidèle" pour que les critères de protection soient le plus directement corrélables aux blessures qu'aurait subi un être humain dans les mêmes conditions d'impact, on peut, en réalisant des essais d'impact de tête du mannequin dans les mêmes conditions de choc que pour les sujets humains, établir des relations entre le HIC cadavre et le HIC mannequin. Pour les chutes libres avec impact direct de la tête, des essais comparatifs ont déjà été réalisés (1). Ils sont reportés sur la figure 10, où il apparaît justifié de choisir le critère de protection proche de la limite tolérable préalablement déterminée.

#### Remarque importante: Utilisation du HIC pour les porteurs de ceintures en choc frontal.

Nous avons vu précédemment qu'il n'était pas justifié de calculer un HIC en l'absence d'impact de la tête. Il est donc indispensable, lorsqu'un occupant ceinturé en choc frontal impacte un élément du véhicule (volant, par exemple), de définir l'instant de contact de la tête pour le calcul du HIC.

#### CONCLUSIONS

En résumant l'ensemble des données présentées plus haut, on a dégagé les rôles respectifs du jerk d'accélération linéaire et de l'hyperextension de la tête, et obtenu des précisions sur les valeurs d'accélération linéaire et angulaire associées à l'absence de blessure cérébrale.

Par contre, lorsque plusieurs de ces paramètres atteignent simultanément les niveaux élevés, le HIC est apparu comme la fonction la mieux adaptée pour définir le seuil d'apparition d'une blessure cérébrale sévère. On associe alors à ce seuil la valeur de 1500.

#### Remerciements

L'essentiel de cette recherche a été effectué dans le cadre d'un contrat de recherche avec le Gouvernement Français par l'Institut de Recherche des Transports; les conclusions présentées sont propres aux auteurs et n'engagent en rien cet organisme.

#### REFERENCES

- (1) "Results of experimental head impacts on cadavers. The various data obtained and their relations to some measures physical parameters", C. Got, A. Patel (IRO), A. Fayon, C. Tarrière, G. Walfisch (Laboratoire de Physiologie et de Biomécanique Peugeot S.A./Renault), proceedings of 22nd Stapp Car Crash Conference, oct. 24-26th, 1978, Ann Arbor Michigan, USA, published by SAE.
- (2) "Complete analysis and Synthesis of a Series of Reconstructions of Five Real-Life Side Impact Collision Accidents", C. Tarrière, B. Hue, A. Fayon, G. Walfisch (Laboratoire de Physiologie et de Biomécanique Peugeot S.A./Renault), part of the general work program of the joint biomechanical research project (K.O.B.), 1982,

#### "Unfall- und Sicherheitsforschung Strassenverkehr"

- (3) Contribution to the consensus workshop on head and neck injury criteria. C. Tarrière, Laboratory of Physiology and Biomechanics Peugeot S.A./Renault, Washington, March 1981.
- (4) "Reconstruction of Side Collisions", C. Tarrière, B. Hue, A. Fayon, G. Walfisch, in Proceedings of the 8th International Technical Conference on Experimental Safety Vehicle, ESV, Wolfsburg, 21 to 24 october 1981, U.S. Department of Transportation, NHTSA, U.S. Government printing office, Washington DC 20402, USA.

5. "Human head tolerance to impact: influence of the jerk (rate of onset of linear acceleration) on the occurrence of brain injuries", G. Walfisch, A. Fayon, C. Tarrière, F. Chamouard, F. Guillon, C. Got, A. Patel, J. Hureau, Proceedings of the 6th International IRCOBI Conference on the Biomechanics of Impact, 8-9-10 september 1981, Salon-de-Provence (France), Secrétariat de l'IRCOBI, Onser, 109 ave. Salvador Allende, 69500 Bron.
6. "Mass, Volume, Center of Mass and Mass, moment of Inertia of Head", L.B. Walker, E.H. Harris, U.R. Pontius, Proceedings of the 17th STAPP Car Crash Conference, S.A.E., 1973.
7. The abbreviated injury scale, 1980 revision, American Association for Automotive Medicine, Morton Grove, Illinois 60053, USA.
8. Significance of Rate of Onset in Impact Injury Evaluation, D. Viano, C.W. Gadd, Biomedical Science Department, General Motors Research Laboratories, in Proceedings of 19th Stapp Car Crash Conference, November 1975, San Diego, California.
9. "Complete analysis and synthesis of a series of reconstructions of real-life car/pedestrian accidents", A. Heger, H. Appel, Institute of Automotive Engineering, Technical University, Berlin, part of the general work program of the Joint Biomechanical Research Project (KOB), 1982:

"Unfall- und Sicherheitsforschung Strassenverkehr

10. Essais préliminaires à l'élaboration du cahier des charges d'un casque d'utilisateurs de deux-roues, J. Sacreste, A. Fayon, C. Tarrière, Laboratoire de Physiologie et de Biomécanique Peugeot S.A./Renault, C. Got, A. Patel, IRO.
11. Synthèse des résultats et conclusions d'une série d'essais de ceintures de sécurité retenant des cadavres, A. Fayon, C. Tarrière, G. Walfisch, Laboratoire de Physiologie et de Biomécanique Peugeot S.A./Renault, C. Got, A. Patel (IRO). Proceedings of the 2nd international IRCOBI Conference on Biomechanics of Impact, September 1975, Birmincham, England (Secrétariat de l'IRCOBI, ONSER, 109 ave. Salvador Allende, 69500 Bron, France.
12. How to further improve the protection of occupants wearing seat-belts, F. Hartemann, C. Tarrière, G.M. Mackay, P.F. Gloyns, H.R.M. Hayes, D. Cesari, M. Ramet, Proceedings of 19th Conference of the American Association for Automotive Medicine (A.A.A.M.), November 1975, San Diego, California, USA.
13. Belted or not belted: the only difference between two matched samples of 200 car occupants. F. Hartemann, C. Thomas, C. Henry, J.Y. Foret-Bruno, G. Faverjon and C. Tarrière, Laboratory of Physiology and Biomechanics Peugeot S.A./Renault, Rueil-Malmaison (92) France, in proceedings of 21st Stapp Car Crash Conference, October 1977, New Orleans, Louisiana, USA.

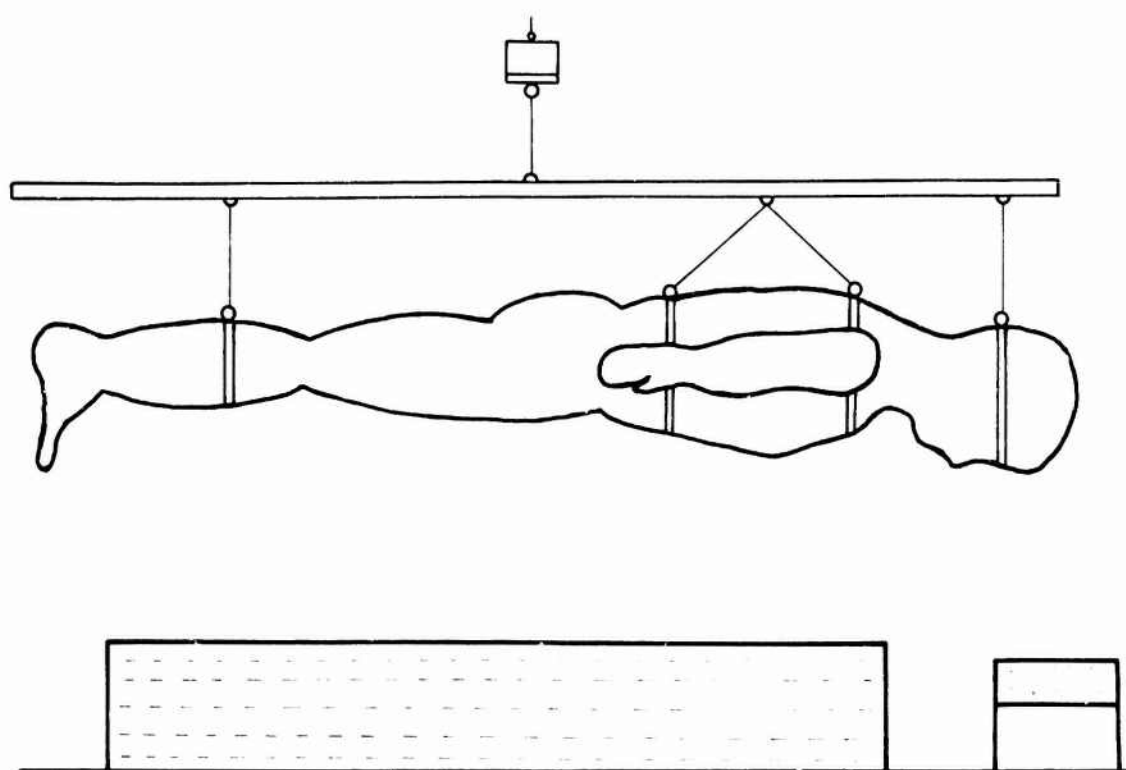


FIG.1. PRINCIPE DES ESSAIS IMPACTS FRONTAUX

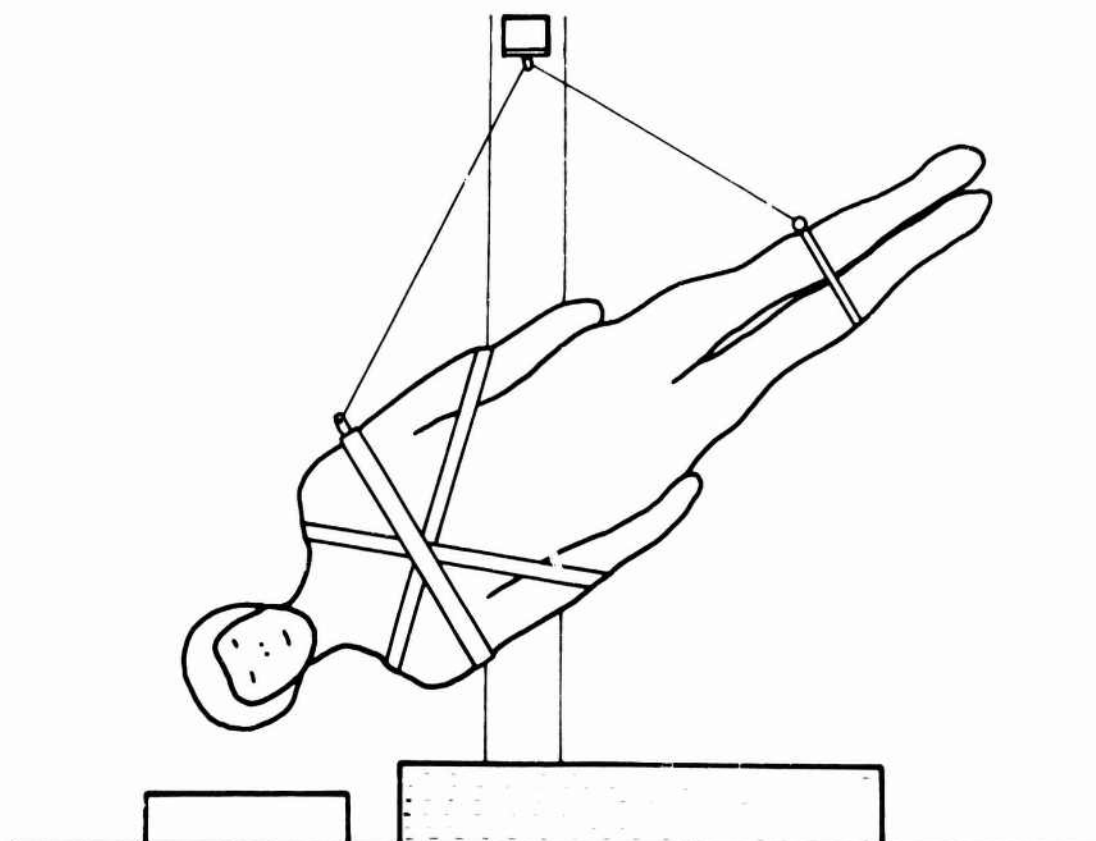
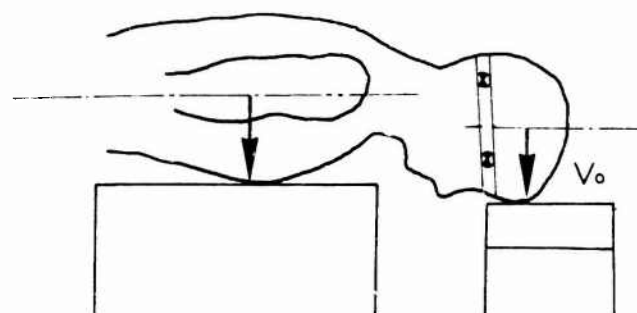
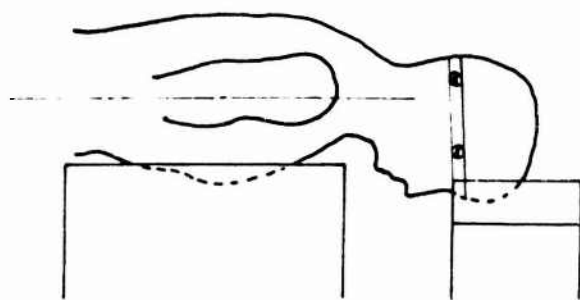


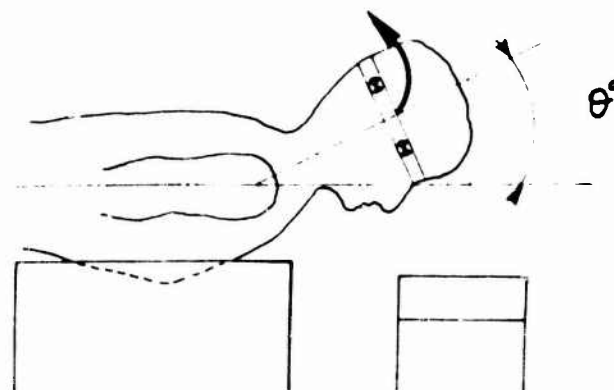
FIG.2. PRINCIPE DES ESSAIS IMPACTS LATÉRAUX



Instant de contact de la tête



Enfoncement dynamique max. de la tête dans le padding



Rebond de la tête

FIG.3. Cinématique de la tête — impacts frontaux.



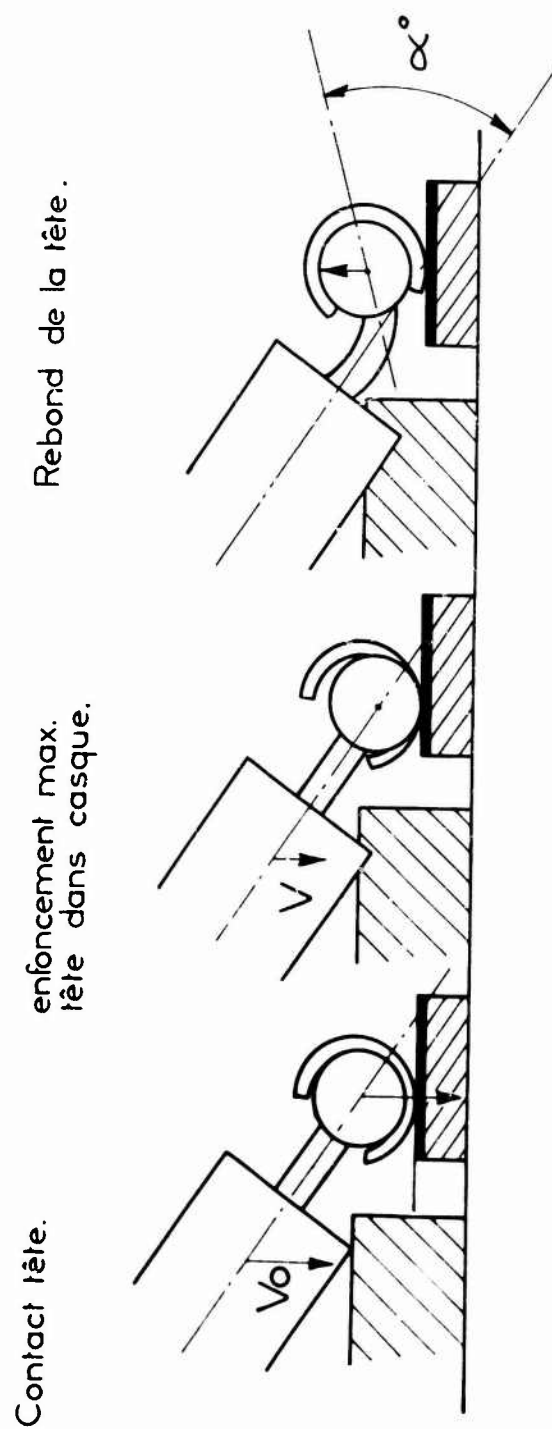


FIG 4 CINEMATIQUE SIMPLIFIEE DE LA TETE.  
IMPACTS LATERAUX.



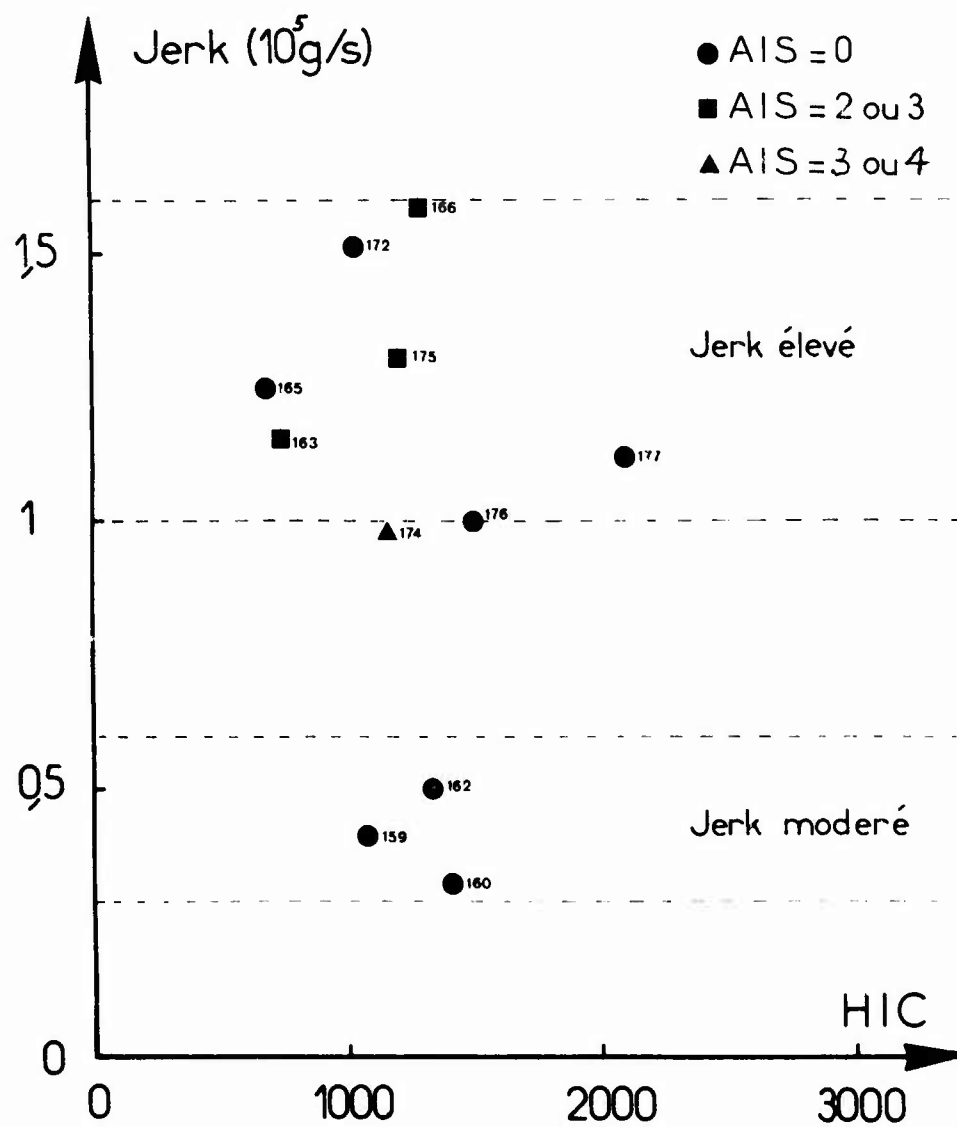


FIG.5. SEVERITE DES BLESSURES CERE-  
-BRALES EXPRIMEES DANS UN PLAN  
JERK/HIC -IMPACTS FRONTAUX

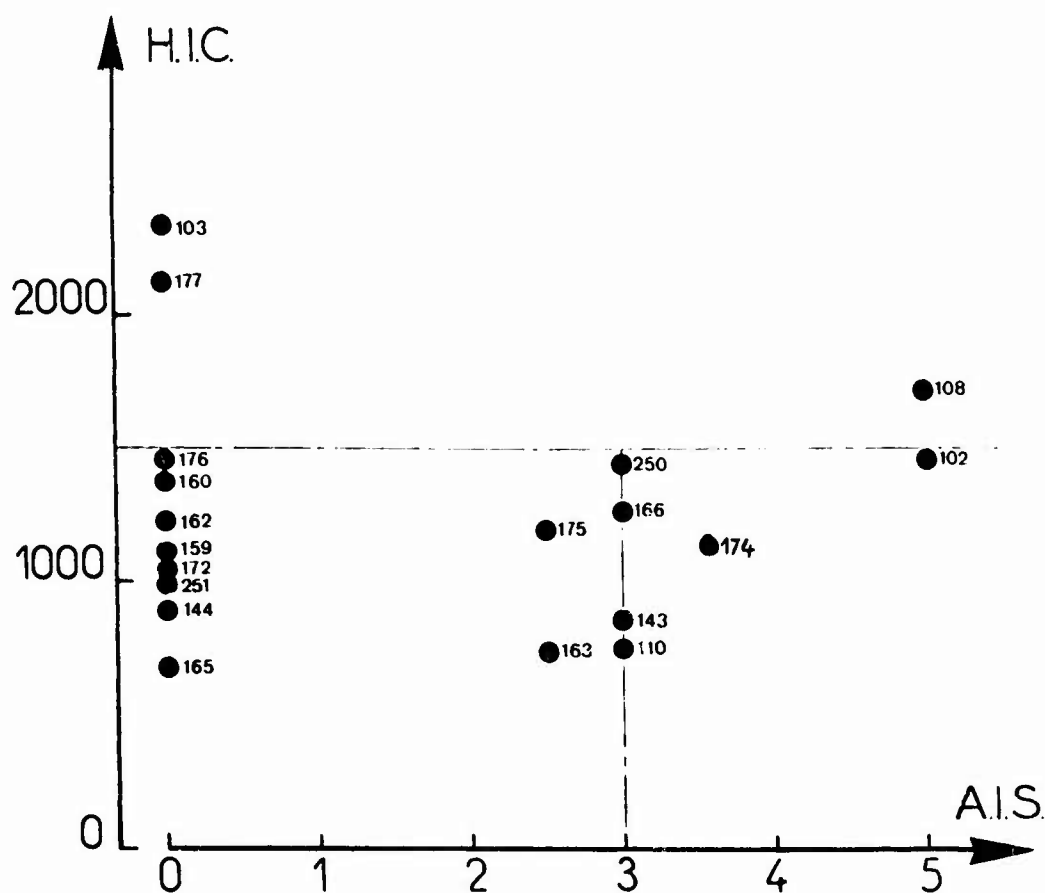


FIG.6. RELATION HIC/AIS-IMPACTS FRONTAUX

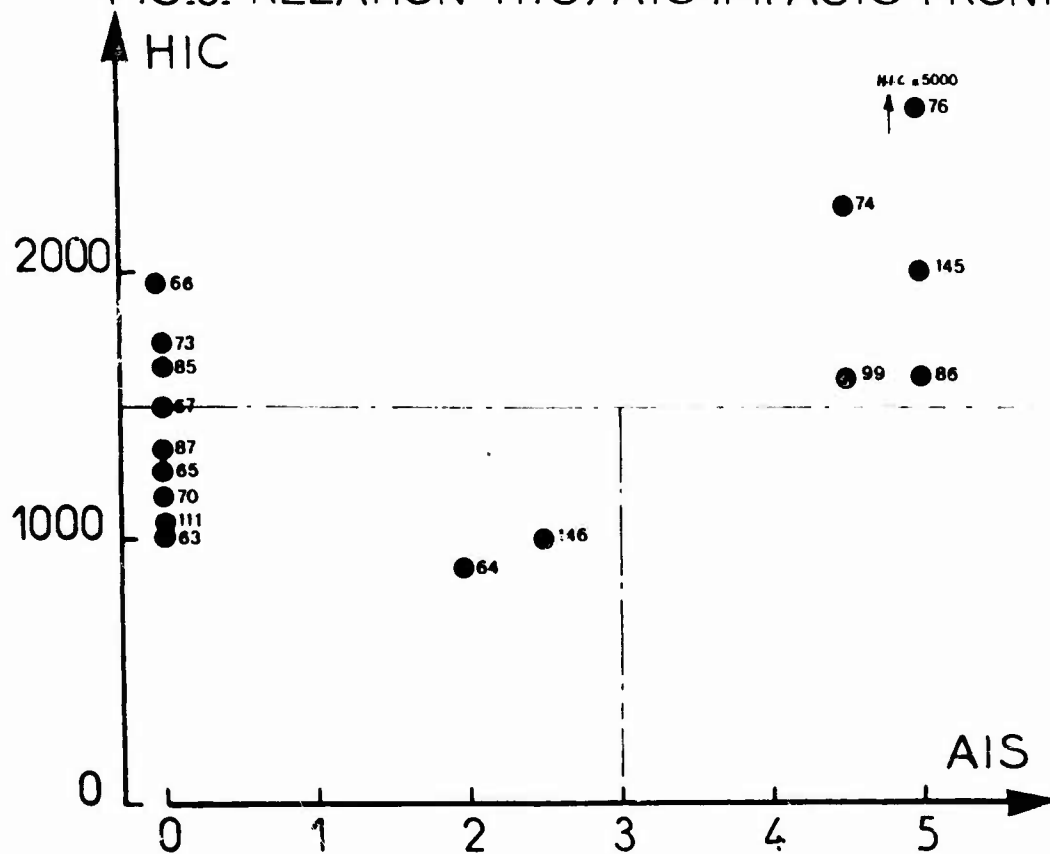


FIG.7. RELATION HIC/AIS-IMPACTS LATéraux

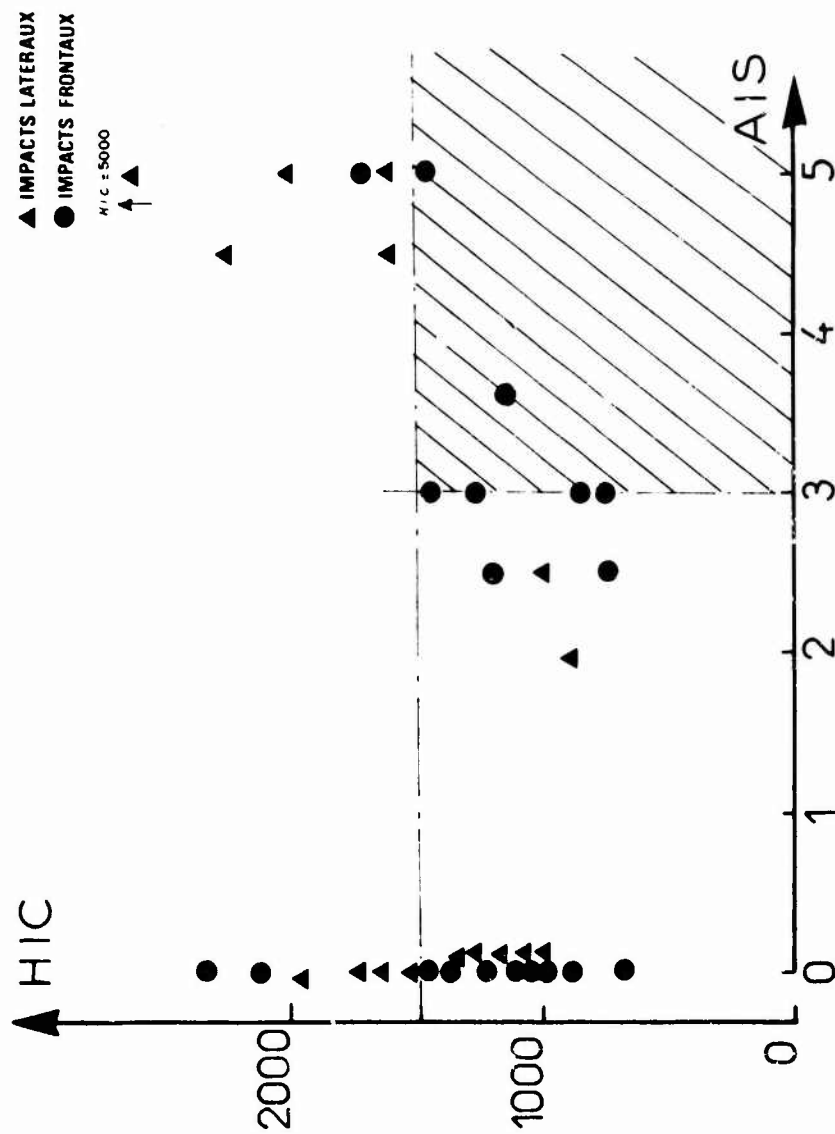


FIG.8. RELATION HIC/AIS  
SYNTHÈSE DES CHUTES LIBRES

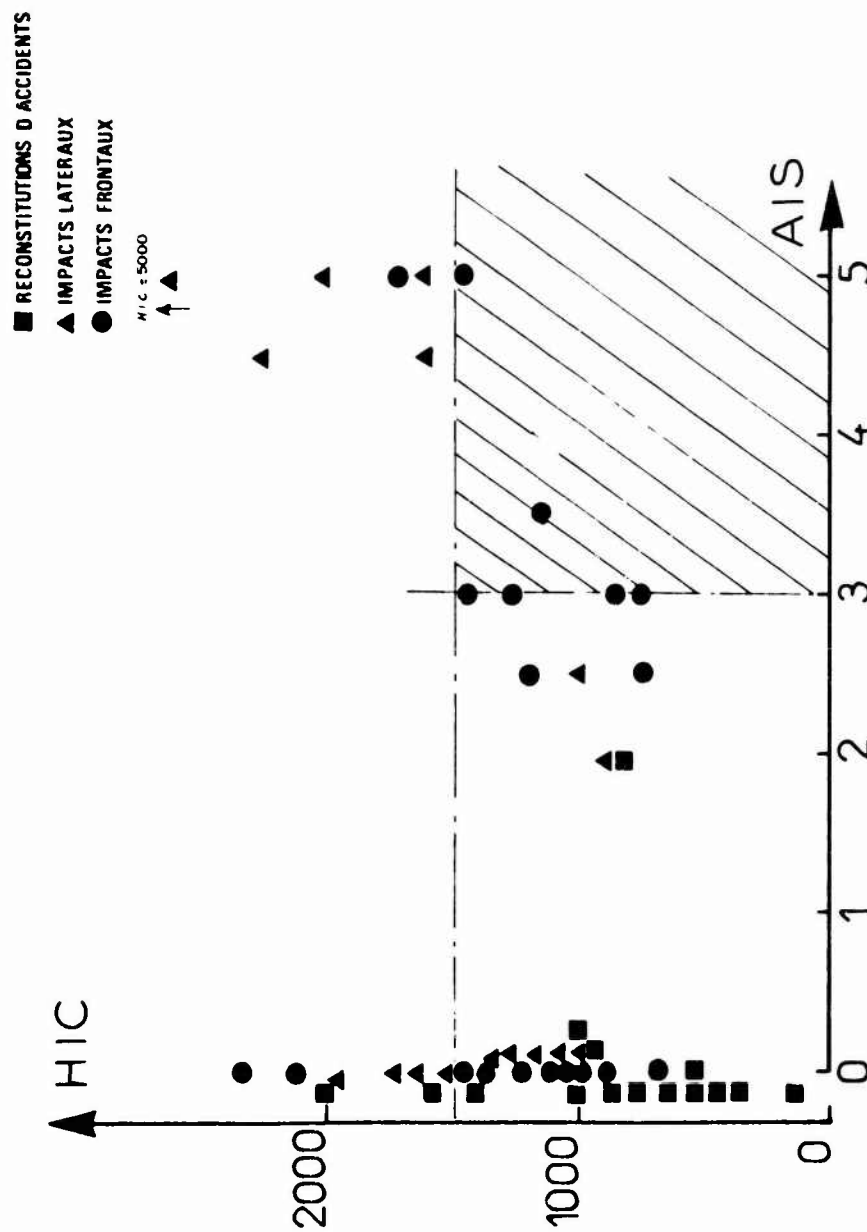


FIG 9 RELATION HIC/AIS.  
 SYNTHÈSE DES CHUTES LIBRES ET DES  
 RECONSTITUTIONS D ACCIDENTS.

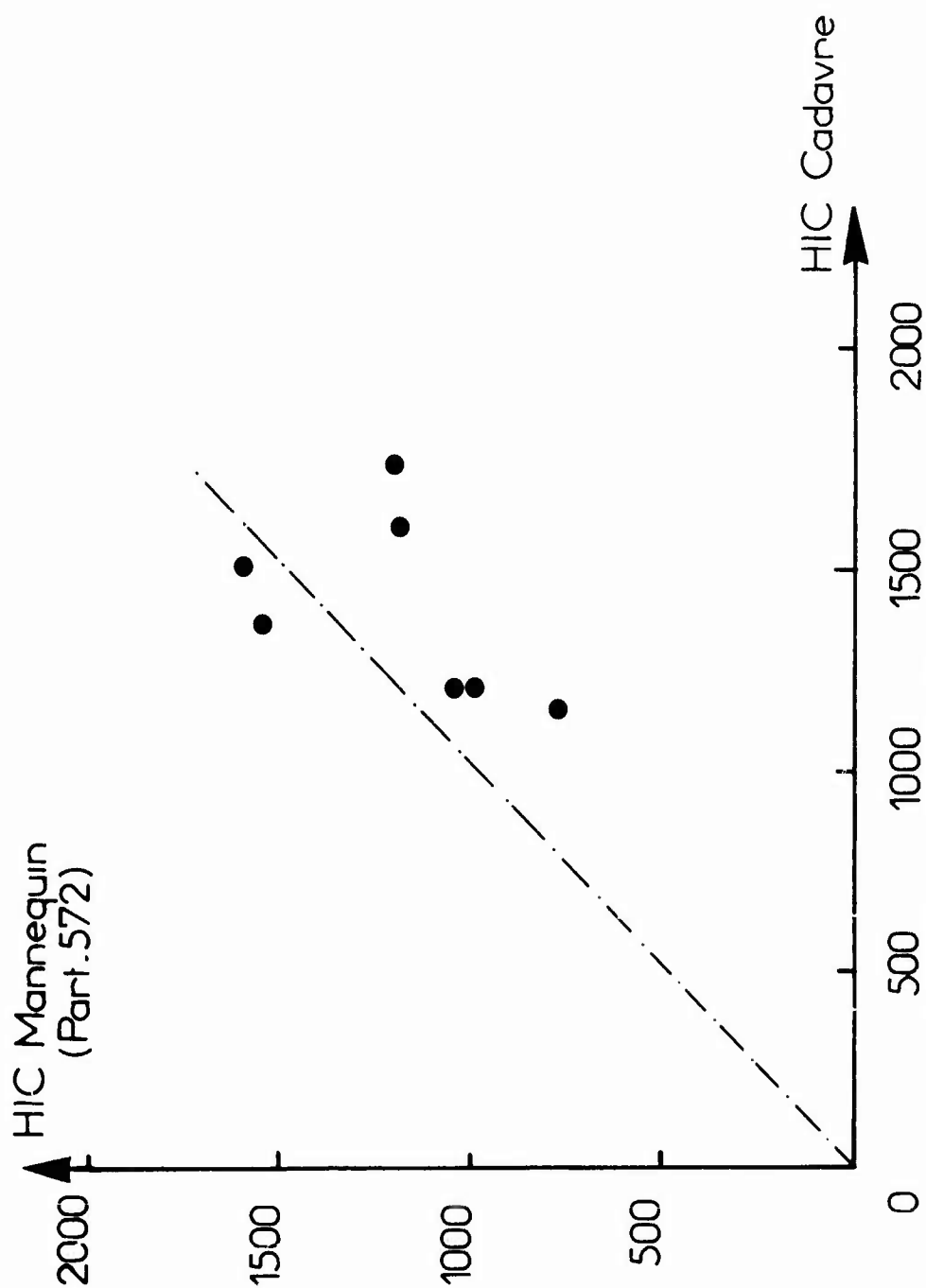


FIG 10 COMPARAISON ENTRE LES HIC MESURES SUR LA TETE DU MANNEQUIN ET CEUX MESURES AU CENTRE DE GRAVITE DE LA TETE DES SUJETS HUMAINS DANS LES MEMES CONDITIONS D'ESSAIS.

TABLEAU 1 - LOCALISATION DES LESIONS CEREBRALES

Type d'impact	Nbre de sujets avec évaluation de l' AIS cérébral	Nbre de sujets blessés	LOCALISATION DES BLESSURES			Lésions cérébrales associées à une fracture du crâne
			Tronc cérébral	Protubérance seule	Autre que tronc cérébral	
pariéto-temporal	17	9	7	4	4	1
frontal	20	10	7	6	3	2

TABLEAU 2 - MESURES ANTHROPOMETRIQUES DE LA TETE DES SUJETS HUMAINS - ESSAIS DE CHUTE LIBRE - IMPACTS FRONTALS

Essai n°	Age	Sexe	Dimensions de la tête (cm)		Circonf. ce	Masse de la tête (kg)		Caractérisation du crâne	
			Diamètre antéro-postérieur	Diamètre transversal		Tête+cou	tête	Minéralisation (g/cm <sup>2</sup> )	Épaisseur moyenne (mm)
102	69	M	17,2	14,8	52,0	4,58	3,33	1,20	5,30
103	68	M	19,5	16,9	61,5	4,30	3,32	1,46	7,67
107	55	F	17,5	13,2	52,0	3,57	2,32	0,62	4,31
108	64	M	18,6	14,7	55,8	5,30	3,78	1,28	6,38
110	49	M	18,7	14,2	54,2	6,22	4,90	1,20	6,50
143	69	M	18,0	16,0	54,6	4,87	3,72	1,33	
144	68	M	18,0	14,5	53,4	4,73	3,92	1,16	
159	60	M	20,5	16,0	60,6	5,61	4,41	0,99	6,32
160	56	M	20,6	16,2	57,2	5,45	4,25	0,97	6,62
162	64	M	19,2	15	54,4	4,86	3,62	0,63	5,04
163	63	M	20	17	59,4	6,56	4,59	1,06	7,45
165	66	M	20,5	15	57,5	5,95	4,31	0,93	6,26
166	59	F	18	15,2	56,4	5,14	4,10	0,68	5,53
172	50	M	19	17	57,5	5,4	4,17	0,69	5,85
174	65	M	18,5	16	55,3	4,78	3,96	0,76	5,33
175	73	M	20,5	15,5	53,6	4,27	3,22	0,78	6,48
176	53	M	20	16,5	57,4	5,69	4,26	1,04	6,20
177	64	F	19	15,5	53,6	4,24	3,30	1,00	5,98
250	66	F	19	15,4	54,5	4,53	3,41	-	
251	38	F	18,4	14,6	54,5	5,05	3,57	1,30	5,25

\*:masse du squelette cranio-facial moins la mâchoire inférieure .

TABLEAU 3 - ESSAIS DE CHUTES LIBRES DE TÊTES - IMPACTS FRONTALS - RESULTATS DE MESURES

Essai n°	Accélération linéaire tête		$\Delta t$ calcul du HIC (ms)	Jerk d'accélération linéaire ( $\mu 105$ g/s)	Vitesse angulaire (rd/s) maxi	Accélération angulaire (rd/s <sup>2</sup> ) maxi	Hyperextension		AIS cérébral
	maxi (g)	3 ms (g)					°	tête/thorax	
103	349	149	3.1	2.49	50.73	35779	15118	65	0
144	126	117	2.3	0.16				56	0
159	214	117	6.0	0.415	25.7	10025	4340	27	0
160	187	150	4.8	0.32	63.3	10546	8989	19	0
162	192	132	6.2	0.51	37.6	21352	1043	56	0
165	163	109	6.2	1.25	21.9	14744	1302	31	0
172	209	102	6.0	1.52	25.2	15240	9000	26	0
176	257	127	4.60	1.00	18.9	8953	5058	20	0
177	255	169	4.70	1.14	23.3	10373	7021	17	0
251	252	129	7.5	0.63	56.2	24265	12079	76	0
110	194	109	8.7	0.52	85.1	40120	9504	78	3
143	292	101	9.2	0.17	48.5	43226	8185	66	3
163	150	102	6.2	1.17				19	2 ou 3
175	190	130	5.3	1.3				21	2 ou 3
166	213	133	5.8	1.59	14.6	11282	5418	22	3
250	202	129	9.7	0.76	96.2	15313	12978	61	3
102	232	147	3.6	0.87	84.1	39336	17222	80	5
107	154	90	10.1	0.55	69.6	18205	10905	70	3 ou 4
108	313	144	3.5	0.50	80.8	20343	12064	67	5
174	182	122	7.4	0.39	23.3	18922	12936	27	3 ou 4



TABLEAU 4 - CHUTES LIBRES DE TÊTES - IMPACTS FRONTAUX - RESUME DES PRINCIPAUX RESULTATS

	Nombre d'essais	AIS = 0			Blessures cérébrales $2 \leq AIS \leq 3$				AIS > 3				
		Nombre d'essais			moyenne			Nombre d'essais			moyenne		
		mini	maxi	moyenne	mini	maxi	moyenne	mini	maxi	moyenne	mini	maxi	moyenne
accélération linéaire maxi	10	126	349	220	6	150	292	206,8	4	154	313	220	
accélération linéaire 3ms	10	102	169	130	6	101	133	117	4	90	147	125	
HIC	10	692	2351	1344	6	750	1460	1050	4	516	1720	1218	
$\theta$ tête/thorax	9	17	76	41	6	19	78	44	4	27	80	61	
Jerk 105 g/s	11	0,16	2,49	0,95	6	0,17	1,59	0,92	4	0,50	0,99	0,74	
Vitesse angu- laire maxi (rd/s)	8	18,9	63,3	36	4	14,6	85,1	61	4	23,3	84,1	64	
Vitesse angu- laire 3ms (rd/s)	8	18,5	61,1	30	4	14,1	74,9	56	4	23,2	83,6	63	
Accélération angulaire maxi (rd/s <sup>2</sup> )	9	8953	35779	16808	4	11282	43226	32485	4	18205	39336	24201	
Accélération angulaire 3ms (rd/s <sup>2</sup> )	9	4302	15118	8161	4	5418	12978	9021	4	10905	17222	13281	

TABLEAU 5 - RELEVÉ ANTHROPOMETRIQUE DE LA TÊTE DES SUJETS HUMAINS - ESSAIS DE CHUTE LIBRE - IMPACTS LATÉRAUX

Essai n°	Age	Sexe	Dimensions de la tête (cm)		Masse de la tête (kg) Tête+cou	Caractérisation du crâne Minéralisation (g/cm <sup>2</sup> )	Épaisseur moyenne (mm)
			Ø antéro-postérieur	Ø transversal			
63	78	F	18,2	15	4,02	3,28 0,53	1,05
64	59	M	19,2	14,5	4,86	3,92 0,55	1,05
65	57	M	19,4	15,5	5,02	4,23 0,88	1,58
66	82	F	18,2	14,5	3,56	2,92 0,53	1,11
67	82	F	18,2	14,1	4,43	3,34 0,69	1,27
68	49	F	18,4	14,5	5,16	3,82 0,79	
69	71	M	20,2	15,6	4,70	3,81 0,80	0,97
70	68	M	19,2	14,1	4,58	3,56 0,75	1,50
73	55	F	17,5	14	4,78	3,68 0,51	1,01
74	74	M	18	13,5	5,22	3,64 0,95	1,67
76	75	M	19,2	14	4,23	3,45 0,75	1,13
83	74	F	19,2	15	4,12	3,33 0,46	0,70
85	65	M	17,2	14	4,62	3,36 0,72	0,84
86	65	M	19	15	3,47	3,00 0,99	1,26
87	73	M	20	15	5,52	3,73 1,25	1,30
99	73	F	18	14,5	4,00	2,80 0,51	0,96
111	52	M	18,4	15,2	4,87	3,64 0,80	1,15
145	68	M	18	15	4,22	3,45	
146	68	M	18	15	4,96	3,91	
147	57	F	19	14	4,42	3,59	

TABLEAU 6 - RESULTATS DE MESURES - ESSAIS DE CHUTE LIBRE - IMPACTS LATÉRAUX

Essai n°	Accélération maxi (g)	Accélération linéaire 3 ms (g)	HIC	$\Delta t$ calcul de HIC (ms)	Vitesse angulaire (rd/s) maxi 3 ms	Accélération angulaire maxi (rd/s) 3 ms (rd/s)	Inclinaison latérale tête/thorax °	A.I.S. cérébral
63	198	110	1000	6,2			32	0
65	175	130	1250	6,1			36	0
66	240	167	1993	4,8	30,3	19219	7138	0
67	210	152	1500	3,8	25,7		61	0
70	160	145	1200	7,1			58	0
73	240	172	1750	4,6			30	0
85	350	172	1665	-	31,3	7042	58	0
87	240	140	1350	5,8		10000	55	0
111	153	109	1000	10,20		13300	55	0
64	165	110	900	7,1			72	2
146	144	125	1000	6,6	31,5	6385	15	2 ou 3
74	459	136	2250	5,3	29,04	4556	39	4 ou 5
99	292	140	1600	7,6	25,4	20626	32	4 ou 5
83	210	143	1255	3,8	24,25	20160	89	4 ou 5
76	580	200	5000	4		8000	53	5
86	211	148	1690	5,4		7500	28	5
145	216	178	2000	5,8		12000	33	5

TABLEAU 7 - RESUME DES PRINCIPAUX RESULTATS - ESSAIS DE CHUTE LIBRE - IMPACTS LATéraux

	AIS = 0			LESIONS CEREBRALES						AIS > 3		
	Nombre sujets	Mini		Nombre sujets	Mini		Nombre sujets	Mini		Mini	Maxi	Moyenne
		Maxi	Moyenne		Maxi	Moyenne		Maxi	Moyenne			
accélération linéaire maxi	9	153	350	218	2	144	165	154	6	210	580	328
Accélération linéaire 3ms	9	110	172	144	2	110	125	117	6	136	200	157
H.I.C.	9	1000	1993	1412	2	900	1000	950	6	1255	5000	2284
Inclinaison tête/thorax $\alpha$	9	30°	64°	52°	2	15°	68°	41°	6	28°	89°	45°

## HEAD AND SPINE INJURIES

Anthony Sances, Jr., Ph.D.  
 Joel Myklebust, Ph.D.  
 Chris Houterman, B.S.  
 Robert Weber, Ph.D.  
 James Lepkowski, B.S.  
 Joseph Cusick, M.D.  
 Sanford Larson, M.D., Ph.D.

The Medical College of Wisconsin and Wood VA Medical Center  
 8700 West Wisconsin Avenue  
 Milwaukee, Wisconsin 53226 USA

Channing Ewing, M.D.  
 Daniel Thomas, M.D.  
 Marc Weiss, Ph.D.  
 Michael Berger, Ph.D.  
 M. Eugene Jessop, D.V.M.  
 Naval Biodynamics Laboratory  
 P.O. Box 29407  
 New Orleans, Louisiana 70189 USA

Bernard Saltzberg, Ph.D.  
 Texas Research Institute of Mental Sciences  
 1300 Moursund, Texas Medical Center  
 Houston, Texas 77030 USA

## SUMMARY

Neurophysiologic and biomechanical methods were used to evaluate axial tension applied to the cervical spinal cord and brain during impact or inertial loading. Because axial forces are often implicated in military accidents, these studies were designed to evaluate physiologic changes in the brain and spinal cord with cervical axial tension applied to the rhesus (*Macaca mulatta*) monkey. Both slowly applied (0.1 to 1 cm/s) and rapidly applied loads (greater than 100 cm/s) were studied in the isolated fresh cadaveric cervical column of the monkey and in the intact living and dead monkey. Similar investigations were conducted on fresh human cadaveric skulls and cervical spinal columns and in the fresh human cadaveric torso. Both axial tension and compression were applied to the human preparations. Thoraco-lumbar sections were also tested for failure in compression. Helmet studies were also conducted to determine the effects with axial loading. A mathematical model was developed using a lumped parameter torso, head and helmet capable of simulating displacement and time dependent applied loads. The model was compared with photographically studied football injuries for validation.

## I. INTRODUCTION

The majority of studies on head and spine injury have evolved damage criteria from biomechanical measurements and pathological findings (33). In contrast, few studies are available which evaluate the neurophysiological parameters of injury in the closed animal model. Most studies of the physiology of head and spinal cord injury utilize techniques similar to the Allen (1,41) method in which the neural tissue is directly traumatized. These methods require the destruction of supporting elements such as vertebrae and ligaments, making biomechanical correlations difficult. Furthermore, the injuries produced often do not correlate with those seen clinically (3,7,19-22).

Consequently, studies have been directed to develop a physiologically controlled closed model of spinal cord injury with axial tension in the subhuman primate. Biomechanical data has been obtained from monkeys and fresh human cadavers to determine the mechanical and physiological parameters of human spinal cord injury (32,34,35).

All of the subhuman primate studies were done with axially applied tension forces. A critical review of the quasi-static and the dynamic films and X-rays demonstrated less than 10 degrees of extension or flexion induced during the experiments. The alteration of the evoked potential secondary to spinal cord distraction was studied in monkeys in whom thoracic osteotomies were done with stimulation of the dorsal columns of the spinal cord.

Cerebral responses were gone within two minutes after complete occlusion of the ascending aorta. The evoked responses recorded from the spinal cord continued for approximately ten minutes and then gradually disappeared. However, the immediate flexion and distraction responses were altered. These findings suggest that mechanical trauma alters the spinal cord evoked potentials and that it should be possible to differentiate a mechanical from a vascular insult (19). In the efferent pathways, stimulation of the motor cortex produces a response which can be measured over the spinal columns reflecting the physiologic integrity of the corticospinal tracts. The corticospinal tracts are altered in the same way as the afferent response by cord flexion, distraction or ischemia. Therefore, the evoked potentials can be used to evaluate spinal cord dysfunction over afferent or efferent pathways (35).

Changes in the spinal and cerebral afferent and efferent evoked potentials were evaluated with axial forces applied between the shoulders and skull of the living male *Macaca mulatta* monkey. The failure loads ranged from 556 Newtons to 1555. The largest cervical stretch was observed in the smallest animals (32). The loads were quasi-statically applied.

The majority of animals demonstrated minimal ligamentous disruption except one animal which had a C3-C4 total disruption at 1112 Newtons. Two animals with posterior muscular transection showed findings similar to the intact animals. The majority of changes appeared to be secondary to mechanical stretch of the cervical medullary junction. Routinely, the evoked potentials decreased prior to or concurrently with changes in heart rate, blood pressure and regional perfusion evaluated with microspheres (34).

Studies in monkeys at high loading rates (up to 110 cm/s) produced failures of the upper cervical spinal column at 1690 Newtons to 2668 Newtons. In these animals, a cervical displacement of 0.5 cm to 1 cm produced a 50% reduction in the evoked potential. Structural failure and alteration in physiologic parameters occurred with displacements of 1.25 cm to 2.13 cm (34).

These studies suggest that the afferent and efferent evoked potentials are sensitive indicators of metabolic or mechanical alterations in spinal and cerebral pathways. Forces required for tissue disruption were approximately twice as great in the dynamic studies compared to quasi-static runs.

The strength of the isolated monkey cervical column was evaluated with slow and rapid loading rates with forces applied between the skull and upper thoracic spine. In quasi-static tests, the columns failed at 325 to 534 Newtons. With rates up to 170 cm/s, the failure loads were 1289 to 1423 Newtons. The anterior ligaments were approximately twice as strong as the posterior and failures routinely started in the anterior ligaments and proceeded posteriorly. The monkey cervical spinal cord failed in tension at approximately 35 Newtons quasi-statically and 90 Newtons dynamically (32,34).

## II. MODEL STUDIES

Analysis of sports injury films indicate various time dependent and position dependent events are required for cerebral or cervical spinal injury. To provide an understanding of the mitigating effects of helmet protection and to estimate the forces upon the necks and accelerations at the head, a model was developed. The computer model simulates player impact conditions with and without helmets with a typical contact surface (Figure A). An external force can be included which often occurs with opposite player contact.

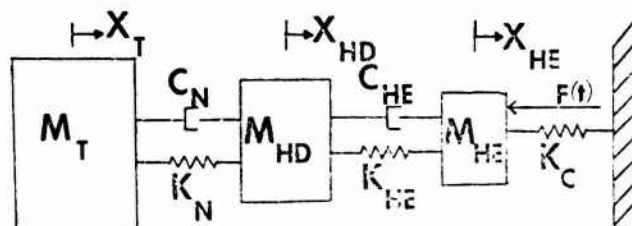


FIGURE A: LUMPED PARAMETER MODEL

where  $M_T$  = mass of thorax (kg),  $C_N$  = damping coefficient of neck (Ns/cm),  $K_N$  = stiffness coefficient of neck (N/cm),  $M_{HD}$  = mass head (kg),  $C_{HE}$  = damping coefficient of helmet,  $K_{HE}$  = stiffness coefficient of helmet,  $M_{HE}$  = mass of helmet,  $K_C$  = stiffness coefficient of contact surface,  $F(t)$  = external applied force to helmet, N = Newtons, s = seconds, m = meters, cm = centimeters.

The model motion is confined to one dimension, is coincident with the spinal axis and neck and helmet compression is not restricted. The muscles and ligaments and overlying tissue offer negligible resistance in compression; and the skull stiffness is neglected. The upper and lower limbs and torso are combined into an effective torso mass (25,35). The torso mass is appropriately reduced to account for the angle of impact of the athlete with another player or a fixed object. The following equations define the acceleration of the thorax, head, and helmet, respectively

$$\ddot{X}_T(t) = \frac{C_N(\dot{X}_{HD}(t) - \dot{X}_T(t)) + K_N(X_{HD}(t) - X_T(t))}{M_T} \quad (1)$$

$$\ddot{X}_{HD}(t) = \frac{C_N(\dot{X}_T(t) - \dot{X}_{HD}(t)) + C_{HE}(\dot{X}_{HE}(t) - \dot{X}_{HD}(t)) + K_N(X_T(t) - X_{HD}(t)) + K_{HE}(X_{HE}(t) - X_{HD}(t))}{M_{HD}} \quad (2)$$

$$\ddot{X}_{HE}(t) = \frac{C_{HE}(\dot{X}_{HD}(t) - \dot{X}_{HE}(t)) + K_{HE}(X_{HD}(t) - X_{HE}(t)) - K_C(X_{HE}(t)) + F(t)}{M_{HE}} \quad (3)$$

For the no helmeted case  $C_{HE}$ ,  $K_{HE}$  and  $M_{HE}$  are zero. Table A compares the impact with helmet (H) and without helmet (WH) for effective torso masses of 34 and 68 kg. The Table indicates that the helmet provides protection; however the neck forces are in the region of injury at velocities of 3 to 4.6 m/s (5,12,14,27,28,33). A review of football injury films demonstrates neck injuries with impact velocities of approximately 5 m/s (35). The helmet provides the greatest neck and cerebral protection for the smaller torso mass. Furthermore, studies with typical commercial football helmets indicate bottoming out with 2 to 3 cm of compression (35). Beyond this compression, substantially higher forces and energy are transmitted to the brain and neck when the helmet bottoms out. Brain injury may occur in the region of the highest impact velocities with a 68 kg mass where bottoming out probably occurs. Table B shows the effects of various stiffness and damping coefficients upon peak neck force, peak head accelerations and peak helmet compression for the typical parameters shown in the legend. The least risk for the head and neck occurs with the smallest values of helmet stiffness and largest helmet damping coefficients, however, a substantial increase in helmet compression is required.

Table C demonstrates an augmentation of neck forces with increasing neck stiffness and compliance, and a decrease in neck compression and acceleration at the head. Table D shows typical stiffness and compliance parameters for six popular commercially available helmets. The model is a single spring with stiffness ( $k_2$ ) in series with a kelvin element with a spring having a stiffness of ( $k_1$ ) and parallel dashpot with a compliance of ( $C_1$ ).

For comparable parameters, this model yields results similar to those published by McElhaney (25). However, his study did not include variation of helmet compliance, neck stiffness, compliance, and compressions.

This model may be useful in evaluating the effects of changes in helmet and neck parameters, and for estimating forces and accelerations in injury. Studies of helmets and human cadavers suggest that the kelvin elements can be approximated with series springs, or two series of kelvin elements. Parametric optimization indicates that the neck model should be replaced with, at least two series kelvin elements with stiffnesses of 900 to 1800 N/cm and 1400 to 2100 N/cm and compliance of 35 to 150 Ns/cm (39).

TABLE A

$M_T$	H/WH	$V_i$	$F_N$	$A_{HD}$	$N_C$	$H_C$
(kg)		(m/s)	(N)	(m/s <sup>2</sup> )	(cm)	(cm)
34	WH	3	6672	762	3.6	--
34	H	3	5338	549	3.0	1.5
34	WH	4.6	9786	1128	5.6	--
34	H	4.6	8006	823	5.1	2.3
34	WH	7.6	16458	1859	9.1	--
34	H	7.6	13789	1341	7.9	3.6
68	WH	3	8896	762	5.1	--
68	H	3	8451	549	4.5	1.8
68	WH	4.6	13344	1128	7.6	--
68	H	4.6	12010	823	7.0	2.8
68	WH	7.6	22685	1859	12.7	--
68	H	7.6	20016	1341	11.5	4.6

Peak values of force on the neck ( $F_N$ ), acceleration of the head ( $A_{HD}$ ), compression of the neck ( $N_C$ ) and compression of the helmet ( $H_C$ ) for torso weights ( $M_T$ ) of 34 and 68 kg, impact velocities ( $V_i$ ) of 3 m/s, 4.6 m/s, and 7.6 m/s, with helmet (H) and without helmet (WH). Constant values for the model were  $K_N = 1751$  N/cm,  $C_N = 1.75$  Ns/cm,  $K_{HE} = 4378$  N/cm,  $C_{HE} = 3.5$  Ns/cm,  $M_{HD} = 4.5$  kg,  $M_{HE} = 0.1$  kg,  $K_C = 4378$  N/cm.  $F(t) = 0$ .

TABLE B

$K_{HE}$	$C_{HE}$	$F_N$	$A_{HD}$	$H_C$
(N/cm)	(Ns/cm)	(N)	(m/s <sup>2</sup> )	(cm)
4378	0.175	20461	1676	4.6
4378	3.5	20238	1433	4.6
4378	17.5	18904	1402	4.3
1791	3.5	16680	1067	9.7
4378	3.5	20238	1433	4.6
8756	3.5	20906	1524	2.5

Peak force on the neck ( $F_N$ ), acceleration of the head ( $A_{HD}$ ), and helmet compression ( $H_C$ ) with changes in helmet stiffness ( $K_{HE}$ ) and damping ( $C_{HE}$ ) characteristics. Constant values for models were  $K_N = 1751$  N/cm,  $C_N = 1.75$  Ns/cm,  $M_T = 34$  kg,  $M_{HD} = 4.5$  kg,  $M_{HE} = 0.9$  kg,  $K_C = 4378$  N/cm,  $V_i = 7.6$  m/s.  $F(t)=0$

TABLE C

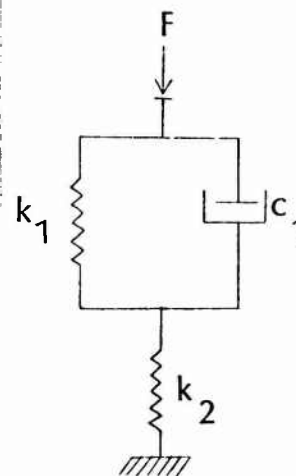
$K_N$	$C_N$	H/WH	$F_N$	$A_{HD}$	$N_C$	$H_C$
(N/cm)	(Ns/cm)		(N)	(m/s <sup>2</sup> )	(cm)	(cm)
146	1.75	WH	2137	1272	8.9	--
146	1.75	H	2039	895	7.9	0.05
1751	1.75	WH	9786	1128	5.6	--
1751	1.75	H	8006	823	5.1	2.3
14447	1.75	WH	15769	768	1.1	--
14447	1.75	H	11506	591	0.8	2.8
1751	0.14	WH	8168	1183	4.8	--
1751	0.14	H	7606	850	4.6	1.3
1751	17.5	WH	8879	666	2.8	--
1751	17.5	H	7652	501	2.5	2.0
1751	73.0	WH	12208	393	1.3	--
1751	73.0	H	9200	277	1.3	2.5

Peak force on the neck ( $F_N$ ), acceleration at the head ( $A_{HD}$ ), neck compression ( $N_C$ ) and helmet compression ( $H_C$ ) for various neck stiffness ( $K_N$ ) and neck compliance ( $C_N$ ). Constant values for model are  $M_T = 34$  kg,  $M_{HD} = 4.5$  kg,  $M_{HE} = 0.9$  kg,  $K_C = 4378$  N/cm,  $K_{HE} = 4378$  N/cm,  $C_{HE} = 3.5$  Ns/cm,  $V_i = 4.6$  m/s,  $F(t)=0$



TABLE D

Helmet	$k_1$ (N/cm)	$k_2$ (N/cm)	$c_1$ (Ns/cm)
Fully padded with foamed plastic in segregated cells			
A.	3383	1817	417
B.	3891	2189	1215
Pneumatic 1			
A.	3015	876	133
B.	1933	721	159
Pneumatic 2			
A.	4782	1007	464
B.	4059	1117	413
Pneumatic 3			
A.	2049	788	170
B.	2418	744	189
Suspension with padding			
A.	6260	1138	739
B.	10474	1445	1431
Hydraulic			
A.	2298	963	196
B.	1366	855	133
One used fully padded with foamed plastic in segregated cells			
1st	2860	1772	926
2nd	18354	1883	1214



Three element helmet model for 2.0 cm displacement at vertex on six different brands of the most popular U.S. football helmets. Helmet on Z90.1 magnesium head form with MTS-810 controller. Ram velocity 120 cm/s. Two helmets of each model (A,B) with exception of used helmet tested twice in succession at bottom. Constants derived from load relaxation curves.

### III. HUMAN SPINAL COLUMN STUDIES

#### A METHODS

Twenty-two unembalmed human male cadaver specimens were studied with forces applied in tension, compression and transverse to the cervical column. The methods have been described elsewhere ( 34 ). Briefly, all specimens were determined to be within normal limits from the medical history and X-ray examinations done prior to the tests. All tissue was X-rayed following each test. Final injury was determined by careful gross dissection with confirmation of the findings by at least two clinical staff members. In the isolated cervical and thoraco-lumbar spinal column studies, the supporting tissues were carefully removed to avoid damage to the ligaments. All tissues were kept at 2°C until studied (1-3 days). Liberal amounts of Ringer's solution were used to keep the preparations moist during the tests. Dynamic axial loads were applied to the human spinal columns with a Series 810 Materials Test System (MTS) at rates up to approximately 152 cm/s. The slow rate studies were applied with the Instron Device at rates of less than 2 cm/s. All forces were applied at a constant rate. In several cadavers a Bourne 118 linear potentiometer was attached between spinous processes or from a spinous process to the base of the skull to measure cervical distraction. Films were taken of the studies at 1000 frame/s with a Hycam camera. The energy absorbed up to fracture (failure energy) by the specimen was estimated for each run. The load deflection curves were approximately linear, consequently this assumption was used for the estimation. The machine energy was calculated from the machine load deflection to failure. The tissue energy was calculated for those runs in which the linear potentiometer readout was available. All recordings were made with a 1858 Honeywell Visicorder. Most of the specimens underwent multiple runs and were remounted in the regions without observable damage. All angles for the isolated cervical and intact torso are measured from the Frankfurt plane of the head with respect to the horizontal. Unless stated, all tests were conducted with a 10 cm piston stroke.

#### Tension

Ten unembalmed human male cadaver specimens were studied, with forces applied in axial tension (Tables 1,2). In five of the preparations (S-1,2,3,4,5, Table 1) tension was

applied between the base of the skull and the lower cervical or upper thoracic elements of the isolated spinal column, both of which were mounted in methylmethacrylate and 1 mm diameter nichrome wire, and attached to the ram or base with a U bolt or a 6.3 mm diameter stainless steel cable. Four of these same specimens (S-2,3,4,5, Table 1) underwent ablation studies upon remounting, with either the anterior ligamentous complex (all anterior ligaments up to and including the posterior longitudinal ligament) or posterior ligament complex (all posterior ligaments up to but excluding the posterior longitudinal ligament) transected (Figure 1). In one specimen (S-9, Table 1), axial tension was applied between the head and lower cervical and upper thoracic elements of the isolated spinal column. A 6.3 mm diameter stainless steel cable in methylmethacrylate anchored the head. In another isolated column (S-23, Table 1), the forces were applied to the anterior longitudinal ligament or the anterior longitudinal ligament and the tectorial membrane, secondary to transection of any ligaments posterior to these (Figure 1). In the whole cadaver torsos (S-6,7,8, Table 2), axial tension was applied between a fixed yoke on the shoulders. The head was mounted in methylmethacrylate and attached to the ram with a 6.3 mm diameter stainless steel cable, with the force applied at the vertex. Axial tension studies were also conducted on cervical spinal cords taken from three of the cervical spinal columns used in the axial tension studies (S-3,4,5, Table 1). The cord was clamped at each end with serrated jaws attached to the Instron or MTS system. The unclamped free cord section ranged from 3.8 to 7.6 cm (Table 1). Diagrams indicate approximate fixation and specimen shape.

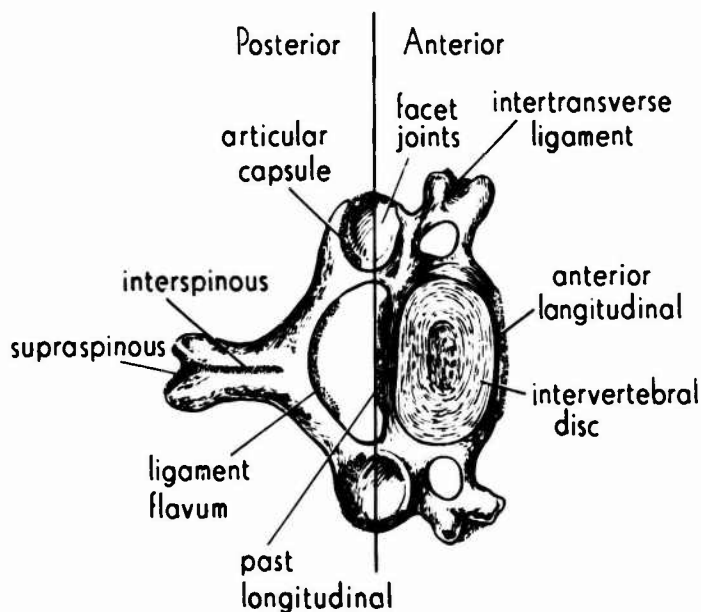


Figure 1: Ligaments of lower cervical spinal column. Vertical line indicates division between posterior and anterior compartments.

#### Compression

In another series, thirteen human male cadaveric specimens were studied with compression of the cervical elements (Tables 3,4). For this series, one specimen (S-20, Table 3) was compressed from C1 to C7, with the isolated column mounted in methylmethacrylate molded into a 15 cm diameter aluminum cylinder with set screws driven into and 1 mm diameter nichrome wire incorporated into the tissues. In four of the isolated cervical columns (S-6,10,19,21, Table 3), the force was applied to the base of the skull by means of a bolt mounted in methylmethacrylate and inserted into the load transducer of the MTS, and the upper thoracic elements mounted in methylmethacrylate molded into a 15 cm diameter aluminum cylinder with set screws driven into and 1 mm diameter nichrome wire incorporated into the tissues. One of these preparations (S-6, Table 3), consisted of the remaining viable cervical column and base of skull from the whole torso axial tension study. For fixation in three preparations (S-14,16,17, Table 4) the whole torso was mounted and supported under the armpits with a rigid yoke with additional compression force applied to the anterior and posterior thorax. The force was applied to the region of the vertex with a 10 cm x 10 cm, 3.6 kg steel plate attached to the ram. In the five remaining specimens (S-11,12,13,15,18, Table 3), a compressive force was applied to the head, with the 10 cm x 10 cm, 3.6 kg steel plate, with the upper thoracic elements mounted in methylmethacrylate molded into a 15 cm diameter aluminum cylinder with set screws driven into the tissues.

For comparison, forces were applied to the isolated thoraco-lumbar columns of seven of the cadaver spinal columns used in the cervical compression studies (S-10,11,12,13, 17,18, Table 5). A compression force was applied between T2 and L5 or L5-sacrum by mounting the upper thoracic and lower lumbar segments in methylmethacrylate molded into 15 cm diameter aluminum cylinders with set screws driven into the tissues. In one preparation (S-11, Table 5), the remaining tissues were transected into two sections, T11 to L4 and

T3 to T10, and compressed with the distal portions of the isolated columns mounted in methylmethacrylate molded into 15 cm diameter aluminum cylinders with set screws driven into the tissues. In another specimen (S-12, Table 5), the remaining viable column was remounted at T10 and the sacrum with methylmethacrylate molded into 15 cm diameter aluminum cylinders with set screws driven into the tissues. Slow and fast compression force rates were applied with the MTS and Instron devices. Moment arm values were calculated from the original vertical spinal axis, between T2 and L5, to the displaced axis at the maximum area of deformation, usually the thoraco-lumbar junction, prior to loading. This moment arm is, therefore, the minimum value acting on a preparation which usually deforms substantially during compression. Diagrams indicate approximate fixation and specimen shape.

#### Transverse

In several cervical and thoracic specimens, forces transverse to the column were applied with a 2 cm x 2 cm steel plate, to determine the shear force required for disruption of the anterior and posterior ligamentous complexes (Table 6). In the cervical studies (S-11, 12, Table 6), the lower cervical elements were mounted in a methylmethacrylate block with the forces applied in either an anterior to posterior or posterior to anterior direction with the force plate at C2 or C3. In one of these tests (S-11, run 4, Table 6), the anterior aspect of C2 and C3, C4, C5, C6 were mounted in methylmethacrylate blocks with the force applied in a posterior to anterior direction at the C2 methylmethacrylate block. In another test (S-12, Table 6), T6 and T9 were mounted in methylmethacrylate blocks and loaded at T9 in an anterior to posterior manner. Moment arm values were calculated from the distance between the point of force application (center of plate) to the junction of where the specimen is mounted in the methylmethacrylate block.

### B. IN VITRO TENSION STUDIES ON ISOLATED CERVICAL SPINAL COLUMNS AND CERVICAL SPINAL CORDS

#### Case S-1 (Isolated Column, Table 1)

This 50 year old isolated column was mounted in the Instron Device and loaded at a constant rate of 0.13 cm per minute. In the first run, the specimen was mounted at C7 and the base of the skull. An endplate disruption was observed at C4-C5 with 1446 Newtons, and approximately 1.14 cm of distention. Failure commenced in the anterior compartment (all anterior ligaments up to and including the posterior longitudinal ligament) and proceeded posteriorly. The remaining tissue was remounted between the base of the skull and C3, C4. With the second application, failure occurred at the C1-C2 junction with disruption of the anterior occipital-atlanto ligament, anterior and posterior longitudinal ligament and right articular capsular ligament. The failure began anteriorly and occurred at 1312 Newtons, and 1.10 cm of distention.

Comment - The anterior to posterior failures were similar to those observed in the isolated cadaveric columns of the monkeys (32). The lower force value for failure between C1 and C2 is probably due to the stress imposed upon the column during the first run.

#### Case S-2 (Isolated Column, Table 1)

This 36 year old, 52 kg preparation was mounted at C7 and the base of the skull during the first run. A circular skull fracture at the foramen magnum occurred at 1779 Newtons with a machine deflection of 2.67 cm and a loading rate of 0.13 cm per minute. For the second run, the specimen was mounted at C1 and C7 and the posterior ligaments were cut at C4-C5 up to but excluding the posterior longitudinal ligament. The anterior complex (disc, anterior and posterior longitudinal and intertransverse ligament) disrupted at 1289 Newtons. For the third run the tissues were mounted at C1 and C4 with the anterior ligaments transected between C2 and C3 up to and including the posterior longitudinal ligament. Failure of the posterior complex (interspinous, supraspinous, ligamentum flavum and articular capsules) occurred at 622 Newtons.

Comment - The basilar skull fracture of the first run shows that the strength of the cervical elements was in excess of 1779 Newtons. The posterior ligament and anterior ligament ablations demonstrate that the anterior ligaments are stronger than the posterior ligaments as found in the monkey (32).

#### Case S-3 (Isolated Column, Table 1)

This 65 year old isolated column was mounted in the MTS device and loaded at a rate of 127 cm/s. In the first run the specimen was anchored at T3 and the base of the skull. An endplate failure at C6-C7, as well as partial disruption of capsular ligaments at C1-C2 and partial disruption of the interspinous ligament at C3-C4 occurred at 1668 Newtons with a machine deflection of 3.3 cm. For the second run, the preparation was anchored at C6 and the base of the skull, and the posterior ligament complex was transected between C3 and C4. The MTS device malfunctioned with no injury to the column and no recorder output. For the third run the remaining tissue was remounted at C3 and the base of the skull. No injury occurred with a load of 1668 Newtons and a distention of 4.4 cm. The preparation was remounted and the test was repeated. In test four a fracture of the odontoid base and through the anterior arch of C2 was produced with 1390 Newtons and a machine deflection of 1.4 cm. The dens and fractured arch were still inserted in the atlas and no occipital-atlanto ligamentous damage occurred. The spinal cord was not visibly damaged.

Comment - Although partial disruption of the articular capsules at C1-C2 occurred in the first run, subsequent runs upon the upper cervical column (C3-base of the skull) were required to bring about failure.

Case S-4 (Isolated Column, Table 1)

This 76 year old, 59 kg preparation was mounted at T3 and the base of the skull for the first three runs. During the first and second runs, loads of 556 and 1056 Newtons were obtained, respectively, with no injuries occurring. During the third run, an endplate disruption at C6-C7 along with partial disruption of the capsular ligaments at C2-C3 occurred with 778.4 Newtons, a machine deflection of 2.4 cm and a 1.46 cm distention between C3 and C7. For the fourth run, the anterior ligaments were transected between C2 and C3, up to and including the posterior longitudinal ligament, with the specimen mounted between C5-C6 and the base of the skull. The posterior complex disrupted at C2-C3 with a force of 444.8 Newtons and a distention of 1.8 cm. The spinal cord showed no damage.

Comment - The lower cervical endplate failure of the third run occurred at 778.4 Newtons. This force is approximately 50% less than the forces obtained for similar lower cervical endplate failures, which is probably due to weakening of the column as a result of the two previous runs. The anterior ablation demonstrated that the anterior ligaments are stronger than the posterior ligaments, as found in the monkey (32).

Case S-5 (Isolated Column, Table 1)

This 63 year old preparation sustained a C6-C7 endplate failure along with disruption of the articular capsules at C1-C2. This occurred with 1835 Newtons, a distention of 2.12 cm between C1 and C7 and a loading rate of 142 cm/s, with the specimen mounted at the base of the skull and T3. The second run was a C2-C3 posterior ablation with the specimen remounted at C6 and the base of the skull. A C3-C4 endplate disruption was observed at 612 Newtons.

Comment - The endplate failure of C3-C4 in the second run must have occurred as a result of the first run, although no apparent damage was observed at that junction after the first run. The force obtained during the second run did not damage the anterior complex of C2-C3, which is consistent with previous data (32,34). No damage was observed in the spinal cord.

Cases S-3,4,5 (Human Cervical Spinal Cords, Table 1)

The remaining cervical cords were removed and mounted into the jaws of the apparatus. For S-3, the isolated cervical cord failed between the jaws at 278 Newtons with a loading rate of 106 cm/s. The free, unclamped region between the jaws was 7.6 cm long. In S-4, the isolated cervical spinal cord was transected at the midcervical level at 167 Newtons with a loading rate of 1.6 cm/s. The length of the cord between the jaws was 3.8 cm. For S-5 the cervical spinal cord was disrupted at the midcervical region at 389 Newtons with a loading rate of 118 cm/s. None of the cords slipped in the jaws.

Comment - The dynamic forces were approximately twice those required for static disruption. Failures were observed at the midsections with approximately 10-26% elongations.

Case S-9 (Isolated Column, Table 1)

This 61 year old preparation had a posterior complex disruption at C6-C7 followed by total disruption of the soft tissues at that interspace. This failure was observed at 1940 Newtons with 0.13 cm/min loading. For the second dynamic test, the machine malfunctioned and only provided a maximum of 2688 Newtons. This force was not sufficient to damage the spinal column. For the third run, a C4-C5 endplate failure occurred with 1601 Newtons and a rate of loading of 0.13 cm/min.



Comment - The dynamic force applied to the isolated cervical column in the second test was at least 40% greater for run one and 70% greater for run three than that required statically, without failure.

Case S-23 (Whole Torso and Isolated Cervical Column, Table 1)

In this 25 year old, 68 kg preparation, the cervical spinal column was isolated from the intact head to C4, and anchored through the anterior portions of the vertebral body of C3 and C4 with steinman pins (run 1, Table 1). The posterior complex, posterior longitudinal ligament, intertransverse ligament, and the posterior and anterior annulus of the disc were ablated, leaving only the anterior longitudinal ligament intact. A tensile load was applied to the anterior portions of the C3 and C4 vertebral bodies at a rate of 0.13 cm/s. A force of 845.1 Newtons and distention of 2.29 cm resulted in disrupting the anterior longitudinal ligament at the C3,C4 interspace. For the second run, the column was remounted at the head and C1, C2. The posterior complex was ablated at the C1, C2 interspace leaving the anterior longitudinal ligament and the tectorial membrane intact. The force was applied along the spinal axis with direct vertical loading, which produced disruption of the anterior longitudinal ligament and tectorial membrane at C1, C2 with 689.4 Newtons.

Comment - The ablation studies of runs 1 and 2 give some indication of the strengths of the anterior longitudinal ligament and anterior annulus. The lower force value for failure between C1 and C2 during the second run is probably due to the stress imposed upon the column during previous runs.

TABLE 1  
IN VITRO TENSION STUDIES ON ISOLATED CERVICAL SPINAL COLUMNS AND CERVICAL SPINAL CORDS

SPECIMEN	WGT (kg)	AGE (yr)	RUN #	PREPARATION DIAGRAM	PREPARATION MOUNTING	LOADING RATE	FAILURE	MAX LOAD		MACHINE DEFLECTION AT FAILURE		FAILURE ENERGY (J)	TISSUE
								N	lbs	cm	in		
S-1 CARDIAC FAILURE	77.1	50	1		Isolated column C7-base of skull.* Anchored at C7-base of skull. Wire and methylmethacrylate used to anchor U-bolts to preparation	0.13 cm/min	C4-C5 endplate failure. Ant. & Pos. Long. lig. and interspinous lig. disrupted	1446	325	1.14	0.45	8.2	--
			2		Isolated column (C3C4)-base of skull.* Anchored at (C3C4)-base of skull. Wire and methylmethacrylate used to anchor U-bolts to preparation	0.13 cm/min	C1-C2, Ant. & Pos. Long. lig., R capsular lig. and Ant. Occipital-atlanto lig. disrupted	1312	295	1.10	0.44	7.2	--
S-2 RENAL FAILURE	52.2	36	1		Isolated column C7-base of skull.* Anchored at C7-base of skull. Wire and methylmethacrylate used to anchor U-bolts to preparation	0.13 cm/min	Circular skull fracture at foramen magnum	1779	400	2.67	1.05	23.7	--
			2		Isolated column C7-C1.* Anchored at C7-C1. C4-C5 Pos. ablation.** Wire and methylmethacrylate used to anchor preparation	0.13 cm/min	C4-C5 endplate disruption. Disc, Ant & Pos. Long. lig. and intertransverse lig. disrupted	1289	290	1.59	0.625	10.2	--
			3		Isolated column C1-C4.* Anchored at C1-C4. C2-C3 Ant. ablation.*** Wire and methylmethacrylate used to anchor preparation	0.13 cm/min	C2-C3 Pos. complex disrupted. Interspinous, lig. flavum, and articular capsules disrupted	622	140	0.88	0.345	2.7	--

\*Refers to entire length of column used

\*\*Interspinous, supraspinous, articular capsules and lig. flavum dissected away to spinal cord

\*\*\*Anterior and posterior longitudinal ligament, disc and intertransverse ligament dissected away to spinal cord

+Linear potentiometer deflection at failure, with area of attachment shown above.

R=right L=left

Ant.=Anterior, Pos.=Posterior

TABLE 1  
(CONTINUED)


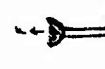
SPECIMEN	WGT (kg)	AGE (yr)	RUN #	PREPARATION DIAGRAM	PREPARATION MOUNTING	LOADING RATE	FAILURE	MAX LOAD N	MACHINE DEFLECTION AT FAILURE cm	FAILURE ENERGY (J) MACHINE TISSUE
S-3 LUNG CANCER	72.6	65	1		Isolated column T3-base of skull.* Anchored at T3-base of skull. Wire and methylmethacrylate used to anchor prep.	127 cm/sec	C6-C7 endplate failure. Partial disruption of articular capsules at C1-C2. Partial disruption of inter-spinous lig. at C3-C4	1668	3.3 1.3	27.5
			2	Isolated column C6-base of skull.* Anchored at C6-base of skull. C3-C4 pos. ablation.** Wire and methylmethacrylate used to anchor prep.	---	None	--	Machine failure	--	
			3	Isolated column C3-base of skull.* Anchored at C3-base of skull. Wire and methylmethacrylate used to anchor prep.	---	None	1668	4.4 1.75	36.7	
			4	Isolated column C3-base of skull.* Anchored at C3-base of skull. Wire and methylmethacrylate used to anchor prep.	142 cm/sec	C1-C2, base of odontoid and Ant. arch of C2 fractured	1390	1.4 0.55	9.7	
			5	Isolated cervical cord 7.6 cm long, clamped in jaws	106 cm/sec	Midpoint	278	0.76 0.3	1.0	
S-4 CARDIAC ARREST	59	76	1		Isolated column T3-base of skull.* Anchored at T3-base of skull. Cables and methylmethacrylate used to anchor prep.	142 cm/sec	None	556	4.9 1.95 C3-C7 1.68 0.66+	13.5
			2	Isolated column T3-base of skull.* Anchored at T3-base of skull. Cables and methylmethacrylate used to anchor prep.	142 cm/sec	None	1056	4.1 1.6 C3-C7 2.19 0.862+	21.6	11.6

TABLE 1  
(CONTINUED)



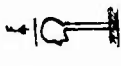

SPECIMEN	WGT (kg)	AGE (yr)	RUN #	PREPARATION DIAGRAM	PREPARATION MOUNTING	LOADING RATE	FAILURE	MAX LOAD N	MACHINE DEFLECTION AT FAILURE cm	FAILURE ENERGY (J) MACHINE TISSUE
S-4 CARDIAC ARREST	59	76	3		Isolated column T3-base of skull.* Anchored at T3-base of skull. Cables and methylmethacrylate used to anchor prep.	132 cm/sec	C6-C7 Endplate failure Partial disruption of capsular lig. at C2-C3	778.4	2.4 0.95 C3-C7 1.46 0.575+	9.3 5.7
			4		Isolated column C6-base of skull.* Anchored at (C5C6)-base of skull (C2-C3 Ant. ablation)** Cables and methylmethacrylate used to anchor preparation	142 cm/sec	C2-C3 Pos. complex disrupted	444.8	100 1.8 0.7 C1-C3 0 0+	-- 4.0
			5		Isolated cervical cord: 3.8 cm long, clamped in jaws	1.6 cm/sec	Midpoint	167	37.5 0.89 0.35	-- 0.7
S-5 HEPATIC FAILURE	56.7	63	1		Isolated column T3-base of skull.* Anchored at T3-base of skull. Cables and methylmethacrylate used to anchor prep.	142 cm/sec	C6-C7 Endplate failure Partial disruption of capsular lig. at C2	1835	412.5 8.3 3.25 C1-C7 2.12 0.83+	75.1 19.4
			2		Isolated column C6-base of skull.* Anchored at C6-base of skull (C2-C3 Pos. ablation)** Cables and methylmethacrylate used to anchor preparation	142 cm/sec	C3-C4 Endplate failure	612	137.5 0.51 0.2	-- 1.6
			3		Isolated cervical cord: 3.8 cm long, clamped in jaws	118 cm/sec	Midpoint	389.2	87.5 1.0 0.4	-- 1.9

TABLE 1  
(CONTINUED)

SPECIMEN	WGT (kg)	AGE (yr)	RUN #	PREPARATION DIAGRAM	PREPARATION MOUNTING	LOADING RATE	FAILURE	MAX LOAD N	MACHINE DEFLECTION AT FAILURE cm	FAILURE ENERGY (J) MACHINE TISSUE
S-9 RESPI- RATORY FAILURE	75.8	61	1		Isolated column T2-head* Anchored at (T1T2)-head Cables used to anchor preparation	0.13 cm/min	C6-C7 Pos. complex disrupted followed by total failure at C6-C7 junction	1940	3.0	29.1
			2		Isolated column C6-head* Anchored at (C5C6)-head Cables used to anchor preparation	100 cm/sec	Machine failure No disruptions	2688	4.0	53.8
			3		Isolated column C6-head* Anchored at (C5C6)-head Cables used to anchor preparation	0.13 cm/min	C4-C5 Endplate failure	1601	4.6	36.8
S-23 CARDIAC ARREST	68.0	25	1		Isolated column head-C4 Anchored through Ant. portions of C3 & C4 body with Steimen pins. Pos. complex, Pos. Long. Lig., intertransverse lig. Pos. annulus and Ant. annulus ablated. Ant. Long. Lig. remains intact. Force applied to Ant. portions of vertebral bodies.	0.13 cm/min	Ant. Long. Lig. Disrupted at C3-C4	845.1	2.29	9.4
			2		Isolated column head-C3 Anchored at the head and (C1-C2). Pos. complex ablated at C1-C2. Ant. Long. Lig. and tectorial mem. intact. Force applied along spinal axis. Direct vertical loading.	0.13 cm/min	Disruption of Ant. Long. Lig. and tectorial mem. at C1-C2	689.4	--	--



## C. IN VITRO HUMAN AXIAL TENSION STUDIES ON INTACT WHOLE TORSOS

Case S-6 (Whole Torso, Table 2)

This 67 year old, 72.5 kg cadaver expired due to smoke inhalation. For this study, the entire torso, including the head and neck were mounted in the frame with a rigid yoke fixed on the shoulders. At a loading rate of 125 cm/s and a peak force of 3780 Newtons, a transverse circular skull fracture occurred at the base of the skull through the sellar region. However, the cervical ligaments did not fail. High speed films of the test show that the specimen underwent direct vertical loading.

Comment - This failure is similar to that of run one, preparation S-2. The circular skull fracture observed for this preparation suggests that the dynamic force is approximately twice that required for a static skull fracture. This study also suggests that this human cadaver neck could withstand at least 3780 Newtons without disruption.

Case S-7 (Whole Torso, Table 2)

The 70 year old specimen was mounted using the entire torso with a rigid yoke fixed on the shoulders. A linear potentiometer was also mounted between the base of the skull and the spinous process of T2. High speed films show that the specimen underwent direct axial loading with less than 30° of rotation. This preparation had four runs, each at a different machine stroke limit. The first three runs were done at 20%, 40% and 50% of the total machine stroke of 10 cm. The fourth run was done at 100% of the total machine stroke. During the first three dynamic runs, no cervical injuries were observed, although forces of 2216.4 Newtons, 1535.4 Newtons, 2780 Newtons and linear potentiometer displacements of 2.82 cm, 2.54 cm and 2.84 cm were recorded for the three runs, respectively. An odontoid fracture (at its base and still inserted in the atlas) occurred at 3892 Newtons and 1.85 cm linear potentiometer distention during the fourth dynamic run. The cruciform, transverse and lateral alar odontoid ligaments were left intact, as were the other cervical ligaments.

Comment - This study shows that the cervical column (T2-base of skull) is able to withstand distractions of approximately 2 to 3 cm without obvious ligamentous damage. The odontoid fracture at 3869.3 Newtons, without ligament failure, demonstrates the strength of the cervical ligaments and is comparable to the forces involved in run one of S-6 (Table 2).

Case S-8 (Whole Torso, Table 2)

This 70 year old, 75.8 kg specimen was mounted using the entire torso in a frame, with a rigid yoke placed upon the shoulders. A linear potentiometer was mounted between the base of the skull and the spinous process of T2, to monitor the amount of cervical distraction. During the first run, the recording device failed. The force and the distention applied to the preparation were unavailable. There was no apparent injury after the first run, although films indicate a direct vertical loading, followed by a slight extension of the neck as the piston came to rest. The specimen was remounted for a second run. An odontoid fracture at its base and disruption of the posterior ligament complex at C1-C2 was observed at 2446 Newtons with direct vertical loading of 129 cm/s.

Comment - The failures of this preparation occurred at approximately 60% of the forces obtained for similar failures (S-6 and S-7, Table 2). The lower forces in run 2, is probably due to weakening of the column during the first run.

## D. IN VITRO HUMAN COMPRESSION STUDIES ON ISOLATED CERVICAL SPINAL COLUMNS

Case S-6 (Isolated Column, Table 3)

This 67 year old preparation was mounted at C7 and the base of the skull with methylmethacrylate. The force was applied along the spinal axis at a rate of 120 cm/s. A load of 4500 Newtons was obtained, producing a C5 burst fracture with anterior subluxation of C5 on C6 (Figure 2A&B). The anterior and posterior longitudinal ligaments and discs were intact, however, the posterior ligament complex was disrupted at the C5-C6 junction.

Comment - This failure is similar to those observed clinically.

Case S-10 (Isolated Cervical Column, Table 3)

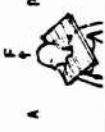


In this 76 year old specimen, the spinal column was isolated from the base of the skull to T2. The cervical section was mounted at the base of the skull and T1, T2 with methylmethacrylate. With the force applied 2 cm posterior to spinal axis, the preparation was forced into extension with a loading rate of 130 cm/sec and a force of 4410 Newtons. A transverse fracture of the odontoid and of the C6 vertebral body with complete avulsion of the anterior longitudinal ligaments was observed.

Comment - The transverse fracture of the odontoid in the cervical test is similar to the failure observed in S-7, run 4 and S-8, run 2 (Table 2) although the force was approximately 20-90% greater in compression than in tension.

Case S-11 (Isolated Cervical Column, Table 3)

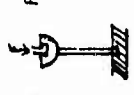
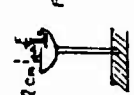


In this 55 year old, 43.1 kg specimen, the spinal column was available from the intact head to T2. The tissues were fixed with a 3.6 kg steel plate on the vertex of the head and T1, T2 mounted in methylmethacrylate. During this run, the plate slipped off

TABLE 2  
IN VITRO HUMAN AXIAL TENSION STUDIES ON INTACT WHOLE TORSOS

SPECIMEN	WGT (kg)	AGE (yr)	RUN #	PREPARATION DIAGRAM	PREPARATION MOUNTING	LOADING RATE	FAILURE	MAX LOAD N	MAX LOAD lbs	MACHINE DEFLECTION AT FAILURE cm	FAILURE ENERGY (J) MACHINE TISSUE
S-6 SMOKE INHALATION	72.5	67	1		Whole torso: yoke on shoulders. Yoke and cables used to anchor preparation	125 cm/sec	Transverse circular fracture	3780	850	2.03 0.8 Cl-T2 Malfunction	38.4 --
S-7 CARDIAC ARREST	88.9	70	1		Whole torso: yoke on shoulders. Yoke and cables used to anchor preparation	152 cm/sec	None	2216.4	498.3	3.8 1.5 Base of Skull-T2 2.82 1.11+	42.1 31.3
			2		Whole torso: yoke on shoulders. Yoke and cables used to anchor preparation	127 cm/sec	None	1535.4	345.2	3.3 1.3 Base of Skull-T2 2.54 1.0+	25.3 19.5
			3		Whole torso: yoke on shoulders. Yoke and cables used to anchor preparation	127 cm/sec	None	2780	625	5.08 2.0 Base of Skull-T2 2.84 1.12+	70.6 39.5
			4		Whole torso: yoke on shoulders. Yoke and cables used to anchor preparation	127 cm/sec	Odontoid fractured at its base and still inserted in Cl. Cruciform, transverse and lateral alar odontoid lig. intact	3892	875	Malfunction Base of Skull-T2 1.85 0.73+	-- 36.0
S-8 CARDIAC ARREST	75.8	70	1		Whole torso: yoke on shoulders. Yoke and cables used to anchor preparation.	120 cm/sec	Recorder failure	--	--	-- --	-- --
			2		Whole torso: yoke on shoulders. Yoke and cables used to anchor preparation.	129 cm/sec	Pos. complex disrupted Cl-C2. Odontoid fractured at its base and still inserted in Cl	2446	550	2.5 1.0 Base of Skull-T2 1.90 0.77	30.6 23.2

†Linear potentiometer deflection at failure, with area of attachment shown  
Ant.=Anterior, Pos.=Posterior

TABLE 3  
IN VITRO HUMAN COMPRESSION STUDIES ON ISOLATED CERVICAL SPINAL COLUMNS

SPECIMEN	WGT (kg)	AGE (yr)	RUN #	PREPARATION DIAGRAM	PREPARATION MOUNTING	LOADING RATE	FAILURE	MAX LOAD N	MACHINE DEFLECTION AT FAILURE cm	FAILURE ENERGY (J) MACHINE TISSUE
S-6 SMOKE INHALATION	72.5	67	1		Isolated column base of skull-C7*. Anchored at base of skull-C7. Force applied along spinal axis. Wire and methylmethacrylate used to anchor preparation.	120 cm/sec	C5 burst fracture with ant. subluxation of C5 C6. Pos. lig. complex disrupted at C5-C6.	4500	3.66 1.44	82.3 --
S-10 RESPIRATORY ARREST	88.5	76	1		Isolated column base of skull-T2.* Anchored at (T2T1)-base of skull. Force applied 2 cm pos. to spinal axis. Wire and methylmethacrylate used to anchor prep.	130 cm/sec	Extension injury: Transverse fracture of odontoid and body of C6. Ant. long. lig. at C6 disrupted	4410	7.4 2.91	163.2 --
S-11 RESPIRATORY ARREST	43.1	55	1		Isolated column head-T2.* Anchored at (T1 T2)-head. Force applied along spinal axis. Metal cylinder and methylmethacrylate used to anchor prep.	---	Flexion injury: pos. complex disrupted at C1-C2. Machine and prep. failure. Load plate slipped off back of head. Tectorial mem. disrupted at C1-C2	400.3 90 Approx value	Machine Failure	-- --
S-12 PNEUMONIA	58.9	57	1		Isolated column head-T1.* Anchored at (C7 T1)-head. Force applied at union with head flexed 30° forward. Metal cylinder and methylmethacrylate used to anchor prep.	152 cm/sec	Flexion injury: Posterior complex disrupted at C1-C2	1779 400	0.64 0.25	5.7 --

\*Refers to entire length of column used

\*Linear potentiometer deflection at failure, with area of attachment shown above.

L=left, R=right, Ant.=Anterior, Pos.=Posterior

TABLE 3  
(CONTINUED)

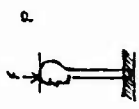

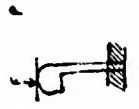
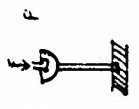



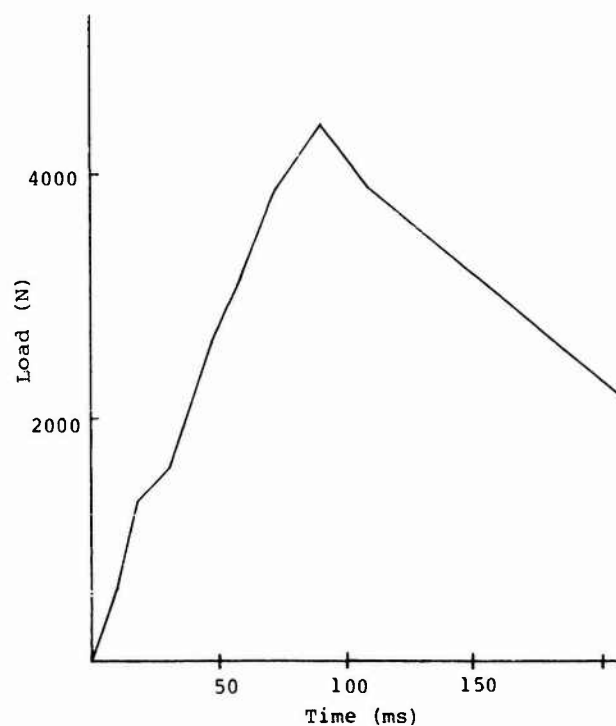
SPECIMEN	WGT (kg)	AGE (yr)	RUN #	PREPARATION DIAGRAM	PREPARATION MOUNTING	LOADING RATE	FAILURE	MAX LOAD N	MACHINE DEFLECTION AT FAILURE cm	FAILURE ENERGY (J) MACHINE TISSUE
S-13 ACUTE RESPIRATORY FAILURE	77.1	84	1		Isolated column head-T2.* Anchored to (T1-T2)-head. Force applied 5 cm ant. to spinal axis. Metal cylinder and methylmethacrylate and cables used to anchor prep.	112 cm/sec	Flexion injury: Pos. complex disrupted, ant. long. disrupted at C2-C3. Partial compression failure of disc at C2-C3.	2309.4	3.71 1.46	42.8 --
S-15 HEART ATTACK	81.6	54	1		Isolated column head-T3.* Anchored at (T2T3)-head. Force applied 2.5 cm ant. to spinal axis with head flexed 20° forward. Metal cylinder and methylmethacrylate used to anchor preparation	122 cm/sec	Flexion injury: ant. long. lig. and disc disrupted at C2-C3 C4-C5 endplate failure. Partial fracture of ant. inf. body of C4	4448	7.52 2.96	167.2 --
S-18 CARDIAC ARREST	79.4	41	1		Isolated column head-T3.* Anchored at (T2T3)-head. Natural curvature of spine eliminated by flexing head and removing the jaw. Metal cylinder and methylmethacrylate used to anchor preparation.	0.25 cm/sec	Articular facets and capsules disrupted on L side from C2-C7. Pos. complex stretched at C1-C2.	644.5	0.48 0.19	1.5 --
S-19 CARDIO- RESPIRATORY ARREST	68.1	61	1		Isolated column base of skull-T3. Anchored at (T2T3)-base of skull. Top of skull removed just above eyes with jaw removed. Force applied along spinal axis. Bolt, methylmethacrylate and metal cylinder used to anchor preparation.	23 cm/sec	Skull was twisted left. Articular facets disrupted at C1-C2.	1601.3	1.12 0.44 Base of Skull-T1 0.18 0.072+	9.0 1.4

TABLE 3  
(CONTINUED)

SPECIMEN	WGT (kg)	AGE (yr)	RUN #	PREPARATION DIAGRAM	PREPARATION MOUNTING	LOADING RATE	FAILURE	MAX LOAD N	MACHINE DEFLECTION AT FAILURE cm	FAILURE ENERGY (J) MACHINE TISSUE
S-19 CARDIO - RESPIRATORY ARREST	68.1	61	2		Same as HS-19, Run 1.	60 cm/sec	Interspinous and supraspinous lig. stretched at C1-C2 Axis fracture of R. ant. arch. Teardrop fracture of ant. body of C2.	1509.2	1.14 0.45 Base of Skull-T1 0.15 0.06+	8.6 1.1
S-20 SEPTICEMIA	65.8	64	1  2		Isolated column, anchored at C1-(T1T2T3) Force applied along spin- al axis. Wire, methyl- methacrylate, metal cy- linder used to anchor preparation  Isolated column, anchored at C1-(T1T2T3) Force applied along spin- al axis. Wire, methyl- methacrylate, metal cy- linder used to anchor preparation	---  92 cm/sec	Rupture of disc at C4-C5  Articular facets and capsules dis- rupted on L side at C3-C4, C4-C5. Partial disrup- tion of ant. long. lig. at C6-C7	---  7434.8	---  0.99 0.39	---  36.8
S-21 RESPIRATORY ARREST	106.1	30	1		Isolated column, anchored at (T3T4)-base of skull. Forced flexion with force applied along spinal axis. Head flexed 25° forward. Metal cy- linder and methametha- crylate used to anchor prep.	25 cm/sec	Flexion injury: Inferior ant. body of C4 and sup. ant. body of C5 fractured	1868.2	2.23 0.88	20.8 --



(A)

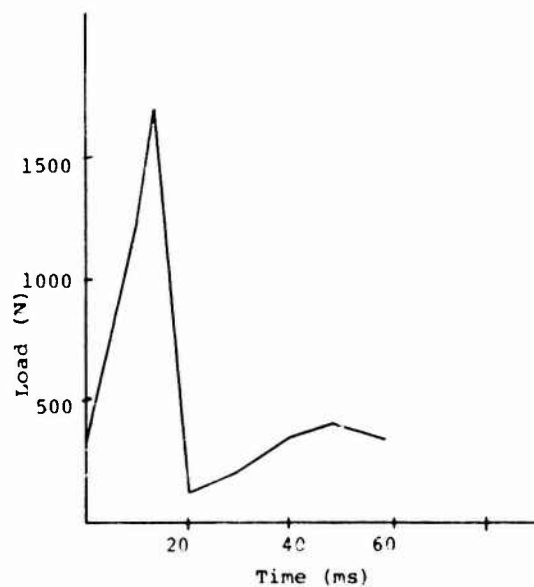


(B)

Figure 2: S-6 (Table 3, Run 1). A) This preparation is shown in a lateral view with the column in extension. The arrow points to the C5 vertebral body which has been fractured and pushed anteriorly upon C6. B) Force versus time plot.



(A)



(B)

Figure 3: S-12 (Table 3, Run 1). A) This specimen is shown in a lateral view with the column in a neutral position. The arrow points to the disruption of the posterior ligamentous complex at the C1, C2 junction. B) Force versus time plot.

the back of the head, moving the head forward approximately 8.9 cm. The continuous force component could not be determined. A machine force of 400.3 Newtons was observed. The posterior ligament complex and tectorial membrane disrupted at C1, C2.

Comment - The axial force measured during this test is probably too low to cause injury to column. The injury sustained was probably the result of the head flexing forward.

Case S-12 (Isolated Cervical Column, Table 3)

The spinal column, from the intact head to T1, was isolated from this 57 year old specimen. The head was flexed 30 degrees forward with force applied at theinion. A posterior ligament complex disruption at C1-C2 with a force of 1779 Newtons at a rate of 152 cm/s was observed (Figures 3 A&B).

Comment - The failure of the cervical column in flexion occurred at a value 2.5 times less than the forces involved in the failure of cervical columns loaded axially (S-6,10,Table 5). The maximum force for this specimen is in the range of the forces observed for axial tension studies of the isolated cervical column.

Case S-13 (Isolated Cervical Column, Table 3)

In this 84 year old specimen, the spinal column was isolated from the intact head to T2. The force was applied 5 cm anterior to the spinal axis, at a rate of 112 cm/s. A flexion injury, at the C2-C3 junction occurred disrupting the posterior ligamentus complex, exposing the spinal cord and disrupting the anterior longitudinal ligament, along with partial compression failure of the disc at a force of 2309.4 Newtons.

Comment - The failure incurred for this preparation included posterior ligament and bony compression. The finding between S-12 and S-13 may be due to the initial position of the plate (Table 3).

Case S-15 (Isolated Cervical Column, Table 3)

The cervical spinal column of this 54 year old specimen was isolated and anchored between the intact head and T2-T3. The head was flexed forward approximately 20 degrees from the horizontal and the force applied 2.5 cm anterior to the spinal axis. The head rotated approximately 35 degrees anteriorly with the force plate coming to rest on the occipital protuberance. A force of 4448 Newtons and a rate of 122 cm/s was observed. A flexion injury occurred with the anterior longitudinal ligament and disc being avulsed at the C2-C3 junction. A C4-C5 endplate failure, accompanied by partial fracture of the anterior inferior vertebral body of C4 was also observed (Figures 4 A&B).

Comment - The force obtained applied to this specimen is approximately two to three times greater than the forces seen in the flexion injuries of S-12 and S-13 (Table 3). This force is similar to the force obtained from S-6 (Table 3).

Case S-18 (Isolated Cervical Column, Table 3)

In this 41 year old specimen, the spinal column was isolated from the intact head to T3 and anchored with a 3.6 kg steel plate on the vertex of the head and T2, T3 mounted in methylnmethacrylate. The natural curvature of the cervical column was eliminated by removing the jaw and flexing the head forward. During this test, the specimen moved forward and laterally (to the right) as a result of the force plate slipping on the scalp. An axial force of 644.5 Newtons and a 0.48 cm distention was observed at a rate of 0.25 cm/s. The articular capsules and facets were disrupted on the left side from C2 to C7 and the posterior complex at C1-C2 was distended beyond its physiologic limits.

Comment - The disruption of the articular facets and capsules from C2 to C7 is the result of the force plate twisting the cervical column to the right.

Case S-19 (Isolated Cervical Column, Table 3)

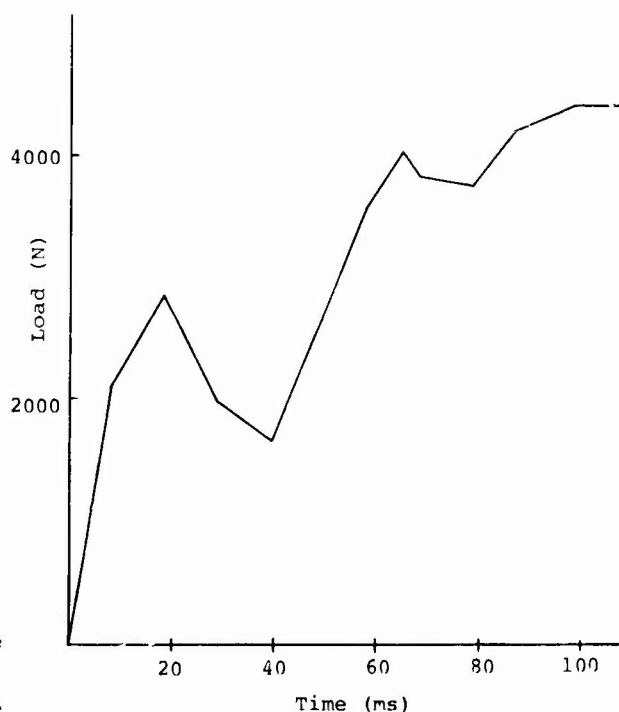
The cervical spinal column was isolated in this 68.1 kg, 61 year old specimen and mounted at the base of the skull and T2, T3 for all tests. A linear potentiometer was mounted between the base of the skull and T1 spinous process to measure cervical distention. The mandible was removed and the force was applied along the spinal axis. This specimen was subjected to a series of twelve tests with the impulse to the piston being a step function. No failures were observed for the first twelve tests at 440 Newtons. Therefore, they are not recorded on Table 3. In the thirteenth test (run 1), a force of 1601.3 Newtons, a machine deflection of 1.12 cm and a rate of 23 cm/s was observed, with the head twisting to the left and the articular facets being disrupted at C1-C2. The specimen was set up again for the fourteenth test (run 2) and loaded at a rate of 60 cm/s. A fracture of the right anterior arch of the axis and a tear drop fracture of anterior body of C2 with stretching of the supraspinous and interspinous ligament at C1-C2 occurred. A force of 1509.2 Newtons and a machine deflection of 1.14 cm was measured (Figures 5 A&B).

Comment - This isolated cervical column underwent direct vertical loading. The forces may be compared to those in S-6, run 1 (Table 3), which are probably due to weakening of the column during the numerous runs.



(A)

Figure 4: S-15 (Table 3, Run 1) A) This preparation is shown in a lateral view with the column flexed forward at the C4,C5 junction. This isolated column underwent a forced flexion test. The top arrow points to the C2-C3 interspace where the anterior longitudinal and intervertebral disc were disrupted. The bottom arrow points to the C4,C5 endplate failure with a partial compression fracture of anterior inferior body of C4. B) Force versus time plot.



(B)

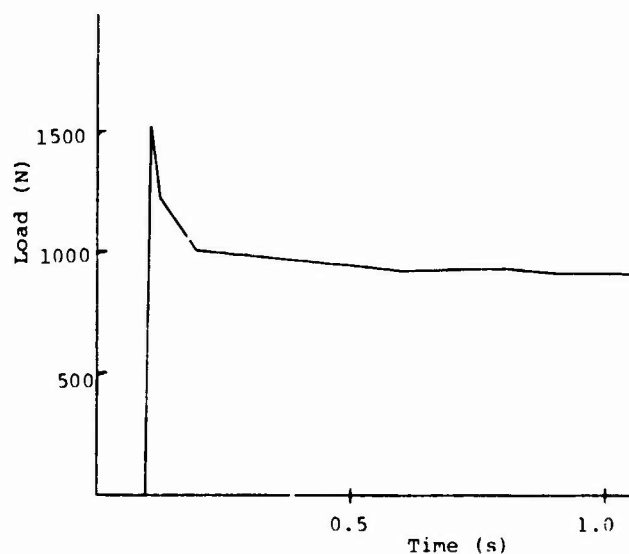


Figure 5: S-19 (Table 3, Run 2). A) This preparation is shown in a lateral view with the column in a slightly extended position. The arrow points to the teardrop fracture of the anterior body of C2. B) Force versus time plot.



Case S-20 (Isolated Cervical Column, Table 3)

This 64 year old preparation expired due to septicemia. The cervical column was isolated and mounted at C1 and T1, T2, T3. The force was applied along the spinal axis during run 1 and a rupture of the disc occurred at the C4-C5 junction. The recorder malfunctioned. The specimen was set up in the same manner for the second run, with the force applied to the spinal axis at 82 cm/s. The articular capsules and facets were disrupted on the left side of the column at C3-C4 and C4-C5, and a partial avulsion of the anterior longitudinal ligament at C6-C7 occurred at 7434.8 Newtons.

Comment - The maximum force of 7434.8 Newtons obtained with this specimen was the highest force level observed with any of the isolated cervical column compression tests. A possible explanation is that a preparation fixed at C1 places the vertebral bodies in direct opposition to one another and distributes the loads over a greater portion of the column.

Case S-21 (Isolated Cervical Column, Table 3)

In this 30 year old preparation, the cervical column was isolated and anchored at the base of the skull and T3-T4. This specimen had a battery of 23 tests at less than 500 Newtons of compressive force and 0.5 cm compression to obtain data concerning the spring constants (k) and damping constants (c) of the cervical column. No failures were observed during the first 22 tests and, therefore, they are not recorded on Table 3. In the twenty-third test (run 1), the column was mounted at the base of the skull to T3-T4 and flexed forward 25 degrees with respect to the horizontal. The force was applied along the spinal axis at a rate of 25 cm/s with a load of 1868.2 Newtons. The column underwent a posterior to anterior angulation of 35 degrees with respect to the horizontal, at the C4-C5 junction and a 70 degree forward flexion of the total column. The anterior inferior body of C4 and the superior anterior body of C5 were fractured.

Comment - The compression fractures of the C4 and C5 vertebral bodies emphasize that most of the flexion/extension of the cervical spine is in the central region. The C5-C6 interspace is generally considered to have the longest range of flexion/extension, but the C3-C4, C4-C5 and C6-C7 interspaces are all able to undergo a considerable range of flexion/extension (40).

E. IN VITRO HUMAN COMPRESSION STUDIES ON INTACT WHOLE TORSOSCase S-14 (Whole Torso, Table 4)

This 71 year old specimen was mounted using the entire torso in the frame with a rigid yoke positioned under the arms. The force was applied at the hairline approximately 7.5 cm anterior to the vertex, with the neck in extension 40 degrees with respect to the horizontal. An endplate failure at C5-C6 occurred with the anterior longitudinal ligament disrupted, the posterior longitudinal ligament intact, an avulsion fracture of the anterior inferior body of C4, a fracture of the spinous process of C6 and a small chip fracture of the anterior superior body of C5, at 1512 Newtons with a force application of 122 cm/s (Figures 6 A&B).

Comment - The type of failure that occurred with this specimen can be classified as an extension injury. The failure of the endplate at the lower cervical level and the force involved is similar to the endplate failures and forces of the axial tension studies of the isolated cervical columns (S-1,3,4,5,9, Table 1), except that the bodies of C4 and C5 are avulsed. The probable explanation for this is that during a forced extension, the anterior portions of the column are placed in tension.

Case S-16 (Whole Torso Column, Table 4)

This 80 year old, 63.5 kg specimen, expired due to a spontaneous subarachnoid hemorrhage. The whole torso was mounted in the frame with a rigid metal yoke placed under the arms. The force was applied along the spinal axis with a 3.6 kg impactor plate, 2.5 cm above the vertex, at a rate of 112 cm/s. The column appeared to undergo a straight vertical loading with the head ultimately going into 15 to 20 degrees of flexion. The supraspinous, interspinous and articular capsules were disrupted at the C1-C2 junction and the posterior occipital-atlanto ligament was stretched beyond its physiologic limits.




Comment - For these high loading rates the ligaments are often distended without bony damage.

Case S-17 (Whole Torso Column, Table 4)

This 65 year old specimen was mounted using the entire torso in the frame with a rigid yoke placed under the arms. The force is applied along the spinal axis with a 3.6 kg impactor plate, 1.9 cm above the vertex of the head. Upon impact, the head moved down and forward. An occiput-C1, and C1-C2 flexion injury occurred with the posterior occipital-atlanto ligament stretched beyond its physiologic limits and the articular capsules and supraspinous ligament disrupted between C1 and C2.

Comment - The failure of the upper cervical region in the whole torso test is comparable to the failure of S-16, run 1 (Table 4). This flexion injury can probably occur with a force of approximately 2000 to 3000 Newtons.

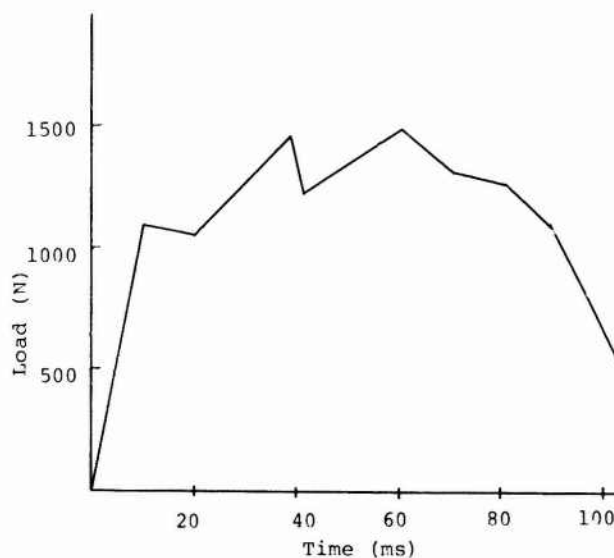
TABLE 4  
IN VITRO HUMAN COMPRESSION STUDIES ON INTACT WHOLE TORSOS

SPECIMEN	WGT (kg)	AGE (yr)	RUN #	PREPARATION DIAGRAM	PREPARATION MOUNTING	LOADING RATE	FAILURE	MAX LOAD N	MACHINE DEFLECTION AT FAILURE cm	FAILURE ENERGY (J) MACHINE TISSUE
S-14 RESPIRATORY FAILURE	49.9	71	1		Whole torso: yoke under arms. Force applied 7.5 cm ant. to spinal axis. Neck is in extension 400 with respect to horizontal. Yoke used to anchor preparation.	122 cm/sec	Extension injury: endplate failure at C5-C6. Ant. long. lig. disrupted at C5-C6. Spinous process of C6 fractured. Avulsion fracture of ant. inf. body of C4. Chip fracture of ant. sup. body of C5.	1512	3.61	27.3
S-16 SPONTANEOUS SUBARACHNOID HEMORRHAGE	63.5	80	1		Whole torso: yoke under arms. Force applied along spinal axis with plate 2.5 cm above vertex of head. Yoke used to anchor preparation.	112 cm/sec	Flexion injury at C1-C2: Supraspinous, interspinous and articular capsules disrupted. Pos. occipital atlanto occipital lig. stretched	2936	9.2	135.0
S-17 RESPIRATORY ARREST -- BRAIN TUMOR	68.1	65	1		Whole torso: yoke under arms. Force applied along spinal axis with plate 1.9 cm above vertex of head. Yoke used to anchor preparation.	142 cm/sec	Flexion injury at occiput -C1-C2: Pos. occipital atlanto lig. stretched, articular capsules and supraspinous lig. disrupted at C1-C2	1868	7.2	67.2

Ant.=Anterior, Pos.=Posterior



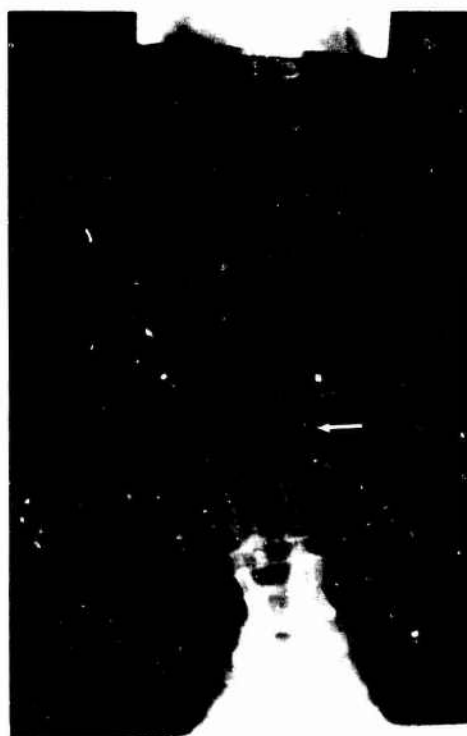
(A)



(B)

Figure 6: S-14 (Table 4, Run 1). A) This is a lateral view of the cervical column after it had been isolated from the intact whole torso. The column is in a slightly extended position. The type of injury incurred is an extension injury. The top arrow points to the avulsion fracture of the anterior inferior body of C4. The bottom arrow points to the endplate failure at the C5,C6 interspace. B) Force versus time plot.

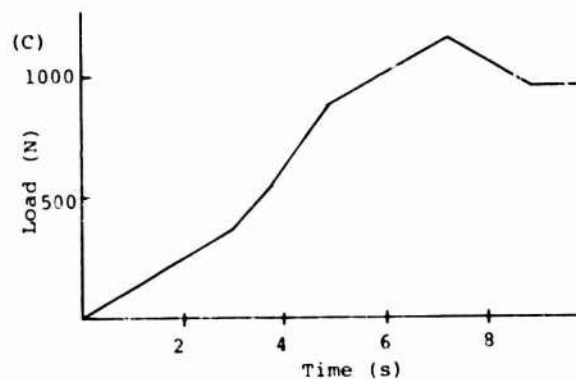
(A)



(B)



Figure 7: S-11 (Table 5, Run 1). A) This is an anterior to posterior view with the column undergoing a slight lateral angulation. The arrow points to the compression ("wedge") fracture of T11. B) This is a lateral view with the column in a slightly flexed position. The arrow points to the compression ("wedge") fracture of T11. C) Force versus time plot.



## F. IN VITRO HUMAN COMPRESSION STUDIES ON ISOLATED THORACO-LUMBAR COLUMNS

Case S-10 (Thoraco-Lumbar Column, Table 5)

For the thoraco-lumbar study, the specimen was mounted at T3-T4 and L5 with methylmethacrylate. The preparation was loaded at 2 cm/s with a blowout fracture of the body of L1, rupture of the anterior longitudinal ligament and unilateral fracture of the left pedicle (root of arch) and transverse process occurred. A force of 1735 Newtons was measured. The column underwent a posterior to anterior angulation. That is, (the column buckled with a 87 degree included angle at the T12-L1 junction) with a 22 degree right lateral column angulation.

Comment - The failure of L1 is consistent with the fact that the thoraco-lumbar junction exhibits the highest torsional stiffness. This makes the T12-L1 motion segment the site of high stress concentration and as such, is the site of the highest frequency of spine injuries.

Case S-11 (Isolated Thoraco-Lumbar Column, Table 5)

The thoraco-lumbar section was mounted at T3, T4 and L5 with the force applied along the spinal axis. The column flexed approximately 60 degrees with respect to the horizontal and the center of the bodies of T11 and T12. A maximum force of 1134 Newtons was measured. An anterior wedge fracture of T11 with avulsion of the anterior and posterior longitudinal ligament was found (Figures 7 A,B&C). The remainder of the thoraco-lumbar section was remounted in two sections, T11 to L4 and T3, T4 to T10 with methylmethacrylate. The T11 to L4 section underwent three runs. The first dynamic run and second static run resulted in no apparent injuries at forces of 4904.8 and 4803.8 Newtons, respectively. With a loading rate of 1.0 cm/s and a force of 4848 Newtons, a disruption of the posterior ligament complex occurred at the T12-L1 junction. The load was applied along the spinal axis of the remaining T3 to T10 section, at a rate of 1.1 cm/s and a force of 3647 Newtons. The column underwent a lateral movement of approximately 30 degrees. The articular capsules were stretched beyond their physiologic limits at the T9-T10 junction.

Comment - The second thoracic segment (T11-L4) underwent three runs with forces ranging from approximately 4800 to 4900 Newtons before failure of the column occurred. These forces are nearly 4.5 times greater than those attained with the intact isolated thoraco-lumbar column. This is probably due to the elimination of the natural curvature of the spine as the result of testing a smaller thoraco-lumbar section. The T3 to T10 segment underwent a force approximately three times greater than those of S-11 (run 1, Table 5). This may be due to the elimination of the natural curvature of the spine and the smaller spinal section.

Case S-12 (Isolated Thoraco-Lumbar Column, Table 5)

The thoraco-lumbar section was mounted at T2, T3 and L5-sacrum with methylmethacrylate. Initially, the spine was flexed forward 30 degrees with the force applied to the center of the vertebral body of T2. The final included angle between the center of the bodies of T10 and T11 was 95 degrees. A force of 978 Newtons was measured. A fracture of the T9 vertebral body just above the disc, and disruption of the left lateral portions of the ligamentum flavum was found. The remaining column was remounted between T10, T11 and L5-sacrum and underwent two runs. A force of 4558.7 Newtons at a rate of 102 cm/s was observed during the first run, but no failure occurred. During the second run, a compression fracture of the body of L2 and disruption of the posterior longitudinal ligament and ligamentum flavum at the L2-L3 junction occurred with a force of 2885.9 Newtons at a rate of 127 cm/s.

Comment - The failure of the second segment (T10-sacrum) occurred at a force of approximately 50% less than the force obtained in the first run of this segment, in which no injury occurred. This is probably due to weakening of the column in the previous runs.

Case S-13 (Isolated Thoraco-Lumbar Column, Table 5)

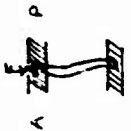
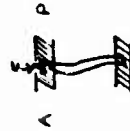
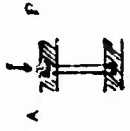
The isolated column was anchored at T3-T4 and L4-L5 with methylmethacrylate, and the force was applied along the spinal axis. The column had a 135 degree final included angle at the T7-T8 junction, and a 35 degree right lateral movement at the T7-T8 junction. A force of 2224 Newtons was measured. A compression wedge fracture of the bodies of T7, T12 and L2 was found. A bone chip was present in the superior anterior portion of the body of T8 along with a fracture of the spinous process of T8. The posterior ligament complex and the anterior longitudinal ligament were disrupted at the T7-T8 junction, exposing the spinal cord.

Comment - The compression (wedge) fractures of T7, T12 and L2 are an indication that the entire column flexed forward, even though the greatest amount of flexion occurred at T7-T8 junction.

Case S-16 (Isolated Thoraco-Lumbar Column, Table 5)

The spinal column was isolated from T2 to the sacrum and mounted in methylmethacrylate. The column was placed with the bodies of T2-T3 angulated forward 35 degrees. The force applied was at a rate of 122 cm/s. A 90 degree included angle at the T10-T11 junction, as well as a right lateral angulation of approximately 30 degrees at failure. A T10-T11 endplate failure with a wedge fracture of T11, disruption of the posterior ligament complex and partial disruption of the spinal cord was observed (Figures 8 A,B and C).

TABLE 5  
IN VITRO HUMAN COMPRESSION STUDIES ON ISOLATED THORACO-LUMBAR COLUMNS

SPECIMEN	WGT (kg)	AGE (yr)	RUN #	PREPARATION DIAGRAM	PREPARATION MOUNTING	LOADING RATE	FAILURE	MAX LOAD N	MAX LOAD lbs	MACHINE DEFLECTION AT FAILURE cm		FAILURE ENERGY (J) MACHINE TISSUE
										5.9	2.32	
S-10 RESPIRATORY ARREST	88.5	76	1		Isolated column T3-L5* Anchored at (T3T4)-L5 Force applied along spinal axis. Metal cylinder and methyl- methacrylate used to anchor preparation	2 cm/sec	"Blowout" frac- ture of body of L1 with rupture of ant. long. lig. and uni- lateral fracture of L pedicle- transverse pro- cess and extend- ing into pedicle	1735	390	5.9	2.32	51.2
S-11 RESPIRATORY ARREST	43.1	55	1		Isolated column T3-L5* Anchored at (T3T4)-L5 Force applied along spinal axis. Metal cylinder and methylme- thacrylate used to anchor preparation	1.2 cm/min	T11-T12: Max. angle of flexion attained 60°. Fracture of body of T11 just above disc. Ant. and pos. long. lig. disrupted	1134	255	1.5	0.59	8.5
			2		Isolated column T11- L4.* Anchored at T11- L4. Force applied along spinal axis. Metal cylinder and methylmethacrylate used to anchor prep.	61 cm/sec	None	4904.8	1102.7	2.26	0.89	55.4
			3		Isolated column T11- L4. Anchored at T11-L4. Force applied along spinal axis. Metal cylinder and methyl- methacrylate used to anchor prep.	1.1 cm/sec	None	4803.8	1080	2.59	1.06	64.6
			4		Isolated column T11- L4.* Anchored at T11- L4. Force applied along spinal axis. Metal cylinder and methyl- methacrylate used to anchor prep.	1.0 cm/sec	T12-L1 pos. complex dis- rupted	4848	1090	3.63	1.43	88.0

\*Refers to entire length of column used

X=Motion

L=left, R=right, Ant.=Anterior, Pos.=Posterior

TABLE 5  
(CONTINUED)



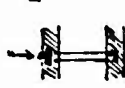

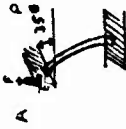


SPECIMEN	WGT (kg)	AGE (yr)	RUN #	PREPARATION DIAGRAM	PREPARATION MOUNTING	LOADING RATE	FAILURE	MAX LOAD N	MACHINE			FAILURE ENERGY (J)	
									DEFLECTION AT FAILURE cm	DEFLECTION in	FAILURE ENERGY (J)		
S-11 RESPIRATORY APREST	43.1	55	5		Isolated column T3-T10.* Anchored at (T3 T4)-T10. Force applied along spinal axis. Metal cylinder and methylmethacrylate used to anchor preparation	1.1 cm/sec	T9-T10 articular capsules stretched	3647	820	4.49	1.77	81.9	--
S-12 PNEUMONIA	58.2	57	1		Isolated column T2-Sacrum.* Anchored at (T2T3)-(L5 Sacrum). Force applied to center of vertebral body of T2 Spine flexed 30° forward Metal cylinder and methylmethacrylate used to anchor preparation	25 cm/sec	T9-T10 fractured body of T9 above disc. L lateral portion of lig. flavum disrupted Spine flexed 95° at T10-T11.	978	220	2.26	0.89	11.0	--
			2		Isolated column T10-Sacrum.* Anchored at (T10T11)-(L5 Sacrum). Force applied to spinal axis. Metal cylinder and methylmethacrylate used to anchor preparation	102 cm/sec	None	4558.7	1024.9	5.36	2.11	122.2	--
			3		Isolated column T10-Sacrum.* Anchored at (T10T11)-(L5 Sacrum). Force applied to spinal axis. Metal cylinder and methylmethacrylate used to anchor prep.	127 cm/sec	Compression fracture of L2. Pos. long. lig. and lig. flavum disrupted L2-L3	2885.9	648.8	7.87	3.1	113.6	--

TABLE 5  
(CONTINUED)

SPECIMEN	WGT (kg)	AGE (yr)	RUN #	PREPARATION DIAGRAM	PREPARATION MOUNTING	LOADING RATE	FAILURE	MAX LOAD		MACHINE DEFLECTION AT FAILURE		FAILURE ENERGY (J) MACHINE TISSUE
								N	lbs	cm	in	
S-13 ACUTE RESPIRATORY FAILURE	77.1	84	1		Isolated column T3-L5* Anchored at (T3T4)-(L4 L5). Force applied to spinal axis. Metal cylinder and methylme- thacrylate used to anchor prep.	122 cm/sec	Compression frac- ture of T7 just above disc at T7- T8, compression fracture of T12, L2 Pos. complex and ant. long. lig. disrupted at T7-T8 Chip fracture of sup. ant. body of T8 and fracture of spinous process of T8	2224	500	3.58	1.41	39.8 --
S-16 SPONTANEOUS SUBARACHNOID HEMORRHAGE	68.1	65	1		Isolated column: T2- Sacrum.* Anchored at (T2T3)-(L5 Sacrum). Force applied to center of body of T2. Forced flexion at 35°. Metal cylinder and methylme- thacrylate used to anchor preparation	122 cm/sec	T10-T11 endplate failure with wedge fracture of T11. Pos. complex dis- rupted T10-T11, partial disruption of spinal cord	1725	387.8	2.39	0.94	20.6 --
S-17 RESPIRATORY ARREST -- BRAIN TUMOR	68.1	65	1		Isolated column T2- Sacrum.* Anchored at (T2T3)-(L5 Sacrum). Forced flexion, line of force is 7.5 cm forward of center of vertebral bodies. Metal cylinder and methylmethacrylate used to anchor prepara- tion.	122 cm/sec	T9-T10 pos. com- plex and pos. long. lig. dis- rupted at T9-T10 Wedge (compres- sion) fracture of T9.	788.6	177.3	0.84	0.33	3.3 59.1 X --
S-18 CARDIAC ARREST	79.4	41	1		Isolated column T4-L5.* Anchored at (T4T5)-(L4 L5). Forced flexion, line of force is 2.5 cm forward of the center of vertebral bodies. Metal cylinder and methylme- thacrylate used to anchor preparation	61 cm/sec	T12 compression (wedge) fracture Pos. complex dis- rupted and spinal cord exposed at T11-T12. Ant. long. lig. dis- rupted at T11-T12	4452	1001	3.15	1.24	70.1 111.3 X --

X=Moment

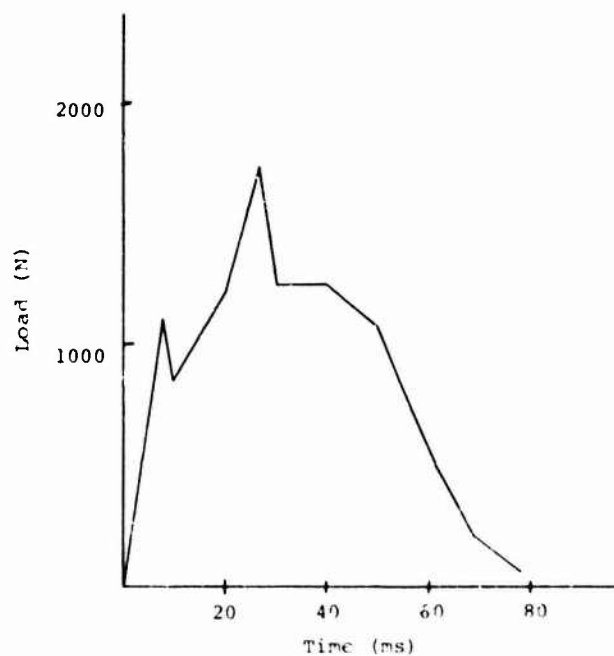


(A)



(B)

Figure 8: S-16 (Table 5, Run 1).  
 A) This is an anterior to posterior view with the column in a slight lateral angulation. The arrow points to the T10, T11 endplate failure. B) This is a lateral view with the column in a flexed position. The arrow points to the T10, T11 endplate failure with a compression fracture to the body of T11. C) Force versus time plot.



(C)



Comment - This test is similar to flexion test of S-12 (run 1, Table 5). Both these preparations were flexed 30 to 35 degrees prior to loading which resulted in a compression (wedge) fracture of vertebral bodies immediately above to the thoraco-lumbar junction.

Case S-17 (Isolated Thoraco-Lumbar Column, Table 5)

The thoraco-lumbar spinal column was mounted at T2, T3 and L5-sacrum with methylmethacrylate. This column had a forced flexion with the line of force 7.5 cm forward of the center of the vertebral bodies. The column was flexed to an included angle of 100 degrees at the T9-T10 junction and a right lateral movement of 30 degrees at a rate of 122 cm/s. A force of 788.6 Newtons and a moment about the center of the vertebral bodies of 59.1 Joules was observed. A wedge fracture of T9 and disruption of the posterior ligament complex and posterior longitudinal ligament occurred.

Comment - The force observed in the forced flexion of the isolated thoraco-lumbar column is approximately 1.5 to 3 times less than the forces achieved with similar columns under straight axial compression. The lower force value may be the result of the moment produced about the center of the vertebral bodies.

Case S-18 (Isolated Thoraco-Lumbar Column, Table 5)

The thoraco-lumbar spinal column was mounted at T4-T5 and L4-L5 with methylmethacrylate. This column was subjected to a forced flexion with the line of force 2.5 cm forward of the center of the vertebral bodies. The column underwent a total angulation of approximately 120 (included angle) at the T11-T12 junction, with a right lateral movement of 30 degrees. A force of 4452 Newtons and a moment about the center of the vertebral bodies of 111.3 Joules was observed. A wedge fracture of T12, disruption of the anterior longitudinal ligament and the posterior ligament complex at T11-T12, exposing the spinal cord was seen.

Comment - The failure of the thoraco-lumbar isolated column is similar to that of S-17, run 1, (Table 5). Both these specimens were loaded in a similar manner, the only difference being the line of force was forward of the center of the vertebral bodies. This distance is 3 times smaller for S-18. The force obtained with this specimen is approximately 6 times greater than that observed for S-17, run 1 (Table 5). This section was also somewhat shorter.

G. IN VITRO HUMAN SHEAR STUDIES ON ISOLATED CERVICAL SPINAL COLUMNS AND THORACIC SPINAL COLUMNS

Case S-11 (Isolated Cervical Column, Table 6)





In this study, the viable tissues that remained from the isolated cervical studies (S-11, Table 3) were remounted and used for studying the characteristics of the column when subjected to transverse forces. In the first run, the column was mounted at C7, T1, T2 with methylmethacrylate, with the force applied at the posterior region of C2-C3. Forces of 845 Newtons at a rate of 122 cm/s produced a compression fracture of the body of C6, fracture of the spinous process of C6 and avulsion of the posterior ligamentous complex at C6-C7, exposing the spinal cord and disc. In the second run, the column was remounted at C4, C5, C6 with only the inferior half of C4 and C5-C6 mounted in methylmethacrylate. The forces were applied at the posterior aspect of C3, producing a disruption of the posterior elements at C3-C4 and fracture of the spinous process of C4 at 1200 Newtons and a 122 cm/s rate. In the third run, the forces were applied on the odontoid with C3, C4, C5, C6 mounted in methylmethacrylate. The odontoid was fractured at the base of its neck, partially into the anterior arch of C2 at 890 Newtons at a rate of 137 cm/s. In run 4, the left anterior and right posterior arches of the axis were fractured with forces applied to the posterior region of C2 at 1068 Newtons at 142 cm/s with the inferior half of C3, and C4-C5 and C6 mounted in methylmethacrylate.

Comment - In runs 1 and 2, a pure flexion injury is simulated, with the majority of the forces imparted to the posterior ligaments. In test 2 the spinous process fracture was probably due to the direct loading upon it. These runs indicate that the strength of the posterior ligament complex for this specimen is in the range of 845 to 1200 Newtons. The third run suggests that the strength of the odontoid is approximately 900 Newtons at the base of its neck. The force values for these tests are probably lower than in a fresh preparation since this preparation had undergone previous testing.

Case S-12 (Isolated Cervical Column and Thoraco-Lumbar Column, Table 6)

In this study, the remaining intact tissues from the isolated cervical and thoraco-lumbar studies (HS-12, Tables 3 and 5) were remounted and forces transverse to the column were applied. In run 1, the column was mounted at C5, C6, C7 and forces were applied to the anterior aspect of C2. The endplate was sheared off at C2-C3 with the anterior and posterior longitudinal ligaments disrupted at 2179 Newtons at a rate of 122 cm/s. In run 2 the other specimen was anchored at T6 and T9 with methylmethacrylate, with the forces applied to the anterior aspect of T9, with no injury to the column at 3167.9 Newtons at a rate application of 122 cm/s. This test was repeated in run 3 with minor stretching of the anterior ligaments at the T7-T8 interspace, with 1970.5 Newtons and a rate of 122 cm/s.

TABLE 6  
IN VITRO HUMAN SHEAR STUDIES ON ISOLATED CERVICAL SPINAL COLUMNS AND THORACIC SPINAL COLUMNS

SPECIMEN	WGT (kg)	AGE (yr)	RUN #	PREPARATION DIAGRAM	PREPARATION MOUNTING	LOADING RATE	FAILURE	MAX LOAD N	MAX LOAD lbs	MACHINE DEFLECTION AT FAILURE cm	MACHINE DEFLECTION AT FAILURE in	FAILURE ENERGY (J) MACHINE TISSUE <sup>F</sup>
S-11 RESPIRATORY ARREST	43.1	55	1		Isolated column: C2-T2* Anchored at (C7/T1/T2) Force applied to C3 in a P-A direction. 5 cm moment arm. Methyl- methacrylate used to anchor preparation	122 cm/sec	C6-C7: pos. com- plex disrupted, spinous process of C6 fractured Compression (wedge) fracture to the body of C6. Spinal cord and disc exposed	845	190	3.61	1.42	15.2
			2		Isolated column: C2-C6* Anchored at (C4/C5/C6). Force applied to C3 in a P-A direction. 2.5 cm mo- ment arm. Methylmethacry- late used to anchor prep	122 cm/sec	C3-C4: spinous process of C4 fractured. Post complex dis- rupted exposing spinal cord	1200	270	2.44	0.96	14.6
			3		Isolated column: C2-C6* Anchored at (C3/C4/C5/C6) Force applied to odon- toid in a A-P direction. Methylmethacrylate used to anchor prep	137 cm/sec	Odontoid frac- tured at base of neck, par- tially into arch of C2	890	200	2.44	0.96	10.8
			4		Isolated column: C2-C6* Anchored at C2-(C3/C4/C5 C6). Force applied to C2 in a P-A direction. Methylmethacrylate and wire used to anchor preparation	142 cm/sec	L. Ant. and R. Pos. arch of C2 fractured	1068	240	1.06	0.42	5.7


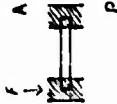
\*Refers to entire length of column used

X=Moment

A=Anterior, P=Posterior

R=right, L=left, Ant.=Anterior, Pos.=Posterior

TABLE 6  
(CONTINUED)

SPECIMEN	WGT (kg)	AGE (yr)	RUN #	PREPARATION DIAGRAM	PREPARATION MOUNTING	LOADING RATE	FAILURE	MAX LOAD N	MAX LOAD lbs	DEFLECTION AT FAILURE cm	DEFLECTION AT FAILURE in	FAILURE ENERGY (J) MACHINE TISSUE
S-12 PNEUMONIA	58.9	57	1		Isolated column: C2-C7. Anchored at C5 C6C7). Force applied to C2 in a A-P direction. Moment arm 1.5 cm. Wire and methylmethacrylate used to anchor preparation	122 cm/sec	C2-C3 endplate failure, ant. and pos. long. lig. disrupted.	2179	490	1.47	0.58	16.0 -- 32.7 X
			2		Isolated column: T6-T9. Anchored at T6-T9. Force applied to T9 in a A-P direction. Wire and methylmethacrylate used to anchor preparation	122 cm/sec	None	3167.9	712.2	1.65	0.65	26.1 --
			3		Isolated column: T6-T9. Anchored at T6-T9. Force applied to T9 in a A-P direction. Wire and methylmethacrylate used to anchor preparation	122 cm/sec	Minor stretching of lig. at T7-T8	1970.5	443	2.59	1.02	25.5 --

X=Motion  
A=Anterior, P=Posterior

Comment - The force to produce an endplate failure at C2-C3 in this specimen was similar to that required to cause a similar failure during axial tension in S-1, run 1 (Table 1).

#### DISCUSSION

The neurophysiological findings indicate that the somatosensory evoked potential is a sensitive indicator of neuronal function and that distraction is an important mechanism in spinal cord injury. Because of this sensitivity, the evoked potential has been applied to the evaluation of neural changes in impact acceleration in the experimental animal (31,37,38). These results can be correlated with subinjury tests in human volunteers (8,26) for evaluation of human injury.

Although the model presented requires refinement, it provides insight into the effects of variation of helmet and neck parameters. Furthermore by comparison of model results with injury films and experimental results more comprehensive and accurate models can be developed. Although this model is limited to axial loading, similar methods can be used to model flexion and extension.

The majority of the results of the cadaver experiments agree with other literature (11,13). While the multiple runs may not represent maximum tissue strength they do however simulate multiple impacts routinely experienced. Short isolated segments of the spinal column require high loads and produce vertebral body failures (30). Greater tissue strength is observed with higher loading rates. With longer segments of the spinal column, or with intact specimens, bending is observed, lower forces are required for failure, and ligamentous damage results (2,36). The relative strengths of the vertebral bodies, ligaments, and discs are comparable to those reported by others (15-17,18a,22a,24,29,40,42).

In extreme cases, the damage is similar to that observed in autopsy studies (4,6,10,23). Upper cervical ligamentous damage and ring fractures around the foramen magnum are routinely observed (6,10,23). Less severe damage is comparable to that seen clinically. Some of the relatively mild damage observed in the cadavers is probably similar to mild injuries which are not detected clinically, yet are painful.

The energies for failure observed in this study are surprisingly low, but are in the range reported by others (15,28). Furthermore, the energies were integrated only to the point of failure, rather than for the entire run. The thoracolumbar studies suggest failure is probably related to the bending movement in contrast to other studies with short segments (15,22a). Furthermore Ewing has demonstrated failure sensitivity with column angulation (9,18).

#### SUMMARY OF RESULTS

- 1) Fresh isolated monkey cervical spines failed quasi-statically in tension between 325-534 N (32) compared to 1446-1940 N in the fresh isolated human cadaver cervical spines. The dynamic loads were 1289 to 1423 N in the monkey (32) compared to 1668-2500 N in the cadaver.
- 2) Intact monkey necks failed dynamically between 1690-2669 N (32) compared to 2450-3900 in the cadavers.
- 3) Circular skull fractures were observed in tension in the cadavers at 1780 N quasi-statically and 3780 N dynamically.
- 4) Fresh monkey spinal cords failed in tension at 36 N quasi-statically and 90 N dynamically (32) compared to 167 N quasi-statically and 278-389 N dynamically for fresh human spinal cords.
- 5) One fresh isolated cadaver cervical spine failed at approximately 645 N in quasi-static compression. In dynamic flexion/axial compression studies the isolated cadaver cervical spines failed at 1779-4448 N.
- 6) Intact cadaver whole torsos failed dynamically in compression at 1512-2936 N.
- 7) Fresh isolated cadaver thoracolumbar spinal columns failed in compression at 1134-1735 N. Short segments failed at 2900-4900 N.
- 8) Shear studies show cervical posterior ligament failures from 845-1200 N with posterior to anterior force and odontoid failure within this range with posterior to anterior or anterior to posterior forces in the isolated column. A failure load of 2175 N was observed with anterior-posterior force application. Loads up to 3168 N did not shear isolated thoracic segments.

#### ACKNOWLEDGMENT

This research was supported in part by the Office of Naval Research Contract N00014-77-CO743.

## REFERENCES

1. Allen, A.R.: Surgery of experimental lesion of spinal cord evaluation to crush injury of fracture dislocation of spinal column. Preliminary report. *JAMA* 57:878-880, 1911.
2. Bauze, R.J. and Ardran, G.M.: Experimental production of forward dislocation in the human cervical spine. *J Bone Joint Surg* 60B(2):239, 1978.
3. Breig, A.: Adverse Mechanical Tension in the Central Nervous System, Almquist and Wiksell, Stockholm, Sweden, 264 pp., 1978.
4. Clemens, H.J. and Burow, K.: Experimental investigation on injury mechanisms of cervical spine at frontal and rear-front vehicle impacts. *Proc 16th Stapp Car Crash Conf*, Society of Automotive Engineers, New York, 1972, p. 76.
5. Culver, R., et al: Mechanisms, tolerances and responses obtained under dynamics of superior inferior head impact, PB-299292, Univ Michigan Highway Safety Research Institute, May 1978.
6. Davis, D., Bohlman, H., Walker, A.E., Fisher, R. and Robinson, R.: The pathological findings in fatal craniocervical injuries. *J Neurosurg* 34:603-613, 1971.
7. DeLaTorre, J.C.: Spinal cord injury. Review of basic and applied research. *Spine* 6(4):315-335, 1981.
8. Ewing, C.L. and Thomas, D.J.: Torque versus angular displacement response of human head to  $-G_x$  impact acceleration. *Proc 17th Stapp Car Crash Conf*, Society of Automotive Engineers, New York, 1974, pp. 309-342.
9. Ewing, C.L., King, A.E. and Prasad, P.: Structural considerations of the human vertebral column under  $+G_z$  impact acceleration. *J Aircraft* 9(1):84-90, 1972.
10. Freytag, E.: Autopsy findings in head injuries from blunt forces. Statistical evaluation of 1,367 cases. *Arch Pathol* 75:402-413, 1963.
11. Got, C., et al: Results of experimental head impacts on cadavers: The various data obtained and their relations to some measured physical parameters. *Proc 22nd Stapp Car Crash Conf*, Society of Automotive Engineers, Warrendale, PA, 1978, pp. 57-99.
12. Haley, J.L., Jr., Shanahan, D.F., Reading, T.E., and Knapp, S.C.: Head impact hazards in helicopter operations and their mitigation through improved helmet design. In Impact Injury of the Head and Spine, C.L. Ewing, et al, eds., Charles C. Thomas, Publ., Springfield, IL, 1981 (In Press).
13. Hodgson, V.R. and Thomas, L.M.: Mechanisms of cervical spine injury during impact to the protected head. *Proc 24th Stapp Car Crash Conf*, Society of Automotive Engineers, Warrendale, PA, 1980, pp. 15-42.
14. Hodgson, V.R. and Thomas, L.M.: A model to study cervical spine injury mechanisms due to head impact. In Engineering Aspects of the Spine, I Mech E Conference Publications 1980-2, pp. 89-96.
15. Kazarian, D. and Graves, G.A.: Compressive strength characteristics of the human vertebral centrum. *Spine* 2(1):1-14, 1977.
16. Kazarian, L.E. and Graves, G.: Compressive strength characteristics of the primate (*Macaca mulatta*) vertebral centrum. Report No. AMRL-TR-79-8, Aerospace Medical Research Laboratory, Wright-Patterson Air Force Base, June, 1979, 25 pp.
17. Kazarian, L.E. and Kaleps, I.: Mechanical and physical properties of the human intervertebral joint. Report No. AMRL-TR-79-3, Air Force Aerospace Medical Research Laboratory, Wright-Patterson Air Force Base, June, 1979, 25 pp.
18. King, A.I., Prasad, P., and Ewing, C.L.: Mechanisms of spinal injury due to caudocephalad acceleration. *Orthop Clin North Am* 6(1):19, 1975.
- 18a. Lantz, S.A., Lafferty, J.F. and Bowman, D.A.: Response of the intervertebral disk of the rhesus monkey to P-A shear stress. *J Biomech Eng* 102:137-140, 1980.
19. Larson, S.J., Walsh, P.R., Sances, A., Jr., et al: Evoked potentials in experimental myelopathy. *Spine* 5(4):299-302, 1980.
20. Larson, S.J.: Unstable thoracic fractures: treatment alternatives and the role of the neurosurgeon. *Clin Neurosurg* 27:624-640, 1980.
21. Larson, S.J.: Bio-engineering analysis of injuries of the nervous system. Chapter in Impact Injury of the Head and Spine, C.L. Ewing, et al, eds., Charles C. Thomas, Publ., Springfield, IL, 1981 (In Press).
22. Larson, S.J.: Lumbar interbody fusion: biomechanical considerations. Chapter in Posterior Lumbar Interbody Fusion, P. Lin, ed., Charles C. Thomas, Publ., Springfield, IL, 1981 (In Press).
- 22a. Lin, H.S., Liu, Y.K. and Adams, K.H.: Mechanical response of the lumbar intervertebral joint under physiological (complex) loading. *J Bone Joint Surg* 60A(1):41-55, 1978.
23. Lindenberg, R., and Freytag, E.: Brainstem lesions characteristic of traumatic hyperextension of the head. *Arch Pathol* 90:509-515, 1970.
24. Little, R.W., Hubbard, R.P. and Hyler, D.L.: Mechanical properties of spinal ligaments for rhesus monkey, baboon and chimpanzee. Report No. AFAMRL-TR-81-40, Air Force Aerospace Medical Research Laboratory, Wright-Patterson Air Force Base, June, 1981, 39 pp.
25. McElhaney, J., et al: Etiology of trauma to the cervical spine. In Impact Injury of the Head and Spine, C.L. Ewing, et al, eds., Charles C. Thomas, Publ., Springfield, IL, 1981 (In Press).
26. Mertz, H.J. and Patrick, L.M.: Strength and response of the human neck. *Proc 15th Stapp Car Crash Conf*, California, 1971, pp. 207-255.
27. Mertz, H., et al: An assessment of comprehensive neck loads under injury-producing conditions. *Physician and Sports Medicine* 6(11), November 1978.
28. Nusholtz, G., Melvin, J., et al: Response of the cervical spine to superior-inferior head impact. *Proc 25th Stapp Car Crash Conf*, Society of Automotive Engineers, Warrendale, PA, 1981, pp. 197-237.
29. Panjabi, M.M., White, A.A., III, and Johnson, R.M.: Cervical spine mechanics as a function of transection of components. *J Biomech* 8:327-336, 1975.

30. Roaf, R.: A study of the mechanics of spinal injuries. J Bone Joint Surg 42B:810, 1960.
31. Saltzberg, B., Burton, W.D., Jr., Weiss, M.S., Berger, M.D., Ewing, C.L., Thomas, D.J., Jessop, E., Sances, A., Jr., et al: Dynamic tracking of evoked potential changes in studies of central nervous system injury due to impact acceleration. Chapter in Impact Injury of the Head and Spine, C.L. Ewing, et al, eds., Charles C. Thomas, Publ., Springfield, IL, 1981 (In Press).
32. Sances, A., Jr., Weber, R., Myklebust, J., Cusick, J., et al: The evoked potential: an experimental method for biomechanical analysis of brain and spinal injury. SAE Transactions 89:3815-3836, 1980.
33. Sances, A., Jr., Myklebust, J.B., Weber, R.C., Larson, S.J., Cusick, J.F. and Walsh, P.R.: Bioengineering analysis of head and spine injuries. CRC Crit Rev Bioeng 5(2):79-122, Feb 1981.
34. Sances, A., Jr., Myklebust, J., Cusick, J., et al: Experimental studies of brain and neck injury. Proc 25th Stapp Car Crash Conf, Society of Automotive Engineers, Warrendale, PA, 1981, pp. 149-194.
35. Sances, A., Jr., Myklebust, J., Larson, S.J., Cusick, J.F., and Weber, R.: The evoked potential - a biomechanical tool. Chapter in Impact Injury of the Head and Spine, C.L. Ewing, et al, eds., Charles C. Thomas, Publ., Springfield, IL, 1981 (In Press).
36. Selecki, E.R. and Williams, H.B.L.: Injuries to the Cervical Spine and Cord in Man, Australian Med Assoc., Mervyn Archdall Med Monograph #7, Australian Medical Publishers, South Wales, 1970.
37. Walsh, P.R., et al: Experimental methods for evaluating spinal cord injury during impact acceleration. Electrotherapeutic Sleep and Electroanesthesia, F.M. Waqeneder, et al, eds., Universitat Graz, 1978, pp. 435-443.
38. Walsh, P.R. and Jessop, M.E.: The evoked potential in sled impact acceleration: Methodologic and neurosurgical considerations. Chapter in Impact Injury of the Head and Spine, C.L. Ewing, et al, eds., Charles C. Thomas, Publ., Springfield, IL, 1981, (In Press).
39. Weber, R.: An introduction to the elements of linear biomechanical modeling. Chapter in Impact Injury of the Head and Spine, C.L. Ewing, et al, eds., Charles C. Thomas, Publ., Springfield, IL, 1981 (In Press).
40. White, A.A. and Panjabi, M.M.: Clinical Biomechanics of the Spine, Lippincott, Philadelphia, 1978.
41. Windle, W.F., ed.: The Spinal Cord and Its Reaction to Traumatic Injury. Marcel Dekker, Inc., New York, 1980, 384 pp.
42. Yamada, H.: Strength of Biological Materials. Robert E. Krieger Publ., Huntington, N.Y., 1973, 297 pp.

## DISCUSSION

DR. HEARON (USA)

During the tests in which the thoraco-lumbar vertebral columns were loaded in compression, were any hyperextension vertebral fractures noted when the column failed?

AUTHOR'S REPLY

No, all failures were in flexion.

UNIDENTIFIED QUESTIONER

You described two sets of experiments, one set in which you preflexed the spine and the first set in which you just provided axial compression of that section of the vertebral column. Did you notice any hyperextension type injuries in that first set?

AUTHOR'S REPLY

Yes, with the isolated columns, we noted cervical hyperextension injuries. I showed a slide with hyperextended avulsion fracture. We also had a chip fracture with an inplate separation at C4-C5 and a teardrop fracture at C4.

## NEUROPHYSIOLOGICAL EFFECTS OF -X IMPACT ACCELERATION

Marc S. Weiss, Ph.D. &amp; Michael D. Berger, Ph.D.

Neurophysiology Division  
 Biomedical Research Department  
 Naval Biodynamics Laboratory  
 Box 29407  
 New Orleans, Louisiana 70189  
 USA

SUMMARY

In 19 experiments, eight unanesthetized Rhesus monkeys, with torsos restrained in a seated position, and with head and neck free to move, were subjected to peak sled accelerations in the -X direction ranging from  $42 \text{ m/s}^2$  to  $963 \text{ m/s}^2$ . Recordings of cortical somatosensory evoked potentials were made using recording electrodes chronically implanted over the somatosensory cortex. Electrical pulse stimuli were delivered at a rate of 5 Hz through spinal electrodes located at L1 - L2. Evoked potentials were recorded prior to impact, through the impact event, and subsequent to impact, then subjected to quantitative analysis procedures which included normalized cross-correlation and exponential regression.

The results of this analysis suggest a neurophysiological effect which holds promise as an indicator of a pre-injurious central nervous system condition. This effect is an immediate increase of 2% to 5% in the latency of the primary surface positive peak of the cortical evoked potential. There appears to be a threshold for these increases in latency at peak sled accelerations in the region of  $600 \text{ m/s}^2$ . This is consistent with previous findings and provides the basis for applying these techniques to human volunteer experiments.

INTRODUCTION

Impact injury involving the head and neck disrupts the normal functioning of the central nervous system (CNS) to an extent dependent upon the severity and nature of the trauma. The often temporary CNS dysfunction, which results from head and neck trauma (identified clinically as "concussion"), is of special interest in the development of a useful injury model. The pioneering work of Denny-Brown and Russell (5) was the first thorough attempt to identify the physiological concomitants of direct head injury and led to numerous subsequent investigations (e.g., 7, 11, 12, 23). These studies shared the following features: (a) the impact blow was delivered directly to the head which was free to move, (b) anesthetized animals (monkey, dog, cat) were subjects, (c) basic vital functions and EEG were monitored. Generally, the results followed a typical pattern, similar to the one described by Denny-Brown and Russell (5) and Williams and Denny-Brown (25). Severe, but non-fatal, blows resulted in a loss of corneal reflex, rise in blood pressure, fall in heart rate, drop in EEG amplitude and frequency, sometimes followed by development of slow waves. These effects could occur in the absence of any apparent brain pathology and have been well reviewed (6, 16, 22).

In the decade following these reports, two important extensions to these basic findings were made. Foltz and Schmidt (8), using unanesthetized monkeys, stimulated the sciatic nerve and recorded evoked potentials (EP's) from the reticular formation (RF) and the medial lemniscus. In six out of eight monkeys receiving severe direct head impacts, the lemniscal response persisted while the RF response was abolished. This first use of the EP in a head injury study indicated that the non-specific brainstem gray matter was functionally more sensitive to impact than the sensory specific ascending pathway. Subsequently, Friede (9) demonstrated that in the cat, both cervical stretch and a blow to the head produced the same loss of reflexes as well as the same neuropathology at the C1 level of the spinal cord. This, again, suggested that the lower brainstem might be the vulnerable site in CNS impact dysfunction.

More recently, Ommaya and his co-workers (10, 14, 15) subjected both the unanesthetized monkey and chimpanzee to non-impact head acceleration while stimulating the median nerve and recording the somatosensory EP's at the cortex. The EP amplitude was more sensitive to head acceleration than the EEG. This occurred in animals that were rendered unconscious (loss of muscle tone, insensitivity to painful stimuli) as well as in some that remained conscious. The duration and intensity of the EP effect appeared to parallel the duration of the unconsciousness, but no relationship to the intensity of acceleration was reported.

These earlier results provided the background for the effort begun in late 1974 when the Naval Biodynamics Laboratory (then the Naval Aerospace Medical Research Laboratory, Detachment #1) undertook the first of many experiments designed to test the neurophysiological effects of indirect or inertial head acceleration using Rhesus monkeys as subjects. In these experiments the restrained torso is accelerated while seated on a sled, with the freely moving head and neck receiving the "indirect" acceleration through the skeletal and soft tissue anatomy. Results from the early experiments (2, 24) indicated that the cortical somatosensory EP showed a decrement in amplitude and an increase in latency following non-lethal impact. These changes appeared to be greater with increased peak acceleration. More recent experiments (4), utilizing EP's recorded from the cervico-medullary junction, suggest the possibility of a threshold for neurophysiological dysfunction in Rhesus in the range of  $700 - 800 \text{ m/s}^2$  -X peak sled acceleration. These results confirm the utility of neurophysiological measures in assessing the effects of inertial forces on the functioning of the brain.



Ultimately, neurophysiological criteria for functional injury to the CNS are desired. The main purpose of the results reported here is to further identify those measures of CNS cortical function which can be the basis for establishing such criteria.

#### EXPERIMENTAL PROCEDURE

The adult Rhesus (Macacca Mulatta, ca. 10 Kg) was selected as the animal model and the somatosensory system as the pathway for testing CNS function. All the experiments were designed to use unanesthetized animals, restrained in a sitting, upright position, with head and neck freely moveable. The restraint system consisted of a nylon suit which covered the entire body except for the head and neck. Straps sewn to the suit firmly restrained the subject to a fiberglass chair which was molded to the shape of the subject's back. The subject was seated on a 410 kg sled which was accelerated by a HYGE system with a one meter stroke. Peak sled accelerations ranged from 42 to 963 m/s<sup>2</sup>. The subject was oriented so that he was accelerated in the -X (17, 18) direction. The sled was decelerated by friction (2 to 3 m/s<sup>2</sup>) over a distance of up to 213 meters. Precise inertial data were obtained from an array of transducers rigidly mounted to the monkey's skull. Physiological data included EKG, respiration, and cervical and cortical EP activity; the exact configuration occasionally varied. Average heart rate was computed by hand from EKG strip chart records.

The eight monkeys used as subjects for these 19 experiments were prepared surgically with chronic in-dwelling electrodes using procedures previously described (20, 21). Briefly, strip disc electrodes were implanted epidurally over the dorsal spinal cord at L1 - L2 and over the cervico-medullary junction. Bilaterally, subdural electrodes were implanted over the primary somatosensory cortex. Three months were allowed for recovery from implantation surgery.

Constant current .2 ms monophasic pulses at a nominal rate of 5 Hz were delivered to one pair of lumbar electrodes. The stimulus intensity ranged from 0.3 to 4.0 ma among animals and was selected for each animal as the highest intensity consistent with the apparent comfort of the subject. Large, but sub-maximal EP's were recorded from the electrodes through a telemetering system with an upper bandlimit of 1500 Hz and a variable lower bandlimit. Table 1 details the parameters used for each experiment.

TABLE 1 Summary of Experimental Parameters

Experiment	Date	-X Sled Peak Acc. (m/s <sup>2</sup> )	Subject	Stimulus Intensity (ma)	Cortical Recording Site	Amplifier			
						Gain (X1000)		Lower Bandlimit (Hz)	
						Cerv.	Cort.	Cerv.	Cort.
LX3008	19578	208	AR0761	.75	left	80	20	30	1
LX3009	19578	796	AR0761	.75	left	80	20	30	1
LX3010	19578	963	AR0761	.75	left	80	20	30	1
LX3027	28478	102	AR4114	.3	left	120	60	50	10
LX3028	28478	407	AR4114	.3	left	120	30	50	10
LX3185	07179	100	AR8857	1.25	right	40	20	50	10
LX3186	07179	810	AR8857	1.25	right	40	20	50	10
LX3695	24780	98	ARNA28	1.5	right	80	2.5	30	10
LX3697	24880	441	ARNA28	1.5	right	80	2.5	30	10
LX3698	24880	435	ARNA28	1.5	right	80	2.5	30	10
LX3699	25380	42	AR8872	4.0	right	40	10	30	10
LX3701	25480	436	AR8872	3.0	right	40	10	30	10
LX3702	25480	434	AR8872	3.0	right	40	10	30	10
LX3703	25580	99	AR8802	2.0	right	40	8	30	10
LX3705	25680	630	AR8802	2.0	right	40	8	30	10
LX3706	25680	624	AR8802	2.0	right	40	8	30	10
LX3713	26680	98	ARNA02	2.0	left	160	16	30	10
LX3714	26680	598	ARNA02	2.0	left	160	16	30	10
LX3715	26680	598	ARNA02	2.0	left	160	16	30	10

EP data acquisition was initiated 30 to 45 minutes prior to impact, was continued through the delivery of impact, and was terminated 45 to 90 minutes after impact. There was a five to ten minute gap in data acquisition ending ten minutes prior to impact. The data were amplified on the sled, telemetered to nearby equipment and recorded on FM tape.

The data were digitized off-line on a hybrid EAI PACER 600<sup>R</sup> computer at a sampling rate of at least 20 kHz. A software-hardware design was used which synchronized digitization with the stimuli. The digitized data were then processed on a UNIVAC 1100<sup>R</sup> series computer.

#### DATA ANALYSIS & RESULTS

Quantitative analysis previously performed on cervical EP's only (4), was extended to include cortical EP's and was used to determine the extent to which the impact produced shifts in latency and amplitude of the early positive peak of the cortical AEP's. Details of the quantitative analysis procedure are described elsewhere (3, 4). Briefly, a baseline AEP was computed for the two minutes preceding impact. Each baseline AEP was an average of approximately 580 individual EP's. To assess the effects of impact, test AEP's (each an average of 10 individual EP's) were computed for the two minutes preceding impact and the five minutes following impact.

A section of the baseline AEP containing the cortical primary surface positive peak was then selected. The latency limits of this section defined the time interval within which each test AEP was searched for a maximum. The amplitude of this maximum defined the peak amplitude for each test AEP. The median latency of the maxima from all the

pre-impact test AEP's was used as a reference for measuring the post-impact shift in latency.

To determine the shifts in latency produced by the impact event, a normalized cross-correlation procedure was used (3). This procedure has a number of advantages over the simple peak detection approach and can reliably detect very small shifts in latency (3). Briefly, a selected portion of the baseline AEP containing the primary positive peak is cross-correlated with a selected portion of each test AEP. The lag at the maximum of the cross correlation function is a measure of the shift in the latency of the primary peak of the test AEP.

As a result of these computations, an amplitude and a latency shift measure was obtained for the primary positive peak of each test AEP. These measures were plotted as a function of time, relative to impact, for the seven minute period starting two minutes prior to impact. Figure 1 illustrates such a plot for the latency shift measure for both the cortical and cervical AEP recorded during one experiment. Actual AEP's for this same experiment appear in Figure 2 (a complete set of AEP's from these experiments has been published previously (4)).

## AEP LATENCY SHIFT

RUN LX3706, 624 M/S<sup>2</sup> N:10

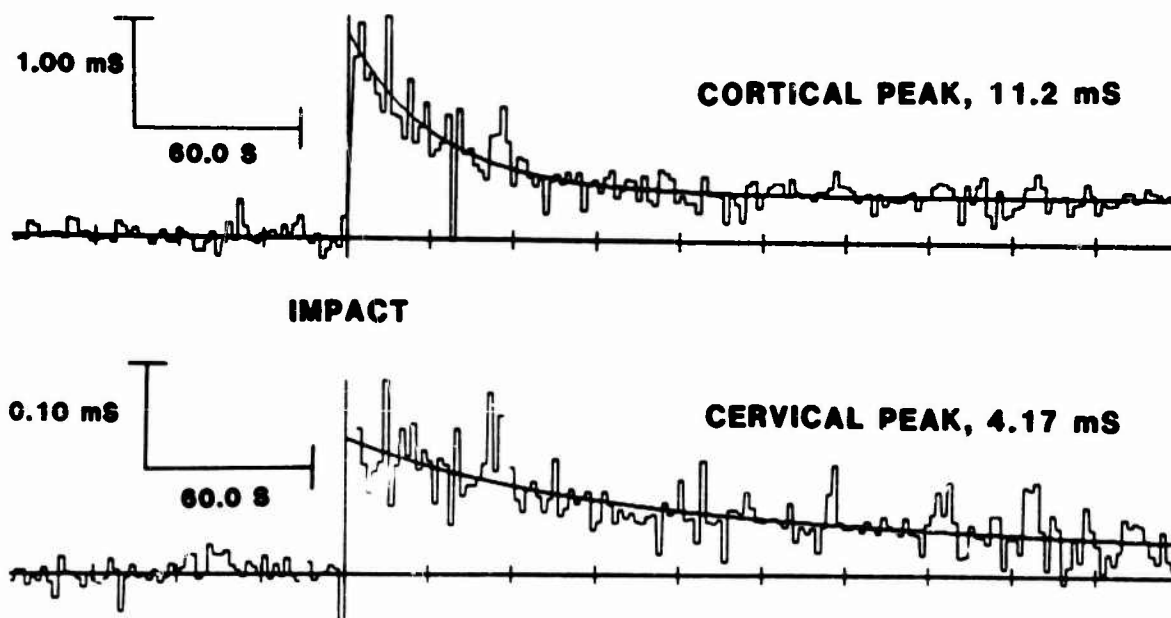


Figure 1. Illustration of the shift in latency of an evoked potential peak produced by an impact acceleration pulse of 624 m/s<sup>2</sup> in the -X direction. The upper graph plots the effect for the positive primary peak of the cortical evoked potential (median pre-impact latency of 11.2 ms). The lower graph plots the effect for a peak of the evoked potential recorded from the cervico-medullary junction (latency of 4.17 ms). The horizontal axis measures time marked in 30 second increments, with a large vertical mark at the time of impact. Exponential regression curves are also superimposed. See text for details.

As can be seen in Figure 1, impact results in a sudden shift in latency which decreases in time. A similar effect though not shown here is found with the amplitude measure. In order to quantify the time course of these changes, an exponential decay function was fitted to the time dependent amplitude and latency shift measurements. The fit for the cortical AEP results took the form of a single exponential plus a constant effect.

$$C = Ae^{t/T} + B$$

Based on this approximation, the initial strength of the effect of impact was estimated from  $A + B$  and the duration of the effect was defined as the negative time constant  $T$ .

The final step in the reduction of these data was to examine scatter plots of the A + B and T measures as a function of peak sled acceleration. The time constant (T) results obtained from analysis of the cortical data showed no consistent pattern and appeared to be unrelated in any obvious way to peak sled acceleration. This contrasts with the initial amplitude (A + B) measure. Figure 3 illustrates the A + B result for the cortical AEP's. The data for the amplitude of the primary positive peak show a decrement at all test levels of impact that is highly linearly correlated (corr. coef. = - .8) with peak sled acceleration. This is similar to the results of Weiss and Berger (24) who found that another correlation measure derived from cortical EP's also decreased with increasing peak sled acceleration. There is a lack of an apparent threshold effect when measuring the change in amplitude. This contrasts with the results obtained from the latency measurements. Examination of Figure 3 suggests that at peak sled accelerations greater than 600 m/s<sup>2</sup>, a substantial increase in latency of the primary positive peak is likely to occur. A linear regression fitted to that portion of the data intercepts the zero axis at 512 m/s<sup>2</sup>. Figure 4 illustrates previously published results (4) showing latency shift results for cervical AEP's from a series of experiments which include those reported here. A similar suggestion of a threshold effect can be seen in the neighborhood of 600 m/s<sup>2</sup>.

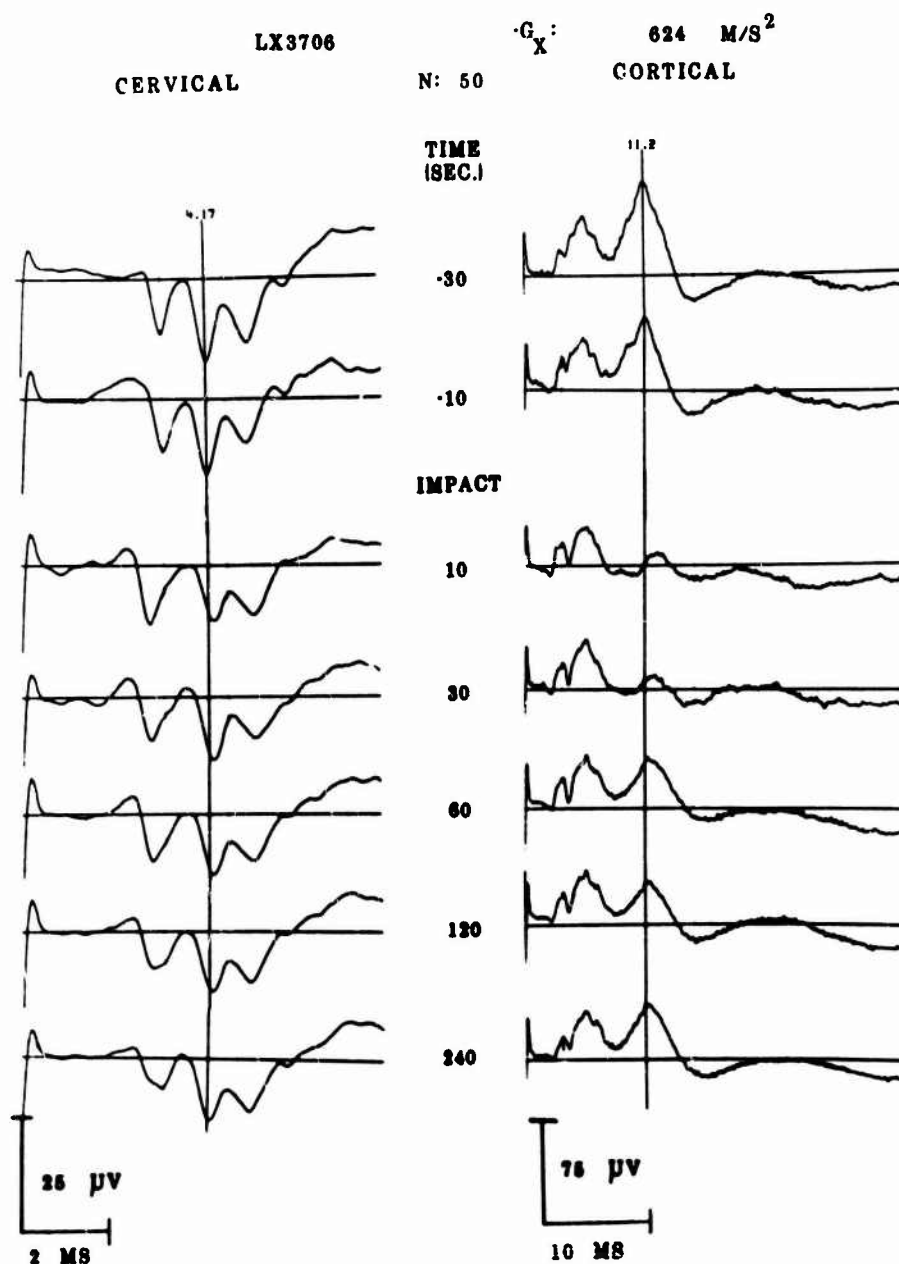
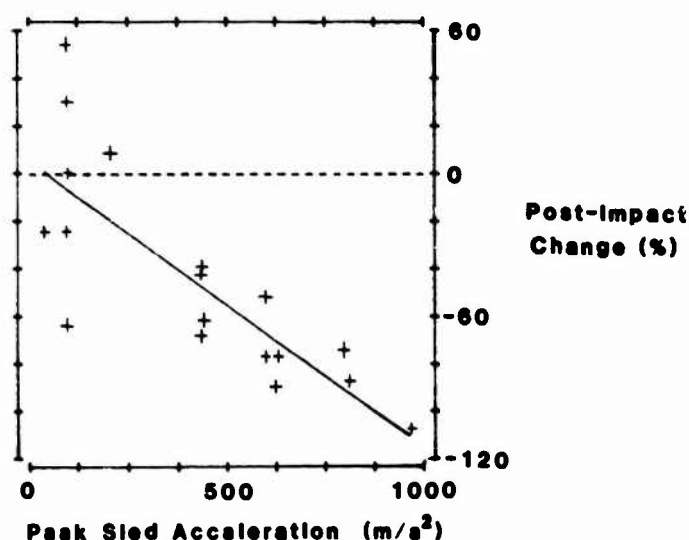


Figure 2:  
Illustration of  
averaged evoked  
potentials for  
the same experi-  
ment illustrated  
in Fig. 1.  
Averages consist  
of 50 individual  
evoked potentials  
and time relative  
to impact is in-  
dicated. The ver-  
tical marker iden-  
tifies the 4.17  
ms cervical peak  
and the 11.2 ms  
cortical peak.  
Note the in-  
crease in la-  
tency fol-  
lowing impact  
and the sub-  
sequent return  
close to the pre-  
impact value.

# CORTICAL POSITIVE PRIMARY RESPONSE

## AMPLITUDE



## LATENCY

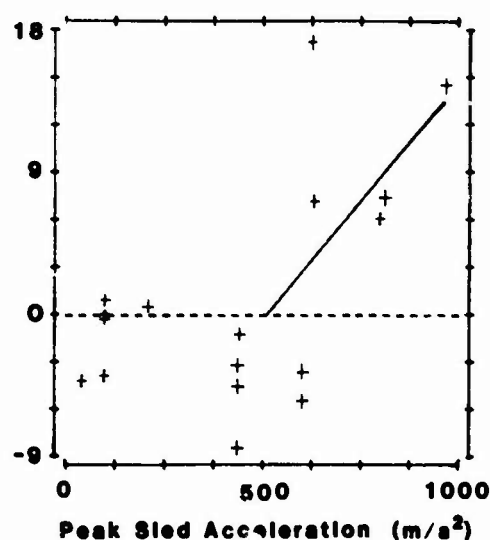


Figure 3: Scatter plots of the amplitude and latency of the primary positive peak of the cortical evoked potential as a function of peak sled acceleration. Change in amplitude and latency is measured as a percentage of the pre-impact median value obtained from the pre-impact test AEP's. See text for discussion.

## CERVICAL AEP'S:

### PERCENTAGE LATENCY SHIFT

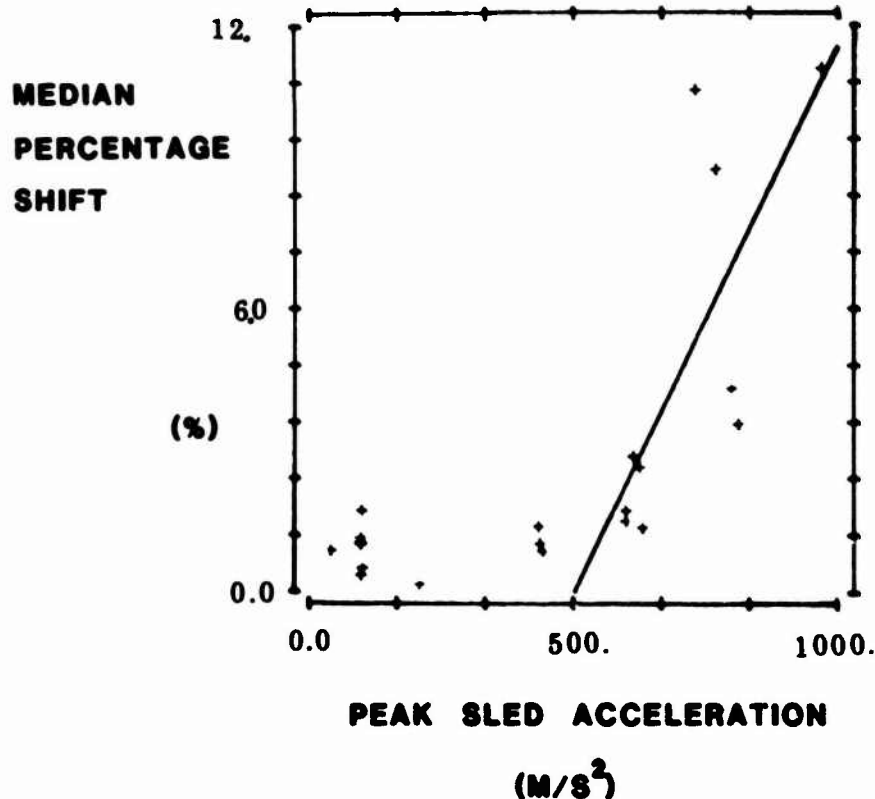


Figure 4: Scatter plot of shift in latency of the peaks of the AEP's obtained from electrodes implanted over the cervico-medullary junction. Details in (4).

## DISCUSSION

Decreases in the amplitude of cortical EP's have been previously reported as a result of direct impact (10, 14, 15) and indirect impact (2, 24). At low peak sled acceleration levels (less than 250 m/s<sup>2</sup>), the present data show increases in the positive primary peak to be equally likely as decreases. This probably reflects the influence of arousal or startle types of behavior which is well documented in other sensory modalities (e.g., 1, 13). The decrement at higher levels of acceleration remains a linearly graded one without a sharp threshold at levels in excess of 700 m/s<sup>2</sup> where injury might be anticipated (19), 70% to 100% decrements in amplitude occur. The amplitude of the primary cortical EP does not appear to be, therefore, a useful criterion for indicating a pre-injury condition.

The latency of the primary cortical EP presents a different picture. The results illustrated in Figure 3 strongly suggest a sharp threshold in the region of 600 - 700 m/s<sup>2</sup>. This closely parallels previous results obtained using EP's recorded from the cervico-medullary junction (also illustrated in Figure 4). This is encouraging in light of the neuropathological findings from these and other NBDL Rhesus experiments (19). The pathology findings indicate no evidence of injury below 727 m/s<sup>2</sup> and a high probability of injury above 825 m/s<sup>2</sup>. In the present experiments, despite the absence of injury, the latency of the primary cortical EP shows a marked increase (greater than 5%) at peak sled acceleration levels above 625 m/s<sup>2</sup>. Thus the increased latency occurring between peak sled accelerations of 625 m/s<sup>2</sup> and 725 m/s<sup>2</sup> may have value as an index of pre-pathological injury. Application and extension of these techniques to the human research program at the Naval Biodynamics Laboratory are currently in progress.

## REFERENCES

1. Anderson, B.W.; Oatman, L.C.: Auditory and visual evoked potentials to irrelevant stimuli during conditioning to a visual stimulus. Neurological Research, 1:281-290, 1980.
2. Berger, M.D.; Weiss, M.S.; A. Sances, Jr.; Walsh, P.R.; Larson, S.J.: Evaluation of changes in CNS function due to impact acceleration. Preprints of 1979 Annual Scientific Meeting of Aerospace Medical Association, Washington, D.C., 1979, pp 135-136.
3. Berger, M.D.: Analysis of Sensory Evoked Potentials Using Normalized Cross-Correlation Functions and Polyexponential Regression, 1981, (submitted for publication).
4. Berger, M.D.; Weiss, M.S.: Effects of Impact Acceleration on Somatosensory Evoked Potential. Impact Injury of the Head and Spine. Thomas, Springfield, Illinois (in press).
5. Denny-Brown, D. and Russell, W.R.: Experimental cerebral concussion. Brain, 64:93-164, 1941.
6. Denny-Brown, D.: Cerebral concussion, Physiol. Rev. 25:296-325, 1945.
7. Dow, R.S.; Ulett, G.; Tunturi, A.: Electroencephalographic changes following head injuries in dogs. J. Neurophysiol. 8:161,172, 1945.
8. Foltz, E.L. and Schmidt, R.P.: The role of the reticular formation in the coma of head injury. J. Neurosurg. 13:145-154, 1956.
9. Friede, R.L.: Experimental concussion acceleration, pathology and mechanics. Arch. Neurol. 4:449-462, 1961.
10. Gennarelli, T.A.; Thibault, L.E. and Ommaya, A.K.: Pathophysiologic responses to rotational and translational accelerations of the head. Proc. 16th Stapp Car Crash Conference, pp 296-307, 1972.
11. Groat, R.S.; Magoun, H.W.; Rey, F.L.; Windle, W.F.: Functional alterations in motor and supranuclear mechanisms in experimental concussion. Am. J. Physiol. 141:117-127, 1944.
12. Groat, R.A.; Windle, W.F.; Magoun, H.W.: Functional and structural changes in the monkey's brain during and after concussion. J. Neurosurg. 2:26-35, 1945.
13. Kitai, S.; Cohen, B.; Morin, F.: Changes in the amplitude of photically evoked potentials by a conditioned stimulus. Electroenceph. Clin. Neurophysiol., 19:122-136, 1965.
14. Letcher, F.S.; Corrao, P.G. and Ommaya, A.K.: Head injury in the chimpanzee Part 2: spontaneous and evoked epidural potentials as indices of injury severity. J. Neurosurg. 39:167-177, 1973.
15. Ommaya, A.K. and Gennarelli, T.A.: Experimental head injury. in Handbook of Clinical Neurology, eds. Vinken, P.J. and Bruyn, G.W., 23:67-90, American Elsevier, New York, 1975.
16. Shetter, A.G. and Demakas, J.J.: The pathophysiology of concussion: a review. Advances in Neurology, ed. R. Thompson, 22:5-14, 1979.

17. Thomas, D.J.; Robbins, D.H.; Eppinger, R.H.; King, A.I. and Hubbard, R.P.: Guidelines for the Comparison of Human and Human Analogue Biomechanical Data, First Annual Report of an Ad-Hoc Committee, Ann Arbor, Michigan, December 6, 1974.
18. Thomas, D.J.; Robbins, D.H.; Eppinger, R.H.; King, A.I.; Hubbard, R.P. and Reynolds, H.M.: Guidelines for the Comparison of Human and Human Analogue Biomechanical Data, Second Annual Report of an Ad-Hoc Committee, San Diego, California, November 19, 1975.
19. Unterharnscheidt, F: Neuropathology of Rhesus monkeys suffering -Gx impact acceleration. Impact Injury of the Head and Spine. Thomas, Springfield, Illinois. (in press)
20. Walsh, P.R. and Jessop, M.E.: The evoked potential in sled impact acceleration: methodologic and neurosurgical considerations. Impact Injury of the Head and Spine. Thomas, Springfield, Illinois. (in press)
21. Walsh, P.R.; Larson, S.J.; Sances, A., Jr.; Ewing, C.L.; Thomas, D.J.; Weiss, M.S.; Berger, M.D.; Myklebust, and Cusick, J.F.: Experimental methods for evaluating spinal cord injury during impact acceleration. Electrotherapeutic Sleep and Electroanesthesia, Vol. V, F.M. Wageneder and R.H. German, Eds., Universitat Graz, 1978.
22. Ward, A.A., Jr.: The physiology of concussion. Clinical Neurosurg. 12:95-111, 1964.
23. Ward, J.W. and Clark, S.L.: The electroencephalogram in experimental concussion and related conditions. J. Neurophysiol. 11:59-74, 1948.
24. Weiss, M.S. and Berger, M.D.: The effect of impact acceleration on the electrical activity of the brain. GARD Conference Proceedings No. 253: Models and Analogues for the Evaluation of Human Biodynamic Response, Performance and Protection, pp. A20-1 - A20-8, 1979.
25. Williams, D. and Denny-Brown, D.: Cerebral electrical changes in experimental concussion. Brain, 64:223-238, 1941.

# INSTRUMENTATION REQUIREMENTS FOR ASSESSING OCCUPANT RESPONSE TO THREE DIMENSIONAL HIGH ACCELERATION ENVIRONMENTS.

Georg D. Frisch  
Naval Biodynamics Laboratory  
New Orleans, LA 70189

Louis A. D'Aulerio  
Naval Air Development Center  
Warminster, PA 70189

## ABSTRACT

Advances in the development of ejection seats address the need to expand the operational requirements to include safe escape from aircraft at low altitudes and high speed. To meet these needs, performance specifications will have to be reformulated to provide safe egress from adverse attitude aircraft at airspeeds of 0 through 600 knots and altitudes as low as 50 feet above ground. Occupant response to increasingly severe acceleration profiles must be addressed early in the development cycle so that seat performance criteria can be effectively defined and delimited to prevent or minimize the possibility of inertial injury. Physiological tolerance assessment has been severely limited by inadequate and incomplete test data to quantify seat performance (in terms of accelerations). Consequently occupant response to acceleration has traditionally been estimated from analysis of anthropomorphic dummy results. Dummy response, however, is highly variable and difficult to correlate to existing human or cadaver tolerance data. Only with an accurate definition of the complete seat-time history (three dimensional) and its variation to changes in environmental factors (airspeed, attitude, occupant restraint, etc.) can an effective tolerance assessment be made. Such minimum instrumentation requirements must be met in all ejection or crash testing if three dimensional seat-time histories are to be evaluated. This paper addresses instrumentation standardization for ejection and crash testing and demonstrates the effectiveness of the proposed methodology in assessing a series of fully instrumented ejections ranging from 0 to 600 KEAS. The effects on seat performance attributable to canopy jettisoning or penetration, rocket ignition, and windblast will be analyzed.

## INTRODUCTION

The behavior of the human body when subjected to high acceleration environments, such as those encountered during ejection from high speed aircraft, has been a topic of intensive interest and investigation dating back to WWI. The development of the ballistically fired ejection seat to cope with the problems of aircrew escape at high speed dramatically increased the safe ejection envelope but also introduced spinal injuries that have plagued us, unabated, ever since. With ever increasing aircraft performance, both the modality and frequency of these injuries is changing and one is rapidly approaching flight conditions for which current escape systems are not designed. This increasing hazard has been expanded to include windblast injuries as well as those associated with unstable ejections due to adverse aircraft attitude and ineffective restraint which allows excessive seat-man interaction.

Evaluation of these systems, in terms of performance and physiological acceptability, is based on track tests employing instrumented dummies, where the monitored inertial data is then used to evaluate tolerance and system performance. To be effective, the data base generated in such tests must be correlated to experimental human test data, if it exists, or to other ejection systems for which some human response is known from accident statistics. The problem with accident statistics is that the reconstruction of the ejection conditions is usually incomplete and ill defined and that the data base is limited, precluding robust statistical analyses to be made.

Attempts to quantify the dynamic response of the human body and the associated injury potential of high acceleration environments has been limited due to the experimental protocols that can be initiated. Human volunteer tests, through necessity, impose limitations on the acceleration levels investigated. Furthermore, seating and restraint systems are optimized to preclude the remotest possibility of injury. Consequently, the best one can hope for is that with precise control over acceleration input, occupant initial position, restraint configuration, and employing sophisticated three-dimensional instrumentation to monitor inertial response of clearly defined anatomical segments, a consistent and quantifiable human response mechanism can be described. Injury potential can then be investigated in terms of the isolated characteristic response.

Another avenue of investigation has centered around the use of cadavers and live nonhuman primates. Although this affords the possibility of approaching the acceleration environment of interest, the significant differences in the response of live humans and cadavers and the questionable validity of predicting human response based on that of human analogues, has not resolved the problem.

Since experimental approaches are limited, mathematical modeling of ejection seat performance and human biodynamic response to high acceleration continues to be an attractive research tool and has been used with varying degrees of success in analyzing the problems associated with the aircraft escape environment (1,2). The effect of overall escape system performance and occupant response with varying anthropometry, restraint configurations, air speed, and aircraft attitude, can be investigated and sensitivity analyses performed to isolate problem areas. Human and human analogue experiments play an extremely important role since they provide the only physical data with which the predicted responses of the analytical models can be compared to establish validity.

Central to any tolerance assessment or validation effort is the quantity and calibre of the experimental data available. Lack of standardization has made relative comparisons between results from different laboratories or test programs virtually impossible. Information regarding instrumentation location, orientation, and pre or post processing of the sensor data is often incomplete or not defined. Furthermore, the amount of instrumentation employed in many experimental protocols is insufficient to reconstruct the three-dimensional time history of occupant response to a given acceleration input. Validation efforts, based on such incomplete or ill defined data, can lead to serious biases, and subsequent computer analyses can further cloud an already confusing issue.

## EJECTION INSTRUMENTATION REQUIREMENTS

In simulating ejections, occupant response to the seat acceleration is affected by a variety of factors, each of which influences the complexity of the instrumentation required and the scope of the analysis to be conducted. In the case of ditching, for instance, the acceleration-time history of the seat and aircraft (driving function) is unaffected by occupant response to that input. Since the mass of the



aircraft is so much larger than that of the crew member, the occupant-seat interaction is not of large enough magnitude to vary the underlying seat deceleration profile. This is also the case during the catapult phase of an ejection. During this time the seat accelerates along a predetermined vector and the acceleration achieved is primarily dependent on ejected weight. Generally, the seat acceleration during these early stages is two-dimensional with no angular components present. At low air speed, the seat acceleration determines occupant response and, given repeatable inputs, this response should also be consistent. Typical results from dummy tower tests are shown in figure 1.

Although the driving function may be two-dimensional, dummy response need not be. Dummy, restraint harness webbing, and cushioning materials, deform and pitching of the dummy in the seat is usually observed. Consequently, the information presented in figure 1 is insufficient to fully assess the dummy response to the well defined driving function. It should be noted that experimentally derived human tolerance to +Gz acceleration is defined in terms of the driving function. Therefore, the commonly accepted human injury threshold of 25G (under ideal seating and restraint) relates to the seat monitored accelerations. Interpretation of track results to determine physiological acceptability should be based on seat data and not on the levels monitored on the dummy, whose response can be altered by changing seat cushioning properties, restraint configurations, and initial position (3,4).

In cases such as through the canopy ejections, seat-acrylic engagement alters the seat driving function and the seat-time history tends to become more erratic. Additionally, possible secondary dummy-aircraft interactions (loading of the head by the canopy acrylic) can also affect the driving function (figure 2). In such cases there is a feed-back mechanism by which occupant response can affect the seat-time history. Now, the driving function need no longer be directly correlated to injury since a secondary occupant loading path has been introduced. Assessing tolerance levels and injury mechanisms in such situations is extremely complex and can no longer be solely based on monitored seat data. When the seat is off the rails, we have a completely closed loop system until rocket burnout (figure 3). Here, occupant motion within the seating and restraint system can significantly alter the seat trajectory achieved, which in turn is the driving function of the seat-man system. Center of Gravity (C.G.) shifts away from the rocket thrust line, excessive slump due to ill fitting or loose restraint, and flailing induced by aerodynamic forces, all tend to increase seat-man interaction and set the stage for instability in the ejection. This differentiation between driving function and response is clearly demonstrated in the following two series of ejection tower tests recently conducted with fully instrumented dummies.

**CATAPULT PHASE** Monitored dummy chest Gz response to six simulated ejections is shown in figure 4. One would have to agree that results are extremely reproducible and demonstrate that given commensurate inputs (seat driving function), dummy response should be consistent. This consistency appears to be further verified when considering monitored dummy head response shown in figure 5. These assumptions are contradicted when one considers figure 6, where monitored dummy chest Gx accelerations clearly fall into two distinct groups. If the dummy restraint system was changed between series 1 and series 2, then one would have to reach the conclusion that series 2 provided the better restraint, minimizing the Gx accelerations. Slight pitching of the dummy within the seat need not be clearly discernable in monitored dummy chest Gz accelerations. Further assumptions can be made when interpreting figure 7. Here, dramatic differences in monitored head Gz accelerations are evident throughout the entire course of the runs. One could propose the argument that since dummy pitching varied between series 1 and 2, the acceleration-time histories of the neck pivot were altered and consequently the head was being driven differently, although consistently, in the two series under consideration. The looser restraint allowed the head to build up greater momentum, resulting in a more

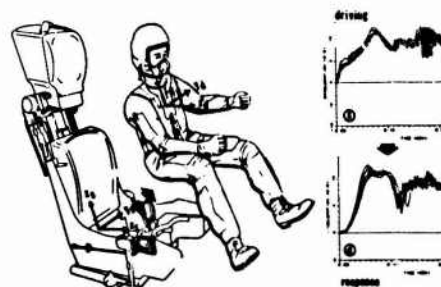


Figure 1. Catapult phase of ejection. Note that occupant response does not affect the seat acceleration (driving function).

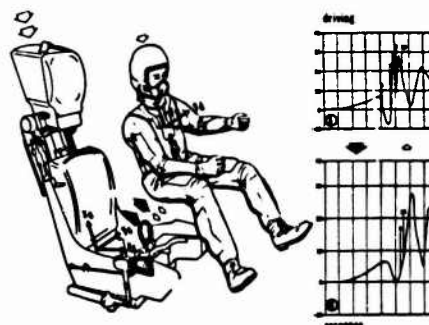


Figure 2. Catapult phase with canopy penetration. Secondary loading of the dummy alters driving-response relationship.



Figure 3. Rocket phase of ejection. Note the closed loop system where occupant response influences seat trajectory.

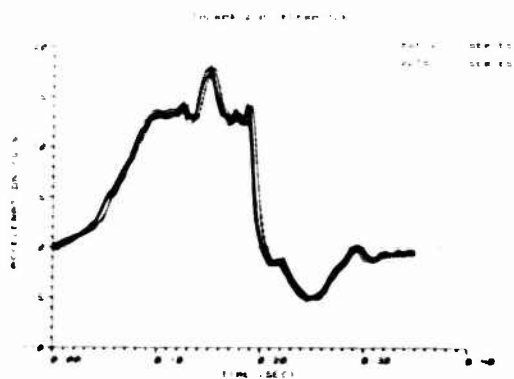


Figure 4. Monitored dummy chest "Gz" response.



severe head-chest interaction (approximately 0.14 sec.), rebound, and secondary impact with the head box (approximately 0.29 sec.). Since the data from the two series of runs was internally consistent and the seat acceleration-time history well known, such results are ideal for mathematical modeling validation. One would vary restraint properties to try to replicate the monitored accelerations. Given enough effort, this curve fitting could be accomplished. The problem, however, is that the results obtained would be completely wrong. The fact of the matter is that all of the previous data came from the same tests, the variability of which is demonstrated in figure 5.

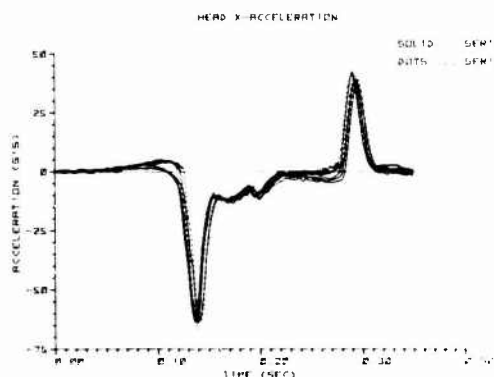


Figure 5. Monitored dummy head "Gx" response.

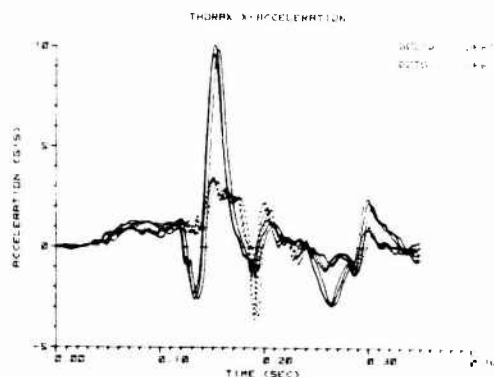


Figure 6. Monitored dummy chest "Gx" response.

The six acceleration profiles, grouped into series 1 and 2, are actually data traces from three tests, employing redundant instrumentation in the dummy's chest and head. The major differences noted are due to instrumentation location. Installation of the sensors is shown in figure 8. Data from the respective head and chest instrumentation clusters (two each) were separately plotted as series 1 and series 2. Chest accelerometers were aligned and mounted on the bottom and top of the dummy chest cavity, while the head accelerometers were mounted on a bracket attached to the head. From the previous example it becomes clear that since dummy response is a complex function of cushioning and restraint properties, the location of the instrumentation must be known to make a relative comparison between tests possible. Indeed, if series 1 and series 2 were data from two different test programs, then, not knowing where the data was monitored, one would interpret these results differently. We see that for the tests considered, the variability in results due to instrumentation location is much greater than that between different tests, given the same instrumentation location.

These between location differences are related to the angular motion of the dummy segments. For the case of the dummy chest accelerations, cluster 2 was closer to the pelvic area of the dummy than was cluster 1. Since the dummy pivoted about the lap belt, the chest excursion at cluster 2 was smaller than at cluster 1 and consequently the linear acceleration due to the angular motion was smaller, as seen in figure 7. Likewise for the head, cluster 1 was closer to the neck pivot point than cluster 2, resulting in lower acceleration values prior to the head contact with the chest (figure 6). When the head bottomed out on the chest, the torque on the head instrumentation bracket forced cluster 1 toward the pivot point (+Gz) and cluster 2 away (-Gz).

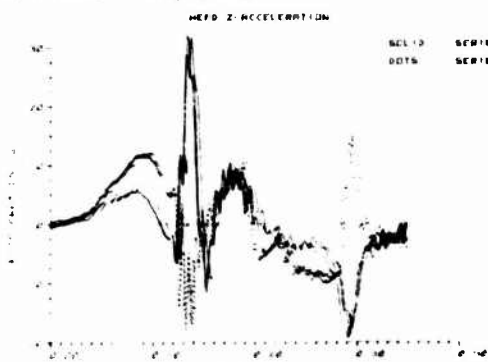


Figure 7. Monitored dummy head "Gz" response.

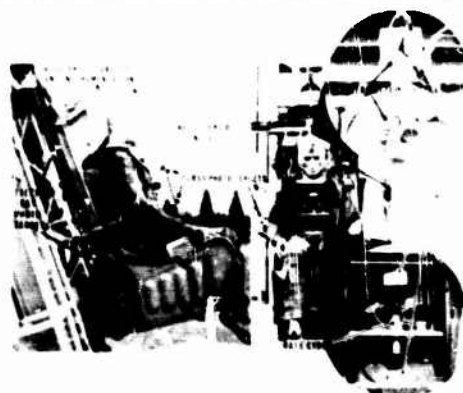


Figure 8. Fully instrumented tower test.

Before comparing data from various test programs or different laboratories, all the instrumentation employed must be related on a well defined coordinate system and hope that both linear and angular acceleration components were monitored. Having both linear and angular information, one can translate the monitored accelerations to other points relative to a rigid body coordinate system. Once translated to a common point, effective comparisons can be undertaken and characteristic responses theorized.

**ROCKET PHASE** As has been noted, once three-dimensional acceleration-time histories are anticipated, both linear and angular rate information must be known to effectively analyze seat-man interaction and ejection performance. Traditionally, ejection system tests have not employed full seat instrumentation but have relied on monitored dummy data to estimate seat performance. The problem with this approach is two-fold. First, human tolerance assessment should be based on seat data up to seat-man separation. Secondly, since seat-dummy interaction affects seat performance, this compliance cannot be quantified unless the seat-time history can be contrasted to that of the dummy. So, in addition to the problem of instrumentation location previously discussed, here we often have insufficient data gathered to make even imprecise comparisons possible. The problems associated with using dummy data as estimates of seat performance can be illustrated in the following example.

The concept feasibility demonstration of the Maximum Performance Ejection Seat (MPES) initiated an ejection from a cockpit section suspended 100 feet above ground level with the cockpit oriented to a 175 degree roll attitude, with 0 degrees being specified as straight and level. Since the dummy's joints were significantly tightened, as was the restraint system, the accelerations monitored on the seat were as close to those on the dummy as can be expected and this example can be considered a best case situation.

As is usually the case with the dummy, in this test the seat was also fully instrumented with both redundant linear accelerometers and angular rate sensors (figure 9). Consequently, both the dummy and seat three-dimensional acceleration profile was known. As can be seen in figure 10, the dummy was well restrained in pitch, with the respective seat mounted and dummy mounted angular rate sensors in close agreement. Roll and yaw rates, however, do show discrepancies, with the yaw differences being more pronounced (figures 11, 12). In determining the seat acceleration-time history at the seat-man C.G. (figure 9), the monitored seat linear accelerations were translated to this remote location using first the seat and then dummy angular rate information. The calculated seat Gx acceleration, expressed in the inertial reference system, is shown in figure 13. As anticipated, the estimate of seat performance, using the seat mounted gyro information, differs considerably from that where the dummy gyro was used. Similar results are evident in the calculated Gy and Gz accelerations (figures 14, 15). The bias introduced by using dummy angular rate information to estimate seat performance is unacceptably high, especially if the data is to be integrated to obtain estimates of seat velocity or displacement. To illustrate the accuracy of results using seat data, the calculated seat displacement-time history was compared to the Bowen trajectory data. Results are shown in figures 16 and 17. Considering that the seat sensor data had to be doubly integrated over two seconds, the results are in excellent agreement.

#### COMPARATIVE ANALYSIS

A major problem in interpreting ejection data is that both dummy and seat acceleration-time histories are effected by a host of parameters such as windblast, extremity flail, and C.G. shift, which are difficult to estimate and can dramatically influence the trajectories achieved. Even at low airspeed, seat angular velocity can effect the linear accelerations monitored. This has made comparisons between tests and different seat types extremely difficult in that instrumentation locations for the various seats tend to differ due to hardware geometry and available instrumentation mounting locations. Although the arrangement shown in figure 9 is sufficient to define the seat-time history, one still has to decide to what location this information should be standardized. Under dynamic yaw, pitch, and roll conditions, the recorded linear accelerations at point "b" will differ from that at point "c". Consequently, when comparing two seats, information must be translated to a common point so that comparisons can be undertaken. The establishment of a seat coordinate system is consequently crucial.

Using the seat-man C.G. (as per figure 9) as the origin of such a coordinate system produces some inconsistencies. During ejection, the dummy will move within the seat and this combined C.G. location will consequently vary in relation to seat structure. This will also be the case when varying dummy weights are used. Use of a seat-man C.G. coordinate system will in effect allow several coordinate systems to exist for a given seat. Consequently, one would want a system which is independent of the occupant and well defined relative to seat structure. Additionally, such a seat coordinate system should be consistent across seat types and easily identified on a given test fixture.

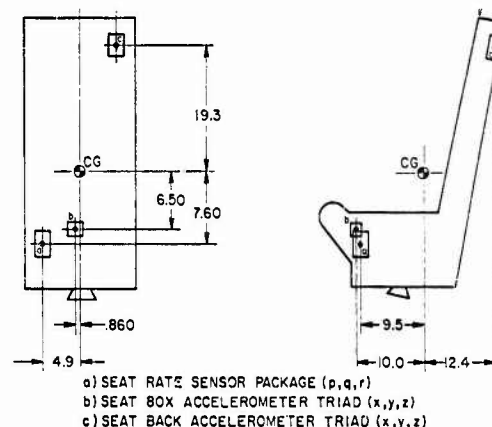


Figure 9. Fully instrumented seat used in MPES test.

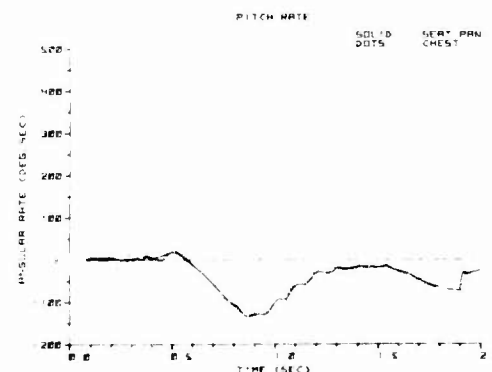


Figure 10. Dummy vs. seat pitch rate.

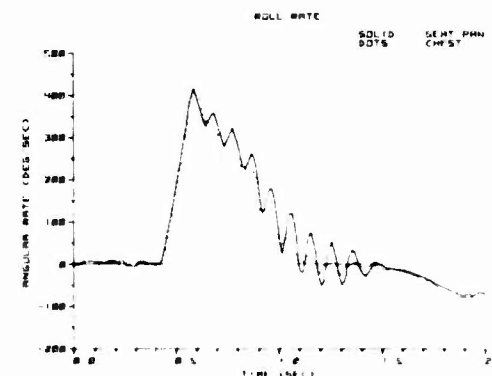


Figure 11. Dummy vs. seat roll rate.

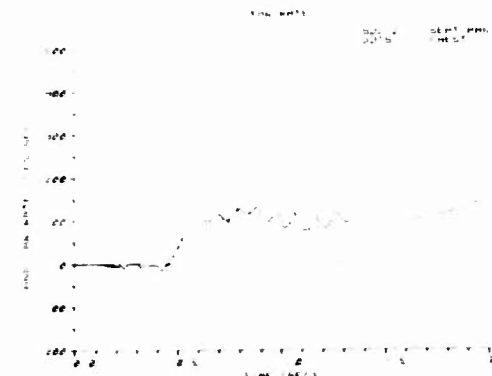


Figure 12. Dummy vs. seat yaw rate.

Such a system is proposed in figure 18. In this coordinate system, the Y-Z plane is coincident with the ejection plane and contains the Seat Reference Point. The X-Z plane bisects the seat and the X-Y plane is orthogonal to the others and also contains the Seat Reference Point. The intersection of these three planes defines a right handed coordinate system that can be located on all seats and is directly related to the hardware. The monitored data (both linear and angular), when localized in this coordinate system, can be extrapolated to the Seat Datum Point (the intersection of the three planes) and results from different tests and seat types can be compared on a common basis. This means that different instrumentation mounting locations used on various seats can be compensated for, as long as the orthogonal sensitive axes of the three angular and three linear rate sensors are aligned with the axes of the seat coordinate system. Dummy motion within this coordinate system can be estimated and seat-man compliance established.

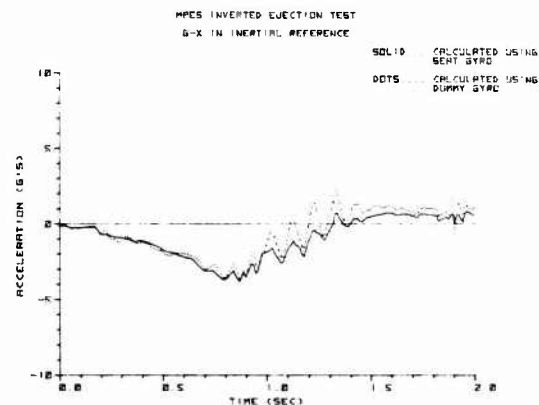


Figure 13. Calculated seat "Gx" acceleration using dummy vs. seat angular rates.

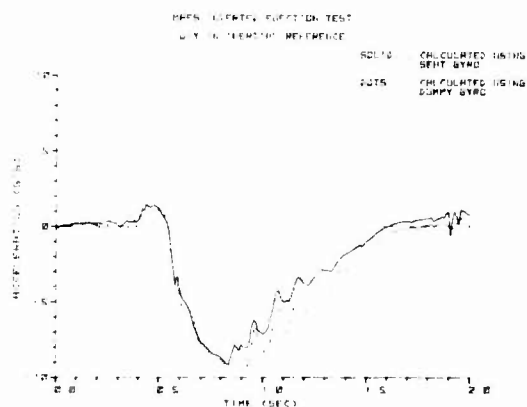


Figure 14. Calculated seat "Gy" acceleration using dummy vs. seat angular rates.

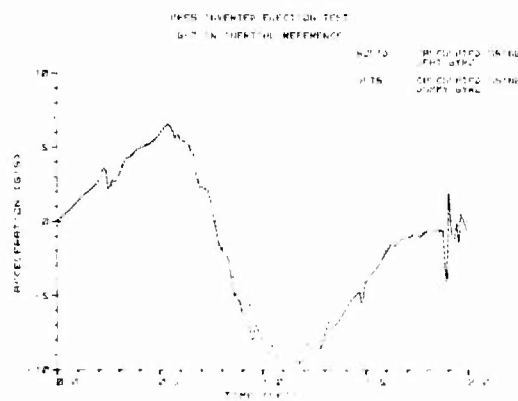


Figure 15. Calculated seat "Gz" acceleration using dummy vs. seat angular rates.

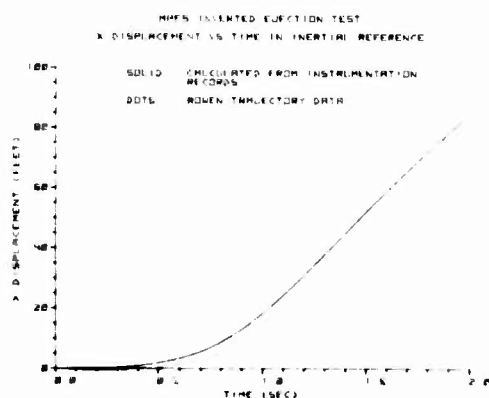


Figure 16. Calculated seat "X" displacement vs. Bowen trajectory data.

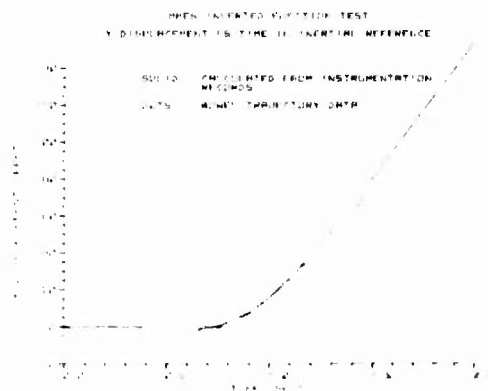


Figure 17. Calculated seat "Y" displacement vs. Bowen trajectory data.

#### APPLICATIONS

In attempting to compare results from different tests, reproducibility of system performance for given test conditions must be established to provide estimates of inherent variability that can be anticipated. If reproducibility can be demonstrated, then monitored acceleration characteristics can be related to specific events and the effects of environmental factors assessed. Figure 19 shows the consistency in results that can be attained. This particular example compares two zero/zero ejection tests (zero altitude, zero airspeed) from an A-7 cockpit, using identical seats and dummies. The seats were fully instrumented, in accordance with the requirements previously outlined. Additionally, redundant orthogonal

linear accelerometers were employed to provide separate estimates of the seat-time history. Seat Z1 vs Z2 (octagon vs triangle) shows the calculated seat-time histories using the two respective accelerometer clusters for a given test. This difference between Z1 and Z2 can be interpreted as error due to location transformation. As can be seen this is negligible for the tests under consideration. Seat Z2 vs Z2 (triangle vs cross) shows the monitored variability between the two tests. The within vs between test variability indicates that, using this instrumentation package, relative differences between tests are real and not artifacts of the instrumentation. Both tests employed canopy penetration and the close agreement in results indicates that the manner in which the seat fractures and passes through the canopy acrylic is repeatable. Analysis of the test films to establish fracturing patterns reinforced this conclusion. The characteristic dip in the monitored seat acceleration, evident at approximately 0.06 seconds, is a direct result of the seat mounted canopy breakers engaging the acrylic, with subsequent seat retardation until the canopy begins to disintegrate. It should also be noted that the large difference in accelerations evident at 0.18 seconds is due to rocket ignition. CPT1 did not activate the rocket after catapult separation.

Test conditions can be changed by altering the ejected weight or ejection air speed. The effects of dummy weight on the trajectory is shown in figures 20 and 21. For each test (zero/zero, 150 KEAS) the monitored aft and front dummy responses were overlaid to corresponding seat first motion. As expected, the front dummies (3%) consistently attained higher G levels than those in the aft location (98%). Within a given test condition, however, both dummy acceleration profiles were consistent with similar frequency response. Given these results, one would appear to be dealing with a stable system, lending itself to comparison and factor analysis. Although one can compare TF-18 SRT1 to TF-18 SRT3 (since the instrumentation mounting locations were the same) these results do not lend themselves to be contrasted against other seat types employing different instrumentation locations. Since no seat angular rate information was monitored in these tests, the data could not be translated to the Seat Datum Point as per figure 18.

TF-18 SRT 1 (150 KEAS) AFT VS FRONT DUMMY ACCELERATIONS.  
DUMMY -2- DATA (CATAPULT JETTISON).

○ AFT DUMMY  
△ FRONT DUMMY

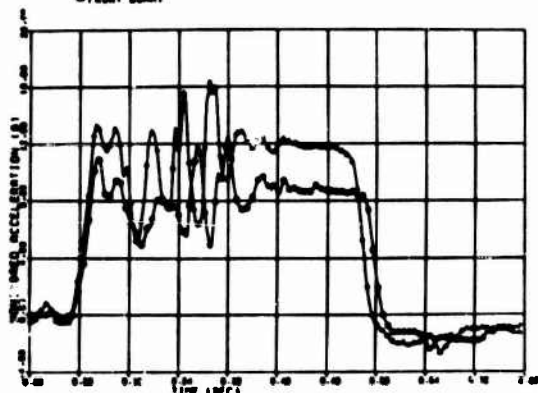


Figure 20. The effect of dummy weight on acceleration. Figure 21. The effect of weight at airspeed.

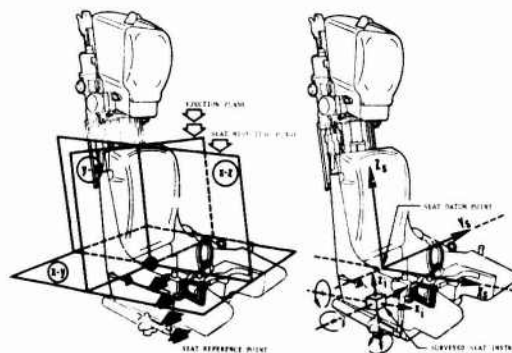


Figure 12. Proposed seat coordinate system.

CPT1 VS CPT1  
100 KEAS CPT1  
○ SEAT -2- A1 ACCEL.  
△ SEAT -2- A2 ACCEL.  
+ SEAT -2- A2 ACCELERATION

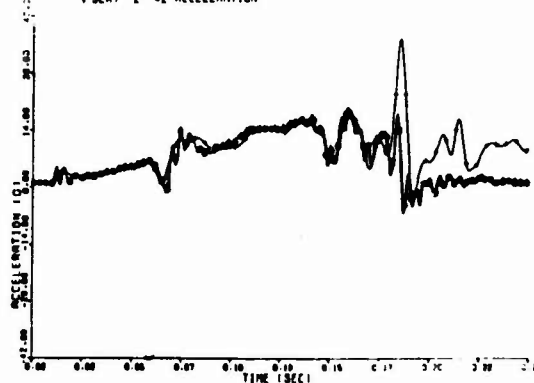
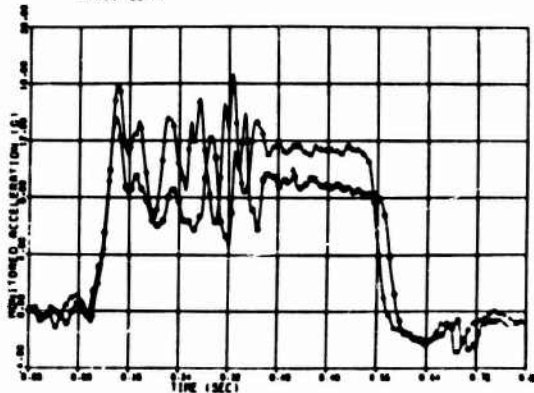


Figure 19. Within vs. between test monitored data variability.

TF-18 SRT 3 (150 KEAS) AFT VS FRONT DUMMY ACCELERATIONS.  
DUMMY -2- DATA (CATAPULT JETTISON)

○ AFT DUMMY  
△ FRONT DUMMY



Attainable reproducibility and stability across varying ejection speeds is further demonstrated in figures 22 and 23. When categorized by dummy weight, results are remarkably consistent. As before, seat-acrylic engagement is clearly evident at approximately 0.06 seconds, resulting in a seat retardation of approximately 4G, followed by an erratic acceleration profile reflecting seat and/or dummy interaction with the remaining unfractured acrylic. Rocket ignition and burn-out can be seen at approximately 0.16 and 0.42 seconds respectively. The large acceleration fluctuations (post 0.6 seconds) seen in SRT1 reflect seat-ran separation and can be discounted in performance analysis, since the dummy is being extracted from the seat by the parachute. This event is delayed in SRT4 due to the higher ejection airspeed. The corresponding dummy responses are shown in figure 23, with the same acceleration characteristics evident. Seat/dummy-canopy acrylic interaction is clearly evident and the acceleration attributable to rocket

ignition has been amplified by approximately 8Gs. From these examples it is evident that the respective ejections are stable, repeatable, and characteristic of this system.

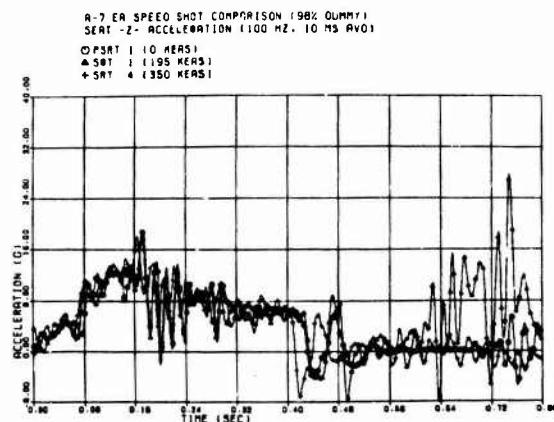


Figure 22. Reproducibility of seat performance across varying ejection air speeds.

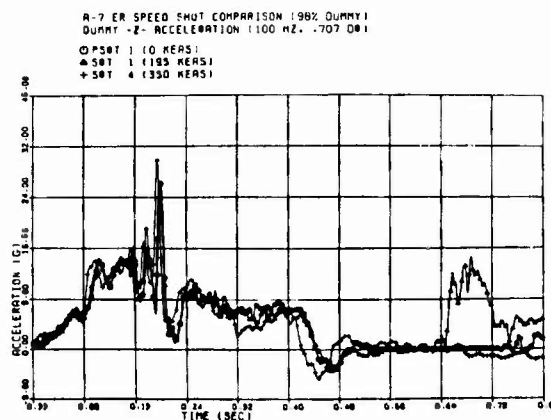


Figure 23. Reproducibility of dummy results across varying ejection air speeds.

The effect of airspeed on system performance and dummy response is directly reflected in the monitored dummy Gx accelerations seen in figure 24. As before, ejections were categorized by dummy weight (3%) and ejection air speeds ranged from 0 to 600 KEAS. The seats were stable and the differences in monitored accelerations can be attributed to windblast and drag. It should be noted that acceleration differences prior to catapult separation (approximately 0.16 seconds) reflect the dummy-seat interaction, since the dummy is not totally free to respond but is pushed into the seat back which is still attached to the aircraft. Only after catapult separation is the seat-man system unrestrained in responding to the wind forces. Two points are noteworthy. First, the increasing (with airspeed) monitored -Gx acceleration prior to catapult separation does indicate that the dummy is pushed into the seat with increasing severity. Secondly, at high speed, the maximum force exerted on the seat-man system occurs well into the rocket phase, indicating that the wind force is not a monotonically decreasing function but that turbulence does significantly affect wind force-time history. The largest acceleration difference between the 0 and 600 KEAS cases occurs at approximately 0.275 seconds. This change of approximately 42Gs can be used to estimate the wind force exerted on the seat-man system. The surface area of the seat-man combination was estimated to be approximately 8 sq. ft. and the ejection weight was 337 lbs. From these values the wind force was estimated to be 1800 PSI (peak). Although somewhat high, this estimate is a reasonable approximation of the dynamic pressure anticipated at this airspeed (1500 PSI), taking into account the compressibility effects of air (5).

Having shown that results for a given ejection system in a particular aircraft configuration are consistent and quantifiable, it is of interest to compare performance across aircraft types, where ejection angles and seat geometries vary. A comparison between test ejections from A-7 and AV-8B aircraft is shown in figure 25. As was the case for the previously discussed A-7 results, the AV-8B tests were fully instrumented, with the three-dimensional acceleration histories of both the seat and the dummy known. The seat data were analyzed in terms of figure 18 to make comparisons on a common basis possible. AV-8B data acquisition varied somewhat in that the telemetry data was pre-filtered to 100 Hz, whereas A-7 results employed a post-test data filtering algorithm to reduce the raw data to comparable values (100 Hz, 0.707 damping ratio). Although the seat geometries and ejection angles vary between the AV-8B and A-7, the propulsion and stabilization systems in the respective seats are identical and both systems employed canopy penetration as the ejection mode. From figure 25, it becomes obvious that seat performance in the respective aircraft was virtually indistinguishable, with seat retardation due to canopy-acrylic interaction clearly evident in both cases (approximately 0.06 seconds). Considering that the respective canopy configurations and compositions (cast vs stretched acrylic) were different, the consistency in results is remarkable.

Subsequent to the first two AV-8B zero/zero tests, the ejection modality was changed from canopy penetration (where only the seat is designed to fracture the canopy acrylic) to canopy fracturing (where detonating chord fragments the acrylic prior to seat penetration). The comparative results are shown in figure 26. It will be noted that the characteristic seat acceleration decay (approximately 0.06 seconds) associated with the penetration tests is conspicuously absent in the fracturing test. The corresponding monitored dummy data is shown in figure 27. Comparison between canopy penetration and fracturing indicates significant improvement to the seat acceleration profile for the latter case. The seat driving function is comparable to canopy jettisoning, where the catapult phase can be characterized by a monotonically increasing function (see figures 20 and 21). This is reflected in monitored dummy response data (figure 27) which is devoid of the acceleration fluctuations typical of the canopy penetration cases. This smooth

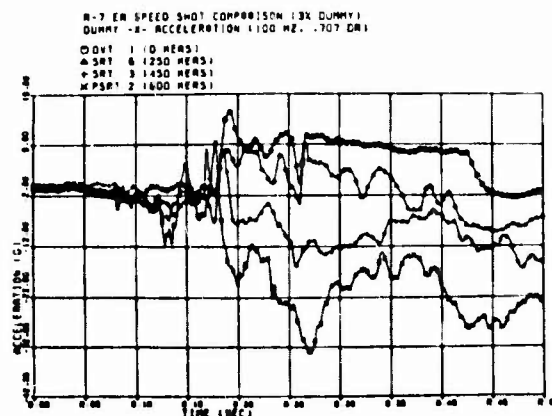


Figure 24. The affect of windblast on dummy "Gx" response.

seat acceleration maintains good seat-occupant coupling and improves spinal loading which can result in increased tolerance and consequently reduced probability of injury during the catapult phase. Additionally, possible secondary loading of the occupant through the head and neck system, due to direct contact with the canopy acrylic, has been virtually eliminated.

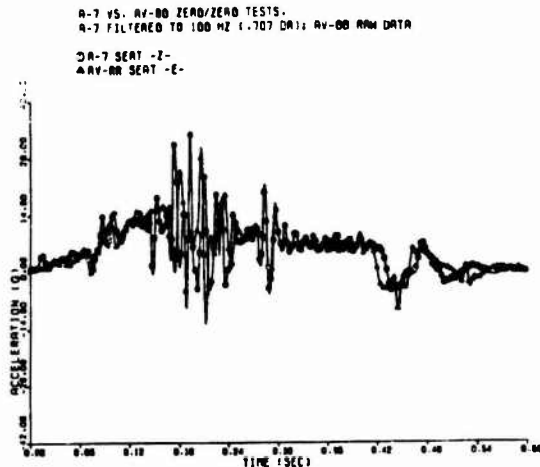


Figure 25. Reproducibility of seat performance across varying aircraft types.

#### CONCLUSIONS

In order to apply available human tolerance information in assessing physiological acceptability of ejection seat performance, both the seat and dummy three-dimensional acceleration-time histories have to be known. This information is required to quantify seat-man interaction and its effect on the seat trajectory. Furthermore, in order to effectively compare results from different test programs involving a variety of seats, the monitored data must be translated to a common point so that the effects of angular rates on linear accelerations can be factored out. This requirement defines the minimum instrumentation that must be employed. Both the linear and angular rates about an orthogonal right handed coordinate system must be monitored for both the dummy and the seat. The ability to translate monitored sensor data to a common point requires definition of a seat coordinate system that is independent of occupant properties, equally applicable to the variety of geometries employed on the various seats, unambiguous, and easily locatable on test fixtures. Such a coordinate system, presently in use on Navy ejection tests, was described. All seat instrumentation must have the sensor's sensitive axes aligned with, and dimensionally located, on this coordinate system.

Initial position and orientation of the dummy instrumentation in this seat coordinate system is also required to fully assess seat-dummy interactions. Consequently, dummy instrumentation must be surveyed onto well defined landmarks so that various test results can be compared on a common basis. As was illustrated, specifying instrumentation location solely by "head" or "chest" does not suffice and can lead to serious biases in data interpretation.

The acquisition and analysis of complete and unambiguous test information is also of primary importance in mathematical modeling, since it constitutes the data base used for validation. Once properly validated, mathematical simulation can be effective in analyzing and expanding the available data and to isolate crucial parameters affecting seat performance. Results from such analyses should be used to aid in the formulation or expansion of experimental designs and isolate parameters that should be monitored.

#### REFERENCES

1. G. D. Frisch, "Simulation of Occupant-Crew Station Interaction During Impact." Chapter 111 (Human Analogues), IMPACT INJURY OF THE HEAD AND SPINE, Charles C. Thomas, Publisher; Springfield, Illinois; 1982.
2. G. D. Frisch, L. A. D'Aulerio, "Bioman - An Improved Occupant-Crew Station Compliance Modeling System." Aviation, Space, and Environmental Medicine, 51(2 -167, 1980.
3. S. Ruff, "German Aviation Medicine in World War II." Prepared Under the Auspices of the Surgeon General, U.S. Air Force, U.S. Government Printing Office. Vol. 1, 1950.

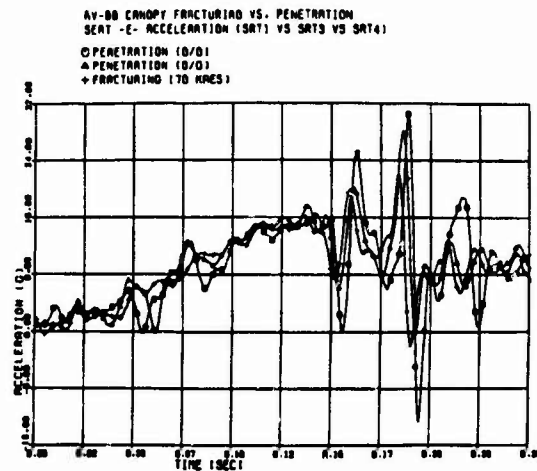


Figure 26. The improvement in seat performance when pre-ejection canopy fracturing is introduced.

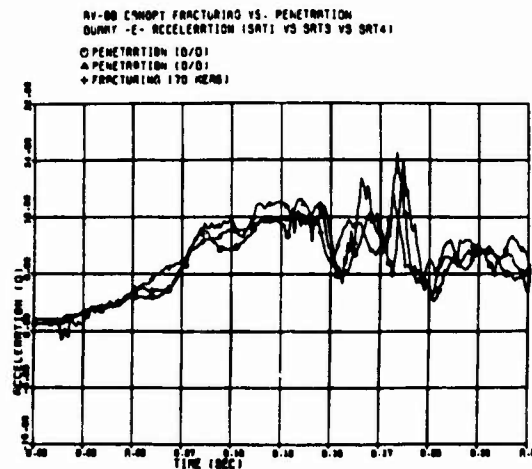


Figure 27. Monitored dummy response in canopy fracturing vs. penetration cases.

4. D. T. Watts, E. S. Mendelson, H. N. Hunter, A. T. Kornfield, and J. R. Poppen, "Tolerance to Vertical Acceleration Required for Seat Ejection." Aviation Medicine, pp 554-564, December 1947.

5. A. M. Koethe, J. D. Schetzer, "Foundation of Aerodynamics." John Wiley and Sons, Inc., New York, 1950.



## DISCUSSION

## UNIDENTIFIED QUESTIONER

Did you survey qualities of various elements as a separate procedure or as a comprehensive total calibration of the complex system as you are using, in which you tried to estimate all the various correlated parameters at once?

## DR. THOMAS (USA) COMMENT

The ejection seat instrumentation is totally different, in terms of the controls, from the experimental instrumentation used in the laboratory. There are major differences. He has discussed the instrumentation for ejection seat testing.

## (UNKNOWN QUESTIONER)

That's the reason I posed the question.

## DR. THOMAS (USA) COMMENT

Is that a sufficient answer?

## AUTHOR'S REPLY

This is one of the reasons we used redundant instrumentation. We filter all the data at 200 hz with a damping ratio of 0.7, because frequencies above 200 hz are not likely to pass into the dummy. The seats are instrumented redundantly to insure an adequate tolerance assessment. Thus, to insure that we were not eliminating any data, we put in the redundant instrumentation with one set filtered at 200 hz, and the other set not filtered, so that we could say that there was no relevant information at 200 hz. We cross-checked the agreement between the filtered and unfiltered and determined the estimate of error involved. I cross plotted them looking at the general differences (within test) versus (between test) difference; the within-test differences were rather small as compared to the between-test differences. I agree that if you want to differentiate or integrate, obviously, you have to do a much better job.

## DR. THOMAS (USA) COMMENT

In the laboratory, working with human subjects, we have a redundant system between the photographic and the sensor measures. You cannot, in practice, achieve this under range test conditions because of the tremendous instabilities in the carriage and difficulty with photographic instrumentation. Some of these tests go as high as 600 knots with tremendous system vibrations; and it's hard to get cameras to adequately function, let alone obtain really good photographic calibration. In summary, our photographic calibration on the range is not nearly as good as the quality we obtain in laboratory tests. I think that may elaborate on your question.



# EVOKED POTENTIAL STUDIES OF CENTRAL NERVOUS SYSTEM INJURY DUE TO IMPACT ACCELERATION\*

B. Saltzberg<sup>1</sup>, W.D. Burton Jr.<sup>1</sup>, N.R. Burch<sup>1</sup>, C.L. Ewing<sup>2</sup>,  
D.J. Thomas<sup>2</sup>, M.S. Weiss<sup>2</sup>, M.D. Berger<sup>2</sup>, A. Sances Jr.<sup>2</sup>,  
P.R. Walsh<sup>3</sup>, J. Myklebust<sup>3</sup>, S.J. Larson<sup>3</sup>, E. Jessop<sup>2</sup>

This paper reports on one aspect of a comprehensive program designed to investigate the effects of various levels of impact acceleration on the functional integrity of the nervous system. The results described are based on the measurement of afferent neural transmission in the Rhesus monkey as revealed by latency and amplitude changes in the evoked potential (EP). In order to track the time course of recovery of latency and amplitude with high time resolution, automated methods for detecting peak amplitude and latency of components of the evoked potential were developed. These methods were applied to EP data recorded during impact experiments on Rhesus monkeys.

## PREFACE

Because of the growing concern for the human and economic cost of vehicular accidents, studies to systematically evaluate the physiological effects of impact acceleration on the head and body are becoming increasingly urgent. Most research in this problem area has been limited in scope because of the complexity of the physiological measurements and the extensive technological resources required to achieve precise recording and control of the large number of mechanical and biological variables involved. In response to this need, a comprehensive program has been developed at the Naval Biodynamics Laboratory (NBDL) for acquiring the fundamental data needed in the development of improved measures to reduce injuries caused by impact accidents. The NBDL facility is equipped with an integrated battery of scientific instrumentation and computers to collect and correlate anatomical, physiological, neurological, radiological, and mechanical data. This paper presents the initial analysis of an electrophysiological data base which is currently being examined and correlated with other physiological and physical measures by specialists in neurophysiology and neuroanatomy at NBDL. The major objective of this continuing analysis is to interpret and model the results of the experiments at NBDL.

## METHODS

Four Rhesus monkeys were subjected to a total of eight sled impact acceleration runs at NBDL to reproduce the dynamic forces which act on the head, and on the spinal column and cord in a lateral (-Y) collision. Each animal was subjected to a 10-G control impact, followed later the same day by a larger impact. The larger impacts were: 30-G for animal AR-8849, 50-G for animal AR-2152, 70-G for animal AR-8695, and 90-G for animal AR-8816. Analyses of only the 30, 50, 70, and 90-G runs are presented here since the 10-G runs showed no significant post-impact EP changes.

Electrical stimulation was applied to the spinal cord with recording of evoked activity from the Left and Right Sensory-Motor Cortex (CXL and CXR). Surgical procedures for electrode implantation were carried out under barbiturate anesthesia with endotracheal intubation and atropine premedication. Stimulating electrodes were a five-in-line lead parallel array placed over the spinal cord. Recording electrodes were placed over the left and right sensory-motor cortex. Details of the electrode configurations and surgical implantation procedures are described in Reference 1 (P.R. Walsh, et al., "Experimental methods for evaluating spinal cord injury during impact acceleration"). All stimuli were constant current rectangular pulses of 0.2 millisecond duration. Current levels (approximately 1.25 milliamperes) were applied sufficient to obtain good afferent evoked potentials.

Copies of the analog data tapes from the NBDL -Y impact experiments were processed at the Texas Research Institute of Mental Sciences (TRIMS) using Average Evoked Potential (AEP) analysis programs written specifically for this project. The analog data consisted of two channels of EEG data, a stimulus marker channel, and a time-code channel. These data constituted the input to a PDP-11 computer equipped with an AR-11 analog-to-digital converter (10-bit resolution). The time code was used to control the digitizing start and stop times relative to experimental impact. The stimulus marker controlled the start of data acquisition for individual responses. In order to achieve high resolution in

\*This work was supported by the Office of Naval Research contract #N00014-76-C-0911.

<sup>1</sup>Texas Research Institute of Mental Sciences, 1300 Moursund, Houston, Texas, 77030, USA

<sup>2</sup>Naval Biodynamics Laboratory, New Orleans, Louisiana, USA

<sup>3</sup>Medical College of Wisconsin, Milwaukee, Wisconsin, USA

measuring the latency of AEP components, the analog tape was slowed to half its normal speed, and appropriate adjustments were made to playback discriminators and the sampling interval. The final digitized data resolution was 25 microseconds per point (equivalent to 40,000 samples per second).

Starting on the rise of the stimulus mark pulse, 2000 digital samples were used to obtain AEPs of 50 milliseconds duration. Initially, 5 individual responses were averaged to create each AEP. The AEPs were written to digital tape for subsequent processing. Preliminary examination of the AEPs (based on 5 responses) immediately following impact revealed a significantly noisy pattern and, therefore, additional averaging was necessary. However, to achieve good time resolution of temporal changes in amplitude and latency of components of the AEPs, it was necessary to minimize (within the constraints of noise) the number of individual responses used to obtain a smooth AEP. Using AEPs consisting of 50 individual responses met both criteria in that the resulting improvement in signal-to-noise ratio gave a smooth AEP while providing a reasonably good time resolution of 10 seconds.

In order to visualize overall changes in AEP waveshape, compressed AEP plots were produced. These plots show the time course of AEPs over a period of 12 minutes, beginning 2 minutes prior to impact. Compressed AEP plots for the Left and Right Cortical Leads (CXL and CXR) from each of the 4 experiments are shown in Figures 1 through 4.

The feature most common to AEPs from the 4 different animals was a peak which occurred in the latency range from 9 to 13 milliseconds following the stimulus. Except in animal AR-2152, used for the 70-G run, this peak was positive-going, and will be referred to as E10. An AEP component in the latency range 15 to 20 milliseconds (designated E15) was found in all animals except AR-8816, the animal used for the 90-G experiment.

Quantification of changes in the AEPs was done by tracking the amplitude and latency of the E10 and, where possible, the E15 peaks. The mean and standard deviation of the measures were computed from 23 AEPs, starting 4 minutes prior to impact. These were used in comparing pre- and post-impact AEP measures. Changes were defined as significant when the measured value for 2 successive AEPs deviated by more than 1 standard deviation from the pre-impact mean. Recovery time for a measure was defined as the time from impact to the first value within 1 standard deviation of the pre-impact mean.

#### RESULTS

Tables 1 through 4 summarize effects on the amplitude and latency of the E10 and E15 AEP components from the 4 acceleration levels studied. Listed in the tables are:

1. The percent relative deviation of the measure during 4 minutes pre-impact (standard deviation  $\div$  mean  $\times$  100),
2. The maximum change post-impact, expressed as percent of the pre-impact mean, and
3. The recovery time

For those instances where the post-impact changes were not significant, the recovery time is reported as zero.

Table 1 shows the effects of impact on the amplitude of the E10 component. At 30-G, the amplitude is reduced in both the CXR and CXL leads. Following 50-G acceleration, the amplitude is reduced more in the Right Lead (76%) than in the Left Lead (70%). The 70-G impact produced an increase in the amplitude of the E10 peak on the left side, and a decrease on the right side.

The largest and most asymmetric effect on amplitude took place at 90-G acceleration, as shown in Figure 5. The amplitude of the Left Lead E10 component increases slightly for 30 seconds following impact, while the positive-going E10 component is completely obliterated from the Right Lead. This effect lasts for 4 minutes post-impact. Between 4 and 5.9 minutes, the amplitude recovers to nearly its pre-impact value before falling again. The amplitude leaves the recovery band again at 6.8 minutes and reaches a reduced stable value by 10 minutes post-impact. Between 10 and 58 minutes, the amplitude exhibits a very slow recovery trend. The amplitude variability from AEP to AEP is markedly less during this time than during the pre-impact period.

For all 4 acceleration levels, the E10 amplitude recovery time recorded from the Right Lead is considerably longer than for the Left Lead. Recovery in the Left Lead following 50-G impact is slightly longer than it takes at 30-G. The Right Lead at 50-G recovers in about half the time compared to 30-G. At the 70-G acceleration, the Left Lead required 5 minutes to recover, while the Right Lead had not recovered during the 6.5 minutes of post-impact data studied. Only 6.5 minutes for this run were used due to a technical problem which is now being corrected. Two recovery times are listed for the 90-G run, the first (5.8 minutes) represents the initial amplitude rebound; the second (58.6 minutes) is for the long-term effect.

Table 2 is a summary of the latency changes for the E10 component of the AEP. There were no significant changes in latency associated with 30-G impact. At 50-G, the Left Lead component shows a 9.2% reduction in latency, while the Right Lead shows a 2.3% increase. The recovery time shown for the CXR lead of the 70-G run is not a reliable estimate because of the small maximum change relative to the pre-impact variability.

The 90-G acceleration gives rise to the most asymmetric effect. As shown in Figure 6, the latency of the Left Cortical E10 component increases 7.9% following impact, and recovery takes place within 1 minute. The left pathway latency increases and decreases again between 4 and 8 minutes post-impact. This time corresponds to the time when the Right Cortical AEP amplitude is rebounding. After 8 minutes, the latency of the left E10 component reaches a mean value which is about 2% less than its pre-impact value.

By comparison, the Right Cortical E10 component of the AEP reappears at 4 minutes post-impact, and its latency is 12% greater than before impact. Latency recovery takes about 7.2 minutes post-impact, a time which also corresponds with the amplitude rebound of this component. From 7.2 minutes on, the latency appears to stabilize to a slightly smaller value than it had pre-impact. This is probably due to the double hump shape of the E10 component in this experiment (Figure 4). Prior to impact, the second hump was consistently larger and was the one detected as the extremal. Following impact, the first hump is larger and, therefore, was detected as the extremal.

Table 3 summarizes the changes in amplitude of the E15 component of the AEP. The higher variability in the measured amplitudes during pre-impact time makes interpretation of this data more difficult. The 30-G impact had the effect of increasing the amplitude in the CXL lead, but had no effect on the CXR lead. At 50-G and 70-G, the amplitude on both sides was reduced, as was the amplitude of the E15 component in the CXL lead of the 90-G experiment. The E15 component could not be reliably detected in the CXR lead of the 90-G experiment. In all runs, recovery of amplitude occurred within 1.7 minutes post-impact.

Table 4 shows that only in the 90-G run is there any effect on the latency of the E15 component of the AEP. The latency increased by 7%, and recovered in 40 seconds.

#### SUMMARY OF FINDINGS

The most striking changes take place in the E10 component.

The recovery time of the E15 component varies directly with the impact intensity. Latency of the E15 component is only slightly affected by impact intensity.

At all 4 acceleration levels, the E10 amplitude component of the Right Cortical response takes longer to recover than the Left Cortical response.

At 70-G acceleration, there is a long-term effect on the E10 amplitude. This effect did not show up at lower impacts. This may be similar to the long-term effect present at 90-G.

The E10 component was obliterated from the CXR lead for 4 minutes post-impact at 90-G. However, small, earlier components remain clear for a considerable time after impact. These early components have latency and frequency characteristics similar to those recorded in human brainstem evoked response studies. At this G-level, these early components are affected quite differently than the E10 component.

#### CONCLUDING REMARKS

Insofar as lateral impact acceleration is concerned, our initial evaluation of the EP data produced in the NBDL experiments reported here indicates that neural propagation from the spinal cord to the sensory-motor cortex is more severely altered along the right pathway than along the left pathway. It should be emphasized that the analysis presented in this paper has been limited to an examination of only two components of the EP, a component at approximately 10 milliseconds latency and a component at approximately 15 milliseconds latency. There are other less prominent components in the range from 7 to 20 milliseconds which have not been analysed as yet, as well as late components which may have neurophysiological significance with regard to understanding the effects of impact acceleration on the motor nervous system. The early components in particular may offer some interesting insights on how brain stem activity is affected. As stated earlier, the electrophysiological results reported here are being integrated and analysed by NBDL in the context of its overall program of biodynamic measurement.

TABLE 1

## SUMMARY OF CHANGES IN AMPLITUDE OF E10 COMPONENT

<u>RUN</u>	<u>MEASURE</u>	<u>CXL-LEFT LEAD</u>	<u>CXR-RIGHT LEAD</u>
30-G	pre-impact relative amplitude deviation	7.5%	6.6%
	Maximum change	-29.8%	-28.8%
	Recovery time	52 seconds	208 seconds
50-G	pre-impact relative amplitude deviation	15.9%	16.7%
	Maximum change	-69.8%	-75.9%
	Recovery time	69 seconds	100 seconds
70-G	pre-impact relative amplitude deviation	33.8%	23.0%
	Maximum change	55.9%	-52.0%
	Recovery time	300 seconds	390 seconds (Note 1)
90-G	pre-impact relative amplitude deviation	20.2%	15.5%
	Maximum change	29.9%	-100.0% (Note 2)
	Recovery time	30 seconds	356 seconds (5.9 minutes) 3518 seconds (Note 3) (58.6 minutes)

NOTES

1. Data for only 6.5 minutes post-impact was tracked for the 70-G run. Recovery had not taken place by that time.
2. The positive E10 component was completely eliminated for 4 minutes post-impact.
3. After the 90-G impact, the amplitude recovered, then fell to a lower, slowly recovering value (see text).

TABLE 2

## SUMMARY OF CHANGES IN LATENCY OF E10 COMPONENT

<u>RUN</u>	<u>MEASURE</u>	<u>CXL-LEFT LEAD</u>	<u>CXR-RIGHT LEAD</u>
30-G	pre-impact relative latency deviation	1.8%	1.0%
	Maximum change	NS	NS
	Recovery time	0	0
50-G	pre-impact relative latency deviation	2.2%	0.5%
	Maximum change	-9.2%	2.3%
	Recovery time	27 seconds	79 seconds
70-G	pre-impact relative latency deviation	0.5%	2.7%
	Maximum change	2.2%	4.4%
	Recovery time	94 seconds	21 seconds
90-G	pre-impact relative latency deviation	1.9%	1.6%
	Maximum change	7.9%	12.0%
	Recovery time	50 seconds	430 seconds

TABLE 3

## SUMMARY OF CHANGES IN AMPLITUDE OF E15 COMPONENT

<u>RUN</u>	<u>MEASURE</u>	<u>CXL-LEFT LEAD</u>	<u>CXR-RIGHT LEAD</u>
30-G	pre-impact relative amplitude deviation	47.7%	65.7%
	Maximum change	119.5%	NS
	Recovery time	41 seconds	0
50-G	pre-impact relative amplitude deviation	24.6%	54.7%
	Maximum change	-78.7%	-100.0%
	Recovery time	100 seconds	69 seconds
70-G	pre-impact relative amplitude deviation	31.4%	20.4%
	Maximum change	-99.4%	-74.0%
	Recovery time	94 seconds	94 seconds
90-G	pre-impact relative amplitude deviation	30.0%	Note 1
	Maximum change	-69.0%	
	Recovery time	60 seconds	

NOTE

1. The E15 component could not be reliably tracked in the 90-G run.

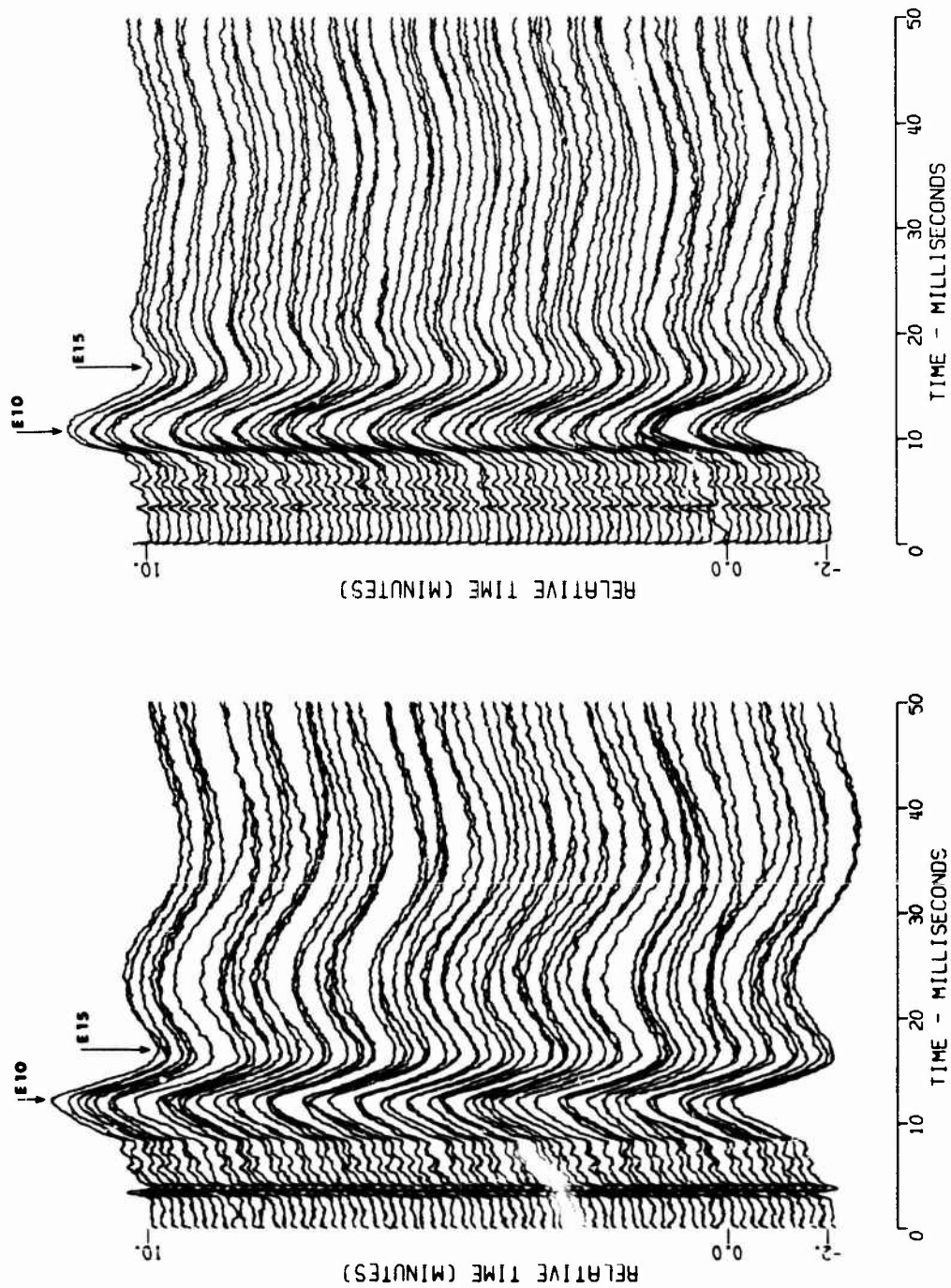
TABLE 4

## SUMMARY OF CHANGES IN LATENCY OF E15 COMPONENT

<u>RUN</u>	<u>MEASURE</u>	<u>CXL-LEFT</u>	<u>CXR-RIGHT LEAD</u>
30-G	pre-impact relative latency deviation	1.8%	2.3%
	Maximum change	NS	NS
	Recovery time	0	0
50-G	pre-impact relative latency deviation	1.7%	1.9%
	Maximum change	NS	NS
	Recovery time	0	0
70-G	pre-impact relative latency deviation	0.7%	0.5%
	Maximum change	NS	NS
	Recovery time	0	0
90-G	pre-impact relative latency deviation	2.9%	Note 1
	Maximum change	7.1%	
	Recovery time	40 seconds	

NOTE

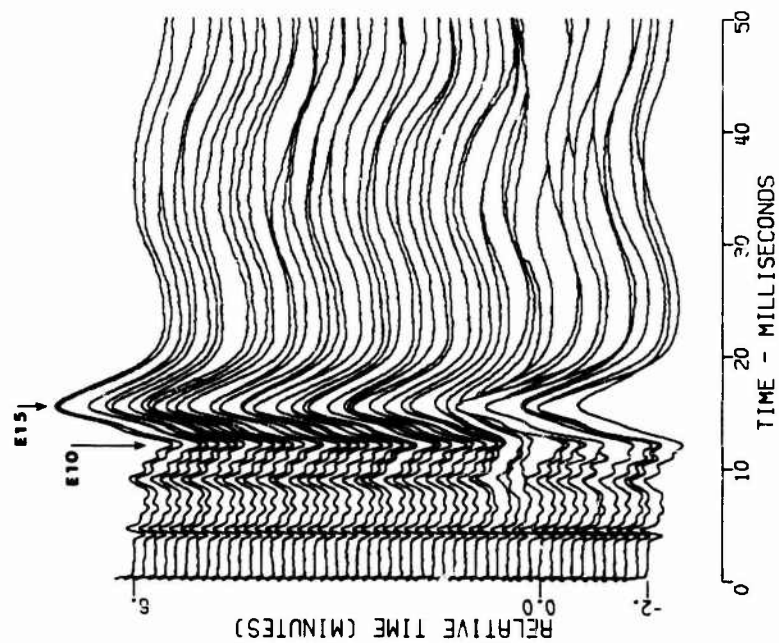
1. The E15 component could not be reliably tracked in the 90-G run.



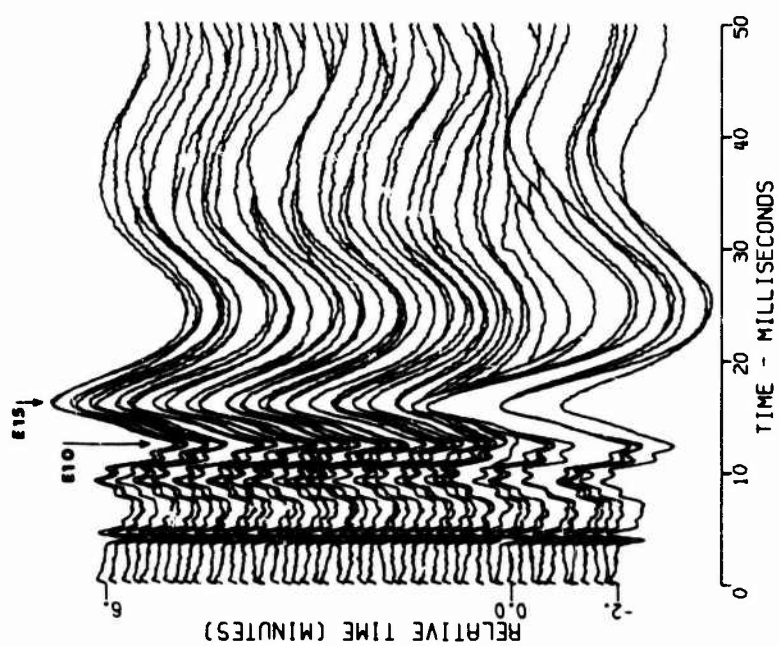
STIMULUS SITE 7, SPINE RECORDING SITE 1, CXR  
LX-3469 30 G - Y 50 RESPONSES AVERAGED

STIMULUS SITE 7, SPINE RECORDING SITE 3, CXL  
LX-3469 30 G - Y 50 RESPONSES AVERAGED

FIGURE 1



STIMULUS SITE 7, SPINE RECORDING SITE 1, CXR  
LX-3471 70 G - Y 50 RESPONSES AVERAGED



STIMULUS SITE 7, SPINE RECORDING SITE 3, CXL  
LX-3471 70 G - Y 50 RESPONSES AVERAGED

FIGURE 2



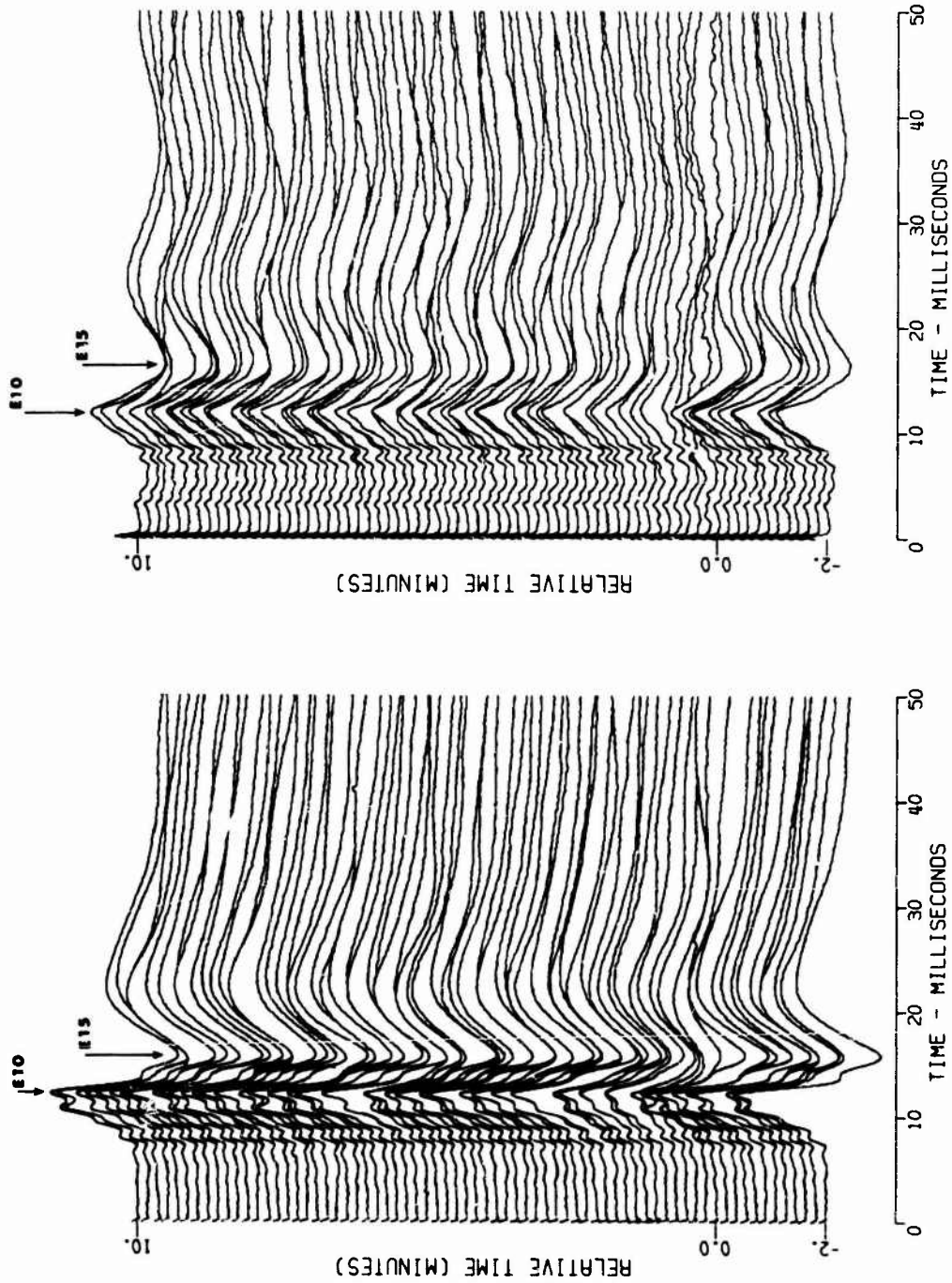


FIGURE 3



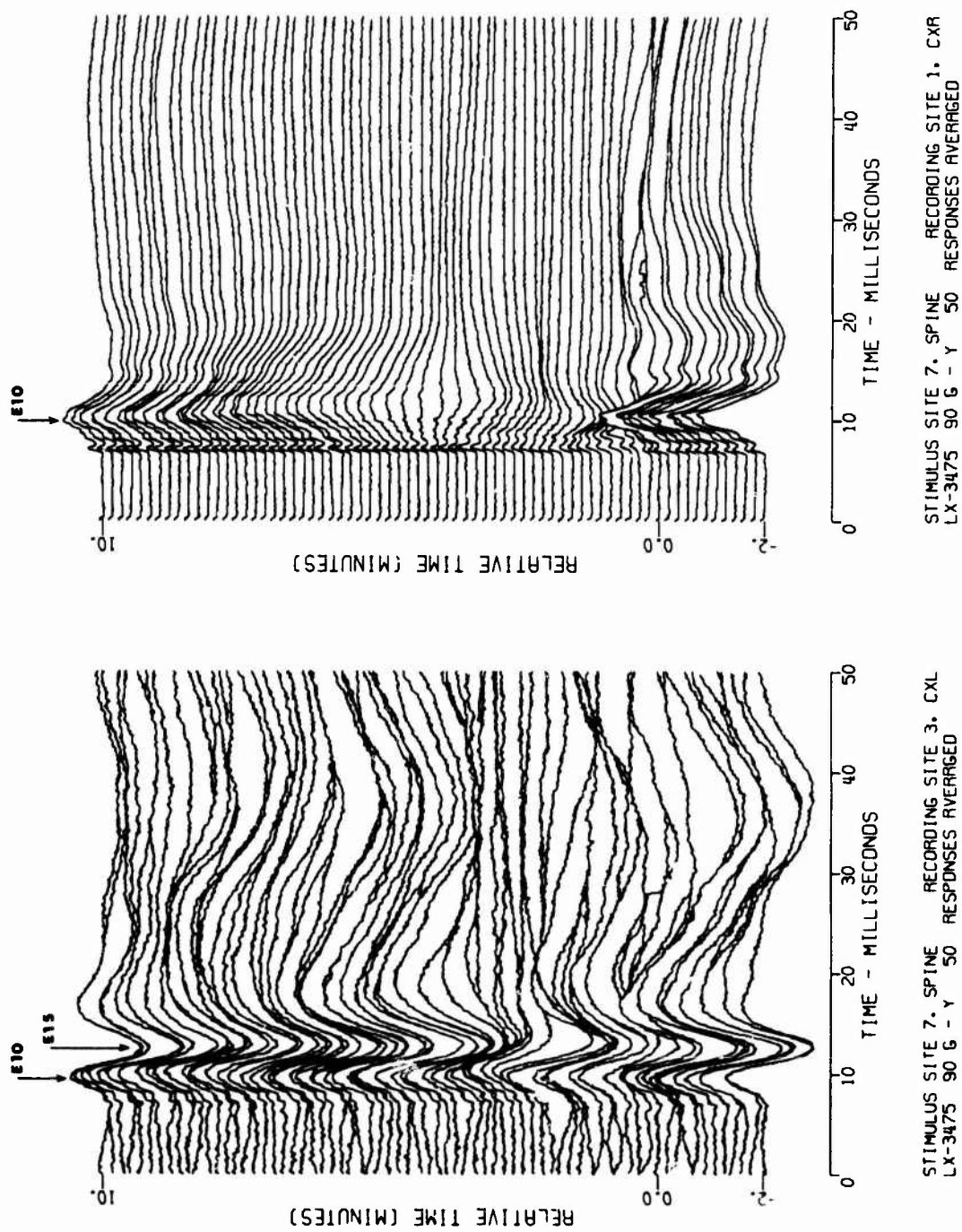


FIGURE 4

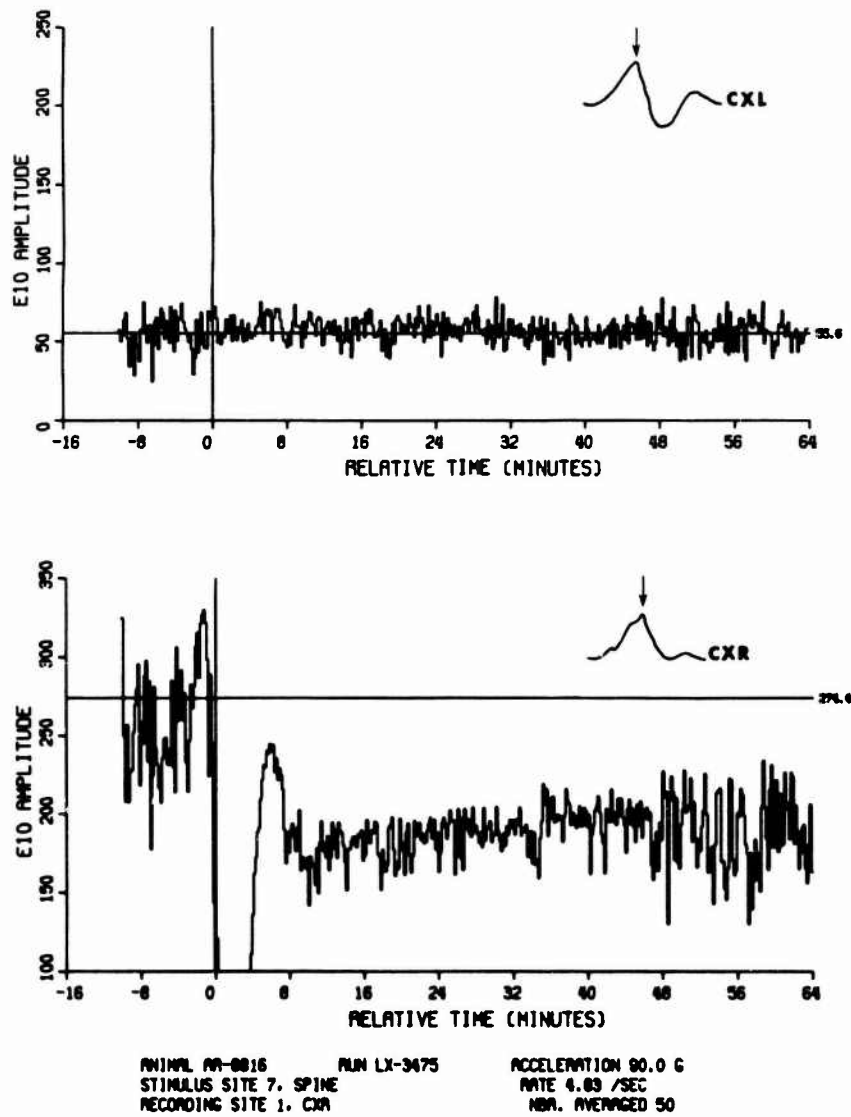
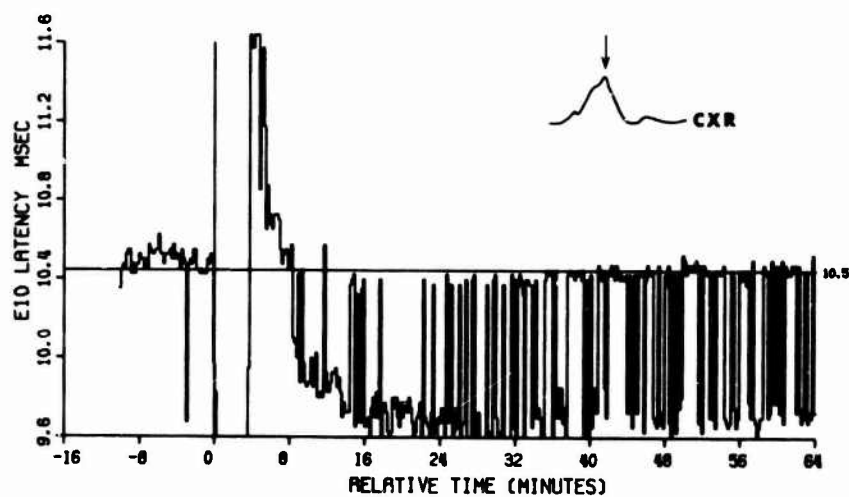
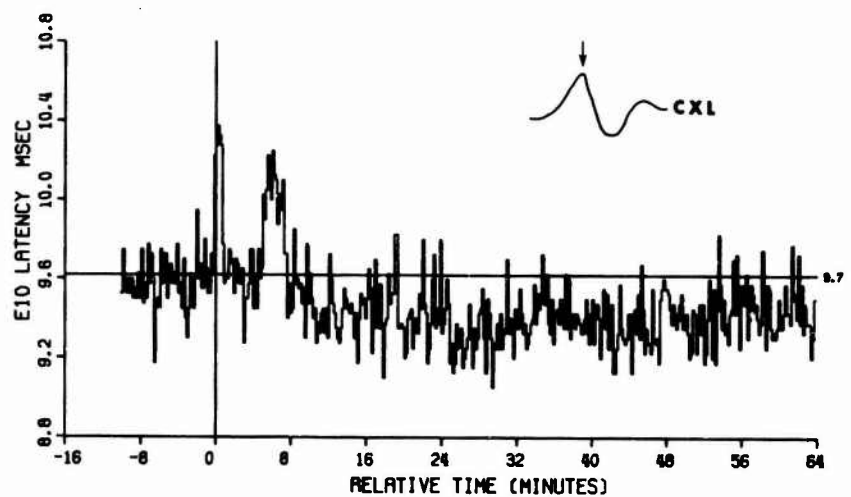


FIGURE 5



ANIMAL RA-8816      RUN LX-3475      ACCELERATION 80.0 G  
STIMULUS SITE 7, SPINE      RATE 4.83 /SEC  
RECORDING SITE 1, CXR      NBR. AVERAGED 50

FIGURE 6

## NEUROPATHOLOGY OF THE RHESUS MONKEY UNDERGOING -Gx IMPACT ACCELERATION

Friedrich Unterharnscheidt, M.D.  
 Naval Biodynamics Laboratory  
 Box 29407  
 New Orleans, Louisiana 70189  
 and  
 Neuroscience, Incorporated  
 3512 Camp Street  
 New Orleans, Louisiana 70115

## SUMMARY

Each vector direction of impact acceleration produces a different and predictable type of injury in regard to quality and distribution.

The specific neuropathological injury pattern in -Gx acceleration transmitted indirectly to the head via the vertebral column consists of tissue damage at the zone of maximum stretch at the atlanto-occipital junction and, if the threshold is reached, incomplete and complete traumatic transection of the spinal cord and rupture of both vertebral arteries and concomitant basilar and spinal subarachnoid and subdural hemorrhages. Furthermore at peak sled acceleration levels low enough that neither incomplete nor complete transections occurred, a local indentation of tissue was seen at the ventral fissure, apparently caused by direct impact of the tip of the odontoid process of the axis. In some instances, subdural hemorrhages over both cerebral hemispheres due to ruptured bridging veins were seen, probably as the result of rotational acceleration. As we have demonstrated before, a neurophysiological and neuropathological continuum from no lesions to severe and lethal ones can be demonstrated, described and quantified. The head-neck and brain-cord systems can be described by input-output relationships. Each effective mechanical input to the head and neck corresponds to a predictable and typical morphological end state.

## INTRODUCTION

Background

Ewing (1964) (1) observed that Naval aircraft crashes might be associated with concussion due to neck stretch, as suggested by the work of Friede, (1960, 1961) (2, 3, 4). In order to further investigate this problem, Ewing obtained Naval Safety Center statistics and analyzed them. These data showed that in the five fiscal years 1959 through 1963, there were 6,974 individuals involved in aircraft accidents involving ejection, bail out, collision with ground or collision with water (which also includes ditchings), of whom 89% were exposed to crash impact accelerations due to collisions with ground or water; while only 11% avoided them by ejection or bail out. Furthermore, 70% of all fatal jet embarked accidents, and 88% of all fatal prop embarked accidents were collisions with water, while only 22% of all jet embarked accidents and only 51% of all prop embarked accidents were collisions with water. The total number of fatalities during this period from collision with water alone was 226.

With the evidence of the severity of the problem in the U.S. Navy, a working paper was prepared by Ewing (1964) (1) which attempted to analyze the cause for the high fatality rate. Ewing stated: "In attempting to determine a reason for the experience quoted above, a study of the literature combined with a study of the aviator's situation during a crash provided the following: (1) the aviator's head and neck are unrestrained, permitting relative motion in a deceleration event between the restrained torso, and the unrestrained head and neck; (2) the crash helmet, worn in all carrier aircraft, has a center of gravity location which shifts the center of gravity of the head-helmet mass superiorly and anteriorly. This would tend to increase the rotational movements of the head on the neck; (3) the crash helmet adds 50% in weight to the normal weight of the head, thus increasing markedly the force exerted on the neck in a deceleration event; (4) an analysis of the various mechanical factors involved reveals that stretch and flexion of the cranio-cervical junction are most important in the mechanics of concussion."

Studies on jet aircraft thrown in the water from the deck of an aircraft carrier have shown, according to Rawlins et al. (1964) (5) that the aircraft usually floats for a maximum of 60 seconds, and then sinks at a minimum rate of 400 ft/min, thus giving a maximum of two minutes for the aviator to escape before being crushed by water pressure, even if he had escaped drowning.

As a result of this analysis, he prepared experimental designs which were funded, of which this study is a part. A new laboratory, the Naval Biodynamics Laboratory, was established in part to perform this work.

This paper is dedicated to Otto Stochdorph, M.D., Professor and Chairman, Department of Neuropathology, University of Munich, School of Medicine, Munich, West Germany.

### Previous Work

Investigations in which uncontrolled and controlled mechanical forces applied to the heads, the spine, and spinal cord of animals, using different impact vector directions are correlated with resulting morphological alterations have been carried out since the last quarter of the last century.

Discussion of the literature and historical reviews were presented by Unterharnscheidt (1963) (6), Unterharnscheidt and Sellier (1963) (7), Unterharnscheidt and Higgins (1969) (8, 9, 10), Unterharnscheidt and Ripperger (1970) (11), Dohrmann (1972) (12), Ducker (1976) (13), Goodkin (1976) (14), Osterholm (1974, 1978) (15, 16). A detailed discussion of the existing literature concerning animal experiments will be given by Unterharnscheidt elsewhere.

In discussing the application of whole body -Gx impact acceleration exposures to Rhesus monkeys the findings presented in the following papers must be considered in detail: (Stapp 1951) (17, 18), Unterharnscheidt (1958, 1963) (19, 6), Unterharnscheidt and Higgins (1969) (8, 9, 10), Friede (1960, 1961) (2, 3, 4), Clarke et al. (1970, 1971, 1972) (20, 21, 22, 23), Osterholm (1974, 1978) (15, 16), Ewing and Unterharnscheidt (1976) (25), Unterharnscheidt and Ewing (1978) (26), Alderman et al. (1980) (24).

### Present Study

The present study reports on a carefully controlled series of experiments with whole body -Gx impact acceleration exposures of Rhesus monkeys with completely restrained torso but unrestrained head and neck. That is, the animal is accelerated with the unrestrained head and neck undergoing flexion. Thus, impact acceleration is transmitted from the sled to the torso by the restraint system, and then via the vertebral column to the head.

The only previous animal experiments using the same vector direction, -Gx, were carried out by Clarke et al. (1970, 1971, 1972) (20, 21, 22, 23) with baboons. These authors in a series of experiments investigated tolerance to abrupt linear deceleration (-Gx) and the subject interaction of baboons, using different restraint systems. In the first series of experiments, restraints used were the Air Force shoulder harness-lap belt; in the second series, a lap belt only; and in the third series, an air bag plus lap belt and also air bag only.

### METHOD

#### Experimental Equipment

A 225,000 Pound Thrust Horizontal Accelerator with sled, control console and enclosed environmentally controlled 700-foot track at the Naval Biodynamics Laboratory, New Orleans, Louisiana, was used. This can impart up to 200 G to the lightweight primate sled for durations of up to 90 milliseconds (ms).

The Inertial Data Acquisition System samples 24 channels of inertial data at 2000 samples/sec/channel, digitizes it, and stores the digitized data in magnetic discs in real time. After the experiment, the digitized data are scaled in the computer using calibration data resident therein. A digital tape is then made of the scaled digitized data for further analysis.

The Physiological Data Acquisition System is designed to acquire ECG, EEG and somatosensory evoked potential for 16 channels via FM/FM telemetry. The ECG band width is 1.0 Hz to 100 Hz ; the EEG band width is 1.0 Hz to 100 Hz.  
The somatosensory evoked potential band width is 30.0 Hz to 1500 Hz.

The Photographic Data Acquisition System includes sled and laboratory mounted cameras, lights and control console, as well as phototarget design which is necessary for obtaining precise three-dimensional photographic displacement data of primate kinematic response. A complete description is published elsewhere (Becker, 1975) (27).

The Transducer Mounting System which was developed for primates permits precise determination of linear and angular acceleration, velocity and displacement at the mounting site. Transformation of the data to coordinate systems fixed in the anatomy is accomplished using the results of biplanar x-ray anthropometry which measures the precise three dimensional spatial position of the instrumentation coordinate system relative to the head anatomical coordinate system (Becker, 1977) (28). The head acceleration was measured by a rigidly mounted array of six linear accelerometers locked to an implanted pedestal bolted to the calvarium capable of measuring angular and linear acceleration and velocity in three dimensions (Ewing and Thomas, 1972 (29); Becker and Willems, 1975 (30); Willems, 1977 (31)).

Sled acceleration was also measured.

Two different types of restraint systems were used: a rigid molded one and a harness vest. There seems to be no difference in the lesions produced, since the head and neck kinematic response is not markedly altered.

### Experimental Procedures

Twenty-eight Rhesus monkeys were subjected to a total of 93 runs with sled accelerations ranging from 5.2 G to 162.8 G in the -Gx vector. Twenty animals were run repeatedly until acutely fatal injury occurred. Eight animals were run only once in order to avoid possible cumulative effects of multiple runs. The results of the injurious run or the solitary run for the animals run once are listed in Tables 1 and 2.

The surviving animals were sacrificed after different survival times. One of these animals was so severely injured (the sled acceleration was 123.0 G) that it had to be euthanized in a moribund state 90 hours after the run. It was determined that this was a threshold case of medullo-cervical injury without subluxation.

Before, during, and after the acceleration, epidural EEG interlaced with somatosensory evoked potential, and ECG were recorded. Non-fatal runs were followed periodically with these neurophysiological recordings. These data will be reported separately (Berger and Weiss, 1982 (32); Saltzberg et al., 1982 (33); Sances et al., 1982 (34, 35)). The ultimate limit for primate survival to -Gx impact acceleration for circumstances in which the head and neck are unrestrained is due to failure of the head-neck junction. The anatomical details, the threshold of injury and the mechanisms of injury were determined for Rhesus monkeys by Thomas and Jessop (1982) (36).

Pre- and post-run x-rays of the entire spine were performed.

Maintenance and utilization of the primates was under the direct control of a specialist in laboratory animal medicine who will report the clinical findings separately (36).

### Autopsy Procedures

The following standardized autopsy method is used for examining -Gx monkeys:

The veterinary pathologist first performs a general autopsy. After evisceration, the torso is dismembered. The neuropathology portion of the autopsy is then begun by removing and opening the underlying muscles and opening the skull in a horizontal plane. Then, the implanted instrumentation pedestal is removed using a rongeur.

The number and location of the epidural electrodes used for recording the EEG and the macroscopic location of intracerebral electrodes are determined and described.

At this point, the removal of the brain is interrupted and preparation begun for removal of the entire brain and spinal cord from the dorsal aspect.

The opening of the spinal column is achieved by a dorsal approach, with the cadaver in the prone position. The lordosis of the spinal column is compensated using a wooden block. After dissecting the skin, a deep incision is made extending from the external occipital protuberance along the spinous process to the middle of the sacral bone. The subcutaneous tissue and the paravertebral muscles are bilaterally removed from the underlying bony structures. The entire bony spine is exposed laterally to the lateral process. Using a rongeur, the spinous process, the dorsal half of the spinal arcs and the lateral process of the sacral, lumbar, thoracic and cervical segments are removed. Only segments C1 and C2 as a whole are left untouched, to be removed later from the entire cervical spine for examination of the ligaments, bones, discs, and vessels at the atlanto-occipital junction (Compare Fig. 8A).

At this point, the removal of the spinal cord is interrupted and the entire specimen with brain and spinal cord in situ is fixed in a 10% solution of formalin for 10 days. The formalin is changed on the second day.

After complete fixation, the exposure and removal of the brain are continued. The base of the skull is gradually removed with a rongeur until the entire brain is exposed. After the cranial nerves have been dissected, the entire brain with the surrounding dura mater is removed.

The remaining parts of the base of the skull and anterior and lateral parts of the neck are then removed in toto. Both cranial ends of the internal carotid arteries are identified and then the area from proximal to distal exposed, downward to the carotid bifurcation.

The dorsal and ventral roots of each spinal cord segment are now carefully cut. The preparation begins at the cauda equina and proceeds upwards to the cervical area. The removal of the last region of C1 and C2 is established by careful dissection of the posterior and ventral roots in the intact spinal canal. This procedure is very sensitive, since this area must be left intact for further study of expected traumatic lesions of the bony and ligamentous structures in the upper third of the cervical area and the atlanto-occipital junction.

After dissecting the uppermost dorsal and ventral spinal roots, the spinal cord with surrounding spinal dura mater is pulled from the spinal canal. It is only at this time that it can be determined whether the upper cervical spinal cord suffered a complete traumatic separation from the lower medulla oblongata, or not. In the latter case, brain and spinal cord are removed en bloc.

Brain and spinal cord are photographed in color as well as black and white at the end of the procedure.

In some instances, the entire specimen is cut in the mid-sagittal using a band saw. This procedure allows an excellent analysis of the location and degree of traumatic lesions of all involved structures since they are left in situ and can be examined and analyzed step by step (Compare Fig. 2-3).

It must be mentioned that it is impossible to give a thorough description of all lesions of the CNS on the one hand and the surrounding tissues of the cervical spine, like muscles, ligaments, bones and discs on the other hand. In order to remove the CNS for histological evaluation, a certain part of the surrounding structures must necessarily be destroyed. In general, a preference was given to the preservation of the CNS to achieve a more thorough insight into the traumatic lesions of these structures.

In further experiments, maceration techniques are planned in order to enhance our existing knowledge about the traumatic lesions of the bony structures and ligaments.

#### Embedding and Staining Techniques

A Spielmeier assortment of tissue blocks for histologic examination is prepared. The following areas of brain and spinal cord are cut from each monkey for embedding in paraplast and celloidin: the frontal-, parietal-, and occipital lobes, the temporal lobe with the hippocampus formation; an entire cerebral hemisphere with basal ganglia, the mid-brain, pons, medulla oblongata, pituitary, the vermis cerebelli and cerebellar hemispheres, and each segment of the cervical, the thoracic, the lumbar, and the sacral spinal cord (using horizontal or coronal sections) and the cauda equina.

Longitudinal sections of the lower medulla and cervical region extending to C2 were cut from a number of animals which showed no traumatic transection between lower medulla and upper cervical spinal cord. Using this technique, a block was cut extending from the posterior part of the fourth ventricle extending to the second cervical segment. This block was then cut in the midline (starting at the ventral fissure) using both halves for histological sections.

Embedding of the spinal cord in paraffin is preferable to celloidin methods from a staining aspect, because, besides the standard staining techniques as Hematoxylin-Eosin and Cresylviolet (Nissl), additional techniques like the myelin method by Heidenhain-Woelcke, axis cylinder methods by Palmgren or Bodian, and Trichrom techniques by Masson, Mallory, Goldner, or Van Gieson can be performed. If the specimen is embedded and dehydrated slowly an uneven shrinkage can be avoided. But in the presence of larger hemorrhages, an embedding in celloidin is preferable because breaks and folds which appear in paraffin do not occur.

It is recommended that longitudinal sections be made at least in a part of the specimens; these longitudinal sections of the spinal cord according to Bodechtel, Krücke, Stochdorph and our own experience generally reveal a better picture of the extent of lesions in disseminated processes and allow the differentiation of focal from funicular lesions.

In this paper, only preliminary histopathological findings are presented. Only those histological specimens which were embedded in paraplast were evaluated. The specimens embedded in celloidin were not as yet available for this evaluation due to the longer embedding periods. Therefore, only preliminary conclusions relating to neuro-histopathology can be drawn.

#### RESULTS

The living animals subjected to -Gx impact acceleration are arranged in a sequence starting with the lowest peak sled acceleration continuing to the highest one using always the peak sled acceleration of the last run when multiple runs were performed on a single animal. For details compare Tables 1 and 2.

#### Summary of Findings: Sled Parameters, Peak Head Parameters. Radiological and Neuro-pathological Findings Due to Each Run and Animal. Summary of Morphological Findings:

Twenty-eight living animals were subjected to a total of 93 runs using -Gx acceleration. The peak sled acceleration ranged from 5.2G to 162.8G. Twenty animals were subjected to multiple runs, and 8 to single runs only. The number of runs per animal in the group with multiple runs varied between 2 and 10.

The peak sled acceleration in the group of animals with multiple runs was normally highest in the last run with 4 exceptions: Animal # 0761 was subjected to peak sled acceleration of 98.3G in an earlier run, with a peak sled acceleration of 21.0G in the last run, the only one subjected to a much higher acceleration in an earlier run than in the last one; animal # 8872 was subjected to a peak sled acceleration of 44.5G in an earlier run, with a peak sled acceleration of 44.3G in the last run; animal # NA28 was subjected to a peak sled acceleration of 45.0G in an earlier run, with a peak sled acceleration of 44.5G in the last run; and animal 8802 was subjected to a peak sled acceleration of 64.3G in an earlier run, with a peak sled acceleration of 63.7G in the last run. The differences in the peak sled acceleration of the last 3 animals in earlier runs as compared to the last one were negligible.



The results of these experiments can be expressed in terms of damage to: (a) Central Nervous System, (b) Vascular System, (c) Skeletal System, and (d) Muscles, Bones and Ligaments.

#### Traumatic Alterations of the Central Nervous System.

Peak sled accelerations ranging from 5.2 -Gx to 63.7 -Gx did not produce clinical or pathomorphological findings. Especially, they did not produce traumatic transections of the CNS at the atlanto-occipital junction and between lower medulla oblongata and upper cervical spinal cord.

The lowest level at which tissue damage occurred was 78.3G. This animal (#0012) which was sacrificed on the same day, and which did not reveal any abnormal radiological findings, showed subarachnoid hemorrhages around the basilar artery and both vertebral arteries. There was no traumatic transection at the atlanto-occipital junction, but a local indentation and brownish discoloration of the tissue at the ventral fissure between lower medulla oblongata and C1 was seen.

The histological examination of the specimen revealed recent and old traumatic alterations in grey and white matter. Another animal (#8790) (Figs. 1A-C) which was subjected to a peak sled acceleration of 87.9 G showed radiologically an incomplete traumatic separation at C1/C2. The run was acutely fatal; there existed no traumatic transection but a local indentation and brownish discoloration of the ventral surface between lower medulla and upper cervical spinal cord. After dissection a mostly centrally located hemorrhage could be seen in the cord.

Another animal, subjected to a peak sled acceleration of 104.5 (#8863) which was sacrificed on the 12th day, revealed no discoloration, but a decreased consistency of the tissue between lower medulla oblongata and upper cervical spinal cord at their ventral aspect, without traumatic transection at the atlanto-occipital junction.

In 6 animals, complete traumatic transections between lower medulla oblongata and upper cervical spinal cord were seen. The lowest level at which a complete traumatic transection occurred was 108.7G (#3921) (Compare Figs. 8B-C). Further complete traumatic transections occurred at peak sled accelerations of 127.4G (#3923), 128.2G (#4099), 131.4G (#3946), 158.4G (#3146), and 162.8G (#3936) (Figs. 2, 3).

In 4 animals, incomplete traumatic transections were seen at 105.3G (#8866), 124.2G (#0764), 126.4G (#4101), and 130.7G (#3951).

Complete and incomplete traumatic transections were found in 10 animals with a peak sled acceleration ranging from 105.3G (#8866) to 162.8G (#3936).

One animal (#3935) subjected to a peak sled acceleration of 123.0G showed severe clinical findings immediately after the run. This animal was involved in another high level run (105.5G) on the same day. The animal was moribund and had to be sacrificed after 90 hours. There was no traumatic transection, but marked central hemorrhagic necroses bilaterally were found in the spinal cord (Figs. 4A-E).

In the group of animals subjected to high level -Gx acceleration, 3 revealed no macroscopically visible CNS tissue damage: animal #3933 (108.6 G peak sled acceleration); animal #3924 (110.4G peak sled acceleration); and animal #4115, (127.3G peak sled acceleration) which was acutely fatal due to a basilar skull fracture. Of the 15 animals who were subjected to peak sled accelerations of more than 100G, 12 revealed severe traumatic alterations. In the remaining three cases, macroscopic traumatic lesions were excluded. A detailed histologic evaluation is underway. The findings will be reported later.

The 2 animals who survived peak sled accelerations of more than 100 G, namely #3933 (108.6 G) and #3924 (110.4 G) were subjected to G levels which were near the threshold level.

Peak sled acceleration levels, with the restraint conditions stated above in the -Gx vector, between 105 G and 110 G represent the threshold zone in which injuries may or may not occur.

Peak sled accelerations of more than 110.4 G in the -Gx vector were acutely fatal and regularly produced, with one exception, incomplete or complete traumatic transections between lower medulla oblongata and upper cervical spinal cord.

The histological examination of the acutely fatal monkeys revealed multiple hemorrhages in the direct neighborhood of the transected area. These hemorrhages can be termed primary traumatic or rhectic. They occurred at the moment of impact, and are the result of ruptures of vessel walls due to the mechanical forces. These hemorrhages were usually more frequent in the gray substance, but they occurred in the white substance, too. These multiple petechial hemorrhages can be so massive that they can form a larger hemorrhage due to confluence of the multiple smaller ones. In general, those hemorrhages were seen only in the direct vicinity of the transected area. In some animals, however, they extended proximally into the upper medulla oblongata, the pons and mid-brain, and distally into lower cervical and upper thoracic segments. They decreased in size and number the more distant they were from the transected zone. If the hemorrhages



were located in the white substance, these primary traumatic hemorrhages were mainly located near the ventral and only rarely near the dorsal surface of medulla, pons and midbrain. There seemed to be an avulsion of vessels at or near the ventral surface of the described anatomical structures due to overstretching. In one case, we observed these hemorrhages at the base of the temporal lobe in the hippocampus formation.

There appears to exist a direct relationship between the severity of the applied forces and the severity and distribution of the pathomorphological findings. The higher the mechanical input expressed as peak sled acceleration, the more severe are the hemorrhages and the larger is the involved area, a finding which has been observed in other animal experiments using other vector directions.

The subdural hemorrhages of the spinal cord seen in the animals with incomplete and complete traumatic transections are large, and normally cover the ventral and dorsal aspects of the spinal cord (Compare Figs. 8C-E) and extend in some instances into the cauda equina. They are the result of the rupture of both vertebral arteries and the anterior spinal artery. The hemorrhage, therefore, extends from proximal to distal, in some cases into the cauda equina.

The pituitary gland revealed no hemorrhages, either macroscopically or microscopically in any of the animals tested. The stalk was intact and showed no traumatic disruption. Subarachnoid and subdural hemorrhages at the base of the infundibulum were the result of disruption of the vertebral arteries extending forward at the base of the brain and skull.

#### Traumatic Alterations of the Vascular System

At peak sled accelerations of more than 110 G, incomplete and complete traumatic transections normally occurred between lower medulla oblongata and upper cervical spinal cord. Above 127.3 G, these transections occurred regularly. Both vertebral arteries and the anterior spinal artery were ruptured and subsequent subarachnoid and subdural hemorrhages were found at the base of the brain and around the spinal cord, extending into different levels, in some cases into the cauda equina.

There are two subtypes of rupture of the vertebral arteries:

(a) The more frequent injury was that in which both vertebral arteries, and in a few instances, the basilar artery, were completely avulsed (Compare Fig. 8B).

(b) The less frequent injury was that in which a separation of the vertebral arteries occurred immediately above the foramen magnum, so that their proximal parts remained intact in the specimen in situ (Compare Fig. 9C).

In this second type, there was a C1 - C2 subluxation instead of an atlanto-occipital separation. Since the cardiac actions in these traumatically transected animals continued for about 20 minutes, relatively large hemorrhages developed which in some instances became space-occupying lesions, and were, therefore, termed hematomas.

The vertebral artery which arises commonly from the subclavian artery has four segments. The first or prevertebral segment ascends posterolaterally between the longus colli and anterior scalene muscles to enter the transverse foramina of the cervical spine at the level of the sixth cervical vertebra. From this point the artery ascends as the second or cervical segment through the transverse foramina to become the third or atlantic segment when it exits from the transverse foramen of the atlas. It then passes posteriorly behind the articular process of the atlas, lying in a groove on the superior surface of the posterior arch of the atlas, and enters the cranial cavity, by piercing the atlanto-occipital membrane and the dura mater to become the fourth, intracranial or intradural segment. This segment ascends anteriorly and laterally around the medulla to reach the midline at the pontomedullary junction, where it unites with the vertebral artery of the opposite side to form the basilar artery (Sheldon, 1981) (58).

The rupture of the vertebral arteries occurs at the point where they pierce the atlanto-occipital membrane and dura mater; the rupture takes place between the third and fourth segment. In some cases, the fourth, intracranial or intradural segment, and in a few instances, the basilar artery, were completely avulsed.

Despite peak sled accelerations up to 162.8 G, no rupture of a carotid artery was observed. Whether traumatic disruptions of the carotid arteries occur when applying higher acceleration levels will be studied in further experiments. The fact that the carotid arteries remained intact and patent could also be deduced from the fact that in some instances subdural hemorrhages developed over both cerebral hemispheres due to ruptured bridging veins (Figs. 9A-B). Since the cardiac actions of the animals with a complete traumatic cord transection continued for about 20 minutes, a patent vascular system of the area supported by the internal carotid artery must exist. Since EEG and ECG were recorded in these cases with the developing and expanding hemorrhages, interesting insights into the neurophysiological aspects can be expected from further data analysis.

### Traumatic Alterations of the Skeletal System

An exact analysis of the status of the ruptured ligaments of the atlanto-occipital junction in a Rhesus monkey is very difficult due to the small anatomical proportions. Furthermore, in order to achieve a thorough knowledge of the traumatic alterations of brain and spinal cord, some structures of the spine and their ligaments must be destroyed in order to remove the CNS.

However, a careful anatomical dissection, using different approaches, allows a quite satisfying description and quantification of the resulting traumatic lesions. It was demonstrated that the dura mater near the foramen magnum (the area where the cerebral dura mater is transient into the spinal dura mater) was partially or completely disrupted.

Small to medium sized hemorrhages, probably due to tears and ruptures of muscles near their origin at the posterior margin of the foramen magnum were seen. Larger hemorrhages existed at the anterior margin of the foramen magnum. The hemorrhages extend into the retropharyngeal space and in some cases into the nasopharynx. This was clearly demonstrated by sectioning entire specimens of head and spine with the spinal cord in situ in the sagittal plane using a band saw (Compare Figs. 2-3).

Data concerning the ligamentous structures of the atlanto-occipital junction in 10 kg Rhesus monkeys are almost non-existent. They are not mentioned at all in the atlas and dissection manual of the Rhesus monkey presented by Berringer et al. (1968) (37), and are only briefly mentioned in the Anatomy of the Rhesus Monkey edited by Hartman and Strauss (1965) (38).

The membrana tectoria and posterior longitudinal ligament normally remained intact, but were completely disrupted in single cases. But after removing these structures, it became evident that the transverse and the proximal parts of the cruciate ligament were ruptured. This led to indentations of the odontoid process of the axis onto a circumscribed area of the ventral portion of the lower medulla oblongata, a lesion which was demonstrated macroscopically and microscopically and which was in some cases survivable as monkeys #0012 and #8863 show. Fractures of the odontoid process were not observed, but we did not utilize up-to-date maceration techniques.

Yet, the complete traumatic transection of the spinal cord between lower medulla oblongata and upper cervical spinal cord cannot be explained by the odontoid process alone. A complex mechanism consisting of stretching, compression, and shearing at the region of the atlanto-occipital junction occurs, combined with rotation of the head on the neck and the neck on the torso. A detailed analysis of the mechanics of transection of the cord is presented below.

### DISCUSSION

A complete traumatic transection of the spinal cord after applying -Gx impact vector acceleration caused hemorrhages mainly in the grey substance but to a lesser degree in the white matter. They are the result of rupture of blood vessels of the spinal cord due to overstretching in the zone of maximum stretch. They can be termed rhectic and therefore primary-traumatic, and occur at the moment of maximum load.

In an incomplete traumatic transection, the grey substance was more affected, and the hemorrhages were more frequent and larger than in the white matter.

Furthermore, at sled peak acceleration levels low enough that neither complete nor incomplete transections occurred, a local indentation was seen at the ventral fissure apparently caused by direct impact of the tip of the odontoid process (Compare Fig. 1C). This local indentation generally produced acute traumatic alterations only in the ventral or anterior fasciculi. Upon these immediate traumatic lesions are superimposed another traumatic alteration which developed only after an interval, but which also were due to the same impact of the odontoid process on the cord. This latter alteration consisted of lesions in the grey substance which led to what may be termed progressive central hemorrhagic necrosis (Compare Figs. 4A-E). Since these traumatic alterations become visible only after an interval of at least hours, they must be termed secondary traumatic.

In order to interpret the pathogenesis of these typical and reproducible lesions (progressive central hemorrhagic necrosis) one must compare them with very similar alterations produced by Osterholm (1978) (16). He found using Allen's method (1914) (39) of dropping a weight on the posterior fasciculi, that traumatic central hemorrhagic necrosis could be produced, affecting mainly the grey substance. There is, in our opinion, no doubt that the same type of lesion could be produced by a direct application of force at the ventral fasciculi by the odontoid process. In our experiments, the odontoid process appears to have the same effect as the dropping weight using Allen's tube, only it affects different tract areas.

The analysis of the specific traumatic lesions caused by -Gx impact allows an additional analysis of the injury mechanisms.

Analyzing the local traumatic alterations at the area of the atlanto-occipital junction, three mechanisms appear to occur during the course of acceleration, simultaneously or consecutively: (a) compression of the spinal cord at the ventral aspect

between lower medulla and C1 segment which leads, in some specimens, to indentation of tissue with or without brownish discoloration or flattening of the specimen in the antero-posterior diameter, if the threshold is reached. This tissue damage is located at the region of the cord in opposition to the tip of the odontoid process and is, without doubt, caused by this structure; (b) stretch along the longitudinal axis of the medulla oblongata and upper cervical spinal cord; combined with (c) a guillotine action between anterior and/or posterior rim of the foramen magnum on the one side and the anterior arch of the atlas (with the directly posterior located odontoid process of the axis) and the posterior arch of the atlas on the other side, which takes place as the head extends on the neck and then rotates relative to the neck. This results in a succession of tension and shear forces at the head neck junction. Failure or subluxation of structures at the head neck junction results in incomplete or complete traumatic transection of the cord tissue.

Looking at normal and transected specimens cut in the mid-sagittal plane, and magnifying them, it can be seen that the odontoid process is located directly posterior to the anterior arch of the atlas (Figs. 5 - 7). In some specimens, its tip extends several millimeters above the highest part of the anterior arch of the atlas.

#### Comparison of NBDL Findings to Clarke et al. Experiments

The only previous animal experiments using the same vector direction, -Gx, were carried out by Clarke et al. (1970, 1971, 1972) (20, 21, 22, 23) with baboons. These authors in a series of experiments investigated tolerance to abrupt linear deceleration (-Gx) and the subject interaction of baboons, using different restraint systems. In the first series of experiments, restraints used were the Air Force shoulder harness-lap belt; in the second series, a lap belt only; and in the third series, an air bag plus lap belt and also air bag only.

In the first series of experiments, 89 deceleration tests were performed with 37 adult male baboons. LD50's were calculated to be 102, 103, and 98 g for the 0.5 ft (0.15 m), the 2.0 ft (0.61 m), and the 3.5 ft (1.07 m) stopping distances, respectively. Since the deceleration pulses were similar, the authors concluded that for the exposure range of these tests, impact lethality is dependent upon the magnitude of peak sled deceleration, irrespective of the pulse duration, sled velocity, or stopping distance. At all stopping distances, the primary cause of death was lower brain stem or cervical spinal cord trauma. The pelvic, abdominal, and thoracic injury patterns were significantly different at the various stopping distances. Animals impacted at the 0.5 ft (0.15 m) stop typically displayed no significant injuries other than head-neck trauma. Pelvic and abdominal trauma were nonexistent. Most of the significant injuries other than to the CNS were directly attributable to the torso portion of the restraint. These injuries included hemorrhage of thoracic musculature and myocardial contusion.

The predominant injuries at the 2.0 ft (0.61 m) stop included pelvic fractures and abdominal myorrhexis, intestinal herniation, urinary bladder rupture, and pelvic fractures in addition to luxation of cervical and thoracic vertebrae. Again, the torso straps of the harness were primarily instrumental in producing the most life-threatening trauma except that to the CNS. These injuries included costal, clavicular, and scapular fractures plus luxation of cervical through thoracic vertebrae.

At the 3.5 ft (1.07 m) stop, the pelvic and abdominal injury patterns were similar to those at the 2.0 ft (0.61 m) stop but compounded in severity. There was a high incidence of transection of the descending colon and musculature or blood vessels in the axillary and cervical regions. Brain stem hemorrhage was a significant finding but there was no evidence of luxation or fracture of cervical vertebrae.

Clarke et al., commented that although the reported injuries were produced directly or indirectly by the safety restraint, its disuse would have resulted in comparable or more severe injuries at substantially lower sled decelerations as shown in the experiment using a lap belt restraint only.

The comparison of our pathomorphological findings with those of Clarke et al. in their first series of experiments, showed that the traumatic transection of the spinal cord of Rhesus monkeys and baboons occur at approximately the same acceleration thresholds.

In our experiments, the incomplete and complete traumatic transections were seen regularly at the level between lower medulla oblongata and C1. Furthermore, the area where the indentations in the tissue occur, near the ventral fissure of the upper cervical spinal cord, was in all instances exactly the same.

In the experiments of Clarke et al., the traumatic transection occurred usually at C1, but in many instances transections were seen at more proximal regions, i.e., in the brain stem, and at more distal regions, i.e., the thoracic and lumbar spinal cord.

In our experiments, the only radiologic findings consisted of atlanto-occipital separation, C1/C2 separation, and basilar skull fractures. The remaining parts of the skull, the spinal column and the other bony structures of the body revealed normal findings.

The experiments of Clarke et al., revealed several cases of avulsion of the atlanto-occipital articulation, which appear to be very similar to our findings which we termed atlanto-occipital separation. But Clarke et al. found many additional fractures and luxations in other anatomical structures in different regions which we did not see. They did describe an avulsion of the basilar portion of the occipital bone. However, other injuries which we did not see included luxations and fractures of the cervical and thoracic vertebrae and spinous processes, luxations of the lumbar spine, avulsion of the odontoid process, fracture of the body of the mandible, fractures of clavicles, ribs, scapulae and sternum, luxation of the sternum, comminuted fractures of the iliac crests and fossae, and transverse fractures of the body of the sacrum.

We found no noteworthy cutaneous harness abrasions and contusions while Clarke et al. found that these traumatic lesions were quite severe and frequent.

It is remarkable that in our experiments, in none of the high level Rhesus exposures did any vertebral fractures occur. There were no significant injuries to the intraabdominal organs as liver, spleen, or intestine; no intrathoracic injuries, and no fractures of the extremities. Yet, these types of injuries are usually the only ones looked for in cadaveric testing. All injuries in our studies were limited to the ligamentous structures of the atlanto-occipital junction or the C1-C2 junction, the CNS and in a few cases, to the skull. These morphological findings have many implications for protective equipment design.

A comparison of the traumatic histologic alterations of both groups cannot be presented since Clarke et al. did not publish histological findings. Also, they presented no discussion of the state of the different ligaments at the atlanto-occipital junction.

Analyzing the traumatic lesions, one can group them in: (1) impact vector specific and (2) supplementary or accidental alterations. In the first group, traumatic alterations are the direct result of the inertial forces; the second group of lesions are the result of insufficient protective or precautionary measures caused by inadequate protective systems.

Since a plethora of inertial data and corresponding morphological findings is available for each increment of peak sled acceleration in a given vector direction in our studies, the thresholds for functional disorders, reversible and irreversible tissue alterations, and death can be clearly defined and quantified.

The species-specific traumatic alterations using Rhesus monkeys are in our opinion convertible to human pathomorphology.

#### Comparison of -Gx Neuropathology with HAD-II Pathomorphology

A comparison of the traumatic spinal cord lesions of the animals subjected to -Gx indirect impact accelerations and those involved in direct impact with nondeforming angular acceleration of the head using Head Acceleration Device (HAD-II) (Unterharnscheidt and Higgins, 1969) (8, 9, 10) reveals different injury patterns.

The squirrel monkeys involved in direct non-deforming angular acceleration of the head using HAD-II did not have traumatic transections of the spinal cord. The three highest applied angular accelerations, namely 327,000 rad/sec<sup>2</sup>, 363,000 rad/sec<sup>2</sup> and 386,000 rad/sec<sup>2</sup> were acutely fatal, but did not produce traumatic transections. Only 2 animals showed relative small subdural hemorrhages in the cauda equina, but not in other parts of the spinal cord. The relationship with the magnitude of angular acceleration could not be clearly established.

The animals involved in non-deforming directly applied angular acceleration of the head, using HAD-II, always showed, with a few exceptions, small rhectic hemorrhages in various segments. The rhectic hemorrhages of capillaries and small veins were found more disseminated in the grey substance. These rhectic or primary traumatic alterations in the spinal cord affected the cervical, thoracic, and lumbo-sacral regions. The severity of these traumatic lesions, too, was related to the angular acceleration and increased with intensity. The correspondence was not as obvious as it was with the cerebrum, cerebellum and brainstem. These spinal cord lesions were not fatal, and the animals showed, indeed, no clinical signs. These small hemorrhages were difficult to discern when stained with the Nissl technique. After five days of survival, these animals showed very little, if any, mesodermal-glial reaction, unlike the more severe rhectic hemorrhages in the cerebellum and cerebrum.

Using both methods, subdural hemorrhages of the brain due to ruptured bridging veins could be produced. These subdural hemorrhages were, however, not regular findings. But it is necessary to take into consideration that the extent of applied impact acceleration ranged from very low intensities which produced no clinical or pathomorphological findings to lethal intensities, in order to describe the entire continuum of possible lesions. However, there is no doubt that the higher the peak sled accelerations, the more frequently subdural hemorrhages could be found.

The animals subjected to direct non-deforming angular acceleration of the head using HAD-II revealed intracerebral lesions in some cases. Five animals, which were exposed to the lowest rotational accelerations (101,000 to 150,000 rad/sec<sup>2</sup>) showed no primary or secondary traumatic morphological alterations in the cerebrum. These were

present, however, in 10 of 13 animals subjected to rotational accelerations from 150,000 to 197,000 rad/sec<sup>2</sup>. The findings included subarachnoid hemorrhages in three animals, combined in one instance with primary traumatic hemorrhages in the oculomotor nerve and tears and avulsions, largely of veins and capillaries in superficial layers of the cortex in eight animals. The subarachnoid hemorrhages were found in the lower range of angular acceleration, while the lesions in the cortex, which must be considered the more severe lesions, were always seen in animals exposed to the higher angular accelerations (175,000 to 197,000 rad/sec<sup>2</sup>) which suffered traumatic lesions in the cortex. This fact indicates that with increasing intensity of the angular acceleration, the primary traumatic alterations extended from the periphery to central portions of the brain. This change in the pattern of distribution of lesions was predicted and foreseen in the analysis of injury mechanics.

The highest angular accelerations administered, i.e., 205,000 to 386,000 rad/sec<sup>2</sup>, caused severe traumatic lesions in the cerebral cortex in four of six monkeys, and in three animals with intensities of 327,000 rad/sec<sup>2</sup> and more, additional primary traumatic lesions in the white substance (located even closer to the cortical pivot). Angular accelerations of more than 300,000 rad/sec<sup>2</sup> were not survived.

The histologic examination of the primary traumatic lesions in the cerebral cortex revealed that these lesions do not represent so-called cortical contusions, a finding that is clearly supported by photographs. Rather, they represent venorrhagic, occasionally capillary- and arteriorrhagic hemorrhages, located predominantly in the more superficial layers of the cerebral cortex. There was evidence of tearing and avulsion of vessel walls. Also, the hemorrhages consistently followed vessel systems running vertical to the cortical surface. The characteristic pin point hemorrhages in a more or less wedge shaped area indicative of cortical contusions in their first stage were not seen. They were always located near the midline, close to the parasagittal fissure of the cerebrum.

Thus, not only is there a difference in quality between primary traumatic cortical hemorrhage associated with directly applied angular acceleration and the so-called cortical contusions found in directly transmitted translational trauma, but there is also a difference in the pattern of distribution of the traumatic cortical lesions encountered in these types of angular and translational acceleration. The alterations due to directly transmitted angular acceleration were located close to the midline, not in a cylindrically symmetric pattern but radially symmetric, as predicted by the injury mechanics. Ommaya et al. (1968) (59) illustrated similar alterations after whiplash injuries in monkeys and described them as cortical contusions. Histological examination indicates that the lesions do not represent the typical so-called cortical contusions, but are caused by tears and avulsions of vessels in superficial layers of the cortex which in turn are produced by the relative rotation of the skull against the (inert) brain. These findings present, in our opinion, substantial evidence against Holbourn's concept that cortical contusions are due to rotational motion. We attribute great importance to angular acceleration, in such cases as the uppercut in boxing, when tearing of bridging veins causes subdural hemorrhage. But we also advance the theory that quality and distribution of lesions after directly transmitted translatory and directly transmitted angular accelerations are essentially different when all the evidence from histological examinations is brought to bear.

#### Comparison of NBDL -Gx Neuropathology with Findings of Friede

Friede (1960, 1961) (2, 3, 4) studied the injury mechanism involved when the head is abruptly displaced with respect to the rest of the body in a series of well-controlled animal experiments on cats. Symptoms were produced in two ways: (1) the animals were given a controlled blow to the head or (2) dropped tail first into a hole in the floor with their heads supported in collars and their bodies allowed to hang free.

Friede's purpose in performing these experiments was to investigate the neuropathology and mechanics of experimental acceleration concussion in cats.

The blow accelerating the head produced an abrupt displacement of the cranio-cervical junction.

Histologic examination of the central nervous system of these cats revealed typical lesions of neuron loss in nuclei of the brain stem. Chromatolysis and loss of nerve cells were seen in the reticular formation, lateral vestibular nucleus, red nucleus and, less often, in other nuclei of the brain stem. These alterations represented an obvious axonal reaction to damage of large fibers in the cervical region. Motor nuclei of cranial nerves were not damaged.

Of greater significance, however, was the demonstration of a typical fiber lesion on the ventral circumference of the first cervical segment of the spinal cord. This circumscribed fiber lesion was found in all cats with symptoms of concussion. Fiber damage was localized in a conical area symmetrical to the ventral median fissure with apex adjacent to the center; maximum damage was seen at the level of C1, grading off rapidly toward the medulla. The damage was primarily localized to large diameter fibers, although in severe lesions fibers of medium and small diameter were occasionally damaged. Myelin sheaths of the thick fibers showed degeneration caudal to the site of the lesion. Sheaths of medium thickness fibers were less affected, showing only slight irregularities. Sheaths of thin fibers were not damaged even if immediately adjacent to damaged large fibers.



The size of the damaged area varied with the severity of the injury.

The partial coincidence of the cervical fiber lesion with the level of the odontoid process could, as Friede (1961) pointed out, be interpreted: (a) since the odontoid process is the most prominent structure in the ventral wall of the cranio-cervical junction, any straining of the cord would show maximal damage at this point; (b) a subluxation of the odontoid process could contribute actively to the mechanics of damage. Friede (1961) summarized his findings: "A subluxation of the odontoid process possibly contributes to aggravation of the damage, but so far there is no evidence for a critical importance of this mechanism."

This series of Friede's experiments indicated that the basic pathologic lesion of experimental concussion was produced by a stretching of the cervical cord around the odontoid process. Cervical stretch may be produced by a sudden blow to the head that displaces the head with respect to the body. The symptomatology of direct cervical stretch was indistinguishable from that produced by a blow to the head. The primary pathology of experimental concussion should be regarded, according to Friede, as damage to large fibers in the ventral surface of the upper cervical cord at the level of C<sub>1</sub>. Changes in the cell structure of the nuclei of the brain stem were secondary to the primary fiber lesion.

Friede (1961) proposed to reserve the term "experimental acceleration concussion," for the specific pathogenetic syndrome he described in detail. He considered the question as to whether the lesion at C<sub>1</sub> could be interpreted as a complicating cord injury or whip-lash injury rather than cerebral concussion. However, in his opinion, the lesions of the ventral fasciculi of C<sub>1</sub> were evidently responsible for the cellular changes in the medulla oblongata attributed to concussion. In his opinion, there was also a definite relationship between histological findings and the generally accepted symptomatology of concussion. Furthermore, the threshold forces required to produce this damage are in the same order as those reported by other authors for concussion. Since histological damage and symptoms changed at the same rate, no discrete symptomatology was left to distinguish a "true cerebral" concussion from the syndrome described by Friede. There is, therefore, according to Friede, no reason to believe that he described a clinical syndrome different in any way from the "concussion" of the majority of physiological experimenters. Several of the individual findings, such as the hemorrhages in the cord at C<sub>1</sub>, have been observed before by other investigators (Denny-Brown and Russell, 1941 (40); A. Jakob, 1912 (41); Peters, 1943 (42). We found and described similar lesions in some of our animal experiments applying direct translational (linear) acceleration (Unterharnscheidt, 1963) (6).

Friede (1961) discussed further the relationship of "experimental acceleration concussion" and clinical "commotio cerebri." In his opinion, this question could be answered only by human neuropathology and it is difficult to answer, indeed, since commotio cerebri is not a fatal condition. Routine pathological material is of little value, since the customary dissection of brain and spinal cord invariably destroys the upper cervical region. In Friede's opinion, there is little doubt, however, that this syndrome will be found as well in man.

It should be noted that in Friede's experiments, complete traumatic transection between lower medulla and upper cervical spinal cord did not occur. Probably the physical forces used were not high enough to produce a complete tissue separation in the cat. It should be recalled that Friede used a different impact vector direction.

The traumatic lesions reported by Friede are unquestionably intravital. They are the morphological end states resulting from several well defined mechanical inputs as described above.

The area of tissue damage presented by Friede is practically identical with that in our experiments. Friede found the area of maximum damage at the level of C<sub>1</sub>. In our experiments, the zone of maximum damage was found between lower medulla and the upper cervical spinal cord, i.e., slightly above C<sub>1</sub> or in the most proximal part of C<sub>1</sub>.

In addition, the area involved in the horizontal plane was similar. Friede found the maximum damage in a conical area symmetrical to the ventral median fissure. This was seen in our monkeys also. In some animals, flattening of tissue or indentations and sometimes brownish discoloration of the tissue could be observed.

The size of the damaged area varied, according to Friede, with the severity of the injury. In severe lesions the damage extended into the lateral portion of the ventral fasciculi. The dependence of the size of the traumatized zone, described as the volume of the involved area, with the intensity of the mechanical input was evident. We clearly demonstrated, that with increasing peak sled acceleration, the damage zone extended from ventral to dorsal, in general only barely involving the dorsal fasciculi, and extending proximally and distally along the longitudinal axis of the medulla oblongata and cervical spinal cord. With increasing peak sled accelerations, we found incomplete and, ultimately, complete spinal cord transections. The transection of the spinal cord in our experiments may have been due to the guillotine action of the foramen magnum, not just to acceleration alone. Since many sled and head acceleration parameters were recorded in our experiments, the thresholds for tissue damage and tissue transection, may be determined exactly, although this analysis is not yet complete.

Comparing and summarizing the findings of Friede and of our experiments, there are indeed many concordant, but some discordant, data. In addition to the localized fiber damage, mainly in the ventral fasciculi, we were able to detect further morphological data in our monkeys. In some animals, quite marked central hemorrhagic necroses in the cord were observed. These centrally located hemorrhagic necroses could be seen with only minimal or no damage in the ventral fasciculi. It is quite possible that these very typical lesions were observed because of the different vector direction and the higher intensities applied.

The injury mechanism will now be discussed. Since the level of the above described traumatic lesions coincides with the level of the tip of the odontoid process of the axis, the occurrence of these lesions has to be interpreted. Friede's interpretation of the cause of the occurrence of these lesions was presented above. Indeed, the odontoid process must be considered the anatomical structure which is most prominent in the ventral wall of the cranio-cervical or atlanto-occipital area. This can be clearly demonstrated using specimens in which the entire monkey is cut in the midsagittal plane. The odontoid process is located in the precise area where we find the tissue indentation and discoloration at the ventral fissure between lower medulla and upper cervical spinal cord. We demonstrated in other specimens, where the spinal cord was removed using the posterior approach, that the odontoid process was protruding beneath the intact posterior longitudinal ligament. Again, this protrusion can lead to indentations and, therefore, traumatic lesions of the area between lower medulla and C1 despite the fact that the posterior longitudinal ligament is intact (Compare Fig. 1A-B). But after dissecting this ligament and folding it backward, it became evident to us that the transverse and the proximal part of the cruciate and the apical ligaments were ruptured.

For the specific pathogenic syndrome which he described in detail, Friede proposed to reserve the term "experimental acceleration concussion."

It is important to draw a distinction between the NBDL experiments and those of Friede. His purpose was to investigate experimental cerebral concussion in cats. Ours was to investigate injury modes and mechanisms in the Rhesus monkey. The similarity of neuropathological findings invite comparison, but it is necessary to agree upon definitions if this comparison is to be apt.

Concussion per se is defined as a morphologically traceless, at least, using light microscopy reversible functional disorder which is therefore only clinically defined.

By this definition, Friede had no cases of concussion in his series, since all of his experiments resulting in "concussion" had fiber damage in the cervical cord, and were therefore not morphologically traceless. Obviously, any observed clinical symptomatology in such cases may be due to the cord damage rather than to concussion per se.

We were not able to observe unconsciousness or lack of responsiveness or abolished reflexes in our experiments except as noted in Weiss and Berger's chapter (32) concerning evoked potential changes. It is unfortunate that the requirement for performing evoked potential measurements precluded any clinical measurement of reflexes in the same experiments in our work. However, clinical observations by telescope from 200 feet away and, after a few moments, clinical observations as to the presence or absence of the grip reflex reveal no evidence of abnormality even in very high level survived experiments.

The evoked potential changes noted by Weiss and Berger (1982) (32) may or may not represent transient phenomena physiologically equivalent to "concussion". Certainly, the evoked potential changes are transient, but we have only just now begun to perform the experiments which will measure evoked potential changes in humans and simultaneously measure their behavioral or performance correlates. It is very difficult, expensive, and time consuming to measure performance correlates of evoked potential changes in primates and the results would be difficult to interpret. On the other hand, the primate investigation was necessary to determine what to look for in humans.

It is possible that the definition of concussion given above is incorrect. The "morphologically traceless" portion may be incorrect, and the definition perhaps should be changed to state that the morphological findings are those limited to cord fiber damage. This would make Friede's cases fit the definition, but it also raises the question of whether the evoked potential changes noted in our experiments fit the definition since at least some of these could be attributed to temporary compression of fiber tracts as demonstrated by Cusick et al. (1977) (43).

These considerations lead to a proposed family of experimental concussion types in terms of nomenclature:

(1) The clinical syndrome of "true" experimental cerebral concussion due to impact acceleration directly applied to the head, using mainly translational acceleration; which can also be termed also experimental cerebral acceleration concussion sui generis, (2) the clinical syndrome of experimental acceleration concussion with extreme neck stretch due to impact acceleration directly applied to the head, and (3) the clinical syndrome of experimental acceleration concussion with extreme neck stretch due to whole body -X indirect impact acceleration exposures with completely restrained toros but unrestrained head and neck. In the last case, the impact acceleration is transmitted from the sled to the torso via the restraint system and then via the vertebral column to the head. It is possible that this type can also

be produced using other impact vector directions, but there have been no animal experiments which demonstrate this.

The first type, the clinical syndrome of "true" experimental cerebral concussion due to direct impact acceleration is the result of an impact directly transmitted to the freely movable head of an animal via an impactor. Classic examples of this type of injury are experiments using a pendulum (Denny-Brown and Russell, 1941) (40) or a concussion gun (Foltz et al., 1953) (44) (Unterharnscheidt 1958, 1963) (19, 6).

In these experiments, essentially translational (linear) acceleration is applied; a certain neck stretch occurs, but it is of negligible importance and does not produce lesions in the spinal cord between the lower medulla and upper cervical area.

In this context, attention is again directed to Friede's experiments mentioned above in which he stressed the point that symptoms produced in the two experimental conditions - (1) the blow to the head, and (2) the neck stretch - were indistinguishable from each other.

We do not agree with Friede, that in both instances, the same mechanism was responsible for the resulting clinical symptoms.

In single cases, primary traumatic lesions in the spinal cord near the occipito-medullary junction did occur as shown by Denny-Brown and Russell (1941) (40), Unterharnscheidt (1958, 1963) (19, 6), and Friede (1961) (2, 3, 4).

If primary traumatic alterations can be seen macroscopically or microscopically, the diagnosis must be based not on the clinical findings but upon irreversible morphological alterations. This is termed in neuropathology a morphological syndrome with primary traumatic tissue alterations of the enveloping structures of brain and spinal cord or of the brain tissue proper. Such typical primary traumatic tissue alterations are epidural-, subdural-, subarachnoid hemorrhages or hematomas, cortical contusions, traumatic intracerebral or intracerebellar hemorrhages, etc. Quality, distribution, and severity of these primary traumatic lesions are impact-vector and acceleration-level dependent. There exists a continuum from severe lesions to immediate death of the animals.

The experimental stretch experiments of Friede should in our opinion be classified under the second type of experimental concussion, namely the syndrome of experimental acceleration concussion with extreme neck stretch due to directly applied impact acceleration. This syndrome was produced by Friede by a direct blow to the head using a striking device and by neck stretch in a drop test.

If the threshold for reversible clinical disturbances in this type of experimental acceleration concussion with extreme neck stretch is exceeded and we are able to detect primary traumatic lesions in the spinal cord we may not use the diagnosis of concussion unless the definition is modified as we suggest above.

To use the term *contusio spinalis* for this morphological diagnosis is not proper, since we can conclude from the analysis of the injury mechanism and the pathomorphological alterations that in addition to the direct impact of the odontoid against the spinal cord, an additional stretch of the spinal cord at the occipito-medullary junction occurred. The tissue damage is caused by impact and stretch.

The third type, the indirect experimental acceleration concussion with extreme neck stretch due to whole body -X impact acceleration exposures leads to a continuum of reversible neurophysiological disturbances and, with higher exposures, to irreversible tissue damage ranging from unremarkable clinical and morphological findings to tissue indentations by the odontoid process of the axis, to incomplete and complete traumatic transections of the spinal cord between the lower medulla and upper cervical areas and ruptures of both vertebral arteries and concomitant subarachnoid and subdural hemorrhages at the base of the brain and in the cervical spinal cord, in some cases, extending into the thoracic and lumbar spinal cord. Only when a detailed histological examination of the tissue specimen does not reveal any macroscopic or microscopic traumatic alterations can this syndrome be considered an experimental acceleration concussion with extreme neck stretch due to whole body -Gx indirect acceleration exposures with completely restrained torso but unrestrained head and neck, unless the proposed revised definition of concussion considered earlier is agreed upon.

In this type, additional neurophysiological data, using somatosensory recordings, etc., may produce other objective findings of reversible disorders.

If the threshold to produce primary traumatic alterations is exceeded we must term these tissue alterations: (1) primary traumatic spinal tissue indentations due to the odontoid process of the axis, and with higher acceleration levels (2) incomplete or complete traumatic transections of the spinal cord between lower medulla oblongata and upper cervical area, eventually with rupture of both vertebral arteries and concomitant subarachnoid and subdural hemorrhages at the base of the brain and the cervical spinal cord.

It is important to stress the point that the quality of the primary traumatic lesions is dosage related; it changes with increments of acceleration levels.



It is possible that a distinction should also be made between the terms cerebral concussion, concussion and commotio cerebri. This area of nomenclature is important because clinicians use one terminology and experimenters another.

Cerebral concussion may be a misnomer except for type one cases. While the symptoms and, therefore, the clinical condition or diagnosis may be identical, it is highly probable that concussion, as pointed out by Friede, can be caused either by direct impact to the head without appreciable neck stretch, or by neck stretch alone without appreciable impact to the head. Therefore, the term cerebral concussion should be used only in cases where very little neck stretch occurred in direct impacts to the head. Commotio cerebri is a clinical term which is frequently used as a synonym for cerebral concussion. The main clinical symptom is immediate unconsciousness. Concussion with neck stretch and no head impact, while clinically indistinguishable from cerebral concussion, is caused by a different mechanism and should never be termed cerebral concussion.

The final definition of concussion by objective criteria of diagnosis must await further experiments. Certainly, the definition of human concussion in terms of "unconsciousness" which in itself is poorly defined physiologically, neurophysiologically and morphologically leaves much to be desired.

We do not agree with Friede that the problem of the clinical syndrome of commotio cerebri can be answered only by human neuropathology. Animal experiments can be used to answer this question, also. In animal experiments, with direct impact of the head against an object using a sled, or using a compressed air gun with an impactor applying linear acceleration, we were able to determine the threshold for producing the clinical symptoms of cerebral concussion (Unterharnscheidt 1958, 1963) (19, 6). Extensive histological examination of the specimens using different survival times and staining techniques failed to reveal any primary or secondary traumatic alterations in brain or spinal cord. There was a complete absence of traumatic lesions at the atlanto-occipital junction. In our opinion, the clinical syndrome of cerebral concussion in animal experiments and the clinical syndrome of commotio cerebri in humans are the result of inertial forces. We do not know the physiological mechanisms which lead to unresponsiveness in animals and altered consciousness in humans. The impacting kinetic energy must produce a certain acceleration with subsequent inertial phenomena which have to reach a certain (known) threshold to produce a clinical syndrome of cerebral concussion or commotio cerebri. There are no pathomorphological findings detectable using the classical light microscopical staining techniques; morphologically, the effects are traceless, as Spatz remarked (personal communication, 1961) (45).

If the histological examination of the CNS of an animal subjected to acceleration concussion shows primary traumatic lesions; e.g., hemorrhages; we can no longer use the diagnosis experimental cerebral concussion; we have to diagnose this entity a contusio cerebri, which is a pathological diagnosis, and describes primary traumatic alterations due to the application of a mechanical load. The inertial data show that the threshold in such a case is higher than that required to produce a cerebral concussion. Therefore, it is imperative that in these animal experiments, exhaustive histopathological examination under standardized conditions be carried out.

H. Adams (1975) (46) discussed the morphological findings of Friede; he wrote: "It has been suggested by Friede (1961) (2, 3, 4) that direct damage to nerve fibers in the upper cervical spinal cord as a result of shear strains of the cranio-cervical junction is a factor in the production of concussion in various experimental animals. It might, therefore, be thought that similar damage would be observed in man, but in a series of 32 fatal blunt head injuries, the author has not been able to find significant numbers of retraction balls or microglial scars in serial blocks of the lower medulla and the upper three cervical segments of the spinal cord (H. Adams 1975)."

Unfortunately, H. Adams presents no details as to which types of fatal blunt head injuries he examined. Many fatal head injuries with a direct impact to the head lead to negligible neck stretch. It would be essential, indeed, to expand the histological examination of the lower medulla and the upper cervical spinal cord of humans to those fatal head injury types with extreme neck stretch.

As to the significance of rotation as a cause of experimental concussion, the experiments carried out by Friede on cats using a device which rotated the heads fore and aft neither produced clinical symptoms of concussion nor neuropathological evidence of damage in the brain and spinal cord. We fully agree with Friede that rotational acceleration does not produce the symptoms of a "true" cerebral concussion, but typical pathomorphological alterations may develop if the threshold for tissue damage is exceeded. The primary traumatic lesions found after rotational acceleration differ in regard to quality and distribution from those seen after translational (linear) acceleration as noted previously in some detail.

In conclusion, it appears that each vector direction of impact acceleration produces a different and predictable type of injury in regard to quality and distribution. This was demonstrated in the experiments where the translational (linear) and rotational acceleration were translated directly to the head (Unterharnscheidt, 1958, 1963, 1970, 1971, 1972, 1975) (19, 6, 47, 48, 49, 50) Unterharnscheidt and Higgins (1969) (8, 9, 10); Ripperger, and Unterharnscheidt (1973) (51) and indirect rotational acceleration was applied Unterharnscheidt et al. (1977) (52); (Unterharnscheidt (1982) (53), and Unterharnscheidt (1973) (51).

Rotational acceleration can be caused by a direct impact to the head, a so-called contact injury when a part of the animal, for example the head, comes in contact with a rigid structure or impactor, by acceleration of the restrained torso while head and neck remain unrestrained (whiplash type injury or indirect impact, i.e., -Gx) or by applying direct rotational acceleration to a helmet in which the monkey's head can be secured; for example, using Head Acceleration Device II (HAD-II).

The specific neuropathological injury pattern in -Gx acceleration transmitted indirectly to the head via the vertebral column consists of tissue damage at the zone of maximum stretch at the atlanto-occipital junction and if the threshold is reached, incomplete and complete traumatic transection of the spinal cord and ruptures of both vertebral arteries and concomitant basilar and spinal subarachnoid and subdural hemorrhages.

Furthermore, at peak sled acceleration levels low enough that neither incomplete nor complete transections occurred, a local indentation of tissue was seen at the ventral fissure, apparently caused by direct impact of the tip of the odontoid process of the axis. This local indentation generally produced acute traumatic alterations only in the ventral fasciculi of the spinal cord. Upon these immediate traumatic lesions are superimposed another traumatic alteration which develops only after an interval, but which also was due to the same impact of the odontoid process on the cord. This later alteration consisted of lesions in the grey substance which led to what may be termed progressive central hemorrhagic necrosis.

In some instances, subdural hemorrhages over both cerebral hemispheres due to ruptured bridging veins were seen, probably as the result of rotational acceleration.

As we have demonstrated before (Unterharnscheidt 1958, 1963, 1970, 1972; Unterharnscheidt and Higgins, 1969), a neurophysiological and neuropathological continuum from no lesions to severe and lethal ones can be demonstrated, described and quantified. The head-neck and brain-cord systems can be described by input-output relationships. Each effective mechanical input to the head and neck corresponds to a predictable and typical morphological end state.

The experiments show very convincingly that more neuropathological examinations, especially of the area between lower medulla and upper cervical spinal cord, must be carried out as a routine procedure in forensic medical examinations. Again, the typical dissection which separates the brainstem from the cervical spinal cord, destroys the most important area. A myelotome, described by Pick, or deliberate tissue saving preparation techniques should be used or developed.

#### RECOMMENDATIONS

As Ewing and Unterharnscheidt (1976) (25) stated, present instructions for Naval autopsies after aircraft accidents are not mandatory and are in effect only routing instructions for the results (54, 55, 56, 57). X-rays are not mandatory for any autopsy case but only for all ejections, ditchings, or crash landings where "significant forces were present."

Recommendations for standardization of autopsy procedures in aircraft accident victims, described from these studies, were outlined by Ewing and Unterharnscheidt (1976) (25).

As a result of our studies, it is recommended that a more comprehensive autopsy be performed, but not be limited to a detailed gross and microscopic examination of all injured organs. In these experiments, as well as those of Friede, the area between lower medulla oblongata and upper cervical spinal cord (i.e., the atlanto-occipital junction) was shown to be the zone of the most extensive stress. Therefore, the brain and spinal cord down to the cauda equina must be removed in toto, leaving the unopened dura mater on the specimen. This is quite important because the level of cranio-cervical junction is suspected as a frequent site of fatal injury in Naval aircraft accidents, but ordinary autopsy procedures destroy this vital area.

#### REFERENCES

1. Ewing, C. L.: Concussion in Naval Aviation: A working paper on the problem. November 1964, unpublished.
2. Friede, R.L.: Specific cord damage at the atlas level as a pathogenic mechanism in cerebral concussion. *J. Neuropathol. Exper. Neurol.*, 19:266, 1960.
3. Friede, R.L.: Experimental acceleration concussion. *Pathology and mechanics.* *Arch. Neurol.*, 4:449, 1961.
4. Friede, R.L.: The Pathology and Mechanics of Experimental Cerebral Concussion. Wright Air Development Division, Air Research and Development Command, United States Air Force, Wright-Patterson Air Force Base, Ohio. WADD Technical Report 61-256, March 1961.
5. Rawlins, J.S.P., Delorme, Seris, and Riddel, I.T.S.: Essais Franco-Britanniques de mesure de vitesse de coulée des avions. (Franco-British Study: Sinking Rate Tests. Measurements of Sinking Rate of Aircraft). Report No. 1 (75104). French Ministry of the Armed Forces (Air), Technical and Industrial Directorate, Flight Tests Center, Registration No. 14, 20 February 1964.

6. Unterharnscheidt, F.: Die gedeckten Schäden des Gehirns. Experimentelle Untersuchungen mit einmaliger, wiederholter und gehäufte stumpfer Gewalt-einwirkung auf den Schädel. Monographien aus dem Gesamtgebiet der Neurologie und Psychiatrie. Heft 103, Berlin, Göttingen, Heidelberg, Springer, 1963.
7. Sellier, K., and Unterharnscheidt, F.: Mechanik und Pathomorphologie der Hirn-schäden nach stumpfer Gewalteinwirkung auf den Schädel. Hefte zur Unfallheilkunde, Heft 76, Berlin, Göttingen, Heidelberg, Springer, 1963.
8. Unterharnscheidt, F., and Higgins, L.S.: Traumatic lesions of brain and spinal cord due to non-deforming angular acceleration of the head. Texas Rep. Biol. Med., 27:127, 1969.
9. Unterharnscheidt, F., and Higgins, L.S.: Pathomorphology of experimental head injury due to rotational acceleration. Acta Neuropath., 12:200, 1969.
10. Unterharnscheidt, F., and Higgins, L.S.: Neuropathologic effects of translational and rotational acceleration of the head in animal experiments. In: The Late Effects of Head Injury. Walker, A.E.; Caveness, W.F., and Critchley, McD. (Edits.). Springfield, Thomas, 1969, pp 158-167.
11. Unterharnscheidt, F., and Ripperger, E.A.: Mechanics and pathomorphology of impact-related closed brain injuries. In: Dynamic Response of Biomechanical Systems. Perrone, N. (Edit.) ASME Monograph. New York, American Society of Mechanical Engineers, 1970, pp 46-83.
12. Dohrmann, G.J.: Experimental spinal cord trauma. A historical review. Arch. Neurol., 27:468, 1972.
13. Ducker, T.B.: Experimental injury of the spinal cord. In: Handbook of Clinical Neurology, Vol. 25, Chapt. 2. Vinken, P.J., and Bruyn, G.W. (Edits.) in collab. with Braakman, R., Amsterdam, North Holland Publ. Co., 1976, pp 9-26.
14. Goodkin, R.: Experimental injuries of the spine. In: Handbook of Clinical Neurology. Vol. 25., Chapter 1. Vinken, P.J. and Bruyn, G.W. (Edits). Amsterdam, Oxford, North Holland Publ. Co. 1976, pp 1-8.
15. Osterholm, J.L.: The pathophysiological response to spinal cord injury. J. Neurosurg. 40:5, 1974.
16. Osterholm, J.L.: The Pathophysiology of Spinal Cord Trauma. Springfield, Thomas, 1978.
17. Stapp, J.P.: Human Exposure to Linear Deceleration, Part 2. The Forward-Facing Position and the Development of a Crash Harness. WADC TR5915, Part 2, Wright Air Development Center, Wright-Patterson AFB, 1951.
18. Stapp, J.P.: Historical review of impact injury and protection research. In: Impact Injury of the Head and Spine. Chapt. 1. Ewing, C.L., Thomas, D.J., Sances, A., and Larson, S.J. (Edits.). Springfield, Thomas, 1982.
19. Unterharnscheidt, F.: Experimentelle Untersuchungen über die Schädigungen des ZNS durch gehäufte stumpfe Schädeltraumen. Zbl. Ges. Neurol., 147:14, 1958.
20. Clarke, T.D., Sprouffske, J.F., Trout, E.M., Gragg, C.D., Muzzy, W.H., and Klopfenstein, H.S.: Baboon tolerance to linear deceleration (-G<sub>x</sub>): Air bag restraint. Paper 700 905. Proceedings, 14th Stapp Car Crash Conference, New York, SAE, 1970, pp 263-278.
21. Clarke, T.D., Sprouffske, J.F., Trout, H.S., Klopfenstein, W.H., Muzzy, W.H., Gragg, C.D., and Bendixen, C.D.: Baboon tolerance to linear deceleration (-G<sub>x</sub>): Lap belt restraint. Paper 700 906. Proceedings, 14th Stapp Car Crash Conference, New York, SAE, 1970, pp 279-298.
22. Clarke, T.D.; Gragg, C.D.; Sprouffske, J.F., and Trout, E.M.: Human head linear and angular accelerations during impact. Paper 710 857. Proceedings, 15th Stapp Car Crash Conference, Coronado, CA, 17-19 November 1971. New York, SAE, 1971, pp 1K-12K.
23. Clarke, T.D.; Smedley, D.C.; Muzzy, W.H.; Gragg, C.D.; Schmidt, R.E., and Trout, E.M.: Impact tolerance and resulting injury patterns in the baboon Air Force shoulder harness-lap belt restraint. Paper 720 974. Proceedings, 16th Stapp Car Crash Conference, Detroit, MI, 8-10 November 1972. New York, SAE, 1972, pp 365-411.
24. Alderman, J.L., Osterholm, J.L., D'Amore, B.R., and Williams, H.D.: Catecholamine alterations attending spinal cord injury: A reanalysis. J. Neurosurg. 6:41, 1980.
25. Ewing, C.L., and Unterharnscheidt, F.: Neuropathology and cause of death in U.S. Naval aircraft accidents. Paper presented at the Aerospace Medical Panel Specialists' Meeting held in Copenhagen, Denmark, 5-9 April 1976. AGARD Conference Proceedings No. 190, B 16-1-6, Recent Experience/ Advances in Aviation Pathology, December 1976.

26. Unterharnscheidt, F., and Ewing, C.L.: Potential relationship between human central nervous system injury and impact forces based on primate studies. Paper presented at the Aerospace Medical Panel Specialists' Meeting, held in Paris, France, AGARD Conference Proceedings No. 253, A18-1-6; Models and Analogues for the Evaluation of Human Biodynamic Response, Performance and Protection, Paris, France, 6-10 November 1978.
27. Becker, E.B.: A photographic data system for determination of 3-dimensional effects of multiaxis impact acceleration on living humans. Proceedings Society of Photo-Optical Instrumentation Engineers, Vol. 57. Palos Verdes Estates, 1975.
28. Becker, E.B.: Stereoradiographic measurements for anatomically mounted instruments. Proceedings, 21st Stapp Car Crash Conference, SAE, Warrendale, PA., October 1977.
29. Ewing, C.L., and Thomas, D.J.: Human Head and Neck Response to Impact Acceleration. Naval Aerospace Medical Research Laboratory Monograph, No. 21, August 1971.
30. Becker, E.B. and Willems, G.: A validated method for instrumental measurement of human head and neck response to impact acceleration. Proceedings, 19th Stapp Car Crash Conference, SAE, Warrendale, PA, 1975.
31. Willems, G.: A detailed performance evaluation of subminiature piezoresistive accelerometers. Presented to the 23rd International Instrumentation Symposium in Las Vegas, 1-5 May 1977. Proceedings of Instrumentation in the Aerospace Industry. Vol. 23, Instrument Society of America. Pittsburgh, PA, pp 531-540.
32. Berger, M.D., and Weiss, M.S.: Effects of impact acceleration on somatosensory evoked potentials. In: Impact Injury of the Head and Spine. Chapt. 11. Ewing, C.L., Thomas, D.J., Sances, A., and Larson, S.J. (Edits.). Springfield, Thomas, 1982.
33. Saltzberg, B.; Burton, W.D.; Weiss, M.S.; Berger, M.D.; Ewing, C.L.; Thomas, D.J.; Jessop, M.E.; Sances, A.; Larson, S.J.; Walsh, P.R.; and Myklebust, J.: Dynamic tracking of evoked potential changes in studies of central nervous system injury due to impact acceleration. Chapt. 10. In: Impact Injury of the Head and Spine. Chapt. 10. Ewing, C.L., Thomas, D.J., Sances, A., and Larson, S.J. (Edits.). Springfield, Thomas, 1982.
34. Sances, A., Weber, R., Myklebust, J., Cusick, J., Larson, S., Walsh, P., Christoffel, T., Mouterman, C., Ewing, C.L., Thomas, D., and Saltzberg, B.: The evoked potential: An experimental method for biomechanical analysis of brain and spinal injury. Proceedings, 24th Stapp Car Crash Conference. October 1980.
35. Sances, A., Myklebust, J., Larson, S.J., Cusick, J.F. and Weber, R.: The evoked potential - a biomechanical tool. Chapt. 7. In: Impact Injury of the Head and Spine. Ewing, C.L., Thomas, D.J., Sances, A., and Larson, S.J. (Edits.). Springfield, Thomas, 1982.
36. Thomas, D.J., and Jessop, M.E.: Experimental head and neck injury. In: Impact Injury of the Head and Spine. Chapt. 5. Ewing, C.L., Thomas, D.J., Sances, A., and Larson, S.J. (Edits.). Springfield, Thomas, 1982.
37. Berringer, O.M., Browning, F.M. and Schroeder, C.R.: An Atlas and Dissection Manual of Rhesus Monkey Anatomy. Tallahassee, Florida, Anatomy Laboratories Aids, 1968.
38. Hartman, C.G. and Straus, W.L.: Anatomy of the Rhesus Monkey. Baltimore, Williams and Wilkins, 1965.
39. Allen, A.R.: Remarks in histopathological changes in spinal cord due to impact. An experimental study. J. Nerv. Ment. Dis., 41:141, 1914.
40. Denny-Brown, D., and Russell, R.: Experimental cerebral concussion. Brain, 64:93, 1941.
41. Jakob, A.: Experimentelle Untersuchungen über die Schädigungen des Zentralnervensystems (mit besonderer Berücksichtigung der Commotio cerebri mit Commotionsneurose). In: Histologische und histopathologische Arbeiten über die Grosshirnrinde. Nissl, F., and Alzheimer, A. (Edits.). 5:182, 1913.
42. Peters, G.: Über gedeckte Gehirnverletzungen (Rindenkontusion) im Tierversuch. Zbl. Neurochir. 8:172, 1943.
43. Cusick, J.F., Ackmann, J.J., and Larson, S.F.: Mechanical and physiological effects of dentatomy. J. Neurosurg. 46:767, 1977.
44. Foltz, E.L., Jenkner, F.L., and Ward, A.A.: Experimental cerebral concussion. J. Neurosurg., 10:342, 1953.
45. Spatz, H.: Personal communication, 1961.
46. Adams, H.: Neuropathology of head injuries. In: Handbook of Clinical Neurology, Vol. 23, Chapt. 3. Vinken, P.J., and Bruyn, G.W. (Edits.) in collab. with Brackman, R., Amsterdam, North Holland Publ. Co., 1975, pp 35-65.

47. Unterharnscheidt, F.: Mechanics and pathomorphology of closed head injuries. Proceedings, Impact Injury and Crash Protection. 9-10 May 1968, Wayne State University, Detroit. Gurdjian, E.S., Lange, W.L., Patrick, L.M., and Thomas, L.M. (Edits.). Springfield, Thomas, 1970, pp 43-62.
48. Unterharnscheidt, F.: Translational versus rotational acceleration - animal experiments with measured input. In: Proceedings, 15th Stapp Car Crash Conference, Coronado, CA. 16-18 November 1971, pp 767-770.
49. Unterharnscheidt, F.: Mechanogenese und Pathomorphologie der traumatischen Hirnschäden. Z. Rechtsmedizin/J. Leg. Med., 71:153, 1972.
50. Unterharnscheidt, F.: Injuries due to boxing and other sports. In: Handbook of Clinical Neurology, Vol. 23., Chapt. 26. Vinken, P.J., and Bruyn, G.W., (Edits.) in collab. with Brackman, R. Amsterdam, North Holland Publ. Co., 1975, pp 527-593.
51. Ripperger, E.A., and Unterharnscheidt, F.: Prototypes of head injuries: Application to animal experiments. International Conference on the Biokinetics of Impact, Amsterdam, 26-27 June 1973.
52. Unterharnscheidt, F., Ewing, C.L., Thomas, D.J., Jessop, M.E., Rogers, J.E., and Willems, G.: Preliminary report on the neuropathological findings in Rhesus monkeys undergoing short duration -Gx acceleration. Abstracts, No. 201, 6th International Congress of Neurological Surgery. Sao Paulo, Brazil, 19-25 June 1977, p 80.
53. Unterharnscheidt, F.: Neuropathology of the rhesus monkey undergoing -Gx impact acceleration. In: Impact Injury of the Head and Spine. Chapt. 4. Ewing, C.L., Thomas, D.J., Sances, A., and Larson, S.J. (Edits.). Springfield, Thomas, 1982.
54. OPNAV Instr. 3760.6K. Navy Aircraft Accident, Incidents, and Ground Accident Reporting Procedures. Navy Department, Office of the Chief of Naval Operations. 25 September 1975.
55. BUMED Instruction 6510.6 series.
56. NAVMED P 5065. Autopsy Manual.
57. SCHAVMED P-19. Manual of Aviation Pathology. U.S. Naval Aerospace Medical Institute, U.S. Naval Aviation Center, Pensacola, FL, 5 December 1962.
58. Sheldon, J.J.: Blood vessels of the scalp and brain. In: Clinical Symposia Ciba, Vol. 33, No. 5, 1981.
59. Ommaya, A., Faas, F., and Yarnell, P.: Whiplash injury and brain damage. J. Amer. Med. Ass. 204:285, 1968.

#### ACKNOWLEDGEMENTS

This project was supported in part by a contract with the Office of Naval Research, Biophysics Program, Washington, D.C., Contract N000 14-78-C0800, and by the Naval Medical Research and Development Command.

Opinions or conclusions contained in this chapter are those of the author and do not necessarily reflect the view or the endorsement of the U.S. Navy nor the sponsoring organizations.

The animals used in this study were handled in accordance with the Guide for the Care of Laboratory Animals, prepared by the Committee of Care and Use of Laboratory Animal Resources, National Research Council.

Sled Parameters				Peak Head Parameters				Results							
Run No.	Animal No.	Peak Sled Acceleration		Dur. msec	Rate of Angular Onset msec	Angular Acceleration Rad/sec <sup>2</sup>	Linear Acceleration msec		Angular Velocity Resultant	Restraint Type	Julian Date	Day of Run	Disposition	Radiological Findings	Gross Neuropathological Findings
		G max	C max				Acceleration	Angular							
3024	4107	10.0		54.4	950				Harness vest	272.78	1	Sacr. 1 d	Normal	No traumatic transection	
3008	0761	21.2							Harness vest	195.78	1				
3009		81.3							Harness vest	195.78	1				
3010		98.3							Harness vest	195.78	1				
3017		21.3			No Inertial Data				Harness vest	200.78	6				
3018		60.1							Harness vest	200.78	6				
3019		42.5							Harness vest	200.78	6				
3020		21.0							Harness vest	200.78	6	Sacr. 7 d	Normal	No traumatic transection	
3027	4114	10.4		49.6	4630	4100	335	42.5	Harness vest	284.78	1				
3028		41.6		24.0	1804		1010	110.8	Harness vest	284.78	1	Sacr. 20 d	Normal	No traumatic transection	
3699	8872	4.3		1.0	352	3200	188	44.0	Harness vest	253.80	1				
3700		5.2		59.6	1453	880	98	19.8	Harness vest	254.80	2				
3701		44.5		25.5	2154	17600	1130	130.0	Harness vest	254.80	2				
3702		44.3		26.3	2201	28800	1060	140.0	Harness vest	254.80	2	Sacr. 11 d	Normal	No traumatic transection	
3695	NA28	10.0		54.9	664	2800	200	40.0	Harness vest	247.80	1				
3696		5.6		53.0	2138	650	90	15.0	Harness vest	248.80	2				
3697		45.0		26.4	2423	16800	900	110.0	Harness vest	248.80	2				
3698		44.5		27.3	1449	18500	1010	114.0	Harness vest	248.80	2	Sacr. 13 d	Normal	No traumatic transection	
3710	NA02	9.9		55.6	641	1120	220	13.9	Harness vest	262.80	1				
3713		10.0		51.0	753	2050	275	29.5	Harness vest	266.80	5				
3714		61.1		17.6	3381	9500	1660	55.0	Harness vest	266.80	5				
3715		61.1		18.3	3677	12700	1340	89.0	Harness vest	266.80	5	Sacr. 10 d	Normal	No traumatic transection	

TABLE 1

Sled Parameters				Peak Head Parameters				Results						
Run No.	Animal No.	Peak Sled		Rate of Onset	Angular Acceleration Rad/sec <sup>2</sup>	Linear		Angular Velocity Resultant	Restraint Type	Julian Date	Day of Run	Disposition	Gross Findings	
		Acceleration	G max			Acceleration msec	msec						Radiological Findings	Neuropathological Findings
3183	8824	10.5	48.9	558	1400	95	11.3	11.3	Harness vest	66,79	1	Sacr. 16 d	Normal	No traumatic transection
3184		62.4	21.5	4111	16000	1475	76.0	76.0						
3703	8802	10.1	53.3	661	3700	170	51.0	51.0	Harness vest	255,80	1			
3704		5.3	76.7	1739	660	56	23.0	23.0		255,80	2			
3705		64.3	17.6	3672	23000	1390	123.0	123.0		256,80	2			
3706		63.7	18.7	3786	24000	1460	122.0	122.0		256,80	2	Sacr. 12 d	Normal	No traumatic transection
3691	0012	10.1	61.2	1470	1850	143	37.5	37.5	Harness vest	255,80	1			
3692		5.3	56.0	986	1100	72	24.6	24.6		255,80	5			
3693		74.2	16.3	4398	16500	1500	92.0	92.0		255,80	5			
3694		78.3	16.1	5111	32000	1500	158.0	158.0		255,80	5	Sacr. 7 d	Normal	Subarachnoid hemorrhages around basilar artery & both vertebral arteries. Local indentation and brownish discoloration of ventral surface between lower medulla oblongata and upper cervical spinal cord; recent and old traumatic alterations in the grey and white substance.

Sled Parameters				Peak Head Parameters				Results						
Run No.	Animal No.	Peak Sled		Dir. msec	Rate of Onset	Angular Acceleration Rad/sec <sup>2</sup>	Acceleration msec	Linear Velocity Resultant	Angular Velocity Resultant	Restraint Type	Julian Day of Run	Disposition	Radiological Findings	Gross Neuropathological Findings
		G	max											
3185	8857	10.2	52.2	641	1310	16?	24.0	Harness	71,79	1				
3186		82.7	15.7	6287	37000	2200	215.0	vest	71,79	1		Sacr. 16 d	Normal	No traumatic transection
1892	3948	83.7	17.1	7342	20700	1630	137.0	Rigid	87,77	1		Sacr. 9 d	Normal	No traumatic transection
1891	3943	83.8	15.8	6334	30000	1950	148.0	Rigid	83,77	1		Sacr. 15 d	Normal	No traumatic transection.
3707	8790	10.0	47.0	726	1050	210	11.0	Harness	260,80	1				
3708		5.2	73.5	1805	1020	81	23.8	vest	261,80	2				
3709		87.9	15.3	5660	34000	2200	145.0		261,80	2		Acutely fatal	Incomplete traumatic separation C <sub>1</sub> /C <sub>2</sub> complete	No traumatic transection Local indentation and brownish discoloration of ventral surface of the specimen between lower medulla oblongata and upper cervical spinal cord; after dissection: recent, mostly centrally located hemorrhage.
3187	8863	10.2	52.2	612	1470	175	19.5	Harness	73,79	1				
3188		104.5	13.7	8180	29000	2600	120.0	vest	73,79	1		Sacr. 12 d	Normal	Indentation of ventral surface between lower medulla oblongata and upper cervical spinal cord. No discoloration, but circumscribed decreased consistency of tissue.

Acutely fatal

Incomplete traumatic separation C<sub>1</sub>/C<sub>2</sub> complete

No traumatic transection

Local indentation and brownish discoloration of ventral surface of the specimen between lower medulla oblongata and upper cervical spinal cord; after dissection: recent, mostly centrally located hemorrhage.

Indentation of ventral surface between lower medulla oblongata and upper cervical spinal cord. No discoloration, but circumscribed decreased consistency of tissue.



Sled Parameters				Peak Head Parameters				Results					
Run No.	Animal No.	Peak Sled Acceleration		Dur. msec	Rate of Onset	Angular Acceleration		Restraint Type	Julian Date	Day of Run	Disposition	Radiological Findings	Gross Neuropathological Findings
		G max	C max			Rad/sec <sup>2</sup>	Linear Acceleration msec						
3189	8866	10.3	56.6	1578	2600	182	35.0	Harness	74,79	1			
3191		10.2	55.0	671	1240	228	17.0	vest	80,79	7			
3192		105.3	13.6	8769	22500	2380	95.0		80,79	7	Acutely fatal	Basilar skull fracture	Incomplete traumatic transection
1894	3933	108.6	14.6	9303	27600	2550	133.0	Rigid	89,77	1	Sacr. 20 d	Normal	No traumatic transection.
1081	3921	10.3	49.6	1533	1190	147	15.2	Rigid	227,75	1			
1082		39.8		872	4300	665	28.6		227,75	1			
1083		38.3	27.2	3512	2005	650	12.8		232,75	6			
1084		38.5	27.3	3832	6800	625	54.0		232,75	6			
1085		38.2	26.9	3478	3200	635	25.6		234,75	8			
1086		39.4	27.3	3829	3450	640	28.9		234,75	8			
1087		39.6	26.6	3.75	5700	730	44.0		234,75	8			
1364		36.9	26.5	1612	5650	680	55.5		68,76	198	Acutely fatal	Atlanto-occipital separation	Complete traumatic transection
1365		108.7	18.5	13398	52000	9200	350.0		68,76	198			
1893	3924	110.4	14.2	9304	31000	2400	140.0	Rigid	88,77	21	Sacr. 21 d	Normal	No traumatic transection.
1562	3935	105.5	21.0	17949	38000	4100	120.0	Rigid	63,76	1	Moribund, euthanized after 90 hours	Normal	No traumatic transection, but central hemorrhagic necroses bilaterally.
1563		123.0	18.7	20762	23000	2000	105.0		63,76	1			

Sled Parameters				Peak Head Parameters				Results					
Run No.	Animal No.	Peak Sled		Rate of Angular Onset	Acceleration Rad/sec <sup>2</sup>	Linear		Restraint Type	Julian Date	Day of Run	Disposition	Gross Findings	
		G max	Dur. msec			Acceleration msec	Angular Velocity Resultant					Neuropathological Findings	Findings
3006	0764	21.5						Harness vest	194,78	1			
3007		80.4							194,78	1			
3011		20.9							199,78	6			
3012		20.8		No Inertial Data					199,78	6			
3013		60.0							199,78	6			
3014		80.9							199,78	6			
3015		97.0							199,78	6	Acutely fatal	Incomplete traumatic transection	
3016		124.2							199,78	6			
1889	4101	34.8	27.5	1614	9700	1460	132.0	Harness vest	77,77	1			
1890		33.3	28.1	1561	5700	615	48.0		77,77	1			
1898		32.5	28.9	1585	4000	670	43.0		79,77	3			
1899		32.5	27.9	1413	3450	580	40.0		79,77	3			
1900		74.8	16.8	5690	14500	1540	90.0		101,77	25			
1901		74.7	16.9	5418	13500	1680	78.0		101,77	25			
1902		75.6	17.1	6232	5750	1770	32.0		103,77	27			
1903		75.3	17.2	6308		1990	40.0		103,77	27	Acutely fatal	Incomplete traumatic transection	
1905		126.4	13.6	13814		2810	53.0		103,77	27			
3031	4115	127.3		No Inertial Data				Harness vest	289,78	1	Acutely fatal	Basilar skull fracture	No traumatic transection.
3025	3923	9.8	51.9	599	2825	148	44.0	Harness vest	275,80	1	Acutely fatal	Atlanto-occipital separation	Complete traumatic transection
3026		127.4	13.2	12922		4300	170		275,80	1			

Sled Parameters				Peak Head Parameters				Results			
Peak Sled		Linear		Angular		Disposition		Radiological Findings		Gross Findings	
Run No.	Animal No.	Acceleration G max	Dur. msec	Rate of Angular Acceleration Rad/sec <sup>2</sup>	Onset msec	Velocity Resultant	Restraint Type	Julian Date	Day of Run	Disposition	Radiological Findings
1359	4099	106.9	19.2	16586		2750	Rigid	58,76	1	Acutely fatal	C/C <sub>2</sub> traumatic separation
1360		128.2	17.2	21427		5200		58,76	1		Complete traumatic transection; subdural hemorrhage of both cerebral hemispheres, right lateral.
1895	3951	130.7	12.9	12698		2880	Rigid	94,77	1	Acutely fatal	Basilar skull fracture
1896	3946	131.4	13.6	14980		2490	Rigid	95,77	1	Acutely fatal	Atlanto-occipital separation
0454	3146	24.0					Rigid	276,74	1		
0650		22.7						9,55	99		
0651		25.9						9,75	99		
0653		50.7						14,75	104		
0654		51.3						14,75	104		
0656		28.7						16,75	106		
0657		108.8						16,75	106		
0659		56.5						21,75	111		
0660		107.5						21,75	111		
0661		158.4						23,75	113		
3032	3936	125.0	13.1	11540		2200	Rigid	290,80	1	Acutely fatal	Atlanto-occipital separation
3033		162.8	11.8	18719		24000	Rigid	298,80	1	Acutely fatal	Complete traumatic transection

Animal No.	Peak Sled Acceleration G max	Disposition	Radiological Findings	Gross Neuropathological Findings
4107	10.0	Surv, no pathology	Normal	No traumatic transection
0761	21.0	Surv, no pathology	Normal	No traumatic transection
4114	41.6	Surv, no pathology	Normal	No traumatic transection
8872	44.3	Surv, no pathology	Normal	No traumatic transection
NA28	44.5	Surv, no pathology	Normal	No traumatic transection
NA02	61.6	Surv, no pathology	Normal	No traumatic transection
8824	62.4	Surv, no pathology	Normal	No traumatic transection
8802	63.7	Surv, no pathology	Normal	No traumatic transection
0012	78.3	Surv, with pathology	Normal	Indentation & discoloration at C <sub>1</sub> subarachnoid hemorrhage around basilar and ventral arteries.
8857	82.7	Surv, no pathology	Normal	No traumatic transection.
3948	83.7	Surv, no pathology	Normal	No traumatic transection.
3943	83.8	Surv, no pathology	Normal	No traumatic transection.
8790	87.9	AF	ITS, C <sub>1</sub> /C <sub>2</sub>	Indentation & discoloration at C <sub>1</sub> central hemorrhagic necrosis.
8863	104.5	Surv, with pathology	Normal	Indentation at C <sub>1</sub> ; no discoloration. Decreased consistency of tissue.
8866	105.3	AF	BSF	Incomplete traumatic transection.
3933	108.6	Surv, no pathology	Normal	No traumatic transection.
x 3921	108.7	AF	AOS	Complete traumatic transection. x
x 3924	110.4	Surv, no pathology	Normal	No traumatic transection. x
x 3935	123.0	Euthanasin, 90 hours	Normal	No traumatic transection, but x
x				central hemorrhagic necrosis. x
x 0764	124.2	AF	AOS	Incomplete traumatic transection. x
x 4101	126.4	AF	AOS	Incomplete traumatic transection. x
x 4115	127.3	AF	BSF	No traumatic transection. x
x 3923	127.4	AF	AOS	Complete traumatic transection. x
x 4099	128.2	AF	TS, C <sub>1</sub> /C <sub>2</sub>	Complete traumatic transection. x
x 3951	130.7	AF	BSF	Incomplete traumatic transection. x
x 3946	131.4	AF	AOS	Complete traumatic transection. x
x 3146	158.4	AF	AOS	Complete traumatic transection, x
x				and old indentation and discoloration at C <sub>1</sub> . x
x 3936	162.8	AF	AOS	Complete traumatic transection. x

AF - Acutely fatal  
ITS - Incomplete traumatic transection  
BSF - Basilar skull fracture  
AOS - Atlanto-occipital separation  
TS - Traumatic separation

----- Peak sled accelerations which do not produce traumatic transections of the cord.

..... Threshold zone, where traumatic lesions in single cases may or may not occur.

----- Peak sled accelerations in which indentations of cord tissue due to the odontoid process may occur.

xxxxxxx Peak sled accelerations which cannot be survived.

TABLE 2

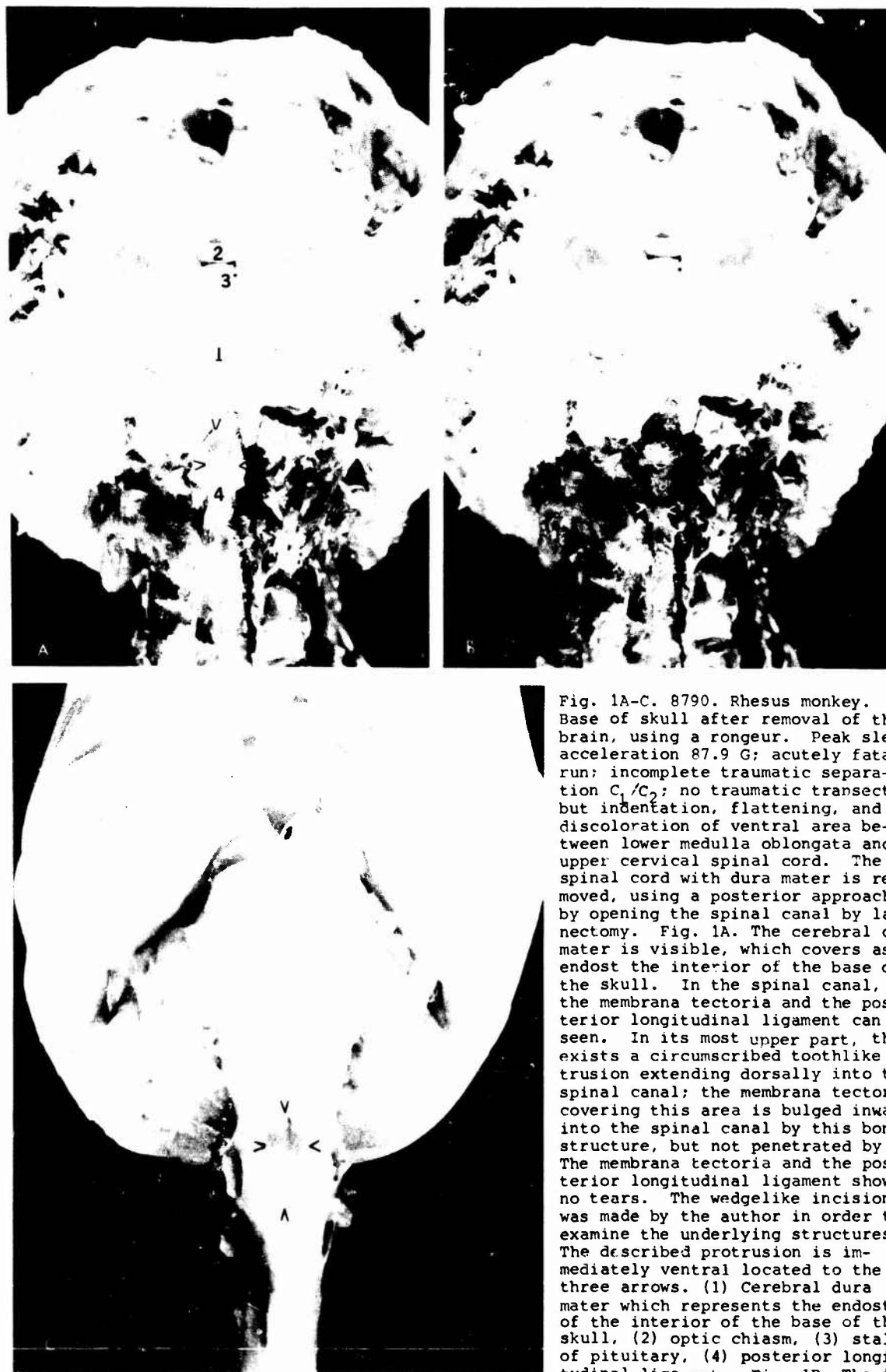


Fig. 1A-C. 8790. Rhesus monkey. Base of skull after removal of the brain, using a rongeur. Peak sled acceleration 87.9 G; acutely fatal run; incomplete traumatic separation  $C_1/C_2$ ; no traumatic transection, but indentation, flattening, and discoloration of ventral area between lower medulla oblongata and upper cervical spinal cord. The spinal cord with dura mater is removed, using a posterior approach by opening the spinal canal by laminectomy. Fig. 1A. The cerebral dura mater is visible, which covers as endost the interior of the base of the skull. In the spinal canal, the membrana tectoria and the posterior longitudinal ligament can be seen. In its most upper part, there exists a circumscribed toothlike protrusion extending dorsally into the spinal canal; the membrana tectoria covering this area is bulged inward into the spinal canal by this bony structure, but not penetrated by it. The membrana tectoria and the posterior longitudinal ligament show no tears. The wedgelike incision was made by the author in order to examine the underlying structures. The described protrusion is immediately ventral located to the three arrows. (1) Cerebral dura mater which represents the endost of the interior of the base of the skull, (2) optic chiasm, (3) stalk of pituitary, (4) posterior longitudinal ligament. Fig. 1B. The incised membrana tectoria is turned

back distally. The circumscribed tooth-like bony structure can now be identified as the odontoid process of the axis; this structure shows no fracture. The superior longitudinal band of the cruciform ligament, the transverse ligament of the atlas and the apical ligament of the dens are ruptured, also the alar ligaments. (1) the odontoid process of the

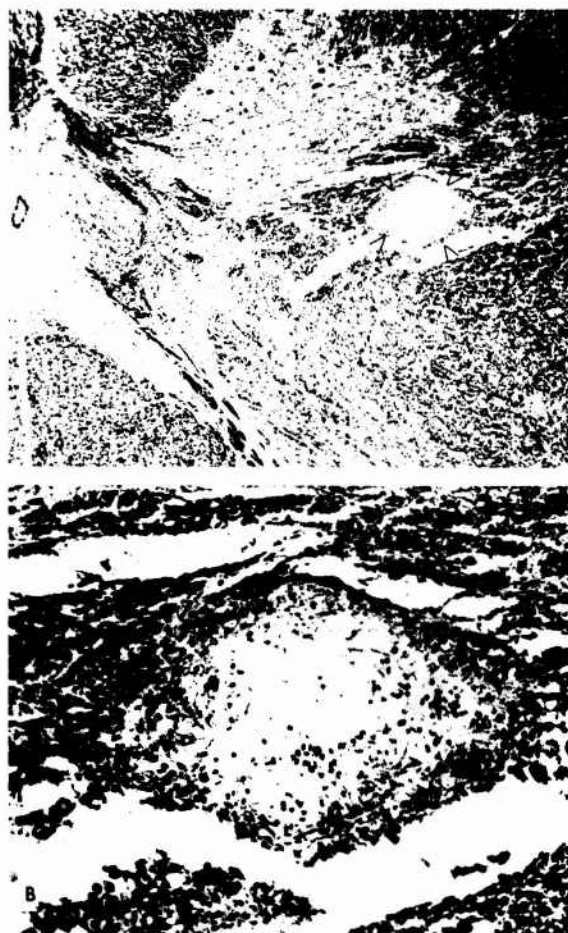


Fig. 2. 3936. Rhesus monkey. Median section through the formalin fixed head, brain, cervical spine, and spinal cord. 162.8 G peak sled acceleration; acutely fatal run; atlanto-occipital separation; complete traumatic transection. (1) head mount, (2) skull, (3) falx cerebri, (4) corpus callosum, (5) cerebellum, (6) midbrain, (7) pons, (8) medulla oblongata, (9) optic chiasm, (10) pituitary, (11) base of skull, (12) basilar subdural hemorrhage due to ruptured vertebral arteries, (13) anterior circumference of foramen magnum, (14) posterior circumference of foramen magnum, (15) posterior arch of atlas, (16) anterior arch of atlas, (17) odontoid process of axis, (18) hemorrhage extending into retropharyngeal space, (19) traumatically transected medulla oblongata, (20) traumatically transected upper cervical spinal cord, (21) spinous process of axis, (22) hemorrhage extending into neck muscles, (23) intervertebral disc between axis and third cervical vertebra. Macrophoto.

Fig. 1A-C. (Cont). axis, (2) the distally turned back membrana tectoria is indicated by white arrows. Fig. 1C. Base of brain and anterior aspect of cervical spinal cord. Brownish discoloration and indentation of the tissue at the atlanto-occipital junction between lower medulla oblongata and  $C_1$ . The tissue in this area is flattened and soft. Due to the impact and sliding movement of the odontoid process of the axis, an ovoid zone (see arrows) of tissue at the anterior aspect of the spinal cord is traumatically damaged. Macrophoto.



Fig. 3. 3936. Rhesus monkey. Median section through the formalin fixed head, brain, cervical spinal cord. Same animals as Fig. 2 but the specimen was distracted, in order to demonstrate the nature of the lesion. 162.8 G peak sled acceleration; acutely fatal run; atlanto-occipital separation; complete traumatic transection. (1) head mount, (2) skull, (3) falx cerebri, (4) corpus callosum, (5) cerebellum, (6) midbrain, (7) pons, (8) medulla oblongata, (9) optic chiasm, (10) pituitary, (11) base of skull, (12) basilar subdural hemorrhage due to ruptured vertebral arteries, (13) anterior circumference of foramen magnum, (14) posterior circumference of foramen magnum, (15) posterior arch of atlas, (16) anterior arch of atlas, (17) odontoid process of axis, (18) hemorrhage extending into retropharyngeal space, (19) traumatically transected medulla oblongata, (20) traumatically transected upper cervical spinal cord, (21) spinous process of axis, (22) hemorrhage extending into neck muscles, (23) intervertebral disc between axis and third cervical vertebra. Macrophoto.



C

D

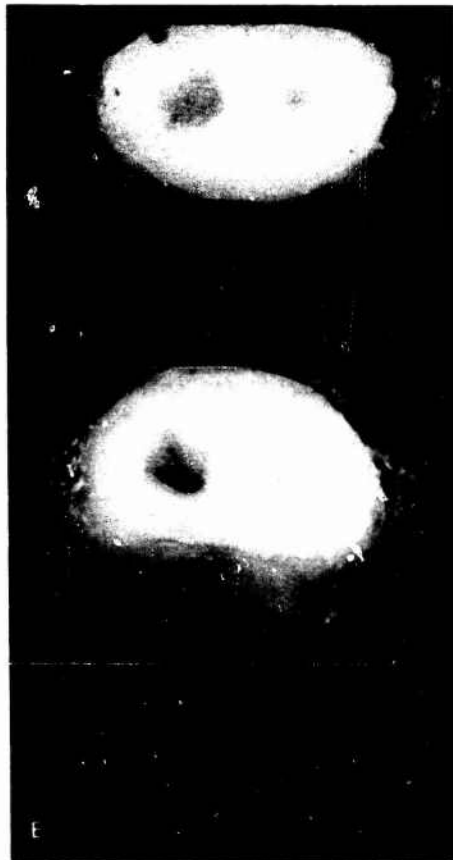


Fig. 4A-E. 3935. Rhesus monkey. Two high level runs on one day; peak sled acceleration of the first run 105.5 G, the peak sled acceleration of the second run was 123.0 G. The animal was moribund and had to be sacrificed after 90 hours; normal radiological findings; no traumatic transection, but centrally located hemorrhagic necroses. Fig. 4A, C<sub>1</sub>. Complete traumatic necrosis of an area of the right lateral column, surrounded by arrows. Partial traumatic necrosis in the neighborhood, especially dorsal. Klüver-Barrera, 30:1. Fig 4B. Enlarged detail from A. Complete traumatic necrosis with invasion of polymorphonuclears. Klüver-Barrera, 120:1. Fig. 4C. Loss of neurons with glial proliferation in the right anterior horn. Multiple recent rhectic hemorrhages in the grey substance. Hematoxylin - Eosin, 50:1. Fig. 4D. Enlarged detail from Fig. A. Loss of neurons with astroglial and microglial proliferation can be seen. There is a marked proliferation of astroglial and microglial elements visible. Remaining neurons reveal loss of tigroid (Nissl) substance; their cytoplasm is opaque staining, the shrunken nucleus peripherally located or completely lost. In this older scar formation, multiple recent rhectic hemorrhages can be seen. Hematoxylin - Eosin, 120:1. Fig. 4E. Area between lower medulla oblongata and C<sub>1</sub>. Both vertebral arteries are visible and attached to the specimen. Bilateral central hemorrhagic necrosis. Macrophoto.



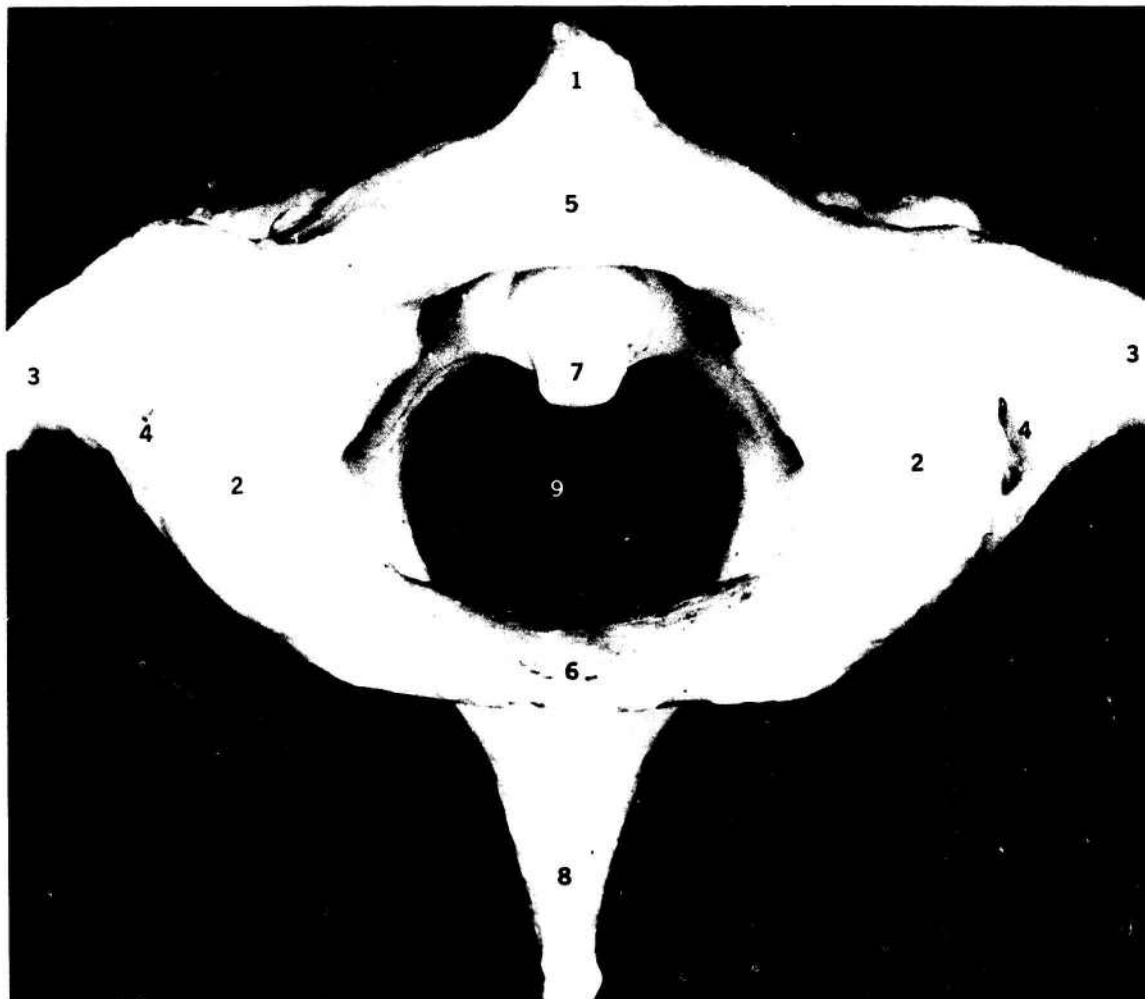


Fig. 5. Rhesus monkey. Control animal. Macerated specimens of atlas and axis seen from above. (1) anterior tuberculum of atlas, (2) superior articular process of atlas, (3) transverse process of atlas, (4) transverse foramen of atlas, (5) anterior arch of atlas, (6) posterior arch of atlas, (7) odontoid process (dens) of axis, (8) spinous process of axis, (9) spinal canal. Macrophoto.



Fig. 6. Rhesus monkey. Control animal. Median section through the formalin fixed head, brain, cervical spine, and cervical spinal cord. (1) skull, (2) falx cerebi, (3) corpus callosum, (4) cerebellum, (5) midbrain, (6) quadrigeminal plate, (7) pons, (8) medulla oblongata, (9) optic chiasm, (10) pituitary, (11) base of skull, (12) retro-pharyngeal space, (13) anterior circumference of foramen magnum, (14) posterior circumference of foramen magnum, (15) anterior arch of atlas, (16) posterior arch of atlas, (17) odontoid process of axis, (18) spinous process of axis, (19) intervertebral disk between axis and third cervical vertebra. Macrophoto.

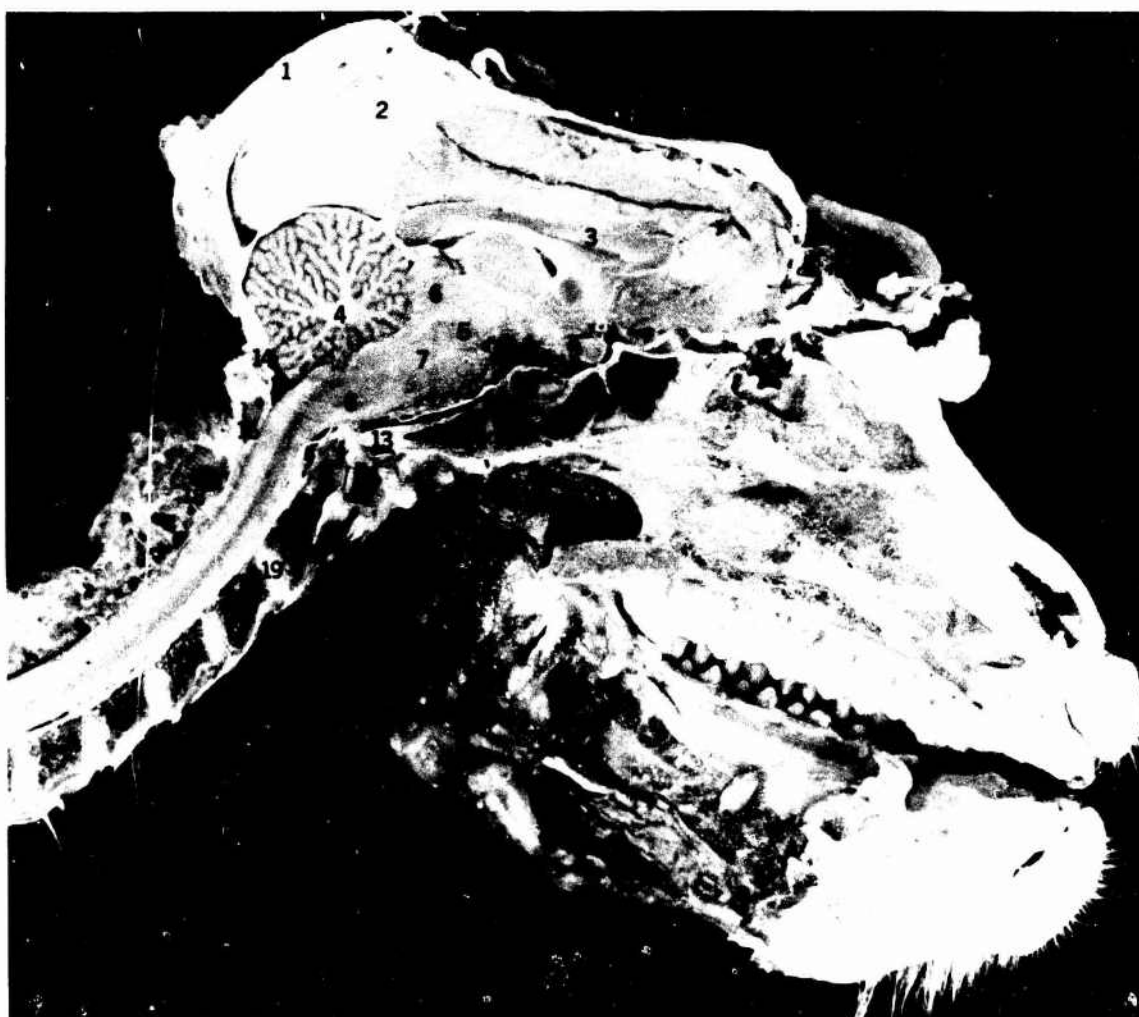


Fig. 7. Rhesus monkey. Control animal, after evisceration and removal of the skin. Median section through the formalin fixed head, brain, cervical spine, and cervical spinal cord. (1) skull, (2) falx cerebri, (3) corpus callosum, (4) cerebellum, (5) mid-brain, (6) quadrigeminal plate, (7) pons, (8) medulla oblongata, (9) optic chiasm, (10) pituitary, (11) base of skull, (12) retropharyngeal space, (13) anterior circumference of foramen magnum, (14) posterior circumference of foramen magnum, (15) anterior arch of atlas, (16) posterior arch of atlas, (17) odontoid process of axis, (18) spinous process of axis, (19) intervertebral disk between axis and third cervical vertebra. Macrophoto.

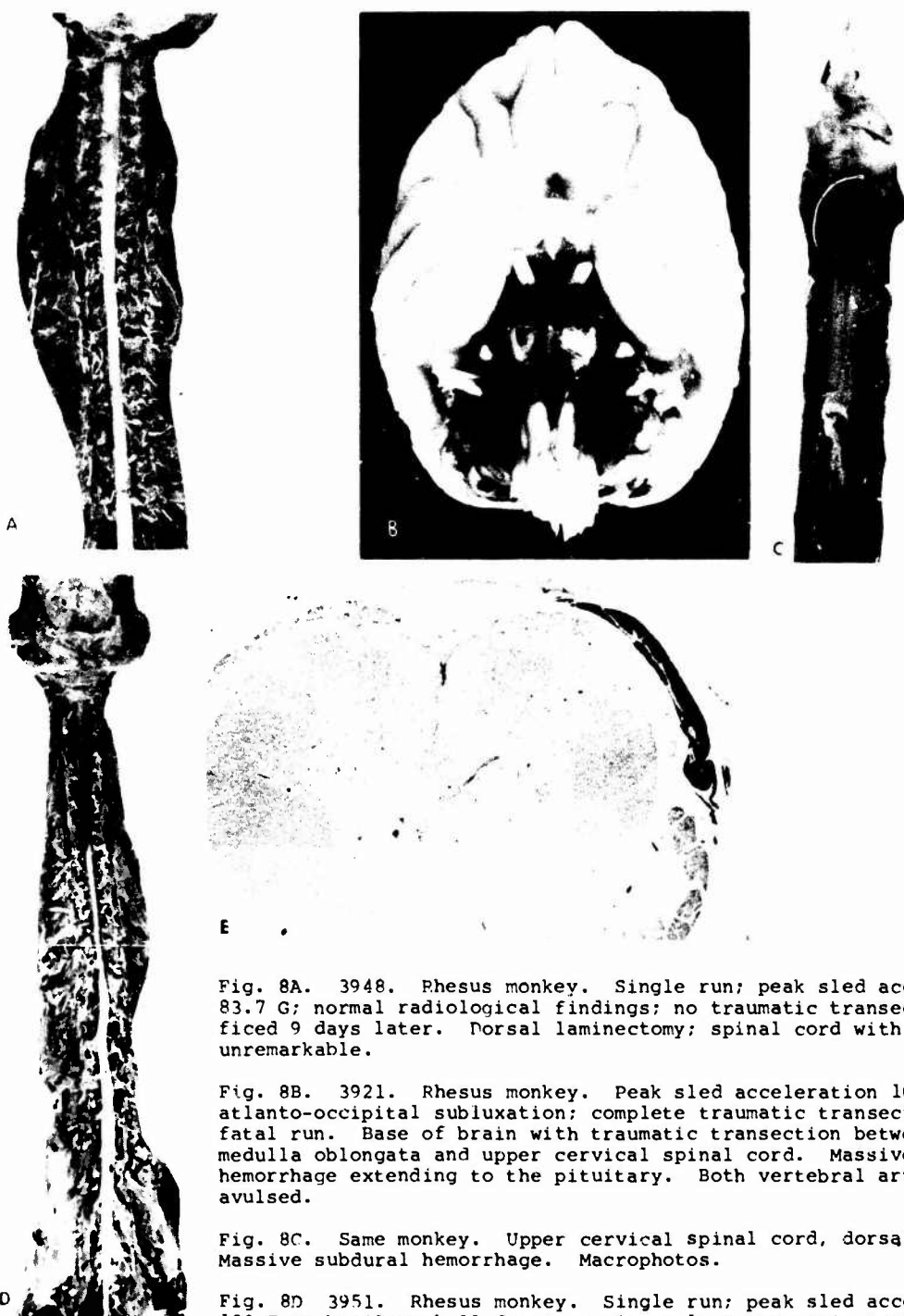


Fig. 8A. 3948. Rhesus monkey. Single run; peak sled acceleration 83.7 G; normal radiological findings; no traumatic transection, sacrificed 9 days later. Dorsal laminectomy; spinal cord with dura mater unremarkable.

Fig. 8B. 3921. Rhesus monkey. Peak sled acceleration 108.6 G; atlanto-occipital subluxation; complete traumatic transection, acutely fatal run. Base of brain with traumatic transection between lower medulla oblongata and upper cervical spinal cord. Massive subdural hemorrhage extending to the pituitary. Both vertebral arteries are avulsed.

Fig. 8C. Same monkey. Upper cervical spinal cord, dorsal aspect. Massive subdural hemorrhage. Macrophotos.

Fig. 8D. 3951. Rhesus monkey. Single run; peak sled acceleration 130.7 G; basilar skull fracture; incomplete traumatic transection, acutely fatal run. Dorsal laminectomy; spinal cord with dura mater. Massive cervical subdural hemorrhage. Macrophoto.

Fig. 8E. Same monkey. Lower cervical spinal cord. Scattered subdural hemorrhage mainly in anterior aspects of the right side. The subdural hemorrhage has not become a space-occupying mass. Grey and white substance reveal no pathomorphological alterations. Hematoxylin - Eosin, 12:1.

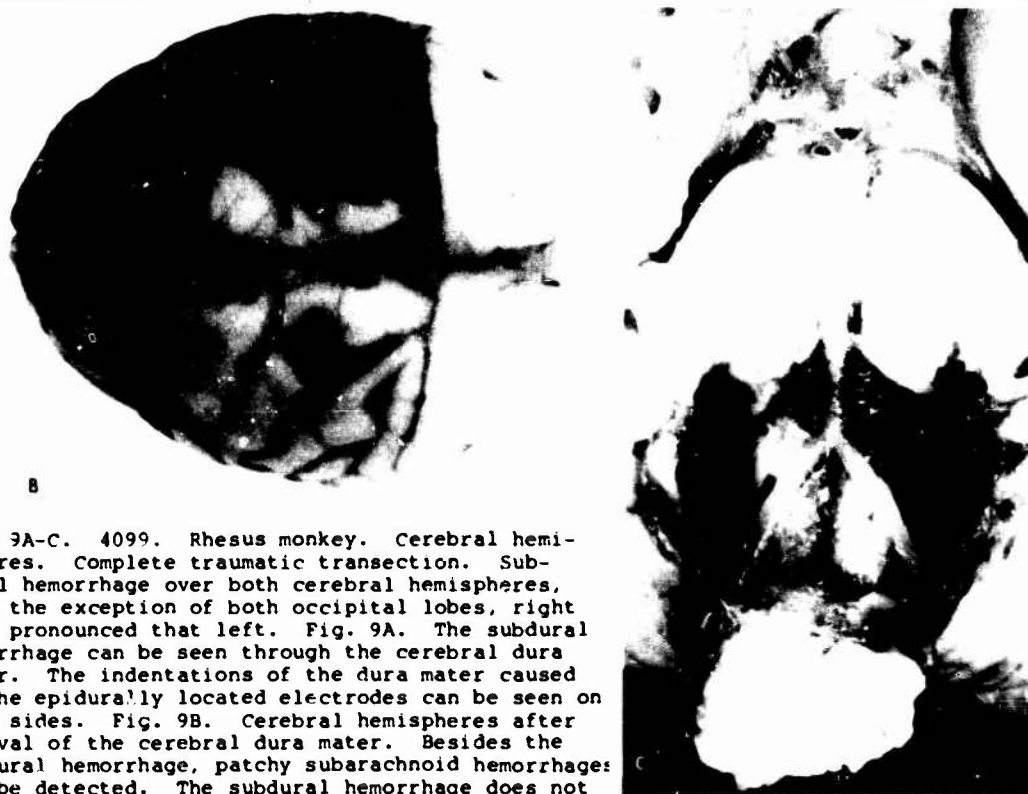
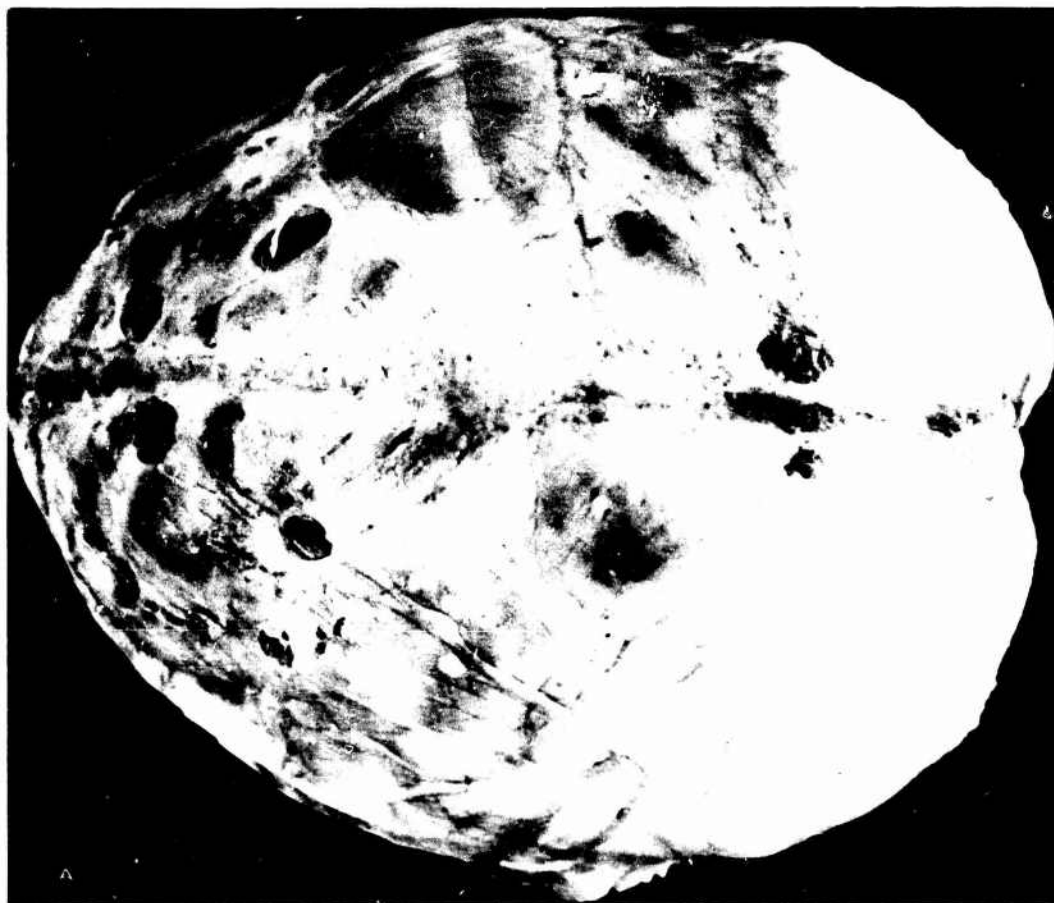


Fig. 9A-C. 4099. Rhesus monkey. Cerebral hemispheres. Complete traumatic transection. Subdural hemorrhage over both cerebral hemispheres, with the exception of both occipital lobes, right more pronounced than left. Fig. 9A. The subdural hemorrhage can be seen through the cerebral dura mater. The indentations of the dura mater caused by the epidurally located electrodes can be seen on both sides. Fig. 9B. Cerebral hemispheres after removal of the cerebral dura mater. Besides the subdural hemorrhage, patchy subarachnoid hemorrhages can be detected. The subdural hemorrhage does not extend into both occipital areas; the parieto-occipital fissure (monkey fissure) represents the borderline. The occipital lobe of the Rhesus monkey shows practically no sulci. Fig. 9C. 4099. Rhesus monkey. Base of brainstem with subarachnoid and subdural hemorrhage. Acutely fatal run: 128.1 G peak sled acceleration; C/C, subluxation; complete traumatic transection. Both vertebral arteries are disrupted at the area of the foramen magnum. The disrupted zone of the lower medulla oblongata reveals an uneven and corrugated surface. Macrophotos.

Recherche concernant la Protection de la colonne vertébrale  
aux accélérations de l'éjection  
F. COUSSAU, AERAZUR EFA, ISSY-LES-MOULINEAUX, B. VETTES et G. BEZAMAT, CEV BRETAGNE  
58, Boulevard Galliéni  
92130 ISSY-LES-MOULINEAUX (FRANCE)

### RESUME

Dans le cadre d'un marché d'études, le Service Technique de la Production Aéronautique a demandé à la Société AERAZUR-EFA de concevoir un équipement soulageant la colonne vertébrale des pilotes de chasse lors d'éjections. Une solution pneumatique fut retenue. Les travaux consistèrent à mettre au point des structures gonflables, dites 'poutres', capables de supporter des efforts importants. Ces poutres furent utilisées pour réaliser un équipement, afin de vérifier la validité des principes retenus. Des essais en centrifugeuse sur mannequin et sujet humain effectués par le Centre d'Essais en Vol, Laboratoire de Médecine Aéronautique, montrèrent qu'un tel équipement était capable de diminuer de 50 % les efforts transmis au siège par la colonne vertébrale. L'étude d'un prototype utilisable dans l'environnement avion, ainsi que son gonflement au moment de l'éjection, a été menée.

### INTRODUCTION

Lors d'une éjection hors d'un avion de chasse, la colonne vertébrale du pilote ou du navigant qui s'éjecte est sollicitée dangereusement. L'accélération linéaire que subit l'éjecté atteignait 20 g en pointe sur les sièges de l'ancienne génération, elle avoisine maintenant avec les sièges de la nouvelle génération, 15 g. Cette valeur est encore largement suffisante pour entraîner dans de nombreux cas, des lésions de la colonne vertébrale. Ces lésions sont d'autant plus graves que la position des sujets avant l'éjection est mauvaise ou que le harnais est mal ajusté. Il ne faut pas oublier la masse de la tête qui provoque une hyperflexion du cou au départ du siège, puis est rejetée brutalement vers l'arrière, dès la sortie du cockpit au contact du souffle.

Dans le cadre d'un contrat d'études, le Service Technique de la Production Aéronautique a demandé à la Société AERAZUR d'envisager les principes qui pourraient être utilisés pour diminuer la gravité des lésions de la colonne vertébrale, lors d'une éjection. La protection devait être assurée en final par un équipement individuel, basé sur les principes retenus.

Pour parvenir à une protection de la colonne vertébrale, l'équipement devrait donc remplir les fonctions suivantes :

- Positionner le torse du sujet, de façon à maintenir la colonne vertébrale le plus parallèlement possible au dossier du siège éjectable qui est également l'axe d'action de l'accélération.
- Soulager la colonne vertébrale de l'effort qu'elle subit, lors de l'éjection.
- Maintenir la tête dans une position normale, permettant d'éviter l'hyperflexion.
- Ne pas gêner l'utilisateur pendant toute la phase inactive de l'équipement : soit le vol normal.

### APPROCHE TECHNIQUE DU PROBLEME

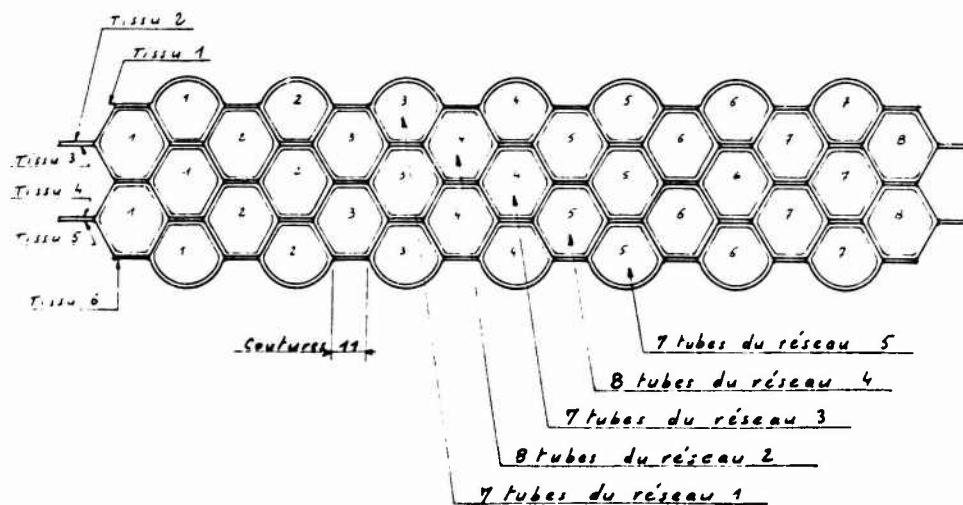
Les fonctions citées ci-dessus, les connaissances antérieures d'AERAZUR dans le domaine du gonflable, nous conduisirent à envisager une solution pneumatique, dont les principes généraux furent les suivants :

- Améliorer les performances mécaniques de la colonne vertébrale, en lui adjoignant une structure gonflable, capable de reprendre mécaniquement des efforts importants, plus particulièrement de compression, soutenir la tête en position normale, provoquer la mise en place obligatoire du torse lors du gonflement de cette structure.

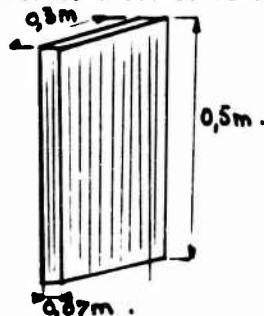
Les efforts qu'il fallait soutenir nous ont obligés à étudier et développer des schémas de structures gonflables très performants. Nous avons intitulé ces structures, des 'poutres' par analogie avec la théorie de la résistance des matériaux.

Les poutres retenues capables de supporter les efforts envisagés, sont à deux composants complémentaires, une enveloppe textile dans laquelle est placée un réseau de tubes obtenu par soudure haute fréquence de deux feuilles de polyuréthane. Les différentes couches de tubes sont imbriquées les unes dans les autres, de cette façon, une section droite de la poutre a l'aspect d'un nid d'abeilles.

## SCHEMA N° 1

Coupe transversale (maquette gonflée)

Les petits diamètres des tubes permettent d'utiliser des pressions internes relativement élevées et de conférer ainsi à la 'poutre' un très bon comportement au flambage par compression. La pression interne d'utilisation de ce type de poutre est de 5 bars; Sa pression d'éclatement est de 11 bars.  
Les efforts de compression maximaux provoquant le flambage d'une poutre de dimensions conformes à celles du schéma sont :



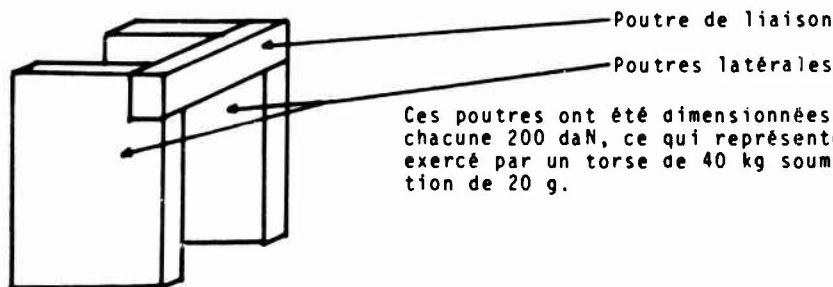
SCHEMA N° 2

500 daN à 5 bars

650 daN à 7 bars

Ces poutres sont donc le matériau qui allait nous permettre de construire notre structure gonflable.

La structure se compose de deux poutres ayant l'aspect de plaques, situées sous les bras et contre les flancs du sujet. Ces poutres sont reliées entre elles au moyen d'une autre poutre de même nature, mais transversale située sur la poitrine du sujet.



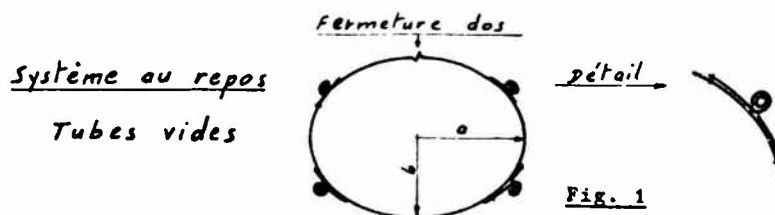
Ces poutres ont été dimensionnées pour reprendre chacune 200 daN, ce qui représente 50 % de l'effort exercé par un torse de 40 kg soumis à une accélération de 20 g.

Il était impossible de reprendre les 200 daN affectés à chaque poutre uniquement sous les épaules, comme le font les béquilles d'un infirme, les épaules auraient été repoussées vers le haut et n'auraient pas retransmis les efforts aux poutres.

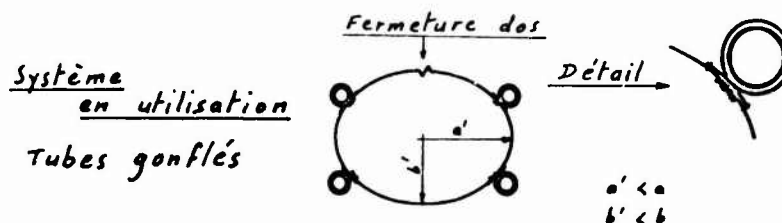
Un vêtement, une sorte de gilet, rendu solidaire des poutres, serrant très fortement le torse lors du gonflement de la structure est chargé de retransmettre une partie des efforts générés par le torse soumis à l'accélération. Le serrage est obtenu par des sortes de cabestans provoquant le raccourcissement des différents périmètres du vêtement lors du gonflement du vêtement.

Vue en coupe d'une représentation du système

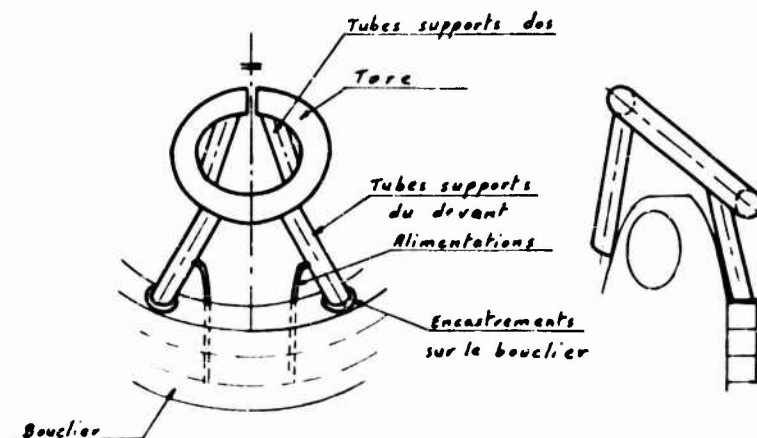
### Sections transversales du torse



Seuls sont représentés le vêtement support et les cabestans



La tête est maintenue sous le menton et autour de la mâchoire inférieure par une sorte de minerve composée d'un tore gonflable diamètre 40 mm soutenu par quatre tubes.



L'ensemble ainsi réalisé ne ressemble guère à un équipement individuel de sécurité d'un pilote. Toutefois, il permettra de tester les principes qui ont été retenus pour soulager la colonne vertébrale lors d'une éjection.





#### EQUIPEMENT D'EVALUATION

##### Première évaluation

Une première évaluation a donc été faite au Centre d'Essais en Vol de Brétigny (France) dans la centrifugeuse du Laboratoire de Médecine Aéronautique sur un sujet humain.

##### DESCRIPTIF DES MOYENS DE MESURE

Une jauge au mercure (longueur 520 mm) est fixée le long de la colonne vertébrale à partir de deux points fixes osseux (vertèbre cervicale - vertèbre lombaire). L'allongement ou le raccourcissement de ce capteur entraîne une variation de résistance qui se traduit par une variation de tension. Les variations de tension ainsi obtenues sont simplifiées, enregistrées et contrôlées sur un voltmètre numérique. L'étalonnage du capteur est effectué et la tension choisie pour les mesures correspondant à des longueurs comprises entre 550 mm et 620 mm.

## DEROULEMENT DE L'ESSAI

Trois types de lancement de la centrifugeuse par moteur électrique sont réalisés, de 1 à 5 Gz par paliers successifs. Le premier avec le gilet non gonflé, le deuxième avec le gilet gonflé et le troisième sans gilet.

La surveillance est assurée par caméra de télévision et écran de contrôle et par liaison "phonie".

## RESULTATS

(voir graphes page suivante)

### Gilet non gonflé

Dès l'accélération de 1,5 Gz, on constate un raccourcissement du capteur jusqu'à environ 3,5 Gz et ensuite un allongement progressif jusqu'à 5 Gz avec pointe maxima au freinage. Dès l'arrêt de la centrifugeuse, le capteur revient à sa position de départ. Ces différentes modifications traduisent un raccourcissement de 4 mm et un allongement de 13 mm. Le raccourcissement correspond au tassement du sujet observé sur l'écran de contrôle et l'allongement à une hyperflexion de la région cervicale dorsale.

### Gilet gonflé - 2 bars

A aucun moment, il n'y a de variation de capteur. Le sujet véritablement bloqué dans le carcan constitué par la minerve et le corset ne subit ni tassement, ni hyperflexion de sa colonne.

### Sans gilet

Comme pour le gilet non gonflé, il y a en premier lieu un raccourcissement du capteur de 1,5 à 2,2 Gz, puis un allongement progressif jusqu'au freinage. Ces déplacements sont du même ordre que ceux obtenus avec le gilet non gonflé, mais s'établissent plus précocement.

L'allongement, comme dans le premier cas, est dû à l'hyperflexion de la colonne cervico-dorsale. Sa précocité d'apparition s'explique par rapport à l'essai avec gilet non gonflé par l'absence de maintien de la tête et du torse par la minerve et le gilet même non gonflé.

## CONCLUSION

Cet essai a permis de montrer l'efficacité du principe de ce type de vêtement sur un sujet humain au cours d'accélération + Gz subies en centrifugeuse. La colonne vertébrale semble être moins sollicitée, lorsque le sujet porte le gilet gonflé.

## MESURE DES EFFORTS EN CENTRIFUGEUSE

A la suite de cet essai favorable, il fut décidé de développer un moyen de mesure s'intégrant dans le siège éjectable, capable de déterminer les valeurs des efforts repris par les poutres et de l'effort transmis au siège. Ce moyen de mesure intitulé 'balancé' est logé dans le baquet du siège éjectable à la place du paquetage de survie.

Le serrage du torse et de l'abdomen provoqué par le vêtement lors du gonflement, la compression des aisselles, donnaient quelques inquiétudes au Corps médical. En effet, les efforts de compression pouvaient engendrer des lésions différentes de celles que nous cherchions à réduire. Le vêtement fut donc instrumenté pour pouvoir mesurer la compression dans la zone sous-mammaire, sous les aisselles et au niveau du creux épigastrique.

Une nouvelle série d'essais en centrifugeuse fut lancée, d'une part, avec un sujet humain et, d'autre part, avec le torse d'un mannequin (Hybrid II 50 percent)

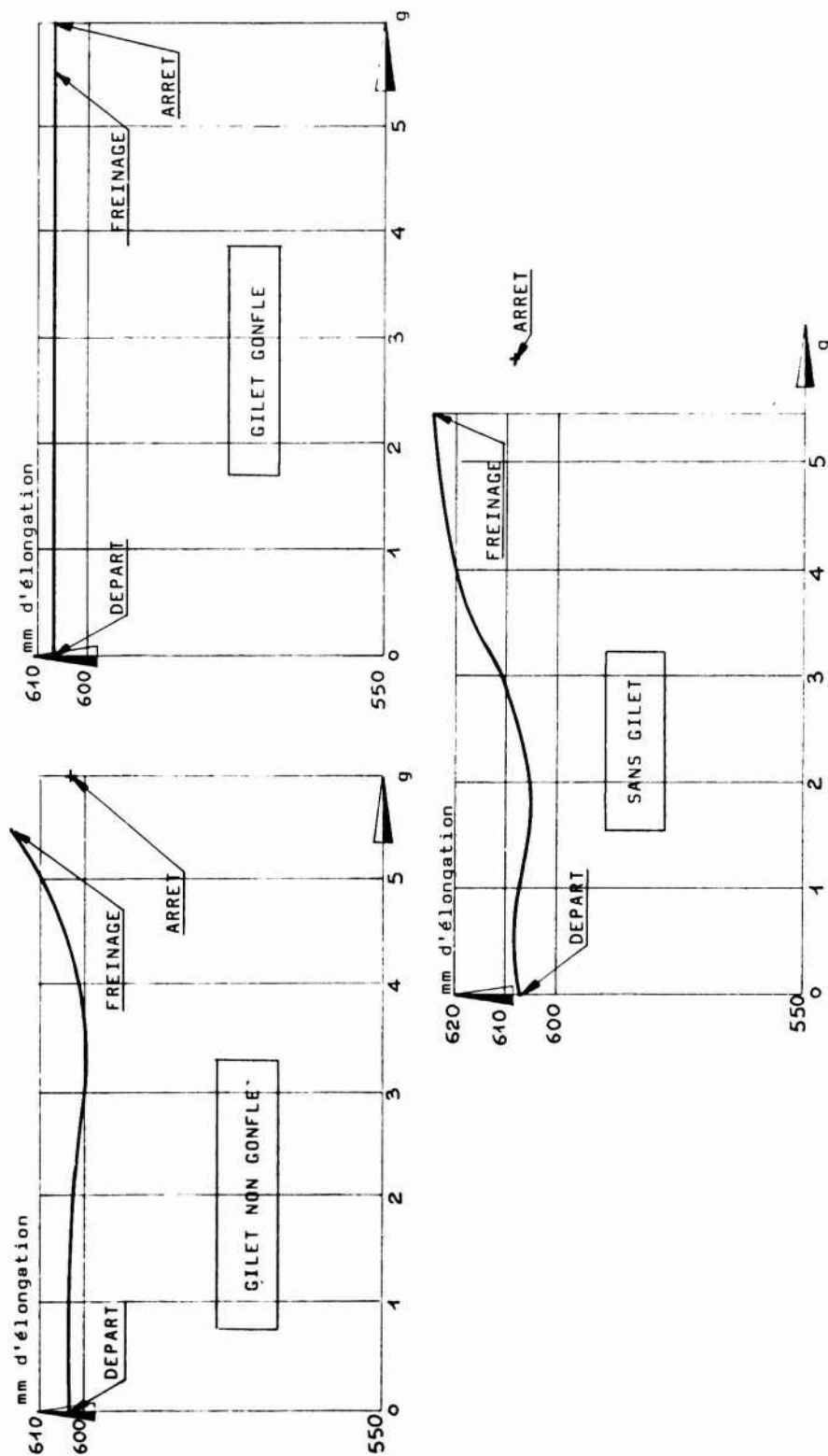
Les mesures suivantes furent effectuées :

Sujet humain et mannequin

- Effort repris par les poutres latérales
- Effort transmis au siège par la colonne vertébrale
- Compressions torse et abdomen par serrage

Mannequin seul

- Effort de compression dans la colonne vertébrale zone dorso-lombaire.



Les paramètres choisis furent les suivants :

- Valeur de l'accélération tête siège
- Pression relative de la structure gonflable du vêtement.

Les valeurs suivantes de ces paramètres furent retenues :

. Accélération

Sujet humain	0 - 5 g
Mannequin	0 - 5 - 10 - 14 g

. Pression relative dans le vêtement

0 - 0,5 - 1 - 1,5 - 2 - 2,5 - 3

Les graphiques résument les résultats obtenus, page suivante.

Le comportement du mannequin ou du sujet humain était suivi à l'intérieur de la cabine de la centrifugeuse par une camera-video qui permettait de bien saisir le déplacement de la tête et l'enfoncement sur le siège. Des caméras rapides filmaient le comportement des poutres, lorsque l'accélération maximale était obtenue.

### ANALYSE DES RESULTATS

Nous pouvons cependant faire quelques remarques pour mettre en relief les résultats les plus saillants.

#### MANNEQUIN (sans les jambes-masse 40 kg)

Prenons les essais effectués à 14 g, accélération voisine de celle exercée par un siège éjectable de la nouvelle génération.

Lorsque le vêtement n'est pas gonflé, le mannequin transmet un effort de 680 daN au siège, l'effort de compression dans la colonne vertébrale est de 440 daN. Ces chiffres sont suffisants pour expliciter les lésions observées sur la colonne vertébrale trop fréquemment obtenues.

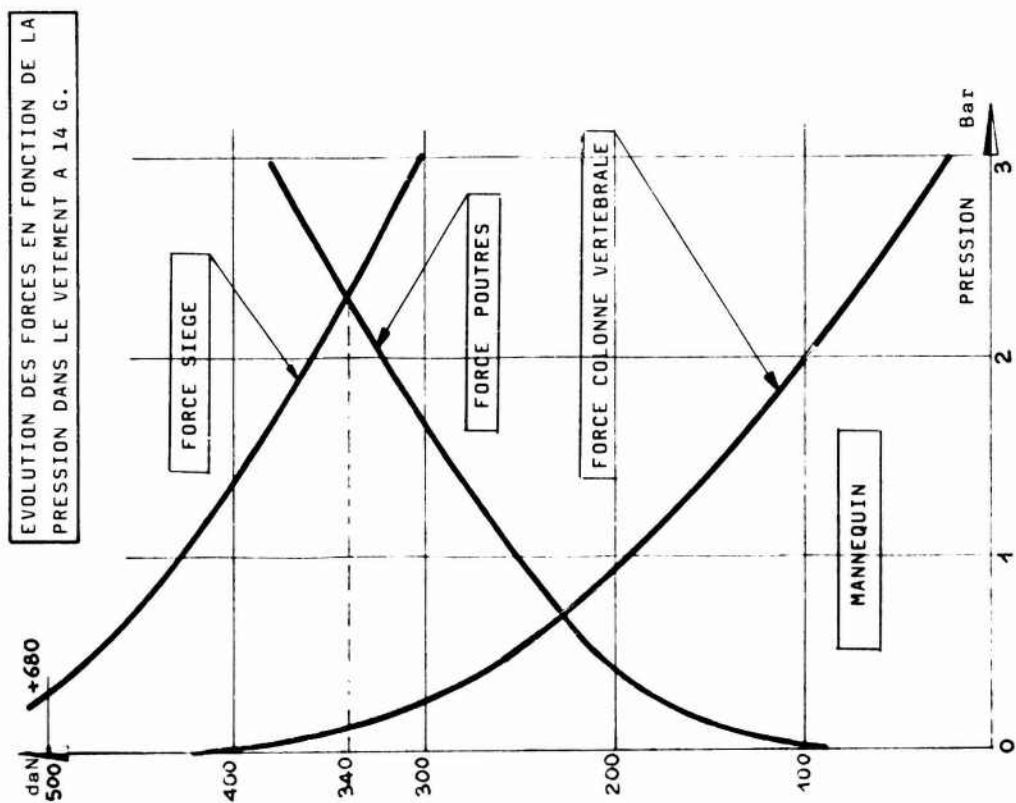
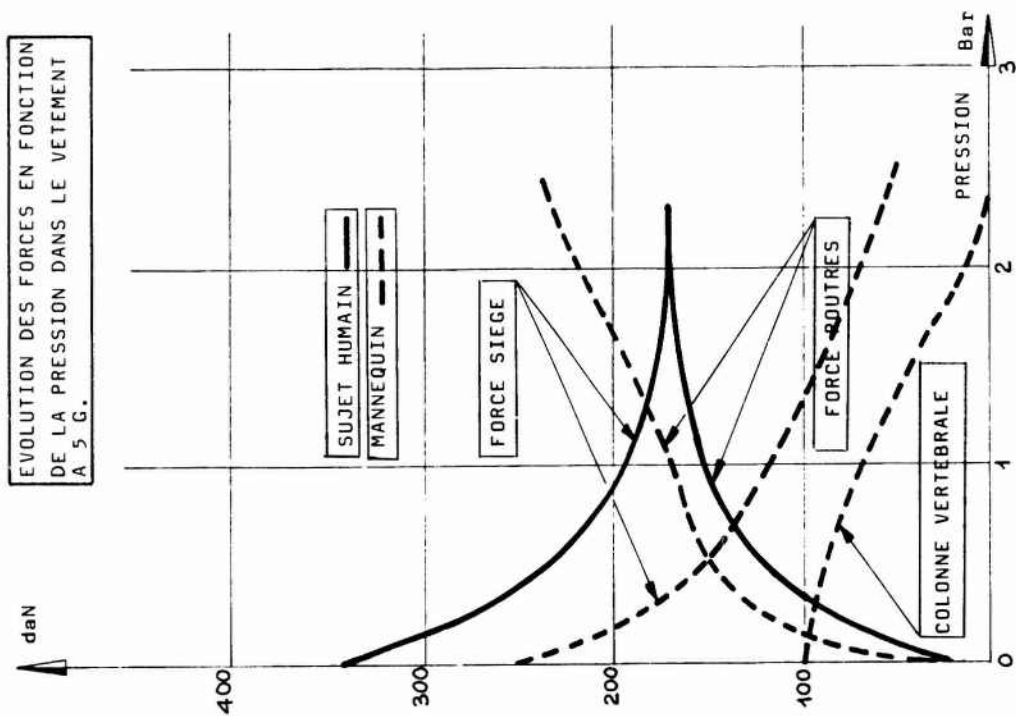
Lorsque le vêtement est gonflé à 2,5 bars environ, l'effort transmis au siège n'est plus que de 340 daN et les poutres reprennent également 340 daN, l'effort de compression dans la colonne vertébrale n'est plus que de 60 daN.

Ceci montre que les efforts résultant des masses situées au-dessus du niveau de la jauge de contrainte positionnée dans la colonne vertébrale du mannequin ont été en partie repris par les poutres. L'effort transmis au siège s'en trouve donc diminué. Le principe de protection de la colonne vertébrale par une structure gonflable porteuse semble être vérifié, tout au moins avec le mannequin Hybrid II - 50 %.

#### SUJET HUMAIN

Pour des raisons de sécurité, lors des essais sur sujets humains, l'accélération a été limitée à 5 g.

Les compressions provoquées par le serrage du vêtement étaient assez faibles pour qu'on puisse les négliger dans le futur.



La première constatation concerne la valeur de l'effort transmis au siège par le sujet humain par rapport à sa masse totale soumise à la même accélération.

La masse du sujet humain est de 85 kg, soit sous 5 g 425 daN pour une accélération de 5 g l'effort maximal repris par le siège est de 340 daN, soit 80 % de la valeur précédente. Le siège ne supporte donc pas uniquement les efforts fournis par le tronc.

L'analyse du graphe représentant les essais à 5 g met en évidence que le vêtement gonflé à 2,5 bars permet de diminuer de 50 % la valeur de l'effort transmis au siège.

L'efficacité est donc également démontrée sur sujet humain, mais à 5 g. seulement.

L'allure générale des courbes relatives au mannequin et au sujet humain est assez différente. En effet, les courbes concernant le sujet humain semblent être asymptotiques à la droite horizontale  $F = 170$  daN, contrairement aux courbes obtenues avec le mannequin qui ne présentent pas d'asymptote commune.

Ceci prouve une fois de plus qu'il est difficile et dangereux d'extrapoler le comportement d'un équipement sur sujet humain à partir de résultats obtenus avec un mannequin.

Les moyens vidéo à l'intérieur de la cabine de la centrifugeuse, la description des sensations du sujet humain, nous permettent de dire que le support de tête dit 'minerve' améliore le maintien de la tête, tout en étant assez gênant au cours des essais pour le sujet.

#### TENTATIVE SUR RAMPE

Une série d'essais de lancers de siège éjectable à la rampe fut programmée et eut lieu ; les résultats obtenus ne furent pas significatifs, étant donné qu'il y avait une trop grande incompatibilité avec le système de brelage du mannequin sur le siège et le vêtement lui-même. Avant d'aborder ce type d'essais, il fallait donc passer par une phase d'élaboration de la définition et d'analyse de compatibilité.

#### CONCEPTION D'UN PROTOTYPE UTILISABLE

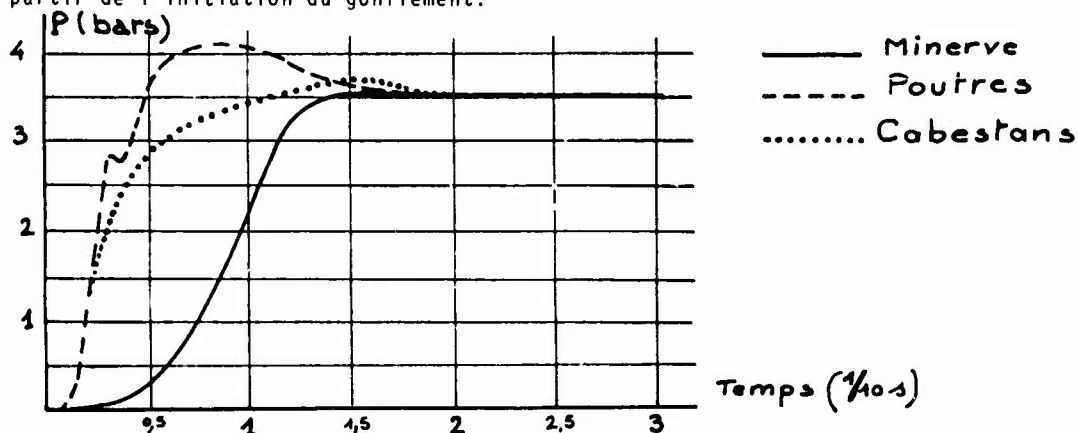
Nous avons donc conçu un prototype assurant les mêmes performances, mais pouvant être testé et utilisé dans l'environnement avion.

L'aspect gonflement au moment de l'éjection de ce vêtement fut également pris en compte lors de cette phase de définition. L'obstacle essentiel fut pour nous la durée de mise en forme. La génération pneumatique retenue est une bouteille contenant de l'azote comprimé sous forte pression, reliée au circuit pneumatique du vêtement par l'intermédiaire d'une vanne, dont l'ouverture est commandée par un système pyrotechnique.

Le circuit pneumatique, élément essentiel du vêtement, d'une part, devait conférer les performances mécaniques aux poutres gonflables, d'autre part, canaliser avec le moins de perte de charge possible, le fluide azote.

Nous sommes parvenus à obtenir de façon fiable un temps de gonflement pour une pression interne relative de 2,5 bars de 0,1 seconde. Ce temps est compatible avec une séquence d'éjection. Il pourra être amélioré dans une phase d'optimisation des performances, en utilisant des containers de gaz, dont les diamètres de passage des gaz soient plus importants et également en utilisant de l'hélium comme fluide.

Le graphe ci-dessous représente l'allure de la montée en pression, à partir de l'initiation du gonflement.



Pour modifier la structure pneumatique du vêtement, nous nous sommes appuyés sur la remarque suivante :

. gonflées à 2,5 bars, les poutres pneumatiques avaient des performances mécaniques suffisantes, alors qu'elles sont capables d'être gonflées à 5 bars, elles sont donc surdimensionnées.

L'équipement ainsi réalisé a donc l'aspect représenté ci-dessous :



Ces travaux ont permis de démontrer la validité d'un principe de protection de la colonne vertébrale et de s'assurer de la possibilité de son application dans l'environnement avion. Cependant, de nombreux problèmes restent à résoudre :

- Intégration de la génération de gonflement dans le siège ou le packaging
- Essais en grandeur réelle sur sujet humain
- Tailles différentes
- Réglages en fonction des mensurations du sujet
- Industrialisation

## DISCUSSION

## UNIDENTIFIED QUESTIONER

Is the sequential timing of the system such that suit inflation occurs in a timely manner?

## UNKNOWN COMMENT

The suit inflation begins at the moment you operate the seat firing handle. The suit is inflated in 0.10 seconds and by this time the body is already fully loaded by the ejection gun; therefore, the body is already slumped in the seat.

## AUTHOR'S REPLY

The suit inflates very fast; I think the timing is fast enough to be effective. (Remainder of tape could not be transcribed).

## DR. HEARON (USA)

Regarding the latest version of your protection device, with the suit deflated, is there any limitation to cervical range of motion? What is the total weight of the garment?

## AUTHOR'S REPLY

No there is no limitation to cervical motion. The weight was not provided.



## THE U.S. NAVY APPROACH TO CRASHWORTHY SEATING SYSTEMS

by

Marvin Schulman

Naval Air Development Center  
Warminster, PA 18974, USA

## SUMMARY

The U.S. Navy has for the past 22 years been committed to the support of a number of research and development programs to improve seating systems in non-ejection aircraft. This commitment has resulted in a family of crashworthy seats which have gone through considerable testing and evaluation to demonstrate their capacity to manage crash loads and to limit those loads transmitted from the aircraft to the crewmembers. The development process has led to crashworthy armored and unarmored pilot/co-pilot, troop, passenger, gunner and specialty seats. However, the demonstration that these seats are effective in increasing the probability of survival during and after a crash does not necessarily mean that they will be adopted for military aircraft. New generation helicopters will require crashworthy seating in accordance with the latest Military Specifications, but retrofitting current operational aircraft with advanced seats is a more difficult undertaking. The acquisition manager must make the final decision and then provide the funding to support the effort.

## INTRODUCTION

A three pronged approach is being used by the U.S. Navy to improve aircrew survivability by way of non-ejection seating systems. First, several exploratory and advanced development seating programs are funded each year with the expectation that new concepts and improved equipment will evolve through the development process and eventually find their way into both fixed wing and rotary wing military aircraft. This is a long term approach aimed at continually advancing the technology. Second, for the nearer term, seating systems and components that have already gone through the initial two phases of the development process and have demonstrated life support equipment improvement, are selectively proposed for new aircraft or as retrofitables for current operational Navy and Marine aircraft. When this approach is used, the "on-the-shelf" equipment is modified and then evaluated for the specific aircraft, through an engineering development program. As a third step toward improving seat crashworthiness, Military Specifications are written or modified as new concepts are proven. These specifications are then imposed on airframe contractors as a control over the acceptability of their equipment delivered to the Navy under an engineering change proposal.

## CRASHWORTHINESS

Although the U.S. Navy has had active programs since the early 1950's to improve the crashworthiness of non-ejection seats in helicopter and fixed wing aircraft (1), the level of funding to support these efforts seemed to always border on modest to austere. Being in the shadow of ejection seat technology with its ability to attract the bulk of research dollars no doubt played an important part in deciding how much of the military fiscal pie would be devoted to the fixed seating community. Table 1 gives a historic review of the U.S. Navy sponsored programs for crashworthy seating over the past 25 years. During this time much of the development activity was devoted to exploratory development programs to demonstrate the feasibility of energy attenuation devices and crashworthy techniques as applied to the complete array of naval helicopter seats.

Prior to the mid 1950's when the term "seating crashworthiness" was used it was understood to mean the capacity of the seating system to withstand imposed crash loads without experiencing failure to its structure. If the seat remained attached to the aircraft floor tracks and showed no gross structural failure, then it was considered crashworthy. Terms such as 20-20-10 G's (2) were used to describe the static load factors in the Gz, Gx, and Gy directions to which the seat and a weight simulating the human (usually a body block) were required to be exposed without extensive damage. If dynamically tested, inertial forces measured on the weight played no part in determining success or failure. It was not until that time that the term "crashworthiness" took on a new significance and meaning among the seating development community. With the development and demonstration of devices to dissipate energy (3) through the controlled deformation or working of metal, a means existed whereby seating systems would not only remain structurally intact but occupant exposure to acceleration could be maintained below a physiologically injurious level. "Crashworthy seating" now became synonymous with survivability and seat structural integrity; a contributing factor rather than the only criteria for judging the success or failure of a seating system. In the later 1960's to early 1970's the U.S. Navy programs for seats had advanced to the point that several systems had gone through a sufficient amount of development tests to make them potential candidates for eventual incorporation into operational aircraft (4) (5) (6). However, the prime importance of this initial work was to support and instill confidence in the private industry sector that crashworthy seating was a technology whose time has come. Along with the development which led to "on-the-shelf" hardware, the Navy published Military Specification MIL-S-81771A (7) for energy attenuating seats in non-ejection seating aircraft.

TABLE 1. U.S. NAVY CRASHWORTHY DEVELOPMENTS

DATE	TITLE	DESIGNER	PROGRAM OBJECTIVE	REF. NO.
1956	CREW SEAT/E/A DEVELOPMENT	AEROTHERM	DEVELOP TUBE & OIE E/A SYSTEM FOR USE IN CREW SEATS	3
1957	F7U-3 EJECTION SEAT E/A DEVICE	NAOC	MINIMIZE BACK INJURIES BY USING SST STRAP	26
1962	WIRE BENOER E/A CONCEPT	VAN ZELM/ NADC	DYNAMICALLY T&E ENERGY ATTENUATION PROPERTIES	-
1964 - 1965	CW TROOP SEAT (SIOE FACING)	BOEING/ VERTOL	DEVELOP TROOP SEAT USING WIRE PULLING LL & FRANGIBLE TUBE LL STRUT	27
1966 - 1967	CW NET CUSHIONED CREW SEAT (PHASE 1)	STENCEL	DEVELOP CRASH ATTENUATING SEAT USING SST E/A RODS & CABLES	28
1968	CW ARMORED CREW SEAT (SERIES 1)	BOEING/ VERTOL	DYNAMICALLY T&E CREW SEAT USING TUBE PLATING E/A STRUTS	29
1969	ENERGY ATTENUATION CRITERIA	NADC	DYNAMICALLY T&E COMMERCIAL E/A DEVICES	30
1969	CW ARMORED CREW SEAT (SERIES 11)	NAOC	MODIFY, T&E SERIES 1 SEAT USING TOR-SHOK E/A STRUTS	4
1969	DESIGN STUDY OF LIGHT-WEIGHT ARMORED HELICOPTER SEAT	BUDD	ESTABLISH DESIGN PARAMETERS FOR ARMORED HELICOPTER SEAT	39
1970 - 1971	CW NET CUSHIONED CREW SEAT (PHASE 11)	NADC	MODIFY, T&E PHASE 1 SEAT USING TOR-SHOK E/A'S	5
1970	MIL-S-81771(AS)	NADC	INTRODUCE DYNAMIC CRASH LOADS REQUIREMENT INTO FIXED SEAT SPECIFICATIONS	31
1970 - 1972	CW TROOP SEAT (FWO/AFT/SIDE FACING)	BOEING/ VERTOL	DEVELOP CW TROOP SEAT USING CEILING ATTACHED WIRE BENOER E/A DEVICES	15, 16
1970 - 1971	ENERGY ABSORBER DESIGN CRITERIA	BETA	DETERMINE OPTIMUM E/A PROFILE I.E. NOTCHED F-O CURVE CUMULATIVE PROBABILITY OF INJURY, ORI	32, 33
1970 - 1971	ARMORED E/A CREW SEAT	ARA	DEVELOP TRI-AXIAL E/A ARMORED SEAT WITH TOR-SHOKS	34
1970 - 1974	IMPROVED PESTPAINT SYSTEM	BUDD	INVESTIGATE USE OF LOW ELONGATION WEBBING FOR RESTRAINTS	35, 36
1971	SURVEY OF NAVAL AIRCRAFT CRASH ENVIRONMENTS	DYNAMIC SCIENCE	IDENTIFY AREAS FOR NEEDED IMPROVEMENT IN STRUCTURAL DESIGN	37
1972 - 1973	UH-1 CW ARMORED PILOT SEAT	ARA	RETROFIT TRI-AXIAL E/A SEAT FOR UH-1 HELICOPTER	6
1974 -	INFLATABLE BODY AND HEAD RESTRAINT	NADC/ THIKOL	DEVELOP CRASH ACTUATED INFLATABLE RESTRAINT SYSTEM	23
1975	MIL-S-81771A(AS)	NADC	INTRODUCE CRASH SURVIVAL DESIGN PULSES & ENERGY ATTENUATION REQUIREMENTS	7
1974 - 1978	CH-46E CW ARMORED CREW SEAT	VERTOL/ ARA	RETROFIT CW ARMORED CREW SEAT (SLEP)	-
1974 - 1978	JAN CW STANDARDIZED CREW SEAT	ARA	DEVELOP ARMORED CREW SEAT FOR ARMY/NAVY AIRCRAFT	38
1975 -	LAMPS SEATING	SIKORSKY	PROGRAM MANAGEMENT OF CFE SEATING EFFORTS	-
1976 - 1977	NOTCHED E/A PROGRAM	BETA/ NADC	DETERMINE FEASIBILITY OF NOTCHED E/A CONCEPT (FABRICATION & PERFORMANCE)	-
1976 - 1978	CW UNARMORED CREWMAN SEAT	ARA	DEVELOP LIGHTWEIGHT CW CREW SEAT	-
1977 - 1978	CW GUNNER'S SEAT	ARA	DEVELOP CW GUNNER SEAT (SIDE FACING) WITH MODULAR ARMOR	18
1978 -	CW MILITARY PASSENGER SEAT	ARA/ VERTOL	DEVELOP CW MILITARY PASSENGER SEAT FOR FIXED WING AIRCRAFT	19, 20, 21
UNDATED	MIL-S-85510(AS)	ARMY/NAVY	NEW CW SPEC FOR TROOP/PASSENGER SEATS	17
1980	CW T&E TROOP SEATS	ARA & BOEING/ VERTOL	T&E TWO TROOP SEAT DESIGNS	14
1980	VARIABLE-LOAD E/A	SIMULA	DEVELOP VARIABLE-LOAD E/A FOR PILOT/CO-PILOT SEAT	25
1981	PARAMETRIC STUDY OF SEAT DESIGN	ARMY/ NAVY/ PAA	SYSTEMATIC APPROACH TO SEAT DESIGN	-

## LEGEND:

DRI:	DYNAMIC RESPONSE INOEX	E/A:	ENERGY ABSORBER	LL:	LOAD LIMITING
SLEP:	SERVICE LIFE EXTENSION PROGRAM	SST:	STAINLESS STEEL	T&E:	TEST & EVALUATE
CFE:	CONTRACTOR FURNISHED EQUIPMENT	CW:	CRASHWORTHY	FD:	FORCE DISPLACEMENT

## CRASHWORTHY PILOT/CO-PILOT SEATS

The opportunity to use this specification for crashworthy seating came when the U.S. Navy decided to improve its inventory of CH-46 helicopters through a Service Life Extension Program (SLEP). As a result of a concerted marketing effort by the Navy's research and development sector, it was able to convince the CH-46 acquisition manager that crashworthy pilot and co-pilot seats should be part of the total helicopter improvement program. The fact that the acquisition manager could examine prototype hardware and review test results to assess the extent of risk to his program, was a major factor in the decision to go with crashworthy seats. However, the success in "selling" these seats was due primarily to a strong requirement born out of the failure history of the two operational seats being replaced. Each of those armored seats weighed approximately 125 kg (275 lbs) as a result of armor modules being mounted onto a conventional tubular unarmored crew seat. It is no wonder that with this increased weight for ballistic protection, a series of seat retention failures took place during hard landings and crash situations. Several changes had been made to improve the seat retention capability with the armored modules installed. The last of these was the inclusion of an inertia reel mounted on the aircraft bulkhead directly in back of the seat with the strap portion attached to the seat. Its purpose was to react some of the load into the bulkhead relieving the load at the seat-track interface. However, the inertia reel proved to be ineffective for retaining the seat on the tracks and principally served to keep the seat and occupant from catapulting through the forward portion of the cockpit.

Since this program was basically a retrofit of new seats into a operational aircraft, many constraints were placed on the seat design, leading to trade-offs in performance. Alteration of cockpit, layout of controls, consoles and equipment were considered outside the scope of the program. Floor structure was to be modified only to the extent that the seat track and its tie-down points could be improved to react to crashloads. Since the eye reference point had to be maintained in its original position, the location and dimensions of the seat were fairly well fixed. A maximum bucket to floor clearance of 16.5 cm (6.5 in.) was available with the seat adjusted to its full down position. This amount of clearance is hardly sufficient to realize the full energy attenuating potential of a properly designed crashworthy seat. However, testing did indicate that the new CH-46 seat with the same ballistic protection as the original but weighing 34 kg (75 lbs) less, performed significantly better than the original. When subjected to a crash pulse representing the 95th percentile potentially survivable accident (48Gz combined axis), the seat stroked fully and maintained its structural integrity and attachment to the aircraft floor. As a comparison, the operational seat which had never undergone dynamic testing, had an "advertized" structural capability of reacting static load factors of 10Gz, 15Gx and 11Gy. Because of the new seat's limited stroking, the dummy decelerative load in the Gz direction exceeded design limits quoted in the literature, although the physiological consequence of doing so is not clearly stated. Gross injury predictors such as the Eiband Curve (8), Head Injury Criteria (9) and Dynamic Response Index (10) are used to set finite acceleration limits for design purposes but certainly need more refinement in terms of experimentation and data base to accurately predict extent of injury. The 16.5 cm (6.5 in.) limitation may have reduced the seats' full effectiveness against the most severe survivable crash pulse but as a retrofittable it vastly improved the marginal performance of its predecessor by making the best use for relative displacement of the seat and occupant with respect to the airframe. Figure 1 shows the seat installed in a CH-46E helicopter.

Another opportunity for the introduction of crashworthy crewmember seating came when the U.S. Navy decided to purchase the Sikorsky SH-60B Seahawk helicopter. Once again MIL-S-81771A was used as the control document for the pilot/co-pilot and sensor operator seats. Unlike the CH-46 retrofit program, the SH-60B is a new aircraft which has been designed to meet the same stringent crashworthy requirements as the U.S. Army's UH-60A Black Hawk. The Army design criteria from their "Aircraft Crash Survival Design Guide" (11), MIL-STD-1290 (12) and MIL-S-58095 (13) resulted in the first U.S. helicopter which truly integrates crashworthy features into the total aircraft at the earliest stages in the design process. The pilot/co-pilot unarmored seat systems in the SH-60B have the capability of stroking a full 40.6 cm (16 in.) from the up position because of additional clearance provided by a floor well beneath each seat. The sensor operator seat can stroke 35.5 cm (14 in.) from its full up adjustment. A floor well is not included at this seat location.

Two more helicopters have just recently been designated for improved pilot/co-pilot seats. Both the CH-53 and H-2 acquisition managers have funded programs to retrofit their aircraft with cockpit crashworthy seating. As with the CH-46 retrofit, the extent of improvement over the replaced seats will depend on dimensional constraints within the cockpit.

## CRASHWORTHY TROOP SEATS

A particularly challenging crashworthy development undertaken by the Navy has been troop seats. Current seats can support a 100 kg (220 lbs) occupant with a static overload factor of 10 in the down direction and 1.1 in the lateral direction. They will stay intact only at the lowest deceleration levels when dynamically tested. Troop seats are fabricated of extremely light materials because of weight restrictions and come in several different configurations, single and multiple bench sizes. The seats must be easily removed and readily stowable. In some aircraft they are mounted so that the

occupant faces forward or rearward. In the larger helicopters, such as the CH-53 and CH-46, they are mounted along the bulkhead with the occupants facing sideward. Obviously these combined features present a formidable design problem to the engineer expected to upgrade their crashworthiness. However, the development challenge has met with varying degrees of success depending on the seat configuration in the aircraft. Crashworthy forward facing troop seats have been developed and extensively tested (14). Although the very ambitious design goals originally set for them to withstand the most severe potentially survivable crash were not quite reached in the Navy program, they were able to perform without failure close to these limits. Side facing seats were also developed and tested (15) (16). They came close to meeting Design goals which were set lower than the forward facing seat because of the asymmetrical loading applied to the aft side of the seat when subjected to a crash in the forward direction. Comparing the low strength operational troop seats to these crashworthy seats, it was evident that dramatic improvements have been made. They not only showed a significant increase in structural integrity but also reduced the acceleration loading on the occupant through energy attenuation techniques. Figure 2 shows one version of a troop seat developed for the Navy.

At a later date, the U.S. Army sponsored a program which took the initial Navy work and with improvements to the design, successfully demonstrated that the seat met the performance criteria of the latest joint Army/Navy specification for troop seats (17). The seat was taken through the entire development process and is currently operational in their UH-60A helicopter. The Navy expects to use a similar version of this seat in their SH-60B helicopter.

Whether crashworthy troop seats move into other operational aircraft depends on the acquisition managers for each aircraft. Ultimately, they must decide where to invest their allocated funds and it is understandable that there are a myriad of other expenditures and potential acquisitions which could be competing with crashworthy troop seats for their support. Aside from cost, a weight penalty is associated with any retrofit of improved troop seats and may well influence any decision. For example, analysis showed that a weight increase of 175 kg (385 lbs) would be incurred in the CH-53E helicopter with the retrofit of 55 seats. This figure is based upon crashworthy troop seats weighing approximately 5.4 kg (12 lbs) each versus the 2.3 kg (5 lbs) seats they will replace. The additional weight could be compensated by the elimination of two stations from the total capacity of the aircraft. Obviously the weight penalty for helicopters such as the H-1, H-2 and H-3 which carry a limited number of passenger's, would be much smaller and not a critical influencing factor in the acceptance of crashworthy troop seating.

#### CRASHWORTHY GUNNER/CREW-CHIEF SEATS

Along with the development of troop seats another effort was directed toward the design of a crashworthy Gunner/Crew-Chief seat for helicopters such as the UH-1, CH46 and CH-53 (18). These seats require more rugged structure than troop seats but are less elaborate than pilot/co-pilot seats. Normally mounted side facing in the aircraft, they are subjected to harder use and must support an occupant wearing an armored protective vest. In addition, the design selected for development featured a modular armored seat pan which could be installed under the comfort cushion for additional ballistic protection. During non-combat missions the armor is readily removable for storage off the aircraft. Total weight of the seat with the module is 24 kg (53 lbs). Without the armored seat pan it weighs 12 kg (26 lbs). The seat was designed to distribute the crash forces between the upper and lower seat tie-downs to the aircraft. Figure 3 shows a drawing of the seat (similar to the troop seat) with its array of floor attached and ceiling attached energy attenuators. These devices are arranged to stroke in series, stabilizing the seat as it moves during the impact. A series of dynamic crash tests conducted on the Navy's Vertical Drop Tower proved the feasibility of this approach. The performance of the seat established that the design met the crashworthiness objective. Integration of the design into a new aircraft would not be a problem. However, using this design as a retrofit for aircraft such as the CH-46 or 53 would be a more formidable task. Since the seat is anchored by energy attenuators from above and below it will require a modification to the aircraft structure to attach the upper seat attenuators into the airframe. Preliminary analysis indicated that installation of a Gunner/Crew-Chief seat can be made with minimal structural reinforcement since the series design of the upper and lower energy absorber configuration reduces the ceiling load reaction.

#### CRASHWORTHY PASSENGER SEATS

The primary objective of this Navy effort was to design and fabricate military passenger seats which demonstrate crash safety and comfort. State-of-the-art seat technology can now offer these features in a cost effective way. It is anticipated that crashworthy passenger seats could prevent nearly 50 percent of the fatalities and serious injuries occurring in survivable transport aircraft crashes without paying a weight penalty for the new technology.

Two types of passenger seats have been developed and tested (19) (20) (21). One is a forward facing seat and the other, rear facing. Each seat is a bench type with separate back rests and is capable of supporting two occupants. A series of dynamic tests performed on both types proved the feasibility of using either approach to react a crash pulse of 24 G's (peak acceleration) with an impact velocity change of 15.2 m/sec (50 ft/sec). A representative seat orientation for a combined horizontal crash of 20° pitch, 10° yaw and 25.8° roll was used for the tests. In the case of the rear facing seat,

floor deformation of the aircraft was simulated by distorting one mounting track 10 degrees in pitch and rolling the other track 10 degrees. This floor distortion was chosen to maximize stresses produced in the seat and represents a realistic crash occurrence. Figure 4 and 5 show the rear facing seat installed on a fixture in its pre and post test position (note floor track distortion).

The technology demonstrated in this Navy program is directly applicable to commercial aircraft carriers. As a matter of inter-agency cooperation, the Federal Aviation Agency (FAA) participated in the program through the use of their Civil Aeromedical Institute test facility. In comparison to the crashworthy passenger seats, the present FAA commercial aircraft requirement for occupant inertia forces relative to seat structure during an emergency landing is; 2.0 G upward, 9.0 G forward, 1.5 G sideward and 4.5 G downward (22). It is evident from these values that a considerable crashworthy improvement could be obtained with new seats designed to the technology shown feasible by this program.

#### RESTRAINT

As a complimentary program to crashworthy seating, the Navy has an ongoing joint effort with the U.S. Army to develop a restraint known as "Inflatable Body and Head Restraint System, (IBAHRS)." Previously designed and developed under a Navy program to show feasibility of approach (23), the services have joined together to accelerate the development of IBAHRS because of the solutions it offers to present day restraint inadequacies. The Army's interest is driven by a concern that during a hard landing or crash of certain helicopters, crewmembers are likely to strike optical equipment directly in front and in close proximity to their heads. IBAHRS holds the potential of reducing this hazard. The U.S. Navy also has the same concern but looks upon IBAHRS as a viable candidate for incorporation in all its helicopters.

Present day crewmember restraint consists of a pair of shoulder harnesses and a lap belt fitted together at a single point release buckle. The normal adjustment of the harness allows some free movement of the occupant during mission performance. If a crash is imminent, the crewmembers are advised to position their backs against the seat allowing the inertia reel to take up excessive strap length. However, some slack will remain in the restraint as a result of its initial adjustment. It has been demonstrated that a slack harness reduces the effectiveness of a restraint, increasing dynamic overshoot and the probability of severe injury during a potentially survivable crash. A loose lap belt could also contribute to occupant submarining, adding to the probability of debilitation.

If the crewmembers have sufficient time and presence of mind, they could lock the inertia reel and then tighten each of their harness straps removing as much slack as possible. It is not likely under the stressful situation of an impending crash that they will go through this procedure. IBAHRS was developed as a passive system which would automatically tighten the harness at the onset of a crash. It uses an inflatable which upon expanding, pretensions the straps and forces the occupant back against the seat. This action reduces the dynamic overshoot effect and restricts the body and head motion of the wearer, lessening his chances of striking cockpit objects. Strap loading concentration on the torso is reduced because of the large bearing surface spread across the wearers body when the restraint inflates. A crotch strap is used to prevent submarining by the occupant.

IBAHRS has three main subassemblies: (a) the harness/bladder, (b) the solid propellant gas generator or inflator and (c) the omnidirectional crash sensor system. Figure 6 is an illustration of the various parts showing the location of the inflators within the bladders and the remote sensor hookup to the aircraft's electrical system. The operation of IBAHRS is as follows: A crash sensor system located on the cockpit floor rapidly detects the occurrence of a helicopter crash (recognizing a crash signature of a particular magnitude) and through a wire connected circuit closure fires an electrical squib in each generator mounted within the left and right hand bladders. The bladders, manufactured of high strength material are attached to the underside of conventional shoulder straps and are neatly folded and held in place so that the appearance of the system shows little alteration from current restraints. Upon detonation, the generators produce a non-toxic gas which unfurls and fills the bladders in less than 20 milliseconds. Figure 7 shows the inflatable bladders and their installation. After approximately one second the gas pressure is relieved within the bladders. Testing of the system under simulated crash conditions has shown significant load reductions on the occupant and the ability to take-up almost any amount of harness slack.

#### A SYSTEMS APPROACH

Crashworthy seating is only one part of an overall approach to crash survivability. It makes little sense to concentrate on seating systems for aircraft such as the CH-46 or CH-53 without considering their compatibility with cargo. It is usual operational procedure to carry a mix of passengers and cargo during a flight. If the cargo should break away from its aircraft tie-down at the onset of a crash, the probability of survival becomes nil. The concern over the interaction of the cargo with personnel is only one of many issues which must be addressed and program managers would be remiss if they do not use a systems approach to crashworthiness. This involves the process of examining all the consequences of a crash that may contribute to injury or fatality. It does no good to survive a crash through a sophisticated seating system only to have the individual subsequently drowned in a sinking helicopter or gravely injured because of fire.



The Navy is addressing the total problem of crash survivability in its Helicopter Aircrew Survivability Enhancement Program, (HASEP). Within this program it is examining different crash scenarios and associated hazards. Crashworthy seating and cargo restraint, helicopter flotation and sink rate retardation, hatch lighting and removal, underwater breathing and crashworthy fuel cells are all being investigated for possible incorporation as retrofittables for operational helicopters and as requirements for new helicopters. Currently, development efforts are underway to provide flotation/sink rate retardation for the heaviest helicopters in the U.S. Navy. Another effort is on-going to develop underwater hatch lighting systems. The initial phase of a program has recently been completed which resulted in the development of a crashworthy cargo restraint system capable of maintaining its structural integrity and tie-down in an aircraft (24). HASEP intends to address all of the potential hazards in a priority order, sponsoring development programs to solve the problems while bringing all these technologies together to optimize crash survivability.

#### ON-GOING DEVELOPMENT

The development of hardware is an iterative process in which products are moved forward to the operational sector while further refinements and improvements are being investigated. As a typical example, the crashworthy pilot/co-pilot seats for the SH-60B will soon be placed in operation but a new exploratory development program is in progress to further improve its future performance. These crashworthy seats are presently constrained by single load limit settings which match the effective weight of a 50th percentile seat occupant. Since the seat must also accommodate the total range of occupant weights ranging from 5th through 95th percentiles, its crash performance is a compromise between these extremes. The heavy occupant therefore receives a "soft" ride during the stroking of the seat while the lightweight occupant is exposed to higher accelerations for any given crash condition. A method has been developed which overcomes this limitation and maximizes the effectiveness of the seat. It adjusts the limit load for the specific weight of the occupant, optimizing the seat system performance for the total military crewmember weight distribution (25).

The SH-60B uses two inversion tube energy absorbers as its load limiters. A device has been conceived, fabricated and tested which will allow the seat occupant to manually select a limit load value corresponding to his weight including equipment. Figures 8, 9 and 10 show the system installed on a seat. By adjusting a manual control dial to this weight, a flexible shaft is rotated and in turn adjusts the energy absorbers to the proper limit load by a constricting mechanism. The mechanism consists of six spherical balls captured by a ball retaining ring and a ball adjustment ring on each energy absorber. The spherical balls are guided within cross holes in the ball retaining ring which is riveted to the energy absorber housing. The adjustment ring has six "cammed" or "ramped" surfaces which, as the adjustment ring is rotated by the flexible shaft worm gear, displaces the balls either towards or away from the centerline of the inversion tubes. The extent of deformation (grooving) to the inversion tubes is determined by the position of the balls, Figure 11. A series of dynamic crash tests were conducted to comparatively test and evaluate the performance of the variable-load energy absorbers against the single-load energy absorbers currently being used on the SH-60B seat. When a 5th percentile seated dummy was exposed to a 48G, 15.2 m/sec (50 ft/sec) crash pulse the variable energy absorbers allowed the seat pan to stroke 36.8 cm (14.5 in.). Under identical conditions, the single-load energy absorbers stroked 24.1 cm (9.5 in.). The 52 percent increase in displacement reduced all plateau acceleration measurements on both the seat pan and dummy chest cavity. Calculation of the Dynamic Response Index also showed a significant decrease for the longer stroking seat. A similar test comparison using 95th percentile dummies resulted in both seats stroking almost the same distance, 28.2 cm (11.1 in.) versus 29.5 cm (11.6 in.), which is within the design range of displacement for the 95th percentile occupant in the full down position. In that position there is 30.5 cm (12 in.) available for stroking into the floor well beneath the pilot/co-pilot stations. Had the seats traveled any further during the tests, they would have "bottomed-out" on aircraft structure. Avoidance of such a happening was a design constraint at the upper range of occupant weights for either energy absorption system and both performed within design tolerance.

#### CONCLUSION

As stated previously, development of crashworthy seating systems has been undertaken to bring the technology up to a level where it would be considered low risk for final point design and development into designated aircraft. By initiating new programs and taking them through exploratory and advanced development, confidence is generated in two very important sectors; 1) private industry, the ultimate supplier of the equipment and 2) the military acquisition manager, the customer for the designated aircraft. Both must be convinced that the development of crashworthy seating systems is achievable before they will participate in the enterprise. Without that confidence, the hardware will remain "on-the-shelf," likely not to advance any further to the user community. Through research and development programs sponsored by the U.S. Navy and Army, crashworthy seating for non-ejection aircraft have been demonstrated to be feasible, cost effective and ready for incorporation into operational aircraft. Albeit a slow process, various crashworthy seats have been accepted into fleet aircraft and it is hopefully expected that all military aircraft will be outfitted with crashworthy seating systems in the near future.

#### ACKNOWLEDGEMENTS

The assistance of Mr. Leon Domzalski of the Naval Air Development Center, in providing information for this paper is gratefully acknowledged.

## REFERENCES

1. Domzalski, L.P., et al, "U.S. Navy Development in Crashworthy Seating," Proceedings of the 18th Annual SAFE Symposium, San Diego California, Oct 12-16, 1980
2. Military Specification, MIL-S-7832A(Acr), "Seats, Pilot's, Adjustable, Short Range Aircraft," of 16 Oct. 1954, Department of Defense, Washington D.C.
3. Langner, F.C., "Conduct Study, Design, Develop and Furnish Prototype of Energy Absorption Systems for Aircraft Seats," Aerotherm Corp. Final Report of 30 March 1960
4. Domzalski, L.P., "Dynamic Testing of an Energy Attenuating Armored Crew Seat," Naval Air Development Center, Warminster PA, Report No. NADC-AC-7001 of 15 May 1970
5. Schulman, M, "Development and Dynamic Testing of an Energy Absorbing Helicopter Crew Seat," Naval Air Development Center, Warminster PA, Report No. NADC-CS-7109 of 30 Dec 1971
6. Mazelsky, B., "A Crashworthy Armored Pilot Seat For Helicopters, Naval Air Development Center, Warminster PA, Report No. NADC-74018-40 of 18 Jan 1974
7. Military Specification, MIL-S-81771A(AS), "Seats; Aircrew Adjustable; Aircraft General Specification For," of 30 April 1975 Department of Defense, Washington D.C.
8. Eiband, A.M., "Human Tolerance to Rapidly Applied Accelerations: A Summary of the Literature," National Aeronautics and Space Administration, Washington D.C. NASA Memorandum 5-19-59E, June 1959
9. Federal Motor Vehicle Safety Standard No. 208 "Occupant Crash Protection," Part 571 Motor Vehicle Safety Standards, U.S. Department of Transportation, NHTSA, Washington, D.C. Aug. 15, 1977
10. Stech, E.L., Payne, P.R., "Dynamic Models of the Human Body," Aerospace Medical Research Laboratory, Wright Patterson Air Force Base, Ohio, AMRL Technical Report 66-157 Nov. 1969
11. "Aircraft Crash Survival Design Guide, Vol. I through V," Applied Technology Laboratory (AVRADCOM) Ft. Eustis VA, Report No. USARTL TR 79-22, 1980
12. Military Standard, MIL-STD-1290(AV), "Light Fixed and Rotary Wing Aircraft Crashworthiness," of 25 Jan 1974, Department of Defense, Washington D.C.
13. Military Specification, MIL-S-58095(AV) "Seat System: Crashworthy, Non-Ejection, Aircrew General Specification," Aug 1971, Department of Defense, Washington D.C.
14. Domzalski, L.P., "Test and Evaluation of Two Crashworthy Troop Seat Concepts," Naval Air Development Center, Warminster PA, Report No. NADC 80197-60 of 30 Sept 1980
15. Reilly, M.J., "Energy Attenuating Troop Seat," Naval Air Development Center, Warminster PA, Report No. NADC-AC-7105 of 24 March 1971
16. Reilly, M.J., "Energy Attenuating Troop Seat Development Report, Addendum, Naval Air Development Center, Warminster PA, Report No. NADC-73121-40 of 8 Jan 1973
17. Military Specification, MIL-S-85510(AS), "Seats, Helicopter Cabin, Crashworthy, General Specification for," undated.
18. Mazelsky, B, "Design Fabrication, and Testing of an Armored Gunner/Crew-Chief Seat System," Naval Air Development Center, Warminster PA, Report No. NADC-80155-60 of June 1980
19. Reilly, M.J., "Crashworthy Passenger Seat Development and Test," Boeing Vertol Corp., Eddystone, Pa. Report No. D210-11845-1 of June 1981
20. Mazelsky, B., "Design, Development and Fabrication of a Military Crashworthy Passenger Seat System," Aerospace Research Associates, West Covina, California, Report No. 194 of May 1979
21. Mazelsky, B., "A Design Study On Crashworthy Two-Man Passenger Seats For Fixed Wing and Rotary Wing Aircraft With Experimental Verification For A Rearward Facing Fixed Wing Configuration," Aerospace Research Associates, West Covina, California, Report No. 224, Aug 1981
22. Federal Aviation Regulations, Emergency Landing Conditions, Part 25 Airworthiness Standards: Transport Category Airplanes, Department of Transportation, Federal Aviation Administration, June 1974
23. Schulman, M. McElhenney, J., "Inflatable Body and Head Restraint," Naval Air Development Center, Warminster PA, Report No. NADC-77176-40 of 30 Sept 1977

24. Shefrin, J., "Demonstration of Advanced Cargo Restraint Hardware For COD Aircraft. Vol. 1," Naval Air Development Center, Philadelphia PA, Report No. NADC-77154-60
25. Svoboda, C.M., Warrick, J.C., "Design and Development of Variable Load Energy Absorbers," Naval Air Development Center, Philadelphia PA, Report No. NADC 80257-60 of 16 June 1981
26. Woodward, C.C., et al, "Investigation, Design and Development of an F7U-3 Ejection Seat Energy Absorption System For Reduction of Crash Force Loads," Naval Air Material Center, Philadelphia PA, Report No. NAMC-ACEL 335 of June 1957
27. Boeing/Vertol, "Final Report on Development of Vertol Mark I Crash-Safety Troop Seat," Boeing/Vertol Co., Eddystone PA, Report No. R-397 of May 1965
28. Schulman, M., "Dynamic Testing of a Developmental Net Cushioned Helicopter Crew Seat," Naval Air Development Center, Warminster PA, Report No. NADC-AC-6819 of Jan 1969
29. Reilly, M.J., "Crash Attenuating Armored Crew Seat Development Report," Boeing/Vertol Co., Eddystone PA, Report No. D8-2431-1 of May 1969
30. Schwartz, M., "Dynamic Testing of Energy Attenuating Devices: Phase Report," Naval Air Development Center, Warminster PA, Report No. NADC-AC-6905 of 9 Oct 1969
31. Military Specification, MIL-S-81771(AS), "Seats; Aircrew Adjustable; Aircraft General Specification For," of 10 June 1970, Department of Defense, Washington, D.C.
32. Carr, R.W., Phillips, N.S., "Definition of Design Criteria For Energy Absorption Systems," Naval Air Development Center, Warminster PA, Report No. NADC-AC-7010 of 11 June 1970
33. Phillips, N.S., et al, "A Statistical Investigation Into the Development of Energy Absorber Design Criteria," Naval Air Development Center, Warminster PA, Report No. NADC-CS-7122 of 30 Dec 1971
34. Mazelsky, B., "An Armored Energy Attenuating Crewman's Seat For Rotary and Light Fixed Wing Aircraft," Naval Air Development Center, Warminster PA, Report No. NADC-72186-CS of 29 Sept 1972
35. Pavlick, M.J., "Prototype Fabrication and Testing of Improved Restraint System," Naval Air Development Center, Warminster PA, Report No. NADC-73002-40 of 31 Jan 1973
36. Pavlick, M.J., et al, "Prototype Fabrication and Testing of a Modified MA-2 Harness," Naval Air Development Center, Warminster PA, Report No. NADC-75034-40 of 30 April 1975
37. Glancy, J., Desjardings, S., "A Survey of Naval Aircraft Crash Environments With Emphasis on Structural Response," Dynamic Science, Deer Park, Arizona, Report No. 1500-71-43 of Dec 1971
38. Mazelsky, B., "Preliminary Design of Armored Crashworthy Crew Seats For Future Army Helicopters," Aerospace Research Associates, West Covina California, ARA Report No. 174 of 12 Aug 1975
39. Gerner, J., "Design Study of Lightweight Armored Helicopter Seat Incorporating Crash Attenuating Supports," Naval Air Development Center, Warminster PA, Report No. NADC-7229-CS; Budd Co. Report No. 9400-196-2964 of 22 Dec 1969





FIGURE 1. Seat Installed in a CH-46E Helicopter



FIGURE 2. Crashworthy Troop Seat - Upper and Lower Energy Absorbers



FIGURE 3. Gunner's Seat with Armored Seat Pan and Upper/Lower Energy Absorbers



FIGURE 4. Rearward Facing Passenger Seat



FIGURE 5. Rearward Facing Seat After Stroking

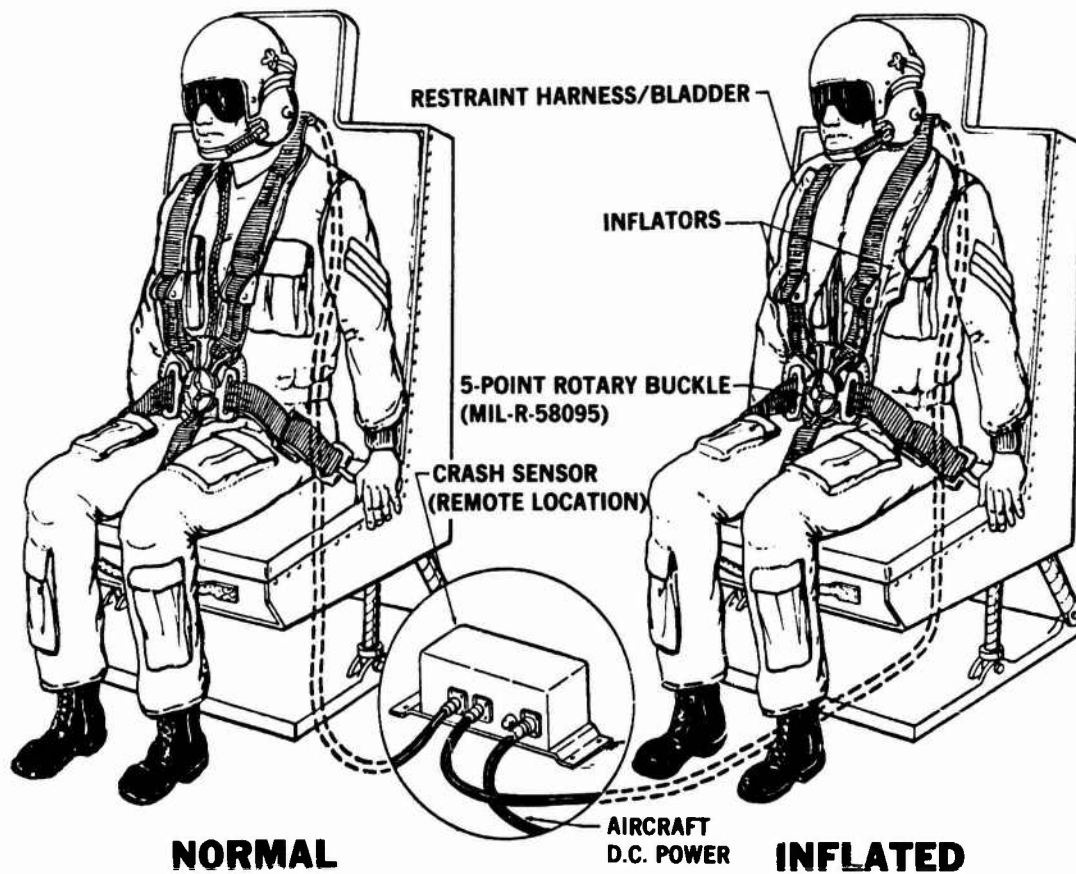


FIGURE 6. Illustration of IBAHRS



IBAHRS Before Actuation



IBAHRS After Actuation

FIGURE 7.



FIGURE 8. Crashworthy Seat with Control Dial on Upper Right Side - Ready for Test

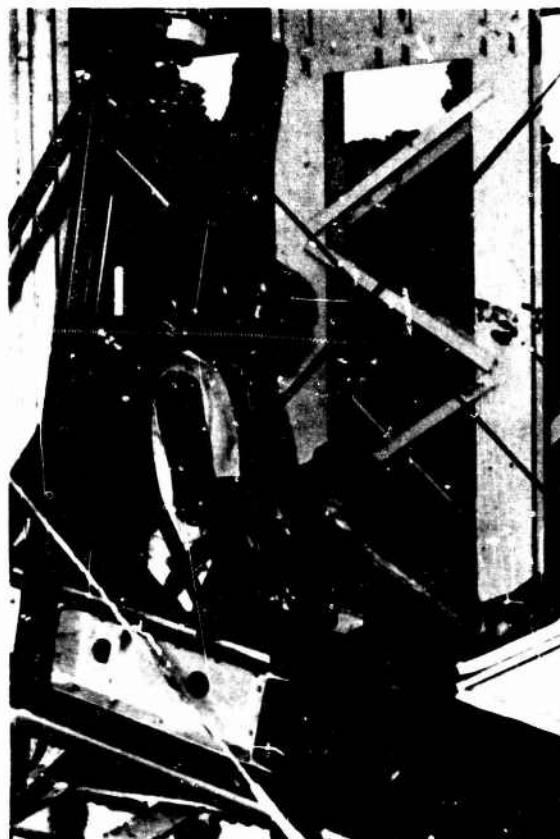


FIGURE 9. After Stroking

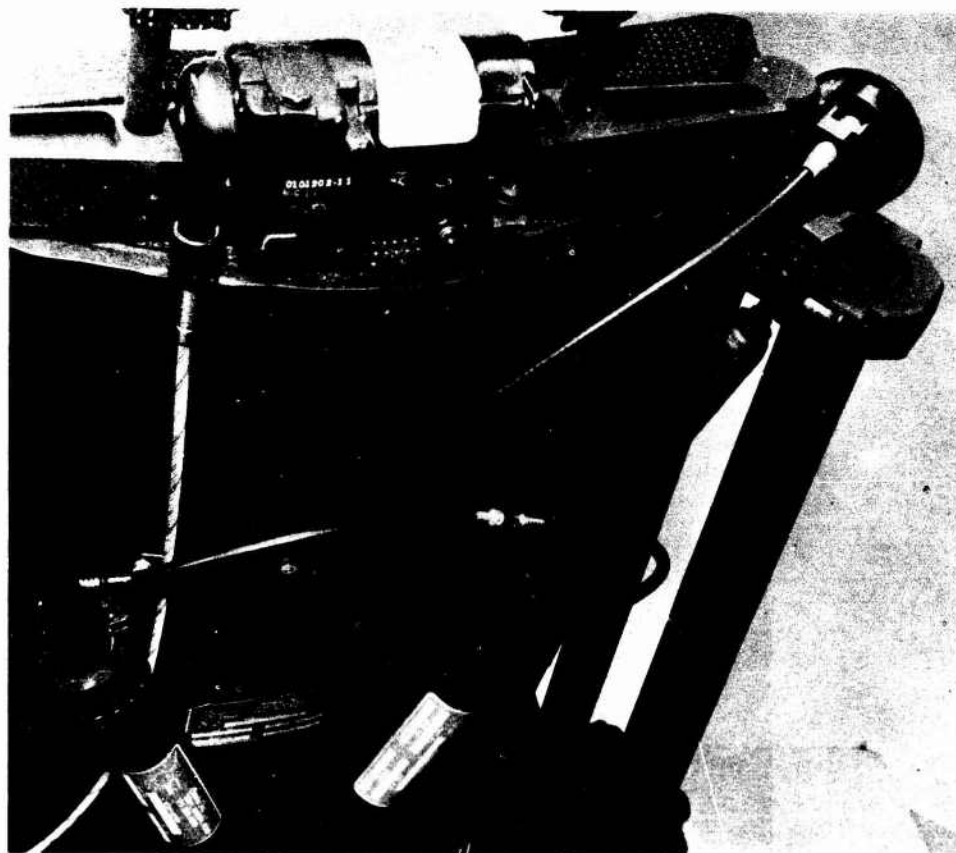


FIGURE 10. Energy Absorbers and Flexible Control Shaft Adjusters

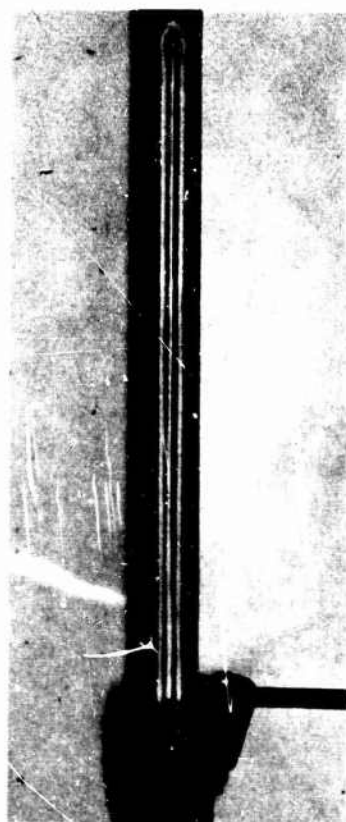


FIGURE 11. Post Test View of One Energy Absorber Showing Grooves

## DEVELOPMENT OF IMPROVED CRITERIA FOR ENERGY-ABSORBING AIRCRAFT SEATS

by  
S. P. Desjardins, President  
J. W. Coltman, Research Engineer  
D. H. Laananen, Manager, Research and Development

Simula Inc.  
2223 South 48th Street  
Tempe, Arizona 85282  
U.S.A.

### SUMMARY

Present criteria for the design and evaluation of crashworthy aircraft seats have been in existence since 1971. Their application has enabled greatly improved seating systems to be developed and put into use in modern U.S. Army helicopters. The experience gained during the development and qualification of these production systems has emphasized the need for more comprehensive criteria. An interagency effort was therefore initiated and sponsored by the U.S. Army to accomplish this goal. Several research efforts are presently underway to provide the needed information to develop more rigorous and comprehensive design and evaluation criteria, to more completely understand the complex response of the human occupant and seating system in the crash environment, and to maximize the efficiency of such systems in providing crash protection to the occupant. The efforts now underway include the acquisition of additional information concerning human tolerance to +G<sub>z</sub> loading, the development of a standardized test dummy, variables testing and a sensitivity analysis to determine the influence of the many variables involved on the seat and occupant response, an investigation of the influence of the test subject considering various anthropomorphic dummies as well as cadavers, and, of course, the overall synthesis and interpretation of the results of these research efforts. This paper summarizes these projects, reports on their status, and presents preliminary results of the research efforts.

### 1. INTRODUCTION

The new generation of U.S. Army helicopters possesses unprecedented crashworthiness, as pointed out in Reference 1. These aircraft are equipped with many crashworthy features, including seats designed both to provide efficient restraint in all loading directions and energy-absorbing stroke in the vertical, or +G<sub>z</sub>, direction. The seats are designed to comply with existing criteria that were developed and documented in 1971 (References 2, 3, and 4). Although these seats are far superior to any prior systems, there are several areas of uncertainty in the design criteria that require additional research to enable further progress to be made in the hardware.

First, knowledge concerning human tolerance to +G<sub>z</sub> acceleration is extremely limited. In fact, little new information concerning human tolerance to acceleration in this direction has been developed in many years. Although extensive effort has been expended on the critical areas of human head and neck response (U.S. Navy) and the effects of restraint system variables on acceleration loads in the forward, -G<sub>x</sub>, and lateral, G<sub>y</sub>, directions (U.S. Air Force), essentially no effort has been directed in this other very critical direction. The need for additional knowledge of +G<sub>z</sub> response is affirmed when it is considered that aircraft occupants can withstand the full 95th-percentile survivable crash acceleration conditions in the lateral and longitudinal directions with no energy absorption, only proper restraint (a complex problem when related to the head), but cannot tolerate the 95th-percentile vertical crash pulse without energy absorption.

The last program of significance to investigate the variables associated with vertical (+G<sub>z</sub>) acceleration of aircraft occupants was sponsored by the U.S. Army Air Mobility Research and Development Laboratory, Fort Eustis, Virginia, (now the Applied Technology Laboratory) in 1969 and 1970. The results of this program are presented in Reference 5. The goal of this earlier program was to evaluate the meager information then available and to develop an achievable criterion to guide the design of crashworthy crewseats for U.S. Army aviation. This task was accomplished, and the resulting criterion has now been in existence for the past ten years.

Techniques used for the design and evaluation of energy-absorbing seating systems are explained in detail in References 1, 2, 4, and 6; however, in summary, the Eiband human tolerance data with upper level ejection seat criteria superimposed (as presented in the Aircraft Crash Survival Design Guide, Reference 7) was taken for the upper limit of tolerable acceleration in the +G<sub>z</sub> direction. Tests and analyses were then conducted to establish the force level necessary on the vertical energy-absorption system to limit the acceleration excursions of the seat pan to magnitudes of less than 23 G for time durations in excess of 0.006 sec as dictated by the tolerance data. The test results indicated that if the energy-absorbing mechanism were set for stroking at a force computed using a 14.5-G load factor, the desired result could be achieved. Test data supporting the conclusions of this analysis are presented in Reference 5.

In seat tests conducted during the ensuing years, a characteristic seat pan z-axis deceleration response was observed. In this characteristic curve, the seat pan deceleration rises sharply during the onset of the input pulse, then drops rapidly, sometimes passing through zero. It then rises sharply and forms a secondary spike before damping out around the load factor used in the design of the energy-absorbing system. In most of the tests conducted during the time period between 1971 (when the criteria were established) and the present, the secondary spikes have exceeded the criteria limit of 23 G and have been a source of concern. One question of concern is whether the secondary spike is a natural response of the seat and occupant spring-mass system, or if it is caused by some external source. Also, it is not known whether the acceleration spike is hazardous to the seat occupant.

The need for answering these questions was confirmed in August 1978, during qualification testing of the U.S. Army's Black Hawk helicopter crewseat, when the secondary acceleration spike once again exceeded the criteria limits. At that time it was decided to research the data available and to attempt, through analysis, to determine whether the secondary spike did, in fact, increase the hazard to the occupant. The results of this analysis indicated that the secondary spike is a natural response of the seating system and, in itself, does not increase the hazard to the occupant. However, the analysis also indicated that the crash pulse might be hazardous to the occupant at times other than during the secondary spike. It was further concluded that the criterion as it now exists is not sufficiently comprehensive, and that additional research should be immediately initiated to both establish the effects of system variables upon seat and occupant response and expand knowledge in the area of human tolerance to decelerative loading in the +G<sub>z</sub> direction. These additional data constitute a necessary prerequisite to establishing<sup>2</sup> a more comprehensive set of criteria controlling the design of crashworthy crewseats. Under the leadership of the U.S. Army Applied Technology Laboratory at Fort Eustis, Virginia (ATL), and the U.S. Army Aeromedical Research Laboratory at Fort Rucker, Alabama (USAARL), a multi-service effort was initiated with goals of performing the research necessary in these areas. The overall program is illustrated in Figure 1. The research efforts were designed to provide at least a minimum level of needed information in each area and to meet the following objectives:

- Establish the sensitivity of seat and occupant response to system variables.
- Determine the effect on system performance of the type of dummy being used for testing and establish an appropriate standardized dummy for seat system evaluation.
- Investigate the performance of the seat with an occupant more nearly representative of the operational occupant than are anthropomorphic dummies. Cadavers were to be used for this investigation.
- Establish, through dynamic testing, additional information concerning human tolerance to acceleration loads in the +G<sub>z</sub> direction.

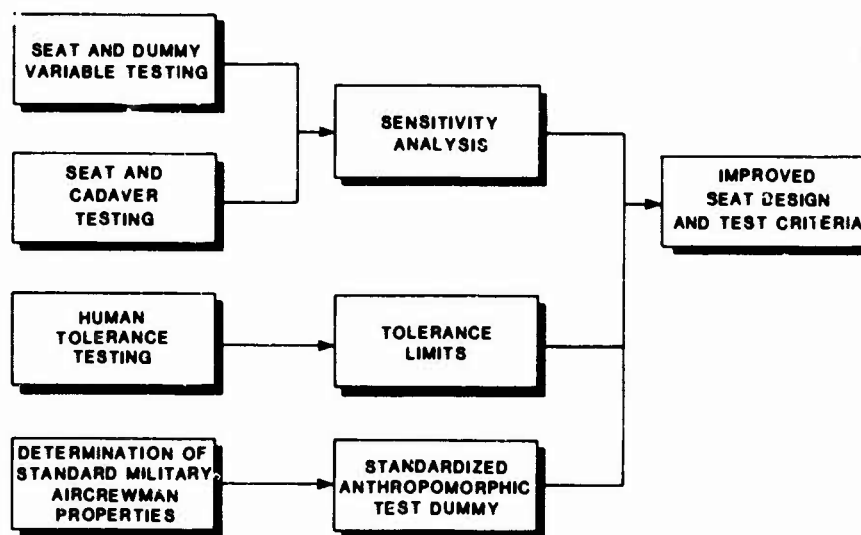


Figure 1. Overall program elements.

The effort to establish a standardized test dummy is being coordinated by USAARL and involves an ad-hoc committee consisting of representatives from both interested Government agencies and the private sector. Research to increase the knowledge of human tolerance to acceleration loads in the +G<sub>z</sub> direction is being performed by the Naval Biodynamics Laboratory, Michoud, Louisiana,<sup>2</sup> with support and sponsorship of USAARL. The other research is being coordinated by Simula Inc., with test and advisory support of many of the other involved organizations, and with the sponsorship primarily of the ATL and USAARL. The overall program is summarized in Table 1.

The purpose of this paper is to summarize the status of this overall effort and to present some preliminary information available from these current programs.

TABLE 1. PROGRAM RESPONSIBILITIES			
Program Objective	Agency/Organization	Responsibility	Sponsor
Establish the sensitivity of vertically (z-axis) stroking seating systems and improve the criteria for their design.	Simula Inc., Tempe, Arizona	Overall responsibility for program direction. Provide all seat hardware, data analysis, data synthesis and interpretation, and report results. Also, perform testing, data acquisition, reduction, and analysis.	Applied Technology Laboratory, U.S. Army Aviation Research and Development Command, Fort Eustis, Virginia
	Civil Aeromedical Institute, Oklahoma City, Oklahoma	Perform dynamic testing support; provide instrumentation and test dummies; record, reduce, and submit data; and advise on other programs.	Federal Aviation Administration
	Naval Air Development Center, Warminster, Pennsylvania	Provide dynamic test support, instrumentation, data acquisition, and reduction.	U.S. Navy
Determine the tolerance threshold limit-load setting for the energy-absorbing mechanism that would not cause spinal injury in cadavers. Also, determine the response of an energy-absorbing crewseat with a human cadaver as an occupant for comparison with the response using an anthropomorphic dummy.	Simula Inc., Tempe, Arizona	Overall program responsibility. Provide test seat hardware, establish instrumentation requirements, perform final analysis of data, interpret and report results.	U.S. Army Applied Technology Laboratory, Fort Eustis, Virginia; U.S. Army Aeromedical Research Laboratory, Fort Rucker, Alabama; Federal Aviation Administration Technical Center, Atlantic City, New Jersey; U.S. Air Force, 6570th Aerospace Medical Research Laboratory, Wright-Patterson Air Force Base, Ohio
	Bioengineering Center, Wayne State University	Acquire cadavers, instrument the cadavers; perform the dynamic tests; acquire, record, and reduce test data.	Same as above
Standardize the seat test dummy.	Ad-hoc committee consisting of representatives from industry and Government	Acquire and select pertinent data for use in establishing the physical parameters of the military aircrewman for use in subsequent development of a standardized test dummy.	U.S. Army Aeromedical Research Laboratory, Fort Rucker, Alabama
Improve knowledge of the tolerance of human subjects to +G <sub>z</sub> accelerative loading.	U.S. Naval Biodynamics Laboratory, Michoud, Louisiana	Overall Program responsibility including performing tests of live human volunteers, followed by surrogates. Acquisition of data, analysis and presentation of results.	U.S. Army Aeromedical Research Laboratory, Fort Rucker, Alabama; U.S. Naval Biodynamics Laboratory, Michoud, Louisiana



## 2. SEAT AND OCCUPANT RESPONSE TO VERTICAL (+G<sub>z</sub>) ACCELERATIVE LOADING

The desired function of crashworthy crewseats is to protect occupants from the decelerative crash load hazards with severities up to and including those of a 95th-percentile survivable crash pulse as defined in Reference 7. Since a properly restrained human can withstand the lateral and longitudinal loads associated with the respective 95th-percentile survivable crash pulses, no load attenuation is necessary, or desirable due to space limitations, in those directions. In the vertical direction, however, crash energy absorption and force attenuation are required since the human spine can withstand only a fraction of the load associated with the 95th-percentile survivable vertical crash pulse.

Various criteria for design of the vertical energy absorption system have been established. Basically, they involve establishing the force level at which the energy-absorbing system should stroke to limit the load in the human spine to a tolerable magnitude. This is accomplished by determining some "effective" weight for the occupant (effective weight is less than the total body weight because part of the body weight - the weight of the feet, lower legs and lower thighs - is carried by the floor of the aircraft rather than by the seat), adding to it the movable weight of the seat, and multiplying the sum by the load factor (G) determined to be tolerable. The criteria included in the 1970 edition of the Crash Survival Design Guide (Reference 8), Paragraph 3.3.3.1, state that "This effective weight plus the weight of the movable portion of the seat should be decelerated at an average level of 18 G or less." Average G is further defined as "The total velocity change of the seat pan ( $\Delta v$ ) divided by the total pulse duration of the seat pan." (Notice that no mention was made of the shape of the deceleration-time history but, rather, only the average deceleration established by dividing the area under the curve by the duration.) However, some researchers felt that perhaps the 18-G average value was too high and would still allow occupant injury. Consequently, in 1969 and 1970, a limited research program was sponsored by the U.S. Army Aviation Materiel Laboratories and conducted by Dynamic Science (AvSER Facility) to try to re-evaluate, verify, and refine the criteria for the design of crashworthy armored crewseats. Results of this program are documented in Reference 5.

Again, the objective of the criteria was to provide design guidance that would help in the development of seats that would limit occupant spinal loads to tolerable levels during crash pulses of severities up to, and including, the 95th-percentile survivable vertical crash pulse. The acceptable acceleration levels specified by Reference 4, which had been based on the Eiband tolerance data and the ejection seat design band (Reference 9), were selected for use. As shown in Figure 2, this criterion limits the headward (+G<sub>z</sub>) acceleration imposed on the occupant to 23 G for time durations in excess of 0.006 sec, where time durations are defined as the length of the plateau between the onset and the offset portions of the acceleration-time histories experienced by the seat pan. The research program was structured to determine and establish the stroke distance and load for the energy-absorbing mechanisms to limit the accelerations imposed on the occupant to values less than those estimated to produce injury according to this criterion. It was thought that if the load attenuation system on the seat would provide such performance, then, within the limits of the seat stroke, the occupant would have as good a chance of avoiding injury as an individual using an ejection seat.

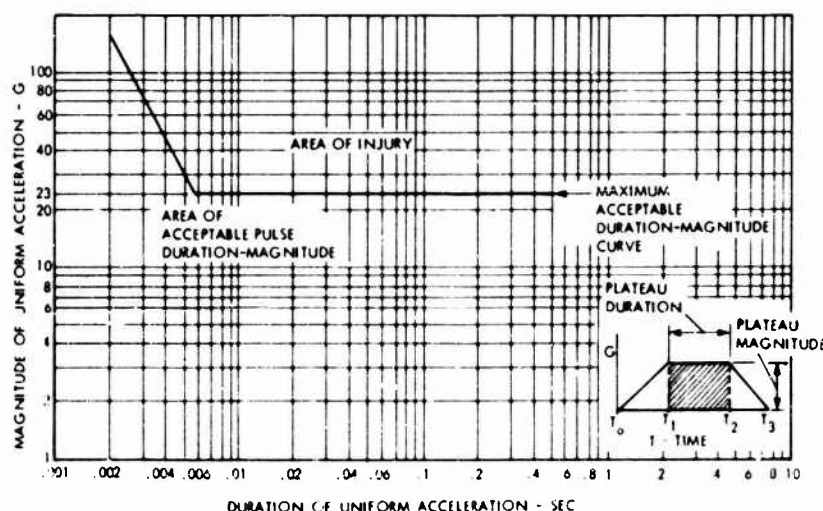


Figure 2. Maximum acceptable vertical seat acceleration (from Reference 4).

The research program mentioned above consisted of analysis followed by a series of eight dynamic tests to develop the criteria for determining the limit load that would produce the desired performance within the prescribed minimum practical stroking distance of 12 in. Because of funding limitations, the program conducted was not sufficient to include a comprehensive investigation of the influence of many of the variables; such as



energy absorber load-versus-deformation characteristics, anthropomorphic dummy variables, rate of onset and input pulse shapes, bottom cushion load-deflection characteristics, and seat spring rate. However, the tests that were run indicated that it should be possible to retain the seat pan deceleration within the limits of the criteria used for ejection seats.

In the years following development of the criteria, several crashworthy seats were developed. As these seats were dynamically tested, a characteristic deceleration-time history was displayed (see Figure 3). The characteristic shape had been evident in the criteria development test data as well, but the magnitudes of the peaks and valleys had been lower. As mentioned in the Introduction, the characteristic shape of the seat pan deceleration-versus-time history includes a high initial spike followed by a deep notch that sometimes passes through zero, actually becoming an acceleration rather than a deceleration. This notch is followed by a second high peak, followed, in turn, by various waveforms damping out and usually centering around the design limit-load factor of the system. This characteristic shape is apparent in all dynamic tests of the various crashworthy seat designs, including the Dynamic Science criteria development seat (Reference 5), the Simula Inc. UTTAS prototype seat (Reference 10), the Simula Inc./Norton Co. Black Hawk production seat (Reference 11), and the ARA Inc. JA/N SEAT (Reference 12).

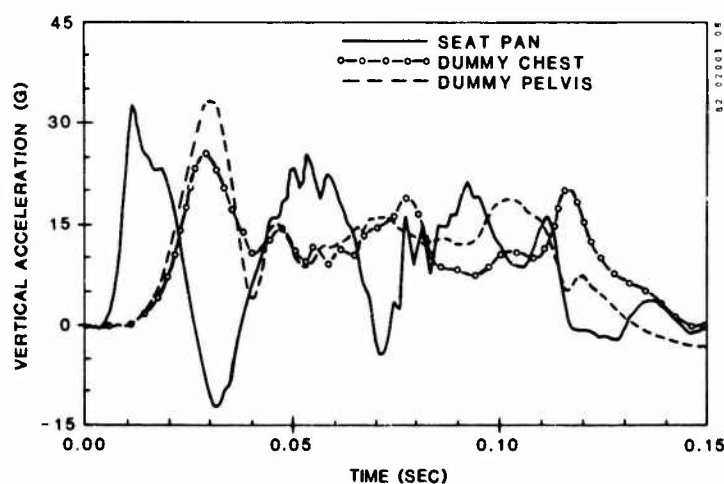


Figure 3. Typical response of seat pan, dummy chest, and dummy pelvis to vertical crash loading.

The explanation of the formation of this characteristic waveform is associated with the inherent dynamic response of the seating system and its occupant. Total coupling of the seat and its occupant (anthropomorphic dummy), is not achieved since the occupant consists of masses connected by nonrigid body members, such as the vertebral column and neck in humans or elastic structural members in anthropomorphic dummies. Further, the dummy is seated on simulated buttocks flesh and a comfort cushion which do not form a rigid connection between the occupant and the seat pan. Since the energy-absorbing mechanism of the seat must be set for a given load (calculated by multiplying the effective weight of the occupant and movable part of the seat by the desired limit load factor of 14.5 G), the actual deceleration measured on the seat pan will vary inversely with the coupled weight,  $w$ , according to the relationship  $a = F/w/g$ . The term "coupled" used here simply indicates that the applicable connecting springs are compressed sufficiently to result in the body segments being decelerated in phase and at approximately the same rate as the seat pan (as would a rigidly attached mass).

A deceleration applied to the seat pan initially decelerates the movable seat mass only; consequently, deceleration of the seat pan reaches a large magnitude. As the cushion and the buttocks "flesh" compress, the deceleration of the lower torso mass increases. As the spinal column compresses, the deceleration of the chest increases. The deceleration of these masses increases as a result of the increased load in the connecting members. Considering the connecting members to be represented by springs, there is then a spring constant involved that defines the relationship between deflection and load; i.e., the further a spring is compressed, the larger the required load to compress it. The body segments react in the same way: the more the compression, the higher the load, and the higher the load, the higher the deceleration of the body segments.

Representing the system by a series of springs and masses, when the initial deceleration of the seat pan commences the springs in the body, which have been subjected to a zero-G environment during the drop, are not compressed, as illustrated in Figure 4(a). This simply means that, since the springs are not compressed when the deceleration first commences, large loads cannot be immediately applied to the body segments. As the pulse continues, the body segments continue to move under the resistive load of the partially compressed springs and thus decelerate more slowly than the seat, building up a relative velocity with respect to the seat pan. Eventually, the velocities of the body segments and the

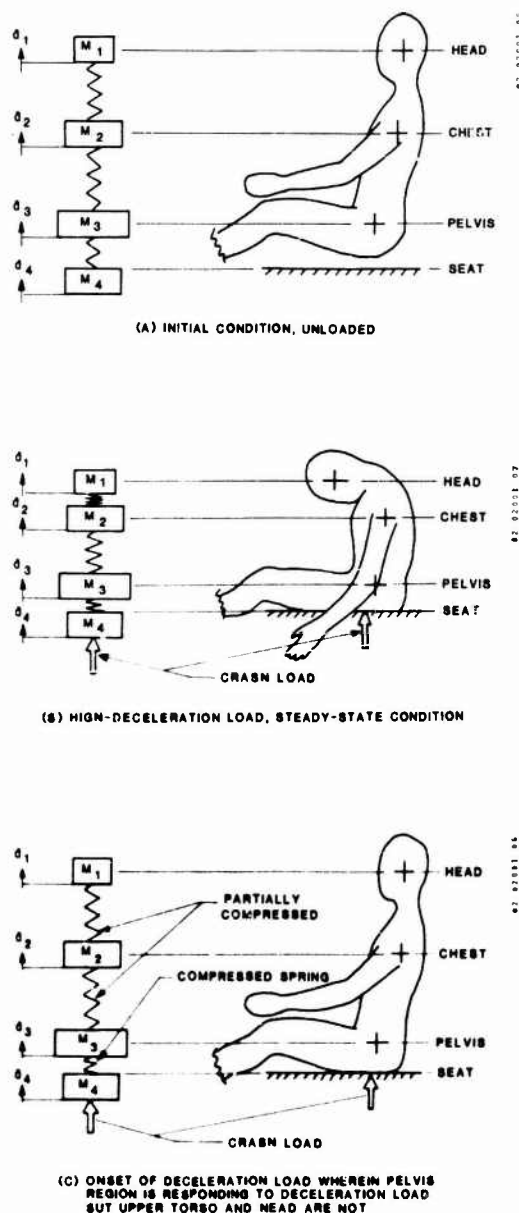


Figure 4. Spring-mass representation of seat-occupant system.

increased compression load in the spine and a build-up of deceleration of the upper torso. Eventually, the springs are all compressed in a quasi-stable state, and the phasing of the decelerations of the various system segments begins to converge toward the average load factor for which the limit load of the energy-absorbing system was designed.

It is important to note that the peak decelerations of the seat pan do not necessarily coincide with peak decelerations of the occupant, pelvis or chest, and thus are not necessarily hazardous to his safety. This apparent deficiency in the existing criteria was known when the criteria were developed, but it was adopted since, from an overall standpoint, the criteria had limited the incidence of injury in ejection seats. However, the Eiband tolerance data used in the criteria do not consider the seat pan deceleration excursions from the average. These data were smoothed in much the same manner as used for calculating average G described in the second paragraph of this section of this paper.

Consequently, the more comprehensive study, described in the Introduction, was undertaken to develop the data necessary to better understand the dynamic response of the seat and occupant systems. This understanding can then be quantified and used to establish more comprehensive design criteria to enable the design of seating systems that will reduce the crash hazard to the occupant, which is, after all, the objective of the crashworthy design effort.

seat pan must all approach each other. This usually occurs later in the sequence, after the second spike (see Figure 4(b)). In the interval, the deceleration of the seat pan responds as a function of energy absorber force, input pulse, and seat and dummy characteristics.

As previously mentioned, initially the measured seat pan acceleration reaches a high value. This occurs because the resistive force in the energy-absorbing system was set at a given value considering the weight of the movable portion of the seat and the occupant. The seat pan is decelerated initially at a magnitude consistent with the force of the energy-absorbing mechanism divided by only the mass of the movable part of the seat, which is considerably less than the design weight for the energy absorption system. The magnitude of initial seat pan acceleration will thus always exceed the limit-load factor for which the composite system was designed.

Eventually, the cushion and buttocks springs are compressed and the load applied to the seat pan by the mass of the lower torso increases (see Figure 4(c)). Because this is a dynamically loaded spring-mass system, the springs associated with the buttocks and the cushion can bottom out, producing overshoot (a higher peak output deceleration than peak input) during the sequence and then, of course, they will again unload. The unloading permits the seat pan deceleration to rise again to the second spike which can be extremely high because of the occupant unloading and the elastic recovery of the seat pan and structure. Note here that the high deceleration of the seat pan does not necessarily correlate with high deceleration of the pelvis or of the chest. From review of both test data and analytical prediction, the opposite generally appears true, i.e., the unloading of the lower torso and/or the chest is the event that produces the spike in seat pan deceleration.

As the seat cushion and buttocks again load up and the pelvis deceleration increases, the high seat pan deceleration of the second spike is decreased. Also, the two characteristic deceleration spikes are usually followed by an

### 3. SUMMARY OF PROGRAM OBJECTIVES AND STATUS

In order to develop the more rigorous criteria needed for the design of energy-absorbing seats, a program of testing and analysis was initiated in 1979 with participation by the U.S. Army, Navy, Air Force, and Federal Aviation Administration. The individual programs include an investigation of the effects of a large number of seat and test variables on seat and occupant response, determination of human response and human tolerance to essentially vertical impact loading, and the development of a standardized and more useful test dummy. For each of these individual research programs, both the objectives and current status are summarized below.

#### SENSITIVITY TESTING AND ANALYSIS

In July 1979, the U.S. Army Applied Technology Laboratory, Fort Eustis, Virginia, initiated a contract with Simula Inc. to conduct a program for development of design criteria for more effective use of stroking distance in energy-absorbing seats. As part of this effort, a matrix of dynamic tests was performed by the Federal Aviation Administration Civil Aeromedical Institute (CAMI), the Naval Air Development Center (NADC), and Simula Inc. Variables that are being investigated through analysis and testing include the shape, magnitude, and rate of onset of the input deceleration pulse; the velocity change; the type and size of the anthropomorphic dummy; the energy absorber limit load; the seat weight; the cushion characteristics; the seat orientation; and the structural spring rate of the seat. Testing has been accomplished using a UH-60A Black Hawk crewseat, which was inspected and overhauled as necessary during the test series to enable successful and repeatable results to be obtained.

CAMI conducted 23 tests with a rigid seat for evaluation and comparison of existing anthropomorphic dummies and 27 tests with the Black Hawk seat for investigation of the effects of the other variables. In order to examine the effects of different test facility types and input deceleration pulse shapes, NADC conducted nine tests and Simula Inc., three. Testing has been completed, and analysis of the data is presently in progress. Some preliminary results are presented in Section 4 of this paper.

#### CADAVER TESTING AND ANALYSIS

Related to the energy absorber criteria research program, testing has been conducted at Wayne State University with human cadavers in a Black Hawk crewseat, as described in Reference 13. That program has been supported by Simula Inc. under a contract with the U.S. Army Applied Technology Laboratory. The primary objectives have been to determine a threshold deceleration tolerance of cadavers and relate this threshold to the U.S. Army aviator population; also to investigate whether the secondary acceleration peak observed in tests of energy-absorbing seats exists when the seat is occupied by a human subject, and if so, to determine whether it presents a hazard to Army aviators.

The first phase of the cadaver testing program consisted of nine tests divided into two series. The first series consisted of a maximum of two dynamic tests with each cadaver. Both tests used a combined-loading mode with the seat pitched forward relative to the impact vector, first 17 degrees and then 34 degrees (orienting the seat back at 4 degrees and 21 degrees relative to the impact vector, respectively) and a 14.5-G energy absorber limit load. The tests resulted in two cadavers successfully passing the first test orientation, but receiving vertebral fractures at the 34-degree pitch; two other cadavers received fractures in the first test. For the remaining three tests in that first phase of the program, 11.5-G energy absorbers were used, with the seat in the more severe test orientation with 34-degree pitch. All three of these subjects also received vertebral fractures. The second phase of the program, which has just started in 1982, includes six tests with the 34-degree pitch orientation, the first three of which will utilize 8.5-G energy absorbers. Two tests have been completed in this phase with one vertebral fracture occurring. Details of the tests in this part of the overall program can be found in the paper by King and Levine (Reference 13). It should be emphasized that bone strength for living humans, especially the aviator population, is significantly higher than for the cadaver population tested. Determination of the bone strength relationship between the cadaver and aviator populations, supported by recent operational experience with energy-absorbing seats, will justify use of a higher limit load than the threshold determined in this program.

#### HUMAN SUBJECT EXPERIMENTS

In order to ensure the validity of both cadavers and dummies in simulating human response to vertical impact, a series of +G<sub>x</sub> tests with living human subjects is to be conducted at the Naval Biodynamics Laboratory.

#### STANDARDIZATION OF DUMMIES

Because the Part 572 anthropomorphic dummy is the only truly standardized test device, it was selected for use in most of the sensitivity testing. However, differences that were noted between the results of the dummy tests and those of the cadaver tests indicate the need for a dummy with more humanlike response to vertical input. Analyses of the data from the sensitivity testing program demonstrated that if probability of vertebral injury is to be used in a criterion for seat evaluation, spinal forces and moments need to be measured directly during the test. Therefore, a dummy to be used in aircraft seat testing should include transducers for measurement of such loads. All anthropomorphic dummies developed in recent years have been designed for automotive uses and utilize

civilian anthropometric data. Should a new dummy be developed for military aircraft seat testing, it would be most desirable to use characteristics of military aircrewmembers. Under the leadership of the U.S. Army Aeromedical Research Laboratory (USAARL), a committee was formed to develop a specification for body dimensions, joint locations, and inertial properties of military aircrewmembers. Membership included representatives of the U.S. Army, Navy, and Air Force, and various civilian organizations. The group agreed that a standard representation for a 50th-percentile male aircrewmember would be developed in the relaxed seated position, with head oriented in the Frankfort plane. During the work of this committee, which was carried out in 1981, the U.S. Air Force drawing board manikin, in the 50th-percentile male size, served as the basis for the development of a set of dimensions and inertial properties. These properties, described in Reference 14, should prove useful both in development of an improved test dummy and in use of mathematical models of the aircraft seat occupant.

Also, under a contract with USAARL, Simula Inc. has modified two anthropomorphic dummies, a 50th- and a 95th-percentile device, for measurement of spinal loads. In December 1981, several of the tests in the sensitivity testing program were repeated at CAMI with the modified dummies. Four tests with the modified 50th-percentile dummy have been conducted at Wayne State University under the conditions used in the first phase of cadaver testing.

#### 4. PRELIMINARY RESULTS

Analysis of the extensive sets of data that have been collected during the dummy and cadaver tests is continuing. Analyses include computer simulation of the tests in order to relate the effects of the various variables and to extrapolate the results to more general conditions. Prior to completion of these analyses, the plotted test data can be examined and several conclusions drawn, as described in the following sections. The basic test configuration is described first, followed by descriptions of individual variables, tests, and their results.

##### BASIC CONFIGURATION

A standard configuration was established for use as the baseline condition in the parametric test matrix. The impact conditions included a 42-ft/sec velocity change, and an input deceleration pulse with a 42-G peak and a rate of onset of 1050 G/sec. The triangular-shaped deceleration pulse which meets these conditions is shown in Figure 5.

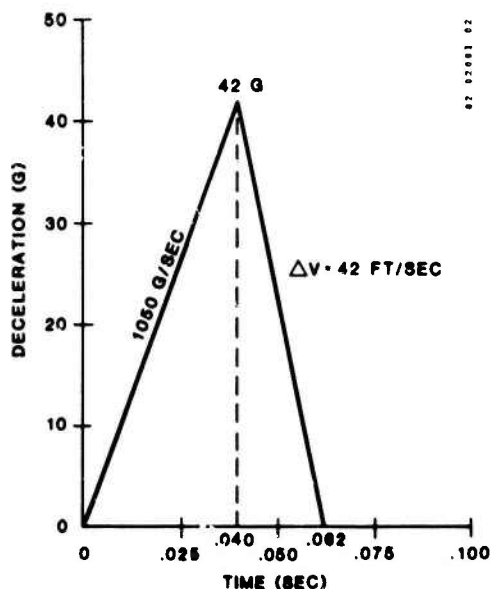


Figure 5. Triangular deceleration pulse meeting prescribed baseline condition.

Test hardware for the baseline configuration consisted of a Simula/Norton Black Hawk crew-seat and a Hybrid II 50th-percentile anthropomorphic dummy. The test seat was a production model which was modified by removal of ballistic armor hardface material from the seat bucket to facilitate modification of movable seat weight. For the baseline test condition, the seat was ballasted with steel plate to maintain inertial properties of the production armored seat. The crewseat is designed to limit inertial crash loads transmitted to the seat bucket and occupant through the use of inversion tube energy absorbers. The inversion loads for the baseline case were set at 14.5 times the effective vertical weight of the seat and 50th-percentile U.S. Aviator, or

$$14.5 \times (60.6 \text{ lb} + 142.3 \text{ lb}) = 2942 \text{ lb}$$

The seat pan cushion was designed to minimize relative motion and rebound between the occupant and seat.

Seat orientation for the baseline case calls for alignment of the seat back with the input velocity vector, as shown in Figure 6. This orientation, which is referred to as vertical in the remainder of the paper, actually represents a 13-degree angle relative to the standard aircraft z-axis. At facilities utilizing a horizontal decelerator, the pitch angle was increased to 17 degrees. The

first 13 degrees of pitch was provided to align the back tangent line with the horizontal surface of the sled (parallel to the velocity vector), in order to eliminate initial extension of the elastomeric spine that would be caused by a downward-oriented seat back angle. The additional 4 degrees of pitch was added to approximately counteract the 1 G of gravity that reduces the overturning moment on the dummy during seat stroking. Since during most of the tests the energy-absorbing mechanism on the seat is set to stroke at 14.5 G, the angle of the resultant deceleration was determined as the angle whose tangent is one divided by 14.5 = 0.069, or 4 degrees. Therefore, under stroking loads, the overturning moment on the dummy should be approximately corrected for gravity, and the response should be similar to that for a seat in an upward-oriented position.

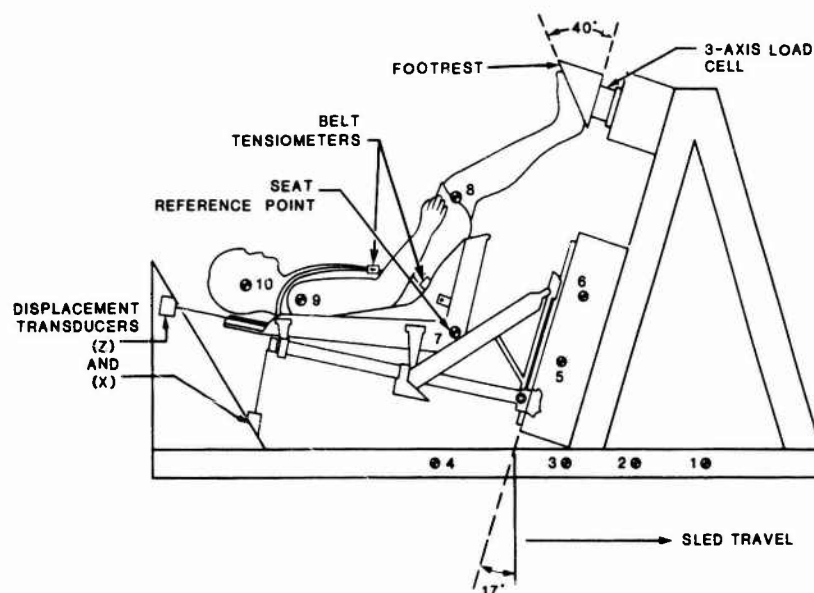


Figure 6. Baseline test configuration (for horizontal decelerator).

#### INPUT PULSE SHAPE

The effect of variation in input pulse shape among test facilities was examined for the baseline test condition. At four facilities, an attempt was made to meet the input deceleration pulse specifications within the constraints of each particular decelerating mechanism. A description of the four facilities is given below:

**CAMI Test Facility:** The CAMI test facility consists of a sled which is accelerated to the desired impact velocity by a cable connected to falling weights and is decelerated by wire-bending energy-absorbing members. The wires are stretched across the tracks and impacted by the sled. To simulate a vertical test, the seat is rotated about its pitch axis until its vertical axis is parallel to the velocity vector of the sled and directed rearward.

**Simula Drop Tower:** The Simula test facility consists of a tower made from two poles, implanted in the ground, with a top crossmember. Two guides extend from the top of the tower to the ground to guide the drop cage, and a concrete drop pad is provided to react the impact load. The test specimen is placed in the drop cage, which is raised to the height that will provide the desired impact velocity. Then, it is dropped on a stack of paper honeycomb shaped to impose the desired force-deflection characteristics and, thus, the desired acceleration-time history on the dropped cage.

**NADC Test Drop Tower:** The NADC test facility consists of a four-sided steel tower in which a drop cage is located. The drop cage is raised to the desired height and then dropped on Van Zelm energy absorbers placed in the path of the dropping cage.

**Wayne State University:** The WSU test facility consists of a sled which is brought to the desired velocity with pneumatic pressure. Deceleration of the sled is provided by a hydraulic snubbing device, in which the pressure can be regulated by changing the cylinder orifice dimensions.

Figure 7 shows the baseline deceleration pulses for the four facilities. The pulse shape for the CAMI, Simula, and WSU test facilities is essentially triangular, while the shape of the NADC pulse possesses characteristic oscillations. A summary of the baseline test facility input pulse characteristics is given in Table 2 for comparison. Occupant and seat response data are given in Table 3 for baseline cases at the four facilities. For three of the facilities, two values are listed to show repeatability of test conditions.

In general, the seat stroke achieved in the baseline tests is consistent for tests at a given facility; however, the stroke varied by as much as 5.3 in. among facilities. Tests conducted at CAMI had significantly higher components of seat and occupant acceleration in the x-direction than for similar tests conducted at the three other facilities. The seat pan Dynamic Response Index (DRI), which is computed from the response of a single-degree-of-freedom damped, spring-mass model of the human torso that has been correlated to ejection seat injury (References 15 and 16), is fairly consistent among facilities. However, the duration of the seat pan vertical acceleration peak above the 23-G limit varied by a factor of more than two between the two CAMI baseline tests. Because input conditions that meet the requirements of existing criteria can produce different results at different facilities, it appears that tolerances on parameters defining standard test conditions need to be further reduced.

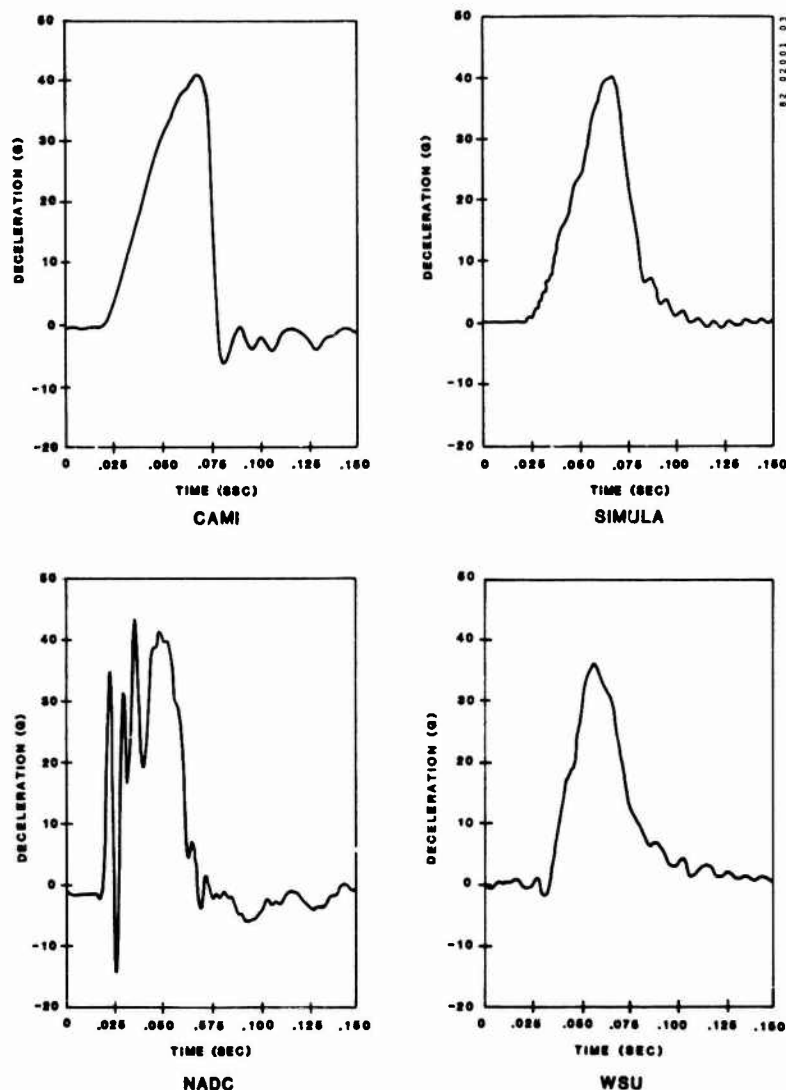


Figure 7. Typical baseline deceleration pulses for the four test facilities.

TABLE 2. COMPARISON OF TEST FACILITY IMPACT CONDITIONS

Test Facility	Peak Input Deceleration (G)	Rate of Onset (G/sec)	Total Velocity Change (ft/sec)	Initial Velocity at Impact (ft/sec)	Percent of Velocity Change in Rebound	Vertical Seat Stroke (in.)
CAMI	40.7	977	44.4	41.8	5.9	10.6
	40.7	982	45.2	42.3	6.8	10.5
NADC	44.6	1370	41.5	36.8	11.3	10.8
	45.0	1340	39.6	36.8	7.1	11.6
Simula	40.0	1050	42.5	31.1	26.8	9.5
	40.8	1070	42.4	31.1	26.6	9.4
WSU	36.1	1700	41.2	41.2	0.0	6.3

NOTE: The baseline conditions were repeated at CAMI, NADC, and Simula; results of both tests are presented here. Data presented for the WSU pulse are from the single baseline test.



TABLE 3. COMPARISON OF SEAT AND OCCUPANT RESPONSE FOR  
BASELINE TESTS AT THE FOUR TEST FACILITIES

Test Facility	Seat Stroke (in.)	Peak Acceleration (G)								Duration of Seat Pan z Acceleration at 23 G (sec)	DRI
		Seat Pan x	Seat Pan z	Pelvis x	Pelvis z	Chest x	Chest z	Head x	Head z		
CAMI Tests	10.6	25.1	26.4	30.5	30.5	18.1	30.4	31.5	36.5	0.007	21.0
	10.5	26.8	29.4	25.1	30.8	24.1	25.8	38.5	36.5	0.016	19.7
NADC Tests	10.8	19.2	36.3	15.4	38.8	10.0	36.1	24.7	40.8	0.006	20.8
	11.6	16.8	34.6	18.7	40.1	14.7	37.4	22.7	42.8	0.007	20.7
Simula Tests	9.5	12.5	22.3	16.2	31.7	10.9	31.3	18.3	36.3	0.	19.4
	9.4	14.1	25.3	12.5	39.8	12.0	36.5	16.7	43.7	0.008	21.5
WSU Test	6.3	15.3	28.9	13.5	39.7	13.3	41.3	21.8	39.6	0.011	18.4

## MAGNITUDE OF INPUT DECELERATION

In order to examine the influence of peak input deceleration, four tests were conducted at CAMI with constant velocity change, and peak accelerations of approximately 22, 32, 42, and 52 G. The predicted trend in seat stroke response was verified. Results of these tests are shown in Table 4. It should be noted that, in order to maintain a constant velocity change, the pulse shape at 22 and 32 G was trapezoidal, rather than the triangular shape used at 42 and 52 G.

TABLE 4. COMPARISON OF TEST RESULTS FOR PEAK INPUT DECELERATION SERIES

Test Pulse Parameters	Test No.	Seat Stroke (in.)	Peak Acceleration (G)								Duration of Seat Pan z Acceleration at 23 G (sec)	DRI
			Seat Pan x	Seat Pan z	Pelvis x	Pelvis z	Chest x	Chest z	Head x	Head z		
21.9 G, 41.3 ft/sec	1	7.0	15.4	22.4	10.7	24.4	12.1	24.1	0.			17.0
32.3 G, 41.8 ft/sec	2	9.5	29.1	24.6	21.1	36.8	31.1	26.5	0.005			18.9
Baseline 40.7 G, 41.8 ft/sec	3	10.6	25.1	26.4	30.5	30.5	18.1	30.4	0.007			21.0
Baseline 40.7 G, 42.3 ft/sec	4	10.5	26.8	29.4	25.5	30.8	24.1	25.8	0.016			19.7
51.5 G, 42.1 ft/sec	5	11.7	28.1	31.8	36.8	45.9	24.8	26.8	0.013			21.4

The magnitude of the dynamic response of the seat and occupant system is due to the interaction of the flexible seat pan and natural frequency of the body. A rigid mass and ideal energy absorbers would produce a peak acceleration solely dependent on the energy absorber limit-load factor. However, for the seat/body system, the peak acceleration is a function of dynamic overshoot and effective mass being decelerated. Therefore, it is not surprising that the peak seat pan z-axis acceleration values listed in Table 4 exhibit a trend of increasing with the input peak acceleration. This fact also indicates the desirability of designing the landing gear/fuselage system to "stroke" at a lower load to reduce peak acceleration values transmitted to the seat attachment points. However, lower loads would require increased stroke distance for the gear and fuselage.

## VELOCITY CHANGE

A series of five tests were conducted to examine seat and occupant response under various velocity change conditions. An attempt was made to maintain a triangular acceleration pulse with a 42-G peak throughout the test series; however, this was not physically attainable for the pulses with lower velocity changes. The results of this test series are presented in Table 5.

TABLE 5. COMPARISON OF TEST RESULTS FOR VELOCITY CHANGE SERIES

Test Pulse Parameters	Test No.	Seat Stroke (in.)	Peak Acceleration (G)						Duration of Seat Pan z Acceleration at 23 G (sec)	DRI
			Seat Pan x	Seat Pan z	Pelvis x	Pelvis z	Chest x	Chest z		
Baseline 40.7G, 41.8 ft/sec	1	10.6	25.1	26.4	30.5	30.5	18.1	30.4	0.007	21.0
Baseline 40.7 G, 42.3 ft/sec	2	10.5	26.8	29.4	25.1	30.8	24.1	25.8	0.016	19.7
40.9 G, 32.3 ft/sec	3	6.4	26.8	28.3	23.4	29.1	24.1	24.4	0.007	20.1
31.0 G, 32.4 ft/sec	4	5.6	20.4	20.9	14.4	26.8	10.7	24.8	0.	17.0
23.5 G, 25.6 ft/sec	5	2.2	14.9	18.4	12.1	25.1	12.7	25.8	0.	18.9

The measured seat stroke in this test series is a strong function of velocity change since the crash energy that must be absorbed during stroking is proportional to the square of the velocity change. Peak seat and occupant accelerations do not appear to be functions of velocity change. The similarity of peak accelerations in Tests 1, 2, and 3, and the reduction in peak values for Test 4 versus Test 3, indicate that the dynamic response of the seat/occupant system is mainly a function of input deceleration magnitude, and that the influence of input velocity change is secondary.

#### RATE OF ONSET OF INPUT DECELERATION

Solution of equations of motion for the seat and occupant indicates a tendency for seat stroke to decrease as the rate of onset of the input deceleration increases. Data presented in Table 2 tend to verify this prediction, as the lowest stroke values were obtained at WSU, where the rate of onset was highest, although it should be noted that the peak deceleration was lower than that for the other facilities. Although a rate of onset is presented in Table 2 for NADC, the irregular nature of the early part of that pulse, as seen in Figure 7, renders its significance questionable. The tests conducted at CAMI specifically to assess the effect of rate of onset appear to exhibit an opposing trend. In this series of four tests with rates of onset varying from 800 to 1700 G/sec, the peak accelerations fell within the normal range of variation among like tests conducted under similar conditions. Seat strokes of 9.5, 10.5, 10.6, and 11.0 in. were measured for tests with rates of onset of 810, 980, 980, 1675 G/sec, respectively, when the velocity change and peak input deceleration were held constant.

#### DUMMY TYPE

Two types of tests were conducted on various, commonly used anthropomorphic dummies. In the first test series, three 50th-percentile dummies, the Hybrid II, VIP-50, and CG-50, were tested in a rigid seat (without cushions) under strictly controlled input pulse conditions with a 14.5-G, trapezoidal-shaped input deceleration. The objective of this series was to remove the dynamic effects of the stroking seat and interaction between the occupant and seat. Tests were repeated three times for each dummy. The average accelerations and seat pan force from the three runs for each dummy are presented in Table 6. For a given dummy, measured accelerations varied by a maximum of  $\pm 1$  G from the average.

TABLE 6. AVERAGE PEAK ACCELERATIONS AND SEAT PAN LOADS FOR RIGID SEAT COMPARISON TESTS OF 50TH-PERCENTILE DUMMIES (AVERAGE OF THREE TESTS)

Dummy Description	Peak Acceleration (G)							Seat Pan z Force (lb)
	Seat Pan z	Pelvis x	Pelvis z	Chest x	Chest z	Head x	Head z	
Hybrid II	15.3	9.6	42.9	6.6	26.2	12.0	33.4	2710
Alderson VIP-50	15.1	10.0	35.3	5.3	37.4	14.7	39.0	2960
Alderson CG-50	15.5	16.9	39.9	14.3	41.3	56.6	46.8	5500



The acceleration values presented in Table 6 indicate that for x-axis response in a vertical test, the Hybrid II and VIP-50 are similar. However, the addition of the elastomeric spine in the Hybrid II significantly alters the z-axis response. The peak z-axis acceleration values for the Hybrid II show a variation among the pelvis, chest, and head, while the essentially incompressible column of the VIP-50 maintains a fairly constant acceleration level throughout the body. Response of the CG-50 dummy is significantly different from the other two dummy types, particularly in the head x-acceleration and loads transmitted to the seat pan, which are presented in Figure 8 for the three dummies.

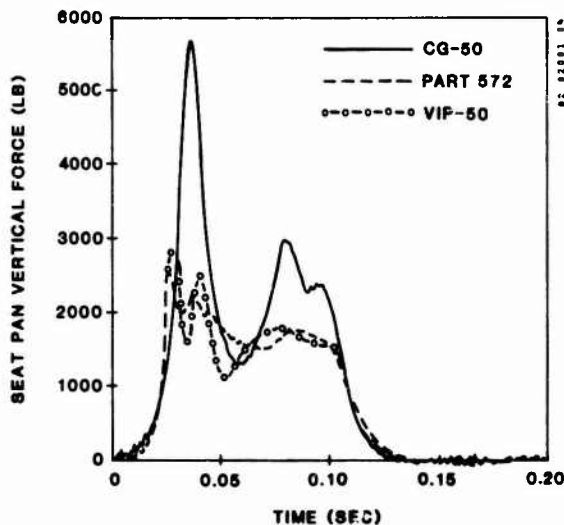


Figure 8. Comparison of seat pan force measured in rigid seat tests with three 50th-percentile dummies.

The second test series used three 95th-percentile dummies commonly used for dynamic qualification tests of energy-absorbing seats: the VIP-95 (with elastomeric spine), the CG-95, and the Sierra 292-895. These tests were conducted with the Black Hawk seat in the baseline test configuration. Results of these tests, presented in Table 7, are inconclusive due to the lack of complete data sets and small sample size. However, the seat pan response appears to be consistent among the three dummies. Variation in seat stroke among dummy types is inconclusive due to the 1.2-in. deviation between the two tests with the same (VIP-95) dummy.

Based on the results of the strictly controlled rigid seat tests, there can be significant differences in the response of anthropomorphic dummies of various types. Therefore, any specification for evaluation of energy-absorbing seats should specify the use of a standard anthropomorphic test device.

TABLE 7. COMPARISON OF RESPONSE FOR 95TH-PERCENTILE DUMMIES IN THE BASELINE TEST CONFIGURATION

Dummy Description	Seat Stroke (in.)	Peak Acceleration (G)								Duration of Seat Pan z Acceleration at 23 G (sec)	DRI
		Seat Pan x	Seat Pan z	Pelvis x	Pelvis z	Chest x	Chest z	Head x	Head z		
Alderson	13.2	29.6	28.1	24.8	34.5	41.5	26.8	-	-	0.012	17.2
VIP-95*	12.0	29.3	25.1	21.8	41.2	15.4	29.8	53.6	32.2	0.005	19.7
Alderson CG-95	13.1	28.4	29.6	-	-	57.0	34.2	-	-	0.012	18.3
Sierra 292-895	11.0	29.8	31.9	22.8	63.3	-	-	-	-	0.010	20.0

\*With elastomeric spine.

#### DUMMY PERCENTILE

Evaluation of seat and occupant performance as functions of dummy percentile was complicated by the lack of similar anthropomorphic test dummies. Two sets of baseline configuration tests were run with a Hybrid II 50th-percentile dummy and a VIP-95 dummy with an elastomeric spine similar to the Hybrid II configuration. Results of this test series are presented in Table 8. In the final test of each series (test numbers 3 and 5) the anthropomorphic test dummies were modified by the addition of a six-axis load cell at the base of the lumbar spine which were used to obtain load and moment data. Measured load and moment data for Tests 3 and 5 are presented in Table 9.

When a 95th-percentile dummy is used in place of the 50th-percentile device the increase in seat stroke of approximately 2 in. is predictable by the increase in vertical effective weight. However, one might also assume that there would be a general decrease in acceleration for the 95th-percentile dummy, although this is not readily apparent from the peak values presented in Table 8. The explanation is that the peak values, due to dynamic overshoot, are not strongly affected by the occupant size, while the average

TABLE 8. SUMMARY OF THE EFFECT OF ANTHROPOMORPHIC DUMMY PERCENTILE ON PEAK ACCELERATION VALUES

Dummy Percentile	Test No.	Seat Stroke (in.)	Peak Acceleration (G)								Duration of Seat Pan z Acceleration at 23 G (sec)	DRI
			Seat Pan x	Seat Pan z	Pelvis x	Pelvis z	Chest x	Chest z	Head x	Head z		
50th Percentile	1	10.6	25.1	26.4	30.5	30.5	18.1	30.4	31.5	36.5	0.007	21.0
	2	10.5	26.8	29.4	25.1	30.8	24.1	25.8	38.5	36.5	0.016	19.7
	3	11.4	32.3	26.0	22.2	28.5	35.5	28.1	32.5	28.5	0.006	19.4
95th Percentile	4	12.0	29.3	25.1	21.8	41.2	15.4	29.8	53.6	32.2	0.005	18.0
	5	13.2	29.6	28.1	24.8	34.5	41.5	26.8	-	-	0.012	17.2

TABLE 9. SUMMARY OF THE EFFECT OF ANTHROPOMORPHIC DUMMY PERCENTILE ON SPINAL LOADS AND MOMENTS

Dummy Percentile	Test No.	Peak Lumbar Load (lb)				Peak Lumbar Moment (in.-lb)			
		x	y	z	Resultant	x	y	z	Resultant
50th Percentile	3	360	60	1220	1220	360	1250	93	1260
95th Percentile	5	593	153	1230	1260	653	1500	107	1510

acceleration during the crash sequence is lower for a heavier occupant (provided that the energy-absorbing limit load is fixed). This is evident from the seat pan DRI which shows a definite trend of lower values for increasing occupant size.

Loads and moments presented in Table 9 are intended for use in validation of computer models and correlation with injury criteria, and not intended for use as a quantitative measure of spinal damage based on known vertebral segment strength distributions. The data presented indicate that axial spinal force (z-axis) is not a function of occupant size, while the moment associated with forward rotation of the body (y-axis) does show an increasing trend with body size. Caution is urged in use of these data because the chest x-axis acceleration measured in tests with the modified dummies shows a substantial increase in peak value. This is possibly an indication that the installation of the load cell may have increased the rotational stiffness of the elastomeric spinal column.

#### CADAVERS VERSUS ANTHROPOMORPHIC DUMMIES

A series of tests are being conducted to establish decelerative spinal fracture loads for occupants of energy-absorbing seats, as discussed in Section 3. The test program is currently in progress and presentation of results is not appropriate at this point. However, enough tests have been completed to determine characteristic response of cadavers in the Black Hawk seat and to justify the use of the Part 572 dummy as a human surrogate for seat testing.

The cadaver test series is being conducted at Wayne State University under the baseline test conditions. Similar tests are being conducted at WSU with a Part 572 dummy that is instrumented to measure spinal forces and moments. Results of comparable cadaver and dummy tests are shown in Table 10. Resultant peak body accelerations are presented for comparison because the accelerometer orientation in the cadaver did not necessarily correspond to the standard dummy coordinate system.

Required seat stroke values presented in Tables 10 and 11 indicate that, in general, the Part 572 dummy requires slightly less stroke distance than does the cadaver. The seat pan vertical accelerations, presented in Figures 9 and 10 for the vertical and combined tests, respectively, show that the interaction between the Part 572 dummy and seat pan is very similar to the response measured with human cadavers. The comparison between body accelerations for the dummy and cadaver does not show a good correlation. Results of this limited comparison seem to indicate that seat performance criteria based on seat pan acceleration may not be as sensitive to occupant type as a criterion based on body segment acceleration. However, it may also indicate that injury mechanisms within the body, e.g., spinal deformation, can not be reliably predicted from seat pan acceleration as internal body response can vary significantly for various occupant types with similar inputs from the seats.

TABLE 10. COMPARISON OF SEAT AND OCCUPANT RESPONSE FOR DUMMIES AND CADAVERS

	Seat Stroke (in.)	Peak Acceleration (G)					Duration of Seat Pan z Acceleration at 23 G (sec)	DRI
		Seat Pan x	Seat Pan z	Pelvis Resultant	Chest Resultant	Head Resultant		
Dummy, Vertical	6.3	15.3	28.9	40.3	43.4	41.7	0.011	18.4
Cadaver, Vertical	7.6	17.5	26.5	33.9	N/A	49.7	0.004	21.8
Dummy, Combined	4.5	27.8	23.9	35.2	31.6	46.9	0.004	17.8
Cadaver, Combined	4.5	37.3	25.4	22.8	N/A	59.6	0.004	22.2
	5.5	40.5	21.0	44.4*	N/A	97.3*	0.	19.3

\*Impact between mouth-mount accelerometer and thigh.

TABLE 11. COMPARISON OF SEAT STROKE FOR CADAVERS AND DUMMIES IN THE UH-60A CREWSEAT

Test Description	Cadaver Tests		Dummy Tests	
	Occupant Weight (lb)	Seat Stroke (in.)	50th% Hybrid II	
			Occupant Weight (lb)	Seat Stroke (in.)
14.5-G E/A, Vertical Orientation, 42-45 G Peak Input Acceleration	166	7.6	164	6.3
	160	7.4	164	7.0
	140	7.1		
	148	7.1		
14.5-G E/A, Combined Orientation, 42-45 G Peak Input Acceleration	166	5.5	164	4.5
	140	4.5		
11.5-G E/A, Combined Orientation, 42-45 G Peak Input Acceleration	218	9.4	164	6.5
	141	7.0		
	160	9.0		
8.5-G E/A, Combined Orientation, 42-45 G Peak Input Acceleration	200	13.1		
	143	9.7		

#### ENERGY ABSORBER LIMIT LOAD

Three different energy absorber limit loads were used in the test program. In addition to the standard 14.5-G devices, both 11.5- and 8.5-G energy absorbers were used, amounting to reductions of approximately 20 and 40 percent, respectively, from the standard load. Unfortunately, no single dummy was used with all three energy absorbers. As shown in Table 12, the 50th-percentile Part 572 dummy caused a seat stroke of 14.2 in. when 11.5-G energy absorbers were used. It was anticipated, and verified by analysis, that with the 8.5-G devices, the 50th-percentile dummy would exhaust all available seat stroke. Therefore, it was decided to use a CG-5 dummy in a test with 8.5-G energy absorbers. The results can be compared with those from a test using the same dummy with the 14.5-G devices. It would be expected that, with energy absorbers of smaller load, the accelerations measured on the dummy and seat would be reduced. As shown in Table 12, the z-components of seat pan and pelvis acceleration show this trend for both dummies, as does the z-component of chest acceleration for the Part 572 dummy. The x-components of accelerations, on the other hand, do not exhibit such a trend.

#### RAMPED ENERGY ABSORBERS

Two tests were conducted using energy absorbers of "ramped" design, whose loads increased with stroke. Although the load-deflection characteristics of the two ramped devices were different, the trends in test results were similar. As shown by the data in Table 13, these special devices performed less efficiently than the standard square wave-type device. The ramped devices caused the Part 572 dummy to utilize more than 1.5 in. additional stroke, while the measured accelerations and calculated DRIs were actually higher.

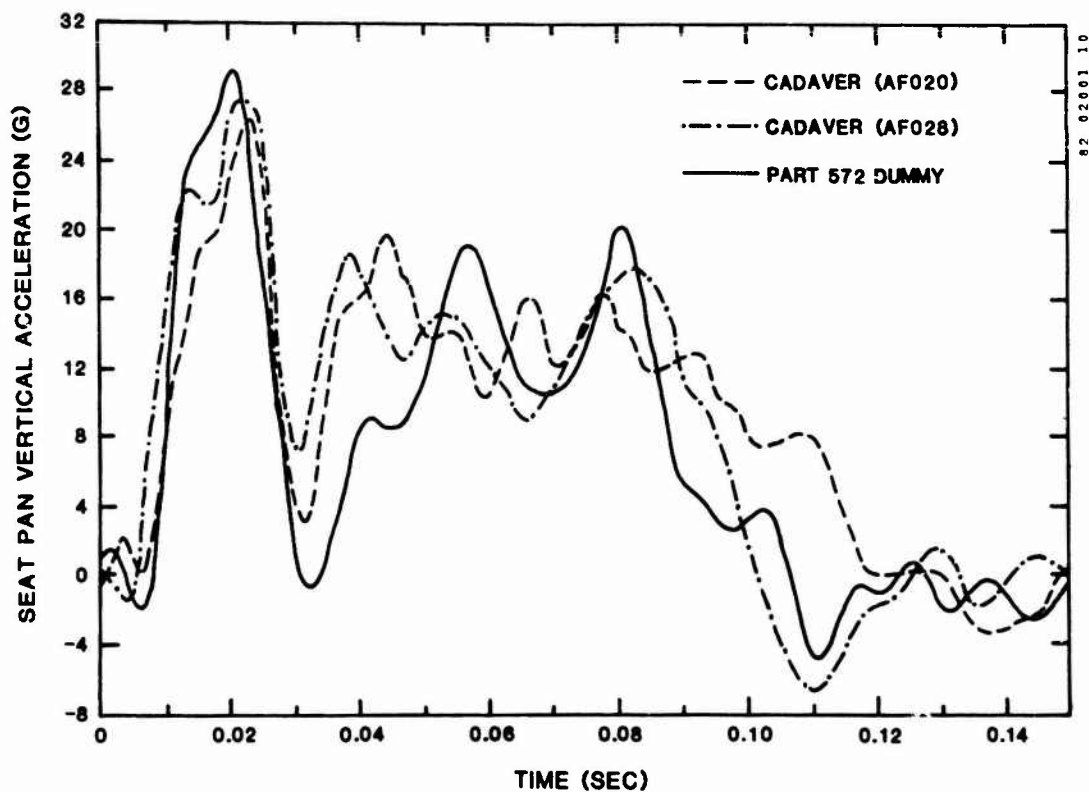


Figure 9. Seat pan vertical acceleration for a Part 572 dummy and two cadavers measured in vertical mode tests with 14.5-G energy absorbers.

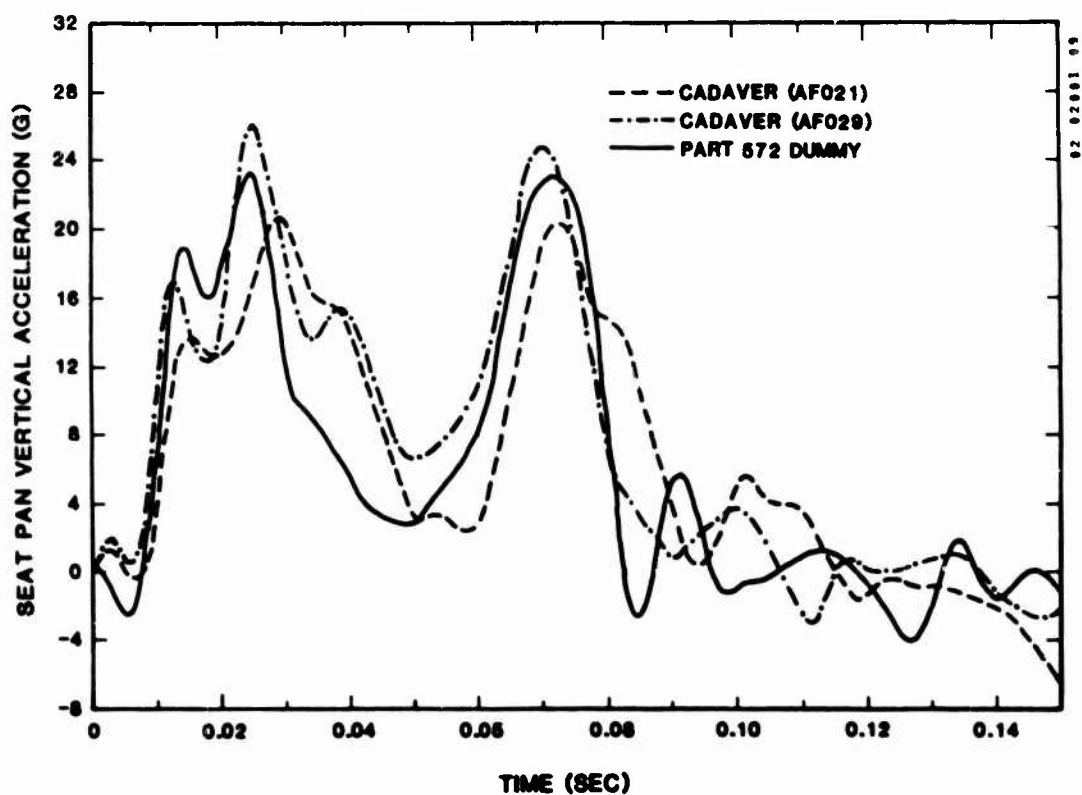


Figure 10. Seat pan vertical acceleration for a Part 572 dummy and two cadavers measured in combined mode tests with 14.5-G energy absorbers.

TABLE 12. EFFECT OF VARYING ENERGY ABSORBER LIMIT LOAD

Test Parameters	Seat Stroke (in.)	Peak Acceleration (G)						DRI
		Seat Pan x	Seat Pan z	Pelvis x	Pelvis z	Chest x	Chest z	
Baseline Test								
50th Percentile Dummy, 14.5-G E/As	10.6	25.1	26.4	30.5	30.5	18.1	30.4	21.0
	10.5	26.8	29.4	25.1	30.8	24.1	25.8	19.7
50th Percentile Dummy, 11.5-G E/As	14.2	24.6	28.1	29.8	20.7	24.1	20.7	19.4
5th Percentile Dummy, 14.5-G E/As	9.9	28.1	31.1	14.4	30.8	32.2	32.1	19.7
5th Percentile Dummy, 8.5-G E/As	16.1	25.0	26.6	24.8	34.5	67.5	68.7	17.8

TABLE 13. EFFECT OF "RAMPED" ENERGY ABSORBERS

Test Parameters	Seat Stroke (in.)	Peak Vertical Acceleration (G)			DRI
		Seat Pan	Pelvis	Chest	
Baseline Tests	10.6	26.4	30.5	30.4	21.0
14.5-G square-wave E/As	10.5	29.4	30.8	29.8	19.7
Ramped E/A, Type 1	12.0	32.3	43.5	26.8	23.7
Ramped E/A, Type 2	12.3	34.8	46.8	34.8	27.5

## MOVABLE SEAT WEIGHT

As mentioned earlier, the basic Black Hawk bucket weight was reduced by removal of the ceramic outer layer of the bucket armor. The movable weight was then adjusted by adding ballast. For the baseline tests, the seat bucket was ballasted to bring its weight and center of mass to approximately those of the production Black Hawk seat. For one test, the ballast weights were removed so that the seat bucket weighed approximately 30 lb less than the production seat, and in another test an additional 55 lb of weight above the baseline case was added. It should be remembered that for these two tests with different movable seat weights, the energy absorber limit loads were held constant, thereby inducing some benefit in terms of acceleration for the heavier seat, and a corresponding penalty for the lighter seat. The trends in acceleration and DRI are as expected, and are shown in Table 14.

TABLE 14. EFFECT OF VARYING MOVABLE SEAT WEIGHT

Test Parameters	Seat Stroke (in.)	Peak Acceleration (G)						DRI
		Seat Pan x	Seat Pan z	Pelvis x	Pelvis z	Chest x	Chest z	
Baseline Tests	10.6	25.1	26.4	30.5	30.5	18.1	30.4	21.0
65 lb	10.5	26.8	29.4	25.1	30.8	24.1	25.8	19.7
120-lb Configuration	14.0	26.5	22.9	26.1	32.8	38.5	21.1	16.4
35-lb Configuration	8.6	35.1	29.6	24.0	42.8	26.7	26.8	21.9

### SEAT FRAME SPRING RATE

For one test, the top of the seat frame was secured rigidly to the sled with steel brackets. It was hoped that comparison of the results from this test with the baseline test would help isolate the effect of seat elasticity on seat and dummy response. Although seat stroke and DRI were unaffected by the frame modification, the x-components of dummy pelvis and chest accelerations were reduced, while the z-components were increased. The results of this test are not particularly conclusive because, although the frame was stiffened, seat bucket elasticity remained a factor.

### SEAT CUSHION STIFFNESS

Two tests were conducted to examine the effects of cushion stiffness. For one test, a block of rigid plastic foam was contoured to cushion shape, and for another, layers of soft upholstery foam were used. An effort was made to adjust the thicknesses of these cushions so that the dummy could be seated in the same position as in the baseline case. Neither of these two tests showed a variation in seat stroke or DRI from those of the baseline case. The rigid cushion increased the natural frequency of the system, so that acceleration waveforms exhibited both higher frequency and higher magnitudes.

### SEAT ORIENTATION

A test was run with a 50-ft/sec, 48-G input with the seat pitched 17 degrees further forward on the sled. This additional pitch combined with the more severe input pulse produced the same vertical component of input acceleration and velocity change as in the baseline case. Seat stroke was reduced from approximately 10.5 in. to 9 in. even though the input acceleration component in the stroking direction was the same as in the baseline case.

### 6. CONCLUSIONS

Criteria developed in 1971 have led to the design and production of aircraft seats with improved crashworthiness. However, testing of these seats has indicated areas where additional rigor in the criteria might aid in achieving more optimum systems. The present research program is directed toward achieving this goal. Although several apparent trends have been noticed in the data, final conclusions are premature at this time. Tests conducted under this research effort indicate that seat performance can vary significantly among test facilities attempting to meet the same input deceleration pulse criteria. This may indicate a need to redefine the deceleration pulse criteria specified in MIL-S-58095(AV) based on recent full-scale crash tests and acceptable tolerances determined from the sensitivity analyses conducted in this program.

### ACKNOWLEDGMENTS

The work described in this paper is supported at Simula Inc. by the Applied Technology Laboratory, U.S. Army Research and Technology Laboratories (AVRADCOM), under contracts DAAK51-79-C-0016 and DAAK51-79-C-0026, where Mr. K. Smith is the technical monitor; and by the U.S. Army Aeromedical Research Laboratory under Contract DAMD17-81-C-1175, where Mr. J. L. Haley is the technical monitor. Mr. G. T. Singley III, formerly of ATL, deserves recognition as being responsible, together with Mr. Haley, for the formulation and coordination of the overall interagency program described herein, as well as obtaining financial support for its initiation.

### REFERENCES

1. Singley, G. T., III, and Desjardins, S. P., Crashworthy Helicopter Seats and Occupant Restraint Systems, in Operational Helicopter Aviation Medicine, AGARD Conference Proceedings No. 255, North Atlantic Treaty Organization, Advisory Group for Aerospace Research and Development, Neuilly sur Seine, France, May 1978.
2. Crash Survival Design Guide, Dynamic Science, A Division of Marshall Industries, USAAMRDL Technical Report 71-22, Fort Eustis, Virginia, Eustis Directorate, U.S. Army Air Mobility Research and Development Laboratory, 1971.
3. Military Standard, MIL-STD-1290(AV), Light Fixed - Rotary-Wing Aircraft Crashworthiness, Department of Defense, Washington, D.C., 25 January 1974.
4. Military Specification, MIL-S-58095(AV), Seat System: Crashworthy, Non-Ejection, Aircrew, General Specification For, Department of Defense, Washington, D.C., 27 August 1971.
5. Desjardins, S. P., and Harrison, H., The Design, Fabrication, and Testing of an Integrally Armored Crashworthy Crewseat, Dynamic Science, Division of Marshall Industries; USAAMRDL Technical Report 71-54, Eustis Directorate, U.S. Army Air Mobility Research and Development Laboratory, Fort Eustis, Virginia, January 1972, AD 742733.
6. Desjardins, S. P., and Laananen, D. H., Aircraft Crash Survival Design Guide, Volume IV - Aircraft Seats, Restraints, Litters, and Padding, Simula Inc., USARTL-TR-79-22D, Applied Technology Laboratory, U.S. Army Research and Technology Laboratories (AVRADCOM), Fort Eustis, Virginia, June 1980.

7. Laananen, D. H., Aircraft Crash Survival Design Guide. Volume II - Aircraft Crash Environment and Human Tolerance, Simula Inc., USARTL-TR-79-22B, Applied Technology Laboratory, U.S. Army Research and Technology Laboratories (AVRADCOM), Fort Eustis, Virginia, January 1980.
8. Crash Survival Design Guide, Dynamic Science, A Division of Marshall Industries, USAAMRDL Technical Report 70-22, Fort Eustis, Virginia, Eustis Directorate, U.S. Army Air Mobility Research and Development Laboratory, 1970.
9. Eiband, A. M., Human Tolerance to Rapidly Applied Accelerations: A Summary of the Literature, Nasa Memorandum 5-19-59E, National Aeronautics and Space Administration, Washington, D.C., June 1959.
10. Domzalski, L., and Singley, G. T., III, Joint Army/Navy Test Program for Black Hawk Seat Systems, Report NADC-79229-60 (Draft), Naval Air Development Center, Warminster, Pennsylvania, 1979.
11. Dummer, R. J., Qualification Test Report, 613-1787 C00L Qualification Testing of Armored Crashworthy Aircrew Seat, RA-305252-1, for Sikorsky Aircraft Contract 576344, Norton Company, Industrial Ceramics Division, October 1978.
12. Chandler, R. F., Dynamic Test of Joint Army/Navy Crashworthy Armored Crewseat, Protection and Survival Laboratory, Memorandum Report AAC-119-80-2, Civil Aeromedical Institute. Mike Monroney Aeronautical Center, Federal Aviation Administration, Oklahoma City, Oklahoma, 25 April 1980.
13. King, A. I., and Levine, R. S., Human Cadaveric Response to Simulated Helicopter Crashes, in Impact Injury: Mechanisms, Prevention and Cost, AGARD, North Atlantic Treaty Organization, Advisory Group for Aerospace Research and Development, Neuilly sur Seine, France, April 1982.
14. Chandler, R. F., and Young, J., Uniform Mass Distribution Properties and Body Size Appropriate for the 50 Percentile Male Aircrewmember During 1980-1990, Civil Aeromedical Institute, Protection and Survival Laboratory, Memorandum Report No. AAC-119-81-4 (Draft), Federal Aviation Administration, Mike Monroney Aeronautical Center, Oklahoma City, March 1981.
15. Stech, E. L., and Payne, P. R., Dynamic Models of the Human Body, Frost Engine Development Corp. AMRL Technical Report 66-157, Aerospace Medical Research Laboratory, Wright-Patterson Air Force Base, Ohio, November 1969, AD 701383.
16. Brinkley, J. W., and Shaffer, J. T., Dynamic Simulation Techniques for the Design of Escape Systems: Current Applications and Future Air Force Requirements, Aerospace Medical Research Laboratory, AMRL Technical Report 71-29-2, Wright-Patterson Air Force Base, Ohio, December, 1971, AD 740439.

# EFFECT OF REEL-TYPE WEBBING RETRACTORS AND SHOULDER-BELT SLACK ON DUMMY DYNAMICS DURING SIMULATED FRONTAL VEHICLE IMPACTS<sup>1</sup>

by  
Timothy J. Bowden, Ph.D.  
and  
James K. Reichert, Ph.D.  
Defence and Civil Institute of Environmental Medicine,  
P.O. Box 2000, Downsview, Ontario, CANADA M3M 3B9  
and  
Adel K. Nassim, P.Eng.  
Road and Motor Vehicle Traffic Safety, Transport Canada,  
28-G Tower C, Place de Ville, Ottawa, Ontario, Canada K1A 0N5

## SUMMARY

A Hy-Ga impact simulator was used for determining the performance of motor-vehicle seat belts equipped with retractors during simulated impacts at 13.5 m/s. The occupant of the seat was simulated by a standard anthropometric dummy. The shoulder strap of the seat belt was pulled various distances up to 25 cm away from the dummy chest before impact and the belt was then anchored near the retractor with fragile tape. The results of this study indicate that a retractor-equipped strap behaves less stiffly than a rigidly-anchored strap, allowing greater forward motion of the body parts restrained by the strap and reducing the peak accelerations of these parts. In a harness in which the retractor is in the lap-belt, the head and shoulder trajectories are similar to those when a harness without retractors is used.

## INTRODUCTION

Within the past decade, public acceptance and use of three-point restraints (lap-shoulder belts) in motor vehicles have been increased considerably by the introduction of reel-type emergency locking retractors (ELR). Harnesses equipped with retractors do not require adjustments of the webbing by the occupant and permit the occupant to move in the seat in order to look behind if necessary.

The effectiveness of the three-point restraint harness has been the subject of a number of reports, both of accident surveys and simulation studies (6,9,11,12). Concern has been expressed about the inability of these harnesses to prevent the occupant from striking his head against the vehicle interior during a collision.

In older three-point harnesses without ELR's, passengers were advised to leave the shoulder strap slightly slack for comfort. Some automobile manufacturers have provided means to leave the shoulder straps of ELR-equipped harnesses slack by defeating the spring tension of the retractor. One paper (11) has reported that such provisions may reduce the ability of the harness to restrain the occupant in a crash and recommended that mechanisms for defeating the retractors be prohibited.

In response to a request from Transport Canada, a series of tests were performed to evaluate the effect of reel-type webbing retractors and belt slack on dummy dynamics during simulated frontal collisions. The study was designed to show how different lengths of slack would affect the performance of a given retractor-equipped harness and how different harnesses would perform with comparable amounts of slack in the shoulder belt.

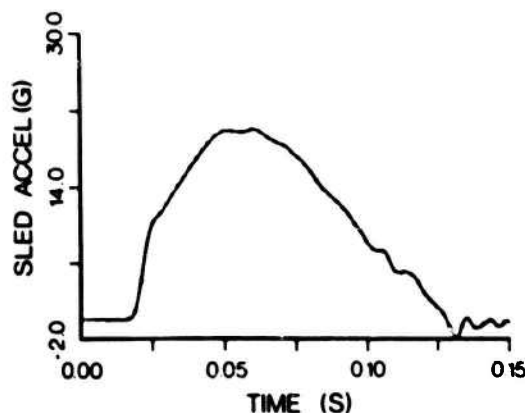


Figure 1 - Sled acceleration as a function of time in a typical test.



## METHODS

The tests were performed using the 12-inch (30-cm) Hy-Ge impact simulator at the Defence and Civil Institute of Environmental Medicine (DCIEM). The Hy-Ge apparatus simulates impacts in "reverse mode"; i.e., a stationary test sled bearing the seat and dummy is accelerated backwards by the controlled action of a pneumatic ram. In these tests, half-sine acceleration pulses with 20 G peak acceleration and 13.5 m/s (48 km/hr) velocity change were used (Figure 1).

The sled was fitted with an automotive bucket seat of a type used in North American "sub-compact" cars. The seat was reinforced to prevent motion or deformation during the test impacts. Belt anchor points, corresponding to those used in "sub-compact" cars, were installed on either side of the seat and behind the seat back at the right side. The occupant was simulated by a standard Part 572 50-th percentile dummy fitted with triaxial accelerometers in the head, chest and pelvic areas (Figure 2). The feet of the dummy rested on a foot brace which simulated the sloping forward part of the passenger compartment floor.

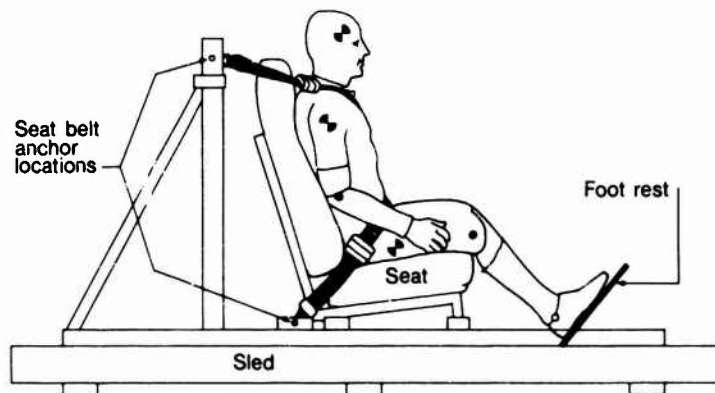


Figure 2 - The test buck with the dummy before a test.

Commercially-manufactured seat belt assemblies with inertially-activated ELR's were obtained from manufacturers through Transport Canada. The inertially-activated ELR has a spring which exerts a tension on the webbing through a torque on the reel axis. When the ELR assembly is accelerated beyond a certain limit in the horizontal plane, a pendulum-like sensor causes a fixed pawl to engage a ratchet on the reel, locking it against the webbing tension.

Two types of restraint harness, both in common use in North American cars, were used. Both had one part in the form of a continuous band of 5-cm-wide webbing, passing from an anchor at the outboard side of the seat through a D-ring attached to the buckle insert, and ending either at an anchor above the shoulder or passing through a D-ring near the shoulder to an anchor below. The second part of the harness was a stub attached to the inboard anchor which carried the other part of the buckle. The Type C belt had an ELR in the shoulder belt and, and passed through a D-ring above the shoulder to the ELR. The Type D belt had an ELR at the outboard lap-belt anchor and was attached rigidly above the shoulder (Figure 3). For comparison, a belt assembly without retractors, similar in pattern to the Type C belt was used; this is called a Type A belt. The naming of ELR-equipped belts this way is adapted from the paper by Dance and Ensarink (5). Polyester webbing was used in all belts.

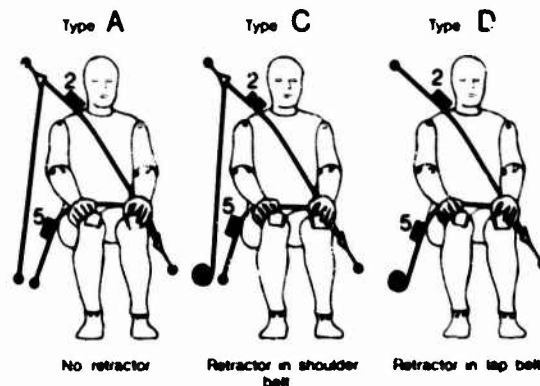


Figure 3 - The three types of harness used showing the locations of belt tension transducers numbers 2 and 5.

After the dummy was positioned in the seat and the belts were installed, the following procedure was used to set a measured amount of slack in the belts. The shoulder strap was drawn over a specially-made gauge placed over the mid-line of the chest of the dummy. This gauge held the webbing at a measured distance from the chest which is called belt slack in the rest of this paper. When the Type C or Type D harnesses were used, the webbing was anchored near the ELR with tape so that it would not be reeled in when the gauge was removed. The extra webbing was drawn in above the shoulder so that the shoulder strap lay across the dummy chest after the gauge was removed. Belt slack lengths of 0.0, 2.5, 5.0, 10.0, 15.0 and 25.0 cm were used in the tests in this study.

In one test of each harness type at each value of belt slack, high speed motion pictures were taken on each side and in front of the dummy at 500 frames per second. The processed films were analyzed to obtain graphic trajectories of targets on the dummy head, shoulders and legs, and to determine the maximum forward motion of the head.

Tensions in separate parts of the seat belts were measured during the impact by five belt tension transducers. One of these, designated tension transducer number 2, was mounted on the shoulder portion of the belt between the dummy chest and the upper D-ring or anchorage point. Another, designated tension transducer number 5, was mounted on the lap strap between the dummy abdomen and the retractor or anchor point beside the seat on the outboard side (Figure 3).

Signals from the belt tension transducers, dummy triaxial accelerometers, and an accelerometer fixed to the sled were amplified on the sled and transmitted to the control room of the Impact Studies Facility.

The data acquisition system at the DCIEM Impact Studies Facility has been described elsewhere (4). The signals passed through analog filters which attenuated frequencies above 1000 Hz (10). They were recorded digitally using Datalab transient recorders (Data Laboratories Ltd., Mitcham, England) at a sampling rate of 10,000 per second.

The digital records were transferred to a computer disk memory for archiving and processing. The records were filtered digitally according to the specifications of SAE Recommended Practice J211b (2) by programs developed at DCIEM (10). Scaled records of accelerations from the triaxial accelerometers were used to calculate resultant accelerations. These accelerations were plotted along with the component accelerations and belt tensions. Maximum values for resultant accelerations and tensions were determined by the computer.

Two tests were performed with each of the three types of seat belts described above at each of the six slack lengths. An additional test was performed at 10-cm slack with the Type A belts when an inconsistency in the earlier results was found.

## RESULTS

### 1. REPEATABILITY

Because two tests were done with each harness at each belt slack setting, it was possible to judge the repeatability of this simulation. Peak accelerations of the head, chest and pelvis of the dummy were compared for the two tests of each type. In most pairs, the differences were less than 5 percent of the actual values, although there were certain exceptions. A larger difference in head and chest accelerations of the two tests with the Type A harness at 10-cm slack led to the decision to repeat the test a third time. The results of this test were very similar to that of one of the previous tests. The overall repeatability of the tests gives some confidence that the differences found with different harness configurations are real effects of the harnesses, rather than the result of experimental artifacts.

### 2. RETRACTOR PERFORMANCE AND WEBBING PULLOUT

All of the retractors used in the tests performed satisfactorily, locking the webbing reel within 20 ms of impact. A certain amount of webbing was drawn from the retractor during impact and this was measured using a wire drawn from a clip by the moving webbing. This is called "belt pullout" and is shown in Figure 4 as a function of belt slack for the Type C and Type D belts. The belt pullout was usually less than 7 cm and decreased with increasing belt slack.

This tendency was a simple consequence of the method used to obtain belt slack. Webbing was drawn from the reel to set the slack; thus, with greater slack, less webbing was left on the reel. A contribution to belt pullout must come from the elastic extension of the webbing on the reel, which itself is proportional to the length of webbing on the reel. The separation of this contribution to belt pullout from that of the motion of the reel itself before lock-up was impossible in these tests. The belt pullout was similar to the maximum extension found in vehicle harness retractors during barrier collisions by Dance and Enserink (5).

### 3. SLACK TIME

A concept which is useful in interpreting evaluations of seat-belt performance is the sleek time which is the time interval between the onset of vehicle deceleration (or sled deceleration, in a simulation such as this) and the onset of webbing tension. The sleek time is related to the "ride-down" time described by Morris (8) in that the sum of the two time intervals is the duration of the crash deceleration in a vehicle collision. During the sleek time, the occupant is not restrained by the harness and will move out of the accelerating seat with increasing relative velocity. Longer sleek times in the shoulder belt are associated with greater excursions of the occupant head and chest and greater peak forces as the occupant is finally caught by the belts. Figure 5 shows the sleek time for the shoulder

strap (belt tension transducer number 2) as a function of belt slack for the three types of belts. The slack time is the interval between the onset of sled acceleration and the onset of tension recorded by the belt tension transducer.

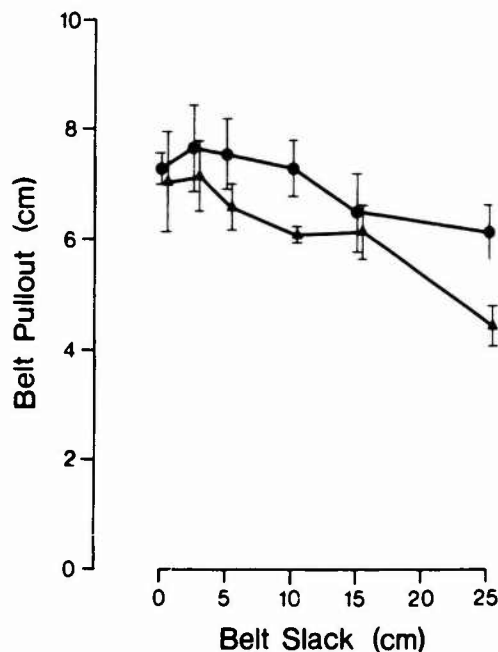


Figure 4 - Belt pullout ( $\pm$  standard deviation) as a function of belt slack;  $\bullet$  - Type C harness,  $\blacktriangle$  - Type D harness.

Figure 5 clearly shows that slack time increases with slack. There is a considerable slack time even at zero slack, 25 ms for the Type A and D belts and 33 ms for the Type C. The importance of this slack time can be seen by considering its relation to the acceleration and velocity of the sled and seat in a typical run. At 25 ms, the sled has reached more than three-quarters of its maximum acceleration and has changed its velocity by 0.23 of the final change. At 65 ms, the acceleration of the sled has begun to decrease and the sled is moving at about two-thirds of its greatest velocity. Thus, it is expected that there will be an increase in the relative velocity of the dummy chest and the seat between 25 and 65 ms of slack time, and a consequent increase in the acceleration of the chest as it is caught by the belt.

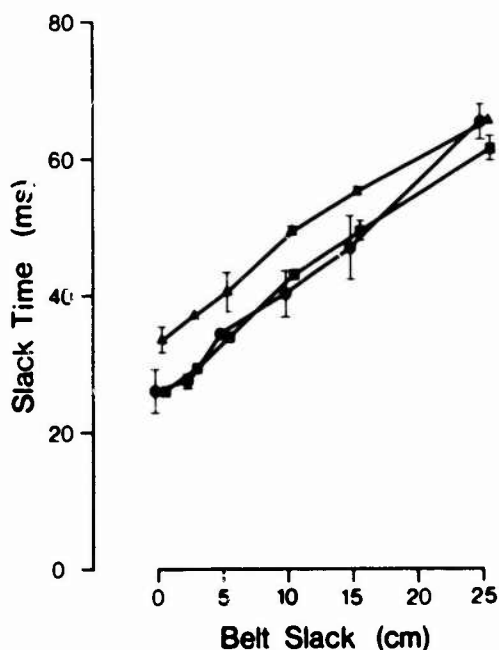


Figure 5 - Slack time ( $\pm$  standard deviation) determined from belt tension transducer number 2 as a function of belt slack;  $\bullet$  - Type A harness,  $\blacktriangle$  - Type C harness,  $\blacksquare$  - Type D harness.

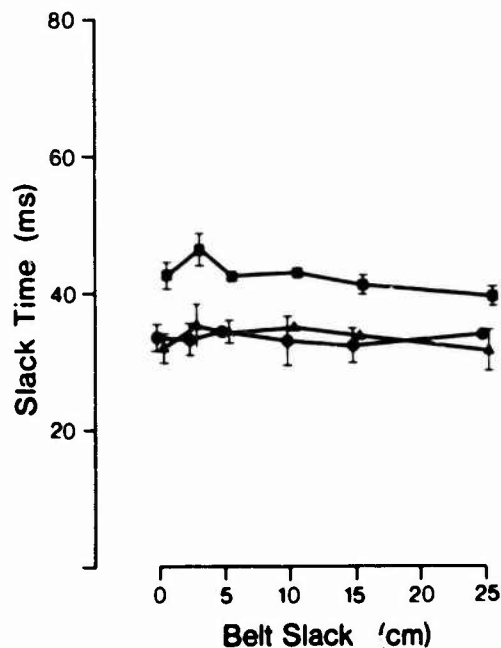


Figure 6 - Slack time ( $\pm$  standard deviation) determined from belt tension transducer number 5 as a function of belt slack;  $\bullet$  - Type A harness,  $\blacktriangle$  - Type C harness,  $\blacksquare$  - Type D harness.

Figure 6 shows the slack time as measured by belt tension transducer number 5 on the lap belt. Here the slack time is nearly constant, indicating that little, if any, of the slack in the shoulder belt passes through the D-ring separating the two parts of the webbing into the lap belt. The slack time for the Type D belts is about 10 ms greater because of the retractor in the lap belt.

#### 4. TRAJECTORIES

The trajectories of three targets on the dummy were measured from the films taken with the right-hand camera. These targets were placed on the head, on the shoulder, and towards the upper end of the femur. A fourth target mounted on the dummy pelvis was impossible to follow because the lap strap obscured it from view.

The positions of the targets, relative to a fixed point on the sled, were measured in selected frames of the film. The times at which the frames were exposed were determined from 10-ms timing marks exposed on the film. Then the positions of the dummy targets at 10-ms intervals from 0.0 ms to 150.0 ms were determined by linear interpolation. These are plotted on an X-Y scale for each of the three belt types and belt slack values of 0.0, 5.0, 10.0 and 25.0 cm in Figures 7 through 18.

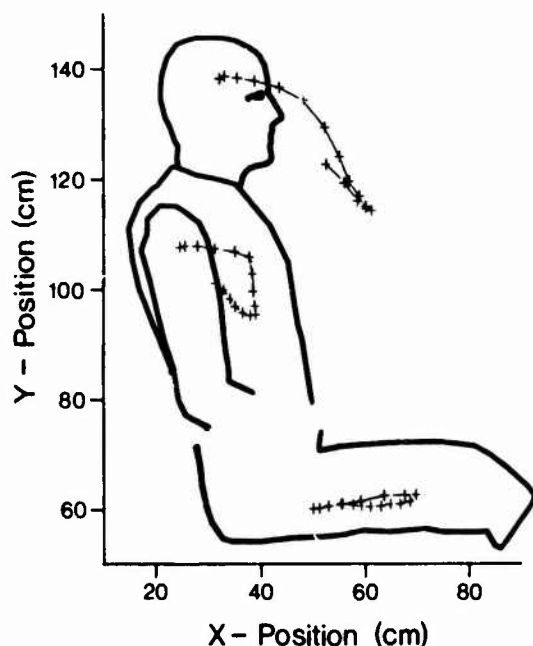


Figure 7 - Trajectory Plot: Type A harness, 0.0 cm slack.

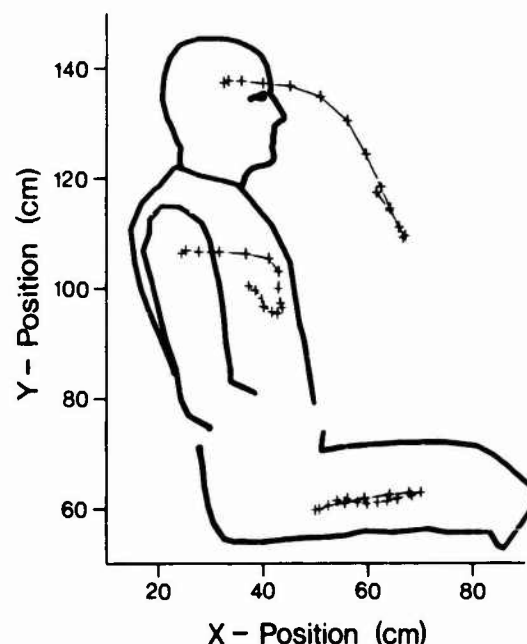


Figure 8 - Trajectory Plot: Type A harness, 5.0 cm slack.

The trajectories show most clearly the effect of the extra slack on dummy motion and the way in which retractors modify this affect. One can see the evolution of the trajectories as the slack increases for each type of belt. Generally, there is greater forward motion of the shoulders and head as the slack increases. At 25-cm slack (Figures 10, 14, and 18), the head is almost in front of the shoulders at the extremity of its forward motion with all belts; with the Type C belt, it is directly above the knee (Figure 14), as if no shoulder strap had been present.

With the Type A and Type C belts, there is no perceptible change in the motion of the leg target with increasing belt slack if the belt slack is 15 cm or less. At 25-cm slack, the forward motion of the leg target increases by about 3 cm (Figures 10 and 14). This indicates that some of the shoulder belt webbing does pass through the D-ring into the lap portion of the belt when the belt slack is 25 cm. In the other cases, the slip of webbing through the D-ring is essentially negligible during a simulated impact; the two parts of the harness behave as fixed lengths of webbing.

Of greater interest is a comparison of the three types of harness when the belt slack is the same. The Type C harness permits greater forward motion of the head and shoulders for a given slack than the Type A harness. This difference is the result of belt pullout, which is about 7 cm, as described above. A comparison of the trajectories obtained with the Type A harness at 10-cm slack (Figure 9) and the Type C harness at no slack (Figure 11) shows that they are almost the same on the forward-moving part, but that the Type A harness draws the head and shoulders back more quickly than the Type C harness. This difference is due to the extra webbing on the reel in the Type C harness, which causes the shoulder strap to respond less stiffly to extension.

In terms of its affect on head and shoulder trajectories, an ELR on the shoulder strap is almost equivalent to 7 cm of slack webbing.

The differences between the trajectories produced by the Type A and Type D harnesses are more subtle. The Type D harnesses allow greater forward motion of the pelvis as demonstrated by the motion of the leg target in Figures 15 to 18. The difference is about 5 cm.

The trajectories also show that the shoulder target exhibits greater downward vertical motion with the Type D harness at all values of belt slack. The trajectory of the head target with the Type D harness is very similar to that of the head target with the Type A harness. The greatest forward motion is slightly less with the Type D harness, and this difference may not be significant.

Figure 19 shows the peak forward excursion of the forward-most point of the dummy head as a function of belt slack for the three harness types. (The forward-most part of the head is not the head target whose trajectory is given in the previous figures, but is of significance, as it indicates the position of a vertical plane in front of the dummy which would be struck by the head in a deceleration similar to the one simulated.)

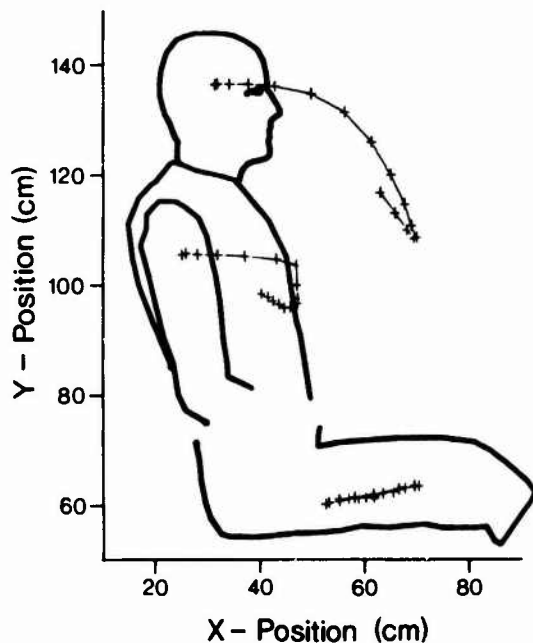


Figure 9 - Trajectory Plot: Type A harness, 10.0 cm slack.

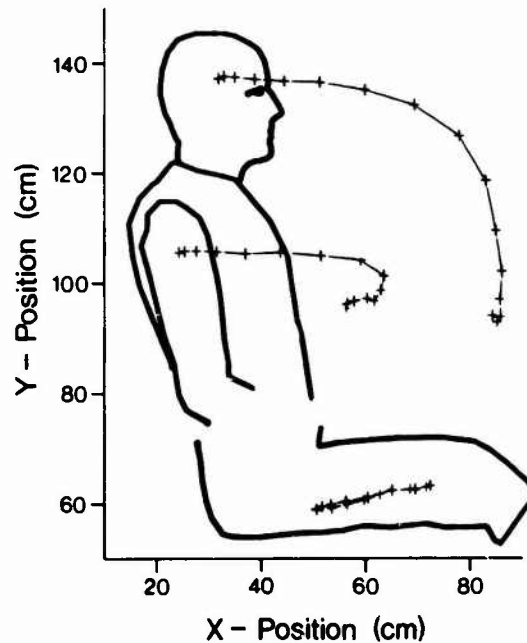


Figure 10 - Trajectory Plot: Type A harness, 25.0 cm slack.

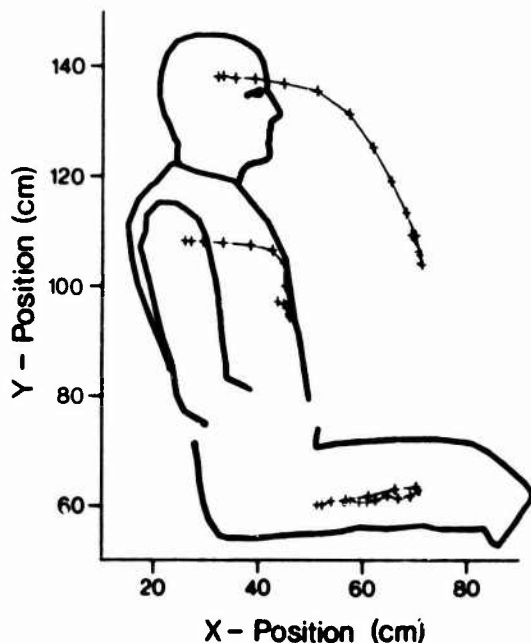


Figure 11 - Trajectory Plot: Type C harness, 0.0 cm slack.

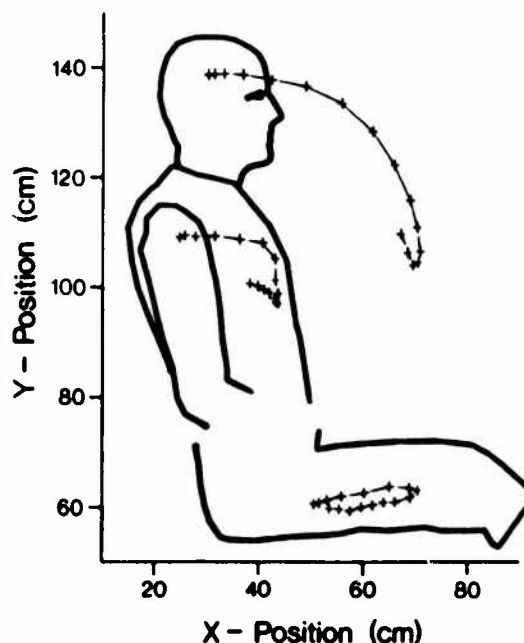


Figure 12 - Trajectory Plot: Type C harness, 5.0 cm slack.

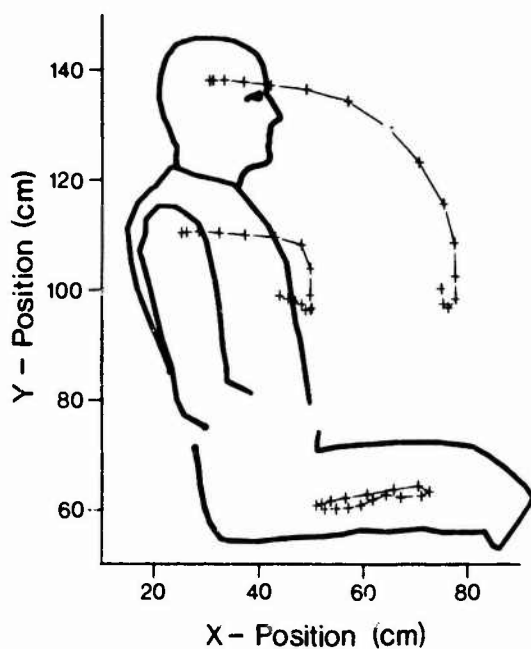


Figure 13 - Trajectory Plot: Type C harness, 10.0 cm slack.

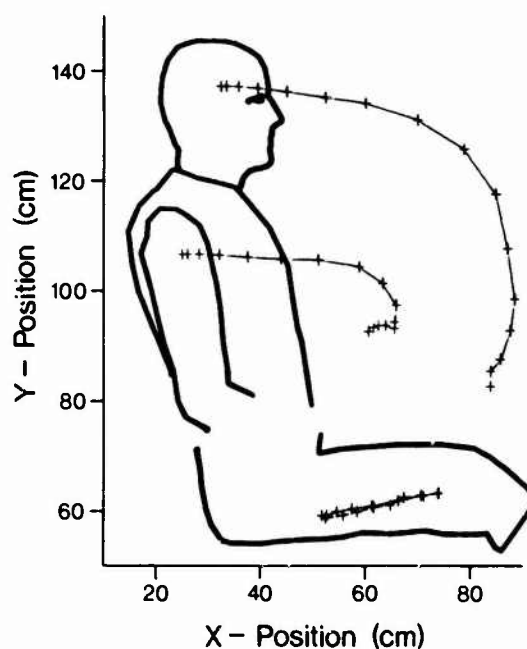


Figure 14 - Trajectory Plot: Type C harness, 25.0 cm slack.

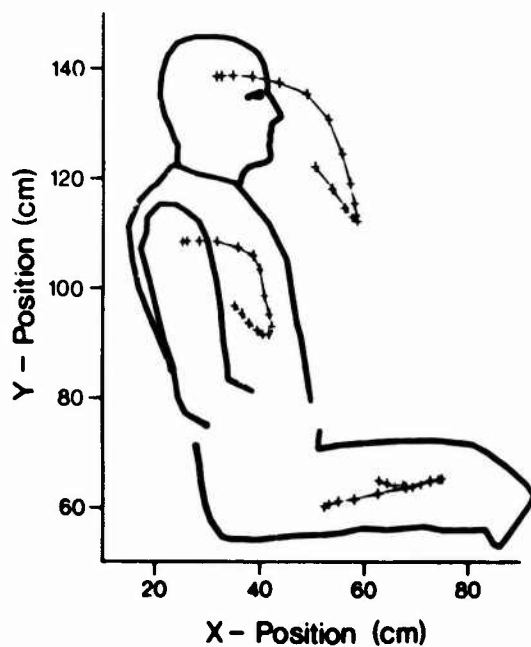


Figure 15 - Trajectory Plot: Type D harness, 0.0 cm slack.

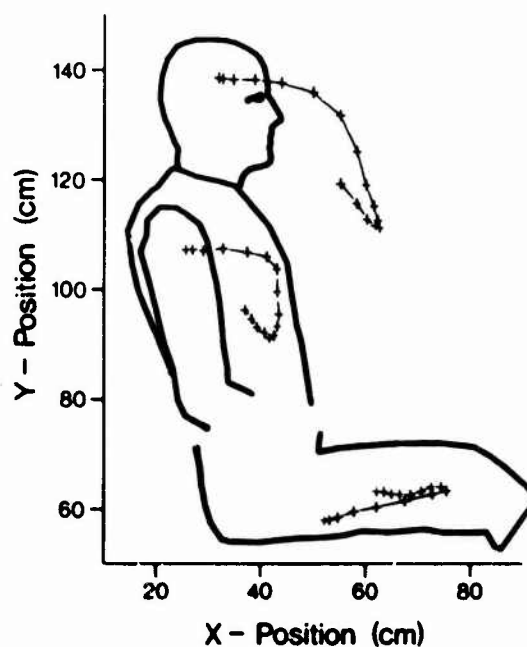


Figure 16 - Trajectory Plot: Type D harness, 5.0 cm slack.

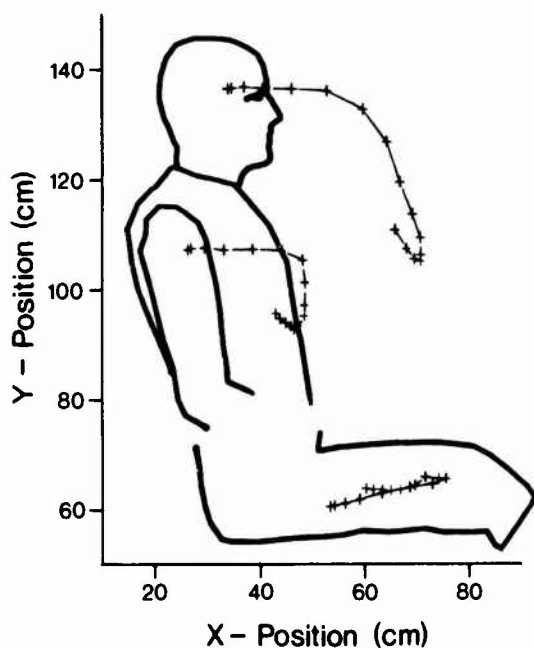


Figure 17 - Trajectory Plot: Type D harness, 10.0 cm slack.

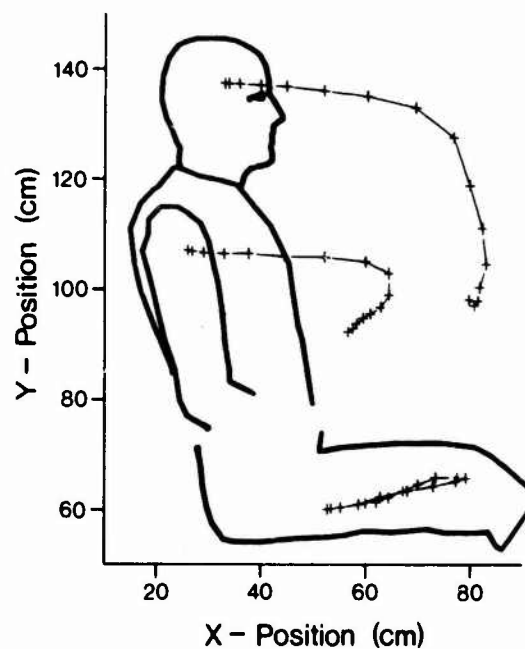


Figure 18 - Trajectory Plot: Type D harness, 25.0 cm slack.

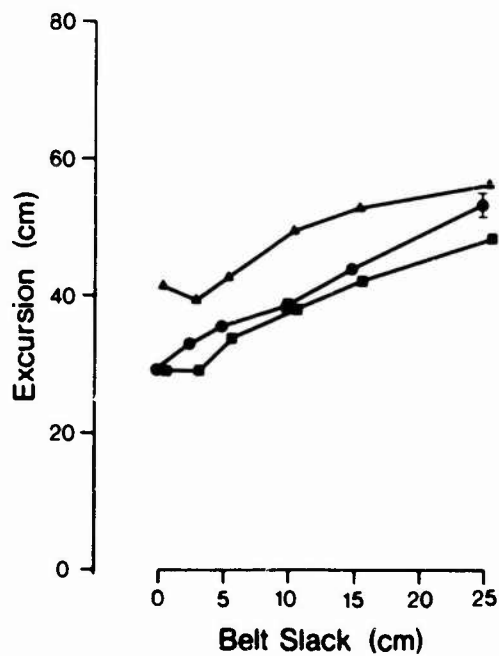


Figure 19 - Maximum forward excursion of the dummy head as a function of belt slack; ● - Type A harness, ▲ - Type C harness, ■ - Type D harness.

## 5. SUBMARINING

The dummy used in these tests was not equipped with any transducer designed to indicate "submarining", such as that described by Leung *et al.* (7). Because the problem of submarining is important in the design of automotive seat and restraint systems, the films were examined to determine whether there was overt submarining in any of the tests; i.e., whether the lap-belt rode above the pelvis and compressed the abdomen.

The films show that the dummy pelvis did tend to rotate forward under the lap belt, and this rotation was most noticeable with Type D belts. However, in no instance did the lap strap ride above the pelvis and bear directly on the abdomen. The rotation of the pelvis is the likely cause of the greater vertical motion of the shoulder target found with the Type D belts.

These observations suggest that the Type D belt may be more likely to induce submarining than the others, but they are not conclusive. Whether or not submarining occurs depends upon the seat and foot restraint as well as the lap-belt.

## 6. ACCELERATIONS

Figure 20 shows the average and standard deviations of the maximum resultant accelerations of the chest recorded in the two tests with each value of belt slack and each harness type. It can be seen that the peak acceleration of the chest increases almost linearly with slack, particularly with the Type A harness.

The acceleration of the dummy chest in a harness in which the shoulder belt is slack should be most similar to the very simple dynamic model for the behaviour of the occupant of a slack belt proposed by Aldman and Asberg (3). These authors discussed the behaviour of a single mass on a spring which attached it to a vehicle which decelerated as in a collision. The spring had some slack, which allowed the mass to move relative to the vehicle without a restraining force. They showed that the peak acceleration of the mass was a complex function of the acceleration of the vehicle as a function of time as well as the slack length. There is no reason *a priori* to believe that the peak acceleration of the mass is a linear function of the slack length. It would appear that the linearity of the above results is a fortuitous consequence of the choice of acceleration-time profile and belt-slack values.

The peak acceleration of the chest is twice that of the sled even at zero slack; this is a consequence of the slack time at zero slack which can only be eliminated by considerable pretensioning of the webbing.

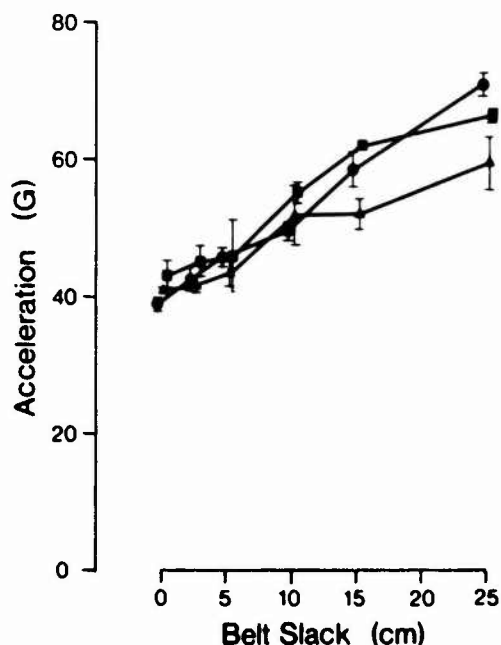


Figure 20 - Peak resultant chest acceleration ( $\pm$  standard deviation) as a function of belt slack;  $\circ$  - Type A harness,  $\Delta$  - Type C harness,  $\square$  - Type D harness.

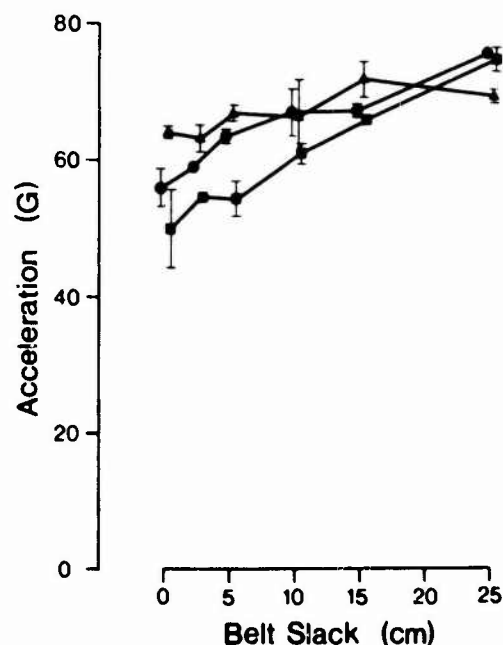


Figure 21 - Peak resultant head acceleration ( $\pm$  standard deviation) as a function of belt slack;  $\circ$  - Type A harness,  $\Delta$  - Type C harness,  $\square$  - Type D harness.



The peak chest acceleration with the Type C harness is about the same as that with the Type A harness at zero slack but increases less rapidly with belt slack so that, at 15-cm and 25-cm slack, the peak accelerations are less than with the Type A harness. The reduced peak accelerations at greater slack are the consequence of the reduced webbing stiffness of the longer webbing of the Type C shoulder strap.

Except at 25-cm slack, the Type D harness produces the greatest chest acceleration at a given value of slack. The difference is not significant.

According to the United States Federal Motor Vehicle Safety Standard 208 (1), the Type A and D harnesses would fail the criterion for chest injury at a belt slack of 25 cm but not at lower slack values. The chest acceleration was greater than 60 G for a period of more than 3 ms in these tests.

The peak accelerations of the dummy head are presented similarly in Figure 21. Peak head acceleration is a more complex function of belt slack and harness type than peak chest acceleration. The expected increase with increasing belt slack is shown with Type A and Type D harnesses but the Type C harness causes the peak head acceleration to be nearly constant.

Although these accelerations are about three times the maximum acceleration of the sled, they are not significant in terms of head injury. Whether the harness would allow the occupant's head to strike a surface within the vehicle with sufficient force to cause injury depends on the particular vehicle and the head trajectories described above.

#### 7. BELT TENSIONS

The belt-tension records obtained in these tests were of interest not only for determining the slack time but also for determining the maximum tension on the webbing as a function of harness type and belt slack. Some investigators have explored the use of webbing tension in automotive harnesses as an indicator of potential injury to the chest and abdomen of the occupant (13). Since the acceleration of the chest is already used as an indicator of potential injury and is an indicator of the net force on the chest, it is of interest to compare the belt loads to the chest accelerations measured in these tests.

The peak belt tension measured by transducer number 2 on the shoulder strap is plotted as a function of belt slack for the three harness types in Figure 22. (No suitable records were available from this transducer in tests of the Type C harness at 25-cm slack.) Although the peak belt tension in Type A and D harnesses does increase with belt slack, the increase is relatively not as great as that of the peak chest acceleration. The peak tension in the Type C harness is independent of belt slack. In both the Type A and D harnesses, the peak tension does not increase from 15 to 25 cm of belt slack; this is likely to be the result of the impact of the chest against the knees taking some of the force required to accelerate the chest.

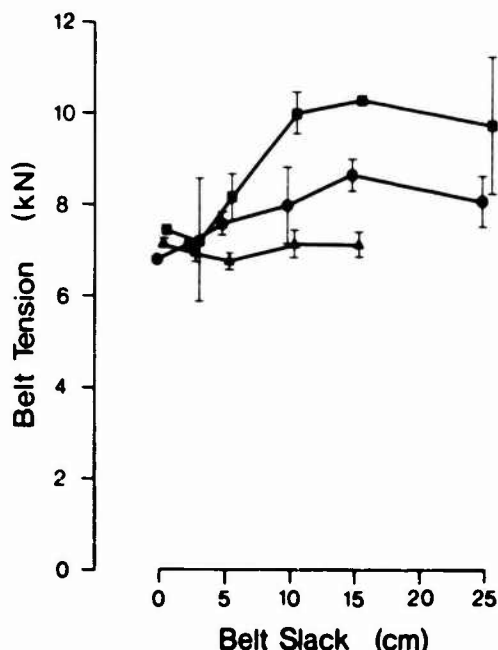


Figure 22 - Peak tension ( $\pm$  standard deviation) recorded by belt tension transducer number 2 as a function of belt slack; ● - Type A harness, ▲ - Type C harness, ■ - Type D harness.

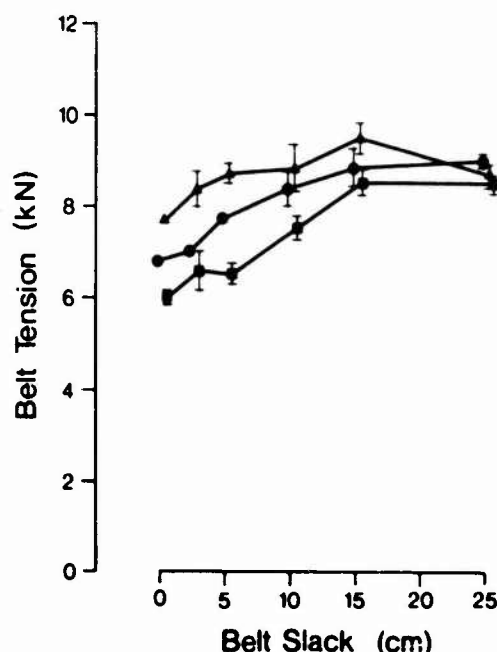


Figure 23 - Peak tension ( $\pm$  standard deviation) recorded by belt tension transducer number 5 as a function of belt slack; ● - Type A harness, ▲ - Type C harness, ■ - Type D harness.

The paradoxical result that chest acceleration increases markedly with slack where belt tension does not can be explained by the fact that the belt geometry at the time of peak tension changes greatly with increasing slack. As the chest moves further forward, the shoulder belt is more nearly parallel to the acceleration of the chest, and, therefore, the force required to accelerate the chest is a greater fraction of the resultant tension in the belt. Viano et al. (13) found a similar result when exploring the belt tension as a function of slack in simulations and mathematical models.

Figure 23 shows that the peak belt tensions recorded by transducer number 5 increased slightly with belt slack. The Type C harness produces the highest tension, except at 25-cm slack, and the Type D produces the lowest. The latter may be the result of the reduced effective stiffness of the webbing on an ELR noted before in connection with the chest acceleration in the Type C harness. The greater forward excursion of the pelvis with the Type D belts would cause the seat to take more of the force accelerating the dummy pelvis.

#### GENERAL CONCLUSIONS

The preceding discussion of the individual measurements leads to a general picture of the effects of belt slack and harness type on the motion of the dummy during simulated collisions.

Increasing belt slack in the shoulder strap allows increased forward motion of the dummy head and chest during impact. At about 25-cm slack, the shoulder strap is almost completely ineffective as the dummy chest begins to contact the femur at its forward-most extremity of motion.

The greater forward motion is accompanied by greater accelerations as the head and chest are arrested by the restraints.

The forward motion of the pelvis is not significantly affected by belt slack, since the belt does not slip through the D-ring separating the lap and shoulder portions of the webbing during a collision, except at 25-cm slack.

An ELR in the shoulder harness has two effects. The webbing is effectively extended by about 7 cm, because this amount is allowed to spool from the ELR. The consequences of this are greater forward motions of the head and chest, with correspondingly greater risks of head injury through striking the vehicle interior. The webbing on the reel reduces the effective stiffness of the webbing, so that although the forward motion of the head and chest are greater than those produced by a harness without retractors, the peak accelerations of these parts are less.

An ELR in the lap belt does not have the same effect as a shoulder belt retractor. It permits greater forward motion of the dummy pelvis, and may make submarining more likely. The head and shoulder trajectories and accelerations are similar to those in a harness without an ELR.

What significance do these findings have for those evaluating restraint systems for military or civilian vehicles? The additional forward motion of the head allowed by an ELR in the shoulder belt can have the most serious consequences if the available space in the upper part of the passenger compartment is limited, as it is with many modern cars (6,12). Similar problems are expected for drivers who have steering wheels or other potential sources of injury within the range of motion of their chests.

In view of these hazards, the users of ELR-equipped restraints should not be advised to leave the shoulder strap slack or defeat the tension of the retractor spring.

It may be impossible to duplicate the easy installation and adjustment of harnesses equipped with ELR's by other means. Retractors may continue to be useful in civilian and military vehicles where these features are necessary to ensure the correct use of restraints. If the headroom is extremely limited and webbing retractors are considered necessary, the designer has the choice between a pretensioning retractor of the type described by Svensson (12) in the shoulder belt, or a retractor in the lap belt.

Each system has potential disadvantages. Pretensioning retractors apparently work well, but may add to the cost of a restraint system and create additional noise hazards. A retractor in the lap belt may allow submarining to occur where it otherwise would be prevented. Retractors fitted this way may be effective if used with anti-submarining seat designs (12) or knee bolsters.

In any case, the importance of dynamic tests, with visual inspection of films, in the evaluation of new restraint systems cannot be overstated.

#### REFERENCES

1. -. U.S. Federal Motor Vehicle Safety Standard 208, Occupant Crash Protection, U.S. Department of Transportation.
2. -. SAE Recommended Practice J211b - Instrumentation for Impact Tests. 1974.
3. Aldman, B. and A. Asberg. Impact Amplification in European Compacts. In: Proceedings of the Twelfth Stapp Car Crash Conference. Society of Automotive Engineers, Inc., Warrendale, PA, U.S.A. pp. 387-401, 1968.
4. Bowden, T.J., J.K. Raichert and J.P. Landolt. The Data Acquisition System at the DCIEM Impact Studies Facility. In: Passenger Car Seating. Society of Automotive Engineers, Inc., Warrendale, MI, U.S.A. June 8-12, 1981. (SAE Paper No. 810812).

5. Dance, M. and B. Enserink. Safety Performance Evaluation of Seat Belt Retractors. In: Passenger Car Meeting. Society of Automotive Engineers, Inc., Warrendale, PA, U.S.A. 1979. (SAE Paper No. 790680).
6. Herbert, D.C., J.D. Scott and C.W. Corben. Head Space Requirements for Seat Belt Wearers. In: Proceedings of the Nineteenth Stapp Car Crash Conference. Society of Automotive Engineers, Inc., Warrendale, PA, U.S.A. pp. 675-704, 1975. (SAE Paper No. 751164).
7. Leung, Y.C., C. Tarriere, A. Fayon, P. Mairesse, A. Delmas and P. Banzet. A Comparison Between Part 572 Dummy and Human Subject in the Problem of Submarining. In: Proceedings of the Twenty-Third Stapp Car Crash Conference. Society of Automotive Engineers, Inc., Warrendale, PA, U.S.A. pp. 677-719, 1979. (SAE Paper No. 791026).
8. Morris, J.B. Seat Belt Performance in 30 MPH Barrier Impacts. National Highway Traffic Safety Administration, Office of Vehicle Systems Research Report DOT HS-802 480, April 27, 1977.
9. Niederer, P., F. Walz and U. Zollinger. Adverse Effects of Seat Belts and Causes of Belt Failures in Severe Accidents in Switzerland During 1976. In: Proceedings of the Twenty-First Stapp Car Crash Conference. Society of Automotive Engineers, Inc., Warrendale, PA, U.S.A. pp. 55-93, 1977. (SAE Paper No. 770916).
10. Reichert, J.K. and J.P. Landolt. Digital and Analog Filters for Processing Impact Test Data. In: SAE Passenger Car Meeting. Society of Automotive Engineers, Inc., Warrendale, PA, U.S.A. 1981. (SAE Paper No. 810813).
11. Shanks, J.E. and A.L. Thompson. Injury Mechanisms to Fully Restrained Occupants. In: Proceedings of the Twenty-Third Stapp Car Crash Conference. Society of Automotive Engineers, Inc., Warrendale, PA, U.S.A. pp. 17-38, 1979. (SAE Paper No. 791003).
12. Svensson, L.G. Means for Effective Improvement of the Three-Point Seat Belt in Frontal Crashes. In: Proceedings of the Twenty-Second Stapp Car Crash Conference. Society of Automotive Engineers, Inc., Warrendale, PA, U.S.A. pp. 451-479, 1978. (SAE Paper No. 780898).
13. Viano D.C., C.C. Culver and B.C. Prisk. Influence of Initial Length of Lap-Shoulder Belt on Occupant Dynamics - A Comparison of Sled Testing and MVMA-2D Modelling. In: Proceedings of the Twenty-Fourth Stapp Car Crash Conference. Society of Automotive Engineers, Inc., Warrendale, PA, U.S.A. pp. 375-416, 1980. (SAE Paper No. 801309).

MADYMO - A CRASH VICTIM SIMULATION  
COMPUTER PROGRAM FOR BIOMECHANICAL  
RESEARCH AND OPTIMIZATION OF DESIGNS  
FOR IMPACT INJURY PREVENTION

by

J. Wismans, J. Maltha, J.J. van Wijk, E.G. Janssen  
Research Institute for Road Vehicles, TNO  
P.O. Box 237, 2600 AE Delft, The Netherlands

## SUMMARY

MADYMO is a compact general purpose computer program package for two or three-dimensional crash victim simulations. The program predicts the kinematic and dynamic behaviour of the victim during the crash, based on data of the victim, the environment, the safety devices and the crash conditions. The package differs from most of the existing CVS programs by its flexibility in choice of number of linkages and number of elements in each linkage. Great flexibility in the modelling of force interactions between elements and environment is assured by the fact that user-defined submodels can readily be incorporated. The package is used for basic biomechanical crash research as well as for the development and optimization of crash safety devices such as seat belts, child seats and vehicle paddings. This paper discusses some recent applications of this program package, with special emphasis on the validity of the model and computer aided design aspects.

## INTRODUCTION

In the field of automotive and aircraft safety research, simulation of crashes to study the effects on the human body is of vital importance in order to evaluate and improve crash safety devices and occupant environment. Most of this work is done by means of experiments, using instrumented dummies, cadavers, and occasionally animals or volunteers.

During the past years more and more emphasis has been placed on the use of mathematical models in this field. Particularly, if such models are used as a complementary research tool to experimental work, they may significantly contribute to the insight in the behaviour of complex biodynamical systems.

This paper deals with models of the type gross-motion simulators, which describe the human body (or other structures) by means of a number of connected rigid bodies. Computer programs for this type of simulations have been developed in the past years by a number of investigators. A review of several of these programs is given by Robbins (1) and King (2). The models vary in complexity and are either two or three-dimensional. They are limited mostly to a fixed number of rigid bodies, all belonging to one linkage system. An exception is the Calspan 3D model that allows definition of more than one linkage system with a varying number of elements.

Some of the crash victim simulation models have intensively been used for aircraft safety related problems. Examples are the Articulated Total Body (ATB) computer model, developed at the Aerospace Medical Research Laboratory, Dayton, Ohio (3) and the Seat/Occupant Model - Light Aircraft (SOM-LA) developed at Ultrasystems, Phoenix, Arizona (4). Both models are 3-dimensional. The ATB model is based on the Calspan 3D model. Several modifications were introduced, like the capability to apply aerodynamic forces to the human body as are experienced during ejection from the aircraft. The SOM-LA model was particularly developed to provide a practical engineering tool for use in crashworthy design and evaluation of seats and restraint systems for light aircrafts. The seat in this model can be represented by means of the finite element analysis technique.

All models dealt with in the review papers of Robbins (1) and King (2) were developed in United States laboratories. The present study describes some aspects of the computer package MADYMO, which has been developed in the Netherlands, at the Research Institute for Road Vehicles, TNO. A review is given of several recent applications of MADYMO in the field of automotive safety. Attention will successively be given to the child's response in a frontal collision, to the simulation of side impacts and to pedestrian accidents. In addition, two examples will be given of the use of MADYMO as a design tool.

## DESCRIPTION OF THE MADYMO CVS PROGRAM PACKAGE

MADYMO is a compact general purpose computer program package for two- or three dimensional simulations of human body gross motions. The program, which is based on rigid body dynamics using Lagrange equations, can be used to simulate one or more linkage systems having no closed loops (see Fig. 1). The number of elements (rigid bodies) in each linkage system can be selected freely. The connections (joints) between the elements in a linkage system are of the hinge type for the two dimensional and of the ball and socket type for the three dimensional simulations. Relative rotations in these joints are resisted by non-linear torsional springs, viscous dampers and coulomb frictions.

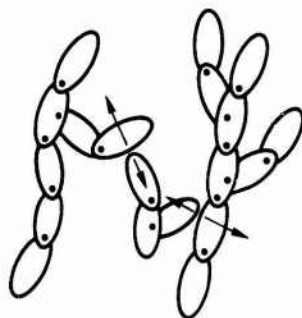


Figure 1 Linkage systems in force interaction.

Various types of external forces can be applied on the segments, like restraint forces, contact forces, gravity and inertia forces. These forces are specified as a function of segment (relative) position, segment (relative) velocity or as a function of time and in general they can act on an arbitrary point of the segment. The program is of a modular structure which facilitates the easy incorporation of user-defined force algorithms. For example, it is possible in this way to simulate more complex joints than the hinge or the ball and socket type, by the introduction of joint force routines that act on two (or more) segments of the same or of separate linkage systems.

The systems response is described by the Lagrange equations of motion as a function of  $n$  independent coordinates  $q_j$  ( $j: 1 \dots n$ ). These coordinates  $q_j$  are generalized coordinates corresponding to the degrees of freedom of the system. The equations of motion are generated by MADYMO and are, for purposes of computation, expressed in the following form (5):

$$\underline{S} \ddot{\underline{q}} = \underline{r}_s + \underline{r}_k \quad [1]$$

where the elements of symmetrical ( $n \times n$ ) matrix  $\underline{S}$  and the column matrix  $\underline{r}_s$  are dependent on the systems position (specified by  $\underline{q}$ ), the mass distribution and the geometry. The elements of  $\underline{r}_s$  in addition are a function of the systems velocity (specified by  $\dot{\underline{q}}$ ). The elements of  $\underline{r}_k$  are generalized forces which are obtained from the joint torques and the external applied forces. The solution of the set of second order non-linear differential equations (Eq. 1) is obtained by numerical integration. The package contains a standard output print option of all input and calculated data. For most simulations the user is interested in only a small portion of the output data, which can be obtained by a simple user-defined subroutine for printing these data. This same routine may be used to generate data files for post-processing plot programs. Fig. 2 illustrates the output of one of these plot programs, a graphic package with hidden line options for the representation of 3D kinematics.

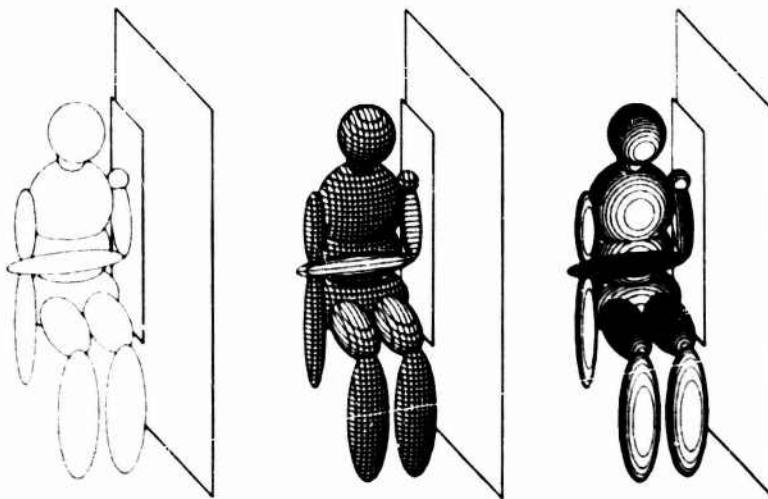


Figure 2 Examples of output of the advanced graphic package for the representation of 3D kinematics.

The MADYMO package contains a two and a three-dimensional option. The size of the standard program files is about 1800 and 2200 Fortran lines for the two and three-dimensional parts respectively (these numbers include the explanatory comment lines). The memory storage needs and the computer run times are dependent on the specific simulation data, such as number of modelled elements, number of contacts allowed etc.

The versatility of the MADYMO program package for a wide variation of applications will be shown now by a selection of simulations that were conducted in the past years.

## SIMULATION OF A CHILD OCCUPANT IN A FRONTAL COLLISION

The first example is the simulation of an impact sled test with a child in a harness type child restraint system (Fig. 3). Details of this study were presented at the 23th Stapp Conference (6). Owing to the 2D nature of the motions the 2D option of MADYMO was used for this analysis. Two linkage systems were defined: one to represent the child and the other for the child restraint system (Fig. 4). The force interactions between the restraint system and the child, and between the restraint system and the sled seat are simulated by a number of springs (representing belts) and ellipse-plane models (representing geometrical contacts).



Figure 3 Test set up of a child in a harness type child restraint system.

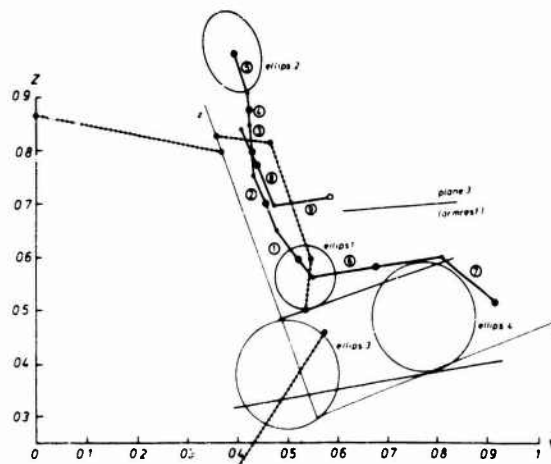


Figure 4 Mathematical representation of a child in a child restraint system.

Model results were compared with two sled tests conducted at the Highway Safety Research Institute in Michigan: one sled test with a 3-year old Part 572 dummy and the other with a child cadaver. To simulate the child dummy, detailed geometrical mass distribution and joint property measurements were conducted at the dummy; for the cadaver only dimensions and total body weight were known, so here estimations, based on data in literature, had to be made for the remaining input data. Fig. 5 shows the belt forces and the resultant accelerations of the cadaver experiment together with cadaver model predictions. In general a satisfactory agreement could be obtained between model and experimental results. Model predictions of the dummy behaviour were, however, found to be more realistic than for the cadaver, which may mainly be due to the great number of estimations that had to be made for the mass distribution and joint properties of the cadaver.

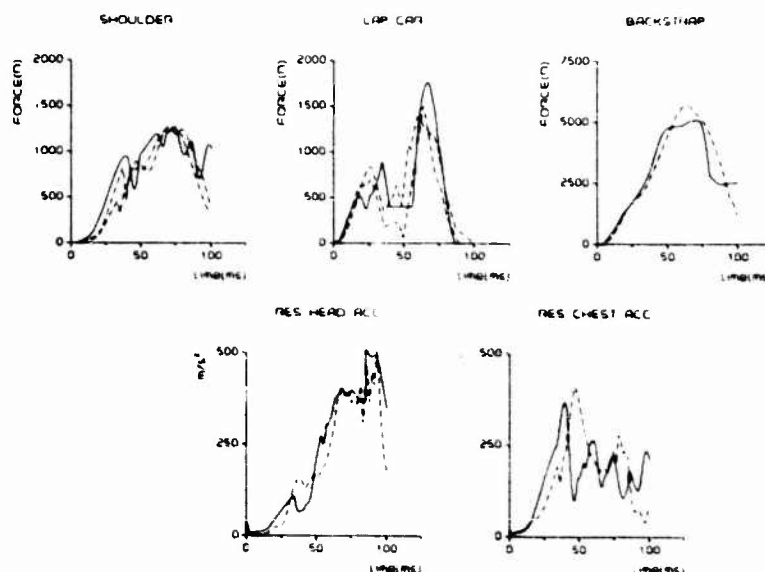


Figure 5 Comparison of belt forces and resultant accelerations of the cadaver experiment with cadaver model predictions;  
— = model; - - - = experiment

## SIMULATIONS OF SIDE IMPACTS

Side impacts produce a significant portion of the present fatality and injury totals. In the past five years injury protection for this type of accidents has become an important research objective. A large part of the present research in this complex field is directed toward obtaining insight in the injury mechanisms, establishment of injury protection criteria and toward the development of lateral impact crash dummies enabling injury detection of the most endangered areas of the human body.

With the MADYMO package several 2D as well as 3D models were formulated enabling the simulation of the occupant in side impacts. Such models can be used for:

- the interpretation and enhancement of biomechanical data obtained from experiments
- computer aided design of dummy components
- improvement and optimization of vehicle side structure and interior paddings.

Models were formulated for two different dummies (the Part 572 50th percentile male dummy and the APROD 80 dummy). The APROD 80 dummy is a modification of the Part 572 dummy with the aim of obtaining a more realistic behaviour in lateral impacts (7). Differences between these dummies are in the shoulder, the arm and the thoracic cage design.

Model predictions were compared with experimental results under relatively simple test conditions: sled tests and drop tests. Details of these simulations are described in reference (8). Fig. 6 illustrates the kinematics of the Part 572 dummy in a rigid wall sled test. Model results like contact loads and head, chest and pelvis accelerations were found to agree quite well with experimental results. That is, model predictions were close to or within the range of experimental repeatability. The differences in behaviour between the Part 572 dummy (stiff shoulder) and APROD 80 dummy (flexible shoulder), as well as the effect of this on padding loads and on padding deformations could clearly be indicated by the model. Differences between the results of 2D and 3D simulations for these simple test conditions (i.e. pure lateral impacts) were found to be small, which indicates that for certain applications the simple and cheaper 2D option can be used with sufficient confidence.

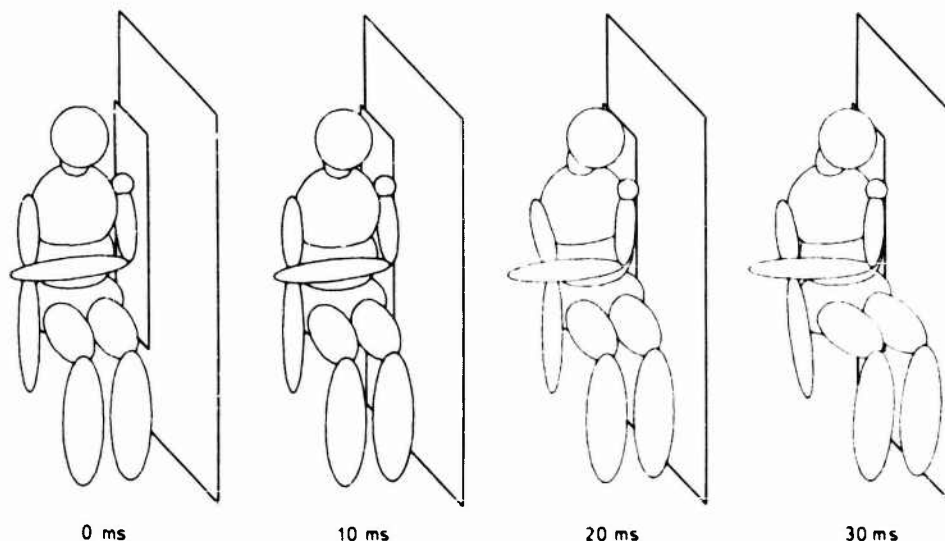


Figure 6 Mathematical simulation of a Part 572 dummy in a rigid wall sled test (25 km/h).

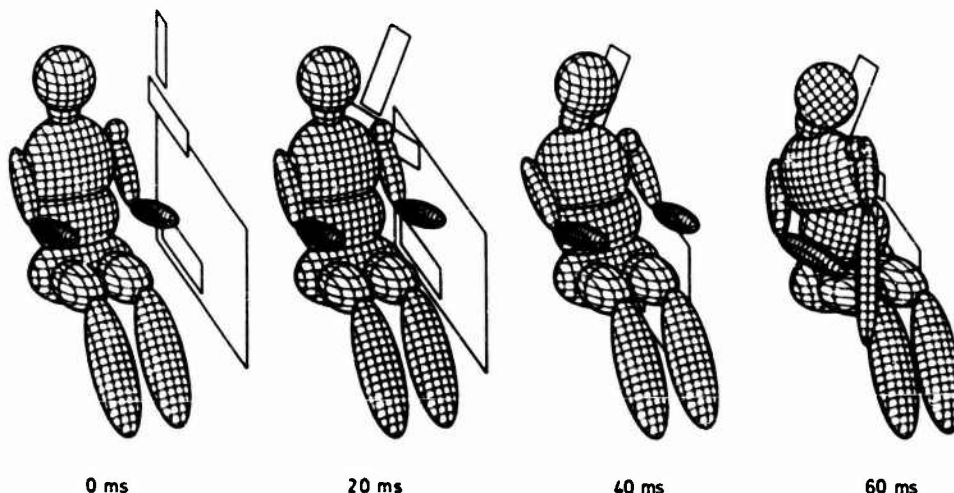


Figure 7 Mathematical simulation of a Part 572 dummy in a Peugeot 504 during a lateral collision (75 km/h).



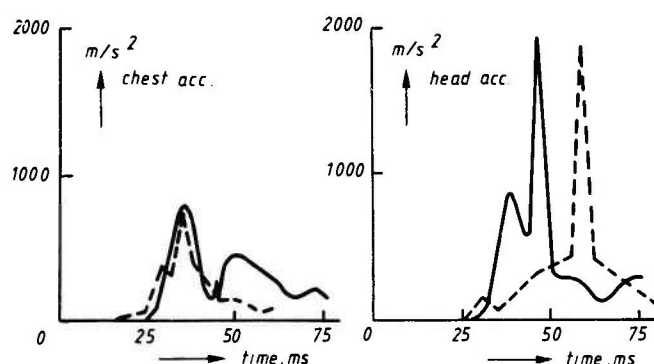


Figure 8 Comparison of resultant chest and head accelerations measured at a Part 572 dummy in a Peugeot 504 during a lateral collision (75 km/h) and corresponding mathematical simulation.  
 — = model; - - - - - = experiment

The 3D side impact model was also used to simulate a much more complicated situation: a real collision between a Peugeot 504 (stationary) impacted on the side (impact angle  $70^\circ$ ) by another Peugeot 504 having a velocity of approximately 75 km/h. For this accident several experimental reconstructions were conducted by the Lab. of Phys. and Biom. Peugeot S.A./ Renault. The mathematical simulation was limited to the interaction between the occupant in the struck vehicle (a Part 572 dummy) and the inside structure of the vehicle. The displacement of the struck door, i.e. the sum of the struck vehicle displacements and structural deformations was used as model input. The stiffness characteristics of door padding and of the arm-rest were determined with a hydraulic tester. The predicted dummy kinematics in this accident are presented in Fig. 7. Model and experimental resultant head and chest accelerations are summarized in Fig. 8. It can be seen that chest accelerations are quite well predicted by the model; the head acceleration-time histories, however, differ considerably from those in reality.

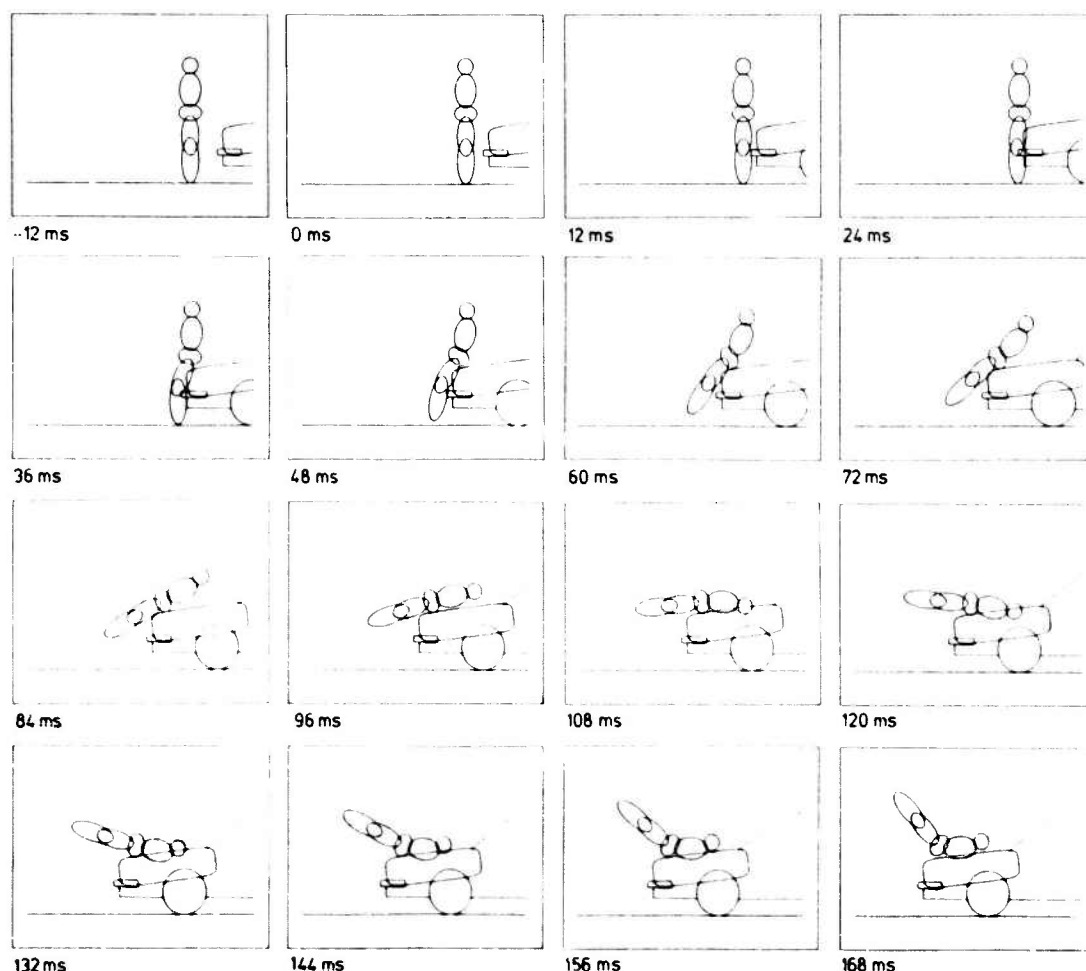


Figure 9 Mathematical simulation of a Part 572 dummy impacted at the side by the vehicle front of an Audi 100 (impact velocity 40 km/h).



## SIMULATION OF PEDESTRIAN COLLISIONS

Since the end of 1980 three research institutes: Bundesanstalt für Strassenwesen (BASt), Organisme National de Sécurité Routière (ONSER) and the Research Institute for Road Vehicles (TNO) have cooperated in the field of pedestrian safety. The aim of this study is to propose a standardized test methodology that can be applied to pedestrian safety tests carried out for research purposes or for compliance testing of passenger cars.

As a part of this project a relatively simple pedestrian-model has recently been formulated with the MADYMO package. The model is two-dimensional and has 5 segments: one for the head, two for the torso, one for the upper legs and one for the lower legs. A new contact model was developed for the simulation of the interaction between pedestrian and vehicle. The external geometries of pedestrian and vehicle are simulated in this model by hyperellipses. Such hyperellipses are particularly attractive, for the representation of the car and bumper geometry, since vehicle edges can quite well be approximated.

The example presented here is a Part 572 50th percentile male dummy impacted by a vehicle of the type Audi 100. The impact velocity is 40 km/h. Since accident analyses show that pedestrians are mostly impacted at their side by the vehicle front, the mathematical model was applied for this situation. In the primary phase of this project no stiffness measurements at the car front were planned, so these model parameters had to be estimated from data in literature.

Model predictions were compared with three experimental pedestrian collisions conducted by BASt with an Audi 100 vehicle. This experiment was not a pure lateral impact since the dummy was slightly rotated in order to avoid a direct impact on the dummy shoulder-arm assembly. Fig. 9 illustrates the kinematics predicted by the model. The impact point of the head on the hood was found to differ 0.15 m from the experimental results. The resultant pelvis, head and chest accelerations for both the model and the experiments (corridor of three experiments) are presented in Fig. 10. In spite of the fact that hood and bumper stiffnesses were estimated for this simulation, model results appear to be quite encouraging.

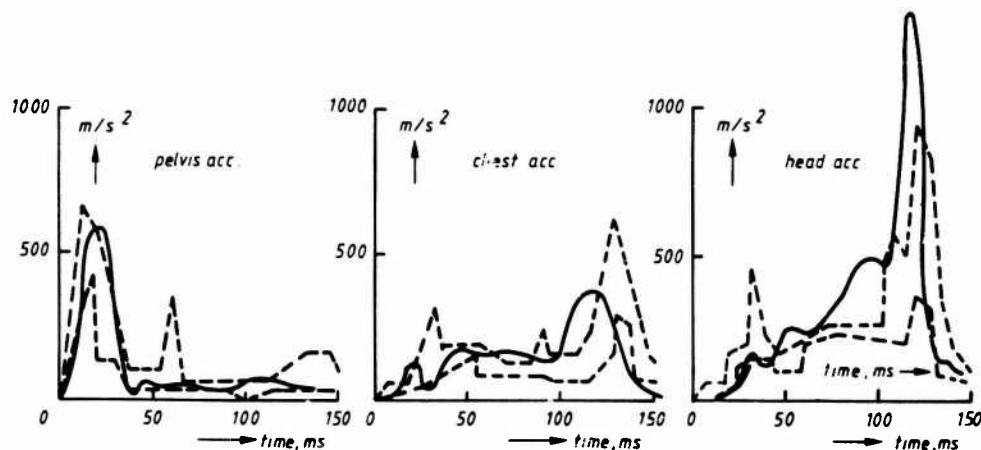


Figure 10 Comparison of model predictions (—) with experimental results (corridor of three experiments denoted by - - - -) of a Part 572 dummy impacted by an Audi 100 (impact velocity 40 km/h).

In the next phase of the project, simulations for different car types and impact velocities are planned. In addition to dummy experiments, cadaver experiments conducted by ONSER will also be simulated. Further it will be analysed to what extent more complex models like a 15 segment 2D model or a 15 segment 3D model can contribute to the improvement of the reliability of the simulation.

## DESIGN OF A DYNAMICAL ACTING CHILD RESTRAINT SEAT

A new concept of a child restraint system was designed and optimized with MADYMO (9). This system features a moving impact shield, which is horizontal during normal use and which pivots upwards during a frontal collision to restrict the forward motion of the child's head and thorax (Fig. 11). The 2D option of MADYMO was firstly used to design and optimize the actuating mechanism for the shield and secondly to optimize the performance of the whole system in a standard ECE 44 50 km/h sled test with a 3-year old child dummy. The shield actuating mechanism consists of a lever arm on the pivoting shield to which a rod with a mass is connected. During the car crash the shield moves into an upright position due to deceleration forces acting on the mass. The downward motion of the shield caused by loadings from head of chest is prevented by a locking device.

Some provisional parameters for this actuating mechanism were selected based on global calculations and engineering judgement. These values were used to formulate a computer model with a linkage of three rigid elements. One element represents the seat shell in interaction with the car seat and car lap belt,

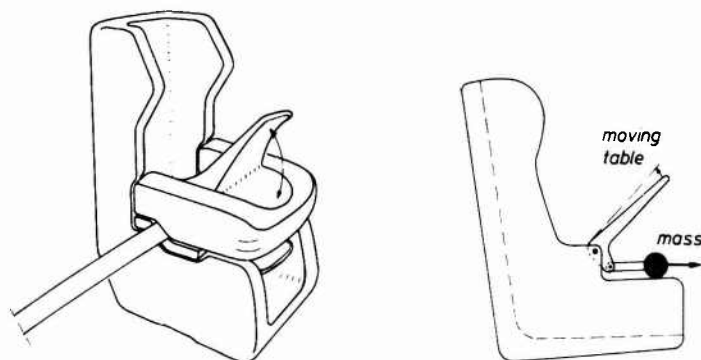


Figure 11 Child restraint system with dynamic acting impact shield.

the other two elements are presenting the pivoting shield with lever arm and the connecting rod with actuating mass. The input for this model was the acceleration-time curve of the ECE 44 sled test.

The first model runs showed that the basic concept could work, the shield could be up and locked within the first 40 milliseconds of the crash. Based on these encouraging results a prototype seat was built and tested without a dummy on the deceleration sled. The model was validated to these tests and was then run for several times with successive changes in the actuating mass, the lever arm length, the mass and moment of inertia of the shield and the belt attachments. The effects of these changes were analysed and finally lead to an optimal and practical combination of the design parameters.

A second prototype based on the above design recommendations was built and tested on the sled, now with the 3-year old dummy in it. This test showed interference of the dummy chest with the moving shield, so that further upward motion of the shield was prevented. Owing to this a next optimization step of the system was required. Therefore the three element model of the seat was completed with a nine element model representing the 3-year old child dummy. An example of the kinematics, predicted by this model is shown in Fig. 12. Special attention was given in this model to the description of the pelvis and chest contacts. Several calculations together with only a limited number of sled tests, finally lead to an optimized child restraint system, which is commercially available today.

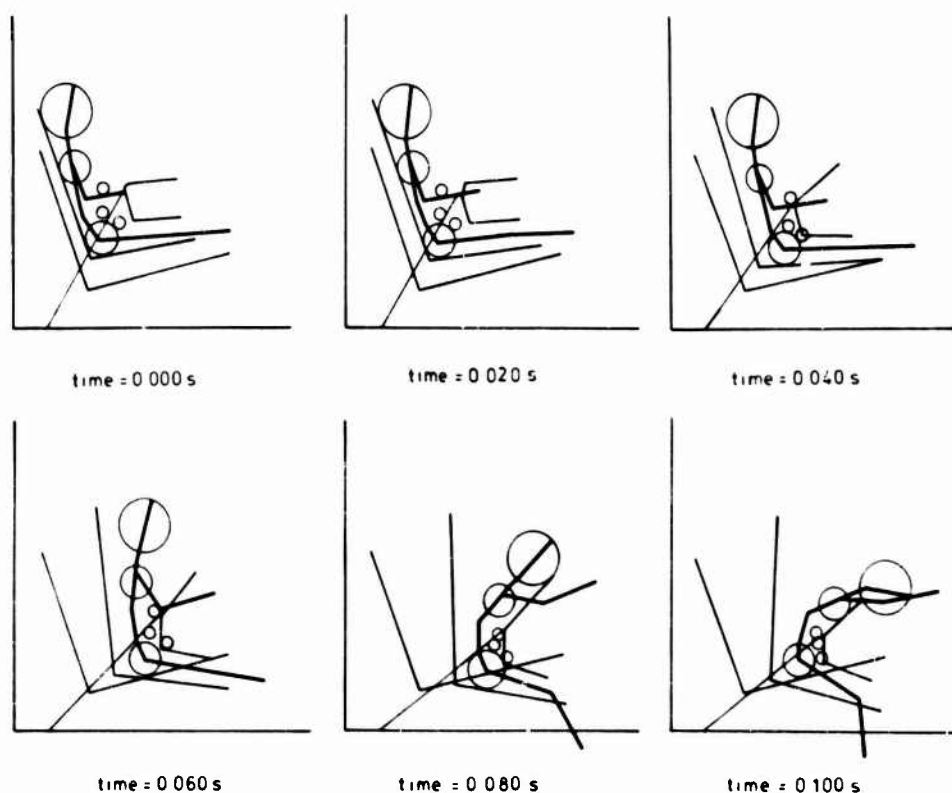


Figure 12 Kinematics of restraint system with dummy for one of the optimization simulations.

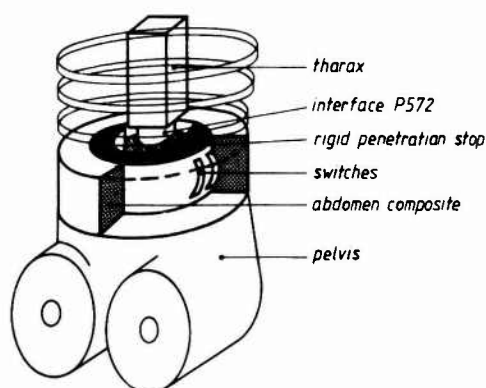


Figure 13 Principle of abdomen section.

#### DESIGN OF A DUMMY ABDOMEN SECTION FOR SIDE IMPACTS

A dummy abdomen for injury detection in side impacts was developed at our laboratory (10). The principle of this design is a rigid drum placed at the critical penetration tolerance level around the lumbar spine, with pressure-threshold contact switches on its surface. This drum is covered by a composite material which should have a dynamic stiffness identical to the human abdomen (Fig. 13). At first the materials urethane and rubber closed-cell foam were chosen because of their expected resemblance to abdominal tissue. After a number of high velocity (6.3 m/s) impacts it was found that none of these materials was able to give responses in the design corridor shown in Fig. 14. This corridor was established from cadaver tests (11).

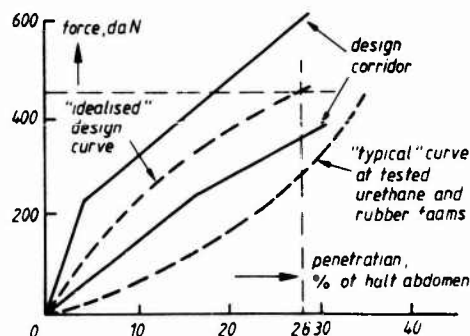


Figure 14 Design corridor for abdomen material.

The solution was to make the outside layer of the abdomen of a relative heavy but flexible material, which is rubber filled with small lead pellets. This mass would initially cause a higher impact force due to its inertia. To avoid the making and testing of a large number of specimens necessary to obtain the correct response empirically, it was decided to use computer simulations to find the design parameters. The MADYMO program package was utilized to formulate a dynamical non-linear finite segment model for 2D impact simulation of the cross section through a half abdomen (Fig. 15).

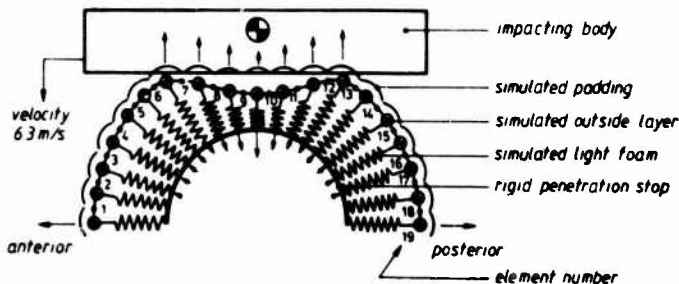


Figure 15 Mathematical model of abdomen.

The heavy rubber-lead outside layer was simulated by an arched chain of 19 rigid joint connected mass-carrying elements. The light underlayer of foam was modelled by 19 massless elements with elastic and damping properties, which transfer the load from the outside elements to the rigid spine connected drum. The impacting body (a rigid arm rest) was a single mass system with a flat contacting plane that could penetrate any of the 19 contact sensing circles attached to the mass carrying elements. These contact sensing circles simulated the outside flexibility of the mass carrying layer. Elastic and damping forces are generated between impacting body and elements as a function of relative penetration and velocity.

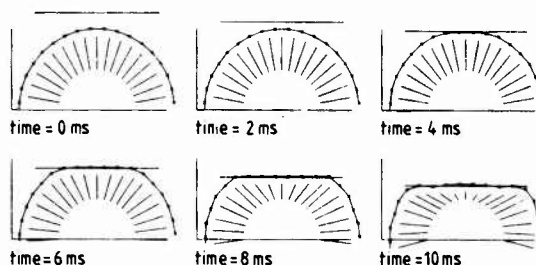


Figure 16 Kinematical response of abdomen model.

This model was exercised with a wide variety of mass distributions and for different impact velocities (Figs. 16 and 17). A few specimens of the most promising combinations were made and tested and were used for validation of the model.

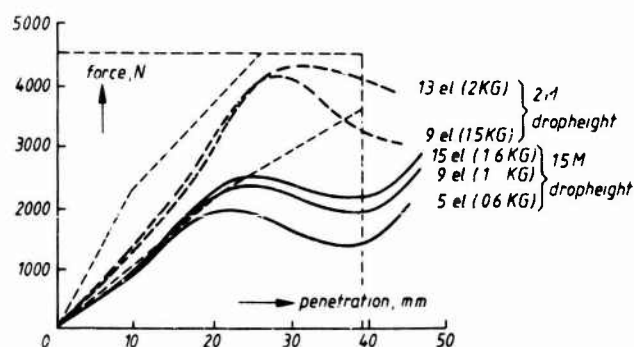


Figure 17 Model response for different mass and impact velocity (drop height).

A prototype abdomen section was build based on the optimal parameters found with the simulation model (Fig. 18) and is now tested in several laboratories in Europe and in the USA.



Figure 18 Prototype of dummy abdomen section for side impacts.

## DISCUSSION AND CONCLUSIONS

Mathematical simulation of the highly complicated gross motion of the human body in an impact environment has gained increasing importance in the past years. One of the computer packages now available for this type of simulation is MADYMO, a general purpose package developed at the Research Institute for Road Vehicles TNO, Delft, The Netherlands. The main features of this package can be summarized as follows:

- a compact FORTRAN source which can be implemented on small computer systems
- a 2D and 3D option
- a variable number of linkage systems
- in each linkage system a variable number of elements
- a set of standard force interaction routines
- easy incorporation of user defined subroutines for specific force interactions and printed and graphic output of calculated data.

Owing to these properties the package is rather flexible with respect to its applicability. This was illustrated in the preceding sections by a number of examples from the discipline of automotive safety. In four of these examples the 2D option was used:

- the behaviour of a child in a child seat
- a pedestrian-car collision
- computer aided design of a new type of child restraint system
- computer aided design of a dummy abdomen prototype.

These model simulations were conducted in close conjunction with experimental evaluations in order to enable judgement of the reliability of the predictive function of these models. It was shown that in most of these simulations the agreement between model and reality was good, which indicates that for this type of applications MADYMO can be a very useful evaluation tool.

Two examples of simulations with the 3D option of MADYMO were presented:

- a rigid wall sled test with the Part 572 male dummy
- a lateral vehicle collision with the Part 572 male dummy as a car occupant.

Both simulations gave a valuable insight in the complex dummy behaviour in side impacts. The highly sophisticated 3D graphic package which was used here to visualize the complex occupant kinematics appeared to be of invaluable importance in these studies.

Most of the simulations presented here were dealing with mathematical models of dummies. In fact data sets presently are available of the Part 572 male dummy (2D and 3D), the APROD 80 dummy (2D), the Part 572 3-year old child dummy (2D), the TNO adult dummy (2D) and the TNO 3-year old child dummy (2D). New data sets are currently being prepared for a dummy representing a 6 year old child and various new side impact dummies. Development and application of mathematical models in the field of automotive safety is a continuous activity in our laboratory. Several programs on further improvement of the MADYMO package are presently being conducted or planned for the near future. Among these are improvements in 3-D joint models, development of hyperellipsoid contact models and a more advanced description of the friction phenomenon.

The application of MADYMO as a computer aided design tool was clearly demonstrated in this presentation. This design approach allows the most important performance parameters to be separated from the lesser important parameters so that the final design can be obtained in a far shorter time than by previous methods of design-prototype test, redesign, retest of prototype etc. Although the examples discussed here all were concerned with automotive safety it is expected, that the MADYMO program package successfully can be applied in other disciplines including the aircraft environment, due to the flexibility of the package and on the basis of experiences of other investigators with similar program packages (3) (4). In fact MADYMO can be used for the analysis of all systems that can be represented by one or more chains of connected rigid bodies undergoing large displacements.

## REFERENCES

1. Robbins, D.H.: "Simulation of human body response to crash loads". In: Shock and vibration computer programs. Monograph No. SVM-10, Shock and Vibration Computer Center, U.S. Dept. of Defense, 1975.
2. King, A.I. and Chou, C.C.: "Mathematical modelling, simulation and experimental testing of biomechanical system crash response". J. Biomechanics, Vol. 9 pp 301-317, 1976.
3. Kaleps, Ints: "Prediction of whole-body response to impact forces in flight environments". AGARD conference proceedings no. 253, Paris, 1978.
4. Laananen, D.H.: "Human body simulations for analysis of aircraft crash survivability". Proceedings of the 5th IRCOB conference on the Biomechanics of Impacts. Birmingham, 1980.
5. Maltha, J. and Wismans, J.: "MADYMO - Crash Victim Simulations, A computerized research and design tool". Proceedings of the 5th IRCOB conference on the Biomechanics of Impacts. Birmingham, 1980.
6. Wismans, J., Maltha, J., Melvin, J.W. and Stalnaker, R.L.: "Child Restraint Evaluation by Experimental and Mathematical Simulation". 23rd Stepp Car Crash Conference, San Diego, 1979.

7. Stalnaker, R.L., Tarrière, C., Fayon, A., Walfisch, G., Got, C., Balthazard, M., Masset, J. and Patel, A.: "Modification of Part 572 dummy for lateral impact according to biomechanical data". 23rd Stapp Car Crash Conference, San Diego, 1979.
8. Wismans, J. and Maltha, J.: "Application of a three-dimensional mathematical occupant model for the evaluation of side impacts". Proceedings of the 6th IRCOB conference of the Biomechanics of Impacts. Salon de Provence, 1981.
9. Stalnaker, R.L. and Maltha, J.: "MADYMO used for computer aided design of a dynamic acting child restraint seat". Proceedings of the 5th IRCOB conference on the Biomechanics of Impacts, Birmingham, 1980.
10. Maltha, J. and Stalnaker, R.L.: "Development of a dummy abdomen capable of injury detection in side impacts". 25th Stapp Car Crash Conference, San Francisco, 1981.
11. Walfisch, G., Fayon, A., Tarrière, C. and Rosey, J.P.: "Designing of an Abdomen for Detecting Injuries in Side Impact Collisions". Proceedings of the 5th International IRCOB conference on the Biomechanics of Impacts". Birmingham, 1980. Secretariate 109 Ave. Salvador Allende, 69500 Bron, France.

#### ACKNOWLEDGEMENTS

The authors wholeheartedly thank Mr. L. Wittebrood for his efforts in running and further improvement of the MADYMO package.

## DISCUSSION

## UNIDENTIFIED QUESTIONER:

First, I would like to congratulate you on a very fine presentation. What computers can be used with Madymo?

## AUTHOR'S REPLY

Madymo can be implemented on all computer systems with a standard Fortran IV compiler. We have experience with Madymo on large computers (Cyber), mini computers (PDP II), and also on micro systems.

## UNIDENTIFIED QUESTIONER:

Is Madymo available for other laboratories and if so, what is the price?

## AUTHOR'S REPLY

Madymo is available for other laboratories. The price for a license contract is dependent on what options are required and on the amount of assistance needed. The price will vary roughly between \$5000 and \$10000.

## DR. KNAPP (USA)

From the simulations presented on the child restraint seat it appeared that the mass-actuated shield made contact with the child's head. Does it? Can the shield cause facial injury?

## AUTHOR'S REPLY

Yes, the head of the child (in the simulation a 3-year, TNO P3 child dummy) does hit the shield, but due to the relatively compliant (soft) tip of the erected shield, the head accelerations are within the tolerance limits for brain or skull injury. What this means for facial injury (for which tolerance levels are expected to be lower for adults) we don't know. However, we have to realize that the 50 km/h ECE 44 sled test conditions are representing worst case conditions, so we are quite confident that facial injury will not occur in real-world crashes. This statement is more or less confirmed by field accident data on fixed-shield systems which have the same injury producing potential.

## UNIDENTIFIED QUESTIONER:

When you speak of ellipses, are these real ellipses or degenerated ellipses?

## AUTHOR'S REPLY

They are high-degree ellipses. It's a normal ellipse in case of two-dimensional simulation, with a high-degree up to 20 eccentricity. The three-dimensional simulation, with a high-degree ellipse, is done in the same manner.

## ADVANCED RESTRAINT SYSTEM CONCEPTS

Reidelbach, W.  
Scholz, H.  
Daimler-Benz AG, 7032 Sindelfingen / Germany

## SUMMARY

Today's lap/shoulder belts with emergency locking retractors provide improvements (automatic belt length adjustment, convenience, and comfort), but also disadvantages (greater webbing elongation and spool-out effect). Compensation of these deficiencies can be achieved by the use of pretensioners, the specifications and possible designs of which will be explained.

The Mercedes-Benz passive restraint system consists of air bags deployed by means of solid propellant gas generators and kneebolsters. The sensor is designed to detect low and high impact severity levels. In a low level impact one of the passenger side generators is triggered, and the second passenger generator only in case of a higher level impact together with or after the driver side generator.

To balance the specific limitations of belt or air bag performances, combined systems have been studied, such as an air bag/knee bolster system with supplementary belt or modern lap/shoulder belt systems, supplemented by an air bag in the steering wheel and a pretensioner for the passenger belt, both of which are designed to prevent head/face impact.

## REVIEW OF SEAT BELT DESIGN

The first seat belts in mass production motor vehicles were modified air craft passenger lap belts offered as an option in the early 50s. A few years later diagonal belts and combined lap/shoulder belts were introduced. In the 60s belt retractors were added to the restraint assembly to provide proper stowage of an unbuckled belt and freedom of movement to the car occupants during normal riding as well as full restraint in case of emergency. Then an intensive development was started aiming at ease of use, wearing comfort, and integrated design of a factory installed belt assembly.

Today the integrated 3-point (lap/shoulder) safety belt with emergency locking retractor (ELR) is standard equipment in all new passenger cars. Fig. 1 shows the actual Mercedes-Benz 3-point belt assembly composed of the seat frame-mounted buckle, the continuous loop belt webbing, and the retractor behind the B-pillar cover. The ELR is located inside of the B-pillar (Fig. 2) and thus protected against dirt and mechanical damage.

## THE PROBLEM OF INDIRECT BELT SLACK

A major task still is the elimination of belt slack. In this respect the manual belt length adjuster of static belts is optimal as it is mechanically simple and lightweight. But since people don't like to be tightly restrained, they refuse to properly adjust static belts. The retractor belt, in principle, provides for automatic length adjustment without slack. But it has one basic deficiency: when crash loaded not only the webbing on the occupant's body is elongated but also the webbing portion between sash guide and retractor. Furthermore the portion which normally is rather loosely wound up on the retractor reel must first be drawn tight around the locked reel before a restraint force can develop. This "spool-out" and additional elongation results in some 10 to 20 cm of webbing running out of the sash guide which means an equivalent additional forward displacement of the occupant's shoulders and head, and consequently an additional injury risk.

## THE SEAT BELT PRETENSIONER

To avoid this, a pretensioner should be added which retracts a certain length of webbing during the first few milliseconds of a crash to compensate for the "spool-out". A pretensioner assembly consists of a crash sensor and a propulsion unit, such as a gas generator, both known from air bag technology.

The mechanism can work longitudinally as was shown with the Mercedes-Benz Experimental Safety Vehicle in 1973 (Fig. 3, pretensioners installed vertically in the mid door pillar, or horizontally along the upper edge of the rear seat back). Another design applies a rapid backward rotation of the retractor reel by means of a pelton turbine wheel driven by water which is propelled towards the wheel by a gas generator as mentioned above (Fig. 4). The basic design specifications are as follows:

Total actuation time period	25 ms	temperature range	- 35 ... + 95° C
sensor reaction time	10 ... 13 ms	reliability	99.9 %
tensioning time	10 ... 12 ms	max. webbing length retracted	280 mm
		max. retraction force	3.500 N

The sensor must react within tolerated time limits when subjected to a standardized sine-wave-like acceleration impulse of about 30 g peak value and about 75 to 80 ms duration. The whole system has to survive severe environmental simulation such as vibration, mechanical shock (pot-holes, curb stones), thermal load, humidity, corrosion. A permanent auto-



matic control (self-monitoring) of all electric circuitry during car operation is provided.

Prototype testing has shown the results displayed in Fig. 5. The accelerations measured on passenger dummies are reduced on the head by 57 %  
on the chest by 16 %  
compared to measurements from testing of usual standard retractor belts. The prevailing effect is the elimination of head contact of the passenger dummy with the dashboard which can still occur at higher impact speeds even though a standard belt is worn. Road accident experience indicates that such contact of a belt restrained passenger, due to already reduced impact energy, does not present severe injury potential but can cause disfiguring lesions which of course should be prevented.

#### AN IMPROVED DRIVER RESTRAINT SYSTEM

The driver is in a particularly difficult situation because his distance to the steering wheel is less than that between passenger and dashboard, and the belt pretensioner may not sufficiently reduce the severity of his head impact with the wheel. Therefore we consider an air bag in the steering wheel as an appropriate supplement to a conventional automatic 3-point belt (Fig. 6), intended to avoid facial injuries, whereas the belt assembly provides the overall protective function in all crash modes. This combined system described in section C takes advantage of the air bag technology which was initiated by the US passive restraint requirement, but which can now also be utilized to improve active restraints.

#### THE MERCEDES-BENZ AIR BAG RESTRAINT SYSTEM

In order to be able to comply with the requirements of former US passive restraint standards, we at Daimler-Benz have developed air bag restraint systems. As early as 1966, we started air bag deployment tests using liquified or pressurized gas as a deployment agent. But the bulky and cumbersome devices available at this time were impracticable for installation in passenger cars, and it was difficult to monitor the operational readiness of the systems and to reduce temperature sensitivity and deployment noise.

In 1970 we therefore turned to an entirely new technology of bag deployment and started the development of a solid propellant gas generator which could be packaged into the hub of the Mercedes-Benz steering wheel without sacrificing the protective function of the energy-absorbing elements of the wheel.

#### AIR BAG AND KNEEBOLSTER

The actual occupant restraining elements of the system are air bags and kneebolsters. The bag on the right front passenger side has a 150 liter volume (Fig. 7), the bag on the driver side a 60 liter volume (Fig. 8). This bag is provided with restraint bands sewn to the inside to control longitudinal expansion and intended to minimize cushion to face contact. Each bag has exhaust vents, providing for a relatively soft and uniform occupant ride-down. The air bag material is Nylon coated with Neoprene.

In addition to the upper torso protection, offered by the two air bags, the Mercedes-Benz system utilizes kneebolsters (Fig. 9) to prevent submarining and to limit the impact loads on the lower extremities. The deformation distance available in our vehicles for this lower torso ride-down is limited to approximately 140 mm in order to maintain seating comfort and leg room. Using a steel tube of circular shape with 145 mm diameter and 0.4 mm sheet thickness the actual peak loads are about 6.000 N which is well below the tolerated value.

#### SOLID PROPELLANT GAS GENERATOR

The compact solid propellant gas generator (Fig. 10) is a steel container 110 mm in diameter and 54 mm height, capable of storing 100 grams of solid propellant needed as the deployment agent for the driver air bag. Two such generators are incorporated in the passenger air bag unit (Fig. 11). The propellant is ignited by an electrical squib fired by an electronic sensor. Gas flowing from the generator does not directly enter into the bag but is filtered out by multi-layer metallic screens.

In addition to dimensional advantages, the solid propellant generator has other advantages as well, such as:

low weight, approximately 1.2 ... 1.3 kg

short inflation time, 25 ms driver / 30 ms passenger

consistency of inflation time. Because of high ignition temperatures, the bag deployment time is not significantly affected by ambient temperatures. Even at minus 40° C, it increases by only 5 ms.

low noise levels, due to flatter pressure increase in the combustion chamber in comparison to Hybrid systems.

greater degree of deployment flexibility. Depending on the array of gas generators used, it is possible to have the bag deployed to an extent determined by the degree of severity of the impact. This kind of incremental deployment controlled by a multi-level sensor is advantageous in low speed impacts and in case of the standing child and the out of position passenger. It also results in a reduction of noise levels.

## ELECTRONIC SENSOR

To trigger the system, we have selected an electronic solid state acceleration sensor designed by Robert Bosch GmbH (Fig. 12). The prime function of the sensor is to rapidly detect an impact and provide the triggering signals to the generator squibs, which in turn fire the propellant. The functional principle is as follows (Fig. 13):

The vehicle acceleration versus time function is integrated during the impact sequence.

In order to avoid inadvertent deployment when the vehicle is in normal operation, the integration process only begins if the acceleration exceeds a minimum threshold  $a_1 = -4 \text{ g}$ .

When the vehicle structure, and specifically the sensor location area, is subjected to heavy shock or high frequency acceleration, the sensor cuts off acceleration peaks beyond a negative limit value  $a_2 = -40 \text{ g}$  and a positive value  $a_3 = 95 \text{ g}$  thus avoiding deployment due to driving over pot-holes and curb stones, or being struck by a hammer or projectile.

If the result of the integration process in the sensor remains below a first threshold  $S_1$ , no bag deployment is initiated. This threshold corresponds to 18 km/h rigid barrier impact speed (BS). If the integration result exceeds this first threshold, but remains below a second limit, only the first increment of the passenger air bag is deployed, being suitable for passenger ride-down from up to 25 km/h BS. The driver in this speed range is securely restrained by the energy absorbing steering wheel and the kneebolster.

If the integration result exceeds the second limit value  $S_2$ , the second increment of the passenger bag and the driver bag are ignited, providing protection up to and beyond 50 km/h BS.

In order to avoid inadvertent deployment due to power surge, whether caused by on-board equipment or high-frequency stray signals, the total electronic sensor system, including ignition cables, is shielded. Extensive testing was conducted to determine surges across the input and output terminals and to design additional shielding circuitry.

The sensor is also responsible for monitoring and registering system readiness. As long as the proper current is passing through the sensor, the system will be constantly monitored at 15 mA for current disconnects and short circuits with any deviation being indicated on the dashboard mounted control lamp.

After an accident has occurred it is possible to determine, by checking registration elements such as safety fuses, the sequence of events (deployment before or after impact). In addition, a coulomb-cell registers the duration of an eventual sensor fail period.

## COMBINED RESTRAINT SYSTEMS

The restraint systems described have certain performance limitations: The conventional lap/shoulder belt, though basically appropriate in all crash modes, can not prevent head impact to dashboard or steering wheel in severe accidents. The air bag/knee bolster system, though very efficient in frontal crashes, can not protect in lateral impacts or rollovers and only to a limited extent in multiple-impact accidents. Obviously a combination of both systems can offer an improved restraint. Then two different designs are to be considered and have been developed.

### THE PASSIVE AIR BAG WITH SUPPLEMENTARY SEAT BELT

An air bag with knee bolster, both designed to meet the passive restraint requirement, i.e. to assure full frontal crash protection without any additional element, have to absorb the kinetic energy of a car occupant at tolerable force levels during the crash event.

An appended seat belt, which we consider indispensable for other than frontal impacts, will also absorb energy and exert additional forces on the occupant. The additional restraining forces from the belt together with those from the bag will be above the "air bag only" forces but can be very close to them, if the belt is "soft", be it due to high elongation webbing or force limiting devices. Actually the selection of the most favourable belt elongation is difficult due to American or European seat belt regulations.

### THE ACTIVE LAP/SHOULDER BELT WITH SUPPLEMENTARY AIR BAG OR PRETENSIONER

If a conventional lap/shoulder belt is the primary element of the restraint providing the basic restraining forces - then only additional head protection is needed. The best supplement to serve this purpose is for the driver an air bag in the steering wheel, for the front passenger a belt pretensioner, as already described.

The wheel bag for this specific application has to be designed to attenuate only the impact of a small mass, the head, instead of the occupant's whole upper torso. So, in this case the bag has to be "soft" which is simply achieved by enlarging the vent diameter. This improved restraint system is actually offered as an option on all Mercedes-Benz passenger cars. Fig. 14 shows typical results of 50 km/h frontal impact tests run on an accel-

erator sled facility using 50 % Part 572 dummies to measure the usual injury risk parameters such as HIC (head injury criterion, computed from the head acceleration versus time function) and maximum resultant chest acceleration. Obviously the restraint system configuration has only minor influence on the chest loading which in all cases remains below the tolerable value. HIC however though also below critical values, reacts more sensitively to system modifications. So, optimization primarily will be based on HIC values. Up to now the best combinations of driver air bags (either designed to meet FMVSS 208 or to support lap/shoulder belt performance) and type 2 seat belts are achieved using high elongation belt webbing not in compliance with current seat belt regulations which therefore should be amended. For the passenger a pretensioned lap/shoulder belt would eliminate head contact with the dashboard and is able to provide protection equivalent to that of the different driver restraint systems.



Fig. 1 - Integrated 3-point safety belt with ELR, Mercedes-Benz 280 E



Fig. 2 - Belt retractor installation in mid door pillar

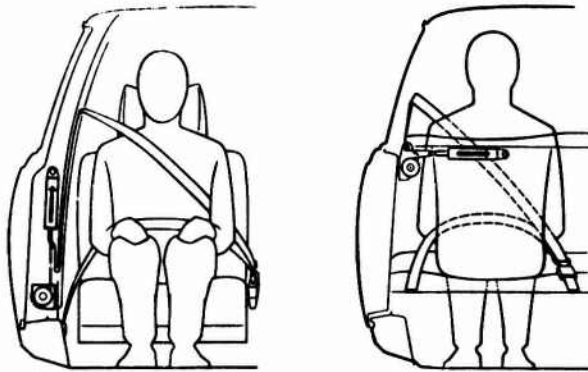


Fig. 3 - 3-point safety belt with longitudinal pretensioner, Mercedes-Benz ESV 22

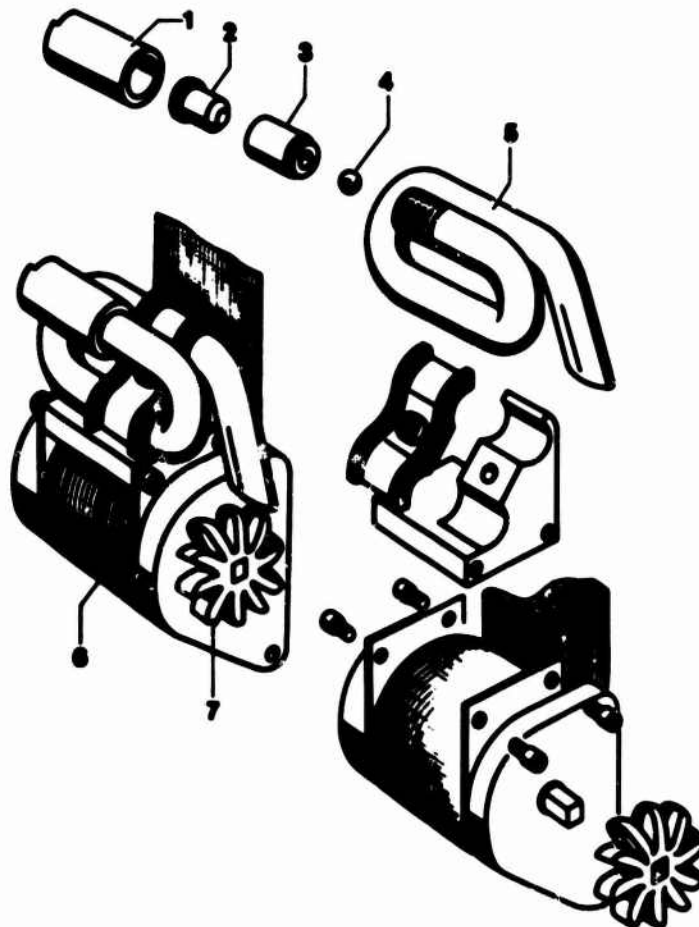


Fig. 4 - Pretensioner assembly added on a standard ELR

- 1 clamping nut
- 2 solid propellant capsule
- 3 gas generator housing
- 4 flying piston
- 5 fluid filled tube
- 6 emergency locking retractor
- 7 turbine wheel

## 50km/h Frontal Fixed Barrier Impact

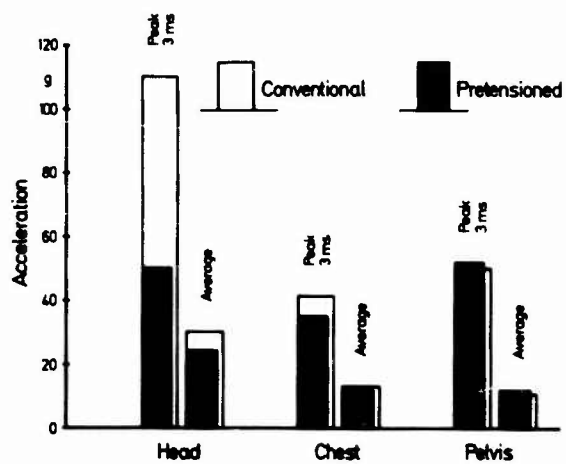


Fig. 5 - Accelerations of dummies restrained by conventional and pretensioned 3-point belts



Fig. 6 - 3-point belt with ELR and steering wheel air bag



Fig. 7 - Passenger air bag

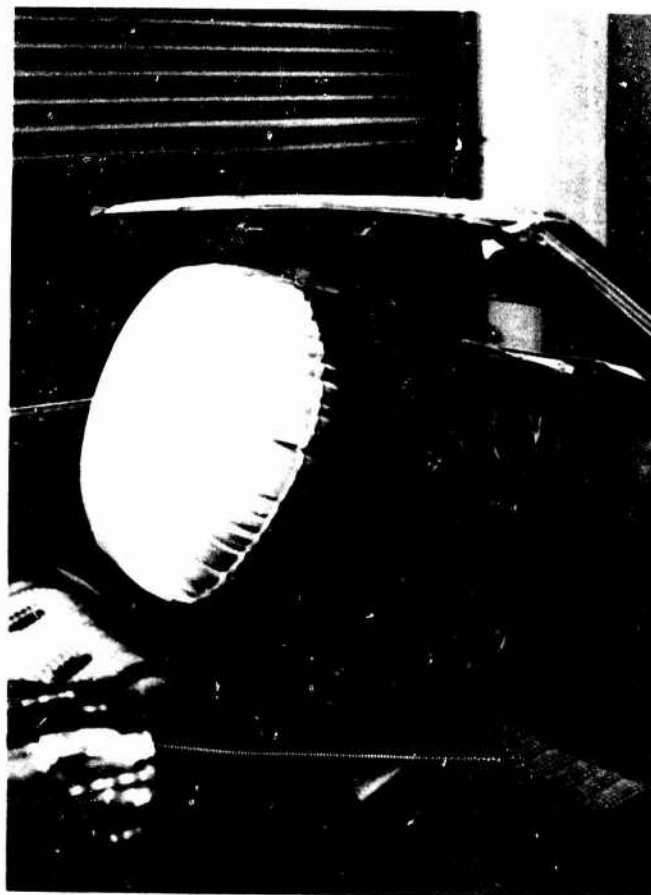


Fig. 8 - Driver air bag



EA 78 75 40

Fig. 9 - Kneebolster, part of Mercedes-Benz passive restraint system

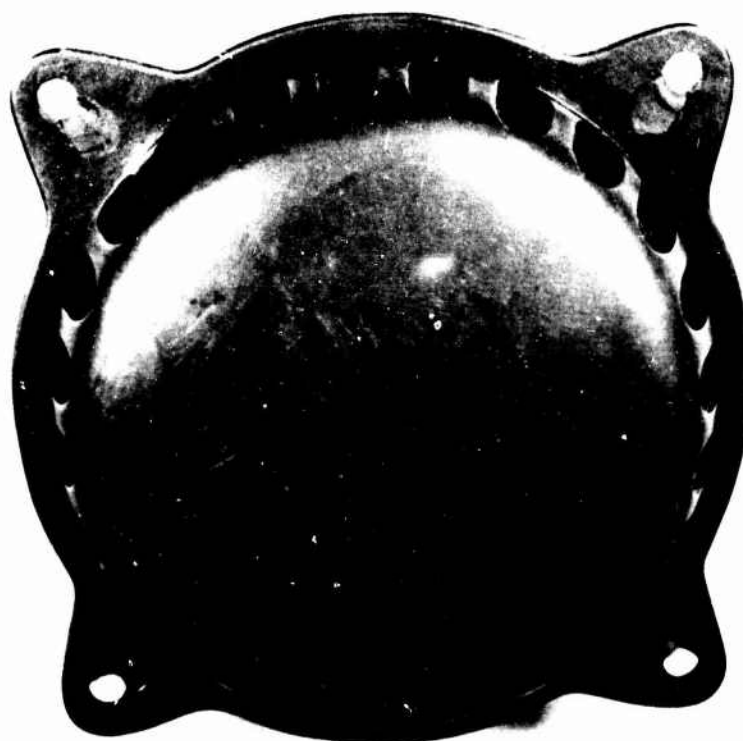
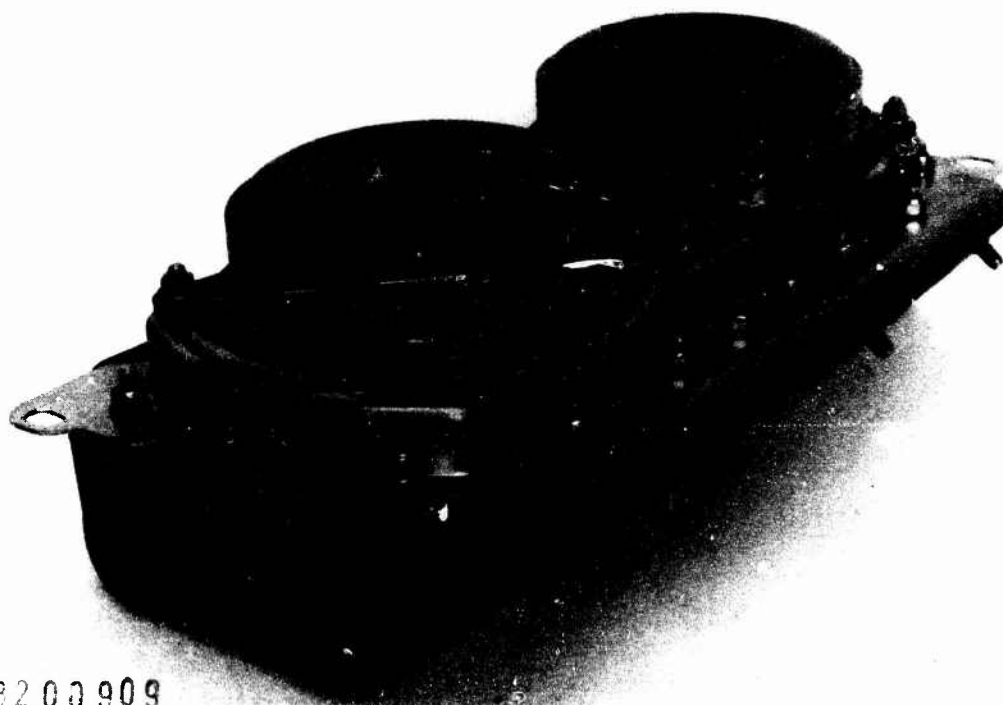


Fig. 10 - Solid propellant gas generator





14.9200909

Fig. 11 - Passenger air bag unit



Fig. 12 - Electronic sensor

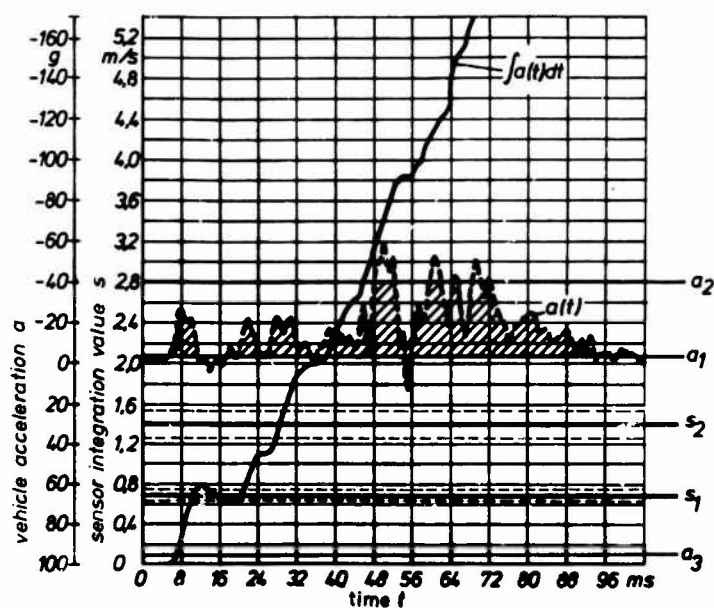


Fig. 13 - Mode of sensor operation

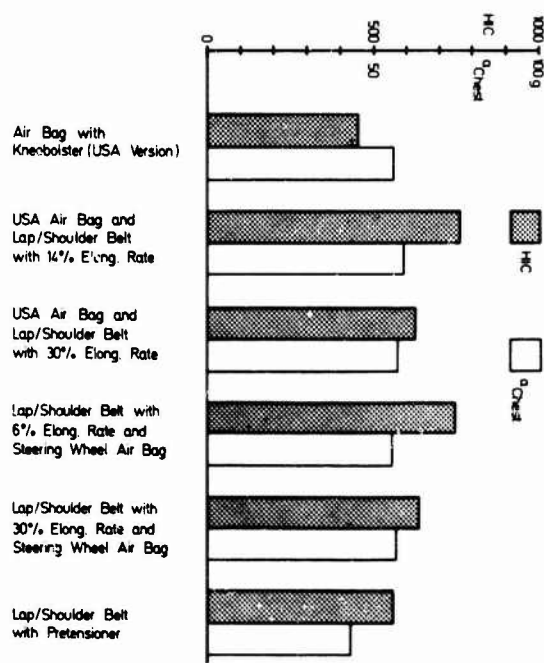


Fig. 14 - Injury risk parameters of different occupant restraint systems

## DISCUSSION

UNIDENTIFIED QUESTIONER

Will the pressure increase in the car's interior using air bag inflation create an injury potential?

AUTHOR'S REPLY

No problems.

MILLER (UK)

Does inadvertant operation induce loss of control?

AUTHOR'S REPLY

Tests indicate no loss of control.

MILLER (UK)

Does airbag impede egress (post crash)?

AUTHOR'S REPLY

Airbag is deflated in 1 second after crash.

SHULMAN (USA)

Will there be a problem of loss of the fluid in the retractor since it must remain in the device (without leakage) for many years?

AUTHOR'S REPLY

We have not experienced and do not expect any loss of fluid. The sealing is very reliable (soldered membrane).

FRISCH (USA)

Do you see any reason why a system such as you described for airbag deployment could not be expanded to include sequencing of longer duration to cover multiple impact cases. This also would imply that the crash sensor would have to work on several occasions. Does protection of this sensor pose a problem?

AUTHOR'S REPLY

In principle, long duration sequencing appears to be feasible. Adding output terminals to and protecting the sensor are the minor problems. The big problem is the need to add a full set of gas generators for each subsequent impact to be covered which in turn presumes that sufficient additional space in specific locations (steering wheel hub) is available which is not the case. Also weight is critical.

DAY (CN)

I am not certain that comfort of the occupant would be significantly reduced by the use of a lap retractor in place of a shoulder retractor. Do you have any comments on this?

AUTHOR'S REPLY

The main comfort feature of retractor belts is the forward torso mobility which enables the car occupant to change seating position, relax muscle-strain, or reach out to the glove compartment, for instance. In case of a lap retractor, any forward motion of the torso leads to sliding of belt webbing across the lap, through the buckle D-ring and across the chest with considerable subsequent friction - very uncomfortable! It would cause rejection of belt use which means a higher loss of safety than the larger possible head displacement in case of a shoulder retractor.

DAY (CN)

In connection with your comment on the improbability of a 25 cm belt slack condition, I would like to point out that many North American automobiles utilize restraint systems with locking mechanisms which defeat the normal retractor operation, allowing any amount of belt slack.

AUTHOR'S REPLY

In case of the belt/retractor design mentioned, large slack is possible. Meanwhile, I believe these designs have been abandoned and are not and will not be installed any more.

D26-2

DESJARDINS (USA)

Have you considered the injury potential of the pretensioning force and retraction rate in the case where the occupant is leaning forward when the pretensioner is activated?

AUTHOR'S REPLY

We have asked volunteers to lean forward and then ignited the system; the reaction does not cause backward motion. The occupant stays where he is; he realizes an increased tension but he is not thrown backwards. The 3000 newtons are not enough to move the human body and there is no injury potential to our knowledge.

DESJARDINS (USA)

What is the approximate cost of the restraint system options you described for the Mercedes auto?

AUTHOR'S REPLY

Approximately 1500 deutsch marks.

## RECENT IMPROVEMENTS IN CRASH RESTRAINT IN UK HELICOPTERS

by  
 Surgeon Commander A P Steele-Perkins  
 Royal Air Force Institute of Aviation Medicine,  
 Farnborough, Hampshire, UK.

## SUMMARY

There is a continuous programme to improve crashworthiness and comfort both in existing and future helicopters in the UK. The introduction of rigid personal survival packs (PSP) in the seat pan, and methods of increasing their comfort and acceptability to aircrew have been detailed recently<sup>(1)</sup>.

This paper describes improvements in other areas - all important for the successful and safe operation of helicopters. The introduction into the RAF Chinook HC1 of crew seats with energy attenuation has resulted in a major advance in crashworthiness, and the principles of the seat are outlined. Shortcomings in the quick release facilities in passenger restraint harnesses are discussed briefly together with suggested improvements. A seat rotation mechanism with good crashworthy features which can be incorporated into any existing seat system is described, and finally the problems of providing an efficient harness for mobile aircrew are discussed and solutions offered.

## CRASHWORTHY SEAT

The Chinook HC Mk 1 has entered into RAF service. This marks a major advance in crashworthiness as it is the first helicopter in the UK to have energy absorption incorporated into the crew seats. The concept<sup>(2)</sup> includes an adjustment which allows for pilots of different weights. Pre-programming the seat to the desired position selects energy attenuating wires, with load characteristics proportional to the weight of the occupant. This allows a crashworthy seat requiring less "stroking" distance than an non-adjustable system - thus overcoming one of the main problems of retro-fitting seats with energy attenuation mechanisms into existing aircraft and avoiding the need for costly modifications to the cockpit floor. A rearwards facing seat provided for the rear crew members also uses the same principle, but because a greater stroking distance is available the added complexity of the adjustable attenuation is not required.

## PASSENGER HARNESS QUICK RELEASE FACILITIES (QRFs)

An area that has been investigated recently is the efficiency of passenger lap harnesses and their quick release facilities. Although the angles at which the buckle should release are specified in civil regulations<sup>(3)</sup> (between 75 and 95 degrees) this is not the case in either UK<sup>(4)</sup> or US<sup>(5)</sup> military specifications. The release angle is important because, if this is too small, inadvertent release can occur through snagging of clothing, or even body movement. A QRF, manufactured by Aerolex Ltd, overcomes these problems (Fig 1). It is operated by a rotary movement and, in the locked position the release mechanism is positively located and is inertia proof. This device will be assessed in a flight trial shortly to prove the overall acceptability of the concept.

## CRASHWORTHY SEAT ROTATION MECHANISM

There is a requirement to increase the crashworthiness of seats for crew members whose task requires them to sit sideways relative to the aircraft. It is accepted that human tolerance to Gy acceleration is poor, and it is common practice to incorporate a rotating or swivel mechanism, to allow the crew member to sit facing forwards (or preferably aft) for critical periods of the flight. However, this is usually a secondary consideration and either results in an expensive modification to the original seat or in a device with limited crashworthiness. An investigation was therefore initiated at the Royal Air Force Institute of Aviation Medicine (IAM) to assess the feasibility of producing a swivelling mechanism which would:-

- a. be compatible with the existing seat and aircraft fittings;
- b. alter the vertical adjustment of the seat as little as possible;
- c. be inherently crashworthy.

Complying with requirement (a) meant that the mechanism must fit between the existing seat and the seat rails. The resulting design (Figs 2 and 3) uses nylon rollers, of equal diameter and length, with adjacent rollers mounted at right angles to each other, in a circular housing. This ensures a very smooth rotating action and also allows crash loads to be spread evenly throughout the unit. With a suitable lever connected to a spring loaded detent position, the seat can be locked at any desired point. The basic concept can be used to modify any existing seat, and the increase in seat height is only 12 mm.

In one aircraft application the seat rails are mounted at right angles to the fore and aft (X) axis of the aircraft. Theoretically, it was considered that the rotation mechanism should enhance crashworthiness, as the interface with the rails would provide a greater area of contact and thus reduce point loading on the rails. Tests are to be performed shortly on the linear decelerator track at the IAM to confirm the crashworthiness of this system. Meanwhile the seat is now in operational use and is well liked by aircrew.

## HARNESS FOR MOBILE AIRCREW

Mobile aircrewmembers in both fixed and rotary wing military aircraft in the UK have hitherto worn a waist type restraint harness ('despatcher's harness') to prevent them falling out of the aircraft, and to provide restraint following such a fall. Disquiet had been expressed for some time by aeromedical authorities on the inadequacies of a waist harness which, even if correctly adjusted, could cause abdominal injuries in a fall. British Safety Standards<sup>(6)</sup> specify that a harness of this type shall only transmit a force of 5G in

a fall of 1.2 m, because of the risk of injury. The IAM therefore devised and produced a prototype restraint system which was incorporated into the standard lifepreserver (Fig 4). Its main features were a strap sewn round the outside of each arm-hole, with a continuous length of webbing across the back, underneath each arm, and over each shoulder of the lifepreserver. The geometry of the device constituted a self tensioning system which would tighten around the shoulders and distribute the load over the whole of the upper torso. The self tensioning mechanism would not operate under normal conditions because it was fixed by a tack (shear) stitch. After a series of tests, a shear stitch with a breaking strain of 73 kg (160 lb) was used to ensure that too high a load was not imposed on a man of light weight, and that a heavy man would not break the stitch carrying out his normal tasks, and so render the harness unserviceable. Drop tests confirmed that the loading applied in a fall was reduced considerably, and dynamic deceleration tests on the linear decelerator showed that a 15G input deceleration was reduced to 6G on the dummy.

Prior to a service trial, an assessment was made in the Royal Navy underwater escape trainer ('Dunker'). Normally, when suspended in air, the wearer is assured that the quick release mechanism is always in the same position and easily reached. In contrast, when underwater, the body weight is supported, taking the load off the restraining straps, and therefore the quick release mechanism can be in any position - usually behind the back. Emergency disconnections were extremely difficult and in many instances the subject required assistance from the safety divers. The flying trials were accordingly restricted to flights over land in order to gain more information on the general suitability of the harness. On completion of the trial a questionnaire survey revealed another major shortcoming. A mobile crewman in a helicopter, when wishing to look out of the cabin door, adjusts the length of the harness restraining strop until he is aware of the tension in his restraint harness. If the harness is of the waist type, he can flex his upper torso, gain an adequate external view, and still be restrained within the cabin. If he does lose his balance, he falls inside the cabin. However, if he is wearing a harness where the restraining strop is attached to the shoulders, he must have a longer strop length to see out of the cabin, which means that the lower part of his body can fall outside the cabin. Because this type of restraint is associated with a full torso harness or jerkin, any fall probably would not result in an injury, but nevertheless this is not a desirable feature of any harness.

In view of the prolonged and circuitous history of the despatcher harness, a list of design aims was discussed and agreed. The objectives are to ensure:

- a. Minimal interference with flight task. The harness should be designed so that it does not compromise comfort or efficiency of other tasks. When in use it should not impede normal movement.
- b. Good upper body mobility. The restraint point, or restraining strop take off point, should be at the waist.
- c. Ease of donning and doffing. The harness should also be compatible with other equipment assemblies worn.
- d. A single handed emergency release, which must be on the wearer's front, and be capable of easy release when under tension. Inadvertent release should be avoided.
- e. Good restraint following a fall.

Two other major factors must also be considered. A harness for mobile aircrew should not be the primary means of crash restraint within the aircraft; this should be provided by the seat harness. Because of the length of strop normally required to operate at the cabin door, the crewman would be liable to injuries caused by impacts within the aircraft cabin structure - which are not effected by the design of the harness. In effect, the main objective of a "restraint" harness for mobile aircrewmen is to prevent the crew member from falling out of the aircraft.

While the assessments were still in progress, the Chinook HCl helicopter had been introduced into RAF service. The harness provided for the mobile crewman was a full torso system of US design (Fig 5). Quite independently the crewman were concerned that the harness was difficult and slow to don and doff, and that inadvertent release could occur through snagging of the release buckles on the cabin floor when lying prone. Since the Chinook does not operate primarily over water, it was considered that the prototype harness designed by the IAM might be suitable, as the problems associated with under water escape should not occur. The harness (Fig 6) had been modified by:-

- a. using the basic skeleton of the lifepreserver only, i.e. without any flotation or other facilities;
- b. re-routing the straps in order to gain more even spreading of restraint loads over the torso;
- c. dispensing with the tear stitch and re-routing the harness so that the restraint take off point was nearer the waist.

The crewman would still be restrained by the upper torso, and the harness would still tighten under load. This was confirmed in drop tests.

Because of the desirability of having a restraint system that could be used throughout all three Services, it was decided to assess this type against both the torso and the waist belt harness. Major modifications had been carried out to the restraining strop portion of the latter. These were as follows:-

- a. improving the mechanism for length adjustment;
- b. incorporating an improved carabiniere type aircraft attachment hook;
- c. including a force attenuating device in the strop.

These improvements were included in both types of harness to provide a more valid assessment of the modifications proposed. The result of the trials indicated an overwhelming preference for the waist harness (Fig 7). Again, the main reasons quoted for the preference were ease of use, and minimum interference with the flight task.

The following table lists the design aims and performance of each restraint system.

	TORSO	JERKIN	WAIST
Ease of don/doff	poor	fair (1)	good
Emergency release	poor	poor	good
Protection against inadvertent release (2)	fair	good	good
Upper body mobility	fair	poor	good
Compatibility with other equipment assemblies	poor	good	good
Preventing fall from aircraft (3)	fair	fair	good
Restraint following fall from aircraft	good	good	poor (4)

#### Notes:

1. If integrated with lifepreserver don/doff not normally required.
2. Depending on quick release mechanism design.
3. If strop adjusted correctly.
4. Improved if force attenuation mechanism included.

Though at first sight it seems illogical that the "restraint" harness chosen should be the least efficient in preventing injury, it must be remembered that the term "restraint" harness is, in this case, a misnomer - as detailed earlier. The improvements noted above are as follows:-

a. Force attenuating system. With a waist harness it is very difficult to limit the load on the body to 5G because this represents a fall of less than 1 m. However, in the context of an aircraft and with a crewman with an adjusted harness, falls in excess of this distance are unlikely. This has been borne out in practice; although the occurrences have been rare, the crewmen were uninjured. An attenuation material, called Plytear is available commercially. It consists of two straps 0.37 m long, joined together by diagonal stitching. When a load is applied to the end of each strap, the stitching tears at a pre-determined load, until either the loading is reduced (Fig 8) or, in a severe case, the stitching is exhausted and the two straps part. To ensure continuity the system is stitched at the same end of each strap to the main portion of the restraint strop. Thus, if the attenuating mechanism were exhausted, any remaining load would be transmitted to the strop. This would, of course, impart a high peak loading on the wearer at this point, but tests have indicated that the drop height would have to be in excess of 2 m for this to occur. The attenuation mechanism begins to operate at approximately 3.1 kN (700 lbf). The full results of the tests are at Table 1 and a typical force attenuation diagram is at Figure 9.

b. Aircraft attachment hook. This must be simple, small, reliable, and have a double action. Hooks in current use are cumbersome and, more important, can sometimes be opened inadvertently. The proposed hook is similar to that used by climbers, but modified so that a rotary action is required before the mechanism is able to open. Once open, it can be held in that position and re-locked simply by releasing the spring loaded lever. The hook is proof loaded to over 10 kN and its ease of action and size have made it well liked by aircrew during the trials.

c. Restraining strop. The requirements for a strop must be ease of adjustment of length and resistance to twisting action. That used originally was 40 mm wide with a proof load of 17.7 kN. The modifications made for the trial were the inclusion of a thicker material which reduced the tendency for the strop to twist, increasing the proof load to 36.4 kN, and the use of an adjustment buckle which was easy to operate and did not have the tendency of the thinner strop to slip under load.

#### CONCLUSIONS

This paper has described improvements in restraint and crashworthiness in widely differing but important aspects of helicopter operations. Efficient harnesses for mobile crewmen, and for passengers, and crashworthy pilots' seats are of equal importance. The improvements described here should lead to a general increase in crashworthiness.

#### REFERENCES

1. Steele-Perkins, A.P. (1980). The Evolution of the Seat Pan Mounted Personal Survival Pack (PSP). AGARD-CP-286.
2. Campbell, R.F. Design of a Crashworthy Crew Seat for the Boeing Vertol Chinook Helicopter. (Source unknown).
3. Civil Aviation Authority Specification 1, Issue 5; Specification for Passenger Lap Belts.

4. Ministry of Defence (Procurement Executive) Specification RDAE 4/2. Manually Operated Quick Release Fittings for Parachute Safety and Restraint Harnesses.
5. Military Specification MIL-S-58095 AV. Seat System: Crashworthy, Non-Ejection, Aircrew, General Specification (1971).
6. British Standards Institution BS 1397:1979. Specification for Industrial Safety Belts, Harnesses and Safety Lanyards.

RUN	DUMMY MASS (Kg)	DROP HT (m)	FORCE AT PLATEAU (kN)	DURATION (Sec)		PLYTEAR USED (%)
				PLATEAU	TOTAL	
1	90	1.2	3.34	0.15	0.38	43
2	90	1.2	3.44	0.16	0.32	43
3	90	1.2	2.99	0.16	0.30	41
4	90	1.2	2.84	0.24	0.35	42
5	90	1.2	3.09	0.18	0.32	50
6	90	1.5	3.24	0.25	0.41	72
7	90	2.0	2.79	0.25	0.45	97
8	90	2.2	2.59	0.20	0.40	100 (1)
9	90	2.2	2.84	0.25	0.43	100 (2)
10	107	1.2	2.94	0.24	0.55	41 (3)

Mean plateau (attenuation breakout) force 3.01 kN SD 0.267 kN Strop length 1.2m

- (1) All attenuation used up: Peak force of 4.98 kN over 0.34 sec from secondary drop
- (2) Safety webbing took up tension during deceleration with 5.48 kN peak over 0.076 sec
- (3) Sierra anthropometric dummy and latest despatcher harness assembly with 3m strop used. Initial peak force of 3.98 kN over 0.04 sec was recorded.

TABLE 1

'Plytear' Attenuator Drop Test Results





Fig. 1

Aerolex (UK) Ltd quick release facility for passenger lap strap harness

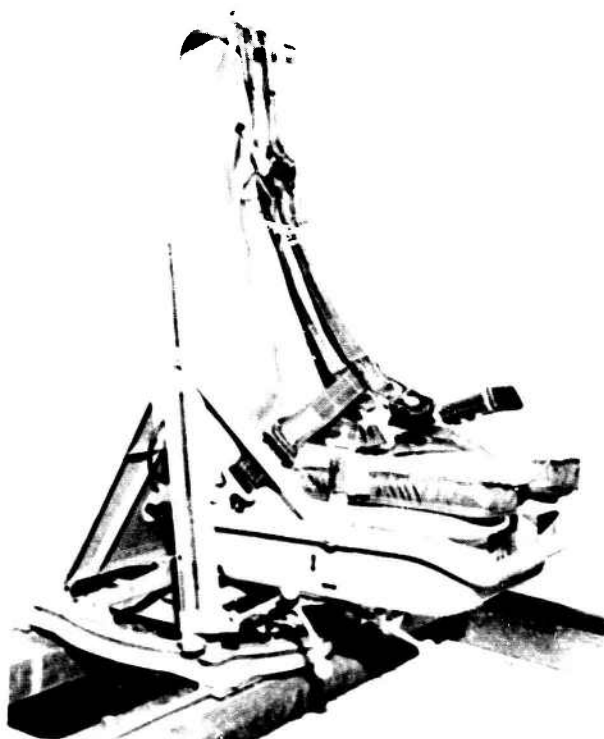


Fig. 2

Sea King Crew seat with crashworthy rotation modification

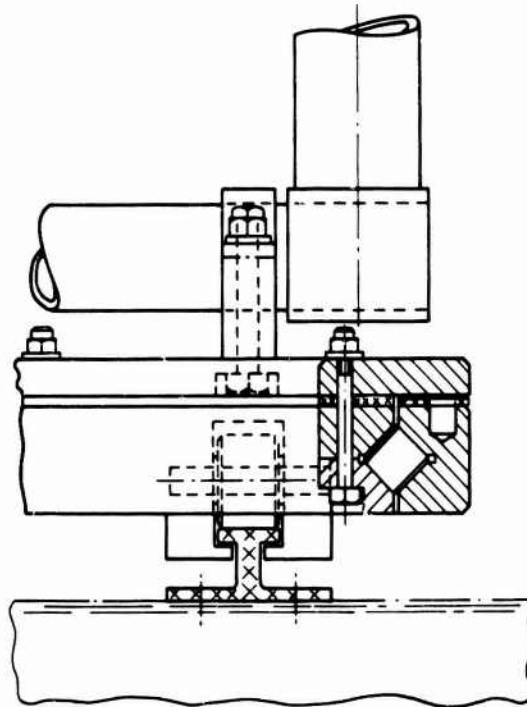


Fig. 3  
Rotating seat - section through  
crossed roller race



Fig. 4  
Prototype harness incorporated into life saving waistcoat



Fig. 5  
Torso harness for mobile aircrew



Fig. 6  
Modified prototype jerkin with re-routed straps

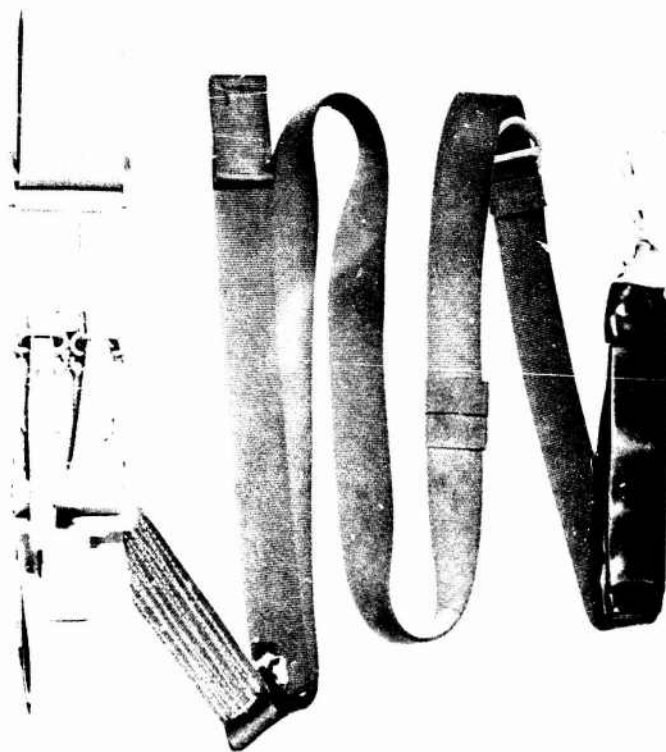


Fig. 7

Despatcher harness with energy attenuator and karabinier hook

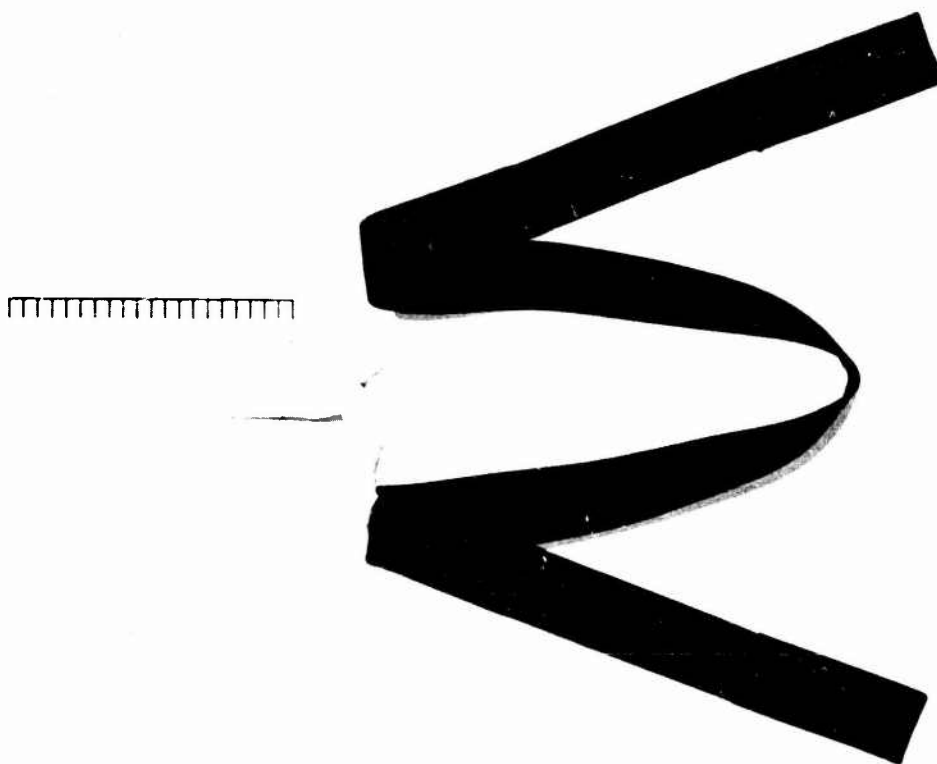


Fig. 8

Attenuator after 1.2m drop with 90 Kg mass

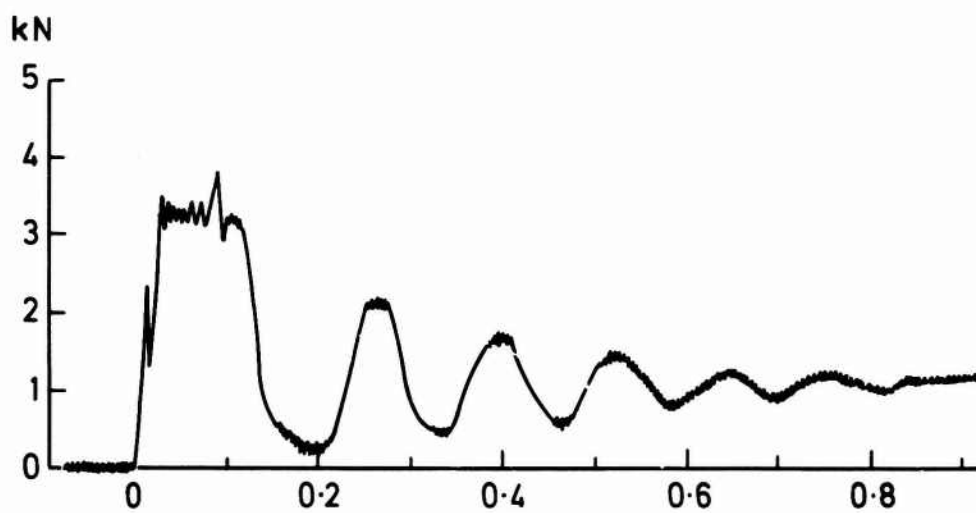


Fig. 9

'Plytear' typical force/attenuation graph

EVALUATION SUR BANC D'ACCELERATION HORIZONTAL ET LORS D'UN CRASH  
SIMULE DE L'EFFICACITE DE SIEGES ANTICRASH D'HELICOPTERES.

ETUDE SUR MANNEQUINS ANTHROPOMORPHIQUES.

par

B. VETTES (\*) et G. BEZAMAT (\*\*)

(\*) - Médecin en Chef - Spécialiste de Médecine Aéronautique  
Laboratoire de Médecine Aéronautique  
CENTRE D'ESSAIS EN VOL  
91220 - BRETIGNY-AIR (FRANCE)

(\*\*) - Expérimentateur Navigant d'Essais  
Laboratoire de Médecine Aéronautique  
CENTRE D'ESSAIS EN VOL  
91220 - BRETIGNY-AIR (FRANCE)

RÉSUMÉ

Dans le cadre des études entreprises en France sur les chances de survie des occupants d'un hélicoptère au cours d'un crash et afin de ramener les accélérations à des valeurs supportables pour l'organisme humain, des sièges munis de dispositifs absorbeurs d'énergie ont été fabriqués.

Trois types de sièges ont été conçus : un siège pilote, un siège troisième homme mécanicien pour le personnel navigant et un siège troupe pour les passagers.

Les essais de qualification ont compris des essais de tenue statique et des essais dynamiques sur banc d'accélération horizontal et au cours d'un crash simulé d'une cellule d'hélicoptère PUMA SA 330.

Le Laboratoire de Médecine Aéronautique du Centre d'Essais en Vol de BRETIGNY/Orge a été plus spécialement chargé d'apprécier l'efficacité de tels sièges à partir de l'enregistrement et de l'analyse des accélérations relevées sur des mannequins anthropomorphiques.

Une méthode automatique de dépouillement et d'interprétation des accélérations relevées sur le siège et le mannequin a été conçue au LAMAS et réalisée par le Centre de Calcul du C.F.V. Elle est basée sur l'évaluation de l'intensité, de la durée des accélérations, du jolt et de la réponse élastique des différentes masses corporelles du mannequin (bassin-thorax-tête).

Les essais sur banc d'accélération horizontal ont été réalisés dans des directions unitaires verticale Z et horizontale X, et dans des directions combinées. Malgré leur sévérité, ces tests ont permis de vérifier le bon fonctionnement des systèmes absorbeurs d'énergie et l'atténuation des accélérations transmises aux mannequins.

L'essai de crash a confirmé ces observations. Les occupants de l'appareil auraient été vraisemblablement sauvés, cependant il subsiste des risques de blessures plus ou moins graves (commotion, fracture, contusion) notamment au niveau de la région cervicale basse (C<sub>5</sub>-C<sub>7</sub>).

I. - INTRODUCTION

Au cours d'un crash d'hélicoptère et lorsque l'appareil reste plus ou moins contrôlé, l'impact au sol se fait à une vitesse horizontale relativement faible et à une vitesse verticale plus ou moins grande. Pour augmenter les chances de survie et ramener les accélérations à des valeurs supportables pour l'être humain des sièges munis de dispositifs absorbeurs d'énergie ont été fabriqués.

Trois types de sièges ont été conçus : un siège pilote, un siège troisième homme mécanicien pour le personnel navigant et un siège troupe pour les passagers.

Les essais de qualification ont compris des essais de tenue statique et des essais dynamiques sur banc d'accélération horizontal et au cours d'un crash simulé d'une cellule d'hélicoptère PUMA SA 330.

Le Laboratoire de Médecine Aéronautique du Centre d'Essais en Vol de BRETIGNY/Orge a été plus spécialement chargé d'apprécier l'efficacité de tels sièges à partir de l'enregistrement et de l'analyse des accélérations relevées sur des mannequins anthropomorphiques.

## 2. - MATERIELS ET METHODES :

### 2.1. - Les sièges anti-crash :

#### 2.1.1. - Le siège pilote (fig.1)

Il est constitué d'une console fixée sur le plancher sur laquelle coulisse un baquet composé d'une armature métallique, d'un revêtement en tôle et d'un coussin. Le guidage du baquet sur les montants verticaux de la console se fait par l'intermédiaire de galets. Le réglage en hauteur peut être obtenu en plusieurs positions. Le siège est équipé d'un harnais cinq points. Il est muni de deux absorbeurs principaux.

#### 2.1.2. - Le siège troupe (fig.1)

Il est constitué d'une armature métallique, d'une assise et d'un dossier en toile tendue et d'un système de câbles permettant la fixation au plancher et au plafond de l'appareil (deux attaches supérieures et quatre attaches inférieures avec six câbles dont quatre sont croisés). Il est muni d'un harnais quatre points. Sa masse est de 7,8 kg.

Les absorbeurs principaux sont situés dans les tubes verticaux. Les absorbeurs secondaires longitudinaux sont composés de deux vérins reliant l'assise aux fixations arrières.

#### 2.1.3. - Le siège troisième homme (fig. 1)

Il est de même nature que le siège troupe et possède la caractéristique d'être repliable.

Pour le siège pilote lorsque l'accélération verticale dépasse un seuil imposé, le baquet est entraîné vers le bas. La limitation de l'effort est assurée par un système absorbeur constitué d'un couteau et d'une cartouche en élastomère enfermée dans un tube métallique. La partie supérieure du tube est liée à la console et le déplacement du baquet produit le déchirement de la cartouche en élastomère par le couteau.

La limitation des accélérations transverses est produite par la déformation en flexion de la partie inférieure des rails de la console et par l'allongement d'une tige en acier inoxydable.

Le principe du fonctionnement des absorbeurs du siège troupe est le même.

### 2.2. - Le banc d'accélération horizontal (fig.2) :

Il est constitué d'un chariot se déplaçant sur des rails dont la mise en vitesse est réalisée à l'aide d'un treuil entraîné par un vérin hydraulique asservi en déplacement. Il est équipé à l'avant de cylindres métalliques creux contenant des tubes de polyuréthane.

Des tiges métalliques fixées à un butoir et équipées d'une olive calibrée à leurs extrémités sont disposées face au chariot. La décélération est provoquée par le laminage du polyuréthane par les olives lors de l'impact. La vitesse d'impact est déduite de la mesure du temps de passage du chariot entre deux repères fixes. La décélération est mesurée par un accéléromètre placé sur le chariot. Tous les essais sont filmés à l'aide d'une caméra rapide.

Les essais dynamiques effectués sur le banc d'accélération ont compris des essais réalisés dans les directions unitaires verticale Z, longitudinale X, latérale Y et directions combinées appelées test 1 et 2 (fig. 3 et 4).

Le test 1 représente un atterrissage d'hélicoptère dur avec maximum d'accélération verticale et des composantes X (30°) et Y (0°). (fig.5).

Le test 2 représente un atterrissage type avion manqué avec un fort dérapage (composante Y) (fig. 6).

### 2.3. - Le crash simulé de l'hélicoptère Puma SA 330 (fig.7) :

L'essai consiste à faire chuter l'hélicoptère d'une hauteur de 5,28 m, selon un mouvement pendulaire, de façon à lui imprimer une vitesse d'impact au sol de composante verticale de 8,5 m/s et horizontale de 5,6 m/s, soit une vitesse résultante de 10,2 m/s. Le crash représente un impact sur un terrain dégagé mais caillouteux (de gros cailloux sont fixés sous la structure au niveau des réservoirs).

Onze mannequins anthropomorphiques ont été utilisés pour cet essai : trois pour l'équipage et huit pour les hommes de troupe.

Vingt caméras rapides disposées dans l'aire de crash et deux caméras rapides embarquées ont filmé la chute de l'impact de l'hélicoptère.

### 2.4. - Les mannequins :

Ils sont du type Alderson - Serem ou Sierra, équipés de blocs d'accéléromètres triaxes Z X Y placés dans la tête, le thorax et le bassin (fig. 8).

### 2.5. - La méthode d'analyse des résultats :

A partir de chaque courbe d'accélération intensité en fonction du temps, filtrée à 100 Hz, nous avons effectué une découpe en tranche de 2,5 g. Chaque tranche représente alors un plateau d'accélération d'une certaine durée. On peut ainsi tracer une courbe de ces différents plateaux. Ces courbes sont alors placées sur les diagrammes de tolérance aux accélérations de durée brève + Gz ; - Gz ; - Gx ; + Gx, établis par WCB en 1964.

Cette opération est répétée pour chaque accélération (chariot - plancher - éléments corporels des mannequins : tête - thorax - bassin).

Par calcul de la dérivée de l'accélération, on peut apprécier le jolt obtenu et par référence au diagramme de EIBAND, avoir une idée des risques encourus.

Pour tenir compte de la réponse élastique des différentes masses corporelles (tête - thorax - bassin) pouvant donner lieu à des phénomènes de déphasage, de résonance (over shoot) ou d'amortissement (COERMAN et coll. 1962), nous avons représenté sur un même graphique, en les superposant, toutes les accélérations d'un même axe.

Cette méthode automatique de dépouillement et d'interprétation conçue au LAMAS a été réalisée par le Centre de Calcul du C.E.V.

### 3. - RESULTATS

Nous prendrons comme exemple les résultats obtenus sur un mannequin assis sur un siège anti-crash troupe subissant sur le banc d'accélération un test 1 et placé face vers l'avant dans le cargo du PUMA.

Pour une accélération de 39 g du chariot, sur l'axe vertical Z, les pics très brefs (1 ms) d'accélérations positives relevés sur le bassin, le thorax et la tête, atteignent 35 à 36 G. Pour le bassin un pic est supérieur à 40 g. Ils sont suivis de brèves pointes négatives de 10 g pour le thorax et de 20 g pour la tête.

Les courbes des plateaux d'accélération rapportées sur le diagramme + Gz de WEBB (fig.9) se situent dans la zone des blessures légères et sur le diagramme - Gz dans la zone d'exposition volontaire pour le bassin et le thorax et dans la zone des blessures légères pour la tête.

Le jolt très important au niveau du bassin n'est plus au niveau de la tête que de 3000 g/s et du thorax de 2000 g/s.

La superposition des différentes courbes n'indique aucun déphasage entre le bassin, le thorax et la tête et témoigne d'un léger amortissement. (fig. 10).

Sur l'axe X les accélérations sont de moindre intensité (pic entre 24 et 27 g sur le bassin et le thorax). Elles atteignent cependant - 38 g et + 38 g au niveau de la tête (brève et brutale oscillation).

Ces valeurs, à l'exception de celles de la tête, prennent place sur le diagramme - Gx dans la zone d'exposition volontaire.

Les courbes d'accélérations superposées mettent en évidence l'amplification au niveau de la tête.

Le jolt n'excède en aucun cas 3500 g/s, valeur bien en dessous des zones de tolérance du diagramme de EIBAND.

Sur l'axe Y les accélérations affectent un mode vibratoire avec des pics positifs et négatifs oscillant entre 8 g et 13 g. Ces oscillations sont particulièrement marquées au niveau de la tête.

Lors du crash simulé du PUMA, sur l'axe Z au niveau du bassin, le choc principal est précédé d'une brève pointe d'accélération négative de 25 g, suivie immédiatement d'un changement de signe (deux pointes à 22 g). Au niveau du thorax et de la tête on retrouve les formes classiques de répartition des accélérations dans le temps. Cependant, les hautes fréquences ne sont pas assez atténuées pour que la tête n'accuse pas de secousses perçues sur le bassin (deux pointes à 15 g pendant 4 ms). Cependant, l'accélération maximale de la tête ne dépasse pas 15 g alors que le plancher est sollicité par un mode vibratoire dont les pointes dépassent 40 g.

Rapportées sur le diagramme de WEBB, ces valeurs se situent au pire dans la zone des blessures légères et sont le plus souvent du domaine du siège éjectable. (Fig. 11).

On observe un jolt important de près de 5000 g/s au niveau du bassin.

La superposition des différentes accélérations fait ressortir la pointe négative du bassin entraînant une amplification d'un facteur 25 par rapport à l'ensemble thorax-tête. Puis l'ensemble bassin-thorax-tête est en phase sans amplification. (Fig. 12).

Sur l'axe X, bien que d'intensité relativement modérée par rapport aux tolérances humaines, les accélérations atteignent 18 g au niveau du thorax. Sur le diagramme de WEBB ces valeurs se situent dans la zone d'exposition volontaire.



#### 4. - DISCUSSION

Lors de l'essai sur banc d'accélération, les valeurs de l'accélération relevées au niveau du bassin sur l'axe Z peuvent faire craindre des lésions pour l'occupant du siège. Il faut cependant signaler que pour le type de mannequin utilisé, le bloc des accéléromètres fixé dans le bassin est également lié à l'articulation du membre inférieur (cuisse et jambe). Ainsi l'accéléromètre qui mesure l'axe Z ne se trouve pas rigoureusement dans l'axe de la colonne vertébrale. Au cours du choc, la course des amortisseurs des montants du siège est très importante et entraîne une projection et une rotation des membres inférieurs. Le décalage angulaire initial de l'axe Z augmente de façon extrêmement variable sans qu'il soit possible de le mesurer.

Il convient donc d'être extrêmement prudent dans l'interprétation de cet enregistrement.

Par contre, les accélérations Gz relevées sur le thorax et la tête sont représentatives des accélérations subies par la colonne vertébrale en cet endroit. Elles indiquent l'effet amortisseur du siège anticrash. En effet, elles sont inférieures à celles du chariot et ne prennent place qu'un très court instant dans la zone des blessures légères.

Le jolt au niveau de la tête est encore grand et se situe sur le diagramme de EIBAND un peu au-dessus des valeurs tolérées par des sujets humains volontaires.

Sur l'axe X la brutale oscillation négative (- 38 g) puis positive (+ 38 g) de la tête provoque un mouvement forcé pendulaire comme le confirment les films cinématographiques. Ce changement rapide de sens entraînant une hyperflexion de la région cervicale basse (C5- C7), suivie d'une extension brutale risque de provoquer des lésions graves (PATRICK et coll. 1965).

Ce phénomène inévitable ne met pas en cause le siège anticrash.

Seul un harnais gonflable pourrait peut être empêcher ces mouvements intempestifs.

Les accélérations Y ne sont pas négligeables. Elles tendent à provoquer une dissymétrie du corps humain qui confère à la colonne vertébrale une attitude défavorable à une bonne tenue aux accélérations verticales subies simultanément. Les oscillations à gauche et à droite de la tête sont des facteurs aggravants (EWING et coll. 1977). Selon ZABOROWSKI 1966, ces accélérations Y sont mal supportées et peuvent être à l'origine de troubles cardiaques.

On peut donc estimer que l'occupant aurait pu être victime de blessures au niveau de la colonne vertébrale dorso lombaire et cervicale avec un état de choc plus ou moins prononcé.

Néanmoins, il convient de signaler qu'il s'agit d'un test extrêmement sévère. La posture qu'il nécessite ne correspond pas à une attitude couramment expérimentée dans la gamme des essais de crash effectués sur différents hélicoptères (sujets normalement assis sur leur siège).

Il représente plutôt un crash d'un appareil non contrôlé heurtant le sol sous n'importe quelle incidence, qualifié jusqu'alors de crash sans aucune chance de survie.

Le crash simulé se rapproche beaucoup plus de cas réel : appareil contrôlé, impactant le sol avec une vitesse horizontale relativement faible et une vitesse verticale importante (autorotation manquée, perte soudaine de puissance).

La superposition des courbes d'accélérations Gz met en évidence le filtrage du siège et son amortissement. Elle montre la transmission amortie des accélérations du bassin au thorax et l'excitation vibratoire de la tête dont les accélérations sont en opposition avec celles du thorax, ce qui indique une sollicitation en traction compression du cou. Le mannequin a été plus secoué qu'écrasé. (Fig. 12).

Sur l'axe X l'accélération du bassin change rapidement de signe. Il a été sollicité successivement dans des sens opposés d'abord projeté en avant par inertie puis poussé en avant par un autre mannequin placé derrière lui (confirmation apportée par l'examen des films). En revanche, le thorax et la tête ont été constamment projetés en avant. Ce mouvement alterné du siège a provoqué des oscillations de tout le corps nettement perceptibles sur l'accéléromètre de la tête. De plus, le choc du mannequin placé à l'arrière a imprimé au siège une rotation de gauche à droite de 60°, ce qui ne peut être qu'un facteur aggravant.

En conséquence, on peut estimer qu'un tel homme de troupe aurait eu la vie sauve avec cependant des risques de lésions au niveau de la colonne vertébrale (fractures) et quelques contusions sinon des douleurs musculaires au niveau du cou.

#### 5. - CONCLUSIONS

Au cours de ces essais dynamiques, le type d'exploitation de ces résultats adopté par le LAMAS du C.E.V. a permis d'apporter des renseignements intéressants sur les chances de survie des occupants et sur l'efficacité des moyens de protection. Les sièges anticrash ont parfaitement rempli leur rôle, les systèmes absorbeurs d'énergie ont amorti les accélérations du chariot et du plancher de l'hélicoptère. Les différentes parties du corps restent en phase durant tout le phénomène. Cependant la combinaison d'accélérations sur les trois axes risque d'entraîner des blessures plus ou moins graves.

Certes de telles expérimentations sont réalisées sur mannequins. Leur transposition à des cas réels est donc sujette à caution, mais elles ont permis de mettre au point une méthode d'analyse, d'interprétation et de fournir une prédiction de la tolérance au crash avec une certaine marge de sécurité. Il est probable que le corps humain dont les structures sont plus malléables et plus souples amortiraient davantage les accélérations enregistrées lors de ces impacts.

BIBLIOGRAPHIE

COERMANN R.R.

The mechanical impedance of the human body in sitting and standing position at low frequencies.  
Human factors 1962 - 4 - 227-253.

EIBAND A.M.

Human tolerance to rapidly applied accelerations : a summary of the literature.  
Nasa Memorandum 5-19-59 E (National Aeronautics and Space Administration) Washington D.C. June 1959.

EWING C.L. et al.

Dynamic response of the human head and neck to + Gz impact acceleration.  
Proceeding-twenty first Stapp Car, Chresh Conference Society of Automotive Engineers.  
New-York 1977 - 547-586.

PATRICK L.M., LISSNER, R.M. and GURDJIAN E.S.

Survival by design-Head Protection, 7 th Stapp car crash Conference Springfield III Charles C.  
Thomas 1965.

WEBB, P.

Impact and vibration in WEBB P. (Ed.)  
Bioastronautics data book NASA SP 3006. 1964  
and NASA SP 3006. 1973

ZABOROWSKI A.V.

Human tolerance to lateral impact with lap belt only.  
Eight Stapp car crash and field demonstration conference.  
Wayne State University Detroit Michigan 1966.

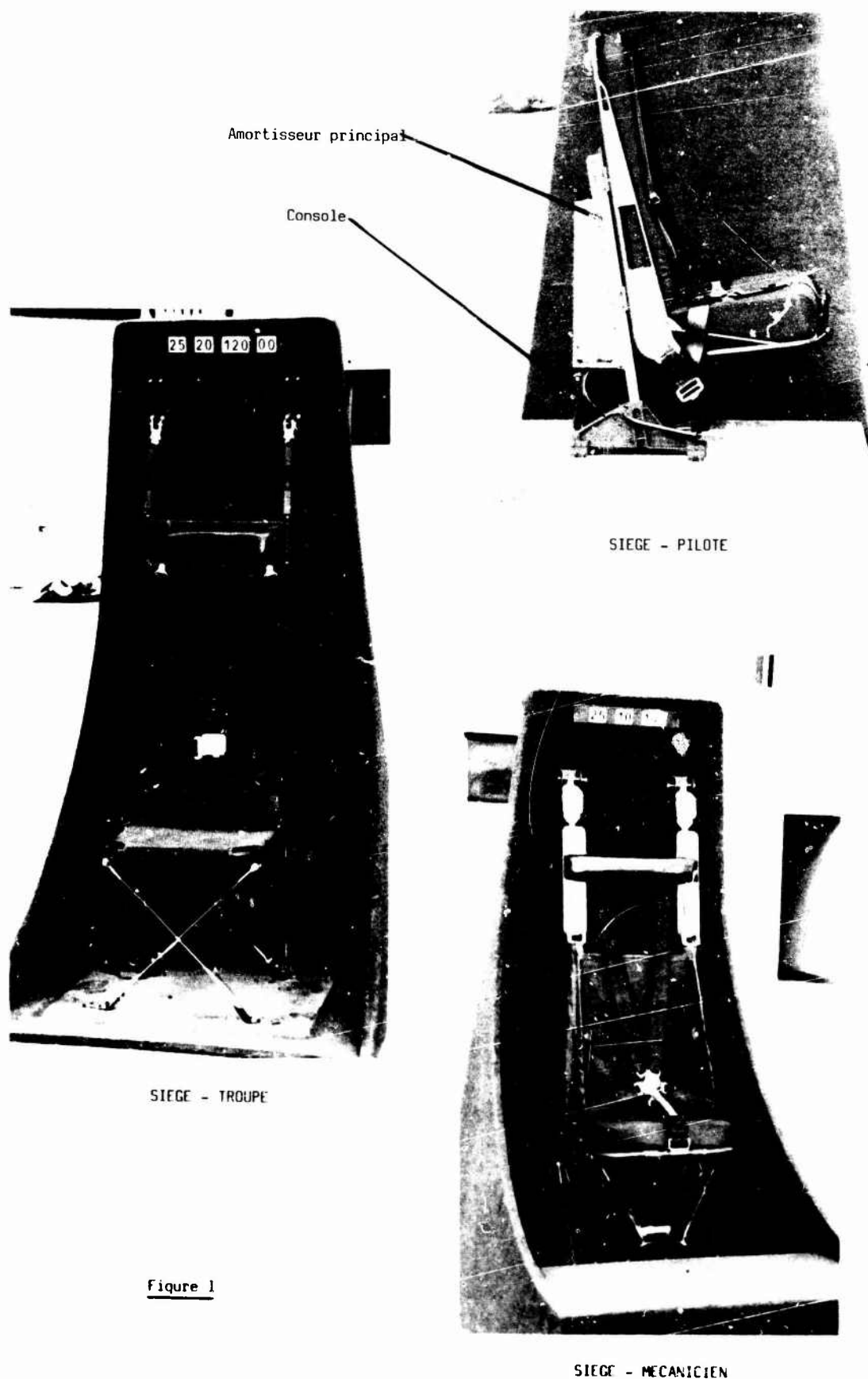


Figure 1

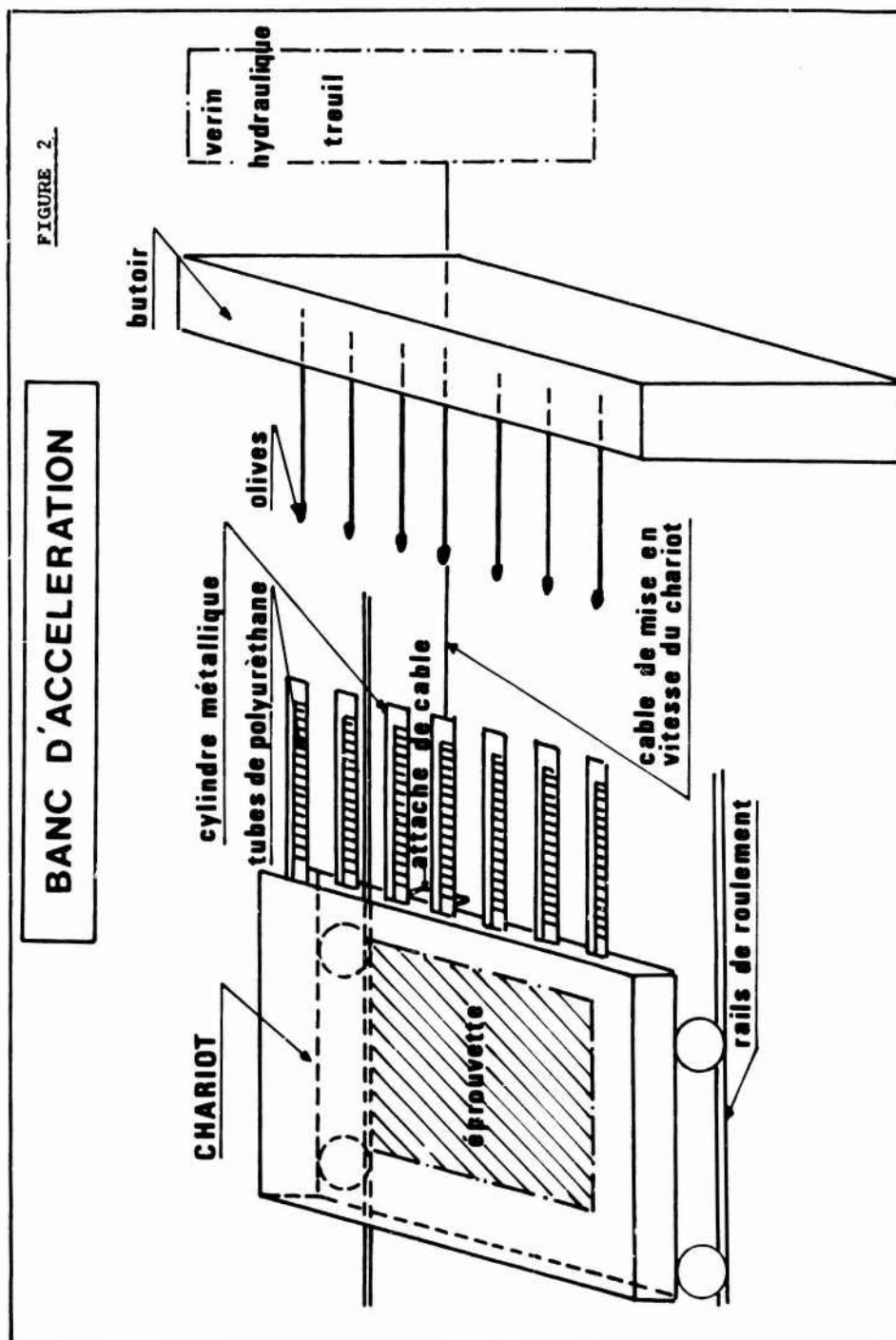


FIGURE 3

# ESSAIS DE MISE AU POINT SUR BANC D'ACCELERATION

CES ESSAIS ONT ETE EFFECTUES DANS LES DIRECTIONS UNITAIRES. X et Z

SIEGE TROUPE (siège monté latéralement sur l'appareil)



SIEGE 3' HOMME

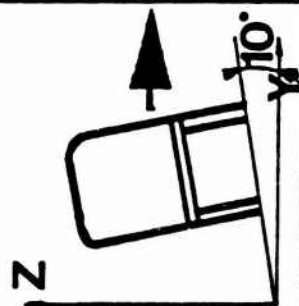
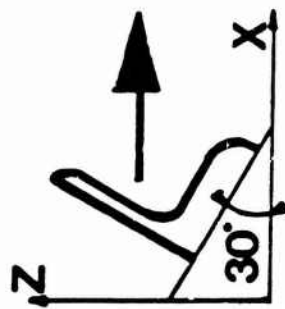


Les sièges ont par ailleurs été essayés en STATIQUE dans les directions d'accélération non validées par les essais dynamiques

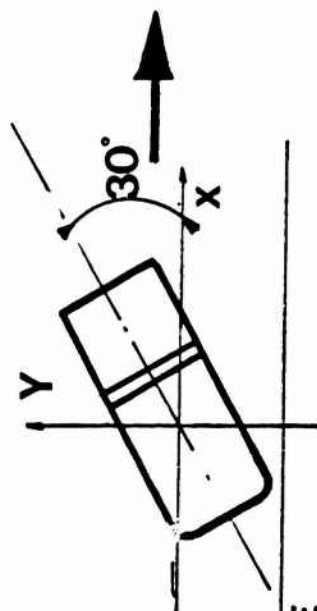
( Z haut, X arrière, Y )

# ESSAIS D'ACCELERATIONS COMBINEES

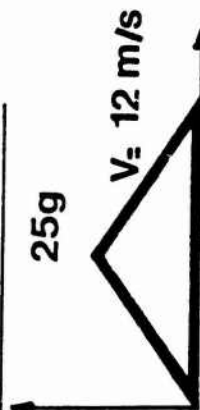
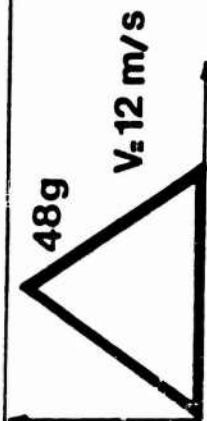
## TEST 1



## TEST 2



### SIEGES PILOTE

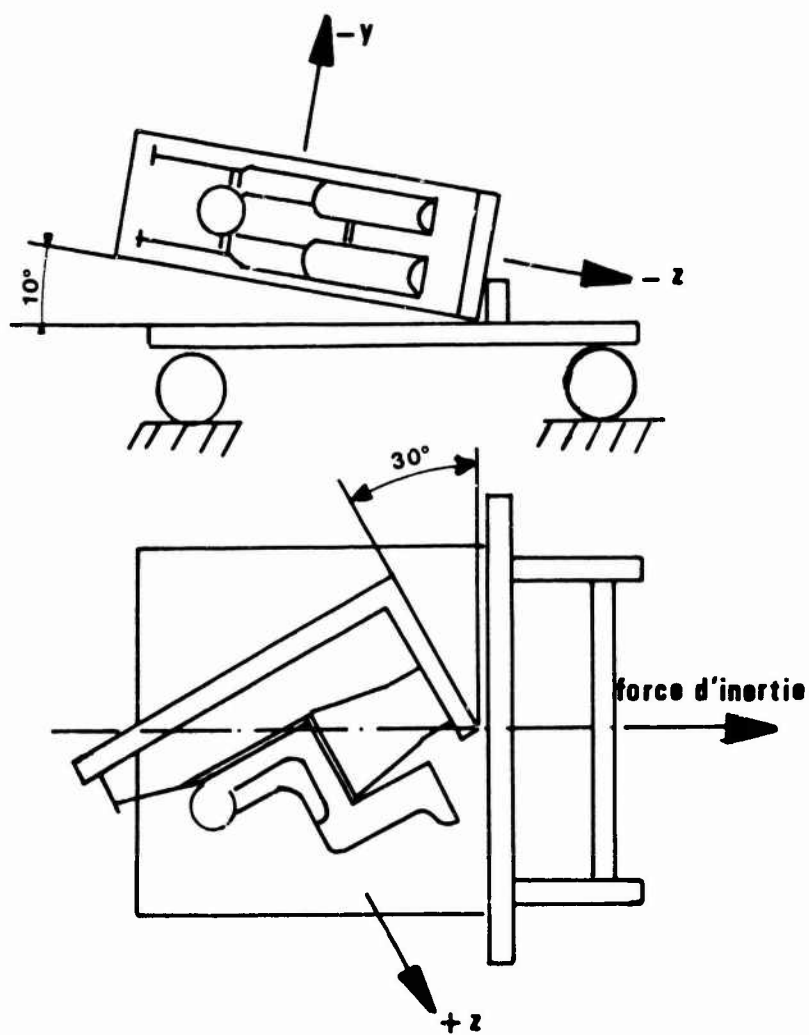


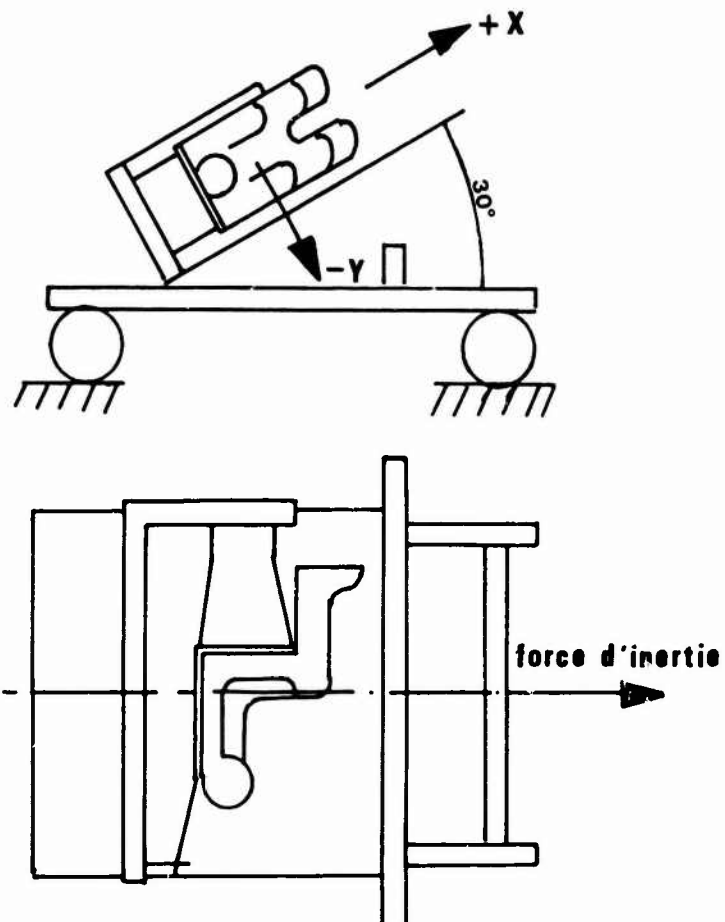
### SIEGES PASSAGERS



FIGURE 4

FIGURE 5

**ESSAI COMBINE TEST 1****Position du siege sur le banc d'acceleration**

**ESSAI COMBINE TEST 2****FIGURE 6****Position du siege sur le banc d'acceleration**



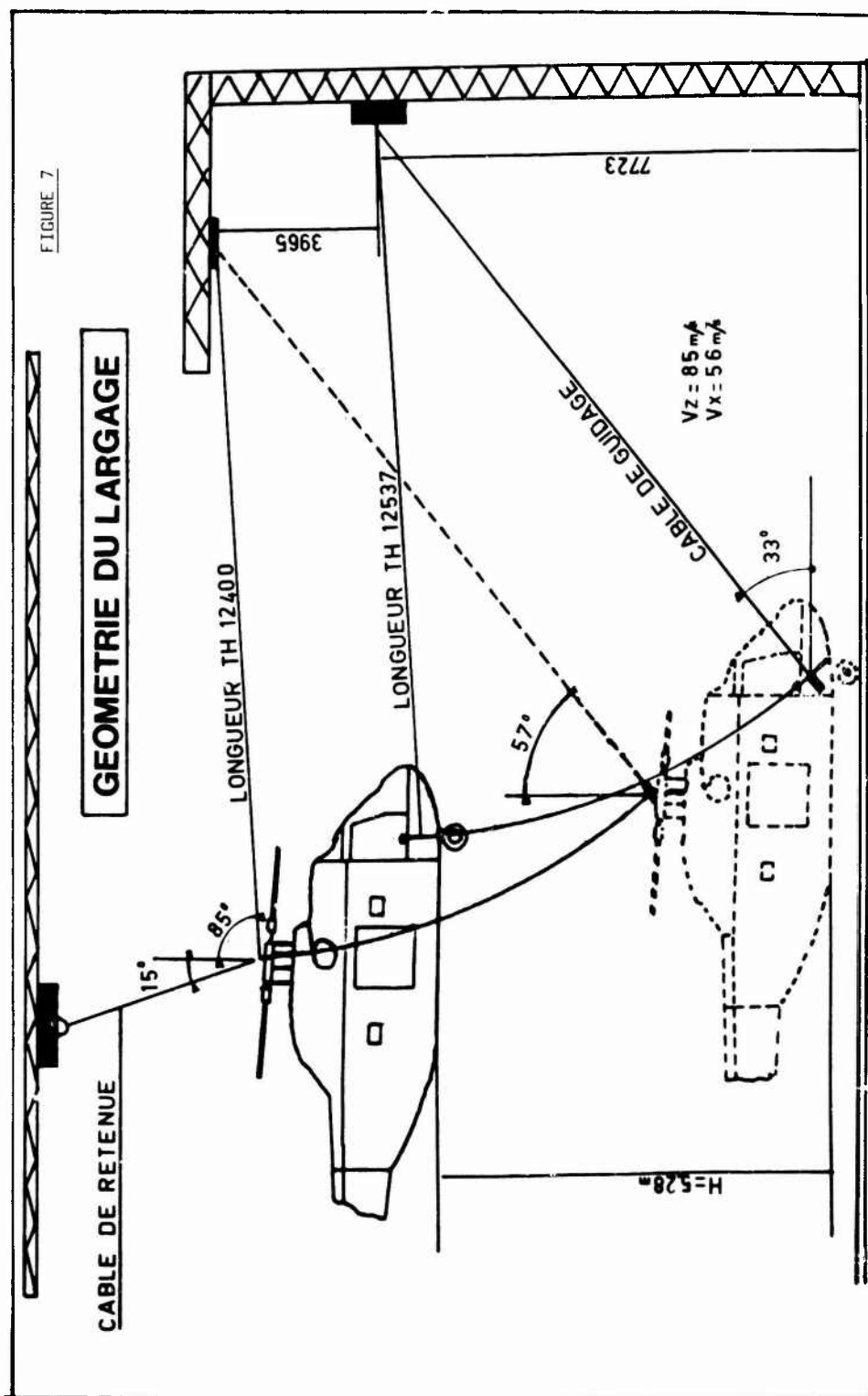
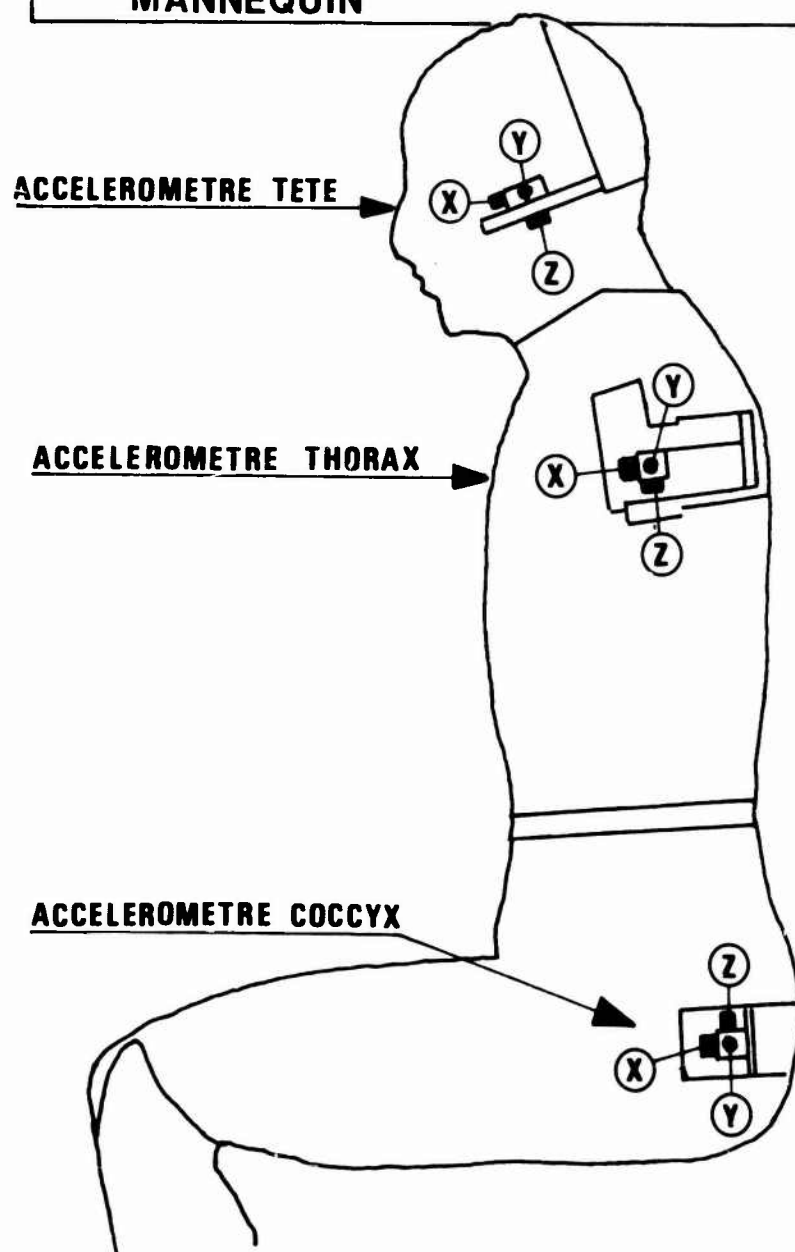


FIGURE 8

**POSITION DES ACCELEROMETRES SUR LE  
MANNEQUIN**



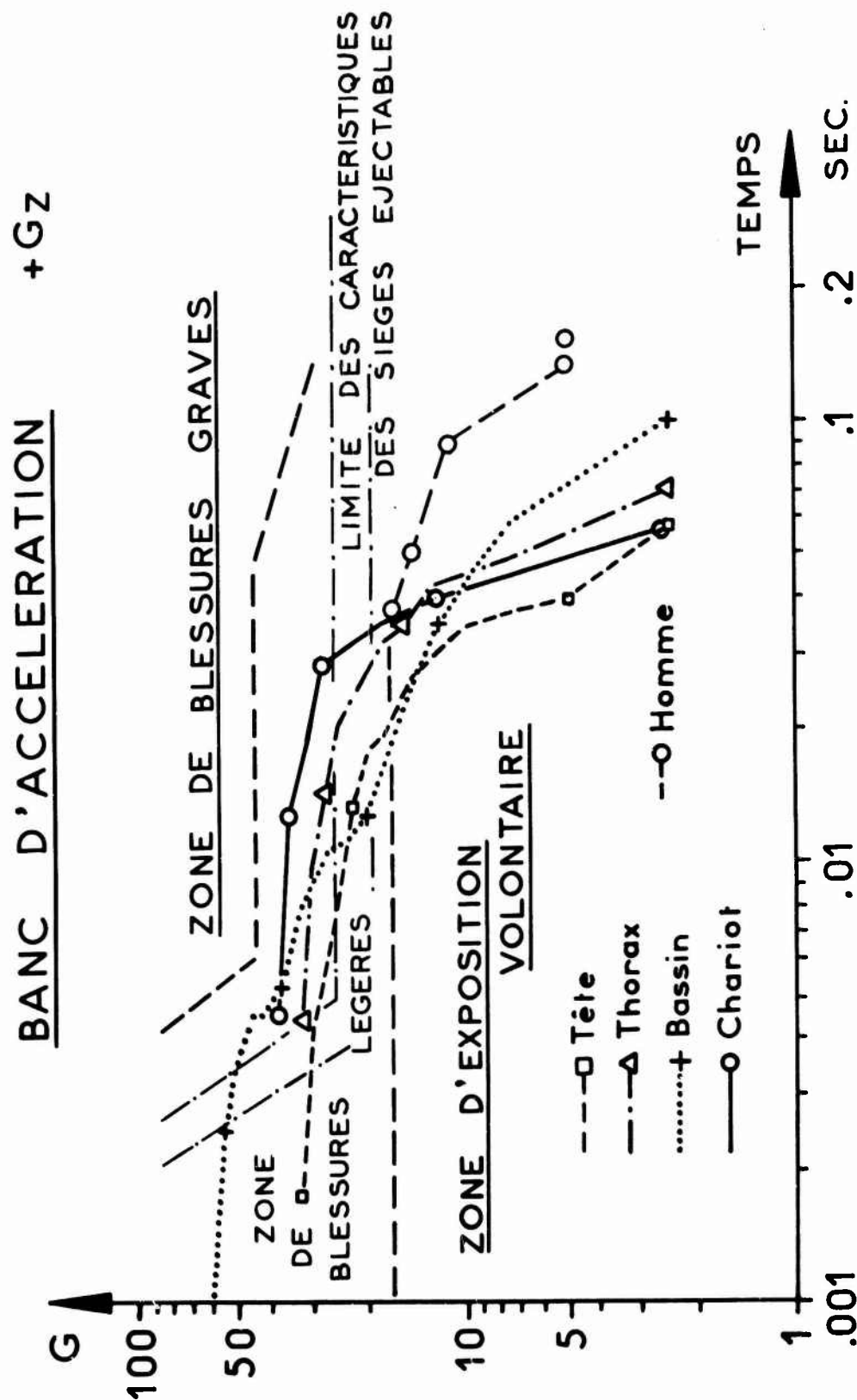
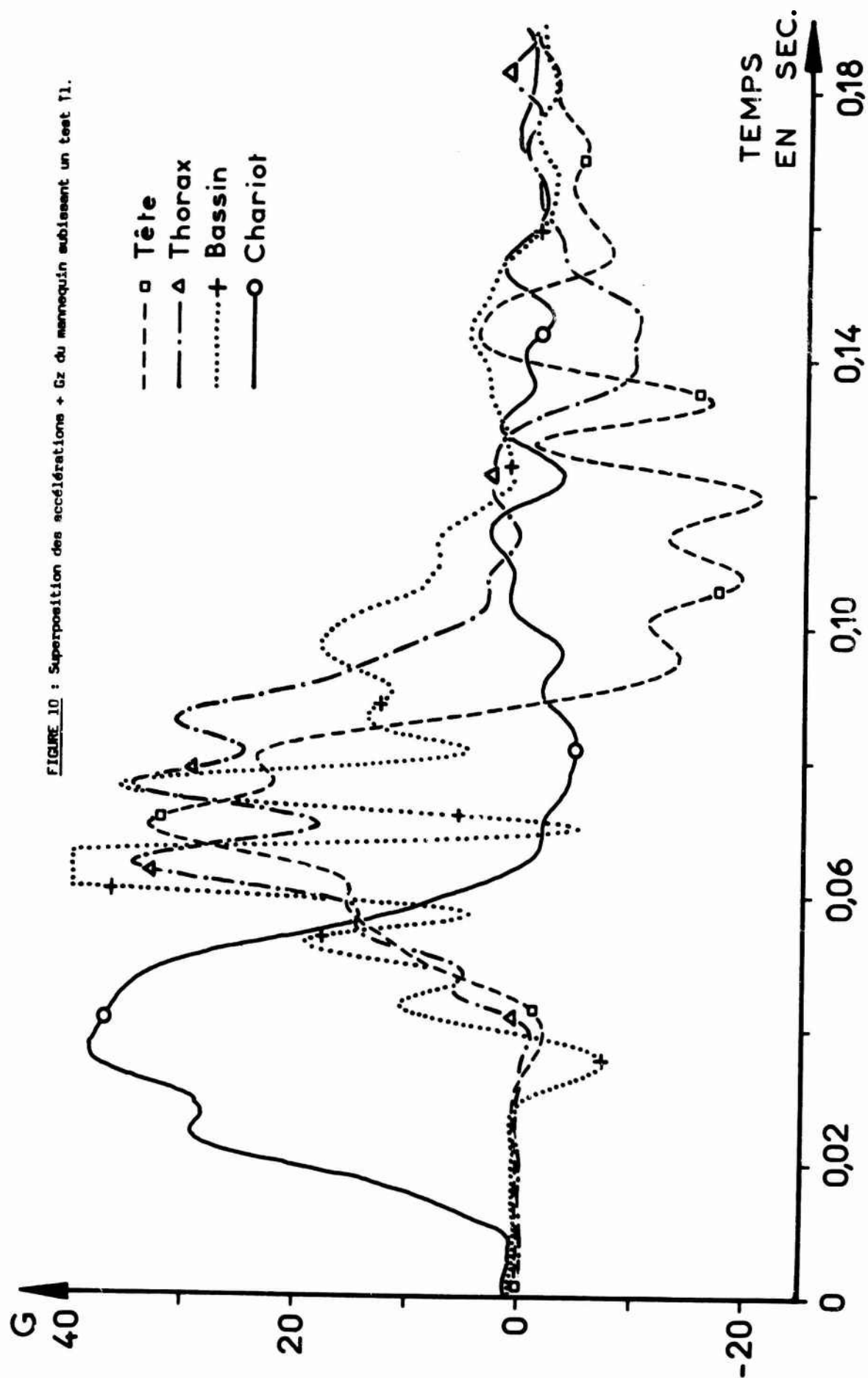


FIGURE 9 : Courbes des plateaux d'accéléérations reportées sur le diagramme de WEBB.



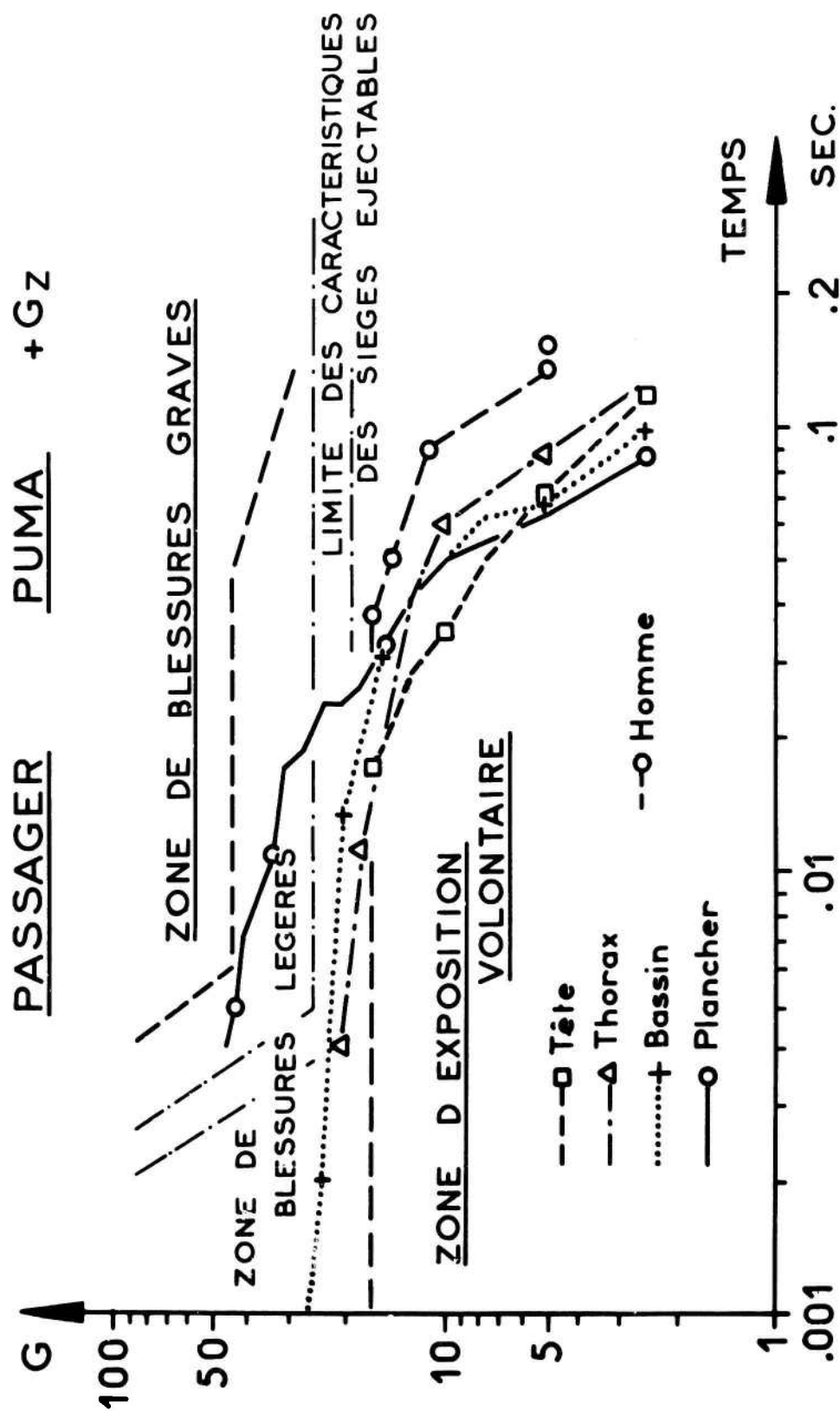
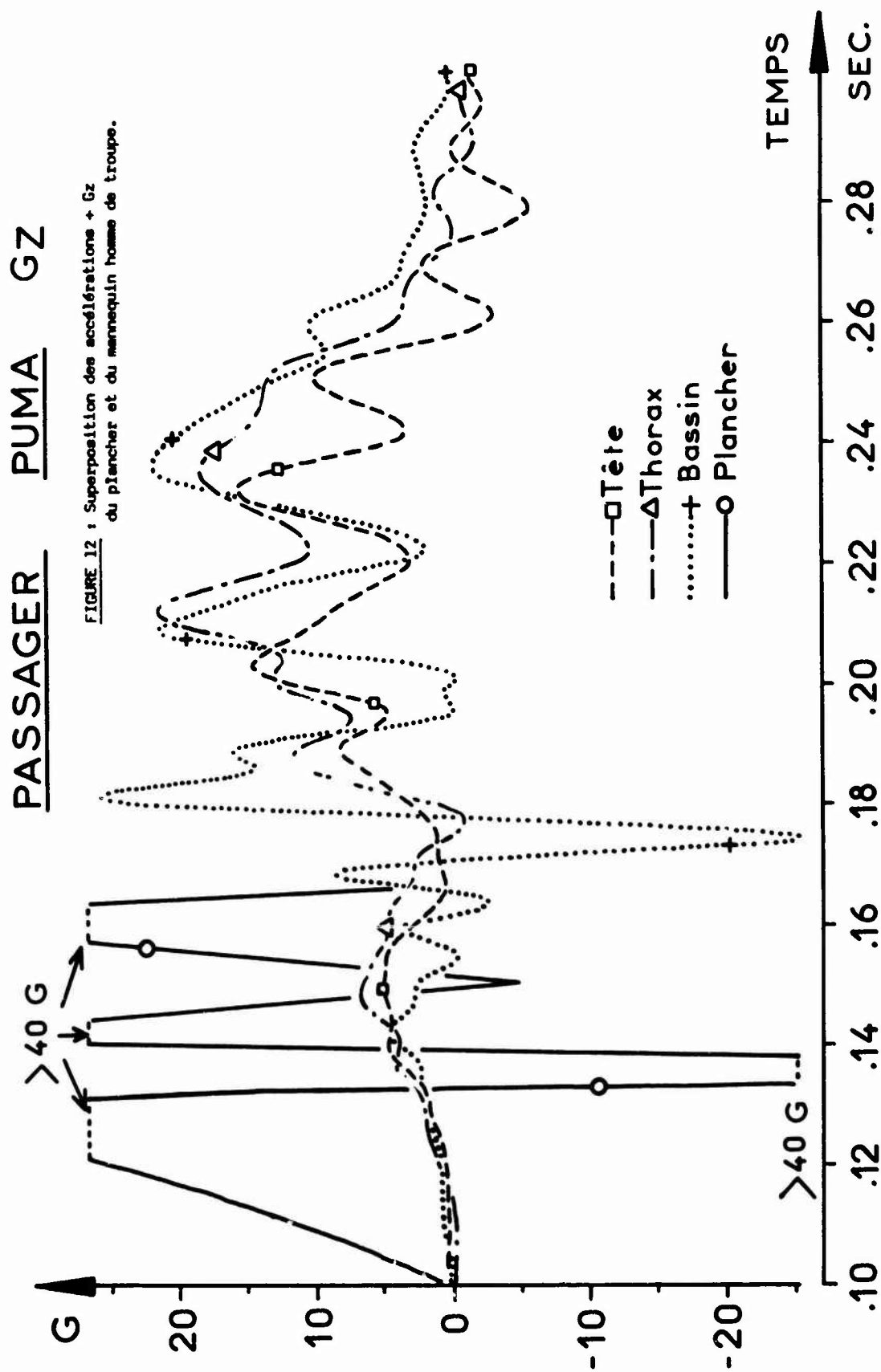


FIGURE 11 : Courbes des plateaux d'accéléérations + Gz du plancher et du mannequin homme de troupe reportées sur le diagramme de WEBB.



## DISCUSSION

STEELE-PERKINS (UK)

Could you explain your philosophy of having the nose undercarriage down but no main undercarriage during the drop of the SA 330?

AUTHOR'S REPLY

The test crash of the Puma SA 330 was organized by the Toulouse Center for Aeronautical Studies, and the SNIAS (Aerospatiale) of Marignane. The CEV (Flight Test Center) of Bretigny was solely concerned with the dummies and their instrumentation. The project directors had, therefore, decided to crash the helicopter with only the nose gear because the crashworthy main undercarriage was not ready for installation at the time of the crash. The crashworthy main gear has been successfully tested since that time at the CEAT de Toulouse with a toboggan.

DESJARDINS (USA)

Why did you refer to the unsurvivability of the test of the Puma when there seemed to be adequate maintenance of livable volume in the aircraft during the crash?

AUTHOR'S REPLY

The crash test of the PUMA SA 330 was considered like a crash having a good chance of survival. It was planned to be an assumed loss of power and a poorly executed autorotation, to produce a slow longitudinal speed and excessive sink speed. The anti-crash seats were intended to further improve the chance of survival by reducing vertical acceleration. It is not necessary that the cabin be crushed to have people killed. They can die sitting in their seats without being crushed.

DESJARDINS (USA)

Does the knife blade in the energy absorbing device you described as being used on your troop seat cut the side wall of the tube during stroke?

AUTHOR'S REPLY

At the moment of impact, the knife penetrates into the elastomeric cylinder, tears it, and absorbs energy, but the tube remains intact.

DESJARDINS (USA)

How did the other seats (not described in the presentation) perform? (Adequate or not).

AUTHOR'S REPLY

The other anti-crash seats, of a different concept, worked more or less satisfactorily. Some fulfilled their role, but one did not work, the dummy remained on it but would have received severe trauma.

SOME LIMITATIONS OF ADULT SEAT BELTS WHEN USED TO RESTRAIN  
CHILD DUMMIES IN SIMULATED FRONTAL IMPACTS

by

A.P. Roy<sup>1</sup>, K.J. Hill<sup>1</sup> and G.M. Mackay<sup>2</sup>

1 - Road Safety Engineering Laboratory, Middlesex Polytechnic,  
The Burroughs, Hendon, London NW4 4BT, England.

2 - Accident Research Unit, University of Birmingham,  
Birmingham B15 2TT, England.

# ABSTRACT

U.K. legislation will require front seat car occupants to be restrained. This may lead to increased use of adult seat belts by children. As a result of safety propaganda and the difficulty of fitting U.K. manufactured child restraint systems in the front seat, the majority of restrained children travel in the rear seating positions.

Since the anatomy of children changes with age, theoretical analyses have suggested at least three categories of restraint systems, each requiring a different design philosophy. Such analyses infer that adult lap and diagonal and lap belt only configurations are unsuitable for infants and, in certain circumstances, unsatisfactory for younger sitting children, whilst in the real world of accidents there is insufficient data to draw any firm conclusions.

This paper seeks to approach the problem of younger sitting children by reporting the results of a series of simulated crash tests using the KL/Middlesex Polytechnic test sled and comparing them with known U.K. accident performance of child restraints complying with BS.3254 - 1960 (designed for the 9 months to 4½ years age range).

The test programme simulated three types of frontal crash pulse with a dummy representing a 50thile 3 year old restrained in adult lap and diagonal belts and adult lap belts. Initial crash velocities were of the order of 50 km/h with sled input pulses ranging from 14 g to 43 g. The results suggest that the adult lap and diagonal configuration was generally satisfactory but for very severe crash decelerations the diagonal strap may load the neck in a manner which does not occur with conventional child restraints. This neck load can be reduced by using a properly located booster cushion but not by household cushions which slip out and leave the child vulnerable to submarining. The lap belt only configuration allows the dummy to jackknife with a possible risk of abdominal injury and of a head contact with the vehicle fascia.

# INTRODUCTION

The Transport Act of 1981 in the United Kingdom has a provision (33B) that persons over the age of one year shall not be transported in the front seats of motor vehicles unless they are restrained, although there are a small number of exceptions which need not concern us here. Child restraint systems on sale in the U.K. are difficult to fit to the front passenger seats of current vehicles because they require four anchorage points symmetrically placed. It is believed, therefore, that increased use will be made of adult lap and diagonal belts by children of ages between one and fourteen years. This paper seeks to examine the suitability of adult lap and diagonal belts for use as a restraint system for children.

A review of the theoretical design considerations of child restraints and field accident data suggests that children in the age range of one year to 4½ years are the least likely to "fit" adult belts and so the simulated crash tests have concentrated on this age range. The performance parameters of the adult restraints have been judged against the appropriate requirements of the two child restraint standards current in the U.K., namely BS 3254 - 1960 and ECE Regulation 44.

# THEORETICAL CONSIDERATIONS

The biomechanical properties of children vary considerably with age and children cannot be considered merely as scaled down adults. In general their growth is characterised by sudden spurts between times of slower and more uniform growth. Individuals of the same age group may show considerable differences in development. Several areas of the body require special considerations at different ages. For instance, the head represents about 25% of the total body length at birth but only about 14% when adult; the brain attains about 75% of its adult size by the end of the second year.

Burdi et al (1969) reviewed the anatomical parameters which must be taken into account when considering the restraint of children in vehicles and concluded that infants and young children relative to adults have:-

- (a) a large head on a thin neck
- (b) a thin skull, thus lacking protection for the brain against direct impact
- (c) a softer and shorter chest
- (d) a large and unprotected abdomen
- (e) a thick layer of subcutaneous tissue
- (f) a small pelvis with undeveloped iliac crests
- (g) a high centre of gravity
- (h) shorter and lighter legs
- (i) an inability to sit up unaided until the age of about 9 months.

These characteristics lead to the following criteria which must be considered in the design of a child restraint:-



- (1) Each age range requires its own type of restraint incorporating ease of adjustment to fit a variety of sizes particularly in the 9 months to 4½ years age group.
- (2) Direct impact of the child with car structures must be prevented, particularly for the head, chest and abdomen.
- (3) Violent deceleration of the child by the restraint must be avoided since it will produce a response from the relatively large head which loads the neck.
- (4) The restraint forces must be spread over a relatively large area.
- (5) Direct forces must not be applied to the child's abdomen.
- (6) The lap belt of a restraint must be prevented from sliding over the abdomen thus allowing the child to submarine.

These anthropometric requirements are reflected in National and International Standards which categorize children into three classes:-

the supine child,  
the younger sitting child, and  
the older sitting child.

Current child restraint standards normally define these classes in terms of the mass of the 50thile child of the given age range. Not all standards agree on the mass and age ranges, except for some measure of agreement on the age range of the supine infant (0 - 9 months). Table 1 shows the age groups specified in BS 3254 and ECE 44 respectively.

TABLE 1

Standard	Lower Limit kg	Upper Limit kg	Distinguished Groups kg	Corresponding Ages (50thile) yr	Date of Issue
BS 3254	9	36	9 - 18 18 - 36	½ - 4½ 4½ - 11	1960 rev.1968
ECE 44	9	36	9 - 18 15 - 25 22 - 36	½ - 4½ 3½ - 7½ 6½ - 11	1981

Table 2 shows the types of restraint commercially available in the U.K.

TABLE 2

Class	Age (years)	Type of Restraint
Supine child	0 - ½	Carry cot Stiffened carry cot
Younger sitting child	½ - 4½	Seat shell with harness - forward and rearward facing
Older sitting child	4½ - 11	Full harnesses, impact shields, adult restraints, booster cushions

Brockhoff (1976) describes a selection of child restraints commercially available.

#### OPTIONS AVAILABLE TO THE PARENT FOR RESTRAINING A CHILD IN THE FRONT PASSENGER SEAT

A study of the options available in the U.K. suggests that the parent may choose to restrain the child using one of the following options:-

- (1) Use a child safety seat or harness which complies with BS 3254 or ECE 44 for the younger and older sitting child. These standards do not cover the supine infant at present.
- (2) Use an adult lap and diagonal belt.
- (3) Use the lap strap only of an adult lap and diagonal, when the parent finds that the shoulder strap passes across the child's face (this may occur for children of age up to approximately 4 years).
- (4) Use a properly designed booster cushion in conjunction with an adult lap and diagonal belt.
- (5) Use an unlocated soft cushion to boost height.

In order to evaluate the results of the simulated tests and put them in perspective, it is appropriate to review the performance of options (1) and (2) using accident data.

#### ACCIDENT DATA

##### The unrestrained child

In accidents of the impact severity simulated in the tests described, accident data show that unrestrained children occupying both the front and rear seating positions are seriously or fatally injured.

In an analysis of 61 high energy frontal impacts, in which at least one child in each car was fatally injured, taken from the files of the University of Birmingham Accident Research Unit, Roy (1980) reported

that children who were not ejected from their Safe Ride Down Envelope (SRDE) received significantly less fatal injuries than those who were ejected. The SRDE is defined as the space in which the occupant may be decelerated without contacting the vehicle structure, thus for a child sitting in the front seating position the dashboard, door and roof represent the limits.

From the total sample of 93 seriously and fatally injured children, it was possible to identify injury agents for 22. Of these, 15 children who were seriously injured reached the limits of their SRDE, 13 of whom contacted a surface which was relatively energy absorbing. Of 7 children who were fatally injured, 5 struck relatively rigid parts of the vehicle. The distribution of injuries for the 93 children is shown in Figure 1. It will be noted that the majority of both non-life threatening injuries (39.2%) and life threatening injuries (12.8%) were to the head or face.

FIGURE 1 DISTRIBUTION OF AIS 1 - 3 (NON-LIFE THREATENING) AND AIS 4 - 6 (LIFE THREATENING) INJURIES GROUPED BY LOCATION FOR UNRESTRAINED CHILDREN - HIGH ENERGY IMPACTS

Total number of injuries - 227

	<u>AIS 1 - 3</u>	<u>AIS 4 - 6</u>
	<u>%</u>	<u>%</u>
Head and Face	39.2	12.8
Neck	1.3	0.9
Arms	11.5	0.9
Chest and Shoulder	9.7	1.3
Abdomen	1.3	4.8
Back	1.8	0.4
Legs	13.2	0.4
Shock Only	0.4	0
	<u>78.4%</u>	<u>21.6%</u>

These data suggest that children should be contained within their SRDE and prevented from contacting the vehicle structure, particularly with the head.

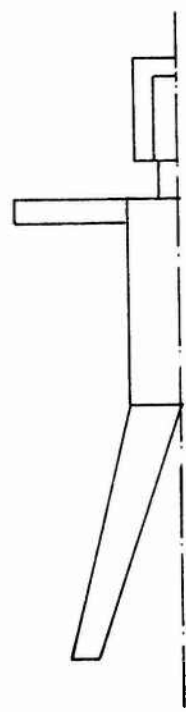
#### The child restrained in child systems

Roy et al (1980) reported the injury pattern of 762 children in accidents, of whom 571 were restrained in safety seats, 80 in harnesses, and 90 were unrestrained. (The safety seats and harnesses complied with BS 3254.) The data was obtained from questionnaire returns organised by TRRL in conjunction with KL Automotive Limited. The majority of the children in seats were within the age range 9 months to 4½ years implied by the standard (BS 3254), but over 50% of the children in harnesses were younger than the minimum age of 4½ years. Overall, the frequency of injury to unrestrained children was of the order of three times greater than for restrained children. The distribution of injuries to both restrained and unrestrained children is shown in Figure 2. The head, face and neck is the zone with the highest percentage of injuries.

The breakdown of injuries by severity for restrained children is shown in Figure 3. A theoretical disadvantage of forward facing restraints in frontal impacts is that the head may apply loads to the neck leading to injury during the time that the child's torso is being decelerated by the restraint. In practice, however, there were no neck injuries with a severity greater than AIS 1 in the restrained sample.

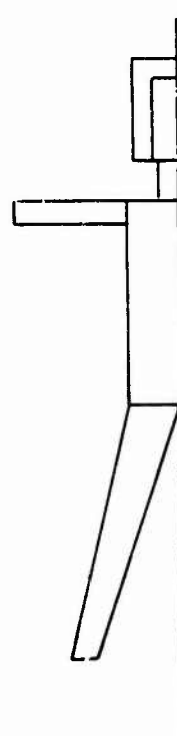
The frequency of neck injuries was of the same order as mouth lacerations and bruises to the torso.

FIGURE 2 SUMMARY OF LOCATION OF INJURIES GROUPED BY HEAD, TORSO AND EXTREMITIES - MEDIUM AND LOW ENERGY IMPACTS



	<u>Unrestrained Children</u>	<u>Restrained Children</u>
	<u>%</u>	<u>%</u>
Head, Face and Neck	63.0	52.8
Shoulder, Chest, Abdomen and Back	8.7	14.8
Arms and Legs	19.6	13.9
Shock Only and Area Unknown	8.7	18.5
	<u>100 %</u>	<u>100 %</u>

FIGURE 3 % OF INJURIES IN GIVEN LOCATION BY SEVERITY FOR CHILDREN RESTRAINED IN CHILD SEATS AND HARNESSSES - MEDIUM AND LOW ENERGY IMPACTS



	<u>Child Seats</u>			<u>Harnesses</u>		
	<u>Severity AIS</u>			<u>Severity AIS</u>		
	<u>1</u>	<u>2</u>	<u>3</u>	<u>1</u>	<u>2</u>	<u>3</u>
Head and Face	42.7	4.9	1.2	24.0	-	-
Neck	8.5	-	-	4.0	-	-
Chest, Shoulder, Abdomen and Back	12.2	1.2	-	20.0	4.0	-
Arms and Legs	9.8	3.7	-	12.0	-	-
Shock Only	4.9	-	-	16.0	-	-
Area Unknown	10.9	-	-	12.0	-	-
	<u>89.0%</u>	<u>9.8%</u>	<u>1.2%</u>	<u>88.0%</u>	<u>12.0%</u>	<u>0%</u>

### The child restrained in adult belts

There is firm evidence that a restraint appropriate to the child's age (and hence stature) is effective. Therefore, it is appropriate to examine accident data as a function of the child's age because it is the younger sitting child who is least likely to fit adult belts.

Comparatively little accident data have been published on the performance of adult belts restraining children, the literature that exists in general comes from sources outside the U.K. Siegal et al (1968) concluded that children of the age range 3 - 4 years may begin to use a standard lap belt, but should not use an adult lap and diagonal belt until they reach a sitting height of about 2 ft. (610 mm), or a standing height of 4 - 5 ft. (1220 mm - 1524 mm). This means an age of at least 6 years for a 50thile male.

Vazey (1977) reported on accidents involving children, mainly below 6 years of age, restrained by adult belts. He reported that 16 out of 37 children (43%) in lap and diagonal belts suffered head injuries of severity AIS 1 or greater and for children restrained by lap belts 6 out of 13 (46%) suffered severe head injuries. From the vehicle damage rating stated only 4 vehicles out of 119 appear to have had an equivalent ETS of the order of 25 km/h or more, which suggests this sample represents impacts of low to medium severity. The frequency of head injury to children in adult belts in Vazey's sample was of the same order as that of those children in child restraints in the Birmingham sample, i.e. 7 out of 18 (38.9%), which were in general high energy impact cases. These frequencies should be compared with 6% of the restrained children suffering head injuries of severity AIS 1 or more in the KL/TRRL sample where impact severity is more representative due to the sample size. Vazey tentatively recommended that adult belts, provided they are adjusted tightly, be used by children. He reported examples of ejection from loosely adjusted 'static' adult lap and diagonal seat belts.

Norin and Andersson (1978) reviewed accidents to 103 children in adult restraints. In this sample only one child was less than the age of 5 years, two of age 6 and four were of age 7, thus 93% were 8 years of age or older. Their report concluded that belted children are not injured more often or more severely than belted adults. In a further report, Norin et al (1979) concluded that adult belts are suitable down to the age of 7 years, possibly with the use of a booster cushion for those of small stature. They recommend that children in the age range 4 - 6 years remain in child seat restraints as long as possible and then use an adult belt with a booster cushion.

### SUMMARY OF CONCLUSIONS FROM PREVIOUS LITERATURE

Theoretical and field evidence suggest:-

- (1) That the age of the child and hence stature is the primary parameter when considering the use of adult belts.
- (2) For unrestrained children, contact with the vehicle structure and ejection are important injury mechanisms.
- (3) Child restraints which comply with BS 3254 are effective in reducing the frequency and severity of injury.
- (4) Both for unrestrained and restrained children, the head and face is the body area with the highest frequency of injury, and in the case of unrestrained children also the body area with the highest frequency of life threatening injuries.
- (5) For restrained children, neck injuries occur with both low severity and frequency and therefore do not seem to constitute a risk.
- (6) Field evidence to date lacks sufficient data on the effectiveness of adult belts as a restraint method for children below the age of 6 years.

These factors led to the conclusion that it would be constructive to conduct crash simulation tests appropriate to the younger sitting child (9 months - 4½ years) because this is the age range for which adult belt restraint may be most inappropriate and where the least field accident data exist.

### TEST FACILITY

The test programme was carried out on the KL/MP dynamic test rig in the Road Safety Engineering Laboratory at the Middlesex Polytechnic. The facility has been described elsewhere in detail, Hill and Roy (1982). In essence the rig consists of a rubber cord powered test sled. The sled can be accelerated in its present form up to a velocity of 55 km/h before impact. It is then decelerated using several different methods.

A block diagram of the instrumentation is shown in Figure 4. The instrumentation and data display system complies in the main with the requirements of SAE J 211. Sled velocity and acceleration are monitored using a timing gate and a uniaxial piezoresistive accelerometer respectively. Dummy head and chest accelerations are monitored using Endevco triaxial piezoresistive accelerometers, the output being displayed on an SE Labs UV recorder. Sled and dummy displacements are obtained from high speed films running at 500 f.p.s. and an eight lens polaroid camera provides an 'instantaneous' assessment of performance.

### TEST PROGRAMME

Simulated frontal impact tests were conducted from impact velocities between 45 km/h and 52 km/h using TNO P3 50thile 'three year old' dummies according to three general requirements, BS 3254, ECE 44 and ECE 16. These are referred to as Series 1, 2 and 3 respectively. Care was taken to simulate a realistic installation and strap configuration. Tests were carried out using either the seat specified in ECE 44 or a British Leyland 'Metro' seat. The anchorage points of the restraint simulated the position found with the Metro front seat at its mid position. Kangol dual safe lap and diagonal belts were used. For comparison purposes tests were also carried out using an 'adult' OPAT dummy of mass 75 kg.

The sled was decelerated from initial velocities of between 45 km/h and 52 km/h using either aluminium

FIGURE 4 BLOCK DIAGRAM OF INSTRUMENTATION

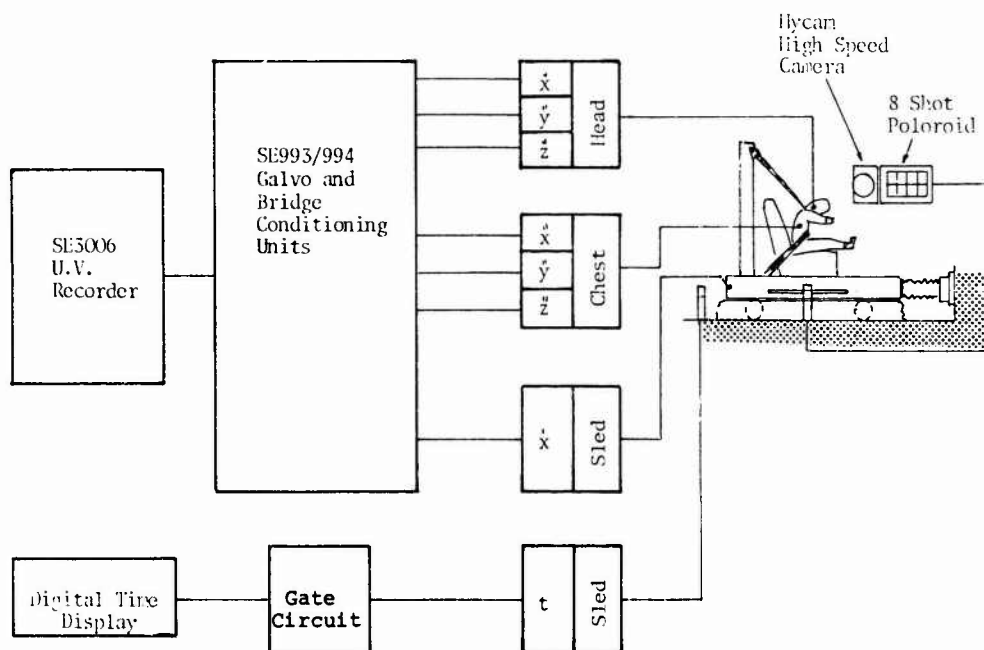
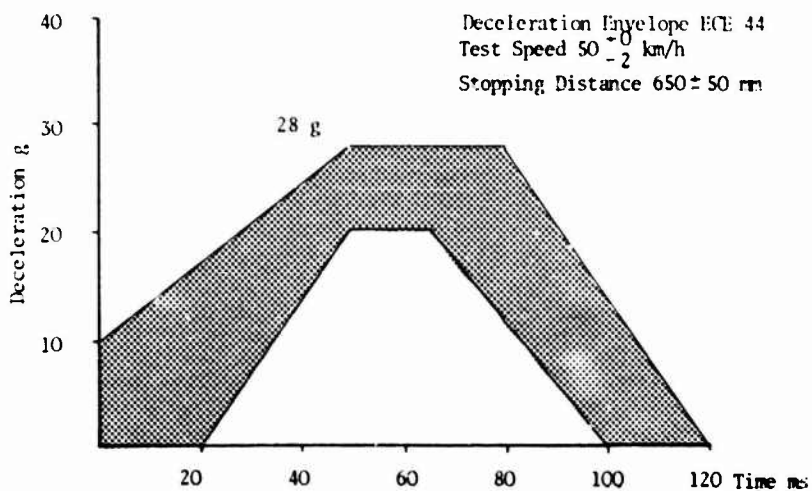
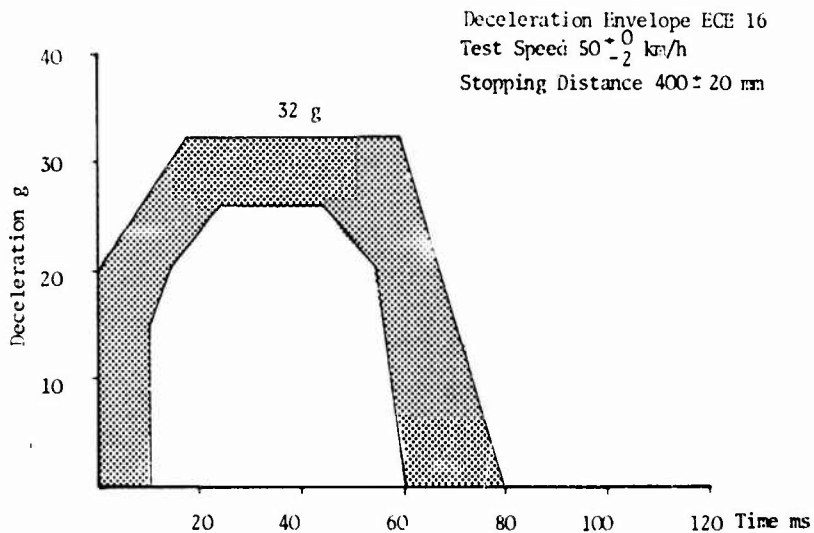


FIGURE 5 DECELERATION ENVELOPES FOR ECE 16 AND 44



crumple tubes or combinations of polyurethane tubes and olives. Thus a range of conditions was investigated which included the specific requirements of BS 3254 (Series 1), ECE 44 (Series 2) and ECE 16 (Series 3) respectively. (See Figure 5.)

#### Parameters measured

The following parameters were measured or derived:-

- (1) Sled velocity, deceleration and stopping distance.
- (2) Dummy head and chest decelerations in the X, Y and Z directions. (See Figure 6 for resultants.)
- (3) Dummy excursion.

The measured ranges of these parameters are shown in Table 3.

FIGURE 6.1 LAP AND DIAGONAL BELT - DUMMY HEAD AND CHEST RESULTANT DECELERATIONS

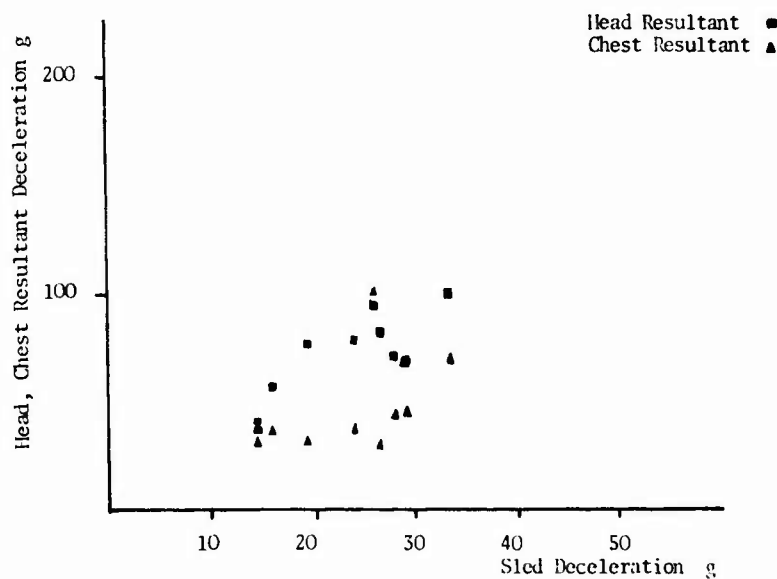


FIGURE 6.2 LAP BELT ONLY - DUMMY HEAD AND CHEST RESULTANT DECELERATIONS

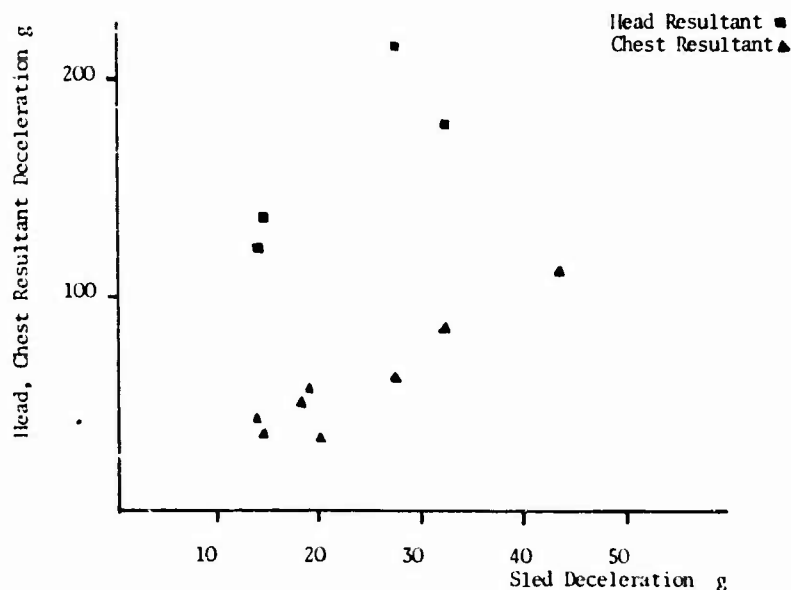


TABLE 3 MEASURED RANGES OF PARAMETERS

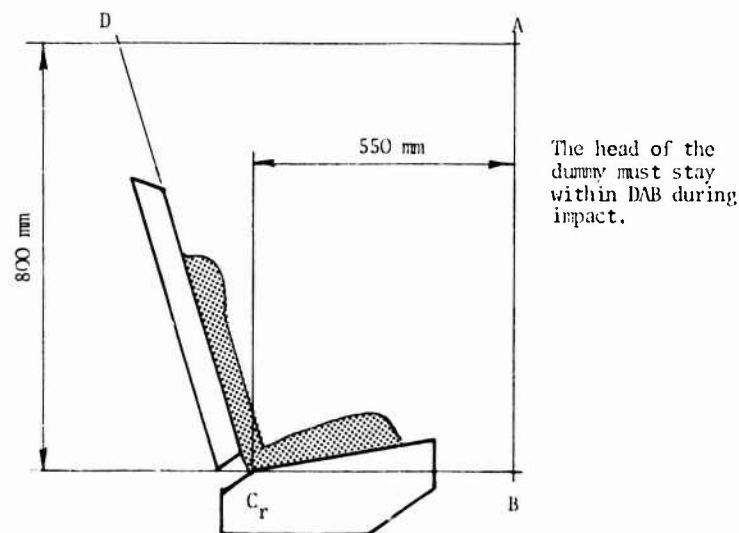
	Lap and Diagonal Belts			Lap Belts Only		
	Series 1	Series 2	Series 3	Series 1	Series 2	Series 3
Sled velocity (km/h)	44.9 - 46.6	47.2 - 52.1	46.0 - 51.2	44.9 - 47.2	49.6 - 51.2	51.2
Sled stopping distance (mm)	599 - 668	550 - 667	469 - 502	623 - 639	608 - 740	502
Sled deceleration (g)	14 - 16	19 - 29	26 - 33	14 - 15	27 - 43	33
Dummy:						
Resultant head deceleration (g)	34 - 59	70 - 80	90 - 97	125 - 136	84 - 216	180
Resultant chest deceleration (g)	30 - 37	30 - 45	70 - 100	35 - 45	61 - 111	85
Forward movement (mm)	< 550	< 550	< 550	> 550	> 550	> 550
Head contact	No	No	No	Yes	Yes	Yes

## DISCUSSION OF RESULTS

The performance of the systems tested have been evaluated in comparison to the requirements specified for child restraints in the various legislative standards for the age range of 9 months to 4½ years. Of those requirements forward movement is probably the most important. Head and chest decelerations are also clearly of great interest and have limits specified in the standards but the biomechanical justification for those limits is not totally clear. ECE 44 specifies a limitation of 550 mm forward movement (see Figure 7) and a maximum resultant chest deceleration of 50 g. This 550 mm critical dimension coincides with the front of the vehicle seat used in most of the tests described (this dimension on the Metro seat was 450 mm).

Measurements of the SRIE in a range of current production vehicles showed that the minimum distance between the C point and the fascia, with the front passenger seat in its maximum forward position, was about 435 mm (see Appendix 1).

FIGURE 7 FORWARD MOVEMENT LIMITATION FOR ECE REGULATIONS 16 AND 44

Lap and Diagonal configuration

In none of these tests did the dummy excursion exceed 550 mm nor was there any head contact. The range of forward movements from 300 mm to 434 mm suggests that in only 2% of vehicles a child could suffer a head contact with the fascia when restrained in the front passenger seat by a lap and diagonal belt. The minimum excursion measured (300 mm) occurred in Series 1 and the maximum excursion (434 mm) in Series 3.

Lap Belt only configuration

In all the lap belt only tests the dummy excursion exceeded the critical 550 mm with a minimum excursion of 608 mm and a maximum of 860 mm; in addition head contact occurred in each case. In contrast to the lap and diagonal configuration, head contact could occur in 86% of vehicles with the seat in its maximum forward position.

Head decelerations

With all restraints the head of the dummy rotates around the lateral Y axis and hence the vertical axis of the triaxial accelerometer tends towards becoming parallel with the ground at the point of maximum head excursion. Hence in lap and diagonal cases where a specific head contact does not occur, the value of the deceleration along the Z axis of the accelerometer tends to have the greatest value.

In the tests where the dummy was restrained by the lap belt alone, head contacts with the seat occurred and

in a number of cases a very high value of deceleration along the X axis of the head accelerometer was obtained.

#### Lap and Diagonal configuration

The resultant head decelerations varied between 34 g and 59 g with average sled decelerations of about 15 g (Series 1), whilst 70 g to 80 g were obtained for sled decelerations around 25 g (Series 2) and 90 g to 97 g when sled decelerations were around 30 g (Series 3). Therefore, the head decelerations in Series 1 and 2 tests were of the same order as those reported by Roy (1980) for child seats, whilst those for Series 3 tests were about 10 g higher.

#### Lap Belt only configuration

In the cases where a lap belt was used to restrain the dummy, very high head resultant decelerations were obtained because of head contacts with the seat. The highest resultants were 136 g (Series 1), 216 g (Series 2) and 180 g (Series 3). These resultants were between two and three times higher than those reported for child seats (ibid).

#### Chest decelerations

##### Lap and Diagonal configuration

For the dummy restrained by a lap and diagonal belt in test Series 1 and 2, the chest resultants were less than 50 g and the decelerations in the vertical direction less than 30 g which are the maxima specified in ECE 44. Hence the lap and diagonal configuration could be considered to comply with these requirements of ECE 44.

##### Lap Belt only configuration

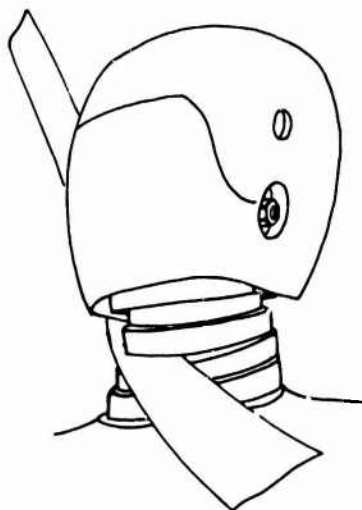
In Series 2 tests where a lap belt alone was used, chest resultants of 61 g to 111 g were obtained and the vertical component exceeded 30 g. Thus this configuration did not comply with the requirements of ECE 44.

#### Neck and Abdominal loading by straps

##### Lap and Diagonal configuration

The dummy was fitted with a plasticine neck collar and abdominal insert. For Series 1 and 2 tests no significant deformation occurred in either neck or abdominal simulations. In Series 3 tests, however, the diagonal strap penetrated the neck of the dummy. (See Figure 8)

FIGURE 8 STRAP PENETRATION OF NECK DISCS WHEN SUBJECTED TO ECE 16 PULSE



##### Lap Belt only configuration

Again although there was no evidence of significant deformation in the Series 1 and 2 tests, there was substantial deformation of the abdominal insert in Series 3 tests.

#### Comparison tests using the OPAT dummy

Comparison tests were carried out using the ECE 16 pulse and an OPAT adult dummy of mass 75 kg, using a lap and diagonal configuration. In none of the tests was the plasticine neck collar damaged or deformed by the belt. This is in line with field experience where neck injuries due to strap loading are not significant.

#### IMPLICATION OF CHILD DUMMY CONSTRUCTION ON PERFORMANCE

There has been much discussion over the risk of neck injury to children using adult belts although actual accident data, so far, does not demonstrate this to be a problem. The biofidelity of the dummy used in



these tests is clearly not at all exact, in particular because of the differences in chest stiffness between the dummy and real children. This is illustrated in the tests using the OPAT dummy which has a much more compliant chest. The results showed that the more the chest compresses the more likely is the diagonal belt to remain on the shoulder rather than load the neck.

Neck loading only occurred in the test series where the sled decelerations were well above those which occur in actual accidents (Ventre 1975). Current cars decelerate at lower levels than the ECE 16 pulse and thus the performance of the child dummy under these extreme conditions probably does not give an accurate insight into the kinematics of real children.

The second aspect of the TNO dummy is the abdominal insert. Again there is no direct relationship established between deformation of the insert and injuries to children. The United States for many years had experience of both adults and children using lap belts only in the front of cars, and up to the present time lap belts are the normal restraint system for rear seats.

The literature indicates that in actual accidents abdominal injuries only occur if some specific factor is present to compromise correct belt function. Such factors are gross obesity, incorrect belt positioning, unusual seat cushion characteristics or peculiar crash force directions, particularly in multiple impacts and rollovers. Hence doubt must be expressed over the interpretation of the performance of the dummy as far as its abdomen is concerned. Clearly submarining under a lap belt carries a risk of abdominal trauma but whether the dummy actually replicates such a motion of an actual child is debatable.

#### CONCLUSIONS

Simulated frontal impact tests using deceleration pulses generally in accordance with the requirements of BS 3254 (Series 1), ECE 44 (Series 2) and ECE 16 (Series 3) and using a three year old TNO 50thile dummy, restrained by either either an adult lap and diagonal belt or a lap belt only in an anchorage configuration simulating a Leyland Metro front passenger seat suggest:-

##### Lap and Diagonal Belt

When the system was subjected to the ECE 44 pulse and the less severe pulse applicable to BS 3254:-

- (1) The forward movement and resultant chest deceleration comply with the requirements of the child restraint standard ECE 44.
- (2) The resultant head decelerations are of the same order as those reported for child seat belt systems which comply with BS 3254 under the same test conditions.
- (3) The plasticine neck collar and abdominal implant showed no evidence of significant deformation or any significant loading by the straps of the restraint system.

When the system was subjected to the more severe ECE 16 pulses:-

- (4) The resultant chest decelerations were of the order of 10 g higher than those for the less severe pulses.
- (5) The forward movement of the dummy was within the requirements of ECE 44, and it is predicted that no head contact would occur in the majority of accidents.
- (6) The shoulder strap penetrated the dummy neck.
- (7) The abdominal insert showed no significant deformation.
- (8) Comparison tests using an adult OPAT dummy showed no similar neck loadings.

Thus the lap and diagonal belt configuration when tested according to the two pulses applicable in the U.K. to child restraint (BS 3254 and ECE 44) complied with the forward movement and chest deceleration limitations of ECE 44.

##### Lap Belt Only

- (1) The resultant chest decelerations were greater than those reported for the child safety seat and the adult lap and diagonal configuration by amounts from 15% (Series 1 tests) to 1.5 times (Series 3 tests).
- (2) The resultant head decelerations were greater than those reported for child seats and adult lap and diagonal systems by a factor of 2.
- (3) The more severe ECE 16 pulse (Series 3) produced major deformation of the plasticine abdominal implant, whilst the less severe ECE 44 (Series 2) and BS 3254 (Series 1) pulses did not.
- (4) In all tests the dummy forward movement was in excess of the critical 550 mm, varying from 10% in the Series 1 tests up to 1.6 times for the Series 3 tests. In all cases head contact occurred with the lower front of the seat or the sled structure.

Thus the lap belt only configuration when tested according to the two pulses applicable in the U.K. for child restraints resulted in excessive forward movement, well outside any SRDE, with a substantial risk of head contact in 86% of current European vehicles when the front passenger seat is adjusted to its maximum forward position. In addition the higher ECE 16 pulse when applied to the particular child dummy used in these tests, suggests that there was some risk of abdominal trauma, but because of reservations about the biofidelity of that body segment the interpretation of that information is debatable.

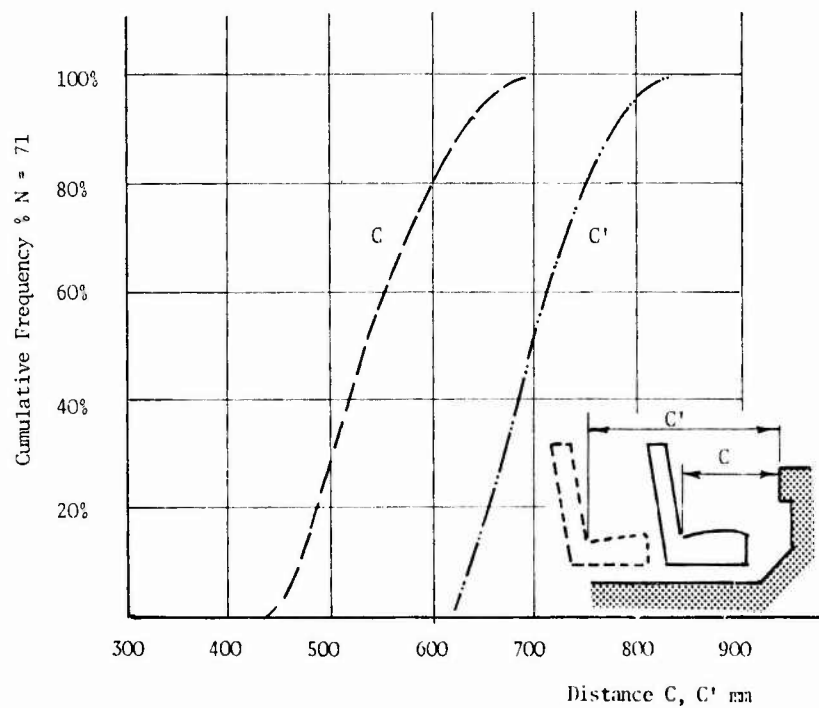
## REFERENCES

1. British Standard (1960). Seat Belt Assemblies for Motor Vehicles. BS 3254 1960. British Standards Institution. London, 1963.
2. ECE Regulation No. 44 (1981). Uniform Provisions concerning the Approval of Restraining Devices for Child Occupants of Power-Driven Vehicles (Child Restraints). E/ECE/Trans/505. Economic Commission for Europe, 1981.
3. ECE Regulation No. 16 (1979). Uniform Provisions concerning the Approval of Safety Belts for Adult Occupants of Power-Driven Vehicles. E/ECE/Trans/505. Revision 2. Economic Commission for Europe, 1979.
4. Burdi, A.R., Huelke, D.F., Snyder, R.G. and Lowrey, G.H. (1969). Infants and Children in the Adult World of Safety Design: Pediatric and Anatomical Considerations for the Design of Child Restraints. *Journal of Biomechanics*, 2, 3, pp 267-280. 1969 (Pergamon Press).
5. Brockhoff, H.S.T., Oudesluys, C. and Bastiaanse, J.C. (1976). Description of Child Restraint Devices. Instituut Voor Wegtransportmiddelen TNO, Report No. 713003-C. Delft, 1976 (TNO/Volvo).
6. Roy, A.P. (1980). Restraint System Performance and Limitations for Child Occupants of Motor Vehicles. M.Sc. Thesis, University of Birmingham, 1980.
7. Roy, A.P., Mackay, G.M. and Gloyns, P.F. (1980). Some Observations on the Modelling of Children in Car Collisions based on Field Accident Investigations. Proc. 5th International Conference of the International Research Committee on the Biokinetics of Impact. Birmingham, September 1980.
8. Siegal, A.W., Nahum, A.M. and Appleby, M.R. (1968). Injuries to Children in Automobile Collisions. Proc. 12th Stapp Car Crash Conference, New York, 1968 (SAE).
9. Norin, H. and Andersson, B. (1978). The Adult Belt - a Hazard to the Child? Department of Traffic Accident Research, AB Volvo Car Division, 1978.
10. Norin, H., Saretok, E., Jonasson, K., Andersson, A., Kjellberg, B. and Samuelsson, S. (1979). Child Restraints in Cars - An Approach to Safe Family Transportation. Paper 790320. Proc. Automotive Engineering Congress, Detroit, February 1979. (SAE)
11. Vazey, B.A. (1977). Child Restraint Field Study. Traffic Accident Research Unit, Department of Motor Transport, New South Wales. Research Report, November 1977.
12. Hill, K.J. and Roy, A.P. (1982). Simulation of the Effects of Vehicle Impacts on Restrained Child Occupants - Part A: A Description of the KL/MP Dynamic Test Facility. *Journal of the Society of Environmental Engineers*, 21, 1, March 1982. (SEE)
13. SAE J211 (1970). Instrumentation for Barrier Collision Tests. Automotive Society Safety Committee Report, New York, 1970. (SAE)
14. Ventre, P. (1975). Proposal of Methodology for Drawing Up Efficient Regulations. Report of Regie Nationale des Usines Renault, May 1975.

## ACKNOWLEDGEMENTS

The authors would like to thank Mr. R. Lowe of TRRL and Mr. G. Rothman of K.L. Automotive Limited for the use of field data for the restrained child. We are also grateful for the continued support of K.L. Automotive Limited for KL/MP Dynamic Test Facility.

FIGURE 9 CUMULATIVE FREQUENCY - DISTANCE C, C'



The distance between the approximate  $C_r$  point and the dashboard in the front seat passenger space was measured in 71 (1981) cars. The results are shown above. C represents the distance with the passenger seat adjusted to its maximum forward position, C' with the seat adjusted to the maximum rearward position. Measurement was to  $\pm 2\frac{1}{2}$  mm although judgement of the  $C_r$  point was to  $\pm 10$  mm.

## DISCUSSION

DR. VONGIERKE (USA)

For equal crash/impact deceleration, is there a higher probability of abdominal injury from lap belts in children compared to adults? What do the accident data show?

## AUTHOR'S REPLY

The injury distribution was such that the proportion of abdominal injuries in the field sample of restrained children was 2 to 4% depending on the type of restraint. (Child restraints were full harnesses) This sample was considered to be reasonable representative in terms of accident severity distribution. Two adult samples that I have found in the literature suggest 4-5%. (Adult restraints were lap and diagonals) A further reference which was concerned with high-energy accidents suggested 6-7%. Hence, I think it reasonable to conclude from the data available that the proportions are the same order due to the lap belt component of a seat belt system. I do not have any data on lap belts only, to make a similar comparison.

DR. WOLTRING (NE)

Would you care to comment on new British legislation relative to mandatory seat belts for front seat children in view of legislation in various European countries forbidding children below 12 years in front seats.

## AUTHOR'S REPLY

Personally, I would rather prohibit children below the age of twelve from the front seats of cars and require that they be restrained in the rear. However, a problem occurs if one has four children in most cars, or if there are no suitable restraints in the rear. Then a choice has to be made between unrestrained in the rear or restrained in the front. Our paper has reported cases of serious and fatal injuries to unrestrained children in the rear, it being noted that some of the children were ejected. Further, in our simulated tests which represented severities of the majority of accidents, the performance of the "3 year old" dummy in lap and diagonal belts seemed reasonable. Thus, it seems reasonable to suggest that children down to this age would be better restrained in the front than unrestrained in the rear. I think we must await more field evidence, however to support this hypothesis.

DR. WOLTRING (NE)

To what extent are child movements in frontal collision predominantly planar, in view of: (1) asymmetric shoulder belts; (2) Falling asleep with head turned sideways, and what is the influence of such factors on the neck injuries referred to with shoulder belts in your paper?

## AUTHOR'S REPLY

In the sled tests the dummies were set up (when restrained in lap and diagonal belts) so that prior to the impact they were symmetrical with respect to the sled centre line. In some of the tests the motion of dummies' head was asymmetric. It therefore seems a reasonable hypothesis, that if the dummy had been set up with the head initially on one side to simulate a sleeping child, then this asymmetrical excursion would have been accentuated. In one of the lap-belt-only tests, the head of the dummy moved sideways to such an extent that it struck the steel support structure of the seat and sustained a "simulated skull fracture" of about 4 cm length.

# VALIDATION OF A BIODYNAMIC INJURY PREDICTION MODEL OF THE HEAD-SPINE SYSTEM

by

Eberhardt Privitzer  
Air Force Aerospace Medical Research Laboratory  
Wright-Patterson Air Force Base, Ohio 45433  
U.S.A.

and

Ronald R. Hosey and James E. Ryerson  
Systems Research Laboratories, Inc.  
Dayton, Ohio 45440  
U.S.A.

## SUMMARY

This paper describes mathematical models of the human and baboon head-spine structures. These models consist of fully three-dimensional assemblages of rigid bodies and deformable elements, for which the equations of motion are solved using a large displacement, small deformation dynamic matrix structural analysis program. A validation program for these models is outlined with particular emphasis on the refinement and validation of the baboon head-spine model. Results are described from a series of drop test simulations which were run to study the effects of variations in the degree of spinal curvature on head-spine system dynamic response.

## INTRODUCTION

Interest in the dynamic response of the human head-spine structure to high vertical ( $+g_z$ ) accelerations dates back to the mid 1940s. It was during this time that jet-powered aircraft began to emerge as the dominant force in military aviation. The relatively large increase in the airspeeds of jet-powered aircraft over the, then conventional, prop driven planes greatly complicated the process of occupant escape from a disabled plane; safely clearing the components of the plane became a major problem. This brought about the development of the ballistically fired ejection seat which, since the spine is the primary path of load transmission between the seat and the head, eventually led to the question of human head-spine structure tolerance to  $+g_z$  accelerations. Performance envelopes of military aircraft have increased substantially since the early jets, and will most likely continue to do so, with the result that crewmembers of these aircraft are (and will be) subjected to increasingly greater and more complex acceleration environments. The need to be able to predict human head-spine structure dynamic response and injury likelihood in these types of environments has, therefore, increased and will continue to do so.

Belytschko et al. [1], Belytschko and Privitzer [2], [3], and Privitzer [4] summarized many earlier studies of human dynamic response to  $+g_z$  impact accelerations. The mathematical models used in these studies were, for the most part, rather simple lumped mass approximations of the head-spine system limited to one-dimensional motion (i.e. along the spinal axis) and to only a few degrees of freedom. The best known of these earlier models, the DRI (Dynamic Response Index) Model, a single-degree-of-freedom approximation of the human head and torso which has been, to some degree, correlated with injury data and drop tower tests, is the analytical tool currently used to represent the occupant in the design of emergency escape systems for military aircraft.

Unfortunately, the one-dimensional nature of the DRI and similar models renders their range of applicability extremely limited. Examples of situations to which these models can not be meaningfully applied include: head-spine system responses in multiple-g environments; situations where the spinal flexural response is significant; interactions between the head-spine system and the ejection seat-back and restraint system; etc. The needs to overcome these shortcomings and to obtain more accurate and encompassing predictions of head-spine dynamic response and injury potential, particularly in light of increasingly greater emergency escape system performance demands, prompted the development of a considerably more sophisticated mathematical model of the head-spine structure, the Air Force Aerospace Medical Research Laboratory's (AFAMRL) Head-Spine Model (HSM) ([1], [2], [3], [4], [5]). The HSM differs from previous models in that it is fully discretized, i.e., the deformation and inertial characteristics of each vertebral level are represented; the structural effects of the rib-cage and viscera-abdominal wall system are accounted for; interactions between the HSM and the ejection seat and the restraint system are accounted for and the governing equations are fully three-dimensional.

Both experimental and analytical approaches have been used to investigate human body tolerance to  $+g_z$  impact accelerations. It is generally accepted that neither approach will stand alone when applied to investigations of human injury levels - they must be logically combined if meaningful results are to be achieved. The initial development of the HSM required the integration of sophisticated mathematical formulations of the governing equations with experimental measurements of material, inertial and geometric properties data required to define the system. The refinement and validation of this model, though also requiring some further mathematical formulations, relies heavily on experimental work, specifically, laboratory tests with human volunteers, cadavers and nonhuman primates and extensive measurements of material, inertial and geometric properties data.

This paper describes the HSM validation program. Particular emphasis is placed on the development, refinement and validation of a model of the baboon (*Papio Anubis*) head-spine structure, the BHSM. This model plays a very important role in the validation of the HSM.

## MODEL DESCRIPTION

## A. The Human Head-Spine Model (HSM)

The HSM has been described extensively in [1], [2], [3], [4] and [5], hence only a brief description is given here. The HSM is a mathematical representation of the human body (specifically the torso and head) consisting of a fully three-dimensional system of rigid bodies interconnected by deformable elements. The rigid bodies represent the inertial characteristics of the head, pelvis, sections of the torso, some skeletal components (such as the ribs) and can also be used to represent obstacles external to the model (such as components of the cockpit environment). Each vertebrae is defined geometrically by a set of 13 points and is contained in a rigid body which represents the inertial properties of a section or a portion of a section of the torso. A section of the torso, corresponding to a specific vertebral level, is defined as the material bounded by parallel planes perpendicular to the vertical (Z) axis and passing through the center of the inferior and superior intervertebral discs and by the torso wall (Liu and Wickstrom [6]).

The rigid bodies interact through deformable elements (springs and beams) which represent the various connective tissues: the intervertebral discs, the spinal ligaments, the articular facets; the viscoelastic properties of the viscera-abdominal wall system; the costovertebral and costotransverse joints, the interchondral cartilage and intercostal tissues of the rib cage.

An ejection seat is defined by a specified number of planes. Interactions between the HSM and the ejection seat are defined by a nonlinear viscoelastic force-deformation relationship. The HSM can be driven through the ejection seat by prescribing the motion of the planes. It can also be driven directly by prescribing either the forces on, or the motion of, any of the rigid bodies' mass centers.

A restraint system can be defined using either spring elements between the ejection seat and the model or by a harness-torso interaction algorithm used for occupant retraction simulations. A new, considerably more general restraint system model will be implemented in the near future. This model will account for loss of contact between the belts and the torso, and sliding of the belts along the torso.

The governing equations for the motions of the rigid bodies and the loadings developed in the deformable elements which make up the HSM are solved using a matrix structural dynamics analysis program. This program is based on a large-displacement, small-strain formulation which uses a rigid-convected or corotational treatment of the deformable elements to decompose the element nodal displacements into rigid body and deformation components (Belytschko and Hsieh [7]). Three solution schemes are available for solving the equations of motion for the displacements, velocities and accelerations of the rigid bodies. The first two are explicit and implicit integration schemes which correspond to the Newmark- $\beta$  numerical temporal integration formulas with  $\beta = 0$  and  $1/4$  respectively (Newmark [8]). The third is a modal analysis approach which uses a standard linear eigenvalue routine to obtain the eigenvalues (squares of the natural frequencies) and eigenvectors (natural vibration modes) of the system.

The HSM has an injury prediction postprocessor which determines the likelihood of spinal injury at each vertebral level due to combined axial compression and bending loads computed during a simulation. The failure criteria currently used are the axial compression (for pure compression) and bending moments (for pure A-P or lateral bending) which would result in the exceeding of the experimentally determined cortical shell compressive yield stress at each vertebral level of the thoracolumbar spine. In developing these failure criteria, the vertebral bodies were treated as elliptical cylinders with inner cores consisting of cancellous bone and .3 mm thick outer shells consisting of cortical bone. Although this approach appears to be reasonable, we are currently conducting an investigation, involving finite-element analyses of vertebral bodies, to gain better insight into the effects of geometric and material property variations on vertebral body stress distributions. Based on these studies, we also hope to formulate a relationship(s) between stress distributions resulting from specified three-dimensional endplate loadings and observed vertebral body failure patterns. The results of this study will be incorporated into the HSM injury prediction capability.

The HSM data base consists primarily of the material property data describing the deformation characteristics of the deformable elements; the geometric and inertial distribution data describing the rigid bodies; connectivity data which aligns the appropriate deformable elements and rigid bodies; and the data which defines the external environment - the ejection seat, restraint system and specified force or motion excitation.

Figure 1 depicts the sagittal plane (right side) and frontal plane (from the back) views of the HSM. Shown are the rigid bodies used to model the head, pelvis, ribs and sternum, and the specified geometries of the cervical (C2 through C7), thoracic (T1 through T12) and lumbar (L1 through L5) vertebrae. Not shown but present within the model are: (1) the deformable elements representing the connective tissues such as ligaments as well as the deformation characteristics of motion segments C2-C3, C3-C4, ... L4-L5 and L5-S1 (a motion segment consists of an intervertebral disc plus half of the inferior and superior vertebral bodies); (2) the rigid bodies representing the inertial effects of sections of the torso; (3) the ejection seat and restraint system. The configuration shown in Figure 1 is representative of the geometry of the head-spine-pelvis structure in a seated-upright adult male.

Figure 1 shows the HSM in its most complete form. Simulations are often run in which the detailed responses of certain components or subsystems of the model are not of primary interest. For these cases, the option exists to replace the detailed models of these subsystems with equivalent simplified representations having similar overall deformation and inertial characteristics. Any subsystem can be replaced with the result that the number of degrees of freedom ranges from 300 [50 primary nodes (rigid body mass centers) times (3 translations + 3 rotations) per node] for the complete model plus ejection seat to 60 for the most simplified HSM plus ejection seat - a considerable reduction in computational effort. The version of the HSM which we currently use most frequently consists of rigid bodies representing the head and pelvis; a single beam element representing the cervical spine; a fully discretized representation of the thoracolumbar spine; and an additional column of nonlinear beam elements representing the secondary loading path along the viscera-abdominal wall-diaphragm-rib-cage system. This model plus the ejection seat has 126 degrees of freedom.

#### B. The Baboon Head-Spine Model (BHSM)

The BHSM is shown in Figure 2. The basic construction of this model is similar to that of the HSM, i.e. a system of rigid bodies connected by deformable elements. The BHSM consists of rigid bodies representing the head; torso segments corresponding to vertebral levels T1 through T12 and L1 through L7; the pelvis; a single deformable element representing the neck; beams representing the T1-T2, T2-T3, ..., L6-L7, L7-S1 motion segment stiffnesses, and a column of nonlinear beam elements representing the secondary loading path along the viscera-abdominal wall-diaphragm-rib-cage system. As for the HSM depicted in Figure 1, the deformable elements of the BHSM are not shown in Figure 2. The BHSM has 126 degrees of freedom.

Belytschko and Privity [2] developed the preliminary model of the baboon head-spine structure. They had very little pertinent data to work with, hence they proceeded to develop just the basic model structure, anticipating that necessary material, inertial and geometric property data would be incorporated into the model as they became available. The model shown in Figure 2, although a refined version of the preliminary model, is still based on a large number of extrapolations and approximations. Further refinements will be made as additional data become available. The following paragraphs summarize the procedures used to develop the present BHSM data base.

**Geometry:** The BHSM configuration depicted in Figure 2 is based on a lateral radiograph of a 25-kg adult male baboon seated upright (tightly restrained) in a vertical drop test vehicle. The dimensions of the vertebrae and pelvis were obtained from the same plus similar radiographs. The head geometry is based on data measured by Reynolds [9] plus measurements, taken by the authors, of an adult male baboon skull.

**Inertial Distribution:** The BHSM mass distribution is based on torso dimensions obtained from the above-mentioned radiographs, direct measurements of the 25-kg adult male baboon (heavily sedated) plus data obtained by Reynolds, who measured the inertial properties of anatomical segments of four frozen cadaver baboons. The mass, mass center and principal moments of inertia at each vertebral level were calculated by sectioning the torso (having overall dimensions assumed to correspond to those of a typical 25-kg adult male) into discrete segments with the number of segments equal to the number of vertebral levels in the model (19). Each torso segment is defined as the material contained in an elliptical cylinder having a height equal to the distance between the midpoints of the inferior and superior intervertebral discs of the contained vertebra and major and minor diameters consistent with the overall torso dimensions. A density of 1 gm/cm<sup>3</sup> was assumed. The head mass, mass center and principal moments of inertia were based on Reynolds' data but were scaled up to correspond to a 25-kg adult male baboon.

**Stiffness Data:** Motion segment axial stiffnesses are based on motion segment compression load deformation curves obtained by Kazarian [10]. No bending or torsional stiffness data were available, hence these were calculated by assuming that the ratio of bending or torsional stiffness to axial stiffness for baboons was proportional to that for humans, resulting in the equation

$$\left( \frac{k_{\alpha}}{k_a} \right)_B C_{\alpha} = \left( \frac{k_{\alpha}}{k_a} \right)_H, \quad \alpha = b, t \quad (1)$$

where the subscripts a, b and t stand for axial, bending and torsion, respectively; the subscripts B and H stand for baboon and human; k stands for stiffness and C, the proportionality constant.  $C_{\alpha}$ , for bending and torsion, were determined by substituting the appropriate expressions for the stiffnesses in (1), yielding for bending and torsion respectively,

$$\left( \frac{EI/L}{EA/L} \right)_B C_b = \left( \frac{EI/L}{EA/L} \right)_H \quad (2)$$

and

$$\left( \frac{GJ/L}{EA/L} \right)_B C_t = \left( \frac{GJ/L}{EA/L} \right)_H$$

Simplifying equations (2) and solving for  $C_b$  and  $C_t$  results in

$$C_b = \left( \frac{I}{A} \right)_H \left( \frac{A}{I} \right)_B \quad (3)$$

and

$$C_t = \left( \frac{J/A}{2(1+\nu)} \right)_H \left( \frac{2(1+\nu)}{J/A} \right)_B$$



where A, I and J are the cross-sectional area and the rectangular and polar area moments of inertia respectively and  $\nu$  is the effective Poisson's ratio. To further simplify (3), it was assumed that  $\nu$  is the same for baboon and human motion segments, and that a typical baboon or human motion segment could be geometrically approximated as a circular cylinder with equivalent radius R. Equations (3) therefore yield

$$C_h = C_t = \frac{R_H^2}{R_B^2} \quad (4)$$

Substitution of this result into (1) and solving for  $(k_\alpha)_B$  yields

$$(k_\alpha)_B = \frac{R_B^2}{R_H^2} (k_\alpha)_B \left( \frac{k_\alpha}{k_a} \right)_H, \quad \alpha = h, t \quad (5)$$

The BBSM geometric, inertial and stiffness data are summarized in Tables 1 and 2. Note that the assumption that the effective Poisson's ratios for human and baboon motion segments are identical, although at first glance seemingly reasonable - i.e. because the geometries and materials are quite similar - may not be all that good. Comparisons of radiographs of human and baboon spines have demonstrated a significant difference in vertebral trabeculae orientation [11]. In human vertebrae, the mean trabeculae orientation is parallel to the vertical axis (inferior-superior), in baboons it is perpendicular to this axis (anterior-posterior). Mean trabeculae orientation corresponds to the axis of greatest stiffness, hence the ratio of axial compression to lateral extension (i.e. the effective Poisson's ratio) for human and baboon motion segments may significantly differ. An investigation of the effects of differences in mean trabeculae orientation on human and baboon motion segment behavior as well as the overall spinal load transmission properties could be quite interesting.

#### HSM VALIDATION PROGRAM

The HSM, once validated for an appropriate range of applications, will be used to develop design criteria for military aircraft emergency escape systems and other impact-inducing systems. The refinement and validation of the HSM involves laboratory tests with human volunteers, cadavers, nonhuman primates (specifically, baboons (Papio Anubis)), evaluation of operational accident data and an extensive amount of material, inertial and geometric properties data acquisition.

Data obtained from low-level laboratory tests with human volunteers can be used for direct comparison to model predictions from simulations of such experiments. These tests consist of impact experiments (e.g. drop tower, sled runs) vibration experiments (e.g. impedance tests) and any other appropriate experiments such as laboratory retraction simulations. A number of these types of HSM simulations have been run and reasonable qualitative and quantitative agreement between HSM predictions and experimental observations has been observed ([1], [2], [3] and [4]). Unfortunately, the low-level experiments which have been simulated to this point were not run for the purpose of measuring parameters to be used in model validation. As a result, any one experiment has supplied only a minimal amount of useful data. It is anticipated that better communication between the model developers and experimentalists will improve this situation.

Although simulations of low-level laboratory tests are necessary to establish the validity of the HSM in noninjury applications, the primary reason for the development of the HSM is to predict human body dynamic response and injury potential in high-level (injury threshold and above) mechanical environments. To validate the HSM for high-level applications requires measured high-level responses. The extrapolation of human dynamic responses involving injury from either low-level testing with human volunteers or high-level testing with cadavers is severely limited in its validity. Major limiting factors include the highly nonlinear behavior exhibited by the human body in the first case, and differences in tissue mechanical properties and muscle tone between humans and cadavers in the second. Operational accident reports are an obvious source of injury-level human response data. However, analyses of these reports has, up to this point, yielded little useful information. Another source of injury-level data are high-level laboratory tests with nonhuman primates. The inference of injury environment human dynamic response data from observed injury responses of nonhuman primates is not an uncommon practice in biodynamic research. The apparent anatomical similarities between humans and nonhuman primates seem to justify this to a certain point. However, it can be shown that those anatomical differences which do exist between humans and nonhuman primates are significant to the point that the direct scaling of injury environment responses of nonhuman primates to humans has limited validity [12].

The requirement for a direct approach to model validation for injury-level environments prompted the development of the baboon head-spine model (BBSM). Observed responses from injury-level baboon drop tests can be directly compared to BBSM predictions from simulations of these tests. The obvious question which comes to mind is that, "Yes indeed, this may result in the direct injury-level validation of the BBSM, but what about the HSM?" The HSM and BBSM are based upon the same modeling concepts, i.e. the formulation of the governing equations, the numerical integration schemes, and the types of data and measuring techniques which define the data base are identical for both models. Hence, injury-level validation of the BBSM validates the HSM modeling concepts for injury-level applications. In addition, appropriate comparisons of HSM and BBSM predictions can provide much needed insight into the relationships between human and nonhuman primate dynamic response mechanisms, and hence into use of nonhuman primates as surrogates for humans in injury environment testing.



TABLE 1. BISM GEOMETRIC AND INERTIAL DATA

Level	Mass Center <sup>(1),(2)</sup> Coordinates (cm)		Mass <sup>(3)</sup> m	Moments of Inertia <sup>(4)</sup>		
	Y	Z		I <sub>x</sub>	I <sub>y</sub>	I <sub>z</sub>
Pelvis	-0.1	3.45	61.5365	23.3629	26.6074	11.3813
L7	0.74	1.885	5.8877	0.6118	1.1276	1.6112
L6	-0.18	5.44	6.1445	0.7132	1.1740	1.7589
L5	-0.83	8.89	6.0455	0.7642	1.1470	1.8011
L4	-1.47	12.14	6.3560	0.9249	1.2029	2.0182
L3	-1.905	15.32	6.5737	1.1221	1.2597	2.2732
L2	-2.37	18.39	6.7742	1.2465	1.2751	2.4186
L1	-3.09	21.19	5.9706	1.1626	1.1113	2.2082
T12	-3.63	23.73	5.9677	1.2131	1.1093	2.2597
T11	-4.40	26.22	6.0144	1.2892	1.1167	2.3452
T10	-5.02	28.65	5.9992	1.3538	1.1122	2.4088
T9	-5.535	30.66	4.1668	0.9300	0.7622	1.6731
T8	-5.93	32.27	3.8605	0.8161	0.7053	1.5053
T7	-6.51	33.86	3.7972	0.7768	0.6938	1.4548
T6	-6.93	35.50	3.9041	0.7313	0.7146	1.4270
T5	-7.17	37.12	3.3046	0.5685	0.6031	1.1592
T4	-7.32	38.63	3.1947	0.4983	0.5832	1.0692
T3	-7.35	40.165	5.7004	0.3998	0.5473	0.9351
T2	-7.29	41.72	5.4429	0.3190	0.5229	0.8428
T1	-7.18	43.34	4.9342	0.2316	0.4744	0.6943
Head	-10.91	52.13	19.4000	6.5414	2.8263	6.5414

(1) X, Y and Z are positive to the left, rear and up, respectively.

(2) All mass centers' X coordinates are 0.

(3) Grams  $\times 10^2$ .

(4) Grams -  $\text{cm}^2 \times 10^4$ .

TABLE 2. BISM STIFFNESS DATA

Motion Segment	Axial <sup>(1)</sup> Stiffness	Bending <sup>(2)</sup> Stiffness	Torsional <sup>(3)</sup> Stiffness	Shear <sup>(4)</sup>
				Deformation Parameter
Neck	0.25	0.49	0.38	0.08
T1-T2	1.95	3.82	2.96	0.52
T2-T3	2.22	4.35	3.37	0.51
T3-T4	2.47	4.84	3.75	0.50
T4-T5	2.67	5.23	4.06	0.54
T5-T6	2.87	5.62	4.36	0.57
T6-T7	3.08	6.04	4.68	0.55
T7-T8	3.25	6.37	4.94	0.53
T8-T9	3.44	6.74	5.22	0.47
T9-T10	3.58	7.02	5.04	0.41
T10-T11	3.77	7.39	5.73	0.33
T11-T12	3.91	7.66	5.94	0.26
T12-L1	3.93	7.70	5.97	0.22
L1-L2	3.96	7.76	6.02	0.18
L2-L3	3.91	7.66	5.94	0.11
L3-L4	3.87	7.59	5.88	0.12
L4-L5	3.83	7.51	5.82	0.12
L5-L6	3.82	7.49	5.81	0.11
L6-L7	3.76	7.37	5.72	0.10
L7-S1	3.51	6.88	5.33	0.10

(1) Dynes  $\times 10^9$

(2) Dyne-cm  $\times 10^8$ ; A-P and lateral bending stiffnesses are currently the same.

(3) Dyne-cm  $\times 10^8$

(4) The shear deformation parameters are combined with the bending stiffnesses because shear effects during motion segment bending are not negligible.

## SIMULATION RESULTS

Figure 3 depicts BISM configurations at times 0, 10, 20 and 30 msec for a preliminary drop test simulation. This run was not made to simulate any specific baboon drop, rather its purpose was to determine if the model behaved realistically for the prescribed input. An approximately trapezoidal acceleration profile having a rise time of 4.5 msec, a constant magnitude of +30  $g_z$  for 8.4 msec and a drop off (to zero) time of 3.6 msec for a total duration of 16.5 msec was prescribed to act on the seatback. Ideally, this same profile would have been prescribed at the seat pan also. At present, however, the highly nonlinear deformation characteristics of the material (primarily the buttocks) which would transmit the seat pan acceleration to the pelvis are not well defined.

The option of prescribing either the given acceleration on the pelvis directly (which would roughly correspond to the instantaneous "bottoming-out" of the buttocks) or that of specifying a vertical force time history on the pelvis were studied through a number of similar preliminary simulations. The force time history was scaled down from a force profile measured using load cells in the seat pan during an actual 70  $g_z$  baboon drop. It was found that when the nonlinear viscoelastic effects of the buttocks were ignored by prescribing the acceleration of the pelvis directly, the computed spinal motion and force responses, particularly in the vicinity of the pelvis, were considerably more severe (as well as somewhat unrealistic) than when the force time history was prescribed. Based on these results, it was decided that all such simulations would subsequently employ a prescribed vertical force time history on the pelvis until a suitable representation of the deformation characteristics of the buttocks is included in the BISM. Although no actual 30  $g_z$  baboon drop test results were available for comparison, the computed motion and force time histories and the BISM configurations shown in Figure 3 are felt to be reasonable for the prescribed input.

Figure 4 shows BISM configurations at times 0, 10, 20 and 30 msec from a simulation of a 70  $g_z$ , 15 msec baboon drop test. Approximations to the vertical acceleration profile of the drop vehicle and the measured seat-pan force time history were prescribed at the seatback and pelvis, respectively. No restraint system was defined for this simulation (nor in the simulation previously described nor for those to be described below). It was felt that no significant loading into the restraint system would occur during the time duration which was considered (30 msec).

Table 3 compares peak resultant accelerations at the head (measured with a rigidly mounted triaxial accelerometer) and vertebral levels L1 and L7 (measured with implanted triaxial accelerometers) measured during the drop to the corresponding accelerations as predicted by the BISM. The measured values appear to be somewhat high, but since some dynamic overshoot (exceeding of the peak input values) is to be expected in an underdamped system, they may be consistent with the drop vehicle acceleration profile. By the same reasoning, the BISM values appear to be somewhat low. This was actually not an unanticipated result, since it was felt that the overall stiffness of the torso might be too low due to the difficulty in accurately accounting for the nonlinear stiffening effects of the rib-cage and viscera-abdominal wall systems. Assuming that the BISM motion segment stiffness data are reasonable, a low overall torso stiffness would result in lower than expected axially transmitted loads and accelerations, and increased bending responses. This is apparent in the model configurations shown in Figure 4, particularly in the neck/upper thoracic and lower thoracic/upper lumbar regions. A more adequate representation of the stiffening effects of the rib-cage and viscera-abdominal wall systems as well as an improved model of the cervical spine are currently being addressed.

TABLE 3. DROP TEST AND BISM PEAK ACCELERATION COMPARISONS

Location	Peak Resultant Acceleration ( $g_s$ )	
	Drop Test	BISM
Head	79	33
L1	110	75
L7	122	72

A number of BISM parameter studies have been run to determine the effects of variations in specified parameters on model response predictions. One of these considered the effects of variations in the degree of spinal curvature. This study was motivated by the observation that the initial (prior to impact) spinal configuration of the subject is very difficult to duplicate from drop to drop even for the same subject. Three initial spinal configurations, depicted in Figure 5, were considered. The "normal spine" is the configuration which was used in the previously described simulations. The "curved spine" configuration was achieved by approximately doubling the curvatures of the normal spine and roughly corresponds to a loosely restrained pre-impact spinal configuration. Since the normal spine configuration is based on radiographs of a tightly restrained seated upright baboon, it is rather doubtful that the "straight spine" configuration, obtained by simply "straightening" the normal spine, could be attained by a baboon seated upright in a drop vehicle. The straight spine configuration was, nonetheless, included for completeness.

Table 4 compares peak BISM axial compressive forces and A-P bending moments for three drop test simulations using the straight, normal and curved initial spinal configurations. The 30-msec model responses for these three configurations are shown in Figure 6. The prescribed seatback acceleration and pelvis force profiles were as described previously. These results demonstrate that 1) peak axial compressive forces decrease with increasing spinal curvature; 2) peak A-P bending moments generally increase with increasing spinal curvature; 3) significantly different responses can occur among what may appear to be nearly identical drops, with regard to drop parameters, animal size, and mass distribution, if care is not taken to minimize differences in the pre-impact spinal configurations of the subjects.

TABLE 4. PEAK LOADS FOR BISM SPINAL CURVATURE VARIATION EFFECTS STUDY

Vertebral Level <sup>(1),(2)</sup>	Axial Compression <sup>(3)</sup>			A-P Bending <sup>(4)</sup>		
	Straight	Normal	Curved	Straight	Normal	Curved
Neck	8.23	5.10	3.23	14.2	12.6	5.54
T2	16.4	14.0	7.50	22.1	27.1	9.07
T3	19.3	17.1	9.82	20.9	30.7	14.3
T4	21.5	20.5	11.9	13.1	17.4	13.7
T5	24.2	23.0	15.4	17.9	4.33	16.0
T6	27.5	25.4	18.4	18.2	4.67	23.8
T7	30.5	27.3	22.2	3.72	9.06	28.2
T8	33.4	30.2	24.1	7.10	11.0	31.6
T9	36.4	31.2	24.6	7.59	7.04	30.3
T10	40.4	35.3	26.6	4.99	6.48	11.2
T11	44.1	38.0	25.6	1.99	12.0	20.9
T12	47.7	41.0	26.5	1.24	17.3	45.1
L2	55.0	46.2	24.7	0.937	29.8	11.5
L4	61.7	53.5	35.2	0.871	18.4	22.9
L6	66.7	58.6	54.7	3.84	29.8	39.9
L7	68.9	62.4	52.7	6.65	33.6	67.7

(1) Refers to inferior intervertebral disc.

(2) Time histories were not output for levels T1, L1, L3 and L5.

(3) Dynes  $\times 10^7$

(4) Dyne-cm  $\times 10^7$

So as not to lose sight of our final goal, the validation of the human head-spine model (HSM), we have included Figure 7 which depicts HSM configurations at time = 0, 40, 60 and 80 msec from a simulation of a hypothetical human drop test. An acceleration profile having a rise time of 14 msec and a constant magnitude of 10 g for 66 msec for a total duration of 80 msec was specified to act at the seatback and directly on the pelvis. The results appear to be both qualitatively and quantitatively reasonable.

Similar drop test simulations with the HSM and BISM have not yet been run. The results shown in Figures 3 and 4 for the BISM and in Figure 7 for the HSM nonetheless provide a significant preliminary indication of disparities in the responses of these two models. These disparities arise mainly from differences in head mass center locations (approximately directly above the neck insertion point in the HSM and approximately 6 cm forward of the neck insertion point in the BISM) and differences in the pre-impact spinal curvatures. The significance of these differences in the models' geometries (as well as the actual geometries of the human and baboon pre-impact head-spine configurations) with regard to dynamic response and injury mechanisms will be addressed in a near-future study.

#### CONCLUSIONS

Three-dimensional mathematical models of the human and baboon head-spine structures have been described. The human head-spine model, the HSM, after appropriate validation will serve as an analytic tool to be used in the development of design criteria for military aircraft emergency escape systems as well as the investigation of detailed head-spine structure responses in complex, potentially injurious dynamic environments in general.

The HSM has been partially validated through simulations of low-level (noninjurious) laboratory experiments with human volunteers. The requirement for injury-level validation of the HSM prompted the development of the baboon head-spine model, the BISM. Validation of the BISM will simultaneously validate the HSM modeling concepts since these are the same for both models.

Results obtained with the BISM, so far, have already demonstrated its considerable potential for providing insight into head-spine structure responses in injury-level impact environments. BISM simulations of a 30 g<sub>x</sub>, 16.5 msec, and a 70 g<sub>x</sub>, 15 msec baboon drop test yielded seemingly reasonable results. Comparison of peak accelerations from the 70 g<sub>x</sub>, 15 msec simulation with corresponding recorded values from an actual baboon drop test, indicated that the BISM predictions were somewhat low. It is felt that the nonlinear stiffening effects of the rib-cage and viscero-abdominal wall systems were not adequately represented in the BISM; this is currently being addressed, along with improvements to the cervical spine model. Comparisons of BISM drop test simulations for three different pre-impact spinal configurations demonstrated the significant effects of variations in initial sagittal plane curvatures on impact-induced head-spine system loads and deformations.

Still in evidence, notwithstanding the apparent progress in HSM and BISM development and validation, are the number of approximations and extrapolations which have been required for the BISM even more so than for the HSM. Some of these data, such as rate-dependent motion segment bending stiffnesses and rate-dependent vertebral body failure characteristics, are obtainable experimentally. These data are essential to, and in fact could help considerably simplify, the model validation process.

## REFERENCES

1. Belytschko, T., Schwer, L. and Schultz, A.B., "A Model for the Analytic Investigation of Three-Dimensional Head-Spine Dynamics," Air Force Aerospace Medical Research Laboratory Report No. AMRL-TR-76-10, 1976.
2. Belytschko, T. and Privitytzer, E., "Refinement and Validation of a Three-Dimensional Head-Spine Model," Air Force Aerospace Medical Research Laboratory Report No. AMRL-TR-78-7, 1978.
3. Belytschko, T. and Privitytzer, E., "A Three-Dimensional Discrete Element Dynamic Model of the Spine, Head and Torso," AGARD Conference Proceedings No. 253, 1979.
4. Privitytzer, E. and Belytschko, T., "Impedance of a Three-Dimensional Head-Spine Model," Int. J. Mathematical Modelling, Vol. 1, 1980, pp. 189-209.
5. Belytschko, T., Privitytzer, E., Mindle, W. and Wicks, T., "Computer Simulation of Canopy-Pilot Response to Bird-Strike," Air Force Aerospace Medical Research Laboratory Report No. AMRL-TR-79-20, 1979.
6. Liu, Y.K. and Wickstrom, J.K., "Estimation of the Inertial Property Distribution of the Human Torso from Segmented Cadaveric Data," Perspectives in Biomedical Eng., 1973.
7. Belytschko, T. and Hsieh, B.J., "Nonlinear Transient Finite Element Analysis with Convected Coordinates," Int. J. Num. Methods Eng. 7, 1972, pp. 255-271.
8. Newmark, N., "A Method of Computation for Structural Dynamics," J. Eng. Mech. Div., Proc. of ASCE, 1979, pp. 67-94.
9. Reynolds, H.M., "Measurements of the Inertial Properties of the Segmented Savannah Baboon," Ph.D. Thesis, Southern Methodist University, 1974.
10. Kazarian, L., Report on measurements of nonhuman primate stiffness data, to be published, Air Force Aerospace Medical Research Laboratory, 1981.
11. Van Sickle, D.C., Personal communication, Air Force Aerospace Medical Research Laboratory, 1981.
12. Privitytzer, E., "Refinement and Validation of a Mathematical Model of the Human Torso," Ph.D. dissertation, University of Illinois at Chicago Circle, 1979.

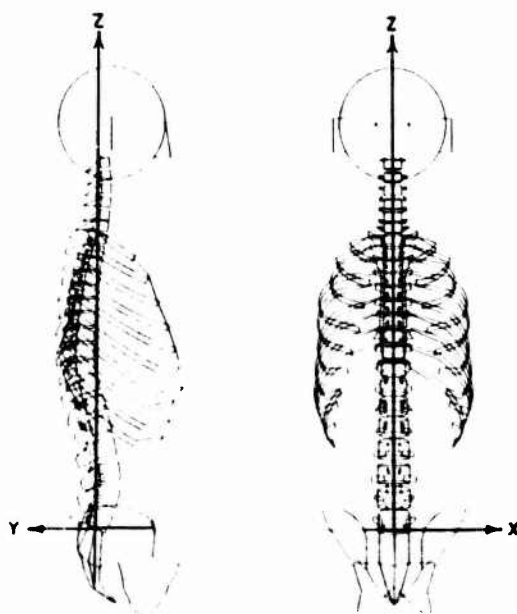


FIGURE 1. SAGITTAL AND FRONTAL PLANE VIEWS OF THE HEAD-SPINE MODEL.

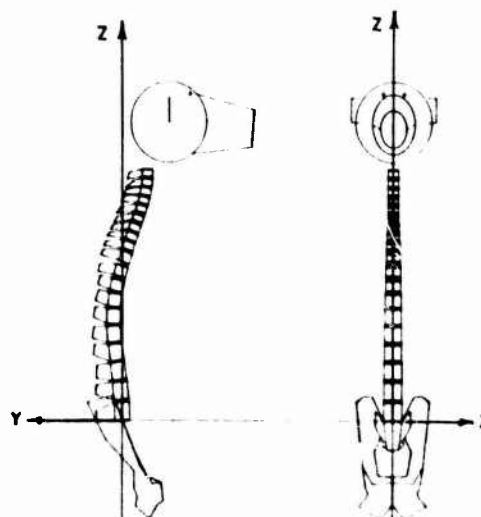


FIGURE 2. SAGITTAL AND FRONTAL PLANE VIEWS OF THE BABOON HEAD-SPINE MODEL.

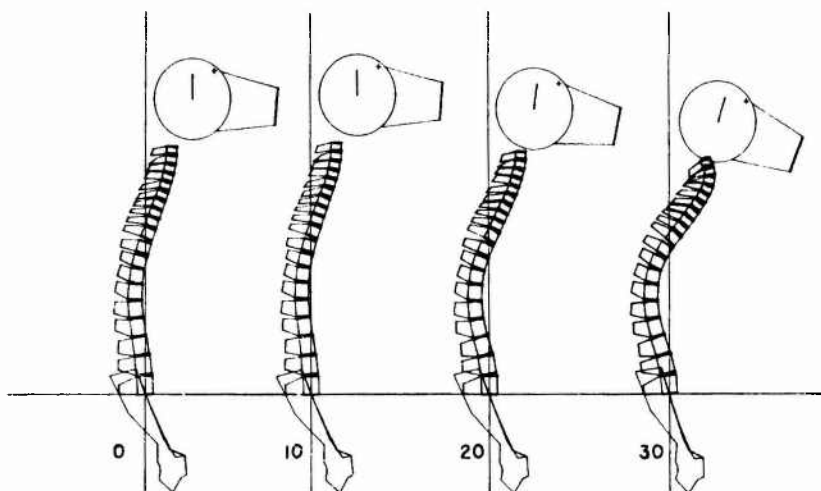


FIGURE 3. BSM SAGITTAL PLANE CONFIGURATIONS AT TIMES 0, 10, 20 AND 30 MSEC FROM A 30  $G_z$ , 16.5 MSEC DROP TEST SIMULATION.

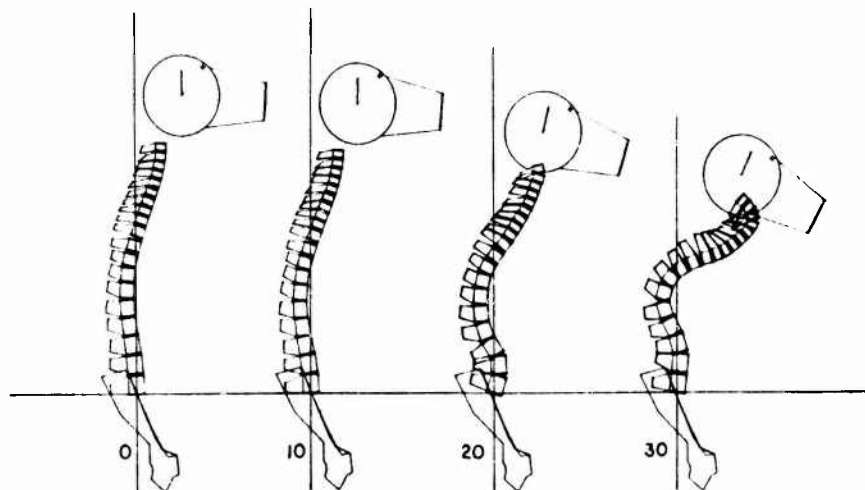


FIGURE 4. BSM SAGITTAL PLANE CONFIGURATIONS AT TIMES 0, 10, 20 AND 30 MSEC FROM A 70  $G_z$ , 15 MSEC DROP TEST SIMULATION.

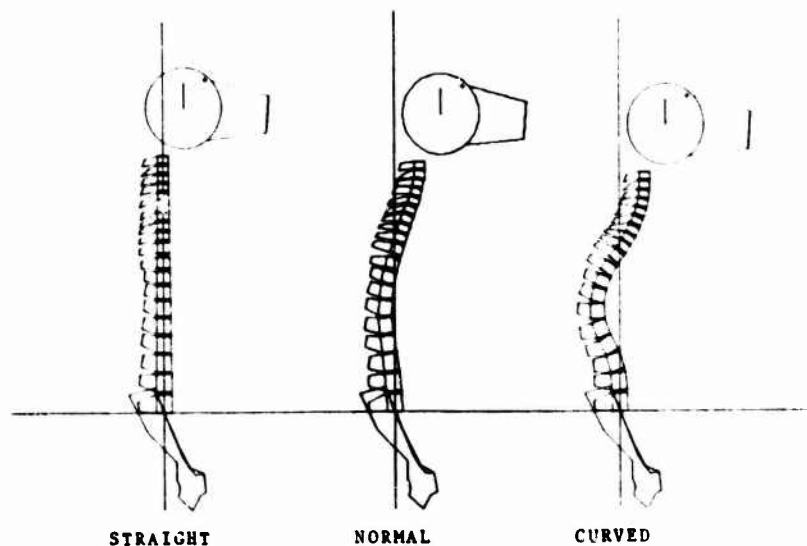


FIGURE 5. INITIAL BSM SAGITTAL PLANE CONFIGURATIONS FOR EFFECTS OF VARIATIONS IN PRE-IMPACT SPINAL CURVATURE STUDY.

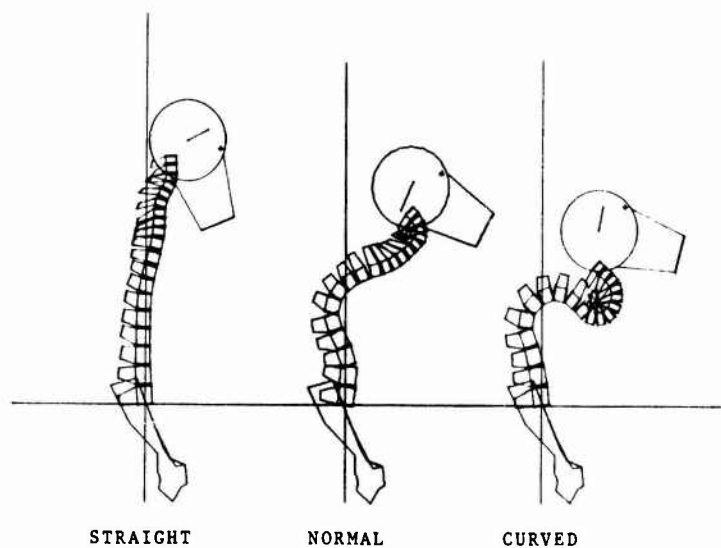


FIGURE 6. 30 MSEC BHM SAGITTAL PLANE CONFIGURATIONS FOR EFFECTS OF VARIATIONS IN PRE-IMPACT SPINAL CURVATURE STUDY.

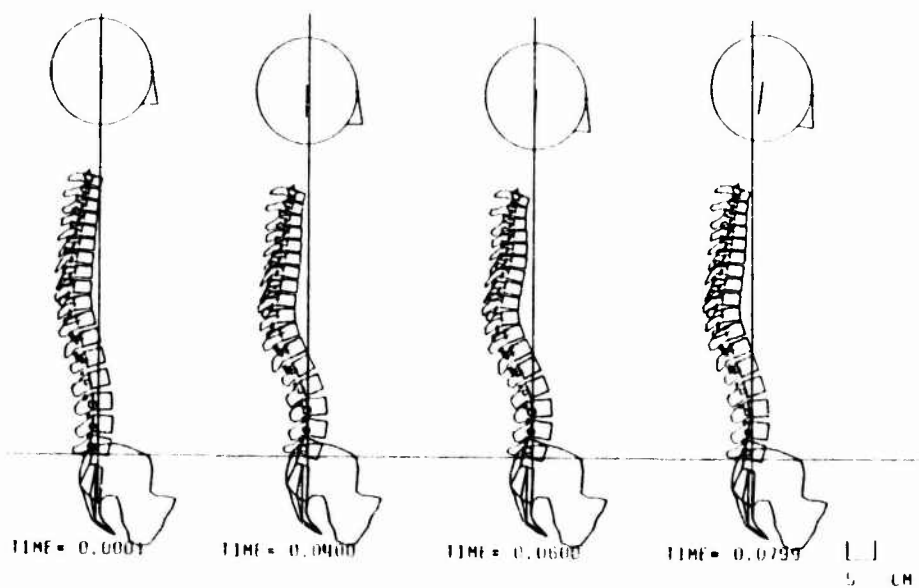


FIGURE 7. HSM SAGITTAL PLANE CONFIGURATIONS AT TIMES 0, 40, 60 AND 80 MSEC FROM A 10  $G_z$  DROP TEST SIMULATION.

## DISCUSSION

MILLER (UK)

The math model has been derived entirely by Z-axis loading. As accelerations will be applied in other directions during ejection, can this model be used for determining spinal reaction to loading in the X and Y axis?

AUTHOR'S REPLY

Yes. The head-spine model and its analysis program are based on fully three-dimensional, large displacement, small strain formulation. Hence, the model is applicable to arbitrary three-dimensional loading environments. Primary emphasis, however, is on the prediction of head-spine system dynamic response and injury likelihood to  $+G_z$  loadings experienced during ejection.

STEELE-PERKINS (UK)

Can you treat the effect of the rib cage as a constant, as surely this will influence the movement of the spine even in a  $G_z$  situation.

AUTHOR'S REPLY

The nonlinear stiffening effects of the rib cage are included. The more complex human head-spine model includes a detailed structural model of the rib-cage in which rigid bodies and beams are used to represent the sternum and the ribs, and beams and springs are used to represent the various joints and connective tissues. In less complex versions of the model, as well as the baboon head-spine model, the detailed rib-cage representation is replaced by a secondary column of nonlinear beam elements which provide a similar nonlinear stiffening effect for the spine.

WISMANS (NE)

This math model seems to be much more advanced than the dummies presently available for impacts in the Z-direction. Are there any plans to incorporate this model in future dummy development programs with respect to the design of the head-spine structure.

AUTHOR'S REPLY

Yes. The only plans which we have with regard to head-spine model applications to dummy development are with respect to the design of a more realistic spine structure for the dummy.

# EVIDENCE FOR THE UTILIZATION OF DYNAMIC PRELOAD IN IMPACT INJURY PREVENTION

Bernard F. Hearon, Maj, USAF, MC, FS  
James H. Raddin, Jr., Lt Col, USAF, MC, FS\*  
James W. Brinkley

Air Force Aerospace Medical Research Laboratory  
and  
Life Support System Program Office\*  
Wright-Patterson Air Force Base, Ohio 45433  
United States of America

## SUMMARY

Dynamic preload is anticipatory acceleration in the same direction as a later impact acceleration. To evaluate the influence of dynamic preload on human impact response, tests with volunteer subjects were conducted on impact facilities at the Air Force Aerospace Medical Research Laboratory (AFAMRL). Test data are presented which indicate that the peak forces and body segment accelerations imposed on subjects during impact accelerations are decreased when those impacts are preceded by dynamic preload. The impact response differences were more striking for comparisons between zero and low levels of dynamic preload than for comparisons between low and higher levels of preload. The threshold for these protective effects is apparently below 0.25 G dynamic preload for the test conditions investigated. In addition, the medical and subjective data support the assertion that dynamic preload is protective when applied prior to  $-G_x$  impact accelerations. Since impacts conducted on decelerator facilities are all influenced by track friction and therefore preceded by dynamic preload, it appears that they are fundamentally different from impacts conducted on accelerator facilities, involving zero dynamic preload. This indicates a need to reassess previous tolerance estimates derived from rocket sled decelerations. Decelerator tests do not appear to predict the more severe results of similar exposures on accelerators. Research efforts are continuing at AFAMRL to further delineate the significance and utility of dynamic preload as a technique in impact injury prevention.

## INTRODUCTION

A number of well recognized factors influence human response to impact acceleration. These include differences in restraint harness materials, geometry, and pretensioning; biological variability among subjects; and variations in subject posture and voluntary bracing. A less well recognized factor of fundamental importance in human impact tolerance appears to be the acceleration-time history imposed on the subject prior to the impact event. Interest in this pre-event history has led to the concept of dynamic preload.

Dynamic preload is defined as an imposed acceleration preceding, continuous with, and in the same direction as an impact acceleration pulse. Some impact accelerations, such as those of a body at rest or a body moving at constant velocity, occur with zero dynamic preload. The pre-impact acceleration in these cases is zero. Other impact accelerations, such as those of a body moving at a decreasing velocity, occur with a variable amount of dynamic preload. Such would be the case in a moving automobile with the brakes applied before striking a barrier.

Dynamic preload should not be confused with static preload, as might be applied by pretensioning a harness restraint system. Static preload has been demonstrated to be useful, and some of the effects are interrelated, but dynamic preload produces additional effects not attainable through the use of harness tension. Dynamic preload should also not be confused with voluntary subject bracing (such as with the extremities) or subject pre-positioning (such as flexing the head forward prior to a  $-G_x$  impact). These techniques have also been demonstrated to influence human impact response. However, unlike dynamic preload, to effectively influence response, bracing and pre-positioning require not only subject anticipation of the impact, but also proper subject performance of the technique as well.

In the conduct of experimental impact testing, facilities have been used which vary in the dynamic preload they impose. Data gathered in the attempt to explore human tolerance limits are derived primarily from experiments conducted on decelerator facilities. The early impact sled tests used rocket thrust to accelerate a sled to a desired velocity (4, 8). The sled then coasted into some form of mechanical or hydraulic braking device which applied the retarding force necessary for the planned impact. During the coast phase, however, retarding forces were already at work in the form of wind resistance and rail friction. These pre-impact retarding forces generally produced sled accelerations in excess of 1.5 G's, sometimes reaching 15 G's. (See Table 1.) The higher levels of imposed dynamic preload often produced dramatic impact responses in the human occupants of the sled well before contact with the brake was made. One of John Paul Stapp's rocket sled exposures, for example, was described as follows.



"At burnout of the rockets, the subject's head and shoulders were pitched forward abruptly into the harness and firmly pressed against the straps throughout the 1.6 seconds of coasting."

The acceleration-time curve for this run demonstrated a 4 to 5 G deceleration of the test sled during the coast phase. Although Lombard (4) suggested over 15 years ago that the timing of this "double punch" profile could be of analytical interest and importance, the protective implications of these data were only recently suggested by Raddin *et al.* (7).

TABLE 1. DYNAMIC PRELOAD AND CORRESPONDING MAXIMUM ACCELERATION TOLERATED DURING  $-G_x$  HUMAN IMPACTS AT VARIOUS TEST FACILITIES

TEST FACILITY	RANGE OF DYNAMIC PRELOADS (G)	MAXIMUM TEST LEVEL (PEAK G)
Rocket Sled Decelerator	1.5 (Calculated Average) to 16.8 (Measured Peak)	45.5 (Measured at seat)
Daisy Decelerator	0.2 - 0.3	34.4 (Measured at sled)†
Accelerators	0	15-16

† Subject incurred multiple vertebral fractures and shock as the result of this exposure.

Other decelerator facilities, such as the Daisy Decelerator at Holloman Air Force Base and the Horizontal Decelerator at AFAMRL impose less dynamic preload on subjects than that experienced during the early rocket sled experiments. The  $-G_x$  impact tolerance work conducted on the Daisy Decelerator (1) resulted in a lower maximum test level than the previous experiments. As shown in Table 1, this exposure level unfortunately resulted in untoward medical effects and thus represented a level of objective tolerance for those test conditions.

Impact facilities designed to produce impact accelerations from a standing start always impose zero dynamic preload. The maximum test levels achieved on such accelerator facilities have been well below the levels achieved on decelerator facilities. In one series of  $-G_x$  experiments conducted on an accelerator (5), the highest level of human exposure reported was 15 G (57 ft/sec). Therefore, as shown in Table 1, previous experience in  $-G_x$  impacts suggests that human tolerance to impact increases with increasing dynamic preload. Although the impact acceleration-time profile for two facilities may be identical, the acceleration-time history prior to the event may differ greatly and may be the basis for differences observed in impact response.

It appears that significant protective benefits accrue to the subject of a test with imposed dynamic preload. At very high levels of preload, body segments are rearranged in advance of the impact, preventing the amplified accelerations associated with the head or other body segment snapping forward during the impact. In effect, the segment moves forward first to avoid snapping forward later, and experiences lower forces during the deceleration. In a similar manner, each small volume of body tissue can be considered to act in some ways like a supported segment. Each volume can be considered to have an associated dynamic preloading threshold which, when applied, can serve to minimize its later impact response. In this way a low level of dynamic preload can be seen to potentially produce beneficial results without associated motion of large body segments or involvement of voluntary bracing.

TABLE 2. NUMBER OF INJURIES INCURRED BY BABOON CADAVERS DURING  $-G_x$  IMPACTS (50 G)

TEST FACILITY	ACCELERATOR	DECELERATOR
Subjects	6	6
Significantly Injured Subjects	4	1
Fractures	1	1
Muscle Tears	4	0
Liver Tears	1	0

Similar apparent differences in tolerance, injuries, and response accelerations have been noted with animal surrogates. For example, 12 baboon cadavers were exposed to nominal 50 G impact accelerations at AFAMRL. As shown in Table 2, of the six subjects exposed on the accelerator, four incurred significant injuries, including one clavicular fracture, one hepatic laceration, and four transections of the rectus abdominis muscles. On the other hand, of the six baboon cadaver subjects exposed to a comparable impact on the decelerator, only one incurred a significant injury. These differences may also be ascribed to dynamic preload.

Comparison of data derived from different impact test facilities, subjects, and conditions has always been difficult. Similar peak G exposures may have very different pulse shapes and, therefore, different velocity changes and pulse energy content. Restraint system designs and materials are often not comparable. Subjects differ in size, weight, and response characteristics. In short, if clear distinctions between responses with differing dynamic preloads are to be made, great care must be taken to assure that all other sources of response variance are well controlled.

The effect of varying the acceleration-time history preceding the impact event while carefully controlling all other sources of response variance is the subject of the present inquiry. The results of matched impact exposures on a decelerator (preload levels of approximately 0.25 G and 0.62 G) and an accelerator (no preload) are presented. The study is also an attempt to establish deceleration exposures as a special case in human tolerance data. Presumed tolerance information derived from tests with high preload would then require interpretation when applied to impact tests with no preload. Tolerance scaling techniques would be required. Furthermore, if tolerance increases with preload, means should be sought to intentionally impose preload as a protective technique in impact exposures.

#### EXPERIMENTAL DESIGN

This experiment was designed to provide a controlled comparison of human response in matched impact acceleration profiles on decelerator and accelerator facilities. The comparable tests were matched for velocity change of the impact sled. The impact acceleration profiles were approximate half-sine waveforms. The tests were conducted on the Horizontal Decelerator and the Impulse Accelerator at AFAMRL. The ready availability of these facilities for use in human testing and the extensive base of comparative test data were prime factors in selecting forward facing ( $-G_x$ ) tests for this investigation.

Volunteer subjects came from the AFAMRL Impact Acceleration Stress Panel. Prior to participation, all subjects successfully completed a thorough medical screening evaluation, including a USAF Flying Class II physical examination, pulmonary function tests, electroencephalogram, exercise treadmill test, and a complete battery of skull, chest and spine x-rays. This screening procedure has been more thoroughly described elsewhere (3). Ongoing informed consent was provided by all subjects throughout the experiment in accordance with the applicable human use guidelines as defined in Air Force Regulation 169-3.

To minimize the potential for injury to subjects, the tests were conducted at presumed subinjury impact acceleration levels. The experimental design matrix is shown in Table 3. The pulses in Test Conditions B and E were preceded by the minimum dynamic preload (approximately 0.25 G) created primarily by friction between the impact sled and the track rails of the decelerator. In Test Conditions A and D, an additional approximate 0.35 G dynamic preload was imposed by the application of sled-mounted braking devices approximately 250 msec prior to impact. There was no dynamic preload in Test Conditions C and F, which were conducted on the accelerator. The 8 G sled profiles are shown in Figure 1 and the 10 G profiles are shown in Figure 2. The forces acting on the subjects at these exposure levels are generally sufficient to overcome the forces of voluntary muscle contraction and, therefore, produce a response which is suitable for comparative parametric analysis. The preload conditions, however, were not sufficient to cause an observable change in subject posture prior to initiation of the impact.

TABLE 3. NOMINAL TEST CONDITIONS

TEST FACILITY	DYNAMIC PRELOAD (G)	CONDITION	
Decelerator	0.62	A	D
Decelerator	0.25	B	E
Accelerator	0	C	F
Sled Acceleration (G)		8	10
Sled Velocity Change (ft/sec)		27	30

The test seat was designed with conventional USAF crew seat geometry with a seat back angle of  $13^\circ$  aft of vertical and a seat pan inclined  $6^\circ$  above the horizontal. Leg bracing was not possible since no footrest was provided. The subjects were restrained by a lap belt and double shoulder strap harness constructed of  $1\frac{3}{4}$  inch wide webbing. The straps were pretensioned to  $20 \pm 5$  pounds. Prior to each impact test, the subject was instructed to assume the same body posture, with head against the headrest, hands resting on anterior thighs without upper extremity bracing, and posterior thighs in contact with the seat pan. During exposures on the accelerator, the subject could hear the countdown to impact in order to assure cognitive anticipation of the event similar to that achieved during decelerator tests.

The test fixture, restraint harness, and subject were instrumented to obtain pertinent objective data during each test. Measured parameters included impact acceleration of the test sled and seat, impact velocity of the test sled, loads reacted at the seat pan, and loads measured at the restraint harness attachment points. Accelerations at the head and chest of the subject were measured by appropriately mounted triaxial translational accelerometers. Photometric data were obtained by two high-speed (500 frames per second) motion picture cameras mounted on the test fixture, permitting assessment of body segment displacements during the impact.

Subjective data were also obtained by means of a post-test questionnaire designed to assess the subject's impression of each impact event relative to other comparable exposures. For example, subjects were asked to characterize head displacement as small or large, shoulder strap pressure as low or high, and overall impression of the impact as comfortable or uncomfortable on an integer scale from -3 to +3, zero indicating a neutral

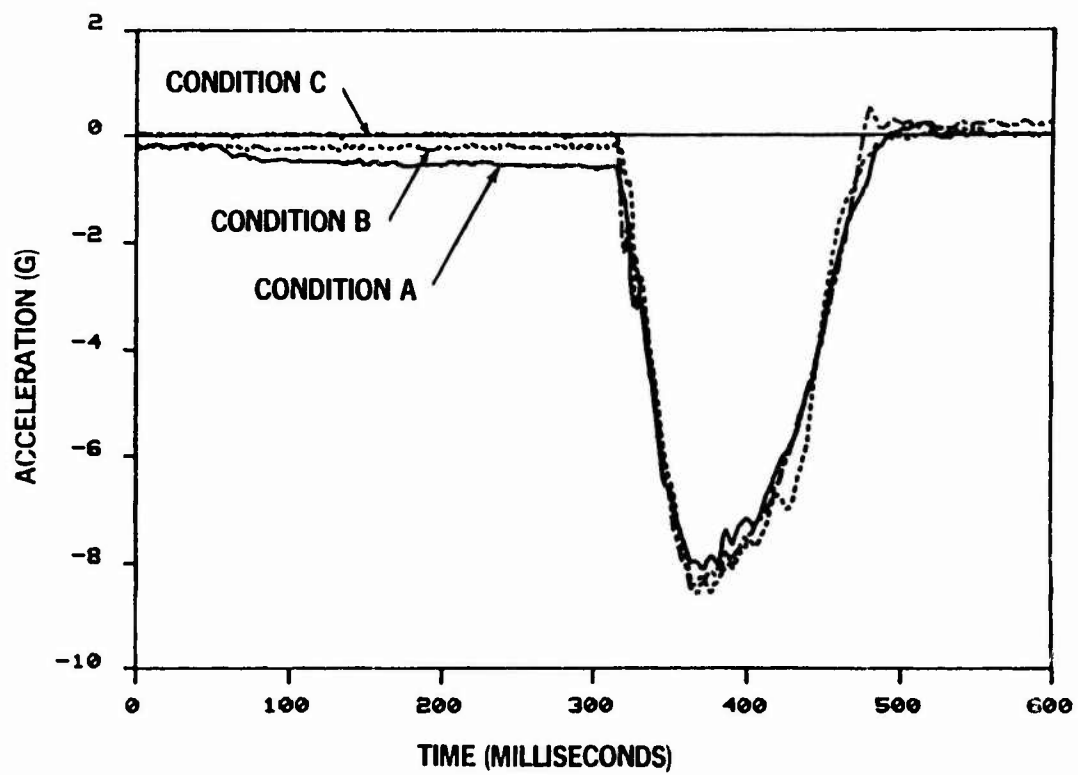


Figure 1. Typical Sled Acceleration Profiles at the 8 G Test Level.

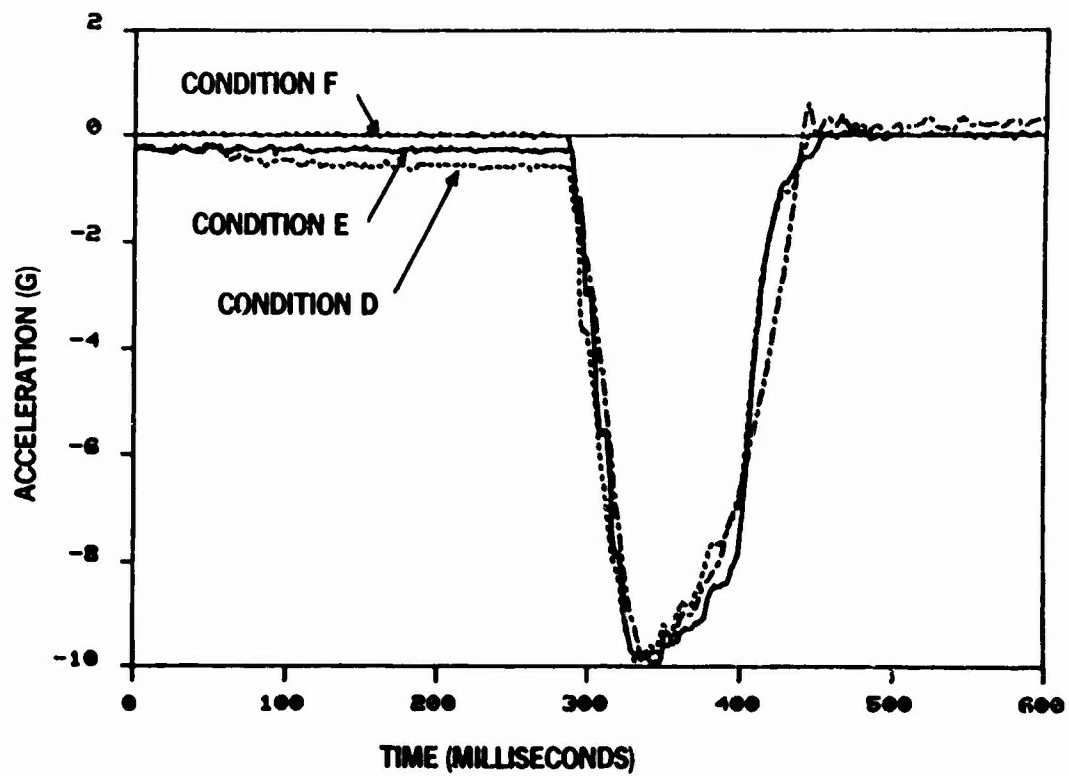


Figure 2. Typical Sled Acceleration Profiles at the 10 G Test Level.

reaction. Subjects were not permitted to review previous post-test responses when completing the questionnaires.

The electronic data were processed by computer and the test results were evaluated using the Wilcoxon paired-replicate rank test (9). This statistical technique was selected to compare the peak values of specific measured parameters and to establish the statistical significance of observed trends in the data. Experimentally measured parameters for each subject were arithmetically compared with the same parameter measured for the same subject in a comparable test condition, in order to establish pair differences. When a sufficient preponderance of ranked pair differences for a parameter changed in the same direction, a trend was established as statistically significant by the Wilcoxon analysis. The 90% confidence level (assuming a two-tailed test) was chosen as the level of statistical significance in this study. This analytical approach established each subject as his own control and thereby reduced the effects of biological variability among subjects.

Evaluation of the entire measured acceleration-time histories of head and chest was also accomplished by calculated severity indices (2). These single parameters, which were derived by a weighted integral of the acceleration-time function taken over the interval of the impact ( $SI = \int a^n(t)dt$ , where  $n = 2.5$ ), were used to compare the overall severities of impact responses. No significance was assigned to the absolute values of these measures. Instead, they were utilized only in a relative sense for comparison.

#### EXPERIMENTAL RESULTS

Data from 100 selected impact tests (54 at the 8 G level and 46 at the 10 G level) conducted between January and August 1981 are presented. The three preload conditions allowed these to be sorted into 92 comparable test pairs which were matched for velocity change of the sled. The difference in velocity change for any given test pair was  $\leq 1$  ft/sec. (The velocity difference in 88% of the 92 matched pairs was  $\leq 0.5$  ft/sec.) Nineteen subjects (17 males and 2 females) participated in the test program and twelve subjects completed all test conditions. Four subjects did not complete the test program since they departed Wright-Patterson Air Force Base for new duty assignments; one subject was temporarily medically disqualified from participation; and two subjects voluntarily withdrew from the program.

Tests on the Horizontal Decelerator were conducted first. The phases of an experimental run on this facility are shown in Figure 3. In these tests, the sled was accelerated to a velocity sufficiently high to achieve the programmed impact velocity at the decelerator following the deceleration experienced during the coast phase. During the velocity control window of the coast phase, the actual sled velocity was compared to a programmed or model velocity. If the actual velocity was higher than programmed, the excess velocity was "trimmed" by the application of sled-mounted braking devices. In this way, the actual sled velocity at impact was assured to be within 1 ft/sec of the desired impact velocity. In Test Conditions A and D, the trim brakes were applied throughout the 250 msec just prior to impact in order to impose an additional approximate 0.35 G dynamic preload on the sled. To achieve the desired impact velocity during these test conditions, it was necessary to allow for the higher velocity change associated with the additional imposed dynamic preload. The sled was, therefore, programmed to leave the velocity control window of the coast phase with a higher actual velocity than in Test Conditions B and E. The 8 G tests were conducted prior to the 10 G tests on the decelerator. Subjects were informed of the impact test level but were not informed of the preload condition prior to each test. The order of presentation of the preload conditions was randomized.

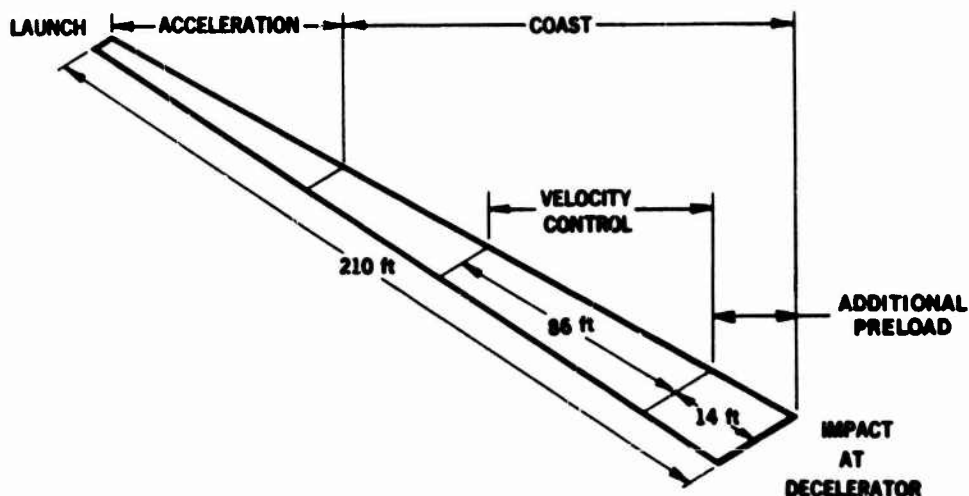


Figure 3. Phases of the Experimental Run on the Horizontal Decelerator.

Tests on the Impulse Accelerator were conducted following completion of all decelerator tests. These tests were not randomized with the deceleration conditions, since transitioning from decelerator to accelerator required substantial facility modifications. However, the difference in mechanization would have prevented blind or double blind presentation anyway. The accelerator tests were designed to produce an impact velocity as close as possible to that measured for the same subject on the decelerator. Since the profiles were almost identical (see Figures 1 and 2), velocity matching implied close correspondence in acceleration as well. However, the mean sled acceleration peak for the 8 G tests was higher on the accelerator (Test Condition C) than for either comparable decelerator condition (Test Conditions A and B). These small differences in the mean sled acceleration peak (0.18 G in comparison B-C and 0.26 G in comparison A-C) were systematic enough to appear as statistically significant in the Wilcoxon analyses. (See tables in Appendix.) To assure that this test bias was not the basis for the observed differences in subject response, 10 G tests on the accelerator were designed to produce slightly lower velocity changes for each subject than had been observed on the decelerator. Sled acceleration peaks for the 10 G tests were, therefore, lower on the accelerator (Test Condition F) than for either comparable decelerator condition (Test Conditions D and E). These small differences (0.36 G in comparison E-F and 0.30 G in comparison D-F) were again systematic enough to appear as statistically significant in the Wilcoxon analyses, but this time, by design, in the other direction. Despite this variation in sled acceleration, response differences at 10 G similar to those documented at 8 G were still observed.

Six comparisons among the test conditions were made. The means and standard deviations of the measured parameters and the statistically significant trends established by the Wilcoxon analysis at the 90% confidence level are presented for each comparison in Tables A1-A6. (See Appendix.) In these tables, an asterisk (\*) indicates a statistically significant change in the designated parameter. Tables 4 and 5 summarize the statistically significant trends in all comparisons of the electronic data. In these tables, the arrow designates the direction of the trend, the number indicates the percentage increase in the parameter mean between test conditions, and an asterisk again designates statistical significance at the chosen confidence level.

TABLE 4  
SUMMARY OF STATISTICALLY SIGNIFICANT TRENDS  
AND PERCENT INCREASE IN PARAMETER MEANS  
FOR COMPARISONS AT THE 8 G TEST LEVEL

TEST CONDITIONS TEST FACILITY DYNAMIC PRELOAD (G)	A		B		B		C		A		C	
	Dec	0.62	Dec	0.25	Dec	0.25	Acc	0	Dec	0.62	Acc	0
SM SLED ACCELERATION												
SLED VELOCITY												
CHEST ACCELERATION												
-X axis												
+Z axis												
Resultant												
CHEST SEVERITY INDEX												
HEAD ACCELERATION												
-X axis												
-Z axis												
Resultant												
HEAD SEVERITY INDEX												
STRAP LOADS												
Total Shoulder Straps												
Total Lap Belt												
SEAT PAN LOADS												
+Z axis												
Resultant												

Comparisons of the 8 G test results revealed statistically significant increases in measured and computed response parameters in the test condition with less dynamic preload. (See Table 4.) In comparison A-B, for example, statistically significant increases in resultant head acceleration, total lap belt load, and resultant seat pan load were seen in the condition with less dynamic preload (Test Condition B). Increases in the same direction were seen for vertical chest acceleration and the chest Severity Index. More dramatic changes in response parameters were seen in the decelerator-accelerator comparisons. In comparison B-C the resultant chest acceleration and chest Severity Index, resultant head acceleration and head Severity Index, total shoulder strap load, total lap belt load, and resultant seat pan load were increased in the exposure on the accelerator. Similar changes, all larger in magnitude, were seen in the A-C comparison. The direction of these trends and the relative magnitudes of the increases observed in this comparison may have been anticipated on the basis of the findings in the A-B and B-C comparisons, since the three comparisons are not independent.

Comparisons of the 10 G test results also indicated statistically significant increases in the measured and computed parameters in the test condition with less dynamic preload. For example, in the D-E comparison, statistically significant increases are seen

in resultant chest acceleration and chest Severity Index in the condition with less dynamic preload (Test Condition E). Although similar findings at the chest are absent in the decelerator-accelerator comparisons, the resultant head acceleration and head Severity Index, total lap belt load, and vertical seat pan reaction load were increased in Test Condition F relative to either comparable test condition on the decelerator (Test Conditions E and D). These findings are summarized in Table 5.

TABLE 5  
SUMMARY OF STATISTICALLY SIGNIFICANT TRENDS  
AND PERCENT INCREASE IN PARAMETER MEANS  
FOR COMPARISONS AT THE 10 G TEST LEVEL

TEST CONDITIONS	D	E	E	F	D	F
TEST FACILITY	Dec	Dec	Dec	Acc	Dec	Acc
DYNAMIC PRELOAD (G)	0.62	0.26	0.26	0	0.62	0
SM SLED ACCELERATION	0		4 <---	*	3 <---	*
SLED VELOCITY	0		0		0	
CHEST ACCELERATION						
-X axis	* --->	3	4 <---		* --->	2
+Z axis	* --->	12	* --->	38	* --->	47
Resultant	* --->	4	---	7	---	9
CHEST SEVERITY INDEX	* --->	9	---	7	---	14
HEAD ACCELERATION						
-X axis	0		* --->	25	* --->	22
-Z axis	---	11	* --->	61	* --->	88
Resultant	---	4	* --->	31	* --->	36
HEAD SEVERITY INDEX	---	5	* --->	56	* --->	62
STRAP LOADS						
Total Shoulder Straps	---	2	2 <---		0	
Total Lap Belt	---	1	* --->	6	* --->	8
SEAT PAN LOADS						
+Z axis	---	2	* --->	6	* --->	8
Resultant	---	2	---	5	* --->	8

These electronic data indicate that forces and body segment accelerations imposed on subjects in impacts preceded even by a minimal dynamic preload are decreased in comparison to those measured during impacts preceded by less dynamic preload. These changes were more dramatic in the decelerator-accelerator comparisons than in the comparisons involving the two decelerator preload conditions. This was true despite the fact that, in the latter comparisons, the difference in dynamic preload between the two decelerator test conditions (approximately 0.35 G) was greater than the difference in dynamic preload between the low preload decelerator case and the no preload accelerator case (approximately 0.25 G). Furthermore, the threshold for significant dynamic preload effects on impact response occurs below 0.25 G. Determining the minimum threshold for these effects would require experiments on a decelerator facility which would impose less than 0.25 G dynamic preload on the test vehicle.

The differences in the statistically significant trends at the 8 G test level (Table 4) relative to those at the 10 G level (Table 5) are probably attributable to variations in test conditions. The variations in sled acceleration peak have already been described. In addition, the pulse duration of the 8 G exposure was different from that of the 10 G exposure, implying differences in the frequency content of these impact waveforms. The mechanical response of the subjects at the two test levels, therefore, should be dissimilar and may account for the differences in observed preload effect.

TABLE 6  
SUMMARY OF OBJECTIVE MEDICAL FINDINGS

TEST LEVEL (G)	8	8	8	10	10	10
TEST CONDITION	A	B	C	D	E	F†
DYNAMIC PRELOAD (G)	0.62	0.25	0	0.62	0.26	0
n =	19	19	16	17	17	12
ABRASIONS	1	1	8	1	2	5
CONTUSIONS	0	0	3	0	2	2
MUSCLE STRAINS	0	1	2	0	0	2

† Two subjects declined this 10 G exposure. Two subjects who participated utilized adhesive tape at the clavicles to prevent abrasions during this 10 G exposure only.

The adverse medical effects of subject participation were confined to anticipated and clinically inconsequential abrasions, contusions, and muscle strains (with the exception of a possible minimal Type I atlantoaxial rotatory fixation in one subject). These data are summarized in Table 6. The abrasions, of course, are observed in areas of subject contact with the restraint straps, particularly at the clavicles, and are easily identifiable post-impact. However, contusions and muscle strains have probably been underestimated, since these effects may not be seen immediately following the impact and may simply not be reported by subjects in follow-up. Nevertheless, the frequency of



these objective medical findings following impact exposures on the accelerator was increased compared to similar exposures on the decelerator at both the 8 G and 10 G test levels. However, the frequency of adverse effects incurred on the accelerator did not increase from the 8 G to the 10 G test level. No attempt was made to differentiate levels of injury severity. The relative scarcity of medical findings in the decelerator tests suggests an effective decrease in the threshold for abrasions with imposed dynamic preload. At higher impact acceleration levels, such as those experienced operationally during aircraft ejection, it is conceivable that a similar beneficial threshold shift may occur, with preload, for the clinically consequential adverse effects of these impacts, such as vertebral fractures.

Analysis of the subject questionnaire responses indicated that subjects, in general, perceived their impact response on the accelerator to be more severe than their response to comparable decelerator tests. For example, in the B-C comparison, 9 of 16 subjects indicated that the overall impact was more comfortable on the decelerator than on the accelerator. Five subjects indicated no difference between the two test conditions and two subjects indicated that the overall response was more comfortable on the accelerator than on the decelerator. Similarly, at the 10 G test level, in comparison E-F, 8 of 12 subjects indicated their overall response on the decelerator was more comfortable than on the accelerator, three subjects indicated no difference and one subject indicated that the overall response on the accelerator was less severe than on the decelerator. The numerical average of the subject responses to this question were computed for these test conditions. These averages indicated the consensus of the subjects that the overall severity of a 10 G impact exposure preceded by nominal track friction (0.25 G) on the decelerator was equivalent to the overall severity of an 8 G impact exposure on the accelerator. In fact, the two subjects who voluntarily withdrew from the test program declined the 10 G accelerator exposure following completion of the 8 G exposure on the accelerator and at least one 10 G test on the decelerator. Interestingly enough, comparison of objective measures of accelerations and forces between 10 G decelerator tests and 8 G accelerator tests for the same subjects supports these subjective assessments. Resultant head acceleration was higher in the 8 G accelerator tests, while resultant chest acceleration, harness loads, and seat forces were higher in the 10 G decelerator tests.

#### DISCUSSION

The test results demonstrate statistically significant increases in severity of human impact response when compared to response measured in similar impacts preceded by higher dynamic preload. These changes are particularly striking when accelerator impacts are compared to matched decelerator impacts. These response differences continue to be statistically significant, in most cases, even when the accelerator event is less severe, as seen in the 10 G comparisons E-F and D-F.

The explanation for the response differences seen in this test program can be understood in part by examining the concept of dead space and the nature of viscoelastic systems exposed to impact. In spite of pretensioning, some structures of the human body are poorly supported by the restraint system. In typical systems, these include the head, arms, legs, and various soft tissue and internal organs. These structures often must displace before direct accelerating forces can be applied through structural attachments. This amounts to a functional "dead space", which effectively delays the onset of acceleration and implies an eventual increased magnitude of acceleration to allow the late-starting member to "catch up". A dead space mechanism such as this is more observable externally in tests with high dynamic preload, such as some reported by Stapp, in which the head and extremities are actually thrown forward during application of preload. In the tests reported here, the dead space mechanism would be less observable and of lower magnitude, but still may occur internally.

The initial conditions imposed on the viscoelastic system of subject, support, and restraint are modified by dynamic preloading. The initial conditions in the decelerator tests are observably different from those in accelerator tests. In the former, loads in harnesses and forces on the seat structure changed during the transition from launch to coast. At impact, therefore, the viscoelastic response of the subject had already begun. All portions of the subject respond to impact partially as springs, and these springs had already begun to deform while under dynamic preload. Such anticipatory deformation has an effect similar to that of removing simple dead space in the sense that the subject response can follow the acceleration of the supporting structure more closely. However, unlike simple dead space, which has no spring constant, viscoelastic deformation of the entire structure must take place under dynamic loading which produces whole body acceleration. The overall effect simply cannot be duplicated by static pretensioning of harness systems or by voluntary bracing.

The apparent protective effects of dynamic preload have two significant implications. The first is that our assumptions about human tolerance should be re-examined. The ability of a human to tolerate a high-energy 45 G impact with significant dynamic preload does not imply that similarly capable subjects can tolerate a similar impact without preload. The acceleration-time history prior to the impact must be specified and scaling laws must be devised in order to improve the comparability of tests conducted on different impact facilities. The second implication of these results is more positive. If dynamic preload makes impact more tolerable, it should be exploitable in impact protection systems.

Practical utilization of dynamic preload requires that the coming impact be sensed in time to allow application of the preload. During this program, in Test Conditions B and E, dynamic preload was applied over a period of approximately 3 seconds of coasting and, in Test Conditions A and D, an additional approximate 0.35 G dynamic preload was applied during the 250 msec immediately prior to the impact event. For practical impact protection, shorter durations of preload application may be required, as well as a means to impose the preload in coordination with the impact. Unplanned impacts, such as crashes, would require impact initiation sensors at the vehicle periphery or beyond it. Planned impacts, such as ejection seat firing, could use preload during the pre-ejection sequence. For either case, the minimum duration of a protective preload pulse must still be determined. The optimum magnitude and duration will depend upon the dynamic mechanical response properties of the subject and restraint system and the characteristics of the impact to be experienced. Furthermore, the direction of the preloading force should be along the impact force vector.

Work at AFAMRL is continuing in order to define practical applications of dynamic preload for use in aircraft escape systems. This application is particularly attractive, since idealized preloading pulses have also been shown to promise improvement in the displacement-time performance of the seat (6). Thus, it may be possible to improve the performance of the seat, and thus its envelope, while at the same time imposing a protective dynamic preload on the seat occupant in order to decrease the probability of injury. The potential for practical and realizable escape systems incorporating dynamic preload will be defined by measuring human response to various characteristic preloading waveforms in vertical impact.

#### REFERENCES

1. Beeding, E. L., Daisy Decelerator Tests (13 July 1959 - 13 April 1960), MDW Test Report No. 60-4, Air Force Missile Development Center, Holloman Air Force Base, New Mexico, July 1960.
2. Gadd, C. W., "Use of a Weighted-Impulse Criterion for Estimating Injury Hazard" in Tenth Stapp Car Crash Conference, Society of Automotive Engineers, Inc., New York, November 1966.
3. Hearon, B. F. and J. H. Raddin, Jr., "Experience with Highly Selective Screening Techniques for Acceleration Stress Duty" in The Effect of Long-Term Therapeutics, Prophylaxis and Screening Techniques on Aircrew Medical Standards, AGARD-CP-310, March 1981.
4. Lombard, C. F., Collected Data on 48 Rocket Sled Experiments (Holloman AFB), NSL 65-94, Northrop Space Laboratories, 1965.
5. Majewski, P. L., T. J. Borgman, D. J. Thomas, and C. L. Ewing, "Transient Intraventricular Conduction Defects Observed During Experimental Impacts in Human Subjects" in Models and Analogues for the Evaluation of Human Biodynamic Response, Performance and Protection, AGARD-CPP-253, November 1978.
6. Payne, P. R. and D. A. Shaffer, An Optimum Acceleration-Time History for an Escape System, AMRL-TR-70-143, Aerospace Medical Research Laboratory, Wright-Patterson Air Force Base, Ohio, 1971.
7. Raddin, J. H., Jr., J. W. Brinkley, and B. F. Hearon, "The Implications of Dynamic Preload in Human Impact Tolerance" presented at the 51st Annual Scientific Meeting of the Aerospace Medical Association (Anaheim, California), May 1980.
8. Stapp, J. P., Human Exposures to Linear Deceleration: Part 2 - The Forward-Facing Position and the Development of a Crash Harness, AF-TN-5915, Part 2, December 1951.
9. Wilcoxon, F. and R. A. Wilcox, Some Rapid Approximate Statistical Procedures, Lederle Laboratories, New York, 1964.



## APPENDIX

TABLE A1

COMPARISON A-B (8 G)  
SUMMARY OF ELECTRONICALLY MEASURED AND COMPUTED DATA FROM WILCOXON ANALYSIS  
(Peak values are tabulated for velocity, accelerations and loads.)  
(n = 19)

TEST CONDITION	A		B		Significant at 90% Confidence
TEST FACILITY	Decelerator		Decelerator		
DYNAMIC PRELOAD (G)	0.62		0.25		
	Mean	SD	Mean	SD	
SM SLED ACCELERATION (G)	8.17	0.20	8.26	0.28	
SLED VELOCITY (ft/sec)	27.9	0.51	27.7	0.45	*
CHEST ACCELERATION (G)					
-X axis	-9.48	1.41	-9.77	0.91	
+Z axis	5.77	1.31	6.40	1.23	*
Resultant	10.6	0.89	10.9	0.74	
CHEST SEVERITY INDEX	18.6	1.92	20.9	2.65	*
HEAD ACCELERATION (G)					
-X axis	-9.86	1.78	-10.4	2.19	
-Z axis	-4.11	1.75	-5.12	2.79	*
Resultant	10.6	1.96	11.6	2.78	*
HEAD SEVERITY INDEX	24.1	6.69	27.8	10.5	
STRAP LOADS (lb)					
Total Shoulder Straps	519	103	534	87	
Total Lap Belt	1230	191	1270	179	*
SEAT PAN LOADS (lb)					
+Z axis	1070	214	1120	215	*
Resultant	1130	210	1180	213	*

TABLE A2

COMPARISON B-C (8 G)  
SUMMARY OF ELECTRONICALLY MEASURED AND COMPUTED DATA FROM WILCOXON ANALYSIS  
(Peak values are tabulated for velocity, accelerations and loads.)  
(n = 16)

TEST CONDITION	B		C		Significant at 90% Confidence
TEST FACILITY	Decelerator		Accelerator		
DYNAMIC PRELOAD (G)	0.25		0		
	Mean	SD	Mean	SD	
SM SLED ACCELERATION (G)	8.23	0.23	8.41	0.16	*
SLED VELOCITY (ft/sec)	27.6	0.36	27.6	0.41	
CHEST ACCELERATION (G)					
-X axis	-9.58	0.79	-9.98	1.23	
+Z axis	6.47	1.09	9.17	4.34	*
Resultant	10.8	0.70	12.5	2.97	*
CHEST SEVERITY INDEX	20.8	2.70	26.0	6.53	*
HEAD ACCELERATION (G)					
-X axis	-10.3	2.29	-14.0	3.29	*
-Z axis	-4.85	2.59	-10.6	2.57	*
Resultant	11.4	2.82	16.8	3.31	*
HEAD SEVERITY INDEX	27.0	9.97	50.8	16.0	*
STRAP LOADS (lb)					
Total Shoulder Straps	535	86	577	102	*
Total Lap Belt	1280	183	1440	239	*
SEAT PAN LOADS (lb)					
+Z axis	1130	224	1220	236	*
Resultant	1190	225	1260	235	*

TABLE A3

COMPARISON A-C (8 G)  
SUMMARY OF ELECTRONICALLY MEASURED AND COMPUTED DATA FROM WILCOXON ANALYSIS  
(Peak values are tabulated for velocity, accelerations and loads.)  
(n = 16)

TEST CONDITION TEST FACILITY DYNAMIC PRELOAD (G)	A Decelerator 0.62		C Accelerator 0		Significant at 90% Confidence
	Mean	SD	Mean	SD	
SM SLED ACCELERATION (G)	8.15	0.21	8.41	0.16	*
SLED VELOCITY (ft/sec)	27.8	0.32	27.6	0.41	
CHEST ACCELERATION (G)					
-X axis	-9.36	1.42	-9.98	1.23	*
+Z axis	5.99	1.30	9.17	4.34	*
Resultant	10.6	0.84	12.5	2.97	*
CHEST SEVERITY INDEX	18.8	1.91	26.0	6.53	*
HEAD ACCELERATION (G)					
-X axis	-9.97	1.87	-14.0	3.29	*
-Z axis	-3.93	1.65	-10.6	2.57	*
Resultant	10.6	2.04	16.8	3.31	*
HEAD SEVERITY INDEX	23.8	6.77	50.8	16.0	*
STRAP LOADS (lb)					
Total Shoulder Straps	526	101	577	102	*
Total Lap Belt	1250	171	1440	239	*
SEAT PAN LOADS (lb)					
+Z axis	1100	215	1220	236	*
Resultant	1160	216	1260	235	*

TABLE A4

COMPARISON D-E (10 G)  
SUMMARY OF ELECTRONICALLY MEASURED AND COMPUTED DATA FROM WILCOXON ANALYSIS  
(Peak values are tabulated for velocity, accelerations and loads.)  
(n = 17)

TEST CONDITION TEST FACILITY DYNAMIC PRELOAD (G)	D Decelerator 0.62		E Decelerator 0.26		Significant at 90% Confidence
	Mean	SD	Mean	SD	
SM SLED ACCELERATION (G)	9.82	0.19	9.85	0.19	
SLED VELOCITY (ft/sec)	30.5	0.29	30.4	0.32	
CHEST ACCELERATION (G)					
-X axis	-11.7	1.14	-12.1	1.31	*
+Z axis †	6.51	1.12	7.31	1.33	*
Resultant †	12.8	0.91	13.3	0.87	*
CHEST SEVERITY INDEX †	28.1	2.72	30.6	3.40	*
HEAD ACCELERATION (G)					
-X axis	-12.3	2.00	-12.3	2.52	
-Z axis	-6.62	3.25	-7.36	4.37	
Resultant	13.8	3.08	14.3	4.20	
HEAD SEVERITY INDEX	40.0	14.4	42.1	18.5	
STRAP LOADS (lb)					
Total Shoulder Straps	666	110	677	113	
Total Lap Belt †	1530	216	1550	219	
SEAT PAN LOADS (lb)					
+Z axis	1290	236	1320	238	
Resultant	1350	235	1380	233	

(† These parameters based on n = 14 due to partial data loss in three tests.)

TABLE A5

COMPARISON E-F (10 G)  
SUMMARY OF ELECTRONICALLY MEASURED AND COMPUTED DATA FROM WILCOXON ANALYSIS  
(Peak values are tabulated for velocity, accelerations and loads.)  
(n = 12)

TEST CONDITION	E		F		Significant at 90% Confidence
TEST FACILITY	Decelerator		Accelerator		
DYNAMIC PRELOAD (G)	0.26		0		
	Mean	SD	Mean	SD	
SM SLED ACCELERATION (G)	9.91	0.19	9.55	0.22	*
SLED VELOCITY (ft/sec)	30.5	0.34	30.4	0.50	
CHEST ACCELERATION (G)					
-X axis	-12.2	1.32	-11.7	1.51	
+Z axis	7.46	0.91	10.3	4.17	*
Resultant	13.3	0.96	14.2	2.70	
CHEST SEVERITY INDEX	31.2	3.33	33.5	6.33	
HEAD ACCELERATION (G)					
-X axis	-12.2	2.42	-15.0	2.70	*
-Z axis	-7.15	3.67	-11.5	2.72	*
Resultant	14.0	3.76	18.4	3.32	*
HEAD SEVERITY INDEX	41.6	17.4	64.8	17.6	*
STRAP LOADS (lb)					
Total Shoulder Straps	676	116	665	99	
Total Lap Belt	1590	167	1680	246	*
SEAT PAN LOADS (lb)					
+Z axis	1330	198	1410	193	*
Resultant	1390	201	1460	193	

TABLE A6

COMPARISON D-F (10 G)  
SUMMARY OF ELECTRONICALLY MEASURED AND COMPUTED DATA FROM WILCOXON ANALYSIS  
(Peak values are tabulated for velocity, accelerations and loads.)  
(n = 12)

TEST CONDITION	D		F		Significant at 90% Confidence
TEST FACILITY	Decelerator		Accelerator		
DYNAMIC PRELOAD (G)	0.62		0		
	Mean	SD	Mean	SD	
SM SLED ACCELERATION (G)	9.85	0.21	9.55	0.22	*
SLED VELOCITY (ft/sec)	30.5	0.32	30.4	0.50	
CHEST ACCELERATION (G)					
-X axis	-11.5	1.19	-11.7	1.51	
+Z axis †	6.79	0.78	10.0	4.50	*
Resultant †	12.8	1.06	14.0	2.92	
CHEST SEVERITY INDEX †	28.7	3.03	32.8	6.74	
HEAD ACCELERATION (G)					
-X axis	-12.3	1.94	-15.0	2.70	*
-Z axis	-6.12	2.39	-11.5	2.72	*
Resultant	13.5	2.38	18.4	3.32	*
HEAD SEVERITY INDEX	39.9	13.5	64.8	17.6	*
STRAP LOADS (lb)					
Total Shoulder Straps	668	108	665	99	
Total Lap Belt †	1550	190	1680	241	*
SEAT PAN LOADS (lb)					
+Z axis	1300	182	1410	193	*
Resultant	1350	185	1460	193	*

(† These parameters based on n = 10 due to partial data loss in two tests.)

## DISCUSSION

S. P. DESJARDINS (US)

Comment: Your findings are of special interest in our understanding and influencing energy-absorbing seat performance. The new crashworthy US Army helicopters include energy-absorbing landing gear which provides the preload and thus perhaps the benefits you describe in your paper. In our qualification drop test of the AH-64A crewseat we simulated the energy-absorbing stroke of the gear in our test pulse. The seat performance was superior with fewer high amplitude transients than measured on other seats where the standard triangular test pulse was used.

AUTHOR

In the helicopter described, the downward, passive stroking landing gear will modify the vertical acceleration measured at the seat. If this modification takes the form of  $+G_z$  acceleration preceding and continuous with the  $+G_z$  impact event, then dynamic preload, by our definition, will have been applied to the seat and occupant. The effects of such anticipatory vertical acceleration on human impact response will be investigated in a future test program at AFAMRL.

However, a distinction must be drawn between downward, passive stroking or energy-absorbing seats and upward, active stroking mechanisms by which vertical dynamic preload conceivably may be applied to a seat occupant. The former appear to impart a beneficial effect during the impact event by limiting the imposed acceleration. On the other hand, the latter would impose an acceleration before an anticipated impact and, in so doing, better prepare the seat occupant viscoelastically for the event. (It may also be conceivable that an upward, active stroke could be utilized in conjunction with a later downward, passive stroke to combine the beneficial effects of each protection technique.) The timing, amplitude, and duration of this dynamic preload pulse would be critical in order to have a beneficial effect. The effects of variations in these preload parameters are the subject of a current AFAMRL human test program.

DR. D. J. THOMAS (US)

1. What was the head and neck initial condition variability within subjects between runs?
2. What was the angular acceleration of the head for each run and was this accounted for in the statistical analysis of the acceleration peaks measured at the mouth?
3. What is unique about the preloading effect that cannot be explained by variation due to initial condition, head angular acceleration response, and forceful loading of the restraint system, all of which are well described from prior experiments?

AUTHOR

1. The test seat and restraint geometry was not varied during this test program. The vertical position of the headrest was varied among subjects, but was the same for a given subject in all test conditions. To further minimize variations in the head-neck initial condition prior to each experiment, subjects were instructed to assume the same body position they had assumed in previous tests. In particular, each subject was asked to keep his head back against the headrest (head up, chin up) and to maintain a mild to moderate amount of neck muscle tension. Proper head position was verified by the test conductor prior to each experiment.

In addition, the effects of variations in initial conditions among subjects on data analysis were minimized by use of the Wilcoxon paired-replicate rank test to establish the statistical significance of results. In this technique, the test results of each subject are compared only to that subject's results in other test conditions. Thus, each subject is his own control, minimizing the influence of biological variability and small differences in initial positions among subjects on data analysis.

2. Direct measurements of angular head accelerations were not made in this study. A triaxial translational accelerometer package was used to obtain the head (and chest) acceleration data. This device, of course, measured translational acceleration components summed with translational components resulting from angular motions. The rotational motion of the head was measured photometrically. These data are being analyzed to derive head angular velocities and accelerations.

3. The static initial conditions in the present study were very carefully controlled to minimize variations in, e.g., subject position and bracing as well as static pretensioning of the restraint. In addition, the impact event profiles at comparable test levels were nearly identical. The observed response differences in the test conditions must, therefore, be attributed to the differences in the pre-event acceleration time history.

Dynamic preload may be distinguished from other impact protection techniques in that it does not require active participation of the subject and, more importantly, in that it involves a whole body viscoelastic preparation of the subject for the impact event. The potential aerospace applications of dynamic preload also set it apart from other protection techniques. If vertical preload pulses can be demonstrated to ameliorate human response to subsequent vertical impact, then utilizing dynamic preload prior to current ejection seat profiles would be expected to reduce crewmember morbidity during emergency escape. At the same time, such an impulsive velocity change will improve the displacement-time performance of the ejection seat. A single modification to the acceleration profile could, therefore, conceivably have two separate, beneficial effects. Similar effects are not seen with other protection techniques.

## DISCUSSION

S. P. DESJARDINS (US)

Comment: Your findings are of special interest in our understanding and influencing energy-absorbing seat performance. The new crashworthy US Army helicopters include energy-absorbing landing gear which provides the preload and thus perhaps the benefits you describe in your paper. In our qualification drop test of the AH-64A crewseat we simulated the energy-absorbing stroke of the gear in our test pulse. The seat performance was superior with fewer high amplitude transients than measured on other seats where the standard triangular test pulse was used.

AUTHOR

In the helicopter described, the downward, passive stroking landing gear will modify the vertical acceleration measured at the seat. If this modification takes the form of  $+G_z$  acceleration preceding and continuous with the  $+G_z$  impact event, then dynamic preload, by our definition, will have been applied to the seat and occupant. The effects of such anticipatory vertical acceleration on human impact response will be investigated in a future test program at AFAMRL.

However, a distinction must be drawn between downward, passive stroking or energy-absorbing seats and upward, active stroking mechanisms by which vertical dynamic preload conceivably may be applied to a seat occupant. The former appear to impart a beneficial effect during the impact event by limiting the imposed acceleration. On the other hand, the latter would impose an acceleration before an anticipated impact and, in so doing, better prepare the seat occupant viscoelastically for the event. (It may also be conceivable that an upward, active stroke could be utilized in conjunction with a later downward, passive stroke to combine the beneficial effects of each protection technique.) The timing, amplitude, and duration of this dynamic preload pulse would be critical in order to have a beneficial effect. The effects of variations in these preload parameters are the subject of a current AFAMRL human test program.

DR. D. J. THOMAS (US)

1. What was the head and neck initial condition variability within subjects between runs?
2. What was the angular acceleration of the head for each run and was this accounted for in the statistical analysis of the acceleration peaks measured at the mouth?
3. What is unique about the preloading effect that cannot be explained by variation due to initial condition, head angular acceleration response, and forceful loading of the restraint system, all of which are well described from prior experiments?

AUTHOR

1. The test seat and restraint geometry was not varied during this test program. The vertical position of the headrest was varied among subjects, but was the same for a given subject in all test conditions. To further minimize variations in the head-neck initial condition prior to each experiment, subjects were instructed to assume the same body position they had assumed in previous tests. In particular, each subject was asked to keep his head back against the headrest (head up, chin up) and to maintain a mild to moderate amount of neck muscle tension. Proper head position was verified by the test conductor prior to each experiment.

In addition, the effects of variations in initial conditions among subjects on data analysis were minimized by use of the Wilcoxon paired-replicate rank test to establish the statistical significance of results. In this technique, the test results of each subject are compared only to that subject's results in other test conditions. Thus, each subject is his own control, minimizing the influence of biological variability and small differences in initial positions among subjects on data analysis.

2. Direct measurements of angular head accelerations were not made in this study. A triaxial translational accelerometer package was used to obtain the head (and chest) acceleration data. This device, of course, measured translational acceleration components summed with translational components resulting from angular motions. The rotational motion of the head was measured photometrically. These data are being analyzed to derive head angular velocities and accelerations.

3. The static initial conditions in the present study were very carefully controlled to minimize variations in, e.g., subject position and bracing as well as static pretensioning of the restraint. In addition, the impact event profiles at comparable test levels were nearly identical. The observed response differences in the test conditions must, therefore, be attributed to the differences in the pre-event acceleration time history.

Dynamic preload may be distinguished from other impact protection techniques in that it does not require active participation of the subject and, more importantly, in that it involves a whole body viscoelastic preparation of the subject for the impact event. The potential aerospace applications of dynamic preload also set it apart from other protection techniques. If vertical preload pulses can be demonstrated to ameliorate human response to subsequent vertical impact, then utilizing dynamic preload prior to current ejection seat profiles would be expected to reduce crewmember morbidity during emergency escape. At the same time, such an impulsive velocity change will improve the displacement-time performance of the ejection seat. A single modification to the acceleration profile could, therefore, conceivably have two separate, beneficial effects. Similar effects are not seen with other protection techniques.

HEAD PROTECTION FOR ROAD USERS WITH  
PARTICULAR REFERENCE TO HELMETS FOR MOTORCYCLISTS

Jocelyn B Pedder : Research Fellow  
Stephen B Hagues : Research Associate  
G. Murray Mackay : Head of Accident Research Unit

Accident Research Unit, Department of  
Transportation and Environmental Planning  
University of Birmingham, P.O.Box No.363,  
Birmingham B15, 2TT, England.

SUMMARY

This paper considers the overall problem of head injuries resulting from road traffic accidents. The mechanism of head injuries and the development of human tolerance criteria is briefly discussed. An accident sample of fatally and seriously injured two-wheeled motor vehicle (TWMV) riders is examined. Data on the performance of the riders' helmets and the nature of the riders' head injuries are presented. This information is used to assess the protective value of current designs worn by the casualties. A comparison of the two groups of riders highlights the outstanding severity of head injuries sustained by the fatalities. In light of this field data, comments are made on the relevance of existing specifications for protective helmets.

HEAD INJURIES

Incidence

Head injuries and attempts to prevent or mitigate their occurrence by the use of helmets have been reported since earliest recorded history (1). In present times, they are a primary contributory cause of death, disability and illness, especially among young people (2,3). Road traffic accidents account for a large percentage of serious and fatal head injuries. They are the most frequent serious injuries inflicted on all major categories of road users; car occupants, pedestrians and motorcyclists.

The real incidence of head injuries resulting from road traffic accidents, however, is difficult to ascertain. National published road accident figures based on police reported accidents are likely to be an underestimation (4). The contribution of 'slight' head injuries to the overall problem is typically overlooked in published statistics although their occurrence may be a considerable drain on hospital resources (5). Furthermore, the type of injury which results in a single overnight stay in hospital may well involve periods off work of between 1 and 5 weeks.

Severity

In practice, a head injury may refer to any degree of harm or damage; from a minor bump which causes no more than slight and momentary discomfort to a violent blow which causes gross injuries resulting in death. In an attempt to quantify the severity of the head injury, several scales have been developed.

The most commonly used measures define the severity of head injury in terms of disturbances to the consciousness. The duration of post-traumatic amnesia (PTA) is a measure developed primarily by Russell who also recognised its limitations (6). PTA must be interpreted and recorded by skilled medical staff and it takes no account of local injury to the brain or cranial nerves. In an attempt to facilitate a more precise definition of the severity of head injury Teasdale and Jennett developed the Glasgow Coma Scale (7). This scale grades observations which can be made reliably by junior medical staff upon whom, in practice, monitoring of head injury often depends.

The Abbreviated Injury Scale (AIS) which was originally developed to provide trauma researchers with a single system for identifying the severity of injuries has recently been substantially modified for the coding of brain injury (8). Brain injuries are now coded in two ways; first they are described in terms of anatomic lesions and secondly, using clinical diagnosis, in terms of level consciousness. The correlation of AIS-80 Brain scores to a series of established severity measures including the Glasgow Coma Scale has been reported to be good (9).

Other measures of severity have been based on the long term consequences of the head injury. Severity has been defined in terms of the physical, intellectual or emotional disabilities, financial or social losses (10, 11). However, because of the complexity and diversity of injury and sequelae international and even national agreement on the parameters for defining the severity of head injury still remain elusive.

The continuing high incidence of head injuries among road traffic accident casualties emphasises the importance of head protection. In order to consider how the head may be best protected, there is a need to understand the injury mechanisms and to establish the human head injury tolerance levels.



Head injuries can be described under the following headings: scalp lacerations or subgaleal haematoma skull fracture either linear, depressed or perforating, intracranial clot either epidural or subdural and brain injury, either contusion, laceration intracerebral clot and concussion (12). They are primarily caused by three types of blow; (i) indirect - caused when the head is accelerated as a result of impacts to other parts of the body; (ii) penetrating - injuries from high speed projectiles, e.g. bullets; (iii) direct blunt impacts - these are the most common cause of head injuries in road traffic accidents.

The most important feature of head injuries both clinically and in terms of ultimate outcome, is the damage sustained by the brain (13). So for these reasons and in view of the concentration of research work into this area the following discussions shall largely concentrate on the mechanisms of brain damage following blunt impacts to the head.

#### Mechanisms

Considerable efforts have been directed at explaining the mechanism of cerebral concussion. This probably reflects both the prevalence and clinical importance of this type of injury to road accident casualties. Three main hypotheses which aim to explain the mechanism of cerebral concussion have been formulated and investigated.

One theory suggests that a combination of stretching and bending of the upper cervical cord may be the primary mechanism of concussion (14). A second theory proposes that deceleration and acceleration forces due to impact, result in pressure gradients (15, 16). These may injure the cranial contacts through shear stresses at the cranio-spinal junction areas or cause negative pressure induced cavitation lesions opposite to the impact site, the so called 'contrecoup' injuries.

A third theory, originally developed by Holbourn in 1943 (17) suggests that there are two main causes of head injury; deformation of the skull with or without fracture causing brain injury close to the impact site, and sudden rotation of the head which results in contrecoup injuries, for some intracranial haemorrhages and for some concussion (18).

An extensive body of research literature has been concerned with the consideration and investigation of the mechanisms of concussion as outlined by these main hypotheses. Recent work reflects the main ongoing debate, that is the relative contribution of translational versus rotational acceleration to brain injuries. However, there is an overall consensus that both components of acceleration may cause brain damage, and in practice, head impacts will typically result in both linear and angular movement.

#### Tolerance

In addition to understanding the mechanism of head injuries it is necessary to establish human tolerance to impact if effective impact protection is to be designed. The establishment of human tolerance data has primarily resulted from work in the following areas; experimental animal tests, cadaver experiments, human volunteers, mechanical models and mathematical models, real accident data. By these methods several types of head injury tolerances have been developed. The two most widely used are:

- (i) The Head Injury Criteria (HIC), (19) currently used in most international standards
- (ii) An Angular Acceleration Limit (20), under consideration for possible inclusion in some European helmet standards.

Newman (21) recently questioned the validity of HIC as a measurement of the likelihood or severity of head injury and considered alternative methods of assessing head injuries. In light of Newman's detailed analyses, there is little value in commenting further on the validity of HIC here. However, it seems likely that in order to maximise head protection devices, several types of tolerance levels will need to be considered.

The ultimate aim of safety design is to prevent a head impact from occurring. If an impact is unavoidable the aim of the safety engineer is to ensure that the structure of the contact surface or the protective head-gear will deform in such a manner that only tolerable forces and acceleration will be applied to the head.

#### HEAD INJURY PREVENTION

##### Car Occupants

One of the main benefits of seat belts is the reduction of the incidence of head contacts. In a sample of insurance claim car accidents, Bohlin (22) showed that the incidence of serious head injuries was reduced by 70% for drivers and 85% for front seat passengers. However, one of the characteristics of even a correctly worn seat belt is the head or face contact with the steering wheel which is unavoidable for the driver in even moderate speed collisions. Current European test methods do not satisfactorily examine this aspect of steering wheel performance (23).

### Pedestrians

A number of studies record the predominance of head injuries in pedestrian casualties (24). Research has shown that life threatening or fatal head injuries are more often caused by vehicle contact than road contact, and that these injuries are more likely to be caused by contacts with the windscreen frame than with the top of the bonnet (25). Ashton (26) examined the likely effects of two types of car modifications on the severity of pedestrian injuries. He concluded that the adoption of fully compliant frontal car structures would overall afford the greatest reduction in injury severity.

### Two Wheeled Motor Vehicles

In the past decade there has been a substantial increase in two wheeled motor vehicle (TWMV) use. With the growth in TWMV use there has been an associated increase in the numbers of TWMV casualties. As fuel and car running costs continue to increase it seems likely that TWMVs will remain a popular mode of transport.

The susceptibility of TWMV riders to serious and fatal head injuries is well documented (24,27). A number of studies have shown that the helmet is an effective means of preventing or mitigating head injuries amongst these road users (28,29). A study of the effect of helmet law repeal in four States in the U.S.A. concludes that unhelmeted riders are two times more likely to incur a head injury of any type and at least three times more likely to incur a fatal head injury than helmeted riders (30). Although the effectiveness of helmets has been clearly demonstrated there remains a need to establish the best method of protecting the head.

### Current Helmet Design

The obvious function of the helmet is to protect the rider's head in an impact situation. Ideally, the helmet should stay on the rider's head throughout the entire accident sequence and provide maximal protection against direct blows, sharp penetration and abrasive surface contacts. In addition to this primary role, the helmet should be comfortable and aesthetically acceptable to the wearer, and it should be financially attractive to both the manufacturer and the rider. Finally, the helmet should fulfil the requirements of safety standards.

The above considerations in conjunction with current manufacturing techniques and materials result in helmets with four main components:

- (i) The Outer Shell. The primary purpose of the outer shell is to distribute the impact load over a large area. It may also provide resistance to penetration by sharp objects and protect the rider's head from abrasive surfaces. In addition, the shell may absorb some of the energy of the impact.
- (ii) The 'Energy-absorbing' Lining. The main purpose of this lining is to absorb the impact energy. Most modern helmets use expanded polystyrene bead foam material; energy-absorption is achieved through the complete or partial destruction of this material.
- (iii) The Inner 'Comfort' Lining. This lining, typically foam-backed fabric, is to ensure that the helmet is a comfortable fit and to accommodate different head shapes.
- (iv) The Retention System. Designed to hold the helmet in position on the rider's head, the most popular method is straps. These are secured to each side of the helmet shell and secured under the riders chin, with a fastening device.

Although contemporary helmets may appear fundamentally similar, there are differences in the outer shell material, the extent of energy-absorbing liner and the type of retention. These differences and the performance of the helmets worn by an accident sample of fatally and seriously injured TWMV riders will be considered in the following section of this paper.

### THE ACCIDENT SAMPLE

The accident sample has been collected by 'in-depth' investigations conducted by a research team within the Accident Research Unit, University of Birmingham. The primary aims of this work are to provide the British Government with information on the patterns of injuries sustained by a sample of fatally and seriously injured TWMV riders, the sources of these injuries, and the protective value of current designs of crash helmets. The first part of the research programme, a study of fatal TWMV accidents, is now complete, whilst the study of seriously injured riders continues.

In this paper the physical behaviour of the riders' helmets is described and then used with associated head injury information and accident data to assess the limits of protection afforded by current designs of helmets.

### British Helmet Regulations

In Great Britain, with the exception of turbaned followers of the Sikh religion, it is compulsory for all TWMV riders to wear protective helmets (31). This headgear must

comply with one of the British Standard Specifications for protective helmets or afford similar or greater protection than specified in these standards. Helmets sold in Great Britain for road use must, however, comply with one of two current British Standards.

The two current British Standards for protective helmets for vehicle users are:

- (i) BS 5361 (32). published in 1976 and replacing previous standards; BS 2001:1972 and BS 1869:1960.
- (ii) BS 2495/77 (33), the 1977 revision of BS 2495 which was first published in 1954.

The main difference between the two standards is the slightly more severe impact test requirements specified in BS 2495/77. The British Standards prescribe a minimum level of performance and a sample of all helmets are tested to ensure compliance with these specifications. The main difference between the British helmet standards and those of other countries lies in the shock absorption test method and the measurements taken. In the British Standards a swing-away test method is used in which a headform is mounted on an arc which pivots about a horizontal axis (34). A recording is made of the deceleration of the striker against time.

The main requirements and corresponding test methods in British Standards and those of other countries relate to:

- (i) The extent of protection and peripheral vision.
- (ii) The shock absorption properties of the complete helmet assembly.
- (iii) The penetration resistance.
- (iv) The strength of the retention system.

The relevance of these specifications will be examined in light of the accident findings.

#### THE FATALITIES

##### The Sample

In an attempt to examine the representativeness of the accident sample, statistical comparisons between certain characteristics of the sample and national data were carried out. There is no significant difference between the sample and national data for the accident location, in terms of 'built-up' areas, road surface conditions and lighting conditions. ( $\chi^2$  values are 0.0005, 0.0543, and 2.3911 respectively).

The age distribution of the driver fatalities in the accident sample (all males) was also compared with equivalent national figures. There is no significant difference between the sample and national data at the 5% level of confidence. ( $\chi^2 = 9.9175$ ).

A total of 197 fatal TWMV accidents involving 205 fatally injured riders were studied, 186 (91.2%) of these riders were aged 16-29 years with 117 (57.4%) in the 16-19 year age group. There were 196 (95.6%) males. The accidents occurred in and around Birmingham. A non-specific sampling scheme was used. Typically, investigations were initiated one or two days after the accident had occurred. The method of investigation is described in detail elsewhere (27). In brief the accident scene was visited, the involved vehicles were examined and whenever possible the helmets were obtained.

##### Helmet Status

Only 4 of the riders were not wearing helmets at the time of their accidents. These casualties, 3 of whom sustained fatal head injuries, have been excluded from the following discussion. A further 3 riders who died as a result of their helmeted heads being run over have also been excluded. It was established that 66 of the remaining 198 helmeted riders lost their helmets at some time during the accidents. The helmets worn by 86 riders remained in position. In the remaining 46 cases there was insufficient reliable information to allow this distinction to be made. The following discussions will consider only the 152 riders whose helmet status following the accident was firmly established.

##### Helmet Type and Certification

There were 89 (66.9%)<sup>†</sup> 'full-face' or 'integral' style helmets and 40 (30.1%) 'open-face' or 'jet' style helmets. In addition, one helmet had a chin guard rivetted to the helmet shell and one full-face design helmet had been 're-styled' by the owner with the removal of part of the chin guard. Two helmets were of the old 'pudding-basin' style. There was no information available on the types of the remaining helmets.

A full break-down of the certification of the helmets is given in Table 1. Only 44 (37.3%) of the helmets were certified to the latest British Standard, i.e. current at the time of the accident.

<sup>†</sup> In this paper percentages are calculated using only known values.

TABLE 1

## HELMET CERTIFICATION BY HELMET STATUS

	Helmet came off		Helmet stayed on		Total	
	N	%	N	%	N	%
BS 2001	4	7.4	6	9.4	10	8.5
BS 1869	13	24.1	7	10.9	20	16.9
BS 5361	14	25.9	13	20.3	27	22.9
BS 2495/60	9	16.7	15	23.4	24	20.3
BS 2495/77	5	9.3	12	18.8	17	14.4
BS label, but number not known	8	14.8	11	17.2	19	16.1
Other certification	1	1.9	0	0	1	0.8
TOTAL	54	100.1	64	100.0	118	99.9
Not known	12		22		34	
GRAND TOTAL	66		86		152	

The basic type of material used in the construction of the outer shell was ascertained for 117 helmets. There were 34 (29.1%) helmet shells made of glass reinforced plastic and 83 (70.9%) were made of thermoplastic material. The main types of thermoplastic material used at the time of this research were polycarbonate and Acrylonitrile-Butadiene-Styrene (ABS). Helmets with shell materials known to be adversely affected by certain paints, solvents and adhesives must bear appropriate warning labels in order to comply with current British Standard requirements. In light of this requirement and the potential disastrous effect of the user decorating certain thermoplastic shells, it seems worth noting that 14.5% of the thermoplastic helmets worn by the fatalities had been painted since manufacture. In a further 34.9% cases, one or more, 'foreign' adhesive labels had been applied to the outer shell.

As far as the investigators are aware, there are no published data on the numbers of helmets generally in use by types, certification or shell material. However, in 1980, of the 600,000 British Standards Institution helmet certification labels released 55% were for full-face helmets, and 45% for open-face designs (35).

Helmets which Came Off

The group of 66 riders who lost their helmets during the accidents represents 43.4% of those cases for which helmet status was firmly established. The reasons for helmet loss were as follows:

1) Shell break-up

In ten (15.2%) cases, the location and brittle nature of the breaks in thermoplastic helmet shells resulted in helmet loss. It is not within the scope of this paper to describe the physical nature of the shell breaks but the main reasons for shell 'failure' were as follows.

- The application of paint by the riders caused two polycarbonate and one ABS helmet shells to shatter on impact.
- The use of a brittle adhesive to attach the rubber trim to the base of the helmet during the manufacturing process caused at least one polycarbonate shell to break in a brittle manner.
- It is known that microscopic crazes and flaws introduced in polycarbonate shells during manufacture are aggravated by certain solvents, for example, petrol. It is difficult to establish whether or not a helmet has been exposed to solvent attack, however, in the sub-sample the four polycarbonate helmet shells which broke from a hole had probably been exposed to solvents prior to the accident.
- Deterioration of the ABS through 'weathering'. In some cases the butadiene phase of the grade of ABS used in the accident helmets had deteriorated through exposure to oxidation and ultra-violet radiation.

2) Retention system failure

There was objective evidence of overload and thus release of some part of the retention systems in 19 (28.8%) of the cases where the helmets came off during the accidents. The nature of the failures are described in more detail in an earlier paper (28).

### 3) Rider error

In four cases the riders had failed to secure their chin straps properly.

### 4) Helmet fit

The reasons for helmet loss in the remaining 33 cases were not immediately apparent. Obviously there must always be some doubt about how the helmets were fastened prior to the accidents, but it was reliably reported that at least eight of these helmets were found with the chin straps still fastened. In this sample of fatally injured riders the security of the helmets' fit on the riders' head was not established. This information, however, was ascertained for a rider in the serious injury sample and the circumstances of this helmet loss will be discussed later.

### Helmets which Stayed On

It was established that in 86 cases, the riders' helmets remained in position throughout the entire accident sequence.

Examination of the helmets worn by accident victims provides valuable information about the nature of the riders' head contacts. The damage suffered by the helmets in conjunction with an inspection of the accident environment and involved vehicles are useful aids in the identification of the likely sources of head injuries. In all, 68 of the helmets which stayed on the riders' heads were fully examined. In view of the helmet retrieval system used in the study, it seems reasonable to assume that the 68 helmets examined by the investigators and described below are representative of this sub-sample. So, the accident performance of these helmets shall be considered in an attempt to assess the limits of protection given by helmets and in order to evaluate the relevance of existing safety standards.

#### 1) The location of impacts on the helmets

Existing specifications for helmets prescribe a region within which the helmet must fulfil certain performance requirements. Although the outer shell and inner energy-absorbing liner may extend beyond this area, in many past and current helmet designs the energy-absorbing lining is reduced in thickness or even absent outside the specified protective area.

In only 31 (45.6%) helmets was all of the shell damage located either at or above the prescribed protective area. In 32 (47.1%) cases at least one blow had been delivered below this region. This information was not ascertained for the remaining five helmets which were examined.

#### 2) Frequency of impacts on the helmets

The 68 helmets which were fully examined had sustained at least a total of 135 blows. In 41 (60.3%) cases the helmets had suffered two or more observable shell impacts. In light of the observation that polycarbonate helmet shells can sustain a blow without visible shell damage the true number of shell impacts is likely to be higher.

Although it is difficult to distinguish different blows to the same site, individual impact marks on the helmet shell often overlapped, and on such occasions it seems likely that the same area of lining (if present) was involved in more than one impact. As the most popular energy-absorbing material used in current helmet designs, may be practically destroyed upon impact, its ability to absorb subsequent blows to the same location must be limited.

#### 3) The type of blow

In impact tests prescribed by current helmet standards, the striker is delivered to the helmet in a near perpendicular direction.

##### Perpendicular impacts

Perpendicular blows to the helmets in position on the riders' heads will typically result in some permanent deformation of expanded polystyrene lining. In 50 (73.5%) of the 68 helmets which remained in position and which were fully examined the linings showed obvious crush damage. This damage was associated with overlying shell damage in all but two cases. These two helmets had polycarbonate shells which had presumably deformed at the time of the impact, but returned to their original position without visible marks of the blow.

Again, true incidence of perpendicular impacts may be higher than that determined from an examination of the expanded polystyrene liners, as it is difficult to ascertain the nature of blows delivered to parts of the helmet shells where there is no energy-absorbing lining materials. Furthermore, an oblique blow may not necessarily cause liner damage.

##### The incidence of oblique impacts to the head

Aldman and his colleagues have stressed the importance of oblique impacts in TWMV accidents resulting in rotational acceleration forces being applied to the skull and brain (36). They have suggested that in most TWMV accidents head impacts would be oblique rather than perpendicular, whether the involved objects were a car, a fixed

obstacle or the ground.

The nature of TWMV riders' most severe head impacts are not easily identified as during the accident sequences the riders' heads frequently suffers more than one blow, each delivered from a different direction. In most situations, however, where the rider hits the ground their head is likely to impact this surface at an acute angle - such oblique impacts are identifiable by marks or road grazing on the outer helmet shell.

The ground was identified as a primary head impact source for 20 fatally injured riders (see Table 2). All helmet shells were marked to varying degrees with surface grazes. The energy-absorbing liners in 14 of these helmets were fully examined. In seven cases there was no observable damage to the liners underlying the outer shell road grazing. It would seem reasonable to conclude that these seven helmets had hit the ground in an oblique fashion, resulting in rotational acceleration forces being applied to the riders' heads. Five of the riders sustained head injuries rated AIS above 3, in four cases without skull fracture. There were no head injuries reported for the other riders.

In practice it seems likely that head impacts usually involve both translational and rotational acceleration, but more rigorous post mortem examinations are necessary before the relative contribution of oblique and perpendicular impacts as sources of head injuries can be realised.

#### 4) The Nature of the Objects Impacted

Most current safety standards prescribe a specified level of energy absorption to both a flat and hemispherical striker. They also require a certain level of resistance to a sharp impactor. The actual objects hit by the riders' heads are obviously an important factor in the resultant head injury, and the striker prescribed by the standard should reflect the shape of the impacted surfaces.

In this class of road user, the object hit is not readily ascertained as during the accident sequence the rider may strike his/her head on a number of different objects. However, in 52 cases at least one identifiable contact between some feature of the accident environments and the riders' heads was established (see Table 2).

TABLE 2.

#### NATURE OF OBJECTS IMPACTED BY HEADS OF RIDERS WHOSE HELMETS STAYED ON

<u>Objects hit</u>	<u>Number</u>	<u>Z</u>
Road surface, ground	20	38.5
Car, car derivative	12	23.1
Heavy goods vehicle	5 <sup>†</sup>	9.6
Brick wall	4	7.7
Tree	3	5.8
Telegraph pole, lamp post, belisha beacon	3	5.8
Road excavations, ditch	2	3.8
Public service vehicle	1	1.9
Agricultural tractor	1 <sup>†</sup>	1.9
Trailer carrying horse	1	1.9
	52	100.0

<sup>†</sup> Includes head impact with sharp object.

The importance of injury producing ground impacts should not be dismissed for any of the riders, as it is possible that in many cases they have been masked by the primary impacts.

So there were a high number of impact with hard flat surfaces. In comparison head impacts with sharp pointed objects were infrequent - noted in only two cases. However, these findings do not necessarily reflect the true incidence of these hazards as they may indicate that helmets afford TWMV riders with adequate protection against sharp penetrating objects, but are less effective in protecting against blunt impacts.

TABLE 3

NATURE OF HEAD INJURIES BY RIDER'S  
HELMET STATUS

<u>Nature of head injury</u>	<u>Helmet came off</u>		<u>Helmet stayed on</u>	
	<u>N</u>	<u>%</u>	<u>N</u>	<u>%</u>
Basal and vault fracture(s)	20	32.3	9	10.5
Basal fracture(s)	21	33.9	25	29.1
Vault fracture	7	11.3	5	5.8
Brain damage (no skull fracture)	6	9.7	25	29.1
No head injuries	8	12.9	22	25.6
TOTAL	62	100.1	86	100.1

Head Injuries

There were four riders who suffered gross head injuries after their helmets had come off; three were runover and one was decapitated. These riders are excluded from the following analyses.

One outstanding feature of the head injuries sustained by the remaining group of 148 fatally injured riders is the high incidence of severe head injuries. The head injuries were assessed using the 1980 Revision of the AIS Scale (8). Head injuries rated above AIS 3 were reported for 90 (60.8%) casualties. Brain injuries with an AIS greater than 2 were reported for 117 (79.5%) fatalities. In 31 (26.4%) of these cases the brain injuries occurred without any skull fractures.

1) Head injuries and helmet status

Head injuries above AIS 2 were sustained by 54 (87.1) of the riders whose helmet came off and by 64 (74.4%) of the riders whose helmet remained in position. The nature and severity of the head injuries sustained by the two groups of riders is given in Tables 3, 4 and 5. However, in considering the data presented in these tables it is important to note that no attempt has been made to match the type and severity of the head impacts sustained by the riders within these two groups.

TABLE 4

THE LOCATION AND SEVERITY OF HEAD INJURIES  
SUSTAINED BY RIDERS WHOSE HELMETS CAME OFF

	<u>AIS Value</u>					
	<u>0</u>	<u>2</u>	<u>3</u>	<u>4</u>	<u>5</u>	<u>6</u>
Skull injuries	14	0	15	29	0	4
Anatomic lesions	8	1	18	14	10	11
Non-anatomic injuries	57	0	0	0	5	0
Highest head AIS (excluding scalp)	8	1	9	20	12	12

TABLE 5

THE LOCATION AND SEVERITY OF HEAD INJURIES  
SUSTAINED BY RIDERS WHOSE HELMETS STAYED ON

	<u>AIS Value</u>					
	<u>0</u>	<u>2</u>	<u>3</u>	<u>4</u>	<u>5</u>	<u>6</u>
Skull injuries	48	2	16	18	1	1
Anatomic lesions	22	0	27	25	5	7
Non-anatomic injuries	79	0	0	0	7	0
Highest head AIS (excluding scalp)	22	0	18	29	10	7

2) The protective value of the helmets

The low number of AIS scores for non-anatomic head injuries reflects the large number of riders who died instantaneously. The severity of the accident sequence is further demonstrated by the high number of severe and fatal head injuries. It was obvious that in many accident situations the loads applied to the helmets were greater than that which any structure of limited thickness could be expected to reduce to a tolerable level.

However, whilst appreciating the limits of protection that can be provided by such structures, the nature of the head injuries, in particular the relatively high number of



basal skull fractures sustained by riders whose helmets stayed on is important. It suggests that the system is adequately distributing the impact load over a large area, but is failing to reduce the forces applied to the head to a survivable level.

### 3) Sources of head injuries

Table 6 shows the contacts which were established as sources of injuries sustained by the skeletal and internal areas of the head.

TABLE 6

#### SOURCES OF THE MOST SEVERE NON-SURFACE HEAD INJURIES SUSTAINED BY THE FATALITIES

<u>Injury Source</u>	<u>AIS Value</u>					<u>Total</u>	
	<u>2</u>	<u>3</u>	<u>4</u>	<u>5</u>	<u>6</u>	<u>N</u>	<u>%</u>
Other vehicle	1	8	12	7	6	34	37.0
Off-road (furniture)	0	3	19	7	4	33	35.9
Road	0	6	7	1	2	16	17.4
Kerb	0	1	2	1	1	5	5.4
Off-road surface	0	0	3	0	1	4	4.3
TOTAL	1	18	43	16	14	92	100.0
Not known	0	9	6	6	5	26	
GRAND TOTAL	1	27	49	22	19	118	

Impact with other vehicles or off-road objects were identified as primary contributory sources of head injury in 67 (72.8%) cases. Ground contacts were established as a major source of head injuries for 20 (21.7%) riders, but as mentioned earlier this may be an under-estimation. It is of note that in this sample of fatalities in no case was any life threatening injury attributed to loading produced by the chin strap. Furthermore, no reported head injuries above AIS 1 were caused by the helmets.

### SERIOUSLY INJURED RIDERS

This part of the paper described a sample of 48 seriously injured TWMV riders studied as part of an ongoing research programme. They represent a sample of casualties injured in accidents within the catchment areas of two hospitals which serve a rural and urban based population in and around Birmingham. The Ministry of Transport (MOT) criterion for serious injuries was used (see Appendix 1). Although, at this stage of the research no attempt has been made to examine the representativeness of the sample, it should be noted that the serious accidents were selected in a non-specific manner.

#### Helmet status

Only one rider was not wearing a helmet at the time of his accident, he is excluded from the following analyses. The helmets worn by 38 (80.9%) of the riders remain in position, the remaining 9 (19.1%) riders lost their helmets at some stage during the accident sequence.

#### Helmet type and certification

There were 34 (72.3%) 'full-face' helmets and 13 (27.7%) 'open-face' helmets. A full breakdown of the certification of these helmets is given in Table 7. There were 17 (37.0%) helmets with glass reinforced plastic shells and 29 (63.0%) were made from a thermo-plastic material, typically either polycarbonate or ABS. The shell material for the remaining helmet was not ascertained.

#### Helmets which came off

It was established that 9 (19.1%) of the 47 helmeted riders who were seriously injured lost their helmets during the accidents. In only one case as a result of loss of integrity of the chin strap system.

Two riders admitted they were wearing their helmets with unfastened chin straps prior to the accident and another rider said he always wore his chin strap loosely fastened. The reasons why the remaining five riders lost their helmets was not immediately apparent, but at least one of these helmets was found with the chin strap still fastened. There was reasonable supporting evidence to the rider's statement that the helmet had been securely fitted and held in place before the accident. The helmet, which was certified to BS 2495/77, had not sustained a major blow and there was no crush damage to the inner lining.

It was found that with the helmet secured on the rider's head it was possible to



remove the helmet by pushing down on the front of the helmet and then rotating it forward. Although there must always be some doubt about how securely a helmet is fastened prior to impact, certain designs of chin strap retention systems and the use of thick comfort padding allow the removal of several makes of helmet in this way. Therefore it seems reasonable to suggest that this is one reason for helmet loss.

TABLE 7

## HELMET CERTIFICATION BY HELMET STATUS

	Helmet came off		Helmet stayed on		Total	
	N	%	N	%	N	%
BS 2001	0	0	3	8.1	3	6.7
BS 5361	2	25.0	12	32.4	14	31.1
BS 2495/60	1	12.5	1	2.7	2	4.4
BS 2495/77 (Pre. and 4)†	3	37.5	14	37.8	17	37.8
BS 2495/77 (+ and 4) +	1	12.5	1	2.7	2	4.4
BS 2495/77 (+ and 5)††	0	0	2	5.4	2	4.4
BS label, but number not known	1	12.5	4	10.8	5	11.1
TOTAL	8	100.0	37	99.9	45	99.9
Not known	1		1		2	
GRAND TOTAL	9		38		47	

† Amendment 4, applies to introduction of dynamic chin strap test implemented on 1st October 1980.

†† Amendment 5, applies to introduction of the so-called 'solvent wipe' test implemented on 1st April 1981.

Helmets which stayed on

Two of the 38 helmets which stayed on were totally undamaged. The nature of the riders' impacts supports the conclusion that neither of these riders suffered a head impact. The helmets worn by 32 of the remaining 36 riders in this group were examined. There was visible shell damage on all these helmets. In 14 (43.8%) cases there was accident damage located below the protective areas prescribed by the helmets' standards. Two or more areas of shell damage were recorded for 15 of the helmets.

In 10 (31.3%) cases there was visible compression of the inner expanded polystyrene lining. Six of the riders wearing these helmets suffered head injuries in only two cases rated above AIS 2. It is of interest to note that four of the riders whose helmet liners sustained crush damage received no head injuries.

Head injuries

In all, 22 riders suffered head injuries but only 3 (6.4%) riders suffered head injuries rated above AIS 2. The location and severity of the head injuries is presented in Table 8. The most severe head injuries suffered by riders whose helmets came off compared to riders whose helmets stayed on is shown in Table 9.

The primary source of head injuries was positively established for 15 of the riders. Ground contacts were responsible for 9 (60.0%) of these riders and impacts with other vehicles for 4 (26.7%). In only one case did the rider's head injury result from impact with an off-road object.

TABLE 8

THE LOCATION AND SEVERITY OF HEAD INJURIES SUSTAINED BY  
THE SAMPLE OF SERIOUSLY INJURED RIDERS

	AIS Value				
	0	1	2	3	4
Scalp injuries	44	3	0		
Skull injuries	45	0	1	1	0
Non-anatomic injuries	26	5	13	2	1
Highest head AIS	25	6	13	2	1

TABLE 9

THE HIGHEST AIS GIVEN FOR HEAD INJURIES SUSTAINED  
BY RIDERS ACCORDING TO THEIR HELMET STATUS

<u>Highest head AIS</u>	<u>Helmet came off</u>		<u>Helmet stayed on</u>	
	N	%	N	%
0	4	44.4	21	55.3
1	2	22.2	4	10.5
2	2	22.2	11	28.9
3	0	0	2	5.3
4	1	11.1		
	9	99.9		

COMPARISON OF HEAD INJURIES SUFFERED BY FATALLY AND SERIOUSLY INJURED RIDERS

In the total sample of fatalities 117 of the riders suffered head injuries above AIS 2 and for 41 (35.0%) of these riders the head injuries were rated AIS 5 or 6. The severity of the head injuries suffered by the fatalities was quite outstanding; frequently the entire skull and its contents were destroyed. In comparison head injuries were less important in the sample of seriously injured riders. In all 25 (53.2%) of these riders received head injuries but only 3 (12.0%) of these were rated above AIS 2.

COMMENTS ON REQUIREMENTS OF HELMET STANDARDS

The following comments are made in the light of the accident research findings presented above.

1) Materials

Most current standards specify certain limitations on the physical properties of the materials used in helmet manufacture. It is stated that materials shall be known not to undergo appreciable alteration in circumstances of use to which the helmet is normally subjected. Shell materials which may be adversely affected by hydrocarbons, cleaning fluids, paints, transfers or other extraneous additions, must carry appropriate warning labels. First it is of note that 11.5% of the inspected helmets, which could have been damaged in this way, had been painted since manufacture and in a further 32.7% one or more 'foreign' stickers had been applied to the outer shell. Secondly the use of a material in a manner which is known to deteriorate in the presence of petrol, one condition commonly encountered in the riders' environment, highlights the inadequacies of descriptive clauses in safety standards.

There would seem to be considerable benefit both to the user and the manufacturer to be rid of the present ambiguities by writing standards as performance requirements rather than as material and design specifications.

2) Extent of Protection

In those cases where the riders' helmets had remained in position throughout the accident sequence, of the inspected helmets 48.4% suffered at least one impact below the protective region prescribed by the British Standards. In view of these research findings it would surely be beneficial to extent the protective area specified in these and other standards.

In addition, with the apparent increase in the use of helmets affording greater head coverage, it is important to ensure that this additional shell area performs in a protective manner. Two other likely benefits of increasing the protective region are:-

- (i) Impact tests over the entire outer helmet surface would highlight 'problem' areas currently located outside the test area but a potential source of helmet failure - for example localised flaws in polycarbonate shell materials introduced during manufacture, such as 'welding lines', surfaces of hole apertures, use of brittle adhesive to attach edge trimmings.
- (ii) In order to fulfil performance test impact requirements it seems reasonable to expect an increase in the amount of energy-absorbing liner in these areas with an associated decrease in the volume of foam comfort padding. This would probably reduce the numbers of poorly fitted helmets.

3) Shock absorption requirements

The severity of the head injuries sustained by the TWMV riders suggests that the distribution of the loads to which they are subjected covers a very wide range. In a substantial number of fatal head injuries, applied loads are such that to provide survival, a ridedown distance of many centimetres would be required. Such conditions are well beyond even the perfect helmet built to current geometrics, and to greatly increase the outside dimensions of helmets is probably not practical.

It is still important however, to optimise protection within current geometries and it is logical to specify acceleration limits by measuring the accelerations actually on the headform. A performance standard of this type is in line with general principles employed in current vehicle design and allows past and present developments of head injury tolerance criteria to be considered. The British Standards mount the accelerometer on the impactor.

4) Type of impact

The relative contribution of rotational versus translational acceleration as a source of head injuries remains unclear (37). However, it seems likely that head impacts suffered by TWMV riders involve both types of acceleration. Most current standards do not take oblique head impacts into account. It would seem sensible to introduce a performance test to simulate blows likely to result in rotational acceleration.

5) Penetration Test

The small number of fatally and seriously injured riders in this sample who suffered sharp penetration blows to their heads does not necessarily reflect the incidence of such impacts for all TWMV riders involved in accidents. An examination of the nature of head impacts sustained by an uninjured accident sample would provide data indicating the exposure of other TWMV riders to penetrating head blows.

6) The Retention System Test

The original retention system test in the two current British Standards has been replaced. The chin strap failures observed in the investigation of fatal accidents reported here were reproduced by Glaister using a modified French designed test (38). In this way a new retention system test was developed. It became effective on 1st October 1980. The amended standards require the helmet retention systems to tolerate the dynamic loads of a 10kg weight dropping through 750  $\pm$  5mm without displacing more than specified amounts.

7) Helmet fit

The problem of securely fastened and appropriately fitted helmets becoming dislodged during the accidents highlights the need for a test to examine overall helmet retention.

CONCLUSIONS

1. Only five riders in this sample of fatally and seriously injured riders were not wearing helmets at the time of their accidents.
2. Helmets came off the riders' heads in 43.4% of the fatal accidents and in 19.1% of the serious accidents, where this information was ascertained.
3. In 28.8% of the fatalities whose helmets came off there was evidence of overload and release of some parts of the helmets' retention system.
4. In 15.2% of the fatalities whose helmets came off, breaks in the thermoplastic helmet shells had caused loss of helmet integrity.
5. In 47.1% of the helmets inspected one or more detected impacts had been sustained below the 'protective' area prescribed by the applicable standards.
6. The nature of helmet damage and injuries in the fatal sample gives some support to the theory that rotational acceleration can cause severe brain injuries in TWMV accidents.
7. In the sample of fatalities, head injuries above AIS 2 were sustained by 87.1% of the riders who lost their helmets and by 74.4% of the riders whose helmets remained in position.
8. Brain damage rated AIS greater than 2 were reported for 79.5% of the fatalities. In 26.4% of these cases, brain damage occurred without any skull fractures.
9. Basal skull fractures were sustained by 64.1% of the 39 casualties whose helmet stayed on and who received skull fractures. Whilst appreciating the limits of protection that can be provided by helmets, this suggests that relatively good load spreading is being achieved but the 'protective system' is failing to reduce

the total loads to a tolerable level.

10. The frequency and severity of head injuries were markedly different for the two accident samples. The head injuries sustained by the fatalities were far more severe and numerous than those received by the sample of seriously injured TWMV riders. The head injuries sustained by the two groups of riders are not evenly distributed up the AIS scale.

#### REFERENCES

- 1) Gurdjian, E.S. Head Injury from Antiquity to the Present with Special Reference to Penetrating Head Wounds, The Beaumont Lecture. Thomas, Springfield, Illinois, 1973.
- 2) Field, J.H. The Epidemiology of Head Injury. HMSO, London, 1976.
- 3) Jennett, B. and MacMillan, R. Epidemiology of Head Injury. British Medical Journal, 1981, 282, 101-104.
- 4) Pedder, J.B., Hagues, S.B. and Mackay, G.M. A Study of Two-Wheeled Vehicle Casualties Treated at a City Hospital. Proceedings of the Sixth International IRCOBI Conference on the Biomechanics of Impacts, September, 1981, 111-127.
- 5) Patel, A.R. Problems for Accident and Emergency Departments. Symposium on Head Injuries, Glasgow, October, 1977.
- 6) Russell, W.R. and Smith, A. Post Traumatic Amnesia in Closed Head Injury. Archives of Neurology, 1961, 5, 16-29.
- 7) Teasdale, G. and Jennett, B. Assessment of Coma and Impaired Consciousness. Lancet, 1974, 2, 81-84.
- 8) American Association for Automotive Medicine. The Abbreviated Injury Scale 1980 Revision. A.A.A.M., Morton Grove, Illinois, 1980.
- 9) Gennarelli, T.A. Analysis of Head Injury Severity by AIS-80. Proceedings of the American Association for Automotive Medicine, 1980, 147-153.
- 10) Jennett, B. and Bond, M. Assessment of Outcome After Severe Brain Injury: A Practical Scale. Lancet, 1975, 1, 480-484.
- 11) Humphrey, M. and Oddy, M. Return to Work After Head Injury: A Review of Post-War Studies. Injury, 1980, 12, 107-114.
- 12) Thomas, L.M. Mechanisms of Head Injury. In Impact Injury and Crash Protection, Edited by E.S. Gurdjian, W.A. Large, L.M. Patrick and L.M. Thomas, Thomas, Springfield, Illinois, 1970, 27-42.
- 13) Adams, J.H., Mitchell, D.E., Graham, D.I. and Doyle, D. Diffuse Brain Damage of Immediate Impact Type. Brain, 1977, 100, 489-502.
- 14) Friede, R.L. Experimental Concussion Acceleration, Pathology and Mechanisms, Archives of Neurology, 1961, 4, 449-469.
- 15) Gross, A.G. A New Theory on the Dynamics of Brain Concussion and Brain Injury. Journal of Neurosurgery, 1958, 15, 548-561.
- 16) Gurdjian, E.S., Lissner, H.R., and Patrick, L.M. Concussion - Mechanism and Pathology, Proceedings of the Seventh Stapp Car Crash Conference, 1965 470-483.
- 17) Holbourn, A.H.S. Mechanics of Head Injuries. The Lancet, 1943, 2, 438-441.
- 18) Ommaya, A.K. and Gennarelli, T.A. Cerebral Concussion and Traumatic Unconsciousness. Brain, 1974, 97, 633-654.
- 19) Versace, J. A Review of the Severity Index. Proceedings of the Fifteenth Stapp Car Crash Conference, November, 1971, 771-796.
- 20) L wenhielm, C.G.P. On Bridging Vein Disruption and Rotational Cerebral Injuries due to Head Impact. Department of Forensic Medicine and the Division of Solid Mechanics, University of Lund, Sweden, 1977.
- 21) Newman, J.A. Head Injury Criteria. Proceeding of the Twenty-Fourth Stapp Car Crash Conference, October, 1980, 701-747.
- 22) Bohlin, N.J. A Statistical Analysis of 28,000 Accident Cases With Emphasis on Occupant Restraint Value. Proceedings of the Eleventh Stapp Car Crash Conference, October, 1967, 299-308.

- 23) Gloyns, P.F., Hayes, H.R.M., Rattenbury, S.J. Protection of the Car Driver from Steering System Induced Injuries, Proceedings of Institute of Mechanical Engineers, London, 1980.
- 24) Ashton, S.J., Pedder, J.B. and Mackay, G.M. A Review of Riders and Pedestrians in Traffic Collisions. Proceedings of the Meeting on Biomechanics of Injury to Pedestrians, Cyclists and Motorcyclists, IRCOBI, September, 1976, 129-171.
- 25) Ashton, S.J. The Cause and Nature of Head Injuries Sustained by Pedestrians. Proceedings of the Second International Conference. Biomechanics of Serious Trauma. September, 1975, 101-113.
- 26) Ashton, S.J. A Preliminary Assessment of the Potential for Pedestrian Injury Reduction through Vehicle Design. Proceedings of the Twenty-Fourth Stapp Car Crash Conference, 1980, 609-635.
- 27) Pedder, J.B., Hagues, S.B. and Mackay, G.M. A Study of 93 Fatal Two-Wheeled Motor Vehicle Accidents. Proceedings of the IVth International Conference on the Biomechanics of Trauma. September, 1979, 24-38.
- 28) Snively, G.G. Head Protection: Preventive Medicine in Traffic Safety. Proceedings of the American Association for Automotive Medicine, 1978, 69-80.
- 29) Newman, J.A. The Protective Value of Contemporary Helmets in the Prevention of Head Injuries. Proceedings of the Scientific Conference on Traffic Safety, Ottawa, Ontario, May, 1974.
- 30) National Highway Traffic Safety Administration. A Report to the Congress on the Effect of Motorcycle Helmet Use-Repeal -- A Case for Helmet Use. U.S. Department of Transportation, NHTSA, April, 1980.
- 31) Department of Transport. The Motor Cycles (Protective Helmets) Regulations 1980, SI 1980/1279 and Amendment SI 1981/374.
- 32) British Standards Institution. British Standard Specification for Protective Helmets for Vehicle Users. BS 5361:1976.
- 33) British Standards Institution. Specification for Protective Helmets for Vehicle Users (high protection). BS 2495:1977.
- 34) Jehu, V.J. Swingaway Helmet Testing Apparatus. Road Research Laboratory Report, LR 407, 1971.
- 35) Personal Communication with J.B. Souter, Senior Certification Officer, British Standards Institution, Hemel Hempstead, England, March 1981.
- 36) Aldman, B., Lundell, B., Thorngren, L. and Turbell, T. Helmet Attenuation of the Head Response in Oblique Impacts to the Ground. Proceedings of the 3rd International Meeting on the Simulation and Reconstruction of Impacts in Collisions, IRCOBI, 1978, 118-128.
- 37) National Highway Traffic Safety Administration, Consensus Workshop on Head and Neck Injury Criteria, Washington, March 26-27, 1981.
- 38) Claister, D.H., Gilks, R. and Kingston, E. High Energy Impact Testing of Helmet Chin Straps, IAM Divisional Record B14, November, 1978.

#### ACKNOWLEDGEMENTS

The authors wish to thank the Department of Transport for financing this work and for the support given by contract officers. Special thanks go to the material scientists Drs. N. Mills and J. Hay of the University of Birmingham for their help in examining thermo-plastic shells. Our thanks also to the late Professor W. Cissane and to Dr. J. Bull at the Birmingham Accident Hospital and to Dr. P. Acland at the University of Birmingham's Pathology Department for their help in the interpretation of the medical data. Post mortem data were collected with the kind permission of Dr. R. Whittington, the Birmingham City Coroner, and other coroners. Finally we are grateful for the assistance given by all other members of the Accident Research Unit.

This paper is published with permission of the Secretary of State for Transport who does not necessarily agree with the views expressed in it.

#### APPENDIX I

The Ministry of Transport's Category of Serious Injury reads: "An injury for which the person is detained in hospital as an 'in-patient' or any of the following injuries whether or not the person is detained in hospital: fractures, concussion, internal injuries, crushing, severe cuts and lacerations, or severe general shock requiring medical treatment".

## DISCUSSION

MILLER (UK)

Do you feel that improved education to cause youngsters to appreciate the limitations of the helmet and the protective mode of operation of the helmet is of considerable value? From my experience, they keep helmets too long and they don't understand the effects of paint and hydrocarbons on the shells. So, I think education is one of the items that ought to be on your list.

AUTHOR'S REPLY

My response is two fold; firstly, I am a cynic with respect to education. To educate people is time consuming and frequently fruitless; there is a considerable amount of documented evidence to show this. Secondly, notwithstanding my cynicism, we all wish to educate people so that they will not throw their helmets away. I can only refer you to the experience that I have had within Britain; the only way for these riders to know that the helmet shell has been degraded by hydrocarbon exposure is the change in the shell's color. In other words, there seems to be a considerable reluctance to provide the basic information necessary to educate riders.

DR. SHANAHAN (USA)

The problem you identified, in terms of helmet retention, is an interesting one to us at the Army Aeromedical Research Laboratory, Fort Rucker, AL. We have also studied the problem of retention, and we had assumed that individuals who did not retain their helmets throughout an entire crash sequence would be more severely injured than those who did. In a study of some 1100 helicopter accidents, we found that there is no significant difference between those flyers who retained their helmets throughout the crash sequence and those who lost their helmets. We concluded that the impact that causes the helmet to be removed from the head is probably the most severe impact received by the individual. I am not saying that we shouldn't strive toward better retention, but I was surprised by that finding in our study.

AUTHOR'S REPLY

We also thought initially that the injury might have occurred, regardless of helmet retention, but the bulk of the helmets that came off the rider's head seemed to have come off without any observable crush damage to the liner and without any observed major impact. Also, in the motorcycle crash situation, it is quite possible that the riders frequently sustain multiple head impacts. We did have quite a few helmets come off the head after a brush with a car and subsequently the rider sustains a head impact on a curb without benefit of helmet protection. Although it is difficult to know at what point in time the rider sustained fatal head injury, in many cases it was almost impossible not to conclude that the fatal head injury had been sustained after helmet loss. So, I think for this (motorcycle) population, the retention is important.

## THE DEVELOPMENT AND INITIAL EVALUATION OF AN OBLIQUE-IMPACT TEST FOR PROTECTIVE HELMETS

by

Wing Commander David H Glaister  
 Royal Air Force Institute of Aviation Medicine, Farnborough, Hampshire, UK.

## SUMMARY

The design of protective helmets is governed by the construction and performance clauses of national and international standards. Performance requirements are based on the assumption that the brain is injured by excessive linear forces, whilst the construction requirements are an attempt to limit rotational forces to a tolerable level.

This paper describes the development of a novel test device in which angular forces are measured (or derived) following off-axis impacts to a helmeted headform, with the ultimate aim of replacing construction requirements by a definitive test.

Prototype and second generation rigs are described and evaluated in tests on several types of helmets using a range of impact surfaces. Preliminary tests suggest that the method can differentiate between various shell materials and, with a modified anvil, surface irregularities can also be examined. Information can be made available relating to the instantaneous levels of friction developed during impacts, on the torque produced, and on the angular acceleration and terminal angular velocity achieved by the helmeted headform. The technique should provide a useful tool for the investigation and further development of protective helmets.

## INTRODUCTION

The design of helmets for civil and, to a somewhat lesser extent, military use, is governed by the construction and performance requirements of numerous national and international standards. A common feature of these is that tests used to evaluate the shock absorbing capacity of helmets are based on three assumptions, namely 1) that the head is a rigid, but freely mobile mass weighing 5 kg; 2) that all impacts are directed at its centre of gravity; and 3) that injury results at a specified level of linear acceleration.

To illustrate these points consider the British Standard 2495:1977 'Protective Helmets for Vehicle Users (High Protection)', though any other standard would serve the purpose. Clause 11 of the Standard describes the shock absorption test in which a helmet is mounted on a headform and impacted by a falling striker. The points to notice are that the centre of gravity of the headform must lie on axis with the striker to which a linear acceleration transducer is mounted with its sensitive axis also coincident. The performance requirement (clause 7) states that under the impact conditions of the test 'the maximum deceleration of the striker shall not exceed 400G'. Over the years and in different standards this pass/fail level has varied somewhat (though the test method has essentially been the same) and there is a case for reducing it to 300G (as in the equivalent international standard (ISO DP 1511)), or even to 150G (Hundlay et al., 1981). However, the point at issue here is that whilst excessive linear acceleration can cause concussion, skull fracture and brain injury, excessive angular acceleration constitutes another important injury mechanism. As Holbourn wrote as long ago as 1943, 'shear strains are the cause of injury, whereas compression and rarefaction strains are not'. Credence is given to this point of view by the observation that it is difficult to produce concussion in cats when the head is fixed (Denny-Brown and Russell, 1941), a finding recently confirmed in experiments on the squirrel monkey (Gennaralli, et al., 1972).

Largely owing to the scarcity of test devices, comparatively little work has been carried out on the effects of angular impact acceleration. Human studies have, naturally, been restricted to accident investigation and, in particular, the analysis of boxing injuries (for example, Untarharnscheidt, 1970). The usually quoted tolerance figures are, for concussion,  $1,800 \text{ rad sec}^{-2}$  (Ommaya and Hirsch, 1971) and, for rupture of bridging veins,  $4,500 \text{ rad sec}^{-2}$  (Löwenhielm, 1977).

It appears that the case for requiring a helmet to protect against the effects of angular acceleration is at least as strong, if not stronger, than for it to protect against linear forces. However, there are at present no suitable test methods and the makers of standards are forced to introduce constructional limitations in the hope that these will reduce the 'sliding resistance' of accepted helmets. For example, the British Standard already referred to (BS 2495:1977) requires that 'the construction of the helmet shall be essentially in the form of a hard shell having a smooth outer surface...in the form of a continuous convex curve', that 'there shall be no external projections greater than 5 mm', and that these 'shall be smooth and adequately fair'd'.

Inevitably, such requirements are restrictive on design and innovation and may not even achieve the desired reduction in sliding resistance. There would be much advantage to be gained by replacing these construction requirements by a performance test or tests. Several attempts have been made - for example sliding friction has been measured, but does not reproduce the high perpendicular forces of an accidental impact. In France, helmets have been dropped onto a test road surface behind a fast moving vehicle, though apparently with the object of investigating abrasion resistance rather than sliding resistance; also a two-axis test rig has been built, though no test results have yet become available. In Sweden, a sophisticated rig has been developed at the Department of Traffic Safety in Gothenberg (Aldman et al., 1976). In this rig the test headform is instrumented with a package of seven accelerometers to give, by computation, three-axis angular accelerations and their resultant. The helmeted headform is dropped in free-fall onto a rotating test surface so that the two velocity components, vertical and horizontal, can be varied independently. Preliminary work has highlighted the influence of road surface texture and shown that realistic impacts may



cause intolerable angular forces. Other experiments have confirmed the use of a free head as being appropriate, since similar results were obtained on whole dummies and even cadavers (Aldman et al., 1978).

The object of the present study was to develop a simple test method in which the 'resultant' impact velocity was achieved by dropping a helmeted headform in guided free-fall, and the two components 'vertical' and 'horizontal' were obtained by impacting an inclined surface. This is the accident situation simply rotated to make the resultant velocity vector perpendicular. This paper describes the development of the method and its preliminary evaluation.

Tests were initially conducted using an instrumented headform, the peak angular acceleration of which was recorded. Various problems led to this approach being abandoned in favour of an instrumented anvil from which both perpendicular and longitudinal impact forces could be monitored. These two phases of the project will be described separately.

#### Phase 1

##### APPARATUS

**Drop tower.** One of the two 10 m tall drop towers in the helmet laboratory at the RAF Institute of Aviation Medicine was modified to provide more anvil area by separating the two vertical guide wires by 20 in (508 mm). A simple drop frame was welded up from 18 mm diameter steel tube with PTFE bushes and the helmeted headform was suspended from this on a harness sewn up from 25 mm wide tape (Fig.1). On impact, the helmet leaves the harness and the frame continues down to be arrested by blocks of energy absorbing foam. The frame also carries a blade which occludes a light beam to trigger the recording system.

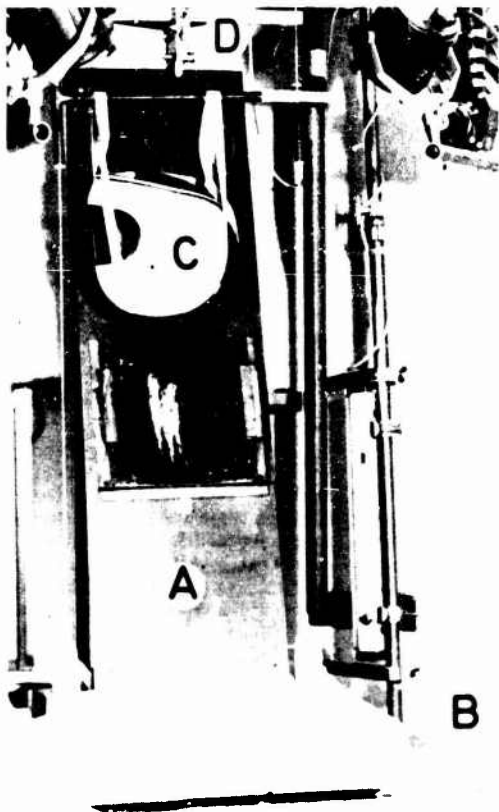


Fig.1. Prototype test rig showing the inclined anvil (A) mounted on a massive monolithic base (B) and carrying a specimen of road surface. The helmet (C) is raised by winch and released from a bomb-slip (D). The helmet is guided during its fall by vertical wires, sliding carriage and a webbing harness from which it bounces clear on impact.

**Headform.** The headform was constructed in hardwood from dimensions given in ECE Regulation No 22 (reference headform K, 580 mm head circumference). This specification was used since it includes dimensions for neck and chin and allows a helmet to be held by its normal chinstrap. A 40 mm diameter hole was drilled vertically up from the neck so that a single-axis angular accelerometer could be mounted at the centre of gravity with its sensitive axis vertical (Endevco Model 7301). The mass of the instrumented headform was then adjusted to 5.0 kg by replacing an appropriate volume of timber by plugs of Wood's metal. Care was taken to achieve a realistic moment of inertia (about the vertical axis) the actual value finally obtained being 165 kg cm<sup>2</sup>. Tests were carried out with the headform horizontal and the accelerometer axis parallel with the anvil surface, so that impacts could take place at any selected point on the horizontal circumference of the helmet.

**Anvil.** This consisted of a sheet of steel, 4.5 mm thick and measuring 1.37 m tall by 406 mm wide bolted against a framework of 40 x 40 x 6 mm steel angle at an angle of 15° from the vertical. The rig was bolted to the concrete monolithic block of the drop tower via a base frame of 70 x 70 x 6 mm steel angle. Differing impact surfaces, each measuring 300 x 300 mm, were mounted on the centre of the anvil using further steel angle (Fig.1). Samples of 'typical' road surfaces were made up by the Transport and Road Research Laboratory at Crowthorne, Buckinghamshire. Following impact, the helmeted headform was caught in a box lined with 100 mm thick energy absorbing Temperfoam. This prevented further damage and limited rotation to about one full revolution.



**Instrumentation.** The output of the angular accelerometer was amplified, stored on a transient recorder (DataLab Series 2000), and displayed on an oscilloscope (Hewlett-Packard 1201B). Permanent records were obtained on Polaroid film.

#### RESULTS AND DISCUSSION

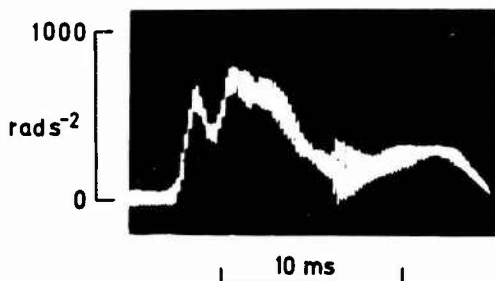


Fig.2. Unfiltered recording of angular acceleration.

A typical oscilloscope recording is illustrated in figure 2. The high frequency component was subsequently removed by the addition of a low pass filter. This record was obtained from a 3.0 m drop of a polycarbonate full-face helmet on to a fine macadam road surface (BS 4967:1973, 6 mm nominal size medium-textured wearing-course macadam). The record shows two peaks lasting for some 7 ms and a longer tail, the total impact event lasting for 16 ms. The peak angular acceleration was  $680 \text{ rads}^{-2}$  and integration of the trace gave a terminal angular velocity of  $5.9 \text{ rad s}^{-1}$  and an overall angular displacement of  $0.053 \text{ rad}$  (about 3 degrees). The record may be compared with the traces left by the helmet as it scuffed along the macadam (Fig.1) which show a double broad mark over 50 mm and a longer narrow tail. At the theoretical impact velocity of  $7.7 \text{ ms}^{-1}$ , the double mark equates with a time of 6.5 ms and the whole event lasted for 16 ms. The impact can be interpreted as consisting of:

1. initial contact of helmet shell with anvil flattens it against the surface giving a broad scuff mark;
2. the shell starts to bounce off the anvil but is rapidly forced back by the inertia of the headform;
3. the headform/helmet combination rebounds from the anvil, and as the force of contact falls, the shell recovers its normal shape and light contact is initially maintained. It may be noted that linear acceleration traces having two peaks are frequently seen in conventional impact tests when forces are measured in the striker (Glaister, 1979).

Many drops were carried out using various helmet and surface combinations, but no comprehensive series of tests was conducted for reasons which included 1) problems with the flying lead which tended to snag and break, 2) limitations of impact site caused by the single axis of accelerometry, 3) damage to the impact surfaces, especially when attempts were made to impact helmet prominences such as studs and rivets, and 4) limited frequency response due to the relative flexibility of the anvil. The method did appear promising, however, and it was decided to modify the test so as to record anvil forces rather than headform forces. The theoretical advantages offered by this approach are that it dispenses with the vulnerable flying lead and can measure, separately, perpendicular and longitudinal impact forces. At the same time the rig was redesigned to be stiffer, to give an improved frequency response.

#### Phase 2

##### APPARATUS

**Anvil.** The anvil (Fig.3) was designed after discussion with the manufacturers of quartz load measuring washers. It consists of a block of cast aluminium measuring  $200 \times 250 \text{ mm}$  by 45 mm thick firmly attached to a second L-shaped block by six load washers (Kistler Instruments Quartz Load Washers Type 9031). A matched set of four of these were evenly spaced behind the anvil to measure perpendicular forces whilst another matched pair were placed at its lower edge to measure longitudinal forces. Each load cell was backed by a PTFE (Teflon) washer, 0.2 mm thick, to allow the necessary slippage (each washer has a stated rigidity of  $6 \text{ kN}/\mu\text{m}$ ) and the surfaces of the blocks were machined to give uniform load distribution. The load washers were individually pre-tensioned to 10 kN by high tensile steel studs using the manufacturer's calibration figures and amplifier (Kistler Instruments Charge Amplifier Type 5007) and the complete anvil was then calibrated using a 250 kN servo press (Mayes), the load washer outputs being paralleled in the two sets of four and two.

The anvil was mounted between two A-frames welded up from  $50 \times 50 \times 8 \text{ mm}$  steel angle and stiffened by 4 mm thick steel plates (Fig.3). The A-frames were bolted to a sub-frame of  $70 \times 70 \times 6 \text{ mm}$  steel angle which in turn was bolted to the monolithic concrete base of the test tower. This somewhat complex design retained rigidity whilst allowing the rig to be removed without disturbing the vertical guide wires. The anvil face was centred 500 mm above the top surface of the concrete base and 130 mm behind its centre line. Slots in the sub-frame provided 80 mm of fore and aft adjustment and allowed impacts to be centred on the anvil face.

**Instrumentation.** The two paralleled outputs from the load washers were fed to two charge amplifiers and thence to two channels of the transient recorder. The previously determined calibration factors were used to set up the amplifiers and were also dialled into a Charge Calibrator (Kistler Instruments Type 5351) which was used to set up and calibrate the entire recording system. The transient recorder was triggered externally from a light beam interrupted just prior to impact or, on occasion, by use of its internal

pre-trigger facility. Outputs from it were displayed on a two-beam oscilloscope (Hewlett-Packard Type 180A) and, when permanent recordings were required, the traces were photographed on Polaroid film.

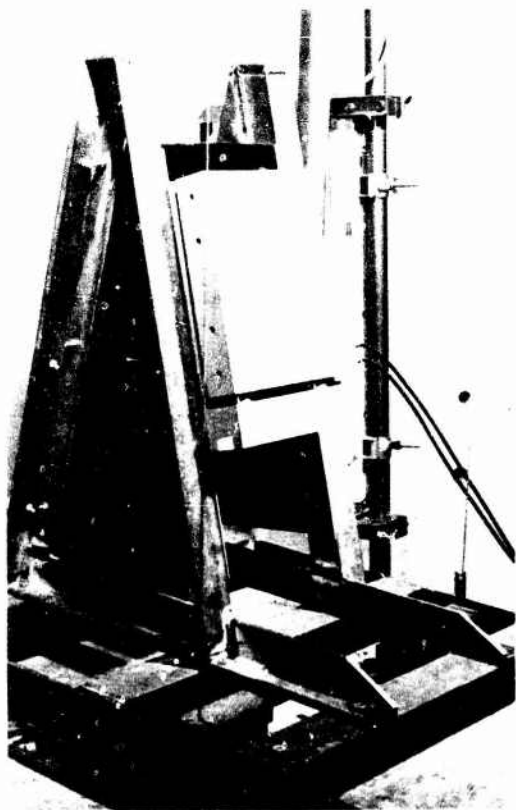


Fig.3. The 'definitive' test rig showing the instrumented anvil mounted between rigid steel A-frames bolted, via a sub-frame, to the monolithic base of the drop tower.

#### RESULTS AND DISCUSSION

Mechanical Performance. Calibration curves for the two transducers' axes are illustration in figure 4. Linearity is excellent and the slopes of the two lines were used to set up amplifier gains for subsequent tests.

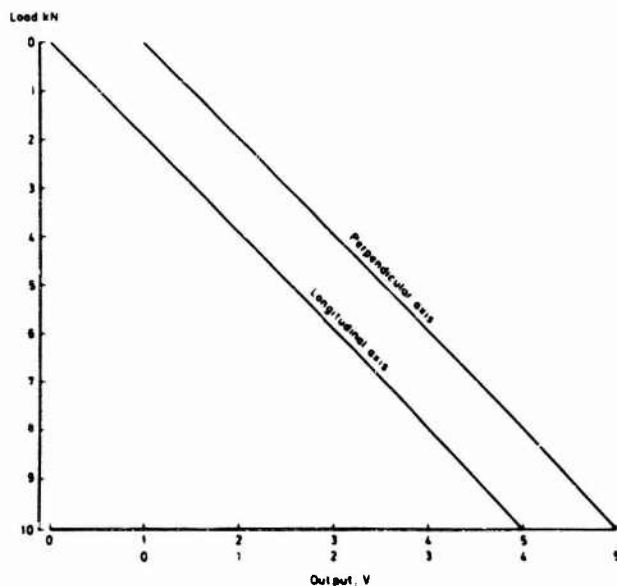


Fig.4. Calibration curves for the two axes of the instrumented anvil.

Resonant frequency was measured by tapping the anvil in either axis with a light hammer and with 180 kHz low-pass filters fitted to the charge amplifiers. With the anvil free standing, values were close to the 9.9 kHz (perpendicular) and 7.0 kHz (longitudinal) calculated from the mass on the anvil and the manufacturer's figures for the rigidity of the load washers. With the anvil mounted, the resonant frequencies fall to 3.4 kHz and 4.0 kHz respectively, but these values are still well outside the channel frequency class 1,000 Hz recommended for head impact studies (ISO 6487-1980). Low-pass filters with a -3 dB point of 1.6 kHz and slope of 12 dB per octave were used with the charge amplifier in all subsequent tests in line with this recommendation.

Cross-talk between channels was investigated by tapping the anvil in either axis using a soft headed hammer. Some flexing of the anvil was demonstrable, despite its thickness, but satisfactory results were obtained over most of its front surface as illustrated in figure 5. Impacts were subsequently arranged so as to avoid the lowermost 50 mm of the anvil where a perpendicular force would have biased the measurement of a simultaneous longitudinal force.

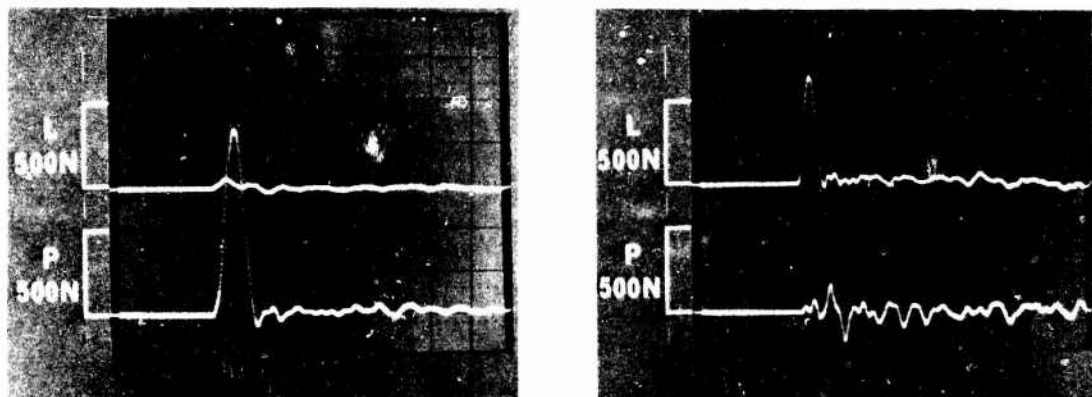


Fig.5. Two axis recordings from the instrumented anvil following (left) perpendicular and right (longitudinal) impacts from a soft-headed hammer.

**Drop Height.** Tests were restricted to a drop height of 5.0 m (compared to 3.0 m in the Phase 1 tests) giving a free-fall terminal velocity of  $9.90 \text{ ms}^{-1}$  (22.2 mph). With an incident angle of  $15^\circ$ , this gives a horizontal component of  $9.56 \text{ ms}^{-1}$  (21.4 mph) and a vertical component of  $2.56 \text{ ms}^{-1}$  (5.7 mph). These impact velocities are relatively low when compared to real accidents, but considered sufficient to evaluate the methodology, and also practical in terms of drop heights available on most existing test rigs. Studies are planned at drop heights of up to 9.5 m, giving horizontal and vertical components of  $13.18 \text{ ms}^{-1}$  (29.5 mph) and  $3.53 \text{ ms}^{-1}$  (7.9 mph) respectively, and also with the anvil less steeply inclined so as to increase the vertical velocity component.

**Anvil Surface.** Impacts were conducted on a variety of aluminium oxide and silicon carbide coated cloth and fibre sheets with particle sizes of grades 24 and 80 (J.G. Naylor and Co Ltd), and on a 3 mm Shellgrip surface having a texture depth of 1.2 mm (BS 4987:1973). All surfaces became clogged after repeated impacts, especially with glass fibre reinforced (GRP) helmets, and clearly needed frequent replacement. Shellgrip gave a very coarse abrasive mark, quite different from the smooth scuffs seen with the road surfaces used in the Phase 1 tests, but comparable to those seen with the grade 24 abrasive. Since the road surfaces varied to such a degree, the finer grade 80 abrasive appeared a reasonable compromise on which to standardise. No difference was apparent between the aluminium and silicon based materials, but it was found that the rigid fibre sheet backed material was easier to support on the anvil. Further tests were, therefore, carried out using a grade 80, closed coat, Resinbond Corolith (aluminium oxide).

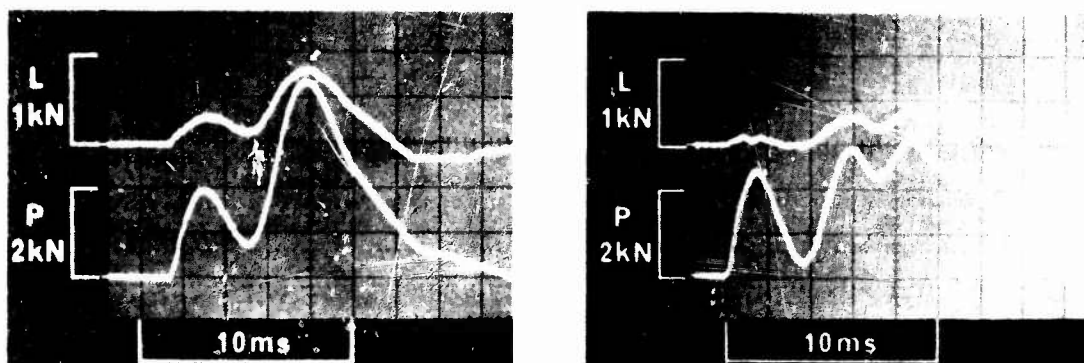


Fig.6. Two axis recordings from the instrumented anvil obtained by dropping (left) a motorcyclist's helmet and (right) an aircraft protective helmet.

**Impact Forces.** Typical recordings are illustrated in figure 6. That on the left was obtained by striking the smooth shell surface of a full-face GRP motorcyclist's helmet; whilst in that on the right the impact point was the aluminium visor mounting of an RAF Mk 3 aircraft helmet. When the traces are compared with results from Phase 1 (Fig 2), it is clear that the second axis of force measurement assists in the interpretation of impact events.

Thus, the longitudinal force provides the rotation inducing torque and is proportional to the induced angular acceleration, whilst the area of the force/time trace is proportional to the angular velocity attained by the helmeted headform. These factors will be related to the risk of injury due to head rotation and, even if absolute tolerance limits are unknown, the greater the forces, the greater will be the risk of resulting injury. The perpendicular force is an indication of the energy absorbing properties of the helmet (as in conventional impact test methods), whilst the ratio of longitudinal to perpendicular forces is a measure of the coefficient of friction at any instant during the impact event.

Comparison of the two recordings of figure 6 show how these several factors can vary from helmet to helmet. With the motorcyclist's helmet, the coefficient of friction remains relatively constant, ranging only from 0.15 at the first peak, to 0.17 in the trough and 0.18 at the second peak. With the RAF helmet, however, the coefficient started at a very low value (less than 0.05) to reach a comparable level (0.13) later in the impact. Figures as high as 0.34 have been seen in helmets with thermoplastic shells (for example, figure 7h).

Integration of the longitudinal force/time traces of figure 6 gives areas in the ratio of 1.0 to 0.5. Assuming equivalent angular inertias in the two tests, this means that the first helmet left the anvil with twice the angular velocity of the second, a further indication of the lower sliding resistance obtained with the RAF helmet.

Digital outputs already available from the transient recorder would allow these factors (and derivatives) to be computed readily for any impact. For example, the coefficients of friction at peak perpendicular force, or at a standard value of perpendicular force, or the maximum value during the impact, as well as the area at the longitudinal force/time curve, could prove to be useful indices for comparing the performance of different helmets.

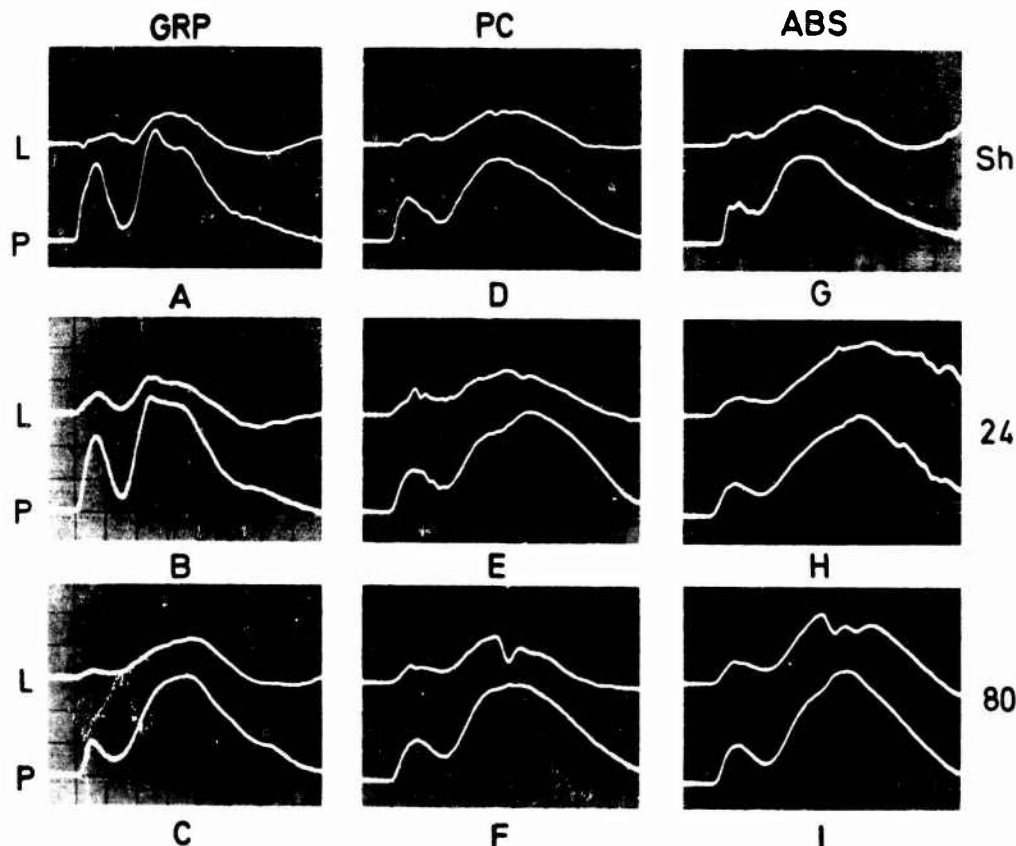


Fig.7. Two axis recordings from the instrumented anvil obtained by dropping glass fibre reinforced plastic (GRP), polycarbonate (PC) and acetyl butadiene styrene (ABS) helmets on to a Shellgrip surface (Sh) and on to grades 24 and 80 aluminium oxide abrasives. The longitudinal scale (L) is 500 N, the perpendicular (P), 1 kN and the time base, 2 ms per division.

**Shell Material.** Figure 7 illustrates recordings for three different helmet shell compositions - GRP, and polycarbonate (PC) and acetyl butadiene styrene (ABS) thermoplastics - and for three impact surfaces - Shellgrip (Sh) and 24 and 80 grade aluminium oxide. All helmets were open-face models of medium size, the GRP one to BS 2495, the thermoplastic ones to BS 5361. Both impact surfaces, shell and anvil, affect the forces developed. Thus, Shellgrip gives lower longitudinal forces though, apart from ABS, the differences are small; whilst ABS gives greater longitudinal forces on all three impact surfaces. Coefficients of friction, estimated at the time of maximum perpendicular force in each case, range from 0.12 for ABS on Shellgrip, to 0.34 for ABS on grade 24 aluminium oxide. ABS also gives greater angular velocities as estimated from the areas of the force/time traces (especially with the abrasives) and this effect is also apparent from examination of the shells post-impact. Figure 8a illustrates an initial scrape followed by a peppery appearance where the shell has rolled against the anvil without further sliding, typical of ABS, and this may be compared with the continuous scrape mark of a GRP helmet (Fig 8b). Similar scrape marks have been seen in helmets worn in real accidents (for example, Aldman et al., 1978, and the Birmingham Accident Research Unit (personal communication)).

A similar conclusion can be drawn from examination of the anvil surface post-impact (Fig 9). Polycarbonate appears to fall between these two extremes, but more tests are required before such generalisations can be firmly established. It may also be noted that a new form of polycarbonate is in production containing a greater concentration of plasticiser than present in the material tested here, and this may affect its sliding resistance.

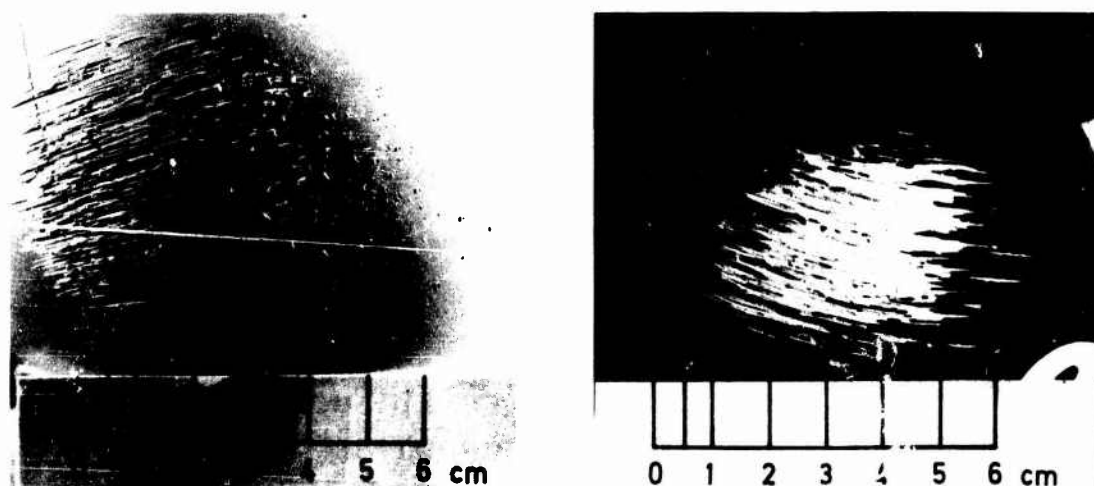


Fig.8. Helmet shell surfaces following oblique impacts against Shellgrip. Left, acetabulene styrene (ABS); right, glass-fibre reinforced plastic (GRP).

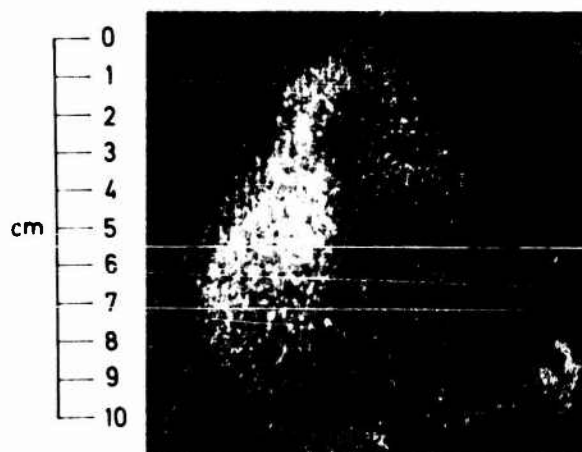


Fig.9. Grade 80 aluminium oxide anvil surface following identical impacts from left, a GRP helmet and right, an ABS helmet. Force recordings are illustrated in figures 7 i and c.

**Shell Profile.** Figure 6 shows that the use of a simple abrasive impact surface does not permit meaningful differentiation between helmets impacted on a smooth part of the shell, or on a rigid projection. Other tests have confirmed that the small impact areas offered by such projections tend to reduce longitudinal forces. Rigid projections (depending on their strength) could, however, catch in a more irregular impact surface and cause increased angular acceleration. This property is to be investigated by use of a modified anvil surface made up from transverse bars of steel with appropriately radiused upper edges.

**Helmet Fit.** A loose fit of the helmet on the headform will allow initial rotation of the helmet alone, followed by helmet plus headform as the slack is taken up. This mechanism offers a further explanation for the double hump recordings previously discussed in Phase 1. In reality, both motions (relative rotation and bottoming of liner on headform) probably take place synchronously. The amount of rotation available will also depend on other factors such as the direction of impact, chin strap tension, and the greater coverage given by a full-face helmet. It is important, therefore, that tests are carried out on the correct size of headform (which should be as anatomically representative as possible) or, until more headforms are available, are restricted to the correct size of helmet.

#### CONCLUSIONS

The oblique impact test rig, as developed through the two phases of this report, functions well with no outstanding major problems.

Preliminary tests indicate that the method can be used to differentiate between various helmet shell materials, but that a special anvil face will be required to examine irregularities in a helmet's outer surface.

Recordings obtained give information on the instantaneous levels of friction developed during impact, on the torque produced on, and angular acceleration induced in the helmeted headform, and on its final angular velocity. All these factors can be readily computed from digital outputs already available.

The technique should provide a useful tool for the investigation and further development of protective helmets.

## REFERENCES

- Aldman, B., Lundell, B. and Thorngren, L. (1976). Non-perpendicular impacts, an experimental study on crash helmets. In Proc. IRCOBI 1st International Meeting on Biomechanics of Injury to Pedestrians, Cyclists and Motorcyclists. pp. 322-331.
- Aldman, B., Lundell, B., Thorngren, L. and Turbell, T. (1978). Helmet attenuation of the head response in oblique impacts to the ground. In Proc. IRCOBI 3rd International Meeting on Simulation and Reconstruction of Impacts in Collisions. pp. 118-128.
- British Standard 2495:1977. Specification for protective helmets for vehicle users (high protection). British Standards Institution, Park Street, London.
- British Standard 4987:1973. Specification for coated macadam for roads and other paved areas. British Standards Institution, Park Street, London.
- British Standard 5361:1976. Specification for protective helmets for vehicle users. British Standards Institution, Park Street, London.
- Denny-Brown, D. and Russell, W.R. (1941). Experimental cerebral concussion. *Brain* 64: 93-164.
- ECE Regulation No. 22/02. Uniform provisions concerning the approval of protective helmets for drivers and passengers of motor cycles and mopeds. Economic Commission for Europe, Inland Transport Committee, Working Party on Road Transport. United Nations, Geneva.
- Gennarelli, T.A., Thibault, L.E. and Ommaya, A.K. (1972). Pathophysiologic responses to rotational and translational accelerations of the head. SAE Paper No. 720970. 16th Stapp Car Crash Conference. November 1972.
- Glaister, D.H. (1979). Measurement of impact forces and accelerations in human crash simulation and protection. In Proc. of the Conference on Weighing and Force Measurement, Institute of Measurement and Control, Brighton, September 1979. pp. 48-65.
- Holbourn, A.H.S. (1943). Mechanics of head injuries. *Lancet*, 2: 438-441.
- Hundley, T.A., Haley, J.L. and Shanahan, D.F. (1981). Medical design criteria for US Army motorcyclist's helmet. US Army Aeromedical Research Laboratory Report LR-81-2-4-1. Fort Rucker, Alabama.
- ISO 6487-1980(E). Road Vehicles - Techniques of Measurement in Impact Tests - Instrumentation. International Organisation for Standardization.
- ISO DP 1511. Protective helmets for road users. International Organisation for Standardization.
- Löwenhielm, C.G.P. (1977). On Bridging Vein Disruption and Rotational Cerebral Injuries due to Head Impact. Department of Forensic Medicine and Division of Solid Mechanics, University of Lund, Sweden.
- Ommaya, A.K. and Hirsch, A.E. (1971). Tolerances for cerebral concussion from head impact and whiplash in primates. *J. Biomechanics*, 4: 13-21.
- Unterscharnschmidt, I. (1970). About boxing: review of historical and medical aspects. *Texas Reports on Biology and Medicine*, 28: 421-495.

## DISCUSSION

DESJARDINS (USA)

Did you account for the inertial effects of the aluminum strike surface on the load cell response? From the pictures it appeared that the impact block had considerable mass which could influence the data.

AUTHOR'S REPLY

Yes. The load washers are extremely stiff; their displacement can be measured in micrometers--so that anvil response can be effectively ignored. The anvil is analogous to the headform used in linear impact tests where transmitted forces are monitored -- only operate in two axes.

STEELE-PERKINS (UK)

In an effort to reduce angular decelerative loads on the head, do you feel that a recommendation limiting the type of material used in the helmet's construction might follow in due course?

AUTHOR'S REPLY

The primary objective is to get away from constructional requirements. What I would like to see is a test similar to that which I have described used to assess prototype helmets (type approve testing). Then, if a certain helmet feature were shown to induce greater angular forces than the established criterion, it would go back to the manufacturer for modification. The final form of the helmet would then be based entirely on its functional performance. Current helmets may not be of the optimum configuration.



## ANALYSIS OF US ARMY AVIATION MISHAP INJURY PATTERNS

by

James E. Hicks, Ph.D., and Billy H. Adams  
 Directorate for Aviation System Management  
 US Army Safety Center  
 Fort Rucker, Alabama 36362

MAJ Dennis F. Shanahan, M.D.  
 Biodynamics Research Division  
 US Army Aeromedical Research Laboratory  
 Fort Rucker, Alabama 36362

## SUMMARY

Recent advances in US Army procedures for the identification and reporting of personnel injuries resulting from aircraft mishaps are reviewed. Mishap injury data requirements based on the needs of retrospective and prospective analyses are discussed. The requirement for these analyses to support engineering management decisions that will implement remedial programs to correct identified crashworthiness deficiencies is discussed. This paper summarizes the US Army process for gathering aviation mishap injury data, describes modifications to procedures and codes for recording injury data, and provides examples of use of the data resulting in fleet-wide improvement programs.

## INTRODUCTION

Since the earliest days of flight, it has been an inescapable fact that aviation mishaps will occur in spite of all efforts to the contrary. This statement is made not in an attempt to detract from the value of mishap prevention but to point out that man is an inherently fallible creature, and he has endowed the equipment and the systems that he develops with the same fallibility. Efforts toward mishap prevention have reduced the US Army aviation mishap rate considerably over the last decade; however, this rate appears to be plateauing toward a relatively constant value (Figure 1). Efforts toward reducing this rate must be continued, but realistically one must assume that the goal of a zero accident rate is not achievable. Furthermore, it is inevitable that crashes will occur as a result of enemy action in a combat environment. Consequently, to minimize these costs both in terms of materiel and personnel losses, it is vital to design crashworthy aircraft and effective life support equipment. Crashworthy designs are, in part, achieved through an understanding of injury mechanisms identified through mishap investigations.

Numerous papers over the past 25 years have reported the incidence and distribution of injuries occurring in US Army aviation mishaps (1,2,3,5,6). Probably the most salient feature of this quarter century of tracking injuries is that the distribution and type of injuries have changed very little, with one important exception. Thermal injury as a cause of death in survivable accidents has been reduced from 41% in 1969 (3) to essentially zero today (7,9) due to the introduction of crashworthy fuel systems in most US Army helicopters in the early 1970's. This rather dramatic achievement occurred through a process of identification and documentation of the problem (mishap investigations) which led to a practical engineering solution. Implementation of a "fix" normally requires a cost justification (i.e., cost analysis), but in the case of thermal injury the nature and severity of the problem was so great that little cost analysis was required.

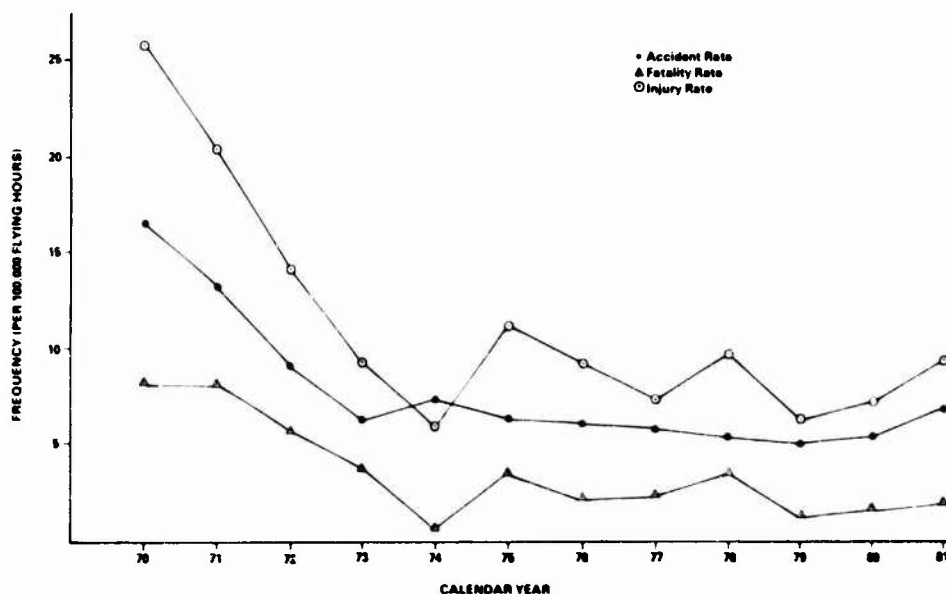


FIGURE 1--US ARMY AVIATION MISHAP EXPERIENCE (CY 1970-CY 1981)



Although this example demonstrates the general method of approaching injury prevention, thermal injury was a rather obvious problem with fairly readily obtainable solutions. Prevention of the most prevalent areas of injury, namely to the head, spine, and extremities (6) is proving to be a far more elusive objective. Solutions to these problems are requiring considerably more detailed and accurate data than has been collected in the past, and the cost effectiveness of proposed solutions must now be readily demonstrable in order to justify their implementation. Identification of mechanisms of injury and their relationship to life support equipment (LSE), i.e., seats, restraints, helmets, have become primary concerns in the quest for means of preventing injury. Furthermore, since this is basically an epidemiological problem requiring the compilation and analysis of relatively large volumes of data, the data should be readily reduced to a form that can be stored and processed by computer. Recognizing these problems, the US Army Safety Center (USASC), together with the Armed Forces Institute of Pathology (AFIP) and the US Army Aeromedical Research Laboratory (USAARL), has developed a system of aircraft mishap injury investigation and analysis that will be described in this paper.

## CRASH INJURY IDENTIFICATION AND REPORTING

### OVERALL MISHAP INVESTIGATION PROCESS

Since 1978, the US Army has used a system of Centralized Mishap Investigation (CMI) wherein USASC provides investigators for the majority of major aviation mishaps. The USASC maintains a number of investigation teams; each consisting of three members (board president, air safety specialist, and recorder). The team serves as the core of the investigation board and draws on local expertise and resources to conduct the investigation. This system of providing a highly trained and experienced team of investigators to direct the investigation of most major mishaps has improved the overall technical quality of investigations by insuring a thorough and standardized approach and uniform reporting methods.

In 1979, through an agreement between USASC and AFIP, AFIP began providing, on a time available basis, an aerospace pathologist to perform the autopsies on fatalities in US Army mishaps. Since the inception of the program, AFIP has performed all but a few of the autopsies. This has vastly improved the quality of necropsy data because these aerospace pathologists are well trained in forensic methods, and they are particularly attuned to the determination of injury mechanisms derived not only through analysis performed at the autopsy table but also through correlation with the kinematics of the crash and damage to the aircraft and LSE. Before 1979, autopsies were performed by local hospital pathologists or medical examiners who may or may not have possessed the necessary interest or training to perform a comparable quality investigation. The flight surgeon assigned to the mishap investigation board assists the aerospace pathologist in his investigation and does a similar injury investigation on all individuals who survived the mishap.

As an adjunct to the onsite injury investigation provided by the investigation board and AFIP, USAARL has established the Aviation Life Support Equipment Retrieval Program (ALSERP) which, by Army regulation, requires that all items of aviation LSE "in any way implicated in the cause or prevention of injury" be sent to USAARL for detailed analysis (8). This program seeks to precisely define the effectiveness of LSE involved in mishaps by correlating damage to the equipment with injuries (or lack of injuries) and other data derived from the field investigation of that particular mishap. This data is coded and stored in a computer for later use in identifying trends or consistent failure modes for various items of LSE. Once problems with a particular piece of equipment are identified, recommendations for changes in design criteria can be made. The major accomplishment of this program to date has been the identification of various failure modes of the current US Army aviation helmet which has, in part, led to the drafting of new aviation helmet design criteria (4). This program is also being used to monitor the functioning of energy-absorbing seat designs which are currently being introduced to the field.

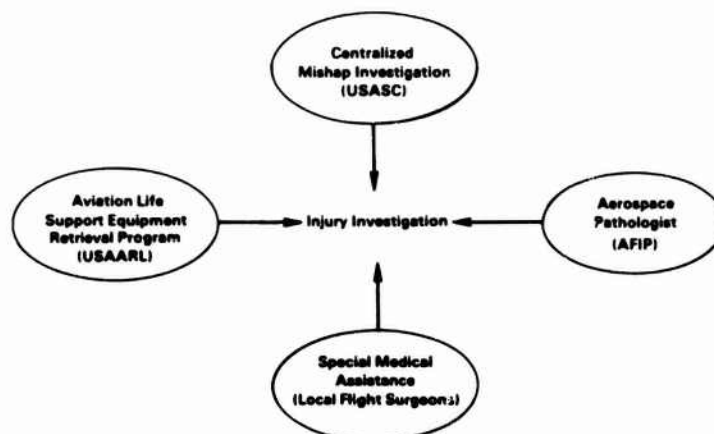


FIGURE 2--INJURY INVESTIGATION

As shown in Figure 2, this combination of centralized mishap investigation, centralized postmortem examination of fatalities, and systematic analysis of retrieved LSE has vastly improved the depth and quality of injury investigation in US Army aviation mishaps through standardization of procedures for data collection and by using experienced and highly trained individuals in key positions.

#### AVIATION CRASH INJURY REPORTING SYSTEM

The aviation mishap investigation process described above provides the overall framework for the identification and recording of aircraft crash injury information. A modified injury coding system has been developed to operate within this framework and provide the necessary medical, engineering, and management information to support required remedies. Completed in 1981, the format and structure of this code are described below.

#### Overall Format of Code

The proposed code is structured to include the four data fields shown in Table I below:

Each one of the data fields will be described separately, after which an example will be provided which demonstrates use of all the data fields together. The proposed reporting system provides that each injury data field will be reported for each separate and distinct injury cause factor as defined below.

TABLE I

OVERALL STRUCTURE OF PROPOSED US ARMY AVIATION MISHAP INJURY CODE

Data Field Number	Nomenclature	Information Provided	Number of Data Elements
1	Identifier	Medical description of trauma	5
2	Mechanism	Physical process of injury occurrence	2
3	Deficiency	Underlying cause(s)	3
4	Cost	Economic impact of lost time, etc.	1

#### Injury Identifier

The trauma incurred by each occupant is reported in terms of a medical description of the injuries and their individual severities. Injuries suffered by those requiring less than first aid are reported as "none." For others, the injury characteristics shown in Table II are reported for each distinct injury.

Actual codes used for each of these data elements are available from USASC. A major departure from previous practice is the proposed identification of injury location in terms of the combination of an overall major body part, its aspect, and the system involved. This is in contrast to the common practice of a specific anatomical identification. This departure greatly enhances the usefulness of the coded data for identification of remedial measures for most injury types. For certain exceptions,

TABLE II

INJURY IDENTIFIER DATA ELEMENTS

Data Element	Nomenclature
1	Location of injury (major body region)
2	Aspect(s) of injured region effected
3	Type of lesion
4	Body system involved
5	Injury severity (established in accordance with (1))

provisions are made for more specific injury location identification. At this writing, there are two exceptions anticipated--the specific anatomical part will be reported for (1) spinal injuries, and (2) for head (skull) injuries. This is necessary in the two cases listed in order to determine the specific remedial measures needed.

#### Injury Mechanism

The mechanism of injury occurrence is used to describe the physical process through which each injury occurred. The injury mechanism is constructed in a subject-verb-qualifier format. Two data elements are used--the mechanism action ("verb") and the mechanism qualifier. The injury location (body part) provides the subject. Thus, a simple sentence is formed from standardized codes to describe the injury mechanism such as spine (L-1) "received excessive vertical force." Multi-year studies of aviation injury patterns were used as the basis for selection of the particular mechanisms to be included in the lists of codes. An attempt was made to balance the requirement for mechanism specificity with needs of engineering analysis. An overly detailed code hampers the identification of corrective actions.

#### Injury Cause Factor

The injury cause factor is identified as that underlying deficiency (or deficiencies) which permitted or caused the mechanism to occur. Injury causes are identified primarily in terms of hazards associated with the design of the aircraft or life support equipment (such as "seat allowed excessive loading"). Operational injury causes are also included such as "failed to use restraint system."

The injury cause factor is constructed in a subject-verb qualifier format in a manner similar to that used for the mechanism above. Thus, the injury cause is formed in a simple sentence from standardized codes.

#### Injury Cost

US Army Regulation 385-40 (10) establishes the economic impact of various injury severity levels based on lost workdays, restrictions from duty, and other similar considerations. Estimates of the cost of each individual injury suffered by each casualty are computed according to these figures and projections by the flight surgeon regarding the prognosis for recovery. Injury costs are calculated by USASC personnel based on data provided by the field investigation. The technique for calculating injury cost insures that each distinct injury is "weighted" according to its individual severity. The sum for any casualty of the weighted costs for all injuries is equal to the overall cost for that individual.

#### Hypothetical Example of Use of The Injury Code

The above components of the injury code are established for each distinct injury suffered by each injured occupant. "Distinct" injuries are defined as those (a) with different cause factors, or (b) occurring to different major body regions. This information provides a description of the injuries, causes, and costs in a format and level of detail which facilitates analysis of critical trends. Thus, an injury code such as the hypothetical example shown in Table III below is established for each casualty.

TABLE III

#### HYPOTHETICAL EXAMPLE OF USE OF INJURY CODE FOR CASUALTY SUFFERING MAJOR INJURIES

INJURY NUMBER	INJURY DESCRIPTION					MECHANISM		CAUSE FACTOR			Injury Cost
	Location	Aspect	Type	System	Severity	Action	Qualifier	Subject	Action	Qualifier	
1	Spine, L1	Inferior	Fracture, comp	Skeletal	Major	Received	Excessive Decelerative Force	Seat	Allowed	Excessive Loading	\$45,405
2	Face	Anterior	Laceration	Skin	Major	Struck	Gunsight	Design	Provided	Inadequate Clearance	\$4,541
3	Hand	Right	Contusion	Skin	Minor	Struck	Structure	Extremities	Failed	On Impact	\$54

Total - \$50,000

#### DEVELOPMENT STATUS OF INJURY CODE

Initial development of the proposed injury reporting and analysis system was completed in early 1981. This code has been partially tested in retrospective analyses of Army aircraft mishap reports performed by USASC with assistance of other Army agencies. In these analyses, the injury code was demonstrated to facilitate the identification and ranking of crash hazards in helicopter designs, as discussed below. Other retrospective analyses, performed by USAARL, of specific head and spine injury

patterns indicated that the initial code lacked sufficient specificity in these two body regions, and the code has been modified accordingly. Evaluations have indicated that the proposed code requires more injury data than the previous system but that the data should be generally available within a mishap investigation.

Results indicate the code provides detailed information regarding injury mechanisms, causes, and costs. This information permits critical cause factors to be rank ordered according to the severity of their effect over selected time periods. This data provides vital management information regarding the need for remedial programs. In addition, the injury causes are described in a format and terminology which facilitates engineering solutions.

## CRASH HAZARD ANALYSES

### RETROSPECTIVE ANALYSES

Two levels of retrospective analyses of crash injury have been performed by the US Army. The first used the coding system described above to identify crash hazards in US Army aircraft. It was envisioned that a primary output of this effort would be an improved direction for crashworthiness research and development including the identification of follow-on research required to define specific design criteria changes necessary to reduce the identified hazards in current and future aircraft and LSE.

Analyses of this type have been completed for three types of Army aircraft; a medium lift cargo helicopter, an observation helicopter, and an attack helicopter (10,11,13). An analysis of a utility helicopter is ongoing and is scheduled for completion during the coming calendar year. The most significant results of one of the crash hazard analyses are discussed below. Emphasis will be placed here on those crash hazards associated with excessive linear acceleration. Supportive information, such as crash impact signatures, will also be provided and related to the injury causes.

### Components of Change in Impact Velocity

Figure 3 shows the longitudinal and vertical components of the change in velocity of the aircraft center of gravity during its major impact for each of the accidents studied. The resulting impact survivability is indicated.

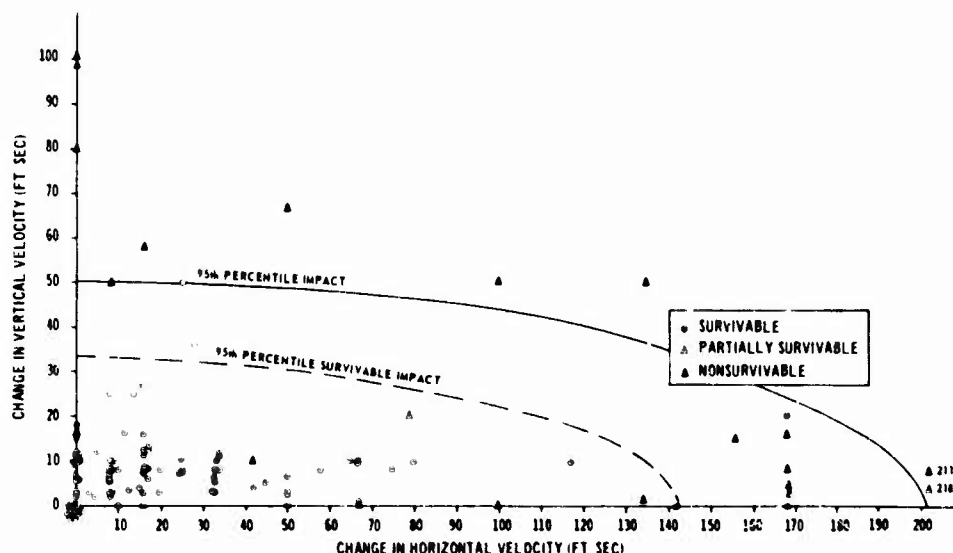


FIGURE 3--VERTICAL AND HORIZONTAL COMPONENTS OF IMPACT VELOCITY CHANGE

Estimated curves for the 95th percentile impact and for the 95th percentile survivable impact are superimposed on the individual data points. The 95th percentile survivable impact curves indicate a "design space" for improvements within the existing aircraft design. The 95th percentile impact is analogous information which may be useful for design and evaluation of crashworthiness features in future helicopters of similar type. This distinction is made because the strength and crushability of the existing airframe forming the "container" for the occupants limit the improvements which can be reasonably proposed for the current aircraft. However, for new aircraft designs, this limitation is not as severe due to potential improvements in the container itself. Thus, crashworthiness improvements for future helicopters should be based on what impacts are expected (such as the 95th percentile impact curve) and not on what impacts were survivable in current aircraft (the 95th percentile survivable impact curve).

### Influence of Impact Conditions on Injury

The strongest influence of impact conditions on injuries was the relationship between vertical velocity change and spinal injuries. Figure 4 depicts the relative frequency of back injuries versus impact vertical velocity change. This data indicates that significant numbers of back injuries occur even in impacts of less than 20 feet per second vertical velocity change. Analysis of these individual cases revealed other factors had significant influence on these low impact cases. These other influences included the longitudinal and lateral components of the impact velocity and the occupant's seating position at the time of impact. However, the strongest influence is shown to be the vertical velocity change. Increasing proportions of all occupants receive spinal injuries as impact exceeds the reserve energy sink speed of the aircraft's landing gear (8 feet per second). These results indicate that ground impact loads are transmitted with little reduction through the fuselage and seat to the occupants.

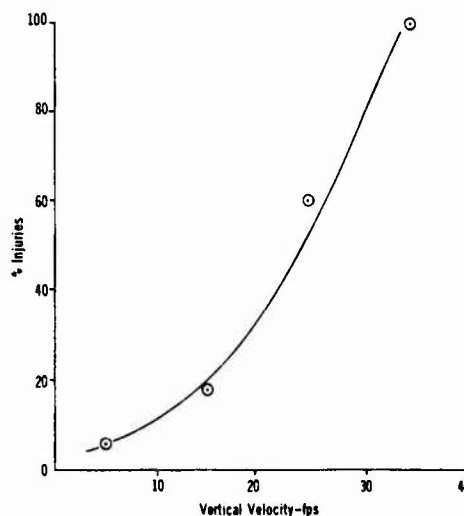


FIGURE 4--RELATIVE FREQUENCY OF SPINAL INJURIES VERSUS CHANGE IN VERTICAL VELOCITY

Figure 5 indicates the relative frequency of spinal injuries versus the vertical component of the peak impact forces (calculated at the center of gravity). Again, this data indicates significant numbers of back injuries occur in relatively mild vertical impacts. This data supports the conclusion that other factors (such as seating posture) have significant influences on spinal injury in even very low vertical impacts (such as less than 10 G's peak). This is important because most spinal injury models consider only the vertical impact component. In addition, this data supports the conclusion that after landing gear collapse, ground impact loads are transmitted directly with little attenuation to the occupants. This lack of energy absorption by the airframe and seat results in nearly 50% of all occupants receiving spinal injuries at peak crash loads of 15 G.

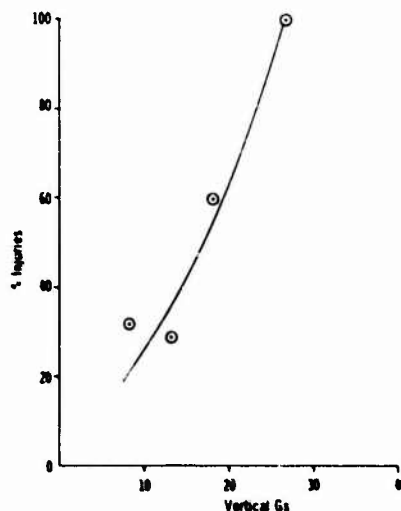


FIGURE 5--RELATIVE FREQUENCY OF SPINAL INJURIES VERSUS VERTICAL FORCE

Figure 6 depicts the frequency of occurrence and cost associated with the most prevalent crash injury mechanisms identified for the aircraft study. All accidents, regardless of survivability, and all injuries, regardless of severity, are included in Figure 6. A breakdown of the more significant injury mechanisms by underlying cause factor is discussed below. Figure 6 indicates that the most frequent injury mechanism was determined to be "body struck structure" while the mechanism resulting in the largest injury cost was "body received excessive decelerative force." After these two, the mechanisms of "body struck by external object" and "body exposed to fire" produced the next largest frequency and cost of injuries.

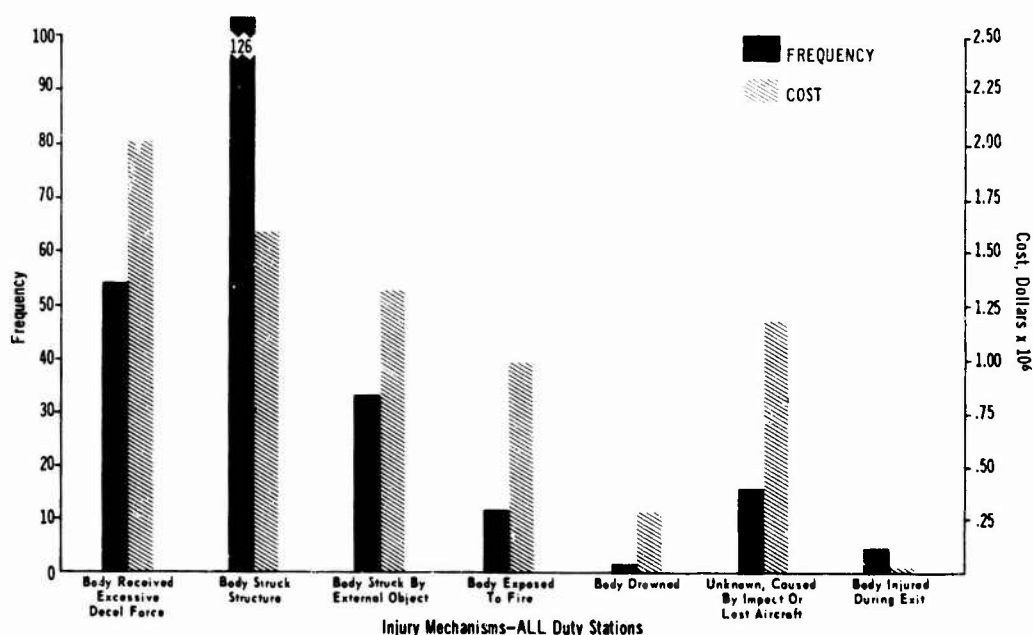


FIGURE 6--FREQUENCY AND COST OF INJURY MECHANISMS

#### Cause Factors Producing the Mechanism "Body Received Excess Force"

The engineering factors which caused the 55 instances of the mechanism "body received excessive decelerative force" are shown in Figure 7. This data indicates that a large majority of the instances and the associated costs of these injuries were caused by the airframe and seat allowing excessive loading of the occupant, i.e., during the major impact the aircraft and seat transmitted peak forces to the occupant which were beyond human tolerance. The energy absorption of the landing gear, airframe, and seat failed to protect these occupants.

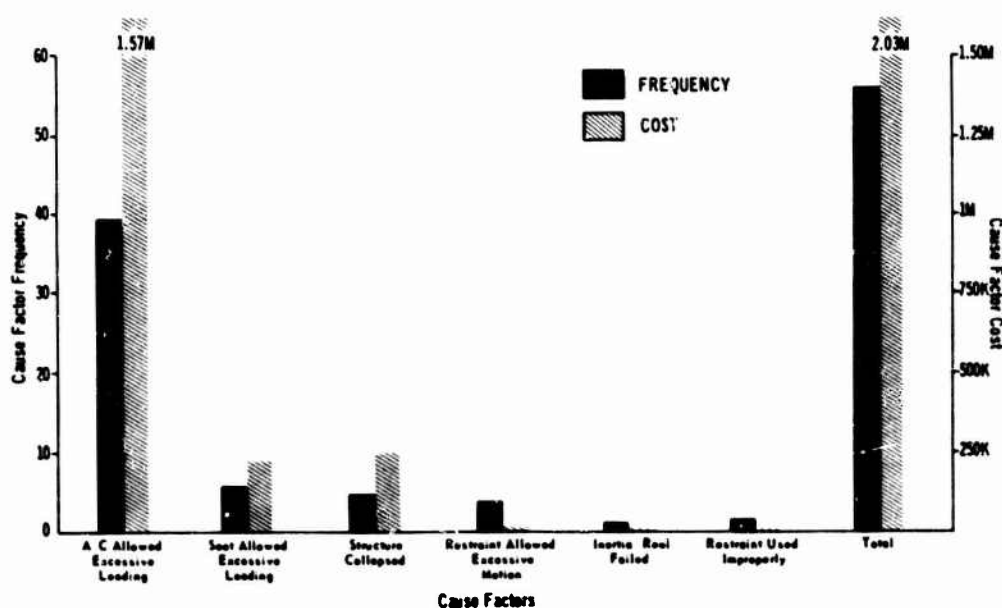


FIGURE 7--FREQUENCY AND COST OF CAUSE FACTORS RESULTING IN "BODY RECEIVED EXCESSIVE DECELERATION FORCE"

### Identification of Crash Hazards

Using a technique discussed in a previous report (13), the combination of the above injury mechanisms and cause factors, frequency, severity, and cost was analyzed to identify the critical crash hazards for this type aircraft. The most significant or highest ranking crash hazard identified was the hazard "body received excessive decelerative force when the aircraft and/or seat allowed excessive loading." As stated above, the energy absorption capability of the landing gear, airframe, and seat failed to protect the occupants. Because any change to the strength and crushability of the airframe and landing gear would require a major modification or redesign, it would not be feasible to effect a change to these systems. Changes would, therefore, concentrate on the seat. Figure 8 depicts the resulting deficiency and the associated 20-year potential cost reduction.

Crew seats transmit intolerable vertical loads to occupants and separate from aircraft, resulting in the spinal injury experience vs. vertical impact severity depicted in figures 4 and 5.	Develop and procure replacement crew seats which will attenuate vertical loading on occupant to tolerable level. The seat design goal should be requirements of MIL-S-58095. Tradeoff studies are required to determine the degree of protection consistent with cost, weight and space constraints.	\$8,992k
<b>DEFICIENCY</b>	<b>CORRECTIVE ACTION</b>	<b>POTENTIAL 20 YR SAVINGS</b>

FIGURE 8---PRIORITY CRASHWORTHINESS NEED (EXAMPLE)

It should be noted that a modified seat cannot be easily designed to absorb sufficient energy for all impact levels shown in Figure 7. It also would not be cost effective because the seat survivability would not be compatible with the survivability limits of the airframe. It, therefore, becomes necessary to optimize the seat providing the maximum protection consistent with cost, weight, space constraints, and the existing airframe survivability limits. The results of this analysis provided sufficient rationale for the initiation and substantiation of an Army program to develop such an optimized seat as will be discussed later.

Returning to the overall types of crash hazard analyses, the second level of analysis was initiated by USAARL and is a more specific analysis of areas of concern identified by the first level analysis. A goal of this type analysis is to refine current criteria for protective hardware for specific body areas and provide a beneficial extension of the Aviation Life Support Equipment Retrieval Program. A study of head, face, and neck injuries in all recent US Army aviation mishaps has been completed and, as mentioned above, contributed to the identification of specific impact hazards and recommendations for changes in helmet design criteria ((4) and unpublished data). Currently, a study of observation helicopter mishaps is in progress and is focusing on specific requirements to reduce injuries to the spine. A major emphasis of this study is to estimate the annual dollar cost of these injuries since approval of any retrofit program to improve seating in this helicopter will depend on an advantageous cost-benefit analysis.

### PROSPECTIVE STUDIES

In an attempt to further improve the quality of injury data collected from mishaps, USAARL has initiated a program to study selected types of injuries in a prospective manner. This program is being developed in order to define modes of injury as precisely as possible in areas where it is believed the best possibilities for LSE and general crashworthiness improvements lie. Currently, this program is focusing on injuries to the head and the spine. This is based on the fact that these two areas encompass over a third of all injuries sustained in US Army aviation mishaps (6) and because of emphasis in the US Army on production of a new integrated flight helmet and the introduction of energy-absorbing seat designs.

Through systematic coordination with USASC, USAARL is informed of all mishaps involving injury, usually within 24 hours of the mishap. If injuries occur in one of the specific areas of interest, the flight surgeon assigned to the investigation is contacted and requested to provide detailed medical information (admission history and physical, photographs of injury, specific measurements of external injury, pertinent laboratory data, radiographs, and reports) as well as all pertinent LSE for analysis. Suggestions may also be made for obtaining any additional onsite data required. This field data is then analyzed by a team of specialists to determine the mechanisms of injury as accurately as possible. An assessment is also made as to practical means of preventing the injury. In this manner, crucial medical information can be collected and analyzed during the first few days after a mishap, and any additional information required can then be sought while it is still available. This program rarely requires



that USAARI send an individual to the scene of a mishap, but that capability exists and is used on occasion when the situation warrants. Medical information gained from these studies is provided to USASC and incorporated into the injury data reporting system previously discussed. Proposals have been made to give this program regulatory authority by revising appropriate regulations.

Since these prospective studies are just beginning, their full impact is yet to be determined. However, this method was recently used during the investigation of a UH-60A Black Hawk mishap wherein a specialized team was sent to the mishap site to assist in the injury investigation. As a result of this investigation, valuable information on the functioning of the energy-absorbing seats installed in this helicopter was collected and certain actual and potential failure modes were identified. Continued detailed investigations will be required to assemble the necessary data to optimize these energy absorbing seat designs.

#### REMEDIES RESULTING FROM USE OF CRASH DATA

The crash injury reporting system discussed here was developed with the objective of not only identifying hazards, as discussed above, but also providing appropriate justification of needed remedial actions. The current austere funding environment makes the conservation of US Army personnel assets more important, but it also reduces the resources available to aid in this conservation. Any program to improve the crash survivability of Army aircraft must compete for funding with all other programs. Priorities of all funded programs are generally established based on their impacts in the areas of cost and operational effectiveness. Thus, the crash injury reporting system is designed to provide output in these management terms. It must be pointed out here that analysis or discussion of the need for eliminating or minimizing a particular hazard to human life would be meaningless based solely on economics. For example, the basic need for aircraft crashworthiness cannot be analyzed adequately on the basis of the economics of crash injury alone.

However, assuming that a decision has been made that a particular hazard is to be controlled, then the next stage in the process regards the selection of the optimum method and hardware for actually doing the job. This is the point where the economics of personnel injury, i.e., cost effectiveness, should enter the decision process. This is due to the fact that the maximum overall reduction in hazard level is desired, but the resources available are usually limited.

The concept of cost-effectiveness can be readily used here to determine the optimum system configuration(s) by spotlighting that system which will provide the greatest relative benefits per dollar of expenditure. The emphasis here is on relative benefits since an absolute, complete value for the monetary advantages of a particular change cannot be calculated whenever human life is involved. These advantages are known only relative to those of alternate system configurations. Thus, the injury reporting system discussed here was designed to provide injury cost data which could be used to either substantiate the need for a remedial action or select an optimum remedy from a set of available alternatives.

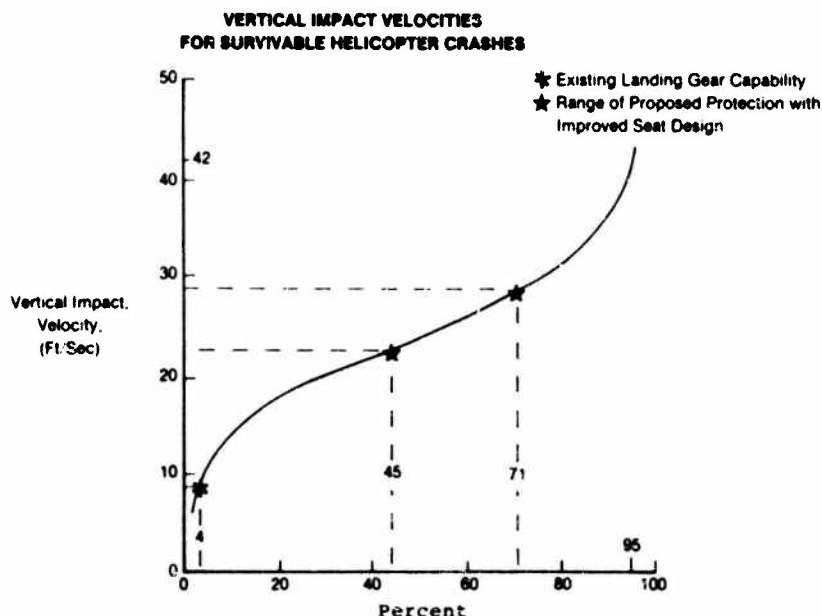


FIGURE 9--CUMULATIVE FREQUENCY OF OCCURRENCE



The identification and substantiation of the hazard regarding excessive vertical deceleration force transmitted to the crewmembers of the Army helicopter discussed above is instructive. As shown, this hazard was identified as the most critical crashworthiness problem in that aircraft. Equally important, the results of this analysis provided substantiating data for the justification of a "fix" in the form of the costs of the resulting injuries. Based partially on this information, an Army product improvement program has been initiated to address this aircraft/seat deficiency. The goal of this program is to enhance the survivability of this aircraft by incorporation of crashworthiness and vulnerability reduction design features. Included is an energy-absorbing seat which provides the maximum vertical stroke feasible within the constraints of the aircraft design. This seat will provide protection for a substantial proportion of survivable impact conditions. Figure 9 indicates a distribution of vertical velocity changes which is generally accepted to describe survivable impacts (14).

Superimposed on this distribution are estimates for the strength of the aircraft landing gear versus the design of the energy-absorbing seat (15). These estimates, taken together with the current injury experience as discussed earlier, indicate that substantial personnel loss and cost reductions will occur when the seat is fielded. It is remarkable that this modification (involving incorporation of an energy-absorbing seat and some modifications to aircraft ballistic armor) will result in little or no aircraft weight penalty. This is certainly a tribute to the aircraft manufacturer's and Army materiel developer's innovative design approach but also to the advanced state of the art of crashworthiness technology.

#### CONCLUSIONS

The current austere funding environment is not anticipated to improve in the foreseeable future. If aircraft crash survivability improvements are to compete with other funding requirements, then all personnel involved in the investigation, analysis or research of crash injuries must strive to achieve an enhanced data base upon which necessary management and engineering decisions can be logically based. An improved crash injury identification and reporting system developed by the US Army as described in this report is felt to be a key element of this requirement. This system appears to provide the following benefits:

- a. Identification of crash hazards in terms readily understandable by the development community.
- b. Prioritization of hazard corrective measures.
- c. Optimization of hazard corrective actions.
- d. Justification of hazard corrective measures.
- e. Adaptation of codes to future data requirements.
- f. Identification of additional research problems in the areas of crash injury and crashworthiness.

The overall goal of any crash injury analysis is to attain improved crashworthiness designs for current and future aircraft. Based upon the benefits described above, the overall impact of this modified system of crash injury identification and reporting will be to provide the responsible project managers with the data required to adopt recommended crashworthiness improvements in new and existing aircraft and life support equipment designs.

#### REFERENCES

1. Berner, W. H., and Sand, L. D. Deaths in Survivable Aircraft Accidents, Aerospace Medicine, Vol. 42, No. 10, October 1971.
2. Beyneh, A. A. Helicopter Versus Fixed Wing Crash Injuries, Aerospace Medicine, Vol. 34, No. 1, January 1963.
3. Haley, J. L., Jr. Analysis of US Army Helicopter Accidents to Define Impact Injury Problems in Linear Acceleration (Impact Type). AGARD Conference Proceedings No. 88, AGARD-CP-88, pp 9-1--9-13, June 1971.
4. Haley, J. L., Jr., (and others). Head Impact Hazards in Helicopter Operations and Their Mitigation Through Improved Helmet Design. In: Thomas, C. C., Impact Injury of the Head and Spine, Springfield, Illinois. (To be published in 1982.)
5. Mattox, K. L. Injury Experience in Army Helicopter Accidents, US Army Board for Aviation Accident Research, Ft Rucker, Alabama, HF 66-1.

6. Sand, L. D. Comparative Injury Patterns in US Army Helicopters. In: Knapp, S. C., Colonel, MC, Operational Helicopter Aviation Medicine: Ft Rucker, Alabama. London: Technical Editing and Reproduction Ltd., pp 54-1--54-7, AGARD-CP-255, May 1978.
7. Singley, G. T. Army Aircraft Occupant Crash-Impact Protection. Army R, D & A. pp 10-12, July-August 1981.
8. Department of the Army, Aircraft Accident Prevention, Investigation, and Reporting, 1975, AR 95-1.
9. US Army Safety Center, Unpublished Data, 1982.
10. Department of the Army, Accident Reporting and Records, 1980, AR 385-40.
11. US Army Safety Center, Engineering Analysis of Crash Injury in OH-58A Aircraft, 1980, TR 79-1.
12. US Army Agency for Aviation Safety, Engineering Analysis of Crash Injury in Ch-47 Aircraft, 1980, TR 78-4.
13. US Army Agency for Aviation Safety, Engineering Analysis of Crash Injury in Army AH-1 Aircraft, 1978, TR 78-3.
14. US Army Applied Technology Laboratory, Aircraft Crash Survival Design Guide, Volume II - Aircraft Crash Environment and Human Tolerance, 1980, USARTL-TR-79-22B.
15. Personal communication between Mr. Roy Fox, Bell Helicopter Textron, and Dr. J. E. Hicks, US Army Safety Center, 5 Jan 82.

#### DEFINITIONS AND TERMINOLOGY

Aircraft Mishap - An unplanned event that results in aircraft damage, personnel injuries, or makes further continued flight impossible or inadvisable. Damage as a direct result of hostile fire is not a mishap but a combat loss.

Crash Force - The maximum value of an assumed triangular crash pulse, determined at the aircraft center of gravity, which occurs during the major impact.

Crash Hazard - A condition due to the design or configuration of an aircraft or life support equipment which may result in injuries to occupants in aircraft accidents.

Crashworthiness - The ability of a vehicle to sustain a crash impact and reduce occupant injury and hardware damage.

Hazard Frequency - The frequency of occurrence of injuries resulting from a particular crash hazard.

Hazard Severity - The severity of the worst credible injury resulting from a particular crash hazard.

Hazard Cost - The sum of the costs of all injuries resulting from a particular crash hazard.

Injury Cause Factor - The design deficiency which caused a specific injury mechanism to occur.

Injury Costs - The economic effect on the operational readiness of the Army due to accidental injuries to servicemembers as calculated according to Reference [2].

Injury Mechanism - The mechanical process through which a specific injury was determined to have occurred, i.e., "what happened."

Major Impact - That impact of the aircraft which results in the largest decelerative forces being transmitted to the aircraft and occupants.

Survivable Accident - An accident in which the following statements are satisfied for at least one occupant aboard the aircraft:

- a. The forces transmitted to the occupant through his seat and restraint system do not exceed the limits of human tolerance to abrupt accelerations.
- b. The fuselage structural container maintains a livable volume around the occupant.

Nonsurvivable Accident - An accident in which neither of the above statements is satisfied for all occupants aboard the aircraft.

Partially Survivable Accident - An accident in which both survivable and nonsurvivable occupant positions exist.

Velocity Change - The change in velocity of the aircraft CG during the major impact.

BACKFACE SIGNATURE FROM BODY ARMOR

by

R. Fred Rolsten, Ph.D., CMfgE. and David J. Karl, Ph.D.  
 Wright State University  
 Main P.O. Box 1604, Dayton, Ohio 45401

Summary

Two types of body armor of light weight have been developed that will prevent perforation. The textile armor will defeat the bullet fired from most handguns. The hard armor will defeat the calibre .30AP. A good correlation has been made between the laboratory testing and field evaluation results as they relate to the rear surface signature and blunt trauma sustained by the wearer. There is concern that a threat greater than calibre .30AP may provide a prohibitive level of impact energy and subsequent blunt trauma injury. The experimental and clinical techniques established for the flexible body armor may be useful as fiducial points in further development.

Wear Body Armor!

It's better for you to wipe sweat while you live,  
 than to have your buddy wipe your blood as you die!

I. BACKGROUND

Combat, whether in the street or on the battlefield, has been a bane to man since his earliest days and has always been characterized by the presence of those who attempt to devise more effective ways to maim and destroy the enemy, of others who strive to protect their comrades from the implements of the foe, and of still others on both sides who devote their efforts to the improvement in techniques for the care and repair of the unfortunates who are the casualties. These three facets of war are interdependent and one group cannot achieve a maximum level of success without the advice and assistance of the other groups.

In the development of personnel armor (head, torso and extremity), the approach is similar to the approach to a disease entity. Primarily, the Medical Service is interested in the treatment and recovery of the casualty and in his speedy return to society or to the fighting force. It is interested in, and vitally concerned with, any methods that can reduce the severity of the wound or in any devices which can bring about complete defeat of a potentially wounding agent.

The use of armor<sup>(1)</sup> as a primary defense for the individual soldier is as old as the history of armed conflict. The body and limbs were natural sequels of man's development of sword and spear, sling and bow. Armor appeared long before the dawn of history; it had attained a high degree of specialization when the shield and buckler and other armor were mentioned in the Old Testament. Medieval armor in Europe developed into an excessively heavy armor of iron or steel plates suitable for jousting on horseback, but poorly adapted to military use. The closing decades of the 15th Century witnessed the introduction of firearms into warfare. Armor yielded slowly to the power of the culverin, falconet and wheel-lock so that when the Thirty Year's War ended, military leaders and tacticians had concluded that armor was outmoded in warfare. It was known that the Japanese wore armor of fairly good ballistic quality up to about 1870. During the Franco-Prussian War, several types of armor were used to a limited degree. Armor appears to have been worn in the Boer War. Well-articulated armors of World War I defended personnel against ball ammunition and were designed to prevent wounds from bullet splash. But, despite worldwide interest in protection, the small-arms armor-piercing (AP) bullet proved a more penetrating foe than designers of body armor could handle during the Spanish-American War, the Russo-Japanese War, World War I and II, and even the Korean conflict.

Capitalizing on the experience of the 17-lb World War II "flak" vest (combination of textile and manganese Hadfield steel), the favorable results in Korea with the 8 1/2-lb flexible (Nylon Army M1952) anti-fragment vest, the U.S. Army used body armor in Vietnam with positive results.

Advances during the early 1960s in both metallurgy and in synthetic materials development, made it possible to produce armor-systems which were ballistically effective and at the same time was of sufficient light-weight to be worn without great discomfort. These armor materials can be conveniently divided into two general categories:

- opaque: there are 4 categories: metallic, reinforced plastic, ceramic and textile. Opaque armor totally rejects the bullet, bouncing it off and dissipating its impact energy through the material itself in combination with the backing material.
- transparent: armor made from glass, polycarbonate or acrylic plastic which dissipates the impact energy through the material.

The need for armor piercing armor protection became especially critical in 1962, when U.S. forces in South Vietnam began extensive combat use of helicopters. In fact, many of the first American casualties were suffered by Army personnel who were flying reconnaissance helicopters as noncombatant advisors and operated in the environment which exposed them to aimed small arms and machinegun fire; i.e., all calibres up to 14.7mm AP1.

The body armor of the 1940s and 1950s provided protection against fragmenting munitions and did not protect against small arms fire; i.e., Cal.30AP. However, the body armor of the 1960s was of two types and the 1960s flexible armor comprised of ballistic nylon, although lighter in weight than previous armor of similar construction was more effective<sup>(1)</sup> against fragments, and the 1960s hard armor comprised of ceramic-fiberglass was effective against<sup>(2)</sup> the Cal.30AP. The hard ceramic armor, known as "Chicken plate" consisted of aluminum oxide (Al<sub>2</sub>O<sub>3</sub>) plate backed by a glass-reinforced-plastic (GRP) and weighed 20- to 28-lbs.

Thus, the armor weight of 20- to 28-lbs was used in World War I to defeat Cal.30 ball and in Vietnam to defeat Cal.30AP.

The dream of the 1901 writers in *Les Armures a L'Epreuve* was attained; i.e., ".....making through scientific gain, that which the earlier armorers were unable to produce in their day, a corselet, light and truly proof, this time, to the test of an armor piercing bullet!"

## II. THE $V_{50}$ LIMIT

Body armor generally has been developed by/for military and then applied to civilian use. It has been heavy, bulky, conspicuous and often not worn unless an immediate danger is foreseen. Military armor is of two types:

- soft material armor (textile) for stopping fragments and low velocity projectiles
- hard-faced armor (steel or ceramic) for stopping high-velocity missiles/bullets.

Historically, armor has been used to stop projectiles in two ways:

way one: the armor may catch and eventually stop the projectile by deformation or by comminution of a portion of the armor.

way two: the armor may deflect or reflect the projectile away from its intended target with little or no energy transferred in the process.

Ideally, in way one, the total kinetic energy of the projectile is permanently absorbed as deformation, fracture, and heat in the armor and projectile. The changes in projectile momentum and, hence, the impulse given the armor is equal to the projectile mass times its velocity ( $mv$ ). Soft steel plates or cotton bales, for example, tend to "catch" soft projectiles and absorb their kinetic energy in this manner. On the other hand, an ideal reflecting armor absorbs no permanent energy, but is subjected to an impulse of  $2mv$  (i.e., the projectile momentum would be completely reversed). Extremely hard and rigid armors tend to operate in this fashion. Several highly idealized projectile impact situations are illustrated in Figure 1, with the energy and momentum transfer given for each. It is the deflection shown in Figure 1-e that provides the "rear signature dose".

Composite ceramic armor behaves initially as a reflector and then as a catcher. The ceramic material on the armor face tends to fragment and to reflect a portion of the projectile kinetic energy trading off energy for increased momentum. The rear face of the composite then catches the residual projectile mass and deforms in order to absorb the remaining kinetic energy. It is the deflection shown in Figure 1-e that provides the "rear signature dose".

Even though two armor materials may appear to be equal in terms of their ballistic limit ( $V_{50}$ ), this only considers a single threat in terms of a single condition (i.e., a specific projectile and its striking velocity). In reality, the projectile may arrive at much higher or much lower velocities.

At higher velocities where the probability of penetration is greater than 50%, the two armor materials may differ in their ability to extract energy from the projectile. The net result is an increase in the residual velocity after passing through the armor, and this can be the determining factor in creating a serious (incapacitating) versus a lethal wound.

The merits of various armor materials should be defined, not in terms of their ballistic limit, but rather in terms of how well they protect people and/or equipment; i.e., in terms of their casualty reduction potential. However, we must recognize that different disciplines have a different basis for modelling the "casualty criteria". The terminal ballistic engineer bases his "casualty criteria", not upon human response, but upon the response of the armor and this response is designated  $V_{50}$ . The  $V_{50}$  is the velocity at which 50% of the bullets are defeated by the armor and 50% of the bullets defeat the armor by penetrating it completely and producing a casualty. The biomedical engineer bases his "casualty criteria", not upon the armor defeat of the bullet, but upon the ability of the human to perform his function after the armor-bullet interaction. This latter "casualty criteria" recognizes that armor can defeat the bullet and transmit a shock impulse\* to the human body; i.e., the rear surface signature of the body armor can result in a blunt trauma injury to the human. The effect of such blunt trauma must be evaluated with the mission since the same blunt trauma injury to various cadre (infantry, tankier, parachutist, pilot, etc.) may have different effects upon the mission. The infantryman may survive an injury that would be fatal to a pilot since the pilot may be incapacitated to the extent whereby he could not fly his aircraft.

## III. THE PROBLEM

Assaults against the lives of public officials and military officers have marred the period starting from the 1960s. This includes the successful/unsuccessful assassination attempts on:

<u>Heads of State</u>		<u>Church</u>
Trujillo (Dominican Republic)	Ford (USA)	Pope John Paul II (Vatican, Italy)
Diem (Vietnam)	Somoza (Nicaragua)	<u>Civil Rights Leaders</u>
Kennedy (USA)	Reagan (USA)	King (USA)                      Jordan (USA)
Shah (Iran)	Sadat (Egypt)	<u>Military Officers</u>
<u>Presidential Candidates</u>		Haig (USA)                      Dozier (USA)
Kennedy (USA)	Wallace (USA)	Kroesen (USA)                      Ray (USA)

$$* \int_{t_1}^{t_2} F dt = mv_2 - mv_1 \quad \text{The total linear impulse on "m" equals the corresponding change in linear momentum of "m".}$$

In Korea, there was a decrease in both the number of battlefield wounded in action (WIA), and killed in action (KIA). There was a decrease in the severity of wounds, which in turn resulted in more rapid and early convalescence and, because of the lightened workload, permitted surgical units to provide better care to those requiring it. While these Korean results and those in Vietnam are gratifying, they most definitely indicate the continuing need for research and development to provide lighter weight armor to those regions of the body which receive the largest number of lethal wounds. Body armor, is now recognized for its life-saving potential and the advantages outweigh factors such as weight and discomfort. The combat troops returning from a "fire-fight" soon learned that "the no-weight and no-bulk armor did not exist" and that "it was better to wipe sweat than blood".

The preponderance of the civil threat is the calibre .22, .32, .38 Special and the Soviet military threat to NATO Cadre can be generalized to the calibre .221(AK-74)\*, .30(AK-47), .50(B-32) and .578(BS-41). Study of the impact energy delivered at the barrel muzzle reveals that the civilian sector can expect a maximum of about 700 ft-lbs of energy to be delivered to soft (textile) armor while in Vietnam the military, with ceramic armor, received .30 cal aimed fire that delivered 3000-ft-lbs of energy\*\*. It can be anticipated as a result of the Vietnam battle field successful testing of ceramic body armor against the .30 cal AP, that these combat results will provide the continued impetus to Soviet Bloc countries to increase the threat from 7.62AP to 12.7mm API and to 14.5mm API.

The energy delivered at the muzzle by 7.62mm, 12.5mm and 14.5mm will be 2979, 11,913 and 23,735-ft-lbs, respectively. Thus, in elevating the threat from 7.62mm to 12.7mm, the ft-lbs of energy delivered at the muzzle will be increased by a factor of four (4) and threat elevation from 7.62mm to 14.7mm by a factor of eight (8). Thus, the military threat may be hypothesized at three levels:

- level one - the ceramic armor defeats the .30 cal AP projectile when 2979-ft-lbs of energy is delivered and momentum/energy transfer at the rear surface usually manifests itself in blunt trauma. The projectile is defeated\*\*\* but the 180-grain projectile does not have a momentum\*\*\*\* exchange with the armor of sufficient magnitude to cause the armor to move at significant velocity, although the wearer is subjected to a substantial dose from the rear surface.
- level two - A hard armor material may defeat the .50 cal API (12.7mm) projectile when 11,913-ft-lbs of energy is delivered and this energy level with the 736-grain projectile may have a momentum exchange with the armor of sufficient magnitude to cause the armor to move at a sufficient velocity and function as a blunt impacting object.
- level three - Case 1: A flexible textile armor may defeat a fragment from an exploding warhead launched in combat or by a terrorist and the rear surface of the textile will become so deformed as to produce a trauma to the wearer.  
Case 2: A flexible textile armor may defeat a round from a handgun and the rear surface of the textile will become so deformed as to produce a trauma to the wearer.

It should be noted that in the previous levels, that the armor defeated the round. Thus, at level one, the human body must contend with the dose from the rear surface of the armor and this dose may be delivered by the deformation of a small area of the GRP backing material. However, at level two, the human body may be placed in a position whereby it will contend with a dose delivered by both the deformation of a small area of the GRP backing material and the impact of the entire armor mass slamming into the body. Level three will subject the human body to a dose delivered by deformation of the flexible textile.

Battlefield testing in Vietnam has revealed that the human body can survive\*\*\*\*\* the blunt trauma dose delivered at the rear surface of 0.30 cal ceramic body armor resulting from impact by a non-penetrating Cal.30AP round. However, many of these combat veterans, upon returning from the combat zone, were immediately hospitalized in order to treat the contusions, hematomas, open wounds, etc., resulting from the blunt trauma due to the gross deformation of the rear surface of the hard body armor.

It should be noted that we have virtually no battlefield experience with the calibre .50, but from the significant increase in the impact energy delivered by the .50 cal API round, one can predict the necessity for altering the body armor weight and design concept if the blunt trauma dose is to be reduced to a level which the wearer can survive. THIS MUST BE EXPERIMENTALLY ESTABLISHED!

While flexible body armor can provide a life-saving function, textile armor normally allows a conical depression to form while ceramic-GRP produces a near-hemispherical depression to form at the armor/human body interface; i.e., rear surface signature. Such a rapidly produced depression and displacement of the human body can cause injury in the form of blunt trauma that covers the range from minor contusion to death. The validity of this statement can be tested by examining the number of law enforcement officers who, while wearing flexible armor, were assaulted by gunfire and the vest defeated the round, but the officer was hospitalized because of blunt trauma.

With both soft (textile) and hard (ceramic) body armor, it has been recognized from field experience that a rear signature dose is administered to the body, but exactly how bad this secondary effect may be, is not easy to determine medically but at best it would appear that beneath the point of bullet impact there may be a severe bruise. At worse, the near term result may be a broken rib or ruptured internal organ (heart, liver, kidney, spleen). There is no doubt that there exists an energy limit threshold above which the human body will always sustain an immediate blunt trauma injury but there is a paucity of data concerning the long term effect.

\* .221 Cal = 5.45mm; .30 Cal = 7.62mm; .50 Cal = 12.5mm; .578 Cal = 14.5mm.

\*\* The wearer of the body armor would receive a jolt of about 1200-ft-lbs.

\*\*\* Refer to references 3-7

\*\*\*\* Refer to Figure 1.

\*\*\*\*\* Some Vietnam veterans surviving a bullet impact on their body armor (chicken plate) are displaying myocardial infarction 10- to 15-years post impact.

#### IV. TRAUMA: CAUSES

Blunt trauma literature is, to a large part, made up of data applicable to auto crashes and blast, typically with total body and total organ or even multiple organ involvement. The differences in mass, velocity, and perhaps dose and dose application times require careful evaluation as to the applicability of these data to projectile-induced blunt trauma with nontotal body involvement or even, more typically, with only discrete areas of single organs involved.

The biophysical response to trauma problem is essentially one of a dose/response nature where the input "dose" is some injury-producing quantity and the "response" is the occurrence of an adverse effect on the human, such as tissue damage, incapacitation, or lethality.

Traumatic injuries to the heart and great vessels are the most lethal injuries sustained by blunt (or penetrating) trauma. Many patients die at the scene or shortly after the injury and other patients reach medical facilities, some of which succumb before or after treatment is instituted.

Many types of blunt trauma to the chest have been incriminated in causing cardiac contusion. These include blows to the chest by:

- the fist
- a club
- a heavy falling object
- a ball travelling at high speed
- a fall from a great height
- kicks by a horse
- compression of the chest between two moving objects
- blast injuries
- contact sports
- "steering wheel injury" (commonest of all in the United States) suffered in automobile accidents.

It is necessary to visualize a brief, but very violent blow, striking the whole surface of the body. Much of the energy of the shockwave is reflected, but part of it is transmitted through the tissues and strikes the internal organs one-by-one during the succeeding milliseconds or so. The tissues vary in their susceptibility to this injury. The homogeneous or more solid tissues are virtually incompressible and simply vibrate as a whole, thus, escaping serious injury.

Compressibility means displacement and wherever tissues of differing densities lie side-by-side, this displacement may cause distortion and tearing of the tissues. Lesions are most severe at junctions between tissues, and at sites, where loose, poorly supported tissue attached to dense tissue is displaced beyond its elastic limits.

A host of methodologies have been described to produce experimental blunt trauma to the torso. Some methods have centered on explaining the pathophysiology of blast injury<sup>(8,9)</sup>, while others have addressed themselves to injuries produced when blunt objects strike the body. Much of the latter work has been directed at characterizing trauma seen in vehicular accidents, such as the steering column injury. These techniques include:

- striking the exposed heart in vivo<sup>(10)</sup>
- striking the perfused liver<sup>(11)</sup>
- striking the precordial area<sup>(12,13,14)</sup>
- ramming the abdomen of a stationary animal with a blunt object<sup>(11)</sup>
- and propelling an animal into a blunt object<sup>(15)</sup>

Much of the blunt trauma experience in the clinical literature is not comparable to that seen behind a pliable textile armor. Series presenting blunt trauma injuries to the heart<sup>(16,17)</sup>, aorta<sup>(18)</sup>, lungs<sup>(19)</sup>, liver<sup>(20,21)</sup>, intestines<sup>(22)</sup> are heavily weighted in vehicular trauma.

However, clinical and research experience in the so-called conventional blunt trauma should not be dismissed when considering blunt injury relative to either soft (textile) armor or hard (ceramic) body armor especially when one considers the foot-pounds of energy delivered by some of the potential bullet threats.

#### V. REAR SURFACE SIGNATURE

The ability of various structural materials to resist penetration by projectiles such as small arms bullets has been extensively studied<sup>(4-7)</sup> and the projectile resistance by body armor is well characterized. However, relatively little has been done to determine whether or not serious wounds can result from the transfer of projectile energy through armor which is not physically penetrated by the projectile. It is evident that a sound understanding of the basic physical interaction mechanisms, particularly with respect to the energy partitioning between transmitted energy to the body and absorbed energy in bullet penetration and deformation, is yet to be established. The greater the energy dissipated by the material, the less absorbed by the body. The localized momentum transfer also comes into play and may be a contributor to blunt trauma.

The test matrix should evaluate dependent variables in the rear surface depression factor (deformation volume, depth, and time) against independent variables of ballistic parameters (velocity, calibre, energy, mass, jacketing); material parameters (denier, plies); and test configuration (stand-off distance, gelatin backing).

Body armor should have the following capabilities:

1. Prevent penetration by the bullet into the chest, abdomen, or back.
2. Any blunt trauma effects should have a mortality risk of 10% or less.
3. The wearer of the body armor should be able to walk from the site of the shooting after the body armor takes a bullet hit.



Let us assume that body armor is meant to cover and protect the thorax, abdomen, and back. Vulnerability then, with regard to body armor, should perhaps refer to that area of the body that will require surgery or intensive care even if the overlying body armor prevents penetration of the particular missile fired. The frontal view indicates that the liver, heart, and spleen would be vulnerable.

The right lateral view indicates the large area occupied by the liver and the small area occupied by the right kidney. Renal contusions, however, are usually managed conservatively and rarely is surgery necessary. Since a patient with a renal contusion would have hematuria, he would be hospitalized and followed closely for signs of blood loss. The left lateral view indicates the vulnerable kidneys, spleen and heart.

The percentage of vulnerable area will vary according to the design of the body armor. Based on earlier testing, the number of layers of flexible Kevlar necessary to convert most of the vulnerable areas into totally invulnerable areas would probably be too heavy to incorporate into a garment that would be comfortable enough for routine use.

Seven plies of Kevlar subjected to assault by a .22 Cal, 40-grain bullet at  $1015 \pm 16$ -ft/sec prevented perforation, but produced an indentation depth of  $2.76 \pm .50$ cm and an indentation volume of  $42.56 \pm 15.83$  cm<sup>3</sup>. The time from bullet contact with the Kevlar to zero velocity was  $0.0010 \pm 0.00016$ -seconds.

Seven plies of Kevlar subjected to assault by a .38 Cal, 158-grain bullet at  $827 \pm 14$ -ft/sec prevented perforation, but produced an indentation depth of  $4.82 \pm 0.33$ cm and an indentation volume of  $148.96 \pm 25.25$  cm<sup>3</sup>. The time from bullet contact to zero velocity was  $0.0018 \pm 0.00019$ -seconds.

Seven plies of Kevlar subjected to assault by a .45 Cal, 234-grain bullet at 804 ft/sec prevented perforation, but produced an indentation depth of 5.55cm and an indentation volume of 234.1cm<sup>3</sup>. The time from bullet contact to zero velocity was 0.0017-seconds.

The test matrix consisted of ballistic test-firings that were divided into six groups and each group was controlled by the variation of one parameter. The resulting conical depression factor (C.D.F.) was determined.

The C.D.F. combines the dimensions of the armor body interface signature into the form

$$C.D.F. = \frac{r^2 h^2}{t}$$
 where the value "r" is the radius (cm) of the depression cone and "h" is the height (cm) of the cone at the time "t" (msec) when the velocity of the axial motion has decayed to 5% of the impacting velocity. This factor was plotted as the ordinate in each test group. The equation is purely empirical.

The change in conical depression factor for the .22 Cal, .38 Cal, and 9mm as a function of Kevlar plies is shown in Figure 2.

As expected, the plot of cone height vs. time after impact were logically spaced and consistent. On the other hand, the plot of base diameter vs. time provided mixed data and indicated the inaccuracy of the assumption of an axisymmetric depression cone. Aerospace shot recoveries into clay back-up for depression measurements revealed a distinct rectangular-based pyramid shape in the clay depressions. High-speed framing camera photographs showed<sup>(23)</sup> the bullet impacting the Kevlar target and revealed the nonuniform strain that led to mixed results in the measured values of the base diameter. The ballistic threat and C.D.F. were reduced, as expected, by decreasing the velocity of impact. In Figure 3 is shown the possible dependence of the C.D.F. on the bullet cross-section area.

## VI. TRAUMA: INJURY

### A. Heart

The heart and great vessels, as other organs, are subject to injury<sup>(24-26)</sup> from penetrating and blunt trauma. The heart is suspended from the great vessels and hangs freely into the pericardial cavity between the anterior chest wall (sternum) and the dorsal spine (thoracic vertebra) and it is thereby subject to injury by the following mechanisms of blunt trauma:

- the heart may be injured by compression between the sternum and vertebral column when the former is suddenly driven in by a forceful blow as in the "steering wheel" type of injury.
- sudden acceleration/deceleration of the chest may cause the heart to be thrust against the chest wall, injuring the heart muscle or tearing the pericardium or great vessels.
- the heart may be subject to damaging force by sudden violent increases in intrathoracic pressure that may produce valvular tears, subendocardial hemorrhages, or actual rupture of the heart wall.

As a result of nonpenetrating trauma, a variety of lesions may occur in the heart and pericardium:

- |  |  |
|--|--|
| - myocardial contusions  | - rupture of the interventricular septum                                   |
| - rupture of the cardiac wall                                  | - coronary artery injury   |
| - tears of the valves, chordae tendineal, or papillary muscles | - rupture of the pericardium and formation of a left ventricular aneurysm. |

### B. Aorta and Great Vessels

The thoracic aorta and great vessels are covered to a small extent with the pericardium and to a greater extent with parietal pleura. The aortic arch crosses over the vertebral column, and the descending aorta descends along the column, giving off the intercostal arteries which then become imbedded in the intercostal spaces. As a result of their anatomic location, the thoracic aorta and great vessels are subject to injury by a variety of forces created from blunt trauma:



- Sudden acceleration or deceleration of the chest may create shearing force between different parts of the aorta, between the heart and aorta, and between the aorta and great vessels --
- the aorta or great vessels may be compressed over the vertebral column.

These forces may precipitate rupture of the aorta or rupture or avulsion of the great vessels (innominate or subclavian vessels, carotid arteries, superior or inferior vena cava, or pulmonary arteries).

#### C. Lungs

Hemorrhages to the lungs are mainly located in the apices and in those parts of the lung which are compressed and contused between the chest wall and the liver, and the chest wall and the mediastinum. The lungs are probably compressed between the rigid spine, the inward moving thoracic wall and the diaphragm.

In the lungs, the alveolar septa are most severely affected since they are torn and the alveolar spaces joined together. The lung parenchyma shears away from the tough vascular tree and the alveolar epithelium is shredded. The epithelium of the bronchioles is stripped away from the basement membrane so that the fluid-air barrier is breached, and blood and edema fluid escape into the alveoli. Air is forced into the pulmonary veins and can be found in the coronary and cerebral arteries. Alveolar-venous fistulae have been demonstrated microscopically. The lung damage varies from pinpoint hemorrhages in survivors to massive intrapulmonary in those who die. At autopsy the pleural surface shows alternate light and dark markings. The light bands correspond to the ribs while the dark-hemorrhagic bands correspond to the intercostal spaces where the lung was not protected by rib-bone.

#### D. Solid Viscera

The solid viscera, most commonly the liver and the spleen, may be damaged by violent acceleration and deceleration forces.

#### E. Surrogate

Based upon goat studies with regard to blunt and penetrating types of trauma, the following assumptions<sup>(27)</sup> were made:

- The 40- to 50-kg goat is a model for a "typical" 70-kg man in body armor. The goat is a satisfactory and conservative model for studies which include the thorax and the abdomen as targets.
- The damage levels of various organs will be similar in goat and man, if the area of impact is equivalent and the same force is applied.
- The goat experiences the same natural course of disease as would the human after similar injury.
- The 70-kg human, with thicker and more resistant abdominal and chest walls, would incur no more damage than would the goat from a given impact. Because of the increased body wall protection, the human would probably incur even less damage.

##### a) Lung

A comparison in respiratory index (RI) and size of lung contusion(s) was made with 67 unarmored goats impacted with riot control missiles and goats armored (either 12-ply ballistic Nylon or 7-ply Kevlar) and impacted with the .38 calibre bullet. Those goats that succumbed had an RI increase of 0.51- to 0.6 and the average size of the lung contusion was 161cc. The Kevlar-protected goats had an average RI of only 0.08 and an average of 5cc of lung contusion, the largest individual contusion measuring 45cc. Based on this comparison, it is unlikely<sup>(27)</sup> that the amount of damage sustained by the Kevlar-protected goats would be of any serious consequence whether it occurred in goat or man.

If one assumes that, if a human wearing a flexible textile (Kevlar) vest was impacted over the chest wall and was treated at a hospital in 1-hour, if a lung contusion does not increase his RI above 4, he should have a 96.5% probability of survival<sup>(28)</sup>.

##### b) Liver

The seven Kevlar armored goats<sup>(27)</sup> subjected to central impacts over the liver (targeted on the 11th intercostal space on the mid-right side) caused contusions averaging 50cc. There was no more than 100cc blood loss in any case.

This injury in the human would also cause intraperitoneal bleeding as well as abdominal pain, tenderness, and muscle rigidity. The victim would probably not be immediately incapacitated, and presumably the patient would be admitted to the hospital within 1-hour after injury. If an abdominal paracentesis were indicated, and it was positive for free blood, surgery would be performed. The liver wound is a minor one and can be handled with a surgical mortality (death within 30 days of surgery) under 50%<sup>(28)</sup>. This should be compared to a central liver wound incurred without the jacket that would incapacitate immediately, and would carry an operative mortality as high as 60%.

##### c) Gut

The data<sup>(27)</sup> infer that if the goat stomach, small or large intestine, under an area of impact is markedly dilated with air, the bullet force transmitted through the textile armor could cause a perforation. Under anesthesia, the goat consistently develops dilatation of the rumen. Perforation of this viscus by the .38 caliber bullet through the 7-ply Kevlar occurred 50% of the time (four out of eight shots). When a portion of gut that was not dilated was impacted (eight times), perforation did not occur. Only a serosal contusion was registered with occasional minimal mucosal contusion.

Any perforation with surgical intervention within 6-hours after injury should have a surgical mortality rate under 5%. The viscus that is only contused would require no operative treatment in almost all cases.

#### d) Spleen

Impacts<sup>(27)</sup> over the goat spleen were difficult in that the spleen was an elusive target. In addition to being a relatively small organ, its orientation and location in the goat is variable enough so that it is hard to hit centrally with consistency. Three attempts were made, and in one shot there was no damage to the spleen; in another there was a 2-cm contusion at the inferior border; and in the last round the spleen was missed.

Since the spleen is easily damaged, we expect that a direct hit over the spleen in the human would probably cause at least a contusion or intracapsular hematoma. Both of these lesions would eventually require surgery, and the surgical mortality should be under 5%<sup>(29)</sup>.

### VII. CONCLUSIONS

1. There is a paucity of medical data pertaining to non-penetrating impacts on body armor.
2. The data which are available do not consider all of the parameters which are medically important in the assessment of blunt trauma (e.g., dose application time and body armor/human body response)..
3. Separate sources of data for similar nonpenetrating projectiles are almost impossible to correlate due to differences in test methods, data acquisition techniques and data recorded.
4. The effectiveness of body armor must be assessed upon the ability of the armor to prevent penetration as well as to significantly minimize serious injury and/or death.
5. The seven ply Kevlar body armor provides protection from the .22 Cal. bullet at 1100 ft/sec and from the .38 Cal. bullet at 800 ft/sec.
6. The blunt trauma dose administered by the .45 Cal, 9-mm, shotgun or higher velocity threats, has been the subject of only partial testing, if tested at all.
7. Experience in Vietnam showed that impact from the calibre .30 AP bullet on ceramic body armor can cause serious, but survivable injury. An impact load of 3000 ft-lbs subjects the wearer to a 1200 ft-lb jolt.
8. The calibre .50 API bullet delivers a 11,913 ft-lb load to the body armor and this large impulsive load may require a carefully conceived armor design in order to preclude the use of body armor that will prevent the bullet from penetrating the human body but will provide a rear signature dose of such magnitude that the wearer cannot survive.

### VIII. RECOMMENDATIONS

1. All shooting events involving body armor should be carefully documented in the same way as the U.S. Army Aeromedical Research Laboratory helmet accident retrieval program.
2. The Medical Department should prove and designate the animal (e.g. goat, swine, canine, etc) to be used as the human surrogate.
3. The Medical Department should provide, to the ballistic engineer, those parameters which must be measured at the rear surface of the body armor.
4. An internal trauma model should be developed and validated so that each point within the human body volume can be assigned a trauma level as a function of impact location, bullet mass and velocity, the impulse spread due to the armor, and the time of dose delivered.
5. The internal trauma model should result in a medical assessment which can be expressed in:
 

- hospitalization cost/time	- temporary disability
- duty time cost	- permanent disability
- retraining cost	- death.
- insurance cost	

### REFERENCES

1. R. F. Rolsten, J. G. Dunleavy, and E. G. Bodine, "Armor Materials for Life Support" ACARD Conference Proc. paper No. 88 on Linear Acceleration of Impact Type, Oporto, Portugal, 23-26 June (1971).
2. J. W. Stangle, R. F. Rolsten and H. H. Hunt, "A Survey of Personal Armor", Law and Order, January (1969).
3. R. F. Rolsten, E. G. Bodine and J. G. Dunleavy, "Breakthrough In Armor", Space and Aeronautics, 50 (1) July (1968).
4. R. F. Rolsten, "The Optimization of Composite Ceramic Armor Materials" Symposium on Ceramic Armor Technology, BML, Columbus, Ohio, January 26-29 (1969).
5. R. F. Rolsten, "Response of Metals and Non-metals Under High Strain Rates", 8th International Symposium on Space Technology and Science, Tokyo, August 25-30 (1969).
6. R. F. Rolsten, "A Study of Shock Loading of Materials", Transactions of New York Academy of Sciences, 36, No. 5, pp 416-480 (1974).

7. M. L. Wilkins, "Third Progress Report on Light Armor Program", Lawrence Radiation Laboratory (LRL), Livermore, Report UCRL-50460, November (1967).
8. I. C. Bowen, E. R. Fletcher, D. R. Richmond and C. S. White, "Biophysical Mechanisms and Scaling Procedures Applicable in Assessing Responses of the Thorax Energized by Air-blast Overpressures or by Non-penetrating Missiles", *Annal. N.Y. Acad. Sci.*, 52, p. 122 (1968).
9. C. S. White and D. R. Richmond, "Blast Biology", *Clin. Cardiopul. Physiol.*, 63, p. 974 (1960).
10. E. F. Bright and C. S. Beck, "Nonpenetrating Wounds of the Heart: A Clinical and Experimental Study", *Ann. Heart J.*, 10, p. 293 (1935).
11. M. L. Trollope, R. L. Stalnaker, J. H. McElhaney and C. F. Frey, "The Mechanism of Injury and Blunt Abdominal Trauma", *J. Trauma*, 13, p. 962 (1973).
12. W. E. DeMuth, E. H. Lerner, and A. J. Liedtke, "Non-penetrating Injury of the Heart: An Experimental Model in Dogs", *J. Trauma*, 13, p. 639 (1973).
13. D. B. Doty, A. E. Anderson and E. F. Rose, et. al., "Cardiac Trauma: Clinical and Experimental Correlations of Myocardial Contusion", *Ann. Surg.*, 180, p. 452 (1974).
14. R. W. Kissane, R. S. Fidler and R. A. Koons, "Electrocardiographic Changes Following External Chest Injury to Dog", *Arch. Int. Med.*, 11, p. 907 (1937).
15. D. R. Erickson, R. Shinozaki, E. Beckman and J. Davis, "Relationship of Arterial Blood Gases and Pulmonary Radiographs to the Degree of Pulmonary Damage in Experimental Pulmonary Contusion", *J. Trauma*, 11, p. 689 (1971).
16. W. E. DeMuth and H. F. Zinsser, "Myocardial Contusion", *Arch. Intern. Med.*, 115, p. 434 (1965).
17. J. W. Jones, R. L. Hewitt, and T. Drapanos, "Cardiac Contusion: A Capricious Syndrome", *Ann. Surg.*, 181, p. 567 (1975).
18. L. F. Parmley, T. W. Mattingly, W. C. Manion, and E. J. Jahuke, "Nonpenetrating Traumatic Injury of the Aorta", *Circulation* 17, p. 1086 (1958).
19. E. Blair, C. Topuzla, and M. Davis, "Delayed or Missed Diagnosis in Blunt Chest Trauma", *J. Trauma*, 11, p. 129 (1971).
20. R. N. McClelland and T. Shires, "Management of Liver Trauma in 259 Consecutive Patients", *Ann. Surg.*, 161, p. 248 (1965).
21. T. Schrock, W. Blaisdell, and C. Mathewson, "Management of Blunt Trauma to the Liver and Hepatic Veins", *Arch. Surg.*, 96, p. 698 (1968).
22. J. Cerise and J. H. Scully, "Blunt Trauma to the Small Intestine", *J. Trauma*, 10, p. 46 (1970).
23. C. A. Honodel, "Soft Armor Test Matrix 1 - Final Report", Lawrence Livermore Laboratory, Univ. of Calif., September 19, (1974).
24. H. D. Leinoff, "Direct Non-penetrating Injuries of the Heart", *Ann. Intern. Med.*, 14, p. 653 (1940).
25. H. W. Hale, Jr. and J. W. Martin, "Myocardial Contusion", *Am. J. Surg.*, 93, p. 558 (1957).
26. C. R. Osborne, "Findings in 262 Fatal Accidents", *Lancet*, 2, p. 277 (1943).
27. M. A. Goldfarb, T. F. Ciurej, M. A. Wienstein, and L. W. Metker, "Body Armor Medical Assessment", National Institute of Law Enforcement and Criminal Justice, May (1976).
28. S. Schwartz, "Principals of Surgery", p. 235, McCraw-Hill Book Company, Inc., N.Y., (1974).
29. R. A. Griswold and H. S. Collier, "Blunt Abdominal Trauma", *S. C. & O.*, 112, p. 309 (1961).

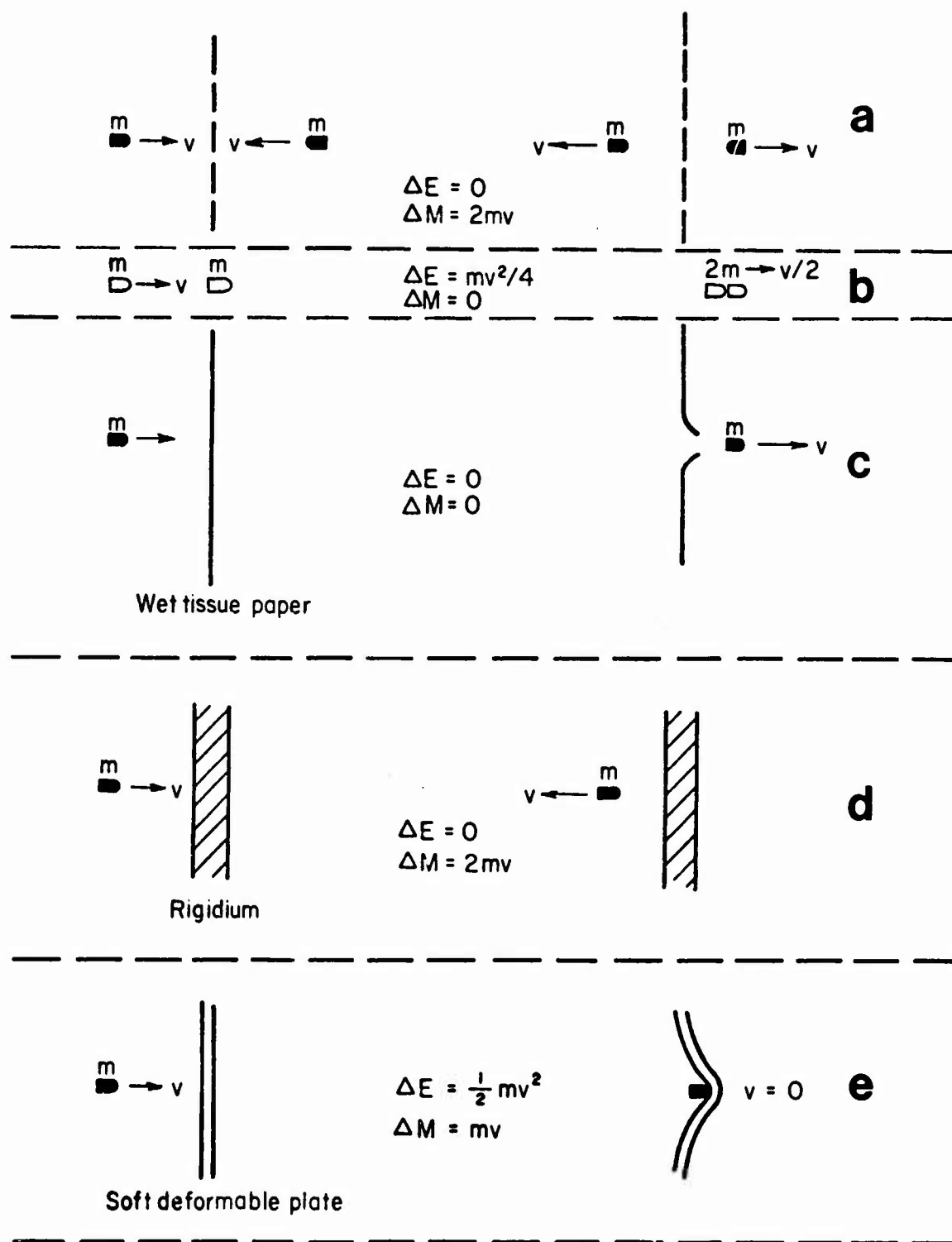


Fig.1 Highly idealized projectile impact situations showing energy and momentum change

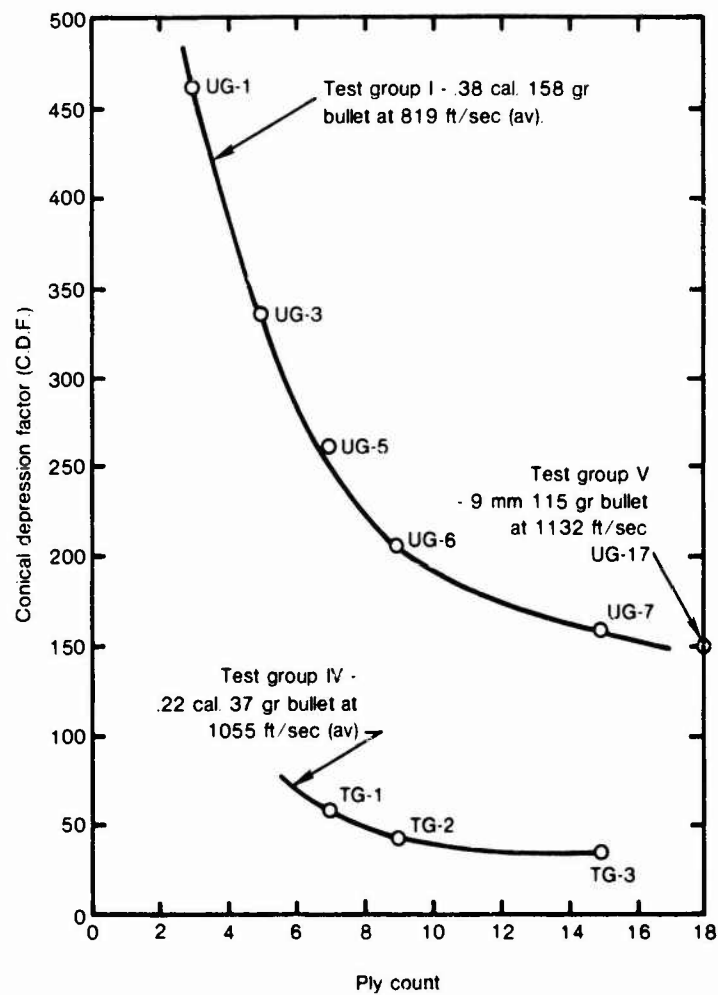


Fig.2 Effect of Kevlar 29, 400 denier, armor ply count on the conical depression factor (C.D.F.) (Groups I, IV, and V)

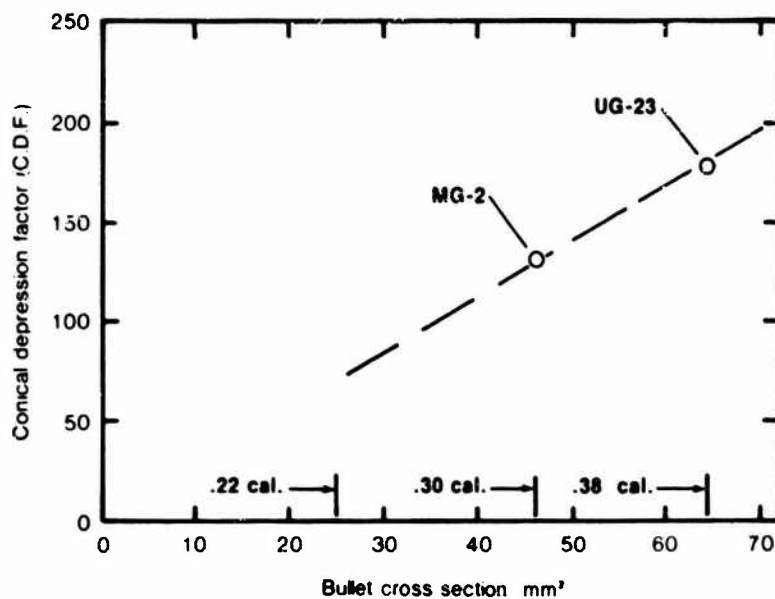


Fig.3 Effect on conical depression factor (D.D.F) of lead bullet cross section at a constant kinetic energy (340 J) on a common target. See Table VIII, Group IV

## DISCUSSION

MR. CARNELL (USA)

Is body armor practical against the anticipated higher USSR threats?

AUTHOR'S REPLY

The chicken plate armor used in Vietnam was adequate against the AK-47 (.30 cal AP). However, additional work must be accomplished in order to provide body armor protection against the BS-42 (12.7 mm) due to the unknown amount of rear signature energy delivered to the wearer.

MR. CARNELL (USA)

Will it be necessary to provide armor on the aircraft or helicopter structure?

AUTHOR'S REPLY

There is certainly a body armor weight which cannot be worn by the individual since he cannot perform his combat duties. In such a case the armor must be carried (supported) by the aircraft.

MR. SCHULMAN (USA)

Is there any difference in the back face signature of Fiberglass backing as compared to the newer Kevlar backing that is being used today?

AUTHOR'S REPLY

Yes, due to the higher tensile strength of the Kevlar one would expect that the energy absorbed in the back-up layer would be greater.

## COST EFFECTIVENESS OF BODY ARMOR

Robert H. Holmes, M. D.  
 Col. (Ret'd) U.S. Army Medical Corps  
 Senior Medical Advisor, International Clinical Laboratories, Inc.  
 155 Spalding Mill  
 Atlanta, Georgia  
 30338  
 U.S.A.

## Summary

Body armor is a common denominator of cost effectiveness. It is the only means we have for further reduction in battlefield mortality and morbidity. Protective devices for materiel and personnel must be continually upgraded. Using KOREA and VIETNAM as references the present day helmet and body armor should provide significant reduction in killed in action and wounded in action. This reduction in casualties can be translated into savings of billions of dollars. A price cannot be placed on human life, but costs can be projected for lost lives and disabilities incurred. The aftermath of war-related expenditures has become so great that societal pressures now challenge the rationale of payment. Protective armor is not just a wise investment, it is a necessity.

Our subject is serious. We share a sense of common purpose, and our cause, we believe, is just. We are uniquely involved in a game that is not for fun, but, rather, a never-ending struggle to outwit the enemy, whoever he may be, and, collectively, we contribute our part, however small, to the continuing drama of survival.

Why are we here? Is that a good first question? Yes, and as a measure of your importance, may it be said that we have a special job to do, and unless we do it, it is quite likely the job will remain undone; and if it is undone, then we shall surely lose some sort of advantage that could be crucial in the next war we hope will never come.

Strategy and tactics comprise the fundamental concepts by which wars are won or lost. Ultimately, these concepts are translated into action, to exercises in logistics, and to operational goals and objectives. It is then that casualties occur, people are wounded, maimed, and killed, fighting strength is reduced, total resources are called upon, and national will is challenged. If war be an extension of politics and diplomacy that have failed, then, surely, all the subtleties of economics as an art, if not a science, must prevail. The total resources of one combatant become locked in mortal combat with the total resources of another. Getting there "fustest with the mostest" is not enough. Whatever it is, wherever it is, it must also work - and work - over and over again.

In the heat of battle cost is given little thought. It is only when supply lines fail that the countdown to certain defeat begins. Cost effectiveness must be applied continuously, before the fact, in the preparation for war, and, after the fact, in the waging of war. Bravery and military skills must be matched by determination and capability to do the most with the least.

Nuclear war, short of total destruction, will, undoubtedly, return man in a short interval of time to a near-primitive state of survival. Any other war, so-called conventional war, could continue indefinitely, draining away life's blood and national resources until the horror of attrition becomes too great and one or the other combatant falls on his knees, starved and worn. A far-advanced technology based on astronomical costs must provide reasonable guarantee of victory, short and swift, or we must go back to a less advanced arsenal of weaponry that will guarantee our staying power, our ability to outlast the enemy. Equipment must be available, durable, and functional, and fighting men must have maximal protection, compatible with accomplishment of mission. Protective armor for men and materiel is not just a wise investment; it is a necessity. It is a common denominator of cost effectiveness.

## Historical Review

In the evolution of human warfare, primitive man was fierce, brutal, gave no quarter, asked for no quarter. It was mostly hand to hand combat - one died, one survived, usually wounded, perhaps to die later. There is ample evidence in the discovery of ancient skeletal remains showing broken bones and caved in skulls that blunt instrumentation had been utilized most effectively. The linear acceleration of a stone axe impacting on an unprotected calvarium left no doubt as to its crushing effect. It is ironic that man, the only animal with the ability to pronate his thumb, and to grasp and hold a tool or a violin, could also hold a weapon for destruction of his fellow man.

As the discipline of warfare progressed through the ages, impact injury from blunt or pointed instrumentation delivered in hand to hand combat gave way to the explosive thrust of gunpowder, and bombardment by missiles that allowed man to fight man at a great distance. Shells made of cast iron and steel burst into fragments with variable mass distribution designed to flood an area and kill or wound. The Russian 120mm shell, so effective in Korea, had a burst velocity of about 3000 ft. per second and a distribution of over 10,000 fragments. Much of the combat involved the shelling of mountain positions and accounted for the major percentage of casualties. Since then, shells have been developed with much higher burst velocities and fragments of much smaller mass. These are highly effective, but must be much closer on target because fragments lose velocity in inverse proportion to their mass.

The ultimate, thus far, in the development of bombardment weaponry, is, of course, the atom bomb used in Hiroshima and Nagasaki, the H-bomb, unused, and the neutron bomb, controversial, perhaps stockpiled, and perhaps available. Impact injury has now become more complicated. Blast, thermal, flash, and radiation energies must be contended with. Crushing overpressures, implosion added to explosion, secondary missiles of immense variety and magnitude, all a composite of linear acceleration contribute to impact injury and destruction of all that comes within an effective range. For only the second time in the evolution of warfare, chemical gas being the first, an agent with a profound delayed wounding effect has added further complexity to this type of explosion, namely ionizing radiation. We are, however, still dealing with impact injury, make no mistake; the missiles we call ionized particles of matter are now of infinite smallness, actually atomic fragments that impact with tremendous velocities and scatter their kinetic energy throughout the body if total exposure occurs. Depending on exposure area and dose, death may occur from disease years and years later.

At the same time artillery weapons were going through their evolution small arms development began. Pistols, rifles, machine guns, automatic weapons of all types made their appearance. The era of the bow and arrow, the cross bow, and the catapult was over. Impact injuries due to linearly accelerated missiles, ogive in design, were new, different, and frequently lethal. Another irony: Dr. Gatling, a physician, applied his genius to development of the machine gun and contributed his part to the opening of our western frontier, the killing of the buffalo and the Indian, and the fighting of modern wars. Such is the stuff of which history is made.

Impact injuries resulting from shell fragments of random configuration and mass are most often multiple and penetrating in type, meaning they have a wound of entrance but no wound of exit. Bullets, more often, produce perforating wounds, meaning a wound of exit as well as entrance - the so-called through and through wound. Shell fragments may range from a mass of near dust-like particles measured in grains to grams, and occasionally to large size slabs of metal which impact with great force over a large part of the body with mutilating effect. Freakish events of all types occur: one incident involved an entire unexploded 20mm shell penetrating the back and flank of a soldier in Vietnam; other incidents involving bullets of all types find the missile almost circling the calvarium or rib cage without deep penetration. Another incident involved a soldier killed in action in Korea without an easily perceivable wound. Finally a wound of entrance was found behind the knee. The bullet tract was dissected along the backside of the thigh, then into the abdomen, the chest, and finally into the left ventricle of the heart.

Studies of war casualties, it must be confessed, have not been performed in the usual manner of true science. Most often the studies have come about because someone in authority eventually got around to thinking that something, nothing very clear-cut, should be done. This is quite understandable, even though not quite reasonable. It is all a question of priority. We tend to enter into warfare emotionally aroused but usually in varying stages of unpreparedness, or, at best, somewhat prepared for the previous war. As the interval between wars, which we call peace, increases and technology advances, we are prone to be in the "midst of being prepared". We are in such a phase now. Development and stockpiling of equipment, weapons, supplies of all types, proceeds in an ever-quickenning pace along with the build up of field forces, training, and the sifting out of personnel for leadership roles. It is the time - very much the time, when a higher priority should be given to planning a program and assembling the characters who will have a primary concern for battle casualty analysis, and a perspective, at least in the general direction, of what such studies could contribute in the accumulation of knowledge about weapon effects, and the mechanism, prevention, and treatment of wounds incurred in battle. It is time to proceed in a well established manner to prepare a plan setting forth goals and objectives and methodology, with biometric evaluation concerning the study to be done. Only in this way will we obtain the data we want, need, and must have.

Many examples in support of the above proposal can be given: the adoption of body armor for field forces in Korea is but one. The concept of armor for the foot soldier was buried under overwhelming opinion that the "soldiers load", emphasized so effectively in book form was simply too great. Nothing more could be added. Better, we should take away. Besides, shell fragments had too great a velocity and mass to be stopped by any wearable material we had available, and stopping small arms fire was out of the question. Wrong! Simply wrong! Battle casualty analysis on large numbers of KIA and WIA showed conclusively that over 75% of the wounds produced by shell fragments were of a penetrating type. This meant that although burst velocity of the fragments was in the order of 3000 feet/second, impact velocity, irrespective of mass, was about 1000 feet/second or less - otherwise the wounds would have been of a perforating type - a through and through wound. We knew this from research in the laboratory. This fact meant that we did have a material capable of stopping these fragments. The prime questions were still present, of course:



Would the soldier wear it? Could he wear it and still perform his duty? A series of field trials in combat showed that the soldier not only would wear the armor but, on occasion, even demanded it. He could perform his duty and with a greater sense of security. He hardly noted the additional weight or heat. He frequently stated, "I would rather sweat than bleed". The most conservative estimate of the effectiveness of present day body armor for the soldier indicates a reduction of at least 75% in thoracic and abdominal wounds. It is now proposed as a standard item of equipment.

A battle casualty analysis performed in Europe on air crew personnel in WWII showed that 86% of the casualties were produced by flak. Only 5% of the casualties were produced by fighter aircraft missiles. The incidence of flak wounds of the thorax and abdomen was reduced 38% by wearing the flak vest. All of this field work was planned expeditiously. Armor was a spin-off. No question remains as to the overall effectiveness of the armor. Although it is quite true that each war has its own peculiarities, its own strategy and tactics, it would still behoove us well to know the lessons of historical experience, or, as it has been wisely said, "we shall be doomed to learn them all over again".

#### Present Perspective

Modern war, really, is the next war, because for many reasons, we have, up until now, tended to fight new wars with equipment, personnel, and ideas pertaining to the last war. As the interval extends between wars this becomes less likely. The passage of time removes combat-experienced leaders from the scene, and new faces, new ambitions, new egos take over, as well they should. Quantum leaps in technology provide new "futuristic" weapons. Scientists of genius probe the mysteries of nature and come up with  $E=MC^2$ . Technologists apply this basic knowledge and produce A-bombs, H-bombs, and neutron bombs. An armed stand-off results. Weapons less capable of national and planetary destruction are developed. Instead of complete annihilation of the enemy in a series of flashes, weapons lower in order of destructive magnitude are developed and man is able to prolong his combat with man through skillful application of strategy, tactics, and heroic exploits on the battlefield which is now land, sea, air, and space.

Unless enormous monies are spent on civilian protective devices and population shelters on a national scale as Russia has done, an assumption must be made that the hazards of nuclear war, blast, thermal, and radiation, will not be experienced or, if experienced, little can be done. THIS COULD BE THE MOST DANGEROUS ASSUMPTION THE FREE WORLD HAS EVER MADE, AND POSSIBLY, THE MOST ENTICING TO OUR PROBABLE ENEMY. It makes sense, however, to argue that if the threat of preemptive nuclear strike is greatly reduced, then a nuclear war based on mutual annihilation will begin to lose its logic. This is happening, apparently, and the tactics of nuclear war now appears directed toward a targeting of specific field forces with a much greater regard toward preservation of cities and mass population. It is heartening, one would think, that an understanding has finally come about, or seems to have emerged, that conversion of the earth to rubble and destruction of modern civilization is hardly a sensible goal for either side. It is an instinctive hope for survival to assume that the standoff is permanent.

If the above conjecture be true, then we are drawn to a battleground of lesser magnitude, and lesser destructive capability, but one that is more personal, based more on skillful maneuver, superiority in weaponry, excellence of communication, brilliance of leadership and training, determination, and heroism of combat personnel.

In the battlefield environment just described, impact injury from linearly accelerated missiles of all types, primary and secondary, will still be the order of the day. Movement of combat personnel quickly from place to place, utilization of specialized weaponry appropriate to the task, and computerized communications will convert warfare into a grim video of gamesmanship. We will enter into an era of even greater need for protective devices for combat personnel and for all modes of transport.

The helicopter, it seems, has become the common carrier for combat personnel and special weaponry bent on task force assignment. There is, obviously, a direct linear relationship between visibility, exposure time and area of vulnerability. The helicopter, as a matter of fact, must depend greatly upon surprise, evasion, concealment, and speed or quickness. These are the intangibles of its survival. Protective armor for crew and vehicle must be continually upgraded.

On the ground the present armored personnel carrier is to be replaced by the Infantry Fighting Vehicle (IFV). Besides a 3-man crew to fire its 25mm cannon and 7.62mm machinegun, the IFV carries six infantrymen in its rear compartment who can fire from ports in the vehicle's armored sides. Each vehicle costs almost one million dollars. Every effort must be made to provide additional personnel protection that will give some chance of survival, even though the vehicle is disabled or destroyed.

Although the current trend is to provide a means for combat personnel to fly or ride with emphasis on mobility, the moment of truth must eventually arrive as stated by Secretary of Defense Casper Weinberger, "In the final analysis, it all is going to come down to the people who advance and take and hold the land that can ultimately determine whether or not the wars are won or the wars are lost. The combat infantryman (in the United States) knows better than anyone of the carnage of war. It is he who carries the burden in times of war and the infantryman has never let us down." The challenge, of course, is for us not to let him down. Planning must be realistic and creative. PROTECTIVE ARMOR FOR PERSONNEL AND EQUIPMENT IS THE ONLY MEANS WE HAVE THAT WILL FURTHER REDUCE BATTLEFIELD MORTALITY AND MORBIDITY.

Modern warfare carries with it such enormous expense that a nation may win the war and then lose the peace through bankruptcy. Analysis of cost effectiveness pertinent to the many variables of war is a worthy objective, but realistically, one must concede that the effort is somewhat fraught with futility. A nation at war does what it thinks must be done at the time, and expense is only of great concern when the shooting is over. None-the-less, consideration of cost before the fact is highly desirable and should be a strong guiding force in all planning, research, and development.

Conventional war is fought with men using modern machines and weapons subject to their command. Nuclear war is still to be triggered by man. To conserve the fighting strength, man himself must be conserved. How cost effective should this effort be to save human life? What is it worth? A well-trained fighting man, a skilled specialist in warfare, represents a tremendous investment in money, time, and talent. It takes a generation to grow such a man - and only an explosive second to kill, maim, or disable this human being so essential to the conduct of war. What is he worth? Simply, everything we hold dear - our heritage, our culture, our future. Without him we lose all.

There are nations with allegedly over-abundant populations who, conceivably, could trade off human life for the expenditure of enemy ammunition and, thereby gain a given objective. Denial of war supplies is a strategy ancient as war itself. It is unlikely, however, that this philosophy will find avid support among military leaders of our time. It is more likely that logistic requirements will be met by other means, no matter the cost.

The cost of a casualty killed in action is the cost of bringing a child to manhood, the cost of his education and training, his equipment, the cost of his retrieval from the battlefield, his treatment, recovery, and rehabilitation, and in event of death, the delivery of his remains to home and loved ones, and future care for his family. In event of disability he is pensioned for life, or until he is no longer disabled. In brief, the cost of an entire military and veterans medical service is pro-rated among those fighting men and women, who may be killed or wounded in action. There is, literally, no end to the cost. One generation fights and dies or lives with its wounds, and several generations then follow to pick up the tab, less and less caring because the dead past buries its dead, we say, but, actually, it never does.

In the deliberation of cost effectiveness as it relates to protective devices whether worn by military personnel or utilized as shielding for combat materiel, one must be acutely aware that whatever is used for the prevention of casualties or in the lessening of wound severity could result in monetary savings of enormous magnitude.

It is axiomatic that one cannot remove the hazard from warfare and it is grimly clear that objectives sometimes must be taken in spite of the expense in human life. Along with the need for protective devices which is so obvious, it is fully appreciated that their usage must be rationalized with the need for accomplishment of the mission. One of the greatest protective measures to be applied is obviously the exercise of wisdom by military leaders in the selection of only those combat objectives that are absolutely essential to winning the war. Simply straightening out battle lines and adjusting boundaries is not enough.

The charge for a single day of hospitalization in the U.S. now averages about 300 dollars. If intensive care is needed the charge may exceed 1,000 dollars. A coronary bypass may cost \$25,000. If one compares such figures to the care of battle casualties in a foreign land, requiring shipment of all equipment and medical personnel the cost becomes staggering. Casualties killed in action are actually less costly than those wounded in action, or those dying of wounds after entering a hospital. In either event, prevention of the wound or lessening of its severity by any protective device is highly cost effective.

In Korea the body armor vest, used only in the latter half of the conflict, probably reduced the killed in action (KIA) by 10 percent. Accurate figures are difficult to obtain. Because of multiple wounds to more than one body region, a lethal wound to a vital area might be prevented and a casualty (WIA) still result from a wound in a less vital area. Also, a wound to a vital area might be reduced in severity by body armor so that a casualty ordinarily KIA would be converted to a casualty WIA. Such circumstances also prevailed in Vietnam, although the battlefield threat of small arms fire was appreciably increased.

In World War II there were almost 300,000 KIA and over a million wounded. In Korea there were 55,000 KIA and 103,000 WIA. In Vietnam, 47,240 KIA and 303,700 WIA. If one assumes that vehicle shielding and body armor together will reduce the casualty incidence even 10 percent, then one can perceive that the dollar savings in medical care will be in the billions, spread over a lifetime.

There is no doubt that a shift in battlefield threat to high velocity small arms, a change in bullet design, and a change in tactics will challenge anew the effectiveness of body armor. This challenge, fortunately, has been anticipated and successfully met. The new Kevlar helmet and body armor vest will provide much more protection than before - and both items will cost less than the treatment of a severe battle casualty for one single day. It is undeniable that all transport vehicles could be made more protective for combat personnel. Not to do so is a flagrant example of "penny wise and pound foolish". A most significant reward, additional to the dollar savings, will be found in the greater sense of security experienced by combat personnel. This will be manifest in increased confidence, improved morale, and better performance.

### Epilogue

If one eliminates nuclear war from our consideration - and it is pragmatic to do so, because the western world, for reasons of its own, has not kept pace in providing realistic protection from its effects - then the battlefield of tomorrow will have much in common with the recent past in terms of wounding agents. Delivery systems will have changed, but shell fragments, bullets, and blast will still prevail. The biodynamics of linear accelerated missiles and of blast phenomena will be essentially the same, but, perhaps, compounded by increased velocities and density, and better targeting.

It is probable that the helicopter has become the most valuable, most versatile, and perhaps most vulnerable of all combat modes of transport. The tank and infantry fighting vehicle share in this vulnerability. Although experience is not yet available to us, logic would surely indicate that inflammable clothing and body armor would provide considerable protection. In terms of cost effectiveness, the enormous expense of weaponry and combat transport can probably be borne by the western allies better than a trade-off of human life. It must be repeated again and again, protective armor for personnel and equipment is the only means we have that will further reduce battlefield mortality and morbidity.

Combat personnel must have light-weight armor to protect the body regions most prone to lethal wounds. This obviously involves the head, neck, thorax and abdomen. It was shown in Korea and Vietnam that shell fragments from mortar, grenade, artillery, and land mine comprised a major percentage of all wounding agents. An estimate of the effectiveness of the armored vest indicated that it probably would have prevented the wound to thorax and abdomen in about 75% of the WIA; might possibly have prevented the wound in 5%; been of questionable value in 10% and would have had no effect in 10%. There is good reason to believe that the new helmet and improved body armor vest will provide even greater protection.

A recent review of soft body armor used by U.S. Police Officers has shown significant effectiveness and cost benefits. Over a five year period (1974-1978) one could assume 288 torso fatalities at a rate of \$200,000 indemnity savings per fatality prevented, and 1,020 torso injuries at \$13,000 savings per injury prevented, leading to a grand total of \$58,860,000. Total expenditure of \$29,300,000 for body armor leaves a net savings of \$29,560,000 over a period of just five years. The improved confidence and performance of the police officer is an added value.

To date, body armor has saved approximately 400 law enforcement personnel from death or serious injury. Under the Public Safety Officers Benefit Act of 1976, \$50,000 is granted to families of personnel who are killed on duty so that any reduction in the number of lives lost represents substantial monetary savings. In this instance, \$20 million. Indemnity costs are now approximately \$200,000 and injury costs \$13,000 per officer killed or wounded. This does not include lost time and disability costs. The actual cost of the body armor, in light of these figures, obviously becomes relatively unimportant.

Let us now assume a casualty killed in action to have a monetary value of \$250,000. This is a highly arbitrary and low figure; life really cannot be given a price. Now let us use the rounded number of 100,000 KIA in Korea and Vietnam, and assume that present day body armor would have saved at least 10 percent, or 10,000. The total savings become 2 billion dollars.

Again, let us assume a casualty wounded in action to have a lifetime medical care and disability value of \$500,000. This is surely low and arbitrary. Assume, now, a rounded figure of 400,000 WIA in Korea and Vietnam, and that present day body armor would have prevented at least 10 percent, or 40,000. The total savings become 20 billion dollars.

The projected savings of 22 billion dollars through the use of body armor in just two of our recent wars sounds impressive but is actually a very low estimate. Overall veterans benefits now run about 15 billion dollars per annum. In truth, the after-math of war related expenditures is so great that societal pressures now challenge our methods of meeting the costs. Still, there is no substitute for victory, and no alternative for the freedom of mankind. Survival is a basic instinct, but way of life gives meaning to that survival.

## DISCUSSION

DR. VON GIERKE (USA)

Are there any operational objections to body armor or are objections based on costs? To what extent does the armor compromise the soldiers' fighting capability, heat tolerance, and overall performance?

## AUTHOR'S REPLY

The fighting man must be able to perform his mission at all times. Body armor design is influenced by these requirements; therefore, no operational objections arise. The heat load will be accepted in view of the protection. The cost of the body armor is acceptable but reduced cost could be achieved by standardization. The overall performance of the soldier is, under certain circumstances, actually improved.

DR. VON GIERKE (USA)

Is there any body armor providing protection to the neck area? It appears to be an important area.

## AUTHOR'S REPLY

It is possible that neck armor can be provided, perhaps as a detachable device to chest armor. Certainly, for some special missions, an armor providing greater neck coverage is feasible.

TRAUMATISMES PAR IMPACT EN SERVICE AERIEN ET APTITUDE AU VOL  
A LA FORCE AERIENNE BELGE

par

Médecin Lieutenant-Colonel FLION A.  
Conseiller Médical du Service d'Enquêtes d'Accidents Aériens  
Force Aérienne Belge  
Quartier Albert I  
B 1130 BRUXELLES  
BELGIQUE

# INTRODUCTION

Dans le cadre des traumatismes par impact en Service Aérien à la Force Aérienne Belge, il nous a paru intéressant de recenser les différents accidents d'impact survenus à des pilotes de Chasse ou d'Ecolage durant une période de 10 années (1968 à 1977 inclus), de les analyser suivant le type d'impact (accidents d'atterrissage-décollage/Mid-Air Collision/Birdstrike/Ejections), d'examiner, dans ces différentes catégories, l'incidence du type d'appareil, la gravité des blessures encourues par les pilotes (légères, moyennes, graves), les rapports entre ces blessures et les circonstances de l'accident, la cause même des lésions, et, enfin, d'étudier les effets de ces accidents d'impact sur l'aptitude au vol des pilotes concernés (inaptitude temporaire totale, limitations d'aptitude et aptitude finale).

Dans nos conclusions, nous examinerons le "Devenir du Pilote" dans l'ensemble des catégories d'impact traumatisants envisagées. L'objet de notre exposé se subdivisera en deux parties à savoir, un aspect statistique relatant les causes et effets des traumatismes d'impact sur les pilotes et un aspect analytique du "Devenir des Pilotes" concernés.

## I. Première Partie : Aspect Statistique.

### 1. Nombre total d'accidents par impact ayant entraîné des blessures chez des pilotes de Chasse ou d'Ecolage entre 1968 et 1977 à la Force Aérienne Belge.

#### a. Accidents survenus lors de : "Atterrissage-Décollage".

- 12 accidents impliquant 15 pilotes ou passagers.

#### b. Mid-Air Collision.

- 4 accidents impliquant 10 pilotes ou passagers.

#### c. Birdstrike.

- 2 accidents impliquant 2 pilotes ou passagers.

#### d. Ejections en vol.

- 13 accidents impliquant 15 pilotes ou passagers.

Nous serons donc amenés, à considérer 31 accidents faisant intervenir 42 pilotes ou passagers (y inclus des occupants de planeurs civils).

### 2. Evaluation statistique de ces 4 catégories d'impact.

#### a. Accidents d'Atterrissage-Décollage

##### (1) Type d'appareil concerné.

	Type d'avion en cause	Nbre accidents	Nbre pilotes
ECOLAGE	MARCONETTI SF 260 M	1	1
	SV4 BIS	1	1
	FOUCA MAGISTER	3	6
CHASSE	RF 84 F	2	2
	F 104 G	3	3
	MIRAGE 5 B	2	2
TOTAL :		12	15

##### (2) Gravité de l'accident.

Ces 12 accidents se subdivisaient en deux catégories :

- Catégorie 5 (avion détruit) = 9 accidents.
- Catégorie 4 (avion gravement endommagé) = 3 accidents.

(3) Gravité des blessures des pilotes.

LESIONS	Nbre Pilotes	ECOLAGE			CHASSE		
		FOUGA	MARCHETTI	SV4 BIS	F 104 G	M 5 B	RF 84 F
INDENNE	1	1	-	-	-	-	-
LEGER	4	3	-	-	-	-	1
MOYEN	3	-	1	-	1	-	1
GRAVE	7	2	-	1	2	2	-
TOTAL :	15	6	1	1	3	2	2
			8			7	

Dans ces 12 accidents impliquant 15 pilotes, nous observons que :

- la moitié, environ de ces pilotes sont des blessés graves (7/15 soit 46,5 %).
- ces blessés graves se répartissent, à peu près, pour moitié dans les avions d'Ecolage (3) et de Chasse (4).
- l'ensemble des blessés se répartit pour moitié dans les avions d'Ecolage (7 + 1 indemne) et de Chasse (7).

Ceci nous amène à considérer que l'Expérience n'intervient pas et que, d'autre part, ces traumatismes d'impact lors de la Phase Atterrissage-Décollage sont graves dans environ 50% des cas.

(4) Relation entre le type de blessure, les circonstances de l'accident et la cause directe des blessures.

LESIONS	CAS	DESCRIPTION	CIRCONSTANCES	CAUSE
(a)	(b)	(c)	(d)	(e)
BLESSÉS LEGERS 4 CAS	1.	Contusions banales Thorax et Membres Supérieurs	Sortie de piste à l'atterrissage	Choc direct contre les commandes et le tableau de bord
	2.	Contusion Cervicale	Atterrissage en urgence dans un verger	Choc de la nuque contre le siège du pilote
	3.	Contusion des membres et du dos	Atterrissage en urgence dans un verger	Choc du tronc contre le siège du pilote
	4.	Plaies multiples superficielles	Overshoot. Au redécollage, heurte des véhicules dans un parking	Choc contre le siège avant d'un biplace
BLESSÉS MOYENS 3 CAS	1.	Brûlures 1° et 2° p'rior-bitaires. Brûlures 1° du dos des 2 mains	Sortie de piste à l'atterrissage. L'avion prend feu	Lésions dues aux flammes. Clear Visor non baissé; absence de gants
	2.	Commotion Cérébrale légère Hématomes des paupières Contusion du cou et du pied	Atterrissage avant le début de piste	Choc contre le tableau de bord; lésions du cou dues aux sangles du harnais
	3.	Angulation du plateau vertébral supérieur de D 5	Atterrissage forcé brutal sur la Base, de nuit	Colonne Dorsale en flexion, lors de l'impact
BLESSÉS GRAVES 7 CAS	1.	Fracture de D 5	Atterrissage sur le ventre, roue non déverrouillée avec sortie de piste	Effet conjugué de forces longitud. et horiz. de l'arrière vers l'avant + flexion antérieure du tronc à l'impact
	2.	Blessures étendues face et occiput. Forte commotion avec coma de 9 jours. Fracture sans déplacement de la cheville gauche	Faute technique de décollage, suivie d'éjection dans des circonstances marginales. Chute du pilote dans un marais parachute non tout-ouvert	Perte du casque. Impact au aol. Cordes parachute enroulées autour de la cheville
	3.	Brûlures 2° frontopariétales et hémiface droites. Fracture extrémité sup. péroné gauche Tassement D 11 - D 12	Ejection à basse altitude à l'atterrissage suite à une panne technique	Chute près du brasier du crash Atterrissage sur le survival Kit. Atterrissage non préparé
	4.	Fracture partie antérieure droite des corps vertébraux de D 8 et D 9	Mauvaise approche d'atterrissage. L'avion heurte les poteaux de lampes d'approche. Le pilote s'éjecte à basse altitude	Flexion antérieure de la colonne dorsale. Ejection non préparée.

(a)	(b)	(c)	(d)	(e)
	5.	Fractures de côtes multiples Fractures des deux malléoles pied g.	Ecrasement d'un SV 4 BIS en mission de remorquage pla- neur, à l'atterrissage	Heurt des structures du cock- pit lors de l'impact
	6.	Commotion cérébrale avec coma de 3 jours. Plaies multiples de la face et du cuir chevelu. Plaies cuisse et jambe droite	Overshoot. Au redécollage l'avion heurte des voitures garées dans un parking sur la base	Choc direct contre les struc- ture du cockpit
	7.	Tassement cunéiforme de D12- L1 avec un écrasement du plateau supér. Léger tasse- ment du plateau supérieur de D11	Atterrissage trop court à proximité de la barrière d'arrêt, étendue sur le sol. L'avion s'y accroche. Le nez de l'avion touche la piste; la roue de nez se brise	Choc à l'impact lors de la rupture de la roue de nez

L'examen de la relation décrite ci-dessus, nous permet de constater que :

(a) Les 4 cas de Blessures Légères :

- surviennent tous à l'atterrissage
- consistent en des contusions ou plaies superficielles liées au choc de parties du corps du pilote contre des structures intérieures du cockpit (siège-commandes-tableau de bord)

(b) Les 3 cas de Blessures Moyennes :

- surviennent tous à l'atterrissage
- consistent en blessures liées au heurt contre les structures du cockpit, en brûlures (avion prenant feu), et en une lésion mineure vertébrale de D5 due à une position défec-  
tueuse de la colonne vertébrale dorsale en flexion lors de l'impact.

(c) Les 7 cas de Blessures Graves se subdivisent en 2 groupes :

- (i) - 3 cas d'éjection à très basse altitude (2 à l'atterrissage et 1 au décollage) ayant entraîné des lésions vertébrales (D8/D9 et D11/D12), commotion cérébrale et frac-  
ture des membres inférieurs (cheville-péroné). Ces lésions sont liées à une éjec-  
tion non préparée, colonne dorsale en flexion, perte du casque et chute sur le sur-  
vival kit non largué par manque de temps.
- (ii) - 4 cas d'impact d'atterrissage provoquant des lésions vertébrales (D5 et D11/12/L1),  
fractures de côtes, commotion cérébrale avec coma, fractures aux membres inférieurs  
et plaies de la face. Ces lésions sont directement liées à l'impact et au heurt du  
pilote contre les structures du cockpit.

b. Mid-Air Collision

(1) Type de collision et gravité de l'accident.

- Cas N° 1 - Collision d'un T33 (Cat 5) et d'un planeur civil (Cat 5)
- Cas N° 2 - Collision entre 2 F84F (Cat 5) dans une formation de trois avions
- Cas N° 3 - Collision entre un F104G 5 B BR (Cat 5) et un planeur civil (Cat 5)
- Cas N° 4 - Collision entre deux T33 (un Cat 5 et un Cat 4) dans une formation de 4 avions

(2) Gravité des blessures.

Ces 4 Mid-Air Collision ont impliqué 7 Pilotes ou Passagers militaires et 3 Pilotes ou Passa-  
gers Civils (planeurs).

CAS	VICTIME	INDEMNÉ	BLESSE			DÉCÉDÉ
			LEGER	MOYEN	GRAVE	
N°1	Pilote T33	-	X	-	-	-
	Passager T33	-	X	-	-	-
	Pilote planeur Civ	-	-	-	-	X
	Passager planeur	-	-	-	-	X
N°2	Pilote F 84 F	-	Xéjec.	-	-	-
	Pilote F 84 F	-	Xéjec.	-	-	-
N°3	Pilote M 5 B	-	Xéjec.	-	-	-
	Pilote planeur Civ	-	-	-	-	X
N°4	Pilote T 33	-	Xéjec.	-	-	-
	Pilote T 33	X	-	-	-	-
TOTAL	10	1	6	-	-	3

Note : éjec. = éjection.



Au vu du tableau ci-dessus nous constatons que :

- les 3 occupants des 2 planeurs civils sont décédés; ce qui n'étonne évidemment pas, compte-tenu du fait de collisions frontales et de l'importante différence de structure existant entre les types d'aéronefs collisionnés.
- par contre nous constatons que les 7 autres pilotes ou passagers sont légèrement blessés voir indemnes. Notons, cependant, que 4 de ces pilotes se sont éjectés immédiatement après la collision.

(3) Relation entre le type de Blessures, les circonstances de l'accident et la cause directe des blessures.

CAS N°	CIRCONSTANCES ACCIDENT	TYPE LÉSIONS	CAUSE LÉSIONS
1. Pilote T33	Le T33 et le Planeur civil à basse altitude volaient, en se rapprochant, sur des caps opposés sur une même trajectoire. Les pilotes NE se sont PAS vus, d'où une collision frontale	Plaies superf. au visage	Débris du planeur projetés dans le cockpit du T33
Passager T33	idem	idem	idem
2. Pilote F84F	Une formation de 3 avions effectue un virage à gauche "VIC". Durant ce virage, le Leader ordonne le passage en échelon à droite. Lors de cette manoeuvre, les N°2 et N°3 s'accrochent et se brisent. Les 2 pilotes s'éjectent. Les 2 ailiers se sont momentanément perdus de vue pendant le changement de formation, volant très près l'un de l'autre	Plaies superf. au front et derrière l'oreille gauche	Perte du casque durant l'éjection
Pilote F84F	idem	Echymoses des épaules. Contusion de D5 à D7	Sangles du parachute Ejection
3. Pilote M5B	Les pilotes du MIRAGE et du Planeur Civil, suivant des trajectoires de collision NE se sont PAS vus en temps utile pour l'éviter. Le pilote du MIRAGE s'éjecte. Le pilote du planeur est tué.	Brûlure cou. Contusion lombaire	Sangle du parachute Atterrissage
4. Pilote T33	Durant une manoeuvre de break, le pilote perd son Leader de vue, dans une formation de 4 avions et le collisionne par manque de vigilance	Plaies 2 genoux. Hématome sous claviculaire g.	Heurte le bord du windshield pendant l'éjection. Dû aux straps

La relation exprimée dans le tableau qui précède nous montre que :

- (a) Dans les 4 cas de collision décrits, l'accident est causé par le fait que les pilotes NF se sont PAS vus (2 collisions avec des planeurs) ou se sont MOMENTANÉMENT perdus de vue lors de changement de place au sein d'une formation de plusieurs avions.
- (b) Les collisions en elles-mêmes n'ont provoqué chez les survivants que des plaies superficielles au visage. Les autres lésions (assez légères) sont directement liées à l'éjection (perte du casque-sangles de parachute-harnais-contact avec le sol-choc contre le bord du windshield lors de l'abandon de bord).

c. Birdstrike.

Sur un nombre très important de Birdstrike survenus entre 1968 et 1977 à la Force Aérienne Belge, nous ne retenons que 2 cas d'accidents, impliquant 2 pilotes et lors desquels les pilotes ont été blessés. Dans ces 2 cas, l'avion en cause était un MIRAGE 5 B.

- Cas N°1

A une altitude de 1000ft environ et à une vitesse de 400kts l'avion entre en collision avec des oiseaux. Le pilote présente des blessures superficielles au visage (sa visière de casque N'était PAS abaissée). Les dégâts à l'avion (cockpit) sont de catégorie 2. Le pilote réussit à ramener l'avion à sa Base.



## - Cas N°2

Durant une mission de navigation à environ 700ft, le pilote ressent deux chocs quasi simultanés. Le second choc est ressenti sur les pommettes et sur l'épaule droite. Surpris, le pilote lâche le stick durant un court instant. L'avion pique et devient incontrôlable. Le pilote s'éjecte. Le pilote présente des éraflures superficielles et des contusions légères provoquées par l'éclatement de la verrière. Le pilote avait sa visière de casque abaissée au moment du birdstrike mais a perdu son casque durant l'éjection (la mentonnière était attachée mais NON tendue).

Dans ces deux cas, les pilotes ne présentent que des blessures superficielles. L'opportunité de la visière de casque abaissée eut permis d'éviter (dans le premier cas) les plaies au visage.

d. Ejections en vol.(1) Type d'appareil concerné.

Entre 1968 et 1977 se sont déroulés 13 accidents Aériens suivis d'éjections impliquant 15 pilotes. Nous n'avons considéré QUE les éjections génératrices de traumatismes d'impact pour le pilote.

Il s'agit de :

- 4 accidents d'avions F 104 G (dont 1 TF 104 G).
- 9 accidents d'avions MIRAGES 5 B (dont 1 MIRAGE 5 B BD).

(2) Gravité des blessures des pilotes concernés.

GRAVITE	F 104 G	M 5 B	Total
LEGER	1	1	2
MOYEN	1	1	2
GRAVE	2	8	10
DECES	1	0	1
TOT. Pilotes	5	10	15

Dans ces 13 accidents aériens suivis d'éjection, nous constatons que sur un total de 15 pilotes, 10 d'entre eux ont été grièvement blessés et 1 des pilotes est décédé. Il ressort que 2/3 des cas de traumatismes d'impact liés aux éjections considérées ici sont des traumatismes graves.

(3) Relation entre le type de blessures, les circonstances de l'accident et la cause directe des blessures.

LESIONS	CAS	DESCRIPTION DES BLESSURES	CAUSE DES BLESSURES
LEGER	1. F104G	Contusion pouce gauche Contusion du bassin Contusion pied gauche Contusion de la nuque	Atterrissage. (chute dure sur les 2 pieds, ensuite chute sur la face. Les 2 visières du casque étant abaissées.
	2. M5B BA	Contusions banales de la nuque	Atterrissage.
MOYEN	1. TF104G	Fracture 1 phalange pouce et annulaire gauches	Durant l'éjection non préparée, casque, gants et bottines arrachés.
	2. M5B BA	Hématomes et éraflures de la racine du nez et du coin interne de l'oeil gauche. Hématome face interne coude droit. Contusions dorsales D9 à D12.	Perte du casque durant l'éjection. Atterrissage dans des arbres.
GRAVE	1. TF104G	Blessures superficielles visage. Contusion bras droit. Tassement D8 et D9.	Casque non attaché, a été arraché lors de l'éjection. Atterrissage sur le survival kit.
	2. M5B BA	Tassement antéro-latéral droit de D 12. Fissurations verticale partie postérieure du corps vertébral de D11.	Blessures liées à une éjection dans une position inadéquate.
	3. M5B BR	Tassement de D12 et fracture L1.	Liées à l'éjection.
	4. M5B BR	Blessure superficielle menton. Tassement vertébral des plateaux supérieurs de D7, D8 et D11 avec légère déformation cunéiforme antérieure des corps vertébraux	Masque O2 arraché. Position défectueuse de la colonne vertébrale dorsale à l'éjection.

LESIONS	CAS	DESCRIPTION DES BLESSURES	CAUSE DES BLESSURES
	5. M5B BR	Ecchymose du cou à droite. Canine supérieure droite cassée. Tassement vertébral D12 et L1.	Suspentes du parachute. Atterrissage. Atterrissage.
	6. M5B BD	Fracture Ischio et Iléo-pubienne droite. Fracture du coccyx.	Lésions liées à un atterrissage sur le survival kit.
	7. M5B BD	Fracture ouverte Tibia et péroné droits. Contusions et hématomes du cou et de l'épaule gauche.	Atterrissage sur le survival kit. Dûes aux suspentes et harnais du parachute.
	8. M5B BA	Eraflures bras dr. et cou à g. Contusion coccygienne. Fêlure péroné gauche. Tassement de D11. Tassement espace L5-S1.	Lésions dues à un atterrissage dur sur le coccyx puis sur le dos, jambe repliée
	9. M5B BA	Hématomes au visage (paupières, narines et commissures labiales). Fracture-tassement vertébrale antérieure de D11.	Lésions dues au casque. Lésions d'éjection (douleur à l'éjection par poignée basse, l'avion étant sur le dos).
	10. F104G	Fracture-tassement de D6-D7 et D8.	Position défectueuse à l'éjection.
DECES	1. F104G	Trauma de la base du crâne. Polytraumatismes des membres et de la colonne vertébrale.	Atterrissage avec un parachute NON ouvert.

Le tableau ci-dessus nous amène à formuler quelques remarques :

- les 2 cas de blessures légères sont du type contusionnel et sont liées à l'atterrissage.
- les 2 cas de blessures moyennes (fractures de doigts et hématomes multiples) sont liées soit à la perte d'équipements durant la séquence d'éjection soit à l'atterrissage.
- les 10 cas de blessures graves se caractérisent par :

- 8 fractures vertébrales dont :

- (i) 3 liées à l'atterrissage (D8-D9 / D12-L1 / D11-L5-S1) chute du pilote en position assise ou sur le survival kit.
- (ii) 5 liées à l'éjection elle-même (D11-D12/D12-L1/D7-D8-D11/D11/D6-D7-D8) en rapport avec une position défectueuse de la colonne vertébrale lors de l'éjection.

- 2 fractures du bassin et des membres inférieurs :

Ces lésions sont en rapport avec un atterrissage dur sur le survival kit, non largué vu les circonstances d'urgence.

En outre, dans ces 10 cas de blessures graves il y a lieu d'ajouter :

- des blessures multiples au visage, liées à l'arrachement du casque ou du masque à oxygène durant l'éjection.
- des lésions contuses au niveau du cou, des épaules et des membres supérieurs en rapport avec les tractions exercées par les suspentes du parachute ou le harnais.

5. Conclusion de la Première Partie statistique.

Dans cette Revue statistique de C.S., couvrant la période de 1968 à 1977 inclus 31 accidents d'impact survenus, en service aérien, à des pilotes de Chasse ou d'Ecolage de la Force Aérienne belge (42 pilotes et passagers) ont analysés.

En fonction des 4 catégories d'impact envisagées, à savoir :

- Atterrissage-Décollage.
- Mid-Air Collision.
- Birdstrike.
- Ejections en vol.

Nous constatons que la gravité des blessures encourues se répartit de la façon suivante :

GRAVITE LESIONS	ATERRISSAGE DECOLLAGE	MID-AIR COLLISION	BIRDSTRIKE	EJECTIONS EN VOL	TOTAL
INDEMNÉ	1	1	-	-	2
LEGER	4	6	2	2	14
MOYEN	3	-	-	2	5
GRAVE	7	-	-	10	17
DECES	-	3	-	1	4
TOT PILOTES	15	10	2	15	42

Le tableau qui précède nous amène aux réflexions suivantes :

1. Sur un total de 42 pilotes ou passagers d'avions de chasse ou d'écologie (y compris 3 occupants de planeurs civils) ayant été l'objet de traumatismes d'impact, nous constatons que 50% sont des traumatisés graves ou sont décédés.
2. que le % relatif des traumatismes graves se trouve le plus élevé dans les impacts liés aux éjections en vol (10 sur 15) suivi par les accidents d'atterrissage-décollage (7 sur 15).
3. que le nombre de décès s'avère le plus élevé dans les Mid-Air Collision, compte-tenu du fait que les 3 pilotes décédés se trouvaient à bord de planeurs civils collisionnés.

Remarque :

Dans cette analyse, seules les éjections ayant entraîné un trauma pour le pilote ont été envisagées.

II. Deuxième Partie : Aspect Analytique du "Devenir des pilotes" concernés.

Préliminaires

Après avoir investigué une série de 31 accidents impliquant 42 pilotes ou passagers d'avions de chasse et d'écologie, survenus entre 1968 et 1977 à la FAé Belge et en avoir décrit les lésions des occupants victimes de traumatismes d'impact, il nous a paru intéressant d'examiner les conséquences de l'accident pour les pilotes en fonction de leur carrière.

L'étude de ce "devenir" des pilotes après l'accident envisagera la durée d'inaptitude temporaire totale, les décisions ultérieures de limitation d'aptitude au vol et l'aptitude finale.

Ces différentes considérations se feront dans chaque catégorie de traumatisme par impact.

1. Devenir du pilote victime de traumatismes par impact dans les accidents d'atterrissage-décollage.

GRAVITE LESIONS	CAS N°	INAPTE TEMPOR TOTAL	APTITUDE LIMITEE	APTITUDE FINALE
LEGER	1.	40 jours	-	TOT. Apte
	2.	-	Après 570 J.	Limité TPT.
	3.	-	-	TOT. Apte
	4.	15 jours	-	TOT. Apte
MOYEN	1.	90 jours	-	TOT. Apte
	2.	30 jours	-	RAYE
	3.	15 jours	-	Limité TPT.
GRAVE	1.	180 jours	-	TOT. Apte
	2.	570 jours	-	INAPTE
	3.	120 jours	-	TOT. Apte
	4.	150 jours	-	TOT. Apte
	5.	150 jours	-	TOT. Apts
	6.	100 jours	-	INAPTE
	7.	130 jours	180 J Lim TPT	TOT. Apte
INDEMNÉ	1.	-	-	TOT. Apte
TOT PILOTES	15	1.590 jours		

Considérations

Le "Devenir" de ces pilotes victimes d'accidents d'impact lors de l'atterrissage-décollage, a été établi comme suit :

Sur un total de 15 pilotes concernés :

- a. L'incapacité temporaire totale a été de 1.590 jours pour ces 15 pilotes après l'accident, soit un % moyen de 106 jours par pilote.
- b. Les limitations temporaires d'aptitude se sont avérées nécessaires dans deux cas (limitation aux avions de chasse sans siège éjectable et avions de transport) l'un, après 570 jours d'aptitude totale suite au développement d'un syndrome cervico-brachial chronique (lors de l'accident, plusieurs douleurs avaient été signalées et le pilote avait été déclaré immédiatement totalement apte au vol), l'autre, après 130 jours d'incapacité totale, a subi une période de 180 jours d'aptitude limitée aux TPT. et a, ensuite, été déclaré Totalement Apte au vol (il avait subi d'un tassement vertébral de D12-L1).
- c. L'Aptitude finale de ces 15 pilotes accidentés a été établie comme suit :
  - 10 sont finalement déclarés entièrement Aptes au vol (66,66 %)
  - 2 sont déclarés Incaptes définitivement (13,33 %)
  - 1 est Rayé par la suite pour raisons professionnelles (6,66 %)
  - 2 sont limités au TPT et aux avions de chasse sans siège éjectable (13,33 %)

2. Devenir du pilote victime de traumatisme par impact dans une MID-AIR Collision.

GRAVITE LESIONS	CAS N°	INAPTE TEMPOR TOTAL	APTITUDE LIMITEE	APTITUDE FINALE
LEGER	1.	-	-	TOT. Apte
	2.	-	-	TOT. Apte
	3.	-	-	TOT. Apte
	4.	-	-	TOT. Apte
	5.	20 jours	-	TOT. Apte
	6.	8 jours	-	TOT. Apte
INDEMNIE	1.	-	-	TOT. Apte
DECES	1.	-	-	DECES
	2.	-	-	DECES
	3.	-	-	DECES
TOT. Pilotes	10	28 jours	-	

Considérations

Le "Devenir" de ces pilotes, victimes de Mid-Air Collision, a été établi comme suit :

Sur un total de 10 pilotes concernés (dont 3 civils)

- a. Les 3 civils occupants de planeurs sont décédés.
- b. L'incapacité temporaire totale a été de 28 jours pour les 7 pilotes survivants, soit un % moyen de 4 jours par pilote.
- c. La limitation temporaire d'aptitude a été nulle.
- d. L'aptitude définitive a été totale au vol pour tous les survivants (à noter qu'un de ces pilotes est décédé, en service aérien, 5 ans après sa Mid-Air Collision).

3. Devenir du pilote victime de traumatisme par impact dans des accidents de Birdstrike.

GRAVITE LESIONS	CAS N°	INAPTE TEMPOR TOTAL	APTITUDE LIMITEE	APTITUDE FINALE
LEGER	1.	-	-	TOT. Apte
	2.	15 jours	-	TOT. Apte
TOT. Pilotes	2	15 jours	-	

Considérations

Le "Devenir" de ces pilotes victimes de birdstrike traumatisant se caractérise comme suit :

Sur un total de 2 pilotes concernés :

- a. L'inaptitude temporaire totale a été de 15 jours soit un % moyen de 7,5 jours par pilote.
- b. Il n'y a pas eu de limitation temporaire d'aptitude.
- c. Ces 2 pilotes ont finalement été déclarés totalement aptes au vol.

4. Devenir du pilote victime de traumatisme par impact dans des accidents suivis d'éjection.

GRAVITE LESIONS	CAS N°	INAPTE TEMPOR TOTAL	APTITUDE LIMITEE	APTITUDE FINALE
LEGER	1.	90 jours	-	TOT. Apte
	2.	3 jours	-	INAPTE
MOYEN	1.	90 jours	-	TOT. Apte
	2.	8 jours	-	TOT. Apte
GRAVE	1.	180 jours	2ème pilote	2ème pilote
	2.	150 jours	-	TOT. Apte
	3.	120 jours	-	TOT. Apte
	4.	210 jours	-	TOT. Apte
	5.	480 jours	-	TOT. Apte
	6.	120 jours	-	TOT. Apte
	7.	330 jours	TPT 360 jours	TOT. Apte
	8.	160 jours	TPT Hélic 240 jours	TOT. Apte
	9.	150 jours	-	TOT. Apte
	10.	270 jours	TPT	TPT
DECES	1.	-	-	-
TOT. Pilotes	15	2.361 jours	-	-

Considérations

Le "Devenir" de ces pilotes victimes d'accidents aériens suivis d'éjection s'est établi comme suit :

Sur un total de 15 pilotes concernés

- a. Un des pilotes est décédé lors de l'éjection.
  - b. L'inaptitude temporaire totale a été de 2.361 jours pour les 14 pilotes survivants, soit un % moyen de 16<sup>h</sup> jours par pilote.
  - c. La limitation temporaire d'aptitude s'est révélée indispensable dans 4 cas (Transport-Hélico ou présence d'un 2ème pilote expérimenté).
  - d. L'aptitude finale de ces 14 pilotes a été la suivante :
    - 11 pilotes ont finalement été déclarés totalement Aptés.
    - 1 pilote a été déclaré définitivement inapte par perte de motivation.
    - 2 pilotes ont été définitivement limités (l'un aux avions de transport, l'autre à la présence obligée d'un 2ème pilote expérimenté lors de ses vols).
5. Devenir des pilotes victimes de traumatisme par impact dans l'ensemble des 4 catégories d'accidents envisagées.

GRAVITE LESIONS	Nbre Pilotes	INAPTE TEMP. TOT	APTIT LIMITEE	APTITUDE FINALE				
				Apte	Limité	Inapte	Rayé	Décédé
LEGER	14	191 jours	1 caa	12	1	1	-	-
MOYEN	5	233 jours	0 cas	3	1	-	1	-
GRAVE	17	3.570 jours	5 caa	13	2	2	-	-
INDEMNÉ	2	-	0 cas	2	-	-	-	-
DECES	4	-	-	-	-	-	-	-
TOTAL	42	3.994 jours	6 cas	30	4	3	1	4

#### Considérations

Le "Devenir" de ces pilotes et passagers d'avions, victimes d'accidents aériens avec traumatisme par impact s'établit comme suit :

Sur un total de 42 pilotes concernés :

- a. 4 pilotes sont décédés.
- b. 2 pilotes furent indemnes et déclarés Totalemt Aptes immédiatement.
- c. Les 36 survivants blessés ont totalisé un nombre total de 3.994 jours d'inaptitude temporaire totale, soit un % moyen de 111 jours par pilote.
- d. Dans 6 cas sur 36 cette inaptitude temporaire totale a été suivie d'une aptitude au vol limitée.
- e. L'aptitude définitive a été TOTALE dans 30 cas sur 42.
  - 4 pilotes ont été définitivement limités.
  - 3 pilotes ont été déclarés Inaptes définitivement.
  - 1 pilote a été Rayé du Personnel Navigant ultérieurement.

#### 6. Conclusions de la Deuxième Partie Analytique.

Dans le cadre de cette Analyse du "Devenir" des pilotes, victimes d'accidents aériens survenus par impact dans des circonstances diverses, nous en arrivons à conclure que sur un total de 31 accidentés ayant impliqué 42 pilotes ou passagers d'avions accidentés l'influence sur la carrière future du pilote s'est établie comme suit :

- 4 pilotes sont décédés soit 9,5 %.
- 30 pilotes sur 42 se retrouvent Totalemt Aptes après des délais divers soit 71,5 %.
- 4 pilotes sont définitivement Inaptes soit 9,5 %.
- 4 pilotes sont définitivement Limités dans leur carrière (passage sur un autre type d'avion) soit 9,5 %.

### III. CONCLUSION GENERALE

Cette Revue de cas de traumatisme par impact en Service Aérien à la Force Aérienne Belge nous permet d'établir les constatations suivantes en fonction du Type d'Impact :

#### 1. Accidents d'Atterrissage-Décollage.

Nous remarquons que 46,5 % des victimes de ce type d'accident sont des blessés graves se répartissant environ pour moitié dans des accidents d'avions de chasse et d'écologie. Les causes en sont pour moitié des éjections à très basse altitude lors d'atterrissage-décollage et pour l'autre moitié des cas d'impact direct avec le sol. Les lésions encourues par les pilotes consistent essentiellement en des lésions vertébrales, fractures de côtes, commotions cérébrales, fractures des membres inférieurs et des plaies de la face. L'inaptitude temporaire totale qui en a résulté pour le pilote a été en moyenne de 106 jours. Le devenir professionnel définitif de ces pilotes s'est révélé être l'aptitude totale dans 66,66 % des cas, l'inaptitude définitive dans 13,33 % des cas, la radiation professionnelle dans 6,66 % des cas et la limitation définitive à un autre type d'avion dans 13,33 % des cas.

#### 2. Accidents de Mid-Air Collision.

Ces accidents ont provoqué le décès de tous les occupants des planeurs civils collisionnés par des avions de chasse. Ils n'ont occasionné que des lésions mineures chez les pilotes militaires accidentés (su visage ou lésions à l'éjection). La cause de ces collisions est due à l'absence de perception visuelle de l'autre avion ou à une perte momentanée de perception visuelle de l'autre avion dans des changements de place lors de vols en formation. L'inaptitude temporaire totale qui en a résulté a été en moyenne de 4 jours par pilote. Les limitations ultérieures d'aptitude ont été nulles pour les pilotes militaires survivants. L'aptitude définitive s'est avérée être totale dans

100 % des cas des survivants.

### 3. Accidents de Birdstrike.

Ces accidents n'ont causé que des blessures superficielles. L'incapacité temporaire totale résultante a été de 7,5 jours par pilote en moyenne. Il n'y a pas eu de limitation ultérieure d'aptitude. L'aptitude finale a été totale dans 100 % des cas de pilotes concernés.

### 4. Accidents d'Ejections.

Dans 2/3 des cas les pilotes ont présenté des blessures graves. Un des pilotes est décédé. Ces traumatismes graves (10 cas sur 15) ont consisté dans 8 cas sur 15 en des lésions de la colonne vertébrale (entre D6 et L1 pour les lésions d'éjection même et entre D8 et S1 pour les lésions liées à l'atterrissage) et dans 2 cas sur 15 en des lésions du bassin ou des membres inférieurs liées à l'atterrissage sur le survival kit non largué.

L'incapacité temporaire totale a été en moyenne de 168 jours par pilote. Le devenir professionnel définitif des pilotes s'est révélé être de 73,33 % d'aptitude totale, 6,66 % d'incapacité définitive, 13,33 % de limitation définitive d'aptitude et de 6,66 % de décès.

Il apparaît donc, que dans l'ensemble de ces 4 catégories envisagées :

- 50 % des pilotes sont blessés graves ou décédés.
- le % de traumatismes graves est le plus élevé dans les impacts liés aux éjections suivies des accidents d'atterrissage.
- les pilotes, victimes de traumatismes par impact à la Force Aérienne Belge conservent un "Devenir" professionnel très satisfaisant puisque, dans l'ensemble des pilotes, ceux qui ont été déclarés finalement totalement Aptes représentent 71,5 % et, ceux qui ont été limités à un autre type d'appareil représentent 9,5 %.
- 81 % des pilotes accidentés ont donc pu poursuivre leur carrière dans le personnel navigant.

Cette conclusion d'une Revue de 31 accidents d'impact traumatisants survenus à 42 pilotes d'avions de chasse ou d'écouleur à la Force Aérienne Belge entre 1968 et 1977 nous apparaît donc comme très positive en ce qui concerne le "Devenir" professionnel des pilotes accidentés.

## DISCUSSION

DR. AUFFRET (FR)

On the bird strike, you have taken only two cases and I would like to ask you whether it was the front canopy of the mirage or the lateral canopy? Recently in France, I have seen two bird strikes which broke the side canopy during very steep banking maneuvers.

## AUTHOR'S REPLY

Well, we kept only two cases in statistics, because the other bird did not enter the aircraft and the pilot was not injured. In these two cases, it was a frontal type of collision, and there was no problem in either banking or turning.



IMPACT INJURIES FROM LINEAR ACCELERATION SUSTAINED BY AN F-5 MAN/MACHINE COLLIDING  
WITH THE TERRAIN AT 45 KIAS

by

Harald T. Andersen  
Institute of Aviation Medicine  
P.O. Box 281, Blindern

OSLO 3

TIGER BLUE, a flight element consisting of two Freedom Fighters, (Northrop F-5A/B) took off in formation from a military air base in southern Norway at 1035 Alpha on bright winter day for a tactical training mission. The mission tasks were as follows:

- planning and executing a flight of two aircraft attacking a minimum of two targets on the ground
- Training offensive and defensive tactical formation flying at altitudes between 200 and 1000 feet with repeated attacks on the targets
- return to homebase with correct approach procedures and landing

The lead aircraft was flown by a senior, very experienced Flight Commander. TIGER-BLUE-2 was a young second lieutenant with a total of 293.5 flying hours, 210 of which in jet aircraft with only 61 hours in the F-5A/B. He had been posted to the squadron one month before the day of the fatal accident. By colleagues he was regarded as an average pilot exhibiting remarkably mature attitudes towards flying duties. His manual skills were appreciated as being better than average, but his progress evidently deliberate, labeling him a slow learner. In retrospect, it is interesting to note the fact that two of the instructors on the squadron, independently of each other, commented in the post-crash interviews, that this young second lieutenant responded much slower than one would expect to new visual inputs when suddenly presented. Moreover, his critical judgement on difficult approaches had sometimes been questioned. Under such circumstances a lack of initiative had been apparent.

The weather report for southern Norway on the day of the accident was very good, a high pressure ridge over Scandinavia giving cold bright winter conditions, but with the sun low over the horizon. Winds were northerly at 10-15 knots in exposed areas. Visibility at the site of the accident was 70 km in bright sunshine and calm. Such weather conditions, with a bright but low sun shining on white snow over sloping hills produce a phenomenon well known to experienced air crew: Behind hills, shadows take on a soft, bluish tint which gives an impression of depth and distance, and the hills themselves appear to be less steep than they in fact are.

The altitude meter setting (QNH) on the air base was 1020 millibars, whereas in the target area the corresponding figure was 1013. With the altimeter set on base, it would read 175 feet too high in the target area and the flight pattern for the attack could consequently be flown 175 feet too low if instruments had to be relied on. This is not likely to have been the case. Such an error of instrumental display cannot have been the cause of the accident. It could hardly have been contributory.

TIGER BLUE flew a defensive formation to the target area and was subsequently cleared for all heights between the terrain and 500 feet. As the formation entered the region designated for low level military flying training 500 feet was selected. The formation was simultaneously changed from defensive to offensive. At initial point (IP), the altitude was reduced to 200 feet and speed selected at 450 knots. The lead aircraft went directly for the target whereas the no 2, according to the briefed procedure, flew a curve to the left of the leader in order to establish a 30 sec separation between deliveries of weapons.

TIGER BLUE-leader dived as had been briefed during the pre-flight preparations 15° on the target - a bridge on the main road - in order to simulate delivery of bombs. TIGER BLUE-two made a similar attack 30 seconds later. Both planes pulled out and returned southwards to the IP, joined in offensive formation and went for the target for a second attack to be flown exactly as the first one. TIGER BLUE-two again flew a course intended to give a 30 sec separation between delivery of weapons and took up position 2 nautical miles behind the leader as TIGER BLUE-one pulled up for the attack. Twenty-nine seconds later TIGER BLUE-two called that he was about to pull up for his second attack on the target. This is his last recorded radio transmission. This time he came in at a very low altitude, approximately 75 feet over the terrain, the lake Breidvatn. He rolled out but continued in horizontal flight passed the target. The tail of the plane struck the ground just below the roadside and with the nose elevated 20°. Then the aircraft bounced over the road, collided directly front-on-terrain and disintegrated.

Some of the larger pieces of the wreckage are shown in the series of illustrations:

- the site of impact overview
- the crash site close-up
- the pilots seat
- the nose cone with pitot tube
- upper part of left tail cone

- upper part of tail fin
- lower part of tail fin

The pilot died in the crash. His body was remarkably well preserved the high speed and mode of impact taken into consideration. Two illustrations show the body from right and the left side wearing flight suit, exposure suit under the flight suit, anti-G garment and flying boots. Likewise the parachute harness and the separate harness with floating devices were left in place.

The right arm is badly torn and ripped off. There is a large lesion in the material over the right thigh, a smaller one over the left thigh and one on the left side near the neck lining. Details of these tears are shown in the three separate close-up views of the flying clothing:

- the tear of the right thigh
- the slit down the left thigh
- the neck-near lesion.

There is one additional small lesion on the back of the exposure suit along the seam. Otherwise the back side of the clothes are intact.

The right and the left boot are shown in the next two illustrations. The heel of the right boot is almost ripped off, the left boot is torn across.

The anti-G garment is torn and the waist separated from the parts covering the lower extremities as is illustrated the next picture. The valve and hose for pressurised gas is virtually uninjured.

The body itself is that of a young male approximately 165 cm with obvious rigor and livor mortis. The head is torn off - it was never recovered - leaving only soft tissue from the right side of the neck and the right ear. The tear continues down the left side of the chest.

The right arm was found beside the body it is torn apart at the middle of the upper arm. Some laceration of both arms and hands are apparent. On the anterior aspect of the right thigh a 20 cm long lesion which involve the underlying muscular tissue. There is a more superficial wound on the left thigh. Both femurs are broken. On the right foot a soft tissue wound is seen extending across. It corresponds to the tear previously shown on the left boot. There are no lesions of the back, the buttocks or the posterior aspects of the lower extremities.

#### FINDINGS ON AUTOPSY.

##### Chest organs.

Left first and second costae were missing, trachea, the esophagus, the left lung and the heart likewise, whereas the right lung was present although lacerated. The aorta was ruptured.

##### Abdomal organs.

The abdominal organs were virtually injured. In the stomach about 30 ml of digested food was found. There were no tablets or parts of tablets in the content. The mucosa was pale with fine, normal foldings. The small and the large intestine were unremarkable. No pathological changes were detected on the examination of the kidneys, the adrenals glands or the pancreas.

A small laceration was evident on the surface of the liver. When sliced the cut surfaces appeared normal, but several lesions could be seen.

There was no damage to the genito-urinary system. The bladder contained 200 ml clear, yellow urine.

Laboratory analysed for alcohol and carbon dioxide were negative.

It appears likely that the lesions of head, chest organs and extremities were caused by the decelerative forces when the plane collided with the terrain. The lesion to the body correspond closely to the external injuries.

Moreover, it is highly probable that the pilot was in control of the plane until it crashed. It has been concluded that the pilot made an unauthorized low pass not reacting quickly enough to clear the sloping hills on the far side of the target and that he died from the multiple injuries caused on impact.



Fig.1 Overview of the impact site



(a)



(b)

Fig. 2 Close-up of the crash site



Fig.3 The pilot's seat



Fig.4 The nose cone with pitot tube



Fig.5 The upper part of the left tail cone



Fig.6 The upper part of the tail fin



Fig.7 The lower part of the tail fin



Figure 8



Figure 9



Fig.10 The flying suit tear on the right thigh





Fig.11 The flying suit slit down the left thigh



Fig.12 The flying suit tears in the region of the neck



Fig.13 The exposure suit tear along the seam



Fig.14 The right boot

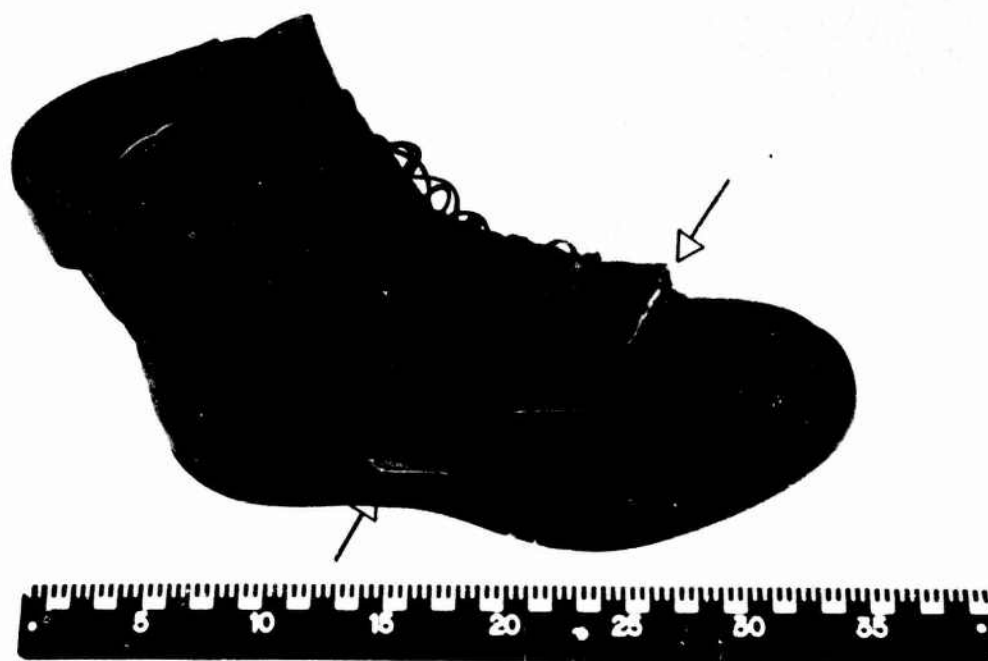


Fig.15 The right boot



Fig.16 The anti-G suit

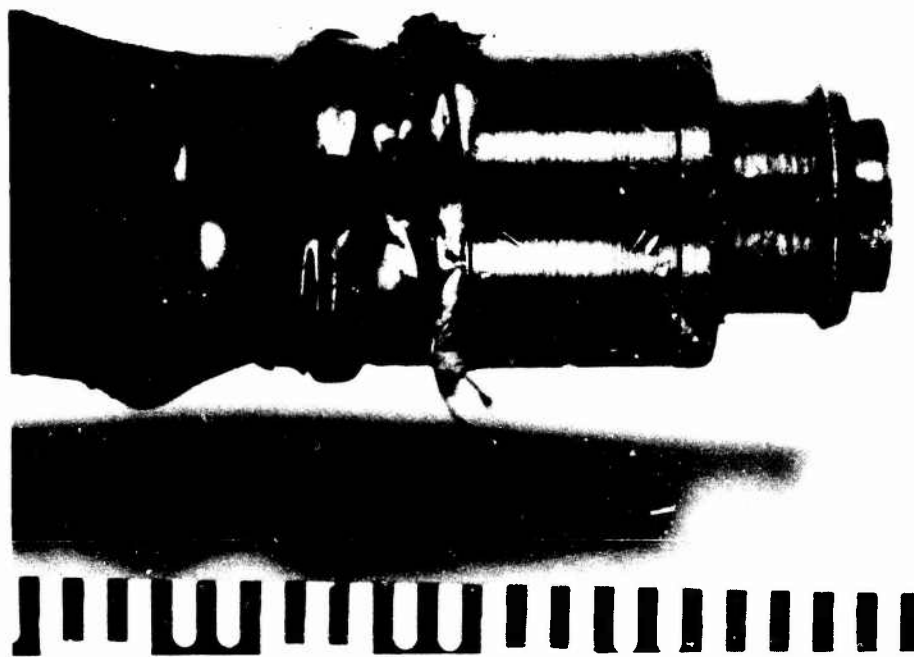


Fig.17 Valve and pressure hoses were virtually undamaged

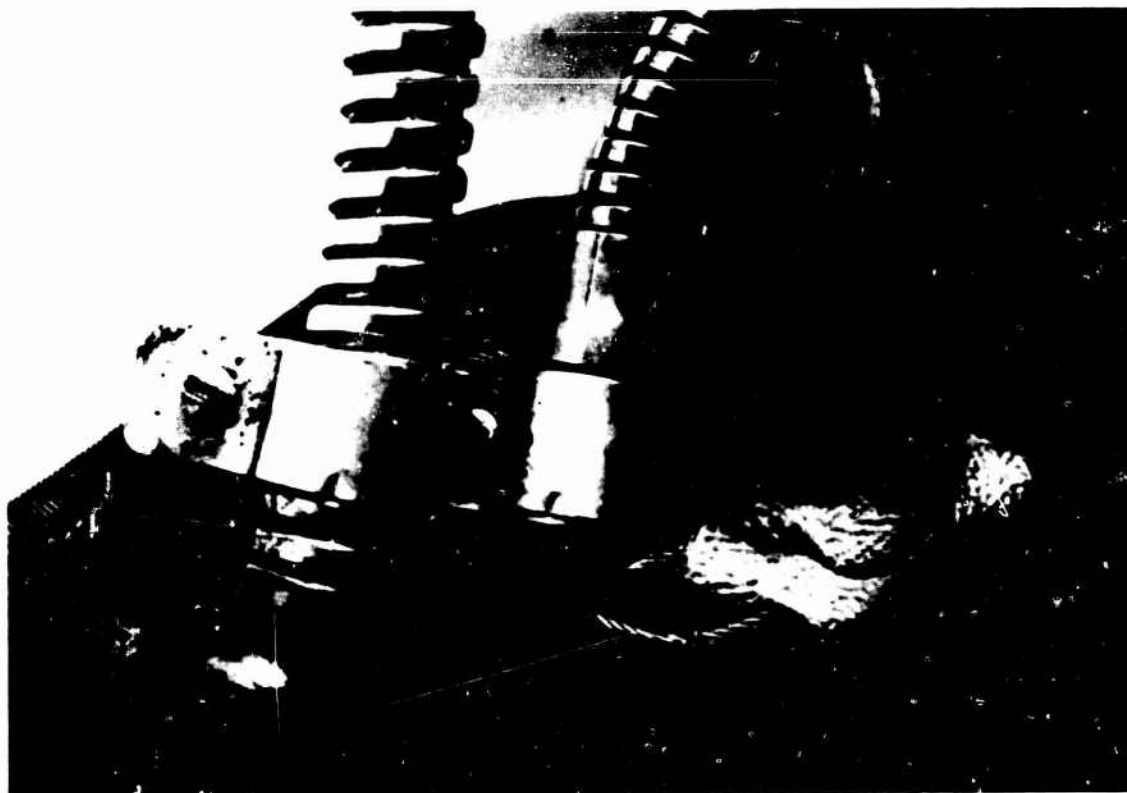


Fig.18 Valve and pressure hoses were virtually undamaged



Figure 19

## PREFACE TO ROUND TABLE DISCUSSION

EDITOR'S NOTE: Dr. D. J. Thomas of the U.S. Naval Biodynamics Laboratory presented a film showing instrumented ejection seat tests at the US Naval Air Development Center. His discussion of the film is noteworthy and is presented here prior to the round table discussions.

DR. THOMAS (USA)

The dummies used in these ejection seat tests were instrumented in conformance with the same standards we use in the laboratory, a three-dimensional coordinate system was established on the seat and on the chest. We specifically did not bother with head-neck instrumentation for the simple reason that we knew the dummies did not have adequate fidelity to make it worthwhile; therefore, we are currently limited with systematically comparing the inertial response of the dummy between seats and between aircraft as Mr. Frisch disclosed in his paper this week. Our Navy tests make it possible for us to rank seats, but we cannot establish absolute levels of safety based on these measurements because of the limited fidelity of the dummy, and the limitation of well validated mechanisms of injury and their thresholds in man. Nonetheless, we have at least proceeded to augment the range testing with laboratory procedures and we have given them a seat ranking procedure, and that is our status of physiological assessment in the Navy. Despite the widely disparate circumstances of these tests and the seats, we are able to get good repeatable response by the careful use of currently available dummies and test standards. In the head-neck area, based on man and animal experiments, we believe that you must know the initial conditions and the entire response of the head-neck system in terms of both its linear and angular acceleration to in any way be able to successfully compare data or to successfully attribute physiological or anatomical structural changes based on the data.

DR. VON GIERKE (USA) COMMENT ON DR. THOMAS' FILM

We should all note the potential for projectile injury with the various fragments you saw floating around in the film. In these ejections, what you saw is why we are looking with some doubt about through-the-canopy ejections because we have no traumatic injury model for this kind of explosion.

DR. THOMAS (USA)

We became involved in round-robin discussions as to whether you would rather break your neck or cut your nose off. It is a very serious problem.

DR. VON GIERKE (USA) COMMENT

In any event, I think that we need a proper model for getting a good probability assessment of this injury mode.

## ROUND TABLE DISCUSSION \*

Chairman: Dr. H.E. von Gierke, US Air Force Aeromedical Research Laboratory, Dayton, OH 45433

Members: Professor Dr. Bier, Forensic Institute, University of Munich, Munich 2, FRG

Dr. D. J. Thomas, Naval Biodynamics Laboratory, New Orleans, LA 70189

Mr. E. Franchini, FIAT Automobiles, Turin, Italy

Mr. B. Carnell, Sikorsky Aircraft Corporation, Stratford, Connecticut 06602

## DR. VON GIERKE (USA) INTRODUCTION:

For this round table discussion, I've taken the liberty to summarize what I consider the major accomplishments of this meeting. Taking as a baseline, the Oporto meeting held 11 years ago, the first obvious point is that progress in automotive crash protection has improved tremendously as evidenced by government programs, regulations, and industry efforts to promote this area and to establish a real international program. We had more papers which were either sponsored or specifically aimed at automotive crash research and fewer papers on general aviation and military impact injuries. As usual, this change in events has its good and bad points. The second point obvious to me, is that we had fewer summary and review papers; we covered the area with specific study results and data presentations which again, has its good points and bad points. Test facilities and blast injuries were covered in CP 88-71, but were left out at this conference with the exception of the armor papers. I don't think this was due to the research not being done, but I think most of us were invited or encouraged to do a paper on the five session topics. Note that this morning, we had some very interesting presentations on body armor and protection against projectiles and we had no papers on projectile injuries or wound ballistics.

As seen in Table R-1 under Injury Mechanisms, there was progress on head-neck injury definition and definition of concussions as noted in several papers. On the other hand, it is clear that we did not get any presentations on a practical head-neck impact injury prediction method, or even numerical quantitative assessment methods of the injury potential of particular impacts. We saw excellent detailed work on concussion and brain injuries in baboons which clarified the various injury mechanisms in general; however, it appears that we still have a long way to go, a lot of research to be done, to establish baboon-to-human scaling laws. I don't know how much is already in preparation, I only know that we worked for quite a while on the scaling of the spine between baboon and man (as heard in paper number 1) and the spine is still simpler than the skull and the neck.

On spinal injury prediction, I think we made considerable progress, and I am very optimistic about what we can do with the verified head-spine model which Dr. Privity presented (paper number 30), and we are pretty far along in scaling the animal data to man and validating the model with human data. However, at the Oporto meeting (CP88-71), we for the first time, presented the Dynamic Response Index (DRI) as a simplified method for predicting injury from emergency escape accelerations, and this has been standardized in various countries and has been accepted as a military specification for systems design in the United States and in other countries, but we realize its shortcomings. We have promised that we would improve the DRI assessment method. We hope that the improvement will grow out of the spinal injury model, but we haven't presented a Design Guide yet to make use of the very much refined and improved technology which has evolved over the last 10 years. In modeling technology, with respect to kinematic models, like the Netherlands (MADYMO) and the United States ATB models, these models are very nicely advanced and have definite areas of applicability. In the future, we need to standardize one particular version or, at least clarify the joint resistance, the joint dynamic qualities, etc. in the model so that when it is used, it is the same model in different services and in different countries. This is a very fruitful area for future standardization. In accident injury investigation, I think we all agree that standard methods are desirable and some international pathology committees have actually made recommendations, but we are still far from general acceptance of one method. Another point which I think was made at the Oporto meeting (CP88-71) is that we use multidisciplinary accident investigation teams, but little progress has been made. In many cases, we do have specialized aviation pathologists conducting autopsies, but we don't have biodynamic experts involved in the evaluation of all accidents.

We heard the paper on the long-term sequelae in the baboon's spinal injuries and the consequences of what we consider sub-injury, sub-tolerance, sub-critical tolerance exposure of baboons, and that after a year, or five years, they can develop into real traumatic diseases. The question was posed at the meeting, and I guess this deserves further study, how much could be benefited from longitudinal studies in this area, and what is the risk/benefit in doing such studies?

I was personally very impressed by the microtrauma techniques which are apparently being used now in cerebral concussion injury research and I think this is an area which is new and which appears very fruitful and should be emphasized in future research.

Table R-1  
Impact Injury Mechanisms

Significant Accomplishments	Future Needs
• Head/Neck injury definition	• Head/Neck impact evaluation criteria
• Spinal injury prediction	• Improved DRI for design
• Modeling technology	• Standardize biodynamic data models
• Accident/injury investigation	• Standardize methods multidisciplinary evaluations
• Long term sequelae	• Longitudinal follow-ups?
• Microtrauma techniques	• Study

Table R-2  
Impact Protection

Significant Accomplishments	Future Needs
• Crashworthy helicopter	• Broader applications of crashworthiness
• Application of EA technology	• Broader applications
• Inflatable restraint harnesses/bags	• Broader applications
• Dynamic/Inertial pre-load	• Study applications

Table R-3  
Msturing of Interdisciplinary Fields

Significant Accomplishments	Future Needs
• Improved automotive dummy*	• Need for aircraft <ul style="list-style-type: none"> <li>a. Inertial response dummy</li> <li>b. Injury assessment dummy</li> <li>c. Instrumentation standard</li> </ul>
• AGARDOGRAPH published on test facilities. no discussion of facilities at this meeting	• Not more facilities, but intenaive use
• Accident and experimental data is better defined	• Standardized accessible Biodynamic Data Banks
• Body armor design and cost effectiveness	• Traumaworthiness? Overall systems approach
• Application of models to windblast effects	• Injury criteria and protection at 1600 Q windblast

\*Not discussed at this symposium, but a significant accomplishment nonetheless.



In the protection area as shown in Table R-2, I think the biggest progress since Oporto (CP88-71) is really the crashworthiness design of helicopters, and I guess these principles deserve partial application in other types of aircraft and should probably extend to crashworthiness of the overall system, including man and his protection. The application of the energy absorption EA principle in crashworthy design was very nicely demonstrated by several papers and I think this is technologically one of the biggest projects in the area. Similarly, inflatable body and head restraint systems (IBAHRs), as restraint systems presented in paper number 21 and the Mercedes-Benz inflatable bag (paper number 26) both appear to offer improved restraint, but there is still hesitation in many quarters to accept air bag and inflatable restraint technology as a practical and economical means of restraint. I can only repeat that when we did the live human studies with air bags with the Department of Transportation, their effectiveness was absolutely fantastic and impressive. If there wasn't the constant doubt about reliability and cost, I think the bags would be very effective crash protection for many applications. By the way, in the joint USAF-DOT sled studies human subjects "impacting" a soft air bag sustained HIC values well over 1000 and perceived it as very mild rebound! So it clearly demonstrates to us, that the Head Injury Criteria (HIC) for this kind of impact into a soft, slow-responding cushion is absolutely wrong.

We heard yesterday (paper number 31) on dynamic or inertial pre-load as a protective mechanism in crash and impact protection. This is a very exciting possibility which certainly deserves further study for applications in horizontal crashes as well as for the ejection exposure.

In general, there was much less discussion controversy and hostility between modelers, theoretical people, experimental people and clinicians. In this meeting, I had the feeling that we were all more or less united, and we all knew what we were talking about, so as a general interdisciplinary field, the area has certainly matured more over the last decade. As seen in Table R-3, a better automotive dummy for automotive crash research was developed. Nonetheless, since our main emphasis and specialty is on aviation, I must say that the automotive crash dummy doesn't solve our problems in aviation impact research. We need, at this point, primarily an inertial response dummy which doesn't have to look like an anthropomorphic dummy but it has to simulate the dynamic load of the human occupant on ejection seats and similar devices. In the long run, of course, we need an automotive and an aviation injury assessment dummy, but one has to keep these different types of dummies separate. (This is my personal opinion; We will not solve this dummy question with one dummy because it will be so expensive that we cannot afford it.) We need to aim at several subcategories of dummies, perhaps an anthropometric dummy as we have used in the past, an inertial response dummy, and an injury assessment dummy. The injury assessment dummy might be subdivided into several injury assessment dummies, because for some situations we are exposing the spinal column to above critical loads and probably wouldn't need detailed head injury assessment. It just wouldn't be cost effective to produce all the desired features in one dummy. We have to make up our mind what particular dummies we need, and then try to accomplish this goal. In some respects, it was almost beneficial that we had no discussions this time about facilities. Many of us now have excellent facilities for crash research in vertical and horizontal devices. Most countries now have test facilities and there are no big arguments about instrumentation. I think maturity technology can be applied to some facilities if the funding is available, but personally, I think with intensive use of existing facilities, we have enough capability for all countries represented. May I note that at the end of the year, we have another AGARDO graph being published to update test facility capability.

Referring to the Tables, note that little discussion occurred on how biological results were measured. I think we have a much more refined method and technology and better standardized instrumentation requirements, although some of these standards are based on automotive standards, and may not be the best for aviation applications. In connection with improved accident and experimental data, I think there is a need of making all of this data available to all potential users by depositary in biodynamic data banks. Several data banks in the various countries would be accessible to all of us and would have at least to some extent standardized formats so that data could be computer-retrieved and analyzed. There is a report available by the US Academy of Sciences on the feasibility of a national biodynamic data bank which discusses some of the problems in executing this.

Progress in body armor design and the cost effectiveness of body armor was discussed as shown in fig. R-3. Not enough material was presented on protective armor trauma (trauma caused by the protective device). Although paper number 36 did discuss this item in general terms. How to get the man out of the armor in post-crash emergencies and how to restrain the armor during crashes and in routine operations are topics worthy of more study. In other words we should make an effort to design the systems more "trauma worthy" in an overall context.

One area not covered at all, but in which we have made some progress is wind blast impact effects caused by ejection systems in high speed aircraft. Some progress has been made, but we are still far from the goal of an ejection system which will provide wind blast protection up to 1600 Q dynamic pressure. This concludes my summary.

DR. BIER (GE)

My background is in automotive accident research. We've done some studies on injuries of belted occupants and injuries of motorcyclists. This prompts me to state another point of view. Currently in the Munich area, we conduct about 2000 autopsies per year at the forensic institute. About 60% of these are road accident victims. In German road accidents, we have about 6,500 killed and 73,000 hospitalized annually. I think this number could be reduced. In the area of West Germany, we did a study yet unpublished and found that in car occupants the safety belt usage rates are between 44% and 70 - 80% and about 4000 occupants are saved annually due to use of the three-point restraint system and about 60,000 prevented from being hospitalized; this is a measure of the effectiveness of current crashworthiness features. The potential is about 3,000 which could be saved if everyone used the available restraint systems, and about 48,000 would not be hospitalized. The unpublished study showed that the reduction of injuries is mainly due to the restraint system, but the reduction in fatalities is also due to other safety measures.

For future design, we are aiming at an optimized vehicle deceleration, we must strengthen the vehicle's weak point in order to increase the G value for safe deceleration. For example, in frontal car crashes there are practically no life threatening injuries to the thorax as long as the protective structure remains preserved. Our aim must be to preserve the passenger car compartment at even higher impact velocities, but there are certain restrictions involved. We must not raise the g value beyond the known human tolerance; however, the exact value of human tolerance, considering head/neck inertial loads is not known. So, what protection measure would best improve human tolerance to forward g loads?

**Usability of Existing Impact Data:** Human tolerance limits are too closely related and in most cases restricted to the various specific mechanisms studied in the laboratory. For future research in the short-term, the most frequent injury mechanisms should be found and very specific tolerance levels for those mechanisms established. This will enable counter measures to be put forward quickly and assist in the validation of models which are in progress. In the long-term the development of more sophisticated models should be continued; basic physical (human tolerance) data acquired including the tolerance of body elements. As to data needed in future research, input data for models must cover the whole variety of injury mechanisms. In addition, laboratory data must be extrapolated from the tolerable up to and beyond the tolerance limits.

In closing, a question, "What can road accident research contribute to the field?" This research can establish data on the most important injuries, with respect to number as well as to severity. However, a considerable amount has been done in this field already, and I think efforts might be reduced; however, road research to evaluate impact safety measures should be continued. Special care must be taken with respect to the integrity of the methods applied and standard methods are necessary. And last, but not least, in-depth case studies should be continued to validate laboratory data; this requires collaboration of pathologists at the scene, scientists in the human/animal test laboratories and mathematicians at the computer to develop the models.

DR. THOMAS (USA)

Let us look at the problem of impact-caused death and mortality from the point of view of public health. The history of public health, the enormous triumphs and the reduction of death and communicable disease were accomplished around the turn of the century. We are still controlling infectious diseases at enormous research costs; however, the one major epidemic left in the young adult population is traumatic death. A recent article by Hartunian, et al, in the American Journal of Public Health, entitled "The Incidence and Economic Costs of Cancer, Motor Vehicle Injuries, Coronary Heart Disease and Stroke: A Comparative Analysis," shows that, in the United States, cancer is the most expensive disease in terms of disability and treatment costs, but the cost of motor vehicle injuries exceeds either coronary heart disease or stroke! There are about 50 people in this room. If we were having an international symposium dealing with the mechanisms, costs and research of either cancer or coronary disease, I am quite sure this room would not provide enough seats!

The number of facilities, internationally, currently involved in the experimental approach to understanding the mechanisms of impact injury may very well never get to the answer, because there are far too few of them and far too few investigators. Each of the investigators are involved in areas where they have specific skills and specific knowledge. In terms of the size and the scope of the problem, I am not sure we will ever get there. If we as an organization don't succeed in getting this point of view across, the resources to continue this sort of research may simply disappear. In the United States Navy, we have tried to take a highly specific and directed approach: to eventually develop an inertial response dummy. All of our efforts and all of our resources have been directed to that goal. Our program was conceived in 1970, based on very preliminary work done in conjunction with the United States Army and Wayne State University. In 1975, the initial sled runs with volunteers began at the United States Navy facility at New Orleans, Louisiana.

#### EDITOR'S NOTE:

Dr. Thomas monitored a series of films showing the relative movement of the head and neck at 15g<sub>x</sub> (forward) impact and 7g (sideward) impacts. The purpose of the films was to illustrate the inertial response of the head relative to the first thoracic vertebral body under circumstances where there is no restraint acting on either the head or neck. Dr. Thomas emphasized in the monitoring of the films that high onset-long duration, low onset-long duration, and high onset-short duration pulses were applied to the restrained volunteers. He emphasized that the head and neck mechanical response were different dependent on the use of forward (g<sub>x</sub>) or sideward (g<sub>y</sub>) pulses.

DR. THOMAS (USA) CONTINUES

The mechanical response of the human volunteers is enormously important from the point of view of modeling and construction of a dummy. The volunteers show fundamental mechanical simplicities within the human structure, an intrinsic dynamic property.

We plan to continue the volunteer response work for different vectors at different levels, and to continue it to find the head response to the first thoracic vertebral body, then the first thoracic vertebral body relative to the pelvis. The response data will be used as the mechanical criteria for the inertial fidelity needed in the construction of models which in turn will be used for engineering specifications for the construction of anthropomorphic dummies.

The next problem is the threshold response. Paper number 14 discusses the rhesus monkey and his response to -x impact acceleration: there is a suspicion from this data that there is a threshold for the interruption of the transmission of neurophysiological signals through the central nervous system of the animal. This is important, because with further analysis, if we find promontory evidence of disruption at very low levels, in the area of physiological change, this may be used as a direct comparison between animal response and human subject experimentation.

If you continue to expose the rhesus monkey to -x acceleration to higher and higher levels of -g<sub>x</sub> (forward) acceleration, you will invariably get head-neck junctional injuries. Three different types of injuries occur: atlanto-occipital separation, C1 and C2 separation and a basilar skull fracture. Our best presumption as to the mechanism of the basilar fracture, is that the basilar-sphenoid junction is not closed in the rhesus so that an instability exists right in front of the foramen-magnum and this can lead to a pull-out fracture

FRANCHINI (IT)

This is a panoramic view of significant problems in automotive safety as related to crashworthiness. Crash safety can be divided into three main areas: Biomechanics, Dummies and Evaluation tests as shown in Fig. R4. Each area is discussed.

I. Biomechanics: We have similar injury definition problems in automotive and aviation crashes.

II. Dummies: An omni-directional, reliable dummy is needed. Today's dummies are designed for longitudinal impact and are absolutely bad for side impact. It's clear that a dummy for the longitudinal impact and another dummy for the side impact is a nonsense, because the man is always the same. Suppose you have an oblique collision test; which type of dummy should you use? The longitudinal type or the side type? Perhaps you must ask the driver to have a front collision but not a side collision! What parameters are to be measured on the dummy? What do your dummy measurements mean in regard to human tolerance? The situation today is that an individual dummy made from a manufacturer and another made from another manufacturer do not agree on the level of impact required to cause an "injury." This is another nonsense.

#### Automotive Crashworthiness

Biomechanics: a. Critical collision types from accident analysis

b. Causes of injury in humans (How do we measure injury severity?)  
Determination of injury causes is a universal problem.

c. Human tolerance criteria not defined completely

Dummies: a. Correlation of tolerance threshold criteria to instrumentation criteria

b. Standard Instrumentation (Measurements)

c. Omni-directional impact, reliability

Evaluation Tests:

a. Standardization of types of car collisions

b. Admissible "injury" levels for dummies in evaluation tests

Figure R-4. Automotive Crashworthiness Factors

III. Evaluation Tests: a. Car Collision Test Types with Dummies: You select the most important type of collision based on the frequency of the collision and the level of severity. You must define a test that can simulate this type of collision. You must put a dummy on board and you must know what you must measure in this dummy to correlate with actual human tolerance; b. Admissible "Injury" Levels for Dummies: First you know from biomechanics the tolerance levels in humans and you have made the correlation between humans and dummies. Now you know what level you can admit as maximum in the test with a dummy.

In closing, I wish to comment on a statement made by Wing Cdr. Glaister in his technical evaluation of the Oporto Linear Acceleration (AGARD CP88-71) meeting to the effect that crashworthiness weight penalties were less important in automobile design. This statement was correct 10 years ago, but not today; the car manufacturer today considers the reduction of weight as a major problem. Reduction of weight means two things; first, reduction of cost and second, reduction of fuel consumption; thus, we limit the energy waste. One other comment, 10 years ago, when you had a safety problem, you concentrated, you suggested modifications, you evaluated the modification, and after that you started production. Today, when you have a safety problem, you concentrate and ask yourself, how much cost? and how much weight? Today, we must combine the safety requirements of cost and fuel consumption. So, in this, the past 10 years has completely changed automotive safety design and evaluation.

MR. CARNELL (USA)

Permit me a general observation on the summaries presented thus far. All of our work is directed towards increasing the safety of occupants in automobile and aircraft accidents, but how can we measure the improvement or increase in safety? To measure the improvement, we must know where we are at the present time; we must know the injury and vehicle damage statistics in a rather well defined way. Most of the injury data I've seen from accidents has not been correlated, as yet, with damage severity. For example, you find a whole "lump" of data related to vertical impact speeds of helicopters, but no definition of when and where the injuries occurred. I suspect that the automobile field has the same problem. So, we really must have injury versus impact severity data to be able to measure where we are to provide the reference point.

As far as design features to improve crash safety, it seems that we are well along the way to incorporating these into automobiles and helicopters. I have not yet seen any real effort done to put such improvements into light aircraft and we would certainly hope to see more crashworthiness in general aviation and much larger transport aircraft. In the United States, regulations are not yet formulated to require significant crashworthy features in fixed wing commercial aircraft. Past history and my experience indicate that aircraft specifications must include crashworthy criteria, otherwise crashworthy features do not get incorporated into the design and don't get the emphasis they should.

If we are going to measure safety improvements, we do need statistical surveys to measure it. We need systems that can tell us the impact severity of each crash. In the United States, the Airborne Information Retrieval System, currently under development will hopefully provide data on how severe a crash is and indeed whether it exceeds to any degree the "crash" capability of the aircraft. The crashworthiness capability of most new "crashworthy" aircraft has not yet been evaluated by actual crash. Some work has been done. Much more needs to be done.

The change over in materials from metallic to composite structures is going to cause a significant change in the type of structural damage and breakup in crashes. We are going to have to be very careful as to how we qualify such change over in aircraft structures.

Data is going to be needed to measure cost effectiveness because we are going to have to measure how many fatalities and how many injuries we have saved. The only real way to get crashworthiness accepted as a discipline is to show that it does pay its own way. It's very difficult to put a price on a human life, but unfortunately, it becomes necessary to do that to convince program managers and others who control the funding for new aircraft designs. I have no doubt that even with just a normal low estimate of the value of human life that crashworthiness is going to prove to be extremely beneficial.

As far as recommendations to improve safety, I think studies to define safe operating limits of aircraft and automobiles are needed; we have some idea of what they are without safety features. I think we need to do some studies to find out what safe operating speeds might be for fully-equipped safety cars. Although we have built-in a much greater degree of crashworthiness in new helicopters, the operational capabilities have increased to the point where we are going to be making full use of that crashworthiness; we must continually review the need for increased crashworthiness limits.

I think we shall see escape systems applied to helicopters. Wirecutters are going to have to be installed because of the wire strike potential of low flight at night, which is becoming a routine operational procedure. Many helicopters are flying over water and floatation systems and emergency underwater escape systems are all going to become of very great value. I have been impressed by the presentations here this week. I think we have come a long way in looking at impact problems, but I think we have a long way to go. I appreciate the opportunity of participating in this meeting.

DR. VON GIERKE REQUESTED QUESTIONS FROM THE AUDIENCE.

DR. WARD (USA)

You said that you did not notice any disagreement between people doing experiments and those doing modeling. I'd like to point out to you that the modelers are almost extinct! When I started modeling, there were probably 10 other people doing head injury models. Today, I am probably the only head injury modeler anywhere and the same may be true in the body as well. To my knowledge there are only 2 thorax modelers. I think this is deplorable and will certainly affect progress in the coming years. It isn't because the modelers that still exist are great. I think it is because of financial considerations. We have grand testing facilities now. They represent a lot of money and they represent a lot of money to keep them going. The modelers have suffered as a result and I think it's sad that it's going to impede the development of a new dummy because everything will have to be done on a trial and error basis.

DR. VON GIERKE (USA)

I agree with you partially. Dr. Thomas has stated that, in general, this field doesn't get enough support and does not have enough people working in it. This is not restricted to just the modelers.

FRISCH (USA)

I think it is pretty safe to say that mathematical modeling has by far outstripped the availability of an adequate data base against which these models can be ranked, tested and evaluated. Modeling has in fact been effectively used certainly within the Navy, to evaluate existing systems. I think we have been very effective in looking at some minor problems in the F-18 and AV8B; that coupled with a lot of other work involved has led to redesigns which otherwise would not have been possible. The problem still is data! Whether experimental or test data, it is either insufficient or inappropriate; this was the basic thrust of my presentation. No matter which model is involved a well defined input is needed; unfortunately, you cannot use dummy response, which is in fact an output, as an input to a model. It just doesn't work that way! Unless an adequate data base is generated in the relatively near future, we will be limited to doing sensitivity analysis and their application to actual application of systems or processes is going to be limited.

My other comment relates to dummy development. Again, the various dummies are going to be very specific to the application. Ejection systems will require not only the development of a better dummy but also the development of accurate instrumentation packages. You can't throw a dummy into near-sonic winds and have it hard wired back to the ground. Transmission of the data back to the receiving station implies calibration headaches. It also implies the problem of where to locate the package: the more sophisticated the model, more joints and articulations, the smaller the volume available to locate the instrumentation. The problem is not in the sensors, but in the telemetry packages. I see absolutely no work being done in this area and if someone gave the best dummy in the world tomorrow, I couldn't use it or certainly I could only use it in very limited applications.

DR. VON GIERKE (USA)

Just one response to your first question about data. I think the ratio of appropriate to inappropriate data has increased showing some progress. I think this progress has occurred primarily from the fact that modelers are working closer with experimental people; some modelers even get their hands dirty from time to time! I think only in this way have we been able to get more appropriate data with which to establish and validate better models.

(UNKNOWN QUESTIONER TO MR. CARNELL)

I feel that not enough people who could look for the accident input data are involved in the on-the-scene accident investigation. The study of the input data for an accident must start immediately after the event happens. So if you wait several hours or maybe several days, you cannot see all that you have to see to find out what happened in this accident. You have to look at the accident place, the accident car, and this should be done as quickly as possible and coordinated with the medical doctor. So we must determine how to get enough people looking for the accident input data and to analyze the accident very properly.

DR. VON GIERKE (USA) RESPONSE TO UNKNOWN QUESTIONER

This is a very good point, similar to the point I tried to make with respect to aircraft accidents when I said we made recommendations sometime ago to field multidisciplinary accident investigation teams to look at accidents. Currently, a lot of effort is expended later, much later, in analyzing inadequate accident data. Speculations don't help really to establish what has happened in an accident.

NEWMAN (CA) QUESTION

My question is based upon remarks made by Dr. Franchini and Dr. Thomas concerning what parameters does one use to establish tolerance limits. Dr. Franchini used examples of acceleration, deformation, force, pressure, etc. Please consider the following hypothetical situation that perhaps is not too far from the truth. If a rhesus monkey were to undergo a change of acceleration of 500 g and sustain a concussion, and yet a human being were to undergo 200 g and sustain a concussion, would that mean the monkey is more tolerant to impact? To elaborate a little further then, since this may sound like a dumb question: If one has criteria which are predicated only on acceleration, one would in fact conclude that a rhesus monkey is indeed more tolerant to impact. Now, how can this be, if in fact, the basic biological materials which comprise the monkey and the human are not really all that different. Please comment on this because I would like to return to it depending upon the reply.

DR. VON GIERKE (USA) RESPONSE

There are many injury models and to each model you have a different tolerance level. One animal can be tolerant to one injury or susceptible to injury and another animal is not.

THOMAS (USA) RESPONSE

I think that in an experimental sense and an application sense, we need to consider the head/neck juncture to be considered the upper limit of tolerance in the primate under minus X acceleration with head-neck unrestrained and no direct impact to the head or to the neck. We feel that this probably applies across all of the primates. So if you run every primate, you'll see that mainly because it has been seen experimentally in the baboon and the rhesus. The levels at which it has been seen are somewhat different, 105 versus 125 g, but this may not be a between-species difference. Differences in the restraint or the way in which the animal was positioned could have caused the difference. Initial conditions are critical, not only for the mechanical head response, but also we suspect with the injury response as we saw in the rhesus. What if we had run a human? At what level would we see the same injuries? There are two particular approaches we take to that problem within the context of the given injury. One is the mechanical comparison between the two, and the other we are attempting to develop is the physiological comparison between the two. There are physiological measurements which constitutes a continuum of response. Dr. Weiss showed some of those measurements in paper number 14. If that same continuum of response is the same across species, there is physiological evidence that, in fact, they are the same. And thresholds for that particular type of injury, may in fact, be the same across species. Certainly the mass of the man is larger, but also his structure is more massive. So those things that are due to the between-geometry difference, between-mass difference, between-strength difference, require further indirect means of comparison between species. We do it structurally, we do it mechanically, we do it physiologically, and we impact test at least two of the non-human primate species in each of the injury modes if we possibly can. But it will always be an indirect problem, and I think that's as close as we can come experimentally to the answer. The impact tests must be done injury mechanism by injury mechanism.



## DR. VON GIERKE (USA) COMMENT

You have considerable differences in injury susceptibility and response in human subjects. You have some difference between male and female, and certainly as we heard at this meeting children have quite different responses, not only mechanical, but also from the physiological standpoint. We know also that impact tolerance limits deteriorate with respect to age.

## NEWMAN (CA) COMMENT

I am in complete sympathy and agreement with Dr. Thomas in the position that he outlines and in fact, all of you really read a little more into my question than I had intended. I did try to be reasonably specific and said that a monkey with a concussion and a human being with a concussion, and I think that most people would agree that it takes a much higher acceleration to cause a concussion in a small monkey than it would in a large man without getting too concerned about the details. The point I was really trying to make was that acceleration is really only part of the story. For example, the mass of the individual will dictate the nature of the inertial loading that takes place within the structure. I am particularly concerned since it's fair to assume that the mass associated with an impact situation plays a dominant role in the eventual injuries; thus, to simply examine acceleration by itself cannot be sufficient to completely quantify an injury criterion. That was the basic premise of my remarks.

## DR. VON GIERKE (USA) COMMENT

I think we all agree that acceleration by itself, doesn't help at all. It's always a complete time course of events and a force application which has to be considered. If we concentrate our efforts on a specific frequency, and duration range or specific type of input, we can restrict ourselves to one parameter like acceleration and use it as a specification perhaps in certain situations. But we must clearly specify the limits of applicability and validity.

## MR. FRISCH (USA)

It's a minor point, but I think it is intuitively obvious to people who conduct experiments that answers are provided for two very basic questions. One is a threshold of something; and the other is the response mechanism. Because when you understand the response, you most likely understand the problem.

## DR. VON GIERKE (USA) CLOSING REMARKS

Thank you for your attendance and participation, and have a safe and good trip home. Hope to see you again when we have the next meeting.

## DR. BANDE (BE) CLOSING REMARKS

Now, just a last point, I think that I can tell the experts here in this room that we expect them in 10 years from now to provide new results. Everything is not sold as we've heard. If all were sold, we could retire. So we expect you back in 10 years from now with more results and more practical results. I wish you a safe journey home or a good stay in Germany.

LIST OF PARTICIPANTS

<u>NAME</u>	<u>TITLE</u>	<u>ADDRESS</u>	<u>ROLE</u>
F.L.V. ALVARES	Brigadier-General	Hospital da Força Aérea Paço do Lumiar 1600 Lisboa (PO)	O
H.T. ANDERSEN	Doctor	Institute of Aviation Medicine P.O. Box 281 Blindern - Oslo 3 (NO)	PM/A
D.J. ANTON	Squadron Leader	RAF Institute of Aviation Medicine Farnborough Hants GU14 6SZ (UK)	O
G. APEL	Doctor	Flugmedizinisches Institut der Luftwaffe Abteilung 5 8080 Fürstfeldbruck (FRG)	O
R. AUFFRET	Médecin en Chef	Centre d'Essais en Vol B.P. N° 2 91220 Brétigny sur Orge (FR)	PM/SO
J. BANDE	Colonel Médecin	Quartier Reine Elisabeth Rue d'Evère 1140 Brussels (BE)	PC
BEIER	Doctor	Munich University (FRG)	O
A.J. BENSON	Doctor	RAF Institute of Aviation Medicine Farnborough Hants GU14 6SZ (UK)	PM
U. BEZ	Doctor Engineer	Porsche AG Entwicklungszentrum Dep EFF Postfach 1140 7251 Weissach (FRG)	O
S.V.A. BLIZZARD	Major	National Defence HQ Surgeon General Branch 100 Metcalfe Street Ottawa, Ontario K1A 0K2 (CA)	PM
E.C. BURCHARD	Generalarzt	Flugmedizinisches Institut der Luftwaffe Abteilung 1 8080 Fürstfeldbruck (FRG)	PM
B.L. CARNELL	Mr	400 Cold Spring Street Apt. D 425 Rocky Hill Connecticut 06061 (USA)	RTD
J. COLIN	Médecin Général	Centre de Recherches du Service de Santé des Armées (CRSSA) 1bis, rue du Lieutenant Raoul Batany 92141 Clamart (FR)	PM
H.F. CORTIER	Lieutenant Colonel	BMVG - JNSAN 1 4 Postfach 1328 53 Bonn 1 (FRG)	O

A - Author

O - Observer

PM - Panel Member

SO - Session Organizer

RTD - Round Table Discussant

PC - Panel Chairman

PDC - Panel Deputy Chairman

PrC - Programme Chairman

<u>NAME</u>	<u>TITLE</u>	<u>ADDRESS</u>	<u>ROLE</u>
F. COUSSEAU	Mr	Société Aératur EFA (Direction Technique) 58, Bd. Galliéni 92130 Issy le Moulineaux (FR)	A
F.-J. DAUMANN	Colonel	Flugmedizinisches Institut der Luftwaffe Abteilung 1 Postfach 172/KFL 8080 Fürstentfeldbruck (FRG)	PM
D.R. DAY	Mr	DCIEM P.O. Box 2000 1133 Sheppard Avenue West Downsview, Ontario M3M 3B9 (CA)	A
S.P. DESJARDINS	Mr	SIMULA Inc. 2223 South 48th Street Suite C Tempe, AZ 85282 (USA)	A
P.F. FALLON	Colonel	HQ USAF (SGES) Bolling AFB, DC 20332 (USA)	PM
A.P.P.L. FLION	Lieutenant Colonel	15 Wing TC 1910 Melsbroek (BE)	A
F. FRANCHINI	Mr	FIAT Safety Center C.so Agnelli 200 Turin (IT)	RTD
G.D. FRISCH	Mr	ACSTD 603/99 Naval Air Development Center Warminster, PA 18974 (USA)	A
T.A. GENNARELLI	Doctor	Hospital of the University of Pennsylvania 3400 Spruce Street Philadelphia, PA 19104 (USA)	A
H. GERDES	Oberstarzt	HQ 3rd (GE) Air Division Römerstrasse 122 4192 Kalkar 1 (FRG)	O
H.E. von GIERKE	Doctor	AFAMRL/BB Wright-Patterson AFB, OH 45433 (USA)	SO/RTD
D.H. GLAISTER	Wg. Cdr.	RAF Institute of Aviation Medicine Farnborough Hants GU14 6SZ (UK)	A/SO
J. GROENENBERG	Doctor	National Aerospace Medical Center (NLRC) P.O. Box 22 3769 Soesterberg (NL)	O
S.B. HAGUES	Mr	The Accident Research Unit Dept. of Transportation and Environmental Planning University of Birmingham P.O. Box 363 Birmingham B15 2TT (UK)	A
J.L. HALEY	Mr	P.O. Box 624 Fort Rucker Alabama 36362 (USA)	PrC
P. HAMPE	Doctor	DFVLR Institut für Flugmedizin Postfach 906058 5000 Köln 90 -F G)	O
B.F. HEALON	Major	AFAMRL/BBP Wright-Patterson AFB OH 45433 (USA)	A



<u>NAME</u>	<u>TITLE</u>	<u>ADDRESS</u>	<u>ROLE</u>
K.J. HILL	Mr	Middlesex Polytechnic Bounds Green Road Bounds Green London N11 (UK)	A
H.A. HOFFMANN	Lieutenant Colonel	Generalarzt der Luftwaffe Postfach 90 2500/522 5000 Köln 90 -FRG)	O
R.H. HOLMES	Doctor	155 Spalding Mill Atlanta, GA 30338 (USA)	A
P. HOWARD	Air Commodore	RAF Institute of Aviation Medicine Farnborough Hants GU14 6SZ (UK)	DPC
P.F. IAMPINETRO	Doctor	AF Office of Scientific Research/NL Bolling AFB, DC 20332 (USA)	PM
E.G. JANSSEN	Engineer	IW-TNO P.O. Box 237 2600 AE Delft (NL)	O
K. JESSEN	Colonel	Danish Defence Command P.O. Box 202 2950 Vedbaek (DA)	PM
J. JUST	Mr	Autoflug GmbH Industriestrasse 10 Postfach 1180 2084 Rellingen (FRG)	O
D.J. KARL	Professor	Wright State University P.O. Box 1604 Dayton, OH 45401 (USA)	A
L.E. KAZARIAN	Doctor	AFAMRI/BBD Wright-Patterson AFB OH 45433 (USA)	A
K.E. KLEIN	Doctor	DFVLR Institut für Flugmedizin Postfach 906058 Linderhöhe 5000 Köln 90 (FRG)	PM
G. KINDERVATER	Mr	DFVLR Pfaffenwaldring 38140 7000 Stuttgart 80 (FRG)	O
G.C. KNAPP	Colonel	US Army Aeromedical Research Laboratory (USAARL) P.O. Box 577 Fort Rucker, AL 36362 (USA)	PM
F.H. KOEHL	Doctor	Messerschmitt-Bölkow-Blohm GmbH Military Aircraft Division Postfach 101160 8000 München 80 (FRG)	O
G. FROM	Engineer	Flugmedizinisches Institut der Luftwaffe Abteilung IV - Ergonomie 8072 Manching (FRG)	O
H.-J. LAUDAN	Lieutenant Colonel	General Flugsicherheit BW Postfach 90 2500/501/07 5000 Köln 90 (FRG)	O
I.A. LEVIN	Lieutenant Colonel	HQ Defence Command Norway Joint Medical Service Oslo Mil/Huseby Oslo 1 (NO)	O
R.S. LEVINE	Professor	Bioengineering Center Wayne State University 418 Health Sciences Bldg. Detroit, MI 48202 (USA)	A

<u>NAME</u>	<u>TITLE</u>	<u>ADDRESS</u>	<u>ROLE</u>
G.K.M. MAAT	Commodore	P.O. Box 453 5700 AL Zeist (NL)	PM
J. MALTHA	Engineer	IW-TNO P.O. Box 237 2600 AE Delft (NL)	A
R. MATTERN	Doctor	Institut für Rechtsmedizin im Klinikum der Universität Heidelberg Voss strasse 2 6900 Heidelberg (FRG)	A
B. MILLER	Mr	Martin Baker Aircraft Higher Denham near Uxbridge Middlesex (UK)	O
J. MYCKLEBUST	Mr	Department of Neurosurgery 8700 W. Wisconsin Wis 53226 (USA)	A
J.A. NEWMAN	Doctor	Biokinetics & Associates Ltd 1481 Cyrville Road Ottawa Ontario K1B 3L7 (CA)	A
W. NISSEN	Oberstarzt	Akademie des Sanitäts- und Gesundheitswesens der Bundeswehr Abt. Studien und Wissenschaft Neuherbergstrasse 55 8000 München (FRG)	PM
R.K. OHSUND	Captain	Office of Naval Research Code 440 800 N. Quincy Street Arlington, VA 22217 (USA)	PM
J.W. ORD	Major General	Aerospace Medical Division (AFSC) Brooks AFB, TX 78235 (USA)	PM
T. PAGALIDIS	Major	Air Force General Hospital Katechaki Street Goudi-Athens (GR)	O
J.B. PEDDER	Ms	Accident Research Unit Dept. of Transportation and Environmental Planning University of Birmingham P.O. Box 363 Birmingham B15 2TT (UK)	A
M. PERKINS	Mr	S.E.M. Martin Baker 49, rue du Captain Guynemer 92270 Bois-Colombes (FR)	O
E. PRIVITZER	Engineer	AFAMRL/BBM Wright-Patterson AFB OH 45433 (USA)	A
P. QUANDIEU	Médecin en Chef	EASSAA et CERMA 26, Bd. Victor 75996 Paris Armées (FR)	A
W. RAABE	Doctor	DFVLR Postfach 906058 Linderhöhe 5000 Köln 90 (FRG)	O
W. REIDELBACH	Professor Doctor	Daimler-Benz AG/Abtlg. A1GS Postfach 226 7032 Sindelfingen (FRG)	A
H.-J. RETHMEIER	Major	FBW 36 Schorlemerstrasse 80/A 4440 Rheine 1 (FRG)	O

<u>NAME</u>	<u>TITLE</u>	<u>ADDRESS</u>	<u>ROLE</u>
R.F. ROLSTEN	Professor	Wright State University Main Post Office P.O. Box 1604 Dayton, OH 45401 (USA)	A
P. ROY	Mr	Middlesex Polytechnic Bounds Green Road Bounds Green London N11 (UK)	A
B. SALTZBERG	Professor	Texas Research Institute of Mental Sciences 1300 Moursund Avenue Houston, Texas 77030 (USA)	A
A. SANCES	Professor	Department of Neurosurgery 8700 West Winconsin Avenue Milwaukee, WI 53226 (USA)	A
M. SCHULMAN	Engineer	Naval Air Development Center Warrminster, PA 18974 (USA)	A
G. SEDLMAYR	Doctor	Autoflug GmbH Industriestrasse 10 2084 Rellingen 2 (FRG)	O
K. SELLIER	Professor Doctor	Institut für Rechtsmedizin Stiftsplatz 12 5300 Bonn 1 (FRG)	O
D.F. SHANAHAN	Major	US Army Aeromedical Research Laboratory (USAARL) P.O. Box 577 Fort Rucker, AL 36362 (USA)	A
D.C. van SICKLE	Professor	Dept. of Anatomy School of Vet. Med. Purdue University W Lafayette, IN 47907 (USA)	A
G. SCHMIDT	Professor	Institut für Rechtsmedizin Voss strasse 10 6900 Heidelberg (FRG)	O
F. SCHUELER	Mr	Institut für Rechtsmedizin Voss strasse 10 6900 Heidelberg (FRG)	O
K. STAACK	Brigadier General	Generalarzt der Luftwaffe Postfach 90 2500/522 5000 Köln 90 (FRG)	PM
A.P. STEELE-PERKINS	Surgeon Commander	RAF Institute of Aviation Medicine Farnborough Hants GU14 6SZ (UK)	A
H.J. STOLZE	Doctor	MMVG - Insau 53 BN 1 Ermekeil SW (FRG)	O
C. TARRIERE	Doctor	Laboratoire de Physiologie et de Biomécanique Peugeot SA/Renault 147, Av. Paul Doumer 92501 Reuil-Malmaison (FR)	A
L.E. THIBAUT	Doctor	University of Pennsylvania Dept. of Bioengineering 462 Moore Building 33rd and Walnut Streets Philadelphia, PA 19104 (USA)	A
D.J. THOMAS	Doctor	Naval Biodynamics Laboratory P.O. Box 29407 New Orleans, LA 70189 (USA)	A/SO/ RTD
F. UNTERHARNSCHEIDT	Professor Doctor	Naval Biodynamics Laboratory 3512 Camp New Orleans, LA 70115 (USA)	A

P-6

<u>NAME</u>	<u>TITLE</u>	<u>ADDRESS</u>	<u>ROLE</u>
B. VETTES	Médecin en Chef	Centre d'Essais en Vol Laboratoire de Médecine Aéronautique 91220 Brétigny Air	A
H.-L. VOGT	Doctor	DFVLR Institut für Flugmedizin Postfach 906058 5000 Köln 90 (FRG)	O
C. WARD	Doctor	Pacific Palisades - Box 722 California 90272 (USA)	A
M.S. WEISS	Engineer	Naval Biodynamics Laboratory P.O. Box 29407 New Orleans Louisiana 70189 (USA)	A
L.E. WILLIAMS	Captain	Naval Air Systems Command (Air S31B) Washington, DC 20361 (USA)	O
J.S.H.M. WISMANS	Doctor Engineer	IW-TNO P.O. Box 237 2600 AE Delft (NL)	A
H.J. WOLTRING	Doctor Engineer	Craeyenbergh 42 6611 AV Overasselt (NL)	O

REPORT DOCUMENTATION PAGE			
1. Recipient's Reference	2. Originator's Reference	3. Further Reference	4. Security Classification of Document
	AGARD-CP-322	ISBN 92-835-0317-0	UNCLASSIFIED
5. Originator Advisory Group for Aerospace Research and Development North Atlantic Treaty Organization 7 rue Ancelle, 92200 Neuilly sur Seine, France			
6. Title IMPACT INJURY CAUSED BY LINEAR ACCELERATION: MECHANISMS, PREVENTION AND COST			
7. Presented at the Aerospace Medical Panel Specialists' Meeting held in Cologne, West Germany, from 26-29 April 1982.			
8. Author(s)/Editor(s) J.L.Haley, Jr			9. Date October 1982
10. Author's/Editor's Address USAARL Fort Rucker, AL 36362, USA			11. Pages 530
12. Distribution Statement This document is distributed in accordance with AGARD policies and regulations, which are outlined on the Outside Back Covers of all AGARD publications.			
13. Keywords/Descriptors  <div style="display: flex; justify-content: space-between;"> <div> <p>Linear acceleration stress</p> <p>Impact acceleration</p> <p>Impact</p> <p>Injuries</p> </div> <div> <p>Biodynamics</p> <p>Protection</p> <p>Vertebrae</p> <p>Head (anatomy)</p> </div> </div>			
14. Abstract <p>Problems dealing with impact injury caused by linear acceleration are covered. Papers cover spinal column injuries caused by <math>g_z</math> (eyeballs down) impact, tensile (eyeballs up) loading of the spinal column, and lower leg injuries, as sustained by front seat occupants in automobile "glance off" impacts at high speed.</p> <p>Head and neck injury mechanisms are discussed both from a physiological and neurological standpoint. Both helmeted and unhelmeted head impacts are analyzed, and helmet test and evaluation methods are covered. Several papers described accident/injury investigation methods, including a helicopter crash test with instrumented dummies aboard. Injury-preventing hardware is covered; papers include restraint harness slack, "dynamic preloading" of the restrained body, testing and evaluation of new shock-absorbing (stroking) helicopter seats, automotive air bag testing, and the use of a "webbing tear" shock absorber on a helicopter crew chief's restraint harness.</p> <p>The validation of a spinal injury model and a more general kinematics (whole body) model are also discussed. Finally, the cost effectiveness of torso armor was discussed in two papers. The conclusions from this meeting will hopefully be applied for improved impact protection.</p>			

<p>AGARD Conference Proceedings No.322 Advisory Group for Aerospace Research and Development, NATO IMPACT INJURY CAUSED BY LINEAR ACCELERATION: MECHANISMS, PREVENTION AND COST Edited by J.L.Haley, Jr Published October 1982 530 pages</p> <p>Problems dealing with impact injury caused by linear acceleration are covered. Papers cover spinal column injuries caused by <math>g_z</math> (eyeballs down) impact, tensile (eyeballs up) loading of the spinal column, and lower leg injuries, as sustained by front seat occupants in automobile "glance off" impacts at high speed.</p> <p>P.T.O.</p>	<p>AGARD-CP-322</p> <p>Linear acceleration stress Impact acceleration Impact Injuries Biodynamics Protection Vertebrae Head (anatomy)</p>	<p>AGARD Conference Proceedings No.322 Advisory Group for Aerospace Research and Development, NATO IMPACT INJURY CAUSED BY LINEAR ACCELERATION: MECHANISMS, PREVENTION AND COST Edited by J.L.Haley, Jr Published October 1982 530 pages</p> <p>Problems dealing with impact injury caused by linear acceleration are covered. Papers cover spinal column injuries caused by <math>g_z</math> (eyeballs down) impact, tensile (eyeballs up) loading of the spinal column, and lower leg injuries, as sustained by front seat occupants in automobile "glance off" impacts at high speed.</p> <p>P.T.O.</p>	<p>AGARD-CP-322</p> <p>Linear acceleration stress Impact acceleration Impact Injuries Biodynamics Protection Vertebrae Head (anatomy)</p>
<p>AGARD Conference Proceedings No.322 Advisory Group for Aerospace Research and Development, NATO IMPACT INJURY CAUSED BY LINEAR ACCELERATION: MECHANISMS, PREVENTION AND COST Edited by J.L.Haley, Jr Published October 1982 530 pages</p> <p>Problems dealing with impact injury caused by linear acceleration are covered. Papers cover spinal column injuries caused by <math>g_z</math> (eyeballs down) impact, tensile (eyeballs up) loading of the spinal column, and lower leg injuries, as sustained by front seat occupants in automobile "glance off" impacts at high speed.</p> <p>P.T.O.</p>	<p>AGARD-CP-322</p> <p>Linear acceleration stress Impact acceleration Impact Injuries Biodynamics Protection Vertebrae Head (anatomy)</p>	<p>AGARD Conference Proceedings No.322 Advisory Group for Aerospace Research and Development, NATO IMPACT INJURY CAUSED BY LINEAR ACCELERATION: MECHANISMS, PREVENTION AND COST Edited by J.L.Haley, Jr Published October 1982 530 pages</p> <p>Problems dealing with impact injury caused by linear acceleration are covered. Papers cover spinal column injuries caused by <math>g_z</math> (eyeballs down) impact, tensile (eyeballs up) loading of the spinal column, and lower leg injuries, as sustained by front seat occupants in automobile "glance off" impacts at high speed.</p> <p>P.T.O.</p>	<p>AGARD-CP-322</p> <p>Linear acceleration stress Impact acceleration Impact Injuries Biodynamics Protection Vertebrae Head (anatomy)</p>

<p>Head and neck injury mechanisms are discussed both from a physiological and neurological standpoint. Both helmeted and unhelmeted head impacts are analyzed, and helmet test and evaluation methods are covered. Several papers described accident/injury investigation methods, including a helicopter crash test with instrumented dummies aboard. Injury-preventing hardware is covered; papers include restraint harness slack, "dynamic preload" of the restrained body, testing and evaluation of new shock-absorbing (stroking) helicopter seats, automotive air bag testing, and the use of a "webbing tear" shock absorber on a helicopter crew chief's restraint harness.</p> <p>The validation of a spinal injury model and a more general kinematics (whole body) model are also discussed. Finally, the cost effectiveness of torso armor was discussed in two papers. The conclusions from this meeting will hopefully be applied for improved impact protection.</p> <p>Papers presented at the Aerospace Medical Panel Specialists' Meeting held in Cologne, West Germany, from 26-29 April 1982.</p> <p>ISBN 92-835-0317-0</p>	<p>Head and neck injury mechanisms are discussed both from a physiological and neurological standpoint. Both helmeted and unhelmeted head impacts are analyzed, and helmet test and evaluation methods are covered. Several papers described accident/injury investigation methods, including a helicopter crash test with instrumented dummies aboard. Injury-preventing hardware is covered; papers include restraint harness slack, "dynamic preload" of the restrained body, testing and evaluation of new shock-absorbing (stroking) helicopter seats, automotive air bag testing, and the use of a "webbing tear" shock absorber on a helicopter crew chief's restraint harness.</p> <p>The validation of a spinal injury model and a more general kinematics (whole body) model are also discussed. Finally, the cost effectiveness of torso armor was discussed in two papers. The conclusions from this meeting will hopefully be applied for improved impact protection.</p> <p>Papers presented at the Aerospace Medical Panel Specialists' Meeting held in Cologne, West Germany, from 26-29 April 1982.</p> <p>ISBN 92-835-0317-0</p>
<p>Head and neck injury mechanisms are discussed both from a physiological and neurological standpoint. Both helmeted and unhelmeted head impacts are analyzed, and helmet test and evaluation methods are covered. Several papers described accident/injury investigation methods, including a helicopter crash test with instrumented dummies aboard. Injury-preventing hardware is covered; papers include restraint harness slack, "dynamic preload" of the restrained body, testing and evaluation of new shock-absorbing (stroking) helicopter seats, automotive air bag testing, and the use of a "webbing tear" shock absorber on a helicopter crew chief's restraint harness.</p> <p>The validation of a spinal injury model and a more general kinematics (whole body) model are also discussed. Finally, the cost effectiveness of torso armor was discussed in two papers. The conclusions from this meeting will hopefully be applied for improved impact protection.</p> <p>Papers presented at the Aerospace Medical Panel Specialists' Meeting held in Cologne, West Germany, from 26-29 April 1982.</p> <p>ISBN 92-835-0317-0</p>	<p>Head and neck injury mechanisms are discussed both from a physiological and neurological standpoint. Both helmeted and unhelmeted head impacts are analyzed, and helmet test and evaluation methods are covered. Several papers described accident/injury investigation methods, including a helicopter crash test with instrumented dummies aboard. Injury-preventing hardware is covered; papers include restraint harness slack, "dynamic preload" of the restrained body, testing and evaluation of new shock-absorbing (stroking) helicopter seats, automotive air bag testing, and the use of a "webbing tear" shock absorber on a helicopter crew chief's restraint harness.</p> <p>The validation of a spinal injury model and a more general kinematics (whole body) model are also discussed. Finally, the cost effectiveness of torso armor was discussed in two papers. The conclusions from this meeting will hopefully be applied for improved impact protection.</p> <p>Papers presented at the Aerospace Medical Panel Specialists' Meeting held in Cologne, West Germany, from 26-29 April 1982.</p> <p>ISBN 92-835-0317-0</p>